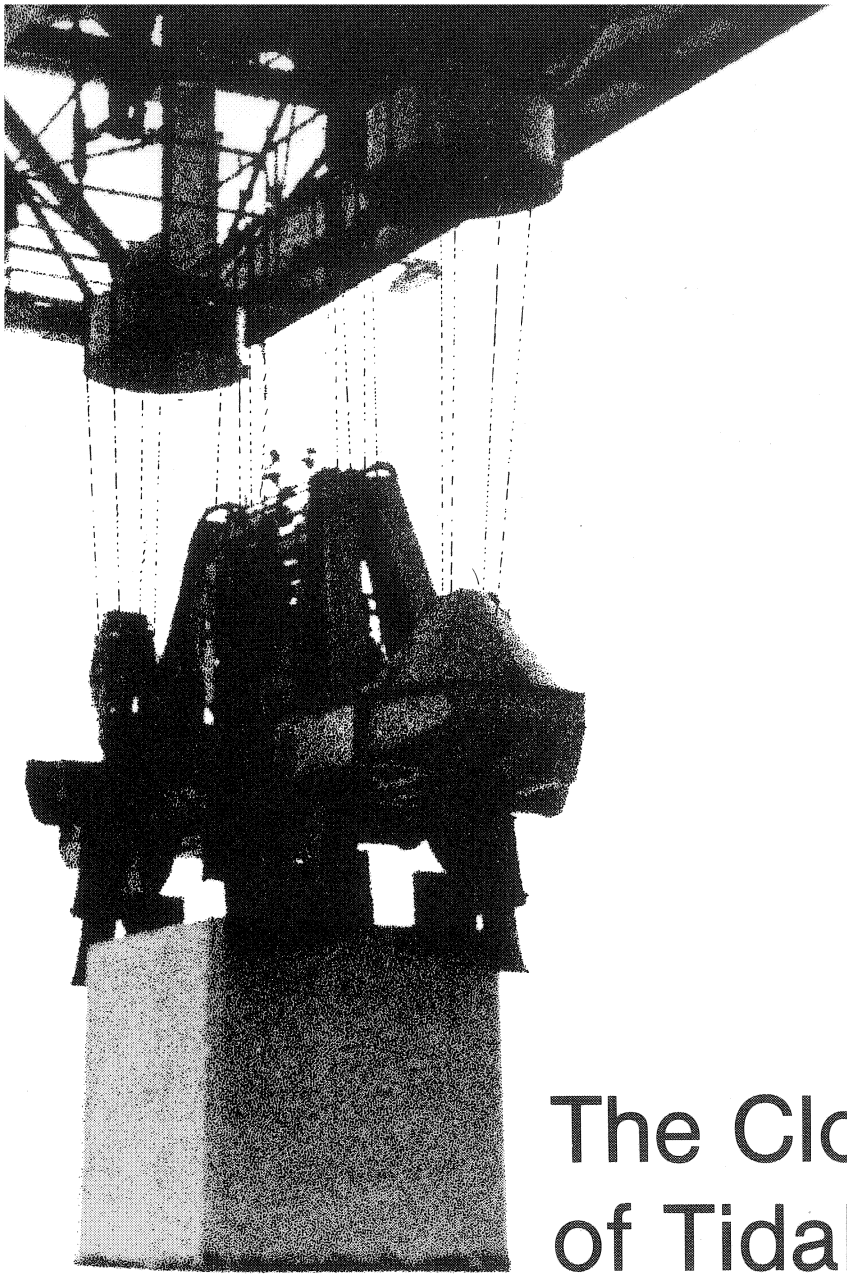

The Closure of Tidal Basins

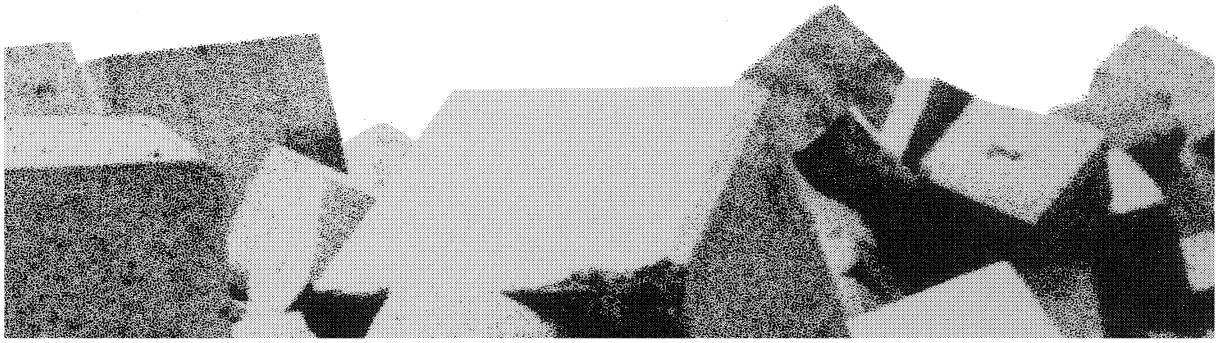

The Closure of Tidal Basins

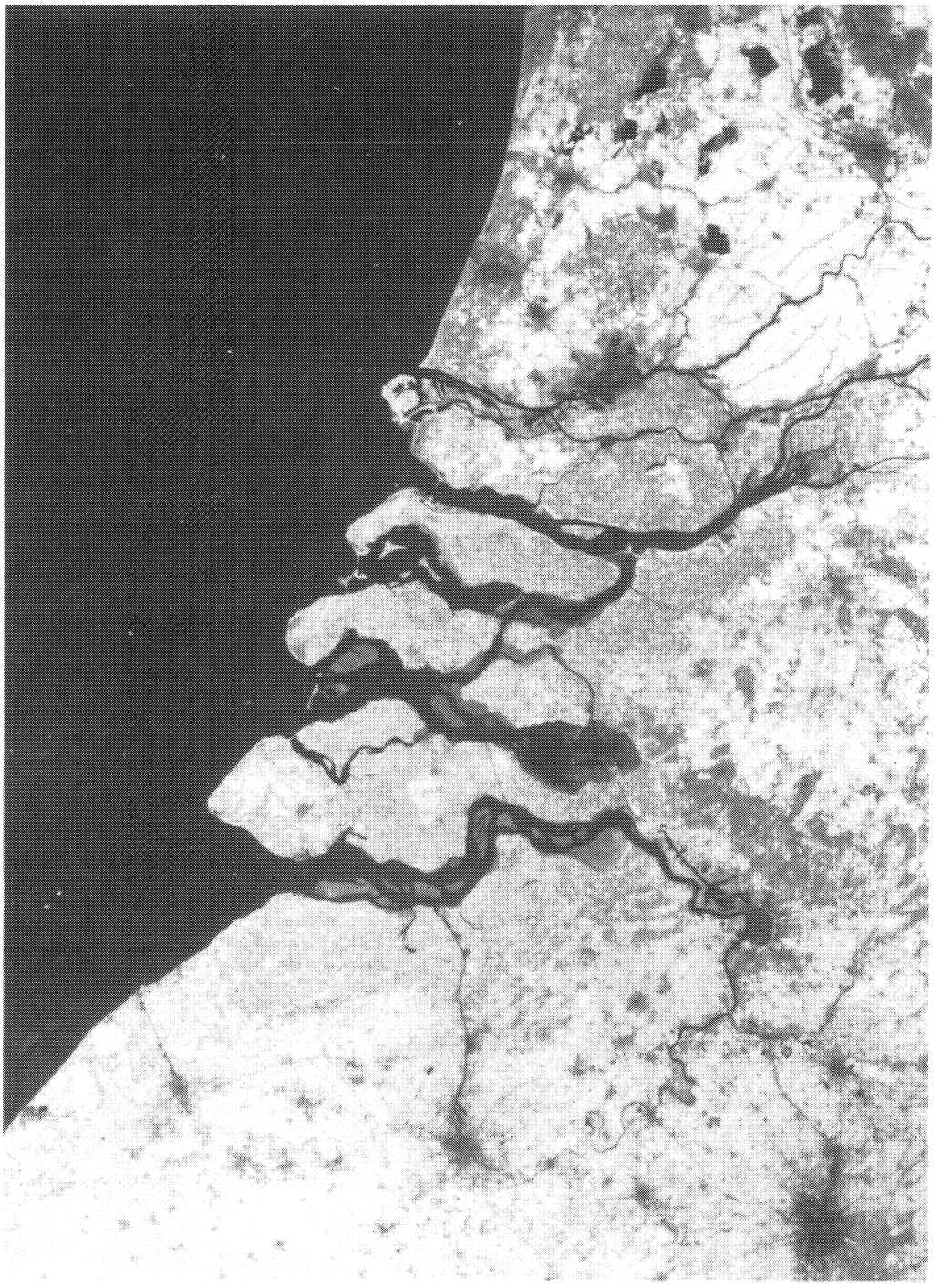

Satellite view of the Dutch Delta Area

The Closure of Tidal Basins

Closing of Estuaries, Tidal Inlets and Dike Breaches

Editorial Board
J.C. Huis in 't Veld
J. Stuip
A.W. Walther
J. M. van Westen

Editorial Co-ordinator
W. van Aalst

Delft University Press/1987

Published and distributed by
Delft University Press
Stevinweg 1
2628 CN Delft
The Netherlands
(0)15 783254

By order of
- Rijkswaterstaat
Ministry of Transport and Public Works
Koningskade 4
2596 AA The Hague
The Netherlands
(0)70 264011

For further information on the subject covered by
this publication and related topics please contact:
- Delft University of Technology
Stevinweg 1
2628 CN Delft
The Netherlands
(0)15 789111
telex: bhthd 38151
- Nedeco, Netherlands Engineering
Consultants
P.O. Box 80508
2508 GM The Hague
The Netherlands
(0)70 469421
telex: 32095
- Ministry of Transport and Public Works
Public Relations
Koningskade 4
2596 AA the Hague
The Netherlands
(0)70 264011
telex: 31043

CIP-DATA KONINKLIJKE BIBLIOTHEEK, THE HAGUE

Closure

The closure of tidal basins: closing of estuaries, tidal inlets and dike breaches/ed. board: J.C. Huis in 't Veld... [et al.]; ed. co-ordinator: W. van Aalst. – Delft: Delft University Press. – Ill.
Publ. by order of Rijkswaterstaat, Ministry of Transport and Public Works, The Hague
With lit.
ISBN 90-6275-287-X
SISO 699.4 UDC 627.5
Subject heading: hydraulic Engineering/Delta Plan

Copyright © 1984, 1987 by Delft University Press, Delft, The Netherlands.
All rights reserved. Published 1984. Second edition 1987.
No part of the material protected by this copyright notice may be reproduced or utilized in any form or by any means, electronic or mechanical, including photocopying, recording or by any information storage and retrieval system, without written permission from Delft University Press.

Printed in The Netherlands

Contents

	Preface	1
	Acknowledgement	2
	Foreword	3
1.	Introduction	7
2.	General Principles	15
2.1.	Project Realization	15
2.2.	Environmental Conditions	41
2.2. 1.	Tides and Currents	41
2.2. 2.	Waves	53
2.2. 3.	Ice	73
2.2. 4.	Hydrology and Geomorphology	85
2.2. 5.	Geological Conditions	111
2.2. 6.	Ecological Conditions	115
2.3.	Site Investigations and Data Acquisition	135
2.3. 1.	Measurement of Stage	135
2.3. 2.	Wave Measurements	147
2.3. 3.	Current Measurements	155
2.3. 4.	Surveying and Monitoring Seabed Morphology	169
2.3. 5.	The Determination of the Suspended Sand Concentration	203
2.3. 6.	Geological and Geotechnical Investigations	213
2.3. 7.	Investigations into Environmental Aspects	257
2.3. 8.	Application of Models in Studies of Ecosystems	269
2.4.	Interaction Watermotion and Closing Elements	281
2.4. 1.	Flow Induced Loads	281
2.4. 2.	Wave Induced Loads	291
2.4. 3.	Ice Induced Loads	295
2.4. 4.	Earthquake Induced Loads	307
2.4. 5.	Stability and Deformation of Closure Foundations	319
2.4. 6.	Stability and Motions of Floating Structures	343
2.4. 7.	Stability of Loose and Cohesive Materials	355
2.4. 8.	Stability of Rock-fill Structures	367
2.4. 9.	Local Scour	387
2.4.10.	Stability of Dredged Trenches	407
2.4.11.	Stability of Revetments	419
2.4.12.	Groundwater Flow	447
2.4.13.	Filters	467
2.4.14.	Environmental Impact on Marine Structures	491
2.4.15.	Some Practical Environmental Points of Attention	495
2.4.16.	Gates	505

2.5. Impact on the Environment 519
2.5. 1. Hydraulic Aspects 519
2.5. 2. Ecological Aspects 539

2.6. Performance Monitoring 561

3. Design and Operations of Closure Works 575

3.1. Approach 575
3.1.1. General 577
3.1.2. Design Phase 578

3.2. Layout of a Closure Dam 583
3.2.1. Positioning of the Dam 585
3.2.2. The Location of Structures in the Dam 587
3.2.3. The Shape of the Closure Gap 588
3.2.4. Cross Section of the Dam 592

3.3. Construction Methods 593
3.3.1. Closure Methods 595
3.3.2. Bottom Protection Works 597
3.3.3. Temporary Works 598

3.4. Gradual Closures 599
3.4.1. Hydraulic Conditions 601
3.4.2. Construction Methods 602

3.5. Sand Closure 611
3.5.1. Sand-fill byHorizontal Pipe Discharge 613
3.5.2. Sand-fill byDumping 621

3.6. Sudden Closure 625

4. Case Studies 641

4.1. Introduction 641

4.2. Closure of Flow Gaps in the Harbour Moles at Zierikzee 645

4.3. Closure of the Brouwershavenschegat by the Construction of the Brouwersdam 663

4.4. Closure of Rivers and Tidal Channels in Bangladesh 729

Photographs

The following photographs are owned by:

pages 7, 9, 10, 11	:	Bart Hofmeester
page 12	:	Cees van der Meulen
page 13	:	Jan van de Kam
Figure 2.2.3.4, 4.6	:	KLM-AEROCARTO
Figure 4.36, 4.38	:	Slagboom en Peeters
Figure 4.42, 4.43	:	Bart Hofmeester

Other pictures are owned by Rijkswaterstaat.

Authors

W. van Aalst,	Staff Engineer, Hydraulics Division, Delta Department, Rijkswaterstaat
J.R. v.d. Berg,	Project Engineer, Hydrographic Section, Hydraulics Division, Delta Department, Rijkswaterstaat
E.L.B. Birnbaum,	Project Engineer, Hydrobiology Section, Environmental Division, Delta Department, Rijkswaterstaat
J. Bruinsma,	Project Engineer, Morphological Section, Hydraulics Division, Delta Department, Rijkswaterstaat
J.C. v.d. Burg,	Project Engineer, Geotechnical Section, Hydraulics Division, Delta Department, Rijkswaterstaat
H. Engel,	Head of Delta Department, Rijkswaterstaat
H.A. Ferguson,	Former Head of Delta Department, Rijkswaterstaat
J.C. Huis in 't Veld,	Chief Project Engineer, Surveying Section, Construction Division, Delta Department, Rijkswaterstaat
D.J. de Jong,	Project Engineer, Biology Section, Environmental Division, Delta Department, Rijkswaterstaat
R.J. Leewis,	Project Engineer, Biology Section, Environmental Division, Delta Department, Rijkswaterstaat
R. Misdorp,	Project Engineer, Landscape Section, Environmental Division, Delta Department, Rijkswaterstaat
H. Mulder,	Project Engineer, Morphological Section, Hydraulics Division, Delta Department, Rijkswaterstaat
J.K. Nieuwenhuis,	Chief Project Engineer, Geotechnical Section, Hydraulics Division, Delta Department, Rijkswaterstaat
C.P. Ockhuysen,	Project Engineer, Hydraulic Section, Hydraulics Division, Delta Department, Rijkswaterstaat
K.W. Pilarczyk,	Project Engineer, Models Section, Hydraulics Division, Delta Department, Rijkswaterstaat
W. v.d. Ree,	Staff Engineer Hydraulics Division, Delta Department, Rijkswaterstaat
D.B. Smith,	Project Engineer, "Dosbouw" Constructors, Burghsluis
H. Speekenbrink,	Project Engineer, Morphological Section, Hydraulics Division, Delta Department, Rijkswaterstaat
P.B.M. Stortelder,	Project Engineer, Chemical Section, Environmental Division, Delta Department, Rijkswaterstaat
J. Stuip,	Senior Scientific Officer, Delft University of Technology
J. Visser,	Project Engineer, Landscape Section, Environmental Division, Delta Department, Rijkswaterstaat
J. Voogt,	Chief Project Engineer, Hydraulic Section, Hydraulics Division, Delta Department, Rijkswaterstaat
H. Vrijling,	Project Engineer, Models Section, Hydraulics Division, Delta Department, Rijkswaterstaat
A.W. Walther,	Head of Hydraulics Division, Delta Department, Rijkswaterstaat
J.M. van Westen,	Project Engineer, Materials Section, Construction Division, Delta Department, Rijkswaterstaat

PREFACE

I share the pleasure of having been involved for many years in the Delta Project with many colleagues from the Rijkswaterstaat, Delft University of Technology, research institutes and contractors. The „Delta workers" certainly wish to impart to others some of the joy they have experienced in their battle with Poseidon. Writers would do so poetically. Engineers try to hide their feelings behind the serious mask of a textbook. However, they secretly hope to convey some of their enthusiasm to colleagues and students who read this book.

This book is backed up by the experiences of a great number of engineers and other professionals. They acquired their knowledge by patient study and experience in the practice of real closures. They learnt their best lessons when the sea outwitted them. In the process they acquired the knack of getting along with water and usually with people as well.

The advantage of working in a small, highly developed country like the Netherlands is that experts in a variety of fields are close at hand. Moreover, since 60% of the population lives below mean sea level interest in hydraulic engineering is shared by many people.

The soon to be completed Delta Project will be the result of fruitful cooperation by the available expertise in the Netherlands. Some of the know-how is brought together in this textbook. I hope it will offer you as much interest and pleasure as the authors experienced in preparing it.

H. Engel
Chief Engineer and
Director of the Delta Division
of Rijkswaterstaat
Ministry of Transport and
Public Works.

Acknowledgement

ACKNOWLEDGEMENT

Many people have contributed to the realization of this textbook. First of all we wish to thank the specialist fellow workers who have put in many hours in writing, discussing and amending the contributions.

Helpful comments and suggestions were obtained from Prof. F. Gerritsen from the Hawai University, on sabbatical leave in the Netherlands and Prof. J.F. Agema from the Delft University of Technology, both currently doing research on the foreground of theory and applications in this area.

For the graphic design we should like to thank L.W.E. Willemstein and G.L. van Graafeiland as well as G.L. Stoové, G. Hiemstra, R. Vransen, A. de Ruyter, S. Verbaan and A. van Dijk who meticulously drew the numerous drawings and graphs and Mrs. Th. Duivestein who did some special typesetting.
We also very much appreciated thecooperation with Mrs. M. van Dorp and T. Verhoef and Messrs. L.J. Cassa and J.C. Wolff of the typesetting section.

We should also like to draw attention to the efforts of the translators and revisors, Dr. J.W. Arriens, Cambridge, and Mrs. M. Hoog who painstakingly tried to interpret the intentions of the authors. For any remaining grammatical errors the authors and editors wish to take the responsibility.

And last but not least the efforts and patience of the typists guided by Mrs. I.Th. Wolff should be mentioned.

The Editors and Authors

Foreword

FOREWORD

Although the damming of running waters is an old art, it could for a long time only be practised on a small scale as the primitive means of technology and the lack of an effective scientific hydrodynamical approach limited the scope.
Only in the last century, when the developments in fluid mechanics could be practically applied, and building technology had made sufficient headway, did it become possible to embark on large dam projects. Since then, thousands of large dams have been built in rivers all over the world, several of them being already more than a hundred years old.
Compared with these activities in rivers, dam building in areas exposed to tides and waves - estuaries and tidal inlets - has lagged considerably behind. Damming in these areas was long confined to the closing of dike breaches that had occurred incidentally. These rough and ready undertakings did not lead to the development of more advanced techniques. Although, perforce, they were often carried out with unusual methods and materials, engineers always returned to the old and well-tried techniques when normal projects had to be designed, for tradition is hard to kill.
Moreover, one of the main reasons for the reluctance to embark on large-scale dam building in tidal waters was the lack of understanding of the phenomena of unsteady flow, which is a characteristic of these waters. It was not until the Zuyderzee project had to be realised that this difficult area of hydrodynamics was so far developed that reliable tidal computations could be executed even over large areas. The basis was then laid for further tidal research which eventually made it possible to design the Delta Plan and other large projects in coastal areas.
However, the Zuyderzee works did not bring about an appreciable change in technology. They were mostly executed in the traditional manner; the willow mattresses balasted with stone that were used only showed small improvements on the old methods.
The first decisive breakthrough from tradition took place during the repair works on the dike breaches on the Isle of Walcheren.
These dikes were bombed by the Allied Air Forces at the end of World War II and confronted the engineers of a completely disorganised and impoverished country with an almost impossible task, which was to close four very large gaps with strong tidal currents in a few months. In this very exceptional situation, recourse has to be taken to revolutionary - till then untried - methods and materials. For instance, concrete caissons entered the field and with them a technique was introduced which, in the course of time, would obtain a firm foothold, notwithstanding strong opposition by those who favoured traditional methods.
Sooner than could be foreseen, the new techniques introduced at Walcheren had their chance for further development when, only eight years later, the flooding of large parts of southern Holland during the storm surge of 1953 called for further applications of the new methods on a much greater scale.

It was, however, the Delta Plan, born as a result of the 1953 storm disaster, that opened definitive roads to revolutionary developments of the art of coastal engineering especially in the fields of damming tidal waters. The significance of this project was not only the exceptionally long period of time it required for its realisation (the Zuyderzee project had required even more time), but especially the structure of the Plan. The Delta Plan consists, in fact, of a sequence of enclosure works of differing size and difficulty, to be executed one after the other, beginning with the smaller closure and ending with the largest: the Eastern Scheldt.
This sequence enabled the engineers to gain gradually more experience and to try different new methods and techniques during the course of the works. Thus, the project could become a kind of school on coastal engineering with ample opportunity to further the different techniques involved, directed especially at the problems concerning the closure of tidal channels. In the course of the project, a wealth of knowledge and experience has been acquired and it would be a pity if this new exper-

Foreword

tise could not be universally shared. This book has therefore been written to make this knowledge available for future use.
It is a reflection of the domination of hydraulic engineers over coastal environments and their ability to adapt and control natural tidal systems in coastal waters and estuaries for the benefit of mankind. This power has caused concern to those who have a keen eye on the important ecological values of these areas for they are afraid that much irreparable damage to the environment could be effected by these huge projects. Fortunately, this book also deals amply with these environmental aspects.
Wide-ranging studies and investigations in the field of ecology have accompanied the civil engineering part of the project and these results are also treated in this book. They may awaken the interest of the coastal engineer in ecological matters and, conversely, open the eye of ecologists not only to adverse but also to possible beneficial effects of coastal engineering on ecosystems.

H.A. Ferguson
Former Chief Engineer and
Director of the Delta Division
of Rijkswaterstaat.
Ministry of Transport and
Public Works.

Foreword

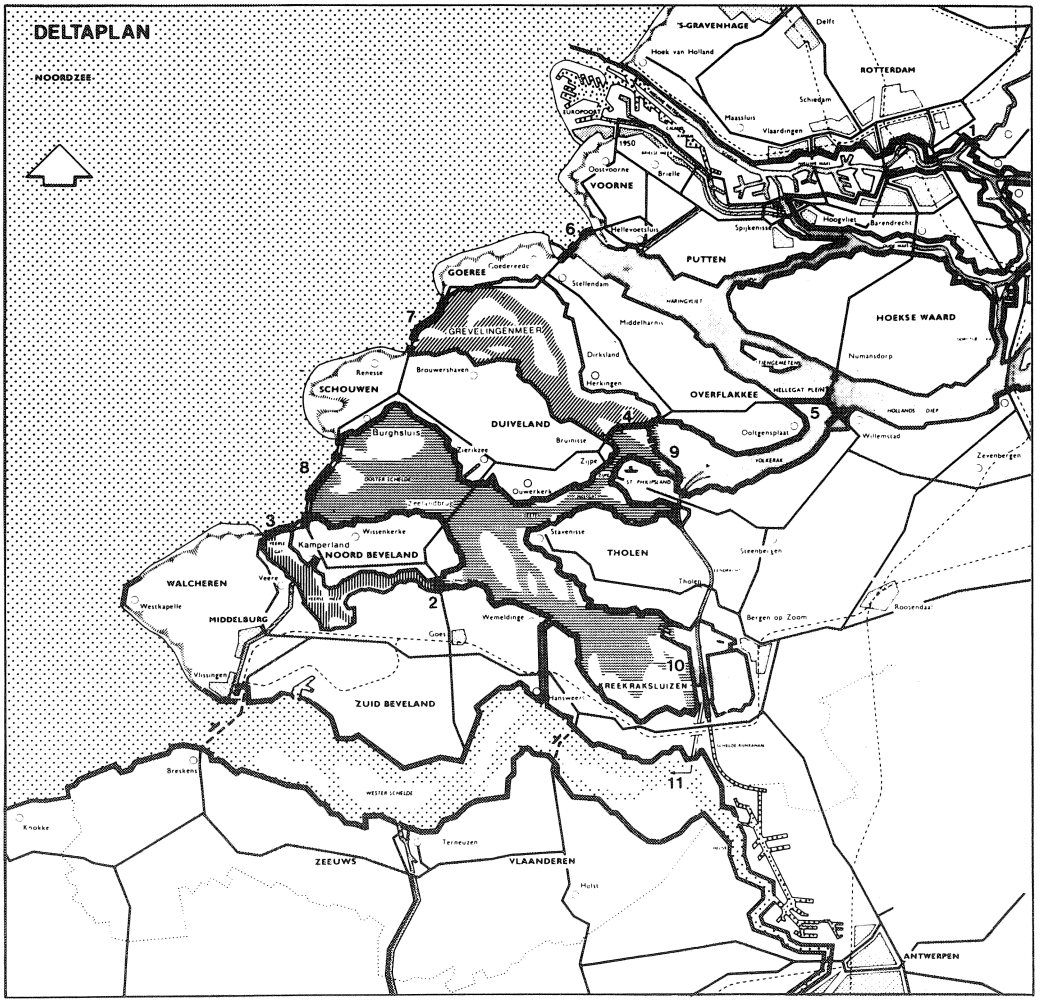

TIDAL, SALT
TIDE-LESS, FRESH
REDUCED TIDE, SALT
SEMI STAGNANT, SALT
SEMI STAGNANT, SALT OR FRESH
HEIGHTENING OF THE DYKES

1 STORM SURGE BARRIER HOLLANDSE IJSSEL (1958)
2 ZANDKREEK DAM WITH SHIPPING LOCK (1960)
3 VEERSE GAT DAM (1961)
4 GREVELINGEN DAM WITH SHIPPING LOCK (1965) AND SLUICES (1983)
5 VOLKERAK DAM WITH SHIPPING LOCKS AND INLET-SLUICES (1970)
6 HARINGVLIET DAM WITH DISCHARGING SLUICES (1971)
7 BROUWERS DAM (1972) WITH SLUICE (1978)
8 EASTERN SCHELDT DAM WITH STORM SURGE BARRIER (1986)
9 PHILIPS DAM WITH SHIPPING LOCKS (1986)
10 OYSTERDAM WITH SHIPPING LOCK (1986)
11 SLUICE BORDERING LAKE (1985)

AT THE SECOND EDITION

Before you is the second edition of 'The Closure of Tidal Basins'. The book easily found its way as a textbook for different graduate and post graduate civil engineering courses in The Netherlands. Sooner than expected the publisher ran out of copies, and faced with a steady demand, invited us to prepare a second edition. We took the opportunity to introduce a small number of minor corrections and the hard cover was replaced by a paperback. The price remained unchanged.
We like to thank the Delft University Press for the efforts to publish this second edition.

The Editors

1. Introduction

Introduction

A.W. Walther

1.1. Hydraulic engineering in the Netherlands

Throughout history the dialogue with the sea has been a matter of life and death for the people in the Netherlands. Yet, the country owes its success in trade to this querulous neighbour and its unique position at the mouths of the rivers Rhine and Meuse. Without coastal defences and dikes, however, half of the country would not even exist.

The first Dutch farms were built in the north of the country by the inhabitants of Friesland on artificial mounds around 400 B.C. Swamps and lakes dominated the country and on the mounds the Frisian people found refuge from the storm surges of the gradually rising North Sea.

Introduction

The first dikes were constructed much later in the eleventh century.
Gradually, the Netherlands arose from the sea. Excess water was pumped out by windmills. Hydraulic engineering was of vital importance to the Dutch and became the „art of the nation".[1]). This can be illustrated by the accounts rendered on disastrous floods throughout Dutch history. In the battle against the sea, this art and tradition live on in the present generation. The principal hydraulic contractors are still established in those areas of the country which have a long history in the battle against the encroaching sea.

---

[1]) Dr. J. van Veen, Dredge, drain, reclaim, the Art of the Nation, The Hague 1950.

Introduction

Since the beginning of the twentieth century, science has provided hydraulic engineers and contractors with new powerful tools. Thus, the closure of the Zuyderzee with a 30 km long dike became possible as a result of the tidal computations by Lorenz. Later on, the Delft Hydraulics Laboratory enabled the study of many hydraulic engineering problems on small scale models. Contractors improved their possibilities by introducing new types of dredgers and special-purpose equipment.

Nowadays, Dutch contractors, consulting engineers and laboratories find their clients in countries all over the world; closing estuaries, constructing dikes, draining marshes, digging canals and building sluices, locks and harbours. The experience with both very small and very large hydraulic engineering projects in the Netherlands has proved to be of value all over the world.

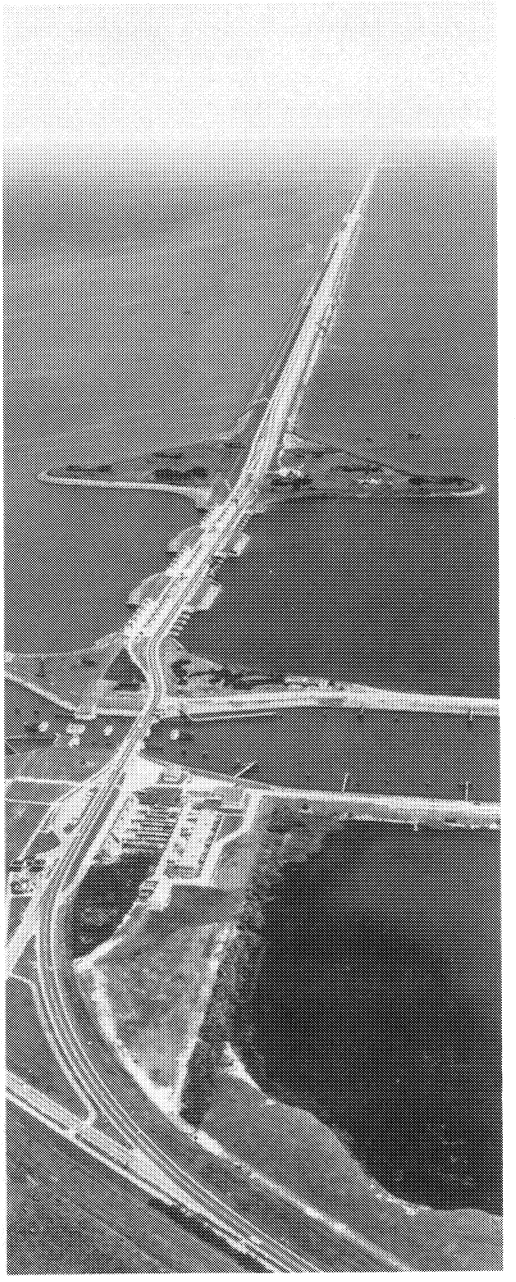

1.2. Ecology and hydraulic engineering

With the gradually increasing possibilities for civil engineers to change the natural environment, awareness arose of the side-effects of their work. Sometimes, these effects were evaluated positively and sometimes negatively.

Therefore, the question arose whether it would not be possible to reduce the negative effects. The fear of negative effects aroused so much attention that many people began to think that a „hands off" policy would be the best. A clear example of this non-intervention attitude in the Netherlands, was encountered by some people involved in the discussion about the Eastern Scheldt project. As a result of the closure of the Volkerak in 1969, the amount of fresh Rhine water entering the estuary decreased. Consequently, the salinity of the Eastern Scheldt water remained fairly constant and high throughout the year. Thus, very favourable conditions were created and the ecological value of the estuary increased. Many opponents of the planned closure of the Eastern Scheldt advocated a „hands off" policy and opposed all human intervention without realizing that the

positive effects of the Volkerak-closure were also the result of humain action. Moreover they did not seem to realize that the area concerned was not the South Pole but a populated part of an industrialized country.

The reader of this book will find that ample attention is given to the negative ecological effects of civil engineering works. With the growing knowledge of ecosystems, however, attention will certainly switch to the positive effects as well.

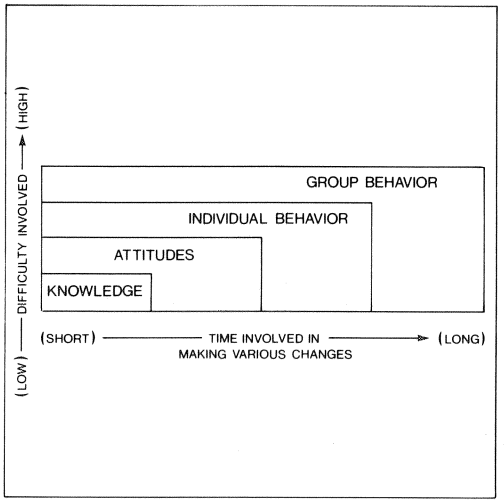

The integration of ecological concepts in civil engineering is still in its infancy. Knowledge is increasing rapidly and attitudes are changing but it will still take a long time before the integration of ecology and civil engineering will be accomplished. This social-psychological process is clearly indicated by Hersey and Blanchard (Management of organizatonal behavior. Prentice Hall Inc. New Jersey.) in the figure alongside. Their plea for the support of behavioral scientists in the application of new knowledge in our society decerves full credit.

1.3. The aim of the book

It is the purpose of the writers to provide civil engineers and students with a guide to one aspect of hydraulic engineering: the closing of estuaries and dike breaches in tidal areas. The starting point of the book is the experience gained in the Dutch Delta Project, which illustrates the growing knowledge of hydraulic engineering and ecology. In the 1960's, the main purpose of the Project was safety against the sea. In the 1970's however, the originally intended total

Introduction

closure of the Eastern Scheldt estuary was abandoned for ecological reasons. Safety combined with the conservation of the ecosystem is the present purpose of the closure with a storm-surge barrier.
The book is concerned with all aspects of closures. Chapter 2 provides the reader with some basic general principles. The phenomena described are: tides and currents, waves, ice, sediment movement and morphology, soil mechanics, geology and ecology. Site investigations and data organisation are dealt with as well as the relations between a structure and its environment. The reader is provided with some basic ways of approaching the problems. The impact of a closure on the environment and the

Introduction

monitoring of the construction after completion are described at the end of the chapter.

Chapter 3 is concerned with closing structures and operations: the location of a dam, the shape of a closure gap and different closing methods. Finally, in order to illustrate the preceding chapters, chapter 4 comprises three different cases of closure: the closure of a dike breach in a harbour at Zierikzee after the 1953 storm disaster, the closure of estuaries in Bangladesh in 1978 and the closure of the Brouwershavensche Gat, one of the largest operations of the Delta Project in 1972.

2. General Principles

2.1. Project Realization

The realization of a project appears to develop along characteristic lines. It is important to be aware of the characteristics of the various stages in the realization process, because each stage has its own specific activities.
This theme is worked out in the following section with emphasis on the realization of projects concerning the closure of estuaries.

Project Realization

J. Stuip

2.1. Project realization

2.1.1. Introduction

It is essential to have a proper idea at the outset of the process of realization. Figure 2.1.1. illustrates this statement in terms of costs; in the beginning of the process the rate of influence on the total cost is high, while during the progress of the project the influence decreases and the cost itself increases. But for other aspects as well the general identification of impacts at the beginning of the process is more effective than at a later stage.

A project realization model may be as follows. The model consists of various stages subdividing the project as far as possible into independent units.

Figure 2.1.1. Influence of cost and costs vs. time.

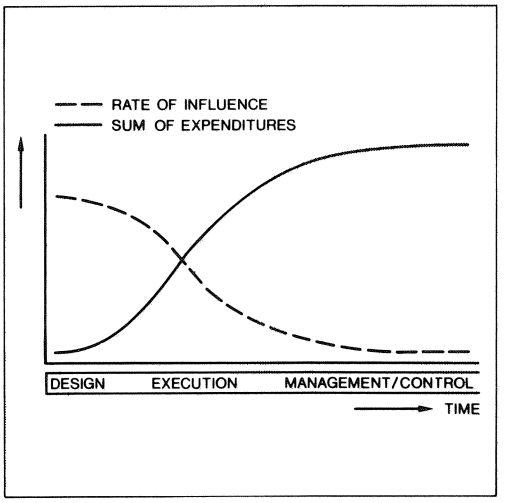

Figure 2.1.2. Realization process.

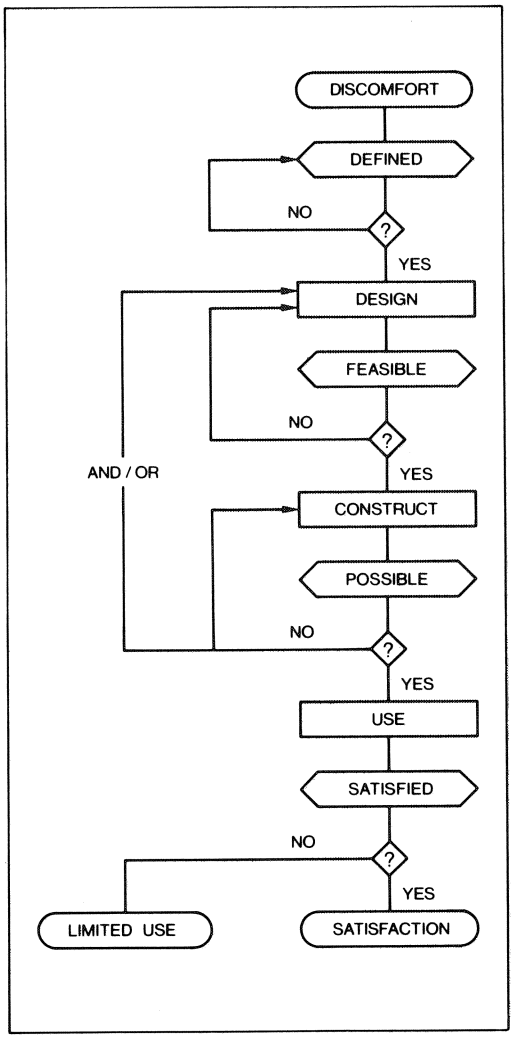

These stages range from interpreting the principal order in terms of environmental, hydraulic, geotechnical and engineering characteristics, to the generation of design concepts, the evaluation of alternative concepts and the exhaustively studied final design, to the construction of the structure with a controlled feedback to design considerations and criteria. After completion, the realization process continues with the systematic supervision of the observance of directions for use and maintenance. Figure 2.1.2. illustrates the model.

The realization of a project generally has an impact on other aspects.
Closing tidal basins involves an essential alteration to the existing environment.
So, considerations other than engineering aspects alone have to be taken into account. In handling environmental problems for instance, „guidance" of specialists is indispensible in the various stages:

- early stage guidance in preparation of decisions between alternatives
- short-term guidance; impacts directly due to project activities;
- long-term guidance; with respect to directly caused changes to the environment that will be present almost permanently upon project completion;
- guidance for management and legalisation of the new environment; the new situation may in many cases require new government powers.

Throughout the realization process it is essential to be thoroughly familiar with the consequences of the various alternatives. Even after project completion, a systematic analysis of the impact parameters should be carried out to check the predictions made during previous stages of the project.
In general the realization process of an engineering structure or even a measure will run along the following lines.
The process starts with a vague feeling of discomfort which is followed by an urge to react. It is clear that in the case of reconstructing a destroyed dike the feeling of discomfort is acute: the land is inundated, keep the water

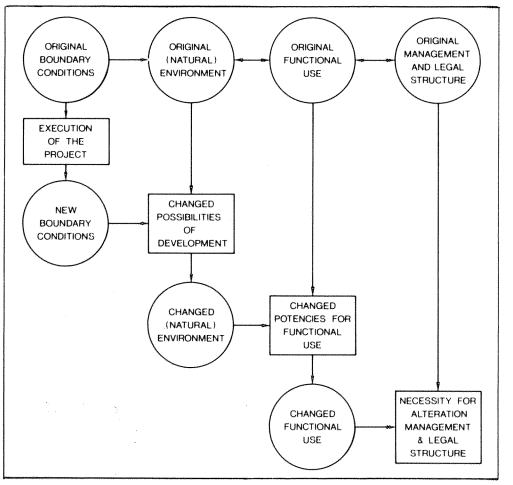

Figure 2.1.3. A chain of results caused by a major human action in the environment.

away! But in the case of closing a tidal inlet or sea-arm the feeling will be less clear-cut and there may be alternatives to a complete closing of the watercourse.
In general, the urge to react results in activities with the objective of changing the given situation. These activities start with a problem formulation in such a format that it is possible to develop alternative solutions. These activities form the beginning of the second stage of the realization process: the design stage. It is obvious that there should be a clear understanding of the characteristic phenomena of the existing situation. Only in this way there is a significant possibility of improving the future situation.
A current definition of design is: to offer the best solution to meet a demand whereby the available means and the natural and social criteria are taken into account.
The design stage itself consists of different

stages such as problem formulation, search for ideas, basic shape development, and dimensioning the final form.
The third stage in the realization process is the implementation of the plans designed in the former stages: the construction or execution stage.
There are many feedbacks to the design stage as there were many thoughts ahead to construction methods in the design stage. It is of great importance to monitor the construction activities in such a way that a controlled feedback to design considerations and criteria becomes possible.
In the fourth stage the structure is finished and ready to be used. The user, the person or community, who in the very first stage was discontented with the existing situation, is now satisfied. In complicated situations, however, the interest of various groups may collide (e.g. comfort or safety of human beings versus environment). As a rule a compromise will be only reached, which means that not all parties will be satisfied.
Monitoring the project remains important both for the construction itself (to check its condition and ability to fulfil the desired functions) and for its environmental impact.

For a sound management of the project it is essential to have available a proper communication and documentation system for all relevant facts and figures gathered during the execution of the project. After completion there should also be a similar system to check the performance of the structure.
Only in this way will a controlled feedback to foregoing stages and to planning for subsequent stages be possible and will the risk of overlooking principal aspects be minimized.
During the initial stages of the design process (and the other stages) a selection usually has to be made from many generated alternatives and, as a rule neither time and money permit complete information about all alternatives to be gathered. It is, however, necessary for a sound assessment that the information gathered on all promising alternatives be of the same level of

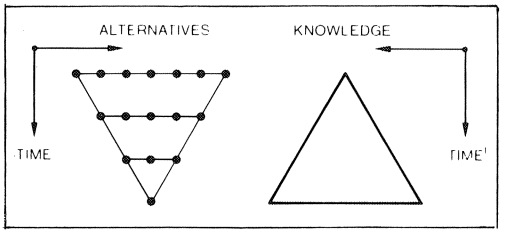

Figure 2.1.5. Decrease of alternatives, increase of knowledge.

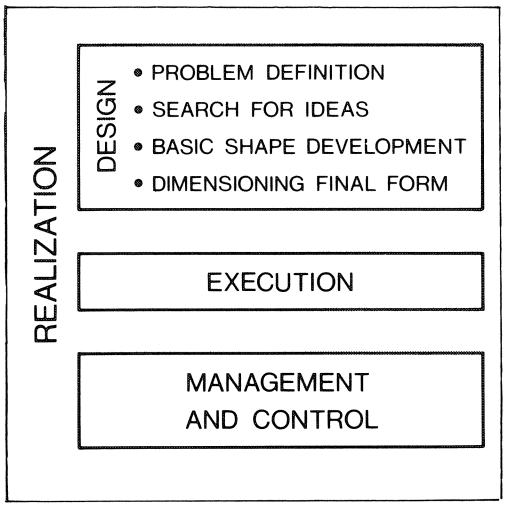

Figure 2.1.4. Stages in project realization.

knowledge; otherwise one risks choosing that alternative about which one knows the least (including the disadvantages) and to reject the best-known alternative (based on the drawbacks of which one is aware).

2.1.2. The initial stage

In this stage the vague feelings of discomfort referred to earlier result in an urge of react.
This vague feeling may for example be a suspected higher probability of being drowned by a stormsurge in a specific area then elsewhere. The urge to react results in the possible actions: maybe the dikes should be reinforced; maybe the dikes should be higher; maybe the water outside the dike should be cut off from the tidal regime; perhaps there should just be a better stormsurge warning system, or perhaps emigration of the population is the best solution, etc.

In the case of a dike breach it is obvious that there is not just a vague feeling but that the urge to react is clear: repair the dike and reclaim the inundated area.
The end of this initial stage will consist of the formulation in broad terms of the objectives of the project.

2.1.3. Design stage

The design stage is a chain of activities with many feedbacks; one tries repeatedly to assess the desired demand and at the same time insight increases into what is really necessary and how those needs can be fulfilled. After formulation of the need this term might be interpreted as objective with certain criteria for the structure (or measure) and its components. During the evolution of the design various alternatives and the criteria for choosing from alternatives and for dimensioning the final design become more and more specific and are expressed in terms of the functional behaviour of the structure.
Within the design process a number of stages can be distinguished:

A. problem formulation;

B. search for ideas;

C. basic shape development;

D. dimensioning the final form.

A. Problem formulation stage
In this stage a clear and exact description of the expected improvement of the existing situation will be given, formulated in such a way that the next stage in the process can start.
The formulation should be expressed in characteristic terms of the phenomena to be altered. For instance the dike should be able to withstand a water level with a probability of exceedance of 10^{-4} per year or the salt content in the water should not exceed 1000 ppm with a probability of 10^{-1} per year.
Formulations such as that the dike should be able to withstand „high-water levels" or the salt content should be „low" are no longer sufficient in this stage.
So, the problem definition stage is characterized by the definition or description of:
- the functional demands resulting from earlier formulated objectives;
- the boundary conditions set by nature (waves, water levels, soil conditions, environment);
- the nature of the criteria on which the conceptual designs as yet to be developed will be judged with, in so far as possible, quantification of these criteria.

B. Search for ideas
Within the framework of the assignment, including time and costs, conceptual designs are generated in this second stage of the design process, which are tested against the already developed criteria and the known boundary conditions.
In this stage the creativity of the designer - „the architect" - is most important, mobilising the available hydraulic, geotechnical, structural and environmental expertise. There are many techniques for stimulating creation of alternative solutions, such as brainstorming, brainwriting, collective note book, bionics, synectis, etc. These techniques are common for inventing new products or solutions for structural concepts.

Besides these techniques, an exhaustive functional analysis of the structure as a whole, as well as the details (carried out during the various stages of the realization) should be the basis for the search for ideas.
At the end of this stage a selection will have to be made from the conceptual designs generated. This selection will be based on a number of criteria such as costs, planning and the extent of uncertainty in both and in meeting the criteria to fulfil the functions.

For this selection procedure, neither time nor money are generally available to gather-through research-complete information about all the alternatives. It is, however, necessary for a sound assessment that the information gathered on the alternatives be of the same level of knowledge. Otherwise one risks choosing the alternative about which one knows the least (including the disadvantages) and rejecting the best-known alternative (based on the drawbacks of which one is aware). At this stage, the probable changes to and the consequences for the various physical, chemical, biological and even social-economical chracteristics of the environment brought about by the various proposed „actions" should be studied. Even if the identification of the inter-relationships between the variables is complicated because of primary impacts followed by secondary ones, a prognosis of future changes is indispensable for decision-making.

An orderly method should be used even for preliminary screening of project alternatives with rapid identification techniques involving checklists, matrices, overlays networks etc. (see Figure 2.1.6.).

Figure 2.1.6. Specimen „water project" check list.

The use of these techniques does not so much require quantified data, as well a general familiarity with the region and the nature of the proposed activities. It is often an aid to the decision-maker in recognizing patterns and trading off disparate impacts. Scorecards can be used if more quantified information is available from field surveys, calculations and simulation models. The scorecard takes a table of impacts and adds colour or hatching to indicate each alternative's ranking for a particular impact. Figure 2.1.7. gives an example of a scorecard of ecological impacts for five alternatives for the discharge capacity of the Eastern Scheldt Barrier.

C. Basic shape development

The next step is to enlarge the data for the selected alternatives, to select the two or three most promising design concepts and to give these a rough basic shape and preliminary dimension estimates. At this stage the insight into the working method and into the details is enlarged, while a quantitative specification of the various criteria becomes more relevant.
Accordingly, more specific criteria will be applied than were previously necessary or possible. This holds for all aspects of the project, including environmental, structural, hydraulic or even organizational aspects.

ILLUSTRATION OF CHECKLIST

ITEMS	NATURE OF LIKELY IMPACT				
	ADVERSE			BENEFICIAL	
	SHORT TERM LONG TERM	REVERSIBLE IRREVERSIBLE	LOCAL WIDE	SHORT TERM LONG TERM	SIGNIFICANT NOMINAL
ECOLOGY					
FISHERIES					
AGRICULTURE					
SILTATION					
EROSION					
EUTROPHICATION					
EARTHQUAKES					
FOG FORMATION					
VECTOR-BORNE DISEASES					
DOWNSTREAM EFFECTS					
LANDSCAPE					
ECONOMIC ACTIVITY					
TOURISM					
RECREATION					
DISPLACEMENT OF PEOPLE					
ARCHEOLOGICAL SITES					

ECOLOGICAL IMPACTS OF THE FIVE NOMINAL ALTERNATIVES

Item	Alternative A3	Nominal Reduced-tide Alternatives (C3) μA = 20000 sq m	μA = 11500 sq m	μA = 6500 sq m	Alternative D4
Key inputs					
Salt basin area (sq km)	369.5	369.3	364.5	352.4	202.0
Tidal range at Zierikzee (m)	3.0	2.9	2.0	1.3	0.0
Primary production (tons/day)	352.9	352.7	348.1	346.1	193.8
Detritus import (tons/day)	546.0	640.0	990.0	916.0	0.0
Primary food availability (% of present)[a]	78	86	116	85	17
Total biomass					
Amount (tons afdw)	21300	24200	29700	27550	5160
Percent of present amount	75	85	104	96	18
Potential abundance of birds					
Benthos-eaters (tons afdw)	6.6-7.3	6.3-9.7	4.9-13.0	3.5-11.7	0.4-1.4
Fish-eaters (tons afdw)	0.0345	0.0445	0.063	0.0566	3.94
Plant-eaters (tons afdw)	Unch.	Unch.	Unch.	Unch.	Incr.
Potential shellfish culture					
Mussels (% of present)	100	90	90	90	13
Oysters (% of present)	100	90	90	90	0
Nursery function					
Shrimp (% of present)	50	150	400	350	0
Fish (% of present)	73	98	133	125	0
Transients					
Rapid kill of benthic biomass (tons afdw)	4220	4231	4491	5148	11492
Rapid kill (% of present benthic biomass)	25	25	27	31	68
Change in average density of benthic biomass from present (g/sq m)	-0.8	7.3	21.9	19.8	-25.0
Time for slow adjustment (yr)	0	4	6	6	6.5

[a]Primary food availability = primary production rate + detritus import rate.

Rankings: Best Intermediate Worst

Figure 2.1.7. Specimen scorecard.

The character of research differs from the former stages in this respect that the study is even more directed to gaining insight into the functioning of more promising designs or the consequences for other aspects, such as environmental and social-economic. At the end of this stage it should be clear what so called limit stages are of importance for the various alternatives. The next stage consists of dimensioning the final form; a thorough study of all limit

states is necessary but up to this point only a comparison made between them. Only an initial evaluation is made of the importance in terms of contributing to the overall probability of failure in the worst possible case, safety, or satisfaction with respect to the „main functional demand". In the study for the limit state one may be confronted with uncertainties. Ruling out these can result in a better (in terms of a less expensive or safer) construction.
Uncertainties can be tackled either by applying a certain rate of over-dimensioning or by simply ruling out the uncertainty itself. In comparing alternative designs, it is often dangerous to use as a criterion the total cost including uncertainties, because they generally have different effects on the total cost. These uncertainties should therefore preferably be presented explicitly, not even expressed in terms of money (this being an extra introduction of uncertainty). Ruling out the uncertainty may be preferable. Especially in those cases where there is only an indication of the uncertainty and no description in statistical terms. Then it is theoretically impossible to give the structure enough strength to meet the prescribed acceptable safety factor or probability of failure.
Figure 2.1.8. gives an illustration of ruling out the uncertainty. The chosen concept for a sea defence work is highly dependent on wave attack. However, in this case there is a marked lack on information on wave characteristics.
Based on the existing (or to be developed) underwater topography of the foreshore an upper limit of the wave characteristics may be calculated.
If the water depth is great and information about the probability distribution of water levels rather scarce, and if even the future development of the foreshore topography is uncertain, the upper limit becomes less valuable. A significant diminution of the water depth may be a useful tool ruling out these aspects. In diminishing the water depth, a bed protection will of course cost money, but the dimensions of these structures are less influenced by (uncertainties in) wave action. It may sometimes happen that the „theoretical" optimum alternative cannot be chosen because of lack of money, materials or skilled labour, etc. In this case the „theoretical" optimum alternative was not the real optimum for those particular conditions.
In giving the plan or the structure its first estimated layout, shape and dimensions quantitative data should already be available. In most cases these data will be based on previous fun-

Figure 2.1.8. Ruling out uncertainty about foreshore development in dam construction.

A. existing situation, erosion of foreshore anticipated
B. dam design too strong for t = o, „good" for expected conditions
C. extension of dam in the future, when expected erosion has occurred
D. fixation of foreshore, limiting wave conditions
E. existing situation, accretion of foreshore expected
F. artificial sandfill on foreshore = future situation, smaller dam.

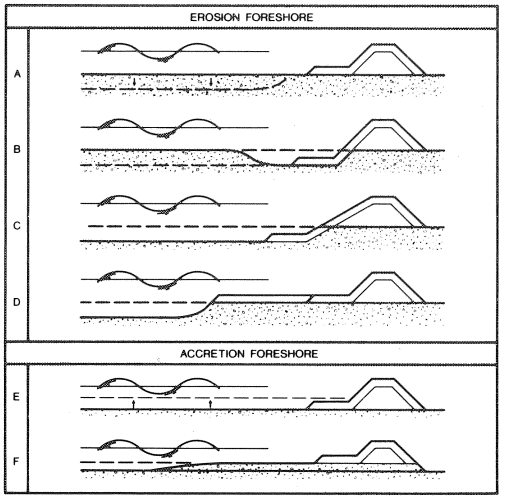

damental research or derived from experience with similar projects. In the literature the relations between various relevant parameters are described and sometimes presented as „design charts". This means that one has to be familiar with the - international - literature.
Only as a very simple example the experimental relationship is given: A(MSL) = 70 x 10^{-6} V, where A(MSL) is the cross sectional area below mean sea level of a tidal inlet and V is the ebb-volume. Many tidal inlets in loose-sediment environments all over the world were investigated and this striking relationship seems to exist if tidal motion dominates. To evaluate the consequence of closing a tidal basin with respect to the morphology of the inlet, or even to evaluate the location of the closure, which will have an effective impact on the ebb volume, this relationship can be used for a first estimate, so in this stage of the project.
Such experimental relationships are available for all kinds of parameters, but if the physical phenomena are well understood and can be described by mathematics, calculations can be made and presented in the above mentioned design charts. Figure 2.1.9. gives an example of the design chart for specifying the stone dimension for various stages of the closure of a specific gap.

The load on the stones is given as the water velocity over the partially completed closure dam. Various stages for the height and width of the dam are given. The strength of the stones is given as a critical value for the water velocity so that a comparison with the actual velocity can be made.
In Figure 2.1.9. the contribution of both is given, worked out for a specific situation and various stone diameters.

D. Dimensioning the final form

In this fourth stage of the design process the functioning of the selected design will be exhaustively studied and tested against the set expectations and criteria. All limit states will be checked and an extensive study made of the failure behaviour of the construction against a broad variety of boundary conditions. The struc-

Figure 2.1.9. Example of design chart: specifying stone dimension for various closure stages.

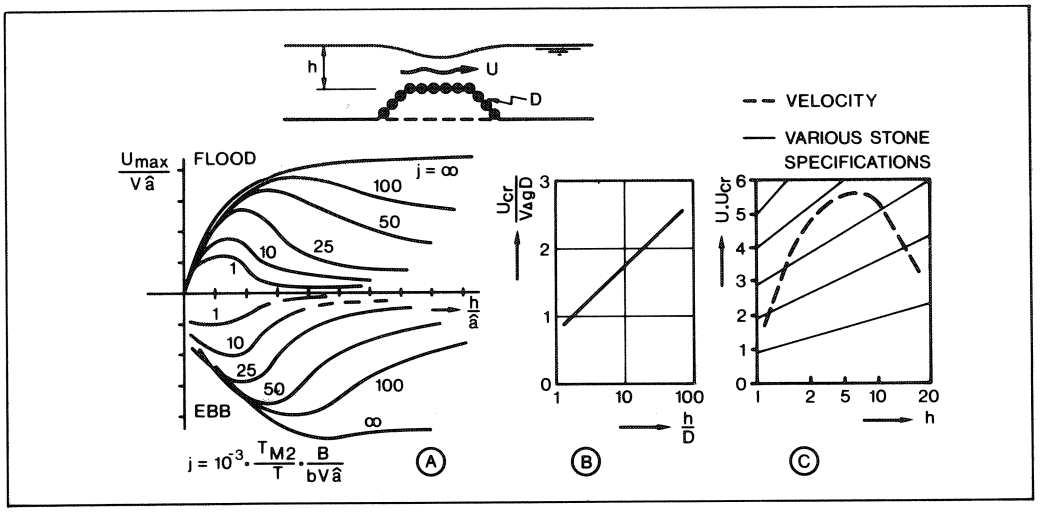

ture will get its final shape and the total structure will be fitted into the existing environment.

Fault tree

In a complicated pattern of relationships a great many aspects arise which necessitate an even more careful and systematic approach. An essential medium, which as a rule can only fully be applied at this design stage in a quantitative manner, is the fault tree. This is a scheme in which the events and their consequences or the errors and causes, which contribute to the probability of failure are arranged in a clear way. Figure 2.1.10. gives an example of a simplified fault tree for an enclosing dike around a polder, consisting of N dike-sections.
In the fault tree all possible modes of failure of elements that can eventually lead to the failure of dike sections and to inundation are listed.

Figure 2.1.10. Example: simplified fault tree for an enclosing dike, consisting of N dike sections.

The fault tree combines four categories of events that may cause the inundation of a polder:
- human failure; management faults;
- aggressive human action;
- „acts of God";
- technical failure of structural elements.

Although all four categories of events are equally important for the overall safety of the polder, te engineer's responsibility is mainly limited to the technical and structural aspects.
Fault trees can be a valuable aid not only for constructional aspects but also for execution activities. Figure 2.1.11. gives an example of a simplified fault tree for the undesired event of a sand closure project being behind schedule.

Limit State

The partial failures are described in the ultimate limit state, where the acting loads are just balanced by the strength of the construction. In quantifying the events in the fault tree the probability of occurrence of this limit state can be found from the convolution integral.
Starting from a probability density function (p.d.f.) of the boundary condition one finds with a transfer function the p.d.f. of the loads on the structural element, F(l). Combining the last-mentioned p.d.f. with the p.d.f. of the strength of

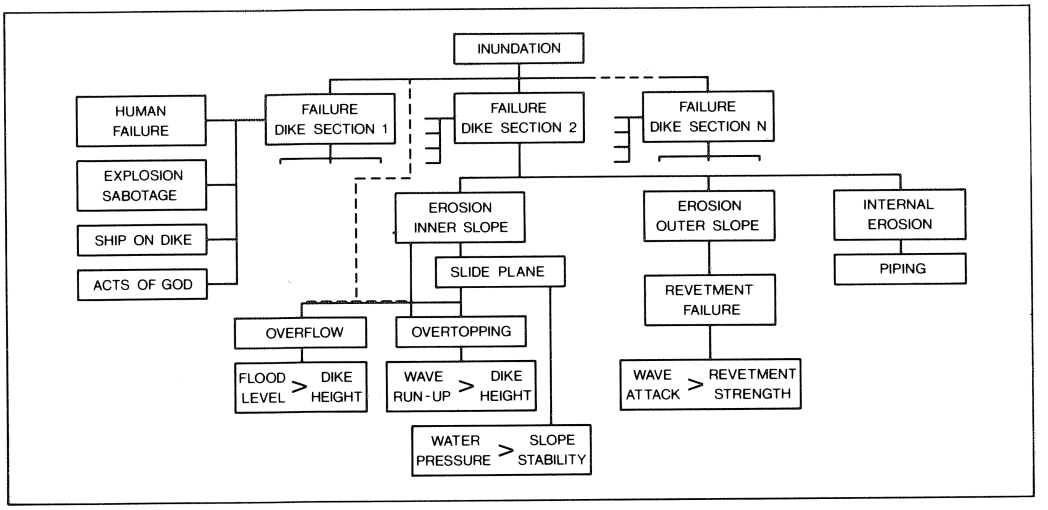

Figure 2.1.11. Fault tree for progress below target for a sand closure.

the structural section, F(s), gives the failure probability p_f of the element:

$$p_f = \int_0^\infty F(s)\,ds\; F(l)\,d(l)$$

This concept is applicable in hydraulic engineering, when the narrow definitions of load and strength are widened to potential threat and resistance.

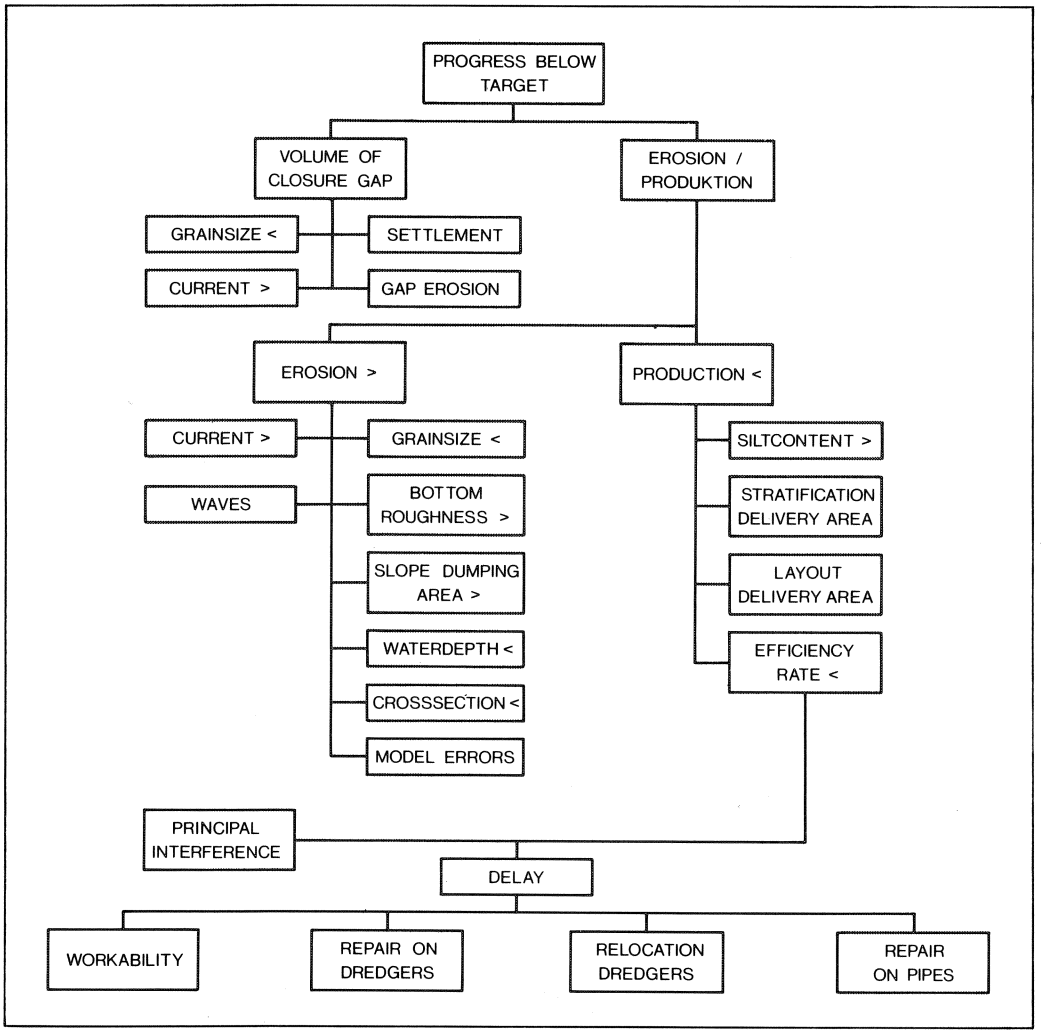

The adapted concept of a failure mechanism is given in Figure 2.1.12.
Besides the loading, structural and failure features, the safety of structures depends on management aspects of the project such as authorization of the organisation, executive management, management guidelines, technology guidelines, control and inspection guidelines and safety evaluation, etc.

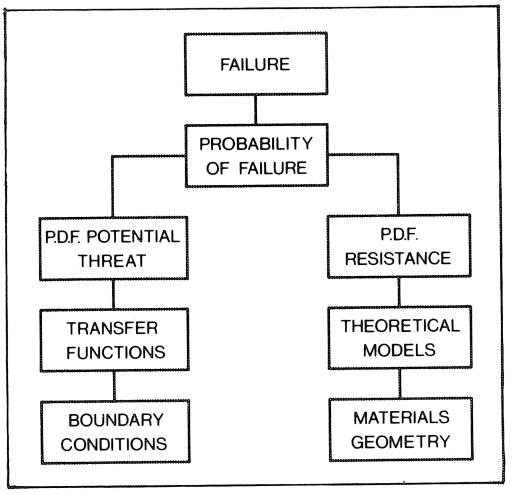

Figure 2.1.12. Concept of the ultimate limit state of a failure mechanism.

There are various limit states such as the serviceability limit state, ultimate limit state, progressive collapse limit state, fatigue limit state and even social limit states.
The last of these are related to the mentality of the local society concerning laws, codes, regulations, customs, policy on the employment of domestic materials and labour, and religion etc. The project itself will of course have a significant impact on the society and the environment: the objective of every civil engineering project is to change or safeguard the social situation and/or environment.

The structures under review in this book consists of closing elements on or in the bed of a watercourse. This watercourse may be made by nature either during long-lasting (periodical) average (not extreme) conditions (e.g. geomorphological processes) or by nature during excessive, short-term actions (e.g. flood disasters, earthquakes) or be man-made during war actions. The structures for closing gullies, gaps in dikes etc. consist of one or more elements based or embedded in the original, in some cases reinforced bed. Some of the limit states for such structures are mentioned below. This list does not set out to be a complete checklist of all relevant items but to illustrate a systematic approach.

In working out these limit states, it is recommended that a distinction is drawn between conditions during the construction stage (inclusive transport) and upon completion of the project (the final stage).

However, for the structures under review the more important limit state will be the ultimate limit state with the following aspects:
- ultimate load carrying capacity (concrete or steel caisson, wooden or steel structure of cofferdam, (reinforced) earth structure of a dike);
- rupture or yielding of a section (bottom of the caisson, cage of a gabion structure, dike section, interface between bottom caisson and foundation bed);
- instability or collapse of single members or elements (slope protection, dike slope, bed protection, partitions of caissons).

Beside the ultimate limit state, there are situations where the ever continuing presence of a load causes a deterioration of constructional resistance in time without any imminent danger of failure.
However, this deterioration of constructional resistance can cause an unexpected failure in extreme conditions. The serviceability of the construction can also diminish without leading to collapse (e.g. settlements, deformation).

The serviceability and fatigue limit state are essentially treated in the same way as the ultimate limit state. However, attention is concentrated on loading situations that occur frequently during the lifetime of the construction rather than on extreme conditions.
Serviceability limit state:
- specifications as regards functional demands, serviceability, durability, etc. (e.g. watertightness, workability of equipment);
- excessive deformation without loss of equilibrium (in the case of large deformations of an open caisson the proper operation of the gates will be obstructed);
- excessive vibrations or motions not associated with fatigue (e.g. vibrations of gates prevent proper gate operation, heavy ship motion diminishes workability);
- damage caused by erosion (e.g. deterioration of organic material in bed and slope protection).

Fatigue limit state:
- accumulated effects caused by cyclic or repeated actions during service life (hysteresis during cyclic loading of the subsoil, freeze and thaw impact);
- disintegration, caused by accumulated fatigue damage and insufficient residual strength from local loss of material (causing higher stresses and consequently more fatigue-sensitive behaviour of the remaining parts of the structure);
- excessive cracking or fracturing of cohesive material or excessive displacement of grains in cohesion less material (penetration of sandy subsoil in filter construction).

A point of great practical importance is that these limit-states can be „solved" in two ways:
1. improving the resistance of the construction to guarantee sufficient strength during the service life;
2. controlled inspection and maintenance procedures with respect to deterioration of constructional resistance.

The second solution, however, introduces a certain non-technical risk, because constructional safety depends on the care of other people than the designers and contractors.
In many cases in hydraulic engineering the application of the limit-state concept is cumbersome because a theoretical description of the transfer function and theoretical models for strength are not available. This is especially true for erosion and scour problems, which govern the design of closure works. Neither are transfer functions to transform waves and currents into forces on grains nor a theoretical model for the „strength" of grains known for cases with a complex geometry of the works. To overcome this problem, models tests are carried out with a simulation of all possible combinations of natural boundary conditions, or even full-scale tests with field data are used.
Then the damage done to the boundary conditions are correlated with the test conditions (Figure 2.1.13.) Of course, field data on boundary conditions, resistance parameters and damage are to be preferred as a basis for correlation if they are available in sufficient quantity.

Figure 2.1.13. Determining limit state by model tests or field data (black box approach).

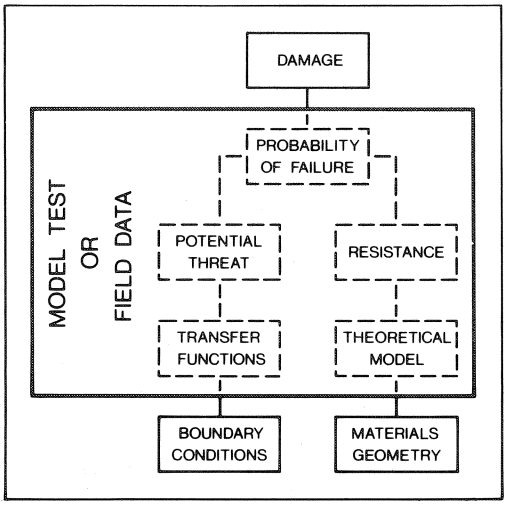

Partial safety factor
In the case where the limit-state concept and the probabilistic evaluation is even with the above mentioned procedure not applicable then at least an approach with evaluation of partial-safety-factors should be worked out.

The partial-safety-factor-format gives three main groups:

I: $\gamma_{s1}, \gamma_{s2}, \gamma_{s3}$: concerning the load
II: γ_{m1}, γ_{m2} : concerning the strenght
III: γ_{c1}, γ_{c2} : concerning the nature and behaviour

γ_{s1} : takes account of the possibility of unfavourable deviation of loads from characteristic external loads, thus allowing for abnormal or unforseen actions; for dams and dikes that are specially build for abnormal loads (e.g. rarely high waterlevels) this factor tends to unity.

γ_{s2} : takes account of the reduced probability that various loadings acting together will all be simultaneously at the characteristic value.

γ_{s3} : takes account of errors in predicting load-effects as a result of inaccurate structural analysis or incorrect design-assumptions, and as a result of neglecting dimensional inaccuracies; to take account of non lineair behaviour where there is a magnification of load effects.

γ_{m1} : to take account of material strengths occasionally falling below the specified charistic value; to take account of possible differences between strength of material in the structure and that determined from control test specimens; to take account of possible weakness in structural material resulting from the construction process.

γ_{m2} : to take account of possible inaccuracy in the assessment of the resistance of a structural element resulting from modelling errors; to take account of effects of poor dimensional accuracy including manufacturing tolerances, in the finished structure on the resistance.

γ_{c1} : to take account of the behaviour of the structure with respect to redistribution of load and strength after (partial) failure of sections or element of the structure.

γ_{c2} : to take account the seriousness of attaining the limit state from other points of view, for example economic consequences, danger to community etc.

With these factors the generalised limit state requirement may then be expressed as: $R > \gamma S$

where $\gamma = \gamma_{s1} \times \gamma_{s2} \times \gamma_{s3} \times \gamma_{m1} \times \gamma_{m2} \times \gamma_{c1} \times \gamma_{c2}$

R = characteristic strength
S = characteristic load

The abovementioned partial safety factor-format have been developped for structrual analysis of steel and concrete structures and is documented in several codes, but it appears to be also applicable for other structures even structures of „loose" material such as dams and dikes.
Besides the faulttree techniques the evaluation of the format gives at least a systematical check of possible errors or in general uncertainties.

Structural Safety
Structures or structural elements should be designed in such a way that, with appropriate degrees of reliability, they
- sustain actions liable to occur during construction and use
- perform adequately in normal use
- maintain sufficient structural integrity during and after accidents

The probability of failure (p_f) is used as a general indication of the safety level to be attained (a low value of p_f indicates a high degree of safety.) The acceptable level of attaining a limit state

should be assessed with regard to social and economic criteria. In general this level should be chosen in such a way that the total resources needed for execution of the structure and for its functioning during its lifetime are as low as possible.

The execution and maintenance of a structure involve expenditures.
A possible structural failure involving a risk of loss, including human life is weighed against these. Increasing the safety decreases the risk. Increasing safety and decreasing risk both lay a claim on limited resources. Although different losses (including human lives) cannot be added mathematically, all have to be considered in order to choose the optimum safety level. The basic principle is shown in fig. 2.1.14.

$E_t = E_i + p_f \times E_f$
E_t = total expenditure
E_i = initial expenditure
E_f = expenditure consequent upon a failure
p_f = probability of failure

In the simple case where a structural failure involves only material losses, the optimum safety level can in principle be found by economic optimization.

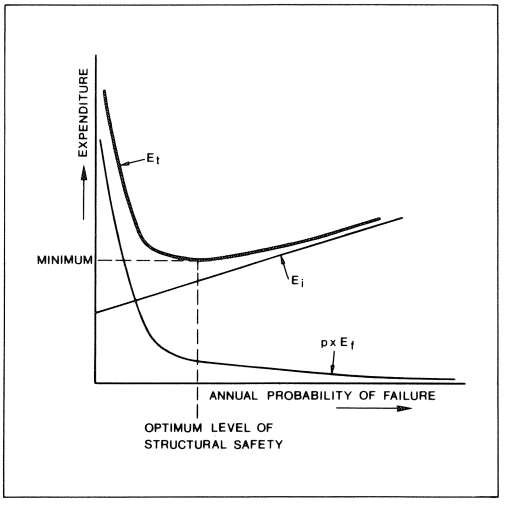

Figuur 2.1.14. Determining optimum level of structural safety.

In this case the initial expenditure for execution, control and maintenance (E_i) are added to the capitalized risk. Risk in this context can be expressed as the product of the probability of failure (p_f), multiplied by the economic consequences (E_f) of the failure.
In the more general case, where a structural failure may involve outside direct and indirect economic losses, death and injury of people, loss of animal life, environmental damage and/or loss of important cultural values, a more complex decision process is needed.
Although some reference value in money may be chosen for the value of a human life this cannot replace the emotional value. The money involved in the death or injury of even a single victim of a building disaster may be considerable. Society tends to put a still higher value on multiple human lives. Dike breaches may, of course, involve a high number of casualties.
In general the starting point for an assessment of the acceptable probability of failure is that to live in the low-lying area behind a dike does not imply a voluntary acceptance of a greater death risk than living elsewhere on higher ground. The probability of failure is linked to the average death-risk per person from other hazards or accidents.
From recent psychometric investigations based on a large number of interviews it appears that the acceptance for one death differs from that for a great number of deaths. Fig. 2.1.15 illustrates the results.

The acceptable level of risk seems to be dependent on:
- degree to which the risk is imposed or is voluntary
- (possibility of) identification of the risk

- personal or social benefits for which the risk is suffered
- possibilities and difficulties of controlling the risk
- historical background of the risk

It seems that an acceptable risk level in Western Europe is the risk of an individual being killed in a traffic accident. This risk level is about 4.10^{-4} per year. In other parts of the world this level may be different.
Figure 2.1.16 gives a rough approximation of the probability of death per person per year in Dutch society. The probability of failure for a structure where a group of victims is involved can be derived as follows:

$$p_f = \frac{\text{individual death risk}}{\text{size of group}}$$

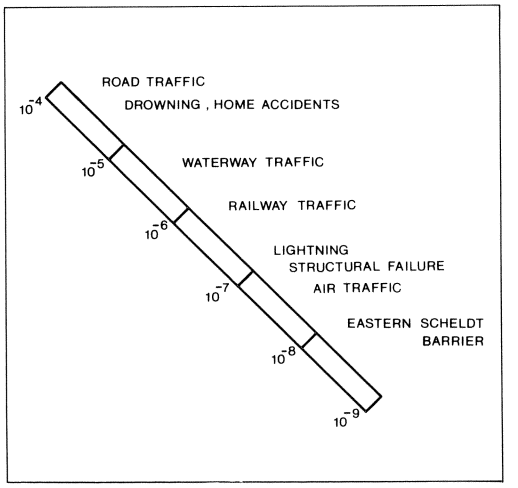

Figure 2.1.16. Probability of death per person per year in Dutch society.

Figure 2.1.15. Acceptable level of risk according to number of victims involved.

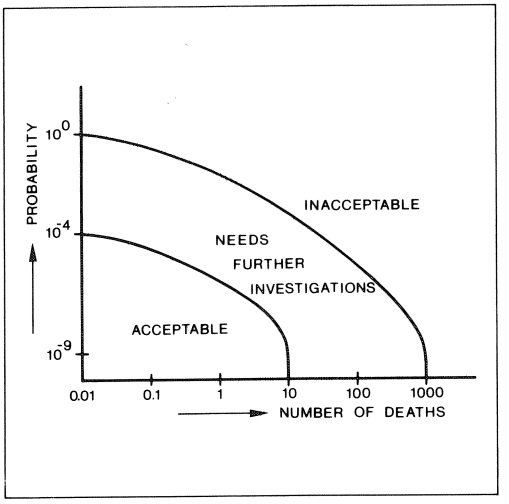

Another procedure for assessing the acceptable level of risk of attaining a limit state is given by CIRIA (Construction Industry Research and Information Association), 1976:

$$p_f = \frac{10^{-4}}{n_r} K_s \, n_d$$

in which:
p_f = probability of failure in a structure's design life.
n_r = the average number of people threatened by the consequences of the failing structure.
K_s = a social criterion factor, given in the table below.
n_d = the design life of the structure in years

nature of structure	K_s
dams, places of public assembly	0.005
domestic, office or trade and industry	0.05
bridges	0.5
towers, masts, offshore structures	5.0

This means that not all structures need the same degree of structural safety and the arguments for differentiating between the safety of different types of structures or structural elements come from the predicted consequences of failure.
However, for the ultimate design and execution of a structure a clear decision is needed. A limited number of safety classes is therefore suggested. The main criteria for deciding on the safety class of a given structure are the same for the assessment of the acceptable level of risk:

- Consequences of failure for human life and limb.
- Economic consequences of a structural failure in comparison with the cost of the structure.
- Consequences of failure for the environment and for other non economic assets caused by a structural failure.

It is common to adopt three safety classes, where class 3 has the highest safety level or the lowest probability of failure. For structures whose failure could cause a major catastrophe (like large reservoir dams) even more stringent requirements may be indicated.
The following matrix table gives the safety classes and their criteria

The safety classes can be compared with values for probability of failure as follows

class 1	$p_f = 10^{-4}$	to 10^{-5}
class 2	$p_f = 10^{-5}$	10^{-6}
class 3	$p_f = 10^{-6}$	10^{-7}
class 3+	$p_f = 10^{-7}$	10^{-8}

It is obvious that the structures under review in this book are classified as safety level 3 or 3+.

However, if measures are taken to prevent high loss of human life or limb the dike may be of class 2.

For example: constructing submersible dikes, erecting safety hills (i.e. higher grounds for refugees) and installing a warning system can decrease the death risk in areas where the flood-wave on a river or estuary is -on long-term base- of an almost unpredictable level and/or in the case where only a limited amount of money is available for erecting robust dikes.

From the flood disaster in Holland in 1953 it appears that the risk of drowning becomes considerably greater once the inundation depth exceeds approximately 2.5 metres (see figure 2.1.17). This means that the acceptable level for the probability of failure or safety class for every dike is not the same, both because of the level of the land behind the dike as because of the water level during the storm.

		consequences of failure for loss of human life or limb		
		scarcely any	a few deaths	many deaths
material damage in comparison with initial costs	- limited	1	2	3
	- appreciable	2	2	3
	- great	3	3	3+

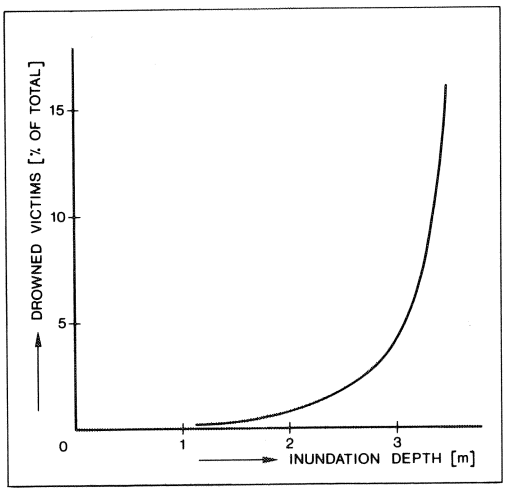

Figure 2.1.17. Proportion of drowned victims in relation to inundation depth

2.1.4. Execution stage

General

A distinction may be drawn between the preparation for the execution operations, the execution operation itself and the control of these operations.

The method of execution depends on many factors, which in turn can influence the design of the closure works. Among these factors are:

- **Available budget** and method of finance. The projects under review are in general financed by governmental agencies. The government will have a policy for the export of foreign currency and for annual or project budgetting etc.
- **Execution time.** In case of a well-balanced design for a closure project all primary and secondary considerations and consequences will be taken into account, and the preparatory stage accepted as being long. In the case of a dike breach, which is an emergency case, the safety of life, goods and chattels is the primary objective. A very fast reaction is of vital interest and the preparation stage and the execution time itself should be as short as possible.
- **Manpower and skilled labour.** Under conditions where there is a lot of (cheap) manpower, (expensive) machinery will preferably be avoided, both for employment and cost reasons. In regions where labour is expensive there will be a tendency to use execution methods which are less dependent on labour. Fig. 2.1.18 gives an example of the relation between various execution methods for scour protection adjacent to closure works -with increasing prefabrication and decreasing manual labour -and the increasing costs of using labour teams.
- **Mentality of labour.** In tropical regions the conditions for hard physical effort are less favourable than in temperate zones. These conditions have over the centuries created a corresponding attitude towards labour.
  This aspect may act as a limiting condition for the execution of a project but can to some extent be influenced by creating favourable and attractive conditions.
- **Mentality of society.** Many countries have special regulations on employment, the use of domestic materials, local labour etc. Laws and codes can restrict the method of execution. Unwritten rules may also be of importance, e.g. the execution of a closure work with a method requiring a lot of labour should not be planned during the harvest period, when harvesting will be given a higher priority, being of vital interest to the people.
- **Materials and equipment.** In the beginning of the design stage the alternatives should be generated as freely as possible.
  Also the development of (special) equipment should not be restricted by the vague feeling for using existing equipment. In the final stage the optimum equipment is compared with that already existing and a decision made, based generally on cost and time con-

siderations, whether new, specially tailored equipment should be constructed or existing equipment used.

- **Auxiliaries.** The execution method and design depend on the support given by various auxiliaries such as a hydrometeo service, research facilities, maintenance facilities for equipment, as well as infrastructure facilities such as land, water, air and railways and harbours etc. and communication facilities in general.
  If, for instance a good warning system is available for storm surges, floods etc. the workability will be higher. A good warning system, being reliable and accurate, will reduce the probability of the warning system failing in terms of lack of or improper warning or poor prediction of the intensity of the event (e.g. the high-water level).
  Even the quality of the warning system can affect the design.
  For example, in the case of a warning system that takes too long to predict a dangerous event, the design should not include any critical operations longer than the period required for predicting the critical event.

Risk analysis of execution operations

As for the design, a risk analysis should also be made for the execution operations. Only a systematic analysis of all operations beforehand can provide a prediction of the risks for (future) execution.

Only in this way the necessity for (costly) improvisation can be minimized, the risks optimized and the quality of the structure be the in accordance with the specifications stated in the design stage. In general the quality of the execution work consists of three elements: quality of the product, execution time and execution costs, of which the first item is the most important. The execution is a dynamic process with time as a governing parameter. Delay is an undesired break in the process and implies in nearly all cases higher costs. Delay may be a result of two main events:

- work is executed, but does not fit within the quality limits.
- work is not executed within the time limits

Figure 2.1.18. Rising labour costs and execution methods for revetments. (Netherlands).

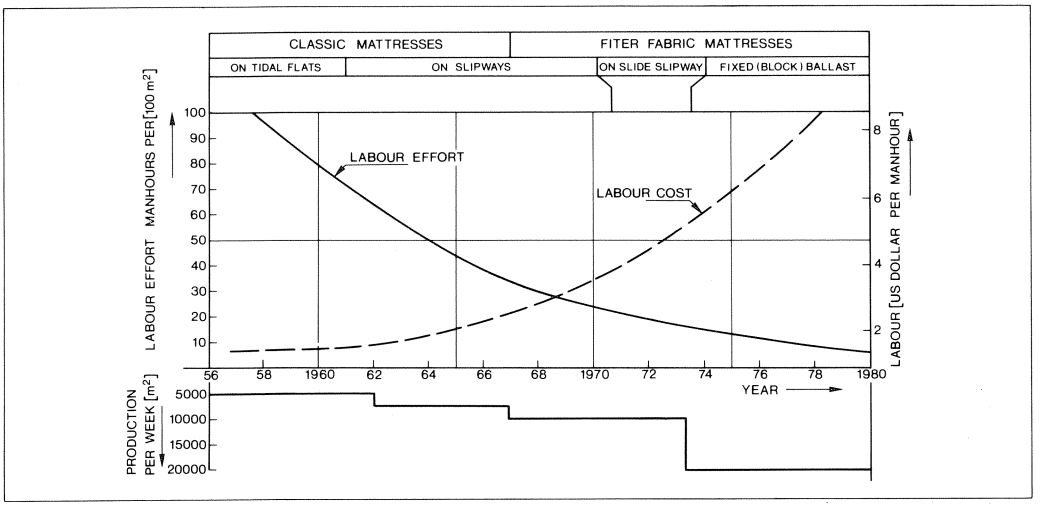

The expected delay caused by variations in the -predicted- planning can be calculated with regular network planning techniques and now with stochastic time parameters. In the base of a best, pessimistic and optimistic guess the critical operations in the network planning can be traced. This analysis will be made with the objective of preparing measures in case of deviations from the expected („mean value") planning. These measures concern manipulation with manpower, materials and equipment. Analysis of the consequences of an initial delay - inducing event can be done with the previously mentioned fault-tree method. In figure 2.1.19. a „standard fault-tree" is given with the undesired top-event „delay" shown on top.
The fault-tree analysis gives the presentation of possible events that can cause a delay with respect to the main (mean) planning. Preparing the data for the fault-tree gives insight into critical operations and events. The technique is worked out for various levels of detail. If all possible events are presented in the fault-tree the analysis becomes too confused, so a step-wise procedure is preferable. In the first step the complex of execution operations is subdivided into a number - say ten to fifteen - of main operations. These can be ranked chronologically.

Figure 2.1.19. example of a standard fault-tree for a delay.

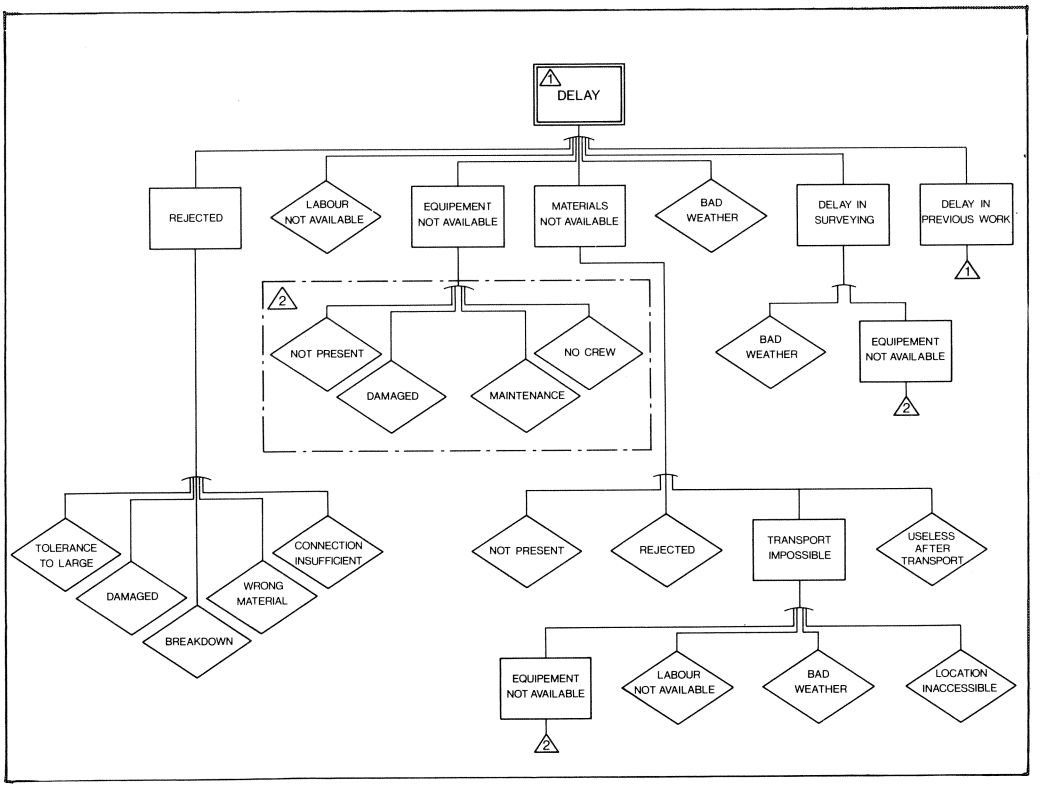

After this a second and eventually a third step deal with the subdivisions only. From the main and sub fault-trees the governing risk-events can be traced and measures to prevent the undesired event be designed; time and cost estimates can be calculated. For a proper communication between all persons concerned these data (critical events, measures, time and cost estimates) should be well documented in combination with the main planning. The partial events can be ranked according to the impact on the undesired delay. Computerization of data processing in preparing the documents is possible. A second and even more steps are necessary for evaluating all the details of the execution operations. Figure 2.1.20. illustrates the various steps in the risk analysis.
A distinction is made between analysis before and after the drawing up of the fault-tree. In the former case emphasis is on the possible event and its probability and consequences, in the second on the measures of a preventive or responsive character for restricting the consequences of delay or inferior quality are scrutinized.
These consequences may be revealed both during the execution stage and in the final stage when the structure is exerted by the load.

Figure 2.1.20. Diagram for risk analysis and counter-measures.

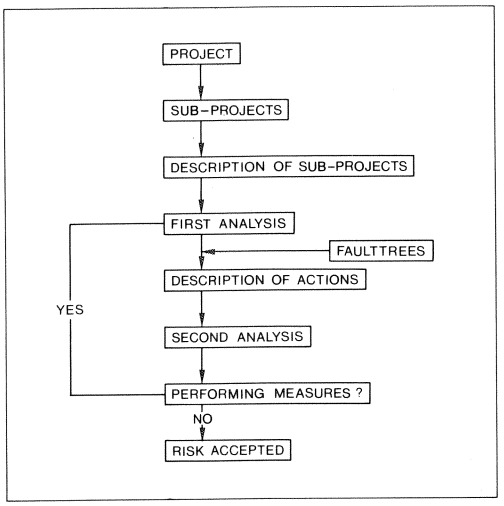

Quality assurance and control procedures
The structure was designed according to many assumptions and specifications, including materials, geometry dimensions and tolerances. During the execution stage an appropriate controlling system is necessary to assess target structural safety. Even after completion of the work a monitoring system is necessary to measure the condition of the structure and to check the predictions of its behaviour.
The safety of a structure is not determined by structural calculations (one of the items of the partial-safety-factor-format) alone. By far the majority of structural failures occur as the consequence of human error, mainly during execution of the work. The assessment of structural safety therefore needs an appropriate quality assurance or control procedure.

The quality can be influenced on the one hand by the active control exerted by the designer, contractor or consultant and, on the other hand by the passive control exerted by for example public bodies or certifying organizations. There is an interaction between the design and the control procedure. The following example may demonstrate the influence of the designer. The foundation of the breakwater at the Hook of Holland, consisting of a gravel layer, was executed by dumping a great number of very thin layers. Due to a „statistical" levelling the probability that the construction of the gravel layer would be distorted by the phenomena of varying fall velocities for various gravel diameters was so low that in-situ testing was omitted. In the case of positioning large single elements under water (e.g. block mattresses as scour protection) a proper control procedure is indispensible because of high requirements for a good connection between those elements. In this case there is no statistical levelling.

Important elements for an appropiate quality assurance are:
- clearly defined requirements
- competent personnel
- clearly defined responsibilities of the people involved
- an adequate information flow

Especially when natural products such as sand, gravel and stones are used, the limits for the qualifications should not be too narrow, but sure exact and clearly defined.

Too narrow limits in general mean more expensive material.
The method for testing samples should be objective and not dependent on the certifying authority. In many cases these methods are prescribed in standard tests.
In the case of controlling stone specifications it is of importance in which stage of the transport from the quarry to the construction site the samples are taken. Because of the many handling operations the stone diameter will decrease. In general the specifications of the stone on the building site is given (according to the design). A control procedure in the quarry will in general be cheaper, but then the rate of decrease of the stone diameter during transport to the site should be known.

In general the higher the safety class or the lower the probability of failure the more stringent the control procedure. A very complex structure will need a more stringent control procedure than a structure with a simple set up.
The control measures will have to give special attention to those aspects that may contribute to a failure with a failure mode that has very severe consequences. „Sensitive" structural details are among them.
For the higher safety class an independent check on the design and the design calculations is necessary. Sufficiently independent supervision on the site and quality control measures must be provided. Fault-trees and event-trees may help in developing a consistent checking procedure that takes into account the influence of deviations from the specified properties in the finished stage of the building project.

Sometimes structures are subjected to a check of the design and quality control procedures on site under the responsibility of an independent certifying authority. This is the case for example for large reservoir dams, (large) ships and offshore structures.

2.1.5. Management and Control

In practice closure dams in estuaries and even dikes protecting low- lying lands are comparable with reservoir dams, although the height of these dams is larger and consequently also the other dimensions bigger.
Great attention has been paid during the last decades to monitoring the performance of reservoir dams. The philosophy behind this approach in safety control is also applicable to other dams and dikes. However, the monitoring system itself is unique to a specific dam. To assure the safety of the dam the links of the (management) chain should be of equal strength and not just the design chain (or stage). (See figure 2.1.21). As stated before the possibilities for inspection and safety evaluation can influence the design. If inspection is not possible after execution, the dam or dike should be of such a design that the probability of a (partial) failure is acceptably low. If the design is based on an inspection procedure then inspection and safety evaluation should be possible (also during bad weather conditions) and should be done.

Management guidelines, technology, management and technical guidelines and authorization and funding are also indispensable after execution of the dam.
Not only the condition of the dam in terms of strength should of course be monitored but also the load on the dam in terms of (high) water levels and wave height or even earthquakes and ice-action. This means that the installation of an inspection and monitoring system for the dam and analysis of gathered data will improve dam safety. The monitoring system in each case must be chosen in accordance with the special requirements of the individual dam. Apart from monitoring the possibility must be kept in mind of installing warning systems which would operate if critical values were exceeded, for

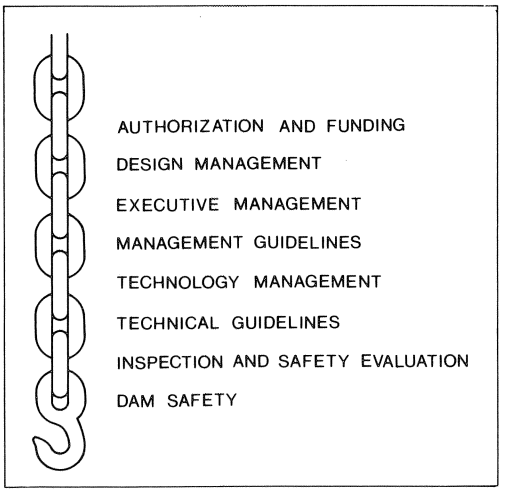

Figure 2.1.21. Dam safety chain

example high water levels, wave run-up, piezometric levels or seepage through the dike. The realization of the dam is based on many assumptions about geology, hydrology, geotechnic, (mechanical) behaviour of the dam etc. The monitoring system gives observed data that can be compared with the assumed (theoretical) values as used during design and execution. This evaluation is of extreme importance for the future response of the monitored dam, but even for new dams to be built.
From inspection of a great number of reservoir dams and also some experiences with dike breaches it appears that most structural failures or cases of poor serviceability have been traced back to human errors.
In particular, the condition of dikes that never have been attacked by severe storms decreases over decades, the dike may get other functions (for habitation, cattle farming, roads, crossings etc.) and „people" (in fact the authorized management) became careless about monitoring the condition and maintenance with regard to the original main function of the dam. According to the „General Principles on Quality Assurance of Structures" the following measures are recommended for avoiding human errors in technology and the use of dams and dikes:

- improving professional education;
- selecting qualified staff;
- improving working conditions and communication between people in the field and in the office;
- protecting responsible people from strain, shortage of time, noise and bad weather;
- taking precautionary measures against unintentional or deliberate human errors and negligence;
- incorporating additional precautions for new designs and new construction methods;
- making systematic use of experienced designers, checkers and controllers, as well as highly qualified independent consultants at all stages, such as during site investigations, preliminary and final designs, analyses, inspections and observations during execution and for the behaviour of the dam during its lifetime in periodical reports;
- carefully planning all the parts of the work to be done from the investigations and design stage to the management stage, the end of the life of the dam or dike.

This means that during the design stage and execution stage the conditions for doing the job should be as favourable as possible (qualified staff, consultants and labour, good communication, protection against bad working conditions, etc.)
During construction careful inspection of the used materials and control of regulations and standards improves the quality of the structure and so the safety of the dam.

The above observation for the safety aspects of the dam itself in fact also holds for the management of the new situation for the environment after completion of the dam.
The closure dam was built to create a new, safer environment behind the dike, but also impacts

on other aspects of the ecosystem, even the socio-economic system undergoes a change. A strategy is therefore required of adaptive environmental assessment, management and design, spanning the entire process starting with the drafting of the project, through its implementation design, execution, and to the monitoring, evaluation and use of the new socio-economic-ecological system. The relationship between the basin behind the closure dam and the - now safer - surrounding low-lying lands is of importance and should preferably be treated as an entity. The task of the former regional management becomes much more complicated in the new situation, because of the new tasks: management of dikes and land and the new and developing ecological situation of the basin. The management authority should have a new legal basis to be able to implement proper regulations. In this way an active management plan for ecology, economy and safety combined should be realized.

References

1. H.L.F. Saeijs, **Changing Estuaries,** Government Publishing Office, The Hague 1982.

2. „General Principles on Quality Assurance of Structures", **JCSS; International Association for Bridges and Structural Engineering,** Zurich, Switzerland; 1981.

3. A. Paape, J. Stuip, W.A. Venis, **Hydraulic Aspects of Coastal Structures,** Delft University Press, 1980.

4. Rationalisation of safety and serviceability factors in structural codes, **CIRIA report 63,** London, 1976.

2.2. Environmental Conditions

In order to predict the effect of the change in natural conditions in estuaries it is necessary to describe the environment in a quantative way with parameters that govern the phenomema and are expected to be most relevant.
In this section a characteristic description of these parameters is given.

J. Voogt

2.2.1. Tides and currents

The continuing rise and fall in water level at the coast of the sea is a phenomenon caused by celestial bodies, i.e. the sun and moon. No local forces are able to generate such water motion: no tidal phenomena occur in lakes. The tide-generating forces of the sun and moon can only generate a perceivable tidal motion on vast water-masses. This is especially true for the worlds oceans. The oceanic tides propagate over the continental shelves to coastal seas, where tides are observed.

To obtain a proper understanding of the tidal phenomenon, we shall first consider oceanic tides in general. The propagation of oceanic tides to coastal seas will be dealt with afterwards. Finally, a method of analysis of the observed tides will be given.

Oceanic tides

As mentioned before, the oceanic tides are generated by the attraction of the moon and the sun. The moon's influence is more than double that of the sun. This is because of the relatively short earth-moon distance in comparison with the earth-sun distance, although the sun's mass is much greater than that of the moon. Let us consider the influence of the moon. In the earth-moon system there are two types of forces: attraction and centrifugal forces. According to Newton's law of gravitation, the earth and moon exert forces upon each other. These forces are balanced by the centrifugal forces due to the rotation of the two bodies around their common centre of gravity. This is, however, only true for the earth as an entity. The distribution of the forces over the earth's surface is shown in fig. 2.2.1.1.

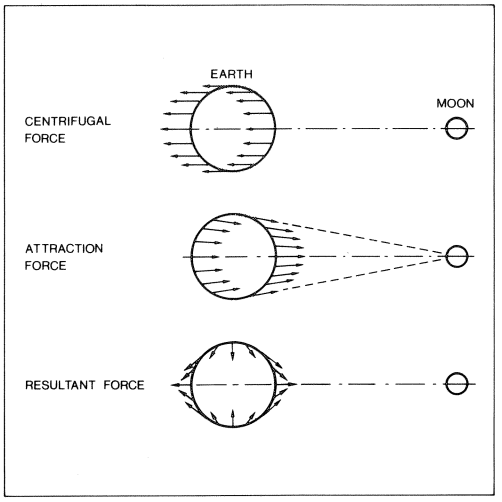

Figure 2.2.1.1. Centrifugal and attraction forces of the earth-moon system.

The forces will cause the water to flow in the direction of the resultant. Thus the water level on the earth will tend to change from a sphere into an ellipsoid. Assuming the earth to be covered completely by water, and neglecting inertia -known as equilibrium theory- **semi-diurnal tides** are explained if we realize that due to the earth's rotation two high waters and two low waters will occur during one day at a certain place on the surface. This tide is called the M_2 tide. The S_2 tide, i.e. the semi-diurnal tide resulting from the sun's attraction force, may be explained in the same way. It is clear that the height of the high and low waters depends upon the relative position of the sun, moon and earth. For instance, when earth, moon and sun are aligned, the effects of the moon and sun are in phase, thus causing **spring tides.** This happens at new moon and full moon. During the first or third quarters, the effects are out of phase, causing a minimum rise in high and low waters. These are called **neap tides.** Figure 2.2.1.2 shows the tidal variation in a lunar month.

Up to now, the motion of the moon has been assumed to be in the plane of the earth's equator. However, the plane of the moon's orbit is at an angle with the plane of the equator. This angle is called the moon's declination.

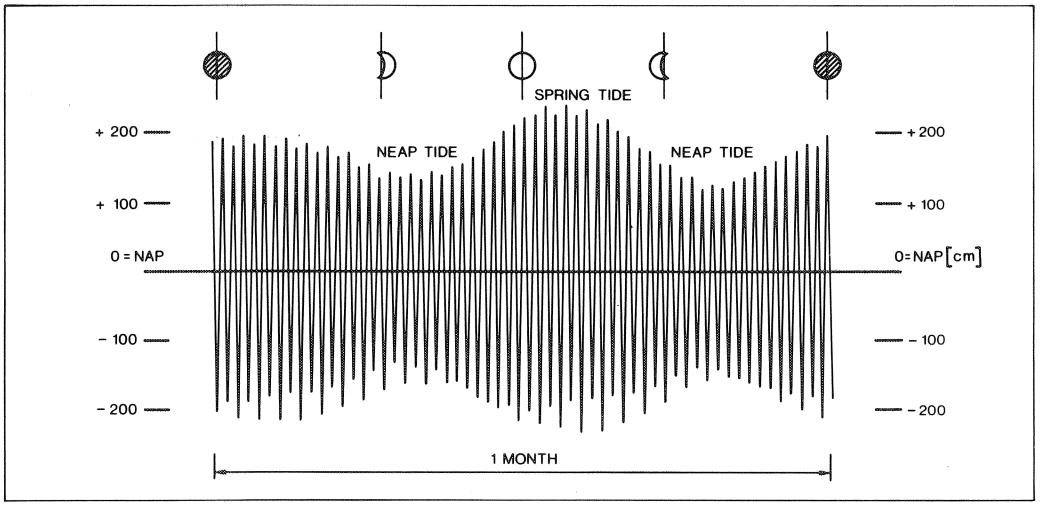

Figure 2.2.1.2 An example of the tidal movement from new moon to new moon at Flushing.

Figure 2.2.1.3 The equilibrium tide.

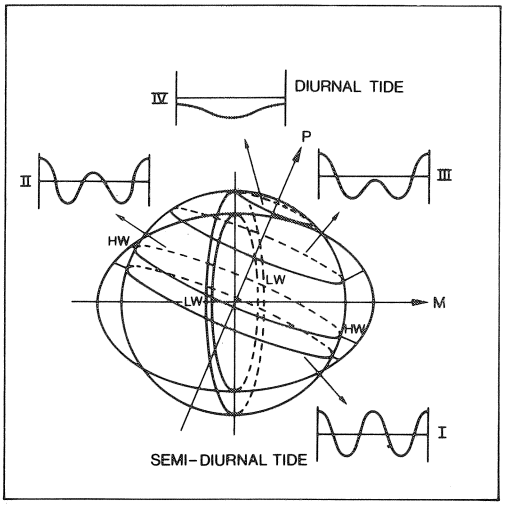

In fig. 2.2.1.3 P is the North Pole of the Earth. From fig. 2.2.1.3, it is apparent that the height of two successive high waters or low waters may differ during the same day. This so-called **daily inequality** is caused by the moon's declination. The effect of the sun's declination is similar. The periodicity of the phenomenon is one cycle/day. The **diurnal tides** may equal or even dominate the semi-diurnal tides (see fig. 2.2.1.3). Examples of diurnal tides are K_1, O_1 and P_1.
The reality is even more complicated. The distance from the moon to the earth, for example, is not constant, which results in varying tide-raising forces. However, these and other effects go beyond the scope of this book. The reader is referred to Dronkers [3].

Shallow water tides
The idealized equilibrium-theory model described in the previous section yielded an explanation for some of the dominant characteristics of oceanic tides. However, one of the most important features not accounted for by this theory is the fact that water-level variations in the ocean propagate with a wave speed dependent on the local depth of the ocean.
When approaching continental shelves and shallow seas, these tidal waves are influenced by the bottom topography and coastline

geometry. This is especially true when the non-linear terms in the dynamic equations which describe the propagation of the tides in the oceans, coastal waters and estuaries, play an important part. Two non-linear phenomena will be mentioned here:

-) distortion of the tidal wave, because its trough is retarded more than its crest as a result of the difference in depth at high and low water. The initially sinusoidal wave can only be described by introducing overtides, e.g. M_4 which is a component with 4 high waters and 4 low waters a day.
-) the bottom friction is assumed to be proportional to $u|u|$. This raises an M_6 component (six oscillations a day).

In these examples an initially sinusoidal M_2 tide is assumed. However, the oceanic tide will usually consist of several astronomical constituents, e.g. M_2 and S_2. Non-linear interaction between these constituents will generate compound tides with frequencies equal to the sum or difference of the frequencies of the original constituents, i.e. MS_4 results from M_2 and S_2.
It should be pointed out that these overtides and compound tides do not have an astronomical origin. They can, however, be very important for coastal seas and estuaries.
In general, no indications can be given as to which components are really important. However, it has been learned from experience that, at least M_4, M_6, M_8, MS_4 and MN_4 have to be considered.

Meteorological tides
Water level variations at the coast are also influenced by meteorological phenomena (atmospheric pressure changes and wind stresses). These phenomena are not usually periodical. Thus, when analysing water level variations, the meteorological effects only show up as random disturbances of the astronomically generated tides.
However, as some meteorological effects are periodical, they can be interpreted as meteorological tides: e.g. 1) monsoons blowing in one direction for half a year and in the other for the rest of the time, or 2) alternating land and sea winds during one day. The tidal period in the former example will be one year, and in the latter one day.
In general, meteorological effects only cause noise in tidal records.

Tidal wave propagation
Tidal waves belong to the class of long waves with wave lenghts of hundreds of kilometres. In general, wave propagation on continental shelves and in coastal seas shows a very complicated character. To gain some insight into this phenomenon, we will restrict ourselves to a wave propagating into a straight canal. Under some simplifying assumptions, a **progressive wave** can be described by the equation

$$z = A \cos(\omega t - kx)$$

with
z = height of water level
A = amplitude of tidal wave
ω = angular velocity = $2\pi/T$
k = wave number = $2\pi/\lambda$
T = wave period
λ = wave length

The propagation speed c of this wave, being λ/T, is

$$c = \sqrt{gh}$$

with
h = water depth

The current velocities to match are given by the equation

$$u = B \cos(\omega t - kx)$$

which implies that the velocity is in phase with the elevation.
See fig. 2.2.1.4

Maintaining this wave requires an infinitely long canal. In nature, however, canals and rivers always are closed at one end. Suppose that at the closed end of the canal total reflection of the wave takes place. A progressive wave travelling in the opposite direction can be expressed by the equation

$$z = A \cos(\omega t + kx)$$

Addition of the two progressive waves gives a wave phenomenon

$$z = 2A \cos kx \cos \omega t$$
$$u = 2B \sin kx \sin \omega t$$

This type of wave is called a **standing wave**

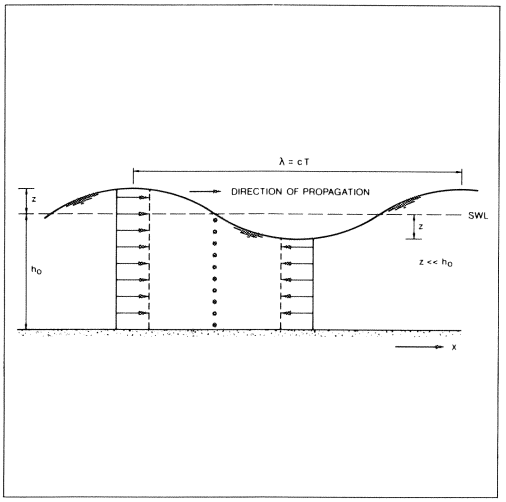

Figure 2.2.1.4 The progressive wave

Fig. 2.2.1.5 shows its characteristics at four successive times ¼ T apart.
It can be seen that the amplitude of the tidal elevation is location dependent: even points with zero tidal movement exist. These are called nodes. Locations with maximum tidal amplitude are called antinodes.

In contrast to progressive waves, tidal velocities are 90° out of phase with respect to tidal elevations: thus maximum velocities occur at the nodes while the velocities are zero at the antinodes. The closed end of the canal will, of course, always show an antinode.
In reality, combinations of progressive and standing waves will generally occur.

Attention should be paid to one specific case. Assume that the length of the canal is equal to an odd number of quarters of a wave length: standing waves will then show a node at the entrance of the canal. In this case, resonance will occur very easily with, in theory, infinite amplitudes and velocities. In nature, friction will prevent this but still impressive phenomena can occur.

Figure 2.2.1.5 The standing wave

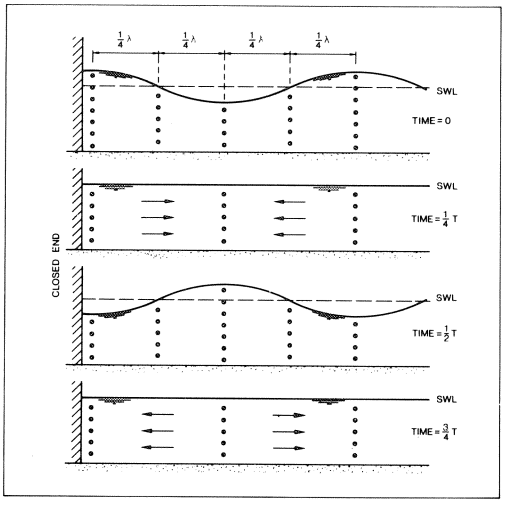

Tides in seas

Some general aspects of tidal wave propagation in straight canals have been dealt with in the previous section. Now we will try to understand tidal wave propagation in coastal seas. One important effect not dealt with up to now is the Coriolis effect. This is due to the rotation of the earth and can be regarded as a force acting perpendicular to the direction of motion. Its magnitude is proportional to the current velocity, with a factor f depending upon the position on the earth.

$$f = 2\,\omega_e \sin\phi$$

with

ω_e = earth's angular velocity = $0{,}73.10^{-4}$ rad/s

ϕ = geographical altitude

The direction of the Coriolis force is to the right of the current velocity in the Northern hemisphere and to the left in the Southern hemisphere. If this Coriolis force is compensated for by a transverse surface gradient, transverse currents will be prevented from occurring.

This can be the case in a wide canal with straight banks and a constant depth. Under these conditions a progressive wave can be expressed by

$$z = A_1\, e^{-\frac{f}{c}y} \cos(\omega t - kx)$$

and

$$u = C_1\, z$$

Here the x-axis is in the longitudinal direction of the canal and the y-axis perpendicular to the bank with y = 0 at the right bank. This wave occurs in a frictionless canal and is called a **Kelvin wave.**

Figure 2.2.1.6 Tides in a wide rotating canal.

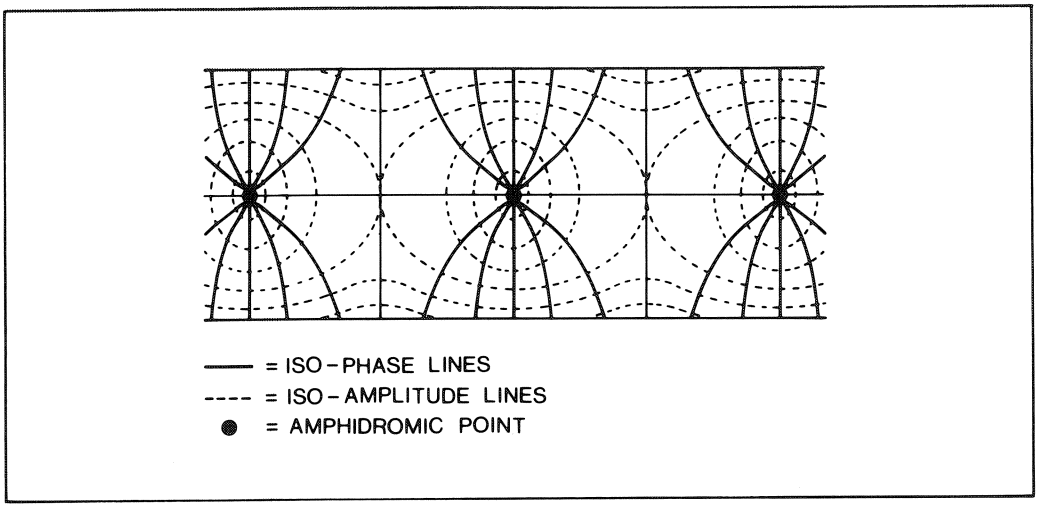

Due to the Coriolis effect the tidal amplitute decreases exponentially with increasing distance from the bank. Similarly, a progressive wave travelling in the opposite direction is given by

$$z = A_2 \, e^{-\frac{f}{c}(W-y)} \cos(\omega t + kx)$$

$$u = C_2 \, z$$

with
W = width of the canal.

Superposition of two waves with $A_1 = A_2$ gives a rather complicated formula. However, the distribution of amplitudes and phases over the canal shows a remarkable pattern with most characteristically a point with zero tidal amplitude, known as the **amphidromic point** (fig. 2.2.1.6).

This case can be regarded as a standing Kelvin wave.

In reality, progressive Kelvin waves can often be observed. Usually they are highly modified due to irregular bed topography, irregular shore geometry and the effect of bottom friction.

Tsunamis
A phenomenon comparable to a tidal wave is the tsunami. Although often miscalled „tidal wave", their only similarity with tides is the long wave character.

The Japanese word „tsunami" has been adopted to avoid confusion with astronomical tides.

Tsunamis are caused by underwater disturbances such as volcanic eruptions or earthquakes.
The generated waves can travel thousands of kilometres across the open ocean. When approaching coastal areas they can attain considerable heights. At Hawaii, tsunami heights of more than 10 metres above sea level have been reported.

Tidal analysis
The tide at a specific location is a combination of the astronomical tide and the meteorological tide. The former is the sun of contributions by different astronomical constituents

$$z = \sum_i A_i \cos(\omega_i t - \phi_i)$$

with A_i = amplitude and ϕ_i = phase of i-th harmonic with angular velocity ω_i.
The values of A_i and ϕ_i are obtained by an analysis of the registrations of tidal recordings. This approach is called harmonic analysis. Different methods can be applied, e.g. the least squares method, the Fourier method, the U.S. Coast and Geodetic Survey method or the Admiralty method. The Admiralty method is preferable when it is sufficient to know the most important constituents. The method, originally developed by A.T. Doodson [1], can be applied to relatively short time series of 15 or 29 days of hourly observations.
Diurnal, semi-diurnal and quarter-diurnal harmonics can be computed by this method. The principles of the method are dealth with in this paragraph.

Let us assume atide consisting of a diurnal, a semi-diurnal and a quarter-diurnal constituent

$$z = A_0 + A_1 \cos(\omega t - \phi_1) + A_2 \cos(2\omega t - \phi_2) + A_4 \cos(4\omega t - \phi_4)$$

with the period of the first harmonic being exactly 24 hours. This expression can be developed into

$$z = A_0 + a_1 \cos \omega t + b_1 \sin \omega t + a_2 \cos 2\omega t + b_2 \sin 2\omega t + a_4 \cos 4\omega t + b_4 \sin 4\omega t$$

with $a_1 = A_1 \cos \phi_1$, $b_1 = A_1 \sin \phi_1$ etc.

The unknown values A_o, a_1, b_1, a_2, b_2, a_4 and b_4 can be obtained if 24 hourly water levels y_o, y_1, y_2..... y_{23} are measured.

With $\omega t = x$ the equations read

$$Y_0 = A_0 + a_1 \cos x_0 + b_1 \sin x_0 + a_2 \cos 2x_0 + b_2 \sin 2x_0 + a_4 \cos 4x_0 + b_4 \sin 4x_0$$

$$Y_1 = A_0 + a_1 \cos x_1 + b_1 \sin x_1 + a_2 \cos 2x_1 + b_2 \sin 2x_1 + a_4 \cos 4x_1 + b_4 \sin 4x_1$$

and similar expressions for y_2 up to and inclusive y_{23}.

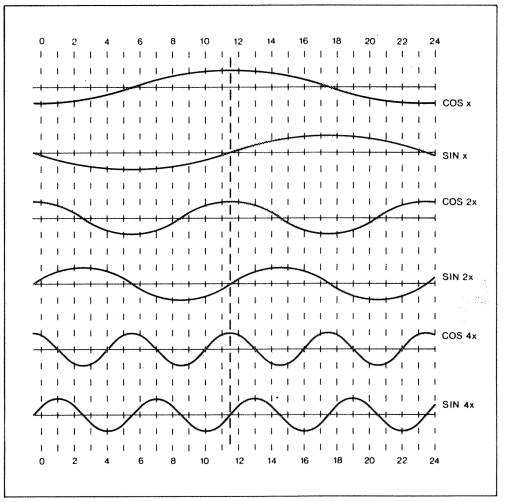

Figure 2.2.1.7 Harmonic curves

The harmonic curves given in figure 2.2.1.7 show some easy calculation rules. For instance, summing cos x_o, cos x_1..... cos x_{22} and cos x_{23} gives a value of zero. So

$$\sum_{i=0}^{23} y_i = 24\ A_0$$

from which A_o can be obtained.

In the same way

$$\sum_{i=0}^{23} y_i * \text{sign}(\cos x_i)$$

can be evaluated. It appears that the coefficients of A_o, b_1, a_2, b_2, a_4 and b_4 are equal to zero, while the coefficient of a_1 is equal 15.322. Furthermore we obtain

$$\sum_{i=0}^{23} y_i * \text{sign}(\sin x_i) = 15.322\ b_1$$

$$\sum_{i=0}^{23} y_i * \text{sign}(\cos 2x_i) = 15.455\ a_2$$

$$\sum_{i=0}^{23} y_i * \text{sign}(\sin 2x_i) = 15.455\ b_2$$

$$\sum_{i=0}^{23} y_i * \text{sign}(\cos 4x_i) = 13.856\ a_4$$

$$\sum_{i=0}^{23} y_i * \text{sign}(\sin 4x_i) = 16\ b_4$$

The notation sign (p) means

$$\text{sign}(p) = +1 \text{ if } p > 0$$

$$= 0 \text{ if } p = 0$$

$$= -1 \text{ if } p < 0$$

The required amplitudes and phases can be computed from the values of a_1, b_1, a_2, b_2, a_4 and b_4. However this method only applies if the tidal period of the first harmonic is exactly one day, and this is only true for the constituent generated by the sun. For the lunar tide the method can be modified to make it equally applicable. The reader is referred to Doodson and Warburg [2].

Observation period and sampling interval

As mentioned above, the Admiralty method can

be applied to relatively short time series of 15 or 29 days of hourly observations, if only information on the most important components is required.
The 15- or 29-day-periods are required in order to compute the two semi-diurnal tides M_2 and S_2. This can easily be understood when the following tidal signal is considered

$$h(t) = \sin(\omega_{M_2} t) + \sin(\omega_{S_2} t)$$

If these two functions are combined

$$h(t) = 2 \cos \frac{\Delta\omega t}{2} \sin \frac{\omega_{M_2} + \omega_{S_2}}{2} t$$

with

$$\Delta\omega = \omega_{S_2} - \omega_{M_2}$$

This signal can be considered as a semi-diurnal tide with a time-varying amplitude A which is equal to

$$A = 2 \cos \frac{\Delta\omega t}{2}$$

During a one day period this amplitude will remain almost constant; therefore, a much longer observation period is required to determine its general behaviour.
Generally, the Rayleigh-criterion is used to estimate a minimum observation period P

$$P > \frac{2\pi}{\omega_1 - \omega_2}$$

ω_1 and ω_2 are angular velocities of two components of different periods.
According to this criterion, the semi-diurnal tides M_2 and S_2 can be separated if observation data over a period of at least 15 days are available. However, separation of the diurnal tides P_1 and K_1 would require an 183-day period of observations. Therefore the 29-day period is sufficient provided that the diurnal components are of minor importance.

Usually, tidal analysis deals with hourly observations. This one-hour sampling interval is used because it is necessary to have at least two registrations during one complete cycle of each tidal component. Semi-diurnal tides would permit a longer sampling interval, but shallow-water tides, going up to M_8 with a period of about 3 hours, require a shorter sampling interval, i.e. less than 1½ hours. In practice, samples are taken every hour.
One must realize, however, that water level variations can also be induced by seiches, which often occur in harbours, and wind waves.These effects should be carefully filtered out before the hourly values are used for tidal analysis. If this is not possible it may be advisable to choose a much shorter sampling interval so that the natural oscillations can be properly analysed.
In conclusion, some observations are made on the accuracy of the tidal analysis results. Disturbances in the hourly observations (e.g. noise) do influence the final results. The accuracy may be limited if the minimum observation period is used; a much longer observation period will usually improve the accuracy of the tidal analysis results.

Tidal prediction
Water levels can be predicted provided amplitudes and phases of the relevant tidal harmonics are available. This is the case at stations where long series of tidal observations have been registered and analysed. Sometimes, tidal predictions are requested for areas where registrations are not available; for example, when civil engineering works are still in the planning stage. Deltadienst personnel have developed a method based on a regression technique for this particular purpose. It can be used if long tidal observations are available at a reference station (e.g. Flushing), and if there are relatively short registrations available at the required station. By correlating the high water levels that occurred simultaneously at the two stations, an equation can be obtained in order to transfer the predicted high water level at the reference station to the high water level at the other station (fig. 2.2.1.8). The same applies to the low water levels and the time differences. The method can even be extended to predict the complete tidal curve at the other station. If the civil engineering works take some years to complete, it would be advisable to install a tide gauge in the area itself to obtain the highest possible accuracy.

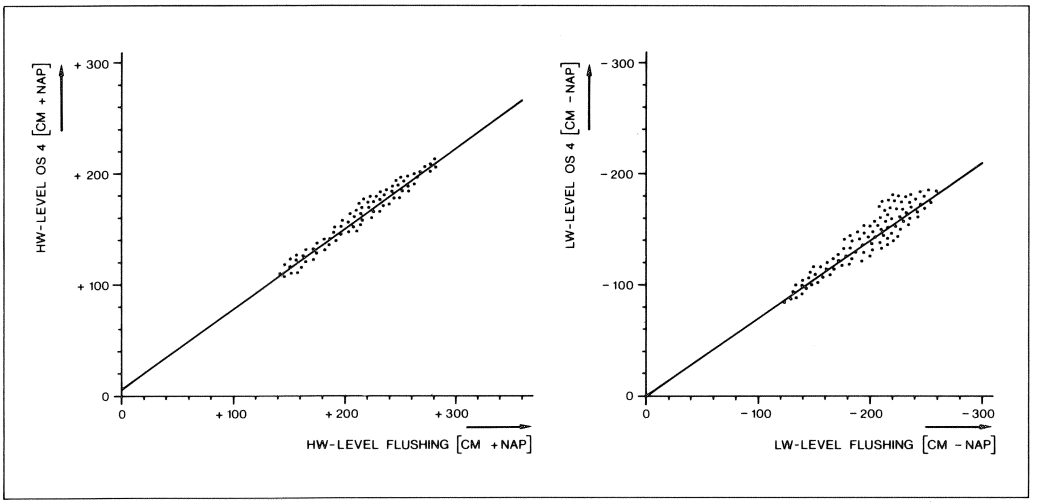

Figure 2.2.1.8. Correlations between high water levels and between low water levels at Flushing and OS4.

References

1. Doodson, A.T., The analysis of Tidal Observations, **Phil. Trans. Roy. Soc. A.227, 1928.**

2. Doodson, A.T. and Warburg, M.D., **Admiralty Manual of Tides,** 1941.

3. Dronkers, J.J., **Tidal computations in Rivers and Coastal Waters,** 1964.

Environmental Conditions

W. van Aalst, J. Bruinsma

2.2.2. Waves

Introduction

The characteristics of surface water waves are a factor of great importance in the design of sea defences, closing structures, harbours, waterways and offshore structures. In this section, only wind-generated waves will be discussed; other wave-phenomena such as tsunamis, seiches and internal waves are omitted.

Among the vast number of existing publications in this field, the „Shore Protection Manual" [1] gives extensive information for practical use. Another excellent introduction to the wave field is the „Handbook on Wave Analysis and Forecasting" [2] published by the World Meteorological Organization (WMO).
A brief description of the basic concepts used in wave-theory and their application in coastal engineering will be given. Its purpose is to explain the various definitions and basic formulae in use for the determination of wave boundary conditions for the design of coastal structures. For theoretical discussions, the reader can consult the monographs by Philips [3] and Kinsman [4].

Finally, a brief description is given of a simple shallow water forecasting model in use in the Netherlands for coastal engineering purposes. In the last section, some probabilistic applications are presented.

Phenomenological description

Simple harmonic long-crested progressive waves are usually characterized by their height H, length L, period T, rate of propagation C, steepness s and direction of propagation θ.
Such waves consist of a series of parallel smooth wave-crests, equidistant from each other and equal in height, moving at a constant speed in a direction perpendicular to the crests without change of shape or speed.

Wave height H is the difference in surface elevation z between a crest and the next trough.
Wave length L is the horizontal distance between successive crests. Wave period T is the

Figure 2.2.2.1. Definitions of wave quantities.

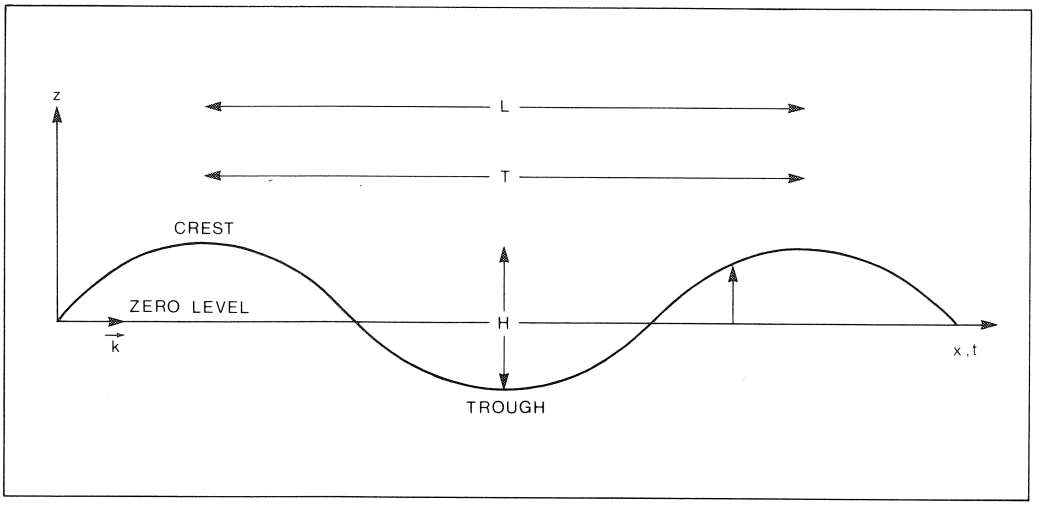

time interval between successive crests, passing a given point.
Rate of propagation C is the speed at which the crests and troughs travel.
Steepness S of a wave is the ratio of the height to the length (H/L).
Wave direction θ is the angle between a vector $\vec{k}$ normal to the wave crests and a fixed direction ($|k| = 2\pi/L$). These definitions are illustrated in figure 2.2.2.1.

However, actual sea waves do not appear as simple as the profile shown in figure 2.2.2.1. The wave pattern at sea appears very irregular and confused. Waves are continually being overtaken and crossed by others. It is hardly possible to determine a wave height, lenght and period.

In figure 2.2.2.2. the water elevation is shown as a function of time for a fixed location.

The wave height H of such a pattern is defined as the vertical distance from a trough to the next crest and the period T is the time distance between two zero downcrossings (figure 2.2.2.2) The wave record in figure 2.2.2.2. shows only one of many possible wave height curves. For other neighbouring locations apparently very different records would be obtained. This is due to the random nature of the sea surface. Fortunately, the statistical properties of the distribution of periods and heights are the same from one wave record to another. Therefore a sea state - that is a wave condition for which a characteristic wave height and period are known - can be described with statistical quantities. The following parameters are often used:

$\bar{H}$ = average wave height.
$H_{z,1/3}$ = significant wave height, that is the average height of the 1/3 highest waves.
$\bar{T}$ = average wave period.

A different way of representing the random appearance of the sea surface is to consider the chaotic wave pattern as a sum of a large number of harmonic-long crested sinusoidal waves, each with its own amplitude (a_n), frequency (f_n) and randomly distributed phase angles (ϕ_n).

$$z(t) = z_o + \sum_{1}^{N} a_n \sin(2\pi f_n + \phi_n) \qquad 1$$

in which

$z(t)$ = elevation of the water level at time t
z_o = mean elevation
f_n = frequency of the n-th wave component = $1/T_n$
ϕ_n = phase angle of the n-th component
N = total number of components

Figure 2.2.2.3. shows the construction of the sea surface from a large number of sinusoidal long-crested progressive waves of different periods, moving in different directions.

Instead of equation (1), the wave pattern is often characterized by a **wave spectrum.** This is the squared amplitude (a_n^2) as a function of the frequency (see fig. 2.2.2.4.a.)

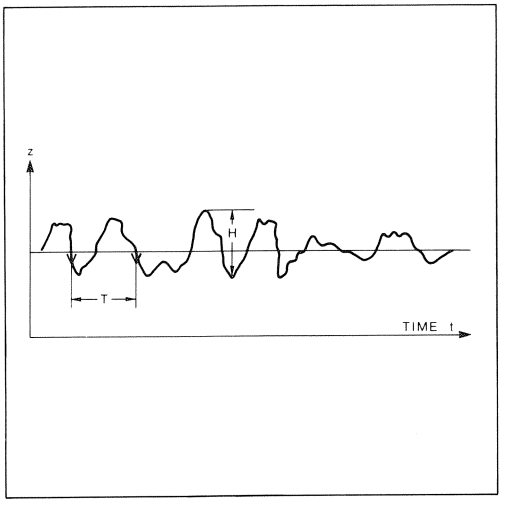

Figure 2.2.2.2. Sample of a wave record.

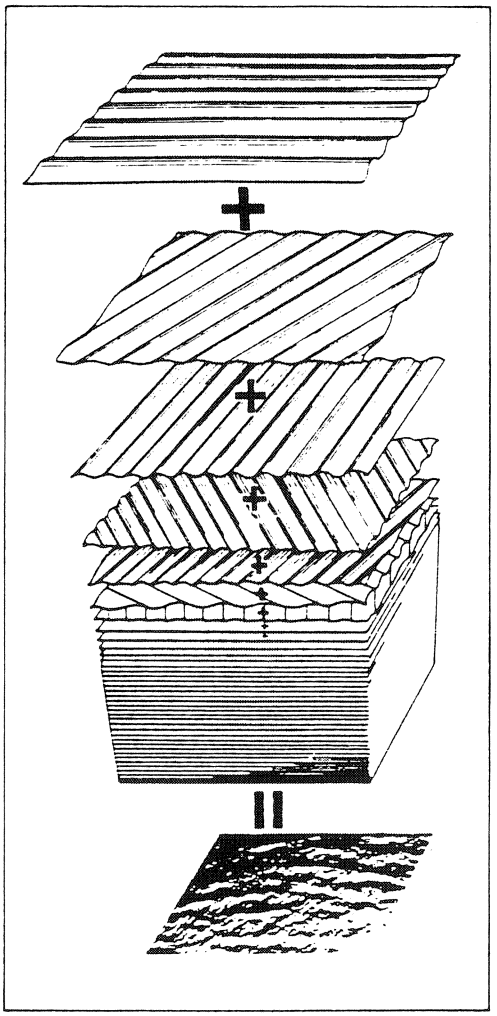

Figure 2.2.2.3. The sea surface obtained from the sum of many sinusoidal waves.

Figure 2.2.2.4 Wave spectrum.

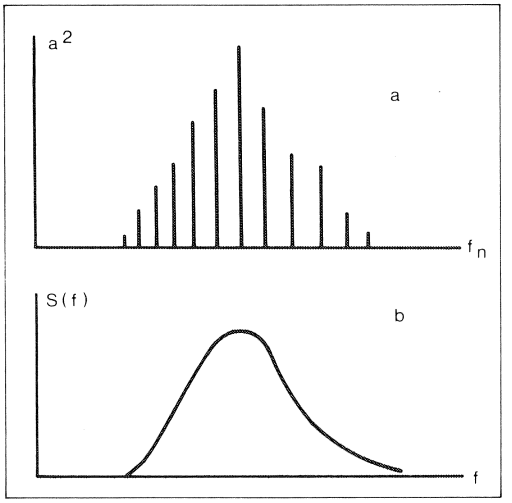

Due to the large number of harmonics, required for the description of a sea state, wave spectra are usually given as a continuous curve connecting the discrete points found from harmonic analysis.
The wave spectrum may not always be as regular as shown in figure 2.2.2.4 b. Complex areas (c.q. delta areas), and also sea states caused by fast changing windfields, give rise to broad spectra which may show several peaks. The representation of the random appearance of the sea surface by means of a wave spectrum has many important applications in coastal engineering.

Not all wave fields show the same characteristics. The following differentiation is commonly used.

Waves generated by local winds are called **„sea"**. Waves that have travelled out of the generation area change into **„swell"**.
„Sea " waves are shaped like mountains with sharp angular tops. The crests are not long and are not all lined up in the same direction. There are many small waves superimposed on larger waves. „Swell" waves have rounded tops. Their pattern is more regular.

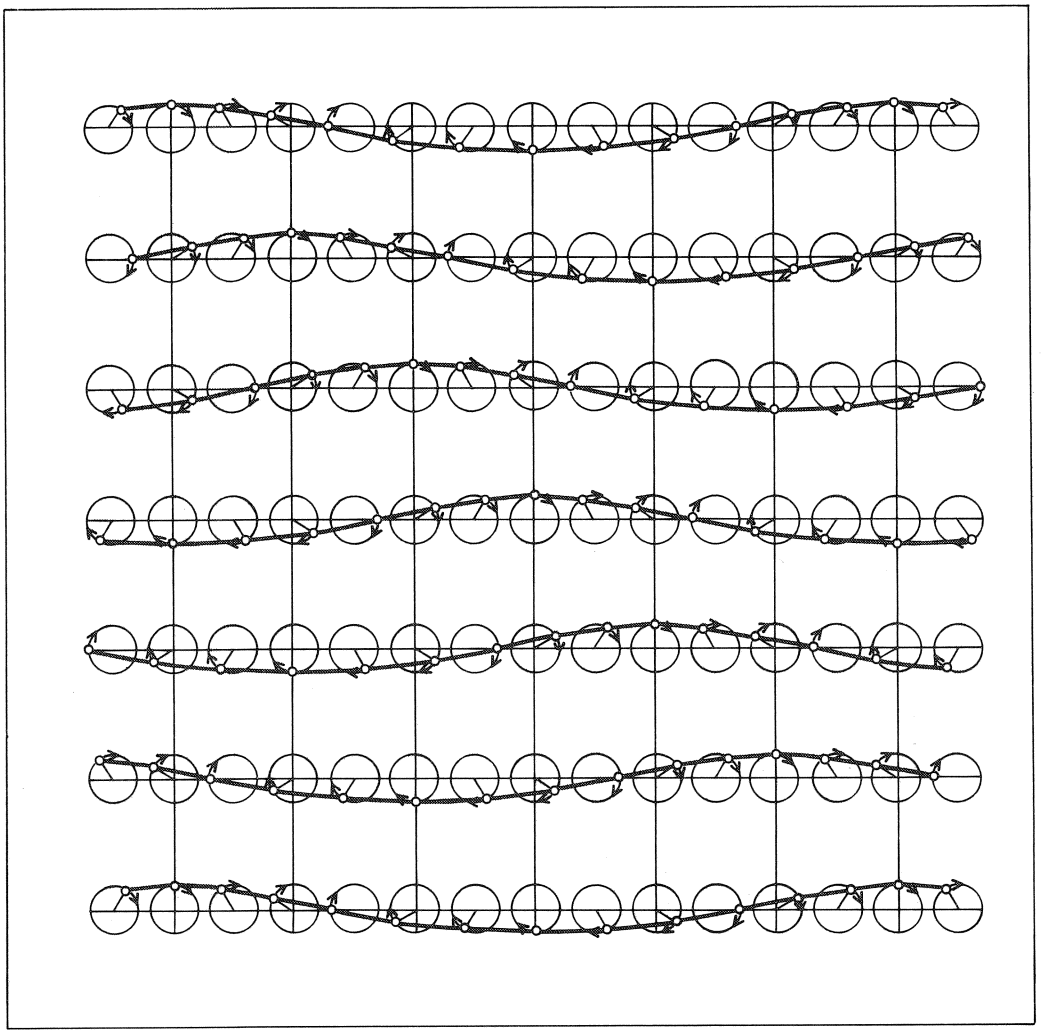

Figure 2.2.2.5 Orbital particle motion, and wave motion progression. Seven snapshots, each with an interval of 1/12th period

Physical description

The water particles in a progressive wave move in approximately circular paths. (fig. 2.2.2.5.)
The instantaneous particle velocity components are:

$$u = \frac{\omega H}{2} \frac{\cosh k(h+z) \cos(\vec{k}.\vec{x} - \omega t)}{\sinh kh} \quad 2$$

$$v = \frac{\omega H}{2} \frac{\sinh k(h+z) \sin(\vec{k}.\vec{x} - \omega t)}{\sinh kh} \quad 3$$

u = horizontal particle velocity
v = vertical particle velocity
ω = radial frequency = $2\pi/T$
$\vec{x}$ = coordinate along the wave direction
z = vertical coordinate
h = water depth
t = time

The energy of water waves consists of kinetic and potential energy and is usually given in energy units per unit of water surface area.
The expression for the total energy per crest length is

$$E_t = 1/8\ \rho\ gH^2 \qquad 4$$

Wave energy propagates at a speed different from that of the wave crests which, in turn, is different from the particle velocities. For instance, take the position of a float on a wave surface, which oscillates about a fixed position while the wave crests move forward at a definite velocity C.

$$C = L/T = \omega/k = \sqrt{g/k\ \tanh kh} \qquad 5$$

When we throw a stone in a pond, we notice the propagation of a group of waves. It seems that waves originate at the rear of the group, move through the group at speed C and die out near the front of the group. This means that the group, as a whole, carrying a certain amount of energy, moves at a speed less than the speed C of individual wave crests.

This speed, at which energy is propagated, is called the group velocity C_g and is given by:

$$C_g = C/2\ (1 + 2kh/\sinh 2\ kh) = nC \qquad 6$$

$$n = 1/2\ (1 + 2kh/\sinh 2\ kh) \qquad 7$$

Due to the particle motions waves are also accompanied by pressure fluctuations. The pressure fluctuation, below the mean water level in a regular wave, is given by:

$$p = \rho\ gH/2\ \frac{\cosh k\ (h + z)}{\cosh kh}\ \cos\ (kx - \omega t) \qquad 8$$

A number of specific phenomena can be observed when waves proceed from deep through intermediate depths to shallow water. To simplify matters, it will be assumed that the depth contours run parallel to the coast.

Shoaling
Waves, approaching the coast perpendicularly, will show wave height changes. The wave heights for two locations differing in depth are coupled by the following equation:

$$H_1/H_0 = \sqrt{C_0/C_1\ \frac{1}{2n_1}} = K_{sh} \qquad 9$$

$$K_{sh} = [\ \sqrt{\tanh kh}\ (1 + \frac{2\ kh}{\sinh 2\ kh}\ )\ ]^{-\frac{1}{2}} \qquad 10$$

K_{sh} = the shoaling coefficient and the phenomenon is known as shoaling. In reality, waves approaching the coast will never increase to infinite heights but will break sooner or later. There are two limitations imposed on wave heights.

Breaking
First, the steepness for a non-breaking wave has a maximum value. For linear theory, this is:

$$S = H/L = 0.142$$

This is the breaker criterion for deep water. The second criterion applies to the wave height, to water depth ratio $H/_h$ which is called the breaking index. From the solitary wave theory, this limiting ratio appears to be:

$$\gamma = H_{max}/h = 2 * 0.78$$

Breaking over the entire range of relative depths from deep to shallow water is covered by Miche's formula:

$$H/L = 0.142\ \tanh\ (2\pi h/L) \qquad 11$$

Refraction
Besides shoaling and breaking, waves undergo other changes when they begin to feel the bottom. The wave crests are forced to turn parallel

to the bottom contours when entering water of variable depths obliquely to the bottom contours. The wave rays (perpendicular to the crests) diverge as the water becomes shallower. Wave refraction is very much like refraction in geometrical optics,where Snell's Law describes the transmission of light through different media.

Refraction also influences wave heights. The heights for two different locations are coupled by:

$$H_1/H_0 = \sqrt{1/2n_1 . C_0/C_1}.b_0/b_1 = K_{sh}.b_0/b_1$$

bo and b1, are distances between two adjacent wave orthogonals (see figure 2.2.2.6.).

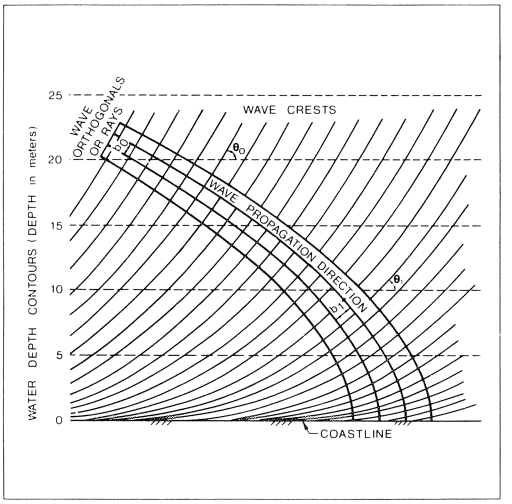

Figure 2.2.2.6. Refraction.

Diffraction.
Diffraction is a phenomenon which causes waves to be spread into the shadow zone of an obstacle. Wave energy seems to be transported along the wave crests. There are no such simple relations between the wave heights of diffracted waves as is the case with shoaling and refraction.

Figure 2.2.2.7. Diffraction.

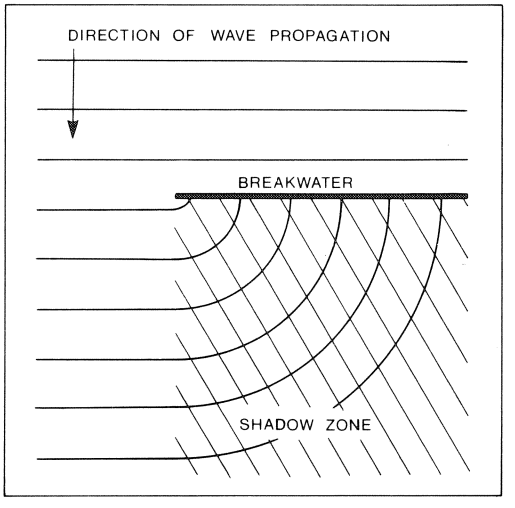

Introduction to wave forecasting models
Designers and builders of coastal engineering structures have a need for wave-forecasting methods. As previously mentioned,there are two different ways of describing a wave field.
In the first method, the irregular wave field is replaced by a fictitious sinusoidal wave having a wave height, period and direction equal to the significant wave height, the average period and the main direction of the irregular wave field. These parameters which, in bygone days, used to be estimated from the visual impression by an experienced observer, were sufficiently accurate for simple forecasting methods. Nowadays, these parameters are obtained from wave records (Figure 2.2.2.2.), measured by wave gauges and waverider buoys. (See chapter 2.3.2.). Such methods give a significant height and period as a function of time and location for waves in a standard windfield. The mean wave direction coincides with the mean wind direction. A standard windfield comprises a region, where a homogeneous stationary wind is blow-

ing at a definite speed U_z, measured at a fixed height z above the mean water level and a straight upper boundary.

The significant wave height and average period of a growing „sea" depend on certain characteristics of the windfield. It appears that the height of waves depends on the duration of the wind. At first, the waves grow rapidly and then, more slowly until a state of equilibrium is realized. After that, the wave height does not increase further. The height of waves, however, also depends on another factor, the „fetch". Each wave, arriving at a certain point, has travelled a certain distance from its point of origin. In the case of a „sea" close to the coast, where a constant off-shore wind is blowing, the generated waves move away from the shore. The farther the waves have moved from the shore, therefore, the higher the waves. Thus, even when the wind has been blowing infinitely long, the wave-height at each point will depend on the distance from the shore i.e. the length of the wind-path or fetch.

In a standard windfield, wave growth is a function of fetch F and duration t. Often, non-dimensional characteristics are selected for calculations of the effects of wave growth:

$$\tilde{H} = \tilde{H}\ (\tilde{F},\ \tilde{t},\ \tilde{h}) \qquad 12$$

$$\tilde{T} = \tilde{T}\ (\tilde{F},\ \tilde{t},\ \tilde{h}) \qquad 13$$

where the symbol $\sim$ over a parameter denotes the non-dimensional character of that parameter:

$$\tilde{H} = gH/U^2;\ \tilde{F} = gF/U^2;\ \tilde{h} = gh/U^2 \qquad 14$$

$$\tilde{T} = gT/U\ ;\ \tilde{t} = gt/U \qquad 15$$

H = wave height
T = wave period
F = fetch
h = water depth
t = time
U = wind speed

For wave growth on deep water, the following analytical expressions are often used:

$$\tilde{H} = A \tanh\ (a\ \tilde{F}^{b}) \qquad 16$$

$$\tilde{T} = B \tanh\ (c\ \tilde{F}^{d}) \qquad 17$$

In fig. 2.2.2.8., empirical relations are given with which wave quantities can be obtained for a given fetch, duration and windspeed. These relations also apply to deep water.
In shallow water, dissipation of wave-energy by the bottom, competes with the atmospheric input of energy by the wind. A simple description is not easy to present, since the shape and composition of the bottom play an important role. For a horizontal bottom and a uniform prolonged constant windspeed, Bretschneider [5] gave the significant wave height as a function of fetch and depth (figure 2.2.2.9.). In practice more complicated situations occur.
For instance, under storm conditions, the horizontal wind forces on the water surface also induce a horizontal current in the wind direction. In shallow water areas, these currents are impeded, causing the water level to rise down wind. This deviation from the normal water level which, under extreme conditions, is of considerable importance, is usually called storm surge or wind setup.

A second method is one in which, besides significant wave height and period, spectral information is also obtained. Each wave spectrum contains a certain amount of energy, has a certain position on the frequency axis and a definite shape. For spectra with a fixed shape, the energy content and position can be characterized by the aforementioned parameters, significant wave height and period.
Frequently other parameters, directly related to the description of spectra, are preferred.
From figure 2.2.8. and also from figure 2.2.9., it can be seen that, for a certain wind speed, a saturation of the significant wave height occurs (for long duration and/or long fetch). Then, the energy dissipation is in balance with the atmospheric energy input.

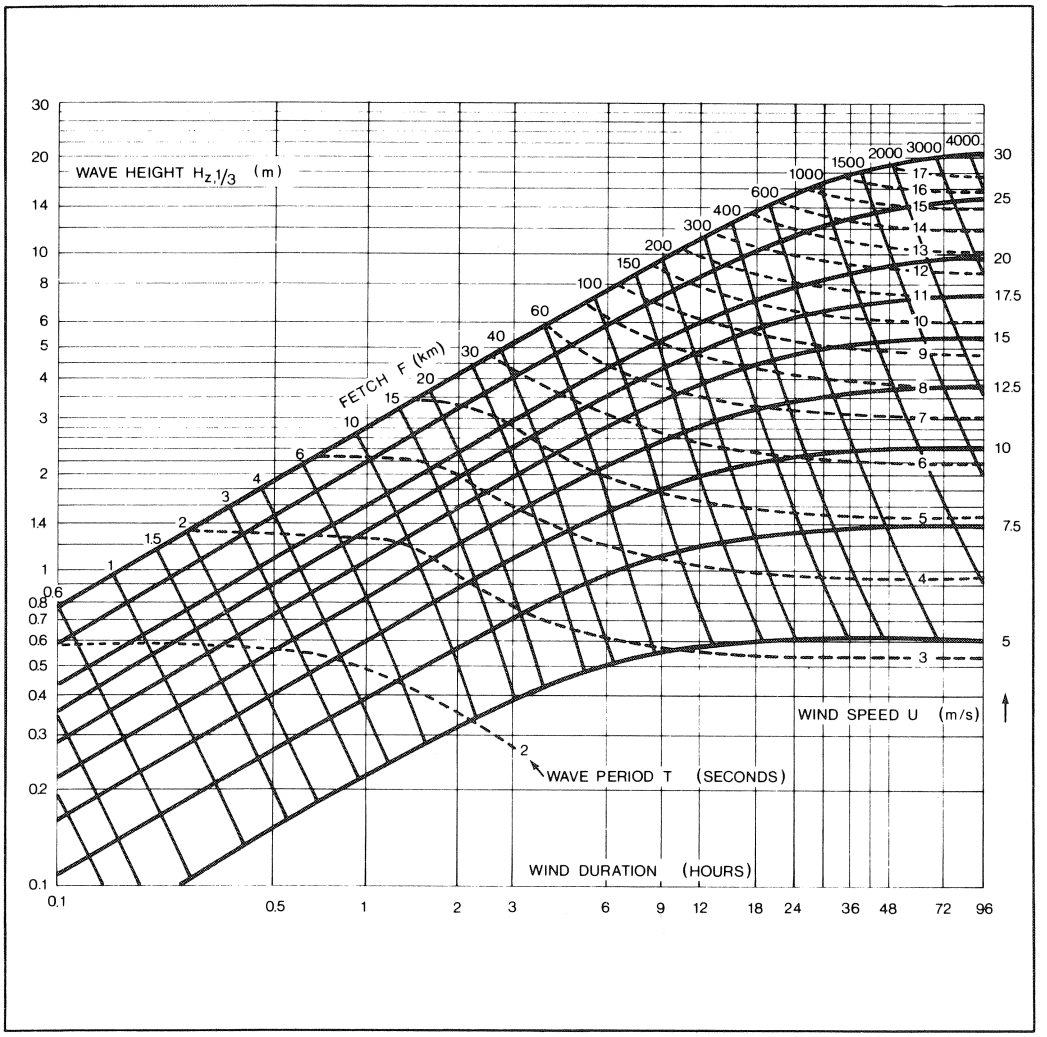

Figure 2.2.2.8 Wave-forecasting diagram.

It is known that, for such a saturation state, which is called a fully developed sea, a fixed spectral shape occurs. The Pierson-Moskowitz is often used for a fully developed sea. In its this spectrum is described by the following formula:

$$S(f) = \frac{\alpha g^2}{(2\pi)^4} f^{-5} \exp\left[-\tfrac{5}{4}(f/f_p)^{-4}\right] \qquad 18$$

in which

S(f) = the energy density
f_p = the frequency at the maximum energy density
g = the acceleration of gravity
α = dimensionless quantity.

However, in growing stages, the sea spectrum is much sharper peaked than the Pierson-Moskowitz spectrum.

During the Joint North Sea Wave Project (JONSWAP)[6], a new spectral shape for growing sea stages was developed:

$$S(f) = \frac{\alpha g^2}{(2\pi)^4} f^{-5} \exp\left[-\tfrac{5}{4}(f/f_p)^{-4}\right] * \exp\left[\frac{-(f-f_p)^2}{2\sigma^2 f_p^2}\right]^{\nu} \qquad 19$$

with

ν = constant, the average value from JONSWAP was 3.3
σ = 0.07 for $f \leqslant f_p$
σ = 0.09 for $f > f_p$

The JONSWAP spectrum is thus obtained by multiplying the Pierson-Moskowitz spectrum with the last factor, the „peak enhancement" factor.

In theory, there is a relation between $H_{z,1/3}$ and the zero order moment of the spectral distribution (M0). This relation

$$H_{z,1/3} = 4\sqrt{M0} \qquad 20$$

with

$$M0 = \int_0^\infty S(f)\,df \qquad 21$$

is only valid for narrow spectra but the approximation, in cases of broader spectra, is sufficiently close for most practical applications.

Figure 2.2.2.9. Relation between the non-dimensional wave height, fetch and depth for a situation with horizontal bottom and uniform prolonged constant wind speed according to Bretschneider [5].

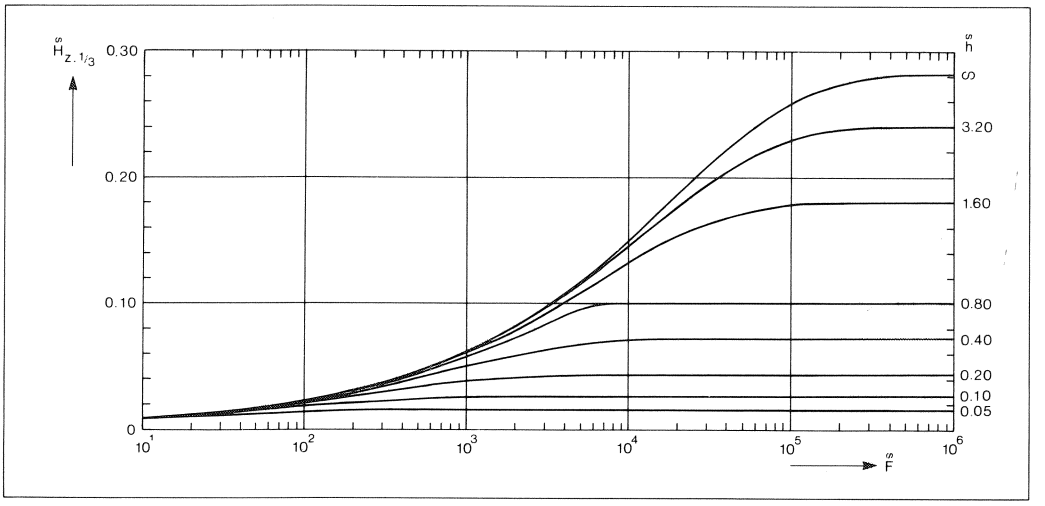

The swell spectrum, at a certain point away from the wave generation area, can be obtained from the sea wave spectrum by taking into account dispersion and angular spreading. The dispersion of waves in the direction of propagation is a result of differences in velocity between various components of the wave spectrum. This important property of water waves is described by the following relation:

$$\omega^2 = (2\pi/T)^2 = gk \tanh kh \qquad 22$$

which says that the radial frequency $\omega = 2\pi f$ depends on the wave number $k = 2\pi/L$ (see also eq. 5).
At great distances from the wave generation area, wave components with low frequencies arrive first to be followed by wave components with higher frequencies. At each time, the swell spectra will be limited to a frequency band of a certain width which shifts gradually to higher values. Often swell spectra will be narrow but this is not always so. This depends strongly on the distance to and the dimensions of the generating windfield.
Finally, wave spectra generation and propagation can be described mathematically by a spectral energy balance equation:

$$dF(\vec{k}, \vec{x}, t)/dt = S(\vec{k}, \vec{x}, t) \qquad 23$$

in which F = energy density of one wave component, S = source term (the sum of energy input and output).

The left hand side indicates the changing of the energy density with time and can be written as:

$$\frac{dF}{dt} = \frac{\partial F}{\partial t} + \vec{C}_g \cdot \nabla F + \frac{\partial \vec{k}}{\partial t} \cdot \frac{\partial F}{\partial \vec{k}} \qquad 24$$

where C_g is the group velocity.

In deep water, the wave number k is independent of time, so the last term will vanish. In shallow water, this term represents the refraction of waves. To describe the source function S, it will be split in three parts:

$$S = S_{atm} + S_{diss} + S_{nl} \qquad 25$$

Here, S_{atm} indicates the energy transferred to the wave component from the atmosphere. The second term S_{diss} represents the energy release through dissipation processes as wave breaking and bottom dissipation. The last term gives the interaction between different wave components. It is called the weak nonlinear interaction. This term is in contradiction with the assumption that the wave surface can be considered as a linear superposition of independent wave components. Non-linear interaction is a weak but very important phenomenon as it is responsible for the shape invariance of wave spectra. During the past thirty years, many mathematical models have been developed to solve the energy balance equation. With these models, the wave climate in deep water (offshore structures) can be forecast. Recently, a number of models became available, which give forecasts of wave propagation in shallow waters [14].
In most cases, a parametrization of the source terms or a parametrization of the wave spectrum is used in these models.
The purpose of a parametrization of eq.23 is to reduce the calculation of the change of a great number (about 100) of spectral points to the calculation of the change of a manageable subset of parameters (α, γ, σ, f_p, see eq. 19). The propagation of the energy density spectrum is then governed by the change of these parameters in relation to fetch, wind speed, bottom configuration etc.

The solution of eq.23 is often approximated by empirical relations as has been shown in figure 2.2.2.9. The disadvantage of empirical relations is that they only give average information. In most cases precise information is required.
Recently Hasselmann et al [7] presented results of an intercomparison of ten wave models for deep water. In this paper, the differences, advantages and disadvantages of the models are given.
One of these models GONO [8], which is also useful for shallow water situations (waterdepth > 10 m), has been used to predict the wave boundary conditions at the seaward edge of the Dutch delta area for the design of closing structures. In the coastal zone of the Dutch delta area, the bottom configuration (bars and

troughs) is so complicated that up to now (1982) no exact description is available. An empirical model, which has been checked against measurements, is being developed and will be described in the next section.
For the **design** of structures, a statistical distribution of wave spectra at the design location gives sufficient information.
Sometimes, the probability of exceedance of an individual wave parameter, such as the wave height of an individual wave, is required. The distribution of wave heights in a sea state can be represented by the „Rayleigh distribution", which is derived from the assumption that the surface elevation (form. 1) is an ergodic Gaussian process. The probability of exceedance of a design wave height H_d by any given wave in a train of Rayleigh distributed wave heights is:

$$P(\underline{H} > H_d) = \exp\left[-2\left(\frac{H_d}{H_{z,1/3}}\right)^2\right] \qquad 26$$

in which
H = stochastic variable
H_d = individual wave height for which the probability of exceedance is required
$H_{z,1/3}$ = significant wave height.

The chance P (1) that the wave height H_d is exceeded at least once in a specific wavefield characterized by $H_{z,1/3}$ containing N waves is:

$$P(1) = 1 - [1 - P(\underline{H} > H_d)]^N \qquad 27$$

Wave conditions for coastal structures in shallow waters
Lack of sufficient measured wave data often forces designers of coastal structures to use wave models. In the Netherlands, field measurements as well as simple mathematical models are in use. For the design and construction of a barrier in the mouth of the Eastern Scheldt estuary (Figure 2.2.2.10.), a wave model has been devised. A description of this model breaks down into two sections (Figure 2.2.2.11.).

- Wave generation and propagation on the North Sea (h > 10 m), resulting in wave conditions at the seaward edge of the coastal zone.
- Propagation of waves from the seaward edge to the structure site over a complicated coastal area and wave generation in that area by local winds.

Due to the shallowness of the coastal zone, the water level strongly determines the penetration of waves from the outside. In areas like the Dutch coastal zone, where the water level varies due to astronomical tide and wind setup, a coupling between the water level and the wave quantities at the seaward edge is apparent.
Moreover, for the design of structures, not only wave quantities but also the water level is of vital importance as a design criterion. There is some dependence between the water level and waves at the seaside because waves and wind setup originates from the same windfield. The complete dependence is disturbed by the astronomical tide, which is independent of the windfield, and by the difference in duration for building up a full grown wave field and a maximum wind setup for a given meteorological situation.

To obtain the wave conditions at the coastal structure, the processes of wave growth, dissipation, breaking etc. should be taken into account. Figure 2.2.2.11. gives a schematic diagram how to proceed.

Wave conditions at the seaward edge
In the above mentioned concept (see figure 2.2.2.11.), the windfield over the North Sea plays a centrale role. It generates both the wind setup (for storm conditions) and the sea. Wave generation and propagation on the North Sea, resulting in wave boundary conditions at the seaward edge, can be obtained from the wave forecasting model GONO [8]. Advanced models are also available for the calculation of the wind setup. However, both models use, as input,the windfield at sea in a large number of gridpoints for a number of time steps. To obtain the design boundary conditions at the seaward edge, a large number of extreme storms should be simulated. Fortunately, in many cases, simple empirical models, which were fitted on

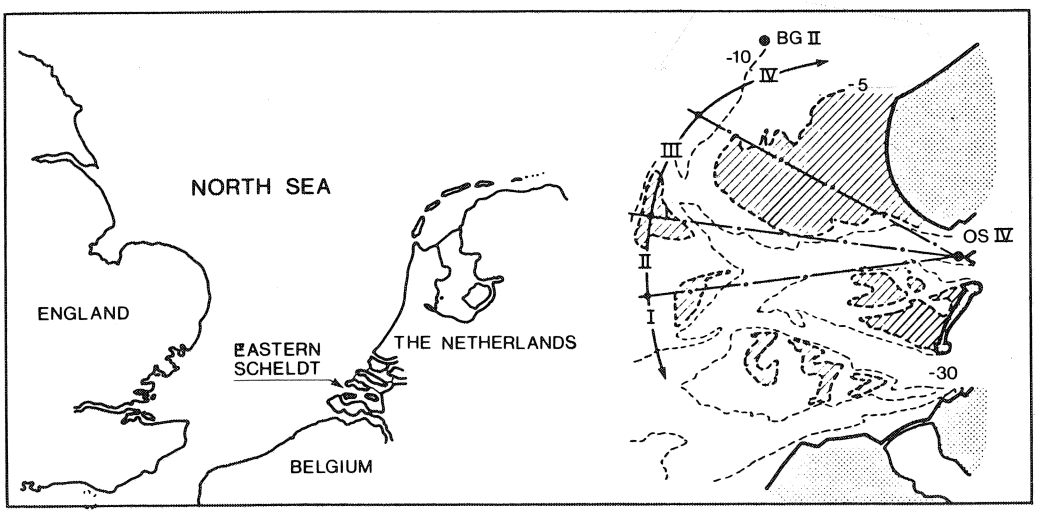

Figure 2.2.2.10 Situation sketch of the Eastern Scheldt estuary and detailed sketch of the Eastern Scheldt with locations of wave stations BGII and OSIV.

Figure 2.2.2.11 Model description.

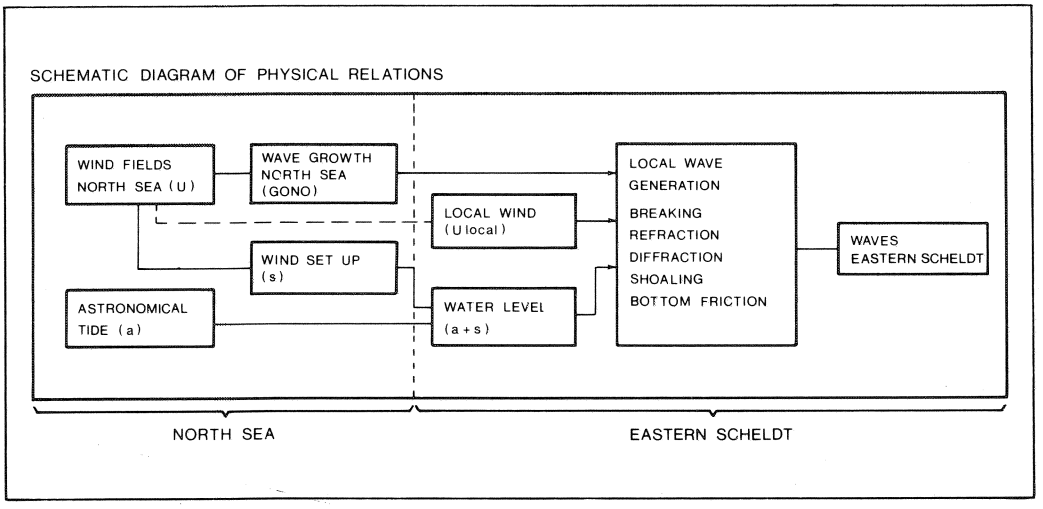

measurements, can be used. The Bretschneider wave model and the Weenink setup model are presented here as an example.
The Bretschneider model [5], [1] starts from the assumption that the windfield at sea can be represented by a constant windspeed U in the direction θ. The significant wave height at the seaward edge of the coastal zone is described by:

$$H_{z,1/3} = 0.283 \frac{U^2}{g} \tanh [0.53 \tilde{h}^{0.75}] . \tanh\left[\frac{0.0125 \tilde{F}^{0.42}}{\tanh(0.53 \tilde{h}^{0.75}}\right] \quad 28$$

Because of the differences in depth and fetch for different directions, a certain schematization of the relevant area is needed for a proper use of this formula. It is then possible, by selecting representative sectors, to calculate the contribution of different wind directions and fetches to the wavefield at a chosen point.

Although this relation applies to wave generation in water of constant depth, it is also a good approximation for smooth varying bottoms using the average depth. In figure 2.2.2.12., the Bretschneider relation has been given for different depths and fetches and also wave measurement results from locations at the seaward edge of the Dutch coast. Except for low local windspeeds, where the deviations are due to swell which is not taken into account, the agreement between calculations and measurements is reasonable.
Statistical information on windspeeds and wind directions is often available. It is then possible to obtain the probability density function of the significant wave height from the wind velocity and direction distribution, by means of formula 28.
The wind setup model of Weenink [9] also schematizes the windfield to avoid lengthy and complicated calculations. Therefore, the North Sea was divided into 5 parts. In this way, the windspeed and direction in each sector can be obtained for any depression field.
(See figure 2.2.2.13.).

According to Weenink's theory, the setup per sector is as follows:

$$s = (c_1 \cos\theta + c_2 \sin\theta) U^2 \quad 29$$

in which c_1 and c_2 are constants, depending on the location. The constants follow from theory or can be obtained from measurements.
The summation of the setups for all five sectors give the setup at a location near the coast.

Wave propagation in the coastal zone
Wave energy, entering the estuary over shoals and gullies, is modified by breaking, bottom friction, shoaling and refraction.
Simultaneously, waves generated by local windfields reach the barrier site. For the calculation of the propagation of wave energy,the area of shoals and gullies was divided in several sectors, each having a characteristic one dimensional bottom profile (Figure 2.2.2.14.).

The irregular wave field is replaced by a sine wave (period T and wave height $H_{z,1/3}$), propagating in the direction of the local windfield.
The transformation of the wave energy is described by the energy balance equation (eq.23) for one wave component.
The dissipative terms are bottom friction and wave breaking. Energy dissipation by bottom friction is assumed according to the relation used in GONO [8]:

$$S_{bottom} = 0.00028 \left[\frac{gk}{\omega \cosh(kh)}\right]^2 \quad 30$$

For breaking, a modified Miche criterion is used (see eq.11):

$$H_{max}/L = 0.093 \tanh 2\pi h/L \quad 31$$

To take care of the influence of tidal currents on wave steepness, a coefficient depending on the current velocity and direction was applied [10].
Wave growth is simulated by the GONO wave growth model which is of the general dimensionless form (see form.16):

$$\tilde{H}_{z,1/3} = 0.22 \tanh [4.62 \times 10^{-4} \tilde{t}^{0.7786}], \quad \tilde{t} \leq 13 \times 10^3$$
$$\tilde{H}_{z,1/3} = 0.22 \tanh [1.91 \times 10^{-3} \tilde{t}^{0.6286}], \quad \tilde{t} > 13 \times 10^3 \quad 32$$

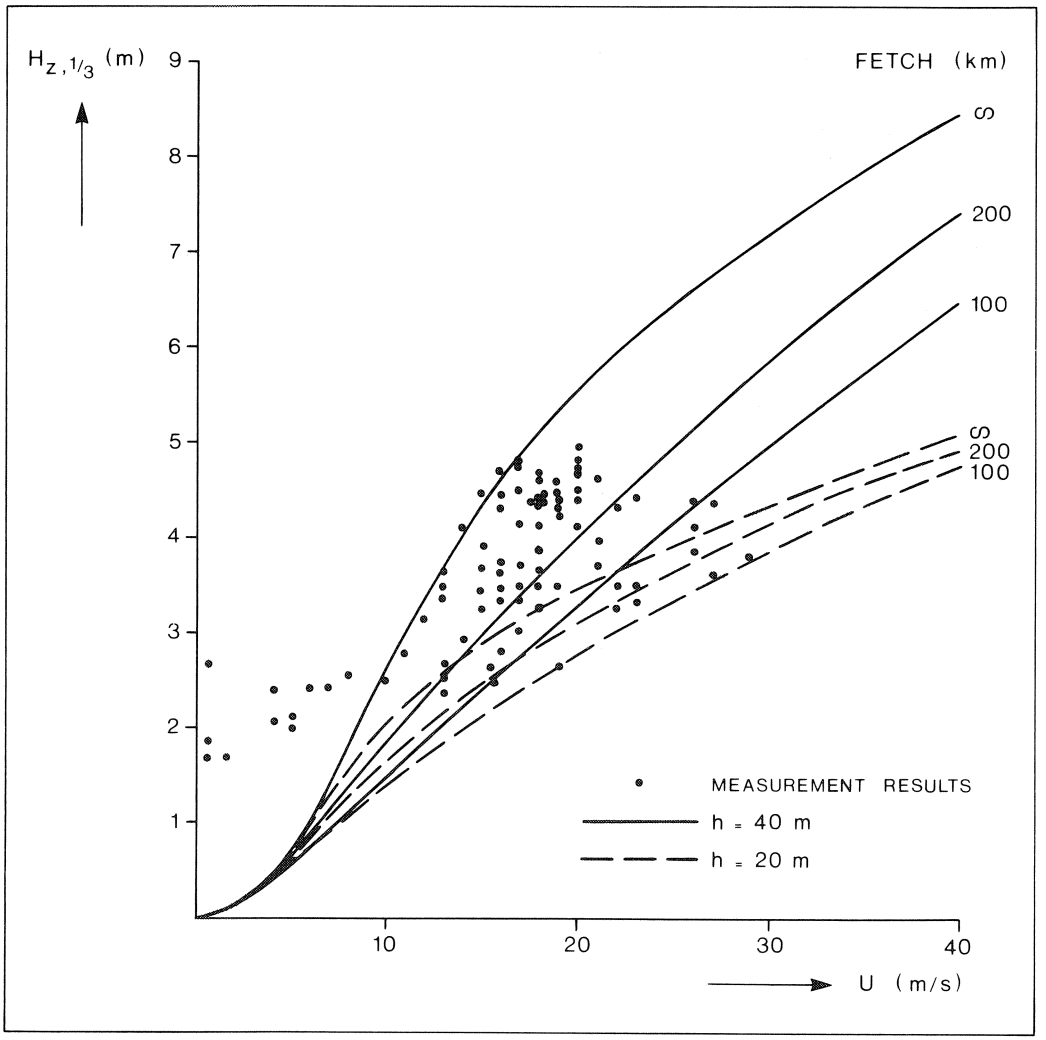

Figure 2.2.2.12 Wave height vs windspeed relations

In order to take care of the complex mechanism of refraction, a bulk coefficient depending on the water depth h was introduced for each sector:

$$H^{ref}_{z,1/3} = H_{z,1/3} \cdot (A + B.h) \qquad 33$$

By selecting for each sector a set of 30 measured significant wave heights that were

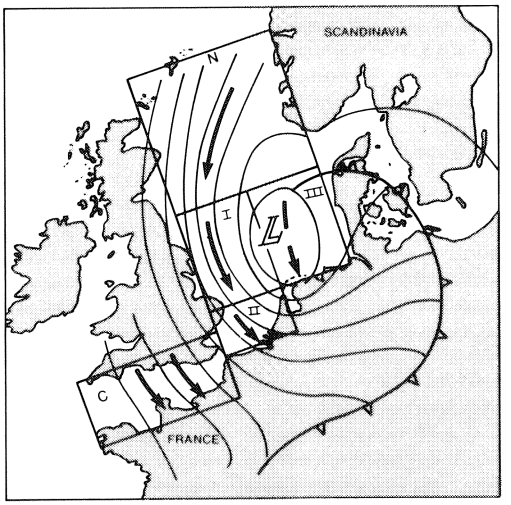

Figure 2.2.2.13 Weenink's schematization for setup calculations

Figure 2.2.2.14 Schematized bottom profile.

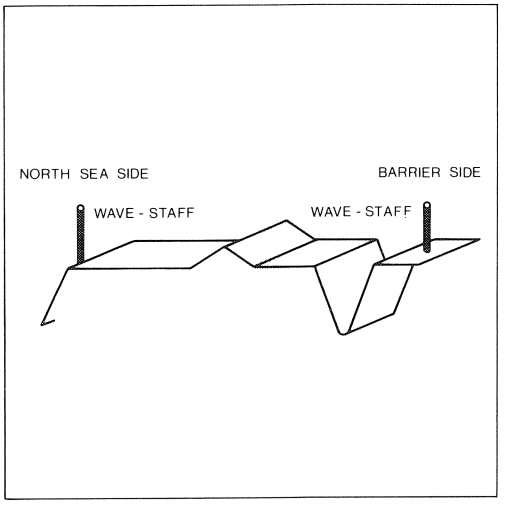

hindcasted against the model calculations by a least squares fit, A and B were determined. Further hindcasts, with fixed coefficients A and B for each sector over a period of several years, showed an overall accuracy of about 15%. A more detailed description has been given in [12] and [13].

Now that the simulation of the significant wave height reaching the barrier site appeared satisfactory, it was expected that, with the introduction of a proper spectral shape, a reliable prediction of the spectral energy density at the barrier site could be obtained.

For that purpose, a relationship between the peak frequency f_p, $H_{z,1/3}$, the waterdepth h and the tidal current V_T was assumed:

$$f_p = f(H_{z,1/3}, h, V_T) \qquad 34$$

and established by the analysis of about 800 spectra.

The chosen spectral shape was:

$$S(f) = \alpha f_p^{\beta-\gamma} f^{\gamma} \qquad f \leq f_p$$

$$S(f) = \alpha f^{\beta} \qquad f > f_p \qquad 35$$

From the same analysis, it was also found that the powers β and γ could be predicted by relations similar to those for f_p:

$$\beta = f(H_{z,1/3}, h, V_T) \qquad 36$$

$$\gamma = f(H_{z,1/3}, h, V_T) \qquad 37$$

It was then possible to simulate, reasonably accurately, the spectral energy density by means of formula 35 (figure 2.2.2.15.)
In some cases (mostly under extreme conditions), the propagation of the wave energy from the North Sea and that originating from local windfields resulted in double peaked spectra at the barrier site.
For windspeeds over approximately 15 m/s, the model provides for separate swell propagation

and generation of sea by the local windfield. By means of the spectral growth formalism of Hasselmann [7], the local sea and the sea coming from the outer region are combined.

Probabilistic Aplications

Loads on structures, due to the attack of sea waves, consist of a hydrostatic component caused by the still water level and dynamic wave forces. During storms, many different combinations of the stochastic variables, water level and significant wave height, occur which result in different combinations of static and dynamic load conditions.

Nowadays, design calculations often have a probabilistic nature,which require the joint probability density of water level and wave height. It is seldom possible to obtain these density functions solely from field measurements, due to the rare occurence of extreme storm conditions. Therefore, some extrapolation techniques are required.

The wave models, described in the last paragraph, offer the possibility to simulate wave heights under simulated meteorological conditions. Here, a simple method will be described for the simulation of the joint probability density function of the high water level h_w and significant wave height $H_{z,1/3}$ under storm conditions,

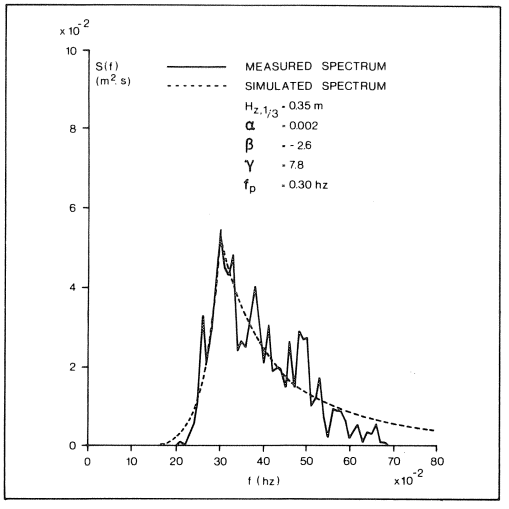

resulting in the joint probability of exceedance of specific values of $H_{z,1/3}$ and h_w

$$P(\underline{H}_{z,1/3} > H_{z,1/3} \text{ and } \underline{h}_w > h_w)$$

As previously mentioned, both wave height and wind setup are caused by windfields over the North Sea. In this concept, water level variations, caused by astronomical tides (a), are coupled to wind setup giving so called high water levels h_W (Figure 2.2.2.16.)

$$h_w = s + a$$

The relation between significant wave height and windfield is, in this case, given by the previously mentioned Bretschneider formula. From these relations, probability density functions can be constructed for both $H_{z,1/3}$ and h_w. The deduction of these relations goes beyond the scope of this article. (See [11]).

Finally, the joint probability density function of

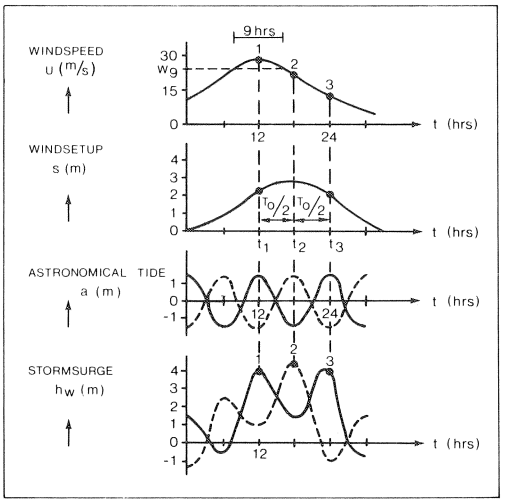

Figure 2.2.2.16. Determination of high water level.

Figure 2.2.2.15 Simulated spectral density

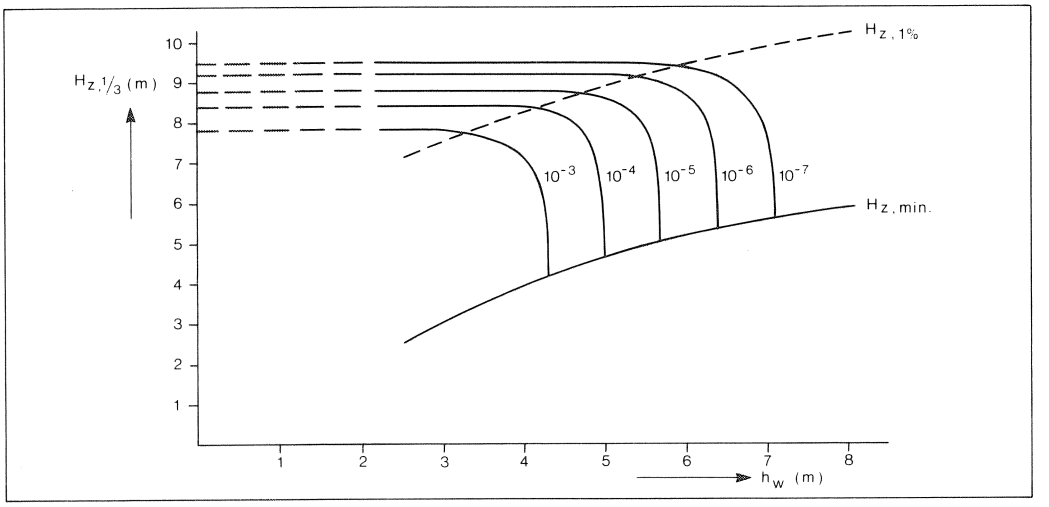

Figure 2.2.2.17. Lines of equal joint probability of exceedance $H_{z,1/3}$ and h_w.

high water level h_w and significant wave height $H_{z,1/3}$ is obtained by multiplication of the high water probability density function and the conditional probability density function of $H_{z,1/3}$ (Figure 2.2.2.17.).

Wave Pattern

The wave height distribution, in a harbour or sheltered bay or in the vicinity of other man-made structures, is often determined by the diffraction and reflection characteristics of the structural components meant for protection from incident waves.

As already mentioned, diffraction of water waves is a phenomenon whereby energy is transferred laterally along a wave crest after a wave train is interrupted by a barrier.

The wave pattern, in the vicinity of a barrier in the path of long crested waves, would show three regions: a region in the lee of the barrier showing diffracted wave energy; a region in front of the barrier showing short crested waves due to the interaction of incident and reflected waves (in the case of waves approaching perpendicular standing waves will occur) and a region of undisturbed waves (Figure 2.2.2.7.).

A quantitative knowledge of the diffraction effect is essential for the design of harbours. A proper location of harbour entrances can greatly reduce the silting problem and harbour resonance.

Reflection of waves is the reflection of wave energy as opposed to energy dissipation. For instance, multiple reflections in a harbour complex may result in a build up of energy appearing as agitation and surging. It is therefore necessary to have protective structures which dissipate rather than reflect energy.

Literature

1. **Shore Protection Manual,** U.S. Army coastal engineering research center, U.S. Government Printing Office, Washington D.C., 1975.
2. **Handbook on Wave Analysis and Forecasting,** World Meteorological Organization, WMO - no. 446 Geneva, Switzerland, 1976.

3. Philips, O.M., **The Dynamics of the Upper Ocean,** Cambridge University Press, second edition, Cambridge, U.K. 1977.

4. Kinsman, B., **Wind Waves, their Generation and Propagation on the Ocean Surface,** Prentice Hall Inc., Englewood Cliffs, New Jersey, 1965.

5. Bretschneider, C.L., Generation of Wind Waves over a Shallow Bottom, **Technical Memorandum nr. 51,** Beach Erosion Board Office of the Chief of Engineers, 1954.

6. Hasselmann, K., Barnett, T.P., Bouws, E., Carlson, H., Cartwright, D.E., Enke, K., Ewing, J.A., Gienapp, H., Hasselmann, D.E., Krusemann, P., Meerburg, A., Müller, P., Olbers, D.J., Richter, K., Sell W. and Waldes H. Measurements of Wind-Wave Growth and Swell Decay during the Joint North Sea Wave Project (JONSWAP) **Deut. Hydr. Z.,** Reihe A(8°), no. 12, 1973.

7. SWAMP Group (Hasselman et al.)
An Intercomparison Study of Wind Wave Prediction Models, Sea Wave Modelling Project (SWAMP), **Proc. Symp. Wave Dyn. and Radio Probing of the Ocean Surface,** Miami, May 1981.

8. Sanders, J.W., Bruinsma, J., Modelling Wind Driven Sea in Shallow Water, **Proc. Symp. Wave Dyn. and Radio Probing of the Ocean Surface,** Miami, May 1981.

9. Weenink, M.P.H., A Theory and Method of Calculation of Wind Effects on Sea Levels in a Partly Enclosed Sea with Special Applications to the Southern Coast of the North Sea, **KNMI, Med. en Verh.,** no. 73, 1958.

10. Battjes, J.A., A Case Study of Wave Height Variations due to Currents in a Tidal Entrance. **Coastal Engineering,** 6 (1982) 47-57.

11. Vrijling, J.K., Bruinsma, J., Hydraulic Boundary Conditions, **Hydraulic Aspects of Coastal Structures,** Delft University Press, Delft, 1980, pp 109-132.

12. Vrijling, J.K., Janssen, J.P.F.M., Bruinsma, J., A practical Method to obtain Wave and Storm Surge Conditions for Predictions and Probabilistic Calculations **North Sea Dynamics, eds. Sündermann/Lenz, Springer-Verlag,** Berlin Heidelberg 1983, pp. 233-247.

13. Janssen, J.P.F.M., Bruinsma, J., van Aalst, W., A Parametric Model for Wave Propagation and wave Growth in very Shallow Waters with Probabilistic Applications. **First International Conference on Meteorology and Air Sea Interaction of the Coastal Zone,** The Hague, (1982) pp 129-131.

14. Vincent, C.L., Shallow-Water Wave Modelling. **First International Conference on Meteorology and Air Sea Interaction of the Coastal Zone,** The Hague, (1982). pp. 87-95

List of symbols

α, β, γ	=	spectral parameters
υ, σ	=	JONSWAP spectral parameters
γ	=	height depth ratio of breaking wave
θ	=	wind direction and direction of wave propagation
ϱ	=	mass density of water
ϕ	=	phase angle
ω	=	radial frequency
a	=	astronomical tide

Waves

a_n = wave amplitude
A, B = empirical refraction coefficients
C = phase velocity
C_g = group velocity
E = wave energy
F = fetch
$F(f, \theta; x, t)$ = energy spectrum with respect to propagation direction θ and frequency f
$\tilde{F}$ = nondimensional fetch
f = frequency
g = gravitational acceleration
h = water depth
h_w = high water level
H = wave height
H_d = design wave height
$H_{z,1/3}$ = significant wave height
$\tilde{H}$ = nondimensional wave height
$\vec{k}$ = wave vector
k = wave number
L = wave length
n = C_g/C
p = pressure
S = wave steepness
s = wind setup
S_{nl}, S_{diss}, S_{atm} = source terms
S(f) = wave energy density function
t = time
$\tilde{t}$ = nondimensional time
T = wave period
$\tilde{T}$ = nondimensional wave period
u, v = coordinates
U = wind speed
V_T = tidal current
$\vec{x}$ = coordinate vector
z = vertical coordinate

Environmental Conditions

K.W. Pilarczyk

2.2.3 Ice (Formation and types of ice)

General

In order to solve the various problems of interaction of ice with engineering structures, it is necessary to have some basic knowledge of the formation and types of ice. This contribution on ice formation will be restricted to the basic information necessary to understand the problem. Ice is, of course, formed when water is cooled to freezing point. There is however a distinct difference in ice formation, growth and melt between freshwater ice and sea ice. The difference lies not only in different freezing points but, more importantly, in variations in the density of fresh and seawater with temperature, and the salt content. In general seawater needs more cooling to form ice than freshwater.

In analysing ice behaviour three distinct periods may be distinguished: (a) the freeze-up period, (b) the ice-growth period, and (c) the ice-melting or break-up period [9] [20]. During the first period the main problem is the estimation of freeze-up dates. During the second period, the main problem consists of estimating the physical characteristics of ice covers, such as ice thickness and structure, which are needed in order to determine ice pressure and bearing strength and to solve water supply problems. During the melting period the main problem is the estimation of the rate of ice break-up and break-up dates. Finally, as ice covers are a product of the weather, all these problems require an understanding of the effect of weather on ice-cover formation, growth and melt.

Figure 2.2.3.1. outlines the general sequence of events during winter and spring break-up periods, ending with the complete disappearance of the ice [21].

Static freshwater ice formation

The cooling of a freshwater reservoir can be divided into two stages:gradual cooling until all the water is at a temperature of about 4°C (the stage of maximum density) and cooling of the surface water from the time the water is isothermal at 4°C until sheet ice forms (below 4°C the density of water decreases with temperature). In rivers, where the current induces a turbulent mass and heat exchange, the formation of ice covers can take place through two different processes. The first might be called the frazil ice evolution process, which starts with the supercooling of water and the production of frazil crystals, the latter gradually developing into ice disks that agglomerate to form porous flocks and floes, finally forming a continuous ice cover. Since water molecules intermix in turbulent flow, the crystallization process, which varies directly with water temperature, takes place at depths over the whole cross-section of the flow. Frazil ice is thus the term used for small disks of ice generally 1-4 mm in diameter and 1-100 μm in thickness that form in turbulent, slightly supercooled water.

The second formation process of river ice might be called the border ice growth process. This may be further subdivided into border ice growth by thermal exchanges alone and border ice extension by frazil flocks. Border ice growth starts in areas of laminar flow along the banks. In rivers and along the seashore ice grows not only from the shore but also around protruding boulders and other obstacles or from anchor ice emerging from the bottom. Fig.2.2.3.2 shows various types of ice covers in rivers according to [10].

Sea ice

The presence of salts in seawater depresses the freezing point, i.e. for a salinity S = 35 $^{o}/_{oo}$ the freezing point is equal to about - 1.9°C. The temperature of maximum density, or inversion temperature, of a saline solution is lower than that of pure water. For normal seawater, the inversion temperature decreases linearly with salinity, and the freezing point and inversion temperature are both equal to -1.3°C for salinity = 24.7$^{o}/_{oo}$ (Fig.2.2.3.6.c). For seawater with a salinity greater than this critical value, the density increases steadily with decreasing temperature, until freezing point is reached. Since there is no inversion temperature to limit convective circulation, a still body of seawater would cool uniformly and no ice could form until the water right at the bottom was at freezing point. It is for this reason that sea-ice forms only in high latitudes and after prolonged periods of cooling.

The mechanism of sea-ice formation is complex.

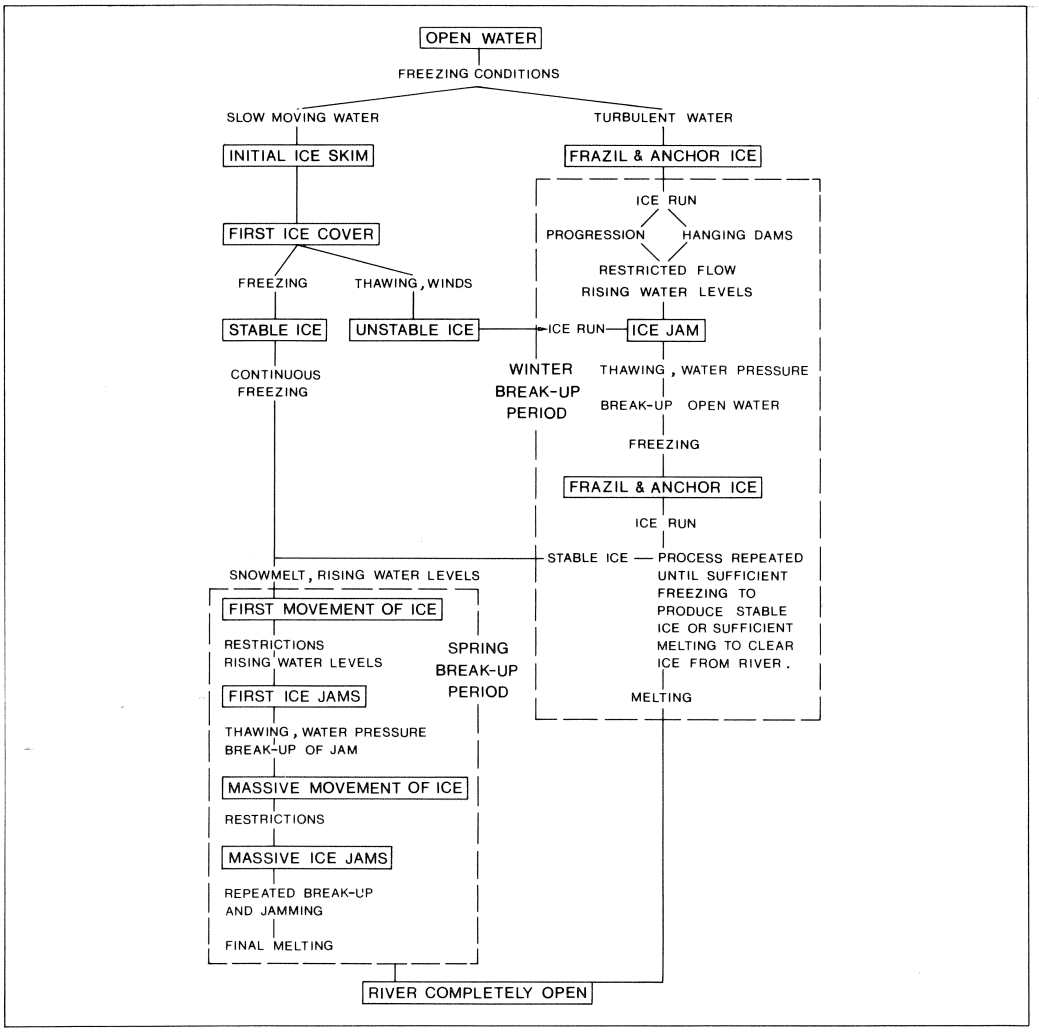

Figure 2.2.3.1 General sequence of events during winter [21].

When the surface layer of seawater is at freezing point, further cooling results in the formation of small discoids of pure ice on the surface. Wind and wave action will compact them, forcing some towards a vertical position, when the ice sheet starts to form. As the seawater freezes, pure ice crystals are formed because foreign atoms or ions cannot apparently fit into the solid H_20 lattice.

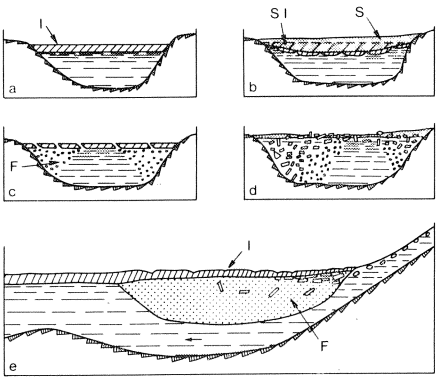

Figure 2.2.3.2(a) Various types of ice covers in a river: a) pure ice cover, b) with snow partly flooded on top, c) with frazil accumulation underneath, d) hummocked ice cover with floes, snow and frazil, e) underhanging dam with frazil, slush and floes [10].

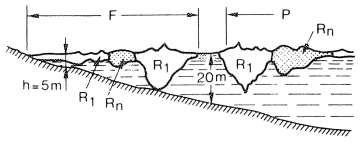

Figure 2.2.3.2(b) Sketch and sea ice in the arctic: P is the Polar Pack ice, F is the fast ice, R_1 are first year partly consolidated pressure ridges and R_n are multi-year consolidated ridges. There is an open lead between the pack and the fast ice [10].

Consequently, if seawater were frozen infinitely slowly, a cover of pure ice would form, with total rejection of the salts into the underlying melt.

The presence of salts in sea-ice thus results from mechanical trapping by the growth of pure crystals, and the amount of salt trapped will depend largely on the freezing rate. The brine in sea-ice is trapped in cells enclosed by pure ice-crystals. The brine cells are usually vertical cylinders.

In any ice sheet with a temperature gradient the brine cells are never in equilibrium. On a cold day, water will freeze out of the brine; on a warm day, the brine will dissolve ice. The net effect is a migration of the cell along the temperature gradient in the direction of higher temperatures. Brine migration considerably reduces the salinity of the upper layers of sea-ice, migration being aided by drainage under gravity in the spring season as rising temperatures cause the brine pockets to enlarge and become interconnected. Most sea-ice is thus honeycombed with a network of large numbers of brine cells and air pockets. The salinity of new sea-ice, very rapidly frozen, may be as high as 20 ‰ but most annual sea-ice has a salinity ranging from 10 ‰ to about 2 ‰. The bulk of sea-ice has a salinity

of around 4°/oo. In general, it can be said that all of the physical and mechanical properties of sea-ice are largely controlled by the brine content and the distribution of the brine cells.

A number of books and general reports have appeared on sea-ice, several of which are listed among the references [1, 2, 3, 6, 10, 12, 14 ,15 ,17 ,18].

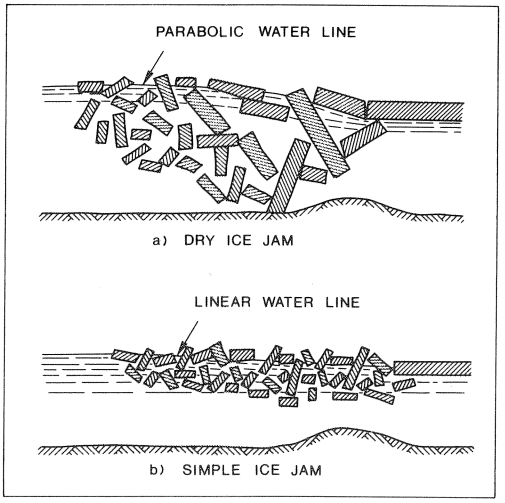

Figure 2.2.3.3 Types of ice jams [9].

Growth of ice

The growth of solid continuous ice in a river, lake or sea from heat exchange with the atmosphere is not always the simple process that it appears at first sight (see Figure 2.2.3.4.). Generalizations about the occurrence and growth of ice throughout the world are of limited value because of variations in climate between maritime and continental regions and from continent to continent. Even local climatic and hydrological differences in the same region can lead to serious differences in local ice occurrence (i.e. rivers with and without heat-exchange with seawater)[2,3,8,9,16,17,19]. Where the network of ground stations reporting ice thickness is sufficient to permit preparation of isoline maps of maximum ice thickness, this method of obtaining ice volumes is recommended.
If the data on representative ice thickness used in the method recommended above are not available, a less accurate estimate can be obtained from climatological data, which are usually accessible. This method, recommended in the 'Guide to world inventory of sea, lake and river-ice'(Unesco/IAHS Paris 1972), is ultimately based on the original theoretical calculation of Stefan (see e.g. Pounder [12]). His equation is that

$$h = \left[\frac{2K}{L\rho_i} \int_{t_0}^{t} \theta dt \right]^{\frac{1}{2}} = \left[\frac{2K}{L\rho_i} S_g \right]^{\frac{1}{2}}$$

Where h is the ice thickness at time t, ϑ is the temperature difference between the surface of the ice (usually, air temperature must be used) and the freezing point of the water (fresh or salt), t_1 is the time of first freeze-up, and K, L, Q_i are the thermal conductivity, latent heat and density of ice respectively. The quantity S_g, called the freezing exposure, is usually measured in degree days. The basic Stefan equation does not apply when there are changes in the heat content of the ice either by absorbed radiation, advection of heat by water currents or other effects. Nevertheless, this equation has been used with considerable success in the modified form

$$h = \alpha S_g^{\beta}$$

Where α is an empirical coefficient dependent on the area in question and the amount of snow cover, and β is another empirical coefficient $\approx$ 0.5.
It is recommended that $\alpha = 2.7$ be used for fresh-lake ice and $\alpha = 2 \div 2.4$ for sea-ice.
If S_g is the freezing exposure in degree-days (Celsius scale) and these values of α, β are used, h will be in cm.

Photo KLM AEROCARTO

Figure 2.2.3.4 Eastern Scheldt. Different stages of ice formation, (1 february 1954), [11].

To apply this method, the area of the country should be divided into regions with a more or less constant winter regime. For each such region, the maximum value of S_g should be calculated (from the data of freeze-up to the date at which the mean temperature rises above freezing) and then the value of h_{max}. An illustration of this method is given in Fig.2.2.3.5 where some literature data are also presented as a function $h = f(S_g)$,[11].

Because of heat generated by hydraulic drag, river ice in an area is usually less thick than lake ice. It is recommended that the volume of river ice in each region be calculated by taking the maximum thickness of river ice to be 15 to 20 percent less than the comparable figure for lake ice in that region. In all cases, the presence of snow on the ice-sheet reduces the speed of ice-growth. For a more rigorous solution of the pro-

Figure 2.2.3.5 Growth of ice, $h = f(S_g)$, [11].

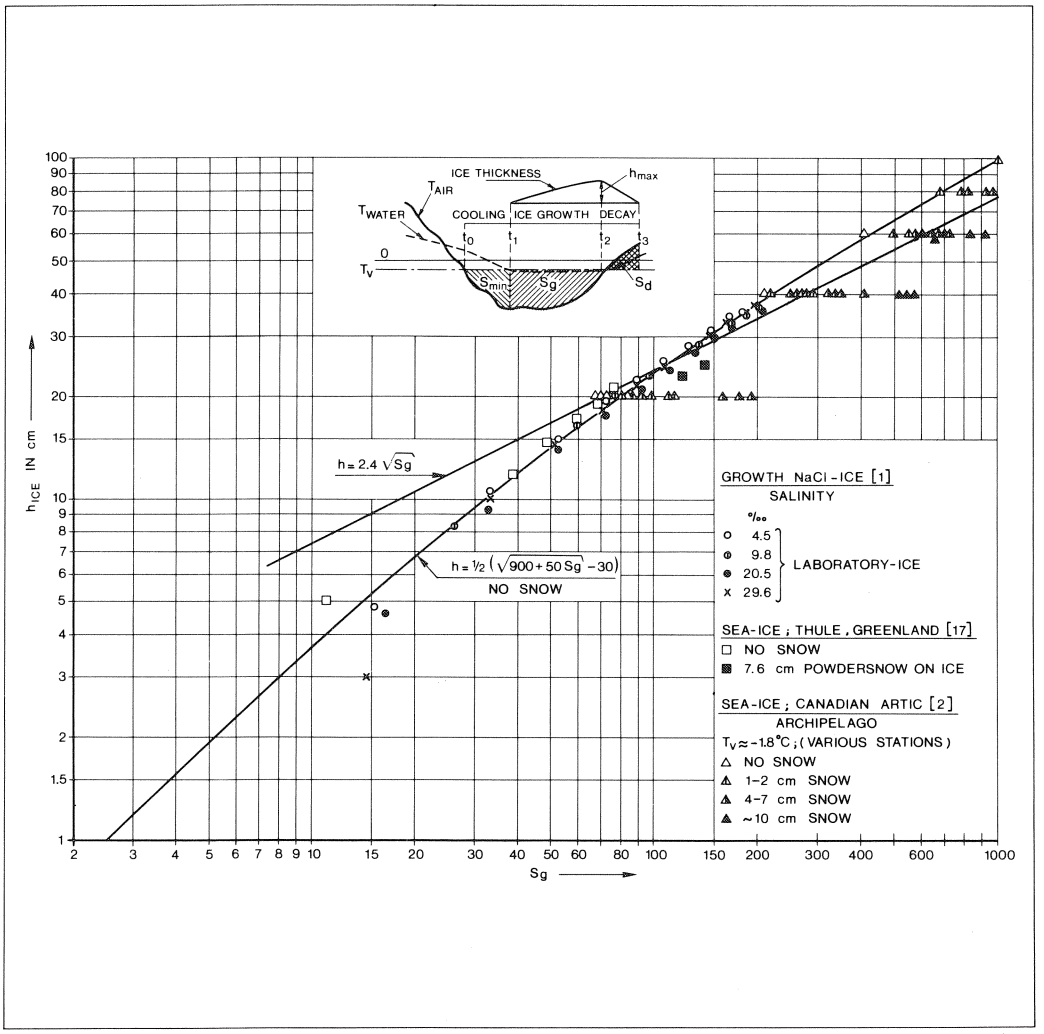

blems of ice growth, the methods suggested by Schwerdtgeger [14,15] or Michel [10] should be applied.These papers clearly show how the thermal properties of sea ice vary with density, salinity and temperature and differ from those of freshwater ice.

Break-up period

The melting and break-up of lake and river ice has been well studied in the past, among others by Williams [20,21] and Michel [9] . The ice first starts to melt on the shore because it is thinner there and because more heat comes from the adjoining ground surface. A free water surface appears along the shoreline leaving the main body of ice floating free. At that time, the ice cover still has considerable strength. Williams describes the further melting as follows:
During the second stage of melting there is melt of the snow and of the snow ice on the floating ice. The melt water flows along drainage patterns on the surface and it drains into the open water at the shore line or into holes that appear to develop preferentially along old thermal cracks.
When the ice cover reaches the advanced stage of melt, where it shows large patches of darkened ice, and so most of the incoming solar radiation is absorbed, it is ripe for breaking by wind and currents and is unsafe for over-ice transportation. The currents created by strong winds will break-up the ice cover and induce circulation that brings the warmer subsurface water to the ice. Some statistical and analytical methods for predicting break-up dates can be found in the Williams papers [19,20].(For sea ice, see[2]).

Although the processes of break-up have been qualitatively well described (see[4] ,[20]), it is difficult to provide any general rules on prediction methods, the main reason being that the break-up of a river is controlled by various meteorological, geographical and geomorphological factors governed by the laws and principles of physics (calorimetry, hydraulics, mechanics, etc.). Moreover, the processes and mechanisms involved are difficult to observe and to predict because of time and space variation.

We quote here the description of break-up periods as given by Michel in [9]. In general the break-up of a river can be divided into three phases, although one or two of them may not fully occur in particular cases. These phases are the pre-break-up period (preliminary destruction) by solar radiation, the drive or break-up which is the generalized hydraulic destruction and transportation of the cover, and the wash or cleaning of residues left by the drive and its ice-jams on banks and bordering lowlands. (see Michel [9]).

Ice jams (see Figure 2.2.3.3.) may form at various sites along the river with increasing discharge, each jam being stopped by a more resistant jam priming site in a lower reach. With the ever-increasing discharge due to snow and ice melt upstream and the ice cover weakening from thermal effects, one of the bigger jams gives way and its impact carries the others along its course, freeing the river of ice in a matter of hours.

The main factors affecting the formation of ice jams are the previous winter conditions, the water discharge at break-up, and the relative position of rapids, fluvial transitions or other hydraulic features. In fact, there is little data at all on ice-jam characteristics in rivers, which are difficult to measure because of the instability of ice cover at that time.

Physical and mechanical properties of ice

This paragraph lists only some of the basic values of the physical and mechanical properties of water and ice. More detailed information may be found in [6], [10] and [12].

Physical properties (Fig.2.2.3.6)

Freezing point or the temperature at which ice starts to form depends on the salinity of the water. Salinity (S) is defined as the ratio of total solids to a total sample of seawater and is expressed in parts per thousands or per mille, denoted by ‰. A salinity of 34.5 ‰ is a reasonably good average for sea-water and is often taken as a standard figure. Freezing point in °C of water is approximately equal to - 0.053 x salinity in ‰ (fig.2.2.3.6.c). Some numerical values are presented as follows:

Salinity,

S °/oo	0	10	20	30	35
Freezing point, T_v °C	0	−0.53	−1.08	−1.63	−1.91

The specific density of pure ice is a function of temperature and pressure. At atmospheric pressure, the specific density ϱ_i can be calculated from the equation

$$\rho_i = 0.9168(1-1.53 \times 10^{-4} T_i) \text{ in kg/m}^3$$

Figure 2.2.3.6 The physical properties of water and ice.

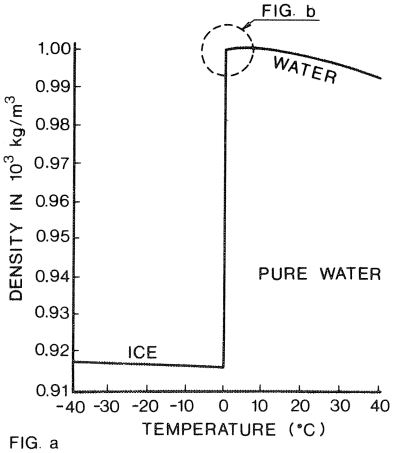

FIG. a
THE DENSITIES OF ICE AND AIR-SATURATED WATER AT ATMOSPHERIC PRESSURE.

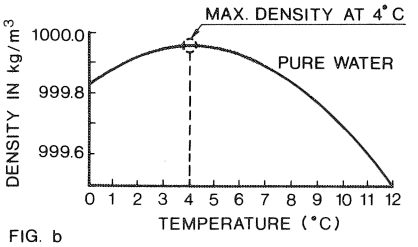

FIG. b
THE DENSITY OF AIR-SATURATED WATER NEAR THE INVERSION TEMPERATURE.

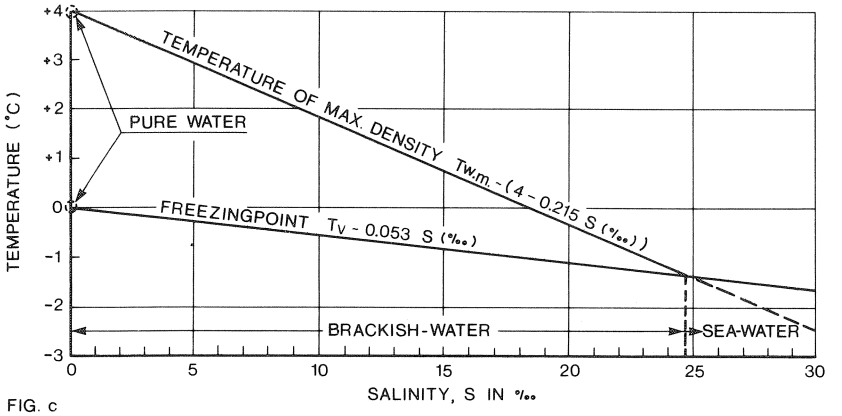

FIG. c
THE VARIATION OF FREEZING POINT AND INVERSION TEMPERATURE WITH SALINITY.

where T_i is the temperature of the ice in °C.
The density of sea ice is more variable than that of fresh-water ice. Reported values range from about 0.85 to 0.94, the lowest figures referring to old surface ice in which considerable brine drainage has occurred and the highest ones to very cold (rapidly formed) winter ice. A typical figure may be taken as 0.91 for winter ice at -15°C.
The typical thermal properties of pure ice and sea ice are listed below. The properties of the sea ice are strongly dependent on the ice temperature, salinity and ice-porosity [14]. The values presented below have to be treated as indicative ones for sea ice with ice salinity of about 4 °/oo (a typical average figure for a cover of annual ice).

Thermal properties	Pure ice	Sea ice(S = 4°/oo
specific heat(water)	C_w = 4.187kJ/kg(1Kcal/kg)	4.187 kJ/kg
specific heat (ice)	C_i = 2.093kJ/kg(0.5Kcal/kg)	variable
Latent heat of fusion	L = 334kJ/kg(79.7Kcal/kg)	297kJ/kg(71Kcal/kg)
Latent heat of melting	L = 334kJ/kg(79.7Kcal/kg)	variable,60-80Kcal/kg as average over ice-growth period
Conductivity(variable)	K = 2.1-2.2 W/m/°C 1.8-1.9 Kcal/m/hr°C at 0°C	2.0 W/m/°C (1.7 Kcal/m/hr.°C)

Mechanical properties of ice
The properties of ultimate strengths, elastic properties and plasticity may be considered to be dependent on the temperature of the ice, its salinity (or brine content), and its crystal structure. These three variables are not, of course, truly independent of each other, the last two being dependent on the freezing rate. In addition to the independent variables listed above, ice is so anisotropic that the direction of stress application is very important. In addition, the rate of stress application (rapid or slow loading) has some influence on the ultimate strength of ice.
An ice cover is an integrated record of the meteorological and oceanographic history of, at least, the preceding part of the winter and the current characteristics of the winter. Any impurities (air bubbles, dirt, organic matter, etc.), the rate of freezing, periodical melting, freezing of snow etc. therefore have a clear influence on the mechanical properties of ice. Because of all of these factors, the mechanical properties of ice, particularly sea ice, show a large scatter in observed values. Experimental inaccuracies (or different methods employed) also contribute to the observed spread of the values.
Because of their practical importance, the ultimate strengths of pure and sea ice in tension, compression and shear have been measured by many observers under a variety of conditions (in the laboratory and in situ) [1,5,13,18].
The ultimate strength of pure ice is generally higher than that of sea ice. The strength of sea-ice increases, however, at lower ice temperatures. The variations in strength with temperature are striking and far from linear.
Slight and abrupt increases in strength have been observed at temperatures of about -8°C and -23°C respectively. These are respectively the temperatures at which $Na_2SO_4 . 10H_2O$ and $NaCl.2H_2O$ start to precipitate from brine. On the other hand, the strength of the sea ice decreases with increasing salinity, air content and impurity levels. Because of the vertical drainage due to the brine, the compression strength of ice in the vertical direction can be up to 3 times as high as in the horizontal direction.
As an illustration of the strength of ice of different origins, some results of Schwarz's investigation [13] on the compression strength of ice are presented below.
Cubical samples of ice (10x10x10cm) were tested. It has to be noted that these results should not be regarded as representative of

those for natural conditions because the loading rate can be very different.
The more or less representative mechanical properties of fresh water ice and some indicative values for the sea-ice with salinity of about 5‰ are listed below. They may be considered to apply to ice samples with a minimum thickness of 5 cm at a temperature of -5°C.

It must be emphasized that any measurement of an individual ice sample may easily be larger or smaller than the tabulated figure by a factor of two or three. The values given are not even theoretically consistent.
Unfortunately, it is still not possible to provide a consistent picture of the physical and mechanical properties of ice, particularly of sea ice. As regards the serious design problems in relation to ice load, especially in northern waters, it is therefore advisable to go into the problem more deeply. In this respect Michel's „Ice Mechanics" [10] is a valuable guide.

Schwarz's data:

Origin of ice	O°C	-10°C	-20°C(ice temp.)
Alster-ice(fresh-water ice)	55 kgf/cm2	103 kgf/cm2	133 kgf/cm2
Baltic sea-ice	21 "	60 "	91 „
Brackish water	14 "	37 "	44 „

Mechanical properties:

Parameter	fresh water ice		sea ice	
	kgf/cm²	kN/m²	kgf/cm²	kN/m²
Tension	15	1500	10	1000
Compression(unconfined)	35	3500	20	2000
Shear	7 700		700	7
Flexure(bending)	17	1700	5	500
Modulusof elasticity(E)	$9x10^4$	$900x10^4$	$(6-8)x10^4$	$(6-8)x10^6$
Poisson's number	0.33	-	0.295	–

References

1. **Assur,A. and W.F.Weeks,** Growth, Structure and Strength of Sea Ice, **U.S.Army Cold Regions Research**, Research Report 135, 1964.

2. Bilello,M.A., Formation, Growth and Decay of Sea Ice in the Canadian Arctic Archipelago, **U.S.Army Snow, Ice and Permafrost Research Establishment**, Research Report 65, 1960 (also Arctic 14 (1), 1961).

3. Bilello, M.A., Method for Predicting River and Lake Ice Formation. **Journal of Applied Meteorology**, Vol.3, no.1,1964.

4. Deslauriers, C.E., Ice Break-up in Rivers, **Proc.Pressures Against Structures**, Quebec, Nov.1966, Canada.

5. Gold, L.W, Elastic and Strength Properties of Fresh Water Ice, **Proc. of Conf. on Ice Pressures Against Structures**, Quebec, Nov. 1966, Canada.

6. Hobbs,P.V., **Ice Physics,** Oxford Univ.Press, Londen, 1974.

7. Martin,S., Frazil Ice in Rivers and Oceans(a review), **Ann.Rev.Fluid Mech.**,13,1981.

8. Michel,B., Ice Covers in Rivers, **Proc.Ice Pressures Against Structures**, Quebec, Nov.1966.

9. Michel,B., Properties and Processes of River and Lake Ice, 'The Role of snow and Ice in Hydrology', **Proceedings of the Banff Symposia**, Unesco-WMO-IAHS,september 1972.

10. Michel,B., **Ice Mechanics**, Quebec, 1978.

11. Pilarczyk, K., Formation and Movement of Ice in the Eastern Scheldt(in Dutch), **Delta Project**, Report W-76.033,1977.

12. Pounder,E.R., **Physics of Ice**, Pergamon Press,1965.

13. Schwarz, J., Uber die physikalischen Vorgänge beim Eisdruck, **Mitteilungen des Franziusinstituts**, Hannover, 1968.

14. Schwerdtfeger, P., The Thermal Properties of Sea Ice, **Journal of Glaciology**, Vol.4, no.36, 1963.

15. Schwerdtfeger, P., The Effect of Finite Heat Content and Thermal Diffusion on the Growth of a Sea Ice Cover, **Journal of Claciology**,Vol. 5, no. 39, 1964.

16. Schulyakovsky, L.G., **Manual of Forecasting Ice-Formation for Rivers and Inland Lakes** (transl.from Russian), Jerusalem, 1966.

17. Weeks, W.F. and O.S.Lee, The Salinity Distribution in Young Sea Ice, **U.S. Army Cold Regions Research Report** 98, 1962.

18. Weeks, W.F. and Assur, A., The Mechanical Properties of Sea Ice, **Proc.of Conf. Ice Pressures Against Structures**, Quebec, 1966.

19. Williams, G.P., Correlating Freeze-Up and Break-Up with Weather Conditions, **Canadian Geotechnical Journal**, Vol.II, no.4, 1965.

20. Williams, G.P., Freeze-Up and Break-Up of Fresh-Water Lakes, **Proc.of Conf. Ice Pressures Against Structures**, Quebec 1966.

21. Williams, G.P.,Break-Up and Control of River Ice, **I.A.H.R. Symposium on Ice and Its Action on Hydraulic Structures**, Reykjavik, 1970.

22. Guide to World Inventory of Sea, Lake and River Ice, Unesco-IAHS, A Contribution to the International Hydrological Decade, **Technical Papers in Hydrology**, no. 9, Paris, 1972.

23. River-Ice Problems, A state-of-the Art Survey and Assessment of Research Needs, Report of the Task Committee on Hydromechanics of Ice, **Journal of the Hydraulics Div.ASCE**, HY1, january 1974.

D. Smith

2.2.4. The Hydrology and Geomorphology of Tidal basins

2.2.4.1. Introduction

The term tidal basin is used in this chapter as an all inclusive term to describe not only the semi-enclosed body of coastal water with its free connection to the open sea and which is subject to tidal exchanges but also the area immediately seaward and adjacent to the inlet entrance.
Geomorphologically the term includes inlets created by eustatic, tectonic, fluvial, glacial and-coastal deposition processes while hydrologically it incorporates both estuaries and lagoons.
The fact that tidal basins are subject to fluctuating tides, river discharges, winds and incoming wave energy means that they are highly dynamic systems which may never reach a state of equilibrium. For engineering projects, such as the development of a harbour or the partial or complete closure of tidal basins, detailed knowledge of currents, circulation, sediment transport and morphological changes is fundamental for assessing the feasibility, the site and choosing a functional design. In most cases the construction of any structure in a tidal basin will introduce immediate and possibly major changes to the hydraulic conditions. These effects need to be investigated so that prognoses of current variations scour or sedimentation rated likely to affect construction, or successive construction phases can be made.

Similarly, these investigations should also be extended for predicting changes likely to take place in the tidal basin, seaward of the closed extrance and along the adjoining coastline once closure has been achieved.
In the following sections of this chapter some simplified concepts and characteristics of circulation, mixing sediment transport and the morphology in tidal basins are presented.
Additional information on the hydrological, morphological and sedimentological dynamics of individual tidal basins can be found in many articles published in the research literature.
Several useful texts that deal with the relevant principles, together with case studies, are also available. These include: Brunn [1], Dyer [2], Fischer et al [3], Officer [4] and Cronin [5].

2.2.4.2. Origin of tidal basins

From a geological point of view most tidal basins are recent features that have developed as a result of changes in sea level.
During the latest Pleistocene Ice Age, about 15,000 years ago, much of the present day ocean water was locked up in continental ice sheets.
At this time world sea levels stood at approximately 100 metres below their present level. This change caused many rivers to incise their valleys. During the Flandrian transgression, when the ice in the continental ice sheets melted and sea level rose by about one metre per century, the incised valleys were flooded. The Flandrian transgression ended about 5,000 years ago although minor fluctuations in sea level have occurred since then.

On submerged and indented coastlines drowned river valleys have lost extensive catchments areas to supply eroded sediment so that many have undergone minor infilling. In plan view these tidal basins have essentially retained the branching and often meandering shape of their original valleys and their entrances are usually controlled within headlands that were formerly valley side ridges. Where infilling has occurred it is usually greatest at the heads of individual arms of the basin, where river deltas form, or near the entrance where sediments transported along the coast have been deposited.

In many cases the entrances to submerged valleys and embayments on deeply indented coasts have been semi-enclosed by spits or tombolos formed from one or both sides of the inlet. Generally these are built up from sand or gravel although in rarer cases they can be formed from boulders. The alignment of the enclosing spit or spits and the position of the tidal basin entrance are generally controlled by the dominant approach direction of waves refracted around headlines, reefs and offshore islands.
Many of the river valleys inundated during the Flandrian transgression and coastal basins

formed by regional tectonic warping or faulting have acted as sediment traps. These have been infilled by both marine and fluvial sediments and in some cases had their entrances closed off by sand spits.
In some cases, such as along embayed coastlines, sediment transported to the coast is reworked by waves and deposited offshore and along the adjacent coastline.

Continued supply of sediment and its subsequent accumulation along the nearby coastline causes the shoreline to prograde seawards. Morphologically this progradation often manifests itself as a series of parrellel dune ridges. In situations where wave energy and tidal currents are low sediments transported through an infilled basin are deposited as a seaward prograding river delta complex.
Coastal regions that have low gradient offshore slopes and a constant supply of sand from longshore drift are often characterised by headland spits and/or barrier islands. Coastal barriers generally form as long sandy islands that are often built up with dunes and dune ridges. These can occur individually or as a string of elongate islands that form a semi continuous coastal barrage. Behind the barrier islands and sand spits separate or interconnected tidal lagoons or estuaries have been impounded. Many of these are connected to the open sea by narrow tidal inlets.
Examination of many coastlines around the world shows that, given a continuous supply of sand and a gentle offshore gradient, sandspit and barrier islands coastlines can form along static, emergent and submergent coasts.

2.2.4.3. Mixing and Circulation in Tidal Basins

Water masses in tidal basins can be broadly divided into two catagories based upon the influence fresh water has on circulation and mixing processes. These are estuaries and lagoons. In this context lagoons have so little or no freshwater discharged into them so that the water mass in the tidal basin esentially maintains the same salinity and density as the water

Figure 2.2.4.1 Schematic illustration of the longitudinal salinity structure and vertical salinity, velocity and net discharge profiles in a well mixed estuary.

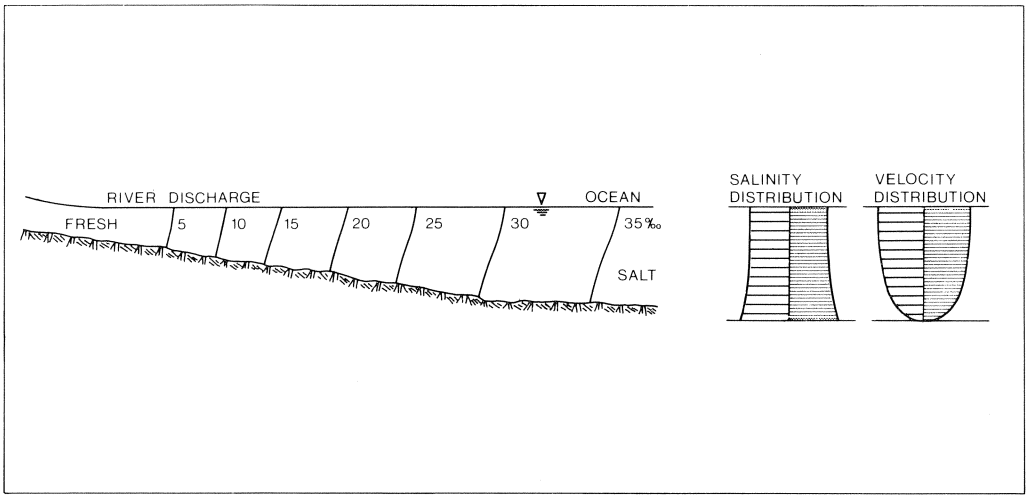

seaward of the basin entrance. In estuaries however saltwater is to various degrees diluted by freswater derived from land drainage.
In concept, the longitudinal profile of the water mass in an estuary can be envisaged as progressing from fresh water riverine conditions at the head, through brackish estuaries conditions along most of the basin, to almost completely marine conditions near the ocean entrance. Density differences between the salt and fresh water masses give rise to a continuum of salinity structures that have a significant influence on both mixing and sediment transport processes. In lagoons however, density differences of this type simply do not occur. They are therefore very much simpler hydrodynamic systems in which tidal exchanges augmented by wind and wave driven currents control circulation.
For classification purposes the continuum of salinity structures found in estuaries has been divided into four distinguishable states: well mixed, partially mixed, highly stratified or salt wedge estuaries and fjords. The characteristic features of these, together with those of lagoons, are outlined in the following sections.

Well Mixed Estuaries
In well mixed estuaries the tidal exchange is very much greater that the river discharge. Turbulance generated by the tidal currents is sufficiently strong to prevent or completely break down any salinity stratification between salt and fresh water so that the water mass within the tidal basin becomes essentially vertically homogeneous. In longitudinal profile salinities steadily increase from the head of the estuary to the ocean entrance while throughout these estuaries salinity depth profiles are very nearly vertical with slighty increased salinities near the bottom.

In the longitudinal direction both weak and strong gradients can develop in well mixed estuaries. The former results from strong large scale horizontal circulation. This is induced by wind, bottom topography, trapping on and between banks and in side channels and tidal phase differences between major channels.

Figure 2.2.4.2 Schematic illustration of the longitudinal salinity structure and vertical salinity, velocity and net discharge profiles in a partially mixed estuary.

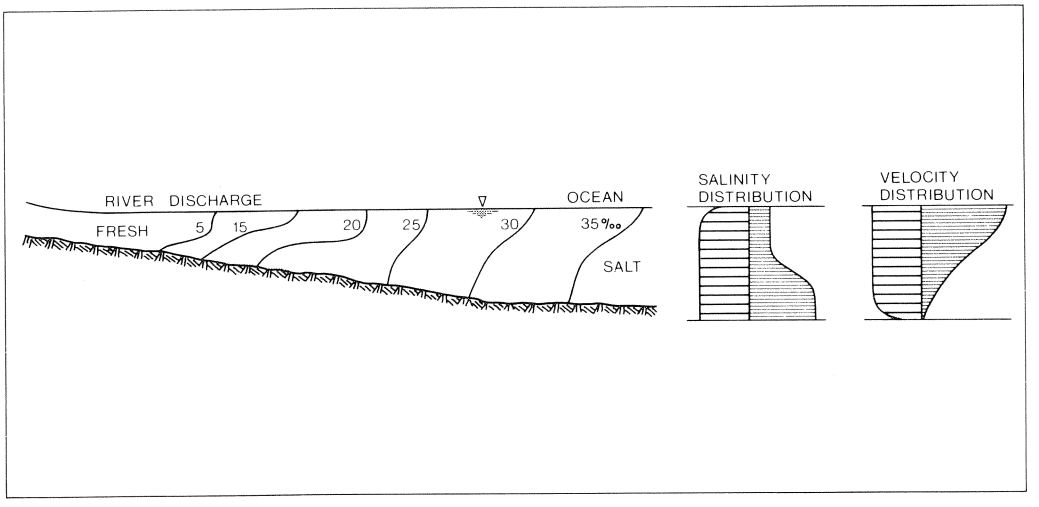

As a result the salinity difference at the mouth of the estuary and at the head is very small. In the case of the latter, where large scale horizontal circulation is less active large differences in salinity can develop between the head and entrance of the estuary (figure 2.2.4.1.). Examples of large well mixed estuaries are: the Eastern Scheldt, the seawards section of the Thames and Chesapeake Bay.

Partially Mixed Estuaries

Water masses in partially mixed estuaries characteristically have, in their upper reaches, an almost homogeneous surface layer of low

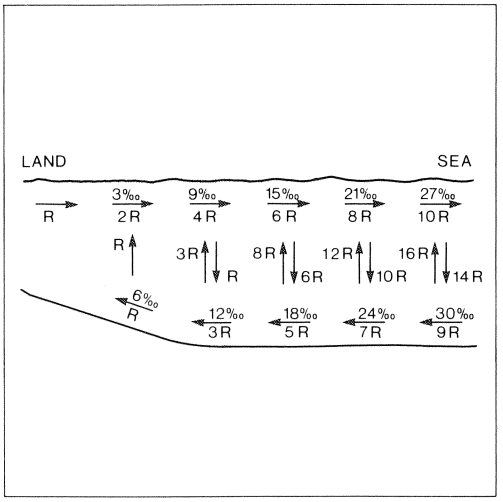

Figure 2.2.4.3 Diagrammatic representation of mixing in a partially mixed estuary. Volume exchange is given in units of river discharge R. (after Dyer [2]).

Figure 2.2.4.4 Schematic illustration of the longitudinal salinity structure and vertical salinity, velocity and net discharge profiles in a salt wedge estuary.

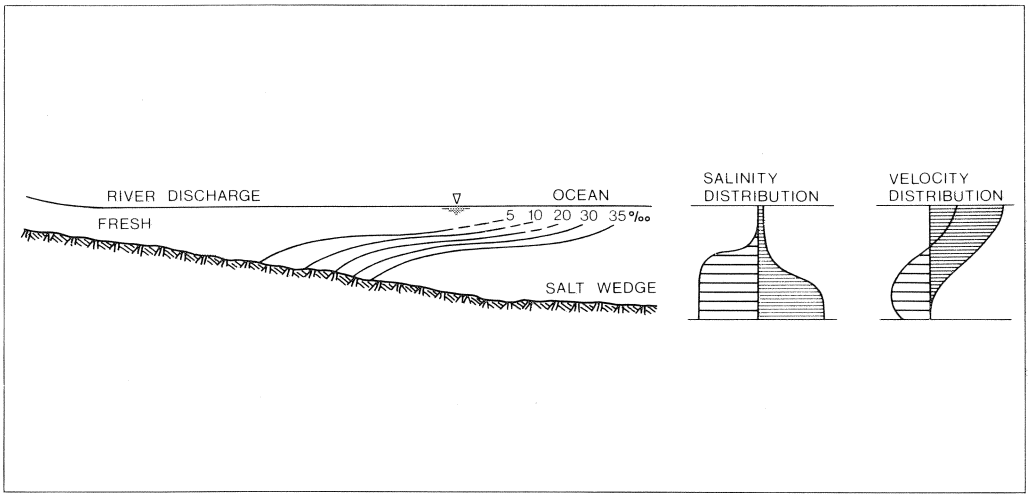

salinity water that is separated from an underlying high salinity layer by a mid depth salinity gradient (figure 2.2.4.2.). In the lower reaches this gradient is weaker and in some cases well mixed conditions can develop.
During the flood tide advection together with turbulence generated by bottom friction cause salt water to be mixed upwards into the overlying and seaward moving freswater layer.
This process tends to create an almost homogeneous water column. The degree to which this is reached varies throughout the estuary. During the ebb bed shear stresses and turbulence decrease. As a result stratification is enhanced. Under these conditions seawater mixed from the underlying layer into the upper seaward moving freshwater layer may in part be compensated for by a weak landward flow of seawater. At the same time the halocline becomes more diffuse and forms at a greater depth. The two layer circulation system, induced by net surface outflow and regulated by fluctuations in river discharge, effectively maintains the nearly horizontal salinity gradient along partially mixed estuaries. Examples of partially mixed estuaries are: the Mersey, Elb, Delaware and the Gironde.

Highly stratified or salt wedge estuaries
Highly stratified estuaries are characterised by a strongly developed sloping halocline that separates a salt wedge of higher density seawater penetrating into the tidal basin from a seaward moving surface layer of freshwater. Vertical salinity profiles usually show that the water masses above and below the halocline are essentially homogeneous while across the halocline itself salinity differences of 20 to 30 o/oo can be confined to vertical distances of less that two metres (figure 2.2.4.4.).

In highly stratified estuaries, the circulation pattern is almost completely controlled by the river discharge. They are best developed in long narrow estuaries with deep channels or where tidal ranges are small. They are therefore a characteristic feature of the lower reaches and delta channels of many rivers.

The salt wedge halocline has an important effect on both internal circulation and mixing processes. During periods when freshwater discharge is low the salinity gradient becomes strongly developed so that mixing of the two water masses results mainly from diffusion and advection processes. With high freshwater discharge inputs, shear stresses developed between the two water masses can cause the halocline surface to become unstable and develop internal waves.
Should these shear stresses become sufficiently great the internal waves break causing saltwater to be injected and subsequently mixed into the overlying seaward flowing freshwater. Saltwater lost from the salt wedge in this way is compensated for by an additional inflow of saltwater.
The position of arrest and length of a salt wedge is primarily controlled by freshwater discharge inputs. It is therefore a dynamic feature that changes its slope and position, migrating backwards and forwards along the estuary, in response to storm and seasonal variations in river discharge. In extreme events, such as floods, the salt wedge can in fact be pushed out of the estuary.

Examples of salt wedge estuaries are:
the Rhone, the Missisippi and the Vellar.

Fjord entrainment type estuaries
Fjord entrainment estuaries can be considered as special cases of highly stratified estuaries that have very deep basins of almost static or slowly exchanging water with a thin, seaward moving, top layer of freshwater (figure 2.2.4.5).
The narrow entrances of fjords dampen the tidal wave so that within fjord basins tidal currents are generally weak. The main flows usually arise as a result of freshwater moving seaward.
These currents fluctuate with changes in the volume of freshwater discharged into the estuary and can be strongly influenced by winds blowing along the fjord.
Salt and freshwater masses in fjord basins are usually separated by a sharp well developed halocline. This extends most of the way along the tidal basin although near the entrance or over the shallow entrance sill it is broken down by increased tidal currents and wave turbulence. In the summer months the halocline can be

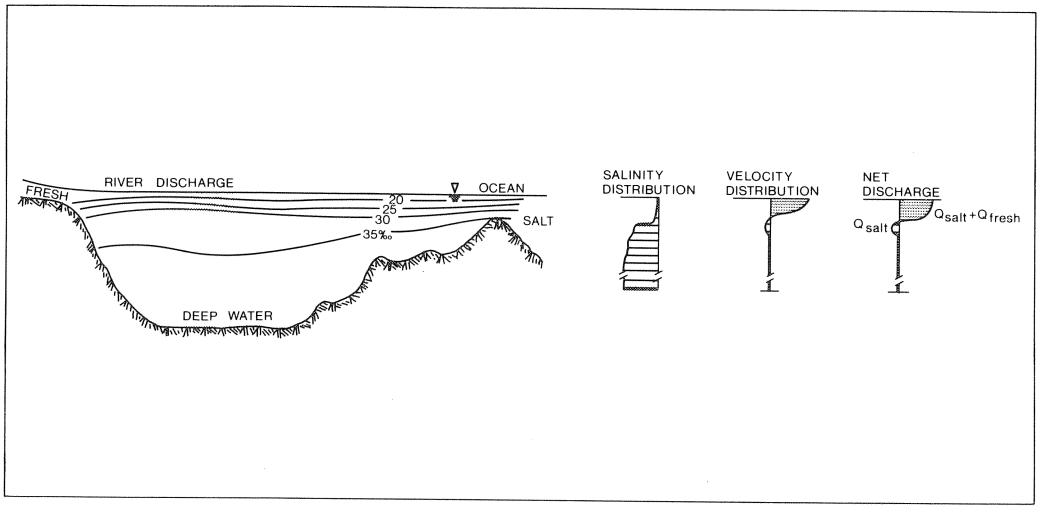

Figure 2.2.4.5 Schematic illustration of the longitudinal salinity structure and vertical salinity, velocity and net discharge profiles in a fjord entrainment type estuary.

strengthened by coinciding with a shallow thermocline while during periods of low freshwater discharge it becomes more diffuse.
Saltwater mixed into the upper freshwater layer is replenished by weak landward flow beneath the halocline. This return flow is strongest nearest the entrance but steadily weakens along the fjord. During very high freshwater discharges however, the surface freshwater layer increases in thickness and becomes almost homogeneous. In fjords with entrance sills density differences limit the depth of this freshwater layer to about that of the entrance sill itself. Under these circumstances return flow replenishment of saltwater lost from basin is periodic.

Lagoons
Lagoons receive little or no freshwater so that the water mass remains essentially as isosaline and homopynal as the seawater beyond the entrance. The exceptions to this are the shallow coastal lagoons found in very dry climates such as along the coast of Mexico and Australia. In these cases high evaporation losses and low flushing rates cause the lagoon waters to become more saline and warmer than the sea or ocean water.
Lagoons that are subject to strong tidal action behave as well mixed estuaries. Circulation and exchange processes are primarily driven by tidal currents.
In microtidal lagoons wind generated currents are frequently stronger than tidal currents. They are therefore the primary factor contributing to circulation.
In interconnected lagoons, such as those formed behind a barrier island chain, wind driven currents can induce a net through flow of water from one lagoon to the next. In these cases time averaged current velocity measurements made in the entrance channels show a net inflow of water through the „upstream" lagoon entrance and outflow from the „downstream" lagoon.

Qantitative classification of estuaries using stratification and circulation parameters.
The descriptive classification of estuarine circulation outlined above is based upon the

relative intensities of tidal and river flows and the physical effects that these have on tidal basin stratification. A first approximation of the mixing status of an estuary can be obtained from basic tide and freshwater discharge data. The Canter Cremers number or estuary number E can be used:

$$\alpha = \frac{Q_f T}{\Omega} \quad (1)$$

$$E = \frac{\Omega F_0^2}{Q_f T} \quad (2)$$

where

Ω = the tidal prism, the volume of water in the basin between the levels of high and low water;
Q_f = freshwater discharge $m^3.s^{-1}$;
T = tidal cycle in seconds;
F_o = Froude number = $U_o/\sqrt{gd}$, where U_o = the maximum flood tide velocity and d is the mean depth at the estuary entrance.

Another indicator is the internal estuary number:

$$E_i = \frac{\Omega F_i^2}{Q_f T} \quad (3)$$

F_i = internal froude number =

$$\frac{q_f}{\sqrt{\frac{\Delta\rho}{\rho} g h^3}} \quad (4)$$

q_f = specific freshwater discharge
ρ = density of fresh river water
$\Delta\rho$ = density difference between fresh and salt water
h = total water depth.

For stratified flow where the interface between salt and freshwater is quite sharp:

$\alpha > 1.0$
$E < 0.005$
$E_i < 0.25$

For partially mixed flow where the salt- and freshwater interface is not clear cut

$0.1 < \alpha < 1.0$
$0.005 < E < 0.2$
$0.25 < E_i < 10$

For mixed flow where no interface is present:

$\alpha < 0.1$
$E > 0.2$
$E_i > 10$

A quantitative classification system based on dimensionless stratification and circulation parameters has been developed by Hansen and Rattray [7], (figure 2.2.4.6A).

In this classification the estuary cross section is assumed to be rectangular.
In addition salinity variations over the width are not taken into account.
In this diagram lines of constant ν, R_z and F_m have been added (B) (Fischer et al. [3]) where:

- ν is the fraction of landward transport of salinity caused by dispersion mechanisms other than the density driven circulation.
- R is a sort of Richardson number („Estuarine Richardson number"), defined by:

$$R = \frac{\frac{\Delta\rho}{\rho} g Q_f}{W U_t^3} \quad (5)$$

where

$\Delta\rho$ = density difference between fresh and salt water
ρ = density of fresh water
g = acceleration of gravity
Q_f = freshwater discharge
W = width of open channel flow
U_t = r.m.s. of tidal velocity

- F_m is a bulk densimetric Froude number, defined by:

$$F_m = \frac{Q_f}{(A [\frac{\Delta\rho}{\rho} g d]^{\frac{1}{2}}} \quad (6)$$

where

A = cross-sectional area
d = mean depth

The stratification parameter for a given position

in the estuary is the ratio of the averaged tidal salinity difference from the bottom to the surface; $S_b - S_s$, to the tidal depth averaged salinity value S. The circulation parameter is the ratio of the residual velocity at the surface U_s to the cross section averaged net river flow velocity, U_r. This classification describes estuarine salinity structures and circulation as a continuum. It is a logical approach in view of the fact that hydrological conditions within an estuary do vary and salinity structures can temporarily change from one type to another.

Hansen and Rattray visualized the steady flow as illustrated in (figure 2.2.4.7a) and assumed that the only tidal effect was to induce vertical and longitudinal turbulent mixing (two-dimensionality). They used data from six real estuaries to relate the effect of internal mixing to bulk

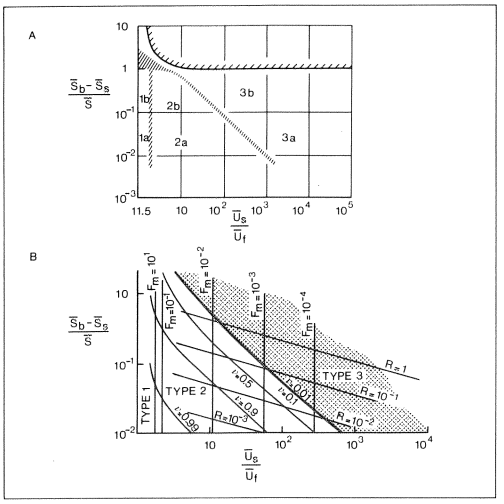

Figure 2.2.6 Estuarine classification diagram from Hansen and Ratray [7], A and Fischer et al [3], B. The regions numbered one to four respectively denote; well mixed, partially mixed, fjords, and salt wedge type estuaries. The subscripts a and b indicate high or low freshwater discharge into the estuary, $S_b - \bar{S}_s$, difference between surface and bottom salinity $\bar{S}$, average salinity in the water column; U_s average surface velocity; U_f, mean flow due to freshwater discharge.

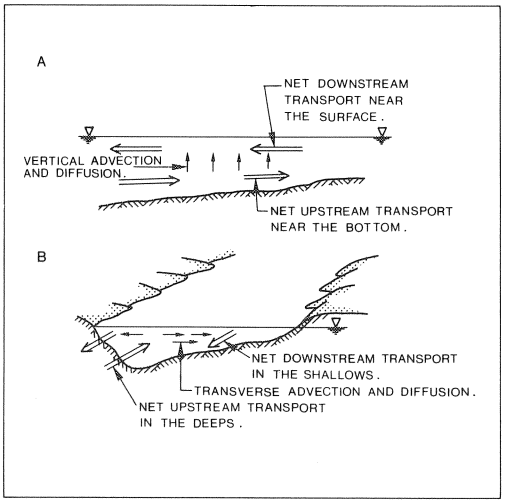

Figure 2.2.4.7 The internal circulation driven by the river discharge in a partially stratified estuary. Currents shown are after averaging over the tidal cycle and are superimposed on the back and forth tidal flow. (A) A vertical section along the deepest part of the channel axis. (B) A transverse section showing the transverse distribution of net currents; (after Fischer et al. [3]).

channel parameters and eliminate the need to specify the mixing coefficients.
The density driven vertical circulation described by Hansen and Rattray does however not account for density induced horizontal circulation. Figure 2.2.4.7.b shows how the upstream flow is expected to be concentrated in the deeper portions of the channel, because the upstream pressure gradient increases linearly with depth below the water surface. The return current is spread over the cross-section and a net transport from the deeper to the shallower section is required to complete the circulation. Thus the channel geometry turns what would otherwise be a vertically two-dimensional circulation cell into a horizontal circulation cell.

Suspended Sediment Transport

The transport and deposition of sediment in tidal basins is intimately associated with internal circulation, current and salinity dynamics. This is especially so in estuaries where river borne suspended sediments, comprised mainly of silts, clays and organic colloidal material, come into contact with brackish water which is instrumental in causing the particles to flocculate into larger aggregates that are more rapidly deposited.
Coarse grained sediment, i.e. terrigenous and carbonate material is mostly transported as bedload along channels and channel margins in the direction of dominant maximum currents.
As already mentioned above fine suspended sediments tend to flocculate when they come into contact with salt water. This process concentrates the suspended material in a turbidity maximum that forms along the middel or upper reaches of the estuary where mixing processes are most active.
Within this zone suspended sediment concentrations are higher than in either the upper reaches or the lower seaward section of the estuary. Turbidity maxima are especially well developed in partially and well mixed estuaries where they are sustained by a semi-enclosed circulation process. Sediment in the upper less dense upper water layer is transported seaward by net downstream flow. During its passage down the estuary some of this material settles into the lower layer of landward residual flow where it is retransported up the estuary. This process has the effect of concentrating and trapping sediment; discharged by rivers, transported in from the sea, or resuspended from within the estuary (figure 2.2.4.8).
Sediment in the turbidity maximum is held in suspension by turbulence but once current velocities decrease at the turn of the tide the suspension settles and slowly consolidates on the bottom. At high water much of this material is deposited on the intertidal flats and bordering saltmarsh or mangrove swamp areas while at low water deposition is restricted to within the tidal channels. When current velocities increase the unconsolidated sediment is resuspended and reworked back into the turbidity maximum. This process results in a constant exchange of sediment in those reaches of the estuary where the turbidity maximum develops. With very high concentrations of flocculated suspended sediment turbulence is reduced and the sediment accumulates along the bottom as a slowly consolidating layer of fluid mud.
This fluid mud layer can be observed on echosounder records and gives a false impression of the true consolidated seabed depth (Kirby and Parker, [11]).
The seaward escape of suspended sediment from estuaries is primarily related to: freshwater discharge, which controls the position of the turbidity maximum in the estuary; the regular tidal exchanges, that pump water out of the estuary during the ebb; and the spring to neap tidal cycle, that continually changes the tidal prism.
Maximum discharge of suspended sediment takes place during flooding when the turbidity maximum is pushed towards the lower reaches of the estuary and stronger buoyant surface flows develop. These are augmented by ebb tidal discharges that pump sediment laden water onto the continental shelf as a semibuoyant turbid plume.

2.2.4.4. Morphology and hydrography of tidal inlets

The morphology of coasts can partly be attributed to the influence the tidal range has on those processes controlling the distribution or accumulation of nearshore sediments.

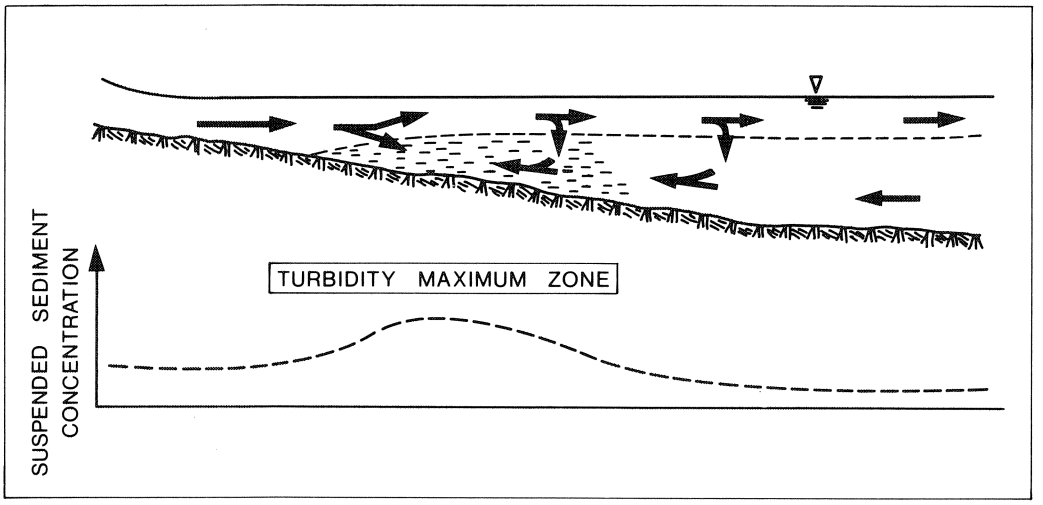

Figure 2.2.4.8 Schematic representation of suspended sediment circulation in an estuary and the resulting turbidity maximum.

This was recognised by Davis, [12], who classified coastlines as:

microtidal, tidal range 0 - 2.0 m (0-6ft),
mesotidal, „ 2 - 4.0 m (6-12ft),
and macrotidal „ > 4.0 m (>12ft).

This classification can generally be applied to tidal basins because their morphologies largely manifest the effects that tidal currents have on circulation and sediment transport. Because of this general relationship between tidal range and morphology, it is possible to describe the morphology and sediment dynamics of tidal basins using a schematic model approach. Models along these lines have been constructed by a number of authors, e.g. Hayes [13, 14] , Wright [15] , Oertel [16] , Allen et al. [17] .
While this is a useful approach, it does suggest that micro, meso and and macrotidal basin morphologies are distinguishable. In reality however, this is not always the case because they often exhibit a number of common morphological features. This is especially so in the case of micro and mesotidal basins. In the following sections the schematic model framework is used to give a broad outline of the morphology, sediment transport and characteristics of tidal flows encountered in micro, meso and macrotidal basins. Before doing this however, it is useful to describe some of the typical morphological features that develop in and near the entrance to a tidal basin. This area, the so called „tidal inlet", is hydrologically and sedimentologically the most dynamic region of a tidal basin and is of course the site where stabilising or closing structures are usually placed.

Tidal inlet morphology
The term „tidal inlet" is generally used to describe the narrow waterway that connects a tidal basin with the ocean and through which reversing tidal flows are concentrated. Morphologically a tidal inlet includes not only the narrow entrance channel but also the intertidal or submarine deltas that can form at one or both ends of the entrance channel. In this sense, a

tidal inlet can consist of three major morphological units: the ebb tidal delta, a lobate sandbody formed seaward of the entrance channel; the tidal gorge, the narrow deep channel at the inlet entrance; and, the flood tidal delta, a shield of sand which develops in the tidal basin, landward of the tidal gorge (figure 2.2.4.9A).

The main morphological features of an ebb tidal delta are: the main ebb channel, channel margin levees, swash platforms with swash bars, marginal shoals, marginal flood channels and the delta terminal lobe.
The main ebb channel, a principal feature of an ebb delta, is formed and maintained by ebb flows that issue from the narrow tidal gorge as a fully turbulent diverging jet over the falling tide. This flow scours the channel and transports sediment seawards onto the ebb delta. Along the sides of the main ebb channel, channel margin levees can develop. These are essentially low relief linear submarine bars that form where the sediment transporting capacity of ebb currents suddenly decreases along the edge of the laterally expanding ebb tidal jet.
Swash platforms are broad low relief sand shoals that can be attached to the headland, spit or barrier beaches on either side of the inlet entrance or, as is sometimes the case, separated from these by shallow channels. They are formed mainly by nearshore wave action and often have migrating swash bars developed on them.
The outer edge of most ebb tidal deltas is often ringed by a complex system of marginal shoals. These form the shallow seaward rim of the ebb tidal delta terminal lobe and are continuously being built up, flattened and reformed by both waves and tidal currents. On coasts with a pronounced longshore drift the „upstream" marginal shoals can develop as one or more long shallow submarine or intertidal transverse bars. In these situations the ebb delta is often aligned in the downdrift direction.
In most cases ebb delta marginal shoals are separated by shallow channels. Along the outer reaches it is not uncommon for a few larger ebb dominated channels to be present, while along the sides and nearer the shore the channels are predominantly flood dominated. The latter, known as „marginal flood channels", carry flood currents towards the inlet during the initial stages of the flooding tide.
In longitudinal profile, the main axis of the ebb channel forms a slightly shallowing ramp towards the outer margin shoals.
Beyond these, the seafloor topography steepens across the terminal lobe of the delta until it joins the more gently sloping continental shelf (figure 2.2.4.9B)
The tidal gorge is the most narrow and generally deepest section of a tidal inlet complex. Both ebb and flood currents are concentrated in the gorge and issue from either side as fully turbulent decelerating jets. The actual geometry of the channel is controlled by a number of factors. These include: the geological origin of the inlet, the supply of sand from longshore drift, the geological substrate through which it passes, and the tidal prism; the volume of water passing through the channel over the flood or ebb tide.

The flood tidal delta, formed on the landward side of the tidal gorge, is built up mainly from sediment transported into the inlet by flood currents. It is usually bordered by ebb dominated channels. The main features of a flood tidal delta are the flood ramp and flood channels, the ebb shield, ebb spits and spillover lobes.
A flood ramp is the steadily shallowing section of the flood delta that begins near the tidal gorge, and, over the shallower sections of the delta, typically divides into a number of shallow diverging channels. Currents passing across these sections of the delta are nearly always strongly flood dominated.
The broad shallow rim to the flood delta, which frequently dries at low water, forms the „ebb shield". Its landward side typically has a steep slope that forms the side of an ebb dominated channel. Over the ebb tide the ebb shield shoal carries most of the water flowing out of the tidal basin around the flood delta. Occasionally the ebb shield is breached by small shallow channels. Sediments carried through these channels during late stages of the flood or early stages of the ebb, accumulate as spillover lobes on the margins of the flood ramp or across the ebb shield.

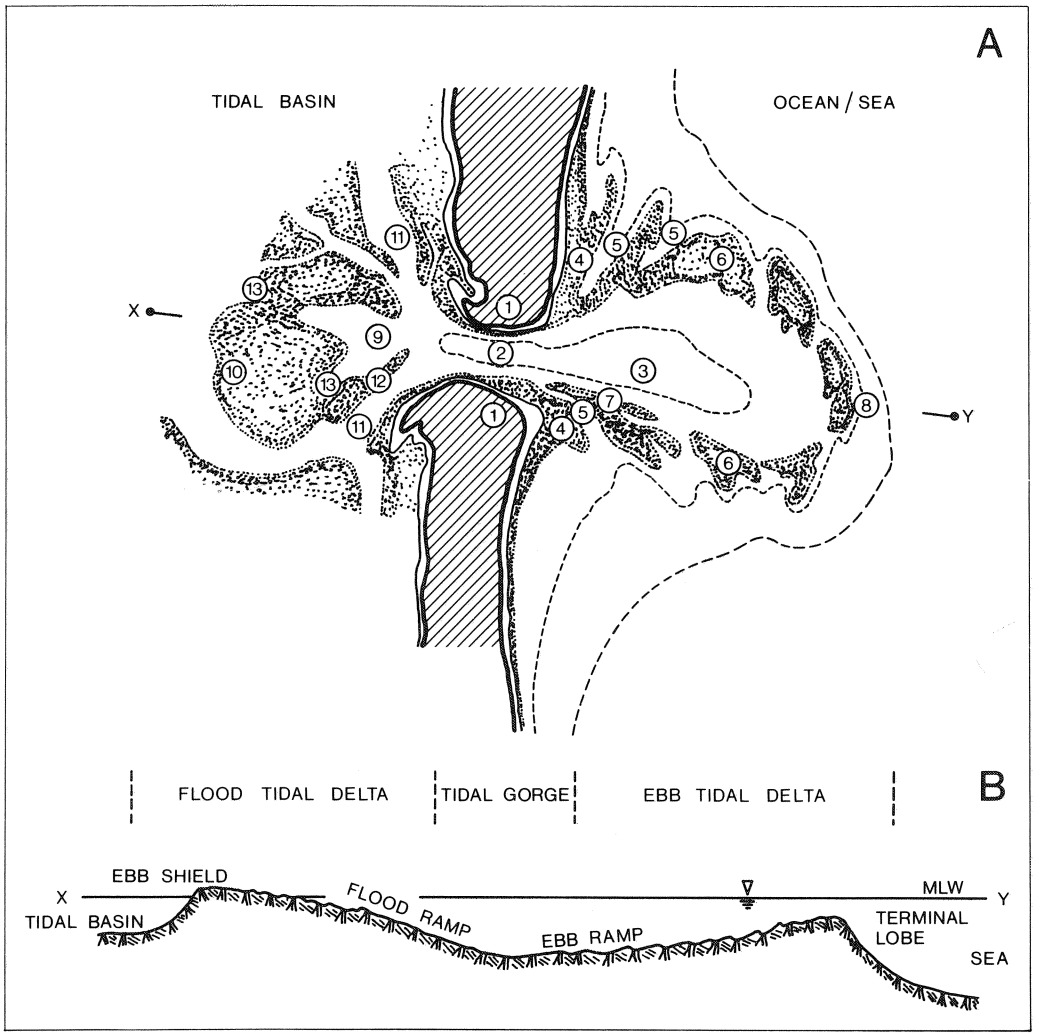

Figure 2.2.4.9 A, schematic diagram illustrating the principal morphological features of a tidal inlet on a sandy coast.
1) coastal barrier or spit headland;
2) the tidal gorge;
3) the main ebb channel and ebb ramp;
4) swash platforms;
5) marginal flood channels;
6) marginal shoals;
7) ebb tidal levee;
8) ebb delta terminal lobe;
9) the flood ramp;
10) the ebb shield;
11) main ebb dominated inner channels;
12) ebb spit;
13) spill over channels.
B, cross section profile from x to y through the tidal gorge and over both flood and ebb tidal deltas.

Ebb spits are elongated accumulations of sediment that become especially well developed on the margins of the flood delta where they effectively separate the flood delta ramp from the ebb flow dominated channels.

Inlet alignment and offset

An examination of aerial photographs of coasts and charts shows that the alignment of spit or headland beaches on either side of tidal inlets can be straight, or offset in updrift or downdrift directions (figure 2.2.4.10). Where beaches are offset, inlet ebb tidal deltas are frequently asymmetrically oriented in the direction of regional longshore drift and dominant incoming waves.

Clearly, the shape and position of individual inlet systems results from those processes moving sediment around them. In general straight inlets can be envisaged as developing from two separate processes, or a combination of both. Firstly, sediment transported by longshore drift is either completely by-passed, or secondly, as sediment accumulates on the updrift side, the total inlet maintains its equilibrium by eroding the downdrift side so that the inlet migrates slowly down the coast.

Offset in the alignment of an inlet entrance may result from geological control where one side of the inlet becomes established against a headland or rock outcrop. On sandy coasts however, inlet offset often results from the complex and dynamic interaction of longshore currents with the ebb tidal jet and waves refracting around the ebb tidal delta (Hayes etal [18], Lynch Blosse and Komar [19]). In the case of downdrift offset, it appears that ebb currents issuing from the tidal basin interrupt the local or regional littoral drift. As a result sand moving in the littoral drift system is mostly deflected out onto the ebb delta marginal shoals although some is transported into the tidal basin. The complex combination of wave and current processes operating over the ebb delta shoals by-pass sand across the ebb delta. Most of this sand is eventually returned to the littoral drift system a short distance „downstream" of the inlet. At the same time waves refracting over the ebb tidal delta interact with ebbing currents. This causes a localised reversal of the littoral drift along the

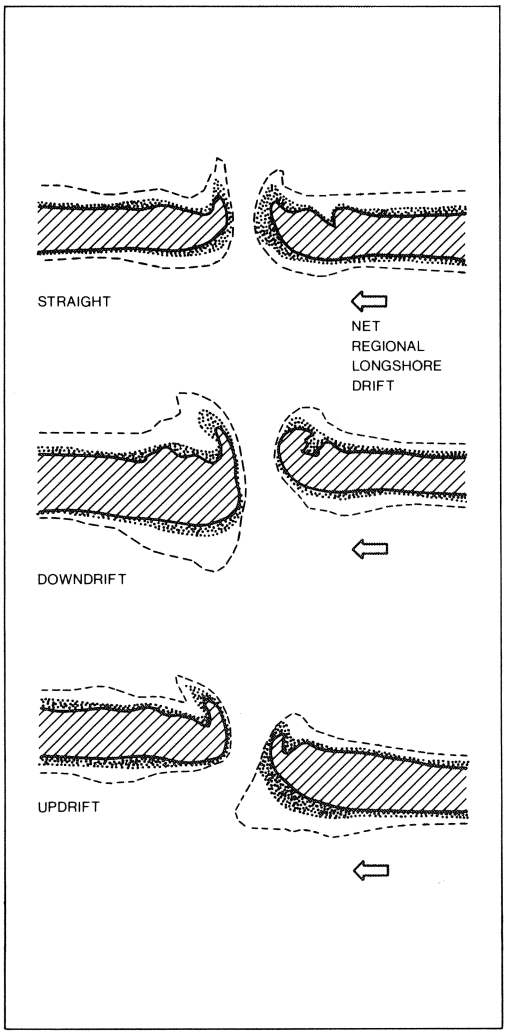

Figure 2.2.4.10 Diagrammatic representation of three types of headland alignment commonly found at the entrances to inlets on sandy coasts.

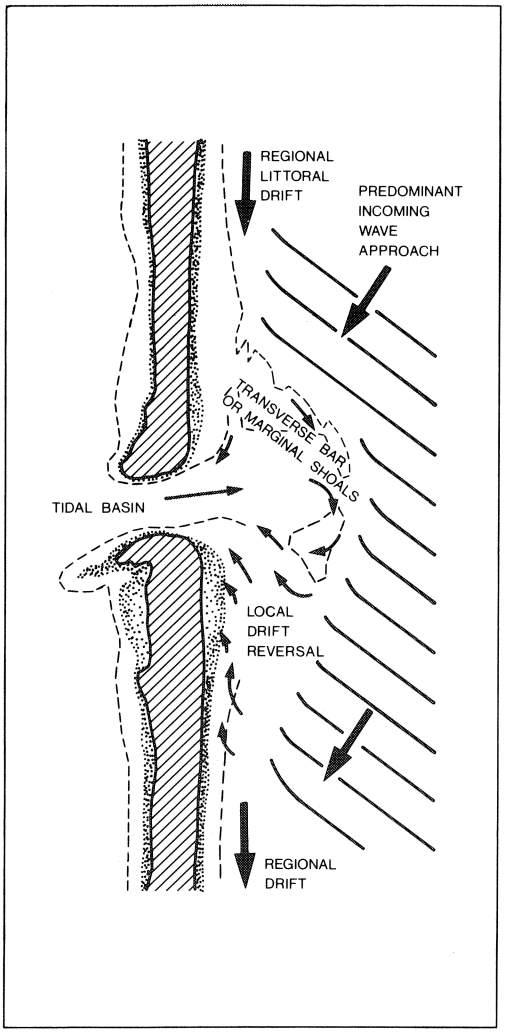

Figure 2.2.4.11 Diagrammatic representation of the local drift reversal typically found on the downdrift side of tidal inlets.

shore immediately below the inlet (figure 2.2.11).
This localised reversal causes some of the sand being by-passed along the outer shoals to accumulate on the swash platforms and as swash bars below the inlet entrance.
These migrate shorewards and, eventually, weld onto the beach below the inlet. Although some of this sand is transported back into the inlet along marginal flood channels, continued accretion along the downdrift shore eventually results in a downdrift offset.

Updrift offsets can develop despite a continuous supply of sand to the downdrift side of inlets. Usually however, other factors such as: the presence of a handland on the updrift side, low incoming wave energy, distribution of the main inner channels, a small tidal prism, migration of the inlet along the coast and net trends in coastal accretion or retreat, play an important role in maintaining updrift offset.
The way in which some of these factors contribute to maintain the updrift offset of a North American tidal inlet has been illustrated by Hine [20]. In this case updrift offset resulted from a slow migration of the updrift barrier along the coast, landward movement of the downdrift barrier, and sand being transported from the downdrift side of the ebb delta into the inlet along a well developed marginal flood channel that ran alongside the downdrift barrier.

Current and sand transport patterns
Segregation of tidal flows over the flood and ebb tidal deltas plays a dominant role in circulation and sediment transport around a tidal inlet complex.
As the water level drops during the ebbing tide, ebb currents are deflected around the flood tidal delta by the shallow banks on the ebb shield. Ebb currents, especially maximum flows which develop near low water, are predominantly carried in the main channels bordering the delta. As a result much of the flood delta remains unaffected by ebbing currents.
This clearly identifiable separation of flood and ebb flows is reflected in the typical dune bedforms that develop in the channels and over the delta. In the bordering channels these are main-

ly ebb oriented although they are often modified during the flood. Over the flood ramp these bedforms nearly always remain asymmetrically oriented in the flood direction. In wide shallow tidal inlets however, the directional alignment of these bedforms can be modified by waves passing into the inlet.
Over the ebb delta evasion of flood and ebb flows also takes place. Here, longshore drift and wave generated currents can both augment or counteract tidal flows.
While the tide is ebbing water is discharged along the main ebb channel of the delta as a laterally expanding and decelerating jet.

The effluent behaviour of this jet and consequent deposition of entrained sediment depends largely on its outflow inertia and buoyancy. These are controlled by both the tidal range and freshwater mixing within the tidal basin.
Because ebb flows are most strongly developed near low water, the outflow of water maintains some inertia over the initial stage of the flood tide. During this period water cannot enter the inlet along the main ebb channel. Initially therefore, flood flows move through the marginal flood channels and enter the inlet peripherally. Later on, at maximum flood, water enters the inlet in an unconfined manner across the whole ebb tidal delta (figure 2.2.4.12).
Sand transport pathways reflect this process. Dune bedforms have mainly flood direction asymmetries in the marginal flood channels and ebb asymmetries along the main ebb channel. Sand transported along the coast by longshore drift is carried along the updrift transverse bars or onto the delta marginal shoals and through the marginal flood channels. Sand moved into the main inlet channel is either transported into the tidal basin and deposited on the flood delta or carried seawards onto the outer shoals of the ebb delta.

2.2.4.5. Micro and Mesotidal Basins

The morphology of micro and meso tidal basins on sandy coasts is strongly influenced by three main factors; incoming wave energy, tide generated currents and sediment supplied by longshore drift. The relative balance between these factors is reflected in the development and distribution of sand bodies around the tidal inlets and within the tidal basins themselves. As a result both micro and meso tidal basins can develop a range of common characteristics. Their geomorphology can therefore be seen as a continuum, ranging from tide dominated to wave dominated with a diversity of forms in between.
Micro tidal basins are generally developed as lagoons or estuaries impounded behind coastal barriers or spits on littoral drift shorelines. They are usually shallow basins that can be separate, such as a drowned river valley, or linked in a series of interconnected basins behind a coastal barrier chain. Often the impounded lagoons or estuaries are partially or almost completely infilled with sediment. In these cases much of the basin area is taken up by saltmarshes or mangroves and extensive areas of intertidal mudflats drained by numerous anastomising and interconnecting channels.
Currents in these basins are mainly tidal and in estuaries these are augmented by freshwater river discharges. Wind driven flows are mainly restricted to the lower more open reaches of the basins although their development is limited to the short period over high water when intertidal areas are inundated. Wind generated waves are also effected by the numerous intertidal shoals. These reduce the available fetch and cause the waves to break and expend much of their energy on the intertidal areas.
In open tidal basins, such as those often formed behind barriers, wind driven circulation and waves can have a significant effect on net circulation. Wind generated surface flows can be greater and move in the opposite direction to tidal currents. In interconnected basins prevailing coastal winds can result in interexchange or a net throughflow of water from one basin to the next.
Wind waves generated in these basins modify the shoreline. Beaches become aligned to the predominant incoming waves while narrow spits and banks develop behind islands and headlands or on the intertidal shoals.

The most changeable area of any micro or meso tidal basin is the tidal inlet and its associated ebb and or flood deltas that constantly shoal,

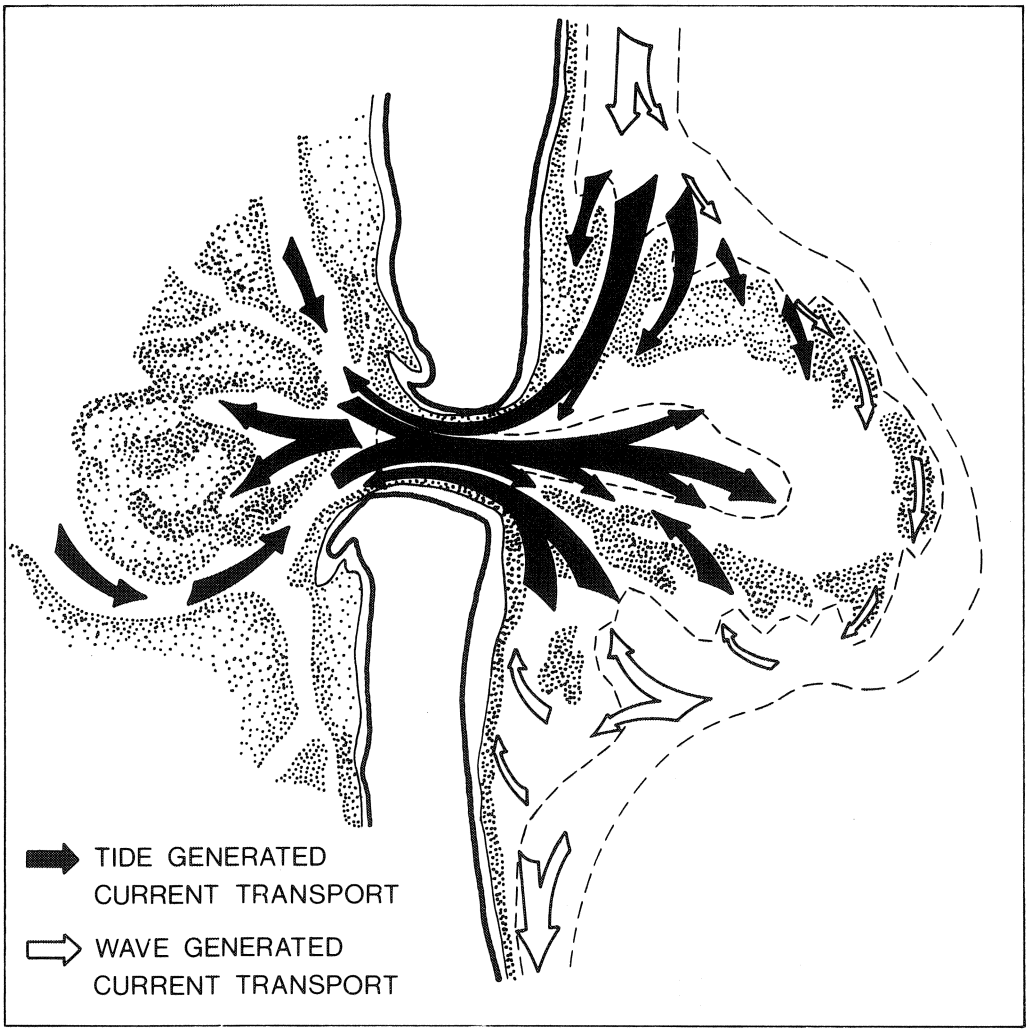

Figure 2.2.4.12 Wave and tide generated current transport pathways around and over the flood and ebb deltas of an idealised tidal inlet on a sandy coast.

deepen or migrate with variations in wave energy and sediment supplied by longshore drift.

Tidal inlet morphologies typical of sandy and barrier island coastlines are shown on figure 2.2.4.13.

Where tidal exchanges dominate or wave activity and longshore drift are weak, the ebb delta develops as a main channel bordered by channel levees and marginal shoals (A). Much of the sedi-

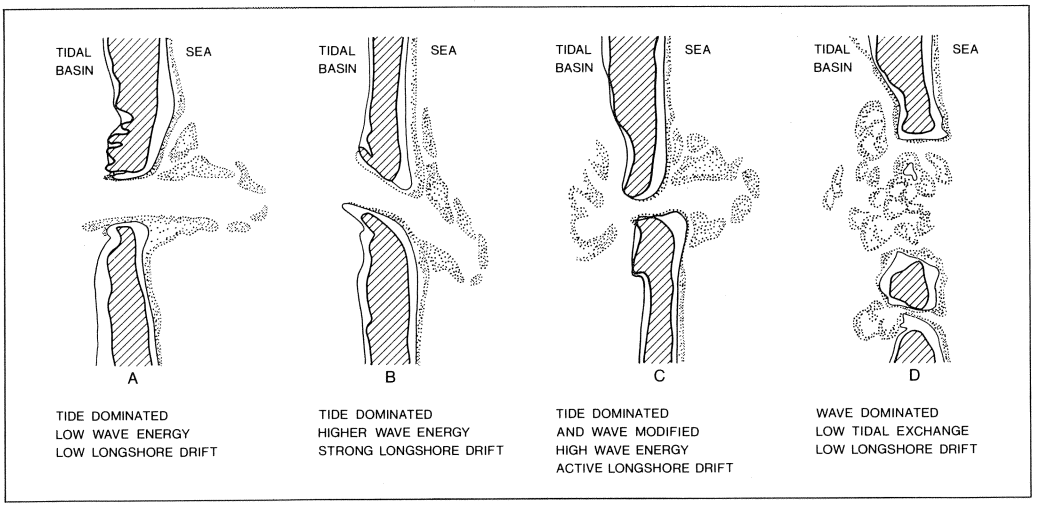

Figure 2.2.4.13 Typical morphologies of tide and wave dominated tidal inlets on a sandy coastline.

ment carried along the shore in the nearshore zone becomes incorporated into the ebb delta.
With increasing wave energy and longshore drift ebb deltas form closer to shore and become oriented with the dominant incoming waves and longshore drift. In these cases a long transverse bar or a series of marginal shoals develop on the updrift side of the tidal inlet (B). Most of the sediment supplied by longshore drift is bypassed along the outer shoals by tide and wave generated currents.
Along shorelines where longshore drift is less active, or wave approach more omnidirectional, ebb deltas form as lobate shoals with a number of diverging main channels (C). Wave and tidal currents carry sediment over the delta as well as into the tidal basin where it accumulates on flood delta shoals.
Wave dominated tidal inlets typically have wide shallow channels with numerous shoals and a poorly developed or non existent ebb tidal delta. The inner side of the entrance usually has spillover lobes of sediment radiating inwards from the entrance (D).
This type of entrance is typical of low barrier coastlines and is usually opened during storm events when storm surge combined with wave attack breaches the barrier. Scour channels develop and typical washover deltas form in the estuary or lagoon behind the barrier. During extreme storms, such as hurricanes or tornadoes numerous shallow channels can be cut through a narrow barrier. Breakthroughs of this sort are assisted by wind blowouts through the barrier dunes.
Generally most storm generated entrances carry insufficient flow to maintain a stable entrance and are eventually choked by shoals and sand transported along the coast by longshore drift.

Those that do remain open are constantly modified by waves that often penetrate into the tidal basin. This is especially so over high water when more shoals in the entrance are submerged.
Unlike inlets on barrier coasts which develop along the open coast, the entrances to inlets formed behind spits on indented and submerged

coasts are often located where wave energy is lowest or geologically controlled against a headland. Within these inlets the flood delta often develops as a shoal bordered by flood and ebb dominant channels.

Although meso tidal basins retain many of the morphological characteristics of micro tidal inlets, features developed by tidal flows dominate those resulting from wave and longshore drift processes.

On barrier coasts inlet channels are deeper and ebb and flood deltas better developed while wide meso tidal basins develop a separate and more distinctive basin morphology (figure 2.2.4.14). The ebb deltas of wide meso tidal basins are broad low relief features with incised main channels. Near the entrance and within the basin large shoals develop. These are usually surrounded by shallow flood and ebb dominated channels that branch from the main deep channels bordering the shoals. The origin of these shoals is uncertain, but comparison of old and new charts usually shows that they undergo slow change. Sediment is actively moved over them in fields of flood or ebb oriented bedforms.

Tidal currents in micro and meso tidal basins typically have a time velocity asymmetry where maximum flood and ebb currents develop before high or low water. This results from differences in tidal range between the ocean and water in the tidal basin and is caused by the flow restricting effect of the narrow inlet entrance (figure 2.2.4.15). As the crest of a progressive tidal wave passes a tidal inlet water drains into the lagoon or estuary basin. This continues for some time after high water until the ocean tide level drops to the water level in the basin. Half a tidal cycle later, when the trough of the tidal wave passes, low water will be slightly higher in the basin so ebb flows continue during the initial phase of the following flood. As a result of this phenomenon the phase and amplitude of the tide within the basin are respectively increased and decreased relative to the the ocean tide (Smith, [21]).

2.2.4.6 Macrotidal Basins

Macrotidal basins are usually funnel-shaped inlets that decrease in width and cross-sectional area at approximately exponential rates upstream from the seaward entrance. Their lower and outer reaches typically have almost parallel 10 to 20 metre deep main channels that are separated by characteristic linear subaqueous and tidally emergent sandbanks. Within these inlets the main channels are bordered by broad sand, but mostly muddy, tidal flats, while near the shore the mudflats are replaced by marginal areas of salt marshes or mangrove swamps. Both the mudflats and bordering saltmarsh or mangrove areas are drained by a network of meandering channels.

Most macrotidal inlets are in fact estuaries formed in the lower reaches of rivers so that the innermost sections usually converge into the tidal reaches of the main river channel (figure 2.2.4.16). The most significant factor controlling sedimentary processes and morphological changes within macrotidal basins is of course the very strong tidal currents. These are strongly influenced by the way the tidal wave is modified as it travels into the tidal basin. As a large amplitude tidal wave enters and moves along a relatively shallow inlet with progressively landward converging sides it becomes both amplified and asymmetrically distorted. This is counteracted along the inner reaches of the inlet by progressively increasing frictional dissipation.

In extreme cases of tidal wave amplification and asymmetrical distortion a tidal bore can form in the inlet. This usually develops as a one to two metre high wave that rapidly progresses up the inlet during the initial phase of flood tide. In certain circumstances tidal bores several metres high can develop.

A consequence of amplification and asymmetric distortion of the tidal wave is that both maximum tidal amplitude and current velocities are found in the middle reaches of the inlet. In response to this distortion tidal currents develop a strong time velocity assymetry which manifests as a short duration high velocity flood phase followed by a longer duration lower velocity ebb.

The degree of asymmetrical distortion to the tide wave and the attendant tidal currents varies over the spring to neap tidal interval. During neap tides, when the tidal wave is less distorted,

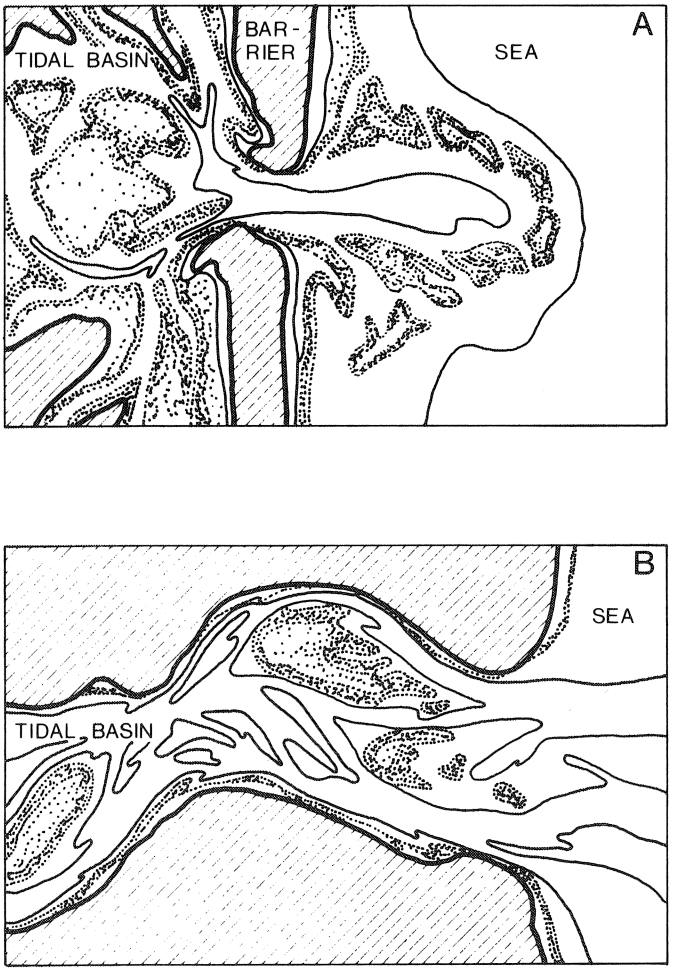

Figure 2.2.4.14 Typical morphologies of mesotidal inlets; A, an idealised inlet on a barrier island coastline; B, a wide inlet developed in a delta or infilled river valley.

the marked contrast between flood and ebb current duration and velocity found during spring tides, is reduced.

Because the tidal prism in macrotidal estuaries is so large, tidal flows are dominant over riverine flows for most of the year. The magnitude of this dominance is illustrated by Wright [22] who found that the tidal prism in the Lower Ord River, Australia, exceeded the mean river discharge by

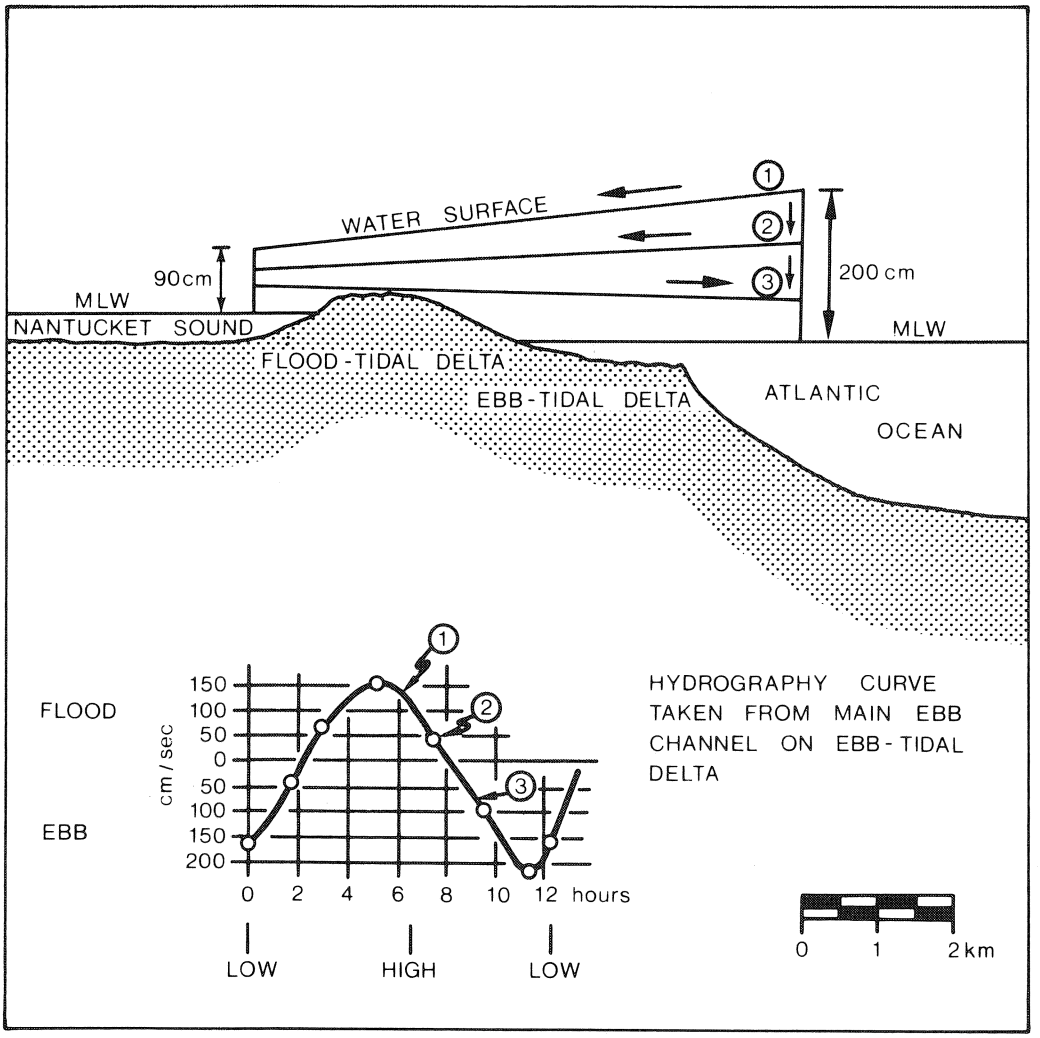

Figure 2.2.4.15 Development of time velocity asymmetry in a tidal inlet.

1) *maximum flood velocity occurs at or near high water;*
2) *over the initial phase of the falling tide water continues to flow in the flood direction;*
3) *hydraulic slope is reversed and ebb flows develop. The volume water discharging into the ocean is progressively restricted as the ebb delta becomes exposed (after Hine [20]).*

nearly 3000 times. Clearly the magnitude of this dominance would vary slightly with seasonal fluctuations in river discharge.
Obviously flood discharges can have an influence on the dominance of tidal flows. For the Seine estuary in France for example, Avione et.al. [23] found that a five fold increase in mean discharge occurred during extreme flood events. Seen in relation to the very large tidal prisms in

Figure 2.2.4.16 Schematic model illustrating the egenral morphology as well as the effect tide asymmetry has on both current velocities and sediment transport in a macrotidal estuary (modified after Allen et.al. [17]).

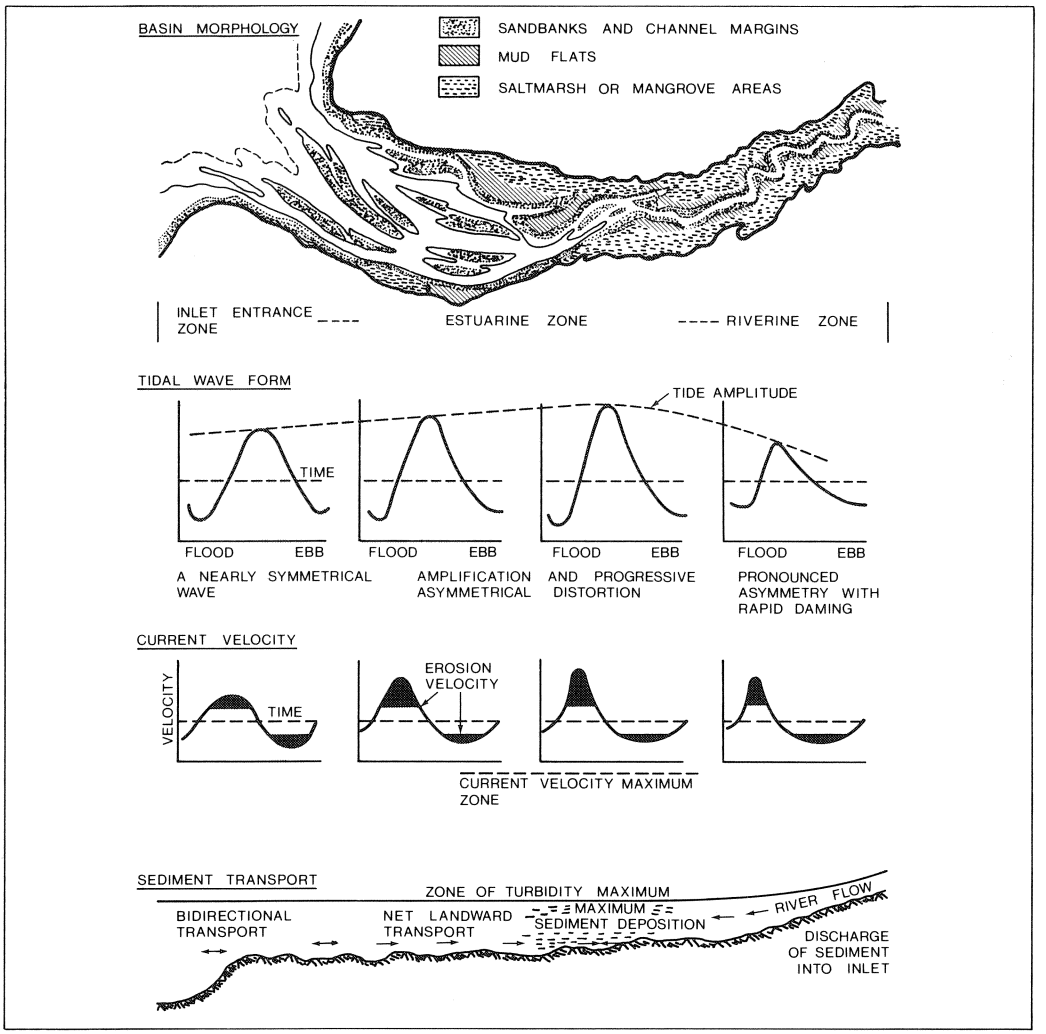

macrotidal estuaries, discharge increases of this magnitude result in riverine flows dominating the innermost reaches of the estuary for only short periods. In regions that have a distinctive wet season the area affected by riverine flows may be considerably extended.

The very magnitude of tidal exchanges in macrotidal basins imposes a significant control on current directions. Moving from the seaward towards the outer reaches of the inlet, tidal cycle current velocity elipses progressively lose their rotational character, flatten and elongate. Within the confines of the inlet itself current directions are almost entirely rectilinear and change nearly 180° from flood to ebb. As a result velocities decrease to almost zero over high and low water. During these slack water periods maximum sedimentation of expended sediments takes place.

In the outermost reaches of inlet channels, where current velocities are least asymmetrically distorted, ebb and flood currents are approximately equal or slightly flood dominant.

Dune bedforms in these areas reverse with tidal flow indicating that bedload sediment transport is bidirectional [24].

In the outer channels dominantly ebb or flood orientated bedforms are often found in separate channels. This is especially so around the sub and intertidal linear shoals and reflects the tendency of ebb and flood flows to follow mutually evasive courses. This phenomenon is a commonly observed feature of channels in inlets (Price [25], Ludwick [26]. The stability and maintenance of the linear banks is probably attributable to this process because sediments transported in opposite directions over and along both sides of the banks are held in a semi-closed sediment circulation system.

In the middle and inner sections of macrotidal basins, maximum velocity flood discharges occur when a portion of the shoals and tidal flats is submerged. In contrast, the longer duration and lower velocity ebb discharges are concentrated in the channels. As a result of this process, channel bedforms often maintain a predominantly downstream orientation while in shallower channel sections and along channel banks mainly flood orientated bedforms develop.

As sediment transport is related by a power

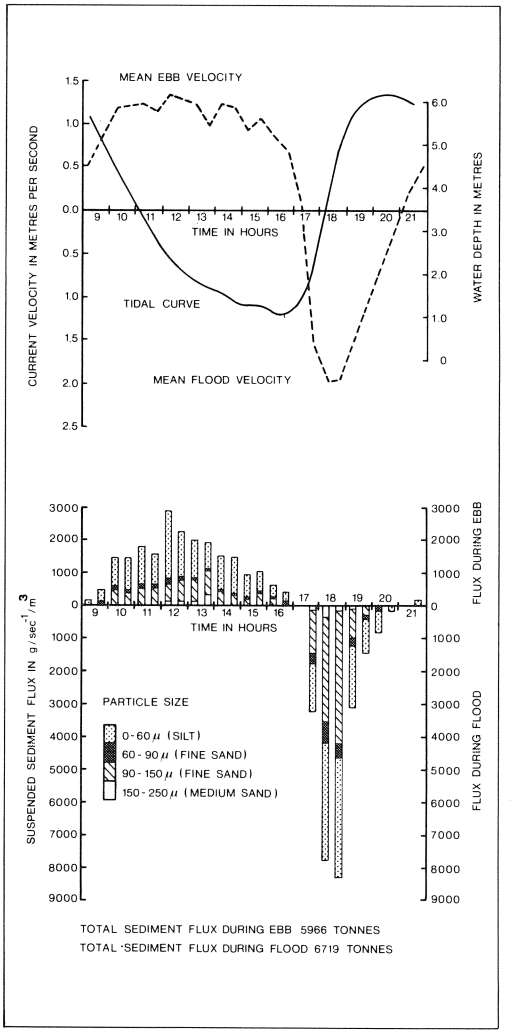

Figure 2.2.4.17 Tidal current velocities and suspended sediment flux over a spring tidal cycle in a channel of the Wash, England (After Kestner [27]).

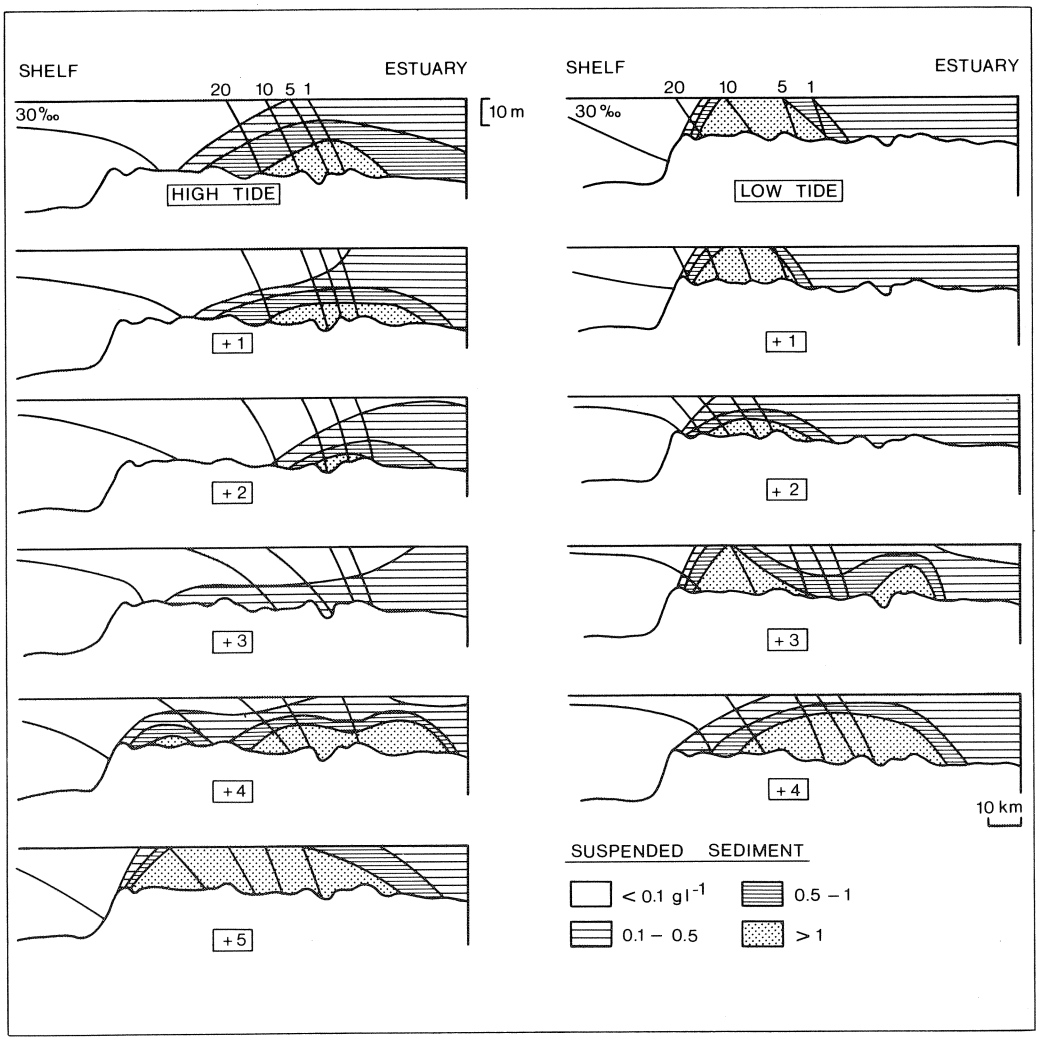

Figure 2.2.4.18 Tidal dynamics of the turbidity maximum in the macrotidal Seine estuary, France, showing its formation in the mixing zone, its growth and decline in the current velocity maximum and its longitudinal migration over a semidiurnal spring tidal cycle. The numbers indicate hours after high or low water at the inlet entrance (after Avione et.al. [23]).

function to mean current velocity, sediment flux is controlled by the balance between the magnitude and duration of peak flood and ebb current velocities over the tidal cycle. In the middle and upper reaches of the macrotidal inlets, where peak flood velocities are much greater than ebb flows, net landward transport takes place. This phenomenon is clearly illustrated by Kestner [27].
For an inner channel of the Wash, England, Kestner found that short duration peak flood velocities, of about twice those that occured during ebb, were associated with a fourfold increase in suspended sediment concentration. The sediment budget at the time of measurement indicated net landward transport and hence trapping of sediment in the tidal basin (figure 2.2.4.17). In the uppermost sections of macrotidal inlets, where the channels are more sinuous and asymmetrical in cross profile, ebb tidal flows backed by riverine discharges are concentrated in the channels.
Ebb flows dominate so that net sediment transport is into the inlet.

The extremely large tidal prism, relative to the discharged volume of fresh water, results in salt water penetrating well into macrotidal estuaries. Over most of the year both strong turbulent currents and large tidal fluctuations in water level restrict the formation of salinity gradients so that well mixed estuarine conditions develop. Where the salt and fresh water masses meet an extensive and variable mixing zone develops.
This, of course, migrates backwards and forwards along the inlet over the tidal cycle and with variations in fresh water discharge. The mixing zone itself is often characterized by a suspended sediment turbidity maxima. This is usually formed by flocculation and concentration of river borne suspended sediments in the convergence zone where bottom salt and fresh water currents meet, but can also form from sediments resuspended by tidal currents in the current velocity maximum region of the inlet. The dynamics of a turbidity maximum in a macrotidal estuary are shown on figure 2.2.4.18.
While much of the suspended sediment discharged into macrotidal estuaries by rivers is deposited large quantities can be transported through the inlets and discharged into coastal waters. The seaward escape of suspended sediment onto the continental shelf is greatest during flood events when the supply of sediment is increased, the turbidity maximum is displaced seaward and increased buoyant surface flow takes place.
During fair weather the greatest discharge of sediment takes places during spring tides when the largest tidal exchanges and maximum current velocities pump sediment seaward. Maximum sediment discharges occur when spring tides and floods coincide.

References

1. Brun, P., **Stability of Tidal Inlets, Theory and Engineering.** Elsevier, 1978, 507 pp.

2. Dyer, K.R., **Estuarine Hydrography and Sedimentation,** Cambridge University Press, 1979, 230 pp.

3. Fischer, H., List, E.J. Koh., R.C.Y., Imberger, J., Brooks, N.H., **Mixing in Inland and Coastal Waters,** Academic Press, 1979, 483 pp.

4. Officer, C.B., **Physical Oceanography of Estuaries (and associated coastal waters).** John Wiley and Sons, 1976 N.Y.

5. Cronin, L.E., (editor), **Estuarine Research,** Academic Press, New York, 1975.

6. Cameron, W.M., Pritchard, D.W., **Estuaries,** In: N.M. Hill (editor), The Sea, 2. John Wiley, New York, 1965.

7. Hansen, D.V., Rattray, M., New dimensions in Estuary Classification, Limnology and Oceanography, 1966, II: 319 -326.

8. Ippen, A.T. (editor), **Estuary and Coastline Hydrodynamics,** McGrawhill, New York, 1966.

9. Ippen, A.T., and Harleman, D.E.F., One

Dimensional Analysis of Salinity Intrusion in Estuaries, **US. Army Corps of Engineers,** Waterways Experiment Station, Vicksburg, Missisippi.
Technical bulletin no. 5, 1961.

10. Rigter, B.P., Minimum length of Salt Instrusion in Estuaries, **Journal of the Hydraulics Division,** A.S.C.E., JS; 1475 - 1496, 1973.

11. Kirby, R., Parker. W.R., Seabed Density Measurements Related to Echosounder records, **Dock and Harbour Authority,** 1974.

12. Davis, J.L., A Morphogenic Approach to World Shorelines, **Zeitschrift fur Geomorphologie,** 1964.

13. Hayes, M.P., Morphology of Sand Accumulation in Estuaries: an introduction to the symposium. In: L.E. Cronin, (editor), **Estuarine Research,** Academic Press, New York : 3 1975.

14. Hayes, M.O., General Morphology and Sediment Patterns in Tidal Inlets, **Sedimentary Geology,** 26: 1980.

15. Wright, L.D., Sediment Transport and Deposition at River Mouths, A synthesis, **Geological Society of America Bulletin,** 88, 1977.

16. Oertel, G.F., Geomorphic Cycles in Ebb Deltas and Related Pattern of Shore Erosion and Accretion, **Journal of Sedimentary Petrology,** 47, 1977.

17. Allen, G.P., Salomon, J.C., Bassoullet, P., Du Penhoat, Y., DeGrandpré, C., Effects of Tides on Mixing and Suspended Sediment Transport in Macrotidal Estuaries, **Sedimentary Geology,** 26, 1980.

18. Hayes, M.O., Goldsmith, V., Hobbs, C.H., Offset Coastal Inlets, **Proceedings of the 12th Coastal Engineering Conference,** A.S.C.E. 1970.

19. Lynch Blosse, M.A., Kumar, N., Evolution of Downdrift Offset Tidal Inlets, A model based on the Brigantine Inlet System of New Jersey, **Journal of Geology, 84, 1976.**

20. Hine, A.C., Bedform Distrubtion and Migration Patterns on Tidal deltas in the Chatham Harbour Estuary, Cape Cod, Massachusetts. In: L.E. Cronin, (editor), **Estuarine Research,** Academic Press, New York, 1975.

21. Smith, N.P., A. comparsion of Tidal Harmonic Constants Computed at and near an Inlet, **Estuarine and Coastal Marine Science,** 10, 1980.

22. Wright, L.D., Coleman, J.M. Thom, B.G., Sediment Transport and Deposition in a Maxrotidal River Channel, Orde River, Western Australia. In: **Estuarine Research, L.E. Cronin (editor), Academic Press, New York, 1975.**

23. Avione, J., Allen, G.P., Nichols, M., Saloman, J.C. Larsonneur., C., Suspended Sediment Transport in the Seine Estuary France, Effect of Man-made Modification on estuary shelf sedimentology, **Marine Geology,** 40: 1981.

24. Hawkins, A.B., Sebbage, M.J., The Reversal of Sandwaves in the Bristol channel, **Marine Gelology,** M7 - M9, 1972.

25. Proce, W.A., Patterns of Flow and Channeling in Tidal Inlets, **Association of Petroleum Geologists,** 47, 1963.

26. Ludwick, J.C., Migration of Sandwaves in Chesapeake Bay Entrance, In: **Shelf Sediment Transport, Process and Pattern,** edited by : D.J.P. Swift., D.B. Duane and O.H. Pilkey., Dowden., Hutchinson and Ross Inc. Pennsylvania: 1972.

27. Kestner, F.J.T., The Loose Boundary Regime of the Wash, **The geographical Journal,** 141, 1975.

Environmental Conditions

J.K. Nieuwenhuis

2.2.5. Geological conditions

All engineering works are built on or in the ground and are often constructed from materials taken from the ground. Any action taken on the ground must produce a reaction from the ground. It is the task of the designer of the structure to predict the nature of this reaction and to understand how the engineering work (the building, dam, tunnel etc.) will behave. There is no circumstance to which the ground will not react. This part of the work is often assigned to the geotechnician, at least for relatively small structures. But not only the prediction of the effect of the structure upon the ground, but also the reverse is equally important. The earth crust is not at rest not just in geological terms i.c. thousands of years, but even in terms of human life.
Movement of the earth and its effects are not restricted to very small areas. It is in this field of science that the (engineering) geologist works. He deals with greater phenomena of the earth than the geotechnician.

To understand his work some definitions are given.

Materials may be rock, soil (in the engineering sense) or fluids or gases (mostly water but perhaps also gas or oil).

Material properties are the geotechnical properties (such as density, strength, porosity, permeability) of the substance. In practice these are determined on test specimens, generally in the laboratory, or are assessed by in-situ testing.

The ground mass is that volume of ground that will be influenced by or will itself influence the engineering work.
The mass influenced by the engineering work is the volume of ground that will be affected, in some way, by the engineering construction.
In case of, say, the construction of a building this could be the volume of ground stressed by the extra load of the building. For a tunnel the mass could consist of (a) the volume of ground affected by the withdrawal of support following the tunnel excavation and (b) the volume of ground from which water is lost by drainage into the tunnel excavation.

The mass which may influence the engineering work is generally much larger than the mass influenced by the work. Dam constructions in valleys may be endangered by the valley sides - these may be of natural origin, unaffected by the construction, but their stability must be investigated. The 'mass' would extend to these landslides, which could be situated well outside the construction area.

All ground masses exist in an environment. The environment includes:
- climate
- stress
- time
- natural hazards

Climate
Climate includes rainfall, in terms of total rainfall, distribution of rainfall in time and rainfall intensity.
The properties of materials may vary significantly depending upon their water content. A material may thus have different properties depending on whether it exists in a wet or a dry climate. Changes in water table level in relation to rainfall will affect mass properties significantly.

Stress
All materials exist under certain stress conditions. Stress on buried materials may arise from

(i) the weight of the material above, which gives both vertical and horizontal stress. Increases in horizontal stress come from the 'Poisson's ratio' effect. If γz is the vertical stress due to weight at a depth z, then horizontal stress equals $K_o \gamma.z$, where

$$K_o = \frac{\mu}{1 - \mu} \text{ where } \mu = \text{Poisson's ratio}$$

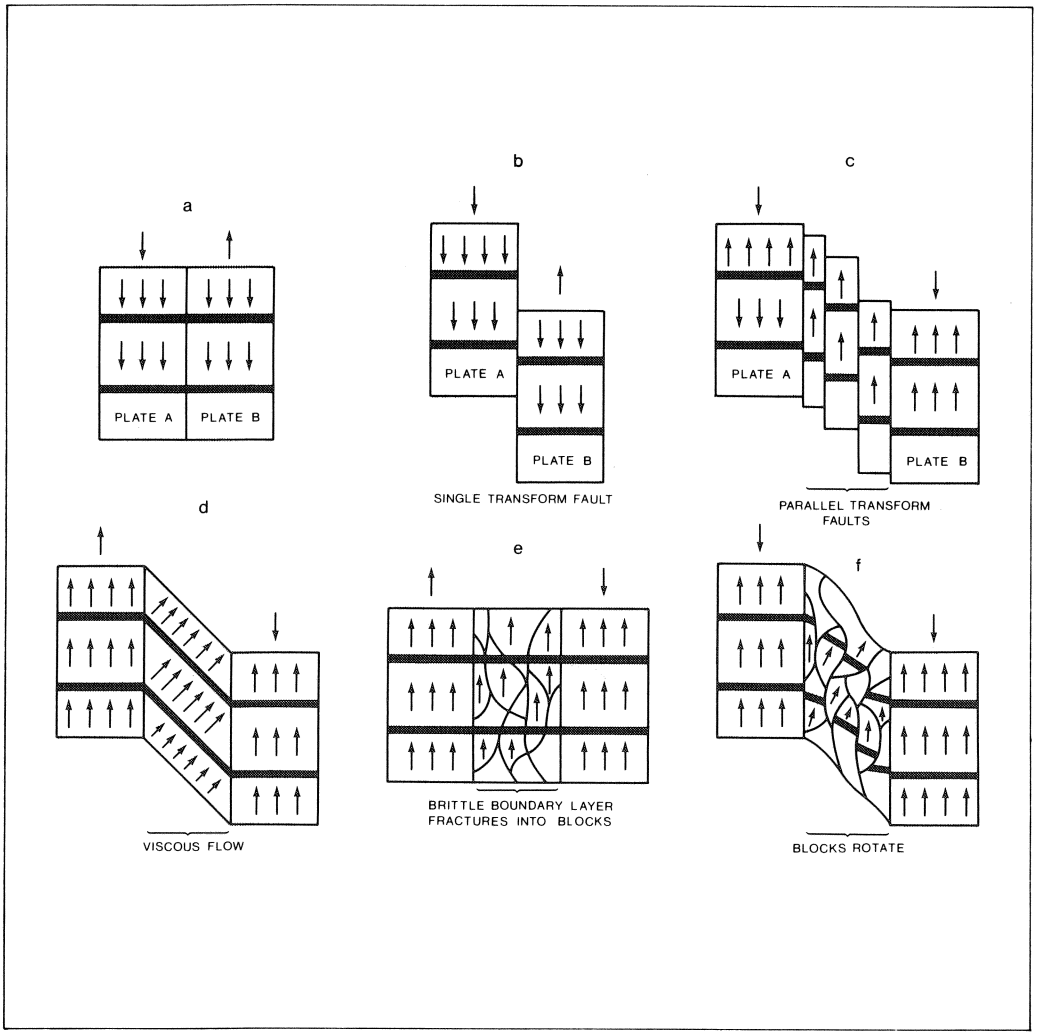

Figure 2.2.5.1 Under the influence of tectonic stresses a variety of deformations can result at a boundary where two plates of the earth crust slide past each other.

This relationship holds for shallow depths.

(ii) tectonic stresses, either residual from past tectonic movements (see fig. 2.2.5.1) or active from present tectonic movements. These stresses appear to be mostly horizontal but are often strongly directional.

(iii) topographic stresses, which are the results of the distribution of stresses in steeply mountainous areas. In Norway 'rock bursts' (explosive failures of overstressed rock) occur in tunnels driven beneath the steep slopes on the sides of fjords.

Time
All things exist in time and change with time. Thus civil engineering works are considered to have a limited economic lifetime after which repairs to decayed construction become more expensive than replacement.
Rock and soil are also subject to decay by weathering and can be expected to retain their properties for but a limited time. Most engineers believe that geological materials will change their properties by weathering in 'geological' time. This is not so and the possibility that the geological mass will decay more rapidly than the engineering work placed upon or in it, must always be considered.

Natural hazards
Catastrophic natural events such as earthquakes, volcanic eruptions, avalanches etc. will affect the ground mass. The possibility of the occurrence of such events may have a major influence on anticipated ground behaviour and the design of engineering structures.

The engineering geological situation consists of mass properties as they exist within the environment.

The engineering work may be an excavation, the construction of a building, of a bridge, of a dam, the withdrawal of groundwater by pumping, deep underground mining, explosions from

Figure 2.2.5.2 Geotechnical profile through the Netherlands.

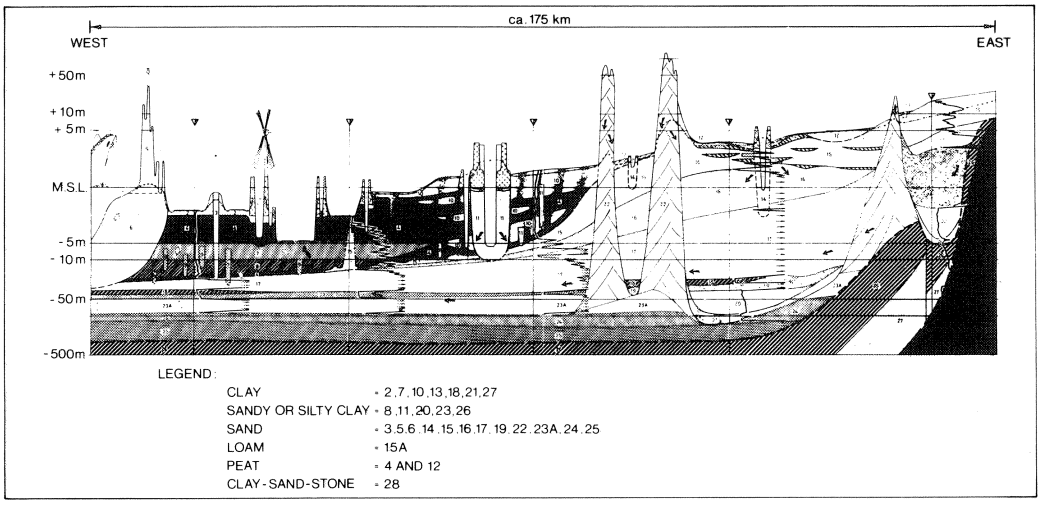

quarrying and many other things. While the engineering work is being constructed and after it is completed changes take place in the mass and the environment. For example, if a dam is built the mass has to sustain additional load while the environment is changed because of the large reservoir lake made behind the dam. The lake may cause changes in climate and the weight of the water may cause earthquakes to occur.

Engineering geologists and geotechnicians seek to determine the engineering behaviours of the ground under the changes imposed by the engineering work. This is necessary because engineering works are designed to function only within a limited range of ground reactions. Thus, when a house is built the ground beneath the house will deform under the weight of the house. If the deformation properties of the ground are not equal beneath the whole area of the house, then the house will settle unevenly. If the structure of the house cannot sustain such deformation, it will fracture and the house may collapse. It is the task of both engineering geologist and geotechnician to determine how the ground will react to the construction of the engineering work so that the engineering work can be designed to function safely and be built as cheaply as possible. The information about the nature of the ground mass and the environment needed to do this is obtained by site investigation. Through such an investigation three objectives are achieved.

- a clear picture of the subsoil with its different types of strata
- soil samples for laboratory testing
- in-situ soil properties by in-situ testing

Fig. 2.2.5.2 represents a cross-section of the subsoil through the Netherlands from East to West. It reveals the geological formation of a delta area, whereby a great variety of subsoil conditions are met over a short distance.

Environmental Conditions

D.J. de Jong, R.J. Leewis, R. Misdorp, P.B.M. Stortelder, J. Visser

2.2.6. Ecological conditions

2.2.6.1. Introduction

This chapter concerns the structure of and the relations between the abiotic and biotic components of estuarine ecosystems.
The term „ecology" stems from the Greek word „oikos", meaning „house„ or „place of living". The ecological system has been defined by Collier et al. [1] as a system „that consists of one or more organisms, together with the various components of their physical and chemical environment".
An ecological system may be analysed at various levels of integration. Collier et al. [1] divide the ecosystem into four levels of increasing complexity. These are: organism level, population level, biotic community level and ecosystem level. Although knowledge of the living conditions of individual organisms, populations and biotic communities is of vital importance for the accurate determination of the structure and the functioning of an aquatic or terrestrial system in a given area, this chapter deals primarily with the ecosystem level. This is because the environmental impact resulting from hydraulic engineering works mostly affects the overall functioning of the system.

The ecosystem may be defined as an environmental unit consisting of various biotic and abiotic components (fig. 2.2.6.1), which are related through interchanges of mass and energy flow.
The principal abiotic components are: the atmosphere, the water and the lithosphere. The atmosphere will not be dealt with here as this component is usually hardly if not at all affected by hydraulic engineering structures. The water has both physical and chemical aspects, whereas the lithosphere may be characterised by its form (morphology), composition and structure.
The principal biotic components may be divided according to their functions in the ecosystem, i.e. the „producers" or green plants, the „consumers" or animals and the „decomposers" or micro-organisms. When analysing an ecosystem (see fig. 2.2.6.1), the structure of the system can be distinguished from the processes influencing it.
The structure is related to the state of the system at a particular moment of time e.g. the number of species and the diversity of species. On the other hand with process aspects the time dimension has to be taken into account as these aspects concern changes that occur within a certain period of time. The time-scale in which these changes occur may differ widely: from less than one second (e.g. water displacement) to decades (geomorphological processes) and thousands of years (evolutionary process).
To make forecasts about the effects of a certain action (e.g. a civil engineering construction) it is essential to have knowledge about what exists in a certain system, as well as about the relations and processes within that system (the functioning of the system).

A given ecosystem does not exist in isolation but is always related to its surroundings. The intensity of these relationships (i.e. the extent of openness of the system) can differ strongly; compare, for example, an „enclosed" lake with an „open" estuary.

Some important relations are:
- the energy supply due to radiation (sun), wind and tidal movement etc.;
- the supply and discharge of water: precipitation, evaporation, flooding, etc.;
- the supply and discharge of matter in the water, in either dissolved or suspended form; the supply of matter by the wind;
- the supply and discharge of plants, remnants of plants and animals by water or wind;
- the migration of animals including the migration of fish or birds;
- the influence of man on the ecosystem: disturbance of the peace, waste discharge, fisheries, encroachment on the environment.

2.2.6.2. Hydrological and physical aspects

Important hydrological and physical aspects include the water level, the supply and discharge of water, the internal water movement, the transparency of the water and the temperature.

Major Components	Some elements	Some variables		
		Subdevision of variables	Structure variables	Processes variables
ABIOTIC				
water	water suspended matter -inorganic -organic (detritus) dissolved components -oxygen -major nutrients -silicium -carbon -nitrogen -phosphorus -(heavy)metals -iron -mercury -cadmium, etc. -chloride -organic substances	waterquantity waterquality -physical - chemical	level volume colour temperature suspended matter/ transperancy taste/odor radio-activity concentration of oxygen organic materials (TOC, BOD, XOD) nutrients chloride heavy metals	flow velocity heating/cooling sedimentation/ flocculation degradation reaeration/ consumption degradation/ production uptake/ exchange processes stratification accumulation
lithosphere	clay sand stones death organic material (peat) nutrients (heavy)metals	morphology composition -physical -chemical	tidal channels shoals salt-marshes particle size/ distribution chemical composition	erosion sedimentation maturing maturing
BIOTIC				
producers (plants)	various green plants -micro-phytoplankton -micro-phytobenthos -sea-weeds and water-plants -terrestrial algae/plants	quantity quality	biomass species diversity	primary production consumption death rate succession
consumers (animals)	various groups of animals 1) -herbivorous animals -omnivorous animals -carnivorous animals 2) -zoöplankton -pelagic animals -bentic animals -suspension feeders -sediment feeders -predators/scavengers -terrestrial animals	quantity quality	biomass species diversity	reproduction growth consumption death rate succession concurrence
decomposers (micro-organisms)	various bacteria and fungi -aerobe species -anaerobe species	quantity quality	biomass species diversity	mineralization

Figure 2.2.6.1. Overview of the major ecosystem components and variables.

Water level

The water level determines which areas must be considered as aquatic or terrestrial systems and if the level is variable which areas will be periodically dry and flooded, i.e. intertidal zone. The water level is important not only for the plants and organisms in the intertidal zone but also via the groundwater for the adjacent terrestrial areas.

The range in water level can vary from very small (centimetres) to very large (10 m or more). These variations can be caused by natural processes such as the tide, wind setup and river discharge. But human intervention can also play a significant part, for instance by employing hydraulic constructions to maintain as stable a water level as possible. In addition, the changes in water level may occur regularly, for instance cyclically due to astronomical tides or very irregularly e.g. due to discharge of a river fed by precipitation. The tidal element usually plays the dominant part in the level variations in tidal areas and estuaries. In estuaries into which a large river debouches, the magnitude of the river discharge can also have a significant effect on the water level in the area involved. In addition to the extent and the possible periodicity of changes in water level, other important factors for the ecosystem include the frequency and duration of flooding (or exposure frequency and duration).

Watersupply and discharge

With the river discharge via an estuary or with the flushing through of a lake and also with the water-exchange due to tidal action a great amount of dissolved or suspended matter is transported. The large transport capacity of water in estuaries, for example, means the availability of large quantities of food for many species of animal life. This in turn permits a great density of animals and enables aquacultures of mussels and oysters. In order to study the ecological processes occuring in the ecosystem, a precise knowledge of the supply and discharge of dissolved and suspended matter is required. Data on the amounts of water supplied and discharged are therefore required.

Internal watermovement

Internal watermovement concerns waves and currents within the system involved. This movement is the result of wind, tide and river discharge. The watermovement in an estuary or sea-arm will mainly be influenced by the tide and the river discharges whereas for a lake the dominant force will be the wind.

Internal watermovement is important for the provision of many dissolved and suspended substances in the waterbody and for a large degree of horizontal transport, as well as vertical mixing of matter. As a result of this movement large differences in temperature and matter, particularly in larger systems, are eliminated. The internal watermovement is also necessary for certain groups of organisms in the waterbody such as plankton. With little or no current, some of these organisms would settle on the bottom. Finally erosion and sedimentation of sand or silt depend strongly on current velocity and wave motion.

Apart from the organisms in the waterbody, creatures that are permanently fixed or live in and on the bed, are current-dependant. While these species will be unable to settle or to remain fixed if the currents are too high, they also depend on a certain current velocity for the supply of food and/or discharge of metabolic products. When the current velocities are too low they will either „starve" or asphyxiate in their own metabolic products or in excreted silt, e.g. mussels which feed on silt and excrete it again in particle-form.

The periodical absence of a current during slack water is of such short duration that it is of minor importance to the living components in the system; moreover, they have adapted themselves to this situation.

An important aspect related to internal watermovement is „stratification". During periods in which the temperature of the upper water-layers rises considerably and thus differs from the lower layers of water or when the salinity of the lower layers increases, a difference in density occurs between the upper and lower strata (see fig. 2.2.6.2.). This causes stratification as a consequence of which the transport of oxygen to the lower layers can be hampered. The consumption of oxygen in the lower layer due to mineralization of dead organic material and respiration continues however, as a result of which a lack of oxygen can occur in this layer. This can in turn lead to a sharply increased discharge of nutrients such as phosphate and ammonia from the sediment - which cannot reach the upper layer through the boundary layer - and even to the formation of toxic sulphite. The consequence of this might be asphyxiation of animals in the lower water-layer

and no growth of phytoplankton in the upper layer.
If the stratified volume is small in relation to the total volume of the waterbody there will be little or no problem. However, if the volume of stratified water is large compared with the rest of the water, the water-quality can deteriorate, particularly if stratification is abruptly raised, due, for instance, to a storm or sudden drop in temperature of the upper layer.

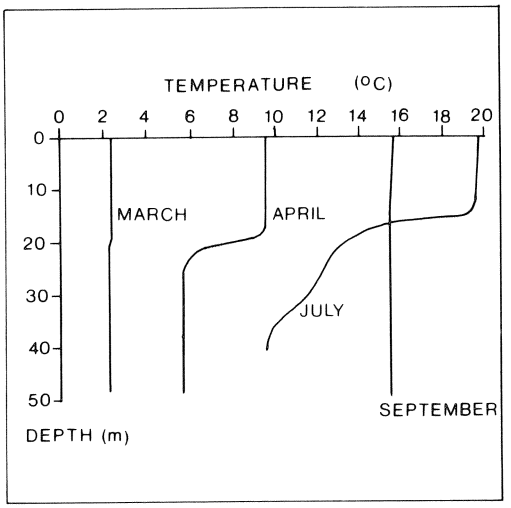

Figure 2.2.6.2. Course of the watertemperature in a lake in relation to the depth. The figure shows a period of temperature stratification in summer which has been raised again in september.

Transparency of the water
Green plants use light as a source of energy for their growth (see also fig. 2.2.6.8.). The quantity of light decreases in relation to the depth of the water. This extinction of light energy under water is described by the following equation:

$$I(z) = I(o)e^{-kz}$$

in which

I (z) = light energy at depth z (joule/m²/day)
I (o) = light energy on the water surface (joule/m²/day)
k = extinction coefficient (m^{-1})
z = depth (m)

The extinction coefficient is determined by the amount of dissolved and suspended particles (silt, dead organic material, algae) in the water. It is assumed that plant growth remains possible to a depth at which one percent of the light energy can penetrate. This zone is named the „euphotic zone". A simple method for determining the euphotic depth is offered by the „Secchi-disc", a white disc of a particular size. The Secchi-depth is defined as the depth at which the disc is still just visible to the naked eye. (But there are also more advanced methods for light measurements available.)
The equation below approximates the relation between the Secchi-depth and the euphotic depth:

$$Z_{euphotic} = 2.5Z_{Secchi}$$

in which

$Z_{euphotic}$ = euphotic depth (m)
Z_{Secchi} = Secchi-depth (m)

Besides light, the speed of the algae growth may be limited by other factors like the concentration of nutrients. When light is the only limiting factor, the rate of algae growth may be approximated as follows:

$$\mu \simeq \mu_{max} \frac{1}{kZ_{euphotic}}$$

in which

μ = the mean growth rate in the vertical (day^{-1})
μ_{max} = the maximum growth rate (day^{-1})
k = the extinction coefficient (m^{-1})

Temperature
The activities of organisms in the water such as growth and reproduction, depend strongly on the temperature. Outside a certain temperature range, which varies from species to species, mortality will occur.
The local climatic conditions e.g. irradiation and air temperature influence the temperature fluctuations of the water to a great extent. The ver-

tical temperature distribution is, to a great extent, determined by the mixing depth of the upper layer, in which heating and cooling occur. In summer water temperature in the upper layer will increase, but in the deeper parts the temperature will remain low (see fig. 2.2.6.2.). Combined with a minimal mixture this can result in stratification (see also „internal watermovement").
The annual temperature fluctuations of the water also depend on the volume and depth of the system: in estuaries and coastal seas the temperature fluctuates more than in oceans and in rivers the fluctuations are even greater. Ice can be formed in estuaries in winter, which can lead to mass mortality of local organisms in shallow areas, e.g. the intertidal area.
Average temperatures can rise as a result of discharges of warm waste-water. Generally, little is known about the consequences of such small rises in average temperature. However to subsist many organisms are not only bound by a critical minimum temperature level, but also by a critical maximum level, above which their activity will decrease rapidly; e.g. in areas with a temperate climate, the maximum temperature ranges between 20° and 25°C.
Finally the temperature also influences the rate at which chemical processes occur.

2.2.6.3. Chemical aspects of water

Of the many chemical aspects which play an important part in the ecosystem, only a few will be mentioned here i.e. salinity, nutrients and toxic substances.
In chapter 2.3.8. there is a brief description of some water-quality models.

Salinity
Salinity is defined as the total amount of dissolved matter in a kilogramme of seawater with the exception of dissolved carbonates and organic matter. Salt mainly consists of NaCl. Salinity is often also expressed as the concentration of Cl^- per kilogramme of seawater (chlorinity), or Cl^- per litre (chlorosity). The following mutual relationships apply:
Salinity = 1.8065 * chlorosity
Chlorinity = density * chlorosity

Seawater contains approx. 18 g Cl^-/l, and freshwater less than 0.3 g Cl^-/l. The intervening salinity range, is described as light-brackish, brackish and highly-brackish or oligohalien (0.3 -3 gCl^-/l), mesohalien (3 - 10 g Cl^-/l) and polyhalien (10-16.5 g Cl^-/l).

In transitional areas and brackish lakes, salinity is determined by:
- the supply of freshwater via rivers, discharges and precipitation. The highly variable discharge of rivers is mainly responsible for the strong shifts in salinity in the estuaries.
- evaporation, as a result of which, particularly in summer, salinity can increase considerably in smaller more or less enclosed systems, even to the point that the natural value of seawater can be substantially exceeded.
- the extent of the exchange with seawater.

The nature of the ecosystem is determined to a great extent by salinity levels and fluctuations. The two most common types are freshwater and saltwater ecosystems, each with totally different plant and animal populations. In the transitional areas, e.g. in the estuaries or permanently brackish lakes, a biotic community develops that is adapted to that particular environment. The salinity therefore, strongly determines which species can live in a particular area. It appears that the number of species present in freshwater and in seawater exceeds that in brackish water. This is illustrated in fig. 2.2.6.3.

The marked difference in density between freshwater and saltwater can result in stratification in a basin when two types of water with a different salinity are brought together. The occurrence of such salt stratification depends, inter alia, on the ratio between the discharged quantity of freshwater, the tidal volume and the morphometry of the basin. In this regard a distinction may be drawn between well mixed, partially mixed and stratified estuaries. (For further details see 2.2.4.).

Oxygen
For a proper functioning of the ecosystem, the water must have an oxygen-saturation of at

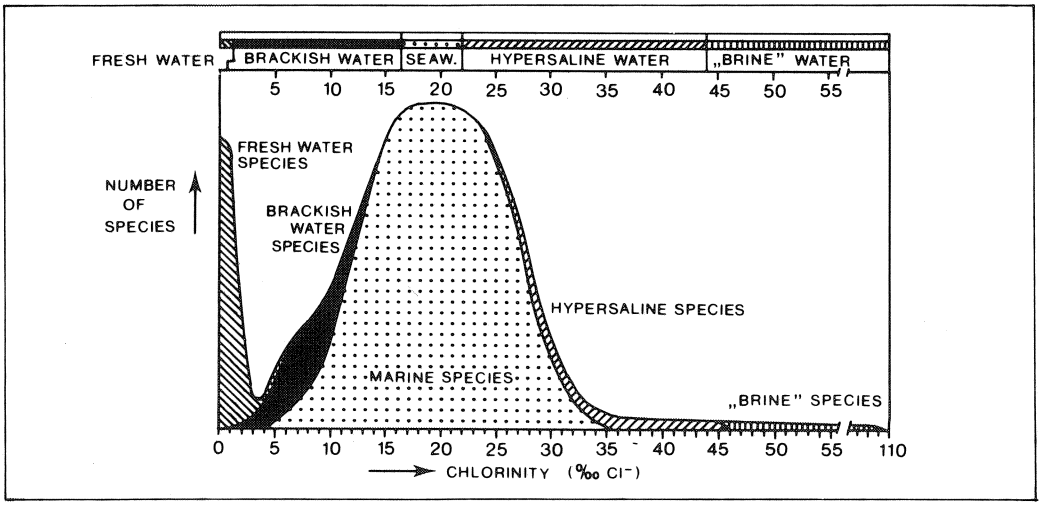

Figure 2.2.6.3. Relation between chlorinity and the number of invertebrates species (after Kinne, 1971 [13]).

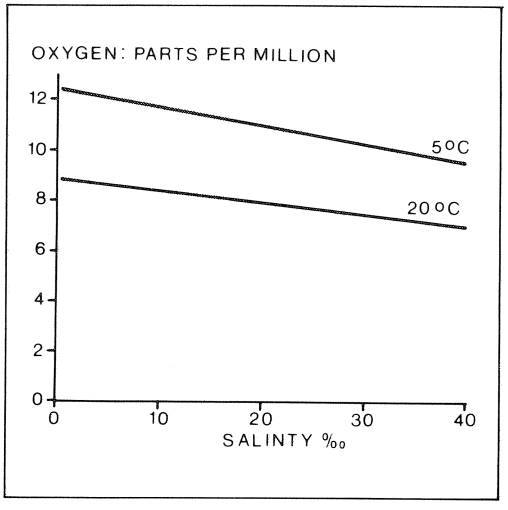

least 80% (a saturation of 100% corresponds with the equilibrium concentration in the water; depending on the temperature and salt content this equilibrium concentration varies between 8 and 12 mg O_2/l). If the temperature and salinity of the water are high, less oxygen will dissolve in the water (see fig. 2.2.6.4.).

Below a concentration of 4 mg O_2/l, the ecosystem will be disturbed and, at an even lower margin of less than 1 mg O_2/l, the biotic community will gradually die.

The most important processes influencing the oxygen concentration, are:

- oxygen production due to photosynthesis;
- oxygen consumption by bacteria during the decomposition of organic matter;
- oxygen consumption by plants (in the dark) and by animals for respiration;
- oxygen supply from the air into the water

Figure 2.2.6.4. Chlorinity and the solubility of oxygen in water satured with air at two different temperatures (after Green, 1968 [26]).

(reaeration), promoted by wind. If the water is over-saturated, the transport will be reversed.

Problems with reference to oxygen concentration arise in particular when excessive discharge of organic matter (c.q. municipal and industrial waste-water) occurs. As a result, decomposition by bacteria will dominate, thus causing a decrease in the oxygen concentration. In the stratified deeper layers of water where there is no supply or production of oxygen, mineralization of accumulated organic matter can also cause oxygen problems. (see also 2.2.6.2.).

Nutrients

The growth elements of green plants are formed by the macro-nutrients: carbonates (C), phosphate (P), nitrogen (N) and silicium (Si). A rough indication of the demand for various nutrients is expressed by:

$$1\ HPO_4^{2-} + 106\ HCO_3^- + 16\ NO_3^- + 16\ H_2O + 124\ H^+ \rightarrow C_{106}N_{16}P_1H_{263}O_{110} + 138\ O_2$$

These figures can however differ for various species of phytoplankton and, depending upon the availability of nutrients, it is even possible for variations to occur within the one species. Silicium is an especially important nutrient for one type of algae, the diatomes. The uptake of nutrients by the algae is reflected in the progress of the concentration. (See fig. 2.2.6.5.).

In spring, when the growth of algae increases due to favourable light and temperature conditions, the concentrations of dissolved nutrients decrease. In autumn the mineralization processes are dominant and, consequently, concentrations will increase. In reality these cycles of uptake and mineralization are completed quite rapidly and recur several times per year. A turnover of 10 - 40 times per annum is possible. This does not apply to silicium; here the turnover is much slower and recurs only once or twice a year, as a result of which diatomes are mainly abundantly present in spring.

The high turnover speed means that very low concentrations of nutrients in summer need not imply that the primary production (i.e. the growth of plants) is limited: the large amount of nutrients discharged as a result of mineralization can immediately be used again for the growth of new algae, so that no change in concentration of the nutrients will occur. On the other hand it is possible that the total phytogenic biomass will decline.

In addition to the factors of primary production and mineralization, the nutrient concentrations are also determined by supply and discharge as well as the exchange with the sediment. Compared, for instance, with the phosphate cycle, the nitrogen cycle is more complicated, as dissolved N can occur in the form of ammonia (NH_3), nitrite (NO_2^-), nitrate (NO_3^-) and dissolved organic N. The mineralization processes determine the mutual relations between these components; e.g. in an environment where oxygen is

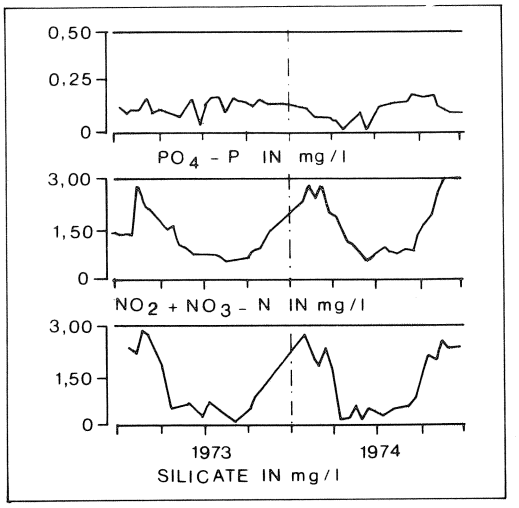

Figure 2.2.6.5. Seasonal fluctuations in the concentration of phosphate, nitrite + nitrate and silicate in a tidal basin in the S.W. Netherlands (Eastern-Scheldt).

abundantly present, NO_3^- will form the principal component.

Up to now, the essential role nutrients play within the ecosystem has been discussed. An excess of nutrients can, however, cause damaging effects. In recent decades the load of nutrients in the water has increased substantially, e.g. via municipal and industrial waste-water discharges and due to the use of fertilizers in the soil. This process of eutrophication has led in freshwater to explosive algae production and changes in algae diversity. Due to this increased algae production (algae bloom) the water becomes more turbid and, intended by a decrease in oxygen concentration, large numbers of fish and other creatures can die, causing offensive odours.
This problem has yet not manifested itself significantly in saltwater, but a continuous excessive load of nutrients may lead in the long run to changes in these ecosystems as well.
Finally it must be mentioned here that certain nutrients (e.g. nitrites and ammonia) are in high concentrations toxic for fish and other animal life.

Toxicants
When the quality of the water with regard to toxicants is measured it should be born in mind that a distinction must be drawn between materials alien to the system and those that belong to it, as well as the extent of the toxicity.
Materials which naturally belong to the system are, in their natural concentrations, harmless (and often essential for the life in the water). However, the natural concentrations of heavy metals, such as mercury and cadmium, are very low. When these concentrations of materials are too high they become toxic i.e. they will disturb the functioning of the organisms.
Substances alien to the system, which include the various types of chemicals produced in recent decades, do not naturally belong to the water and can, depending on various factors, cause damage to the environment.

The extent of the pollution of an ecosystem caused by toxicants can be determined according to the following criteria:

- toxicity : the extent to which the function of an organism is adversely affected by contact with the toxicant;
- bio-accumulation : the extent of accumulation of the toxicant in the tissues of living organisms;
- ecological activities : the extent of the impact on the ecosystem by factors other than direct toxicity;
- persistency : the extent of the toxicant's resistance to chemical changes - whether or not activated by living organisms;
- mobility : the extent and rate of distribution of the toxicant in the ecosystem.

Among the most toxic substances are organohalogen compounds, organosilicon compounds, mercury and mercury compounds, cadmium and cadmium compounds, radioactive waste and carcinogenic substances. Other substances which require special care are arsenic, lead, copper, zinc and their compounds, cyanides and fluorides, pesticides and their by-products and oil and oilproducts.
When assessing the toxicity the combined effect of various minor pollutants should also be taken into account. To prevent pollution of the water there are international conventions concerning the dumping of toxicants, e.g. London (1972), Oslo (1972) and Paris (1976). In a lot of countries there are also national conventions.

Water-quality
A great number of physical and chemical aspects of water-quality have been discussed in the previous pages. For water-quality management, however, the question arises as to when the quality of the water may be described as good and when it may be called polluted. In effect, which ranges of physical properties and concentrations of chemicals are acceptable? It is difficult to provide a satisfactory answer to this question. A first (although somewhat vague) criterion is that an adequate composition and functioning of the ecosystem must be possible, including in the long run. One of the terms of reference to be used could be the natural - not yet polluted - situation. In [5] a review is given of

the natural composition of fresh- and saltwater. The values quoted in this review are however averages. The natural value can vary greatly locally. There are for instance numerous transitional situations from fresh- to saltwater and from high to low phosphate- and nitrogen concentrations. This applies in particular to estuaries and coastal seas, making the determination of water-quality standards in these areas even more complex. In addition, there are various systems, created or changed by human action, for which no natural terms of reference exist. In order to assess water-quality, the psysical and chemical aspects have to be considered in relation to biological life.
A second criterion for water-quality is the suitability of the water for various purposes, such as drinking, swimming, agriculture and horticulture, cooling, processing, aquacultures, etc. Each purpose reguires its own specific standards of quality. Relevant guidelines have been drawn up both by the Environmental Protection Agency in the United States of America and by the European Community. In the Netherlands the European Community guidelines have been incorporated into an „Indicative Multi-year Programme for combatting waterpollution", which is revised and published every five years.

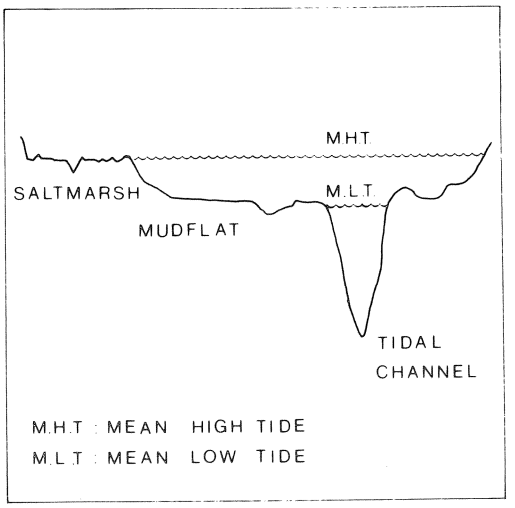

Figure 2.2.6.6. Cross-section of a tidal basin.

2.2.6.4. Morphological and soil mechanical aspects.

A tidal area can be divided into:
- salt-marshes;
- tidal flats and shoals;
- channels

Their elevation in relation to tidal amplitude is illustrated in fig. 2.2.6.6.

Salt-marshes
As evident from fig. 2.2.6.6., salt-marshes have a relatively high elevation in the tidal area. They are characterised by a dense vegetation which usually starts at about 20 - 40 cm. below the mean high-water line. The highest parts of the salt-marshes lie above the mean high-water line but never exceed the highest local flood level. A particular morphological feature of salt-marshes is that they are intersected by numerous creeks, which are sometimes bordered by higher ridges known as natural levees.
Various factors affect the accretion and erosion of salt-marshes, such as:
- sediment supply;
- altitude of the tidal flat;
- location in relation to current and wave impact;
- vegetation;
- current velocity, tidal amplitude and waves.

Generally, salt-marshes are developed from tidal flats in sheltered areas. At places where the silt accumulation is sufficient, pioneer vegetation manages to establish itself. This in turn encourages the accumulation of silt and leads to the formation of salt-marshes. During the process of sedimentation, a relatively stable system of discharge channels - the future creeks - will develop, via which the accumulation is con-

tinuing. When the circumstances are sufficiently undisturbed, i.e. if the erosive forces of currents and waves do not dominate, the initial phases in the development of a salt-marsh can occur after five to ten years.

The described sedimentation process indicates that the soil of the salt-marsh generally contains more clay than the subsoil, which itself usually contains more sand. Within the salt-marsh there are often internal differences in soil composition depending on the accumulation process via the creeks. Thus, as a rule, the natural levees usually consist of more sand than the flood basins behind them, where, as a result of the more quiet sedimentary environment, the soil contains more clay.
As soon as a salt-marsh has been formed, the accumulative factors are joined by erosive elements. These are not only induced by currents but also by wave action. The speed at which wave action can erode a salt-marsh depends on its position in relation to the prevailing wind direction, the width of the tidal flat in front, the speed of the rise and fall of the tide, the transport capacity of the water, the consistency (i.e. composition) of the soil and the density and strength of the roots in the soil.

Shoals and tidal flats.
Shoals and tidal flats consist mainly of unvegetated sand and silt areas which generally lie between mean high-water and mean low-water. Little is in fact known about either the manner in which they are built up in estuaries or about the exchange of sediment between shoals and tidal flats on the one hand and tidal channels on the other. Sediment transport occurs in both directions, sometimes towards the intertidal area, which can increase or raise the shoals and tidal flats, or towards the channels, which results in a decrease. In addition, situations can arise in which there is a certain equilibrium in sediment exchange and yet there is still a geographical shift of the total shoal area. The tidal velocities and the inherent transport capacity of materials are important for this process, as well as the presence of ebb and flood channels and secundary flow. In this connection, the transverse water-level gradient over a shoal is also important; this is brought about when, during a certain phase of the tidal cycle the water level in the channels is different on either side of a shoal. Wave action can cause great disturbances of material, which is then transported by currents over either short or long distances. Sediment transport on shoals and tidal flats is also influenced by algae and other plants, which to a certain extent can impede the movement or transport of sediment, while the zoobenthos is also of importance.

The composition of the sediment is very closely related to the hydraulic parameters mentioned above. At very exposed places, i.e. at places subjected to high current velocities or strong wave attack, coarse sand material is brought in, as a result of which large sand ripples and relatively great differences in elevation, so called megaripples can occur. At less exposed places or in well-sheltered areas the sediment consists of finer materials such as fine sand, silt and possibly even clay. The micro-relief will therefore be less pronounced in these areas (no ripples, even large areas without relief, few discharge channels, etc.).
From the previous text it can be assumed that the sediment composition and the presence of shoals and tidal flats are the result of active processes. However, paleo-phenomena, e.g. the geological character, can also influence the situation. The presence of resistant clay and peat layers can, for example, cause shallows with surface relief and sediment compositions which have not been formed by the actual processes.

Channels
The area of the tidal channels actually comprises the total area below the mean low-water level. In the transitional area between the tidal flat/shoal and channel, either very large or very small shallow zones may occur, in which processes such as secondary waves and currents appear of importance to both the formation of the channels and the shoals.
The underwater morphology is fairly varied. The water depth, for instance, can vary from 5 to 40 m or more. Various types of channels, such as the ebb-, flood- and indifferent-channels may be

distinguished, with longitudinal shallows between them. In ebb- and flood-channels, the ebb and flood currents respectively are dominant. In indifferent-channels, the ebb and flood flows are of about similar strength.
The channels' morphology is the combined outcome of natural developments and artificial interventions.
The principal determining aspects are:
- tidal amplitude and current;
- sediment transport;
- human intervention (dikes, dams, excavation of sand and dumping of dredged material).

In an estuary their will always be a trend towards a certain morphological balance, which can be expressed by a relation between the tidal volume and the size of the wet cross-section. In the Netherlands' Delta area for instance the quotient of the tidal volume and the size of the wet cross-section is approximately constant. Since there has been repeated human intervention in many estuaries over the years, it is often difficult to speak of one original situation. Due to (repeated) activities, the system is subject to continuous morphological changes, and nature constantly adapts in an attempt to re-establish equilibrium. The speed of these morphological changes is mainly due to the sand transport in the estuary itself or to possible sand import from the sea.

The sedimentological composition of the bed in an estuary depends on many factors:
a. human activities: excavation and dumping;
b. geological structure of the basin;
c. the impact of the river;
d. wave action;
e. the vertical tide and derivative tidal currents.

ad a. The estuaries are usually densely populated areas in which a multitude of human activities are taking place, such as shipping and infrastructural and industrial developments. In a growing economy these activities lead to an ever-increasing amount of human intervention in the natural system. This particularly applies to the excavation of (coarse) sand for infrastructural and industrial building activities, which is primarily excavated from channel beds and exposed shoals. This type of excavation can affect the morphology in that as excavation can cause instability of the slopes and subsequent collapse: a natural adjustment to the hydraulic forces. Shipping usually requires the removal by dredging of finer sand and silt sediments and its dumping at sea or in conveniently situated deeper areas in the estuary.
Consequently, the sediment composition will be artificially refined in those (deeper) areas which are created by the erosive action of strong tidal currents and in which, generally, coarse sand prevails.

ad b. The geological composition of the bed of the estuarine basin can influence sediment composition and the morphology since the deeply eroded channels can (for instance) cut into layers of clay and peat; as a consequence, sediment layers are coming out to the channel walls which are in imbalance with the prevailing hydraulic conditions.

ad c. The influence of a river loaded with fine sediment flowing into an estuary has been dealt with in paragraph 2.2.4. Particularly in brackish transition zones, where the salt seawater and freshwater from the river meet, there will be considerable settlement of the river's silt, due to coagulation (physico-chemical processes).

ad d. Wave action will influence the exposed parts of tidal flats and shoal edges. Depending on the extent of exposure and the shear and depth of the waterbody affected by the wind, sediments of coarse sand can, in conjunction with tidal currents, occur locally along the shoals and tidal flats. Conversely, on less exposed areas sediments of fine sand or silt can settle.

ad e. Finally, the composition of the sediment in an estuary can be determined by:
- Density currents, resulting from marked differences in temperature and salinity;
- Wind-induced longitudinal and transverse currents which can manifest themselves in the shallow areas along shoals and tidal flats;
- Tidal currents; the strenght of these tidal currents is determined by the extent of the tidal amplitude and the surface area of the basin.

In those parts of an estuary where density currents are absent or practically non-existent (i.e. a homogenous tidal inlet), the principal sediment-transporting mechanism is activated by tidal currents.
The basin geometry will also determine the shape of the current-velocity curve during the tidal cycle. In relation to this of particulary importance for the general sediment composition is the length of the period during slack high- or low-water in which the flow velocity is less than the threshold of movement of the sendiment.
In entrance areas of relatively simply constructed, elongated sea-arms, it can happen that the slack high-water period is shorter than the slack low-water period. As a consequence, a gradual seaward sediment transport can occur. Conversely, at the upstream end of an elongated basin, the current velocity pattern may be such that the slack high-water period is longer than the slack low-water period. This can be an explanation for landward sediment transport.
If the basin is long enough, this transport mechanism can bring about such a sediment distribution pattern, that „cells" are created each with its own individual composition of bed-sediment.
This general mechanism can be „disturbed" locally by tranverse circulation over the shoals and by secondary flow along the shoal and tidal flat edges. This can inter alia result in differences in depth-dependent sediment-gradients; the deeper channels will have coarser sediment, whereas finer grained sand will settle on the shoals.

The great diversity in the characteristics of an estuary such as current velocities, waves, geological composition and human action, will lead to wide differences in the sediment composition of the bed and in the morphology.
This applies not only to the higher, general level that determines the distribution of shoals/tidal flats and channels, but also to the lower level, such as the occurrence of ripple patterns in sandy sediments in channels and on shoals.

2.2.6.5. The biological system (flora and fauna)

An estuarine or other ecosystem generally comprises a great number of food chains, each in turn consisting of a number of links.
In such a food chain the preceding group will be consumed by the next group, e.g.

phytoplankton
↓
zooplankton
↓
shellfish
↓
fish
↓
birds/man.

In this example five links are shown, each representing a food or trophic level. In reality there are both within individual chains, and from one chain to another, many short-circuits, side-paths and double-functions.
The chain quoted, in fact, looks like this:

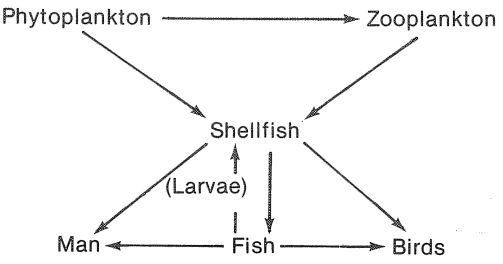

It would therefore be more exact to talk about a foodweb composed of many, interrelated, food-chains. Fig. 2.2.6.7. roughly indicates the appearance of a foodweb for an estuarine ecosystem such as the Eastern Scheldt. For further general schemes of foodwebs, see also Green, 1968 [26].
Within such a foodweb, the energy transport - or the transport of matter - in the biological system can be expressed in quantitative terms (i.e. the process side of the system description). This is shown schematically in Fig. 2.2.6.8. This diagram shows that the transport of matter is, in

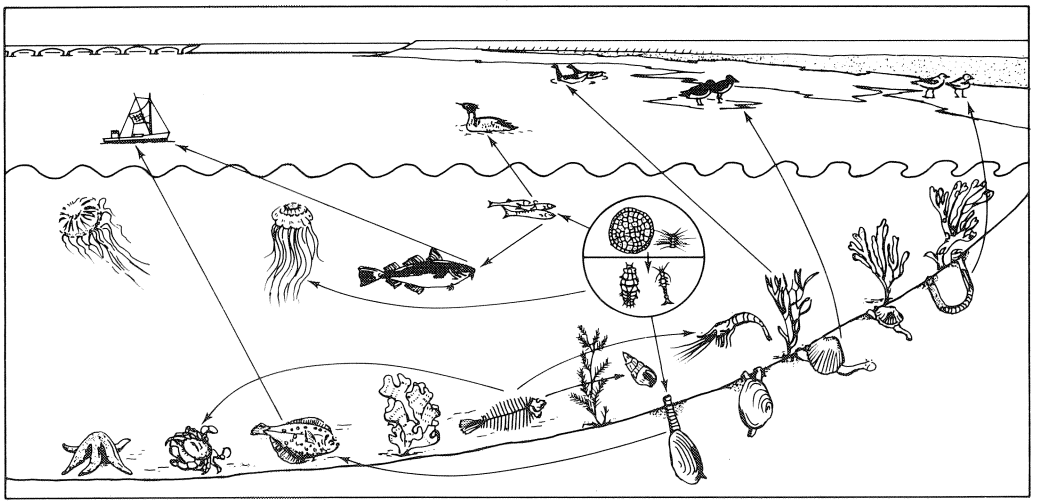

Figure 2.2.6.7. Some examples of food chains in an estuarine food web.

Figure 2.2.6.8. Diagram of the energy cycle in an ecosystem.

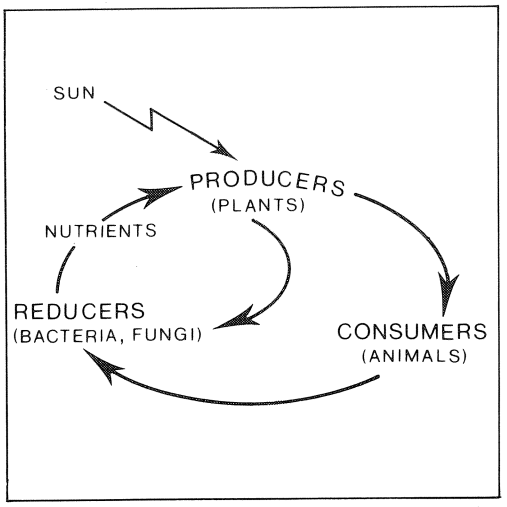

fact, a cycle. In this cycle, producers, with the aid of nutrients and sunlight, form plant matter, i.e. primary production or the first trophic main level. This plant matter is consumed by animals, which also prey upon another, i.e. the secondary production or the second trophic main level. The dead plants and animals will finally be converted (or reduced) into the original nutrients by fungi and bacteria: the third trophic main level. The cycle, thus closed, is regenerated by the sun, the supplier of energy.
In the following section the three previously mentioned trophic main levels will be briefly described, with emphasis on the first two levels, plants and animals.

First however, some of the terms used will be explained.
On closer examination, it is apparent that there are various types of „environment" in an estuary; for instance, the water, the sandbed and the stone bed. These environmental types are called „habitats". These habitats support plants and animals that often specifically belong there. In addition, it appears that certain species of organisms are always found near each other being, in a specific way, interdependent. This may be a „predator-prey" relationship, but also a „parasite-host" relationship. A

third possibility is real „symbiosis", i.e. a situation in which both partners mutually benefit. Thus, groups of organisms are formed which are often found together: these are called „biocoenoses".

The biological producers - the plants

The organisms in this „basis of the foodchain" all contain chlorophyll, the green substance at the heart of the photosynthetic process. This group comprises the following categories:

- in the water:
  - micro-phytoplankton - the unicellular algae suspended in the water, usually forming the largest category
  - micro-phytobenthos - the unicellular algae, which exist on, and in a thin layer under, the soil surface
  - multicellular sea-weeds and waterplants;
- on land:
  - unicellular algae;
  - multicellular plants (herbs, ferns, trees, etc.)

In saltwater, within the phytoplankton and even more so within the micro-phytobenthos, a very important group is formed by the diatoms. These possess selfmade minute shells of silicium covered with often extremely beautiful structural patterns. As these patterns are nearly always characteristic for one species, they can be easily recognized. In addition, plankton contains many dinoflagellates. Certain representatives of this group can cause the more or less toxic „water bloom" or „red tides" (named after the colour that massive occurrences of some of these species will give to the water). Many species of this group also produce shells, but in this case of a horn-like substance; other species are „naked" (i.e. without a shell).
In addition to these two large groups of algae, still other smaller groups exist which, however, will not be discussed here.

In freshwater other species exist than in saltwater.
The groups of phytoplankton in freshwater are, broadly speaking, the same: diatoms, dinoflagellates and micro-algae. A few of the groups are only found in freshwater. One group which can cause problems when it creates „algae-bloom" is the bacteria-related group of blue-green algae. This type of „blooming", which is peculiar to certain freshwater areas, can be toxic and in addition, when it dies off it can cause lack of oxygen for aquatic animals. Moreover, these waters filled with blue-green algae are often unattractive for holidaymakers. Finally, it is remarkable that, in freshwater, fewer multicellular weeds exist than in the sea, whereas, conversely, more higher plants are found in freshwater.
In addition to the saltwater species, an estuarine system will also contain freshwater and brackish water species. Their number will decrease in proportion to salinity, i.e. the nearer one gets to the sea. Some of the very salt-tolerant freshwater species can be found in the open sea, where they will eventually die, although they can remain alive for weeks. They are often indicative of freshwater inflow into the sea.

Throughout the world there are many thousands of species of phytoplankton. Within one estuary alone hundreds of species may exist. The numbers in which they are found can also be illustrative: from only a few specimens to millions of specimens per ml., whereas, per species, they may number from a few hundred to tens of thousands per litre.
Finally, the size of the individuals ranges roughly between a few μm and 500 μm. Many of the species form colonies which are sometimes so large that they are visible to the naked eye.

The third group of water-plants comprises the seaweeds, those are multicellular algae with something resembling stalks and leaves, sometimes fixed, sometimes in suspension, but never with a real root-system, and the higher forms of plantlife (the cryptogams and seed plants) such as eelgrasses in saltwater and various well-known water-plants in freshwater.

In principle the „terrestrial" algae hardly differ from the „water,, algae. The „terrestrial" plants, however, are provided with so-called supportive tissues, which are necessary as gravitation plays an important role above the water. The

plants generally consist of a root system, stems, branches and leaves and have an internal transport system for water and nutrients.
With regard to the terrestrial plants the higher zones of the intertidal area i.e. the salt marshes, will chiefly be described. In this zone, surface water, in addition to the specific terrestrial aspects, still plays a dominant role. Tidal difference, flooding frequency, salt and nutrients content, supply and/or discharge of silt and sand and the position in relations to wind and currents are important factors which determine whether or not vegetation can occur and which species of plants are able to live there.
The importance of, for instance, the flooding factor on the composition of the vegetation of a salt-marsh will be explained by the following example (fig. 2.2.6.9.).
A salt-marsh is intersected with creeks, bordered with higher-lying natural levees and lower-lying clay-basins. The flooding frequency and the period of flooding of a certain part of the salt-marsh is determined by its elevation: the higher the elevation, the lower the flooding frequency. The flooding frequency, in its turn, determines to a great extent the composition of the soil,the extent of maturation of the soil and the level of and fluctuations in soil salinity. When the flooding frequency is high, the soil is usually immature (soft and without oxygen) and the soil-salinity will hardly fluctuate; at a low flooding frequency, however, the soil is usually mature (firm and well-aerated), whilst the soil-salinity can show considerable fluctuations. In addition, one plant species will be better equipped to withstand periodic inundations than another. This combination of factors, i.e. soil composition, soil-maturation, soil-salinity, flooding frequency and duration, determines which plant species can grow in a certain part of the salt-marsh. Thus in fact, the flooding frequency plays a highly dominant role. Accordingly, the various plant species mainly occur in narrow zones parallel to the contour lines and with that to the flooding frequency. A more detailed description of this aspect is given in Chapman, 1977 [24].

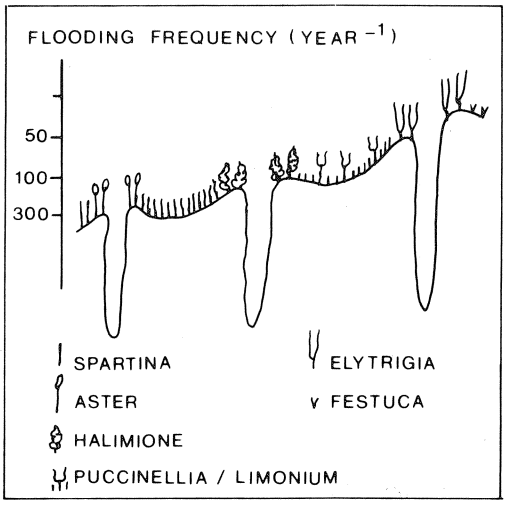

Figure 2.2.6.9. Cross-section of a salt-marsh, showing the distribution of some plant-species in relation to the flooding frequency.

The biological consumers - the animals
The primary production - plant growth - forms the food for the biological consumers. These can be divided into various groups: animal (zoo)plankton, shellfish, worms, fish, birds, etc. These groups, in turn, can be sub-divided into plant-eating (herbivorous), flesh-eating (carnivorous) and both plant- and flesh-eating (omnivorous) animals. As with plants, animals can also be divided into categories.
These are:
- animals passively floating in the water -zooplankton;
- animals actively swimming in the water -pelagic animals;
- animals living in and on the sea bed - benthic animals;
- terrestrial animals, whereby, in this context, special attention is paid to birds.

Fig. 2.2.6.10 illustrates some representatives of the three principal groups.

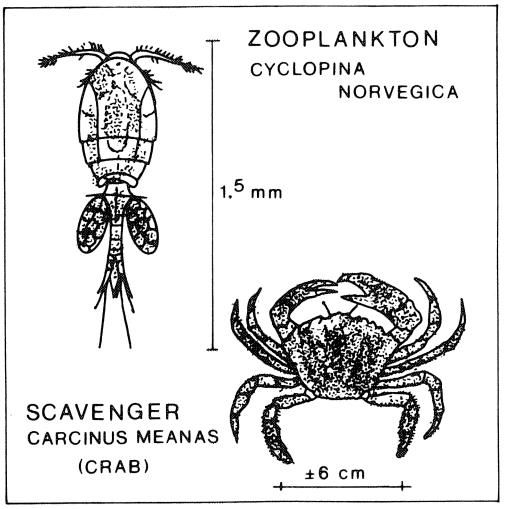

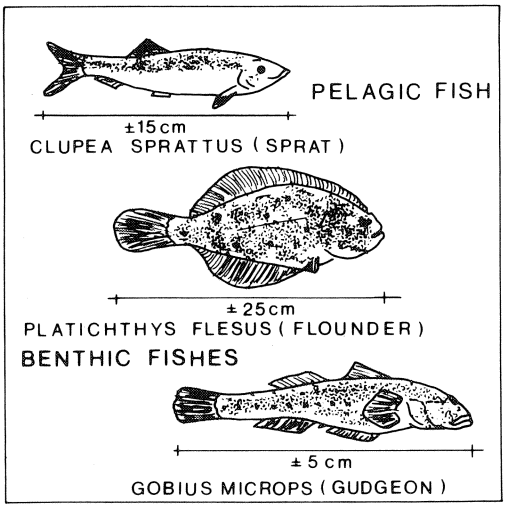

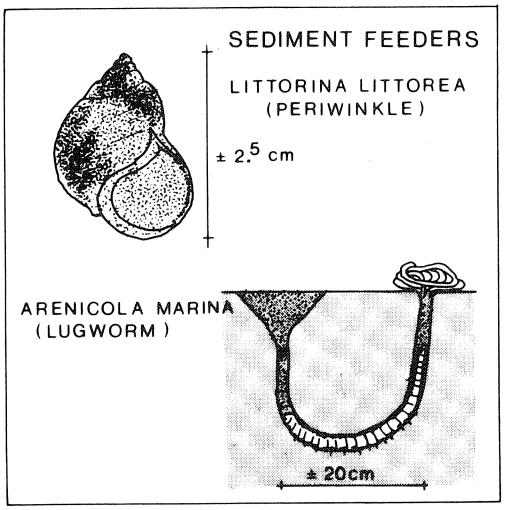

Figure 2.2.6.10. Examples of some groups of estuarine invertebrates (after Green, 1968 [26]).

The smaller zooplankton comprises, in particular, the Copepods and larvae of various species of animals. These larvae often live for a while (a few days to weeks) floating in the water, feed on phytoplankton and sometimes on other zooplankton and meanwhile gradually transform (by metamorphosis) into adult creatures such as crab, lobster, shellfish, starfish, sea-urchins and worms. Fish eggs and very tiny immature fish also belong to this type of plankton and they are eagerly eaten by many animals, especially fish. A typical and abundant member of the larger zooplankton is the jelly-fish, which is to a large extent at the mercy of currents. Jelly-fishes primarily feed on smaller zooplankton and sometimes also on smaller fish which they catch and stun with their tentacles in which nettle-cells are embedded that, when touched, release small poisonous darts. The stings of some sorts of jelly-fish can also be dangerous to man.

The group of pelagic animals mainly concerns fish, i.e. the „round fish" (in Western Europe, e.g. herring, anchovies, sea-pike, mackerel, sprat, etc.) Within this group, there is also a predator-prey relation.

In the group of species living in and on the sea

bed - the benthic animals or zoobenthos - a number of animal groups of a widely divergent nature can be found: the tunicates, the coelenterates, (such as sea-anemones and hydroid polypi), bryozoans, sponges, the coral type animals, worms, shellfish (such as bivalves and snails), the echinoderms (such as sea-urchins and starfish), the crustacea and fish. All play a specific role within the system as a whole. They are often subdivided into three groups: suspension feeders, sediment feeders, predators and scavengers.
Suspension feeders filter their food from running water or from water pumped „through their bodies". This food consists of small particles in suspension, of which both phytoplankton and „detritus" (dead organic matter) form an important part. E.g. Mussels, oysters, tunicates and sponges are equipped with a pumping system. On the other hand sea-anemones and other coelenterates as well as tube-worms are provided with a crown of tentacles that, standing out in the water, serves as a filter. Tube-worms are worms with a tube-like "shell", made from calcareous material, sand or pieces of shells, which they enlarge during their own growth-process.

One example of a sediment feeder is the lug-worm, which engulfs the sediment, digests the nutritious part and excretes the rest; as a result of this process worm-casts are created that sometimes completely cover particular parts of an intertidal area. Some bivalves, such as the baltic tellin, graze the bed with a small „trunk" (the sipho) in search of micro-phytobenthos and detritus. The periwinkle, a snail, does the same but instead of a sipho it uses its tonque, which is like sandpaper, to scrape small layers of algae from stones.
Predators and scavengers are animals that feed on larger living or dead animals. It is often difficult to differentiate between those two groups. Species, belonging to these groups include whelks, dog whelks (both snails), and the larger crabs, shrimps and lobsters. The shore-crab, a very common type of animal, subsists for instance on both carrion and live prey and even on plants; it is therefore sometimes called „the vacuum cleaner of the sea".

Finally, an important group of benthic animals are fish, which can be divided into two groups:
- the ones living on soft substrata, particularly flatfish (plaice, flounder, sole, etc.); whereas
- the hard substrata form the habitat for many „resident" fish. The fish in this group tend more or less to form their own territory. They are often confined to a „burrow" into which they can withdraw; this sometimes happens only during the breeding period, as with fish which attach their spawn to a base and then guard it until the eggs hatch.

With regard to „terrestrial animals" particular attention will be paid to birds, as many estuaries fulfil an important function for them, particularly waders, ducks, gulls, terns, etc.
Sometimes these birds can be found in large numbers in an estuary, usually as a result of the abundant food supply. Estuaries are important as breeding and moulting areas, and as feeding areas during the migration or wintering period. Within an estuary, the intertidal areas are particularly important as food sources for waders. It appears that each of the species of waders has its own specialised method of foraging for certain types of zoobenthos: the shape and lenght of the bill for instance partly determines the method of foraging and the type of food-organisms taken (see also fig. 2.2.6.11).

The principal abiotic aspects for plants and animals in an estuary are indicated in 2.2.6.2./3/4. These paragraphs indicate the way the individual aspects generally influence plants and animals. It will be clear, however, that the various abiotic aspects influence one another in their relations with the biotic components. For the salt-marsh vegetation this is already indicated, but it can also be observed in animals. As these correlations are very complicated and can differ per species or even within one species according to condition and/or stage of life, it is only possible to mention this aspect here. An example of such a correlation is shown in fig. 2.2.6.12, in which the relative growth of mussel-larvae is indicated as a respons to various combinations of temperature and salinity of the water.

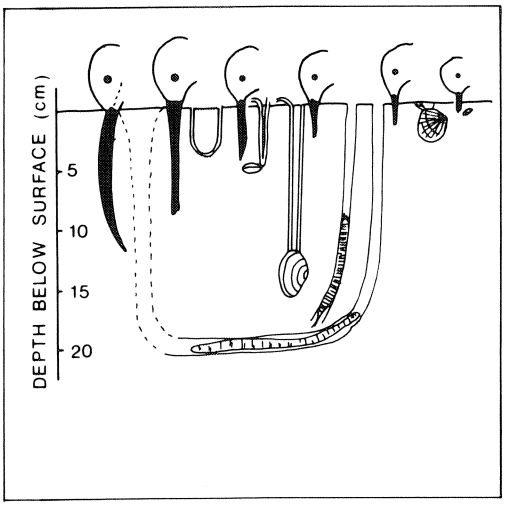

Figure 2.2.6.11. Relation between the length of bill of some common waders and the type and depth of burrows of some common mud-dwelling invertebrates (after Green, 1968 [26]).

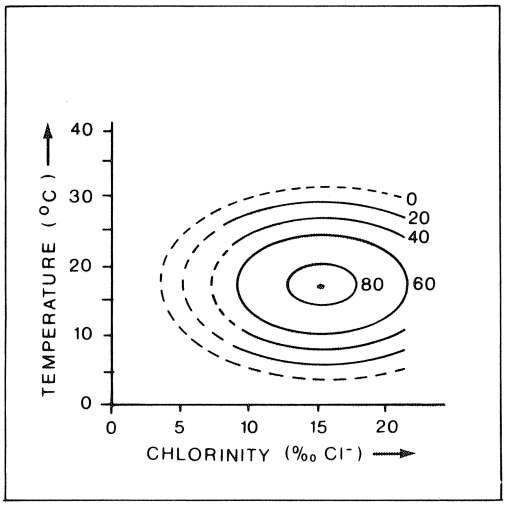

Figure 2.2.6.12. Growth of mussel-larvae for different combinations of temperature and chlorinity. Growth over a period of 16 à 17 days after the fertilization of the eggs, expressed in % of the greatest average increase in length per factor-combination (after Schmidt-van Dorp, 1980 [30], modified after Lough, 1974 [28]).

2.2.6.6. Literature

For a more detailed explanation of the fundamental aspects of aquatic ecosystems, reference can be made to [1,2,3]. [6] is considered to be the standard-work on the subject of physical and chemical water-quality in relation to biological processes in freshwater, but [7,31] can also be used as a good handbook. [8] offers a simple introduction into estuarine chemistry and [9, 10, 11, 32] provide a more profound analysis of both the abiotic and biological aspects in estuaries and coastal waters. Standard-works on chemical and biological aspects of marine systems are [12] and [13] resp. Useful sources of information on toxic substances are [14, 15]. [16, 17, 18, 19, 20, 21, 22] describe the morphological and soil mechanical processes, of which [16, 17] are more simple versions. [23, 24, 25, 26, 27], of which [26, 27] are more simple versions, describe in more detail the biotic component of the ecosystem. In [28, 29, 30] the combined influence of abiotic aspects on animals is discussed.

1. Collier, B.D., G.W. Cox, A.W. Johnson & P.C. Miller., **Dynamic Ecology**, Prentice/Hall International Inc., London, 1974.

2. Odum, E.P., **Fundamentals of Ecology**, Third Edition, W.B. Saunders Company, Philadelphia, 1971.

3. Barnes R.S.K. & K.H. Mann.,**Fundamentals of Aquatic Ecosystems**. Blackwell Scientific Publication, Oxford, 1982.

4. Redfield, A.C., B.H. Ketchum & F.A. Richards., The Influence of Organism on the Composition of Sea Water. **The Sea**, Vol. 2. Interscience, New York, 1963.

5. Burton, J.D., Basic properties and processes in Estuarine Chemistry. **Estuarine Chemistry**, J.D. Burton and P.S. Liss, (ed.). Academic Press, London, 1976.

6. Hutchinson, G.E., **A Treatise on Limnology**, Vol. 1 en 2. Wiley-Interscience, New York, 1957-1967.

7. Golterman, H.L., Physiological Limnology. **Developments in Water-Science 2**, Elsevier Scientific Publishing Company, Amsterdam, 1975.

8. Burton J.D. & P.S. Liss (ed.), **Estuarine Chemistry**, Academic Press, London, 1976.

9. Cronin, L.E., ed. **Estuarine Research,** Vol. 1 and 2, Academic Press Inc., New York, 1975.

10. Wiley, M., ed., **Estuarine Processes**, Vol. 1 and 2, Academic Press, Inc. New York, 1976.

11. Livingston, R.J., ed., Ecological Processes in Coastal and Marine Systems, **Marine Science**, Vol. 10. Plenum Press, New York, 1979.

12. Riley, J.P., G. Skirrow & R. Chester, ed., **Chemical Oceanography**, Vol. 1 - 7, Academic Press, London, 1975-1978.

13. Kinne, O., ed., **Marine Ecology**, Vol. 1 - 4, Wiley-Interscience, London, 1970-1978.

14. Förstner, U. & G.T.W. Wittmann., **Metal Pollution in the Aquatic Environment**, Springer-Verlag, Berlin, 1979.

15. Hutzinger, O., **The Handbook of Environmental Chemistry**, Vol. 1, 2 and 3, Part A. Springer-Verlag, Berlin, 1980.

16. Reineck, H.E. et al, **Das Watt. Ablagerungs- und Lebensraum**, Waldemar Kramer, Frankfurt am Main, 1970.

17. Mclusky, D.S.,**Ecology of Estuaries**, Heineman Educational Books Ltd., London, 1971.

18. Ranwell, D.S., **Ecology of Salt-marshes and Sanddunes**, Chapman and Hall, London, 1972.

19. King, C.A.M., **Beaches and Coasts**,Edward Arnold Ltd., Nottingham, 1972.

20. Ginsburg, R.N. ed., **Tidal Deposits**, Springer Verlag, New York, 1975.

21. Zenkovich V.P., **Processes of Coastal Development** (Steers, J.A. ed.)., chapter 7,8, Oliver and Boyd, Edinburgh, 1967.

22. Morgan, J.P., Depositional Processes and Products in Deltaic Environment, Deltaic Sedimentation, Modern and Ancient (Morgan, J.P. ed.), **Soc. of Econ. Paleont. and Mineralogist**, Special Publ. no. 15, 1970.

23. Remane, A., Die Brackwasserfauna, **Verh. Deutsche Zoöl. Ges.**, 7:34-74, 1934.

24. Chapman, V.J. ed., **Ecosystems of the World**, Vol. 1, Wet Coastal Ecosystems, Elsevier Scientific Publ. Comp., Amsterdam/Oxford/New York, 1977.

25. Whittaker, R.H., **Communities and Ecosystems**, Macmillan Publ. Co. inc., New York, 1975.

26. Green, J., **The Biology of Estuarine Animals**, Sedgwick & Jackson, London, 1968.

27. Perkins, E.J., **The Biology of Estuarine and Coastal Waters**, Academic Press, London/New York/San Fransisco, 1974.

28. Lough, R.G., A Re-evalution of the Combined Effects of Temperature and Salinity on Survival and Growth of Mytilus edulis Lar-

vae using Response Surface Techniques, **Proc. Nat. Shell-fis. Ass.** 64: 73-76, 1974.

29. Lehnberg, W., Theede, H., Kombinierte Wirkungen von Temperatur, Salzgehalt und Cadmium auf Entwicklung, Wachstum und Mortalität der Larven von Mytilus edulis aus der westlichen Ostsee, **Helgoländer wiss. Meeresunters.** 32 (1-2): 179-199, 1979.

30. Schmidt-van Dorp, A.D., De invloed van de watertemperatuur en het zoutgehalte op de groei van de mossel en andere makrozoöbenthossoorten, (Influence of Water-temperature and Salinity on the Growth of Mussels and other macro-zoobenthos species), **Hydrobia Research b.v.**, Sept. 1980 (in Dutch).

31. Wetzel, R.G., **Limnology**, W.B. Saunders Company, Philadelphia, 1975.

32. Mann, K.H., **Ecology of Coastal Waters, A System Approach**, Blackwell Scientific Publications, Oxford, 1982.

2.3. Site Investigations and data Acquisition

If the parameters that govern the most relevant phenomena are described in a format suitable for calculations, the parameter value under natural conditions should be measured.
Preliminary data processing and presentation should be carried out to prepare the data for generating project alternatives and decision making.
In this section various principles of measuring techniques and examples of data processing and presentation are given.

Site Investigations and Data Acquisition

W. van de Ree, J. Stuip

2.3.1 Measurement of stage

General

Water levels, stage or gauge height is the height of the water surface referred to a fixed zero level. Water levels are measured continuously or intermittently by depending on the object of measurement.

Objects of stage measurements may be:

- continuous
- stage-discharge relationship;
- establishing height of hydraulic structures;
- navigability (water depth);
- general statistics;
- intermittent
- reference level for bathymetric surveys, discharge measurements;
- checking relationships;
- determining lowest/highest water levels.

The accuracy of the measurement depends upon the purpose. For instance, observations for navigational objects may be less accurate than for checking a hydraulic model for an estuary.

Neap Tides: When the Sun and Moon are in quadrature, the two tidegenerating forces are acting at right angles to each oth producing a tide which has a higher low water than average a range which is smaller than at other periods.

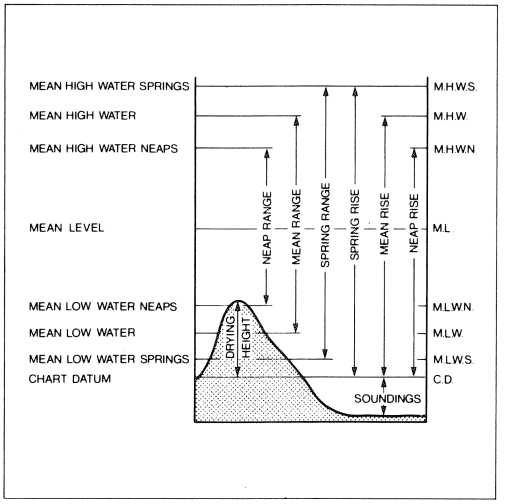

Figure 2.3.1.1. Diagram of specific tidal heights, stages and levels

Chart Datum is the plane from which the depths of all features either permanently or nearly permanently covered bij the sea are measured. It is also the plane from which the heights of all features, periodically covered and uncovered by the sea, are measured. The former are known as soundings, and the latter, are distinguished on the chart from soundings by underling known as drying heights. It is a fixed level below which all „soundings" on a chart are given and above which all „heights of the tide" are given in the tide tables.

Lowest astronomical tide (L.A.T.) is the lowest level which can be predicted to occur under (a) average meteorological conditions and (b) any combination of astronomical conditions. The level of L.A.T. is reached only occasionally and not every year. Lower levels than this can occur with particular meteorological conditions such as stormsurges.

The range of the tide is the difference between the level of any high water and that of the preceeding or succeeding low water.

The rise of the tide is the difference between the level of any high water and that of chart datum.

Mean high water springs or neaps is the average level of high water at springs or neaps.

Mean low water springs or neaps is the average level of low water at springs or neaps.

Mean level may refer to mean sea level, which is the average level of the sea at all states of the tide or to mean tide level, which is the mean of M.H.W.S., M.H.W.N., M.L.W.S and M.L.W.N.

The height of the tide is the vertical distance, at any moment, between the level of the sea surface and Chart Datum. Note that the tide tables give predicted heights which should not be confused with the depths of water.

Soundings on a chart are depths of water below the level of Chart Datum or mean sea level.

Drying heights on a chart are the heights above Chart Datum of all features which are periodically covered and uncovered by the sea.

The dept of water is the sum, at any moment, of the charted sounding and the height of the tide (or the difference, at any moment, between the height of the tide and the charted drying height).

The Height of the Barometer: When the atmospheric pressure is increased, sea level is lowered and vice versa. A varation of one inch (approximately 34 millibars) in the height of the barometer causes a variation of about 0.3 metre in the height of sea level.

The Direction of the Wind: In some areas sea level is raised on the coast towards which the wind is blowing and vice versa. If steady wind conditions are established these conditions will remain static until there is a change in the force or direction of the wind.

Stormsurges: These are phenomena caused by strong wind effects and may give rise to tides which rise or fall up to one metre above or below their predicted heights. These stormsurges occur for example in the southern part of the North Sea where, under exeptional circumstances, even greater variations may occur, particularly in the Helgoland Bight, on the Dutch coast and in the Thames Estuary. These surges occur when conditions, that have caused a raising or lowering of sea level in one part of the North Sea, are replaced in a short space of time by conditions with the reverse tendency. Such changes cause the sea level to oscillate between a high and a low level, the oscillations gradually dying out as conditions become stable again. Surges are generally caused by a deep depression travelling eastwards past the northern entrance to the North Sea.

The difference in specific electrical conductivity of air and water can also be used in the same way as for the wave measurements (electric stage gauge).

The presentation of the stage measurements may be analogue or digital, the system used depending on the data required. The table below provides a comparison between visual, analogue and digital measurement/presentation for various aspects.

Table. Evaluation of measuring techniques for various aspects

aspect \ method	visual	analogous	digital
reliability	observer dependent	instrument dependent	instrument dependent
accuracy	variable	variable	variable
frequency	low	infinite	high if desired
decision*	logic	programmed	programmed
costs	low	higher	highest
computer compatible	mostly not	no	mostly yes

*whether to make a registration or not

Measurement of Stage

Definition of various stages

Tidal Definitions
The Lunar Tide: The result of the tidal force arising from the gravitational effect of the Moon only. Due to the relative proximity of the Moon it is the major tidal force.

The Solar Tide: The result of the tidal force arising from the gravitational effect of the Sun only. The solar generating forces are less than half those caused by the Moon.

Spring Tides: When the Sun and the Moon are in conjunction (New Moon) or in opposition (Full Moon) the two tide-generating forces are acting on the same meridians, so the height and range of the tide will be greater than at other periods. Spring high waters tend to occur at about the same time at any one place.

Stage or gauge height observations are used in combination with other parameters and relations for monitoring the behaviour of the river, estuary or basin.
For rivers a series of gauge readings over a year gives a hydrograph.
A series of hydrographs gives the duration curves, i.e. the probability of occurrence of waterlevels for the particular station. If the relation between stage and discharge is known from measurements, duration curves can be transformed into discharge duration curves.
The gauge height record of a basin, lake or reservoir provides, in addition to data on elevations, indeces for surface area and volume of the water body.
In tidal areas the stage in the estuary gives information about the tidal motion.
based on historical data, predictions can be made for the cyclic tidal motion.
If the relation between velocity, discharge and the stage is known, predictions for the horizontal tidal motion can also be made. The impact of meteorological effects can be studied from historical data if (hindcast) predictions for the water level elevation are available.
In this way the probability of occurrence of wind set-ups can be obtained.
For the operation of a stromsurgebarrier, sluices and also navigation locks, short-term predictions and consequently actual measurements of gauge height readings are indispensable.
Stage data are also of direct use for navigation, flood predictions, water management and acceptable waste disposal etc.

A record of stage may be obtained by systematic observations of a non-recording gauge or by means of a water-level recorder. The advantages of the non-recording gauge are the low initial cost and ease of installation. The disadvantages are the need for an observer and the lack of accuracy of the estimated continuous stage graph drawn through the plotted points of the observed stage. For long-term operation the advantages of the recording gauge far outweigh those of the non-recording gauge and the use of the non-recording gauge as a base gauge is not therefore recommended. However, at a recording gauge station, one or more non-recording gauges should be maintained as auxiliary gauges for the operation of the station. Telemetering systems are used to transmit gauge height information to points distant from the gauging station.

Datum of gauge

The datum of the gauge may be a recognised datum, such as mean sea-level, low-water-spring, or any arbitrary plane chosen for convenience.
As a general (practical) rule a permanent datum for all stations should be maintained to avoid possible confusion by evaluations of historical data for various stations.
To maintain a permanent datum each gauging station requires at least two or three reference marks; that is, permanent points of known gauge height elevation that are indepedent of the gauge structure.
The datum at each gauging station is periodically ckecked by running levels from the reference marks to the gauges at the station.
If an arbitary datum plane is used, it is desirable that it is referred to a bench mark of known elevation above mean sea level, so that the arbitrary datum may be recovered if the gauge and reference marks are destroyed.

Site selection

The selection of gauging sites is dictated by the need for water level data. The location of the gauge is, for example, immediately fixed if discharge data are needed for the operation of a sluice.

In the case of a general study of the hydrology of an area, however, careful judgement will be required.

There are, therefore considerations for determining the general location of the stations in a network, and considerations for the precise location for obtaining reliable data referring to the complex hydraulic conditions at a given station.

The literature provides guidelines for gauging-station network design (see e.g. Meteorological Organisation, 1974: Guide to Hydrological Practices, WMO-nr. 168).

In general, a water resources development network will consist of primary and secondary stations. The primary stations operate permanently to establish the behaviour of the river over time, including dry season flow, peak floods, trends etc. The secondary stations operate long enough to establish the hydrological characteristics of the region.

General coniderations for the proper installation of a specific gauging station are given in World Meteorological Organisation, 1980: Manual on Stream Gauging and International Standard Organisation; 1969: Establishment and Operation of Gauging Stations and Determination of Stage-Discharge Relation.

In general the following considerations are suggested:

- reasonably straight river reaches should be selected in order to avoid transverse slopes of the water surface, especially under high discharge conditions. If, for any reason, the location of a gauge in a river bend cannot be avoided, the possibility of siting gauges near both banks, thus enabling the determination of the mean water level in the cross-section, should be considered.
  This may be often the case in estuaries:
- the site should not be unduly exposed to the wind. The effects of waves and turbulence can be avoided by application of special devices;

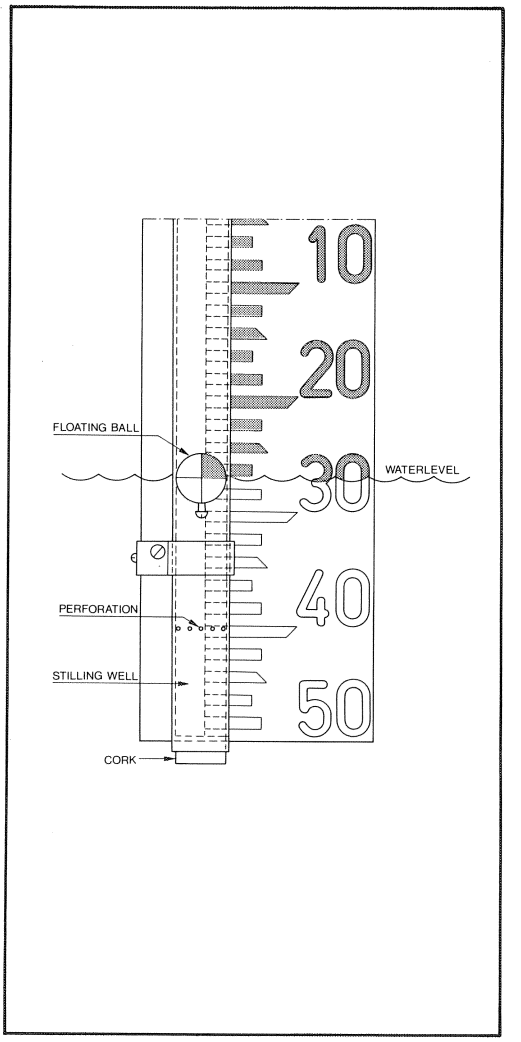

Figure 2.3.1.2. Simple stilling well, floating ball and graduated scale.

- the site should be easily accessible, preferably even under high-water conditions.;
- the lengths of the gauges should cover all variations in water level;
- if gauges are placed expressly to provide data on water level during floods, they should be located near critical points;
- normal gauges measure the static head; sometimes a stilling well is preferable to give the water level in order to dampen fluctuations caused by wind and turbulance and to protect the gauge.

Instruments

In general a gauge consists of two elements: a device to monitor the interface between air and water, and an instrument that shows directly, by analogue or digitally the level of the interface with respect to a reference datum.

As air and water have significantly different physical properties, various principles to detect these can be used. The most widely used property is specific density: water is approximately 1,000 times heavier that air.

Other techniques make use of difference in sound propagation (echosounder upside down) and differences in electrical resistance (also used or wave-height measurement).

These principles have been used by various manufacturers in a wide range of instruments. Details may be found in the manufacturers' specifications and in the general literature (eg. the WMO publications as referred to above.)

Instruments may be grouped in recording and non-recording gauges or stations.

The staff and wire-weight gauges are of the non-recording type.

The staff gauge consists of a graduated gauge plate fixed vertically or at an angle to a stable structure.

Sometimes there is a stilling well with a floating index to the gauge (see figure 2.3.1.2).

The float-tape, electric-tape, chain-gauge are variations on the wire-weight method, where a body is lowered until it floats on the water to be gauged and a reading is taken from a marker or a scale.

The presentation of the sensing (monitoring) of the level of the air-water interface with these

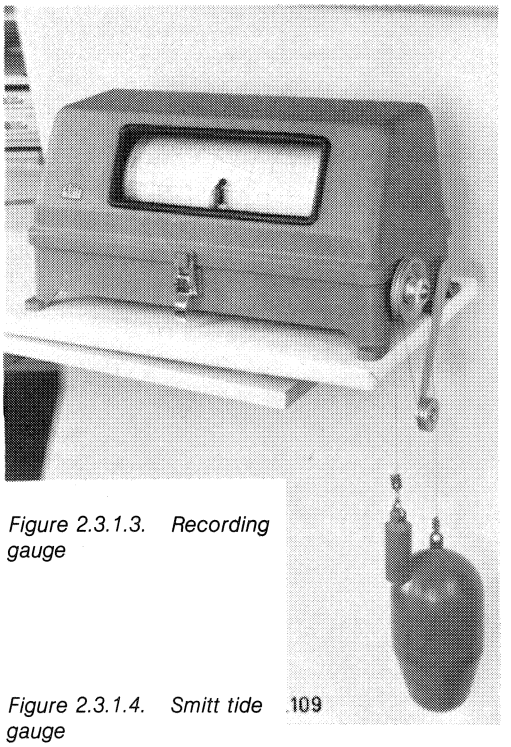

Figure 2.3.1.3. Recording gauge

Figure 2.3.1.4. Smitt tide gauge

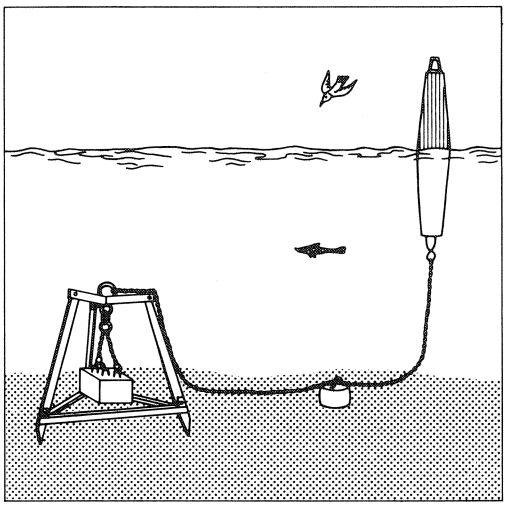

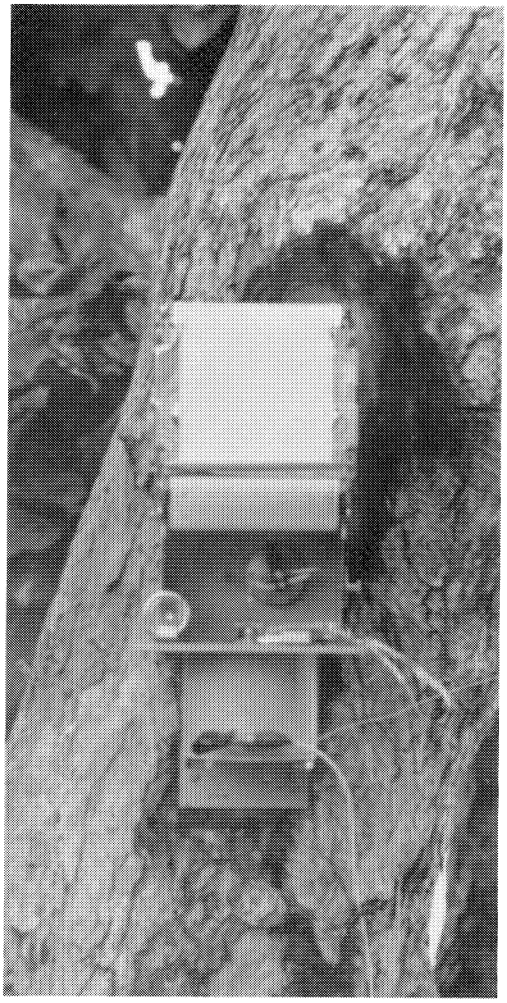

Figure 2.3.1.5 Shore based recording gauge, pneumatic type

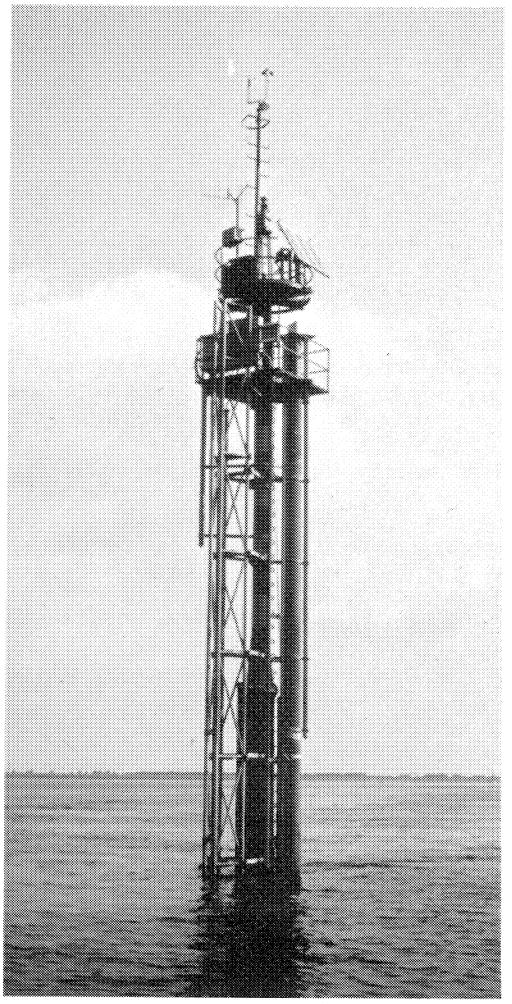

Figure 2.3.1.6 Date collecting platform at Haringvliet.

type of gauges can be recorded at an analogue (electrical or autographic) or digital manner.
Then the instrument is a recording gauge (see figure 2.3.1.3).
Also the so called pneumatic gauges can be recording instruments. In this type the weight of the column of water is measured either by a diaphragm fixed at a certain depth or by a pressure which is needed to produce bubbles from an orifice of a tube at a certain elevation in the river. These types of instruments do not need stilling wells.

The recording units may be installed under water (e.g. the so-called Smitt tide gauge) shore based or on platforms in the water (see figure 2.3.1.4).

The required accuracy of a gauge-height measurement is in the order of 0.5 to 2 cm depending on the object of the measurement.
The precision of the various instruments is given by the quality of water-level measurements and the recording instruments. The accuracy of measuring the gauge-height with reference to the datum also depends on the accuracy of the levelling of the zero index on the gauge with respect to the datum. Due to settlement or uplift of the gauge structure or its support (bridge, pier) the gauge datum and consequently the accuracy of the measurement, may be disturbed.
For wire-height and float-tape gauges, slippage of graduated discs or indices may introduce erroneous readings. Twisting and untwisting of the wire is another source of error.
The accuracy of float-operated instruments is influenced by:

- float-lag; there is a force required to move the float, the float-lag being proportional to the diameter of the float;
- line shift: the weight of the float tape passes the float pulley and changes the depth of flotation;
- the submerging of the counter-weight.

The inaccuracies inherent in bubble-gauge systems stem from gas friction, variations in bubble feed rate and variation of the gas column with stage.

Figure 2.3.1.7 Probability of exceedance of high water level in the Eastern Scheldt.

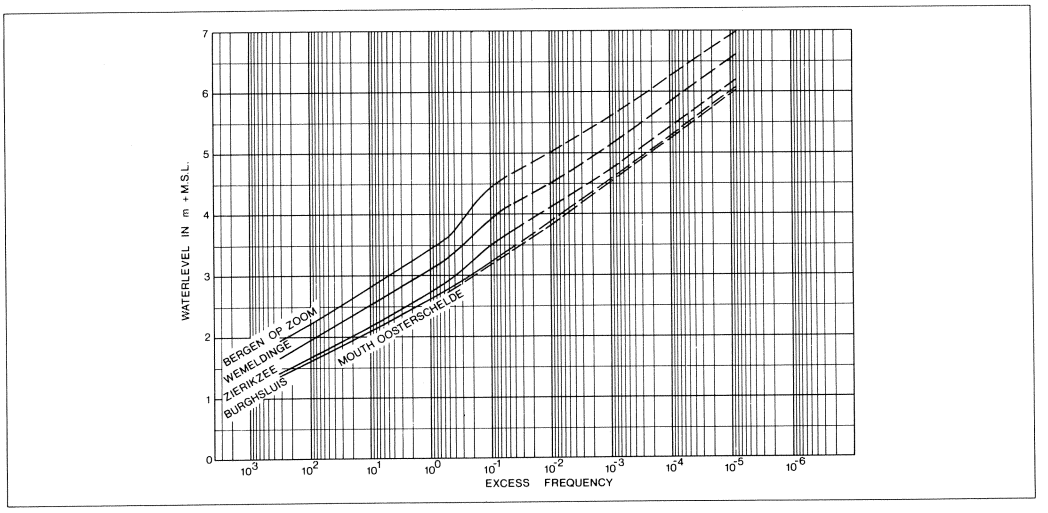

Data processing

Data processing starts with the collection of data in a specific form from the (recording) instrument or even from the note-book of the observer.

After transportation it then passes through the administration of an office or division and is stored in files.

Some basis statistics may already have been compiled for presenting and storing the data in a comprehensive way.

The data are then used and calculation made for special studies.

During the process from data recording to data processing there is a high risk of error.

Many persons and steps are involved. The persons who play a part include the engineer or scientist who asks for the data, the person responsible for daily maintenance, tape replacement etc., the local coordinator, technicians for maintenance of the data transporter, persons involved with initial ckecking of the data, analysing and retrieving faults, and the data user.

The proper operation of the whole system is moreover complicated by the fact that observation errors are often only discovered weeks later by persons miles away from the point of observation.

Strict attention should therefore be paid to the early detection and correction or- better still- prevention of faults before any substantial degree of processing.

Apart from these more or less organisation-induced faults, the quality of recorded data depends on the observation interval and is affected by errors in recording or punching etc.

The time clock in the instrument may be slow or fast, there may be an interruption so that the series of data seems too short, errors may occur in punching for administrative purposes or of the phenomenon, etc.

Errors due to improper measurements or sensing will also result in inadequate data.

It will be clear that checks or even double checks should be made to improve the reliability of the gathered data as soon as possible after collection and certainly before processing.

Methods have been developed to check reliability, such as sequence of process values, double

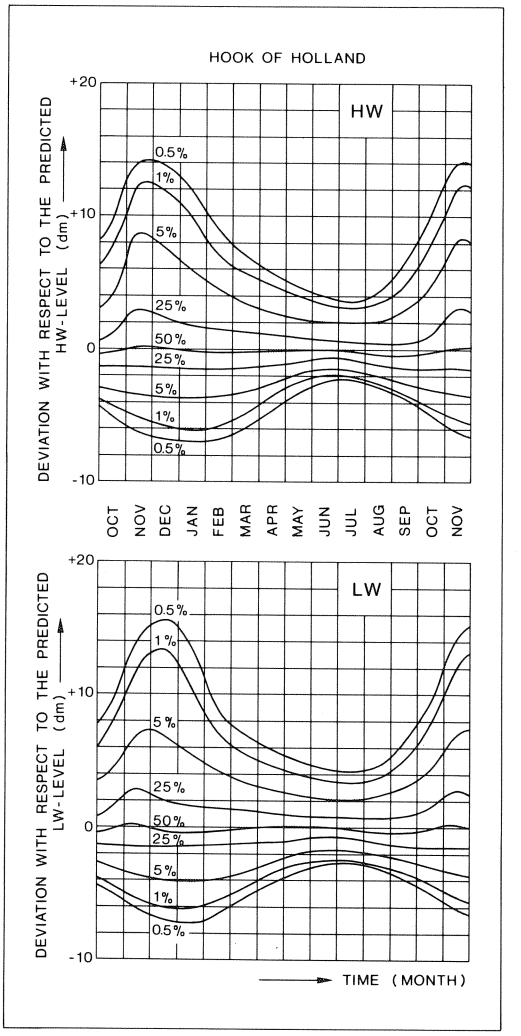

Figure 2.3.1.8 Probability of deviation from predicted astronomical tide for station Hook of Holland and low tide for the same station

mass curve techniques and exceedance of physical limits etc.
The length of the measuring interval greatly depends on the nature of the phenomenon. In many cases, discrete data are collected in equidistant series. Sometimes however, non-equidistant series yield much less data without appreciabele loss of information.
The actual processing of checked data depends on the character and use of these data and is merely a transformation of the collected data in a form that meets the requirements of the user.

Processed data about water levels can be presented in the form of a hydrograph. This is mainly suitable for river stretches. In delta areas, where tidal motion governs the behaviour of water level fluctuations, processed data are presented as tidal constituents, or as the probability of exceedance of a certain (high or low) water level (see figure 2.3.1.7).
Tidal constituents may be calculated from the time series of water level observations.
With these data, tide predictions can be made with respect to astronomical tides.
The effect of meteorological conditions can be calculated with physical models or with the aid of historical data and regression analysis of the parameters.
If these conditions statistically known for a specific station, actual deviation from the astronomical tide can be predicted with a certain prohability.
Figure 2.3.1.8 gives a probability diagram for high and low tide for the station of Hook of Holland.

The relationship between stations along the river can be presented in stage-relation curves.
In these curves stage at a specific station is given with reference to the stage in a base or reference station.
This method holds only when fluctuations in the river are slow and gradual, i.e. for steady conditions.
The approximate travel time of flood waves is indicated in the stage-relation curves (see figure 2.3.1.9).

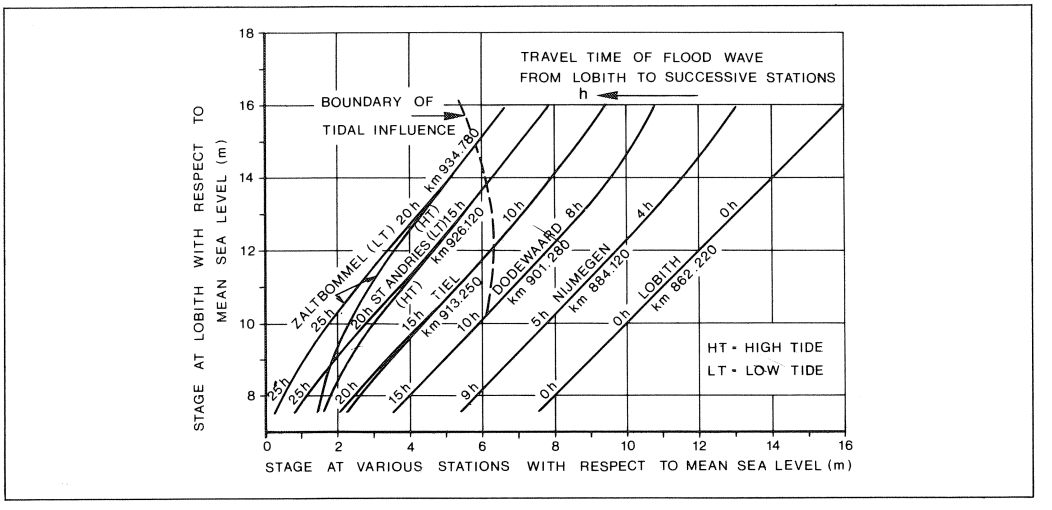

Figure 2.3.1.9 Stage-relation curves along a river (Waal, Netherlands).

In tidal regions these stage-relation curves are determined by the tidal constituents and the geometry of the basin. The tidal wave is attenuated due to bottom friction and amplified due to narrowing of the tidal channels and reflection at the end; resonance may occur.

Site Investigations and Data Acquisition

W. van de Ree, J. Stuip

2.3.2. Wave measurements

1. General

In general wave-height observations can be made either directly or indirectly.
Directly means a visual observation of the fluctuating interface between air and water. The accuracy of visual observations can be improved with the aid of a reference level and a graduated scale.
Indirect measurements are based on the difference between the physical properties of water and air, viz. the specific density or specific electrical resistance.
This chapter provides some examples of instruments based on the various principles but does not pretend to be a complete treatment of all available wave measuring equipment.
The methods have been classified in terms of their historical development, starting with the older instruments based on visual observations. These are followed by the group of mechanical-measurement instruments, with manual evaluation of data. Finally the category of electronic equipment and computer data processing is discussed.

2. Visual wave-height estimation

Before equipment was available, estimation of the wave height by eye was the only available method. It is clear that this method, without any aids or appliances, is extremely difficult and inaccurate. This inaccuracy increases with the wave height; under these conditions waves are nearly always judged to be higher than they really are.
In 1956, however, the location of the Haringvlietdam in the Netherlands and the height of the cofferdam around the building site for the sluices were determined based on such conventional wave measurement observations. Twice a day a survey vessel manned with observers left Hellevoetsluis and took position near the mouth of the Haringvliet close to some navigational buoys and judged the wave height visually.
Due to the length and frequency of the observation periods the results were more or less acceptable.

Fixed or floating wave beacons provided a reference level, thus increasing the accuracy of the estimates.

A floating wave beacon consists of a closed aluminium tube with decimeter callibrations in different colours. The beacon is connected by means of a thin cable to a large, flat damping plate anchored below water level in a shallow channel at a depth of between ½L (L = wave length) and (as a maximum) ¼L. This means that the plate will be in a water layer no longer affected by orbital motion.
In order to facilitate retrieval, the beacon is attached to a buoy by means of a heaving line (see figure 2.3.2.1). Observations with a floating wave beacon are generally made form a measuring vessel.

Observations with these gauges should preferably be performed by two observers: one

Figure 2.3.2.1 Floating wave beacon.

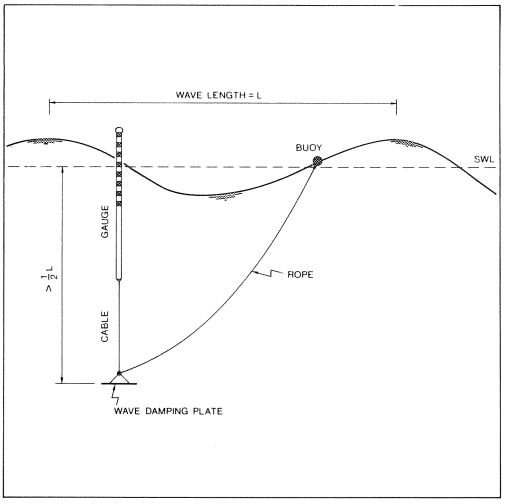

to observe and the other to enter the data read to him on the data sheets. First the height of the wave crest next to the wave trough is read.
From a series of 100 observations the significant wave height can be determined. The significant wave height is defined by taking the average of 1/3 of the highest waves in the observation period.
It is emphasized that the significant wave height determined by the above method is less accurate than when defined by instruments to be dealt with later.

3. Wave registration

The previous methods of observation are far from ideal. Some of disadvantages are that the information obtained is limited as regards both duration and accuracy; the method employed is cumbersome and it is practically impossible to measure waves during storms. In order to circumvent these difficulties we should avail ourselves of an instrument which - attached to a gauge - is able to register wave movements continuously.
The complicated wave movement at a fixed point on the surface can be considered as a point where wave trains coming from different directions pass by. This passing manifests itself in quick, successive changes in water level. The measurement of waves can be considered as the measurement of fluctuations in water level. Based on the above considerations three instruments were developed:

- wave-amplitude recorder;
- electric stage-gauge;
- wave buoy.

Wave amplitude recorder

The wave amplitude recorder was developed by P.J. Wemelsfelder and is often referred to as the Wemelsfelder recorder.
The instrument at the gauge records wave movement by means of a float.
To this end a tube housing the float contains vertical slits 2 cm in width and 60-80 cm in length forming a spiral. Each successive slit is moved 90° from the preceding one. In this way the position of the float tube is indifferent to the current and wave direction.
The vertical movement of the float is converted into horizontal movement of a steel recording pin by means of a wire and wheel attached to the float and a wormgear. The pin scratches the wave movement on waxed paper. The recording pin movement is reduced to 1:50 of the float movement.
The range of the instrument should cover the lowest wave at LLW to the highest wave crest at HWS.
Saving registration paper, and thus extending the period over which observations can be recorded, forms the reason why the instrument is constructed in such a way that of an integrated vertical movement of 300 m only 60 meters are recorded and 240 meters are not. Each time, the wave amplitudes are recorded in a compact shape of 6 mm covering a 60 meter wave-height integration. The next 240 meter wave-height integration is not recorded and no paper transport takes place. The wave registration consequently appears as a number of consecutive blocks.
Of every tenth block the first part is registered in an extended form.

To make this kind of recording a spring is wound by the waves and is released once every 3000 meter wave-height integration with the result that the registration paper is moved with a speed of 1mm/sec. during 72 seconds, thus producing a time wave-height diagram.
When the recordings are analysed the „extended" recordings serve a very good purpose.
In coastal areas a single roll of recording paper is sufficient to cover an observation period of 3 to 4 months.

Nowadays a modified version is available in which the pin and the waxed paper are replaced by an electrical signal and a magnetic tape.
The moving pin operates a potentiometer which in its turn governs the frequency of an electric signal. The clockwork governs the signal of an other frequency generator. Both signals are stored on a magnetric tape and can be processed by a computer to evaluate the date in statistical terms of the measured wave time series.

The electric stage-gauge

This instrument was developed by the

„Technisch Physische Dienst TNO T.H.", Delft, Netherlands.
The electric stage-gauge consists of a bundle of electric wires, strengthened by steel wire and bound by smooth vinyl tape, the ends attached to 200 electrodes spaced 4, 5 or 6 cm apart.
The action of the electric stage-gauge is based on capacity measurement making sure of the difference in conductivity between water and air. In the air - above water - the electrodes are isolated from each other outside the cable but inside the cable are connected in parallel by a series of 200 condensors.
By means of self-induction, the electric stage gauge as a whole forms a circuit with a variable frequency of resonance. Wave action causes one or more electrodes to be short-circuited. Depending on the number of electrodes thus affected a change is instigated in the resonance frequency.
The frequency varies between 1000 and 3000 Hz. The capacity of the condensors is chosen in such a way that the changes in frequency are in 200 even stages of 10Hz. each.
In the original set-up the electrodes were like stems sticking out from the main „tree" with seaweed adhering to them causing „shortcuts". These were later replaced by circular electrodes which do not protrude from the „smooth tree". A disadvantage of this smooth type, however, is that oil floating on polluted water can stick to the gauge, thus causing shortcuts between the electrodes and affecting the registration.
Shore based registration is used. The changing frequency, modulated on a frequency of a carrier wave 420 à 450 MHz, is transmitted by a battery fed transmitter on the gauge to the receiving station ashore.
Signals are transmitted each 0.2 seconds. The signals thus transmitted are received by a receiver situated ashore.
The signals thus received are futher dispatched by telephone line to the office responsible for analysis and measurement. The signals once received are converted and recorded as changing water levels or wave action (figure 2.3.2.3).

Actual registration is performed by a pen recorder (Sefram-recorder) and on punch tape. Signals are transmitted each 0.2 sec. while

Figure 2.3.2.2. Wemelsfelder wave height recorder.

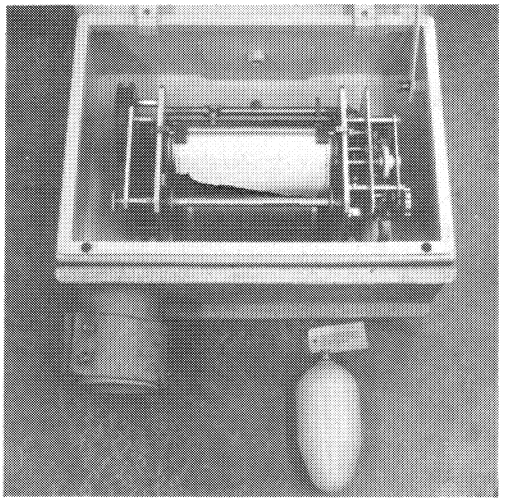

fivetimes a second a coded figure is punched in a tape; this code corresponds with the number of electrodes submerged at that time. The analogue Sefram-recorder performs in a similar way, recording the number of „shorted" electrodes at that particular moment.
This visual registration is necessary as punchtape registration without visualisation makes the tracking of any irregularities extremely difficult.

„Waverider" buoy
The „waverider" is a buoy containing an inertial accelerometer for wave-height measurement. The buoy has been designed for moored and free-floating operation.
The acceleration from the vertical displacement at sea is measured. The accelerometer is pendulous, suspended in a special damping fluid. This acceleration is transformed in the buoy into

Figure 2.3.2.3 Wave height registration in a central recording office.

a frequency-modulated signal on a subcarrier of 259 Hz. The signal is then fed into the transmitter, is operating in the 27 MHz. band. The complete waverider system consists of a stainless steel buoy, a ¼ L polyester glassfibers whip-antenna, (¼ L= transmitter wave length) fastened into the detachable roof-hatch and a mooring line of polyopropylene or nylon-covered steel rope, with a special rubber cable, with stainless steel terminals and swivels.

Figure 2.3.2.4 Waverider (Datawell buoy).

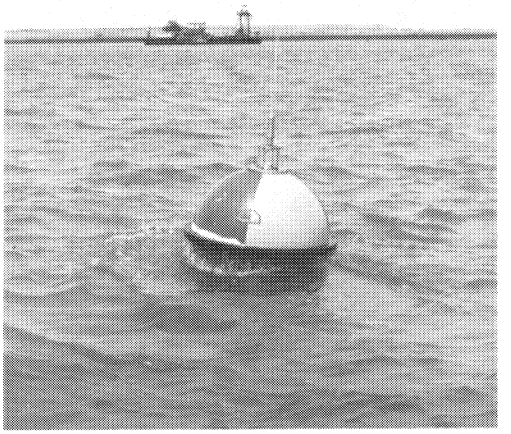

Due to the elastic anchoring system a larger force from the floating buoy is needed for shallow waters. This means a larger buoy for undeep water. Wave recording is given to the receiver ashore, so that information is directly available and the proper functioning of the buoy can be checked daily.
If the receiver is connected to a tape recorder the signal can be stored on magnetic tape for further computer processing via an analogue-digital convertor.
Waveriders transmit continuously on a battery pack lasting 9 months while at the receiving station the receiver can be programmed to record the wave information at certain schedules or continuously.The instrument is very useful both for long term and short term acquisation of data about wave period and height for offshore engineering coast protection studies, and harbour designs etc.

Evaluation
With regard to the performance of the aforementioned instruments the wave-amplitude-recorder is extremely reliable. As such it may be recommended for gathering monthly and yearly statistics. The recordings have, however, to be elaborated manually.
Little use can be made of these recordings for detailed studies of wave motion. The most frequent cause of interrupted recordings is the breaking of the - nylon - float thread.
Given the availability of punch tape, however, the electric-stage-gauge offers the possibility of computer processing and is therefore suitable for extensive studies of wave action.

The wave buoy has in general the same advantages as the stage gauge but installation is easier.
The precision of the measurements can be affected by currents, which can exert a horizontal force on the buoy and hamper the buoy motion used for measuring wave movement.

Wave measurements based on pressure fluctuations due to wave action are suitable for deep water-conditions where wave gauges are expensive or even impossible. A range of these type of instruments is available with various methodes of registration and data processing.
By averaging water-level fluctuations due to (wind) wave action over 3 to 4 minutes it is also possible to determine long periodical (tidal) fluctuations.

4. Use of aerial and radar photographs
Most wave-measurements instruments determine wave-height and period as a function of time. The direct measurement of wave direction has not proved feasible so far.
An important aid in determining wave direction consists of aerial and radar photography. This provides a particularly useful means of tracing changes in wave direction resulting from changes in water depth.
Determining the wave pattern by means of aerial photography is, however, subject to distinct limitations, being as it is highly dependent on the altitude of the cloud cover, the position of the sun and visibility. In heavy winds - when the observation of wave patterns is particularly im-

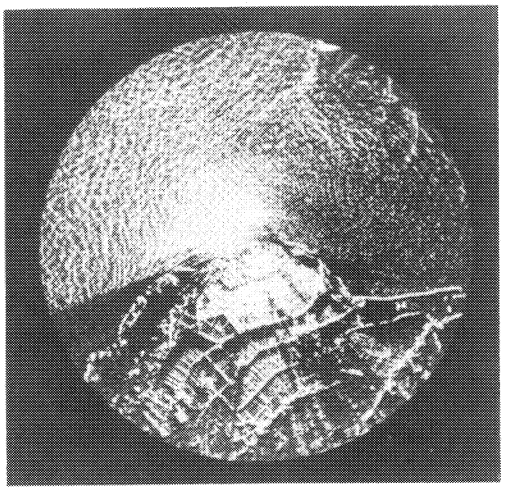

Figure 2.3.2.5 Radar image and interpretation of wave field „Veerse Gat" (south-west Netherlands).

Figure 2.3.2.6 Frequency curve of significant wave height Haringvliet (South-West Netherlands).

portant - it is often impossible for aerial photography flights to be made.
This technique is moreover very costly, so that only occasional observations can be made, thus limiting the usefulness of aerial photography for wave research.
A superior method for establishing wave patterns consists of the use of radar, with which observations can be made during a storm or at any time desired. Radar with a wavelength of 8 mm is particularly effective for recording radar beams reflected off waves. The reflective capacity derives not so much from the shape of the wave fronts themselves as from the minor wind ripples superimposed on the overall wave pattern.
In addition the leading wave shields the succeeding trough, so that the radar beam will only reach and be reflected by the area immediately in the vicinity of the wave tops. The result is that a wave crest will appear on the radar screen as an illuminated line, with succeeding crests showing up as separate, parallel lines. The image appearing on a radar screen can whenever desired be captured in photographic form.
Radar photographs of this kind are not directly suitable for interpreting the wave pattern: the principal lines of the wave movement need instead to be transferred onto a map by projecting

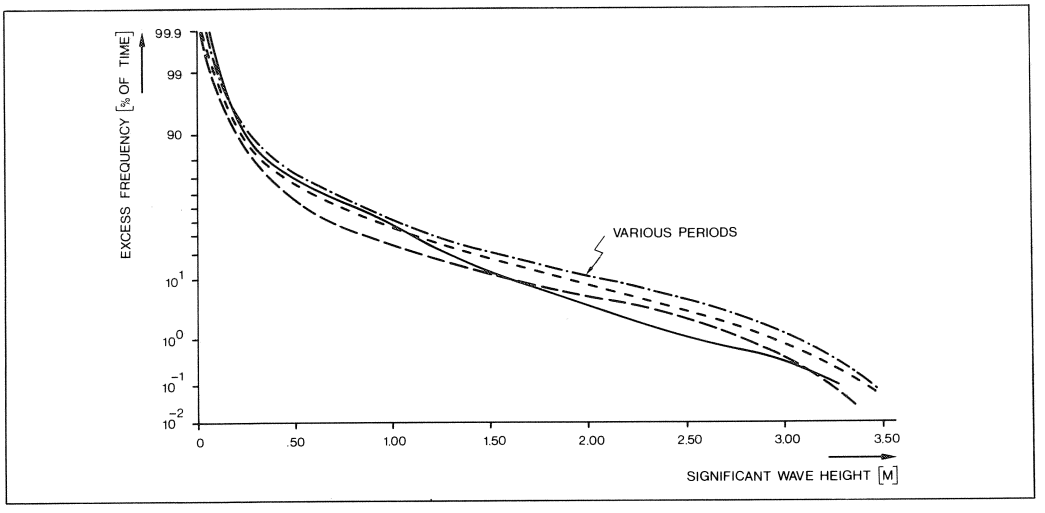

the photograph. Figure 2.3.2.5 shows a radar image and the wave-pattern map derived from it for the mouth of the Veerse Gat in the Eastern Scheldt. The map also indicates the position of a recording wave-measurement post. With the aid of the data recorded by the post (i.e. wave height and period) and the idealized pattern constructed from the radar observations, it is possible by calculation to determine the wave-height and period at any selected point in the surrounding area. The range covered by radar for determining the wave pattern depends heavily on the height of the radar unit; at a height of 20 metres it is around 1.5 km.

5. Presentation of wave data

Wave data gathered for the realization of hydraulic structures contains information on wave height and wave period, both preferably in terms of statistics. These parameters are related to water level (water depth) wind direction, and wind speed. In many cases the statistics for or prediction of these parameters are better known or more reliable than the wave parameters. These relationsships are often used for determining wave loads, workability, etc.
Figure 2.3.2.6 gives a frequency curve of significant wave height for a location in Haringvliet. Figures 2.3.2.7 give a polar presentation of wind speed, wind direction and significant wave height for a location in the Eastern Scheldt.
Figure 2.3.2.8 gives a wave spectrum for a location in the Brouwershavense Gat (BG2).

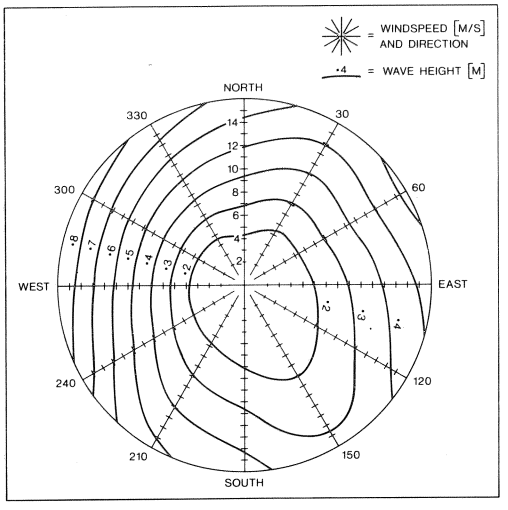

Figure 2.3.2.7 Windspeed, wind-direction and significant wave height, locations WR 4 and BGI (South-West Netherlands).

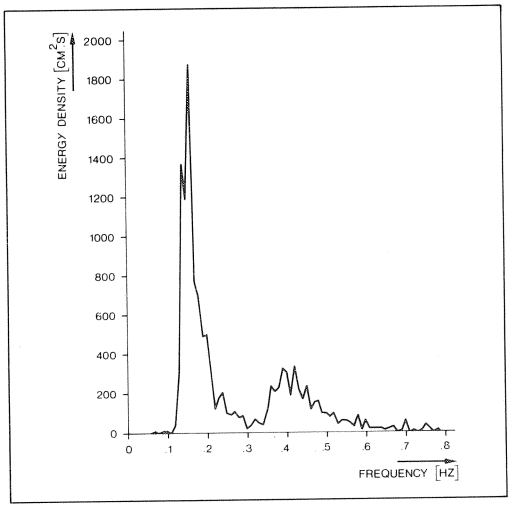

Figure 2.3.2.8 Wave energy spectrum location BG2 (South-West Netherlands).

Site Investigations and Data Acquisition

W. van de Ree, J. Stuip

2.3.3. Measurement of currents

1. General

Within the scope of the subject of this book, the current velocity is mainly of importance for calculating the stability of the estuary or dike breach during closing operations, but also for the stability of closing elements, working boats, pontoons etc. Furthermore current velocities are measured to determine the discharge, which is of importance for obtaining detailed knowledge about the filling and emptying of the basin behind the closure gap.

Usually measurements for the determination of discharge are part of a series taken at various stages of the tide or river flow.

Obviously the cross-section should be taken perpendicular to the direction of the flow and the measuring site should be selected so that the distribution of flow is reasonably regular. Arrangements must be made to define the cross-section on both banks by markers which are clearly visible and readily identifiable at all stages.

Gauges must also be installed on both sides of the cross section and read at intervals throughout the period of measurement.

For calibration mathematical model gauges in the nodes of the model upstream and downstream of the cross section is essential.

In rivers beyond the tidal zone, once a stage discharge curve has been established, the discharge of the river is simply determined by measuring the water level, unless the river-bed has changed considerably.

In tidal regions this is not possible due to the mutual influence of the river run-off and tidal motion which determine the strongly time dependent flow caused by:

- a continuous change of water level due to the tidal effect
- greater velocity gradient in the longitudinal direction than in rivers with flow in one direction
- change in distribution of velocities over time
- during the transition period from ebb to flood current, or vice versa there is a change in direction of the current
- the occurrence of high and low water may not take place at the same time as the change in the direction of the current
- the change in direction of the current does not take place at the same time throughout the whole cross-section
- there may be stratification of flow by density current with the upper strata flowing in one direction and the lower strata flowing in the reverse direction
- sometimes large and rapid variation of width and capacity of section may occur due to successive covering and uncovering of banks by the tide.

Detailed knowledge about the flow pattern during the various construction stages in the axis of and adjacent to the closure gap is necessary to design a proper layout and sequence of construction of the closure works. For this purpose the magnitude and direction of flow should be measured at a number of points. The set-up of these measurements differs from the discharge measurement: different instruments, elaboration and presentation of data and required accuracy.

The purpose of the velocity survey, the site conditions, the type and number of vessels thus determine the method of measurement.

Propeller instruments, pendulum meters, floats or a combination of these instruments can be used. In freshwater regions it is also possible to determine velocities and/or discharges by using dilution methods.

2. Instruments

A profound study of all available current measuring instruments is beyond the scope of this book. To make it possible to choose between the various instruments or at least to be able to judge whether an available instrument is suitable in a specific case the principles of various instruments and a few examples are given.

The main working principles may be:

1. to make the force acting on the sensor element of the instrument in such a way that this force can easily be monitored,
2. measuring the distance between two stations and the time interval that a tracer travels from one station to another downstream,

3. dilution of a tracer caused by the mixing capacity of the current,
4. measuring the effect of an obstruction in the stream on the water level,
5. Measuring the time interval between emission of radiation and reflection of radiated waves,
6. Measuring the effect of the velocity of the water body as a medium for electromagnetic waves.

Figure 2.3.3.1 Working principles of dilution methods.

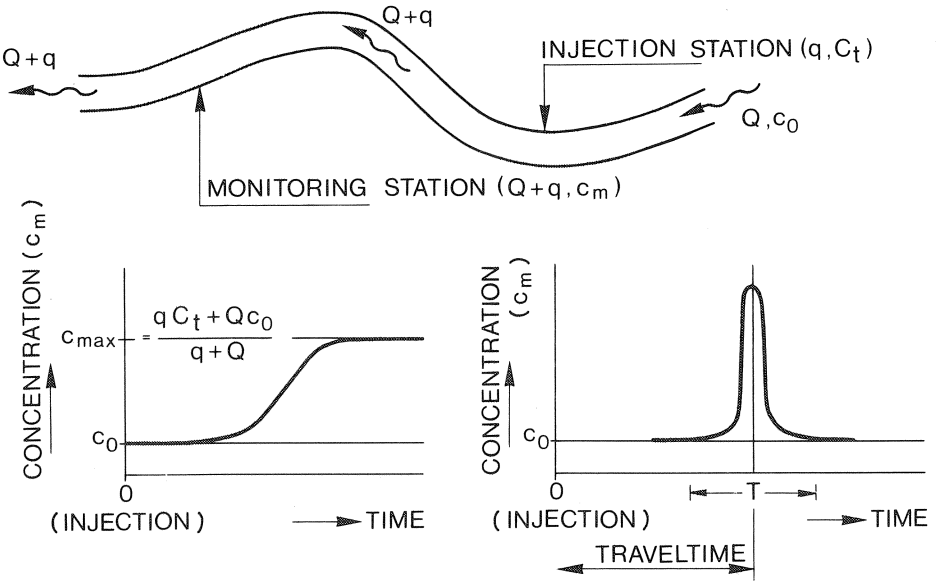

a) CONSTANT RATE INJECTION.

$$Q = \frac{C_t - c_{max}}{c_{max} - c_0} \cdot q$$

C_t = CONCENTRATION OF TRACER.

b) INSTANTANEOUS INJECTION.

1. TRAVELTIME

2. $$Q = \frac{M}{\int_0^T (c_m - c_0)\, dt}$$

M = TOTAL AMOUNT OF TRACER.

In general the measuring techniques are indirect. This means that a calibration should be carried out so that the relation between the current velocity and the reading on the instrument is established.
The reading is acquired by monitoring a phenomenon that is the consequence of the current velocity. The working principles of the second and third group are used in freshwater areas because salt mainly is used as the tracer. In tidal, saltwater areas the salt variations induced by the measurement procedure are hardly detectable. The method is sometimes used for field surveys in small watersheds where the discharges are not as high as in rivers and estuaries.
Floating elements can also be used as tracers, but theoretically they belong to the working principle of the first group
Figure 2.3.3.1 gives the principle of the dilution method.
The principle of the fourth group is based on the variation of the water level due to acceleration and deceleration of the current passing an obstacle in the stream. If the obstacle has a suitable shape and dimensions the instrument or sometimes structure will present the difference between energy head and water level (= velocity head)in a predescribed range and accuracy, from which the mean velocity can be derived. This measuring method is mainly used for discharge-regulating structures and not for closure works. The energy head sensors as pitot tubes are used in the laboratory. The velocity head rod is used for field measurements in small streams (no wind waves). Weirs and flumes are measuring structures respectively without and with constriction and have a calibrated relation between energy head and discharge.
Figure 2.3.3.2 gives some examples of this working principle.

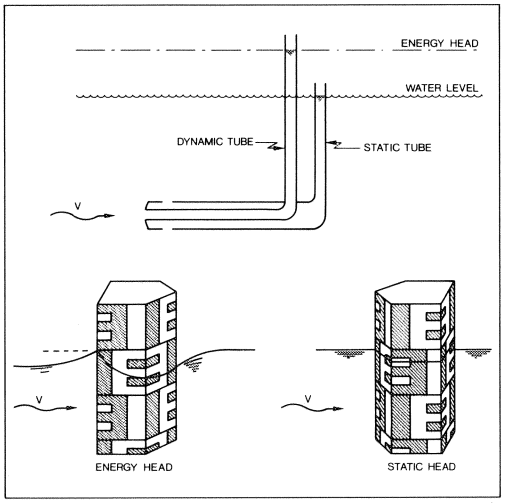

Figure 2.3.3.2 Working principles for energy head-static head conversion.

The fifth group is based on measuring the time taken for electromagnetic pulses to travel across the river. Transducers capable of transmitting and receiving the pulses are staggered on both banks of the stream in such a way that the acoustic path is at approximately 60° to the direction of the flow. The stream velocity is related to the difference in time taken between the pulses crossing upstream and those crossing downstream. It is obvious that the velocity is an „overall", a mean velocity of the river, the medium for transmitting the electromagnetic wave. This method has emerged from the experimental stage, but has not yet found an application in measurements associated with closure works.
The sixth group of working principles is based on Faraday's principle of electro-magnetic induction. This phenomenon shows that an electrical conductor in motion (water in the channel) in a magnetic field (produced by an artificial system) induces an electrical potential. The magnetic field generating system may use an already existing or specifically made cable system in the bottom of a stream or on a smaller scale embedded in a transmitting element and receiving instrument.

The larger systems based on this principle are used for specific cases, mainly discharge measurement in systems carrying polluted water. The small scale-instrument - only a probe, cable and a box housing the electronic part and dials - has already become a standard instrument for hydrographic surveys. If two pairs of sensing electrodes in the probe are used, the direction of the velocity can even be measured. Far the most important principle is that of the first group. Within this group a subdivision can be made while as the characterising parameter is used the way of converting the force on the sensor into a suitable reading:

1.1. floaters
1.2. pendulum
1.3. propellor

ad 1.1. The horizontal, current induced force acting on the floater or a resistance body attached to it makes that the instrument is carried away by the current. Depending on the set-up of the equipment the surface velocity or average velocity is monitored float with resistance body, float rod, chain float (see Figure 2.3.3.3).

The resistance body can be a plywood cross or a canvas sack with ribs. The float with resistance bodies at lower levels can touch the bottom. Then consequently the float velocity is lower than the water velocity.
The float can be attached to a thin rope with distance markers on it. The rope is released from a survey vessel at anchor and the time interval between the passings of the distance markers („knots") is measured. Another method is to fix, at specific intervals, the position of the float in its track from a fixed shore-based location from an anchored survey vessel. The position can be determined with sextant angles, theodolite bearings from ashore or even from radar images. It is also possible to follow the float with the survey vessel and to determine the position of the vessel with respect to reference stations.

ad 1.2. The horizontal current induced load acting on a resistance body makes an equilibrium with the horizontal component of the weight of the body suspended on a cable that is deflected by the force on the body and the cable itself.

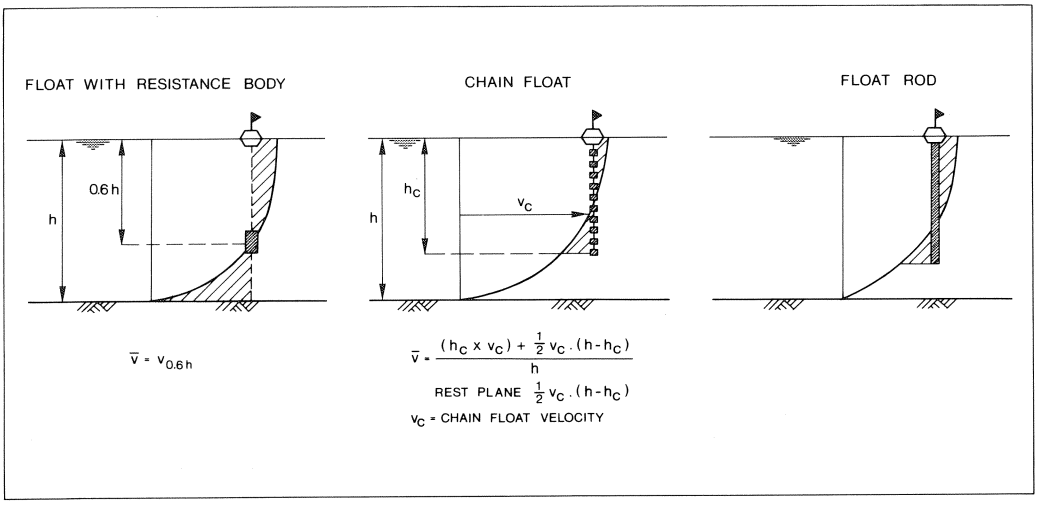

Figure 2.3.3.3 Various types of floats.

These deflections are calibrated for various depth and shapes of the body. The delfections can be read from a reference frame fixed outside the survey vessel and give both current velocity and current direction. This type of instrument is called dynamometer or pendulum current meter. The so called Planeta is a specific design developed by the Delft Hydraulics Laboratory.

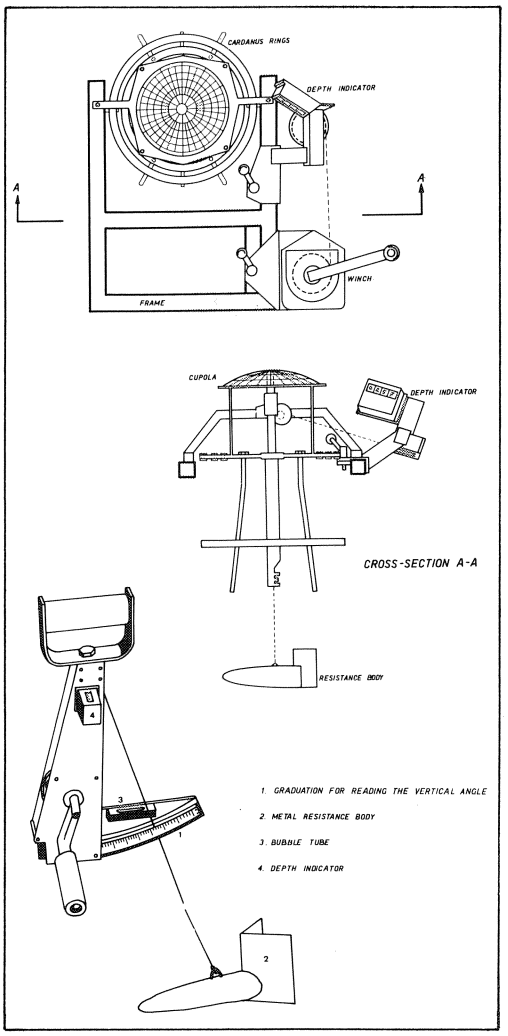

Another instrument designed according to this principle is a pendulum but now having a reacting component induced by buoyancy. A sensor is anchored in the seabottom and obtains an inclination from the vertical position due to the current-induced force. The inclination is monitored and stored on a storage medium inside the instrument.

ad 1.3. The current induced load on a propeller fixed on an axis causes the propeller to turn. Depending on the current velocity, angle of approach and pitch, the propeller runs at a certain angular velocity.
This velocity is measured by counting the revolutions of the propeller in a certain time interval. This is regularly done by the opening and closing of electrical contacts by mechanical, magnetic or photo electric means. The axis of the instrument may be vertical. This type is called a cup type. With a horizontal axis it is called a screw type or propeller-type current meter.
The instruments with a vertical axis are not critical to the horizontal direction of the current. For instruments with a horizontal axis a valve downstream of the propeller steers the axis into the current direction. Due to the turbulence the direction (and magnitude) of the current can fluctuate.
Propellers have therefore been developed which can measure over a range of 40° to 60° the component of the velocity perpendicular to the cross-section. The instrument can be fixed in the watercourse on a rod or suspended from a cable. This cable can be released from a derrick on board a survey vessel, bridge or even cableway. If the anchored survey vessel should be yawing the afore mentioned propellers which are little influenced by the angle of approach are indispensible.

Figure 2.3.3.4 Pendulum current meter.

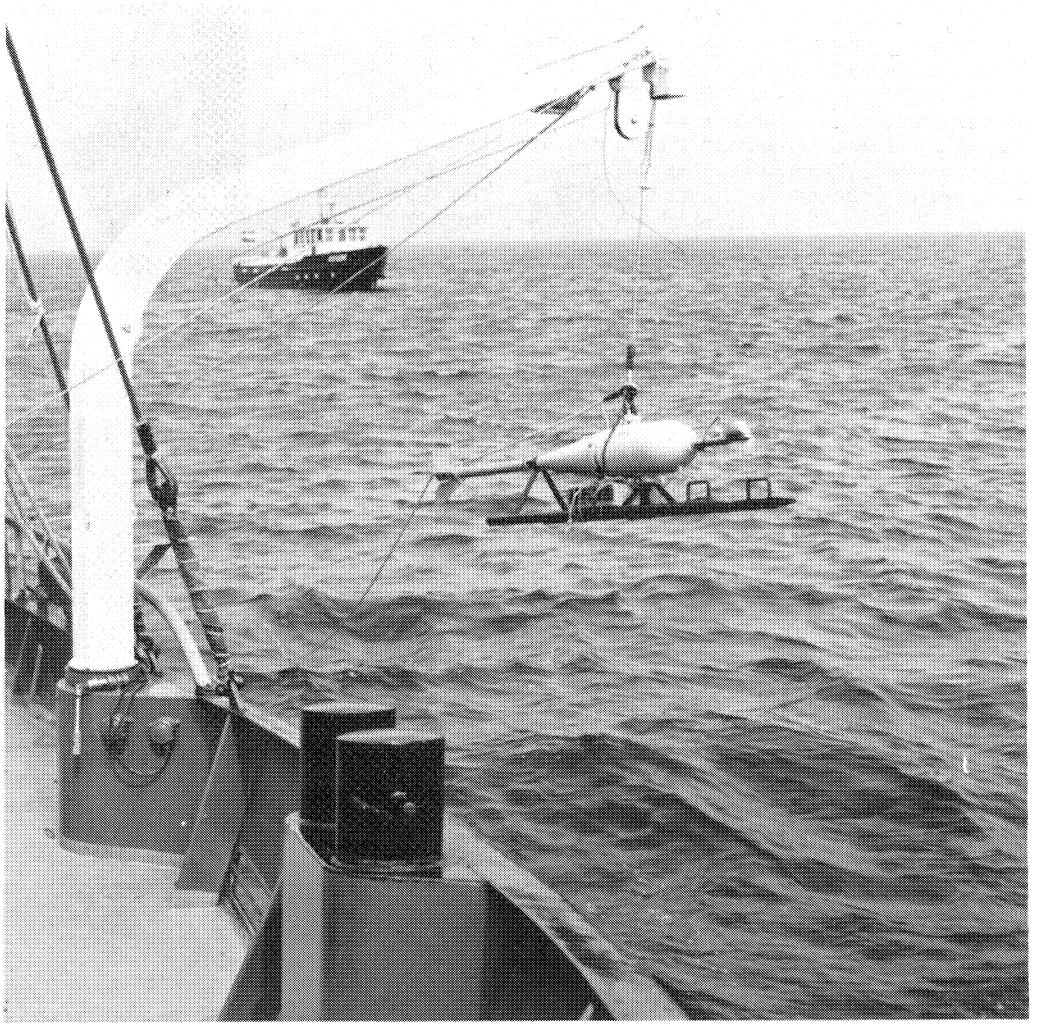

Figure 2.3.3.5 Ott propeller current meter.

In deltaic areas the current velocity and direction are changing continuously due to the tidal motion. Continuous records are sometimes necessary for special studies. Equipment has been developed to monitor and store these parameters for a certain period of weeks or even months. The up and downward motion of the survey vessel is less important because of the rather symmetrical deviations.

Figure 2.3.3.5 gives an example. The so-called Flachsee meter stores compass bearings, the number of revolutions and time on a film which is developed and read out after a certain time. The Flachsee is anchored to the bottom.
As stated before all instruments should be calibrated from time to time. The condition of the propeller instrument can be checked with a negative model consisting of two parts. A regular check of the condition of the elements other than the propeller of the instrument could be made with the so called spin-test. In this test the decay of the angular velocity is measured after a certain initial rotation speed induced by hand or blowing.
A number of factors are reflected in the choice of the instrument and measuring technique such as:

- importance of the measurement and its required reliability
- dimensions of the watercourse
- degree of turbulence, pollution, floating matter etc.
- availability of skilled personnel
- tradition
- accessibility of location
- auxiliaries for maintenance and repair
- cost

Under conditions as under review in this book the propeller instruments are normally used for velocity and discharge measurements. Floats are used for determining (horizontal) flow pattern. A combination is possible.

3. Sampling the velocity profile

In general the flow pattern or the velocity profile is neither uniform nor steady. This implies that the pattern or profile should be sampled continuously and with a dense network to determine characteristic values. In practice only a limited number of observations can be carried out.
From a statistical point of view the question will arise how large the sample should be to be representative with a certain confidence limit for the population (=velocity profile or pattern). From the results of discharge measurements in a large number of rivers without tidal motion of different sizes all over the world, it appears that

Figure 2.3.3.6 Cross-section of a river on a non-distorted scale.

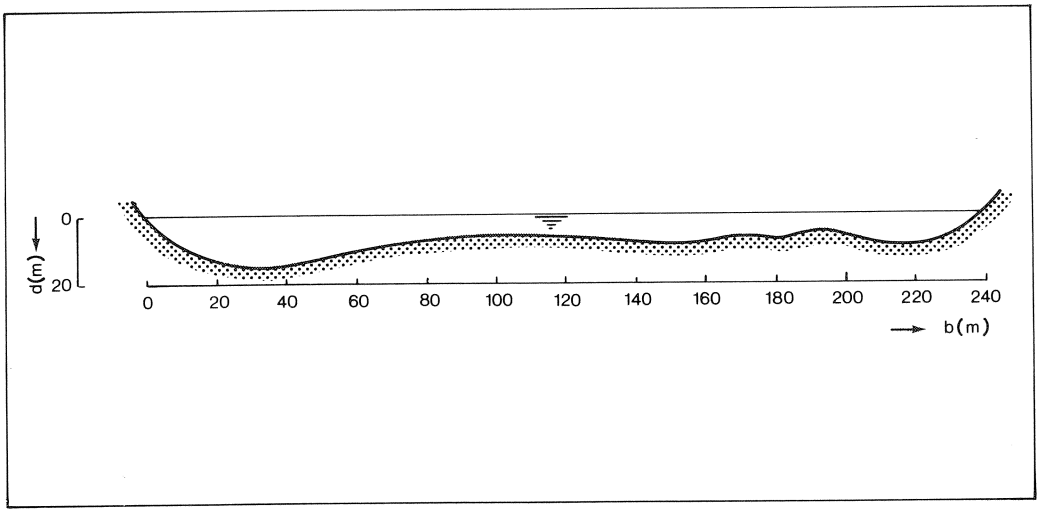

to determine the river discharge it is more advisable to sample the velocity profile with many verticals in the cross-section than to observe only a few verticals with many velocity measurements in each vertical.
This is obvious, from a sketch of a cross-section of a river on a non-distorted scale; the depth of the river is in fact only a fraction of the total width.

The investigations reported by the International Standard Organization indicated that discharge sampling error can be reduced considerably if information on the continuous bedprofile between the measured velocity profiles is used. Furthermore it seems that for non-tidal rivers the number of measuring points in the vertical plays a minor role.

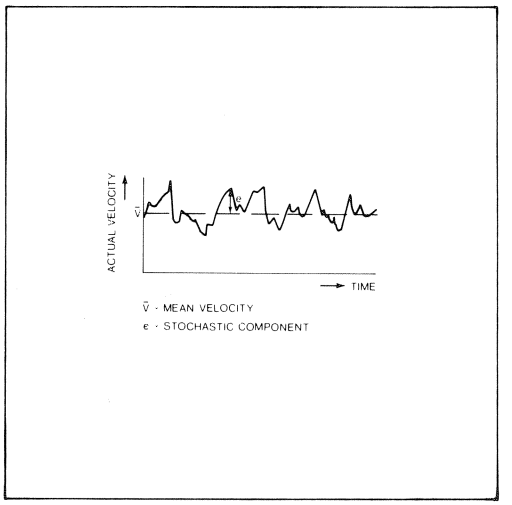

Figure 2.3.3.8 Current velocity, average component, stochastic component.

Figure 2.3.3.7 Arrangement of measuring points in a vertical according to the experience in tidal regions of the Hydrographic Survey Department of the Delta Division of Rijkswaterstaat.

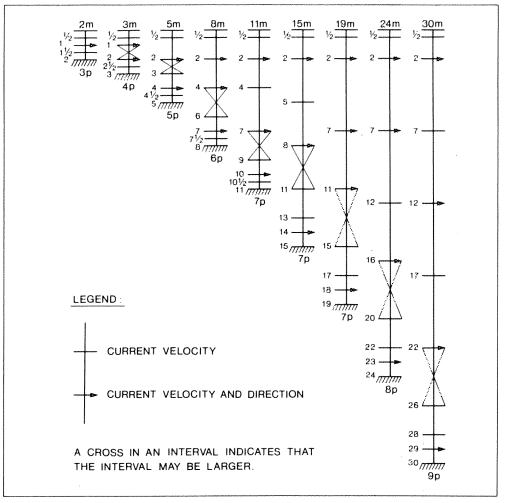

Figure 2.3.3.9 Accuracy and precision.

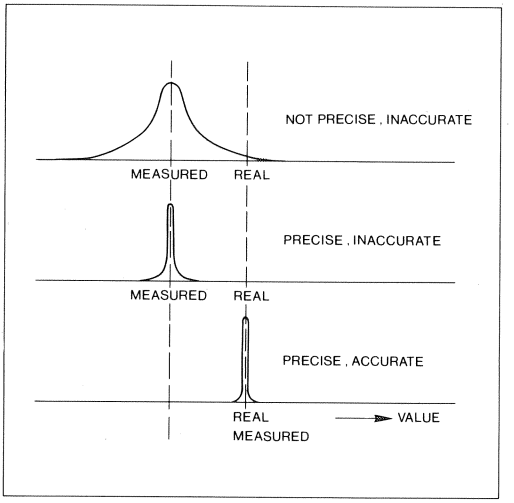

Current Measurements

The velocity at a given depth does not have a constant value but fluctuates due to turbulence. The actual water velocity can be decomposed in an average component (deterministic) and in a stochastic component.

Using a propeller current meter, the average velocity for a short period (seconds or minutes) is obtained by counting the number of revolutions of the propeller in a given time period and is used as the velocity for one moment. It seems that an observation time of at least 60 seconds is advisable to determine mean velocity, so reducing the stochastic component.
In tidal regions, however, the velocity profile is subjected to density currents and acceleration and deceleration in various ways.
Therefore it is advisable to take velocity measurements at closer intervals. According to the experience of the Hydrographic Survey Department of the Delta Division of Rijkswaterstaat the best arrangement in tidal regions for the measuring point in a vertical is a relatively short interval near the surface and the bottom of the channel. Between these a wider spacing may be used, a good interpolation between the measuring points being possible (see Figure 2.3.3.7). An important factor is that each point measurement takes at least 60 and preferably 90 seconds. The complete vertical is measured in downward and upward direction.
For evaluation of the measured data into discharge or flow patterns the time of measurement is taken half-way the downward and upward series of point measurements. The tide -and hence the current velocity - is continuously changing; this means that the monitoring period for a complete vertical cannot take too long and that therefore the number of measuring points in the vertical is limited. For deeper waters the inclination of the cable released from the survey vessel has to be taken into account for determining the position of the instrument.

4. Evaluation and presentation of data

Instruments and the method of evaluation of data are subject to error. An error is a difference between a measured value and the real value. A presentation of a measured value is reliable if the error is small. Reliability consists of accuracy and precision.
Accuracy is a measure of the difference between the mean of the measured values and the real value. Precision is related to the variation of the measured values (See Figure 2.3.3.9).
Measurements with a precise instrument give for every measurement the same value (variation in measured values is small). Measurement with an accurate instrument give the real value, provided that the variations due to an infinite high precision is zero.
Errors are not only caused by instruments but also by human (in)activities. Errors may be of a random or systematic nature.
Random errors could be reduced by repetition: the precision of the average of n times repeated measurements will improve by a factor $n^{1/2}$.
Systematic errors are introduced by an incorrect monitoring of the phenomenon, e.g. improper installation or faulty calibration of the instrument.
Of course the phenomenon itself that is monitored may have a stochastic character, see abovementioned paragraph, sampling the velocity profile.
The use of the velocity data depends on the objective of the measurement. For closure works velocity data are often used to design structure elements, then the maximum velocity at the bottom or along the banks or at locations in the cross-section is of importance. For designing closure operations the slack water period, so low velocities are of more importance.
Consequently also the presentation of current measurements can be done in various ways. Figure 2.3.3.10 gives some examples of presentations:

- flow pattern (top view of surface velocity or mean velocity)
- velocity profile
- current rosette (vector presentation for current velocity for various stages of the tide)
- current velocity and direction tidal graph
- relation between tidal differences and maximum velocity
- velocity profile across the channel (at the dam-axis or edge of scour-protection or along other relevant lines)
- velocity and discharge vector for various stages of the tide
- tidal discharge graph.

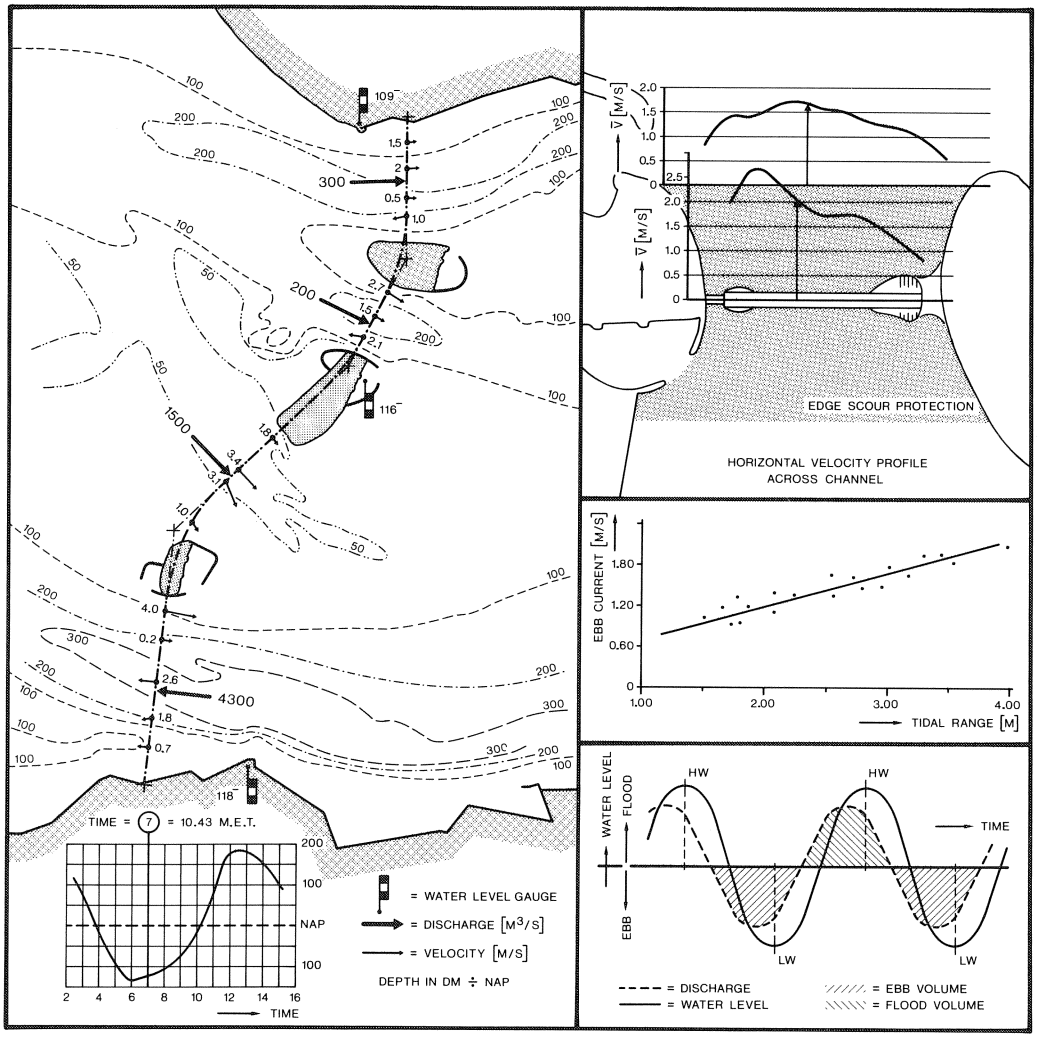

Figure 2.3.3.10 Various presentations of current velocity data

Current Measurements

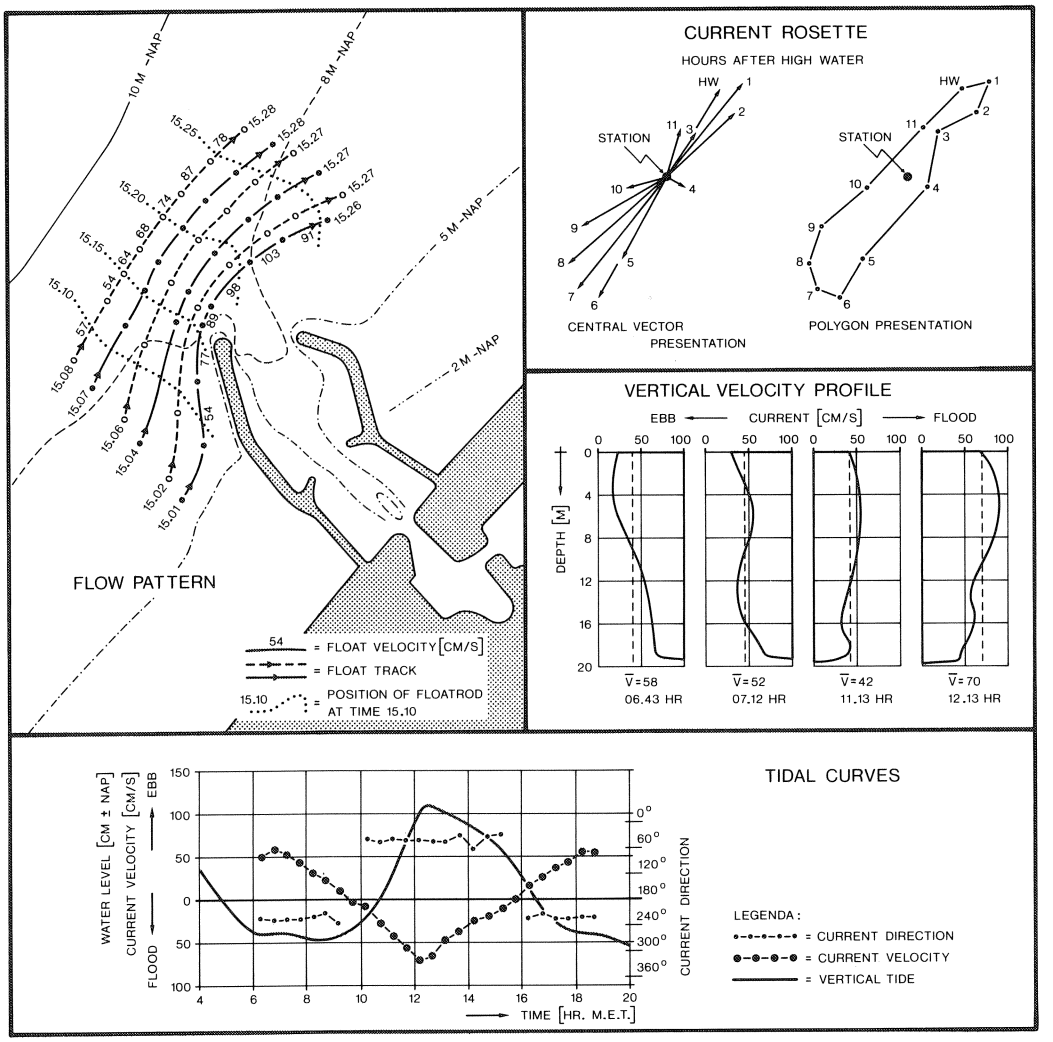

5. Calculating the discharge

As stated before some principles for measuring the flow velocity are worked out in an „overall" measurement of the average velocity. The set up of the installation or equipment can be calibrated in such a way that the value of the discharge is presented.

Measuring the discharge by means of „joint" velocity measurements means a sampling of the

Figure 2.3.3.11 Various methods for computing the discharge.

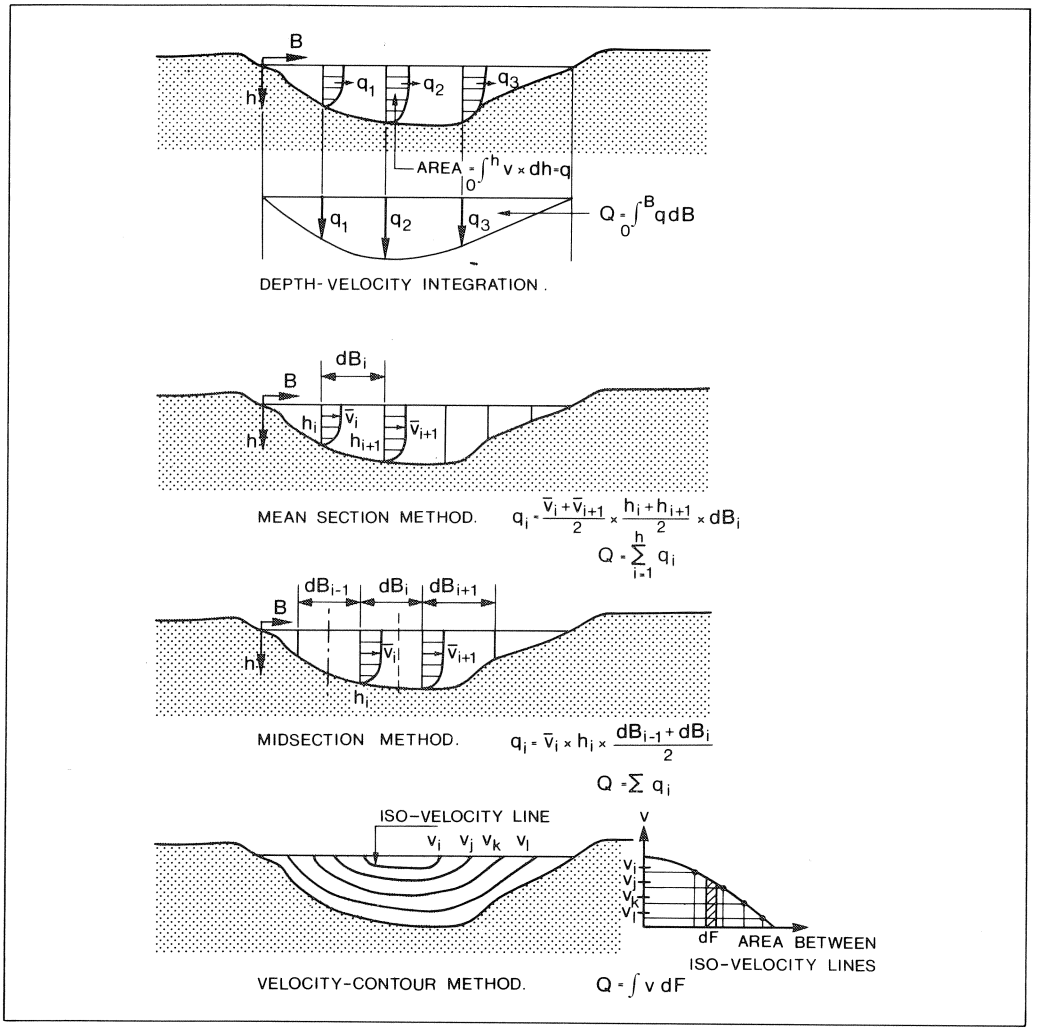

velocity profile of the total cross-section. This may introduce an error. Research was carried out to determine an „optimum" number of sampling points in the vertical as well as the number of verticals in a cross-section. This optimum depends also on other factors, e.g. the availability of instruments, personnel, survey vessels etc. As most rivers and estuaries are rather flat in general it is more advisable to sample the velocity profile with many verticals than only a few verticals with many velocity measurements in each vertical. An exception could be made for deeper streams with an irregular velocity-depth profile as there can be in estuaries, especially during closing operations. In the case of point velocity measurements with propeller or cup instruments or even floats the discharge can be calculated by integrating the values over the cross-section of the watercourse.

There are many methods for calculating the discharge:

- graphical depth-velocity-integration method (per meter river section the discharge vector perpendicular to the cross-section is calculated and plotted vs. the width, then the area of the graphic is measured with a planimeter)
- mean section method (integration over the width of the river of the mean velocity in the vertical of a river section)
- mid section method the discharge per river section is based on the measured velocity profiles on both sides of the section
- velocity-contour method (lines of equal-velocity in the cross-section are determined from the measured and integrated velocity profile).

The velocity profiles are measured at regular intervals in the cross-section. Near river banks and especially near a steep, deep bank the spacing between the profiles is smaller (so called gradient measurements).
According to the experience of the Hydrographic Survey Department of the Delta Division the first method is preferable.

References

1. F. J. Hayes, Stuip, J., Manual for hydrographic and hydrometric surveys, **Delft Hydraulics Laboratory Publication** no. 145, 1975.

2. Jansen, van Bendegom, van den Berg, de Vries, Zanen, **Principles of River Engineering,** Pitman, London 1979.

3. Manual of Stream Gauging, **Operational Hydrology Report** 13, vol. I-Field Work, World Meteorological Organization, Geneva, 1980.

4. L. Horst, B.A. Herfst, Hydrometry, **International Institute for Hydraulic and Environmental Engineering,** Delft 1981.

D.B. Smith

2.3.4. Surveying and monitoring seabed morphology for tidal basin closing projects.

2.3.4.1. Introduction

Closure of the entrance to a tidal inlet, be it partial or complete, will result in extensive changes to current flows and major concomitant variations to the pattern of sedimentation both within the inlet and seawards of the closing structure. Measurement of the distribution and trends in erosion or sedimentation over these areas is essential for: planning the position and design of the closing structure, implementing the construction phases and forecasting possible long term changes that could occur once the inlet has been closed. The possibility that accelerated sedimentation and or erosion may take place near structures at a different time scale than overall morphological changes in a tidal basin means that the density of the network and the frequency of sounding surveys can vary depending on the subject of inquiry.

In this section some aspects of bathymetric surveying relevant to mapping seafloor morphology are outlined. In addition, techniques used to analyse and predict trends in morphological changes, together with their advantages and limitations, are presented.

For more specific material on sea surveying the reader is referred to Ingham [1].

2.3.4.2. Bathymetric surveys for morphological mapping

For major engineering projects, such as the closure of a tidal basin entrance, production and analysis of bathymetric charts is essential for identifying and measuring changes to the sea floor morphology. This information is particularly valuable for monitoring the performance of individual construction stages as well as providing a base from which future changes can be measured and forecast.

A schematic diagram showing the planning, data collection and analysis stages for bathymetric surveys is presented in figure 2.3.4.1.

Bathymetric surveys for nautical purposes are aimed at mapping the general seafloor topography but are primarily concerned with surveying the shallowest sections of shipping lanes. In and near the entrances to tidal basins, these surveys concentrate on the main channels while side channels, intertidal banks and shoals are infrequently surveyed and seldom in great detail.

Surveys for morphological purposes differ from the nautical approach in that a greater amount of recorded data is retained in order to define the seabed topography accurately.

This means that channels, banks and shoals need to be surveyed with the same degree of detail.

2.3.4.3. The survey problem

To fulfill the survey objectives of monitoring morphological changes satisfactorily prior to, during, and following closure of a tidal entrance, means that bathymetric survey programmes must be designed with three levels of coverage, detail and survey frequency.

Large area surveys

A large area survey programme is aimed at establishing a frame of reference survey network which can be used to monitor changes that take place during and after construction. This is valuable for following anticipated morphological changes and identifying any unexpected deviations in large-scale trends that may result from changes to the hydraulic regime as the tidal inlet is being closed.

Should recent and historical bathymetric records be available, data from a large area network survey can be used as a reference for identifying where changes have taken place over the last few decades. These are useful for outlining those changes likely to take place in the following decade and are therefore particularly valuable for deciding where a closing structure will be placed.

The very size of the area to be covered, coupled with the fact that areas with distinguishable morphologies have to be covered, means that the survey area often has to be divided into irregular subsections and that, based also on an

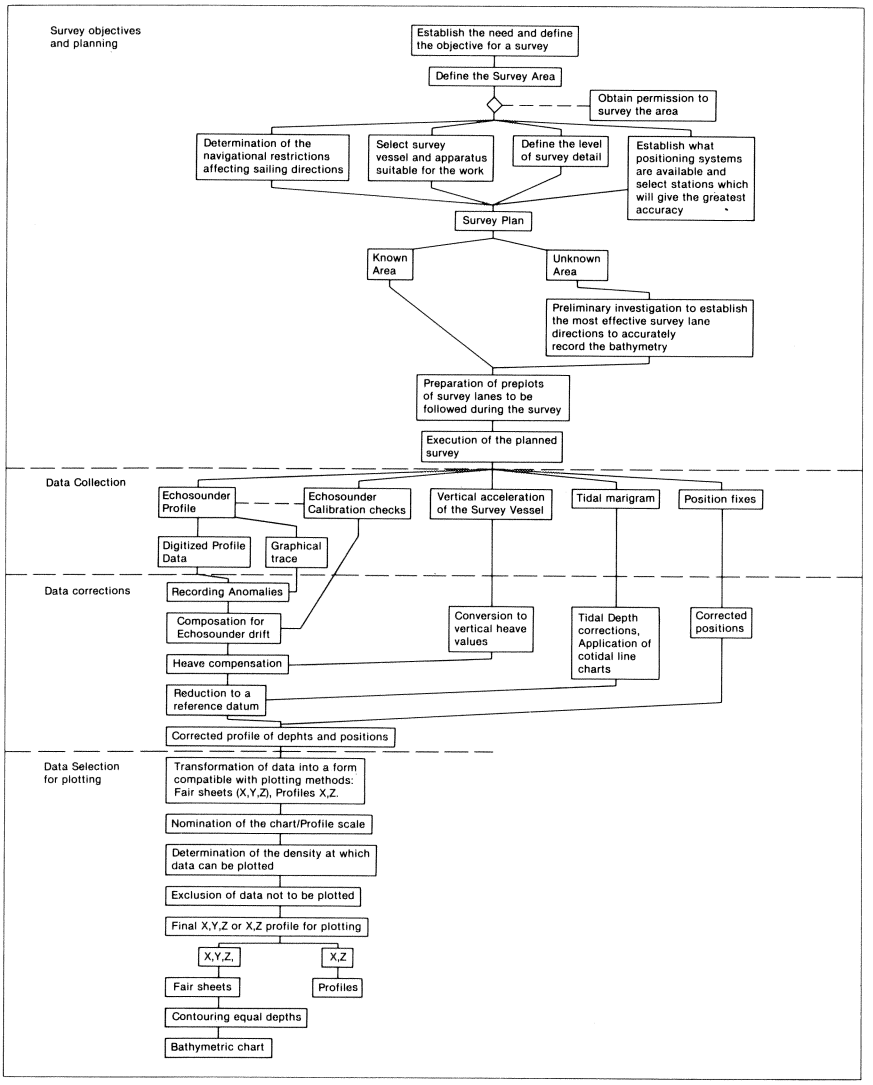

Figure 2.3.4.1 A generalised Flowchart illustrating the various steps involved in planning, data collection and data analysis to produce profiles of the seabed topography, fair sheets and bathymetric charts.

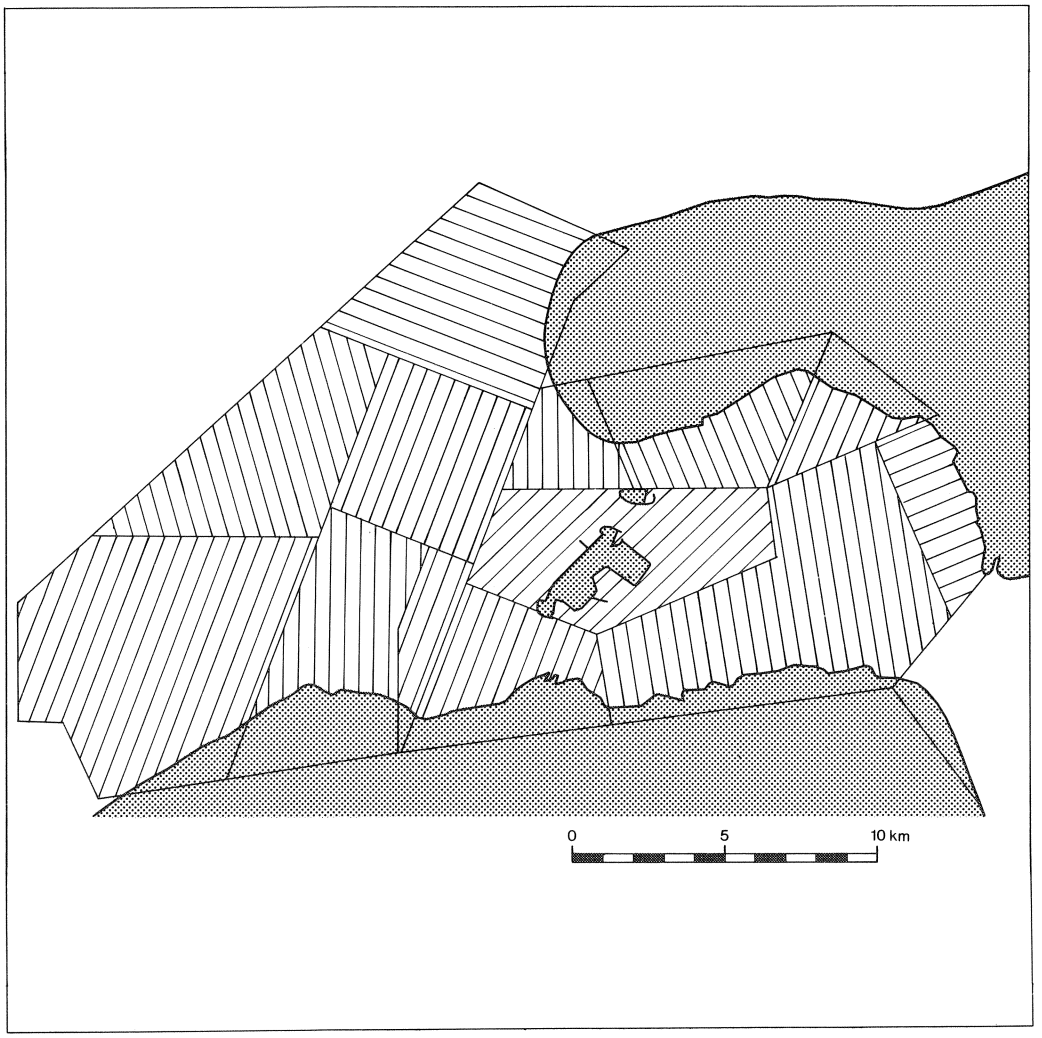

Figure 2.3.4.2 A seaward section of the large scale bathymetric survey network designed for the Eastern Scheldt inlet closing project in the Netherlands.

analysis of historical records, an optimisation of survey line density and surveying frequency must be made.
The two most important criteria that determine the design of a large-scale survey network are:

- that it covers the whole tidal basin, coast and offshore areas of interest, and
- that it can be successfully used to monitor

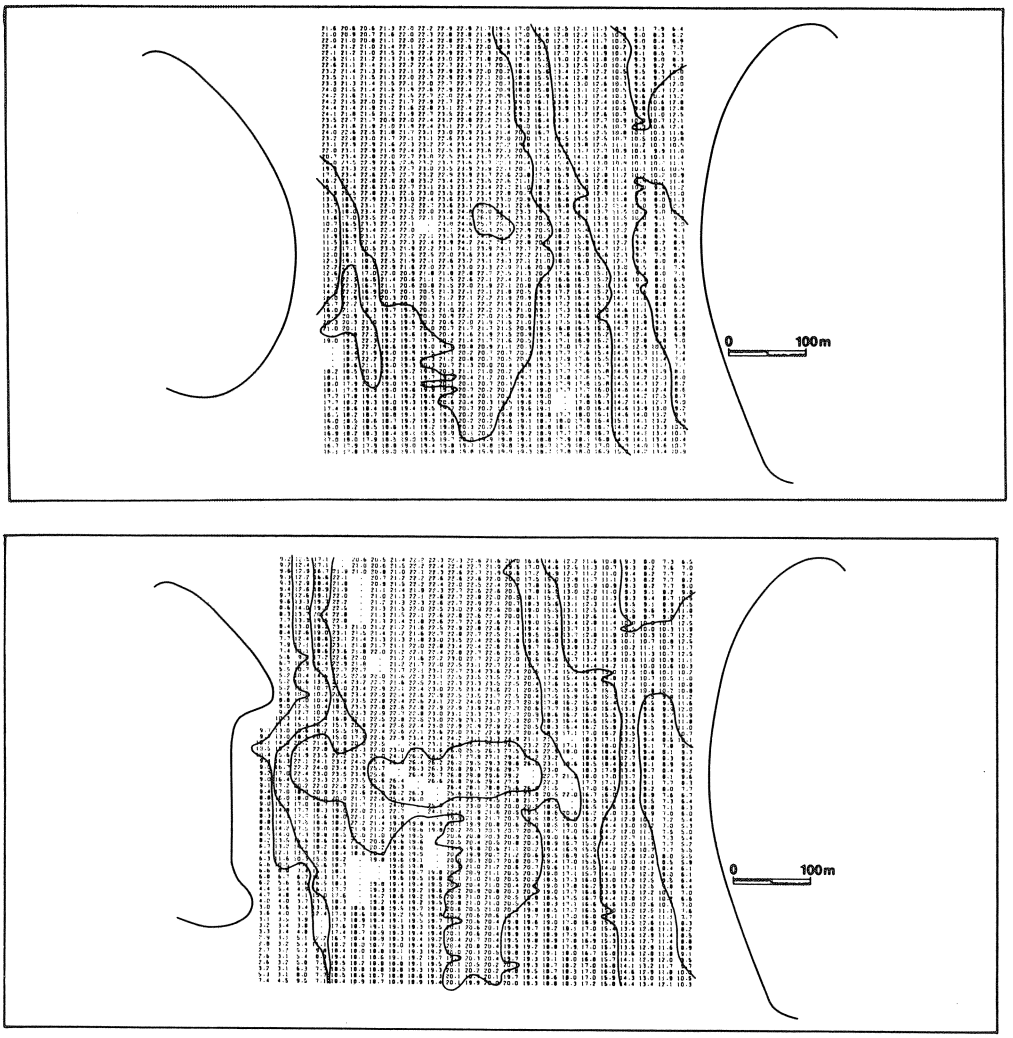

Figure 2.3.4.3 Examples of detailed bathymetric surveys carried out to monitor the effectiveness of dredging and subsequent infilling of a foundation trench in a channel of the Eastern Scheldt inlet, the Netherlands.

changes that take place in all morphologically distinctive areas.

In practice this amounts to designing a network that covers not only the tidal basin and it's entrance but also the adjacent coastal zone (figure 2.3.4.2). Within each subsection of the network the orientation and density of tracks to be surveyed are established to most effectively cover the submarine and intertidal topography.

Surveying a network of this scale is generally carried out on an annual basis.

Intermediate area surveys

Intermediate area surveys are directed towards monitoring those areas that are most likely to be affected during or following completion of an inlet closing structure.

Near the inlet entrance, attention is paid to monitoring changes to the adjacent coastline and nearshore zone as well as to the channels and shoals on both the flood and ebb tidal deltas. Within the tidal basin itself, areas of economic importance, such as access channels to harbours and prawn, oyster and mussel fisheries are examined in detail.

These surveys are primarly used to form a prognosis of their continued viability which could be threatened by increased sedimentation of silt or mud once the inlet has been modified.

Intermediate area surveys usually cover selected sections of the large-scale network. These are usually surveyed at monthly to annual intervals.

Small area surveys

Detailed, high density bathymetric surveys are usually confined to the area where the closing structure is to be built. Surveys of this type are used to monitor the efficiency and effects of construction operations, especially during preparation of the closing structure foundation. This usually involves monitoring scour or sedimentation in dredged trenches, and near abutments, piers, piles etc. (figure 2.3.4.3).

Detailed surveys may, depending on the need, be repeated at intervals ranging from a few hours, such as during a tidal cycle, to one or two months.

2.3.4.4. Survey systems

Within the established survey areas soundings can be made using either free ranging or parallel line systems. Free systems are usually used to chart large areas of often unknown bathymetry. The survey vessel may be kept on a chosen heading for each run or, as is often the case,

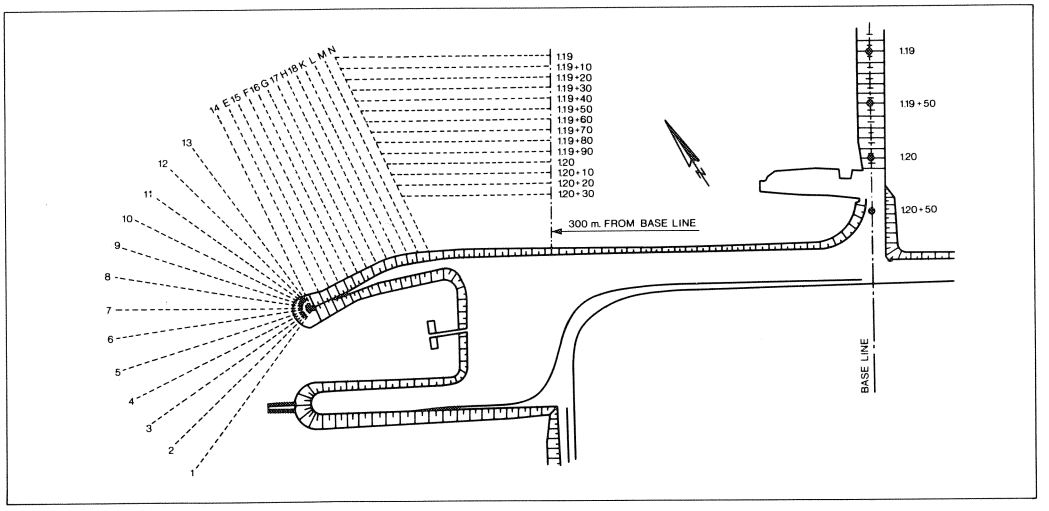

Figure 2.3.4.4 Surveying line systems

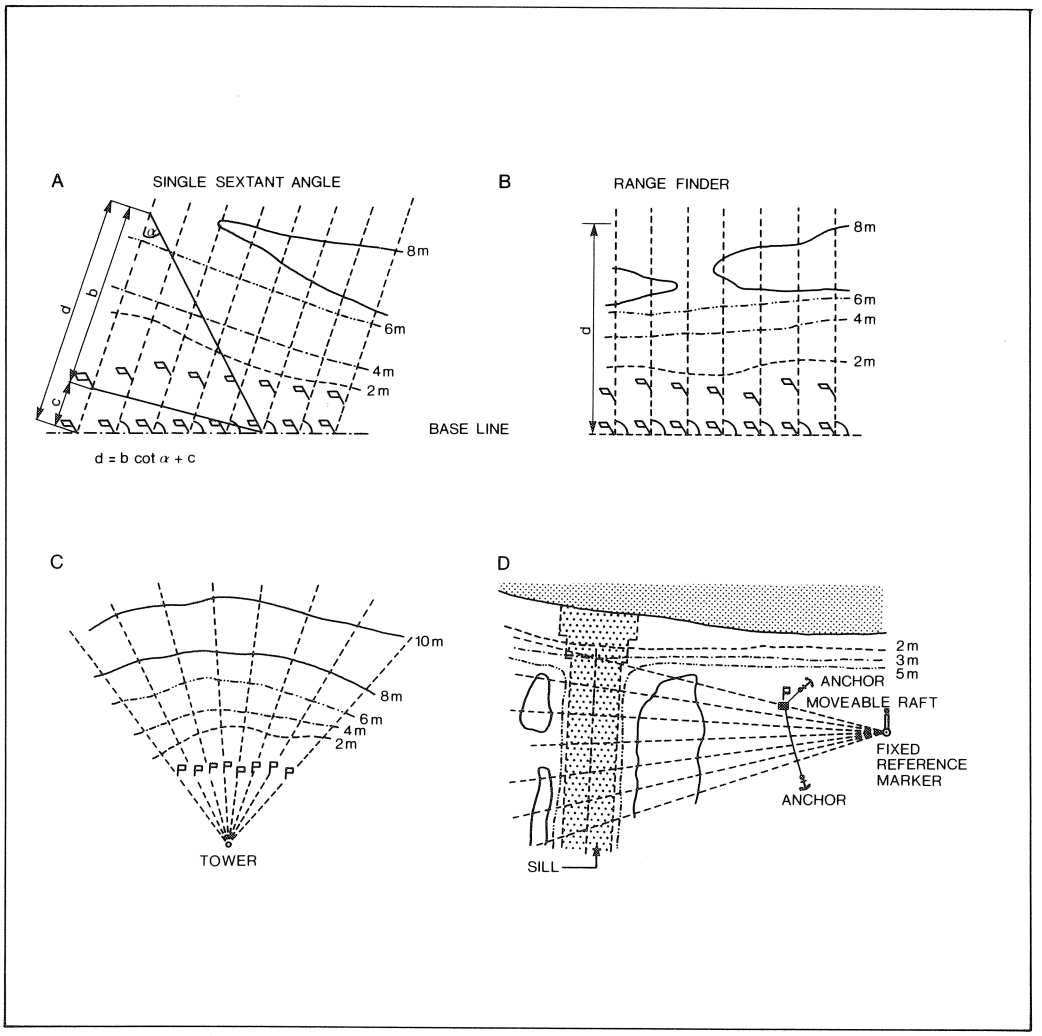

Figure 2.3.4.5 Surveying line systems using fixed or variable point transit lines.

follow a zigzag course until the survey area has been covered in sufficient detail.

For more detailed work, such as monitoring the state of shoaling is an access channel to a harbour or the erosion around a breakwater, parallel or radiating line systems are employed (figure 2.3.4.4). Here the problem is that the lines have to be „pegged out" on the water. With an electronic positioning system

this poses few problems. The helmsman can hold the vessel on course with the aid of a left-right indicator or a track plotter.
When an electronic positioning system is not available, as is often the case for coastal surveys, range bearing techniques can be employed. Each transit line extends from two widely spaced and clearly visable markers. Working from land these can be flags telegraph poles etc. On the water fixed buoys or a movable raft system may be used (figure 2.3.4.5).

2.3.4.5. Measurement of water depth

General
All physical principles used to observe an alteration in density can be applied for monitoring the level of the seafloor or a riverbed.
The simplest method is using the difference in bearing capacity of water and bottom material, for example by a pushing a rod into the water or using a weight on a wire or a chain.
The sounding rod is a wooden rod graduated in centimetres, decimetres or tenths of a foot. A base plate is attached to the bottom end of the rod. This not only prevents it from sinking into the bed but also serves as a weight to keep the rod in an upright position on the bed. Sources of error are deviation of the rod from the vertical and the stagnation head related to the flow velocity, especially where there are strong currents.
The sounding line is used if flow velocity or depth prevent the use of the rod. It consists of a chain or wire to which a lead weight is attached. Tags are tied to the line to indicate the depth in decimetres or feet. Corrections have to be made to the measurements to allow for deviations from the vertical above and below the water surface.
The depths which can be measured using a sounding line are restricted to about 12 to 15 m. Sources of error arise from penetration of the lead into the bed and the variations from the ideal conditions for which the corrections for wire bending have been calculated. Furthermore, it may be difficult to judge whether the lead weight is actually in contact with the bed because in soft sediments the weight can sink into the upper layer.

The principle of reflection of acoustic waves at an interface between two media with different density characteristics is used in echosounder equipment. An echosounder measures the two way travel time of acoustic pulses transmitted from a transducer oscillator mounted underwater on or alongside the survey vessel hull. The time lapse between the transmission and reception of the reflected signal is converted into a water depth and traced onto electrically or heat sensitive paper by a vertical or radially moving stylus. When linked with digitizing and data logging equipment recorded depths can be simultaneously recorded on punched paper or magnetic tape. The frequency at which depths are measured can often be varied from one to as many as ten recordings per second.
Echo-sounding equipment can be permanently mounted on board the survey vessel but it is also available in light portable versions that are particularly useful for small shallow draught vessels working in shallow lagoons or estuaries. Transmission frequencies of echo sounders generally fall in the 30 to 210 kHz range. The lower transmission frequencies are usually used in areas where the seabed is built up of relatively low density material such as fluid mud. In turbid waters laden with high concentrations of suspended sediment most echosounders are rendered ineffective. Under these conditions the sounding line is often the only method available for undertaking or completing a survey.
Survey echo sounders are usually fitted with transducers that have a wide and a narrower emission beam angle which can be set on the recording instrument. For general purposes, such as locating only the shallowest depths, transducer emission beam widths of 20 - 30° are employed.
Narrower beam widths of about 7° are used for more precise measurement of the seabed topography. Special „pencil beam„ transducers with beam angles of 2-3° are also available for very detailed work. These are best employed with a stabiliser to minimise errors arising from pitch and roll movements of the survey vessel.

2.3.4.6. Echo sounder calibrations

Sea water density, which varies with changes in

temperature and salinity, alters the transmission velocity of echo sounder acoustic pulses. To maintain survey accuracy therefore, the echosounder must be calibrated for these changes. Ideally, this should be done in the survey area.

Calibration of echo sounders with hull-mounted transducers is usually made by using the „bar check". For this, a metal plate and or a sealed steel tube, „the bar", is lowered on calibrated lines so that it hangs directly beneath the transducer (figure 2.3.4.6).

The bar is then lowered to a number of depths which are then recorded on the echo sounder. Depths recorded on the graphical trace are then plotted against the actual depth of the bar. On the basis of the results so obtained, the echo sounder zero setting is adjusted to eliminate the measured error (figure 2.3.4.7).

In open water surveys, echo sounder calibrations should, at the very minimum, be carried out before and at the end of each survey. By doing this, echo sounder errors realised during the survey can be compensated for at the depth reduction stage of data analysis. In estuaries, where water densities can change more rapidly, echo sounder calibrations should be made more frequently.

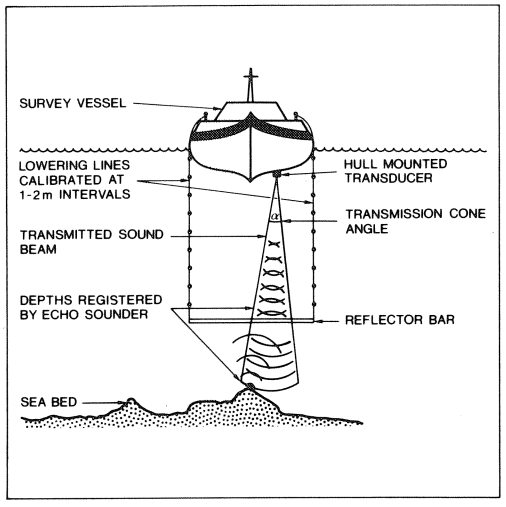

Figure 2.3.4.6 Bar check calibration of an echo-sounder on a survey vessel with a hull-mounted transducer.

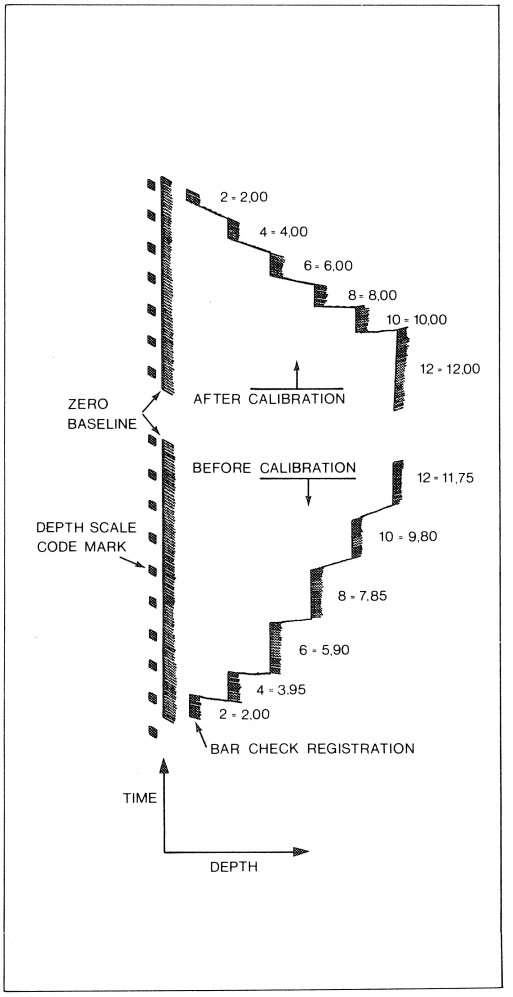

Figure 2.3.4.7 An echo-sounder trace of a bar check used to calibrate the echo-sounder.

2.3.4.7. Datum levels

The measured zero depth of a calibrated survey echosounder is, once it has been corrected for ship squat, the actual water surface. This level varies with the tide and corrections must be made for these variations when reducing the recorded depths to a defined chart datum. For navigational purposes, a chart datum that approximates to a mean low water tidal level, such as the lowest astronomical tide, is often used.
Datums defined on the basis of the local tidal range are not altogether suitable for morphological investigations within inlets and along the adjacent coastline because these levels can vary over short distances with changes to the form and amplitude of the tidal wave (figure 2.3.4.8.).
In order to ensure that the same level for the whole survey area is used, a national or locally established datum must be used.
National datums usually offer the advantage of being related to most tide gauges.
For projects where these levels are not available, depths can be reduced to an established construction site datum. This ensures conformity between onshore and offshore surveys.
Tidal reductions to depth recordings are made using tide levels recorded over the survey period. Recorded depths are corrected for these variations and then reduced to the defined survey datum. For surveys covering large areas, especially within tidal basins where the phase and amplitude of the tidal wave can vary, several tidal gauges may be needed to maintain reduction accuracy. Surveys made some distance from the nearest tide gauge are corrected using time and range correction factors taken from cotidal line charts which are based on reference coastal tide gauges.

Figure 2.3.4.8 Diagram illustrating changes in chart datum and low water levels relative to ordnance datum (O.D.N.) along the Severn Estuary, Great Britain (after [3]).

2.3.4.8. Position-fixing

General
There is a wide variety of positioning systems that can be used in and around tidal basins

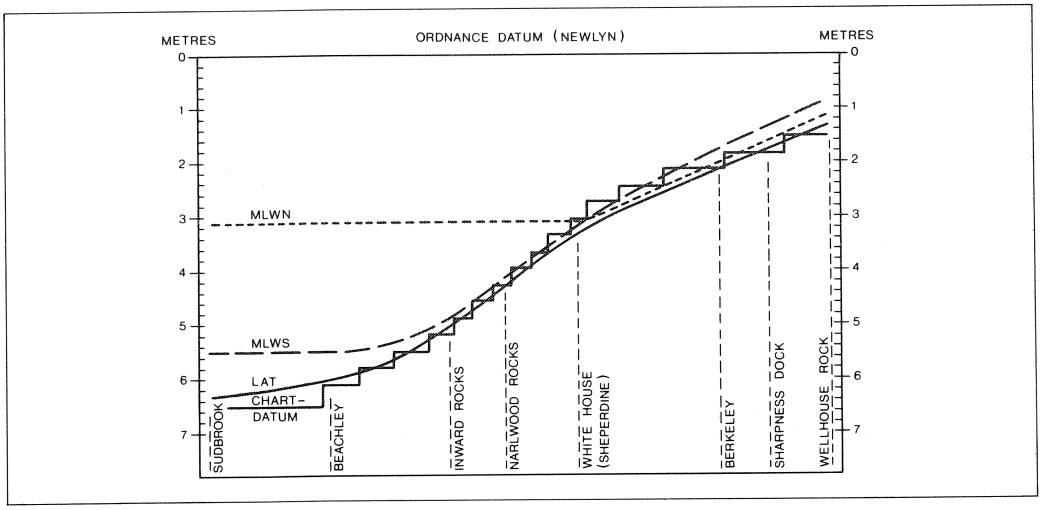

for bathymetric surveying or for fixing positions during sampling or data recording programmes.

Optical methods
The simplest systems and cheapest positioning are the optical methods. These can be divided into three basic variations: double angle resection, single angle + transit line and theodolite intersection methods (figure 2.3.4.9).

Double angle resection
The double angle resection method is based upon simultaneous measurements of the two angles subtended by three prominent shore positions using horizontal plotting sextants. This is usually done by two observers standing close together on the survey vessel. The position given by the two recorded angles can be plotted on the chart in a number of ways. The simples is by using a „station plotter"; a three armed protractor which can have its two outer arms set to the observed sextant ngles. The plotter is then moved about on the chart until all three arms pass exactly through the plotted positions of the three fixed reference masks.
The fixed position then coincides with the centre of the instrument.
For comprehensive or repetitive surveys, that use a few prominent land marks, lattice charts with arcs of circles for constant subtended angles can be prepared.

Using the fixed sextant angles, the corresponding arcs are followed on the lattice chart. The fixed position is located where the arcs intersect (figure 2.3.4.10).
Alternatively, a programmed desk top calculator can be used to convert the two sextant angles into chart coordinate eastings and northings. Unlike the lattice chart approach, where sextant angles must be recorded from a restricted number of preselected points, the fixed reference points to be varied to achieve the optimum positioning accuracy.

One danger of angle resection positioning is when the two position arcs drawn from the three reference marks coincide (i.e. all three reference marks lie on the same circle). This can be avoided by ensuring that the centrale reference point is always closest to the survey vessel or much further away than the other two.

Transit line sextant angle
Using this method, positions are located by measuring the angle subtended from two fixed points across a transitline extending from two widely separated landmarks (figure 2.3.4.9b). Each position is located where the position circle for the recorded subtended angle cuts the transit line. These can be quickly plotted by using a station plotter or predrawn lattice arcs of constant subtended angles.
An alternative to using a sextant angle is the range-bearing approach. In this case, the position is measured along a known transit line - a bearing measured with a theodolite - while the range is recorded by using an optical or electronic range-finder. This method requires radio contact between the ship and shore to match the measured position with the depth on the echosounder trace.

Theodolite intersection
For this method, two or three theodolites, set up along the shore, are used to measure the angle between a fixed land-point and the survey vessel (figure 2.3.4.9c). As with the range bearing approach, good radio communication is needed to coordinate positioning with on board recordings. Course positions can be plotted by using predrawn bearing lines radiating from the theodolite positions or they can be calculated directly if the baseline for the measured angles XYP and YXP extends from one theodolite position to the other.

Electronic systems
The scale, detail and frequency at which bathmetric surveys for large tidal basin closing projects must be made necessitates the use of semi or completely automatic positioning procedures. Electromagnetic positioning systems offer the advantages of very good accuracy, excellent reproducibility and continuity.
Positions can therefore be randomly fixed or continuously recorded on either a time- or

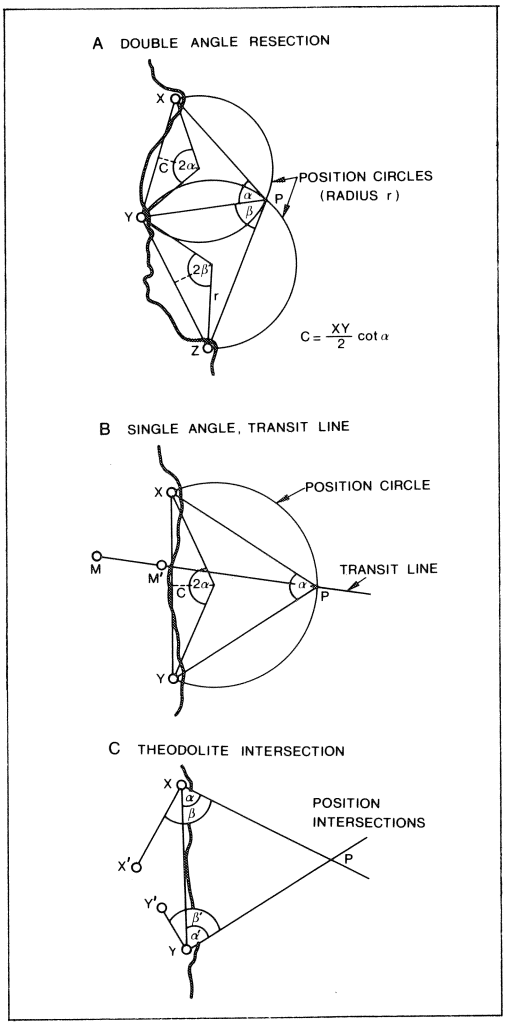

Figure 2.3.4.9 Optical positioning methods using horizontal plotting sextants or theodolites. A, construction of position circle arcs of subtended angles from three fixed marks; x, y, z. B, construction of the position circle arc of an angle subtended from two fixed points (x, y) across the transit line through M -M'. C, theodolite intersections from two reference points (x, y) using a closed triangle, angles x, x', or radiating lines; angles B, B'.

distance interval basis together with measured depth data.
Recording both positions and depth data simultaneously increases the accuracy of surveys.
Mainly due to the rapid expansion of offshore activities over the last decades, a bewildering variety of electronic positioning systems are now available. The effective range of these systems varies from about 10 km to worldwide while their accuracy can vary from one decimeter to several hundred metres.
These factors are primarily determined by the operating frequency used. As such it is common practice to classify systems into separate frequency bands.
Most distance-measuring or position-fixing systems may be classified into four different frequency groups:

1. Low frequency systems (10 to 300 kHz).
   Omega, Decca Navigation and Loran (long-range navigation systems).
2. Medium frequency systems (1-2 mHz).
   Decca Hi-Fix, Lorac, Ray-dist, Toran, Hydrotac and Autotap.
3. UHF Systems (400-600 mHz).
   Syledis, Maxiran, Trident.
4. Micro-wave systems (100-10.000 mHz).
   Trisponder, Motorola Mini Ranger, Cubic Autotape, Tellurometer, Artemis.

The frequency band selected has a major influence on both range and accuracy. (Table 2.3.4.I) Range performance depends primarily on the presence of three distinctly different methods of electro-magnetic propagation (figure 2.3.4.11).

Ground-wave propagation
This is one of prime methods of propagation for frequencies in the 30-300 kHz band. Ground-wave propagation is greatly dependent on the

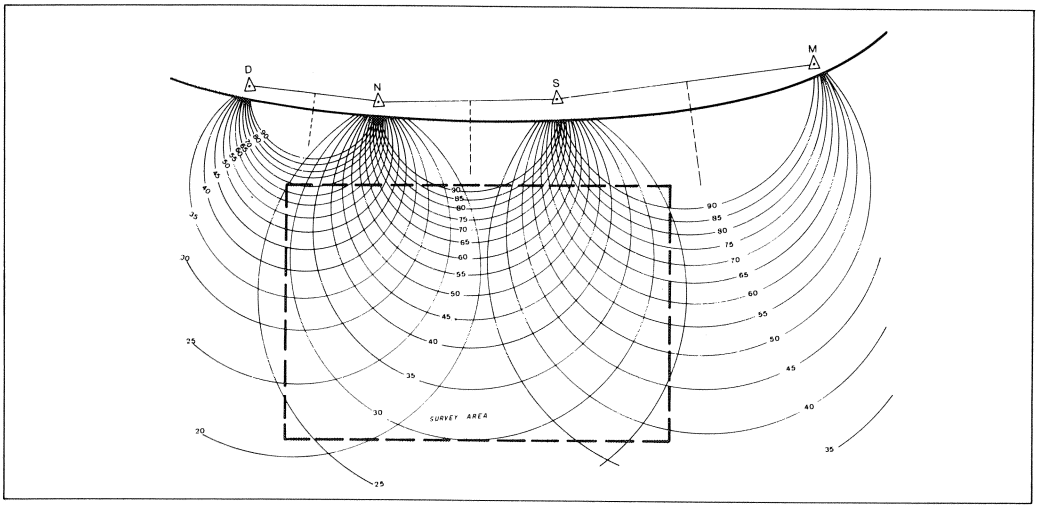

Figure 2.3.4.10 A lattice chart with arcs of circles for constant subtended angles from fixed reference points.

conductivity of the ground through which a wave travels. At very low frequencies ground-wave attenuation is slight and usable signal strengths are obtainable at distances of several hundred miles.

Table 1 Various electronic position-fixing systems and their characteristics

SYSTEM	USE	METHODS	POWER	RANGE	FREQUENCY	ACCURACY
Toran	Multi-user	Hyperbolic	10 Watt 100 Watt	± 100 km ± 550 km	1.6-3.8 kHz	± 1 m. ± 5 m.
Syledis	Multi-user	Circular/ Hyperbolic	20 Watt 400 Watt	± 130 km ± 450 km	420-450 MHz	± 2 m. ± 15 m.
Sea-Fix	Multi-user	Hyperbolic	5 Watt	± 150 km	1.6-3.0 MHz	± 5 m.
Hi-Fix	Multi-user	Hyperbolic	10 Watt 40 Watt	± 150 km ± 300 km	1.7-2.0 MHz	± 3 m. ± 8 m.
Loran-C	Multi-user	Hyperbolic	250 K.Watt 3 M. Watt	± 2000 km	100 kHz	± 150 m.
Autotape	Single-user	Circular	1 Watt	± 80 km	3 GHZ	± 2 m.
Trisponder	Single-user	Circular	1000 Watt	± 80 km	9.2-9.6 GHZ	± 3 m.
Mini-ranger	Single-user	Circular	400 Watt	± 30 km	5.4-5.6 GHZ	± 3 m.
Artemis	Single-user	Polar	0.15 Watt	± 30 km	9.2 GHZ	± 5 m.

Accuracies as stated are repeatability figures as given by the manufacturers.
These accuracies are obtainable only under optimal conditions.

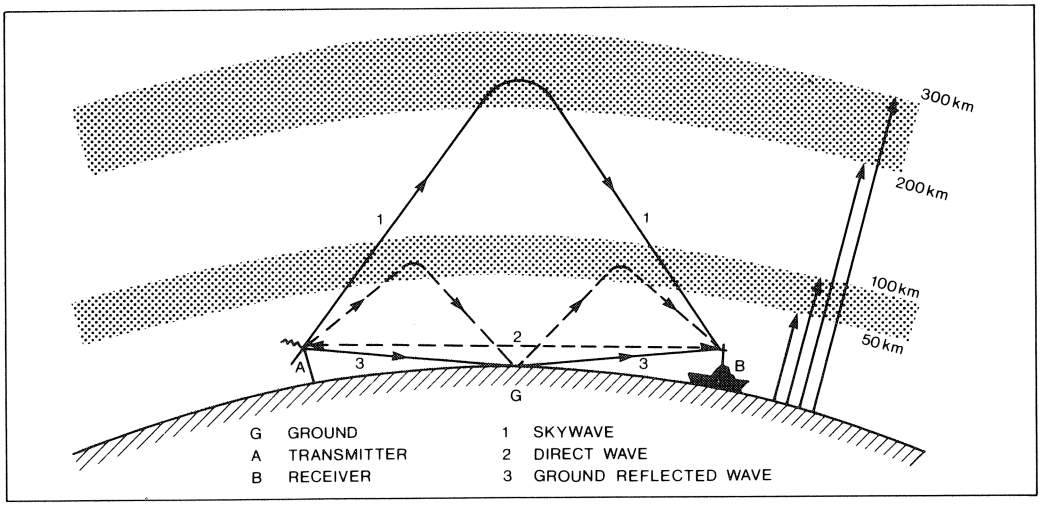

Figure 2.3.4.11 Schematic illustration of electromagnetic wave propagation.

Sky-wave propagation
Sky-wave propagations is caused by transmission reflected off the ionosphere; a region of ionised gasses extending from altitudes of about 50 to 400 km above the earth's surface. The ionosphere is a major natural phenomenon which makes long-distances radio transmission possible at frequencies which would otherwise be very limited.

Direct-wave propagation
Direct-wave propagation exists at lower frequencies of 1 to 2 mHz and is effectively cancelled by the radiation reflected from the earth's surface which undergoes a phase shift of about 180° on reflection.
At high frequencies the reflection coefficient of the surface is lower and the difference in path length in terms of wave length, much greater.
Although this cancellation effect can still cause fading in the 1,000 to 10,000 Hz band, its effect is generally lower and decreases with increasing frequency. One major advantage of frequencies in this band is that it becomes possible to design directional antennae of reasonable size, thereby reducing the effects of reflection off nearby objects. This in turn allows much greater accuracies to be obtained.

Frequency systems
In general the characteristics of the various frequency systems may be summarised as follows:

Low frequency systems
Very long range due to extensive ground-wave propagation. Large antenna and high power requirements.
Accuracy is relatively low due to poor resolution and effects of terrain and conductivity.

Medium frequency systems
Medium-range performance utilizing ground-wave propagation. Night-time range limited to below 150 km by sky-wave interference. Relatively large antenna and power requirements are needed.
Improved accuracy due to higher resolution.

Micro-wave frequency systems
High accuracy due to possibility of directional

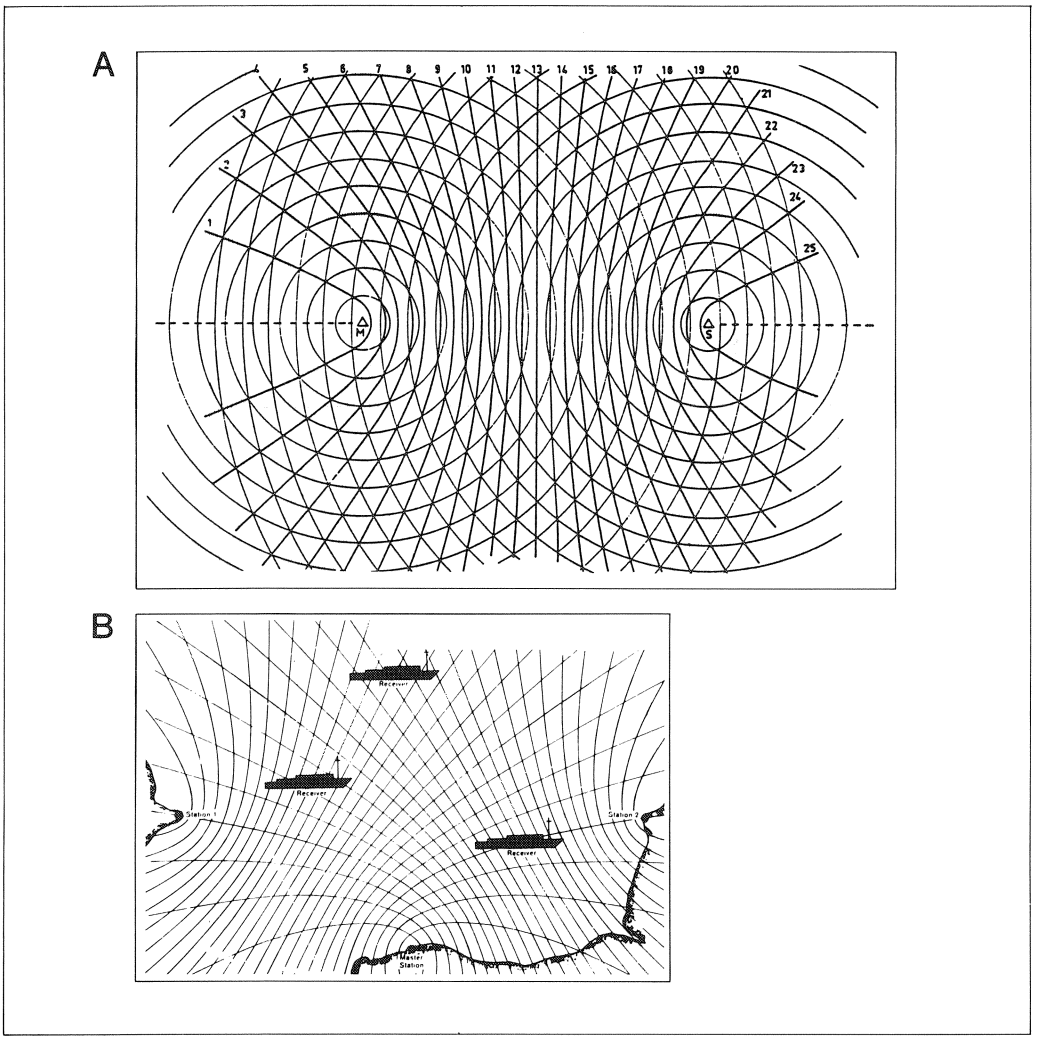

Figure 2.3.4.12 Schematic diagram of the signal patterns for hyperbolic mode megahertz positioning systems.

antennae and propagation free of terrain and ionospheric effects.
Low power requirements due to the use of small-size high-gain antennae. Range performance limited to near line-of-sight conditons.
Range performance affected by weather at the upper end of the frequency band.

It may be seen from the above summary that when accuracy is required there is little choice other than the use of micro waves, and that limitations such as line-of-sight range performance must be accepted.

Geodetical systems
The three basic geodetical systems used for eletronic positioning are:

- Hyperbolic systems,
- Circular systems,
- Polar systems.

Distances are measured using pulse transit time or continuous wave phase difference measuring techniques.

Hyperbolic systems
Hyperbolic systems measure the range difference from three or more synchronised landstations (Master and Slaves) and obtain their fix from the intersection of two hyperbolic position lines. (figure 2.3.4.12A).
The concentric electro-magnetic wave fronts (circles) drawn around M and S have an interval equal to the wave length used and represent the loci of points where the phases are zero.
The curves connecting the intersection points as shown in figure 12B will be homophocal hyperbolae since these have the geometric property that on each point on the hyperbolae the difference in distance from the transmitters remains constant.
The method requires a minimum of three transmitters at known positions on shore, and a receiver on board the mobile station (e.g. Loran-A, Loran-C, Omega, Decca Main Chain, Hi-Fix). A major advantage of hyperbolic systems is that any number of vessels can use the system at the same time.

Circular systems
Position fixing using the circular, or so called range method, is effected by measuring the distance from the survey vessel master transmitter to two or more slave transmitters located at known positions on shore (e.g. Cubic Autotape, Motrola). Each position fix is obtained by intersection of two or more circular range lines, each with the slave transmitter located at its respective center. (figure 2.3.4.13). In this mode generally only one vessel with a master transmitter can be used although a second vessel can sometimes be operated on a time-sharing basis.
It should be noted that, with the hyperbolic and circular methods, the intersection of two position-lines is generally found at two points. This means that, in principle, one pair of measurements gives rise to two solutions for the vessel's position. When these two points are positioned at large mutual distances, and the approximate position of the vessel is known (e.g. by means of dead-reckoning), the ambivalence is resolved; otherwise, a third measurement will be required to select the proper position.

Polar systems
For the polar or „Range-bearing" method the

Figure 2.3.4.13 The pattern for range-range mode positioning systems.

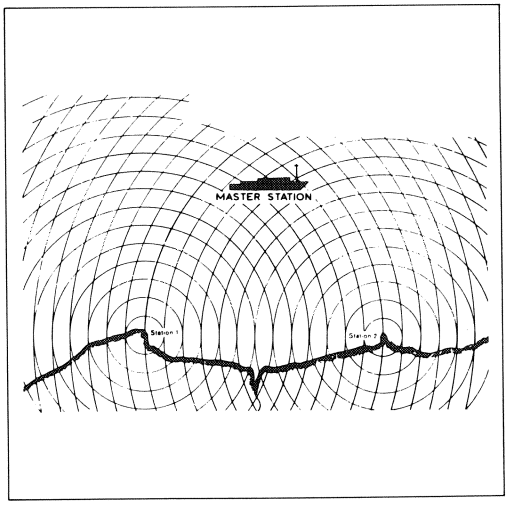

distance between the vessel and the fixed station at known position as well as the angle between the vessel and a reference direction is measured (e.g. Artemis).
A position fix is obtained by intersection of a circular range-line, with the fixed station as its centre, and a straight line through the location of the same fixed station. (figure 2.3.4.14).

2.3.4.9 Data correction and plotting

The first stage of mapping is the production of fairsheets (maps of the seafloor with a high density of recorded depths) which can be used directly for measurements or be contoured to produce bathymetric charts. To produce fairsheets, the recorded soundings must be corrected prior to plotting.
In surveys where the depths and positions are recorded only on the echo-sounder trace, the data for fairsheet plotting must be transcribed manually or with a digitizer.
Corrections for anomalies, such as fish and waves, can be subjectively smoothed from the record and tidal reductions can be effected by making stepwise changes to the depth baseline of the recorded trace prior to data transcription. Today these tedious and time consuming tasks have largely been eliminated by employing automatic recording, analysis and plotting techniques.
Modern automatic survey equipment usually incorporates a digitizer and data logger so that depth, position and vertical acceleration of the survey vessel can be simultaneously recorded on magnetic tape. Depth corrections and plotting can then be handled automatically using a computer and a computer controlled plotter.
Removal of anomalies from automatically recorded depths may be made using time series techniques. Filters, with specific frequency cutoff bands and predetermined tolerance ranges, are used to locate anomalies and if needed, substitute realistic values in their place. The latter approach is however not without its problems.
Anomalous reflections such as weed or fluid mud cannot be eliminated. For weed, manual

Figure 2.3.4.14 The polar method of positioning.

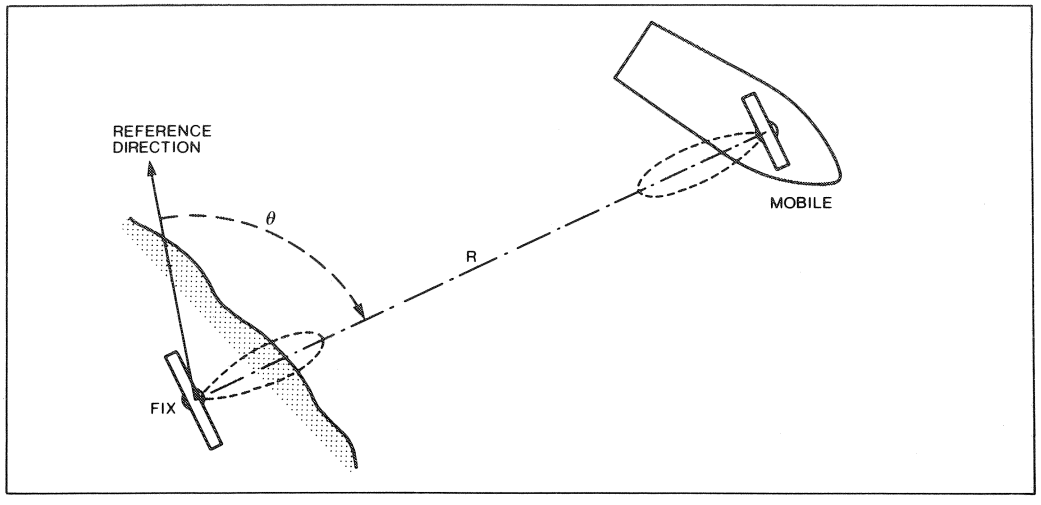

corrections can usually be made by comparing the graphical echo sounder trace with a plotted profile of the automatically recorded depths.

Correcting for fluid mud is a particularly difficult problem to solve and can only be done if density measurements are made to define the depth of consolidated sediment.
Depth errors arising from ship movement in waves, can be corrected by subtracting ship heave, calculated from recorded vertical accelerations of the survey vessel (figure 2.3.4.15).
Another error, ship squat, caused by the settling of the survey vessel as it moves through the water, must also be allowed for. This is usually estimated from the draught and speed of the vessel during the survey.
Tidal range corrections are made by using the tidal height changes, recorded over the survey period, corrected for distance variation using cotidal line charts.
Corrections are usually made in stepwise increments of + 0.01 m. Echo sounder errors are considered to be linear over the survey interval and corrected for accordingly. The final stages of depth correction involve accounting for the depth of the echo sounder transducer and reduction to a datum plane.

Figure 2.3.4.15 A, an automatically recorded depth profile corrected for tidal variations. B, the same depth profile corrected for sea and swell. (after [2]).

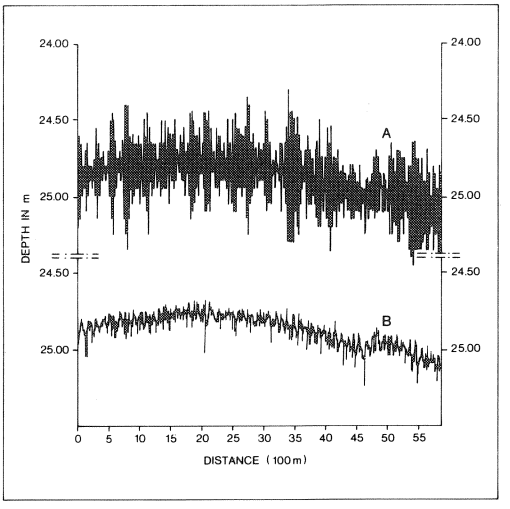

The resulting corrected data sets can be used for (X, Y) or (X, Y, Z) plots of profiles and fairsheets respectively.
Ship heave and tidal correction accuracies are generally within ± 0.15 m and 0.10 m respectively. Allowing for minor errors, such as ship roll and roundoff, the accuracy of measured depths for a well controlled survey are generally better than ± 0.3 m in water 10 to 40 metres deep. Accuracy is further improved within inlets where wave disturbances are reduced and tidal corrections can be more accurately calculated.
Automatic data collection systems always record more data than can be plotted for hydrographical or morphological purposes.
This means that, even on a large scale, more data are recorded than can usually be plotted. A selection of soundings to be plotted must therefore be made. The overriding control for selecting soundings to be plotted on fairsheets is the scale because it regulates the density of depths that can be plotted.
In principle, the selection of soundings is made in two stages:

- identifying depths that will definitely be plotted; i.e. significant peaks and troughs,
- selecting depths not chosen at stage 1 but which can be plotted because the spacing on the fairsheet between already selected soundings is large enough to accommodate additional depths.

A good description of the method and criteria for automatic depth selection for nautical charts is given by Brouwer [2].

2.3.4.10 Highly-detailed surveys

Some aspects of detailed bathymetric surveys used to monitor changes in the seafloor

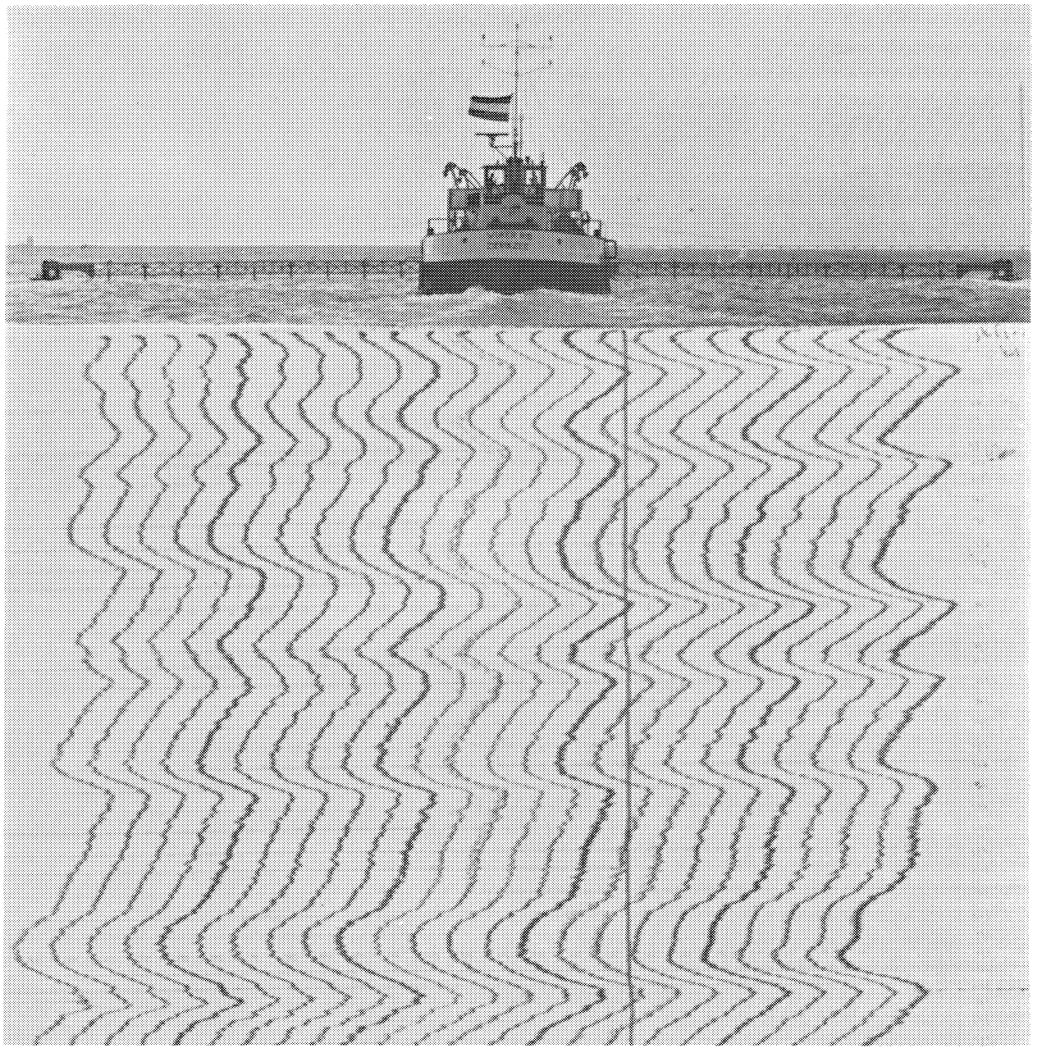

Figure 2.3.4.16 An echo-sounder trace showing 24 simultaneously recorded profiles made by the survey vessel „Wijker Rib''. The height and alignment of bed forms developed in a dredged trench are clearly shown.

topography, and an unusual approach to this problem, together with its limitations, are worth mentioning here. The three principal features of this type of survey are:

- that survey sounding lines be closely spaced so as accurately to record the seabed topography on underwater structures such as sills or scour protection,

- surveying navigation must be very accurate, and
- the time between and plotting of the bathymetric fairsheet must be very short.

These factors mean that when using conventional surveying methods the survey lanes need to be spaced at distances of about 10 to 50 metres. In order to do this adequately, surveying at high or low water is preferred in order to reduce drift of the survey vessel. The rapid data analysis requirement calls for data collection, analysis and plotting to be automated, using data logging and computer techniques.

In addition to conventional surveying, where a single transducer is used, special survey vessels equipped with a great number of transducers can be employed for very detailed and accurate detection of bedforms and accretion or scour around obstacles on the seabed. The transducers are mounted transversely beneath the vessel and buoyant outriggers which can be retracted by being folded alongside the vessel. Between 40 and 100 variable beam transducers may be installed depending on the nature of the survey. These are spaced at anywhere between 1 and 2.5 m apart and positioned about 1.5 m below water level. All transducers operate simultaneously and are connected to an electronic control unit with as many channels as there are transducers. An automatic amplifier control unit may be used to adapt the beam width of the transducers to the water depth therebye ensuring that the area covered by each beam remains constant.

The recorded depth data can be graphically recorded as: instantaneous cross section profiles, longitudinal profiles drawn next to each other (figure 2.3.4.16), or as seabed contour lines. At the same time these data can also be recorded on magnetic tape. Other refinements such as automatic compensation for tidal level changes, that are transmitted to the survey vessel from a telemetry buoy, can also be implemented. Errors introduced by sea and swell can be substantially reduced using a heave compensator. Both tidal and wave data can be fed into a computer which then applies the corresponding corrections to the depth data.

For the closing of the Eastern Scheldt inlet in the Netherlands a survey vessel of this type was needed to monitor changes in and around the foundation being prepared for the closing structure. This vessel, the 54 m long „Wijker Rib", was fitted out with 24 (4-10°) variable beam echosounder transducers mounted 2-5 m apart (figure 2.3.4.17).

In transit and when manoeuvring the outriggers were stowed on deck. When surveying the outriggers, supported at one end by the ship and at the other end by floats, were brought into position by steel cables. With a beam of 9.8 m without outriggers and 66 m with the outriggers spread lanes 60 m wide could be surveyed.

For position fixing Decca or mini ranger electronic systems were used. The vessel was driven by two propellers of 300 hp and fitted with two Schottel navigator active rudders of 260 hp (aft) and 510 hp (forward)to compensate for lateral drift due to currents. One of the problems encountered with this type of surveying is the enormous quantity of data collected which has to be analysed. For example Speekenbrink et al. [4], using this technique to monitor large bedform migrations, made 26 half hourly surveys over one tidal cycle. This survey alone generated 624 profiles for analysis.

2.3.4.11 Side-scanning sonar and seafloor mapping

A major breakthrough in mapping the surface topography of the sea floor has been the development of sideways-looking sonar.

This „side scanning sonar" detects relief features on the seabed by converting reflections from obliquely transmitted signals into distances. These are recorded as a graphical trace -a sonograph - that depicts seafloor topography up to 500 metres on either side of the lane being surveyed.

This ability to map seafloor topography over large areas has proved to be extremely valuable for a wide range of underwater engineering and scientific applications. These include: locating wrecks and obstructions during bathymetric surveys, surveying pipelines, cables and seafloor constructions as well as identifying

Figure 2.3.4.17 The Wijker rib in action, Eastern Scheldt inlet, the Netherlands.

bedforms and the direction of sediment transport on the sea bed. Modern sidescan sonar systems consist of a dual channel recorder, a towing cable and a hydrodynamically stable towed transducer unit or „fish" (figure 2.3.4.18).

A transducer is built into each side of the tow fish. From these a number of very narrow sonar beams are directed obliquely downwards over the seabed and upwards to the water surface (figure 2.3.4.19). Signals relfected from the sea bed and water surface are plotted at their respective slant ranges. The intensity of these marks is proportional to the strength of the reflected signals which vary with different bottom materials.
Low reflief features, e.g. sand, mud or gravel patches, can be differentiated by tone variations on the sonograph. Objects with strong relief, such as wrecks, boulders, rock outcrops or bedforms, are recorded as dark patches with white acoustic shaddows (figure 2.3.4.20).

The heights of detected objects are readily calculated from; the length of the acoustic shaddow, the height of the fish above the bed, and the slant range (figure 2.3.4.21A).
Detected objects are recorded at slant range distances on the sonograph. This introduces a distortion that must be corrected for when making measurements from the recordings. At the same time compression of expansion distortions introduced by sloping topography must also be taken into account (figure 2.3.4.21B).
Many of the distortions inherent in sidescan sonar recordings have in part been eliminated in new „sea floor mapping" instruments.
These work in essentially the same way as sidescan sonar except that a microprocessor is used to correct slant range to a true distance from beneath the sonar fish. In addition the sonograph may be printed at a rate proportional to the speed of the survey vessel. In this way the true relative positions of features on the sea floor are mapped. This allows closely spaced recordings to be combined into a mosaic map of the seabed that may be complemented by superimposing depth contour lines.
The technique of combining seafloor mapping

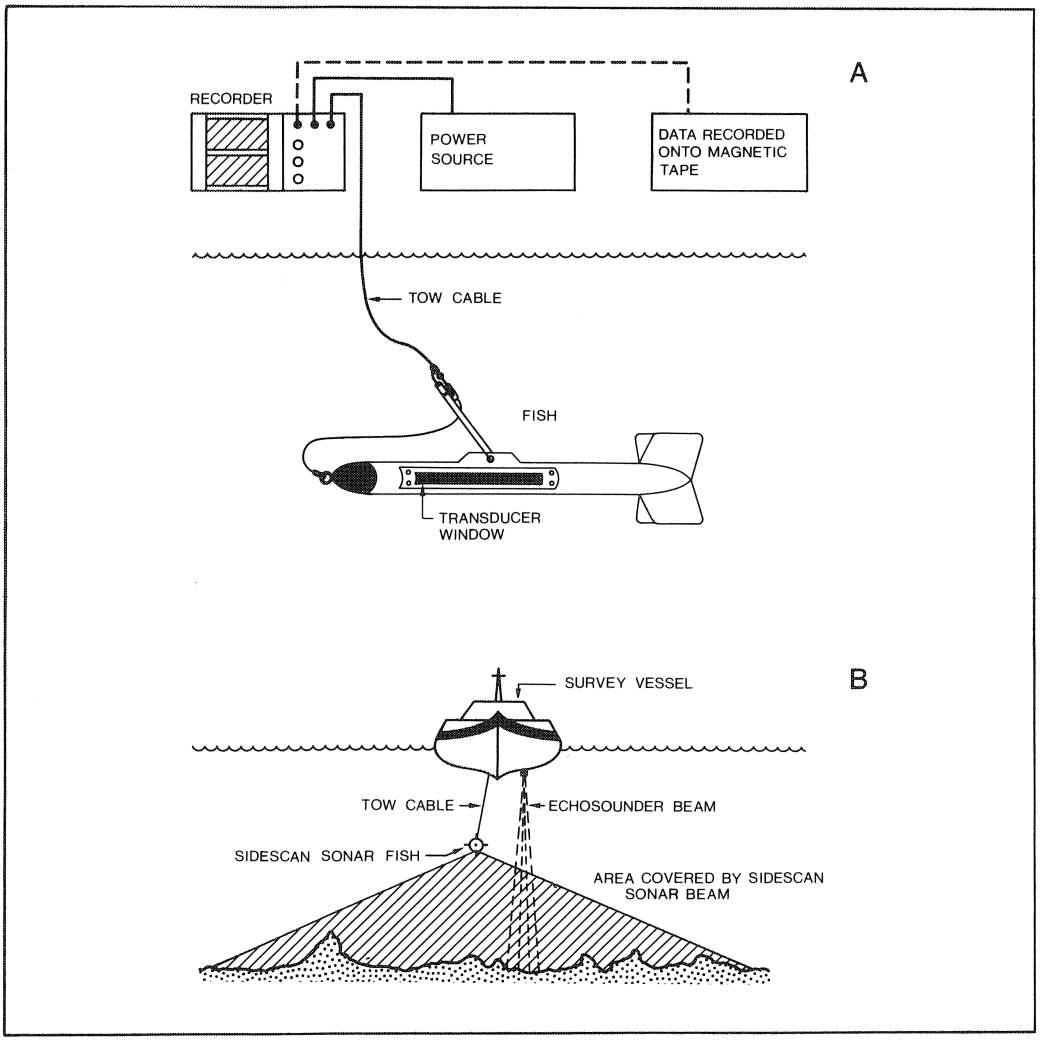

Figure 2.3.4.18 A, diagrammatic illustration of a sidescan sonar system consisting of: the transducer carrying fish, the tow cable, the sonograph recorder with power source and the optional tape data recorder. B, schematic illustration of the area scanned by sidescan sonar beam relative to that covered by a conventional echosounder.

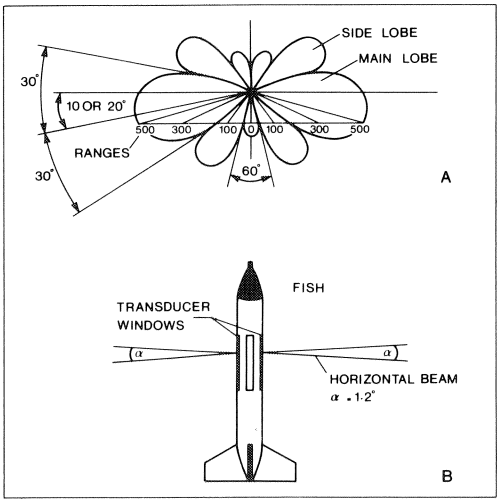

Figure 2.3.4.19. A, schematic illustration showing the vertical distribution of the main and side sound lobes transmitted from a towed sidescan sonar fish.
B, a plan view of the ultrasonic beam emitted from both sides of the fish.

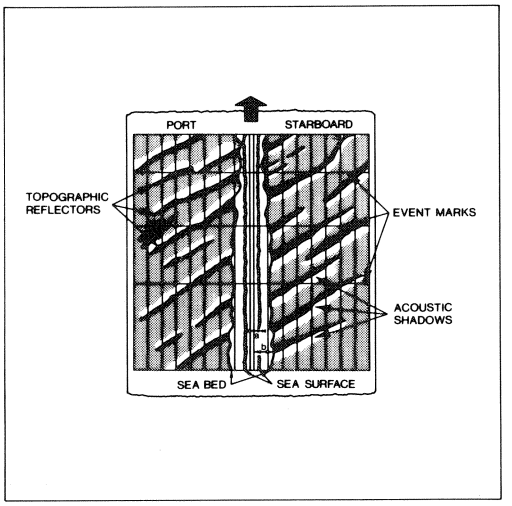

Figure 2.3.4.20 Schematic representation of a sidescan sonar sonograph. Sharp relief features appear as dark marks that typically have white acoustic shadows behind them.
a, depth of fish below water surface; b, height of fish above the seabed; total water depth = a + b.

with bathymetric survey data is extremely valuable for dredging projects. Areas not dredged or poorly covered can be immediately identified. This can head to a significant improvement in dredging efficiency.

2.3.4.12 Determination and prognosis of sedimentation and erosion in and near tidal basins based on historical surveys.

Present knowledge of sediment movement, under the complex hydrodynamics of tidal currents, has not yet reached the stage where large-scale changes to the seabed morphology, such as the formation or migration of channels and banks, can be reliably predicted. Shortcomings in the theoretical treatment of predicting sea-floor morphological changes has necessitated a pragmatic approach to the problem. This is based upon extrapolating trends found in existing data on the assumption that the identified trends will continue in the near future.

The highly dynamic nature of sediment movement in inlets and around tidal entrances implies that an element of uncertainty is inherent in any prognosis made of sea floor morphological development. This is especially so for regions where currents have a strongly three-dimensional character or interact with waves. The irregularity in distribution, form and rate of sediment erosion or accretion of the seabed calls for a multidimensional approach to identify and analyse morphological developments. Some of the basic one, two and three dimensional techniques used to analyse and extrapolate trends of sedimentation or erosion identified from recorded data are outlined below.

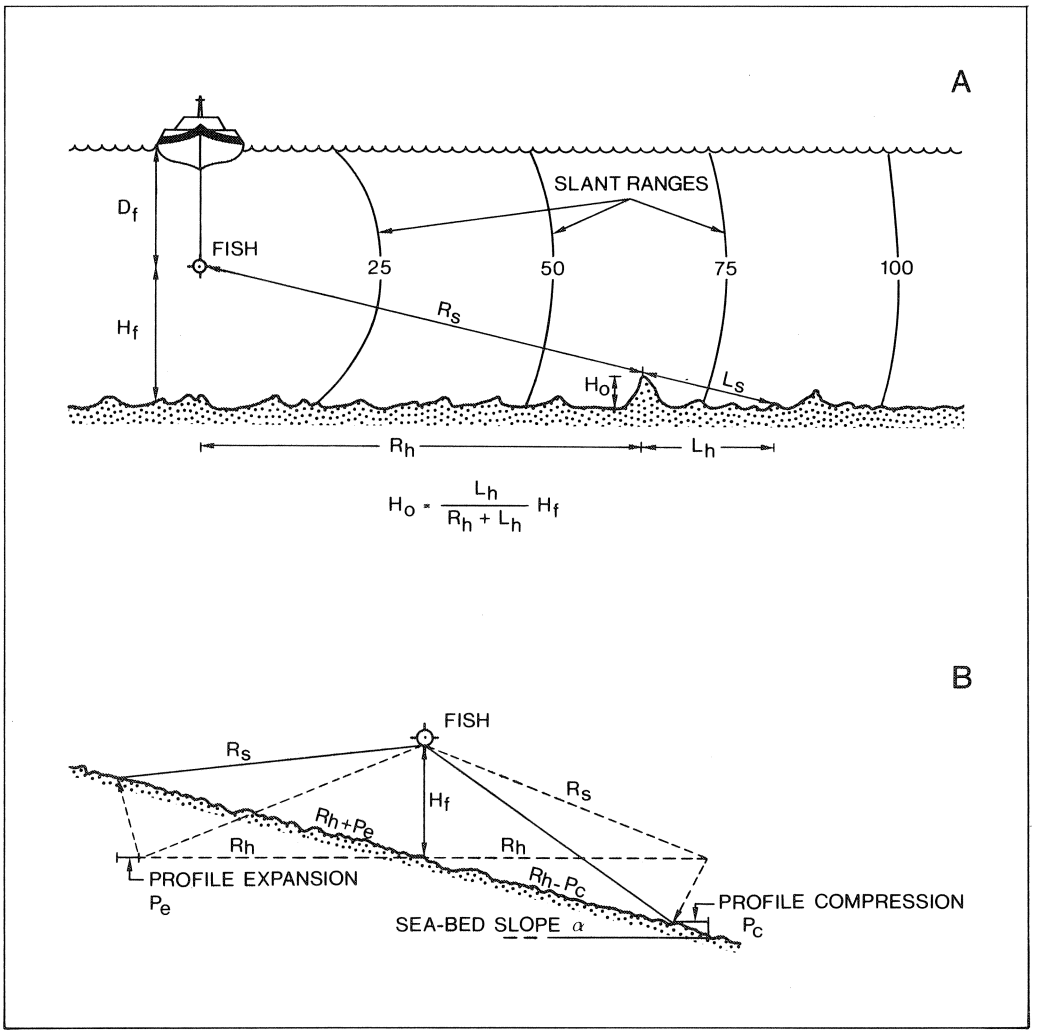

Figure 2.3.4.21A Calculating the height of a sonar contact from the length of the acoustic shadow. Df, depth of fish; Hf, height of fish above seabed; Rs, slant range; Ls, length of the acoustic shadow; Rh, horizontal range; Ho, height of contact.

B, illustration of lateral distortion that occurs when recordings are made over sloping surfaces. Upslope range = Rh + Pe, downslope range = Rh - Pc.

Historical chart comparison
Should historical charts be available, the scale and pattern of changes that have taken place in and seawards of a tidal basin over perhaps the last 100 years can be determined (figure 2.3.4.22).
Comparison of the positions of channels and banks on a large scale quickly shows the magnitude of these changes and where they

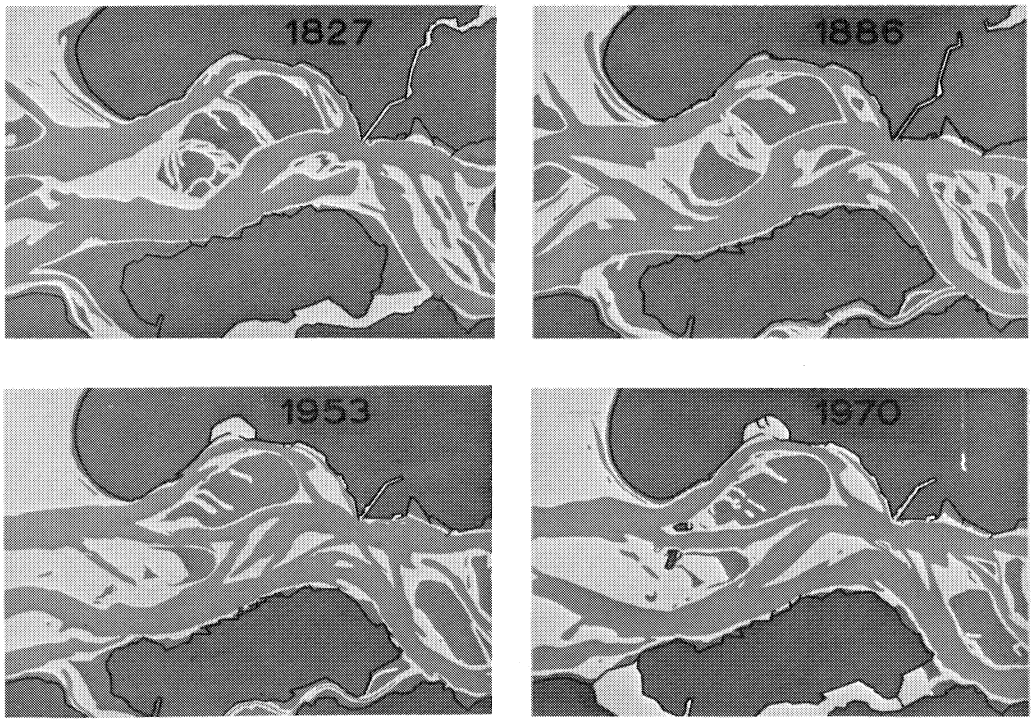

Figure 2.3.4.22 Historical charts that clearly illustrate large scale changes in the position and alignment of shoals and channels near the entrance of the Mesotidal Eastern Scheldt inlet in the Netherlands.

have occurred in the past. Identifying these changes can be particularly important for planning the position of a tidal basin closing structure because contemporary changes are likely to continue during the initial phases of construction. Should these changes be sufficiently large or rapid, they could interfere with the construction programme.

Figure 2.3.4.23 Example of a contour difference chart (Haringvliet, Netherlands, period 1970 - 1975).

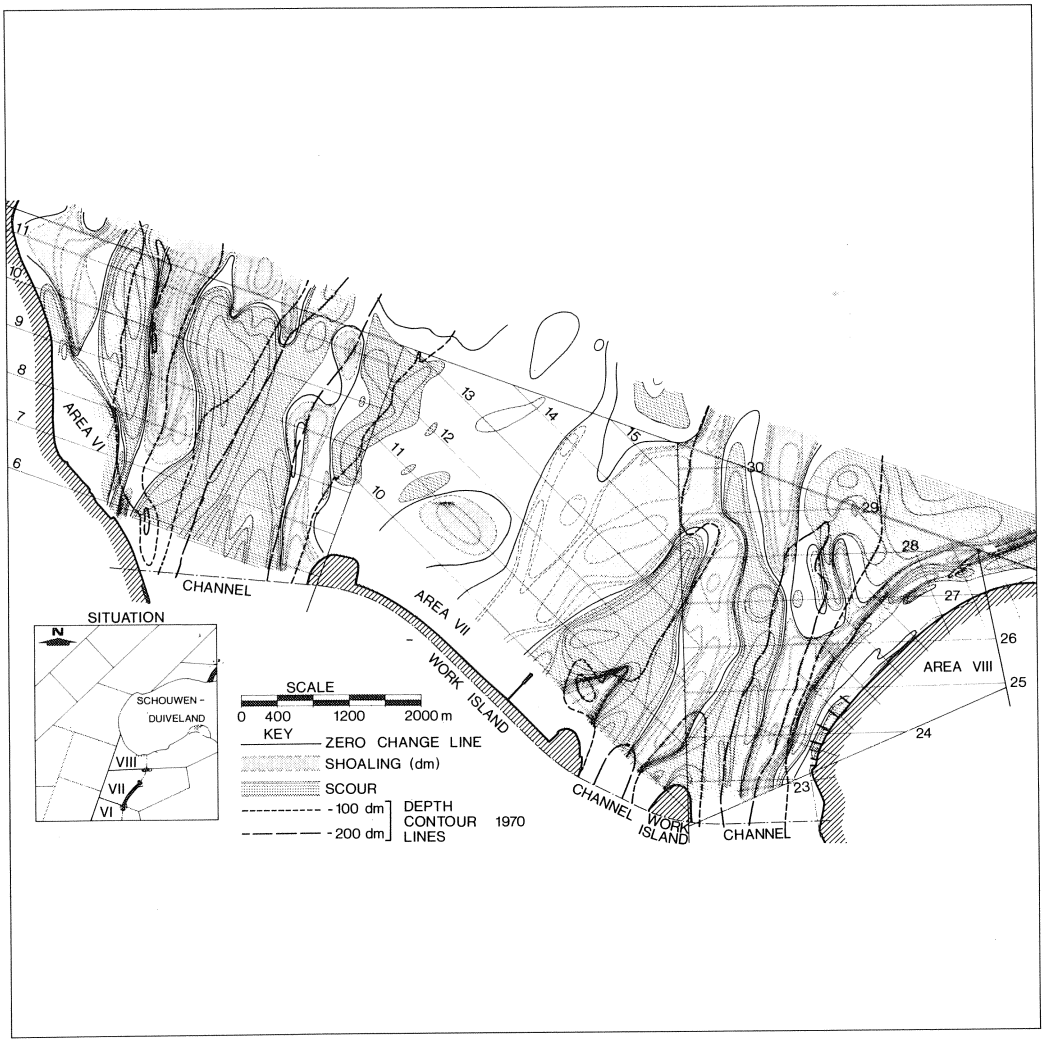

Analysis of historical and recent bathymetric charts can also yield additional information on changes to the volume of the tidal prism and the capacity of tidal channels within the inlet to carry flows.For this work, particular attention must be given to reducing the available surveys to a common datum.

Contour difference method

Contour depth difference charts are constructed from the measured depth changes between two bathymetric surveys (figure 2.3.4.23).

Bathymetric charts to be compared are overlayed and the depth differences systematically noted on a transparent overlay or directly onto the latest bathymetric chart. Changes can be measured by using: a graphical network, individual depth contour lines, or, as in the case when working with uncontoured fairsheets, along the lanes actually surveyed.

Depth changes are contoured and the resulting difference chart clearly defines the position and shape of areas undergoing change.
Analysis of depth differences can be approached in two ways.
The first, long-term measurement, considers only the net change between the first and last surveys.
The second, a more detailed approach, where depth differences between successive surveys are mapped, identifies the localised trends of morphological change by following the development with time of the alignment, shape and position of areas showing the greatest accretion or erosion.

This technique is particularly useful for monitoring developments such as the formation of scour holes after each construction stage during the closure of a tidal extrance.
Another important application is in channel and harbour-dredging programmes because the areas showing marked accretion are quickly located and the quantity needed to be dredged can be readily estimated.
One disadvantage of the method is that it is usually done by hand and is therefore, particularly time-consuming.

Profile differences

Nett changes in depth or alternatively the volume of sediment in survey network areas established within and seawards of a tidal basin are calculated by comparing consecutive survey profiles (figure 2.3.4.24.). The calculated nett changes are then analysed for trends. Where these are found, a prognosis for sections of the survey network can be made.
This method has the advantage of monitoring large areas with a minimum of data collection and analysis. On a large scale however it is restricted because historical survey profiles, if in fact there are any, seldom follow the same profile lines established for a closing project. On the large scale therefore, this approach is used to follow the changes that take place once a tidal entrance has been closed.

Network elements

For this approach, the investigation area is divided into a grid of equal areas, usually squares, and an average depth for each area is calculated. As with profile differences, prognosis is based on trends in differences observed between consecutive surveys (figure 2.3.4.25).
A critical feature of this method is deciding how large to make the squares in the grid network.
Ideally, each square should cover or be contained within areas with distinguishable morphologies. This minimises the occurrence of areas covering two morphological zones, where different hydraulic and sediment processes operate.
In principle, this method can be used at any scale but it does have a number of practical disadvantages. One of the most significant, which arises from the choice of square size, is the vast amount of depth data that has to be analysed and the density at which it is collected in the first place. Another problem is the inaccuracy of survey reductions. These can introduce spurious results that may obscure trends. This type of error can usually be recognised when apparent changes show an almost uniform trend over the whole survey area. This is not always the case however and even if errors are found it usually entails a great deal of additional work to remove them.

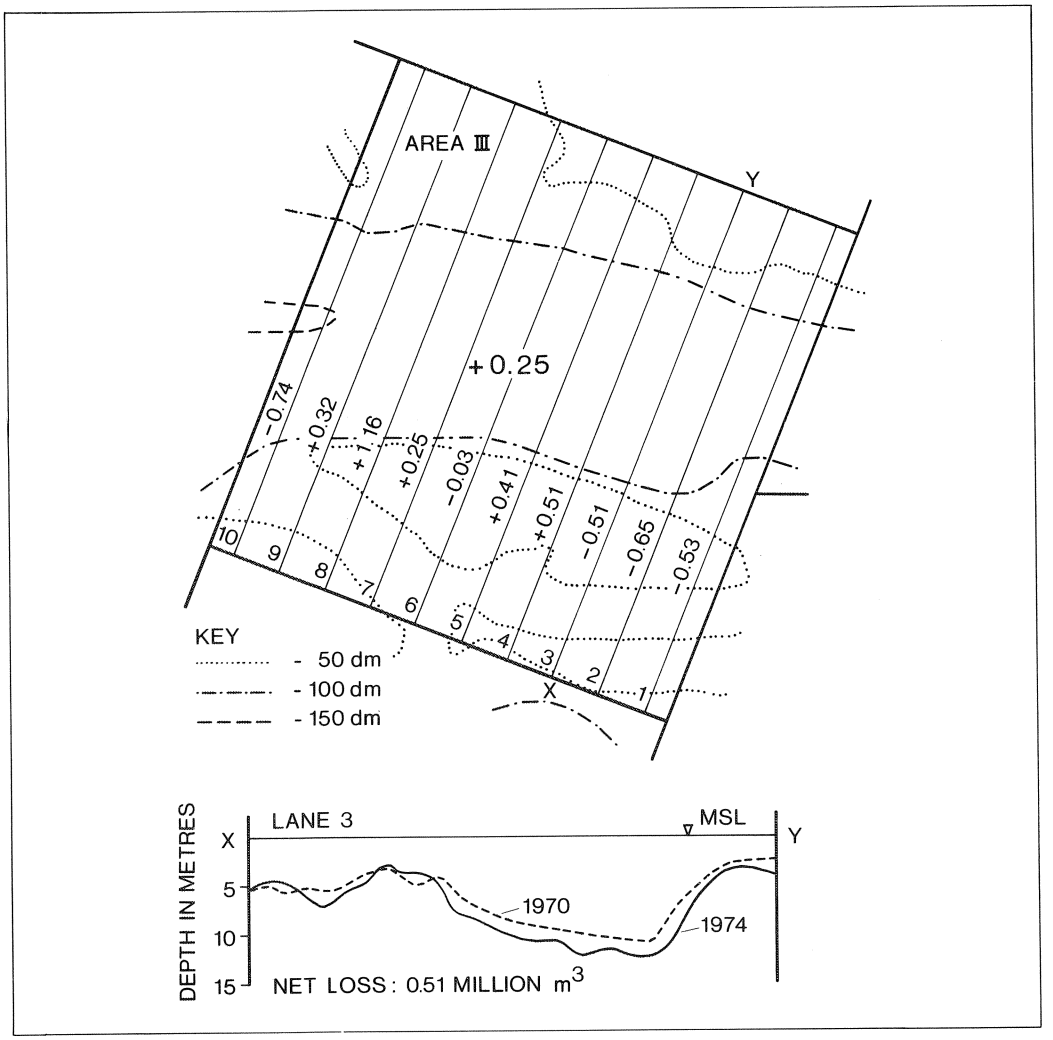

Figure 2.3.4.24 Accumulation and loss of sediment over a four year period along 10 survey lines in a large scale survey network area covering a main channel. Changes along each profile and net change for the whole area are given in millions of cubic metres.

Position, depth or volume lightning graphs

Lightning graphs are used to follow depth, position or volume changes with time. Amid the many random fluctuations, trends in stability or movement of the sea floor can emerge.

A number of variations to this technique exist. These are:

- variations of depth at a fixed point (figure 2.3.4.26),

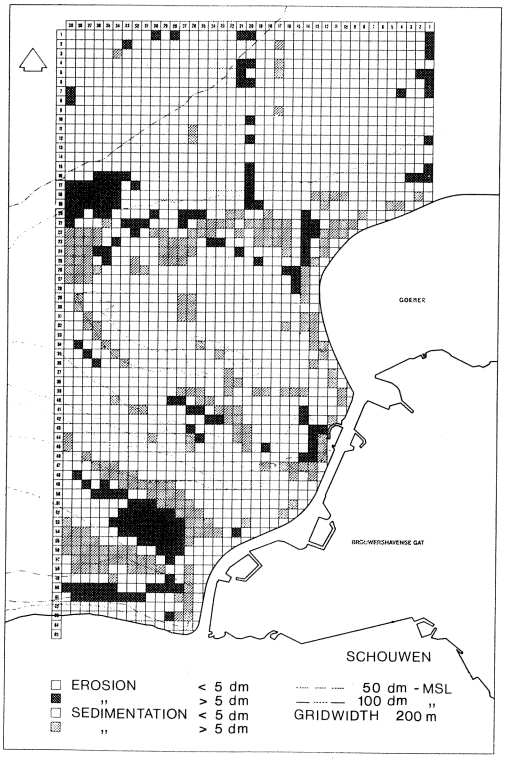

344

Figure 2.3.4.25 Example of the network element method. (Brouwershavense gat, the Netherlands)

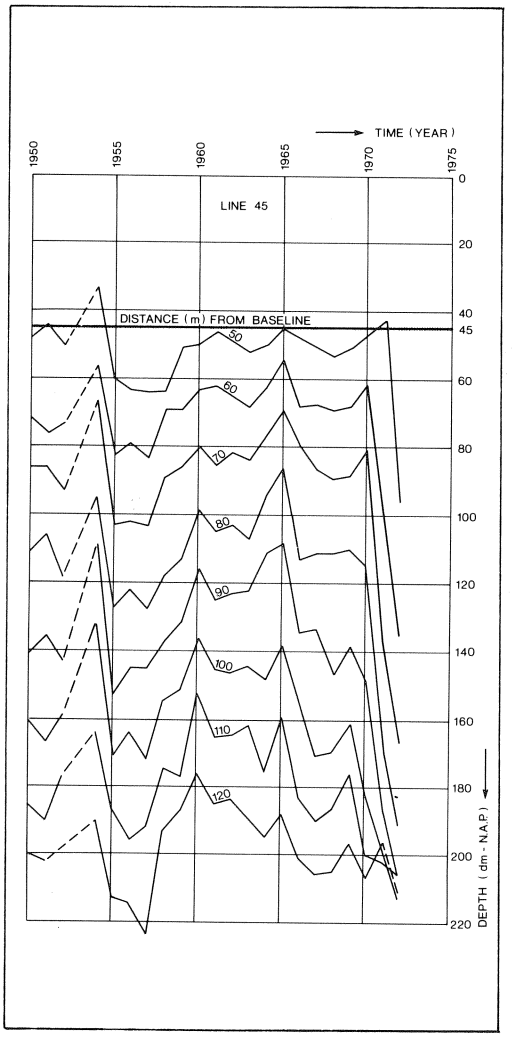

Figure 2.3.4.26 A lightning graph showing changes in depth at fixed distances from a reference line.

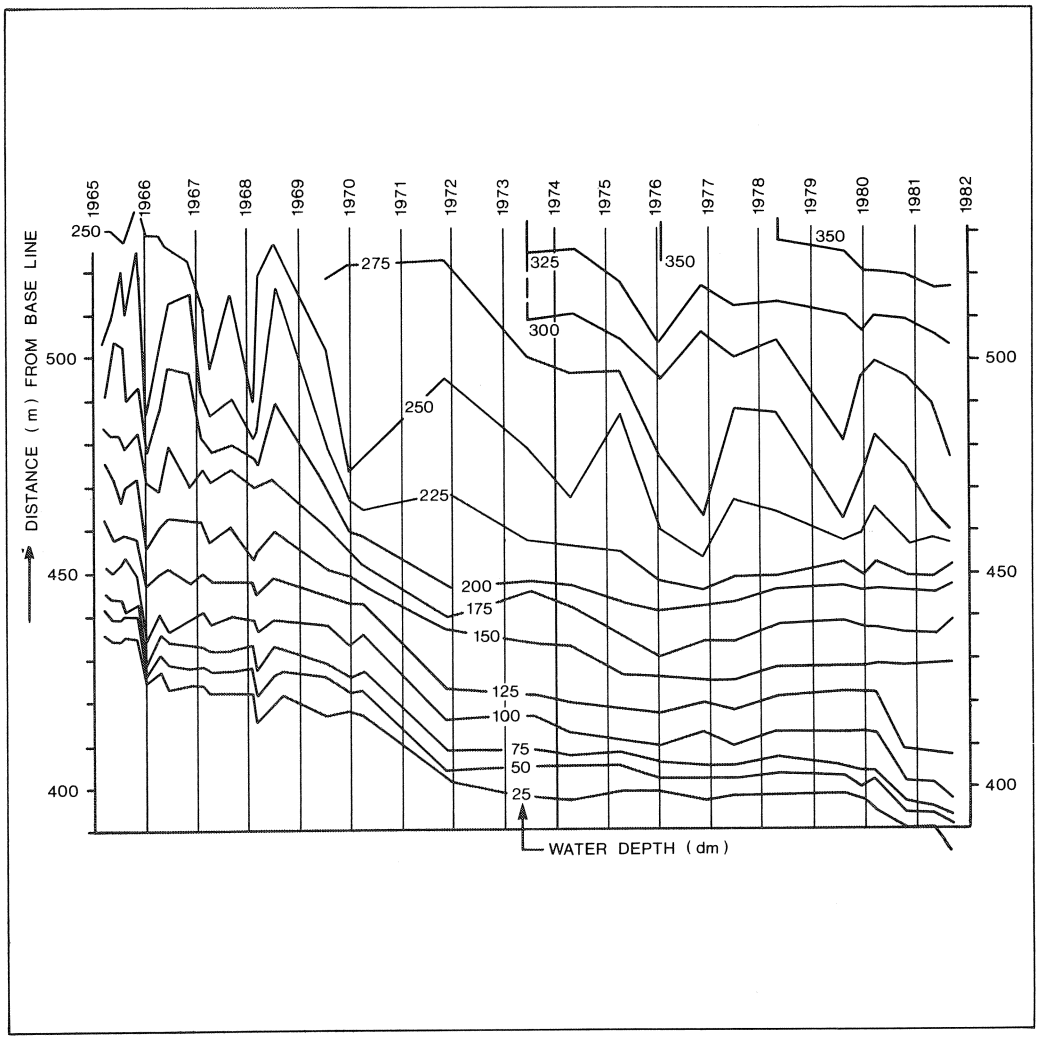

Figure 2.3.4.27 Changes in the distance to a defined depth contour line.

- horizontal movement of depth contour lines (figure 2.3.4.27),
- changes in depth or position of distinctive topographic features such as the deepest points of a channel (figure 2.3.4.28) and
- changes in volume along a surveyed profile.

Interpretation of the graphs is based upon the principe that the seabed will respond to the prevailing hydraulic regime, providing the

sediments are sufficiently incohesive to respond. Changes to the hydraulic regime will therefore eventually manifest themselves as changes to the sea bed. If this action response relationship holds, as could be expected on a sandy coast, then variation of trend slopes on the lightning graphs will indicate changes in seabed stability.

Changes to graph slopes are particularly useful for monitoring phases of instability induced by individual stages of an inlet closing structure and the eventual return of the seabed to a new and probably dynamic equilibrium.

Contour line displacements

One of the simplest ways of forming an impression of changes taking place on the sea bed is to measure and extrapolate measured displacements of depth contours (figure 2.3.4.29).More elaborate vertical and horizontal analyses of cross section profiles can also be made. Prognosis of vertical changes to cross section profiles can be made by simply extrapolating the differences found between two profiles recorded from the same location (figure 2.3.4.30). The recorded differences are assumed to represent a continuing trend in erosion or accretion along the profile.

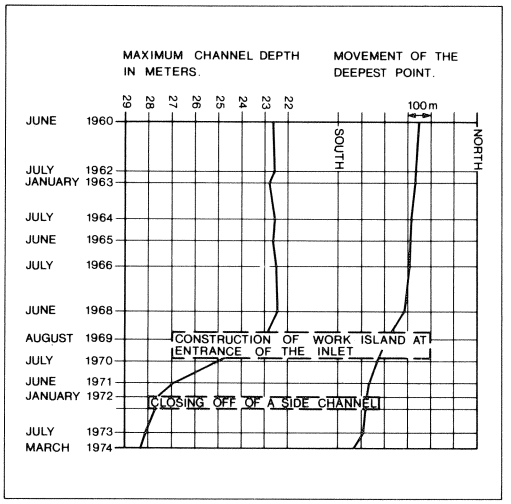

Figure 2.3.4.28 Examples of a position-depth-time graphs.

Figure 2.3.4.29 Extrapolation of measured differences in the position of depth contour lines.

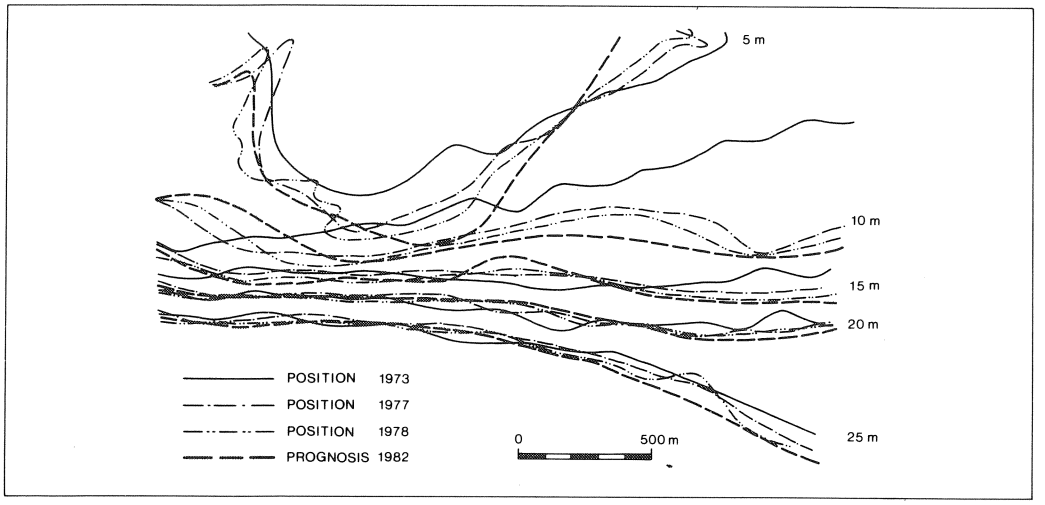

Two limitations restrict the confidence in the extrapolations made using this approach.
Firstly, the assumption that measured changes represent a continuing trend cannot account for periodic phases of sedimentation or erosion. Consequently vertical extrapolations, especially for accretion on sandbanks, sometimes give improbable results.

Secondly, horizontal variations such as the realignment of channels are not accounted for. Profile shapes and channel alignment can be predicted by extrapolating the measured horizontal displacements of: the deepest point, individual depth contour lines and the shallowest points along the channel edges. For each available survey, the position of every reference point on a profile is transferred on to a linear scale and then plotted against time (figure 2.3.4.31). A regression line or a polynomial is then calculated from these points for each contour depth, shoal or channel and drawn onto the graph. In this way the future position and profile of a channel can be estimated. One disadvantage and limitation of this approach is that sometimes the extrapolated lines cross, thereby indicating the development of overhanging slopes.
By applying a mean vertical extrapolation value, calculated by using only the deepest and/or shallowest points of the channel and banks respectively, a three dimensional prognosis of the channel profile can be made (figure 2.3.4.32). As subsequently recorded data become available they can be incorporated into the calculations and the profile prognosis checked and modified.

A useful approach when frequently collected data are available is to base the regression calculation on the last few measurements or alternatively over a fixed time interval. In this way a „moving window" extrapolation, based on the most recent data, defines the trend and not the whole data set.

Figure 2.3.4.30 A prognosis for the development of a channel cross section made by extrapolating measured vertical changes.

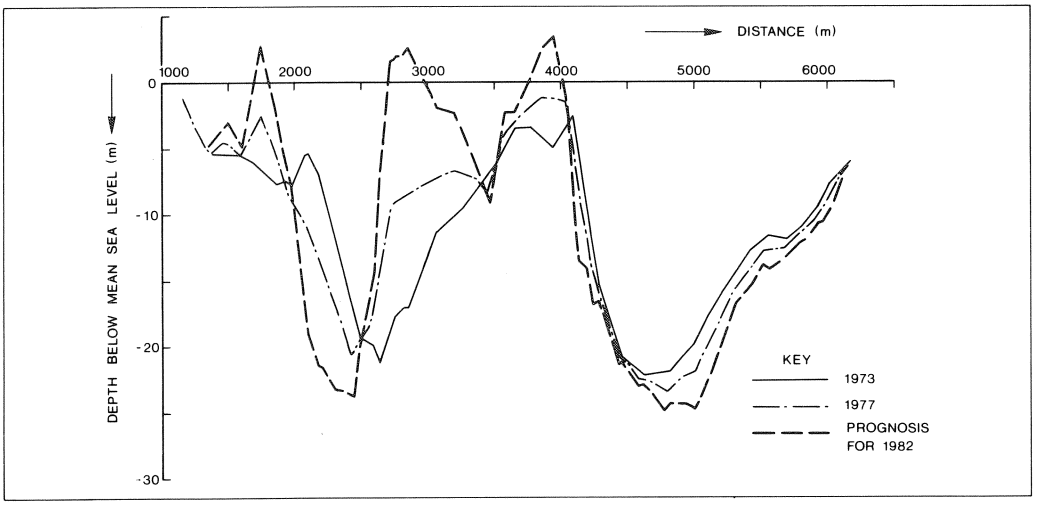

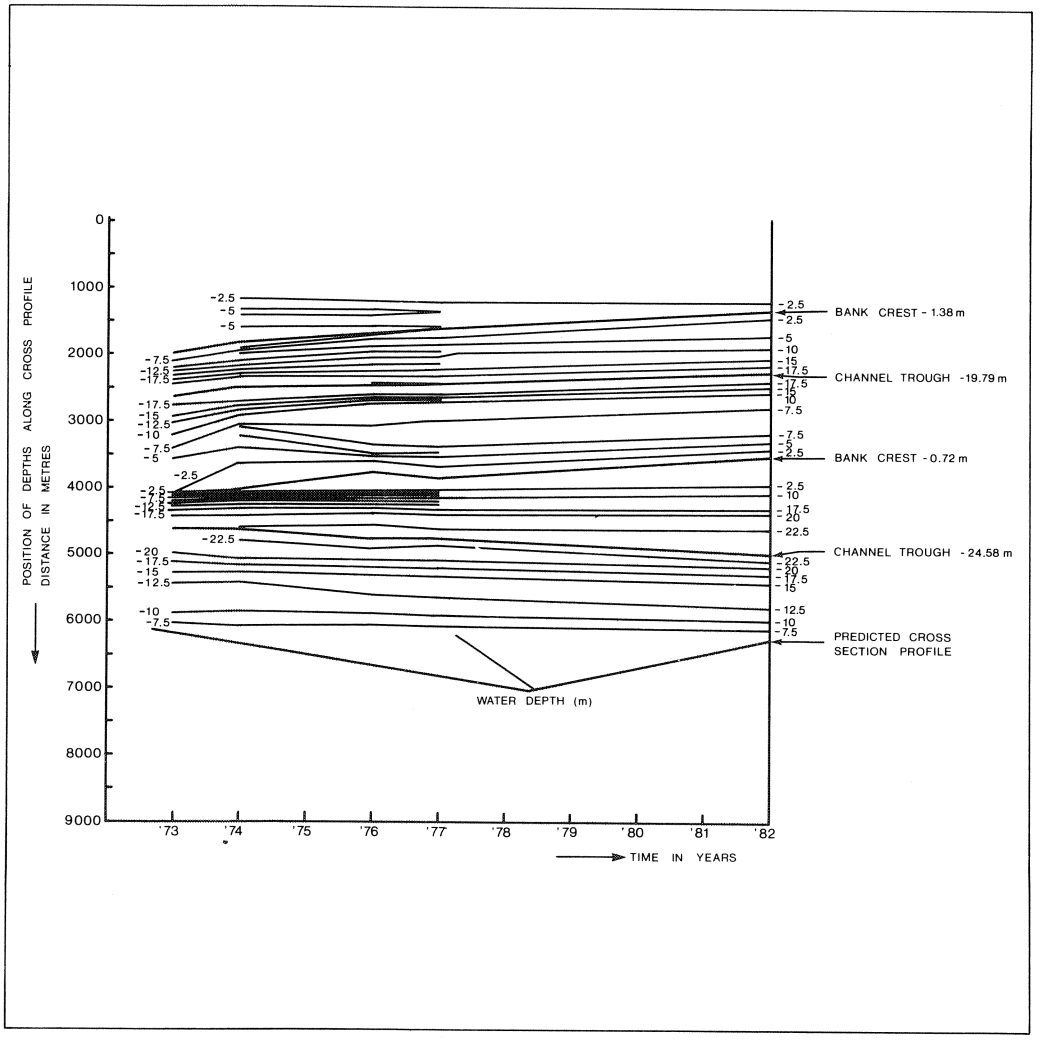

Figure 2.3.4.31 Predicting a cross section profile by extrapolating trends in the horizontal displacement of depth contour lines.

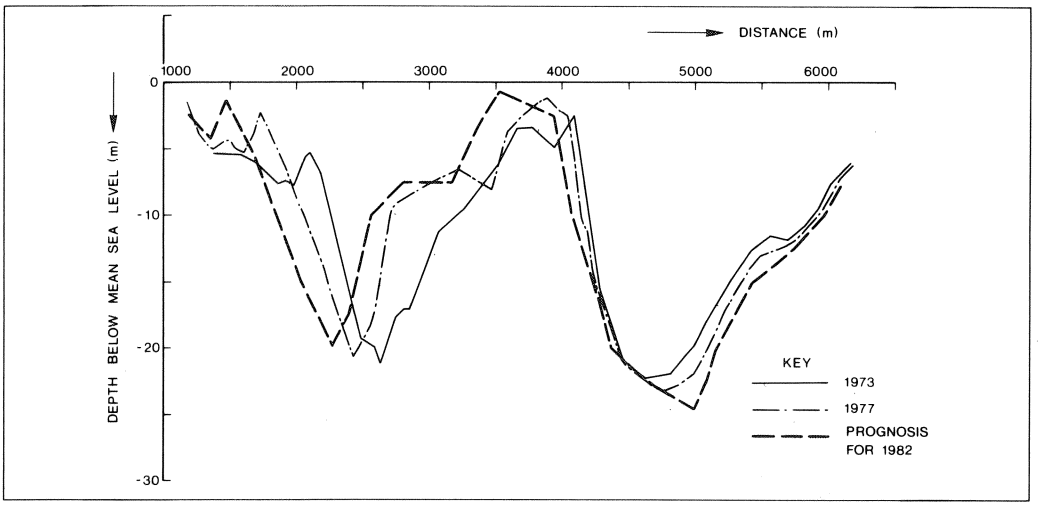

Figure 2.3.4.32 A predicted cross section profile calculated from measured trends in horizontal displacement together with the vertical trends exhibited by the channel troughs and bank crests.

References

1. Ingham, A., **Sea Surveying,** John Wiley and Sons, London, 1975, Vols 1 and 2.

2. Brouwer, G.K., **Automated Depth Selection for the Fairsheet,** International Review, Monaco, L III: 87 - 94, 1976.

3. Glen, N.C., Tidal Measurement. In: Dyer, K.R., **Estuarine Hydrography and Sedimentation.** Cambridge University Press, 1979, 230 pp.

4. Speekenbrink, H., Bliek A.J., Boon, T.J., Svasek, J.N., Van Wijngaarden, N.J, Sedimentation in dredged trenches pp. 215 -233, In **Hydraulic Aspects of Coastal structures, Developments in Hydraulic Engineering,** Part 2, Delft University Press, 1980, 235 pp.

Site Investigations and Data Acquisition

J.H. v.d. Berg

2.3.5. The determination of the suspended sand concentration

2.3.5.1. Introduction

Accurate prediction of morphological problems like siltation in dredged trenches and navigation channels in rivers and estuaries can only be made if the relationship between the sediment transport and the flow velocities is known.
In general this knowledge cannot be obtained with sufficient accuracy from theoretical sediment transport formulae. Preference should be given, therefore, to direct field measurements.
The different mechanisms of sediment transport gives rise to a distinction between bed load and suspended load. For sampling these types of sediment load specific instruments have been developed.

2.3.5.2. Bed load

Bed load transport is defined as movement of material by rolling or creeping along the bottom surface, and therefore refers to a very thin layer with a thickness of several times the median diameter of the sediment involved.
In fact there are no instruments by which the bed load concentration can be measured in an reliable way. The main problem in designing such a sampling system is always that the instrument itself disturbs the hydraulic conditions that govern the bed load transport. A frequently used bottom sediment catcher is the Bottom Transport Meter Arnhem (BTMA). The BTMA consists of an 0,4 m long, 0,05 m high basket sand filter which is pressed on the bed by a frame (Fig. 2.3.5.1).
It has to be stressed that in this way not only bed load material but also suspended load may be trapped. The instrument can not operate in muddy environments because of rapid filter blocking by the fine sediment particles. For the same reason large sand catches provide unreliable results. Since large spatial differences in concentration generally occurs in relation to bedforms, a great number of random measurements is necessary to obtain a more or less accurate impression of the near to the bottom sand concentration.
In unidirectional current situations (rivers) the magnitude of the bed load transport can sometimes be deduced from the ripple migration derived from accurate echo soundings.
When coarse sands are involved and suspended load is unimportant the use of tracers can be taken into consideration.

2.3.5.3 Suspended load

Under natural conditions the solids in suspension consist mostly of silt ($< 50\ \mu m$) and fine sand ($50 - 200\ \mu m$) in varying proportions. To measure this wide variety of sediment types, several devices have been developed.
With respect to the sand load two different types of simple bottle samplers and a pump sampler are being used. A new sophisticated instrument has also been developed recently for measuring the sand concentration by means of ultrasound scattering.
These sampling and measuring techniques are treated briefly below.
Some remarks are also made as to the accuracy of these methods and their use under different environmental conditions.

The Flushing Bottle (Vlissingse Fles, VF)
The VF is an ordinary one litre bottle with a neck diameter of 0.017 m.
(Fig. 2.3.5.2). Within the bottle a small ball of cork is present closing the bottle as it is filled under water. One or more of such bottles may be placed in a frame. After sealing off the bottles by a rubber plug the frame is suspended in the water and is sunk to a measuring position. To take a sample with the bottle it is uncorked by pulling a cable wich is attached to the rubber plug.

The Delft Bottle (Delftse Fles, DF)
The DF is a streamlined bottle with a small neck which is oriented to the flow direction by a tail-fin mounted at the back of the bottle (Fig. 2.3.5.3).
The form of the sampling body induces a low pressure at the rear face in such a way, that the water enters the nozzle of the sampler with almost the same velocity as the undisturbed ambient flow. In the wide body of the sampler the

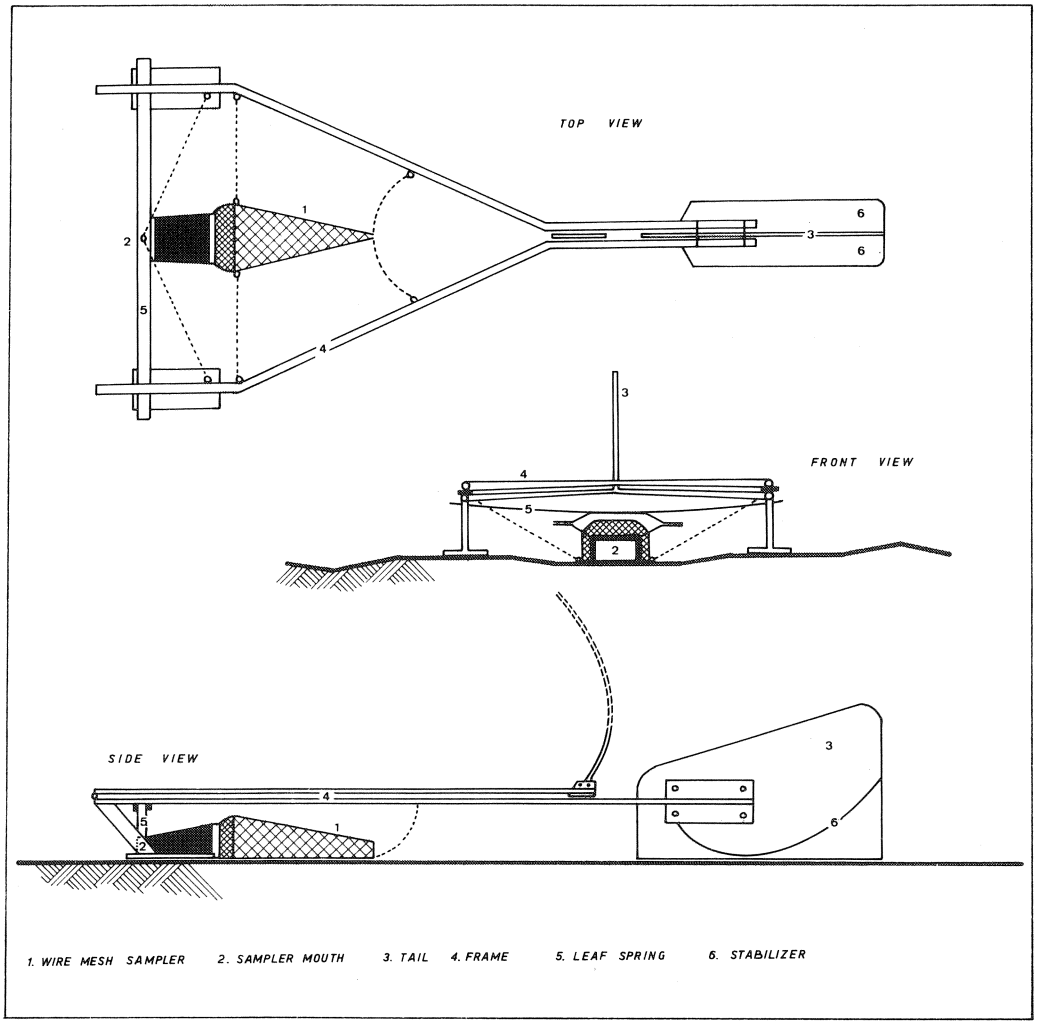

Figure 2.3.5.1 Bed Load Transport Meter Arnhem

flow decelerates and sedimentation takes place. The „dépôt" largely will consist of sand, most of the mud will leave the bottle with the water outflow.

The Pump Filter Sampler (PFS)

The sampling unit of the PFS consists of a streamlined heavy ballast body (150 - 250 kg.) at which an intake nozzle is installed. For pumping

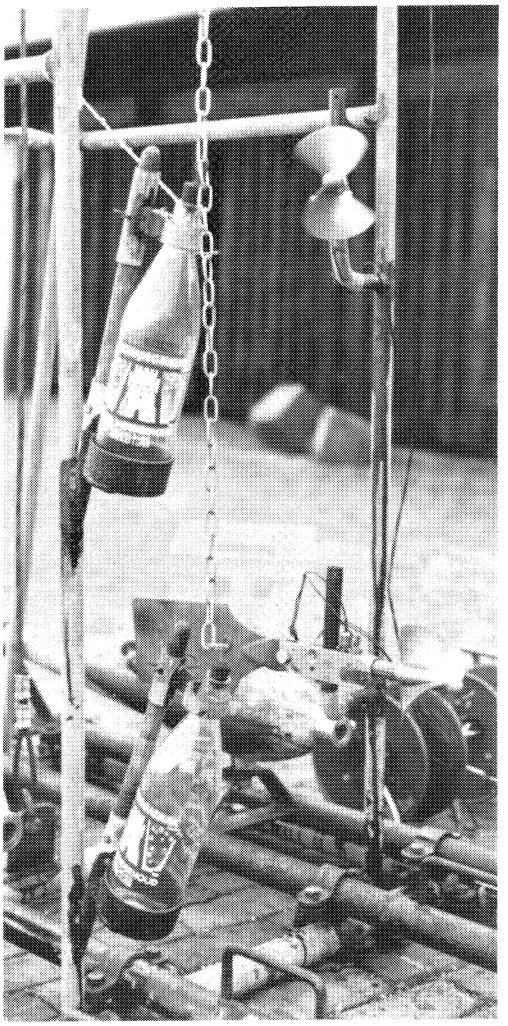

Figure 2.3.5.2 Flushing Bottles in a frame

a pump mounted on the deck is used. The pump is connected to the intake nozzle by a suction hose. The volume of the water sample is recorded by a volume meter based on the flow-through principle. The separation of water and sand is done by forced filtration through a nylon filter (Fig. 2.3.5.4).

The Acoustic Sand Transport Meter (AZTM)

The conventional sampling methods treated above all have in common that they provide data of average concentration over a certain sampling period, that sampling is discontinuous and that the current velocity is measured separately and not exactly at the sampling location. The main feature of the AZTM is the continuous and simultaneous determination of mass concentration and velocity of the suspended sand in the same small volume of water. The concentration and velocity are determined from respectively the amplitude and frequency of one and the same scattering signal.

The measuring principle of the AZTM is shown as a diagram in Fig. 2.3.5.5. The transmitter-receiver (TR) transducers are identical piezo-electric ceramic disks. The dotted area is the effective volume.

The sand particles within the effective volume scatter part of the acoustic energy back to the receiver.

The resulting electric signal contains all relevant information on particle transport. When the sand particles are moving, due to the Doppler-effect a frequency f_1 is observed on the receiver, which has been slightly shifted relatively to the frequency f_0 that has been transmitted by the transmitter. The Doppler shift $\triangle f$ is directly proportional to the particle velocity.

At high concentrations of 1 gram of sand per liter or more, the received signal is considerably weakened by absorption in the area between the TR transducers and the effective volume. The same holds for very high concentrations of mud. To eliminate this effect, a third transducer is added to the AZTM configuration which receives directly part of the transmitted energy (fig. 2.3.5.6).

The sensor head is mounted on a streamlined carrier containing the high frequency electronics (Fig. 2.3.5.7) and is connected by an elec-

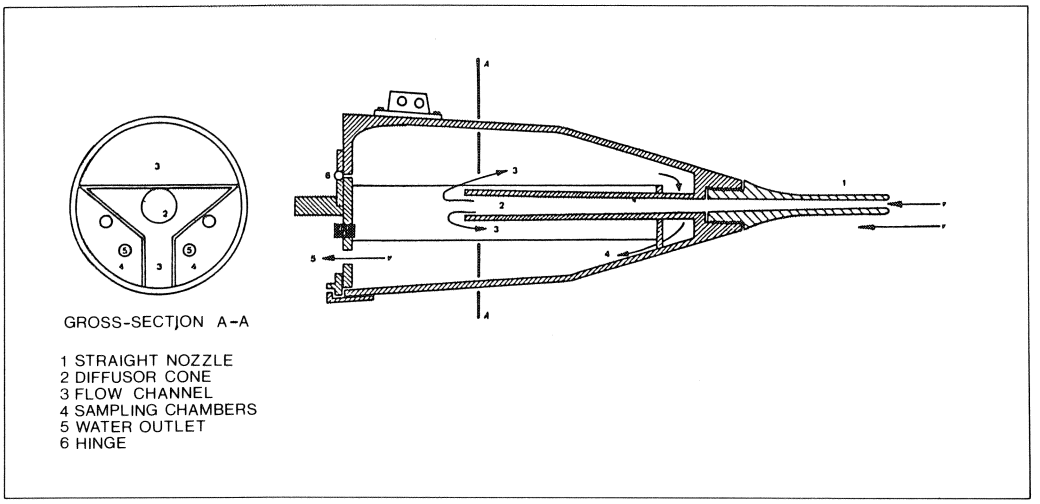

Figure 2.3.5.3 Delft bottle

Figure 2.3.5.4 PFS Filtration Unit

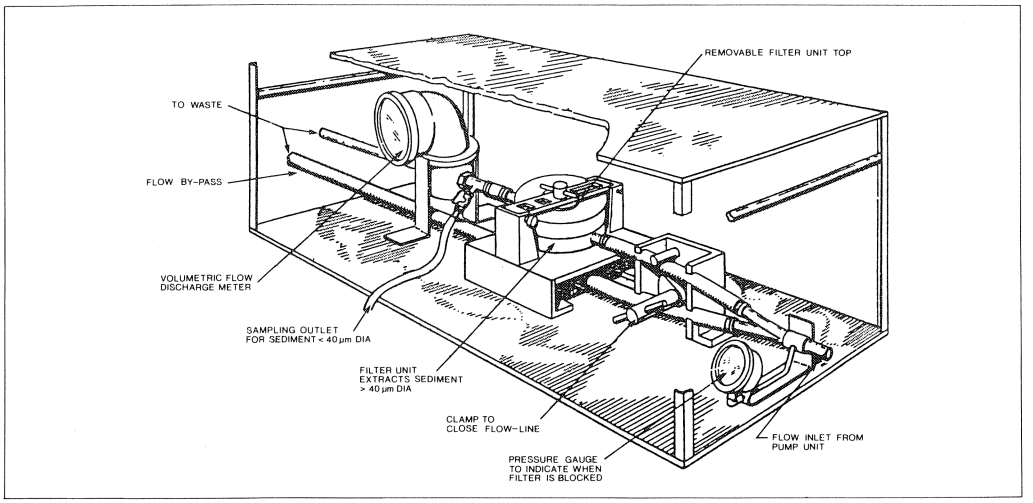

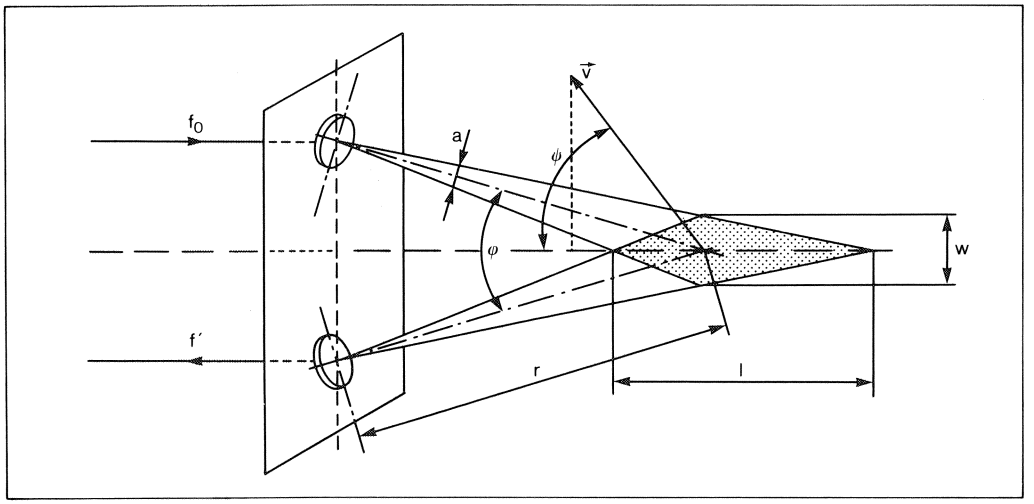

Figure 2.3.5.5 AZIM Geometry of the measuring principle

Figure 2.3.5.7. AZTM monitor

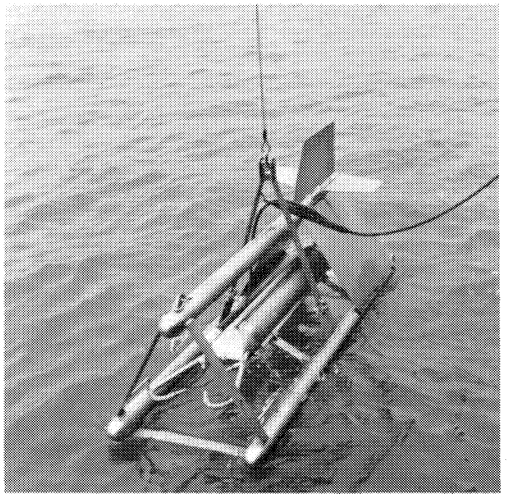

tric cable to a low frequency processing unit on the measuring vessel or platform [1]. The one-dimensional velocity measurement is related to the carrier orientation which follows the mean flow direction. The orientation is measured by a magnetic compass and the vertical position by a pressure gauge and a echosounder, mounted on the carrier.

2.3.5.4 Use and efficiency of the sampling methods.

The sampling efficiency of the VF depend on the current velocity and the inclination of the bottle. Flume tests revealed that no systematic deviation from the concentration in the ambient flow is measured at an inclination of 33° [2]. As the bottle is more oriented to the current the sand catch becomes too high.

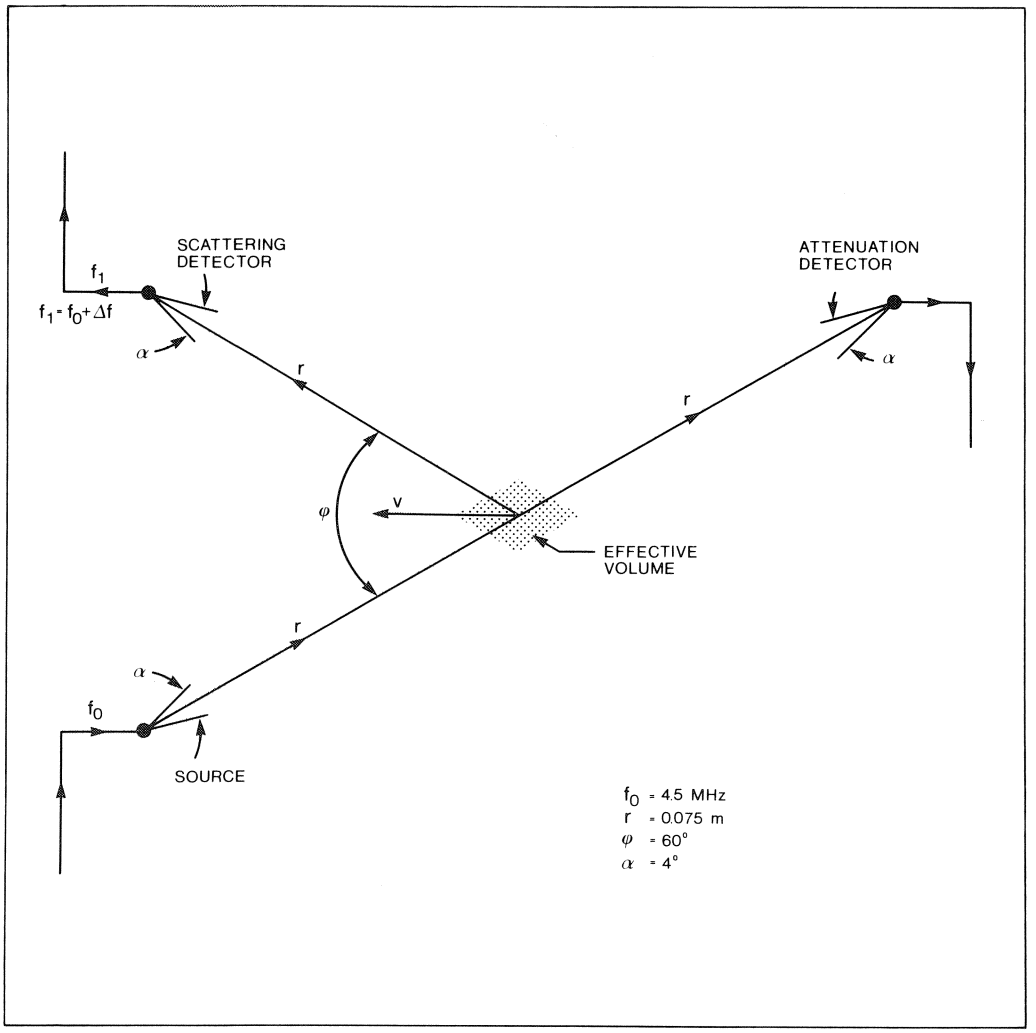

Figure 2.3.5.6 AZTM transducer configuration (geometry not to scale)

With no inclination (axis of bottle vertical) the measured concentration is less than that present in the ambient flow. At an inclination of 33° the sampling time ranges from 30 s at still water up to about 110 s at current velocities of 1.5 m/s. In case of well-mixed suspensions with almost uniform concentration profiles the use of the VF offers a simple solution. However, in tidal condi-

tions this method will result in the handling of a large number of bottles.
Another disadvantage of the bottle is the short sampling time, resulting in an unreliable measurement in a statistical sense. In case of low concentrations the accuracy of the measurements will be reduced and sieve analysis of the sample will be hindered by the small sediment catches.
Conversely, sampling at a higher velocity results in a lower concentration (Fig. 2.3.5.8). Since the intake velocity of the DF approaches the velocity of the ambient flow only in a small range of flow velocities depending on the internal diameter of the intake nozzle several nozzles are used. For measuring in moderate and high velocities a small diameter of 1.55 cm is currently used, whereas a nozzle with a diameter of 2.2 cm is to be applied at lower current velocities [3]. Much time is lost by handling the DF, especially when measurement in deep water is required; after sampling the DF has to be hoisted op with a velocity of 10-20 cm/s. Faster hoisting up causes loss of sediment.
Ideally the intake velocity of the water and sediment at the nozzle of the DF and the PFS should be equal to the velocity of the ambient flow.
Sampling at lower velocities results in a higher sand concentration than in the present stream due to diverging flow lines which cannot be followed by the sediment particles.

In steady flow conditions the intake velocity of the PFS can be adapted to the local flow velocity by adjusting the pump capacity. However, to avoid settlement of sediment particles in the suction hose, a minimum intake velocity of about 1 m/s is required. In unsteady flow conditions it is not practical to equalize continuously the intake velocity to the flow velocity. Consequently sampling errors may occur. Laboratory experiments show errors less than 10% for intake ratios (= intake velocity/local flow velocity) from 0.5 - 1.5 (Fig. 2.3.5.9, [4]).
The filtration method is not suitable for operation in silty or muddy environments because of rapid filter blocking by the fine sediment particles.
The main advantages of the AZTM have been quoted already. In addition to this it may be remarked that a series of measurements with

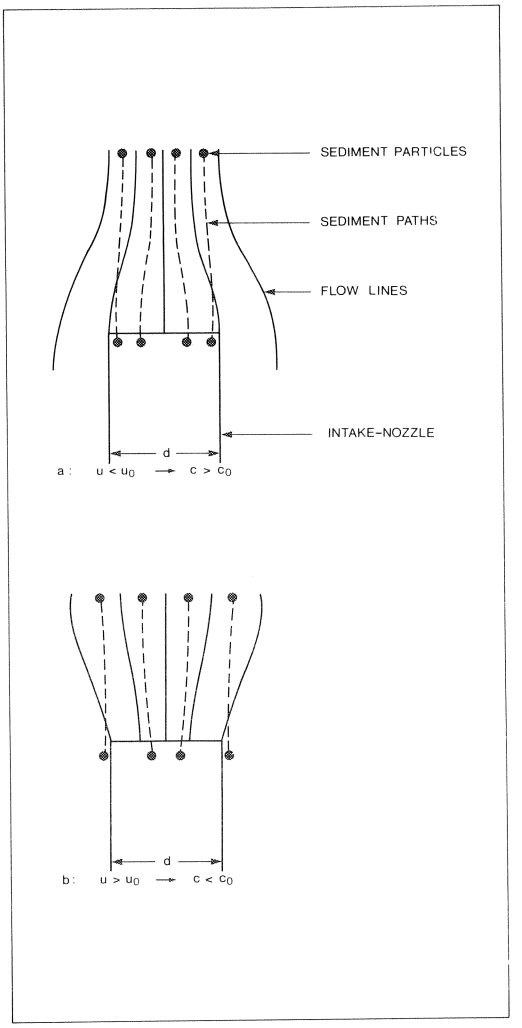

Figure 2.3.5.8 Influence of the intake velocity on the sediment paths

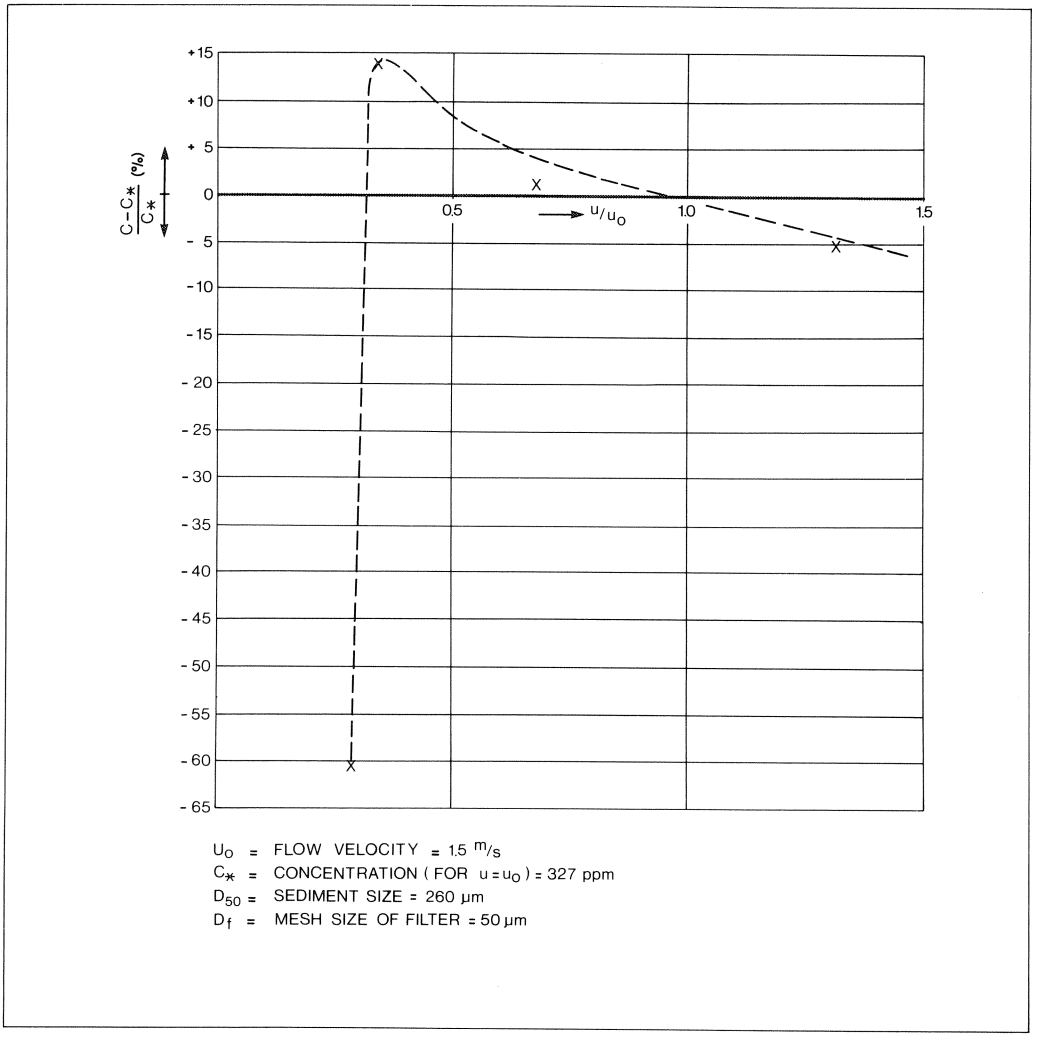

Figure 2.3.5.9 Sampling error in the concentration measured by the PFS as a function of intake ratio

this instrument is not followed by extensive and time-consuming laboratory- work (analysis of dry weight, percentage organic material and fraction 50 μm) as is always the case with the conventional methods. Instead, concentration data are directly available and stored on tape, together with current data and data of the position of the measuring fish in the water column.

As disadvantages of the AZTM can be mentioned:

a. - the complicated nature of the prosessing unit making higher demands upon the operating skill;
b. - the high initial expenses of the system and the high cost of replacing parts;
c. - the vulnerability of the ultrasonic sensor and the electronic units.

References

1. Jansen, R.H.J., **The in-situ Measurement of Sediment Transport by means of ultrasonic scattering,** Delft Hydraulic Laboratory, publ. 203, 1978.

2. Jansen, R.H.J., **Onderzoek Vlissingen Fles,** (in Dutch; Research on the Flushing Bottle) Delft Hydraulic Laboratory, report M 1710, 1980.

3. Hayes, F. Ch., **Guidance for Hydrographic and Hydrometer Surveys,** Delft Hydraulics Laboratory, publ. 200, 1978.

Site Investigations and Data Acquisition

J.K. Nieuwenhuis

2.3.6 Geological and geotechnical investigations

2.3.6.1. General

For major structures a good geological analysis, based on the overall geological structures of the country, is of the utmost importance for an understanding of the geophysical and geohydrological conditions.
The most important geological aspects are:
- geological stratification, formation and history
- groundwater regime
- seismicity

The most important questions which a geotechnical investigation has to answer are:
- what kind of soil is found and at what depth; i.e.: soft soils such as sand, clay and peat or hard soils such as limestone and calcareous sandstone, or very hard soils such as quartzite and basalt.
- what are the mechanical properties of the various soils with respect to their strength and deformation characteristics.
- how pervious is the soil and does it contain water.
- is the soil fissured or weathered.
- will the soil degrade in (short) time

The first step is to organize and design SITE INVESTIGATIONS.
The field programme forming part of the site investigation is complemented by LABORATORY TESTING and GEOTECHNICAL CALCULATIONS.
The last and perhaps most difficult step is the integration of the result of the investigations and structural design, resulting in the ultimate FOUNDATION DESIGN.

There are no rules or laws prescribing the extent or type of investigations necessary for the design, other than the judgement, intuition and experience of the engineer conducting the site investigation programme of the project.
Several standardized investigation techniques have, however, been developed, of which the geological and geotechnical engineer can make use for obtaining the relevant data for his basic calculations and design criteria.

2.3.6.2. Organisation and design of site investigations

General
Practical experience has shown that for a site investigation to be successful it must be well planned and undertaken in an orderly manner using appropriate and well maintained field and laboratory equipment operated by experienced and skilled personnel.
Expertise in the 'mechanics' of investigation (boring, testing etc.) is a routine requirement in all investigations. The most difficult problem is how and where and when to use the various 'tools' available to the site investigator. A 'philosophy' of site investigation has been built up over recent years which proposes the idea of the developing investigation advancing in stages to a satisfactory conclusion, each stage being built on a sound foundation of knowledge established by the previous stage.

Preparatory investigation
After the decision to initiate a project a desk study is undertaken of all available geotechnical, geological and topographical data.
The proposed site and its environments should be examined by an experienced engineering geologist. The objective of this stage is to try to identify potential problems that may arise from site geotechnical conditions in relation to the proposed engineering work.

The topographical, geological and geotechnical data should include
(i) all available topographical maps
(ii) all available geological and hydrogeological maps, records and published articles in scientific journals
(iii) aerial photographs at all scales
(iv) records of natural hazards
(v) site investigation and construction reports for adjacent engineering projects; published articles on the geotechnical properties of the geological units to be found on the site; hydrogeological data.

Site Investigations and Data Acquisition

Reconnaissance
Evaluation of work carried out during the project conception stage may reveal significant gaps in basic knowledge of the site. This in turn will mean that likely problems cannot be foreseen. In such a case some investigation may be required to establish the basic knowledge. This investigation would be undertaken using relatively simple and inexpensive techniques, such as geological and engineering geological mapping, geophysics and perhaps some boreholes. The boreholes could be undertaken partly as an experiment to determine the best method for the boring, sampling and in situ testing to be undertaken in the main stage of investigation. At the end of this stage there should be sufficient knowledge of the site to allow design of the main investigation.

If a number of sites are being investigated prior to choosing one for development the reconnaissance or feasibility investigation may yield sufficient information to allow the choice to be made.

As part of the reconnaissance a site visit is essential.
The engineer will often be the first person to inspect a site for a new engineering work and should return to his office from this trip with information to help engineering geologists and geotechnical engineers with their preliminary studies and investigation design.
This is particularly important when the site is in a distant country which can only be revisited at great expense.

It is always useful to bring back:
1) topographical maps of the site area
2) geological maps and reports
3) aerial photographs
4) details of transportation services
5) addresses of government agencies
6) photographs of the site

Samples of rock and soil will often be required, particularly if the project includes the use of natural materials for construction purposes.
These samples must be of a size adequate for testing purposes.

Main Investigation
In the main investigation stage the work done should recover the information required to design the engineering project. This information is obtained by whatever means are appropriate to the ground conditions and nature of the engineering work. It is possible that some of the investigation work may be difficult and expensive to undertake because of problems of access to the locations of boreholes or in situ tests.
These problems are often easier to overcome during the construction of the project when earthmoving equipment is readily available, so there is a great temptation to postpone necessary investigation until construction begins. This temptation should always be resisted. It is always possible that postponed items of the main investigation could reveal ground conditions which could invalidate the project design. No project should be designed on the assumption that the ground conditions will prove to be satisfactory.

Construction and Post Construction Investigation
One of the unfortunate facts of site investigation is that the forecasts made in the investigation reports resulting from the main investigation are seldom absolutely and totally correct. The construction of a project will quite often reveal discrepancies between the forecast ground conditions and those actually encountered. However, if the investigation is properly done these variations should not cause significant project re-design. The ground conditions encountered must be monitored, recorded and assessed. If no satisfactory assessment can be made on the basis of the information recorded then additional investigations must be undertaken to obtain further data and thus resolve any anomalies.

The behaviour of the completed engineering work will have been computed on the basis of data acquired in the earlier stages of investigation.
Certain features of behaviour, such as settlement, may take many years to become complete after construction of the project. If observed

behaviour is not the same as anticipated behaviour this may indicate that the properties of the ground are affected by some unforeseen and previously undetected factors. Further investigations may be required to resolve this anomaly.

Design of investigations

While the concept of the development of site investigations in stages provides a philosophy of investigation procedure, it does not answer the question - 'what do I do?' - which is so often asked by engineers when confronted with the need to decide what should be done for an investigation of a particular project.

The purpose of investigation is to determine the behaviour of the ground in response to the construction of the engineering work.

This behaviour is determined by calculations based on knowledge of the properties of the ground and the location of ground materials which have those properties.

This knowledge is built up into **a geotechnical 'model'** which holds all the information necessary for calculations and describes the mechanism of the interaction between the structure and ground. The size of the model will depend upon the volume of ground which will influence or be influenced by the construction of the engineering work. To complete the model the investigator must discover the nature and distribution of the materials of which the ground mass is composed, the nature and distribution of the discontinuities that ramify the groundmass, and the engineering properties of materials and mass appropriate to the engineering project.

The number of different materials and the regularity of their distribution depend upon the complexity of the geology of the site.

The extent of investigation will depend upon this complexity - uniform simple geological situations generally require less extensive investigations than more complex geological situations.

All geological units must be 'sampled' and their appropriate properties determined by laboratory or in-situ testing.

The 'sampling' is mostly undertaken by boreholes, which may also serve as means of access to 'samples' to be tested in situ. Trial pits, tunnels and shafts are other means of access to 'samples'.

The materials identified in the samples belong to geological bodies which exist between boreholes. The shape of these bodies is of great importance for they determine the distribution of materials. Shape can be assessed by correlation between boreholes.

This assessment can be helped by using GEOPHYSICAL techniques (such as the resistivity or seismic refraction or reflection methods) to determine the shape of the surfaces of the geological bodies. The 'model' distribution of materials built up from this information must then be tested for geological credibility, i.e. whether the way the groundmass is built up seems likely in the light of the known geological history and structure of the region.

The process of building up the geotechnical model begins with a preliminary understanding of the geological structure based on existing geological information or new geological mapping. The first model is then examined by boring or other means of sampling for verification of the original concept. This is then modified and examined by additional boreholes and other forms of investigation.

Examinations and reviews of the model take place as part of the phased progress of the investigation. The type of boring used in the investigation will depend upon the quality of samples required for testing and identification. This quality is related to the degree of accuracy and reliability of test results required. The degree of precision required in the assessment of ground conditions relates to the likely magnitude of ground reaction consequent upon the construction of the engineering work. If the reaction is likely to be such that the success of the engineering project is in doubt then the quality of testing and sampling must be of the highest grade.

It is extremely unlikely that similar engineering works will be built upon similar geology. It follows that each site investigation is unique.

There is no standard form of site investigation for a particular engineering work. Each site investigation should be regarded as a completely new venture.

A high quality investigation must be economically efficient in the sense that the cost of the investigation must be money well spent.
The investigator must be able to justify each and every item in the site investigation in terms of the value of that item in building up the geotechnical model. The investigator should be able to show good and sufficient reason for undertaking each part of the investigation.

2.3.6.3. Geological and engineering geological maps

Geological maps
Geological maps show the distribution of the geological material exposed on the earth's crust. They are usually constructed to show:
(a) the age of the soil or rock
(b) the type of the soil or rock
(c) the areas where particular types of material occur

Maps are made on various scales. Small scale maps (1 : 100.000 or larger) show the general geology of countries or continents and are used for general geological understanding. Large scale maps (1 : 50.000 or less) show the geology for use in mineral exploration or for planning engineering works. Very large scale maps are made of particular engineering sites (1 : 5000 - 1 : 500). Geological maps show the structural and geological history of an area. Thus a geologist, looking at the map in the figure, could deduce the presence of synclines, anticlines and faults, understand the geological history of an area and be able to predict the depth of particular strata beneath the surface. These maps are very useful to geologists and engineers but mostly they are concerned with the **AGE** of the material while for engineering purposes we are concerned with the **PROPERTY** of the material. Special maps are prepared by engineering geologists for engineering purposes. These give geological data of engineering value. (see figures 2.3.6.1 and 2.3.6.2)

Engineering geological maps
There is a need to produce special maps for engineering geological purposes.
These fall into two types

1. Special maps produced by government agencies which are arranged to show geological features of particular engineering importance.
2. Maps of particular engineering sites arranged to show features of importance only to one type of engineering work or one particlar engineering problem.

Category (1) maps may display engineering geology features appropriate to a particular investigation, or be used to display engineering recommendations. Category (2) maps are usually undertaken for those engineering works which are likely to be inspected from time to time to ensure their continued safety e.g. dams. These maps are usually at scales of 1 : 1000 to 1 : 100.

Details of engineering geological maps of the government agency type are given in the Unesco publication (nr 15) 'Engineering geological maps - a guide to their preparation' published in Paris in 1976. A useful guide to site maps and plans is given in 'The preparation of maps and plans in terms of engineering geology', Geological Society of London, Quarterly Journal Engineering Geology, vol. 5, nr. 4, 1972.

Aerial photographs
Aerial photographs are one of the most useful tools for geological and engineering geological mapping, for they allow geologists to view the ground in three dimensions using a stereoviewer and to see the shape of the land. The tone (the density of greyness) of the black and white photographs will very often depend on the nature of the underlying materials and such features as faults and fractures may be readily seen if conditions are suitable.
The detail in which the geology may be examined depends upon the height of the aircraft, which determines the scale of the photograph. For wide scale geological work, to understand the geology and large areas, small scale photographs are used. For mapping for an engineering purpose very large scale photographs (1 : 1000) may be required. Terrestrial photographs may be taken of slopes or cliffs to aid solution of stability problems.

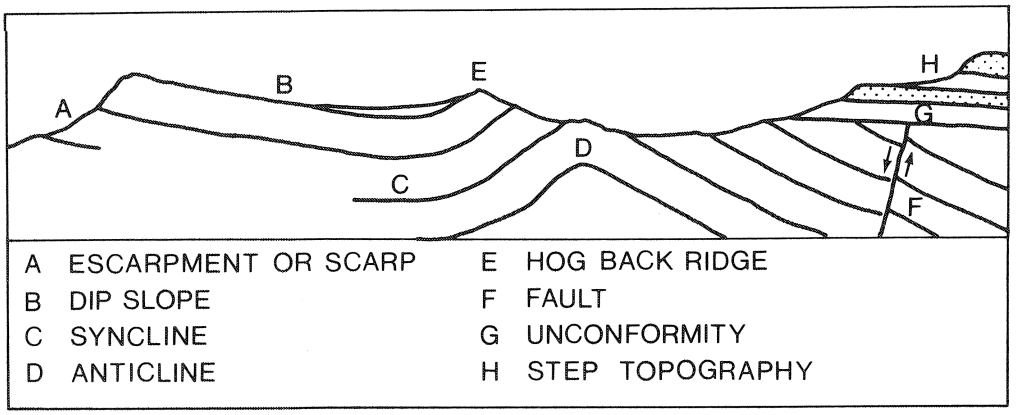

Figure 2.3.6.1 Structure and scenery

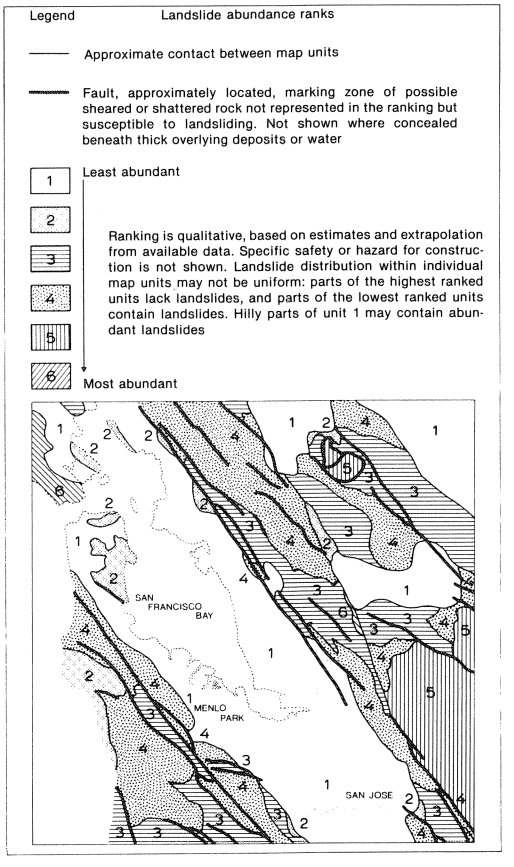

Figure 2.3.6.2 Landslide abundance map of the area around San Francisco Bay. (An example of a government agency map emphasizing a particular geomorphological feature)

Government agency maps

These may be:

a) maps which are modifications of existing stratigraphical maps (in the conventional style) to show lithology rather than stratigraphy
b) maps which emphasize particular geological or geomorphological features (figure 2.3.6.2)
c) maps which serve as a source for documentary research

d) maps which give opinions or describe certain problems that are of engineering significance.
e) maps which give engineering data
f) maps which give engineering opinions.

The types of maps that are published in any particular country depend greatly upon the social, political and legal systems in that country, since, if engineering works are planned and located on the basis of these maps, the question arises as to who takes the responsibility for any error in the maps.
Can claims for erroneous information be made against the government agency? Each of these maps is made from a very large amount of data, and to complete a map, the agency must be prepared to undertake work in areas that have not been investigated by others.
It is also necessary to have a social organisation which makes it obligatory for those undertaking geotechnical work to file the results of this work with the government agency.
Generally the scale of these maps is not larger than 1 : 5000.

2.3.6.4. Geophysical methods in site investigation

Geophysics has played the major role in the exploration for oil. At the end of the 1940's the application and value of geophysical surveys to investigations onshore and offshore for engineering purposes has increased considerably.
This is not, however, universally appreciated, on the one hand because it is not recognized as such, and on the other because geophysical surveys are not used properly by designers.
Geophysical surveys are carried out to help study the geology.
It is not always possible to determine in advance which of the many geophysical techniques will be the most appropriate for a survey.
Many techniques are complementary. It is up to the geologist or geophysicist to deploy the various techniques during the survey.
This requires a good mutual understanding between client and the geophysicist, whereby the geophysicist is given some freedom of choice.
The following geophysical methods are most commonly used:

1. Seismic - refraction
   reflection
2. Electric resistivity
3. Magnetic

The frequency with which each method may be used in any particular area or country depends on geology and topography. See table 2.3.6.1.

Seismic method
If a seismic impulse is generated at the surface by artificial means e.g. explosives or hammer blows, energy radiates into the ground and is reflected (following the laws of optics) back to the surface from any distinct geological boundaries that may be below the ground.
Each material allows the seismic wave to pass through it at a certain velocity. Generally the stronger the material the greater the velocity e.g. velocity through granite is greater than velocity through clay.
If the contrast in velocity between two materials is good, there will be good refraction or reflection from the boundary between the two materials.
(See fig. 2.3.6.3 and Table 2.3.6.2).

In refraction seismic methods a shock is generated at the surface and the return of the wave to the surface is recorded by geophones.
The seismograph measures the time taken for a wave to travel from the shot point to a geophone. 'First arrivals' are recorded. Since the speed of the seismic wave depends upon the nature of the material through which it passes, waves passing through deep high velocity beds (V_1) underlying a low velocity bed (V_0) will eventually arrive at a geophone before those travelling directly through the V_0 material. If the time of travel to each geophone is known a time-distance graph may be drawn and the depth to various strata calculated (see fig. 2.3.6.4).
Seismic reflection methods are mostly used by the oil exploration industry for determining the geological structure deep underground. However, they are also used for engineering purposes when a survey has to be conducted over water (e.g. for dredged channels, underwater tunnels, dam sites on major rivers etc).

Table 2.3.6.1 The application of geophysical techniques to engineering problems

Problem		Example	Method and remarks
Geological	Stratigraphical	Sediments over bedrock.	**Land**
		(i) Sands and gravels over bedrock, water table low in sands and gravels.	Seismic refraction
		(ii) Sands and gravels overlying clay, water table high in sands and gravels.	Resistivity
		(iii) Clay over bedrock.	Resistivity or seismic refraction
		Sediments over bedrock generally	**Marine.** Continuous seismic reflection profiling
	Erosional (for caverns see shafts below)	Buried channel.	Seismic refraction. Resistivity for feature wider than depth of cover.
		Buried karstic surface	Resistivity contouring.
	Structural	Buried fault, dykes	Resistivity contouring. Seismic reflection or refraction. Magnetic gravimetric (large faults)
Resources	Water	Location of aquifer. Location of saline/potable interface.	Resistivity and seismic refraction
	Sand and gravel	Sand, gravel over clay.	**Land.** Resistivity
		Gravel banks	**Marine.** Continuous seismic profiling, side scan sonar, echo sounding
	Rock	Intrusive in sedimentary rocks	Magnetic. (Weathering may give low resistivity.)
	Clay	Clay pockets	Resistivity
Engineering parameters	Modulus of elasticity, density and porosity	Dynamic deformation modulus	Seismic velocity at surface, or with single or multiple boreholes. (Cross hole transmission.) Borehole geophysics
		Check on effects of ground treatment	
	Rock rippability	Choice of excavation method	Seismic (velocities at surface)
	Corrosivity of soils	Pipeline surveys	Surface resistivity. Redox potential.
Buried artifacts	Cables	Trenches on land	Magnetometer. Electromagnetic field detectors.
	Pipes	Submarine trenches	Echo sounding, side scan sonar.
		Submarine pipelines	Side scan sonar, magnetic, continuous seismic profiling (especially if thought to be partially buried) with high frequency pinger
	Shafts, adits and caverns	Shaft, sink holes, mine workings	Resistivity. Magnetometer contouring, infra-red air photography on clear areas. Cross hole transmission. Detailed gravity for large systems.

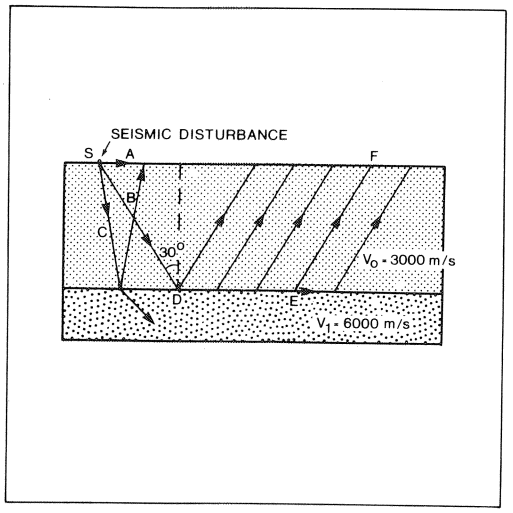

Figure 2.3.6.3 Seismic reflection (SCB) and refraction (SDEF)

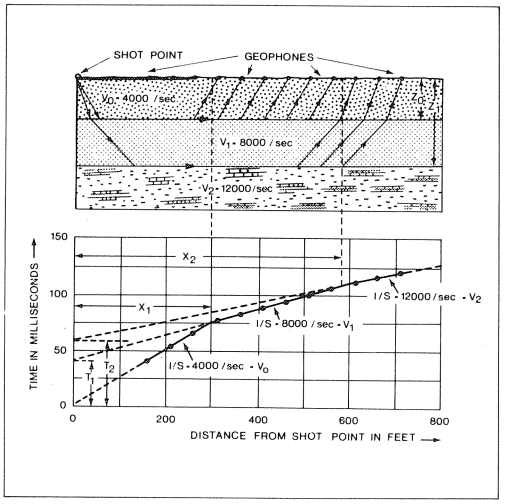

Figure 2.3.6.4 Seismic refraction profile

	Velocity (ft/sec)	Velocity (km/sec)
Alluvium	1,640 - 6,600	0.5 - 2.1
Clay	3,600 - 8,200	1.1 - 2.5
Loess	980 - 1,200	0.3 - 0.6
Sand	650 - 6,600	0.2 - 2.0
Glacial till	1,300 - 5,600	0.4 - 1.7
Granite, quartz monzonite, granodiotrite	15,100 - 19,700	4.6 - 6.0
Gabbro, diabase, basalt	16,400 - 22,000	5.0 - 6.7
Sandstone, shale	4,600 - 14,800	1.4 - 4.5
Limestone:		
soft	5,600 - 13,800	1.7 - 4.2
hard	9,200 - 21,000	2.8 - 6.4
crystalline	18,700 - 21,000	5.7 - 6.4
Anhydrite, gypsum, salt	11,500 - 18,000	3.5 - 5.5
Slate	11,500 - 14,400	3.5 - 4.4
Schist and gneiss	11,500 - 24,600	3.5 - 7.5

Table 2.3.6.2 Seismic velocities of some natural materials

Continuous Seismic Profiling (CSP) devices are used. In these continuously repeated shocks are made in the water and recorded by 12 or more geophones towed behind a boat. These produce a picture which closely resembles the geology beneath the sea or river bed.
Various devices are available such as 'Sparker', 'Pinger', 'Boomer', which produce profiles as accurately as possible depending upon the depth of water, depth of penetration required etc.
Seismic profiling or sub-bottom profiling is indispensible for offshore projects, where subsurface exploration by other means is difficult and expensive. If the general geological and sedimentological setting of the area under investigation is known, much information can be obtained through sub-bottom profiling. The most suitable sub-bottom echosounder is the light (c. 1 kjoule) Sparker or Boomer. These penetrate 40 to 450 metres depending on the type of source and the sediments encountered (see fig. 2.3.6.5).
Interpretation of the records is not easy and requires an experienced geophysicist. Attention must, for example, be paid to the multiples (= repeated signal on the record). These multiples can be very strong and make the data arriving later unsuitable. In engineering works, where interest is concentrated on the relatively thin layer of sediments overlying bedrock this does not usually create a problem.
An expensive alternative is to record the data magnetically and process them afterwards.
Apart from the echosounder and data-recording sub-bottom profiling requires the correct alignment of the records with the ship's position. For that a great variety of positioning systems exists.

Electrical resistivity techniques
In theory, electrical resistivity is more versatile than other shallow geophysical exploration methods in respect of the range of geological situations with which it can deal, but its many practical and interpretative limitations restrict its application to comparatively simple cases on land. Magnetic methods on the other hand can be used over water.

Figure 2.3.6.5 Seabed geology from Sparker Profiles, offshore Louisiana, U.S.A.

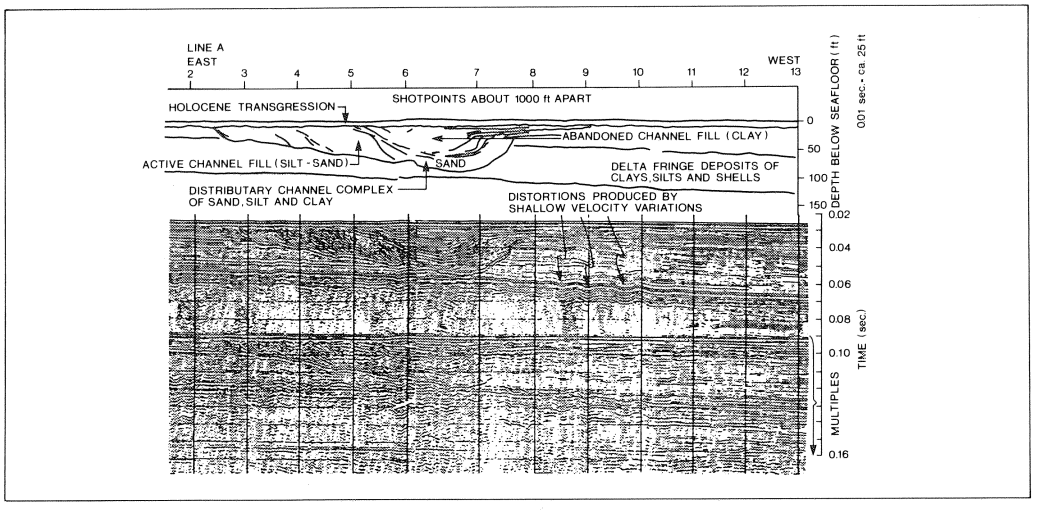

There are many variations in technique, but all are based on passing a current through the ground between certain (current) electrodes and measuring the potential difference resulting between their potential electrodes set up in the path of the current, from which a quantity termed 'apparent resistivity' can be calculated. Changes in apparent resistivity should reflect changes in soil or rock type and moisture content. A commutated current is always used to prevent polarisation at the electrodes which would distort the observed potential differences. Vertical changes in resistivity are detected by expanding the electrode separation about a fixed central point. This increases the depth reached by the current, and the resulting potential difference across the potential electrodes will vary if the resistivity varies with depth. Lateral changes are observed by using a fixed electrode separation and moving the whole electrode array between each reading, a procedure known as 'constant separation traversing'. Where the full three-dimensional pattern of soil variation is required, both techniques should be used, but if the object of the survey is to locate a near-vertical feature such as a fault or open fissure, constant separation traversing alone may suffice. The principle of the most frequently used electrode array (known as the Wenner configuration comprising four equally-spaced electrodes in line) is illustrated in figure 2.3.6.6.

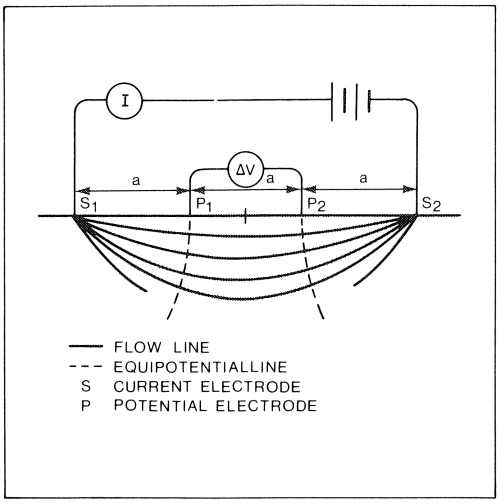

Figue 2.3.6.6 Principle of the electrical resistivity surveying using Wenner electrode configuration

Magnetic techniques

These measure local variations in the earth's total magnetic field strength. This is of the order of 74 000 gammes (1 gamma = 10^{-5} Oersted) at the poles and 30 000 gammes at the equator. Local variations are either induced and due to changes in the magnetic susceptibility (the magnetic equivalent of density) of the underlying soil or rock material, or they are permanent and caused by the presence of permanently magnetised bodies. The size and shape of an induced magnetic anomaly will be due not only to the susceptibility contrast, but to the orientation of the causative feature relative to the earth's field. Thus linear features will be hard to detect if aligned to magnetic north and south, but equidimensional features will be unaffected by this restriction. In engineering practice, magnetic methods are mainly used for the following application:

1. Locating basic igneous dykes below a cover of superficial deposits. Basic dyke-rocks usually contain magnetic iron oxides and show a susceptibility contrast with the surrounding ground.
   These dykes often have some engineering significance: for example, they may be associated with sudden changes in rockhead level, or form jointed and permeable zones in a tunnel drive below the water table.
   Buried landforms cut by erosion into magnetic rocks may be detected by magnetometry.

2. Locating abandoned mineshafts. There is often a good susceptibility contrast between the shaft lining and/or filling and the surroun-

ding ground, especially where the lining is brick or the infilling contains burnt shale, since the firing of caly also tends to form magnetic iron oxides. In fact, the proton magnetometer was originally developed for archaeological surveys because of its sensitivity to buried pottery or brick.

2.3.6.5 Geotechnical methods for site investigation

1. Borings

Most site investigation include boreholes, which are drilled to gather information about the nature and distribution of ground materials and the discontinuities that ramify the ground mass. They may also be used as a means for in situ tests, to allow inspection of the strata exposed in the walls of the borehole, or to install in situ instrumentation which records changes in the condition of the ground.

The nature of the samples recovered depends upon the character of the ground mass and the requirements of the investigation.

Descriptions of the geological nature of the materials penetrated by the boreholes can sometimes be achieved by taking 'disturbed' samples, that is to say samples whose condition in no way represents the condition of the material in situ as the result of disturbance due to the sampling procedure. Samples required for description in terms of both geology and geotechnical properties are taken by special sampling devices and are then termed 'undisturbed'. **No samples are truely undisturbed** for extraction from the borehole almost always implies a change in the conditions of stress under which the sample existed in situ.

Ideally sampling should be continuous and provide a complete sample of all the strata penetrated by the borehole. This is possible to limited depths in soft soils by means of special long samplers, pushed into the soil, such as the Delft continuous sampler or the longer piston samplers and in rocks by rotary core drilling.

Unfortunately most soils are too strong for deep continuous sampling and too weak or bouldery for successful coring, while the soil-like layer of weathered rock overlying fresh bedrock is also difficult to core. In such circumstances recourse

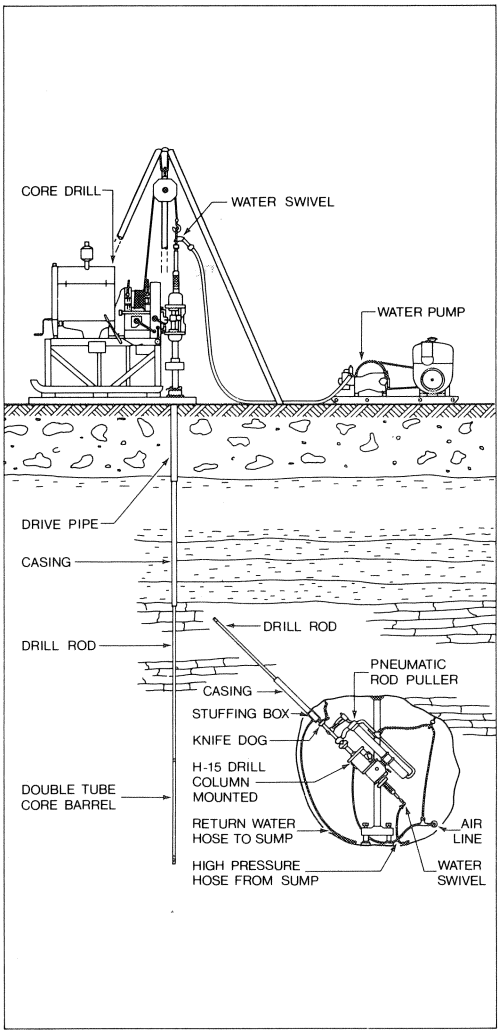

Figure 2.3.6.7 Rotary core drilling equipment

must be had to discontinuous sampling (mostly driven tube sampling) techniques. In such a case the location of samples must be decided before drilling the borehole, or is left to the discretion of the driller acting within a framework of instructions given by the investigator.

Boring in rock

The best way to drill a hole in rock and recover samples, is by means of rotary core drilling.
Rotary core drilling machines contain mechanisms which impart both downward pressure and rotation to a sampling tube which is armed with a cutting bit, so that the sample is cut from the ground. The design of the bit is arranged to produce the best recovery and least disturbance to a particular material type. Reaction to the downward pressure of the sampling tube on the bottom of the borehole is provided by the weight of the drilling machine on the ground.

A typical drilling machine is illustrated in figure 2.3.6.7. In general terms the size of the sample that may be obtained is related to the power and weight of the drilling machine. Drilling manufacturers usually quote a depth rating for a machine which gives the maximum depth to which the machine may be expected to drill for a minimal core size. Examples are given in the table 2.3.6.3. The maximum rod size does not correspond to the maximum core that may be obtained by a particular drill. Larger cores may be obtained but to lesser depths.

Core barrels

Coring in rocks is undertaken using a core barrel armed with a drilling bit. Core barrels may be single, double or triple tube. In the single tube barrel the core is retained in the same tube that serves to rotate the bit. If the cored material is weak, the material in the barrel will be disturbed by the rotation of the tube and bit, so this type of barrel is suitable only for the strongest, most intact materials.

Double tube core barrels have an internal tube that is connected to the main barrel by a roller bearing. The sample passes into this tube, which remains effectively stationary, while the outer tube rotates, because of friction against the core sample by the corelifter at the bottom of the inner tube.
In some materials such as clays, this friction is not always enough to prevent rotation so triple tube core barrels may be used to prevent inner tube rotation.

Core Bits

The core is cut out by the grinding or cutting action of the core bit.
The nature of the cutting edge of the bit depends upon the hardness of the material being drilled. In hard rocks (such as quartzites, granulites and granites) bits are armed with closely spaced small industrial diamonds (bort) set in a strong alloy matrix.

Manufacturer and Model	Engine Power (HP)	Maximum Drillrod Size	Depth rating for maximum size (m)	Weigth of machine (kg)
Boyles X-ray	9	BW	23	112
Craelius D75	8.9	BW	75*	112
Edeco Mark VI/3	27	NW	230	1600
Longyear 34	36	HW	190	1500
Failing 1500	140	HW	460	15270**
Craelius D2000	80	HW	900	5130

* with aluminium rods
** including truck

Table 2.3.6.3 Depth ratings for some drilling machines

Flushing medium
Rock cuttings from the bit are pressed to the surface by the flushing medium. This is commonly water but may be drilling mud (a mixture of water and bentonite) or air. The flushing medium is pumped down the centre of the drill string, between the outer and inner tube of the core barrel, over the bit and thence passes up to the surface via the space between drill string and hole wall.

Rock drilling machine
Other rock drilling equipment is available on the market. The difference with the core driller is in that they produce no coherent samples but **just a hole.** These machines are often truck mounted, may use compressed air motors, hydraulic motors or conventional motors and commonly use compressed air as a drilling fluid. The only samples they produce are the cuttings from the drill bit, which is usually of rock roller design (tricone bits). Accordingly, a geologist has to be in full-time attendance on the drilling rig to log the cuttings as they return to surface and prepare a borehole record.

In many designs of these rigs the rock is cut by the rotation of the bit pressed against the bottom of the hole by the weight of the machine. In others, a compressed air operated device gives a hammering action at the bottom of the hole as well. These are rotary percussive machines. In most of these rotary open hole machines there is no facility for casing the hole.
In one, however, the Atlas Copco Lindo drill, casing is taken down just behind the drill bit so the machine can drill in caving ground.

Boring in soft soil
The rotary core drilling system as described above can be used for soft soils too. But there is a great variety of methods to produce a hole in the ground, whereby samples can be taken during the process of penetration at any depth. As already mentioned sinking a borehole in soft soils is inseparable from sampling. Samples are needed for geotechnical testing. To be able to take samples within the hole the borehole has to be cased temporarily thus preventing the hole from caving in.

There are two main techniques for making a borehole:
a. removal of the crushed material, either at intervals by means of bailing (dry boring) or continuously by means of water circulation (hydraulic boring)
b. crushing the material at the bottom, either with a falling bit (percussive boring) or a spinning bit (rotary boring).

There are therefore four means of making a borehole, although dry percussion boring and hydraulic rotary boring are the most commonly used. Each of these methods is in turn broken down into a great many variants designed to obtain optimal results in differing conditions (e.g. composition of the ground, the availability of equipment and manpower, accessibility, depth and diameter of the boring).

Percussive boring
The oldest form of boring is the dry percussion method, using a shell or bailer. See fig. 2.3.6.8. If the soil cannot be bailed out of the hole easily, a chisel is used to loosen it. Boring is undertaken by repeatedly dropping the chisel or bailer out and into the ground with the assistance of a motorised winch. As the hole advances the casing is pushed down. For deep holes friction on the wall of the casing can become so great that further penetration is impossible.
To overcome that problem a second smaller casing in inserted. At regular intervals drilling is stopped in order to take samples.

In most parts of the world samples of soil are recovered by hammering or pushing sample tubes into the ground. Driven samples are usually taken when the driller observes changes in strata lithology or at intervals. The interval is usually not more than 3 m and not less than 1m between sample tops. Samplers are usually 'open drive' samplers. They consist of a tube whose lower end is armed with a hard steel cutting shoe. The tube is attached to the drilling rods at its upper end by a device which contains a non-return valve which allows the exit of water or air from the tube while the sample allows the exit of water or air from the tube while the sample is driven inside it. The valve and cutting shoe

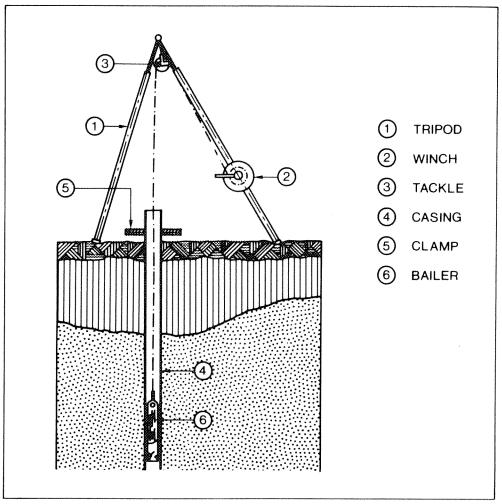

Figure 2.3.6.8 Percussion boring

Figure 2.3.6.9 Delft Continuous Sampler

are detached when the filled tube is brought to surface and the ends of the sample are sealed with wax to prevent loss of moisture.
Such sample tubes are commonly about 400 mm long and 70 mm diameter. Smaller sample tubes may also be used. The American Shelby tube is about 75 mm diameter and does not have a detachable cutting shoe.
Sampling is a discontinuous process because, except in very soft ground, sufficient force cannot be generated to hammer or push long tubes into the ground without the sample being very disturbed. An exception is the Delft Continuous Sampler. This Sampler, developed by the Delft Soil Mechanics Laboratory (the Netherlands) takes a continuous sample of 29 mm or 66 mm diameter. The 29 mm sampler, is pushed into the ground with a conventional 200kN Deep Sounding machine (fig.2.3.6.9). As the sampler is advanced, the sample is fed automatically into a nylon stockinette sleeve, made impervious by a vulcanising process. The sample within its impervious sleeve is maintained in position by a tension cable fixed to the top of the sleeve and a bentonite barytes supporting fluid. With both sizes of sampler a continuous sample of about 18 m long can be taken. At this depth the sample is removed in 1 metre lengths within the sampler extension rods or within its own plastic tube in the case of the larger samples. Samples are placed in purpose-made cases and should be described and sampled for moisture content and other index tests as soon as possible after sampling.
The samples are usually split and one half only sampled. They are then described and photographed in a semi-dried state when the fabric is more readily identified. Only index property

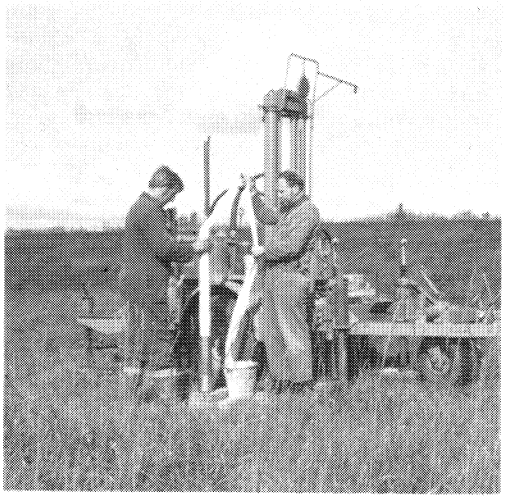

tests can be carried out on the smaller samples while the larger are suitable for a wide range of laboratory tests.

Other methods of boring in soft soil

Continuous Flight Augers
A continuous flight auger is illustrated in the figure 2.3.6.10. Even larger versions exist which

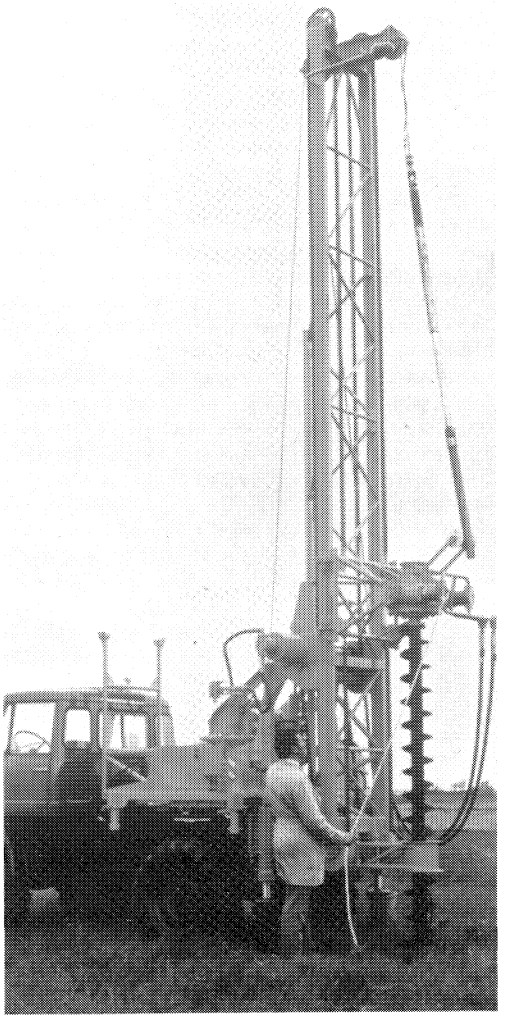

Figure 2.3.6.10 Truck mounted auger

can drill up to 50 cm diameter holes; these are usually truck mounted. Commonly in these larger versions the centre of the flight auger is hollow so that tube samplers can be pushed into the ground below the bottom of the auger. Augers can be found in many varieties.There is a simple auger operated by one or two men. In soft ground it may penetrate up to 5m depth, but its utility is limited because it cannot use casing.

Hydraulic boring

In the case of hydraulic boring (fig. 2.3.6.11) the crushed bottom material is continually removed from the borehole, so that the drilling process does not have to be interrupted (wash boring). A water level is maintained in the borehole at a depth of several metres above the natural groundwater level. The silting up of the wall of the borehole limits water losses and a pressure difference is produced at the side that enables the borehole to be kept intact without the need for casing, even when working in unconsolidated formations (except for a short distance near ground level). These two factors enable high boring speeds to be maintained in unconsolidated formations of up to twenty or thirty metres an hour, so that depths of several hundred metres can be attained in the space of a few days. In unconsolidated formations the bottom material is loosened by means of a rotating bit at the bottom of a hollow drilling tube. With the aid of a pump the water flows upwards in the tube at a high velocity of 3-4m/sec, sufficient to transport large stones etc. to the surface. After the suspended matter has settled, the water descends again in the circular space between the side of the borehole and the drilling tube. In the case of suction drilling as shown in the right-hand half of fig. 2.3.6.11, a suction pump maintains the water circulation. The suction height is however limited to a theoretical 10 m water column, a significant part of which is used up for the difference in height between the highest point of the drilling tube and the water level in the borehole. This means that only a limited amount of pressure is available for overcoming the frictional resistance, whereas the high velocity means that this resistance is high. This sets a limit to the depth of suction drilling of 50 to 100 m.

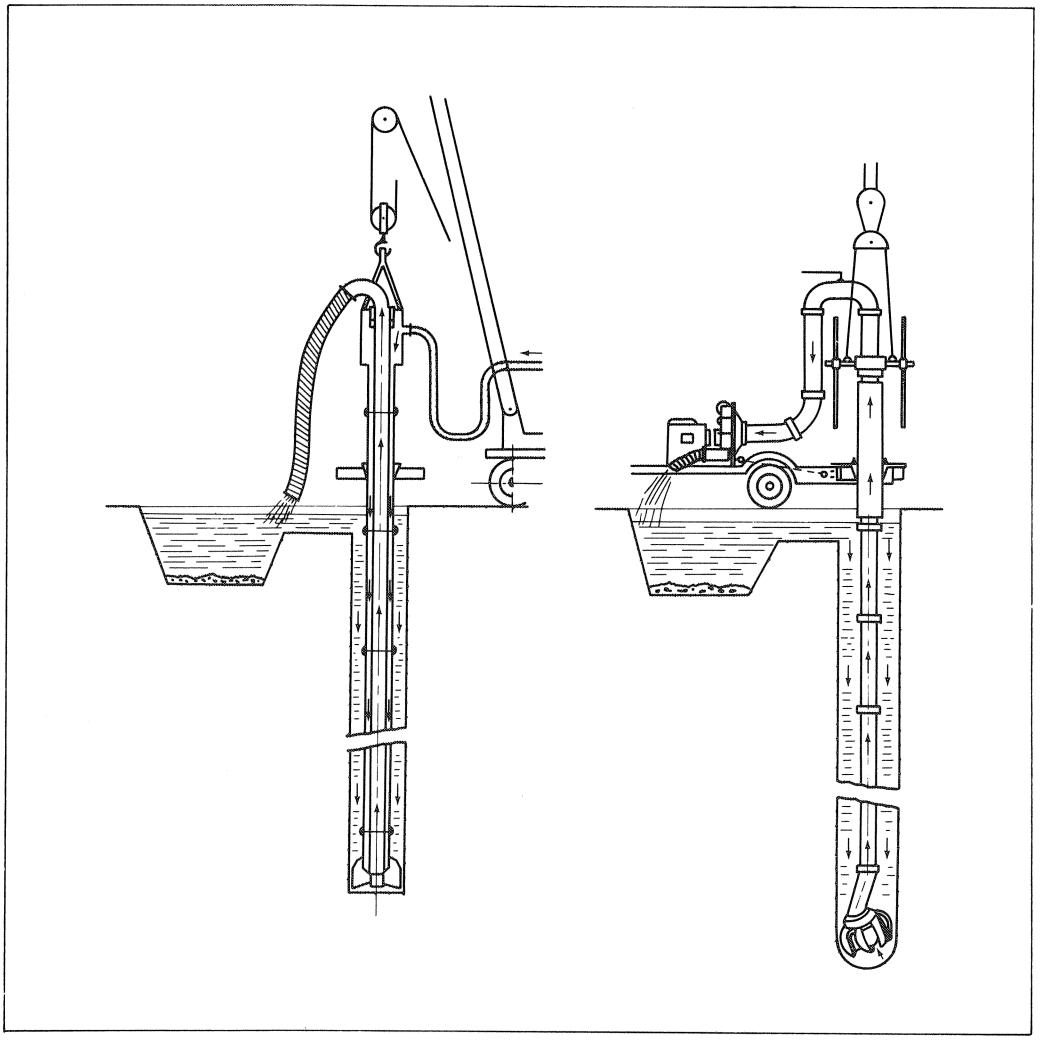

Figure 2.3.6.11 Hydraulic rotary drilling in unconsolidated soil

If greater depths have to be reached the flushing auger system shown in the left half of fig. 2.3.6.11 may be employed, in which water circulation is maintained by an air-lift. The yields obtained with this mammoth pump an dthe compressor required for compressing the air are, however, low, and the energy requirements correspondingly higher.

In between the penetration the process is stopped and driven samples are taken or in-situ tests performed. In shell and auger boring, samples of material used to identify the sequence of strata (disturbed samples) are taken from the drilling tools. In wash boring the nature of the strata is determined by examination of the cuttings brought up by the wash water.

Borehole records

Most materials are described from samples taken from borel oles.
Their description s are given in borehole records which should give a complete account of:

(1) the method and progress of boring;
(2) the samples taken;
(3) in situ tests made in the borehole;
(4) the nature of the strata encountered.

An example of a good standard of borehole record is given in figure 2.3.6.12. (Normally records are produced on A4 size paper). A useful guide to the preparation of good quality borehole records is the Report of the Working Party of the Engineering Group of the Geological Society of London on „The Logging of Rock Cores for Engineering Purposes" (Q.Jl.Engineering Geology, vol. 3, 1970, pp. 1-24).

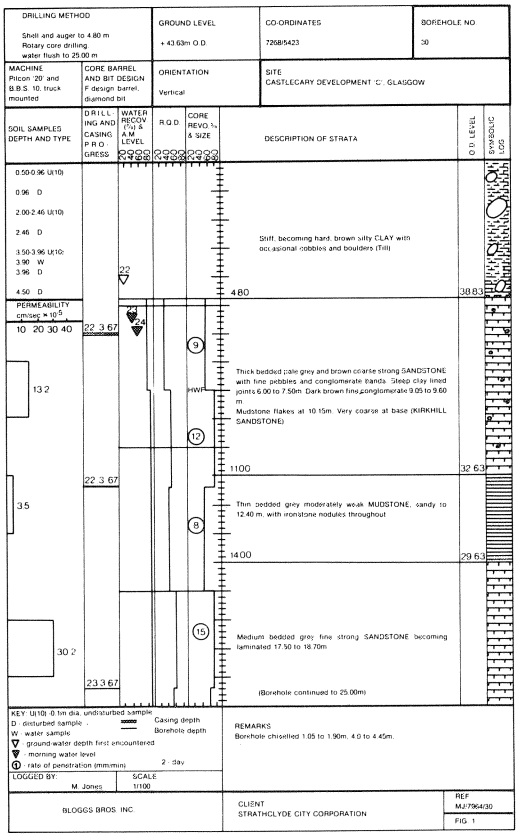

Figure 2.3.6.12 Standard of borehole record

2. Penetration tests

Because of the difficulties of obtaining samples of a quality suitable for laboratory testing and of testing samples large enough to include discontinuities much testing is undertaken of ground in situ. Access to the body of ground to be tested (the in situ 'sample') is arranged by boreholes or by pushing a sensor into the soil. Making a hole releases the stress containing the material adjacent to the borehole sides and relaxation, opening joints and other discontinuities and general loosening of the mass occurs.

Water or air used for boring purposes may alter the moisture content of the materials exposed. These factors are so important that in-situ measurement through penetration tests are performed in soft soils where penetration is possible. Penetration tests are increasingly used because of their economy compared to borings, their reliability and increased sophistication.

Standard Penetration Test (S.P.T.)
This is a dynamic penetration test, carried out in a borehole using a standard procedure and standard equipment. The test was initially introduced by the Raymond Pile Company in the United States to provide an indication of the in situ relative density of sand. It is widely used internationally. The equipment consists of a 50 mm diameter split spoon (barrel) sample of standard dimensions, weighing 66.7 N. This is driven into the soil at the bottom of a borehole by an automatic triphammer, which allows a 622.7 N weight to drop through a height of 762 mm. The number of blows is counted to give a penetration of 300 mm after the tool has been driven through an initial depth of 150 mm of soil, which is assumed to have been disturbed by the boring tools.

The test, which is empirical, has been widely practised and there is much published information linking the results of the tests with other soil parameters and with the performance of structures. The main purpose of the test is to obtain an indication of the relative density of sands and gravels It has also been used to obtain an indication of the consistency of other soils such as silts and clays and of the strength of weak rocks. Other correlations have been produced relating the number of blows N to deformation moduli. One such correlation is illustrated in figure 2.3.6.13.

Procedure of carrying out the test
The test is almost always carried out in a borehole made by shell and auger methods or sometimes by rotary washboring. The bottom of the borehole must be carefully cleaned out, particularly if the test is carried below groundwater level for soils may be loosened by the action of the boring tools and by pressure differences between groundwater and the water in the hole. Such disturbances may be minimized by careful use of the boring tools and by keeping the level of the water in the borehole higher than that of the groundwater.
The number of blows recorded are counted for successive penetrations of 75 mm into the soil. Thus the N values recorded by a driller for 450 mm penetration might read 6, 5, 7, 8, 8, 7 from

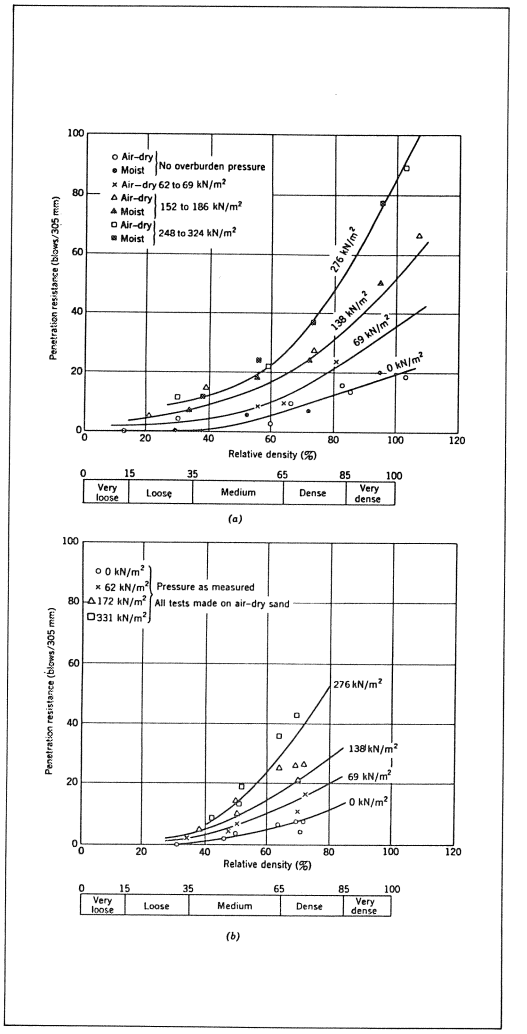

Figure 2.3.613 results of standard penetration tests; (a) Course sand, (b) Fine sand. (Form Gibbs and Holz, 1957)

which the N value recorded in the borehole record would be 30 (7 + 8 + 8 + 7). Recording the number of blows in this way allows the driller to see if there is a change in strata within the test section, for this would be reflected in the 75 mm N values.
The sample retained in the split tube may be used for particle size analysis.

Advantages and limitations of the S.P.T.
The principal advantage of the test and the main reason for its widespread use is its simplicity and cheapness. There is also a great body of information, built upon experience, about the use of the tests results in relation to foundation design. The test is undoubtedly primitive and the values obtained are somewhat approximate and unreliable, but many engineering projects have been successfully designed and constructed on the results produced by this test.

Figure 2.3.6.14 Schematic conception of a dynamic penetrometer

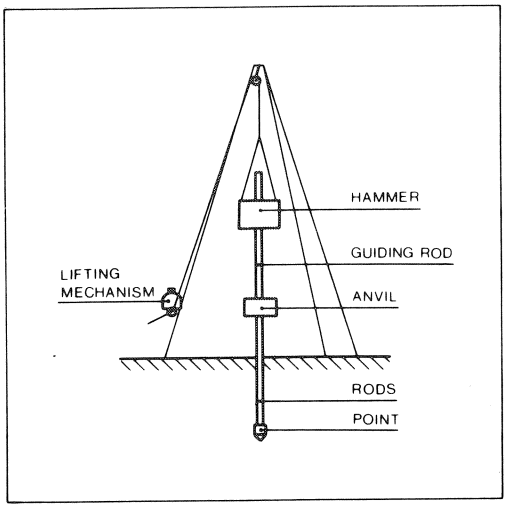

Dynamic cone penetration test (D.P.T)
This test is utilized in gravels, cobbles and boulders. The driving shoe of the split spoon sampler is replaced by a solid cone (with 60° angle at the apex) and the test is conducted in the standard way.
Comparison between standard penetration tests and dynamic cone penetration tests in sands have shown that the dynamic cone penetration tests tend to give slightly higher N-values than the standard penetration tests. However, when the dynamic penetration test is applied on gravels it is usual to attach the same significance to the N-values as is normal for the N-values from standard penetration tests in sands. If the dynamic penetration test is conducted in coarser materials, such as coarse-gravel, cobbles or boulders, it is always uncertain whether or not the cone may be driving a boulder or a cobble ahead of it down the borehole. For this reason dynamic penetration test N-values in coarsely granular soils should always be regarded with some caution.

The dynamic penetration test has many varieties with regards to shape of cone, weight of hammer and drop-height. They can be performed in a pre-drilled hole or directly from the groundlevel. Examples are:

- the S.P.T. in a predrilled hole
- the D.P.T. Swedish Ram Sounding and German Ram Sounding, from groundlevel

Fig. 2.3.6.14 shows schematically the Swedish Ram Sounding device: The weight of the hammer is 63,5 ± 1 kg and the drop height is 0.6 ± 0,1 m.
The rods are 32 mm diam., while the point has a cross-section of 16 cm² over a length of 90 mm.

The static cone penetration test (C.P.T.)
All static cone penetration tests (C.P.T.) consist of pushing a rod into the ground and assessing the physical properties of the material through which the rod is pushed by measuring the resistance at the cone. A very wide variety of static cone penetrometers are available throughout the world but that most widely used and with which people have the most experience are the two type developed in the Netherlands, the

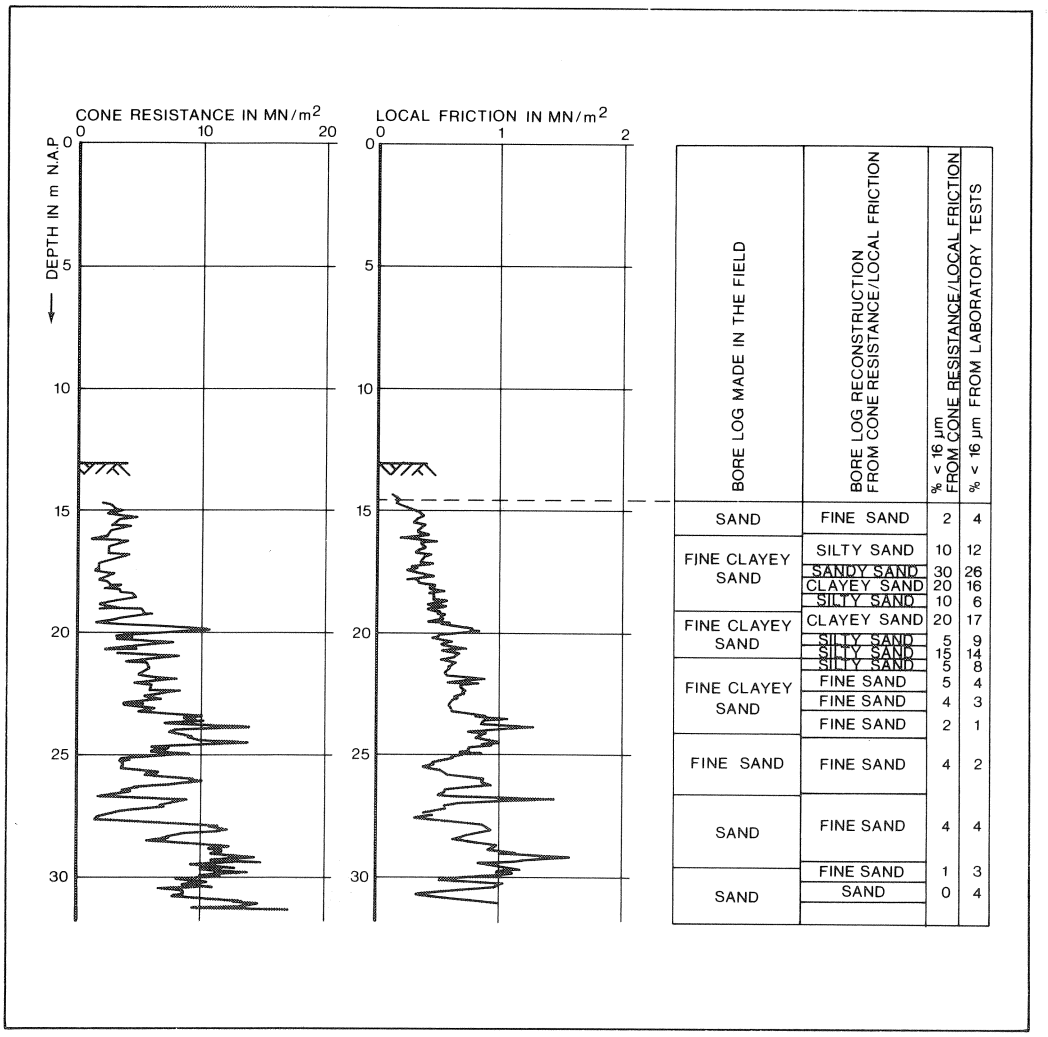

Figure 2.3.6.15 Results of a cone penetration test

mechanical and electrical cone. They both are now standardized. The test was designed to enable a cheap and rapid assessment to be made of the length and diameter of piles necessary to carry a given load. In the original mechanical version the apparatus consists of a rod with a cone end and a tube that surrounds the rod, so arranged that both cone and tube

may be advanced together or separately. They are both forced into the ground by means of a static load. The cone is then advanced ahead of the tube to measure end resistance alone, and if the friction jacket type of cone is used the local friction and cone resistance are also measured. The results are expressed graphically in depth of penetration versus cone resistance plus local friction charts. See fig. 2.3.6.15.

Test results
It is important to note that the test does not give samples to allow direct assessment of the type of soil being penetrated but it may be possible to estimate this from the resistance values and the local friction values. By comparing boring logs and c.p.t.'s it was found that the ratio of local friction and cone resistance provides an identifacition of the lithology. See fig. 2.3.6.16. This implies that the use of the test in site investigation is confined to those areas in which the geology is well known or has been subject to an earlier investigation by boreholes.

Developments
An important development was one in which the original purely mechanical arrangements for measuring cone and tube resistance were replaced by load cells operating electrically (electric cone).
The introduction of electrically operated load-cells at the tip of the sounding rods has opened the way for other improvements, such as the piezometer cone and the density penetrometer. With the piezometer cone the water pressure during penetration can be registered. This type of information provides a very accurate stratigraphy of the soil. The density probe informs about the density or porosity in-situ. In sands, for instance, the porosity-measurement in-situ through borings is not of any value. By means of the density probe correct measurement can be done and reliable values presented.
The electric cone has also opened the way to in situ testing in deep water. Developments in that direction have just started and the keyword will be „remote controlled".

Application of test results
Apart from the stratification and **soil identification** as mentioned above, the measured cone resistance q_c and local friction f_s, also provide a basis for the assessment of **parametric values for** geotechnical computational models. These are:

- Parameters for the bearing capacity of a pile at the point, which is directly related to q_c and the friction along the pile, which is also directly related to f_s, in the case of a straight pile.
- Parameters for the settlement prediction
  According to Terzaghi the settlement of a soil-layer due to a load increment will be:

$$s = \frac{h}{C} \ln \frac{\sigma_0' + \Delta\sigma'}{\sigma_0'}$$

s = settlement
h = thickness of the soil layer
σ'_0 = the initial effective stress of the soil particles in that layer
$\triangle\sigma'$ = the effective stress increase
C = compression modulus

The compression modulus C is related to the q_c by: $C = A.\ q_c$
in which A depends on the type of soil as follows:

A	Soil
10 - 5	coarse sand
6.6 - 3.3	fine sand
5 - 2.5	sandy clay, loam
2.5 - 1.25	clay
1.25 - 0,6	peat

- other parameters such as:
. the angle of internal friction ϕ in granular soils
. Young's modulus of elasticity E_s (E_s = 1,5 à 2 q_c)
. the apparent cohesion c_u in clay (q_c = 14 c_u)
. density and porosity

Advantages and limitations
A great advantage of the C.P.T. is that measurements are independent of the operator. With almost all tests operation is subject to skill

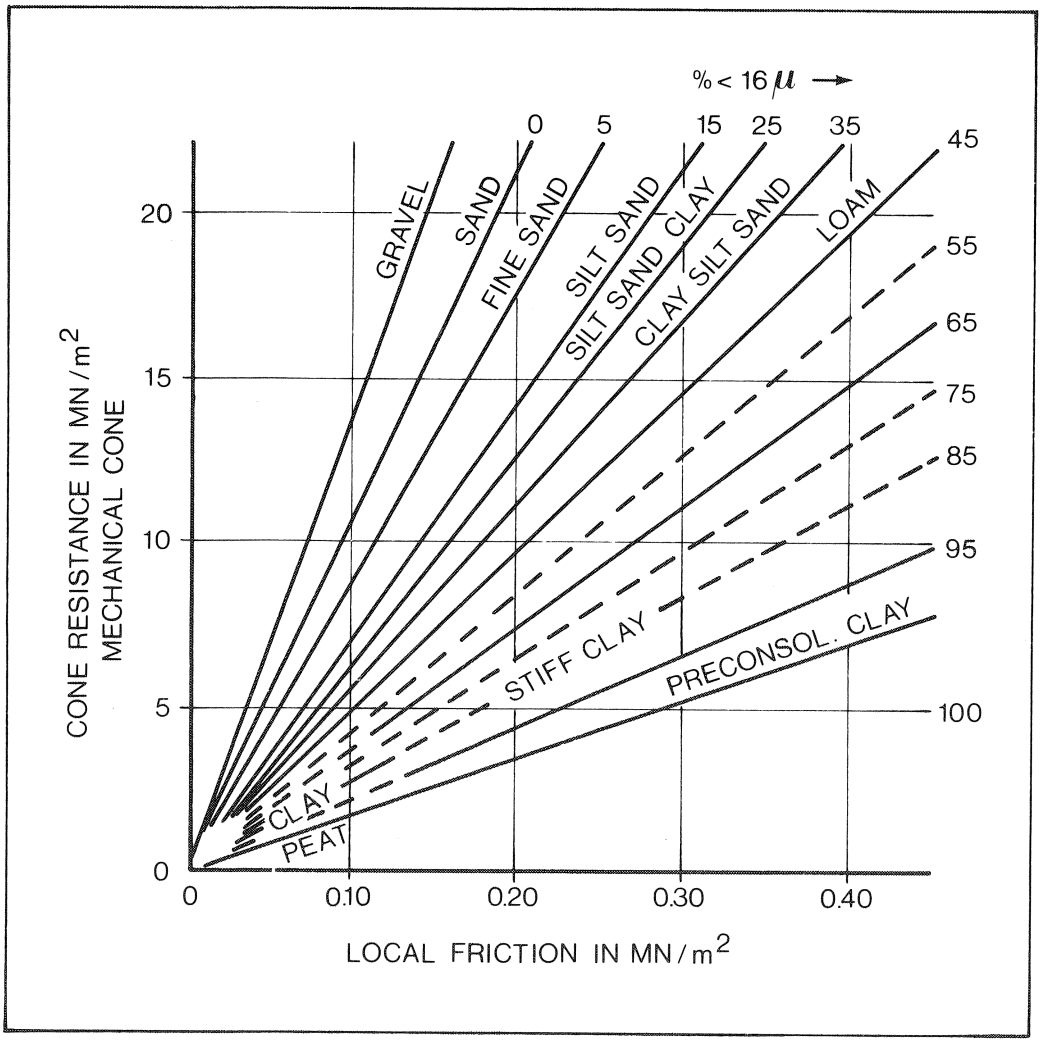

Figure 2.3.6.16 Soil indentification by cone resistance vs local friction

or personal preference and the data obtained must therefore be interpreted cautiously.
Other advantages are that many tests can be performed in a short time, making the test economic compared to boring. Also very important is that the test gives little disturbance of the soil, thus providing accurate in-situ measurements. A limitation, like all penetration tests,

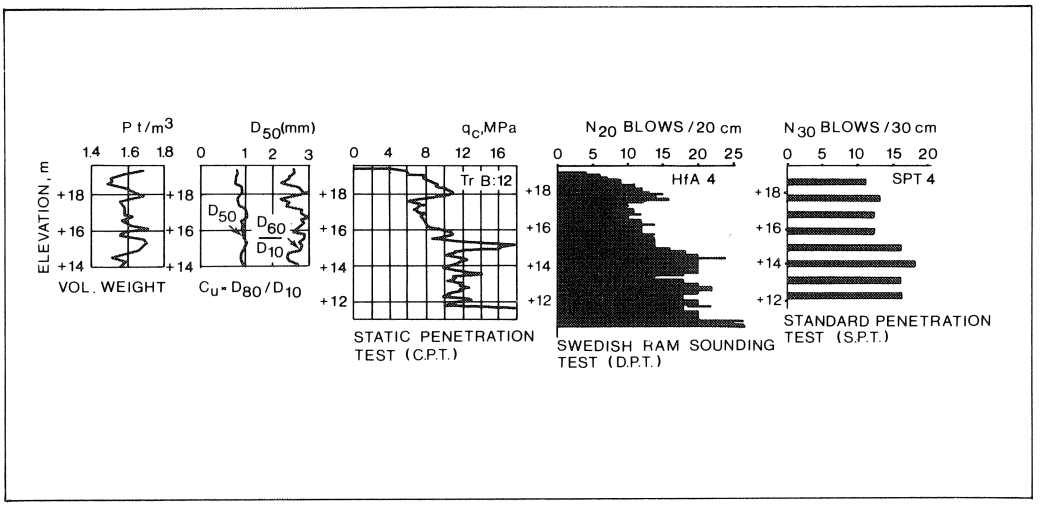

Figure 2.3.6.17 Typical results from different penetrometers

is that hard, consolidated formations cannot be tested.

Fig. 2.3.6.17 shows test-results at one location with the standard penetration test (S.P.T), the Swedish ram sounding (D.P.T.) and the static cone penetration test (C.P.T.).

The vane test

General

A cruciform vane on the end of a solid drill rod is forced into the soil below the bottom of the borehole and then rotated. The torque required to rotate the vane can be related to the shear strength of the soil.

The test is normally restricted to fairly uniform cohesive fully saturated soils and is used mainly for clays having shear strengths of up to about 100 kN/m². The results are of doubtful value in stronger or fissured clays.

The field vane used at the bottom of a borehole is shown in the figure 2.3.6.18.

Advantages and limitations

The main advantage is that the test itself causes little disturbance to the ground and is carried out below the bottom of the borehole in virtually undisturbed ground. This is particularly apparent in sensitive clays where the vane tends to give higher shear strengths than those derived from laboratory tests on samples obtained with a tube sampling device. Under these conditions the vane test results are generally considered to be more realistic.

Vane equipment is also available for use in the laboratory and hand vane equipment may be used in the field to determine the strength of soils exposed in trial pits.

Calculating the shear strength:

The shear strength of the clay may be calculated using the formula:

Torque (T) at the point of failure

$$T = c_u(\pi\, dh)\frac{d}{2} + c\left(\frac{\pi d^2}{4}\right)\frac{d}{3} \times 2$$

where h = length of the vane
d = diameter of the vane
c_u = shear strength of the soil (assuming ϕ = o°)

In the formula the first term relates to the shear strength mobilised by the vertical sides of the vane and the second term relates to the shear strength mobilised by the circles of soil at both ends of the vane.

Pressuremeter test

General
Pressuremeters are devices that expand in boreholes and deform the sides of the borehole. The pressure expanding the device and the deformation of the borehole are measured in order to produce a stress-strain graph. In soils sufficient pressure may be applied to cause shear failure so that a study of the results may serve to indicate settlement and bearing capacity characteristics of the soil. In rocks it is very difficult to develop sufficient pressure to cause failure; generally only deformation characteristics can be measured.

Pressuremeters for soil testing
The typical soil pressuremeter consists of a rubber tube expanded underwater or oil pressure. This fits closely into the borehole or in very soft soils, may be driven into the ground. The Menard Pressuremeter is one of the first instruments of this type developed and is widely used with a reputation for reliability. See fig. 2.3.6.19.
The Menard Pressuremeter consists of two components:

- The probe
  This is a cylindrical metal body with rubber membranes stretched over it and attached in such a manner as to effectively form 3 independent cells.
  The central measuring cell contains a liquid under gas pressure, the upper and lower cells are pressurized with gas only. The deformations are measured by the central cell only where conditions of plane strain are deemed to exist due to the presence of the guard cells.

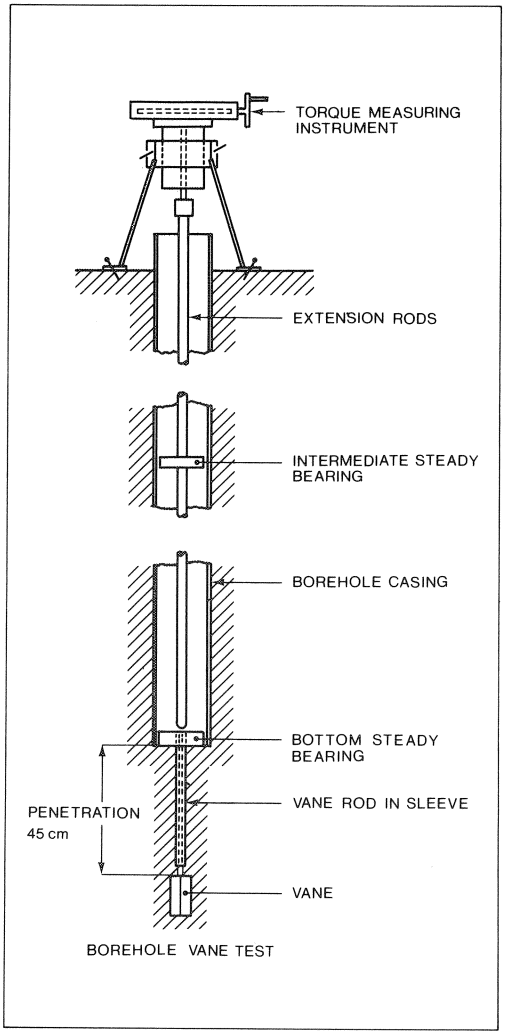

Figure 2.3.6.18 Field cone used in a borehole

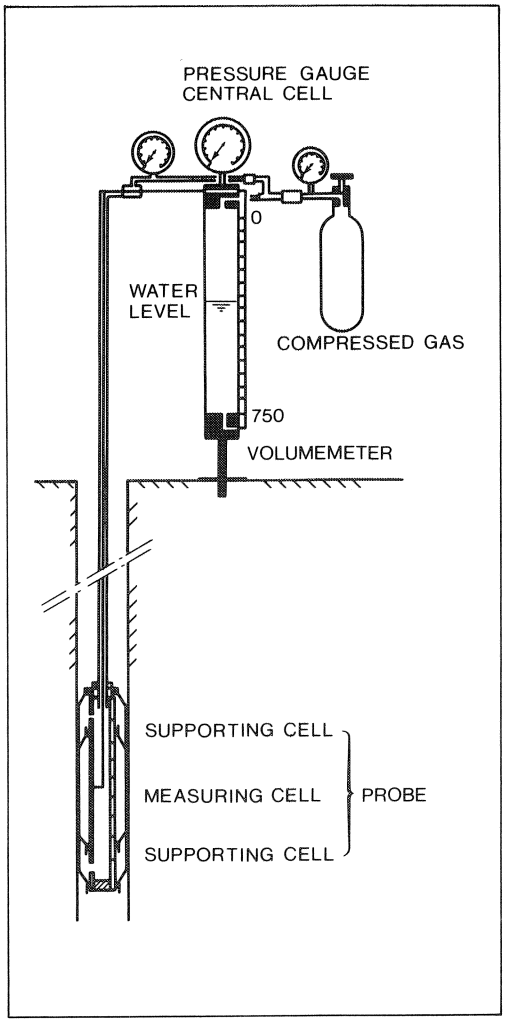

Figure 2.3.6.19 Pressure meter test set-up

In order to minimize the possibility of the rubber membranes being punctured by sharp aggregate, these are generally protected by a shield of overlapping longitudinal metal strips.
The probes are available in various diameters to suit the standard borehole dimensions; the most common dimensions are Ax, Bx, Nx.

- The volumemeter
This is a metal cylindrical, water-filled reservoir equipped with pressure gauges and regulators. It permits the controlled injection of water and gas into the central and guard cells respectively.
The pressure meter provides information of the in-situ strength property of the soil, which is the elasticity in a horizontal direction. Fig.2.3.6.20 shows the relation of readings and elasticity

3. Site investigation on water

The methods used for soil exploration on land are in principle applicable to situations on water. Usually it is a matter of moving the workfloor from the ground surface to a floating surface or to the deck of a temporary fixed platform. As long as the water is not deep or moving the condition for investigation can be dealt with.

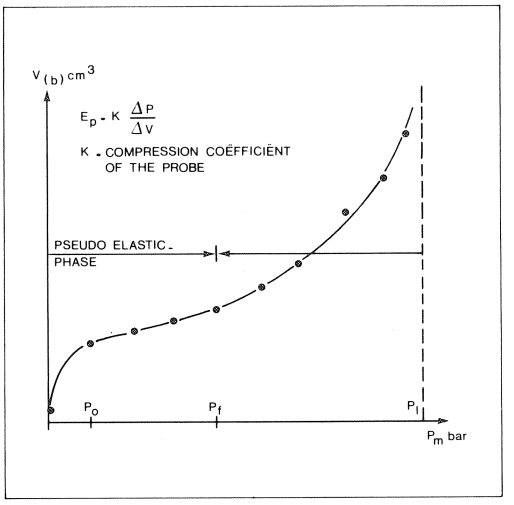

Figure 2.3.6.20 Result of pressure meter test (uncorrected curve)

If waterdepths become great, if there is a strong current and if waves and swell occur soil exploration becomes a venture in itself.

In most cases of investigation over water a pontoon is used. When exploration has to be executed off shore a sea-worthy ship becomes necessary. The big handicap with both situations is that the deck moves in respect to the bottom, which means that all activities in the borehole have to be done independently from the movement of the workfloor. This can be achieved by putting a casing provided with a heavy weight on the bottom.
This casing extends above the deck and stands freely from the pontoon.
Fig. 2.3.6.21 shows the principle and arrangement for boring and penetration testing on a pontoon.
When the waterdepth exceeds 30 meters, investigation with such an arrangement becomes hardly possible. The rotary drill system is instead the appropriate solution. This method is derived from the oil exploration industry. Use is made of a drill-string, which is lowered from the deck of the ship and penetrates the soil. The drill-string has enough flexibility to allow for some dislocation of the ship. This type of boring can be designated as rotary wash-boring. At intervals drilling can be stopped and drive samplers can be lowered to the bottom of the hole through the hollow drill string to take samples.
Instead of a sampler a wireline penetrometer can be lowered. With such a penetrometer a cone penetration test of 1,5 m in length can be performed at the bottom of the hole. Fig. 2.3.6.22 shows the system of drill-string, sampler and penetrometer developed by Fugro, The Netherlands, on board of a ship.

The need for better and more economic methods of soil exploration, especially for offshore conditions, has been and still is stimulated by oil exploration and the construction of large structures near the coast. A sophisticated instrument for site investigation was the result of such a demand. It is the diving bell used for site investiga-

Figure 2.3.6.21 Drilling Pontoon

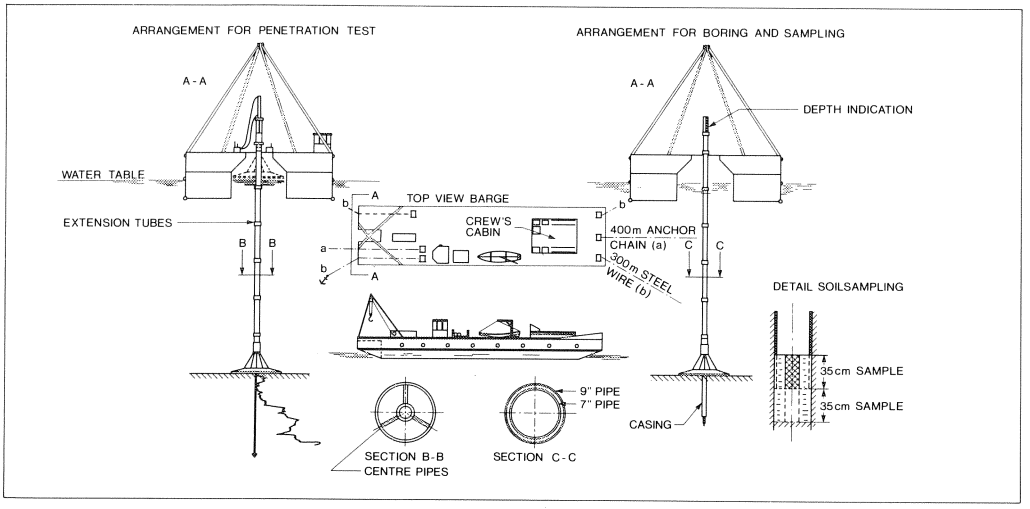

tion in the Eastern Scheldt estuary in the Netherlands, where the Rijkswaterstaat is building a large storm surge barrier. With such a bell, cone penetration tests and density tests can be performed; long continuous samples can also be taken.

Fig.2.3.6.24 presents the result of a cone penetration test made from the bell.

Figure 2.3.6.22 Drill string with Wison Cone penetrometer

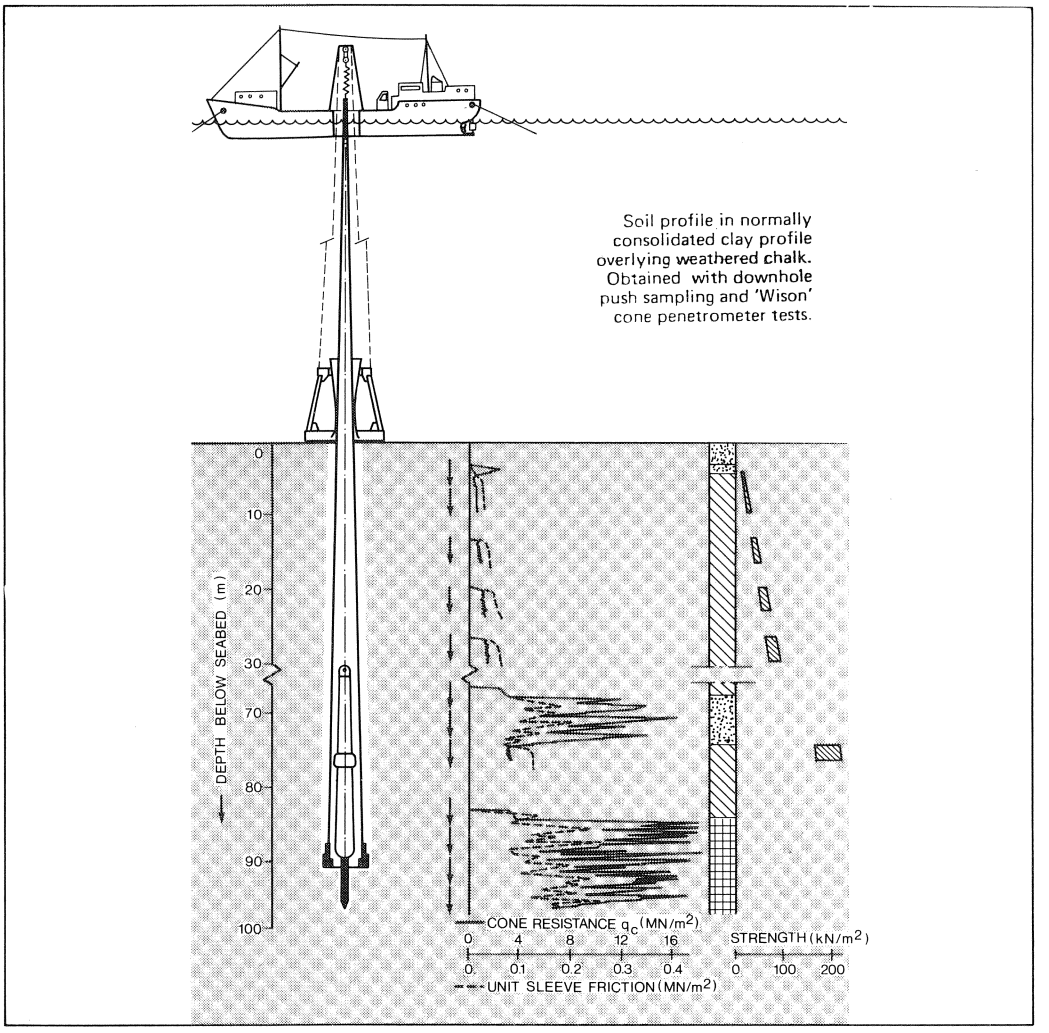

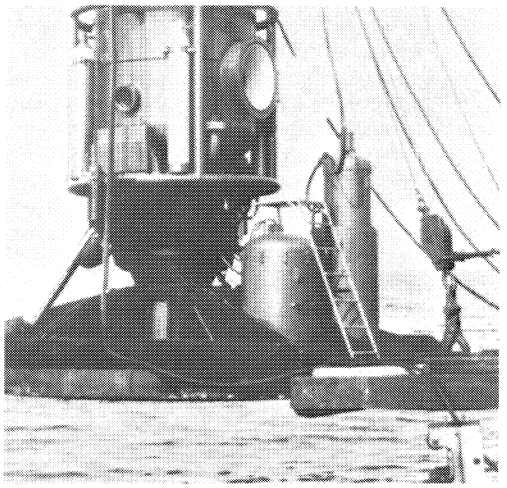

Figure 3.6.23 Diving bell for seabed investigation

Advantages and limitations
The major advantage of a large drilling pontoon or drill-ship is that there are hardly any restrictions to the depth of penetration.
The same penetration as on land can be in principle achieved. What may cause a limitation is the cost involved. Drill-ships or specially built pontoons such as the one for the diving bell, which has a weight of max. 70 tonnes, are the biggest cost factor of the site investigation.
A lot of effort has therefore been put into improved sub-sea soil investigation apparatus which can be handled comparatively easily.

Shallow seabed exploration
As a result a great variety of boring and penetration equipment for seabed testing has been developed especially during the oil boom in the North Sea.
The development of all this equipment is based on the principle that testing should be done from the seabed, independently of the ship's movement. Operation is then remotely controlled. The success has not so far been very impressive. For shallow investigation some equipment works quite satisfactorily and can be used well, i.e. the vibracorers as shown on fig. 2.3.6.25 and fig.2.3.6.26 or the 18 ton Stingray of Mc Clelland Engineers, fig.2.3.6.27.
With the Marine vibracorer a sample of 9m can be taken in waterdepths of up to 200m. With the Geodoff a wash-boring of 11 m can be executed in waterdepths of up to 100m. The Geodoff can be altered for the performance of a short cone penetration test.
With the Stingray cone penetration tests of 30 m have been executed in waterdepths up to 200 m. By intermittent drilling the penetration depth can be extended considerably.

2.3.6.6. Laboratory testing

1. General.
Laboratory testing is carried out to assess properties of a soil sample. In this context soil should be regarded as ground material which influences or is influenced by a man-made structure, whether this structure is built from concrete, steel or from soil. The structure may be situated above or in the ground. The type of ground which poses the greatest problems is generally the sedimentary soils. This section therefore applies mostly to this type of formation.
The civil engineer working with soil must design his structure not only for the properties of the soil as it exists at the start of the project but also for the entire design-life of the structure. He thus needs to know both the properties of the soil at the start of the project and how these properties will vary during the design-life. Both the size and shape of a given deposit and the engineering properties of the soil in the deposit may change very significantly. Many of these changes occur independently of man's activity, whereas others are brought by the construction activity itself. The significant changes in engineering behaviour that can and do occur during the life of soil make soil engineering both difficult and interesting. The engineer soon

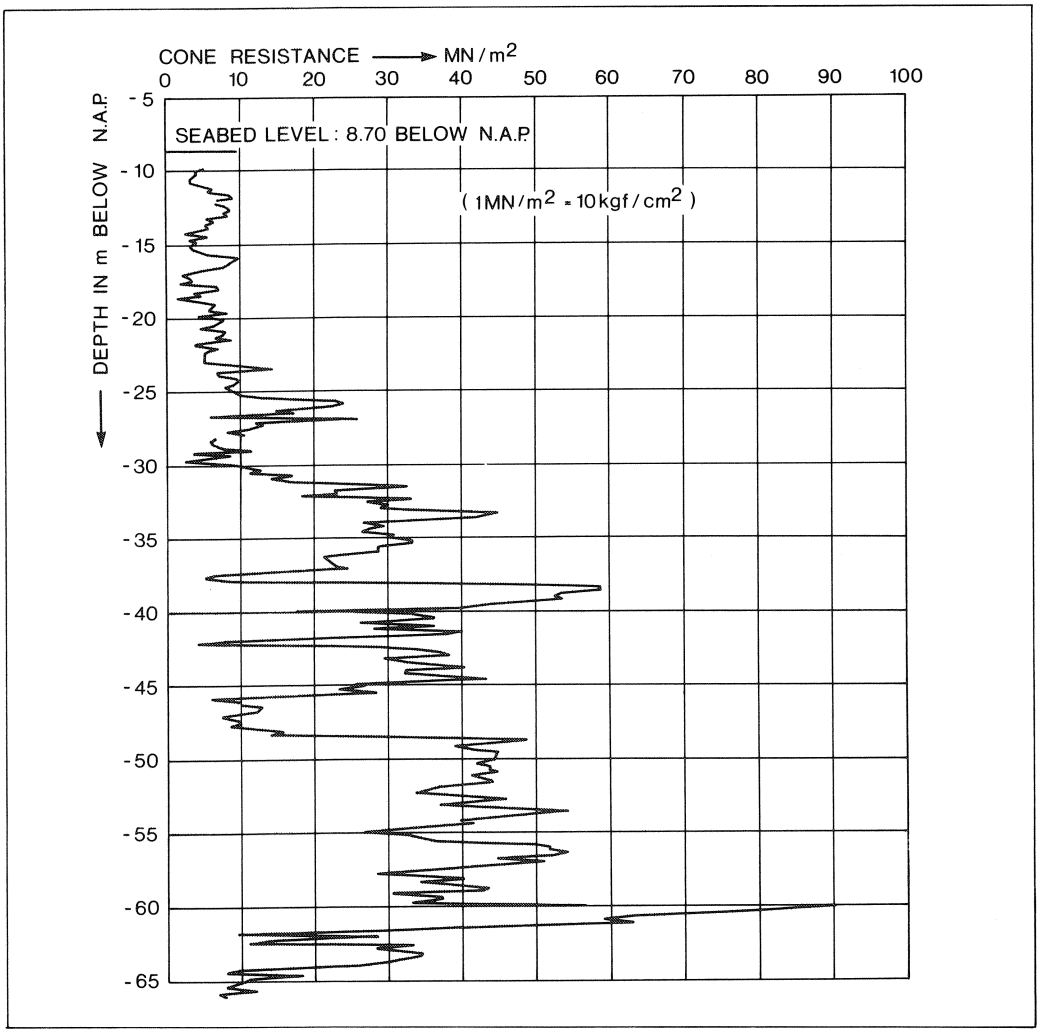

Figure 2.3.6.24 Result of an electrical cone penetrometer test to a depth below - 65 m NAP (seabed level was - 8.70 m NAP), performed with the diving bell (NAP = Amsterdam water reference level)

learns that soil is not inert but, instead, very much alive and sensitive to its environment.
The factors with the greatest influence on the behaviour of soil are:

a. Stress

In general, an increase in stress on a soil element causes an increase in shear strength, a decrease in compressibility and a decrease in

The basic construction consists of two vertical pillars, down which the vibrator house slides, mounted onto a rectangular frame and strengthened by wire braces fixed to the top and base of the frame. The frame is equipped on one side with two vanes to keep it from turning by the sea current during Hoisting and Lowering, and to give it the most stable position on the sea-bed.
The electric corer has been manufactured in several size/versions: a. a very small and light aluminium one for transport by air b. a large and heavy one for corers upto 9 metres long. Normally the more heavy corers are equipped with the often more effective system of the Vibro Hammer. The lighter versions are equipped with the less expensive Vibro Hammer. At the present time three types of the electric vibrocorer are standarised.
With optional extra's it is possible to increase the corelengths and diameters. Core Barrels can be obtained with or without PVC liner.
The barrel consists of a seamless mild-steel tube with a core catcher soldered into a replaceable cutting shoe with a flange at the top. A coarse threaded collar slides over the barrel and engages it to the motor housing.
The waterproof motor house consists of two electric motors mounted side by side and delivering vibrations via two eccentric fly-wheels. The motors counter rotate.

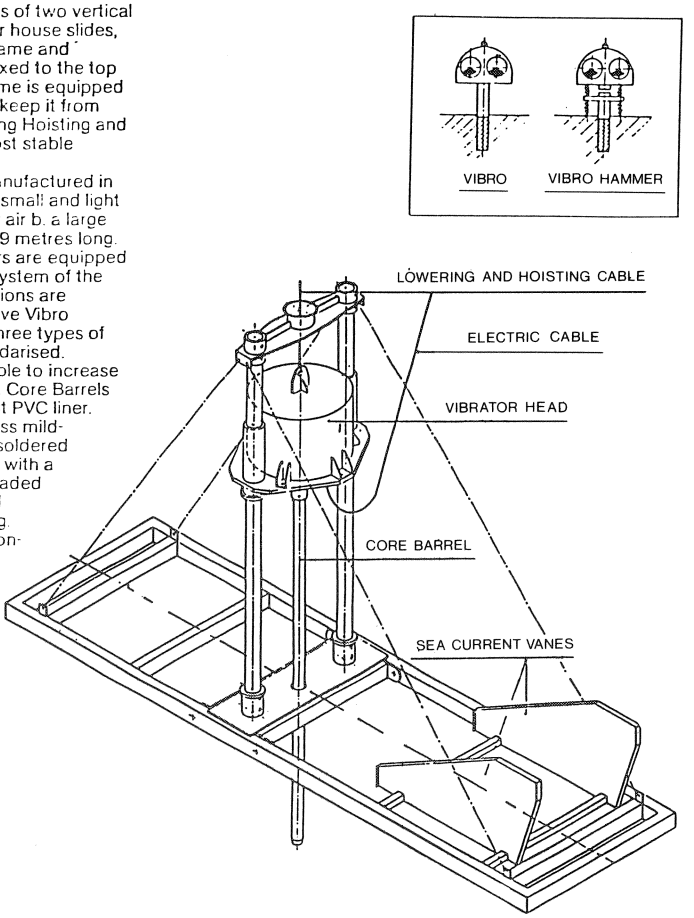

Figure 2.3.6.25 Electric driven vibro and vibro hammer corers

permeability; a reduction in stress causes the reverse. The changes brought about by a stress reduction are usually less than those caused by a stress increase of equal magnitude.
Note that there is a distinct difference between various types of discontinuous rock masses with regard to the stress distribution, as can be seen in figure 2.3.6.28.
During the formation of a sedimentary soil the

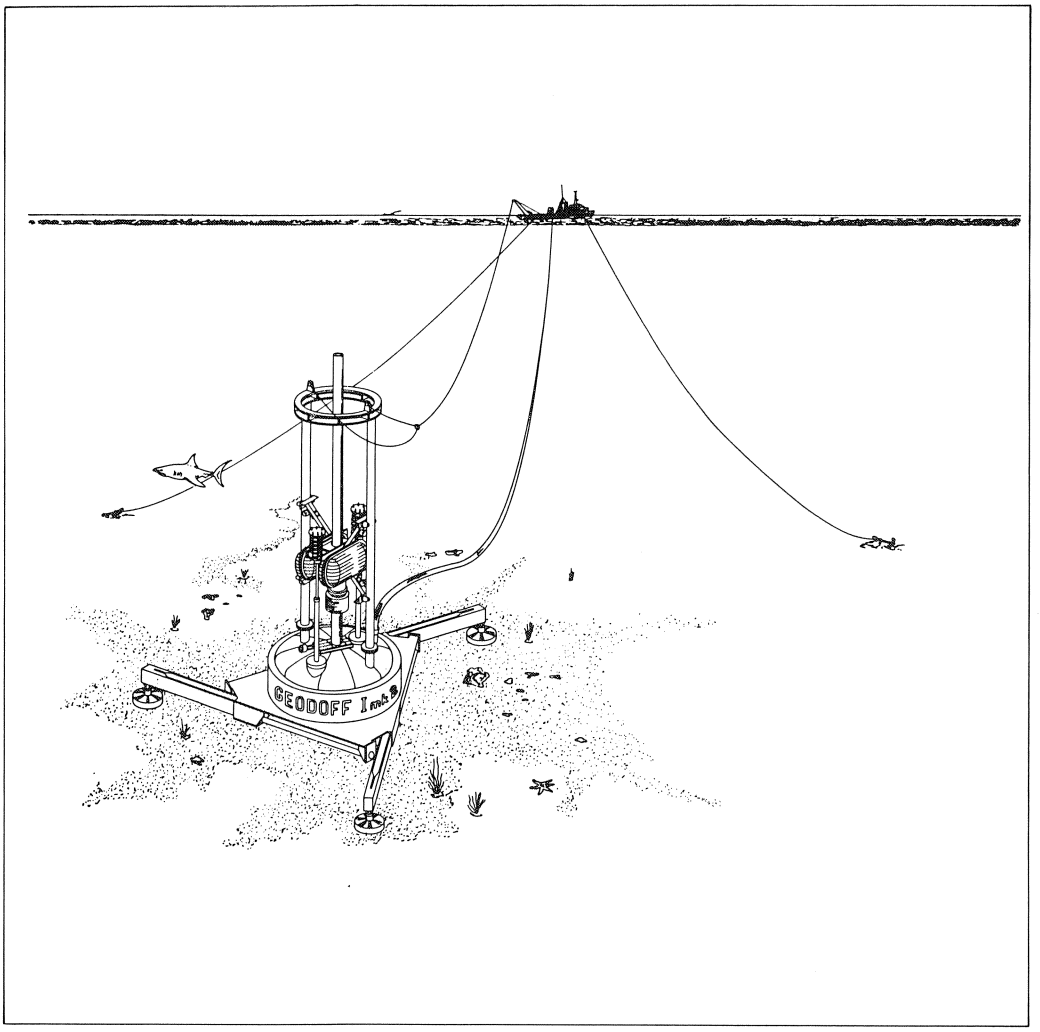

Figure 2.3.6.26 Geodoff vibrocorer

total stress at any given elevation continues to build up as the height of soil over the point increases. Thus the properties at any given elevation in a sedimentary soil are continuously changing as the deposit is formed. The removal of soil overburden, e.g. by erosion, results in a reduction of stress. A soil element that is at equilibrium under the maximum stress it has ever experienced is normally consolidated,

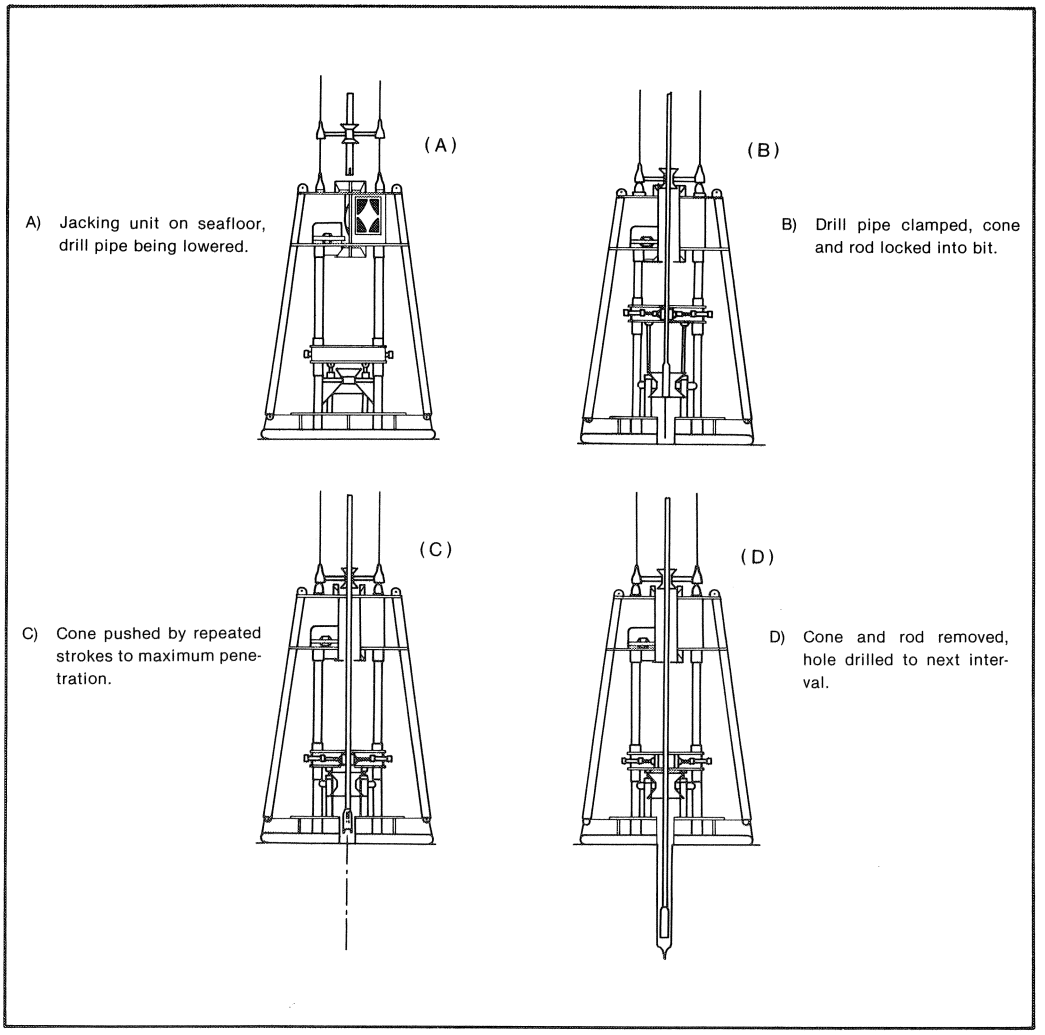

Figure 2.3.6.27 Cone testing with Stingray

whereas a soil at equilibrium under a stress less than that to which it was once consolidated is overconsolidated.

There are construction activities that result in an increase of the confining stress on soil and there are others that result in a reduction of stress. For example, the dam shown in Fig. 2.3.6.29 caused a very great increase of vertical stress on the soils underneath the dam. When

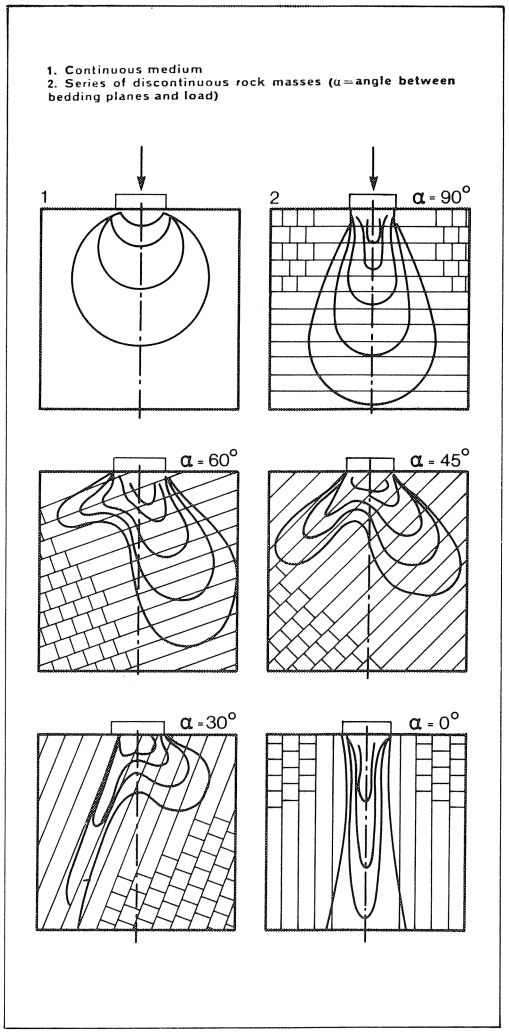

Figure 2.3.6.28 Distribution of stresses in a jointed rock mass of varying bedding dips under an applied external normal load (Gaziev and Erliken)
1 Contimous medium
2 Series of discontinuous rock masses (x = angle between bedding planes and load)

equilibrium was reached under this load, the soil underneath the dam had become much stronger. On the other hand, the excavation for the Panama Canal (Fig. 2.3.6.30) resulted in considerable unloading of the soil in the canal and immediately adjacent to it. This unloading resulted in a decrease in the strength of the shale immediately adjacent to the canal and contributed to the slides that occured along the canal.

b. Time.

Time is a dependent variable for the other factors contributing to change in soil behaviour (especially stress, water and environment). For the full effects of a stress change to be felt, water must usually be extruded or imbibed in the soil element.

Because of the relatively low permeability of fine-grained soil, time is required for water to flow into or out of this type of soil. Time is an obvious factor in chemical reactions such as those occurring during weathering.

c. Water.

Water can have two deleterious effects on soil. First, the mere presence of water causes the attractive forces between clay particles to decrease. Second, pore water can carry applied stress and thus influence soil behaviour. A sample of clay which may have a strength approaching that of a weak concrete when it has been dried can become mud when immersed in water. Thus increasing the water content of a soil generally reduces the strength of the soil. The activities of both nature and man serve to alter pore water conditions. In many parts of the world, there is a very marked variation in water conditions during the year. During the hot, dry season, there is a lack of rain and the groundwater level drops; during the wet season there is surface water and general rising of the groundwater. This seasonal variation in water conditions causes a marked change in soil properties throughout the year.

There are many construction operations that alter groundwater conditions. For example, the dam shown in Fig. 2.3.6.29 impounded a reservoir, which subjected the foundation soils to a great increase in pore-water pressure. Not only

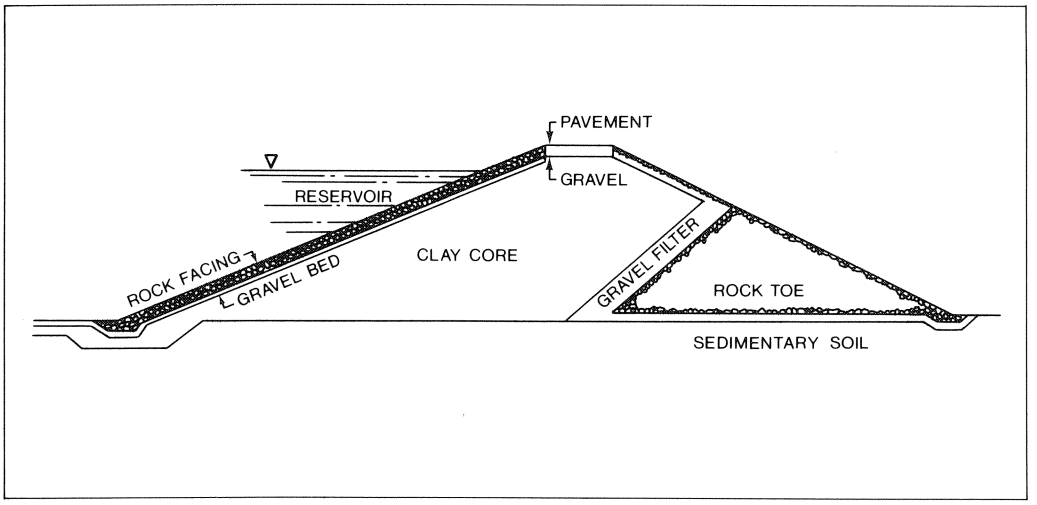

Figure 2.3.6.29 Earth dam

Figure 2.3.6.30 The Panama Canal; Cross section through East Culebra Slide

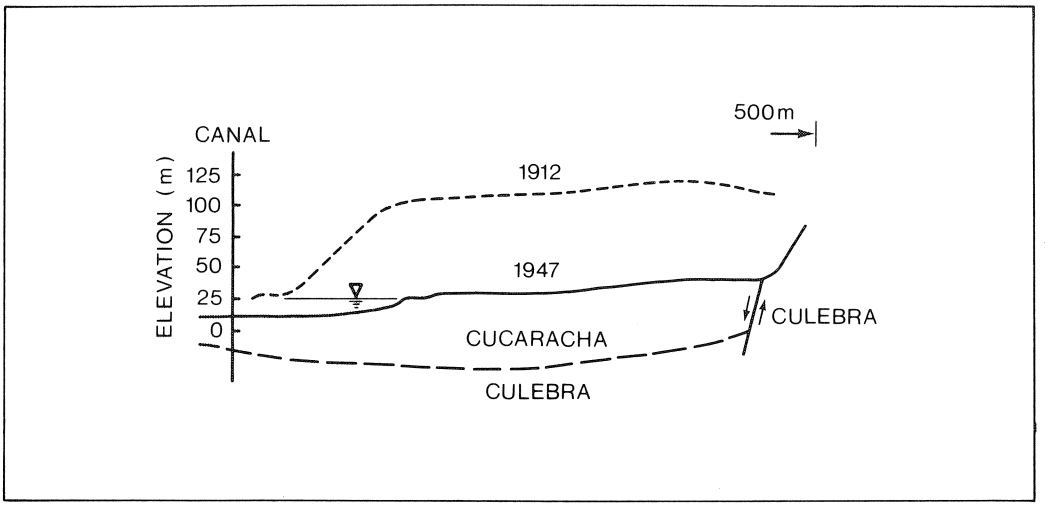

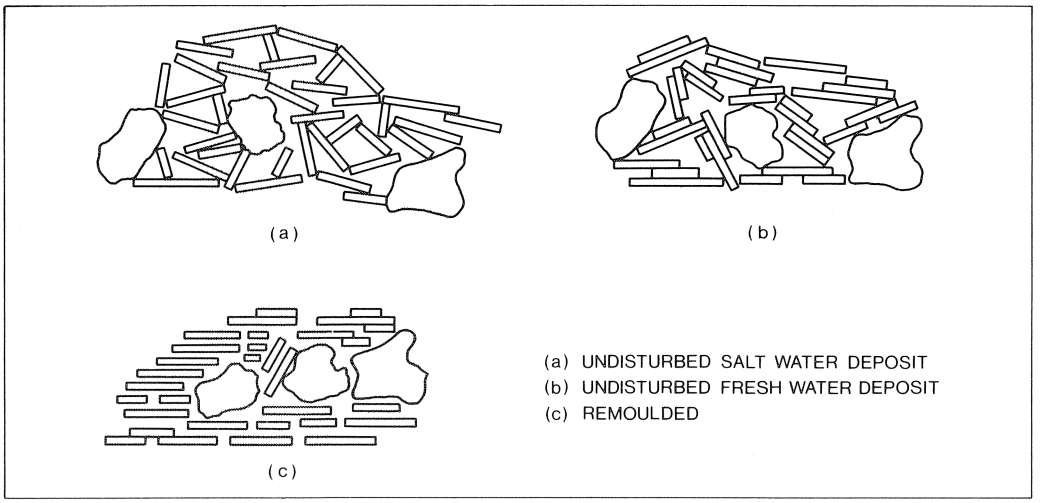

Figure 2.3.6.31 Structure of natural clay

were the foundation soils given an increase in pore pressure, but many dry soils which had never been inundated were submerged with water from the reservoir.

d. Environment

There are several characteristics of the environment of a soil which may influence its behaviour. The two considered here are the natural pore fluid and temperature. A sedimentary clay or compacted clay can be formed with a pore fluid of a certain composition, and at a certain temperature; both of these can change during the life of the deposit. One example is a marine clay laid down in water high in salt, 35 g of salt/liter of water for a typical marine environment.

A marine clay is frequently uplifted so that it is above the level of the sea, and the groundwaters percolating through the clay are of much lower salt content than the sea water. Thus during the life of the sedimentary clay there can occur a gradual removal of the salt in the pore fluid so that, after many thousands of years and leaching, the pore fluid can be quite different from that at the time of sediment formation. Reducing the electrolytic content of the water around the soil particles can reduce the net attraction between them. In other words, leaching of the salt in the pore fluid can cause a reduction in shear strength.

The most dramatic example of a reduction in shear strength brought about from pore water leaching is exhibited in the „quick clays".

These marine clays were deposited in a highly flocculated condition. Despite the resulting high water content, these clays developed a moderately large strength because of the bonds that formed at the edge-to-face contacts. These clays then had most of the electrolyte in their pore fluid removed by years of leaching.

For this new environmental condition, the clay would tend to be in a dispersed condition (see Fig. 2.3.6.31c), and for the same water content it would have very little strength. However, this change does not show up fully until the clay is subjected to enough disturbance to break the bonds built up by years of confining stress.

Upon disturbance, the clay may lose all of its

strength and become a soil-water slurry with zero shear strength. These quick clays have caused many engineering problems in the Scandinavian countries and in Canada where they are widespread. The disastrous landslide near Rissa, Norway, 1978 occurred in a quick clay.
A remarkable circumstance is that this was the first large-scale landslide ever filmed from start to end.
The change in temperature from time of deposit formation to a given time under consideration can result in a change of soil behaviour.
Thus a clay deposit in a glacial lake undergoes a general warming during its life. Further, a soil existing at great depth in the ground, sampled and brought into the laboratory for testing, may undergo property changes due to the difference in temperature between the ground and the laboratory. Increasing the temperature of a cohesive soil normally causes an expansion of the soil as well as a change of the dissolved air content.

The engineer can see from the discussion in this section that he must give thought to how the properties of the soil might change during the life of his structure, and not expect to make a proper design on the basis of the properties of the soil as it exists prior to construction. He could be faced with a disastrous failure if he designed his earth dam on the basis of the strengths of the soil which exist prior to the construction of the dam. He must also select the proper values of strength, permeability, and compressibility to be used in a given soil problem. This implies that not only a possible degradation should be taken into account but also that samples should be tested in the laboratory under future site condition, at least as closely as possible resembling that condition.
Fig. 2.3.6.32 illustrates how the type of tests is related to the expected soil condition when a pile is axially loaded.

2. Tests

Several types of tests may be carried out in order to predict the behaviour of the soil in future conditions. Often these tests are not all required, especially when the general geological condition is known. A distinction can be made between:

a. Mineralogical testing by means of microscopy, x-ray and chemical analysis.
b. Mechanical testing, through which the properties of the soil samples are determined.
c. Model testing on a small scale either under normal gravity conditions (1g) or under increased gravity conditions, i.e. in a centrifuge (more than 100 g). This type of test is mostly applied when the configuration of soil and structure is complicated and a good prediction of the interaction between soil and structure is wanted.

It is not possible to describe all the kinds of tests. Reference is therefore made to the relevant publications, which are freely available. Some routine tests, mostly of category b, will, however, be mentioned briefly.

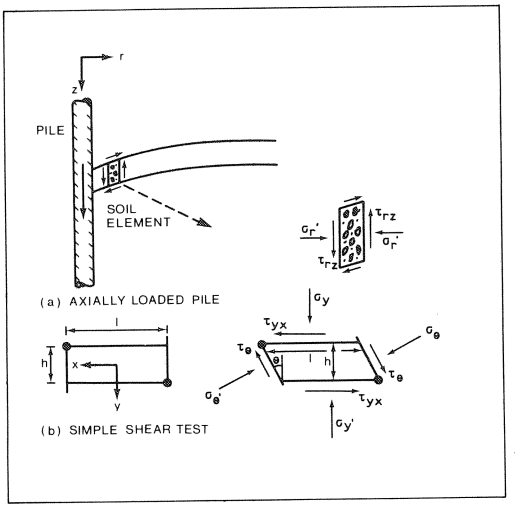

Figure 2.3.6.32 Analogy between shearing of soil around an axially loaded pile and soil in a simple shear test

2.3.6.7 Composition and classification of soil types

Granular analysis
The purpose of the test is to define the grain-distribution-diagram. The test is performed, inter alia, to investigate the soil compaction possibilities; to examine to what extent the soil can be used for hydraulic fill; to assess the quality of the soil for road- construction and earth fill. The test can be applied to both sand and clay. The grain-distribution-diagram is defined on the basis of results from sieve tests and/or hydrometer tests (see fig. 2.3.6.33 and 34).
The practical significance of the sieve curve is that, from the curvature data can be derived on the grain-size and the distribution of the material and that a general insight can be gained on the permeability.

Chemical analysis
To supplement the granular analysis, the humus and lime contents can be defined by a chemical analysis.

2.3.6.8 Mechanical-physical properties

Density
It is possible to determine:

a. the specific gravity, the weigth of volume and the water content of clay samples; simultaneously, the consistency limites are also defined. This is done in order to assess the workability of clay and to investigate its water retaining capacity. If the water content is lower than required for the plastic limit than the clay is not suitable. Nor is it suitable if the water content exceeds the liquid limit.
b. Maximum-minimum density
In order to get an impression on the possibility of compacting the sand, the maximum and minimum density of a sample can be determined.
The density is expressed in porosity percentage.

Permeability
The permeability of the soil is also important for

Figure 2.3.6.33 Grading curves of a very fine sand and a very coarse sand

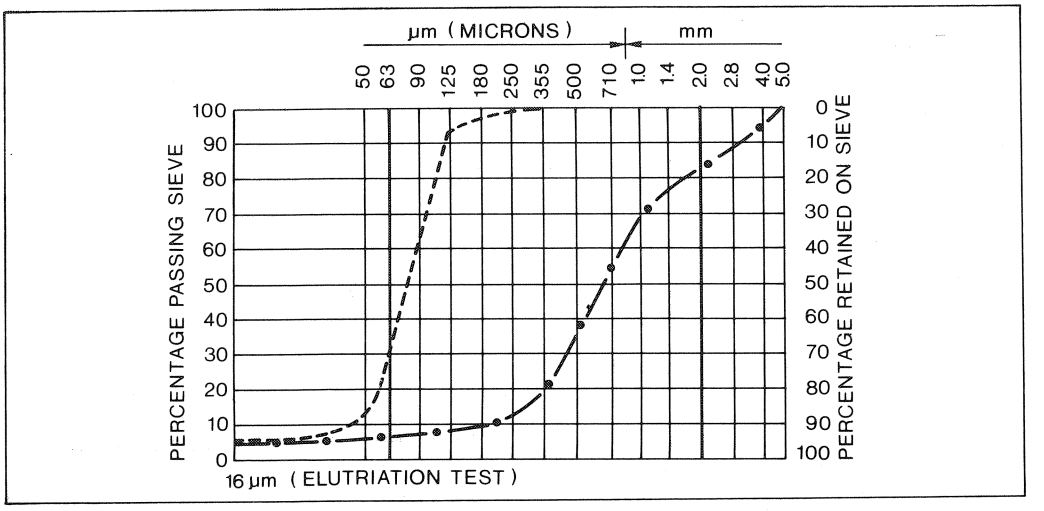

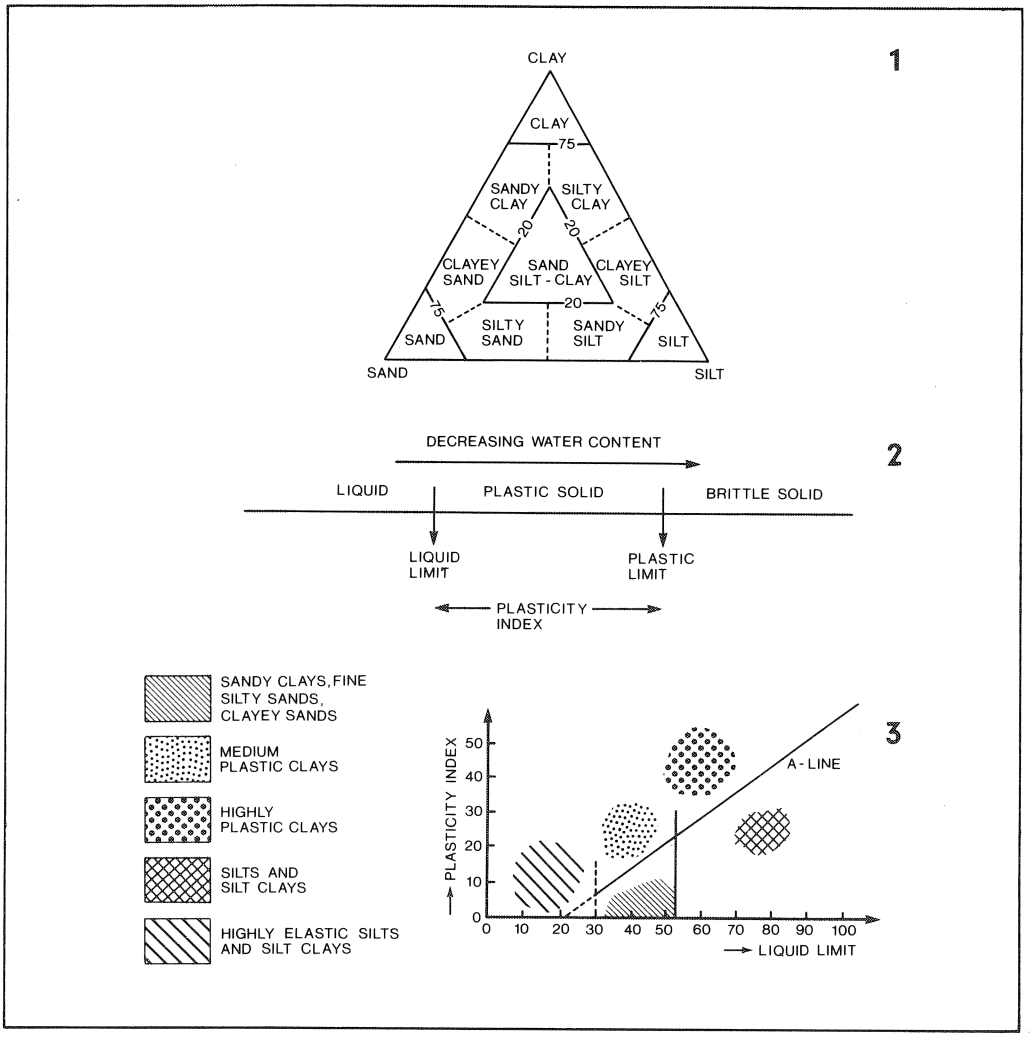

Figure 2.3.6.34 Classification of sediments

1. *Nomenclature based on sand-silt-clay percentage (Shepard, 1954)*
2. *Behaviour of cohesive soil over range of water contents*
3. *Plasticity chart (Lambe, 1954)*

determining the settlement rate of the soil under the influence of an applied load.

Another field for which the permeability is important, is the dimensioning of dewatering wells. The permeability strongly depends on the composition of the soil and can therefore differ from area to area.

In cohesive soils, the permeability tests are performed on undisturbed samples obtained from

borings specially taken for such tests.
For non-cohesive soils, it is practically impossible to take undisturbed samples. Therefore, the permeability is determined from samples with varying density. The relation between the density and the logarithm of the permeability is linear.

The permeability of soils normally differs both in horizontal and vertical direction; as an exception, they are equal in both directions.

Permeability tests in cohesive soils are therefore performed both horizontally and vertically. The permeability can also be determined from the results of the consolidation tests.

In addition to the permeability, the capillary rise can also be determined. This parameter is of importance for, inter alia, the drainage lay-out, the determination of the construction height of road foundations with regard to freezing, etc.

The capillary rise in sand amounts only to a maximum of a few decimetres, whereas in clay the rise can be from some to 20 or 30 decimetres.

Consolidation
The soil consolidation properties are investigated by testing a 2 cm high sample that must be subjected to various vertical loads. If the sample is water-saturated, the settlement resulting from the load, will be retarded, depending on the permeability of the soil. During the test, the progress of settlement for each top load is constantly monitored.
Apart from the consolidation constant C, according to Terzaghi's formula, the hydrodynamic period can also be determined. The consolidation constant C depends on the load and is therefore, in fact, not a constant. The settlement calculations will gain in accuracy if this factor is taken into account.
The stress situation in a laboratory is one-dimensional. In practice however, particularly on the edges of the loaded area, the subsidence will occur more rapidly than according to the one-dimensional consolidation theory.

The hydrodynamic period of sand is very short; as the permeability of the soil decreases, water drainage will be impeded and the duration of the hydrodynamic period will be increased.

Friction properties
The aim of determining soil friction properties is to assess the stability of earth planes for e.g.
- the stability of earth fill
- the soil pressure on earth-retaining structures;
- the bearing capacity of soil.

In these categories, the angle of internal friction ϕ' and the cohesion c' play important roles as friction properties.

The shear stresses prevailing in the soil depend on the normal stresses. As long as the shear stress is lower than the shear resistance, no stability loss will occur.

In order to define the friction properties, various tests can be performed in which the vertical load is varied and the relevant shear resistance is measured. The relationship between the normal stress and the shear resistance can be expressed in the formula below: (see also 2.4.5.1.).

$$\tau_f = c' + \sigma' \tan \phi'$$

In which:
τ_f = shear resistance
σ' = normal effective stress
ϕ' = angle of internal friction
c' = cohesion

cohesion c:
The cohesion c can be divided into two forms, i.e. the actual cohesion and the apparent cohesion, which is caused by, inter alia, capillary stresses.

The following tests can be performed to determine the friction properties:
a. The direct consolidated shear test.
   For each top load, the sample is consolidated prior to the performance of the shear test.
   The shear plane is horizontally orientated. This needs not necessarily be the most unfavourable direction. Consequently, the

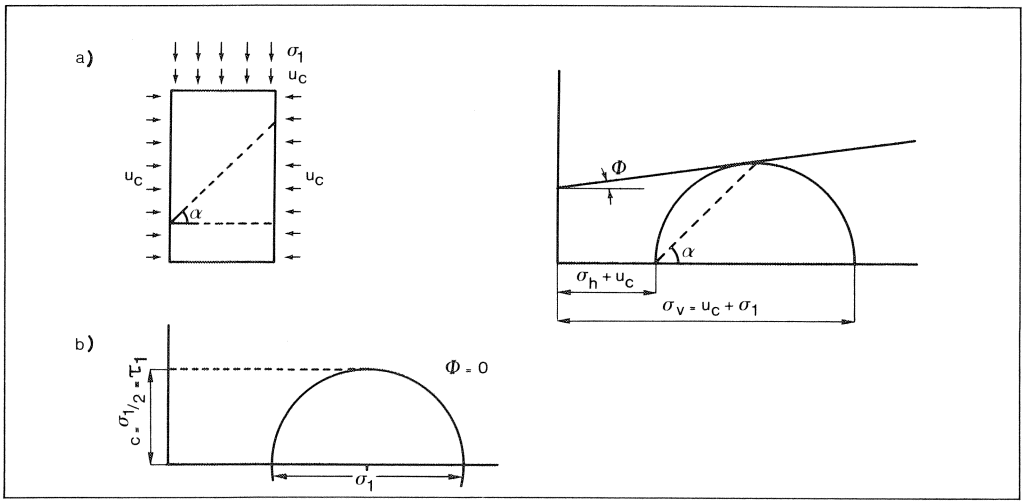

Figure 2.3.6.35 Unconfined compression test

values obtained from this test may yield too favourable a result. For peat, however, which usually is found in horizontal layers, the test can give a good indication of the shear resistance.

b. The direct not (completely) consolidated shear test.
If no consolidation has yet occurred then $\phi = 0$ occurs. This situation compares with the phase immediately after a load has been applied. In this situation the apparent cohesion c is also determined.
The apparent cohesion can also be roughly determined by the Vane test.
By means of a standardised apparatus, a set of vanes inserted into the soil is rotated until the soil slips off the vanes.
The force required to achieve this is a parameter for the apparent cohesion.
The Vane test can also be used to perform an in-situ field test. The best results are yielded by clay. The peat test results are unreliable.

In order to obtain more accurate test results on the shear resistance of the soil, cylindrical samples are taken.
The advantages of this method as compared to that of the direct sheartest, are:
- The most unfavourable shear plane can develop freely. Its direction is not, as in the direct shear test, determined by the test procedure.
- it is possible to get an image of the total stress situation of the sample.

The cylindrical samples are vertically loaded, whereby it is possible to exert horizontal confining pressure. The purpose of this test is to investigate the horizontal/vertical pressure combination at which the sample collapses. By using the method, developed by Mohr, of incorporating the pressure combinations in a diagram, it is possible to gain an impression of the friction properties of the sample.
Tests performed on cylindrical samples are:
- the unconfined compression test
- the triaxial test.

c. The unconfined compression test.
The unconfined compression test is perform-

ed on samples without any side pressures. The horizontal pressure is supplied by a capillary pressure u_c on all sides. The sample is vertically loaded until it collapses. See fig. 2.3.6.35a. It can be seen that the location of the circle on the τ-axis is actually not definite as the value of $\tau_h = u_c$ is unknown. If the direction of α is known, it is possible to assess the angle of internal friction.

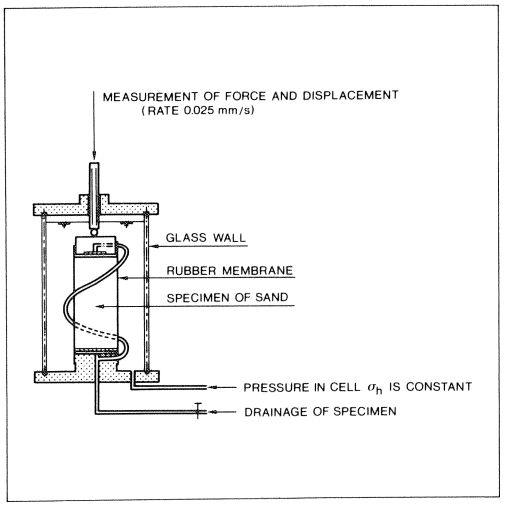

When performing an unconfined compression test on sand, the consolidated ϕ' is measured. When tests are performed on clay or peat the completely unconsolidated situation is measured: $\phi = 0$. The apparent cohesion c then amounts to $\tau 1$ see fig. 2.3.6.35b. The values for the friction properties, obtained from this test, can be used for preliminary calculations. The accuracy is limited as the pressure of the samples is generally not in accordance with the pressure situation of the terrain. An advantage of the unconfined compression test is that it can be performed rapidly and easily in the field.

d. Triaxial test
In a triaxial test the drainage of porewater can be blocked completely in order to measure the water pressures in the sample.

Figure 2.3.6.36a Principle of the triaxial test apparatus

Figure 2.3.6.36b Stress-strain diagram and critical stress circle in Mohr's diagram obtained in the triaxial test

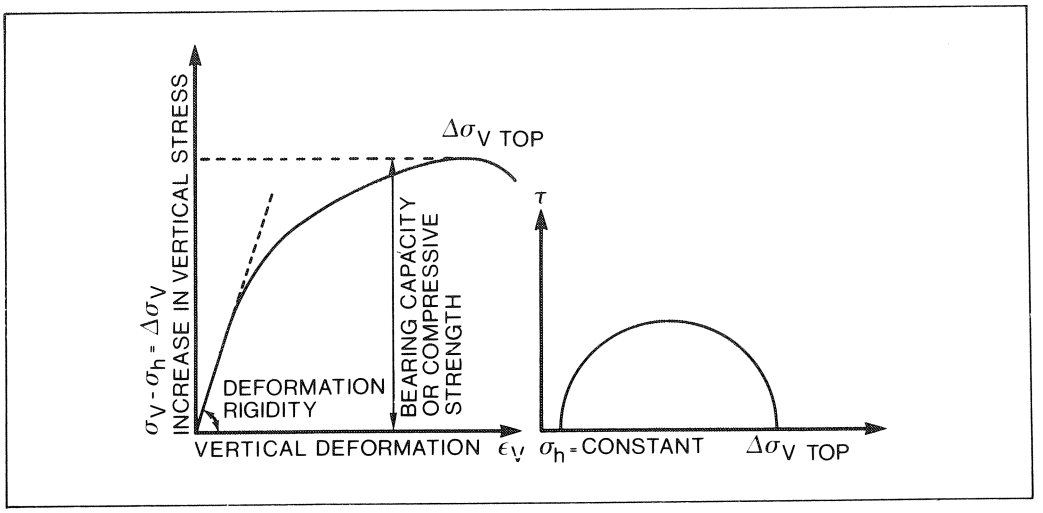

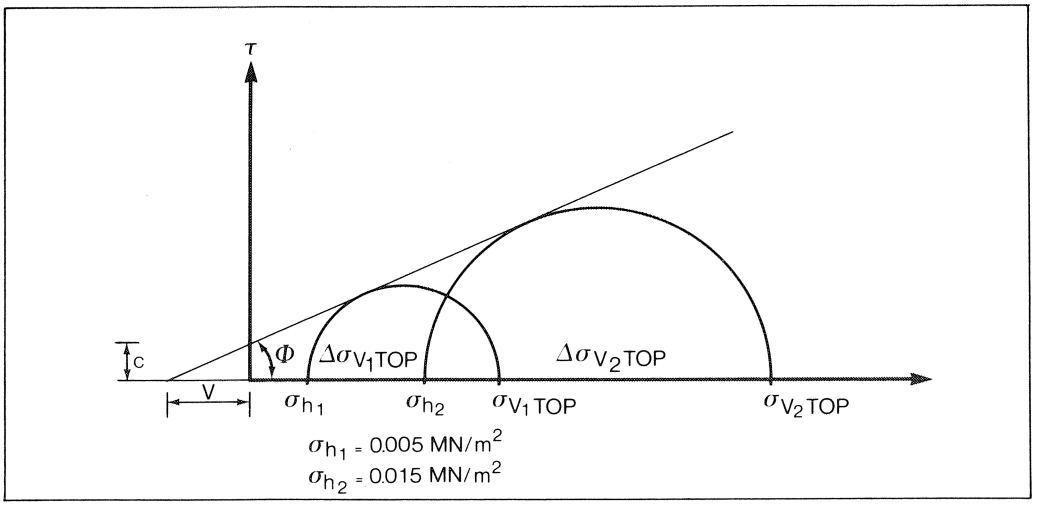

Figure 2.3.6.36c Determination of the angle of internal friction, and the cohesion from two triaxial tests

There are three different types:

- The drained test.
  Here the porewater can be discharged. The test is performed after the sample has been completely adjusted to the applied vertical load. This test takes a very long time.
- Unconsolidated test.
  In this test, the drainage of the porewater is blocked completely. As a result, excess water pressures will arise in the sample.
- The consolidated undrained test.
  The sample is consolidated according to the load. However, when the load is increased, the outflow of water is impeded as a result of which excess water pressures occur.

Figures 2.3.6.36a, b and c show a set-up of the triaxial test and its results in the form of a stress-strain diagram as well as the determination of ϕ and c when two tests have been performed.

3. Testing of rock

Although it is not the aim of this book to deal with rock mechanics, there are some remarks about the general approach regarding the assessment of the property of a rock sample.

Rock mechanics

One of the tasks in the discipline known as „rock mechanics" is to describe the tensions and deformations occuring in rock formations. Any attempt to make an accurate description makes one realise that this discipline is a tricky labyrinth of possibilities and difficulties. It is therefore advisable to make use as much as possible of the existing description methods: elements from the elasticity theory and soil mechanics are regularly applied. Conversely, the plasticity theory and rheology are as yet not generally used. In order to include the fracture mechanism of rock, views on the „cataclastic and clastic processes" are taken into consideration. As a first step, the manner of fracturing is determined by the „fracture and the fracture plane" analysis.

Subsequently, the structure is determined based on the fracture types and the degree of fracturing of the rock. Based on these factors, movements and displacement of rock formations can be analysed. Practical experience shows that, in this manner, a logical and satisfactory picture can be formed on complex situations. It can then be decided which theory is best suited to describe (approximatively) the problems (or its components) namely:

1. with elements from the „elasticity" theory
2. with the „fracture" theory, and the theory on „clastic and cataclastic deformations"
3. with elements from „soil mechanics".

Site Investigations and Data Acquisition

P.B.M. Stortelder, D.J. de Jong.

2.3.7 Research into environmental aspects

This chapter deals with the environmental research required for the various building stages of a hydraulic structure. Subsequently, the differing research strategies and, in brief, some of the research techniques are reviewed. Finally, some special points of interest regarding environmental research and the presentation of data are discussed.

2.3.7.1 Research phasing

The total execution of a hydraulic structure can be subdivided into three phases. These are:
- the planning phase;
- the design and construction phase;
- the operational and managerial phase.

In all three phases, environmental aspects play a role.

The planning phase

In the planning phase the preparation (of the execution) of the project is commenced. In this phase the environmental aspects have to be taken into account, together with the economic and social aspects, in order to help decide whether or not to continue with the plans and to assess the best means of realizing the project. At this stage, the environmental research is focussed on the prediction of the environmental consequences of the plan or of various alternative plans. The generation of plans that are more favourable for the environment can also form part of the research in this phase. In order to make the advantages and disadvantages of a plan as explicit as possible, it is recommended that the „zero option", i.e. the maintainance of the actual situation, also be included in the preparatory plans. In some countries it has become obligatory for an „environmental impact statement" to be drawn up, in which the possible repercussions of the proposed plans for the environment are analysed as an aid to decision-making. In the ideal situation, wide-ranging and detailed ecological research will be carried out to investigate the possible consequences of the proposed plan(s). However, such research, in which all possible environmental aspects (see par. 2.2.6. and fig. 2.2.6.1) and their mutual relations, as well as the functional uses of the system for man, are investigated, requires a very large staff and a great deal of money and will take many years.
In practice therefore decision-making is usually founded on the „best available knowledge", sometimes supplemented by more thorough subsidiary research concerning the more critical environmental repercussions. In addition to the data gathered in the area itself, experience gained with similar impacts in comparable areas can also be used in some cases.
Given the necessity to weigh the new plans against the „zero option", a thorough knowledge of the structure and the functioning of the prevailing system is essential. Such knowledge is moreover indispensable for making forecasts about the expected environmental impacts.

The design and construction phase

In the design and construction phase the emphasis is put on the environmental supervision of the works themselves, i.e. indicating and minimizing the negative consequences for the environment of the final design and its construction. Examples of the aspects that must be taken into consideration during this phase include:
- the trace and shape of the dams;
- the location and capacity of the discharge equipment:
- the choice of materials (with regard to the possibility of release of toxic substances);
- the selection of locations for temporary facilities such as working harbours and transport roads;
- noise pollution (e.g. with regard to breeding birds, fish);
- the selection of terrains for sand-excavation and dumping of dredged materials;
- the repercussions of possible animal and plant growth (i.e. mussels) for the stability and the design;
- calamities.

The environmental aspects being investigated in this second phase vary from project to project. It is impossible to issue general directives for this purpose.
In order to be able to indicate possible en-

vironmental problems at this stage, it is imperative that - experienced - environmental experts are kept up-to-date with any proposed building plans and activities. This requires close and continuous collaboration between the engineers involved with the design and construction and the environmental experts.
In addition the environmental research started in the first phase will continue during this phase, especially if insufficient time was available during the first stage.

The operational and managerial phase
In the operational and managerial phase, the environmental research focusses on the actual environmental consequences of the project. This will not only enable the forecasts to be tested but, even more importantly, will allow additional measures to be taken to counter unexpected, adverse developments so as to achieve optimal results - also environmentally - with the project. The environmental preparation for this phase, which must result in actual physical plans and management plans (see also 2.1 and 2.6) should be initiated as soon as the planning phase starts.
By means of environmental research during the actual construction it is possible, to reduce the remaining uncertainties in the prognoses made during the previous phases. The research in this third phase should not be confined to the ecosystem, but must also include the relations existing between the ecosystem, the functions the system offers to man and governmental policy.

2.3.7.2 Research strategies

Before an extensive environmental research project is started, the literature will be surveyed to investigate the questions:
- what information is available on the area in question?
- what information is available on similar areas elsewhere?
- has the proposed action been executed before and what were the consequences?

Thus a general idea can be obtained of what is already known, based on which a research plan can be drawn up for supplementary environmental research. A general ecological model will be an important aid for drawing up such a research plan. An example of the results of such a model is presented in figure 2.3.8.9. With the aid of such a model, it is possible to trace gaps in knowledge in certain fields so that, subsequently, the research can be focussed on these gaps. [18].

A number of differing strategies are available for the actual research, e.g. field studies, experimental studies and mathematical models.

Field studies concern observations made or measurements taken in the field either with or without laboratory back-up. Examples include measurements of temperature and water-quality, bird-counts, vegetation research and soil and geomorphological investigations. An advantage of this method is that it rapidly yields information on the system involved without actually causing any severe disturbance to it. The disadvantage of these field studies (especially inventorial studies) is that it is often difficult fully to comprehend the processes, as a result of which the information gathered with this research method is often inadequate for making forecasts of the consequences of particular actions.

Experiments are useful for investigating the specific consequences of a particular action. In principal, these can be divided into the following three categories:
- in a field experiment one element in the field will be changed temporarily, e.g. a temporary increase of the freshwater discharge in order to investigate the impact of a decrease in salinity on the organisms living on the bottom. Nature itself also sometimes offers the possibility of getting data about the effects of certain interventions, e.g. comparing the environmental consequences of an extremely dry or extremely wet year with the annual average and a severe winter with a moderate one.
- in a simulated experiment a natural system with all aspects relevant for the research, will be simulated on a small scale as accurately as possible. The advantage of this method is

that various systems can be set up simultaneously and that it is possible to measure the consequences of an action very directly (see also 2.3.8. for further information).

- in a laboratory experiment one specific process only is tested under highly controlled conditions specially created for this situation. Simulated and laboratory experiments

Figure 2.3.7.1. Principal research strategies and their costs and specialized equipment requirements.

strategy	costs of research set-up	additional cost per experiment	specialized equipment requirements
field study	high to low	high	measuring ship, analysis equipment, considerable manpower
field experiment	high to low	high	idem
simulated experiment	very high to limited	high	sampling and analysis equipment, and sometimes considerable manpower
laboratory-experiment	limited	low	accurate measurement and manipulation techniques
mathematical model	high	low	computer capacity, data with regard to calibration and verification

are, for example, very important for testing the consequences of discharges of toxic substances on organisms.
In addition to the above-mentioned research methods for gaining insight into the ecosystem and environmental impacts, via observations and measurements, mathematical models have become increasingly important. This model research will be discussed in more detail in 2.3.8.
Fig. 2.3.7.1 provides a comparative survey of the approximate costs of each of the above-mentioned methods. A distinction has been drawn between the initial costs required for setting-up the research and the additional cost of a supplementary experiment. In addition, some indications are given of the specific equipment required for each research method.

2.3.7.3 Research techniques

In recent decades a wide range of techniques has been developed for environmental research. These techniques can vary from very simple, inexpensive and easy-to-use apparatus to very advanced, expensive equipment requiring highly trained personnel.
On the one hand the choice of technique will be influenced by what measurements have to be taken and where and the degree of accuracy required, and on the other by the availability of funds, laboratory facilities and qualified personnel.

It is impossible to provide a brief, overall impression of all the available techniques and their applications. This section only describes the principal groups of techniques, with examples of their possible applications. References to the literature enable further information to be obtained on the available techniques for measuring specific components, organisms and processes in the ecosystem.

With regard to the techniques, a distiction can be made between remote-sensing techniques, techniques for executing direct measurements in the field, sampling techniques and laboratory techniques for specific physical, chemical and biological analysis and, finally, apparatus for data storage, analysis and presentation.

Remote-sensing techniques
Remote-sensing involves the application of aerial survey techniques for observing phenomena on the earth's surface. These techniques can be divided into:
- photographic techniques such as true-colour and false-colour photography, which are used specifically to make topographical, morphological and vegetational maps and to detect phenomena induced e.g. by disease or moisture deficiency;
- multi-spectral scanning (MSS), whereby the reflected solar beams in the visible part of the spectrum and the nearby infra-red can be registered. Two possible applications of this technique are the determination of the biomass quantity and vegetation mapping;
- infra-red line-scanning (IRLS), whereby a thermal-sensitive sensor records the surface of the earth line by line. This thermal picture furnishes information on sea-currents, the dispersal of cooling- and river-water, the shortage of moisture for crops, etc;
- radar, which can be used for various purposes including the examination of the geometry and the moisture content of the earth's surface. Radar can also be used to observe bird migration.

These examples show that remote-sensing techniques can be applied to various aspects of the environmental research whilst a great number of potential uses are being investigated. The use of remote-sensing techniques is particularly recommended for preliminary site exploration and/or when the study covers large and sometimes almost inaccessible areas. In most cases, however, field measurements will also be necessary, particularly if more detailed or more specific data are required.
A detailed manual on remote-sensing has been published by the American Society of Photogrammetry [10]. Verstappen [11] has described the applications in geomophology and Johnson [12] those in ecology.

Techniques used for direct measurements in the field
Numerous appliances and purpose-designed

measuring equipment are available for direct field measurements and observations. Some examples of aids used in biological research which are indispensable for visual observation when exploring and mapping terrains are binoculars and low-flying aircrafts for the counting of birds, diving equipment or diving bells for research into submarine flora and fauna and vessels with fishing equipment to study the behaviour of fish. A number of abiotic elements may also, or must, be measured in situ with purpose-designed equipment.
Some of the most important items of measuring equipment are:

- current velocity and direction gauges;
- wind velocity and direction gauges;
- the Secchi-disc for measuring the transparency of the water;
- photo-sensitive cells for measuring the radiance and penetration of light under water;
- thermometers;
- turbidity gauges;
- side-scan sonar for recording the profile and structure of the bed [19];
- various types of electrodes; these are sensitive sensors which, depending on the concentration to be measured, induce changes in the potential difference between the two poles of the electrode.
  Electrodes have been developed to measure among other things oxygen, pH, sulphide and conductivity. Salinity, chlorinity and chlorosity can be deduced from the combined result of the conductivity and temperature measurements. In addition, special salinometers can be bought on the open market.

Sampling equipment

The analysis of the measurements of a great number of environmental variables is so time-consuming and/or reguires such specialized equipment that this has to take place in laboratories. For this purpose, samples have to be gathered. Various types of appliances have been developed for taking standard samples. A survey of some of the water-sampling apparatus is given by Grasshoff [15].
For continious sampling of, for instance, a debouching river, automated sampling equipment can be used with which - if necessary in proportion to the discharge - sub-samples can be intermittently taken. Because there is a time difference between the moment of sampling and the moment of analysis, it is necessary for a standardized method to be used for conserving samples. Otherwise certain processes may occur which can greatly influence the variables to be measured, for instance, bottom organisms that die and decompose, a decrease in the oxygen concentration due to mineralization processes, and oxidation of such components as H_2S and NH_3.

In taking samples particular attention must be paid to the setting up of an efficient sampling scheme. To obtain the desired results on a statistically sound basis, this scheme must be attuned to the often large and rapid variations -both in time and space - in the various environmental variables. For further information on this subject, see Jeffers [3] and Green [4].

Laboratory techniques

These can be divided into manual and automated techniques and are applied to both water and soil research. Some of these techniques and their application are explained below:

- manual techniques:
  - destructions to dissolve fixed components so as to arrive at certain analyses;
  - sieve-analysis to determine the grain-distribution of the soil-sample;
  - fluorimetry to determine chlorophyl;
  - centrifugating to gather silt for further analysis;
  - filtration $< 50\mu$ and $> 50\mu$;
  - spectrophotometry;
  - atomic absorption to determine heavy metals;
  - polarography to determine heavy metals;
- automated techniques:
  - colorimetry (as part of an auto-analyser) for various nutrients
  - sedigraph, coulter-counter } to determine the distribution of particle-size;
  - chromatography to analyse pollution of micro-organic matter;

micro-organic matter;
- potentiometric titrations e.g. for chloride content;
- ion-selective electrodes e.g. for oxygen, conductivity and pH.

Fig. 2.3.7.2. shows a scheme for the analysis of a water sample in a laboratory.
Books relating to measurements in the field [1], biological studies [2, 5, 13], chemical and physical analysis of freshwater [5, 14] and seawater [13, 15] and soil/sediment analysis [16] are included in the literature.

Equipment used for data storage, analysis and presentation
In recent years, there has been enormous development in the equipment used for data storage, analysis and presentation. This development is still underway and at such a rate that it is of little or no use making any recommendations on the subject. One development might, however, be of interest. It appears that smaller equipment, such as micro-computers and desk-top computers, offers increasing possibilities for the storage of data by means of cassettes, floppy discs or disc-units, for greater calculation speed and for the presentation of data on monitors and by plotters. In this way, fairly extensive data-sets can be adequately analysed without having to invest in a „large" computer.

To conclude this section, an example is given in fig. 2.3.7.3. of an advanced measuring system in which these various elements have been included. The system consists of a measuring ship that is capable of performing continiously a large number of measurements such as oxygen content, temperature and conductivity.
These data are directly stored in a computer system on board and, if necessary, analysed. In addition, the ship is equipped with a more extensive system for taking samples of the water (at various depths) and the soil for further analysis in the laboratory. A centrifuge forms part of this sampling equipment. In a computer centre, the data are stored, analysed and presented in consultation with specialists. A special group of

Figure 2.3.7.2. Example of a scheme for the analysis of a water-sample.

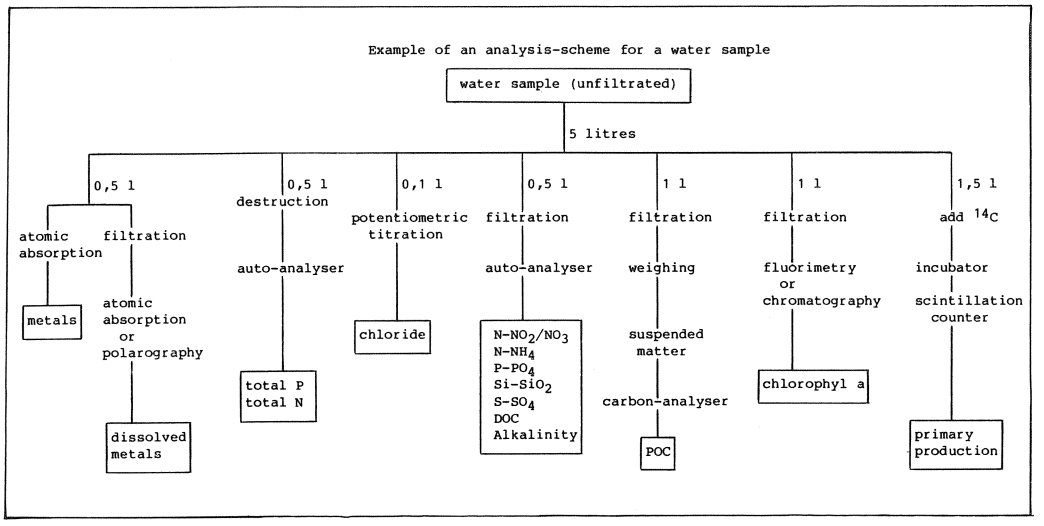

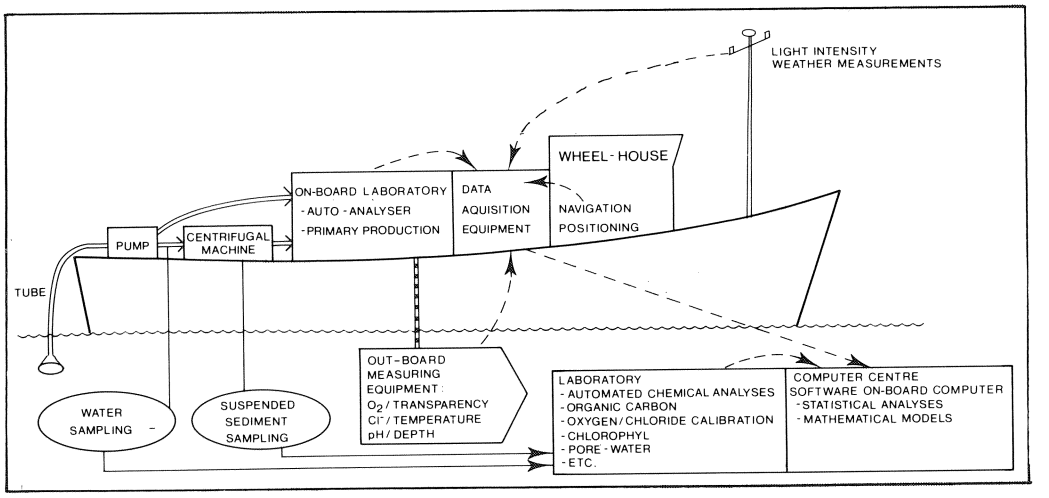

Figure 2.3.7.3. Scheme of a highly automated water-quality measuring system consisting of a ship with on-board equipment for water sampling, chemical analysis and data storage and comprehensive on-shore laboratory and computer facilities for data analysis.

Figure 2.3.7.4. Example of a computer-made graph. (isopletes of oxygen in Lake Grevelingen) (after de Vos et al, 1980 [7]).

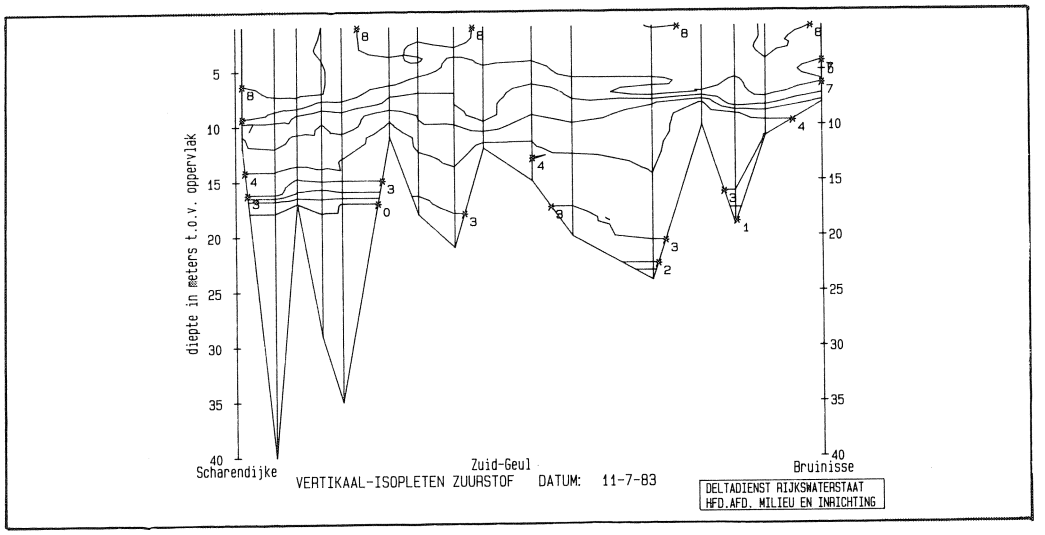

people looks after the maintenance of the measuring equipment. By using this automated system, part of the results can be presented immediately after measurements have been taken. (fig. 2.3.7.4.)

2.3.7.4 Some special points of attention

When carrying out environmental research, some important and more or less general phenomena must be taken into account.

- A primary point is that many processes show periodical fluctuations. The seasonal variation, with a periodicity of a year, is one of the most clear examples. In addition, there is the diurnal cycle (day-night) and, in the tidal areas, there is the tidal cycle. In addition, most organisms have a natural cycle with a periodicity of several years, i.e. the natural numerical variation. This variation can, in its turn be influenced by external factors such as climatic fluctuations (severe/mild winters, etc.)
- A second point is that the study into relations and processes requires integrated research in which many disciplines collaborate, including hydrologists, chemists, morphologists and biologists. This implies that many parameters must be jointly measured and analysed - often continuously - over a long period. This requires a sound research plan in terms of content and organisation.
- A third point is that various species of organisms (particularly animals) depend upon several areas for their life-cycle, e.g. migratory birds, fish, sea-mammals (see also fig. 2.3.7.5.) As a consequence, it is to a certain extent necessary to have some understanding of the relations between the area under research and the other areas. It is often very difficult and time-consuming to obtain sufficient insight into these relationships as the animals often have to be caught and marked and facts about their distribution can only be established after reported sightings (e.g. ringing of birds).

Figure 2.3.7.5. The main autumn migratory routes of arctic wader species; the map shows the relation between the breeding areas in the arctic region and the more southerly wintering areas (after Saeijs en Baptist, 1980 [17]).

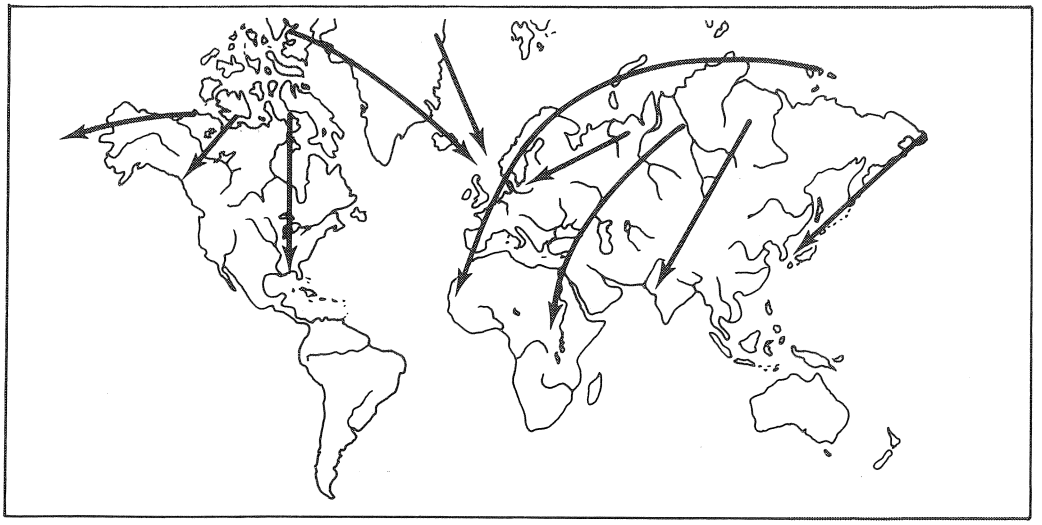

2.3.7.5 Presentation

In addition to the gathering and analysis of research data, the presentation of the results is of great importance.
This must be done in a manner comprehensible not only to specialists but also to non-specialists. Important aids in this respect are maps and graphs (fig. 2.3.7.6.), but a combination of maps and graphs is also possible (fig. 2.3.7.7.).
Apart from an objective presentation of the data, which requires the user to have a certain amount of background knowledge, it is also possible to present the information with some weighing of the various data. This is illustrated in fig. 2.3.7.8. with respect to „the species-count" and „variations in the salinity level" resulting from interventions in the environment.

Figure 2.3.7.6. Example of a graph (relationship between chlorinity and the species count of 7 groups of invertebrates in the S.W. part of the Netherlands, see also fig. 2.2.6.3.) (after Schmidt van Dorp 1979 [8]).

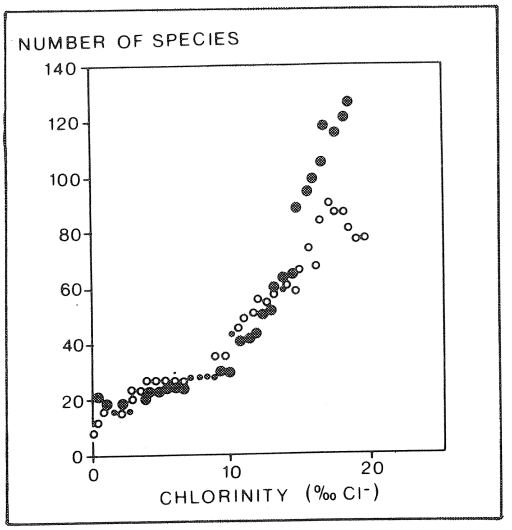

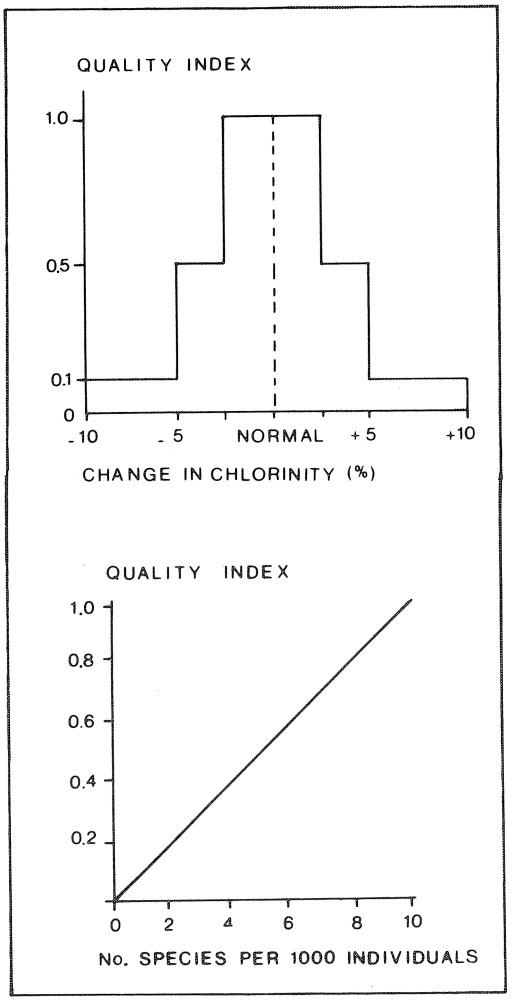

Figure 2.3.7.8. Examples of „quality-index" graphs (after Canter & Hill, 1979 [6]).

Figure 2.3.7.7. Example of a combination of a map and graphs (distribution of heavy metals coming from the rivers Rhine and Meuse in the Delta of the SW Netherlands, Rhine-contents are 100%) (after Anon, 1982 [9]).

The drawing-up of such „quality index" graphs requires a proper understanding of the significance of the parameter in question for the ecosystem as a whole and for the function in question.

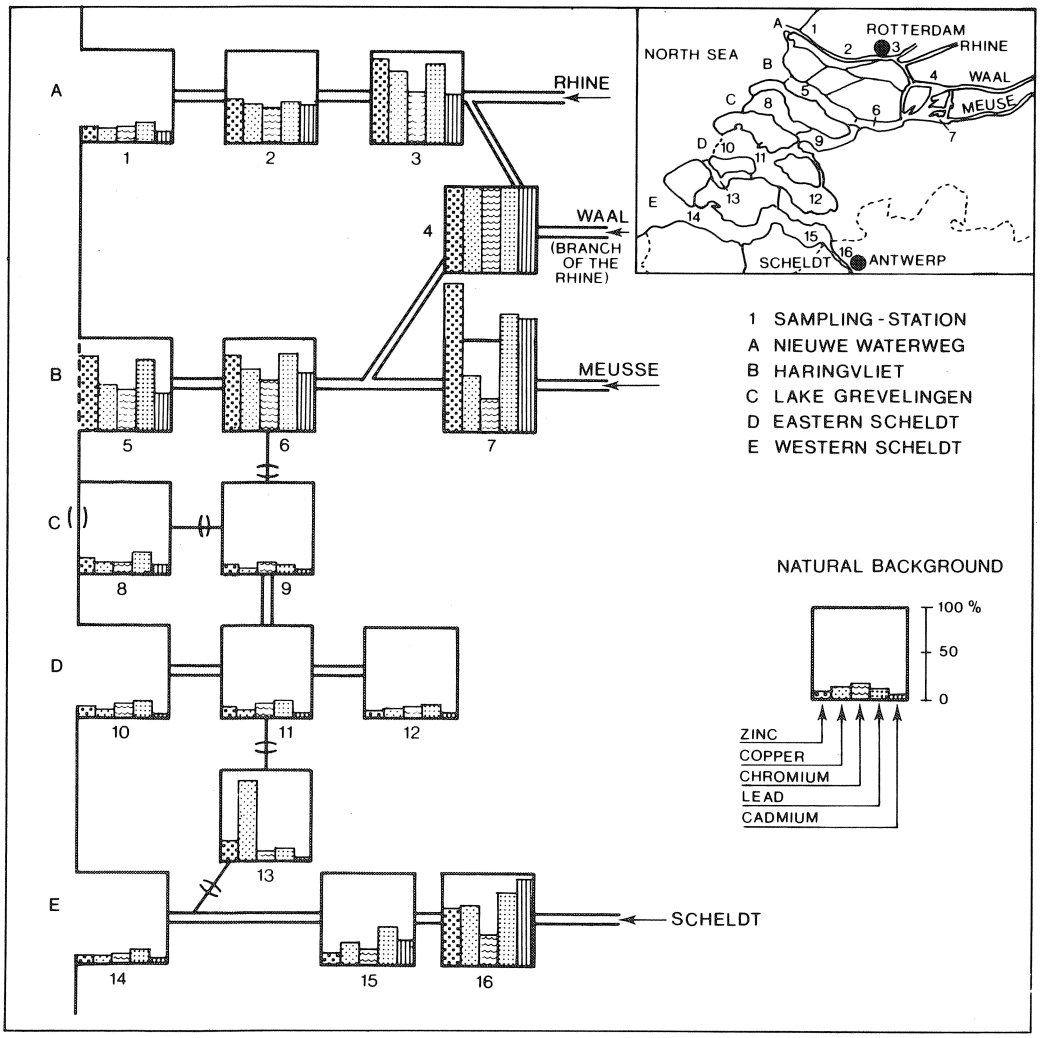

Literature

1. Dyer, K.R., ed., **Estuarine Hydrography and Sedimentation**, Syndics of the Cambridge University Press, Cambridge, 1979.

2. Schlieper, C., **Methoden der Meeresbiologischen Forschung**, VEB Gustav Fischer Verlag, Jena, 1968.

3. Jeffers, J.N.R., Sampling (Statistical Checklist 2), **Inst. of Terr. Ecology**, Merkwood Research Station, Grange-over-Sands, Cumbria, U.K.

4. Green, R.H., **Sampling Design and Statistical Methods for Environmental Biologists**, John Wiley & Sons, New York/Chichester/-Brisbane/Toronto, 1979.

5. I.B.P. Handbooks; Blackwell Sc. Publ. Oxford:

   - Vollenweider, R.A., ed. **A Manual on Methods for measuring Primary Production in Aquatic Environments.**, part 12, 1969.
   - Edmondson, W.T. & G.G. Winberg ed., **A Manual on Methods for the Assessment of Secondary Productivity in Fresh Waters** part 17, 1971.
   - Sorokin, Y.I. & H. Kadota eds. **Techniques for the Assessments of Microbial Production and Decomposition in Fresh Waters** part 23, 1972.
   - Golterman, H.L., R.S. Clymo & M.A.M. Ohnstad, **Methods for Physical and Chemical Analysis of Fresh Water** part 8, 1978.

6. Canter, L.W. & L.G. Hill, **Handbook of Variables for Environmental Impact Assessment**, Ann. Arbor Science, Michigan, 1979.

7. Vos, C.P. de, J.S.L. Vink, B.A. Bannink & J. Leentvaar, Water Quality Impacts Exchanging Water between Sea and a Closed Estuary, **Prog. Water Tech. Vol. 13**, pp 271-285, Pergamon Press Ltd., 1980.

8. Schmidt van Dorp, A.D., Literatuuronderzoek naar de soortenrijkdom van het makrozoöbenthos in relatie tot het zoutgehalte. (Research of Literature on Species-richness of Macro-zoobenthos in Relation to Salinity). Rapport 1979-5, **Delta Inst. v. Hydrob. Ond.** Yerseke, 1979 (in Dutch).

9. Anon., **Het Delta Boek,** Natuur & Techniek, Maastricht, 1982 (in Dutch).

10. Reeves, R.G. et al ed., **Manual of Remote Sensing Vol I + II,** American Society of Photogrammetry, Falls Church, Virginia, 1975.

11. Verstappen, H. Th., **Remote sensing in geomorphology**, Elsevier Amsterdam, 1977.

12. Johnson L.P. (ed), **Remote Sensing in Ecology**, 1969.

13. Strickland, J.D.H. & T.R. Parsons, **A practical Handbook of Seawater Analysis,** Fisheries Research Board of Canada, Ottawa, 1972.

14. Anon, Standard Methods for the **Examination of Water and Wastewater,** American Public Health Association, Washington, 1971.

15. Grasshoff, K., **Methods of Seawater Analysis**, Verlag Chemie Weinheim, New York, 1976.

16. Black, C.A. et al, ed., **Methods of Soil Analysis, Parts 1 and 2,** American Society of Agronomy Inc., Madison, USA, 1965.

17. Saeijs, H.L.F. & H.J.M. Baptist, Coastal engineering and European wintering wetland birds, **Biol. Cons. 17**, p63-83, 1980.

18. Bigelow, J.H., J.C. de Haven, C. Dzitzer, P. Eilers and J.C.H. Peeters, **Protecting an Estuary from Floods, A Policy Analysis of the Oosterschelde,** Vol. III, Assessment of long-run Ecological Balances, R 2121/3-

Neth. Rijkswaterstaat, The Hague/Rand, Santa Monica, 1977

19. Flemming, B.W., Side-Scan Sonar: a practical guide, **Intern. Hydrographic Rev.**, L III (1) Monaco, 1976.

P.B.M. Stortelder

2.3.8. Application of models in studies of ecosystems

2.3.8.1. Mathematical models

In the last 20 years, mathematical models have become much more important in the management of water bodies and studies of ecosystems. First, they provide a more systematic and quantitative description of initial relations and processes present in an ecosystem, thus enabling the structure as well as the behaviour of ecosystems to be understood better. Furthermore, changes due for example to pollution and overfishing may be analysed more rapidly and exactly.
A second reason, connected closely to the above, is the wish to predict consequences of natural and human interference in ecosystems, such as the effects of a reduction of wastewater discharges, closing estuaries, and impacts on water-quality by increasing the inlet flow in a lake.

2.3.8.2. Simple relation models

In general, models give a strongly simplified schematic description of only a part of very complex (eco)systems. In a highly simplified case, the relation between only two system variables is described, excluding all variations in place and time within the system itself.

Example 1. Relations concerning the algae biomass
Based on analysis in many lakes around the world, Vollenweider [14, 15, 16] and O.E.C.D. [29] have derived equations for the relation between the phosphate concentration in the inlet water, the phosphate concentration of the lake and the algae biomass (as chlorophyll-a, a pigmentation, used as weight for the algae biomass).

$$P_m = P_i \frac{1}{1+\sqrt{\tau}} \quad (1)$$

and

$$F = 0.37\ P_m^{0.79} \quad (2)$$

in which

P_m = phosphate concentration in the lake (g/m^3)
P_i = phosphate concentration in the inlet water (g/m^3)
τ = mean water residence time ($year^{-1}$)
F = chlorophyll-a concentration in the lake (mg/m^3)

Application of these models is restricted to completely mixed lakes, in which the phosphate loading does not fluctuate in time. Furthermore, suitable results are only obtained in the case of the limitation of algae biomass by phosphate concentration.
The equations have been tested and new relations have been formed [17, 18, 19]. In general, however, there is a loss of accuracy due to a high standard deviation in the analysis (fig. 2.3.8.1), meaning that the formation of unambigious equations for a large group of lakes is

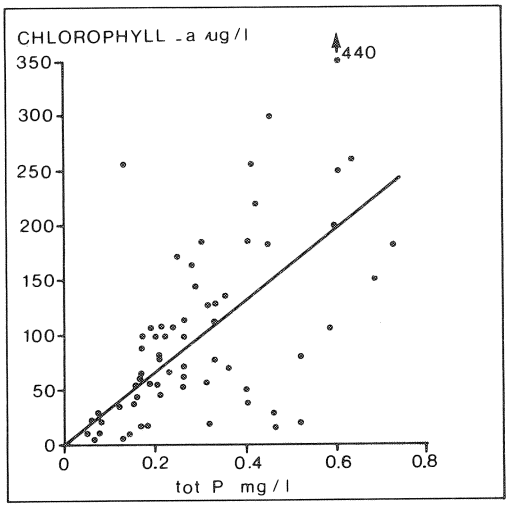

Figure 2.3.8.1. The calculated relation between chlorofyl-a and total phosphorus concentration based on the measured concentrations in some Dutch Lakes (correlation line y = 0,32 x + 2).

difficult. This may better be done for certain groups of lakes, for instance for lakes with certain equivalent characteristics.
The above-mentioned model was of major importance in analysing causes of excessive growth of algae. The model is still being used in a predictive way (e.g. on the effects of dephosphating waste-water).
Besides the concentration of phosphate, the biomass of algae is controlled by other factors such as the concentration of nitrogen and light. Studies on the prevention of excessive algae-growth in Dutch lakes [20] gave the following equations concerning the limitating factor for algae-growth:

$$\text{light} \quad : F = \frac{530}{H} - \frac{40.38}{S_o} \qquad (3),$$

$$F_{max} = \frac{985}{H} - \frac{94.71}{S_o}$$

$$\text{nitrogen} \quad : F = -89.6 + 89.6N \qquad (4),$$

$$F_{max} = -33.87 + 112.9N$$

$$\text{phosphorus} \quad : F = -15.53 + 776.32P \qquad (5),$$

$$F_{max} = 1206.9P$$

in which
F = average concentration chlorofyll-a (mg/m³)
F_{max} = maximum concentration chlorofyll-a (mg/m³)
H = depth (m)
S_0 = water-transparency by absence of algae (m)
N = average concentration of total nitrogen (g/m³)
P = average concentration of total phosphorus (g/m³)

After determination of H, S_0, N and P, the limiting factor is given by the lowest result in (3), (4) and (5).
For instance, if nitrogen is limitating, a further reduction of the nitrogen loading will immediately result in a decrease of algae biomass. In this case, reduction of the phosphorus load will only be effective if the limitating role of nitrogen is overtaken by phosphorus.

It is difficult to provide a common valid standard for the level of the chlorophyll-a concentration as it depends on the trophic characteristics of the lake. Oligotrophic lakes have a chlorophyll-a concentration of less than 1 mg/m³. A ten fold increase of the chlorophyll-a concentration as caused by an increase of the nutrient load may result in a remarkable change of the structure of the ecosystem. A chlorophyll-a concentration of more than 50-100 mg/m³ (which may be observed as the upper limit concentration for eutrophic lakes) may cause severe damage to the ecosystem, such as a decrease of species diversity, strong fluctuation in the oxygen concentration or even anaerobic conditions, and mortality of organisms. In the case of high algae biomasses the transparency is limited to a few decimetres, which makes a lake less attractive for recreational activities. High algae biomass also creates many problems for the preparation of drinking water.
The influence of the chlorophyll concentration on the transparency can be approximated by the following equation

$$\frac{1.9}{S} = \frac{1.9}{S_0} + 0.016\,F \qquad (6)$$

in which
S = transparency (m)
F = chlorophyll-a concentration (mg/m³)

Example 2. Some relations in estuaries
Going from salt to fresh in an estuary, the changes in water-quality may first be analysed in a relatively simple way by plotting the concentration of any water-quality component against the chlorosity of the water.
In figure 2.3.8.2 point A represents the concentration of component C in freshwater; the concentration in saltwater is given by point B. A straight line of the measured concentration of C between A and B indicates that the water-quality in terms of C can explained by dilution of the saltwater by freshwater.
The addition (e.g. by discharge) or removal of the component (e.g. by sedimentation) results in deviation from the straight line (the points lying

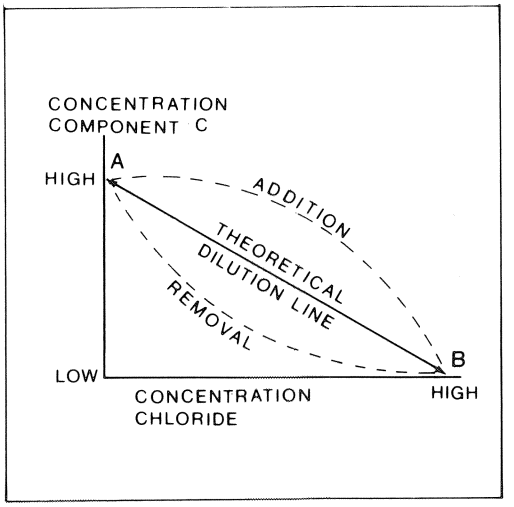

Figure 2.3.8.2. Idealized representation of the relationship between the concentration of a dissolved component and the chloride concentration for an estuary with single sources of river- and sea-water and in the case that the concentration of component C in river-water is higher than in sea-water.

above or under the straight line respectively). If processes of addition and removal take place at the same time the interpretation of the results becomes more complicated. For example, if addition and removal are of the same magnitude, a straight line will be the result of this method, as in the case of pure dilution [2].
The same method is used to analyse the quality of the sediment, by plotting the concentration of C against the percentage of sea silt in the sediment (instead of the chlorosity of the water). This percentage can be measured by using the natural differences in composition of sea and river silt as traced by differences in mineralogy and chemical and/or isotope-geochemical composition. A positive deviation from a straight line indicates accumulation processes (adsorption/precipitation). A negative deviation is caused by removal processes.
Examples for the concentrations of cadmium, chromium and phosphorus (relative to aluminium) in the sediment of the river Scheldt are illustrated in fig. 2.3.8.3.

2.3.8.3. Mass balance calculations

In modelling an ecosystem, use is often made of mass balance calculations. For a bounded compartment in a system, the basic mass balance equation for any component is:

$$\text{Accumulation} = \text{mass inflowing} - \text{mass outflowing} \pm \text{source/sink}. \quad (7)$$

The accumulation term describes the change of the total mass of a component in a fixed time period and compartment. Instead of accumulation, a component can be removed. In principle, such an equation can be derived for any component (e.g. phosphorus, alsgae or fish). The in-and outflowing mass concerns for instance loading by rivers and discharges by rain, polders, industry etc. The source/sink term represents all processes in the system causing changes in the contents of any component other than by in- and outflow. Some examples include accumulation, nutrient uptake by algae and consumption of shellfish by fish.

2.3.8.4. Mixing models

To be applicable, these mass balances need a definition of the system size. At its simplest the mass balance covers the complete system. In this case only scant attention is given to the mixing in the system. With respect to such mixing, there are big differences between a lake, a river and an estuary. In the next examples three rather simple models for describing the mixing process as well as an application of the mass balance equation are given.

Example 3. Ideal-mixed model
An ideal-mixed system is characterized by the absence of concentration gradients in place. This means that the concentrations are con-

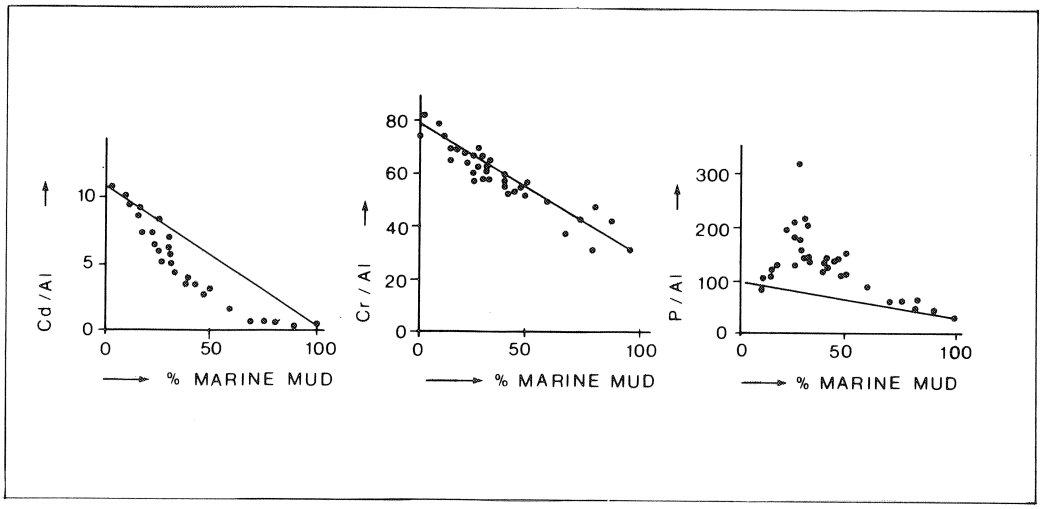

Figure 2.3.8.3. The measured cadmium, chromium and phosphorus concentration relative to the aluminium concentration of the sediment of the Scheldt estuary related to the percent of marine mud of the sediment, and compared with the theoretical conservative mixing of river- and marine-sediment.

sidered to be equal throughout the system (fig. 2.3.8.4). The concentration of the outflowing water is therefore the same as the in-lake concentration. The mass balances for an ideal-mixed system are:

$$\text{component C: } \frac{d(VC)}{dt} = Q_i(t)C_i(t) - Q_u(t)C(t) \pm \text{source/sink} \quad (8)$$

$$\text{water : } \frac{dV}{dt} = Q_i(t) - Q_u(t) \quad (9)$$

in which
V = volume ideal mixed reservoir (m^3)
Q_i = inflowing volume (m^3/s)
Q_u = outflowing volume (m^3/s)
C_i = concentration in inlet water (kg/m^3)
C = concentration in reservoir (kg/m^3)

The source/sink term represents all processes in the system which can affect the concentration of component C. These processes can be included in the mass balance equation by a separate term. However, each process requires a specific description. A „first order decrease" model is often used. In this model, the decrease of the concentration of the component is directly proportional to the concentration of the component. The equation is completed with the term KCV in which K is the reaction's rate constant. An example of such an approach is the decrease in the concentration of organic matter due to consumption by bacteria.
In order to obtain a quick impression of a problem, the so-called steady-state is often first used in model investigations. This state suggests that there is no change in process rates and inlet, meaning that:

$$\frac{d(VC)}{dt} = 0 \text{ and } \frac{d(V)}{dt} = 0 \quad (10)$$

giving the next mass balance equations:

$$0 = Q_i C_i - Q_u C - KCV \quad (11)$$

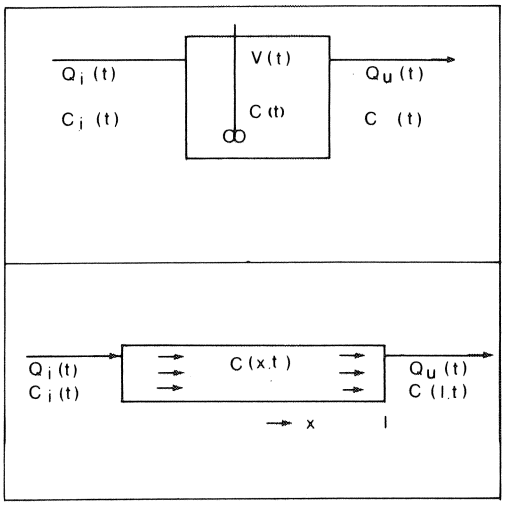

Figure 2.3.8.4. Model of a ideal mixed reactor (for explication: see text).

Figure 2.3.8.5. Model of a plug flow reactor (for explication: see text).

$$Q_u = Q_i \quad (12)$$

If Q_i, K and C_i are known, it is simple to compute the concentration in the mixed system:

$$C = \frac{Q_i C_i}{Q_i + KV} = \frac{C_i}{1+K\tau} \quad (13)$$

in which τ is the mean residence time (time^{-1}). The equation shows a decreasing concentration when τ increases.
If C, $C_i$and τ are known from measurements, K can be calculated. Ideal-mixed models are applicable to lakes which are well mixed by wind. A number of lakes linked by canals can be regarded as a scheme of more ideal-mixed reservoirs. Deep lakes are often not ideal-mixed. In the case of vertical gradients in concentration, the lake is „stratified". When a stratification consists of two layers (upper and lower layer) it might be possible to consider these layers as ideal-mixed, but the exchange of water and material between both layers must then be estimated.

Example 4. Plug-flow model
A plug-flow model is characterized by the presence of a gradient in the x-direction only and the absence of back-mixing (fig. 2.3.8.5.). By a constant cross-section area, the mass balance equations are:

$$\text{Component C: } \frac{dC}{dt} = -\frac{1}{A}\frac{d(QC)}{dx} \pm \text{source/sink} \quad (14)$$

$$\text{water: } Q_i(t) = Q_u(t) \quad (15)$$

in which
A = cross-section area (m²)
x = distance (m)

Under steady-state conditions with a first order decrease of component C the equation is

$$0 = \frac{Q}{A}\frac{dC}{dx} - KC \quad (16)$$

giving the solution:

$$C(x) = C_i \exp\left[-\frac{KA}{Q}x\right] \quad (17)$$

Rivers and canals may be described as plug-flow systems, assuming a one-dimensional flow in the x-direction and gradients in the x-direction only. The latter needs instantaneous mixing of a discharge in the cross-section.

Example 5. Advection-dispersion models
Most systems are often better described by an intermediate form of the above mixing models. In chemical process engineering non-ideal mixed systems are described by a cascade and/or parallel connection of ideal-mixed systems, or by a plug-flow with axial dispersion.

The mass balance equations for a plug-flow system with axial dispersion are:

$$\text{component C: } \frac{\partial (AC)}{\partial t} = - \frac{\partial (QC)}{\partial x} + \frac{\partial}{\partial x} \left(AD \frac{\partial C}{\partial x}\right) \pm \text{source/sink} \qquad (18)$$

in which D = dispersion-coefficient
The steady-state equation assuming first order decreases in concentration and place independency for A, Q and D is:

$$0 = - Q \frac{\partial C}{\partial x} + AD \frac{\partial^2 C}{\partial x^2} - KC \qquad (19)$$

The solution of this equation is

$$C(x) = C_0 \exp [\lambda_1 x] \text{ for } x < 0$$

$$C(x) = C_0 \exp [\lambda_2 x] \text{ for } x > 0$$

with

$$\lambda_{1,2} = \left(1 \pm \sqrt{1 + 4 \frac{KA^2D}{Q^2}}\right) \frac{Q}{2AD} \qquad (20)$$

and

$$C_0 = \frac{M}{Q\sqrt{1 + 4 \frac{KA^2D}{Q^2}}} \qquad (21)$$

in which
C_o = concentration at x = o
M = discharged amount of component C at x = o
Q = water discharge at x = o.

This solution in illustrated in fig. 2.3.8.6 for different values of D, Q and K.
An analytical solution of the advection-dispersion equation is only possible in a few cases; a numerical solution method is often required.
The one-dimensional advection-dispersion equation is applicable specially to vertically mixed estuaries and for rivers and canals with a low water flow and/or strong back-mixing.
In applying these models, special attention has to be given to determining the value of the dispersion-coefficient. This can be done by measuring the gradient in the concentration of a component with a conservative behaviour (i.e. a compound which is not subject to different processes, but is transported only) such as chloride. Solving the advection-dispersion equation for a conservative component, the source/sink terms are eliminated by definition. After a prototype measurement of the distribution of the concentration by a known in and outflow, the dispersion-coefficient is the only unknown factor.

CURVE	D (km^2/d)	Q (km^3/d)	K (d^{-1})
A	10	10^2	0.1
B	5	2×10^2	0.1
C	2	5×10^2	0.1

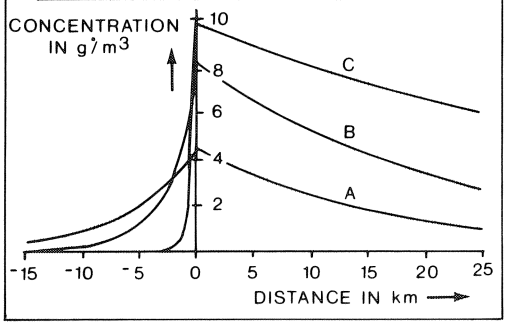

Figure 2.3.8.6. Calculated concentration distribution in a river or estuary in the case of a continuous discharge of water (Q) at point 0 and with a concentration of 10 g/m³ for different dispersion coëfficients (D) and a decay rate (K) of the component of 0.1 d^{-1}.

2.3.8.5. Coupled models

Example 7. Algae/BOD/oxygen/phosphate model
A strongly simplified model, with four equations is given in fig. 2.3.8.7.
The parameters in this model are algae species,

		growth	death	BOD-decay	reaeration	reaction
algae	$\frac{dA}{dt} =$	$+ k_1 F_n A$	$-k_2 A$			
BOD	$\frac{dL}{dt} =$		$+Y_1 k_2 A$	$-k_3 L$		
oxygen	$\frac{dC}{dt} =$	$+Y_2 k_1 F_n A$	$-Y_3 k_2 A$	$-k_3 L$	$+k_4 (C_s - C)$	
phosphorus	$\frac{dP}{dt} =$	$-Y_4 k_1 F_n A$	$+Y_5 k_2 A$			$-k_5 P$

k : rate coefficients
Y : conversion factors
F_n: $F.P/(P_k + P)$
F : light factor
P_k: Michaelis-Menten factor for phosphorus
C_s: dissolved oxygen saturation concentration

Figure 2.3.8.7. Simplified model equations (after van Straten, 1979 [1]).

BOD (Biological Oxygen Demand, a measure for the amount of decayable organic matter) and the oxygen and phosphate concentration. These equations also give the mutual relations. For instance, the change in oxygen concentration, does not only depend on the actual oxygen concentration due to the reaeration process but is influenced also by the BOD concentration, via the BOD decay process by which oxygen is consumed, and by the concentration of algae, as growing algae produce oxygen while dead algae consume it as they decay.
Although the illustrated model is still rather simple, its application requires the knowledge of five rate coefficients and five conversion factors. This is one of the biggest problems in applying reliable ecological models. Besides the wide range of the values given in the literature, these coefficients and conversion factors are not constant but appear to be dependent on for example temperature or the kind of algae species.

Example 8. Algae/zooplankton models
A general equation for algae-growth, discriminating for natural death and for decay by consumption by other organisms (grazing) is given as follows

$$\frac{dF}{dt} = (\mu - s - g)\ F \qquad (22)$$

in which
F = algae biomass (mg chlorofyll/m³)
μ = growth rate (s^{-1})
s = natural death rate (s^{-1})
g = grazing rate (s^{-1})
For zooplankton the following equation can be derived

$$\frac{dZ}{dT} = agFZ - d_z Z \qquad (23)$$

in which
Z = concentration of zooplankton (mg/m³)
d_z = death rate of zooplankton (s^{-1})
a = efficiency factor
The rate coefficients in the equation may be considered as constants in rough approximations. However, for applications which need more accurate results, the variability of these coefficients has to be taken into account. The growth rate of algae can for example be described by the following equation:

$$\mu = \mu_{max}(T)\,G(I)\,F\ (\text{nutrients}) \qquad (24)$$

in which
$\mu_{max}(T)$ = maximum growth rate (temperature dependent)
G(I) = light reduction function.
F(nutrients) = nutrients reduction function.

Descriptions of G(I) and F(nutrients) are provided in various references, for instance by Golterman [27].

In practice, a good description of algae/zooplankton relations can hardly be given, on account of the dynamic character of the ecosystem and the numerous initial relations and reverse connections. To illustrate the dynamic character of the system, the algae and zooplankton concentrations measured during a year in an experimental reservoir have been drawn in figure 2.3.8.8. This shows that an increase of the algae biomass is not always followed by an increase of the zooplankton biomass as might be expected on the basis of the higher amount of available food. For instance, it appears that the

Figure 2.3.8.8. Seasonal variations in the total concentration and dominant species of phytoplankton and zooplankton in an experimental reservoir.

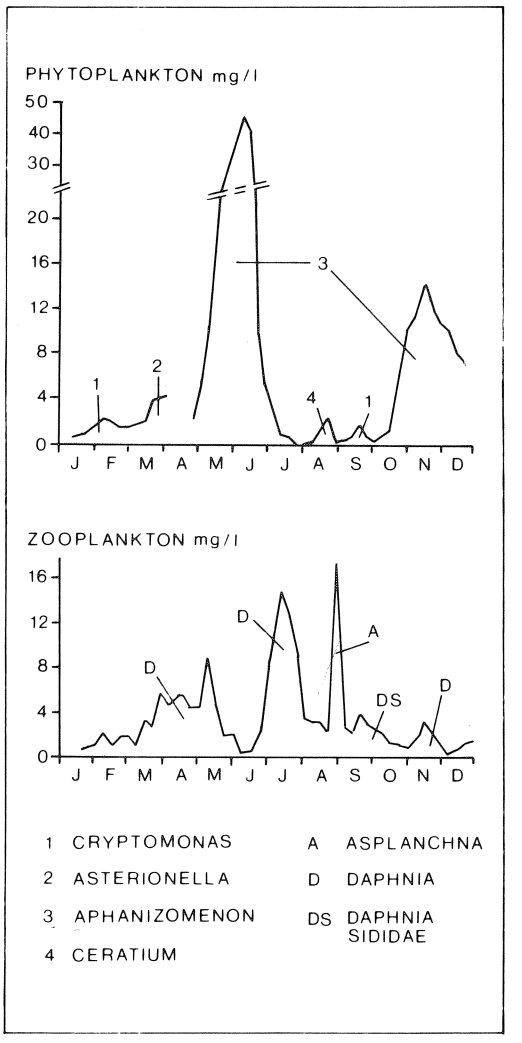

algae Aphanizomenon is hardly consumed by zooplankton.
This makes it necessary to develop a more detailed model, for instance by discriminating between different algae species.

2.3.8.6. Ecosystem models

In the above examples only part of the ecosystem has been modelled. The complete complex food web in an ecosystem includes not only algae and/or zooplankton, but also shellfish, birds and fishes. Attempts have, however, been made to develop general ecosystem models, including all groups of living species and mass flows. Bigelow et al [16] have developed an ecosystem model, in which equilibrium circumstances have been calculated. First results are illustrated in fig. 2.3.8.9. However, the model has not yet been calibrated and verified sufficiently. Park [22] has developed a dynamic model, named Cleaner. Di Toro et al [23], Bierman [24], Kremer and Nixon [25] and Canale [26] also developed ecological models. However, the development of general ecological models is still in the initial phase, in which much attention still has to be paid to the description of the system and calibration and verification of the models. In calibrating these models, scale models may play an important role. These are discussed at the end of this chapter.
On account of the large number of components and process rates playing a role in models, the calibration and verification of the models may take a very long time. Models, capable of general application are not to be expected in the near future. Compared with the development of hydraulic models, the development of ecological models has only just begun. For the time being specific problems may be solved by using submodels. The development of such submodels, concerning for example phytoplankton, zooplankton, macro-zoobenthos, eelgrass and predator-prey relations is being actively undertaken.

2.3.8.7. Relation between hydraulic and ecological models

The relation between hydraulic models on the one side and water-quality and ecological models on the other is nearly always unidirected. An ecosystem variable is influenced by current, amounts of water and water level but generally does not influence these hydraulic parameters. One of the very few examples of the latter is the presence of density currents due to gradients in chloride concentration or temperature. Except in the case of density gradients, water velocity equations can be solved independently of the equations for conservation of material. For this reason, calculations in an ecological model may be limited to the equation for conservation of water and of the ecological parameters considered, while the solutions of the water velocity equations are used as input. Developing these models, it is often not necessary to know the complete three-dimensional flow pattern. A simple description of mixing, as mentioned in the examples above, will often be sufficient for an ecological model. If a more exact description of a system is needed, it may be necessary to verify the ecological model in a two or three-dimensional hydraulic model. However, further detailing of the ecological model in this direction has to be balanced against other possible improvements of the ecological model, for instance of the rate coefficients and conversion factors.
Several two and three-dimensional ecological models are being developed at the present time. Jörgenson [11] has presented an overview of a large number of ecological models and their characteristics either available or in the process of development.

2.3.8.8. Scale models

Scale models are used to represent parts of the natural system on a smaller scale. Examples are the hydraulic tide model for the Rhine delta and models for isolated reservoirs for experiments in an ecosystem.
Much insight into a system can be obtained by measuring during manipulation of the boundary conditions of a system. In hydraulic modelling, it is possible to do many experiments in a short time. In ecological modelling this causes problems, because of the long time scale of the processes. For this reason, a number of parallel ex-

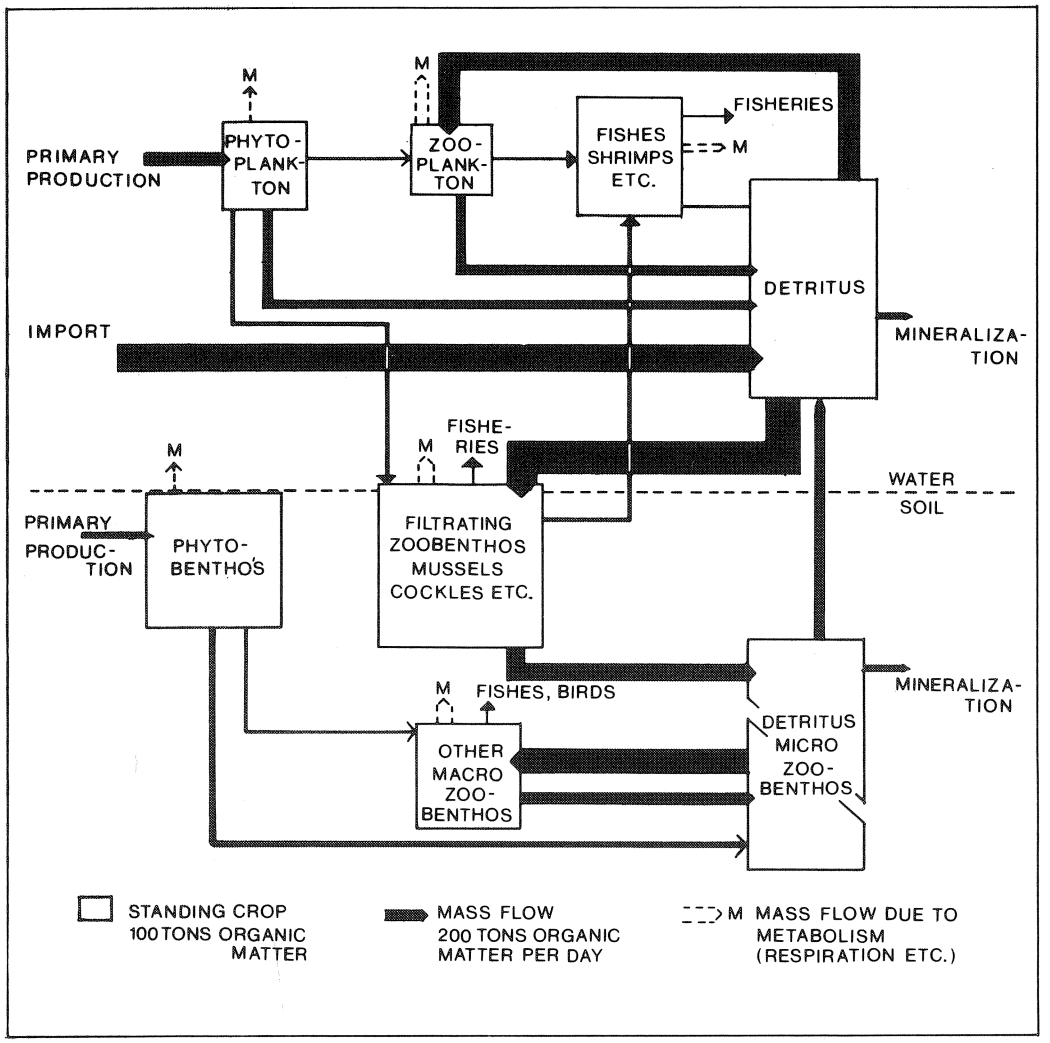

Figure 2.3.8.9. Scheme of an ecosystem model, showing the major components and energy flows (based on Bigelow et al, 1977 [21]).

periments are carried out (cf. experimental fields for agriculturel purposes). The use of scale models often requires large-scale investment in money and manpower, while the results will be obtained relatively slowly. Besides this, one has to consider the possibility of scale effects, for instance the growth of mussels against the wall of an experimental reservoir.

Although scale models have specific benefits

(e.g. possibilities for three-dimensional analysis, controlled circumstances, easily measurable responses compared with natural-measurement, parameter estimation) the development of mathematical models has progressed remarkably in recent decades, partly due to the increased availability of fast computers. Once developed, these mathematical mdels have the advantage of being able to carry out a large numer of model experiments rapidly and inexpensively. However, the necessary analysis for sound calibration and verification often demands a long measurement campaign. Scale models are very useful in this respect in addition to field measurements and small experiments in laboratories.

2.3.8.9. Literature

The elementary principles of the above mixing-models are described in [4]. Introductions to the application of water-quality models for lakes, rivers, estuaries and seas may be found in [5, 6, 7, 8 and 9]. A recent 'state of the art' for river models has been published in [10] and for lakes in [12]. Chammuneau et al, cited by Jörgenson [11] have made overviews of ecological models in the process of development, classified according to the number of components considered and the physical representation of the system. Jörgenson et al [13] have published a „Handbook of Environmental Data and Ecological Parameters".

1. Straten, G. van, Hydrological Aspects of Oxygen Behaviour and Algae-blooms in River Systems. In: **the Relation between Water- quantity and Water-quality in Studies of Surface Waters,** Proceeding of Technical meeting 35, Versl. Meded. Comm. Hydrol. Onderz. TNO 25. The Hague, 1979.

2. Liss, P.S. Conservative and Non-conservative Behaviour of Dissolved Constituents during Estuarine Mixing. In: **Estuarine Chemistry**, J.D. Burton & P.S. Liss, ed. Academic Press, London, 1976.

3. Salomons, W., Impact of Civil Engineering on the Pathways of Heavy Metals from Rivers to the Southern North Sea. Proceeding of the International Conference **Heavy Metals in the Environment**, Amsterdam,Sept., 1981.

4. Levenspiel, O., **Chemical Reaction Engineering**, Second Edition. John Wiley & Sons Inc., New York, 1962.

5. Thomann, R.V., **System Analysis and Water Quality Management.** McGraw-Hill Book Company, New York, 1972.

6. McDowell, D.M. & B.A. O'Connor, **Hydraulic Behaviour of Estuaries**, Civil Engineering Hydraulics Series, The MacMillan Press Ltd, London 1977.

7. Lyklema, L., Theoretical Aspects of the Relation between Water-quantity and Water-quality Aspects of Surface Waters, In: **The Relation between Water-quantity and Water-quality in Studies of Surface Waters**, Proceeding of Technical Meeting 35, Versl. Meded. Comm. Hydrol. Onderz. TNO 25, The Hague, 1979.

8. James, A. ed., **Mathematical Models in Water Pollution Control**, John Whiley & Sons Inc., New York, 1978.

9. Goldberg, E.D., I.N. McCave, J.J. O'Brien & J.H. Steele, eds., The Sea Volume 6: **Marine Modelling**, John Wiley & Sons Inc., New York, 1977.

10. Hahn, H.H. & B. Eppler, Models of Rivers, In: **State of the Art in Ecological Modelling**, S.E. Jörgenson ed., Pergamon Press Ltd., Oxford, 1979.

11. Jörgenson, S.E., State of the Art of Ecological Modelling of Lakes, paper presented at the **International Symposium on Modelling the Water Quality of Hydrological Cycle**. Baden 11th - 15th Sep. 1978.

12. Jörgenson, S.E., State of the Art of

Eutrophication Models, In: **State of the Art in Ecological Modelling**, S.E. Jörgenson, ed., Pergamon Press Ltd., Oxford, 1979.

13. Jörgenson, S.E., **Handbook of Environmental Data and Ecological Parameters**, ISEM, Copenhagen, 1979.

14. Vollenweider, R.A., **Scientific Fundamentals of the Eutrophication of Lakes and Flowing Waters, with Particular Reference to Phosphorus and Nitrogen as Factors in Eutrophication**, O.E.C.D., Paris, 1971.

15. Vollenweider, R.A.,Advances in Defining Critical Loading Levels for Phosphorus in the Lake Eutrophication, **Mem. Ist. Ital. Idrobiol**. 33, 53 - 83, 1976.

16. Vollenweider, R.A., The Concept of Nutrient Load as a Basis for the Internal Control of the Eutrophication Process in Lakes and Reservoirs, **Zeitschrift für Wasser- und Abwasser-Forschung 12 (2)**: 46 - 55, 1979.

17. Dillon, P.J., A Critical Review of Vollenweider's nutrient Budget Model and other Related Models, **Water Resources Bull. 10**, 969 - 989, 1974.

18. Larsen, D.P. and H.T. Mercier, Phosphorus Retention Capacity of Lakes, **J. Fish. Res. Board Can. 33**, 1742 - 1750, 1976.

19. Jones, J.R. and R.W. Bachmann, Prediction of Phosphorus and Chlorophyll Levels in Lakes, **J. Water Poll. Contr. Fed. 48**, 2176 -2182, 1976.

20. Coördinatiecommissie Uitvoering Wet Verontreiniging Oppervlaktewateren, Werkgroep VI, **Ontwikkeling van grenswaarden voor doorzicht, chlorophyl, fosfaat en stikstof. (Development of Limits for Transparency, Chlorophyll, Phosphate en Nitrogen).** Rijksinstituut voor Zuivering van Afvalwater. Lelystad 1980 (in Dutch).

21. Bigelow, J.H., J.C. de Haven, C. Dzitzer, P. Eilers and J.C.H. Peeters, **Protecting an Estuary from Floods, A Policy Analysis of the Oosterschelde.** Vol. III, Assessment of long-run Ecological Balances. R 2121/3-Neth. Rijkswaterstaat, The Hague/Rand, Santa Monica, 1977.

22. Park, R.A., **A Model for Simulating Lake Ecosystems**, Rep. No. 3 Center for Ecological Modelling, Rensselaer Polytechnic Inst. New York, 1978.

23. Di Toro, D.M., R.V. Thomann, D.J. O'Connor and J.L. Mancini. Estuarine Phytoplankton Biomass Models - Verification Analysis and Preliminary Application, **The Sea Vol. VI, Marine Modelling**, E.D. Golfberg et al. ed. Wiley - Interscience. New York, 1977.

24. Bierman, V.J., Mathematical Model of the Selective Enhancement of Blue-Green Algae by Nutrient Enrichment, **Modelling Biochemical Processes in Aquatic Ecosystems**, R.P. Canale, ed. Ann. Arbor Science Publishers Inc., Michigan, 1976.

25. Kremer, J.N. and S.W. Nixon, **A Coastal Marine Ecosystem**,Springer Verlag, Berlin, 1978.

26. Canale, R.P., L.M. De Palma and A.H. Vogel, A Plankton-Based Food Web Model for Lake Michigan. In: **Modelling Biochemical Processes in Aquatic Ecosystems**, R.P. Canale, ed. Ann. Arbor Science Publishers Inc., Michigan, 1976.

27. Golterman, H.L.,Physiological Limnology, **Developments in Water Science 2**, Elsevier Scientific Publishing Company, Amsterdam, 1975.

28. Bannink, B.A., J.H.M. van der Meulen, J.C.H. Peeters and J.C. van der Vlugt, Hydrological Consequences of the Addition of Phosphate Precipitants to Inlet Water of Lakes, **Hydrobiological Bulletin Vol. 14**, 1/2, p. 73 - 89 (1980).

29. Eutrophication of Waters, **Final Report O.E.C.D.**, Paris, 1982.

2.4. Interaction Watermotion and Closing Elements

The realization of structures under review introduces a change in natural conditions. This in turn brings about an impact on the structure itself: a load on the structure or in general on the system.
In this section a number of subjects is dealt with, with emphasis on phenomena adjacent to the closure site.
In general a distriction is made between the load on the structure exerted by the environment and the strength. The combination of both gives an indication of safety or probability of failure of the structure, structural elements or system.

Interaction Water Motion and Closing Elements

J. Stuip

2.4.1 Flow-induced loads

1. Introduction

Generally, forces exerted on a structure induced by a stream coursing past this structure can have a component normal to and in the direction of the flow. These forces can either be steady or fluctuating depending on the shape of the structure, the Reynolds number and the turbulent character of the flow. The forces are induced by friction in the boundary layer along and pressure gradients over the structure.

Where circular cylinders such as bridge piers, pylons and also ropes, pipelines etc. are present the flow will pass on both sides and thus the flow pattern will by symmetrical and, consequently, the pressure distribution around it. In this case there is only a component in the direction of the flow (drag force). If there is an angle between the alignment of an elongated structure and the flow direction, or if a current passes only on one side of the structure, the flow pattern is asymmetrical and a force will occur in the direction normal to the flow (lift force).

However, if the flow pattern is unstable, the force will fluctuate. This phenomenon can be described by the Strouhal-number.

As the shape of the structure is of great influence, model tests with the appropriate Reynolds number will provide the most accurate prediction of the specific forces on these structures. However, in the following sections data gathered from previous experiments are given as guidelines for preliminary design activities.

Figure 2.4.1.1. Flow regimes, depending on Reynolds-number (Blevins, [7]).

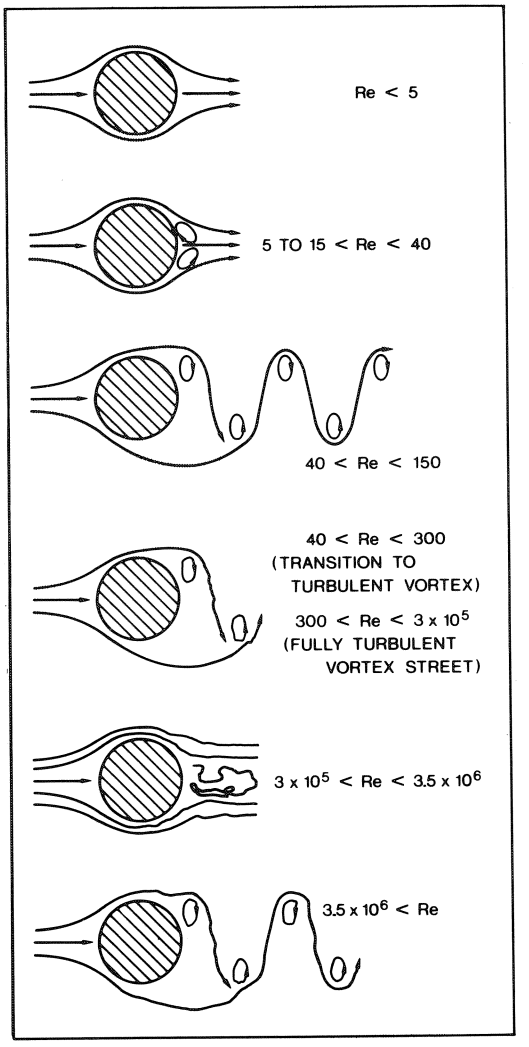

2. Steady lift and drag forces

Flow-induced forces occur not only when the water flows past piles, beams and piers, but also past ropes, anchor cables, guide wires or braces for stiffening that form elements of a complete structure, bore pipes, pipelines etc. When a fluid particle flows towards the front of a cylinder, the pressure in the fluid particle rises from the undisturbed stream pressure to the pressure in the stagnation point of the cylinder. This high pressure impels a boundary layer on both sides of the cylinder. According to the Reynolds number

$$R_e = \frac{vD}{\nu}$$

where:

D = diameter (m)
v = velocity (m/s)
υ = viscosity ( )

the pressure may or may not be able to force the boundary layer around the cylinder (see Figure 2.4.1.1.).

In the case of a cylinder at high Reynolds numbers the boundary layer separates from each side of the cylinder and from free shear layers that trail aft in the flow.
For smooth circular-shaped bodies the separation point for these vortices is not well-defined and a regular fluctuating pressure distribution may occur.
This phenomenon may interact with the struc-

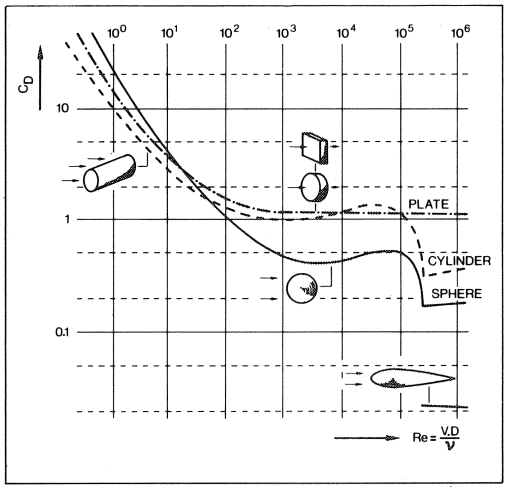

Figure 2.4.1.2[A] Drag-coefficients, $C_D = f(Re)$.

Figure 2.4.1.2[B] Drag-coefficient for cylinders, recommended for design[4].

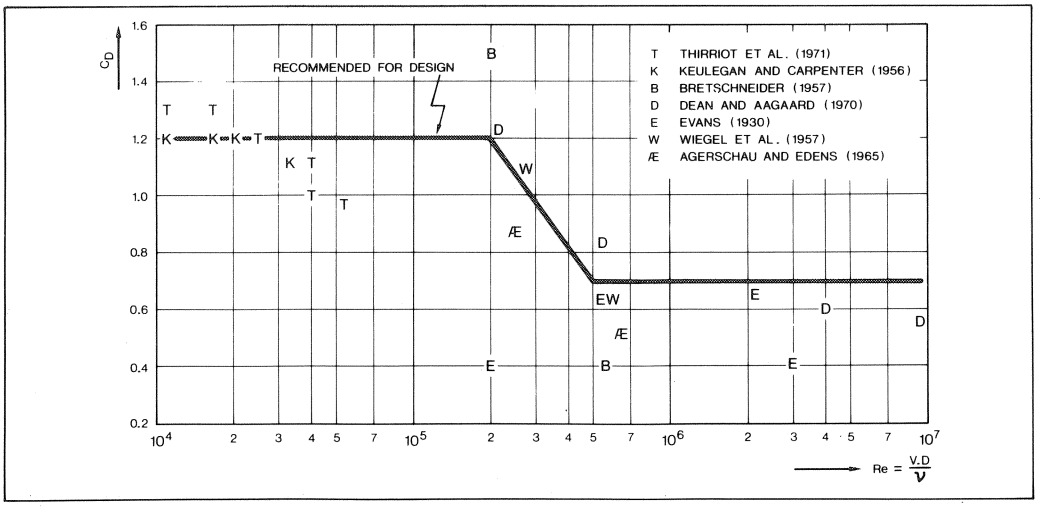

ture motion.
In the case of sharp-edged bodies the separation point for the vortices is more defined and the probability of the formation of regular fluctuating forces very low.
A high turbulence intensity of the approach flow has a similar effect as the well-defined, sharp edge of very rough structures.
In the case of an asymmetric presssure distribution a force transverse to the flow direction still occurs (= steady-lift force).
The drag force acting in the direction of the undisturbed flow is defined as:

$$F_D = \tfrac{1}{2}\rho v^2 C_D A$$

and the lift force acting in the direction perpendicular to the flow is defined as:

Figure 2.4.1.3 Drag- and lift-coefficient for a floating caisson and a submerged body (Nakamura and Mizota, 1971 [2]).

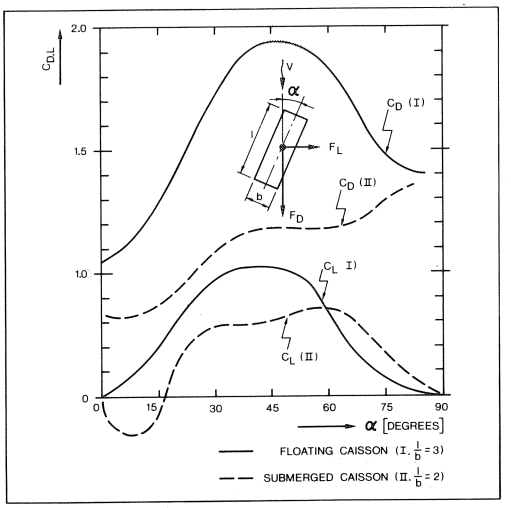

$$F_L = \tfrac{1}{2}\rho v^2 C_L A$$

where:

C_D, C_L	=	drag, lift coefficient (1)
ϱ	=	specific fluid density (kg/m³)
v	=	undisturbed approach velocity (m/s)
A	=	cross sectional area perpendicular to the flow direction (m²)

As stated before C_D and C_L are highly dependent on the shape of the structure and should for final design purposes be determined with the aid of physical model tests.
In Figures 2.4.1.2. a and b, and 2.4.1.3. some data of experiments are given, while figure 2b gives recommended data for the design of cylindrical piles [4].
These data are only valid if no obstacles (such as seabed, caisson floor etc.) are present near the structure.
If the surrounding flow is hampered by other structural elements, this has a significant effect on C_D and/or C_L.

Figure 2.4.1.4. gives the results of experiments for bridge piers. In this case the river bed is a boundary for the water flow.
Figure 2.4.1.5. gives the results for C_D and C_L for a caisson that is lowered onto the sill.
These coefficients greatly increase when the caisson almost reaches the sill. Note that, in the final stage (caisson on the sill), the „drag force" is formed by the difference in head over the caisson (the waterflow is now completely blocked).
For sharply edged structures and in the direction of flow a small dimension, C_D decreases (approx. 20%) if the turbulence intensity increases (from approx. 1% to 10%), see Figure 2.4.1.6.
For rectangular rods (length/width > 1) a reattachment of the flow occurs so that C_D has a lower value than in the case of a square rod. In that case the effect of the turbulence-intensity will be less.

3. Flow-induced vibration on circular-shaped structures

As shown in Figure 2.4.1.1. for 300 < Re < 3 x

10^5 (which generally occurs in hydraulic structures) a regular fluctuating pattern of vortices is formed.
The formation of these vortices in the wake of the structure causes an alternating force in a direction normal to the flow direction, which may interact with the structure motion.
The frequency of this vortex shedding (f_s) is given by:

$$f_s = \frac{V}{SD}$$

where:
S = Strouhal-number
v = approach, undisturbed velocity
D = characteristic transverse diameter.

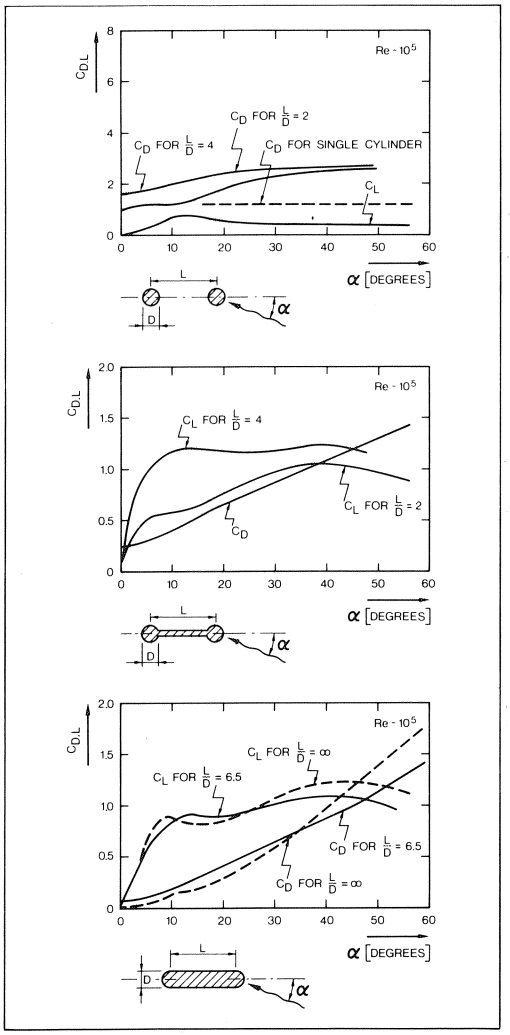

Figure 2.4.1.4 Drag- and liftcoefficients for bridge piers vs. angle of approach velocity (Apelt and Isaacs, 1968 [1]).

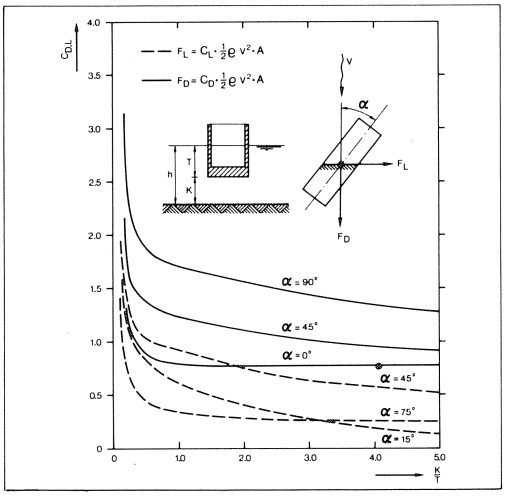

Figure 2.4.1.5 Effect of real clearance on C_D and C_L (after model tests for a caisson 42,5x15x4.8 m³, Delft Hydraulics Laboratory, M878).

This frequency is defined as a dominant frequency of a broad-band of shedding frequencies.
The Strouhal number varies with the shape of the object, but is independent of the Reynolds number above Re ≅ 10^3 for shapes with sharp edges since in this case the turbulent flow pattern in the wake does not vary. However, for rounded shapes the Reynolds number can have a great effect on the Strouhal-number. For preliminary design and for checking design calculations for relatively stiff structures the following relation, based on model experiments between the Strouhal number and drag-coefficient, may be used:

$$S = 0.21\ C_D^{-0.75}$$

If this phenomenon plays an important role for a specific structure, physical model investigations are preferable for the final design.
Not only the shape of the upstream edge of the structure will influence the vortex but also the shape of the trailing edge.
In general, sharp ended trailing edges will induce less shedding (their amplitude being smaller) than rounded edges. This phenomenon makes it possible to reduce the amplitude of the vortex-induced vibration. This can also be achieved by increasing the mass or internal damping, by avoiding resonance and by changing the cross section. Damping can be increased by using concrete instead of steel, or by incorporating materials with high internal damping properties such as wood, rubber or sand fill.
A reduction of vortex-vibration can also be obtained by trying to prevent resonance which could be achieved by dimensioning the structure in such a way that $f_n/f_s > 1$, where f_n = natural frequency, f_s = shedding frequency. This means a relatively stiff structure (higher frequency than the vortex frequency).

The natural frequency is given by the formula:

$$f_n = C_n \sqrt{\frac{EI}{m_v L^4}}$$

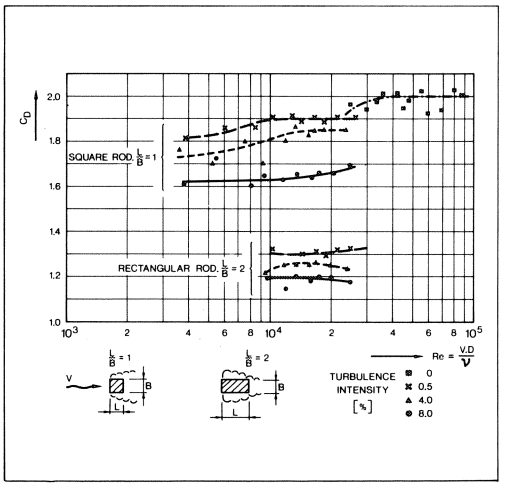

Figure 2.4.1.6. Drag coefficient vs. Reynolds number for square and rectangular rod with various intensities of turbulence (Roberson [3]).

where:

C_n = factor depending on the support system of the structure from 0.56 for a cantilever up to 3.57 for a beam clamped at both ends (see Figure 2.4.1.7.)

E = modulus of elasticity (N/m²)
I = area moment of inertia (m⁴)
m_v = virtual mass per unit length (kg/m)
L = length (m)

The virtual mass consists of the mass of the structure (m) and the mass of water around it that is accelerated by the motion of the submerged structure:

$$m_v = m + m_H$$

m_H is the hydrodynamic mass or added mass.

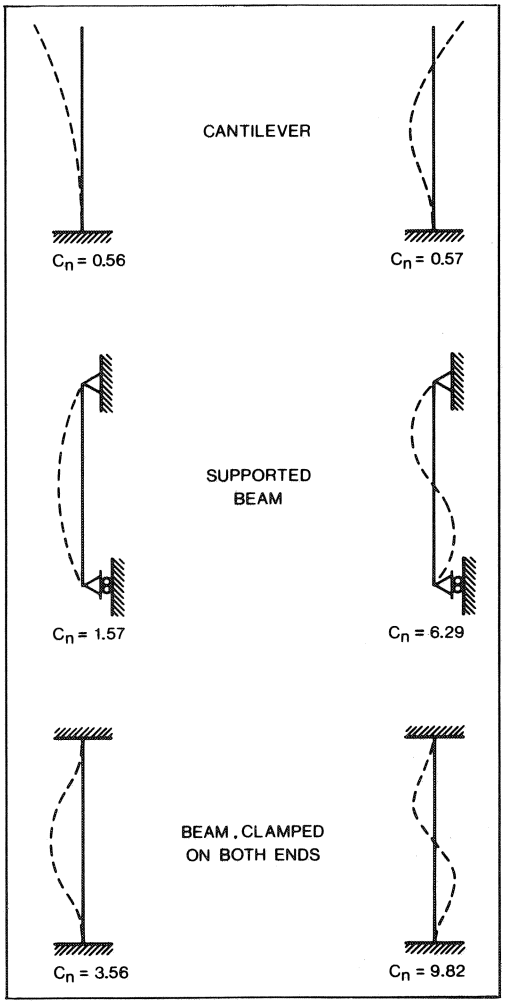

Figure 2.4.1.7. C_h factors for various systems.

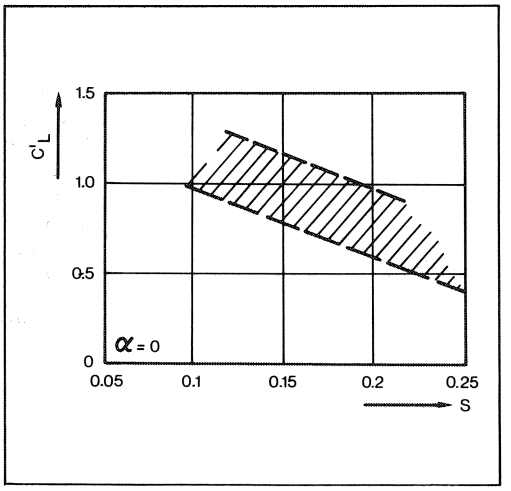

Figure 2.4.1.8. C_n vs. Strouhal-number (after Pennino, 1981 [8]).

Figure 2.4.1.9. Drag-coefficient vs. Reynolds-number for a plain and shrouded cylinder (after Blevins, 1977 [7]).

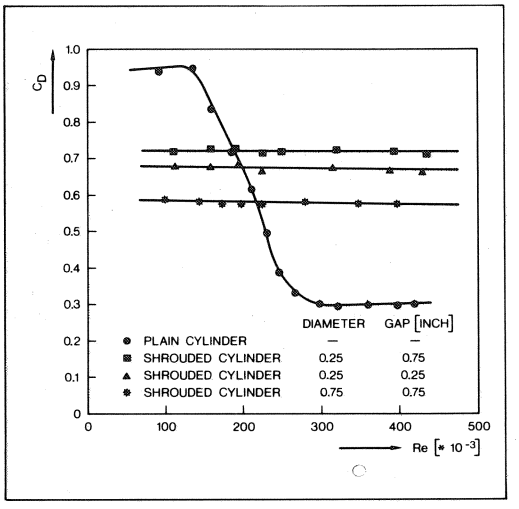

A rough estimation for the added mass for circular piles is twice the volume of the pile.
If vibrations occur, these will increase the drag and lift forces in comparison with a steady condition:

$$F_D = (C_D + C'_D)\,\tfrac{1}{2}\rho v^2 A$$

$$F_L = (C_L + C'_L)\,\tfrac{1}{2}\rho v^2 A$$

where:

F_D = drag force (N)
C_D, C'_D = steady resp. fluctuating drag force coefficient
ϱ = specific density of fluid (kg/m³)
v = approach velocity (m/s)
C_L, C'_L = steady, resp. fluctuating lift force coefficient

As to the fluctuating force coefficients, various references give various results. In general for non-resonant conditions ($f_s/f_n > 1$).
C'_D is about 10 to 25% of C_D. C_L is a not yet completely known function of the Strouhal-number and is given in Figure 2.4.1.8. as a range.
Furthermore C'_L depends on the ratio f_n/f_s. For cylinders C'_L can double or triple as the vortex frequency approaches the structural frequency. The designer should preferably avoid fluctuating lift forces and conditions where $f_s/f_n \approx 1$ because even relatively small forces can excite the structure near resonance. By changing the cross-section of the structure, for instance by streamlining, separation of water particles from the boundary layer along the edge of the structure will be prevented and consequently also vortex formation. Streamlining is only effective if the approach angle of the flow to the structure is constant.

Relatively small modifications in the cross-section along the structure and perpendicular to the flow can also reduce vibration. In fact, this measure is a variation of the Strouhal number (viz. D = characteristic transverse diameter). If this Strouhal number does not have the same value along the structure, resonance is „nearly" impossible.

Shrouds and small rectangular plates fitted at intervals prove to be successful but increase the drag forces of the structure (see Figures 2.4.1.9. and 2.4.10.).

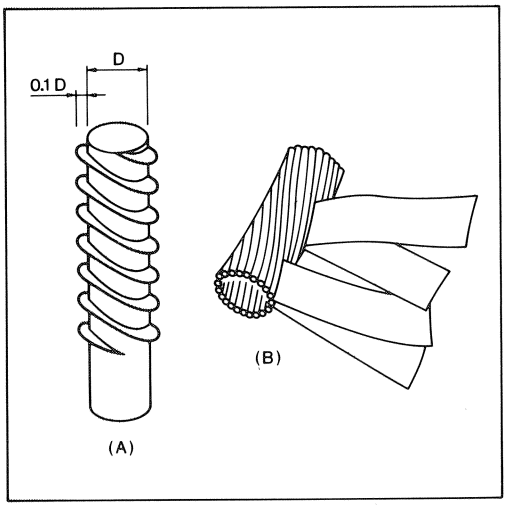

Figure 2.4.1.10. Methods of reducing vortex-induced vibrations: (a) stack with spiral, (b) ribboned cable (Blevins, 1977 [7]).

References

1. Colin J. Apelt and Lewis T. Isaacs, Bridge piers-hydrodynamic force coefficients, **Journal of Hydraulic Division**, proc. ACSE, HYI, January 1968.

2. Y. Nakamura and T. Mizota, Aerodynamic Characteristics and Flow Patterns of a Rectangular Block, **Rep. Res. Inst. for Applied Mechanics** Kyushu University 19(65), 1971.

3. John A. Roberson, Turbulence Effects on Drag of Sharp-edged Bodies, **Journal of Hydraulic Division HY7**, 1972.

4. **Shore Protection Manual**, U.S. Army coastal Engineering Research Center, Virginia, 1973.

5. Research Investigation for the Improvement of Ship Mooring Methods, **The British Ship Research Association**, Report NS. 386, 1973.

6. John A. Roberson, Clayton T. Crowe, **Engineering Fluid Mechanics**, Houghton Mifflin Company, 1975.

7. Blevins, R.D., **Flow-Induced Vibration**, Nostrand Reinhold Company, New York 1977.

8. Pennino, B.J., Prediction of Flow-Induced Forces and Vibrations **Water Power and Dam construction**, February 1981.

J.K. Vrijling

2.4.2. Wave induced loads

2.4.2.1. Wave forces on vertical walls

The pressure fluctuations below still water level (s.w.l.) caused by a progressive sinusoidal wave can be written as:

$$p(z,t) = \rho g \frac{H}{2} \frac{\cosh kz}{\cosh kd} \cos \omega t$$

for $0 < z < d$

If the wave encounters a vertical wall it is nearly completely reflected. The percentage of the wave height, that is reflected is denoted by α. The incoming and the reflected wave together form a standing wave in front of the vertical wall. The pressure fluctuations in the standing wave below s.w.l. are given by

$$p(z,t) = \rho g \frac{H}{2} (1+\alpha) \frac{\cosh kz}{\cosh kd} \cos \omega t$$

for $0 < z < d$

Above s.w.l. the pressure fluctuations may be approximated by

$$p(z,t) = \rho g \left[\frac{H}{2} (1+\alpha) + d - z\right] \cos \omega t$$

for $d < z < h$ or

$d < z < d + \frac{H}{2} (1+\alpha)$

The force exerted by the wave on the wall is found by integrating the pressure diagram over the height of the structure.

$$F = \int_0^h p(z,t)\,dz$$

Below s.w.l. the result of this integration for the time maximum is

$$F_1 = \rho g \frac{H}{2} (1 + \alpha) \frac{\sinh kz}{k \cosh kd} \Big/_0^d$$

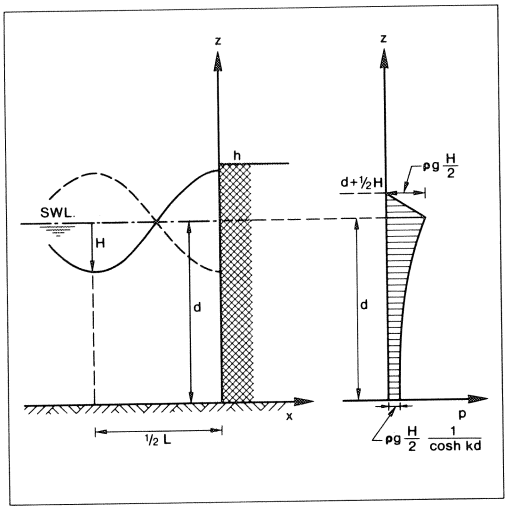

Figure 2.4.2.1 The height of the standing wave does not reach the top of the wall.

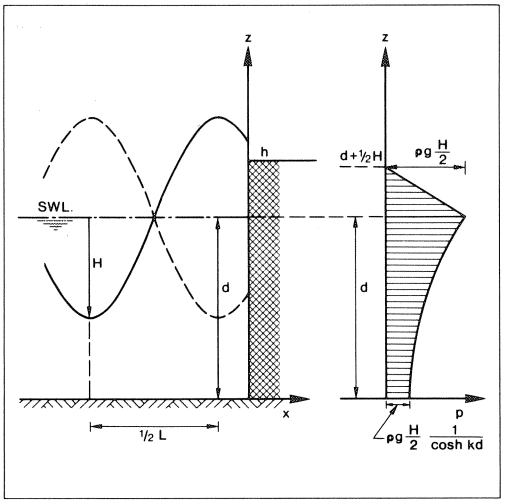

Figure 2.4.2.2 The pressure diagram if the height of the standing wave exceeds the top of the wall.

The integral of the pressure diagram above s.w.l.

$$F_2 = \rho g[\{ \frac{H}{2} (1 + \alpha) \} z - \tfrac{1}{2} z^2] \Big/_{d}^{h}$$

The total force F is now derived by summing the two parts

$$F = F_1 + F_2$$

2.4.2.2. Wave forces on vertical piles

In a wave field the flow is unstationary and exerts a fluctuating load causing drag and inertia forces fluctuating with a period similar to that of the wave on structures surrounded by water.
For objects with a characteristic diameter D, smaller than the wave height H (H/D > 1), drag and inertia forces both are of importance, see Figure 2.4.2.3.
For conditions where H/D < 1, for instance for gravity type offshore structures, drag forces may be neglected since inertia forces can be obtained directly from an integration of the wave pressure on the surface of the structure. Figure 2.4.2.3 gives results; the horizontal force T may be used as a transfer function for a spectral approach of the wave forces, i.e. drag and inertia forces on the structure with a period similar to that of the wave. The total force per unit length of a vertical cylindrical pile with a relatively small diameter viz. approximately D/L < 0,1 may be expressed as :

$$F = \tfrac{1}{2}\rho C_D D U|U| + \rho C_m \frac{\pi D^2}{4} du/dt$$

where :
C_d = drag coefficient
ϱ = specific density of fluid
D = diameter of pile
u = horizontal orbital velocity =

$$\frac{H}{2} \frac{gT}{L} \frac{\cosh [2\pi(z+d)/L]}{\cosh (2\pi d/L)} \cos (\frac{2\pi t}{T})$$

z = depth (above still water)
d = waterdepth
L = wavelength
H = waveheight
C_m = inertia coefficient

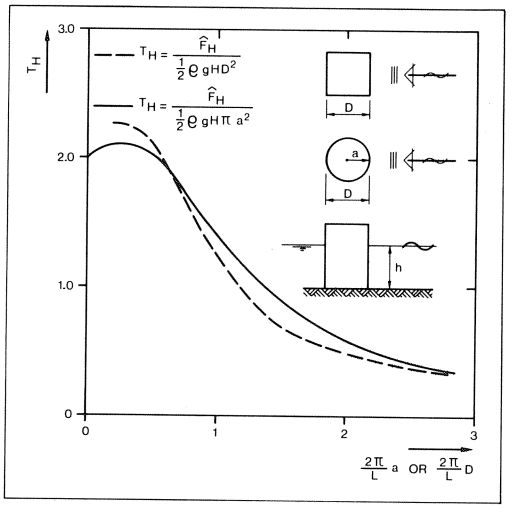

Figure 2.4.2.3a The horizontal force on a large diameter pile as a function of relative wavelength. (inertia force prevails)

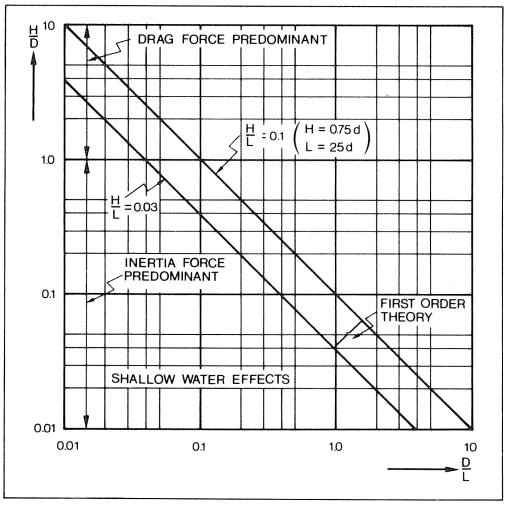

Figure 2.4.2.3b The relative importance of the drag force and the inertia force as a function of the ratio's of waveheight wavelength and pile diameter.

$\frac{du}{dt}$ = horizontal orbital accelation =

$$\frac{g\pi H}{L} \frac{\cosh\left[2\pi(z+d)/L\right]}{\cosh(2\pi d/L)} \sin\left(\frac{-2\pi t}{T}\right)$$

The maximum value of the drag force component coincides with the passage of the wave crest (t = o). The inertia force component is at a maximum when the wave passes the still waterline (t = ¼ T, where T = wave period). See Figure 2.4.2.4.) Figure 2.4.2.5 a and b give values for C_d and C_m as a function of the Reynolds number and for various Keulegan - Carpenter numbers $K = \frac{Um\ T}{D}$

where u_m = maximum orbital velocity.

For practical purposes often C_m = 2, while for the wave drag coefficient the steady flow drag coefficient is taken, which is allowed if A/D > 10

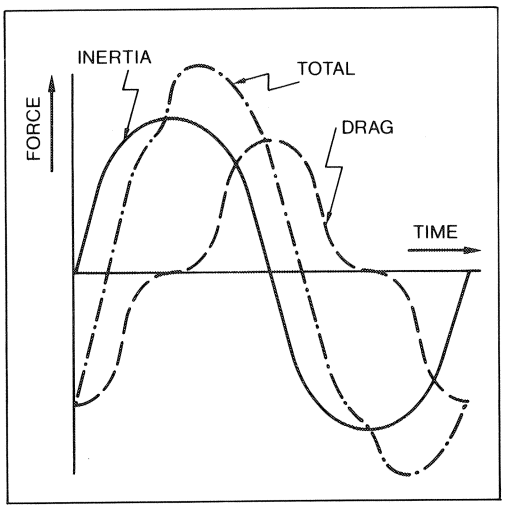

Figure 2.4.2.4 The inertia force, the drag force and the total force as a function of time.

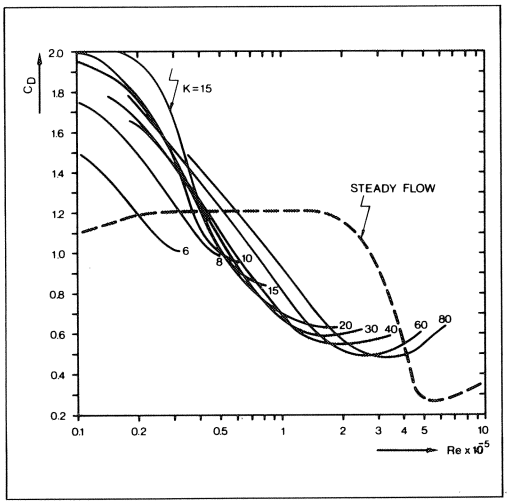

Figure 2.4.2.5a The drag force coefficient C_d as a function of the Reynolds and the Keulegan-Carpenter numbers.

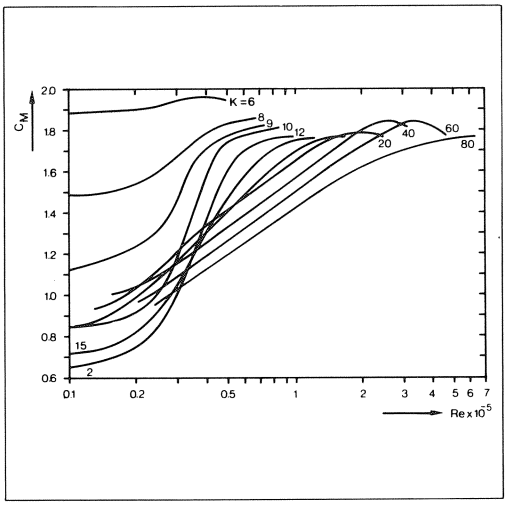

Figure 2.4.2.5b The inertia force coefficient C_4 as a function of the Reynolds and the Keulegan-Carpenter numbers.

where A = amplitude of particle motion of the wave:

$$\frac{HgT^2}{2\pi L} \frac{\cosh\,[\,2\pi(z+d)/L]}{\cosh\,(2\pi d/L)}$$

and D = diameter of the pile.
For shallow water (ratio waterdepth to wavelength <0.04) and breaking waves it is suggested that C_d should be increased by a factor of 2.5.
For deep water (ratio waterdepth to wavelength >0.5) and breaking waves this coefficient does not need adjustment.
In the case of a relatively close space between piles (4 < times pile diameter) the wave force increases with respect to a solitary pile. The table below gives an indication of the increasing effect.

References

Morison, J.R., Design of Piling: **Proceedings of the Conference on Coastal Engineering,** Long Beach, California (1950).

A Critical Evaluation of the Data on Wavecoefficients, **The British Ship Research Association Contract Report** No. W 278. D.o.E. Report OT/R/7611, 1976.

Table 2.4.2.1 Factors for close spaced piles. (C_d (row of piles) = factor x solitary pile).

$\frac{d}{b}$ = $\frac{\text{space (c.t.c.)}}{\text{pile diameter}}$	2	3	4
row of piles parallel to wave crest	1,5	1,25	1,0
row of piles perpendicular to wave crest	0,7	0,8	1,0

Interaction Water Motion and Closing Elements

K.W. Pilarczyk

2.4.3. Ice induced loads

Introduction

One of the most important forces in the design of an hydraulic structure in the colder climatic regions is the thrust applied to it by ice.
The force that ice will exert on a structure is determined by four factors [6].
These are:

1) the characteristics of the ice cover and properties of the ice;
2) the relative motion between the ice and the structure;
3) the response of ice to stress;
4) the response of the structure to an imposed load.

The latter factor is determined primarily by the design, but the engineer has little control over the first three, and it is about these that additional knowledge is required.
Ice covers are a product of the weather. Their characteristics, such as thickness, quality of the ice and type of crystal structure, are subject to a variability that depends on weather conditions.
For a particular site, several years of observations on the characteristics of the ice cover and the weather are usually necessary to establish the statistical information required.
Because of the size of the area involved and limitations imposed by time and human resources, these observations are usually not available, and so the engineer must make do with the more general information that is already available in the technical literature.
Experimental results and calculation methods are summarized in the literature by Starosolszky [15], Michel [10] Neil [11] and Carstens [20].

Reasons for considering ice forces [20]

Before one can accurately predict ice forces on a structure some preliminary considerations have to be made.
One should be aware for instance that the forces transmitted to a structure by the ice are generated by natural forces such as winds, currents or thermal strains. These natural forces can be concentrated on the structure by large ice sheets and represent an upper limit for the ice forces. The usually considered upper limit for the ice forces, is the force to fail the ice against the structure in the easiest mode of ice failure. Sometimes one can select the mode of failure which gives the lowest force but often one has to check several modes.
Another consideration relates to the clearance of ice around the structure; if ice rubble builds-up on the structure the mode of ice failure (and hence the force) can change.
A suggested logic for considering some of the above mentioned points is presented in figure 2.4.3.1.
Environmental forces can be calculated separately and compared with ice interaction forces to indicate the design force. Environmental forces are not easily estimated to any degree of accuracy, but they are usually much greater than the ice interaction forces so that accuracy is not so important.
Sometimes a short cut to the environmental force can be made by using observed ice velocities and floe sizes to estimate kinetic energy prior to impact. If this energy is much greater than the work done in deforming the ice to reach the maximum interaction force then the latter force governs the design force.

Environmental forces such as the rate and magnitude of ice movement also input to other parts of the logic diagram as shown.
For the ice interaction force, the mode of ice failure is the most important factor to consider. Intuitively one can expect ice against vertical structures. However it is well known that thin ice can buckle at lower forces than crushing. Furthermore ice rubble in front of a vertical structure can lead to bending failure in a way similar to the formation of first-year ridges. Bending failure will occur against a sloping structure, but the presence of re-frozen rubble or high friction due to the freezing of ice to the structure can lead to ice crushing at higher loads. All these possibilities may have to be considered.
The ice-type governs both the failure mode and the actual interaction force. Such factors as thickness, ridge shapes and sizes, crystal structure, salinity, and temperature are known to be important and will need to be specified.
For sloping structures the friction between the ice and the sides is also important in determining the horizontal force.

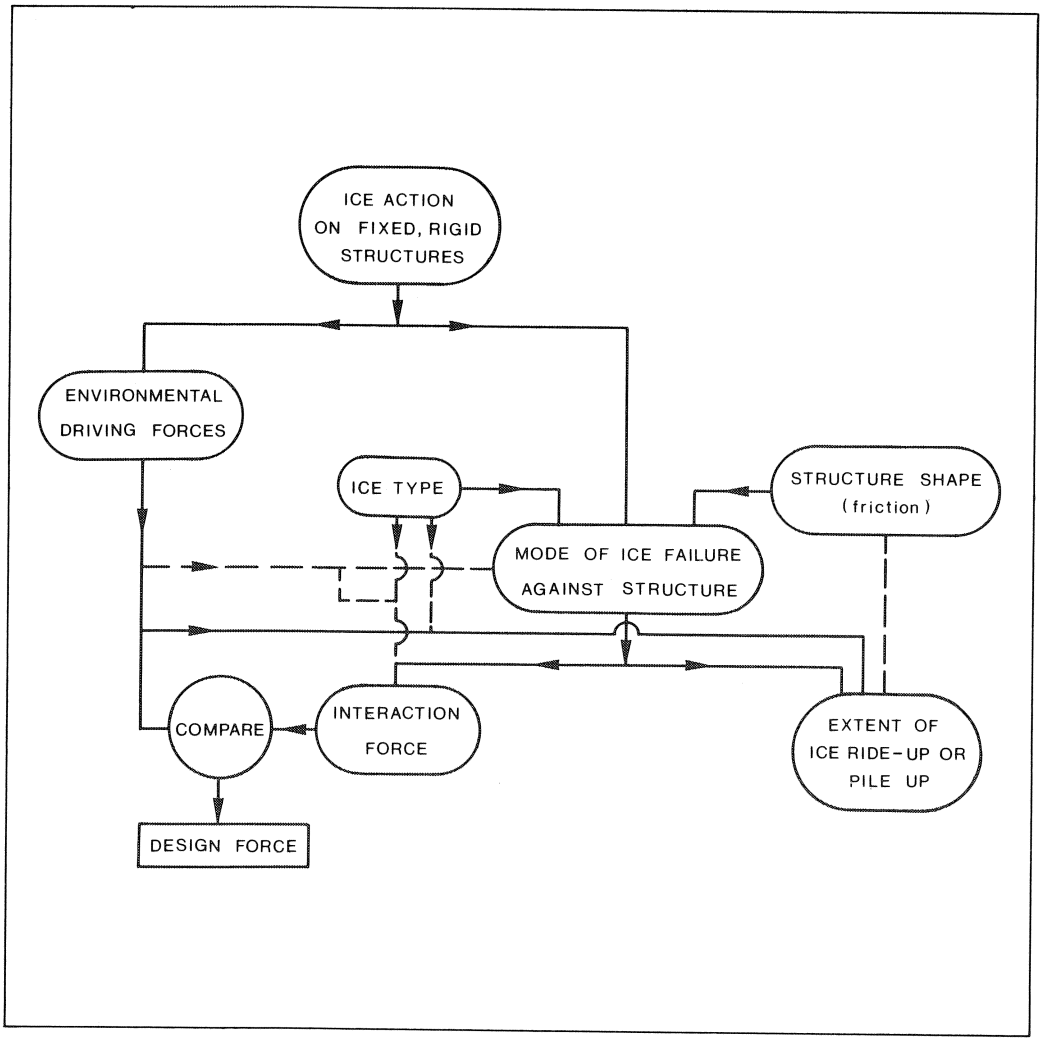

Figure 2.4.3.1. Logic for considering ice action on fixed, rigid structures.

In addition, the width of the structure will influence two things: first the way ice rubble clears around the structure; and secondly whether ice failure occurs simultaneously across the full width of the structure.

For certain low-freeboard structures the problem of ice encroaching onto the structure may have to be seriously considered. As shown in the

logic diagram such factors as structure shape, extent of ice movement and characteristics such as strength or thickness will all have to be considered in determining the extent of ice ride-up or pile-up on the structure.

Types of ice forces

According to Michel[10] and Neil [11], there are essentially four modes of ice action against

Table 2.4.3.1 Principal modes of ice action [11]

No	DESCRIPTION	TYPICAL ENVIRONMENT	ILLUSTRATION
1	STATIC PRESSURE FROM EXPANDING OR CONTRACTING SHEETS	LAKES, SHELTERED COASTAL WATERS. TEMPERATURE CHANGES AND JACKING BY REFREEZING OF CRACKS	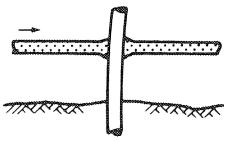
2	IMPACT OF MOVING SHEETS AND FLOES	RIVERS AT BREAK-UP, COASTAL WATERS WITH APPRECIABLE CURRENTS	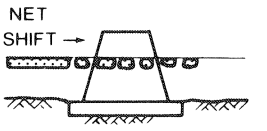
3	SLOW PRESSURE FROM ICE PACK OR JAM	EXPOSED COASTAL WATERS, RIVERS	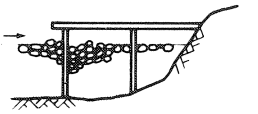
4	VERTICAL MOVEMENT	TIDAL LOCATIONS WITH HEAVY ICE BUILD-UP	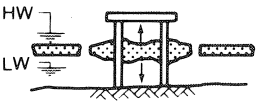

marine and hydraulic structures, namely (see also Table 2.4.3.1.):

1) Static pressure from expanding or contracting ice sheets. This type of ice movement, caused by air temperature changes, induces important stresses in the ice and reactions on the structures. This pressure is particularly important in the case of constrained ice sheets and acts principally in lakes, reservoirs and sheltered coastal areas on dams, dikes and retaining structures.
2) Impact of moving ice sheets, pressure ridges and ice islands.
This movement may be caused by wind and/or water currents. They are particularly important for slow-moving large masses of cold ice.
These forces are observed in very large rivers at break-up, in coastal waters, large estuaries and in the Arctic seas. They affect all types of marine structures and ships; piers, piles, offshore structures, ship hulls, etc, One of the worst conditions is slow-moving pressure ice containing large continuous ice masses.
3) Pressure exerted by unconsolidated ice accumulations.
When the floes are too small, they will accumulate under the influence of wind and currents. The forces are transmitted to the marine structures by friction between the ice pieces instead of by the actual crushing of the ice. The ice accumulations may be in the form of jams or pack ice acting on many types of hydraulic or marine structures.
4) Vertical forces exerted by ice.
The main cause is the movement of an ice sheet adhering to a structure, due to a variation in water level. Vertical forces are also caused by the weight of ice caps adhering to the structure.

In the following section, only some basic information on the first two above mentioned types of ice forces will be given. The more detailed information necessary for design purposes can be found in [10, 11 and 20].
Very valuable information on the interaction between ice and coastal (offshore) structures in the arctic regions can also be found in the papers of Kivisild [3], Per Bruun [12], Peyton [13] and POAC '77 [19].

Force of an expanding ice sheet
Rising air temperature causes an ice sheet to expand. Thermal expansion may give rise to considerable stresses in the ice cover as well and, since the frictional resistance of the underlying water is practically negligible, the expansion is unrestricted as long as no firm barrier is encountered.
The average linear expansion coefficient of ice is $5.5.10^{-5}\ °C^{-1}$, implying that an ice cover of 1 km length expands 5.5 cm if its temperature is raised by 1°C. The rate of expansion is determined by the rate of temperature rise.
If the stress in the ice cover attains the ultimate strength of the ice during the ice expansion, plastic deformations will occur in the expanding phase. The ice will fail mostly in bending and the structure will no longer be subjected to the full thrust due to the expansion of the cover.
There are many theoretical and experimental methods for predicting the magnitude of the ice thrust due to thermal expansion [1,2,7,10,15,17], but there is still no method which can be chosen for the definitive design.
For this reason this problem will be illustrated only by figure 2.4.3.2. which has been developed for conditions peculiar to the Soviet Union [15]. This figure is valid for a 50m wide ice cover. For ice covers longer than 50m, allowance is made for failure due to buckling by introducing the following reduction factors:

length of the cover L (m)	to 50	51-75	76-100	101-150	151
reduction factor, r	1	0.9	0.8	0.7	0.6

From measurements taken on reservoirs in the United States, the ice thrust of relatively thin sheets was found to range from 5.4 to 8.6 tons/m run while, with thicker sheets, it was from 14 to 25 tons/m.
Similar tests have been done in the Soviet Union in the Ges Reservoir of the Dnieper River. The maximum recorded ice thrust was 12.5 tons/m.
In the Soviet Union, 30, 20 and 15 tons/m² respectively are recommended as first approximations of ice pressure for design purposes for the Siberia, Leningrad and Caucasus regions. In Norway, the recommended value of ice pressure is from 2 to 9 tons/m², whereas in Sweden 15 to 20 tons/m² are considered necessary.

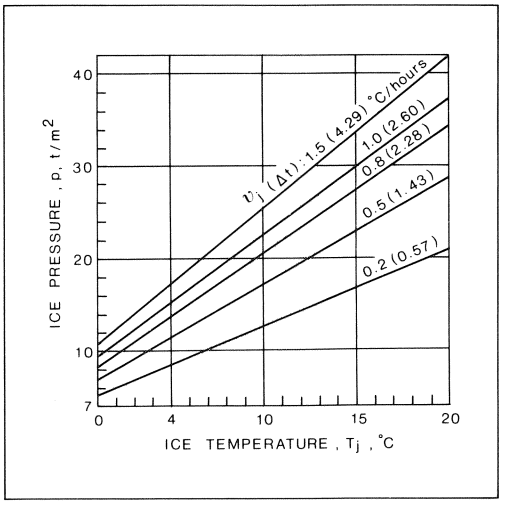

Figure 2.4.3.2. Ice pressure as function of rate of ice temperature „v_j" and change of air temperature ($\triangle$t)

The values of ice thrust used by Canadian engineers vary between 15 and 22 tons/m for rigid structures. For more flexible structures such as sluice gates, values in the vicinity of 7 tons/m are commonly used.
The importance of a proper allowance for ice thrust is appreciated when it is realized that for a dam 12m high, an ice thrust of 22 tons/m has the same tendency to tip the dam as the design water pressure.

Michel [10] also reports different methods of prevention against static ice pressure.
Two of these are mentioned below.
At an existing dam, designed with no allowance for ice pressure, the following procedure may be used for protection against expanding ice.
Generally, all dams are designed for the full reservoir condition with the water surface at or very near the top of the dam. It is possible to compensate for the effect of ice thrust by lowering the reservoir level during the season when ice pressure may exist, so that the total load at the critical section is no larger than for the full reservoir condition.
The best-known method of preventing an ice sheet from pushing on a dam is to maintain an open water gap in front of the structure. This can be done in various ways. A permanent solution is to install a system of piping along the edge of the wall at the bottom of the reservoir so that compressed air can be used to create a vertical current bringing the warm water at the reservoir bottom to the top, thus preventing ice formation. This system works well as long as there is an adequate vertical temperature gradient in the reservoir. In turbulent flows, this gradient is very small and there is normally not enough heat stored in the bottom of the water to prevent ice formation at the top.

Moving ice sheets of dynamic ice thrust
The destruction of an ice floe by a structure (e.g. a pier) occurs in different ways, depending mostly on the stored kinetic energy of the floe and its strength. Michel [10] describes this ice-structure interaction in the following way. Upon impact with a pier, a small ice floe is crushed locally, stops and then continues to move across an adjacent opening. A slightly larger floe generally collapses by splitting, while a large ice field is cut without splitting. Finally, under certain conditions, the ice buckles at a certain distance from the face of the pier. During the penetration of a pier into a large ice field, the width of indentation gradually increases and attains a maximum value equal to the total width of the pier, after which it remains constant.
For a better understanding of the ice-structure interaction, we quote Michel's derivation of the general relationships.
If we consider an ice floe hitting a pier, the energy transmitted to the obstacle is made up of the energy of deformation inside the ice floe and the energy required for its crushing. As the energy of deformation is negligible when compared with the energy of crushing for sizable impacts, the fundamental relationship of mechanics gives:

$$F\,dx = m\,v\,dv$$

where F is the force exerted on the obstacle for a displacement dx of the floe, and m and V are the mass and instantaneous velocity of the floe.
On the other hand, at crushing, we have:

$$F = \sigma_i\, y\, h$$

where σ_i is the crushing strength of ice by indentation, y is the width of the failure zone and h is the thickness of the ice.(See fig. 2.4.3.3.)
For an ice floe, with an initial velocity V_o, that is completely stopped by the pier we get:

$$\int_{x=0}^{x=x_0} h\sigma_i(x)\, y\, dx = \frac{1}{2} m v_0^2$$

Because of the geometry of the pier, the term on the left has an upper limit when x = d and y = B where d is the length of the pier nose and B is the total width of the pier.If the kinetic energy is adequate to attain this upper limit, the floe will not stop and the maximum force will be given by:

$$F_{max} = \sigma_i\, B\, h$$

In the case where the indentation strength of the ice can be taken as independent of the indentor width y, the force required to stop an ice floe of a limited size can be easily computed:

$$A_0 = \int_0^{x_0} y(x)\, dx = \frac{mv_0^2}{2\sigma_i h}$$

A_o is thus the horizontal crushed surface of the ice floe when it stops as shown on Fig.2.4.3.3. and can be determined for any type of pier shape (Michel et al.,[8,10]. Actually, y_0 is the pier width corresponding to the A_o area.

For the case of a triangular-nosed pier of angle 2α attacked by an ice floe along its axis, we obtain the Petrunichev [10] formula for limited size floes:

$$F_{max} = v_0\, h\sqrt{2\rho_i \sigma_i \Omega \tan\alpha}$$

Figure 2.4.3.3. Crushing of an ice floe against a pier.

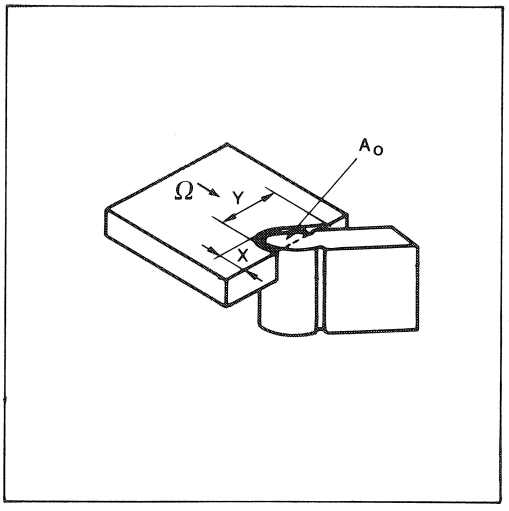

where

F_{max}	-	maximum horizontal force
V_o	-	water velocity
h	-	ice thickness
ϱ_i	-	density of ice
Ω	-	area of the ice floe
σ_i	-	crushing strength of ice (by indentation)
α	-	half the angle between centre line ice floe and pier

The relatively simple case of indentation of ice by vertical face structures shows that the largest forces are associated with crushing along the contact perimeter in a more or less continuous manner. The force acting on the structure is usually defined by the effective ice pressure, p:

$$F = p\, b\, h$$

F - force on the structure
p - effective ice pressure
b - width of the structure
h - thickness of the ice

The main question, then, is to relate the effective ice pressure to the actual crushing strength of the ice and other geometrical factors.

Tests done by Michel and Toussaint[9] with ice plates at -10°C, indented with a square edge indentor, have shown that the failure mechanism differs considerably in function of the rate of indentation.

The problem of defining the effective ice pressure 'p' is a complex one. The detailed description of this problem relating to the different failure mechanisms of ice, dimensions of ice floes and the geometry of structure can be found in [10].

For a quantitative illustration of this problem, the generally known and broadly applied method of Korzhavin [4] will be presented below (acc. to [20]).

Korzhavin suggests the following empirical relationship for P.

$$p = I\, m_s\, k\, \sigma_c$$

where

σ_c = the ice strength in compression
k = a contact coefficient which equals 1.0 for perfect contact
m_s = a shape factor which is close to 1.0 for circular piers
I = an indentation factor which tends to 1.0 for a wide structure and is equal to 2.5 for narrow structures (b/h = 1.0).

In Korzhavin's original equation a velocity term was included, but it is generally accepted that this can be omitted if the ice strength is specified for the appropriate velocity or strain rate.

The usefulness of the above equation to the engineer is limited because of the need of a value for the ice compressive strength. Compressive strength measured on small ice blocks is notoriously variable, being highly sensitive to crystal orientation, degree of confinement, temperature, strain rate and size of sample.

However, despite this limitation, this equation includes some useful concepts for ice pressure on piles. It suggests that for wide structures, with I = 1, the maximum pressure approaches the uniaxial ice crushing strength, and for narrow piers, the ice pressure could be 2.5 times greater. The equation also tells us that the ice pressure is a function of the „goodness" of contact between the ice and pier.

The practical value of the formula has been verified by Korzhavin in tests performed on rivers in Siberia with floes of different size and shape, and floe velocity $0.5 < V_o < 1.5$m/s. It is not advisable to use this formula for $V < 0.5$ m/s because it leads to a high over-estimation of the real thrust.

Design values according to Korzhavin for the ultimate strength of ice during an ice-run are given in the table below.

Character of Interaction	Rivers of the North and Siberia			Direction of force toward the axis of crystalization
	Vo = 0.5 m/sec	Vo = 1.0 m/sec	Vo = 1.5 m/sec	
1. Compression	65	50	45	Normal
2. Local bearing	160	125	110	Normal
3. Bending	60	45	40	Normal
4. Shearing		30-40		Parallel
5. Tension		70-90		Parallel

Table 2.4.3.2 Design values of ice ultimate strength, t/m².

It has to be noted that many of the observations, reported in the technical literature, are of little general value because of insufficient information about the character of the ice and the details of the experimental method employed. They can only be used for climatic and local conditions similar to the conditions reported.
More detailed information may be found in [11] and [20].

When designing low freeboard structures with sloping beaches such as artificial islands, it is important to be able to assess the likelihood of ice ride-up. Factors which may limit ice ride-up and suggested procedures for designing against ice ride-up are examined below.

Consider the configuration shown in Figure 2.4.3.4. where P is the force necessary to move the ice pieces up the slope [20].

Now if
m = the mass of each piece
n = the number of ice pieces on the slope
α = the angle of the slope from the horizontal
μ = the coefficient of friction
g = the acceleration due to gravity

then,

$$p = \sum_{1}^{n} mg\ (\sin\alpha + \mu\cos\alpha)$$

In another form, for a simple two-dimensional system,

$$P = L\ h\ b\ \rho_i g(\sin\alpha + \mu\cos\alpha)$$

Where, L is the length of slope covered by ice, h is the ice thickness, ρ_i is the density and b is the width of the ice on the slope.

Ice motion in large bodies of water is caused mainly by wind stress. The resulting environmental driving force can be calculated separately and compared with the slope resistance to indicate the design force.

If the steady state environmental driving force (F) is greater than the horizontal component of the slope resistance then the potential for ice ride-up exists. That is, the potential for ice ride-up exists if,

$$\frac{F}{P\ \cos\ \alpha} \geq 1$$

A typical environmental driving force (F) might be derived using the classical expression for wind drag on an ice surface.

$$F = C_{10}\ \rho_a g v^2 A$$

where:
C_{10} = drag coefficient at the 10-metre level
ϱa = air density
V = air velocity at the 10-metre level
A = „fetch area" (= area of ice cover, Ω).

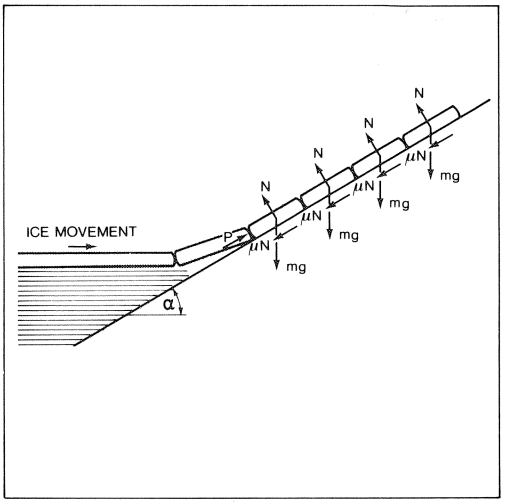

Figure 2.4.3.4. Forces for simple ride-up.

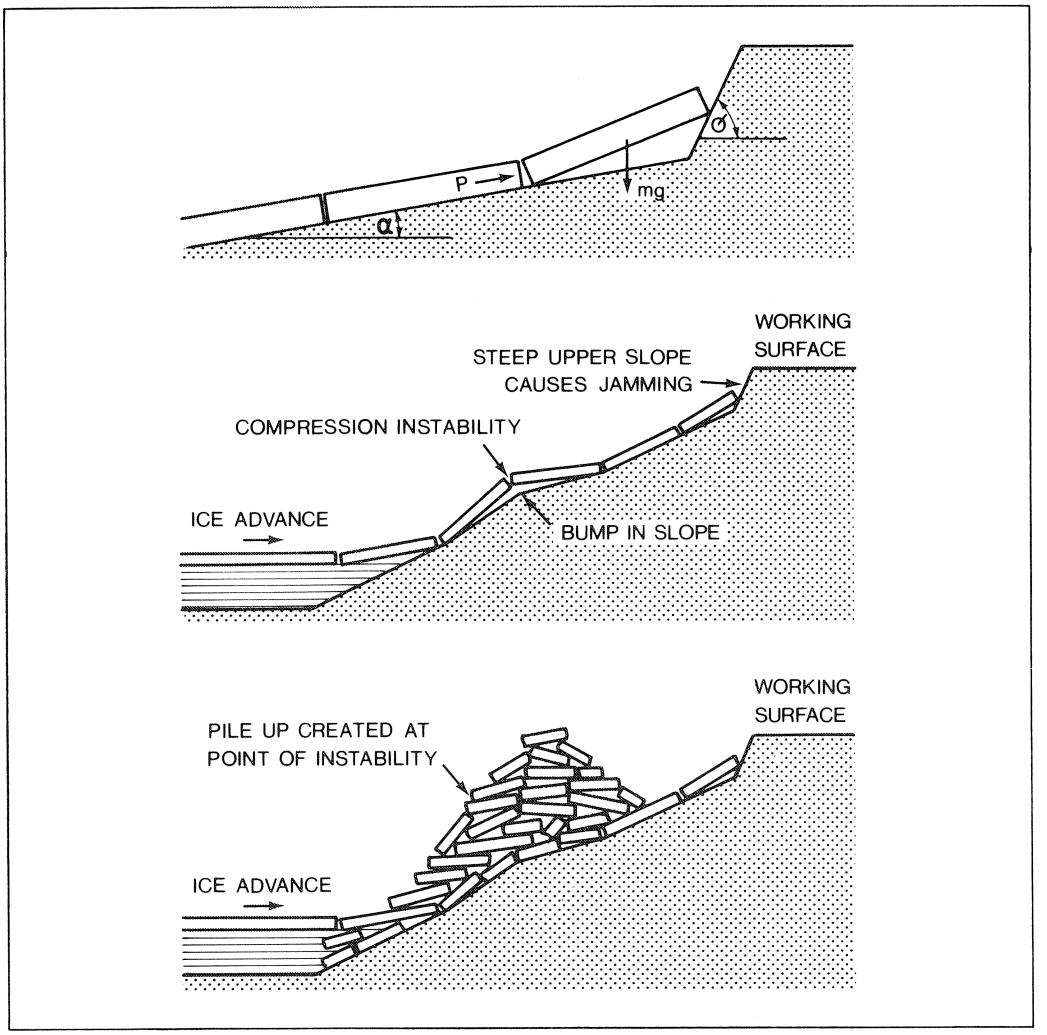

Figure 2.4.3.5. Design to resist ice ride-up.

An average value of C_{10} for a rough ice cover is given as 0.0022, [20]. For ridget arctic sea ice a value of $C_{10} = 0.005$ has been recommended. Some typical sheet sizes needed to impose critical ice forces on various structures are given in Table 2.4.3.3. For ice sheets sizes greater than those shown the ice forces will be governed by the ice failure mechanism and not by wind

stress. It can be seen that only on relatively small bodies of water will the wind induced ice force control the design load for the structure.

For floes of limited extent moving at a velocity determined by the current or wind, ice forces can be calculated using energy considerations. The initial kinetic energy of the floe is equated to the work done in failing the ice as the edge of the ice floe is penetrated by the structure. Floes below a certain size will be brought to rest before full penetration at lower-than-maximum ice force. However this condition is unlikely to govern ice design criteria.

Structure	Typical Force for Ice Sheet Failure (KN)	Ice Sheet Size to Generate Ice Force (For V = 15 ms^{-1}) (m) x (m)
Conical Light Pier (3 m diameter)	1500	1600 x 1600
Conical Drilling Platform (60 m diameter)	30000	2630 x 2630
Cylindrical Pier (4 m diameter)	10000	4150 x 4150
Dredged Island (150 m diameter)	500000	18600 x 18600

Table 2.4.3.3 Ice sheet sizes to generate typical ice forces [20]

Although the force necessary to push the ice pieces up the beach is caused by the environmental driving force, it is the ice sheet just in front of the beach which transmits the force. If the force due to slope resistance causes edge failure of the ice sheet then pile-up will occur at the water line and ride-up will be inhibited.
Features can be built into an island to discourage ice ride-up. An obvious solution is to raise the freeboard of the island and steepen the side slopes, but this approach is expensive because of the additional construction material needed.
Obstacles can be placed on the beaches to inhibit ice ride-up. This solution was used on a dredged island in the Beaufort Sea where steel piles were placed in the beach to protect the drilling rig during spring break-up. However, it turned out that the ice was so weak that rubble formed at the water-line never reached the piles.

Perhaps the best approach is to alter the geometry of the island beach in order to encourage instability of ice pieces trying to ride-up.
A design using this approach is illustrated in Figure 2.4.3.5. The steep upper slope of the beach causes a jamming action which leads to sufficient force being generated to trigger a compression instability at the point of change in slope of the beach. The resulting pile-up is centered on the point of change in the slope which can be positioned so that the pile-up does not encroach onto the island surface.

References

1. Assur,A., Maximum Lateral Pressure Exerted by Ice Sheets, Seminar no.1, **Proc.8th Congress IAHR,** Montreal, 1959.

2. Drouin,M., Static Ice Force on Extended Structures, **Proc.Ice Pressures Against Structures,** Quebec,1966.Canada.

3. Kivisild,H.R., Offshore Structures in Arctic Ice, BOSS'76.Vol.II,1976. **The Norwegian Institute of Technology.**

4. Korzhavin.K.N., Ice Affecting Engineering Structures on the Siberian Rivers During Ice-Run,**8th Congress IAHR,** Montreal,1959.

5. Korzhavin.K.N., Dynamic Ice Pressure and Deformation of Structures, **IAHR, Symp. on Ice and Its Action on Hydr.Structures,** Reykjavik,1970.

6. Legget R.F. and L.W.Gold., Ice Pressures on Structures, A Canadian Problem, **Proc.Ice Pressure Against Structures,** Quebec,1966.

7. Lindgren,S.,Thermal Ice Pressure,**IAHR, Symp. on Ice and Its Action on Hydr.Structures,**Reykjavik,1970.

8. Michel, B.,Drouin,M., Impact of an Ice Floe on an Obstacle, **Proceed. Inter. Ass.for Hydraulic Research,**Vol.5, 1965.

9. Michel,B. and Toussaint N., Mechanisms and Theory of Indentation of Ice Plates, **Journal of Glaciology 19,**no.81,1977.

10. Michel,B., **Ice Mechanics,** Les Presses de L'Université Laval, Quebec, 1978.

11. Neill,C.R., Dynamic Ice Forces on Piers and Piles, An assessment of Design Guidelines in the Light of Recent Research, **Canadian Journal of Civil Engineering,** Vol.3, 1976.

12. Per M.Bruun and P.Johannesson, The Interaction Between Ice and Coastal Structures, **Conf. on Port and Ocean Engineering under Arctic Conditions,** Tech.Univ.of Norway, 1971.

13. Peyton,H.R., Ice and Marine Structures, **Ocean Industry,**(3),no.3,9 and 12,1968.

14. Schwartz,J., The Pressure of Floating Ice-Fields on Piles, **IAHR, Symp. on Ice and Its Action on Hydr.Structures,** Reykjavik 1970.

15. Starosolszky, J., Ice in Hydraulic Engineering, **Techn.Univ. of Norway,** Trondheim, 1968-1969.

16. Weeks,W.F. and D.L. Anderson, Experimental Study of Strength of Young Sea Ice, **Am. Geophysical Union,** Trans., Vol.39, no.4, 1958.

17. Ice Pressures Against Dams, A Symposium .1954, **Trans.Am.Soc.Civil Eng.,**119.

18. Standarization of Testing Methods for Ice Properties, Working Group of the IAHR Section on Ice Problems, **Journal Hydraulic Research** (IAHR) Vol.18,no.2.1980.

19. --------(1977). **4th International Conference on Port and Ocean Engineering under Arctic Conditions.** Newfoundland, Canada, 1977.

20. Carstens, T. Working Group on Ice Forces on Structures (T, Carstens, Editor) Special Report 80-26, **IAHR, section on ice problems,** 1980.

J.K. Nieuwenhuis

2.4.4. Earthquake induced loads

Introduction

In some areas of the world (fig. 2.4.4.1) construction has to withstand additional loads due to the occurrence of earthquakes. Many phenomena may cause earthquakes, e.g. volcanic activity or explosions, but the most important earthquakes

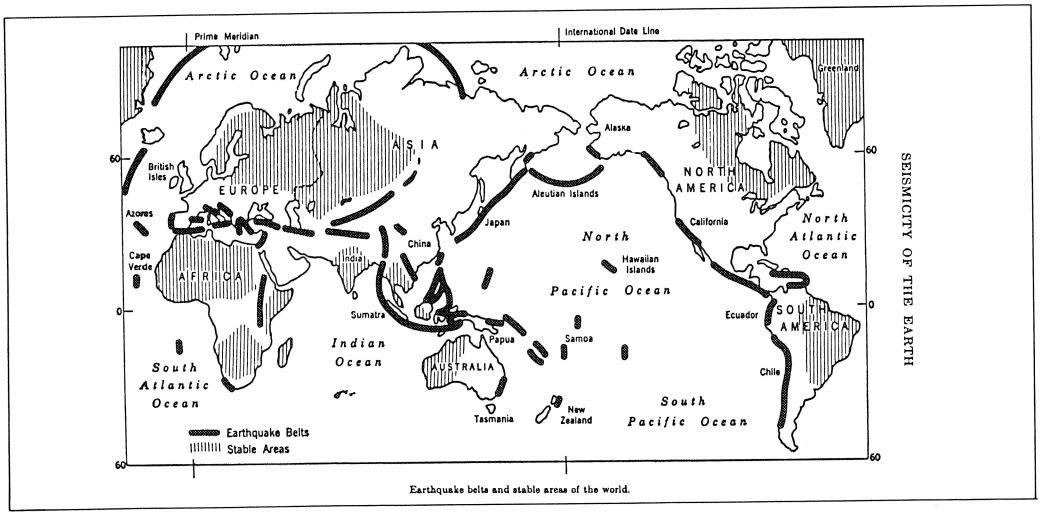

Figure 2.4.4.1 Earthquake belts and stable areas of the world

are of tectonic origin. These tectonic earthquakes are associated with large-scale strains in the earth's crust.
Earthquakes can also be induced e.g. by a large water-reservoir, which is or has been created behind a recently built dam.
The point in the crust of the earth where the first seismic waves originate is called the hypocenter and the vertical projection of this point on the earth's surface is the epicenter. (see fig. 2.4.4.2). The location of a hypocentre is determined by mathematical analysis of travel lines of compressional or P and shear or S-waves. Thus:

$$T = \frac{S}{V_s} - \frac{S}{V_p} = S\left(\frac{1}{V_s} - \frac{1}{V_p}\right)$$

where

S = distance of observation point from hypocentre
V_s = velocity of S-waves
V_p = velocity of P-waves
T = difference in arrival time between P and S waves ($V_p > V_s$)

For the design of a man-made structure such as dams in an earthquake affected region the most difficult question is to assess the earthquake risk and to translate the event into a „design earthquake" or rather into an appraisal and analysis of soil-structure interaction during seismic events and to predict the effect of ground shaking on site conditions.

Description of earthquake waves

The seismic waves that emanate from earth-

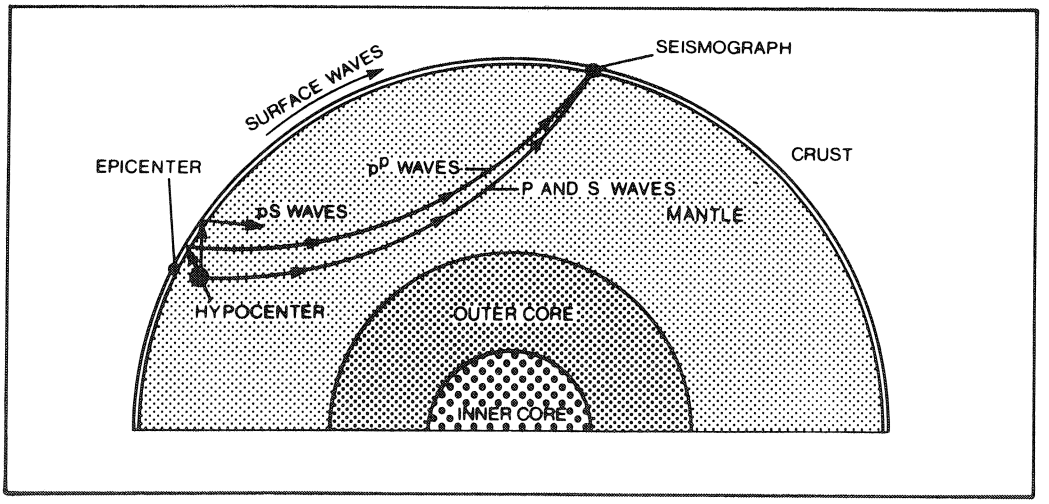

Figure 2.4.4.2 PATHS OF SEISMIC WAVES are traced on a cross section of the earth. Body waves from an earthquake or an explosion travel through the crust and mantle along the curved paths labeled P, S, pP am pS. A pP wave is a compressionel wave that is produced by the reflection of a P wave from the surface of the earth just above an earthquake or an explosion; a pS wave is a shear wave that results from the conversion of part of the compressional energy of an upward P wave into transverse energy as the P wave is reflected from the surface. Surface waves such as rayligh waves and Love waves diminish rapidly in amplitude with increasing depth. The hypocenter is the focal point of an earthquake or an underground explosion from which the waves radiate. The epicenter is the point on the earth's surface directly over the hypocenter.

quake sources can be approximately divided into two types of waves, body waves and surface waves, and it is the relative proportions of these two waves that determine the general character of earthquake ground motions.
Body waves consist of compressional (P) and shear (S) waves, which radiate in all directions from earthquakes and whose propagation paths follow the laws of geometric optics at high frequencies.

Because body waves radiate in all directions from earthquakes, the energy carried in a body wave decays as $1/r^2$, where r is distance along the propagation path, neglecting reflections and ray focusing and defocusing caused by variations in velocity structure along the path, and neglecting anelastic dissipation. Surface waves, on the other hand, are waves that are trapped on surfaces of major velocity discontinuities in the earth and cannot be observed far from the interfaces. On land the major discontinuity along which surface waves propagate is the earth's surface, although at sea surface waves can propagate along the sea floor. Because these waves spread along a surface, the energy they carry decays approximately as $1/r$.
Consequently, at a large epicentral distance they may be the dominant wave observed. In general, surface waves start to become important at epicentral ranges which exceed three times the earthquake depth.
Surface waves with a tremor period of 0.1 to 5 seconds have the greatest impact on structures.

In an earthquake an enormous amount of energy is released. A measure of this released energy is the magnitude, usually given on the scale of Richter. The formula by which magnitude may be calculated was devised by by Richter [1] and depends upon the amplitude of the maximum

seismic wave recorded on a special seismograph. It is precisely defined as „the logarithm (to base 10) of the maximum seismic wave amplitude (in thousands of millimeter) recorded on a special seismograph called the Wood-Anderson at a distance of 100 km from the earthquake epicentre". Magnitudes may be expressed as Richter magnitude and range from 0 to almost 9. Commonly the lowest magnitude recorded by conventional seismologists is about 2 which represents something close to the smallest earthquake that can be felt by human beings. Annually there are some 18000 to 22000 earthquakes of magnitude 2.5 or greater.

The determination of the damage under earthquake loading proceeds along a number of different steps:

a The source function: determination of the seismicity in the region as a function of location, time and magnitude and the correlation with other zones of recent tectonic motions.
b The medium: determination of the influence of the medium on the dampening of the motions in relation to the epicentral distance.
c The seismic risk: determination of the relationship between earthquake parameters and the probability of occurrence of specific intensities, accelerations, velocities and motions.
d The local subsoil: determination of the influence of the subsoil structure on shape and magnitude of the incoming signal.
e The frequency characteristics of the structure to be built. These properties to a large extent determine the vulnerability of the structure for the incoming earthquake signal as modified by the local subsoil.

Items a, b and c belong to the domain of the seismologist in cooperation with the geologist, for item d the soil engineer is responsible and item e belongs to the constructor.

For the determination of the ultimate risk involved not only the occurrence of a specific acceleration but also the value and vulnerability of the structure and the loss in case of damage should be taken into account.

Risk : Probability x value x vulnerability

This relationship shows for example that the risk for a single building has a different value from that for a whole town.
To obtain the latter risk all the individual risks for separate structures should be summed.
Consequently, for a dike not only the value of the structure itself should be taken into account, but also the value of the hinterland.

Impact of earthquakes on structures

In the foregoing section earthquake phenomena were explained briefly.
For the design of a man made structure in an earthquake affected region the most difficult question is to assess the earthquake risk and to translate that risk into a „design earthquake" or rather into an appraisal and analysis of soil-structure interaction during seismic events and also to predict the effect of ground-shaking on site conditions with emphasis on phenomena such as liquefaction, consolidation and slope failures.

The most important limit states in the analysis of a dam, dike or embankment are:

- instability as a result of a fault on which the dam is built
- sliding of the slope as a result of subsoil tremor.
- progressive development of piping as a result of loss of cohesion of the foundation or interior of the dam or through cracks induced by the earthquake motions.
- overtopping of the dam as a result of seiches or surges induced by an underwater earthquake at sea or induced by a large soil mass sliding into a reservoir behind the dam.

Fig. 2.4.4.3 presents the procedure of risk-analysis according to Chaplow [3], which can be summarised as follows:

a) Initial assessment from the atlas of Crampin et al [2]
b) A check to see if the area is covered by an earthquake code
c) Collection of teleseismic events from international agencies and local records
d) Geological study to reveal active faults and

types of strata that could cause magnification

e) Establishment of a local network of seismic monitoring stations.

Methods to analyse stability

There are two major mechanisms, which will negatively affect the stability of a structure (i.e. a dam) during an earthquake.

Figure 2.4.4.3 Methodology for defining seismic risk at dam sites

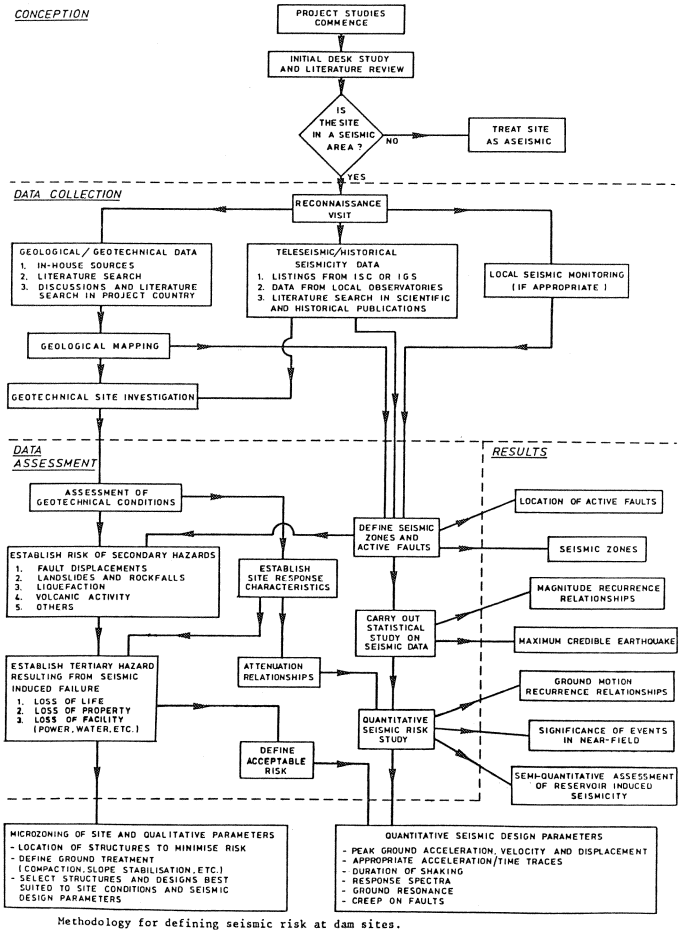

Methodology for defining seismic risk at dam sites.

These are:
- additional inertial forces will act on the structure because of groundmotion.
- soil material, in or underneath the structure, may loose its bearing capacity permanently or temporarily.

The first mechanism is taken in consideration through the pseudo-static analysis of the stability of the structure. The second mechanism must be determined by an analysis of the dynamic behaviour of the soil with emphasis on the reduction of shear strength and the liquefaction potential of the granual soils.
In designing structures like earth dams these mechanisms cannot be left out [4] and [5].
In the 19th Rankine Lecture given by Seed [6] an outstanding and comprehensive „state of the art" on earthquake-resistant designing is presented. Some aspects of this lecture are presented in the following section.

Method of pseudo-static analysis of the safety of earth dams

For the past 40 years or more, the standard method of evaluating the safety of earth dams against sliding during earthquakes has been the so-called pseudo-static method of analysis in which the effects of an earthquake on a potential slide mass are represented by an equivalent static horizontal force determined as the product of a seismic coefficient, k or n_g, and the weight of the potential slide mass, as illustrated in Fig. 2.4.4.4 Terzaghi [7] described the method in the following words:

„An earthquake with an acceleration equivalent n_g produces a mass force acting in a horizontal direction of intensity n_g per unit of weight of the earth. The resultant of this mass force, n_g W, passes like the weight W, through the centre of gravity O_1 of the slice abc. It acts as a leverarm with length F and increases the moment which tends to produce a rotation of the slice about the axis O by n_gFW. Hence the earthquake reduces the factor of safety of the slope with respect to sliding from G_s ($G_s = \frac{s.l.R}{E.W.}$) to:

$$G' = \frac{s\ l\ R}{E_W + n_g F_W}$$

Figure 2.4.4.4 Convenient method for computing effect of earthquake on stability of a slope (after Terzaghi, 1950)

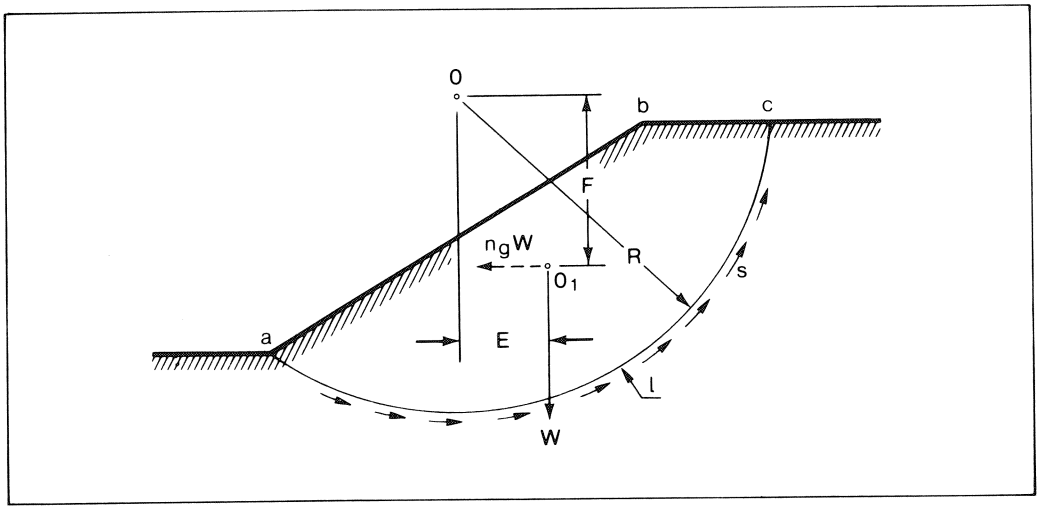

The numerical value of n_g depends on the intensity of the earthquake.
Independent estimates (Table 2.4.4.1) have led to the following approximate values:

Severe earthquakes, Rossi-Forel scale IX: $n_g = 0.1$
Violent, destructive, Rossi-Forel scale X: $n_g = 0.25$

Table 2.4.4.1 Approximate relationships, earthquake intensity, acceleration, and magnitude

Rossi-Forel Intensity Scale (1883)	Modified Mercalli Intensity Scale (1931, Wood and Neumann)
	1. Detected only by sensitive instruments
I The shock felt only by experienced observer under very favorable conditions	2. Felt by few persons at rest, especially on upper floors; delicately suspended objects may swing
II Felt by a few people at rest: recorded by several seismographs	3. Felt noticeably indoors; but not always recognized as earthquake; standing autos rock slightly; vibration like passing truck
III Felt by several people at rest; strong enough for the duration or direction to be appreciable	4. Felt indoors by many, outdoors by few; at night some awaken; dishes, windows, doors disturbed; motor cars rock noticeably
IV Felt by several people in motion; disturbance of moveable objects; cracking of floors	5. Felt by most people; some breakage of dishes, windows, and plaster; disturbance of tall objects
V Felt generally by everyone; disturbances of furniture; ringing of some bells	6. Felt by all; many frightened and run outdoors; falling plaster and chimneys; damage small
VI General awakening of those asleep; ringing of bells; swinging chandeliers; startled people run outdoors	7. Everybody runs outdoors; damage to buildings varies depending on quality of construction; noticed by drivers of automobiles
VII Overthrow of moveable objects; fall of plaster; ringing of bells; panic, without great damage to buildings	8. Panel walls thrown out of frames; fall of walls, monuments, chimneys; sand and mud ejected; drivers of autos disturbed
VIII Fall of chimneys; cracks in walls of buildings	9. Buildings shifted off foundations, cracked, thrown out of plumb; ground cracked; underground pipes broken
IX Partial or total destruction of some buildings	10. Most masonry and frame structures destroyed; ground cracked; rails bent; landslides
X Great disasters; ruins; disturbance of strata; fissures; rockfalls; landslides, etc.	11. Few structures remain standing; bridges destroyed; fissures in ground; pipes broken; landslides; rails bent
	12. Damage total; waves seen on ground surface; lines of sight and level distorted; objects thrown up into air

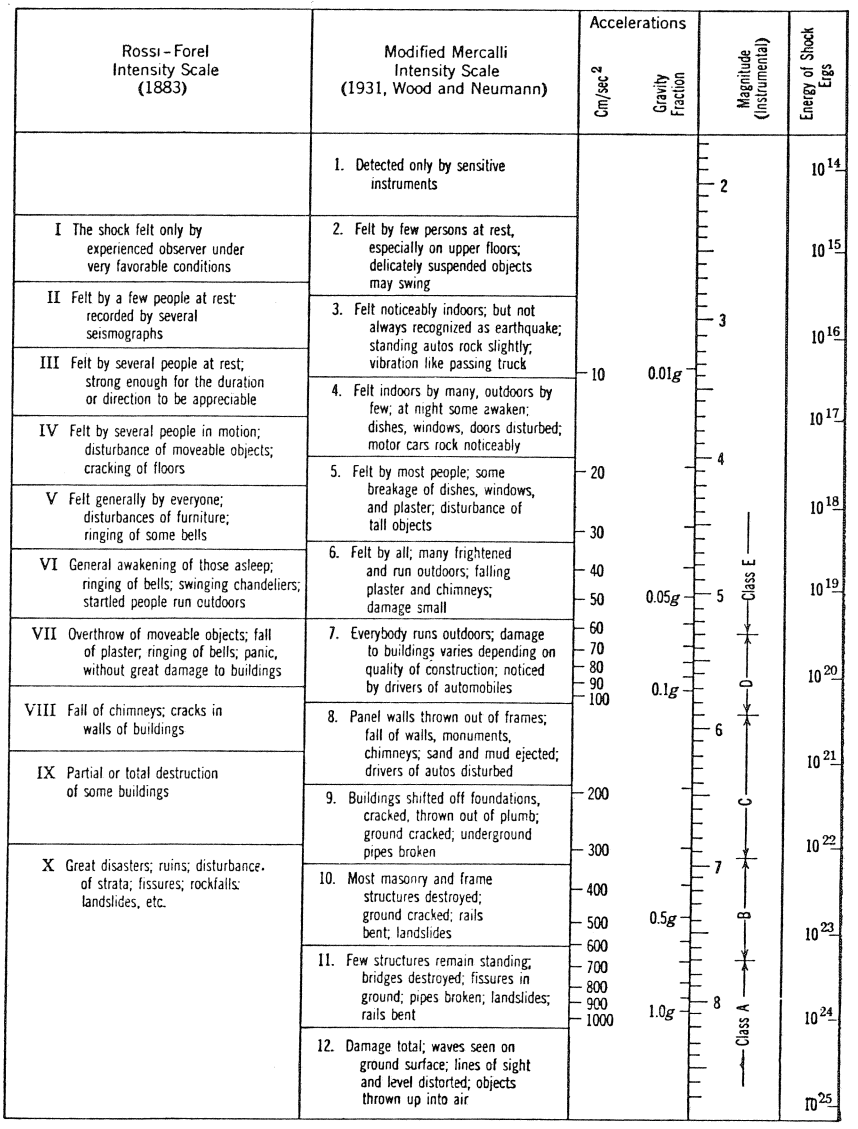

Catastrophic: $n_g = 0.5$

The theory is based on the simplifying assumptions that the horizontal acceleration $n_g g$ acts **permanently** on the slope material and in **one direction only.** Therefore the concept it conveys of earthquake effects on slopes is very inaccurate, to say the least. Theoretically a value of $G_s = 1$ would mean a slide, but in reality a slope may remain stable in spite of G_s being smaller than unity and it may fail at a value of $G_s > 1$, depending on the character of the slope-forming material.

Detailed studies of the failures of dams during earthquakes seem to provide convincing evidence of Terzaghi's original statement that the pseudo-static method of analysis is not necessarily indicative of the seismic stability of an embankment dam even if the computed factor of safety exceeds unity.

The general conclusion which seems to follow from the close study of embankment dam performance during earthquakes is as follows:

- hydraulic fill dams have been found to be vulnerable to failures under unfavourable conditions - in particular shaking produced by strong earthquakes;
- many hydraulic fill dams, however, have performed well for many years and when they are built with reasonable slopes on good foundations they can survive moderately strong shaking - say up to about 0.2 g from magnitude 6.5 to 7 earthquakes with no harmful effects;
- virtually any well built dam can withstand moderate earthquake shaking, say with peak accelerations of about 0.2g and more, with no detrimental effects;
- dams constructed of clay soils on clay or rock foundations have withstood extremely strong shaking ranging from 0.35 to 0.8g from a magnitude 8.25 earthquake with no apparent damage;
- two rockfill dams have withstood moderately strong shaking with no significant damage and if the rockfill is kept dry by means of a concrete facing they should be able to withstand extremely strong shaking with only small deformations;
- since there is ample field evidence that well built dams can withstand moderate shaking with peak accelerations up to at least 0.2 g with no harmful effects, we should not waste our time and money analysing this type of problem but should concentrate our efforts on those dams likely to present problems either because of strong shaking or because they incorporate large bodies of cohesionless materials (usually sands) which, if saturated, may lose most of their strength during earthquake shaking and thereby lead to undesirable movements;
- for dams constructed of saturated cohesionless soils and subjected to strong shaking, a primary cause of damage or failure is the build-up of pore water pressures in the embankment and the possible loss of strength which may accrue as a result of these pore pressures. Great caution is required in attempting to predict this type of failure by pseudostatic analysis, and dynamic analysis techniques seem to provide a more reliable basis for evaluating field performance, and,
- the fact that a number of dams have failed in periods up to 24 h after an earthquake suggests that piping through cracks resulting from earthquake shaking may well have been responsible for the failure. This fact reemphasizes the need to provide an adequate system of filter materials in constructing dams in seismic regions to ensure that progressive erosion through continuous cracks cannot occur.

So there is a very clear difference between the seismic resistance of dams constructed of clayey soils and those constructed of saturated sands or other cohesionless soils. For example, it is noteworthy that no failures have been reported in dams built of clayey soils even under the strongest earthquake shaking conditions imaginable, and that all cases of slope failure reported have involved sandy soils. This is also apparent in laboratory tests on soils subjected to cyclic loading. In general, while some types of clay show a degradation in strength due to cyclic loading, samples of clay of the type used

for dam construction do not seem to show significant changes in pore water pressure due to cyclic loading with numbers of cycles of the order of those produced by earthquakes, and the strength of the soil, both in terms of peak strength and residual strength, does not seem to change appreciably as a result of the earthquake type loading.

It is also of special interest that embankment failures are reported to have occurred some time after the earthquake motions had ceased. This may have been due to the progressive development of piping through cracks induced by the earthquake motions but it may also have been due to the time required for a redistribution of pore water pressures to bring about a failure condition. In any case it suggests that post-earthquake stability is a major factor to be considered in evaluating the earthquake resistance of embankment dams.

A knowledge of field performance data of this type can provide a valuable supplement to analytical studies in the final assessment of the seismic stability of an earth dam and in some cases can eliminate entirely the need for analytical studies. In fact such knowledge of past performance, combined with guidance provided by dynamic analysis when appropriate, and the application of good judgment are the tools required to reach final decisions on the seismic stability of dams at the present time; with the aid of such information, it should indeed be possible to provide a higher degree of safety of dams against the damaging effects of earthquakes than ever before possible.

Procedures involving dynamic analyses of embankments:
In recent years procedures have been developed to predict the dynamic behaviour of embankments due to earthquakes.
In the Rankine Lecture of 1965, Newmark [8] first proposed the basic elements of a procedure for evaluating shaking. In this important development he envisaged that slope failure would be initiated and movements would begin to occur if the inertia forces on a potential slide mass were large enough to overcome the yield resistance and that movements would stop when the inertia forces were reversed. Thus by computing an acceleration at which the inertia forces become sufficiently high to cause yielding to begin, and integrating the effective acceleration on the sliding mass in excess of this yield acceleration as a function of time, velocities and ultimately displacements of the slide mass could be evaluated. The method has proved to be particularly useful in cases where the yield resistance of the soil can be reliably determined, as in Fig. 2.4.4.5 for example, and therefore for the analysis of situations where pore water pressures do not change significantly as the earthquake motions continue or shear displacements occur.

By examining the dynamic response of embankments it has been found that the effective peak accelerations on a potential slide mass decreases with increasing depth of the slip surface within the embankment and that values of effective peak acceleration k_m or k_{max} on slide masses extending to different depths within an embankment can be estimated by curves such as those shown in Fig. 2.4.4.6 [9]. In this figure k_m is expressed as a fraction of the peak acceleration developed at the crest of the embankment, ü max.
Once such values have been established, together with a value for the acceleration causing yielding of the soil to occur, k_y, it is a relatively simple matter of double integration to determine the displacements that will develop for representative forms of earthquake motions.
Computations of this type have been made by Ambraseys, Sarma and Makdisi and Seed for earthquakes having a magnitude of about 6,5 and the results are remarkably similar as shown in Fig.2.4.4.7.

With the aid of charts such as those shown in Figs. 2.4.4.6 and 7 it is a relatively simple matter to evaluate potential displacements during shaking for embankments in which the yield acceleration is reasonably **constant.**
Typical examples of computed displacements for earth embankments which do not lose more than 15% of their original strength during earthquake shaking (i.e. many clayey soils, some

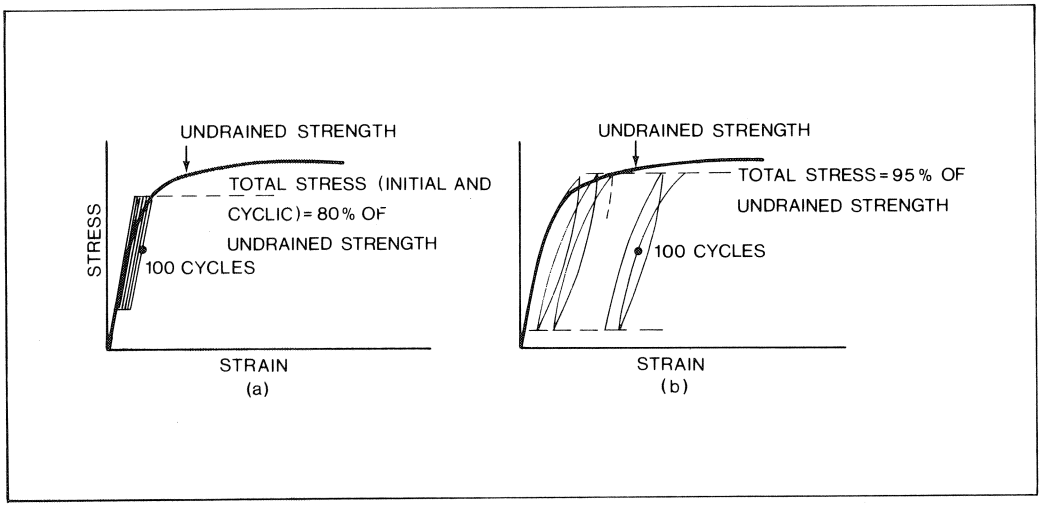

Figure 2.4.4.5 Determination of yield stress for sample of clay

Figure 2.4.4.6 Comparison of several attennation expressions

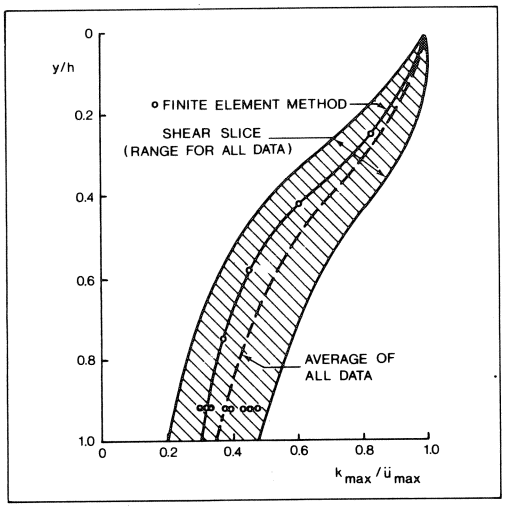

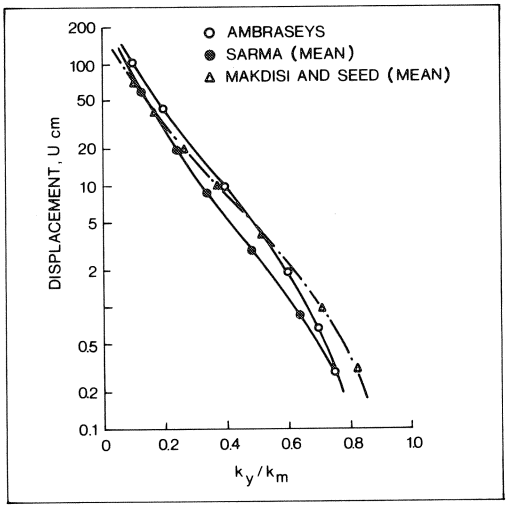

Figure 2.4.4.7 Computed displacements of embankment dams objected to magnitude 6 earthquakes for sorts having little or no strength loss due to earthquake-induced deformations

Table 2.4.4.2 Probable upper bound displacements for embankment dams subjective to magnitude 6,5 earthquakes (little or no strength loss).

	Crest acceleration	km	Factor of Safety (FS) = 1-15 for k = 0.05 15% strength loss	FS = 1.15for k = 0.1 15% strength loss	FS = 1.15 for k = 0.1 No strength loss
	1.0g	≈0.4	≈4.0 ft	≈1.8 ft	≈1.0 ft
Probable upper bound of accelerations for most earth dams	0.75 g	≈0.3	≈2.7 ft	≈1.2 ft	≈6.0 in.
	0.50 g	≈0.2	≈1.7 ft	≈6.0 in.	≈1.0 in.
	0.25 g	≈0.1	≈6.0 in.	0	0

Probable upper bound dispacements for embankment dams subjected to magnitude 8¼ earthquakes (little or no strength loss)

	Crest acceleration	km	Factor of Safety (FS) = 1.15 for K = 0.1 15% strength loss k, = 0.10	FS = 1.15 for K = 0.15 15% strength loss k, = 0.15	FS = 1.15 for K = 0.15 No strength loss k, = 0.20
	1.00 g	≈0.4 ft	≈17 ft	≈7 ft	≈3 ft
Probable upper bounds of accelerations for most earth dams	0.75 g	≈0.3	≈10 ft	≈3 ft*	≈8 in.*
	0.50 g	≈0.1	≈3 ft*	≈4 in.*	0*
	0.25 g	≈0.1	0*	0*	0*

* Acceptable performance.

dense saturated sands and clayey sands) are shown in Tables 2.4.4/2. It may be seen that if the soil does not build up large pore pressures and change strength substantially during shaking and if the embankment is initially designed to withstand an inertia force of about 0.1 or 0.15 g without yielding, the computed displacements for most earthquakes producing crest accelerations less than about 0.75 g are within acceptable limits.

If this is in fact the case, then to ensure acceptable performance it is only necessary to perform a pseudo-static analysis for a seismic coefficient of 0.1 g for magnitude 6,5 earthquakes (0.15 g for magnitude 8 earthquakes) and obtain a factor of safety of the order of 1.15 to ensure that displacements will be acceptably small.

Thus the application of this procedure will invariably result in tolerable displacements if the pseudo-static analysis procedure is followed for the criteria shown in Table 2.4.4.3 and if the soils do not lose more than 15% of their initial strength due to earthquake shaking and associated displacements or build up large pore pressures.

Seed-Lee-Idriss analysis procedure

In recognition of the limitations of the pseudo-static analysis approach and the difficulties of evaluating a yield stress criterion for many saturated cohesionless soils, an alternative approach to the evaluation of deformations in earth dams was developed. The details of the general procedure have undergone many improvements since that time [10], primarily through the development and application of finite element procedures but also through the development of improved testing procedures.

In spite of the improvements, however, the basic principles of the procedures have remained unchanged and involve a series of steps which might be summarised simply as follows:

(a) Determine the cross-section of the dam to be used for analysis.

Table 2.4.4.3 Design criteria: for embankment constructed of soils which do not build up large pore pressures due to earthquake shaking or show more than 15% strength loss (usually cohesive soils such as clays, silty clays, sandy clays or very dense cohesionless soils), based on acceptable deformations due to earthquake shaking crest acceleration less than 0.75 g.

Earthquake magnitude	Design criteria
6,5	FS = 1.15 for seismic coefficient = 0.1
8	FS = 1.15 for seismic coefficient = 0.15

(b) Determine, with the cooperation of geologists and seismologists, the maximum time history of base excitation to which the dam and its foundation might be subjected.

(c) Determine, as accurately as possible, the stresses existing in the embankment before the earthquake; this is probably done most effectively at the present time using finite element analysis procedures.

(d) Determine the dynamic properties of the soils comprising the dam, such as shear modulus, damping characteristics, bulk modulus or Poisson's ratio, which determine its response to dynamic excitation.
Since the material characteristics are non-linear, it is also necessary to determine how the properties vary with strain.

(e) Compute, using an appropriate dynamic finite element analysis procedure, the stresses induced in the embankment by the selected base excitation.

(f) Subject representative samples of the embankment materials to the combined effects of the initial static stresses and the superimposed dynamic stresses and determine their effects in terms of the generation of pore water pressures and the development of strains.
Perform a sufficient number of these tests to permit similar evaluations to be made, by interpolation, for all elements comprising the embankment.

(g) From the knowledge of the pore pressures generated by the earthquake, the soil deformation characteristics and the strength characteristics, evaluate the factor of safety against failure of the embankment either during or following the earthquake.

(h) If the embankment is found to be safe against failure, use the strains induced by the combined effects of static and dynamic loads to assess the overall deformations of the embankment.

(i) Be sure to incorporate the requisite amount of judgement in each of steps (a) to (b) as well as in the final assessment of probable performance, being guided by a thorough knowledge of typical soil characteristics, the essential details of finite element analysis procedures, and a detailed knowledge of the past performance of embankments in other earthquakes.

This procedure lends itself naturally, however, to somewhat simplified versions of the method, which have often been used for reason of time and economy.

The ultimate simplification is, of course, the total elimination of all analysis procedures and a simple evaluation, based on a knowledge of the materials comprising the dam and the judgement resulting from conducting many previous analyses and observing the performance of existing dams.
In the most modern versions of the method, the assessment of pore water pressures during and following an earthquake shaking may involve studies of simultaneous pore pressure generation and dissipation.
The particular procedure used in any given case should depend on the complexity of the case being considered, the margin of safety provided for, the level of earthquake shaking likely to develop, and the judgement and experience of the engineer responsible for the study.

References

1. Gutenberg, B. & Richter, C.F.,: **Seismicity of the earth,** Princeton University Press, 1954., 2nd ed., 310 pp.

2. Crampin, S., Fyfe, C.J., Bickmore, D.P. & Linton, R.H.W.: Atlas of Seismic Activity 1909 - 1968, **Seismol. Bull. Inst. Geol. Sci.,** No. 5, 1976., HMSO

3. Chaplow, R.,: The definition of seismic risk at dam sites. **Proc. Conf. Design of Dams to Resist Earthquake.** Instn. Civ. Engrs., London, 1980, pp. 7-13

4. Ambraseys, N.N. 1960: The seismic stability of earth dams, **Proc. 2nd World Conf. on Earthquake Engineering,** Vol.1, pp. 1960 331-356

5. Sherard, J.L., Woodward, R.J., Gizinski, S.F. and Clevenger W.A. **Earth and Earthrock Dams,** John Wiley, N.Y. 1963.

6. Seed, H.B. 1979 Considerations in the earthquake-resistant design of earth and rockfill dams, **Geotechnique,** Vol. 29 No. 3, 1979, pp. 215-263.

7. Terzaghi, K. 1950, **Mechanisms of landslide.** The geological survey of America, Engineering Geology.

8. Newmark, N.M. 1965. Effects of earthquakes on dams and embankments, **Geotechnique** 15, No. 2, 1965, 139-160.

9. State of California Dept. of Water Resources (1979). The August 1, 1975 Oroville Earthquake investigations, **Department of Water Resources Bulletin,** No. 1979, 203-278.

10. Seed, H.B., Duncan, J.M. & Idriss, I.M., **Criteria and Methods for Static and Dynamic Analysis of Earth Dams, Criteria and Assumptions for Numerical Analysis of Dams** (Naylor, D.J., Stagg. K. & Zienkiewicz, O.C., Eds). Swansea ; University College 564-588.

11. Ritsema A.,R. **On Earthquake Risk for Nuclear Power Plants** Publ. 153, K.N.M.I., de Bilt 1976.

12. Lane, R.G.T. 1979; General Report on Seismicity and Aseismic Design of Dams. **Trans. 13th Int. Congress on Large Dams,** New Delhi, Vol. 4, 1979, pp. 669-726.

13. Seed, H.B., Makdisi, F.I. & DeAlba, P. (1978). Performance of earth dams during earthquakes. **J.Geotech. Engng Div.** 104, No GT7, Proceedings Paper 13870.

14. Seed, H.B. & Martin, G.R. (1966). The seismic coefficient in earth dam design. **J. Soil Mech. Fdn Div.,** Am. Soc. Civ. Engrs 92, No. SM3, Proceedings Paper 4825, 59-83.

15. Ambraseys, N.N. & Sarma, S.K. (1967). The response of earth dams to strong earthquakes. **Geotechnique** 17, No. 3, 181-213.

16. Makdisi, F.I. & Seed, H.B. (1978). Simplified procedure for estimating dam and embankment earthquake induced deformations. **J. Geotech. Engng Div.,** Am. Soc. Civ. Engrs, 104, No GT7, Proceedings Paper 13 898, 849-867.

17. Lee, K.L. (1978). Seismic stability considerations for Tailings Dams adjacent to San Andreas Fault. **Proc. 1st Central American Conference on Earthquake Engineering,** San Salvador.

18. Seed, H.B., Lee, K.L., Idriss, I.M. & Makdisi, F.I. (1975). The slides in the San Fernando Dams during the earthquake of February 9, 1971. **J.Geotech. Engng Div.,** Am. Soc. Civ. Engrs 101, No GT7. Proceedings Paper 11449, 651-688.

J.K. Nieuwenhuis

2.4.5 Stability and deformation of closure foundations

The constructions used for the closure of sea-arms may be divided into two main types:

a. Constructions formed by a large number of small „elements" such as sand, clay, stones and blocks, or what are known as flexible constructions;
b. constructions made up of large, internally stable elements such as caissons, or what are known as rigid constructions.

In many cases a closure gap is first of all temporarily sealed by means of a construction consisting of blocks or caissons, after which these elements are incorporated into a much larger dam consisting of locally available granular or cohesive materials. Figure 2.4.5.1 shows a cross-section of a construction of this kind. The principal geotechnical aspects that must be taken into consideration in both sorts of construction are:

- stability (1)
- deformation (2).

These two phenomena are indicated in fig. 2.4.5.2. These aspects may be defined by means of various calculation methods based on the laws of soil mechanics. A number of soil parameters must be known when taking them into account.

With respect to stability calculations the most important parameters are cohesion $\bar{c}$ and the angle of internal friction ($\bar{\phi}$).
In the case of settlement calculations the coefficient of compressibility (m_v) is an important soil parameter, while permeability (k) is an important factor with respect to the time-dependent consolidation process of clay and peat.

The determination of the soil parameters and the various calculation methods are discussed below. This requires in the first place a sound understanding of intergranular stress and pore-water pressure.

Figure 2.4.5.1 Cross section of a sea dike (Brouwersdam)

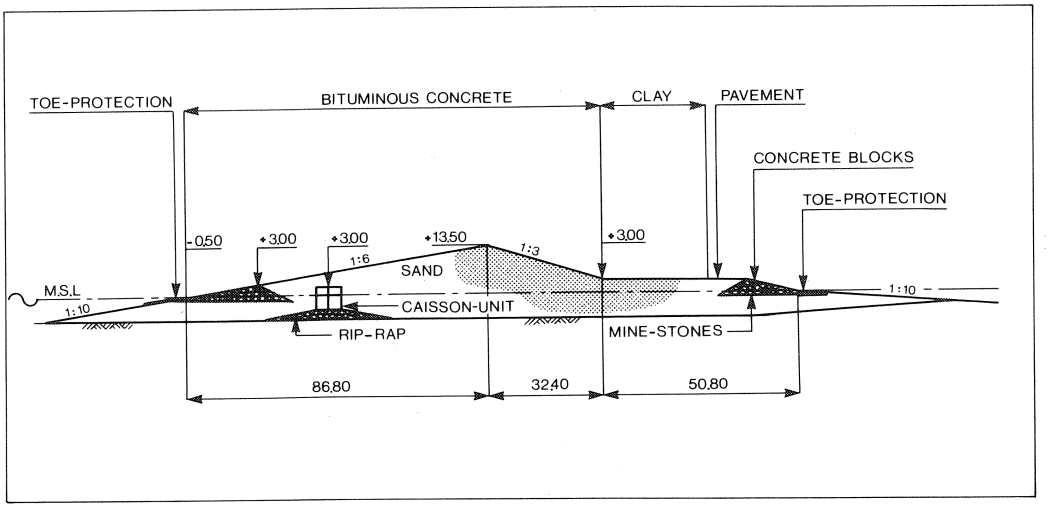

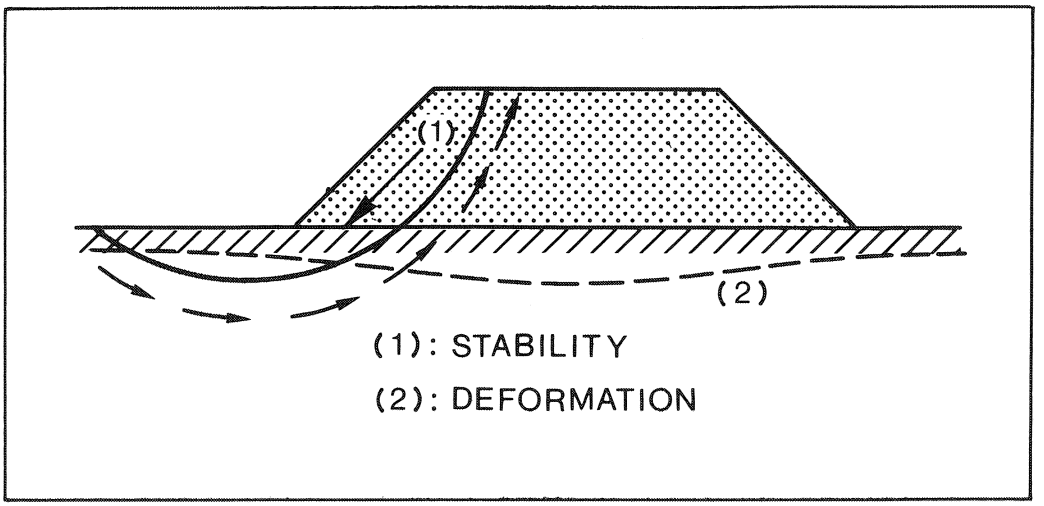

Figure 2.4.5.2 Phenomena of stability and deformation

Intergranular stress and pore-water pressure
For stability purposes, it is of great importance when constructing a dam to know the material of which the subgrade is composed. If the sub-grade consists primarily of a permeable material such as sand, the increase in stress resulting from the weight of the overlying dam will be converted almost directly into an increase in intergranular stress in the sub-grade. The pore-water pressure will not change.
If the sub-grade consists of a relatively impermeable material such as clay, the increase in stress will result in a direct increase in pore-water pressure. After the passage of time the water pressure in the sub-grade will decline as part of the pore water flows away, leading to an increase in shear strength. It follows from the above that in the case of a dam built on a sand sub-grade the safety factor against failure will not alter under unchanged conditions, whereas in the case of a dam built on clay sub-grade the safety factor will increase over time.
In the case of the layered construction of a dam it may be assumed that if the sub-grade is comparatively impermeable, there will be a certain amount of sub-grade adjustment to the increase in effective stress. The degree and speed of the adjustment may be calculated by means of consolidation theory (see 2.4.5.2).
It is also of importance to know the direct adjustment of an impermeable sub-grade to an increase in stress. This direct adjustment is affected by the presence of gas bubbles in the pore water, since a gas-water mixture is compressible. The adjustment may be calculated by means of laboraroty tests and generally amounts to 10-30% of the final increase in effective stress.

1 Stability

1.1 Soil parameters for stability calculations

A simple test for determining the shear resistance of soil is a direct shear test (see fig. 2.4.5.3).
Measurements are taken to determine the horizontal force T required to cause the soil to

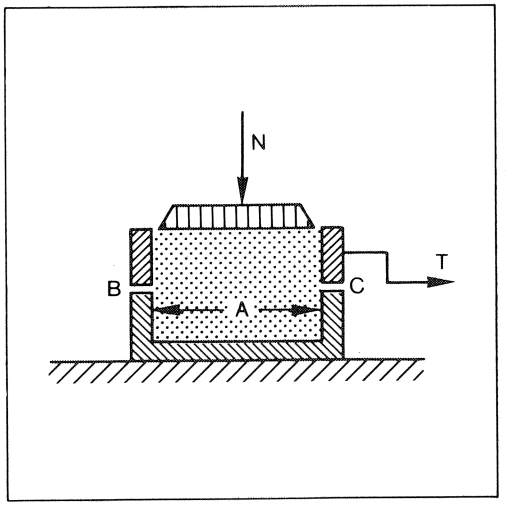

Figure 2.3.5.3 Direct shear test

Figure 2.4.5.4 Coulomb's stress-shear relation

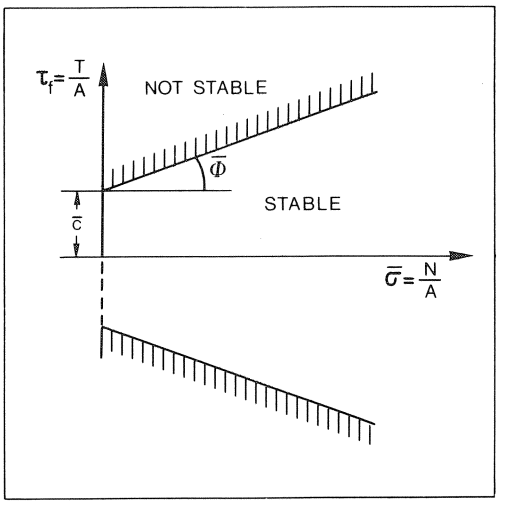

slip at various values of N. The slip is assumed to take place along the plane BC. Dividing this by the surface area A yields the normal stress $\sigma = N/A$ and the maximum shear stress $\tau_f = T/A$. If it is ensured that the pore-water pressure u during the test is equal to zero, the resultant normal stress σ will be equal to the intergranular stress $\bar{\sigma}$. If the related values for $\bar{\sigma}$ and τ_f are plotted on a chart (fig. 2.4.5.4), the two turn out to have a linear relationship. This law, discovered by Coulomb in 1776, may be expressed by the following equation:

$$\tau_f = \bar{C} + \bar{\sigma} \tan \bar{\phi}$$

The line obtained by means of this equation represents the boundary between two areas: points in the area below the boundary line indicate stress combinations where the soil is in equilibrium, while points above the line represent stress combinations that give rise to shear. It may also be noted that a similar boundary line may be drawn below the σ – axis, in this case associated with shear in the opposite direction. This test is subject to a number of disadvantages, namely:

- the plane of shear is fixed;
  the stress conditions of the sample are not fully known.

For this reason other tests to determine shear resistance, such as the triaxial compression test, are generally carried out in the laboratory (see section 2.3.4.6). The shear strength parameter is the most important and difficult factor for stability calculations.

1.2 Stability considerations with flexible constructions

In the case of flexible closure constructions the following stability aspects have to be taken into consideration:

a. stability of the outer slope of the dam;
b. stability of a part of the dam body;
c. stability of a section of the dam located at such a depth as to include part of the subgrade.

Re. a During storms the outer slope of the dam will be attacked by waves. If the quality and dimensions of the outer slope are inadequate to resist the attack the slope will be eroded and the dam will breach.
Appropriate preventative measures must therefore be taken.
These can take various forms:

1. in the case of a sandy coastline, artificial construction of a dune profile. Wind and wave action lead to the formation of beaches running at a gentle angle (1:40) into the sea, accompanied in many cases by dune formation. In closing off a sea-arm in a dune area, a closure construction may be selected with a cross-section similar to that of a dune. The outer slope of a dam construction of this kind can be left largely unprotected as long as the erosion process during the stormy season and the natural sanding-up process in the quiet season are in equilibrium with one another.

2. installation of closed revetment.
A loss of stability may occur as the results of shearing and uplift. Shearing occurs when the shear resistance along a slope falls as the result of hydrostatic excess water pressure beneath the revetment caused by waves and the high level of the sea. In extreme cases the excess water pressure from inside the body of the dam can become so great that the revetment is pushed up. Local exceedance of the **shear criterion** will result in local tensile stresses in the revetment of unacceptable magnitude in certain circumstances. Exceedance of the **uplift criterion** will lead to tensile stresses over a large area and hence to equally unacceptable fissure formation. In both cases failure of the revetment can result in unacceptable erosion of the dam and, ultimately, to its failure. This erosion process occurs particularly rapidly in a sand body.

3. installation of an open revetment.
The advantage of an open as opposed to a closed revetment is that the build-up of excess pressure beneath the revetment is avoided.
Instability of an open revetment occurs when the large (stone) elements on the outside are removed by wave action, thus exposing the finer layers below to erosion. Instability can also be caused by inadequate operation of the filter, when the fine particles in the lowest layers wash out through the upper layers. The revetment will settle and cease to function properly, whereupon failure of the dam may occur as described under 2 above.

Re.b and c The outer slope may also be attacked even more rigorously if one of the outer layers should slip (see fig. 2.4.5.5). This phenomenon occurs when the driving moment, formed by the weight of the failure mass and the arm A, exceeds the resisting moment produced by the shear resistance along the sliding surface. Particularly after protracted high water levels, when the soil is saturated with water, the driving moment can become too large once the water level returns to normal or less than normal.

The stability of the outer slope may be ascertained by means of sliding surface calculations. For these calculations data are required on the extreme water levels, the path of the phreatic surface in the dam, pore-water pressures in the dam and subgrade and the weight by volume of the soil. Apart from these stress variables, data must also be available for the strength parameters, such as the angle of internal friction $\bar{\phi}$ and cohesion $\bar{c}$.
In many cases the sliding surface will be more or less circular, as in figure 2.4.5.6 (a). The shape of the sliding surface is, however, affected by discontinuities in the subgrade (i.e. the existence of weak layers).
In the cases of slopes of limited height, calculations have to be made on the basis of circular planes or planes made up out of straight lines. There are a large number of stability analysis methods based on:

a. a circular sliding surface, where the overall equilibrium of the potential failure mass is taken into consideration.
b. a circular sliding surface, where the potential failure mass is divided into slices, e.g. by the methods devised by Fellenius, Bishop and Spencer.
c. straight shear planes, where the potential failure mass is divided into triangles and squares.

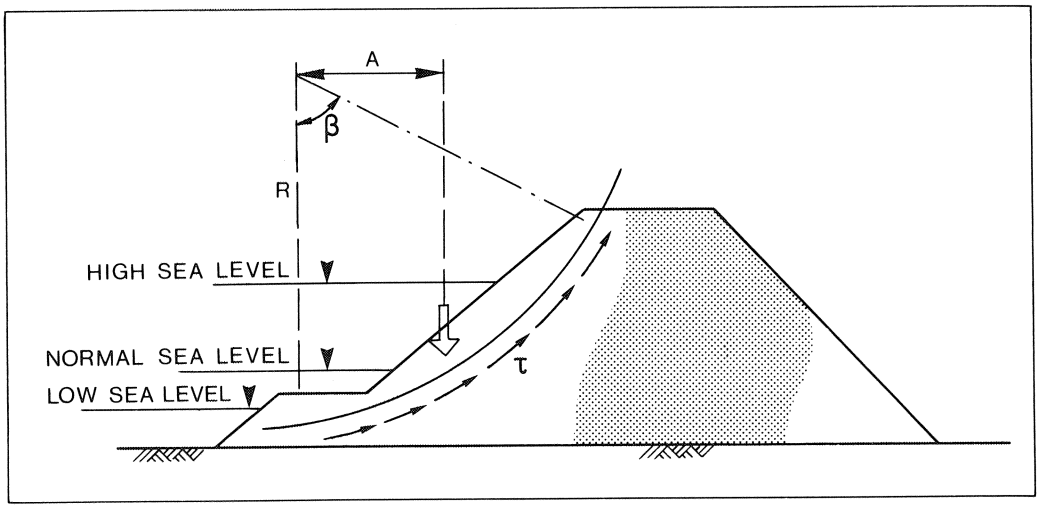

Figure 2.4.5.5 Stability under varying sea level

The last of these methods is suitable for a situation such as that shown in figure 2.4.5.4 (b). All these equilibrium calculations are based on a two-dimensional situation.

Calculation model

Special attention is given to the simplified Bishop method of slices; this method is com-

Figure 2.4.5.6 Sliding zones

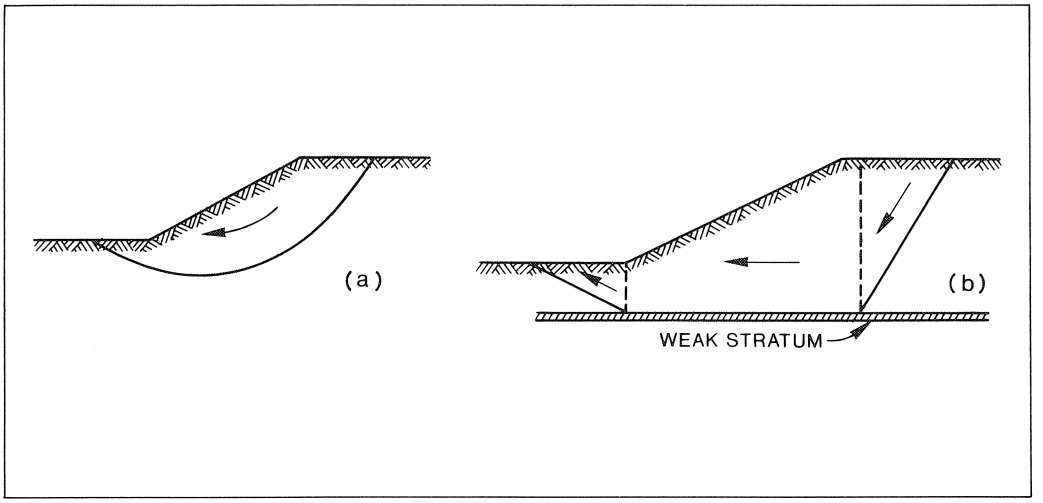

paratively easy and gives good results. The normal stress acting at a point of the failure arc should be influenced mainly by the weigth of soil lying above that point. This reasonable statement forms the basis for the method of slices. In this method the failure mass is broken up into a series of vertical slices and the equilibrium of each of these slices is considered. Figure 2.4.5.7. shows one slice with the

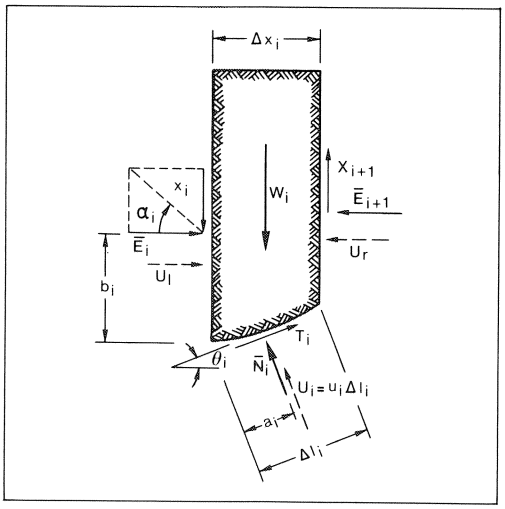

Figure 2.4.5.7 System of forces acting on a slice

unknown forces that act on it. These forces include the resultants X_i and E_i of shear and normal effective stresses along the side of the slice, as well as the resultants T_i and N_i of the shear and normal effective stresses along the failure arc. Also acting on this slice are the resultants U_l and U_r of the pore water pressures against the sides and U_l against the failure arc. These pore water pressures are assumed to be known.

In all methods, the safety is defined in terms of moments about the center of the failure arc:

$$F = \frac{M_R}{M_D} = \frac{\text{Moment of shear along failure arc}}{\text{Moment of weight of failure mass}} \quad (1)$$

The denominator is the driving moment and may be evaluated as in the next example. Note that the moment arm for the weight of any slice is equal to r. sin θ_i.

$$M_D = r \sum_{i=1}^{i=n} W_i \sin \theta_i$$

where r is the radius of the failure arc, n is the number of slices, and W_i and θ_i are as defined in Figure 2.4.5.8. Similarly, the resisting moment may be written as

$$M_R = r \sum_{i=1}^{i=n} (\bar{\sigma}_i \tan \bar{\phi} + \bar{c}) \Delta l_i =$$

$$r(\tan \bar{\phi} \sum_{i=1}^{i=n} \bar{N}_i + \bar{c}L)$$

where Δl_i is the length of the failure arc cut by the i^{th} slice and L is the length of the entire failure arc. Thus Eq. (1) becomes

$$F = \frac{\tan \bar{\phi} \sum_{i=1}^{i=n} \bar{N}_i + \bar{c}L}{\sum_{i=1}^{i=n} W_i \sin \theta_i} \quad (2)$$

Simplified Bishop Method of Slices

In this method it is assumed that the **forces acting on the sides of any slice have zero resultant in the vertical direction.** The forces $\bar{N}_i$ are found by considering the equilibrium of the forces shown in Figure 2.4.5.8.

A value of safety factor must be used to express the shear forces T_i, and it is assumed that this safety factor equals the F defined by Eq. 2 Then:

$$\bar{N}_i = \frac{W_i - u_i \Delta x_i - (\frac{1}{F}) \bar{c} \Delta x_i * \tan \theta_i}{\cos \theta_i [1 + (\tan \theta_i \tan \bar{\phi})/F]} \quad (3)$$

Combining Eqs. (2) and (3) gives

$$F = \frac{\sum_{i=1}^{i=n} [\, i\, \Delta_{x_i} + (W_i - u_i\, \Delta_{x_i}) \tan \phi][\, 1/M_i(\theta)\,]}{\sum_{i=1}^{i=n} W_i \sin \theta_i} \qquad (4)$$

where

$$M_i(\theta) = \cos \theta_i \left(\frac{1 + \tan \theta_i \tan \bar{\phi}}{F} \right) \qquad (5)$$

Equation 4 requires a trial an error solution since F appears on both sides of the equation. However, convergence of trials is very rapid. Example illustrates the tabular procedure which may be used. The chart in Figure 2.4.5.9. can be used to evaluate the function M_i.

To illustrate the simplified method of Bishop the following example is presented.
Example:
Given: the slope, failure surface, flow net and strength parameters in fig. 2.4.5.10
Find: the safety factor
Solution: the first step is to find the weigth of the free body above the failure surface. This may be done conveniently by breaking the free body into a series of vertical slices as shown in the

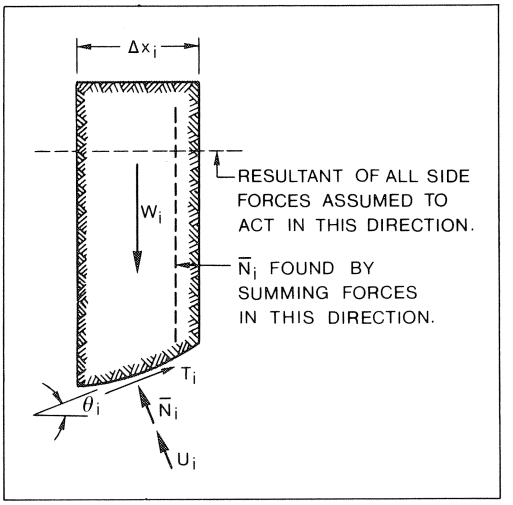

Figure 2.4.5.8 Forces considered in Bishop's simplified model of slices

Figure 2.4.5.9 Graph for the determination of $M_i(\theta)$

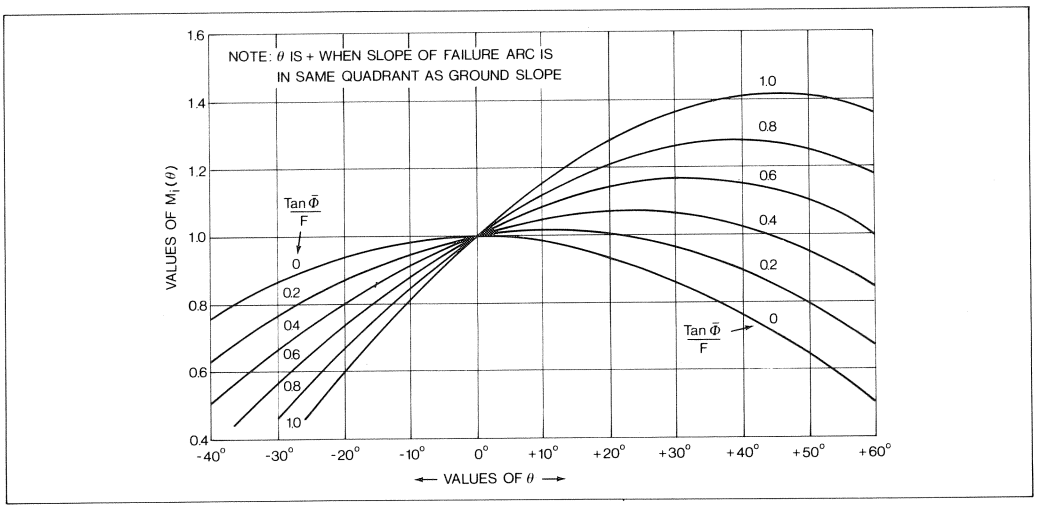

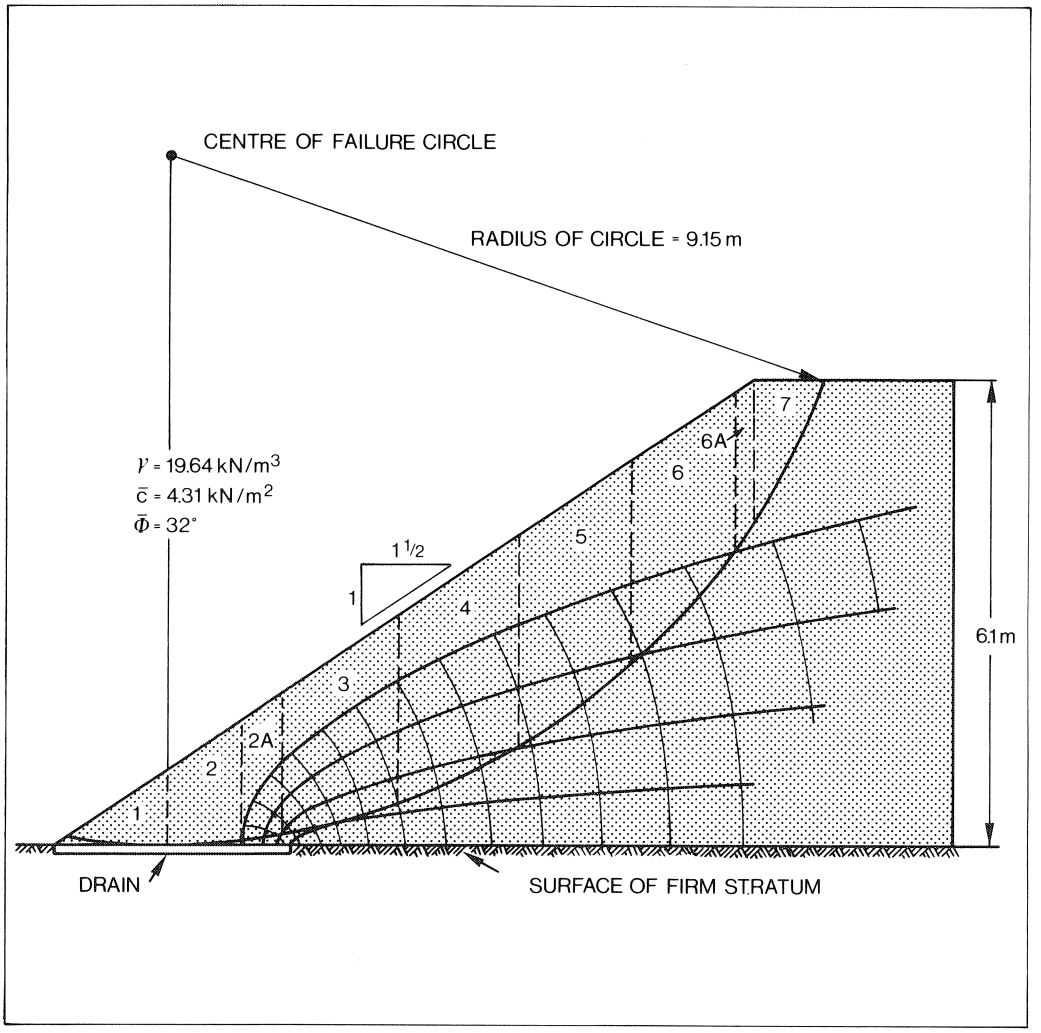

Figure 2.4.5.10 Example of slope stability

figure. Slices 2 to 6A are approximately trapezoids, and their weigth can be computed by multiplying the unit weigth of the soil times the width of the slice times the average heigth of the slice. Slices 1 and 7 may similarly be treated as triangles. The calculation of the resulting weigth is given in Table 2.4.5.1.

The next step is to determine the pore water pressure at the base of the slices. See Figure

Table 2.4.5.1 Example of the calculation of the safety factor by the simplified method of Bishop

(1) Slice	(2) Width $\triangle x_i$ (m)	(3) Average Height (m)	(4) W_i (kN)	(5) $\sin\theta_i$	(6) $W_i \sin\theta_i$ (kN)	(7) $\bar{c}_i \triangle x_i$ (kN)	(8) μ_i (kN/m)
1	1.37	0.49	13.2	−0.03	−0.4	5.9	0
2	0.98	1.28	24.6	0.05	1.2	4.2	0
2A	0.55	1.77	19.1	0.14	2.7	2.4	1.4
3	1.52	2.26	67.5	0.25	19.6	6.6	10.0
4	1.52	2.74	81.8	0.42	34.4	6.6	13.9
5	1.52	2.84	84.8	0.58	49.2	6.6	12.0
6	1.34	2.56	67.4	0.74	49.9	5.8	5.3
6A	0.18	2.04	7.2	0.82	5.9	0.8	0
7	0.98	1.16	22.3	0.87	19.4	4.2	0
					181.9		

(9) $\mu_i \triangle x_i$ (kN)	(10) = (4)-(9) $W_i - u_i \cdot \triangle x_i$ (kN)	(11) $\tan\Phi$ (kN)	(12) = (7) + (11) (kN)	(13) M_i F = 1.25	F = 1.35	(14) = (12) ÷ (13) F = 1.25	F = 1.35
0	13.2	8.3	14.2	0.97	0.97	14.6	14.6
0	24.6	15.4	19.6	1.02	1.02	19.2	19.2
0.8	18.3	11.4	13.8	1.06	1.05	13.0	13.1
15.2	52.3	32.7	39.3	1.09	1.08	36.1	36.4
21.1	60.7	37.9	44.5	1.12	1.10	39.7	40.5
18.2	66.6	41.6	48.2	1.10	1.08	43.8	44.6
7.1	60.3	37.7	43.5	1.05	1.02	41.4	42.7
0	7.2	4.5	5.3	0.98	0.95	5.4	5.6
0	22.3	13.9	18.1	0.93	0.92	19.5	19.7
						232.7	236.4

For assumed $F = 1.25$ $\quad F = \dfrac{232.7}{181.9} = 1.28$

$F = 1.35$ $\quad F = \dfrac{236.4}{181.9} = 1.30$

A trial with assumed $F = 1.29$ would give $F = 1.29$.

2.4.5.11. After this the safety factor is obtained as shown in Table 2.4.5.1.

It is necessary to make a trial and error search for the failure surface having the smallest factor of safety. When using circular failure surfaces, it is convenient to establish a grid for the centers of circles, to write at each grid point the smallest safety factor for circles centered on the grid point, and then to draw contours of equal safety factors. Figure 2.4.5.12 shows as example of contours of equal safety factor. In making

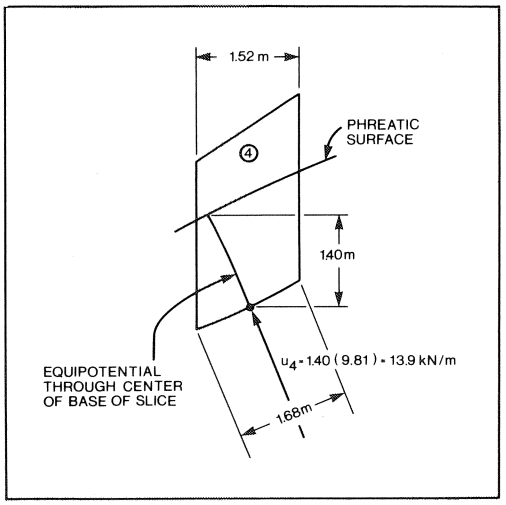

Figure 2.4.5.11 Pore-water pressure determination

Figure 2.4.5.12 Contours of safety factor

this analysis, only circles passing tangent to the underlying firm stratum were considered, but in many problems it would also be necessary to consider shallower circles.

The method of analysis described in the foregoing section considers only the stresses in a single vertical cross section through the slope. There is no rigorous method for treating three-dimensional effects. If three-dimensional effects appear to be important, the best available approach is to consider three parallel cross sections through the slope, compute the safety factor for each, and then compute a weigthed safety factor using the total weigth above the failure surface in each cross section as the weighting factor (see Figure 2.4.5.13).

Other methods of stability analysis

There are other methods of stability analysis in addition to those mentioned before. Methods have been developed for failure surfaces which are spirals (Terzaghi. 1943). A graphical version of the ordinary method of slices is often used (May and Brahtz, 1936) and is subject to all the errors and limitations of that method. Methods based upon finite difference and finite element procedures are or have been developed. The main result of studies based on such more

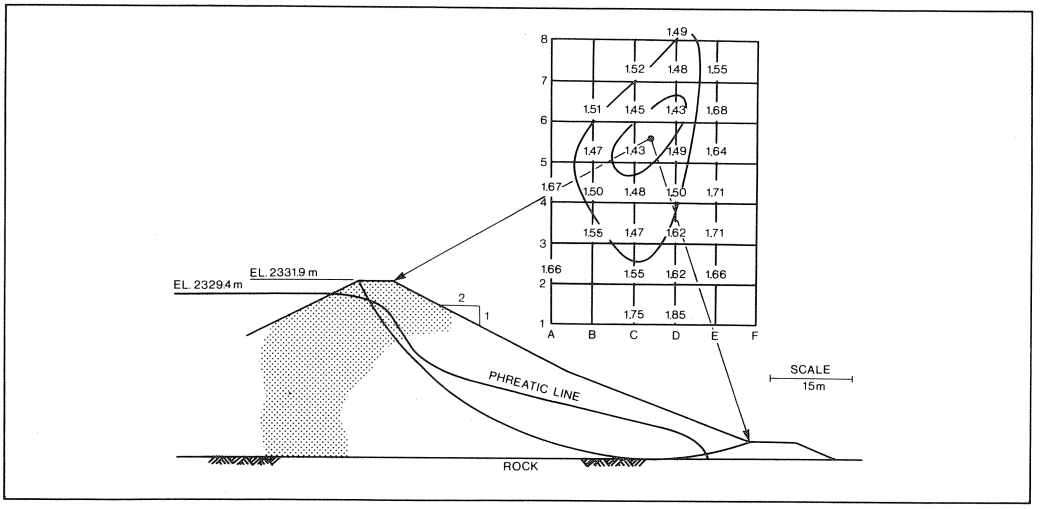

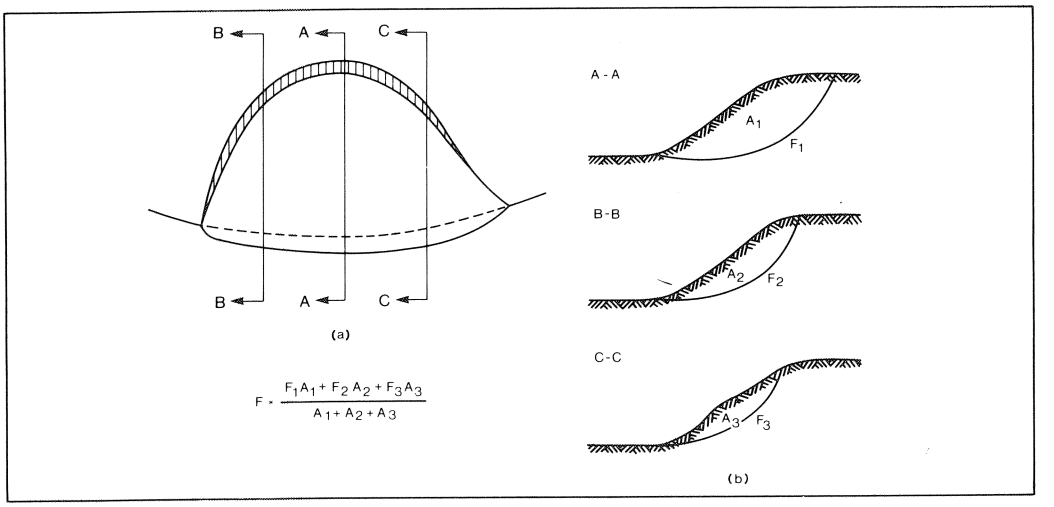

Figure 2.4.5.13 A weighed factor of safety F for a restricted failure

sophisticated methods is to learn how to use the simpler methods more effectively. With proper attention to detail, the simpler methods (Bishop's simplified method of slices, the wedge method, and sometimes the ordinary method of slices) will give safety factors within ± 10% of being correct for the assumed strength parameters. Thus the main uncertainty in slope stability analysis lies in the **proper choice of strength parameters.**

In the past, slope stability calculations have involved considerable tedium.
This situation has been relieved by the widespread availability of computers. Stability charts, giving combinations of $\overline{c}$ and $\overline{\phi}$ required for stability in typical situations, are available and are quite useful for preliminary analysis (Taylor, 1948; Bishop and Morgenstern, 1960).
In order to obtain rapid insight into the stability of a slope use may be made of a calculation method developed by Taylor. This is based on the following assumptions:

1. pore-water pressures are neglected;
2. homogeneous grain structure;
3. sliding surface takes a circular form;
4. no upper load (can be introduced however by increasing the value of H or γ).

In the calculation a distinction should be drawn between the following two cases:

1. Circular failure surfaces through the toe of the slope ($n = 0$, $D \neq 1$), where once again two situations may be distinguished, viz.:
   a) the sliding surface remains above the toe
   b) the sliding surface proceeds beyond the plane of the toe, to a depth $D \times H$ (fig. 2.4.5.14).
2. Circular failure surfaces running underneath the toe of the slope and intersecting the groundlevel ($n > 0$, $D > 1$).

Taylor has calculated the slope gradients (α) at which equilibrium is just retained for a wide variety of soil properties ($\gamma, \overline{\phi}, \overline{c}$). The values found for the most dangerous sliding surfaces have been plotted in a diagram as shown in Fig. 2.4.5.15. It may be seen from the diagram that to the left of the line $D = 1$ the sliding surfaces run through the toe while to the right of the line they

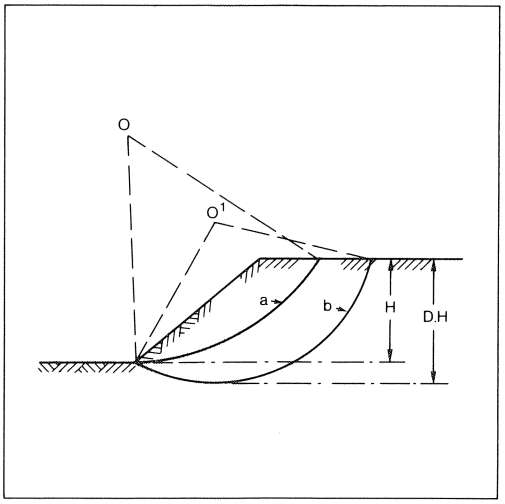

Figure 2.4.5.14 Failure zone through toe of slope

Figure 2.4.5.16 Squeezing

run underneath the toe. To the left of the line n = O the sliding surfaces start at the toe of the slope. When using the diagram for an initial survey of the stability of a slope a distinction may be drawn between three situations:

1. slopes above water
2. slopes under water
3. slopes in transitional areas.

For slopes above water, the value for the weight per unit volume is used for γ, taking account of the (air-filled) voids.

For slopes under water, allowance is made for the fact that the voids are now filled with water and for the specific mass of the grains under water. In transitional areas it is assumed that the voids are filled with water. Refinements may be introduced by making allowance for the outflow of groundwater.

Squeezing

This may be regarded as a special form of instability in which the construction as a whole is abruptly subjected to vertical displacement. Squeezing is taken to mean the lateral extrusion of very weak soil upon the imposition of a load. Squeezing may occur when constructing the foundation for a heavy engineering construction or storage tank onto a base containing a zone of very weak soil in between a more or less firm surface layer and a load-bearing layer at greater depth. In these circumstances the weak layer may be squeezed out laterally in the same way as a tube of toothpaste. The process is sometimes referred to as the ice-water effect (fig. 2.4.7.16).

Clearly, water pressures play a large part in this process: if the load is imposed quickly it will give rise to water excess pressure in the weak layer, which will in turn give rise to low sliding resistance.

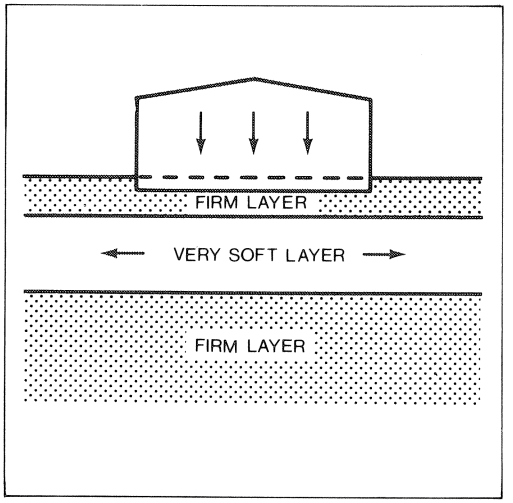

1.3 Stability aspects with rigid closure constructions

Rigid closure constructions may be built on a shallow foundation, on caissons or piles. Where possible preference should be given to a shallow foundation since with piles or caissons a con-

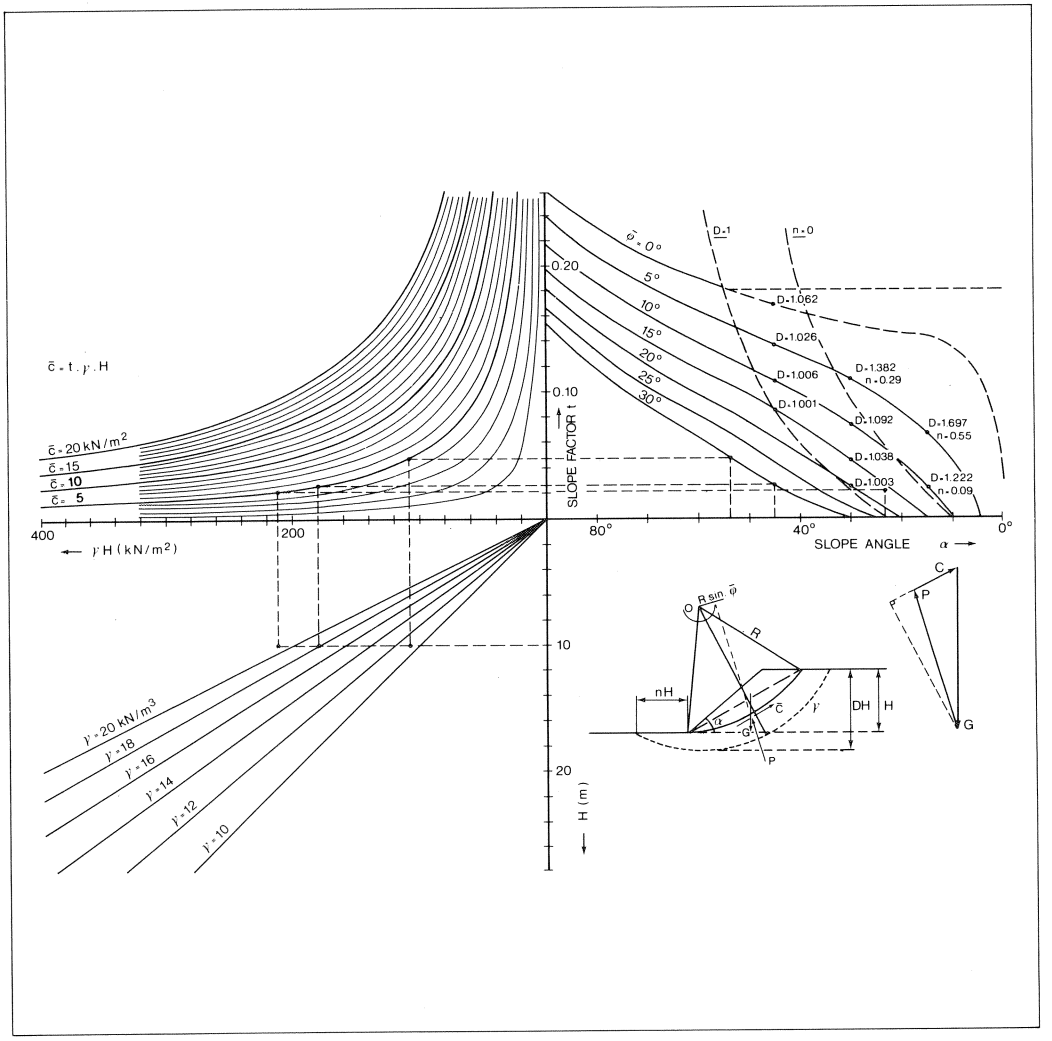

Figure 2.4.5.15 Taylor's diagram for slope stability calculation

struction pit has to be used. As shown in fig. 2.4.5.17, the transfer of stress to the underlying layer differs in the two types of construction.

This section is confined to shallow foundations, especially for a caisson.
The stress on a sluice caisson with the sluices closed takes three forms, viz.:

- static or dead-weight stress (W)

- quasi-static, horizontal, resultant water pressure (H_s)
- cyclic wave stress (H_d)

A construction built on a shallow foundation derives its stability against horizontal stress from the weight of the construction
Possible failure mechanisms include:
a) horizontal shifting of a caisson over the sill
b) shifting along a shallow sliding surface in the sill and subgrade whereby the caisson is displaced both horizontally and vertically.

Which of these mechanisms arises depends on the size of the relationship between the horizontal load H resulting from head loss and wave loads and the vertical load W resulting primarily from the dead weight of the caisson and the sliding resistance and load-bearing properties of the foundation layers. A major factor in this respect is the coefficient of friction f between the caisson bottom and the sill.
In the case of horizontal slip H must exceed f.W.

The foundation pressure rises rapidly during placement of a caisson. In the case of permeable or semi-permeable soil, the pore-water pressure beneath the caisson will increase, which may adversely affect stability. Comparatively high shear stresses may occur in the upper layer of the soil, especially in the case of a thin sill.
If the soil should consist of recent sea-sand deposits it will generally contain a high voids ratio and thus be sensitive to the build-up of pore-water pressure under cyclic alternating shear stress.
This in turn can lead to higher water pressure in the pores than might otherwise be expected at the sea level in question.
In the case of loosely-packed sand, contraction will occur, whereas dense sand will expand. Shear stresses can only be resisted by the granular structure and not by the water between the grains (i.e. the pore water), which is however subjected to the consequences of the change in volume. Because water is virtually incompressible it will resist the change in (pore) volume, thus resulting in an increase or decrease in water pressure. In the case of loosely-packed sand the

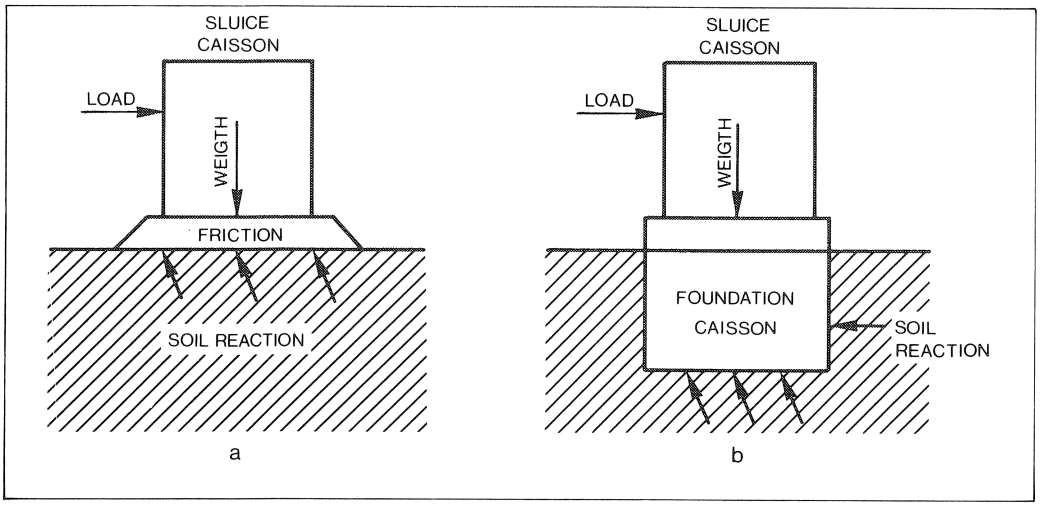

Figure 2.4.5.17 Transfer of loads to the subsoil

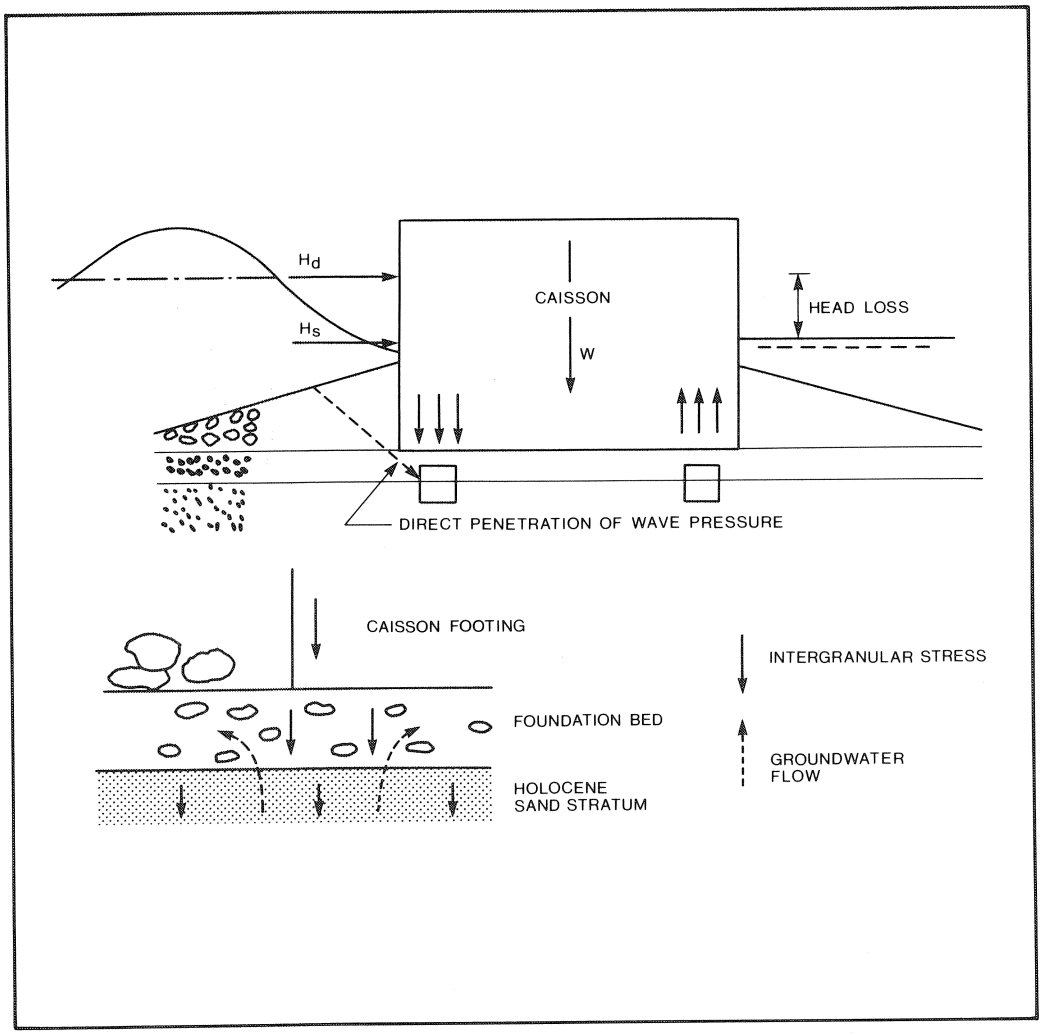

Figure 2.4.5.18 Schematized view of the pore pressure evoking phenomena under a caisson loaded by waves and head loss

result will be excess water pressure and hence a reduction in grain friction, with a consequent reduction in the sliding resistance of the grain structure.

Fig. 2.4.5.19 illustrates what happens upon a change in volume in loosely-packed and dense sand.

The excess water pressure in the grain skeleton will lead to a temporary reduction in the bearing

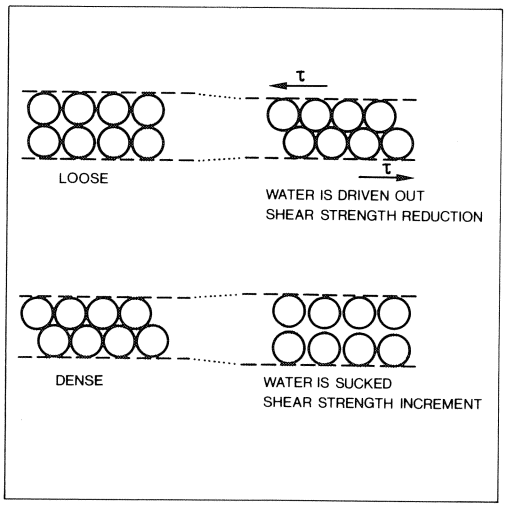

Figure 2.4.5.19 Volume changes in loose and dense sand

Figure 2.4.5.20 Relation between water velocity and flow area decrease

capacity of the soil, the precise extent depending not just on the voids ratio but also on the pattern of storm loads and on the water flow-off. This aspect forms a vital part of stability and deformation analysis.

Another aspect with regard to stability and deformation of a structure built on a shallow foundation, is the erosion of the subsoil underneath the structure.

In order to prevent the subsoil from scouring a filter construction is frequently used. This filter built under the structure on top of the sand has to withstand three types of loading. First a stationary flow due to a static head loss, secondly the instationary flow due to the direct penetration of waves and thirdly the cyclic pore pressures due to the structure movements. The last type of loading may introduce high pore pressures in the sand (with low permeability) and much lower pore pressures in the coarser filter layers (with high permeability). Due to this difference in permeability, cyclic hydraulic gradients result in the interface sand-filter (see figure 2.4.5.18). If the filter is not properly constructed, sand will be washed out through the filter. The sand transport can be considerable and result in unacceptable deformations of the structure.

A thorough filter analyses, including the deter-

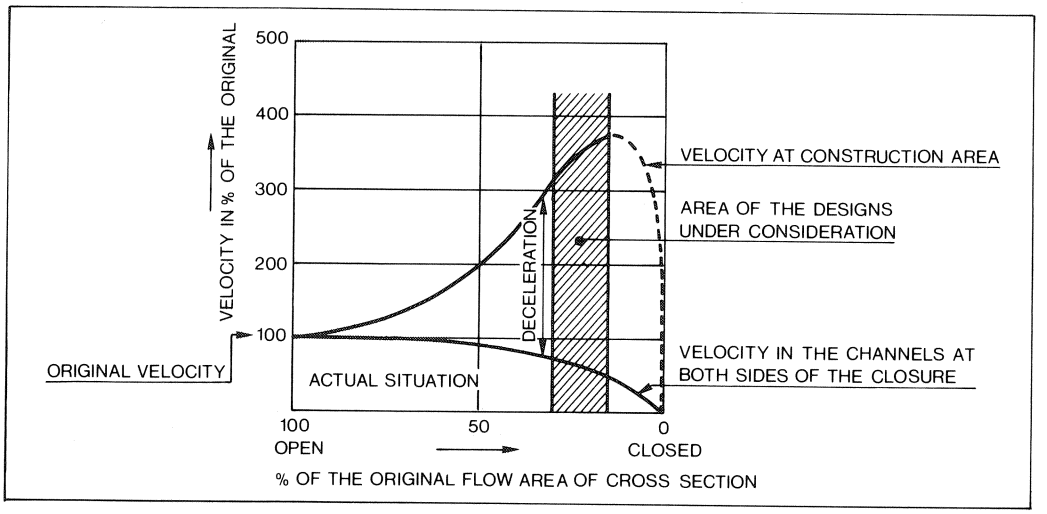

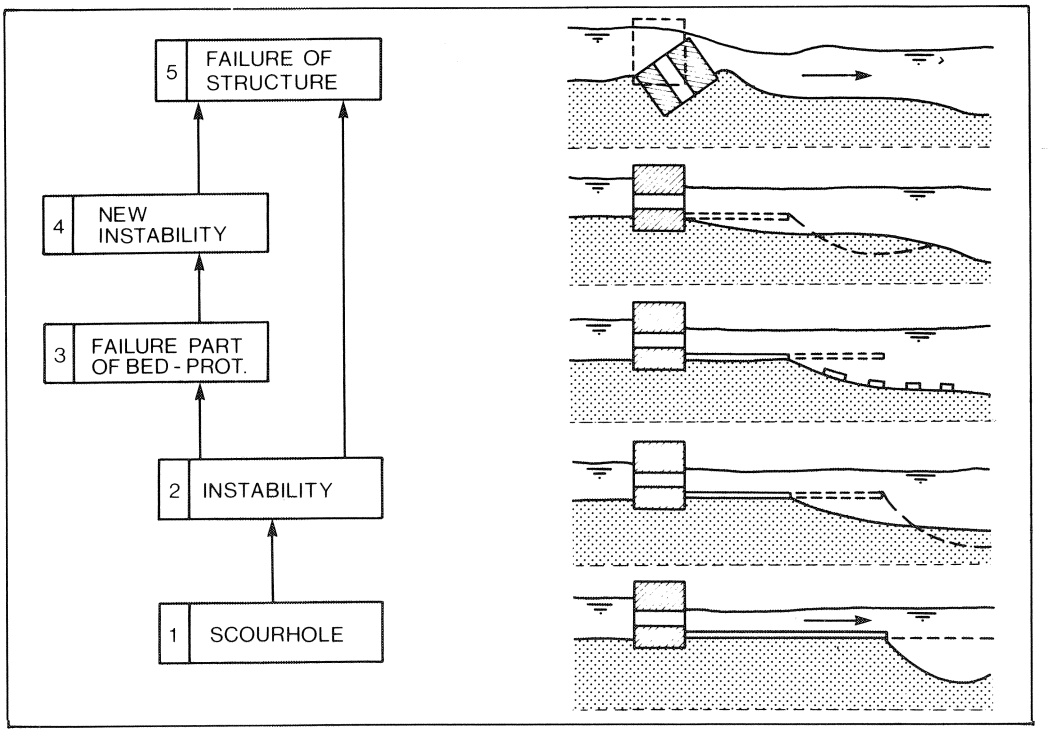

Figure 2.4.5.21 Erosion, at end of bed protection

mination of the maximum static and cyclic hydraulic gradients should therefore be performed.

1.4. Erosion-induced instability of a closure construction

One further stability factor should be mentioned of relevance to both rigid and flexible closure constructions. Fig. 2.4.5.20 illustrates how the current velocity in a dam increases as the gap is narrowed. Because the channel profiles on either side of the dam remain the same as the discharge declines, the velocity on either side of the dam decreases.
This means that the difference between the high velocities in the immediate vicinity of the dam and the low velocities further away becomes steadily greater as the gap is narrowed.
The delay the current is forced to undergo before flowing through the dam therefore increases as the closure gap is narrowed. Delay is coupled with energy conversion, kinetic energy being converted into potential energy, heat and turbulence.
An immediate consequence of the increase in turbulence is that the current is able to pick up and transport steadily more sand. This can lead to erosion on either side of the gap. In order to limit the extent of the erosion or scour, bottom protection is installed on sandy bottoms. Even so, scour holes will be created on both sides of the dam at the edges of the bottom protection. If the slope of such holes should become sufficiently steep, the embankment may slip. This in turn could lead to flow slides in the sand

deposits. This phenomenon is related to the tendency for loosely-packed grains of sand to contract in response to sudden changes in stress. This tendency is counteracted by the pore-water, which destroys the mutual contact between the grains. The sand softens and begins to act as a thick fluid. A large quantity of sand from under the bottom protection can then flow away, thus threatening the stability of the dam. Even if the flow slide does not run right through to the dam or if the soil slip does not result in sand flow, a potentially dangerous situation can be created because the bottom protection becomes damaged. Damage of this kind can work inwards progressively until the dam itself is threatened. This process is illustrated in fig. 2.4.5.21.
Various measures can be taken at the edge of the bottom protection to limit the size of possible soil slip and hence of any flow slide. These measures include:

- densification of the sand deposits to prevent flow slide
- filling the scour holes with rubble to prevent soil-slip
- fitting the bottom protection with a special type of edge that keeps the slopes of the scour holes as shallow as possible, thus eliminating the risk of slip.

2 Deformation

2.1 General

Deformation is taken as meaning:

1. distortion of the soil **with** a change in volume
2. distortion of the soil **without** any change in volume of significance.

The first of these covers settlement and the second squeezing and shifting.

In order to calculate the amount of settlement likely to result when a load is imposed on a bed, soil compression tests are generally carried out in a laboratory. In these tests a laterally restrained soil sample is subjected to a vertical load and the resultant compression measured. The lateral restraint prevents deformation in the horizontal plane. Compression and any outflow of water can only occur in the vertical plane. While this is therefore a one-dimensional case, it is also a situation which may be approximated in the field in certain instances, e.g. if an extended horizontal site is evenly stressed over its entire surface area. The results of a compression test can accordingly be used in such cases to calculate or extrapolate the anticipated degree of settlement.

Example:
Assume that an extended horizontal surface consisting of a layer of sand resting on a firm subgrade (e.g. rock) is stressed with a load over its entire surface area. The settlement of the ground level may be calculated by means of Terzaghi's formula:

$$\varepsilon = \frac{1}{C} \log \frac{p2}{p1}$$

The coefficient of compressibility C can be determined by means of a compression test. In this equation p1 and p2 represent the effective stresses before and upon the imposition of the load, and are therefore indicated as $\overline{\sigma}_1$ and $\overline{\sigma}_2$. Since $\overline{\sigma}_1$ is a function of depth z ($\overline{\sigma}_1 = \gamma.z$) the settlement of the site must be calculated by means of integration.
Consider for this purpose the compression of a layer dz located at a depth z (see fig. 2.4.5.22).

$$\Delta(dz) = dz \frac{1}{C} \log \frac{\overline{\sigma_2}}{\overline{\sigma_1}} =$$

$$\frac{1}{C} (\log \overline{\sigma}_2 - \log \overline{\sigma}_1) \, dz$$

The total settlement becomes:

$$\Delta h = \frac{1}{C} \int_0^h (\log \overline{\sigma}_2 - \log \overline{\sigma}_1) \, dz$$

This integration can be carried out simply by graphical means by plotting $\overline{\sigma}_1$ and $\overline{\sigma}_2$ on a logarithmic scale. In this case ($\log \overline{\sigma}_1 - \log \overline{\sigma}_2$) dz = dF, so that the total settlement Δ h is equal to 1/C x the area between the two curves.

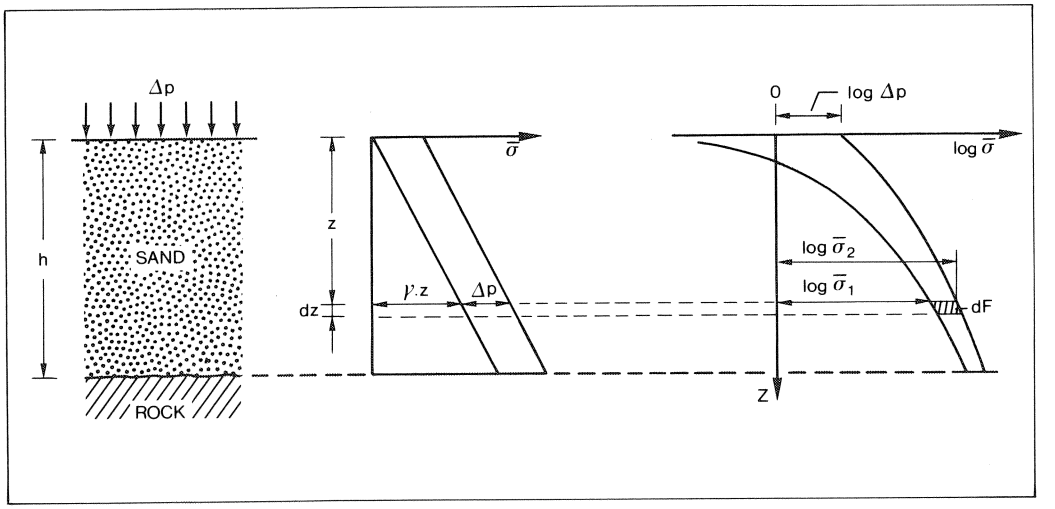

Figure 2.4.5.22 Compression of dry sand under loading according to Terzaghi

Figure 2.4.5.23 Compression for 2 layers of soil with groundwater

This graphic method may also be effectively used for more complex cases, e.g. if groundwater is present and/or the soil consists of layers with varying properties (C,γ). An example is shown in Figure 2.4.5.23.

For weak soils the effect of loading is more complicated. Clay and peat are much more compressible than sand, besides which the com-

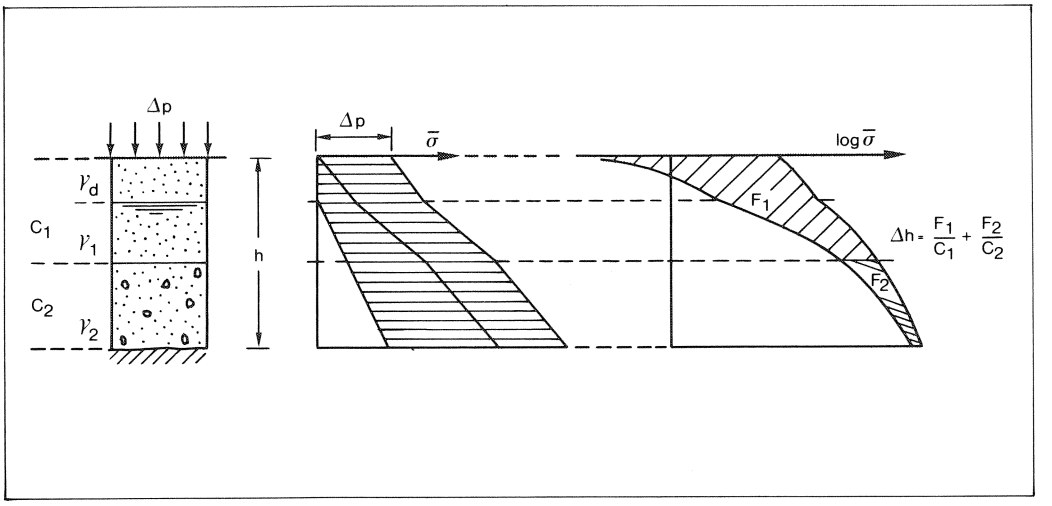

pression is highly time-dependant (see fig. 2.4.5.24).
With respect to compression tests on peat and clay two phenomena may be distinguished:

1. consolidation.
   During this period the water is subject to excess pressure. As this water is released the excess water pressure declines and the effective stress increases, thus causing settlement.
2. secular or secondary effect.
   Upon completion of consolidation, when the excess water pressure has virtually disappeared, settlement can continue to occur over very lengthy periods in many kinds of clay and peat.

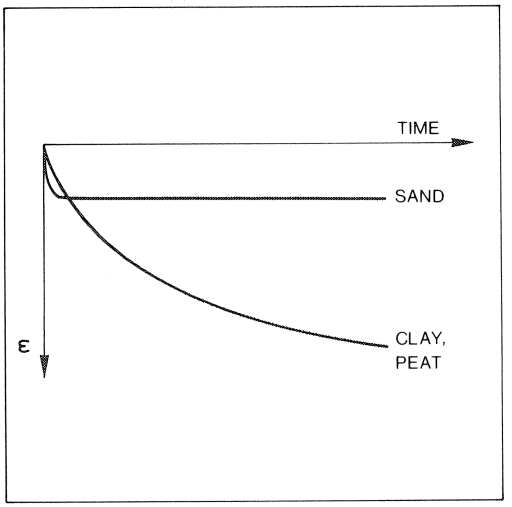

Figure 2.4.5.24 Compressibility of sand compared to that of clay and peat

2.2. Consolidation and the secondary effect

With respect to consolidation, a theory was devised by Terzaghi on the basis of certain simplified assumptions. Consolidation theory seeks to provide an explanation for the time-lag that occurs when a saturated soil is compressed. It is assumed that both the material of the grains and the water are incompressible, from which it follows that compression of the soil can only arise if the grains become more thigtly-

Figure 2.4.5.25 Loading in a oedometer

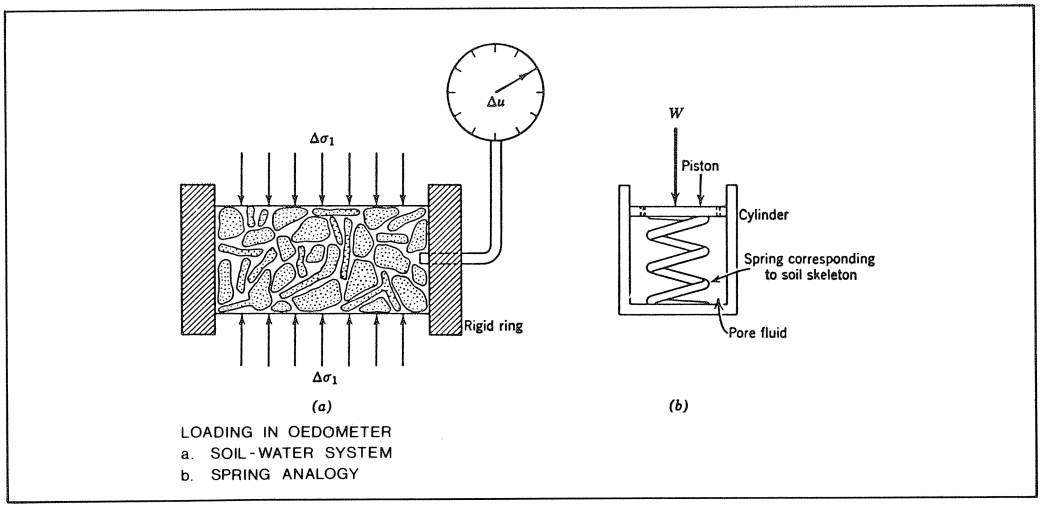

LOADING IN OEDOMETER
a. SOIL-WATER SYSTEM
b. SPRING ANALOGY

packed. This in turn means that the voids ratio declines, so that pore-water must be expelled. The outflow of the water through the narrow voids takes time, however, which explains why the compression of the soil is subject to delay.
This one-dimensional process may be illustrated in terms of the following model. In a cylinder filled with an incompressible liquid (see fig. 2.4.5.25) it is possible for a perforated piston to move up and down without friction, the piston being supported by springs. If the pistion is subjected to a load W, the springs will only be able to absorb this load after they have been compressed a certain distance.
Before this can happen, however, the liquid will first have to be squeezed out through the perforations in the piston, which takes time.
As long as this process is uncompleted the sprıngs will be unable to provide the full counterforce and part of the load will be borne by the liquid. This places the liquid under greater pressure, thereby causing it to flow out. In this model the springs represent the compressibility of the granular skeleton while the outflow of the water through the perforated piston my be compared with the groundwater flow through the pore channels, On the basis of the principle described above the consolidation process may now be described mathematically.
For a one-dimensional case, i.e. one where the compression and water flow can only take place in the vertical direction (upwards and/or downwards), as in the case of a compression test, Terzaghi arrived at the following differential equation:

$$\frac{\partial w}{\partial t} = \frac{k}{m_v \gamma_w} \frac{\partial^2 w}{\partial z^2}$$

$\frac{k}{m_v \cdot \gamma_w}$ is termed the coefficient of consolidatîon, c_v.
The properties of the soil that determine the pattern of the consolidation process are contained in the coefficient of consolidation:

$$c_v = \frac{k}{m_v \gamma_w}$$

It may be noted that k and m_v are not constant but decline over the course of the consolidation process. As a result c_v is also not constant, although the variations are more limited since they are determined by the relationship k/m_v.
The differential equation may be solved either analytically or graphically.
Solutions for the equation may be found in most handbooks dealing with soil mechanics. The solution may also be found by an oedometer test, where the water in the pores can flow upwards and downwards (see fig. 2.4.5.26).
According to the formula the end of the consolidation will in theory never be reached. In practice the consolidation time t_e is related to the point where 99% of the final settlement is reached.

It may also be seen from the formula that the consolidation takes longer:
- the greater the compressibility m_v,
- the smaller the permeability k, and
- the greater the layer tickness h.

In order to provide an impression of the order of magnitude of t_e, the latter has been worked out in table 2.4.5.2 for four cases of sand and clay, in each case for a 20 mm thick sample and a 2m thick soil layer.

It is evident from these figures that the consolidation time may virtually be ignored in the case of permeable sand-layers, but that for clay it can be extremely lengthy.
The anticipated rate of settlement may be deduced if the coefficient of consolidation c_v of the soil type in question is known. The latter may be determined from the results of a compression test, using either Taylor's $\sqrt{}$ t-method or Casagrande's log t-method.
According to consolidation theory, settlement should take place asymptotically towards a final value S_u, which is virtually reached at the practical end of consolidation. In practice, however, this is not borne out; tests on clay and peat have shown settlement to continue beyond the practical end as well. In some cases a final value was still not obtained even in tests lasting a number of years. Keverling Buisman termed this phenomenon the secular effect.
The secular or secondary effect may be shown most clearly by plotting the settlement measu-

	h (mm)	k (mm/s)	m_v (m^2/kN)	γ_w (kN/m^3)	c_v (m^2/s)	t_e (s)	
sand	20	10^{-1}	10^{-4}	10	10^{-1}	0,002	
,,	2000	,,	,,	,,	,,	20	
clay	20	10^{-7}	10^{-3}	,,	10^{-8}	1.10^4	= 5.5 hours
,,	2000	,,	,,	,,	,,	2.10^8	= 6.3 years

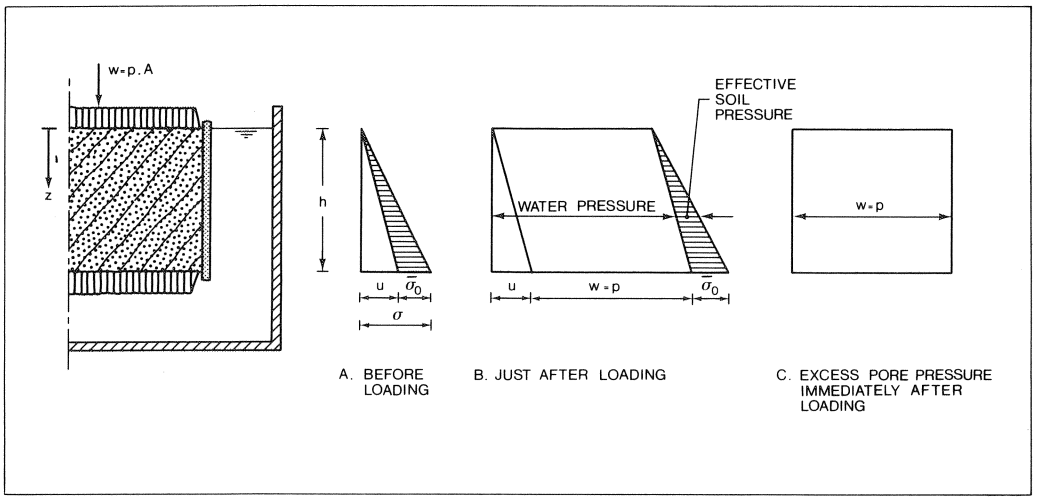

Figure 2.4.5.26 Pressure development in saturated soil by loading

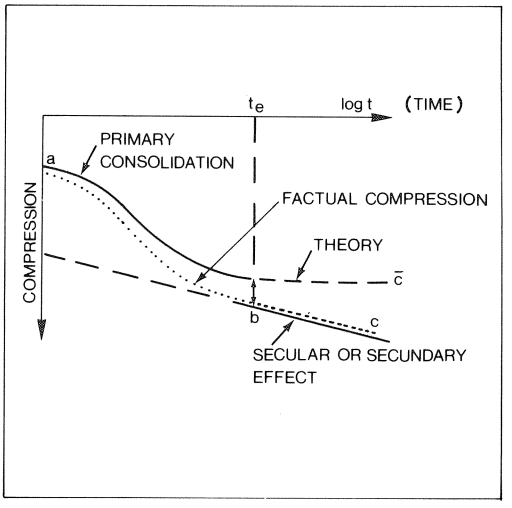

Figure 2.4.5.27 Primary and secondary compression

red in the course of a compression test against the logarithm of time. This produces a curve as shown by abc in fig. 2.4.7.27. The section ab of the curve is s-shaped and more or less corresponds with the settlements calculated by consolidation theory if these are also plotted against log t. According to the theory the curve should run more or less horizontally beyond the point b (bc'), but the actual settlement path (bc) differs markedly.

Consolidation and the secondary effect have been taken as successive phenomena described by totally different formulae.
This gives rise to inconsistencies if the results of a compression test on a 2 cm thick sample are applied for calculating the compression of a much thicker layer in the site.
This particularly concerns the two following points:

- the theory of consolidation provides for a layer-thickness effect but this is absent in the equation for the secondary effect.
- the theory of consolidation assumes a linear relationship between load and settlement, whereas Terzaghi assumes a logarithmic relationship.

As a result the settlement curve for a thick layer as calculated by consolidation theory will not in general correspond with the path determined on the basis of the secondary effect.
In practice, of course, a continuous consolidation settlement takes place.

As was seen, Terzaghi's theory of consolidation assumes vertical pore-water flow out of the soil. It is possible, however, for there to be horizontal flow or a combination of horizontal and vertical flow.
Such a situation may for example occur if vertical sand drains are used to accelerate the consolidation process:

- the consolidation due to horizontal flow may be calculated according to Kjellman's formula:

$$t = \frac{D^2}{8\,c_h}\left(\ln\frac{D}{d} - \frac{3}{4}\right)\ln\frac{100}{(100 - U_h)}$$

in which:

t = time
D = distance between the drains
d = diameter of the drains
C_h = coefficient of consolidation for horizontal flow
U_h = average consolidation due to horizontal flow.

- the consolidation due to vertical flow may be calculated using Terzaghi's formula.
- Barron's formula may be used to determine the resultant consolidation U_c when the consolidation due to vertical flow (U_v) and horizontal flow (U_h) are known, i.e.:

$$U_c = 100 - \frac{(100 - U_h)(100 - U_v)}{100}$$

3. General remarks

The foregoing paragraphs about stability and deformation deal only with basic soil mechanics in simplified situations i.e. one or two dimensions. The state of the art is, however, further developed.
More sophisticated numerical methods are available using finite element principles, with which complicated soil-structure configurations under static or dynamic conditions and even for three dimensions can be calculated.
In some cases these advanced methods are justified, in other cases not. The engineer should only use advanced prediction-methods when he has sufficient insight into the situation; i.e. the engineering work including the construction process and the soil parameters. It is pointless to try to increase the accuracy of prediction by 10% using advanced methods while soil parameters may vary between 100 and 300%. This is often the case. But not only are the soil parameters insufficiently determined, the requirements of the structure, e.g. loading conditions, are often not well defined.
We would therefore conclude that a knowledge of basic soil mechanics, combined with experience and sound engineering judgement, should enable a construction work such as the closure of an estuary to be properly and economically designed and constructed.

H. Mulder

2.4.6 Stability and motions of floating structures and equipment

2.4.6.1. Introduction

The stability and motions of floating structures are extremely complex. In practice nowadays, the calculation of motions and forces is done by large computer programs. It is therefore not possible to discuss the subject here in detail. Only some simple cases and principles concerning free floating vessels and moored vessels will be dealt with in this section.

2.4.6.2. Free floating structures

1. Stability.

The weight of a vessel is in equilibrium with the upward force according: m.g. = ϱ.g.V where

m = mass of the vessel	kg
g = gravitation constant	m/s²
ϱ = density of water	kg/m³
V = volume of displaced water	m³

The weight is acting in the centre of gravity G (see figure 2.4.6.1) while the upward force acts on the pressure point B.

When a rotation is given to the vessel B will move to B¹. N is called the false metacentre. The moment of stability M_s = m g GZ where GZ is the arm of static stability . Also M_s = g V GN sin Φ. When Φ approaches zero N becomes M, the metacentre. Hence $M_s = \varrho$ gV GM Φ where GM is the metacentre-height. When M is above G the equilibrium is stable. The equilibrium is indifferent respectively unstable when M = G and M is below G. The moment of stability can be divided into the form stability (ϱ gVBM Φ) and the weight stability (ϱ gVBG Φ). The value of BM can be determined by I/V, where $I = \int xy^2dy$ is the moment of inertia (x is the longitudinal and y the transverse axis; for rectangular vessels $I = 1/12\ Lb^3$, where L is the length and b the width). For low values of Φ (< 15°) the arm of static stability can be described by the Scribanti formula: $GZ = GM \sin\Phi + BM\ tg^2\Phi/2 \sin\Phi$. When $\Phi \rightarrow 0$ $dGZ/d\Phi$ = GM or GM determines the tangent in Φ = 0. When a vessel contains liquid with density ϱ', there will be a reduction of GZ of $I_t\varrho'/V.\varrho$ where I_t is the transverse moment of inertia.

Figure 2.4.6.1 Stability of a vessel

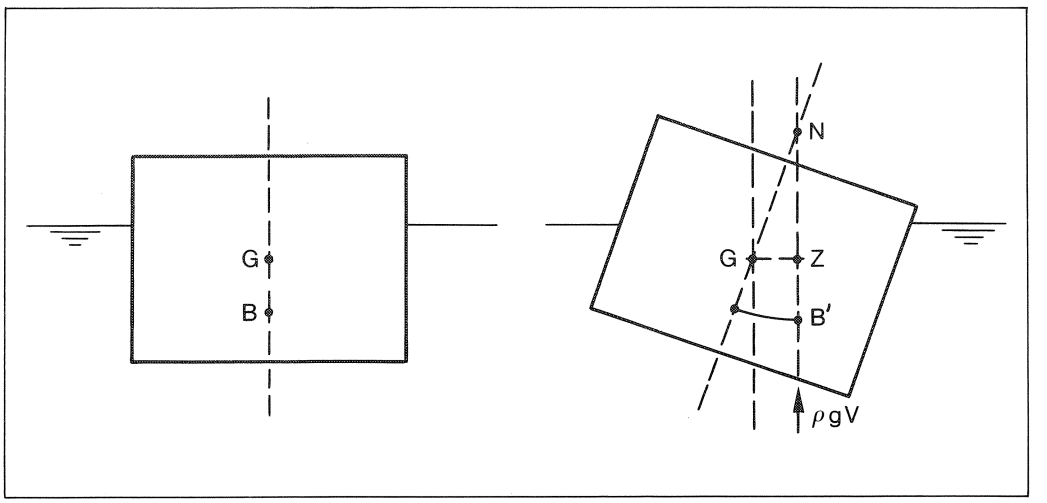

2. Motions

Vertical motions.
The vertical motions in still water can be caused by waves and the forward speed of a vessel. The speed induced motions are squat - a uniform sinking due to a drop in the level of the surrounding water as a result of the return flow; and trim - a rotation about the transverse axis as a result of asymmetry of the return flow pattern. The wave induced motions are heave - a uniform vertical motion; pitch -a rotation about the transverse axis; and roll - a rotation about the longitudinal axis.
Current induced motions are inverse speed induced motions.

Horizontal motions
These motions, caused by waves, are sway - a motion along the transverse axis ; surge - along the longitudinal axis; and yaw - a rotation about the vertical axis.

Thus, there are three rectilinear and three rotational motions. A freely floating vessel has three natural periods (heave, roll and pitch), with the restoring force being gravity (or buoyancy).
A first approach to the behaviour of vessels in waves is usually the oscillation due to transverse waves the equation of motion being given by:

$$a_\phi \frac{d^2\phi}{dt^2} + b_\phi \frac{d\phi}{dt} + c_\phi \phi = M(t) = M_a \cos(\omega t + \varepsilon_M)$$

where
a_Φ = hydrodynamic coefficient for virtual mass (mass vessel in water and added mass of water)
b_Φ = hydrodynamic coefficient (damping)
c_Φ = hydrostatic coefficient (restoring)
M(t) = moment induced by waves
The solution when $\Phi = \Phi_a e^{i(\omega t + \epsilon_\Phi)}$ gives:

$$f = \frac{\phi_a}{\phi_{st}} \frac{1}{\sqrt{(1-\mu^2)^2 + \nu^2\mu^2}}$$

$$tg\ \varepsilon_\phi = \frac{-\nu\mu}{1-\mu^2}$$

where:
f = enlargement factor
Φ = amplitude characteristic
Φ_{st} = static oscilation angle = M_a / c_ϕ
μ = resonance factor = ω/ω_e
ω = wave frequency
ω_e = natural frequency = $\sqrt{c\Phi/\alpha\Phi}$(no damping)
ϵ_Φ = phase characteristic
$\nu = b_\Phi/\sqrt{a_\Phi c_\Phi}$

The natural frequency can be calculated with

$$\omega_e = \frac{\pi\sqrt{GM}}{K_{\phi\phi}}$$

where $K_{\Phi\Phi}$ = transverse inertia radius (for rectangular vessels $K_{\Phi\Phi} \sim 0.45$ to 0.55 b).
Analogous to rotation the equation of motion for translation is given by:

$$a_x \frac{d^2x}{dt^2} + b_x \frac{dx}{dt} + c_x x = F(t)$$

where x = direction of translation

The computation of the motions can be done by using a response function method. In nature a wave field consists of single sinusoidal waves with their own period, phase and amplitude. The field can usually be characterized by an energy spectrum: $S_h(\omega)$ [m²s]. This spectrum must be transformed with respect to the encounter-frequency instead of the wave-frequency. A response spectrum is then determined by submitting the vessel to a series of constant frequency excitations: $R(\omega)$ [m/m]. The motionspectrum is given by $S_X(\omega) = R^2(\omega) . S_h(\omega)$ [m².s].
The response function is usually found by model-tests. It is generally safe to assume that the chance of exceeding a certain motion amplitude is given according to the Rayleigh distribution by:

$$P(\phi \geq \phi_a) = e^{-\phi_a^2/2m_0}$$

where m_o = area under the S_Φ -curve

Furthermore

$$\phi_{sign} = \phi_{0.135} = 2\sqrt{m_0}$$

or

$$P(\phi \geq \phi_{sign}) = 13.5\%$$

3. Forces

A floating structure can be submitted to forces caused by wind, current and waves. These forces have a dynamic character.
Forces due to wind and current can be described by $F = F_I$(inertia) + F_{II}(dragforce)
where
$F_I = C_m \varrho V \, dv/dt$
$F_{II} = \frac{1}{2} C_d \varrho A v^2$
and
C_m = inertia coefficient = a/m
a = virtual mass
m = mass of displaced medium
ϱ = density of medium
V = displaced volume of medium
v = velocity
C_d = drag coefficient
A = area of impact
C_d depends on roughness, shape and Reynolds number.
The pressure in a wave is given by

$$P = -\rho g z + \tfrac{1}{2}\rho g H \frac{\cosh[k(z+d)]}{\cosh(kd)} \cos(kx-\omega t)$$

where
z = vertical axis from M.S.L. upwards
H = wave height
k = wave number = $2\pi/\lambda$
λ = wave length
d = depth (bottom at z = -d)
x = horizontal axis in wave direction from wave crest
t = time
ω = wave frequency
T = wave period
Integrating the pressure over the wall of the vessel (z = -D to z = o) results in the force:

$$F = \tfrac{1}{2}\rho g D^2 + \tfrac{1}{2}\rho g \frac{H}{K} f_k \cos(kx-\omega t)$$

where:
f_k = [sinh(kd) - sinh (kd - kD)]/ cosh (kd)
D = draft of the vessel

2.4.6.3. Moored vessels

The problem of a moored vessel is more complicated than the problem of unrestrained vessel motion. There are three additional periods (surge, sway and yaw) and the restoring force (elasticity and cable weight) is nonlinear.

The basic equation of motion is:

$$a_x \frac{d^2x}{dt^2} + b_x \frac{dx}{dt} + (c_x + d_x)x = F(t) + F_p$$

where
d_x = spring coefficient mooring cable
F_p = pretension force in cables

The spring coefficient is the ratio between the cable-force and the extension of the cable. The relation between these parameters is given by:

$$V_B = \tfrac{1}{2} l w + d_1 \sqrt{\left(\frac{W}{2}\right)^2 + \frac{H_B^2}{(\ell^2 - d_1^2)}}$$

$$V_A = V_B - lw$$

$$R = \frac{2H_B}{w} \operatorname{arctgh}\left(\frac{d_1 w}{V_A + V_B}\right)$$

where
V_B = vertical load at the chain (see point B in figure
V_A = vertical reaction force at point A
R = horizontal distance A-B
l = length of the cable
w = weight of the cable per unit of length
d_1 = vertical distance A-B
H_B = horizontal load at B
see figure 2.4.6.2
It is important that $V_A > o$. When H_B is low the cable will lie on the bottom, which means V_A = o and a reduction of l (now unknown instead of V_A). See figure 2.4.6.2.

A H_B-R diagram is called the chain-characteristic and is nonlinear. Because dH_B/dR increases with H_B and R, it is possible to prevent large displacements by pretensioning the chain. However, when the pretension force is high the total chain force due to load will be extra high and heavier chains will be needed.
Because of the complexity of the calculations some simple cases only will be discussed here.

The following assumptions are made:
- roll, pitch and heave are ignored (vertical motions)
- the pressure due to the orbital motion is ignored

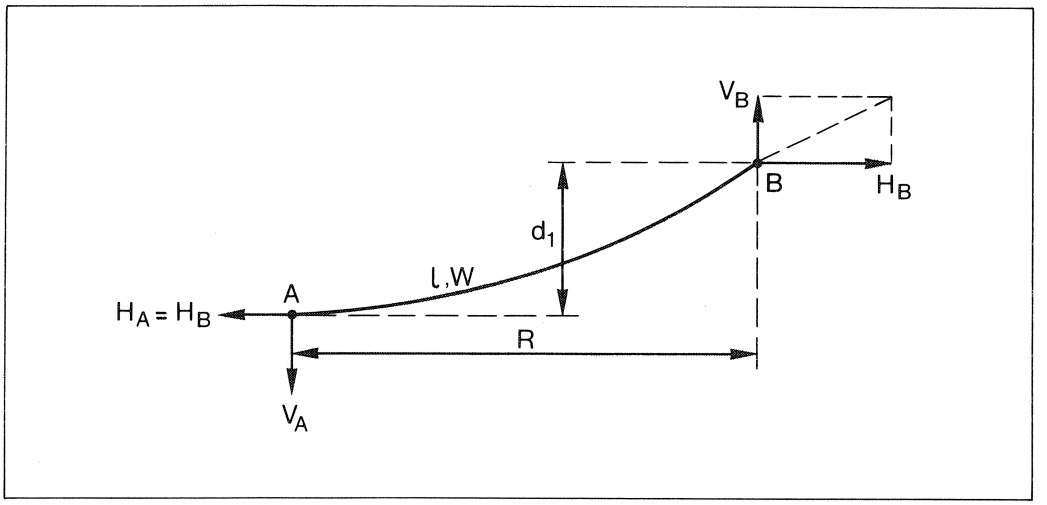

Figure 2.4.6.2 Example of a cable

the water level along the side of the vessel is described by:

Z_W = 1/2 H cos ($k_1 x$ - Φ) (see fig. 2.4.6.3)

where

k_1 = $2\pi/\lambda_1$

λ_1 = $\lambda/\cos\alpha$

α = angle between side and direction of propagation

x = horizontal axis with x = o, halfway the vessel

Figure 2.4.6.3 Schematization of a wave along the side wall of a vessel

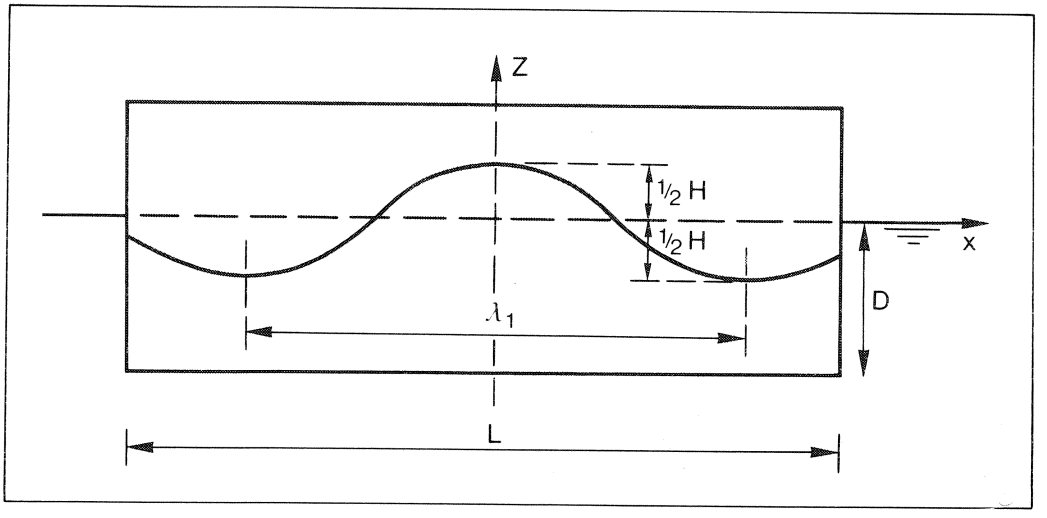

- the wavelength λ_1 is equal on both sides of the vessel
- the waveheight H is different on both sides of the vessel:
  H at „attack" side and H^1 at the other side
- $\Phi = o$ and $\Phi^1 \neq o$; because of $\lambda_1 = \lambda_1^1 : \Phi^1 = kb\sin\alpha$

Now the resulting horizontal force is given by:

$$F(x) = \tfrac{1}{2}\rho g \{\tfrac{1}{4}H^2 \cos^2(k_1 x) + HD \cos k_1 x - \tfrac{1}{4}(H^1)^2 \cos^2(k_1 x - \phi^1) - H^1 D \cos(k_1 x - \phi^1)\}$$

The resulting force over the total length can now be calculated. For instance when $H^1 = o$ this results in:

$$F_R = \tfrac{1}{2}\rho g L \{\tfrac{1}{8}H^2 (1 + \frac{\sin(k_1 L)}{k_1 L}) + HD \frac{\sin(\frac{1}{2}k_1 L)}{\frac{1}{2}k_1 L}\}$$

when $\alpha \rightarrow 90°$ then $k_1 \rightarrow o$ and $F_R = \frac{1}{2}$ pg L H D (1 + $\frac{1}{4}$ H / D)
However when $\alpha = 90°$ and $Z^1_w = -\frac{1}{2}$ H continuously along the side then $F_R = \varrho g H D L$ (maximal force).
It is also possible to calculate the yaw moment (M_z):

$$M_z = \int_{-\frac{1}{2}L}^{+\frac{1}{2}L} xF(x)\,dx = -\tfrac{1}{8}\rho g \frac{H^2 L}{k_1} \{A_1 \sin(2\phi^1) + A_2 \sin(\phi^1)\}$$

$$A_1 = \tfrac{1}{4}(\sin(k_1 L)/k_1 L - \cos(k,L))$$

$$A_2 = \frac{4D}{H}(\sin(\tfrac{1}{2}k,L)/\tfrac{1}{2}\,k_1 L - \cos\tfrac{1}{2}\,k_1 L)$$

The maximum moment with respect to Φ^1 (or α) occurs when $dM_z/d\Phi = 0$, or $\Phi^1 = \arccos(-\beta \pm \sqrt{\beta^2 + 0.5})$ where $\beta = 1/8\ A_2/A_1$.
For the horizontal motions a simple method can be used to calculate the displacements when the total horizontal force and moment are given (steady state)

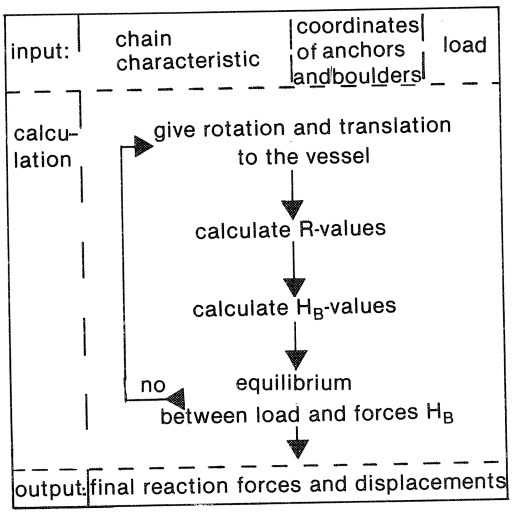

Figure 2.4.6.4 Scheme of calculation of forces and displacements in steady state

This method does not account for dynamic forces, in which case a response function is required. The method above must therefore be repeated for any change in load, draft, water level, specification of the chain and geometry of the mooring system.

For calculations, the most attractive mooring system is a symmetrical one. Again, assumming a static force in both horizontal directions (F_x, F_y) and chains at the sides of the vessel only, the optimal angle between the chains and the side wall is $\gamma = \text{arctag}\ {}^3\sqrt{F_y/F_x}$ (x = longitudinal direction). The chains are there by considered to conduct as bars.

To design a mooring system the next scheme can be useful:

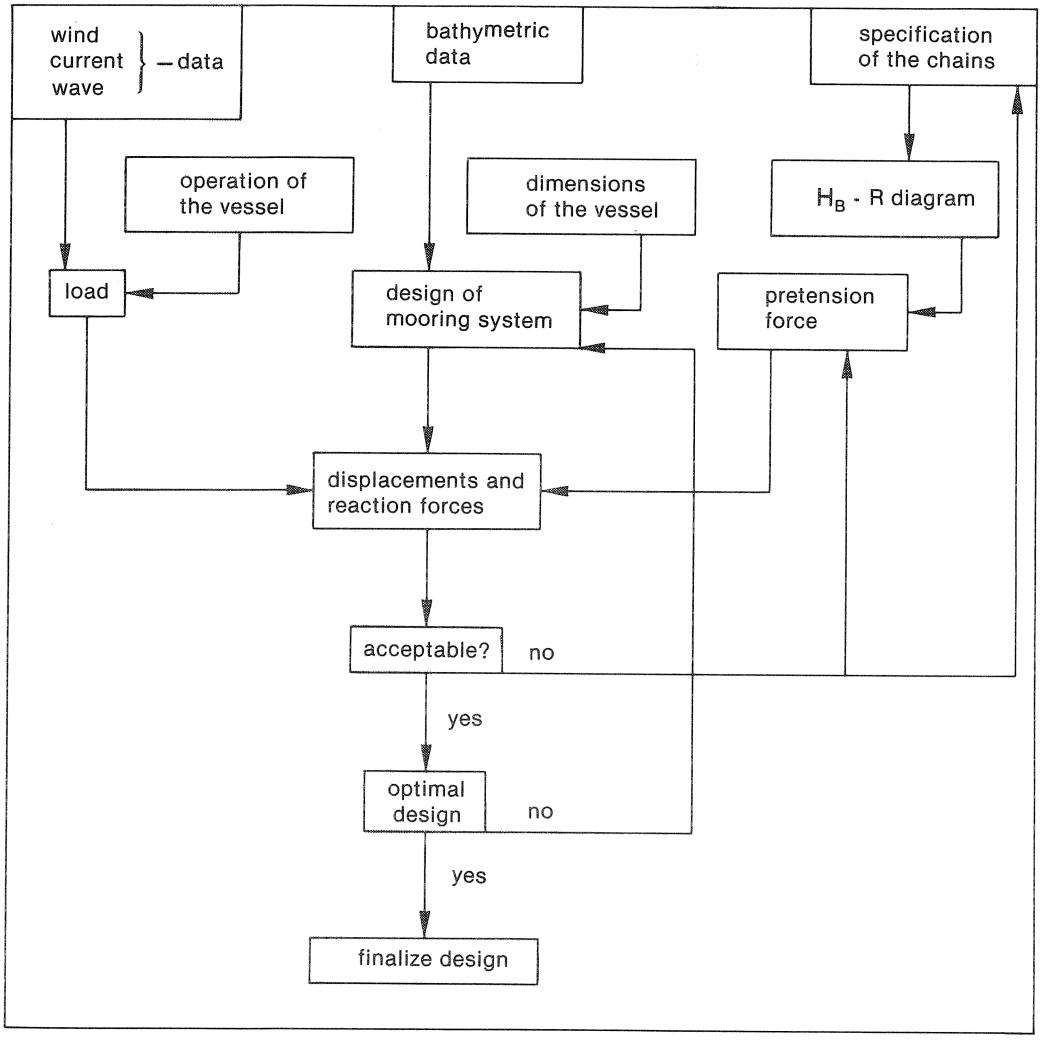

Figure 2.4.6.5 Flow diagram for designing a mooring system

2.4.6.4 Examples

1. **Stability**
   Suppose a vessel with $m = 45.10^6$ kg and with $L * b * d = 150 * 30 * 15$ m.
   Hence $V = m/\varrho = 45.10^3$ ($\varrho \approx 1000$ kg/m^3) and the draft $D = V/(l * b) = 10$ m
   $I = 1/12\ L\ b^3 = 337.5.10^3$ m^4

Hence BM = 7.5 m
Suppose G is 7.5 m above the vessels bottom and B at 0.5 D = 5 m above the bottom.
Then BG = 2.5 m en GM = 5 m.
In figure.

Figure 2.4.6.6 Pressure and centre points

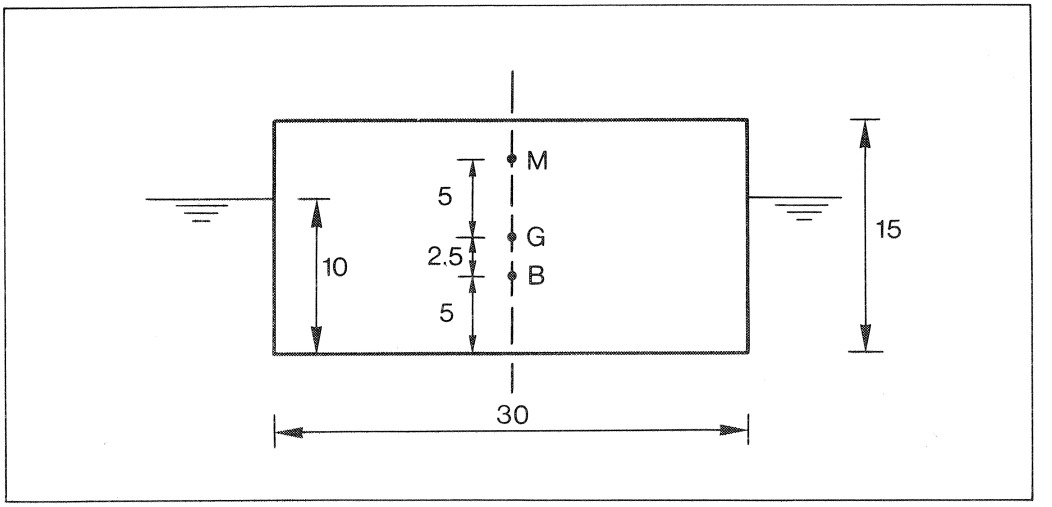

If $\Phi < 15°$ the arm of static stability becomes:
$GZ \approx (5 + 3.75\,tg^2\,\Phi)\sin\Phi$ (calculated until $\Phi = 15°$) or in figure

Figure 2.4.6.7 Relation between arm of static stability and rotation

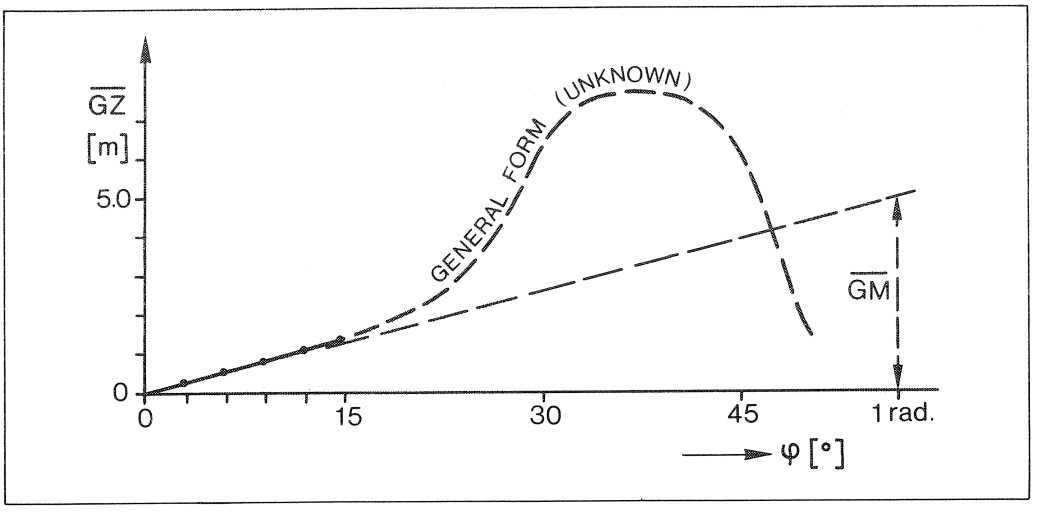

2. Motion

Suppose $K_{\Phi\Phi} = 15$ m.
Thus $\omega_e = 0.468$ [s^{-1}] and $T_e = 13.4$ s.

When the waves have a period of 5 sec., then $\omega = 1.257$, thus $\mu = \omega/\omega_e = 2.69$ (resonance factor). In case of waves only (transverse) $\Phi_{st} = kH = 2\pi H/\lambda$
In deep water $\lambda = 1.56\,T^2 = 39$ m ; with for instance H = 2.5 m (waveheight) it follows that $\Phi_{st} = 0.40$ rad $= 23.1°$.

When ν is relatively small (little damping) then the enlargement factor becomes $f \approx 0.025$ and $\Phi_a \approx 0.6°$.

3. Forces

Suppose the same vessel as above and $C_D = 1.4$, $C_m = 1.2$.

Windforce

ϱ	$\approx$	1.2 kg/m^3 (air)
V	=	5 * 150 * 30 = 22.5 * 10^3 m^3
dv/dt	=	5.10^{-3} m/s^2 (assumption)
v	=	40 m/s
A	=	5 * 150 = 750 m^2
F_I	=	162 N
F_{II}	=	10^6 N

Current force:

dv/dt	=	0.3. 10^{-3} m/s^2 (assumption)
v	=	2 m/s
A	=	10 * 150 = 1500 m^2
F_I	=	16.10^3 N (dominates wind-force f_I)
F_{II}	=	4.2.10^{6}N

Wave force:

D	=	10 m
H	=	2.5 m
λ	=	39 m
d	=	30 m(waterdepth!)
F	=	491.10^3 + 61.10^3 cos (kx - ωt) N/m

4. Moored vessels

For the simple case we assume:

$\alpha = 45°$; H = H^1 = 2.5 m; λ = 39 m; D = 10 m; L = 150 m

Hence: $\lambda_1 = 55.15$ m ; $k_1 = 0.114$
$\Phi^1 = 3.42$

Now: $F_x = 12.10^3$

$$\{\tfrac{5}{8}\,[\cos^2(k_1x) - \cos^2(k_1x-\phi^1)] + 10\,[\cos(k_1x) - \cos(k_1x-\phi^1)]\}$$

while: $F_R = \int_{x=-\frac{1}{2}L}^{x=\frac{1}{2}L} F(x)\,dx$

it follows that:

$$F_R = 12.3.10^3\,\{\tfrac{5}{8}\,.\,\tfrac{1}{2}\,[L + \frac{\sin(k_1L)}{k_1} - L - \frac{\sin(k_1L-2\phi^1)-\sin(k_1L-\phi^1)}{2k_1}] + 10\,[\frac{2\sin(k_1L)}{k_1} - \frac{\sin(\frac{1}{2}k_1L-\phi^1)-\sin(-\frac{1}{2}k_1L-\phi^1)}{k_1}]\} =$$

$$= 12.3.10^3\,\{47.681 - 47.675 + 51.59 - 26.04\} = 12.3.10^3\ 25.55\ (N) = 314\ KN$$

the yaw moment $M_z = 9.63\ 10^6$ Nm.
When $H^1 = o$; $F_R = 12.3.10^3\{47.68 + 51.59\} = 1.22.10^3$ kN.

When $Z^1w = -\frac{1}{2}$ H and $\alpha = 90°$; $F_R = 36.8.10^3$KN.

Example of chain-characteristic (H_B-R diagram):
Suppose the cable length l = 120 m; w = 1.1617 KN/m^1 and d_1 = 26.7, 23.9 and 14.8 m. The result is given in figure 2.4.6.8.
Chains and anchors must be chosen according to their proof/breaking load and holding power. The figures 2.4.6.9/2.4.6.10 show some possibilities.

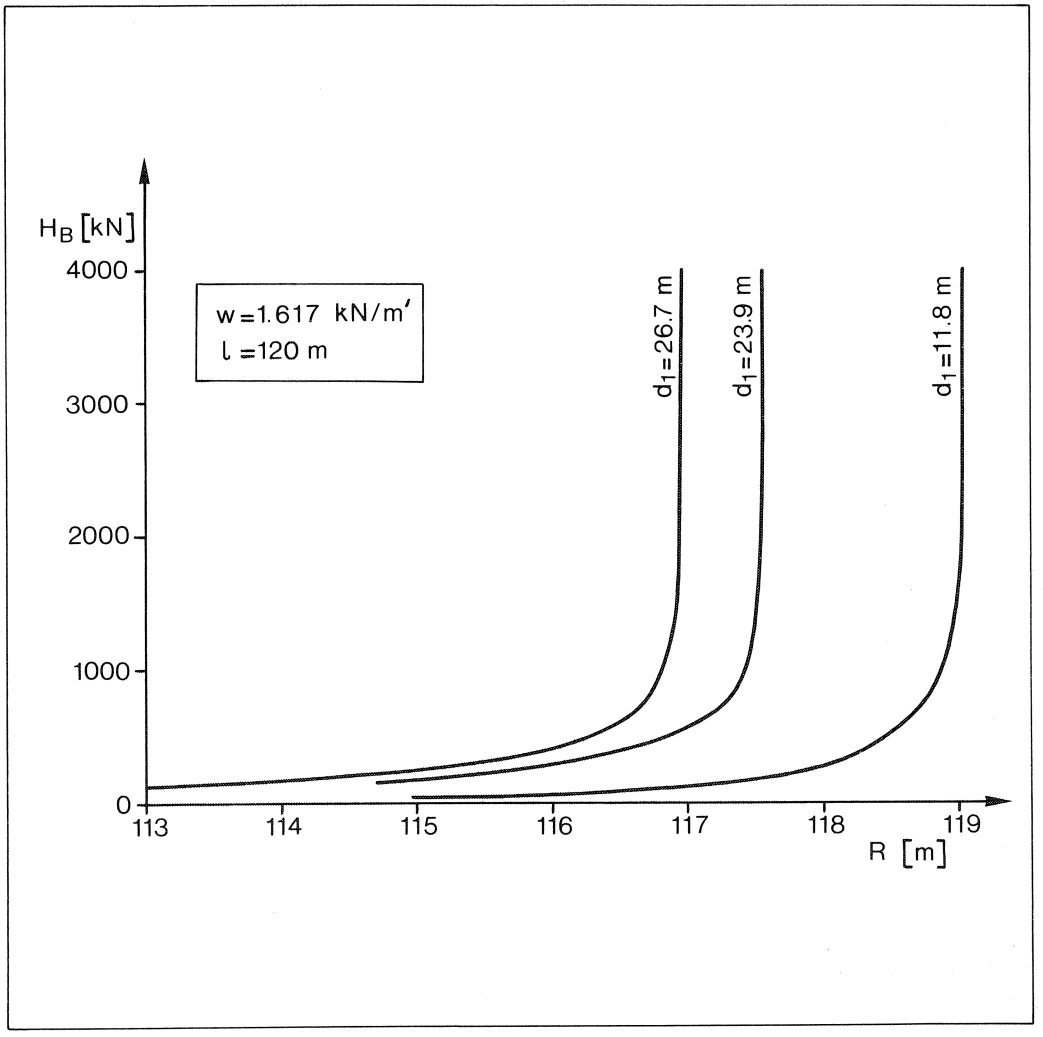

Figure 2.4.6.8 Chain-characteristics

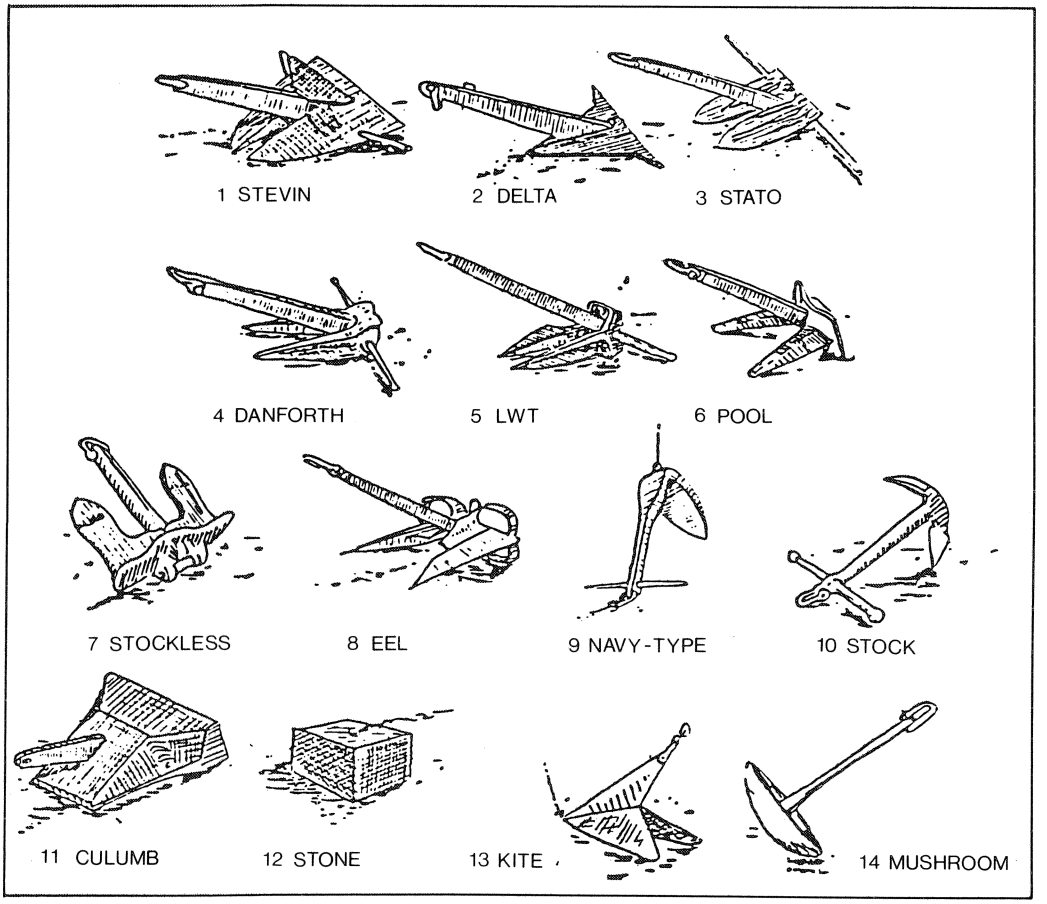

Figure 2.4.6.9 Anchor types and their holding power

	Holding power (x its own weight; tonnes)	Soil Analysis
1. Steving	17	normal - hard
2. Delta	15	normal
3. Stato	13	normal
4. Danforth	11	normal
5. U5 navy-type LWT	8	normal
6. Pool	8	normal - poor
7. Stockless	5	normal
8. Eel	7	normal
9. Flinstone	2 – 4	normal - hard
10. Stock	3 – 5	normal - hard
11. Culumb	6 – 8	normal - hard
12. Stone	2 – 3	all
13. Kite	30 – 100	mud
14. Mushroom		

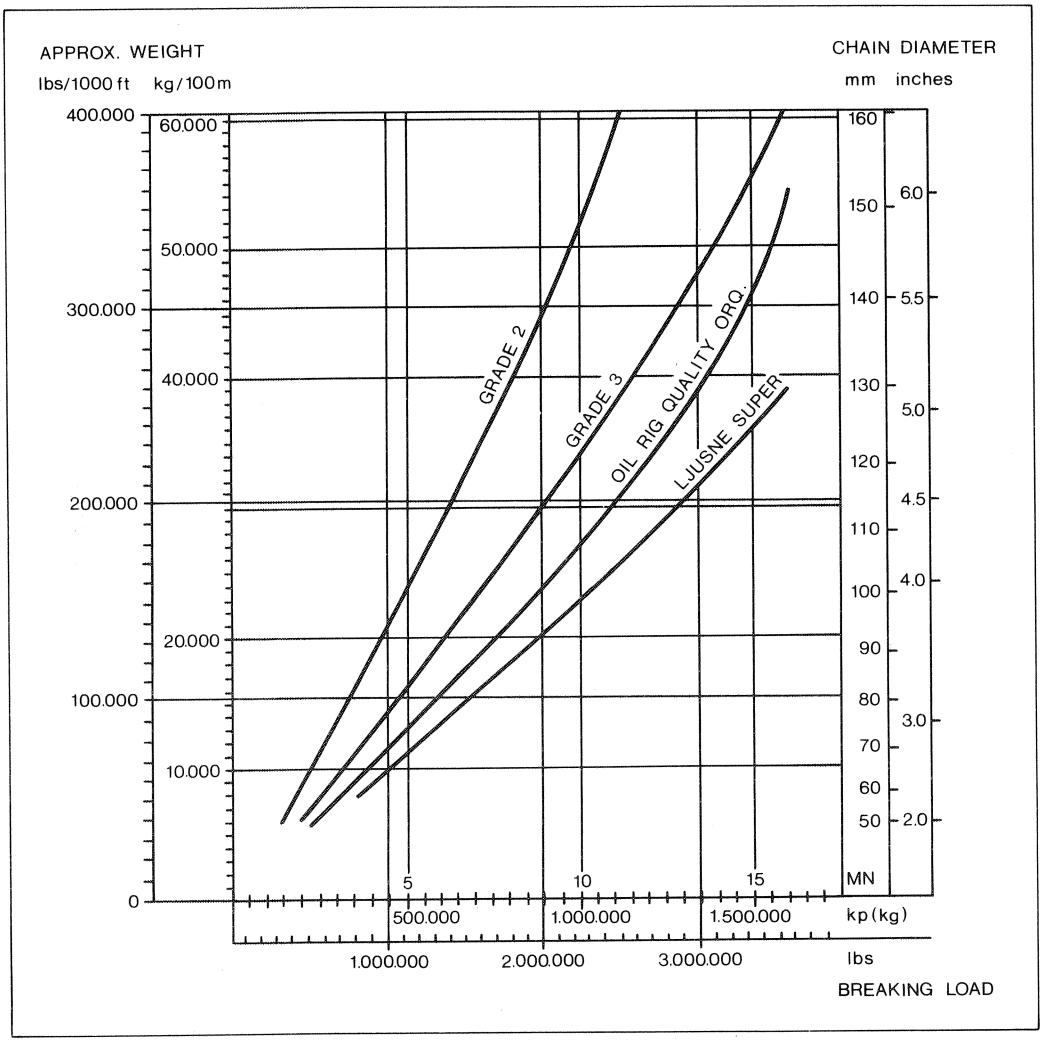

Figure 2.4.6.10 Comparison of chains

References

1. Robert L.Wiegel, **Oceanographical Engineering,** Prentice Hall, inc, 1964

2. **Hydraulic Aspects of Coastal Structures,** part 2 Delft University Press, Delft, Netherlands, 1980.

3. **Hydromechanical Aspects of Floating Offshore Constructions part 2,** Ships Hydromechanics laboratory, Delft, University of Technology, report no 458 - 1977 (Dutch text).

4. **Ship motions in waves** Ship Hydromechanics Laboratory, Delft, University of Technology, report no 502 K-1980 (Dutch text)

5. H.F. Metz, G. Kranendonk, **Calculation of Anchor Chain, Polytechnical Magazine, 2/5/1973 (Dutch text)**

6. J.J. Myers, C.H. Holm, R.F. McAllister, **Handbook of Ocean and Underwater Engineering,** 1969, McCraw-Hill.

7. **Principles of Naval Architecture,**Society of Naval Architects and Marine Engineers, 1967.

K.W. Pilarczyk

2.4.7. Stability of loose and cohesive materials

2.4.7.1. Initiation of particle motion. Basic principles

The water current acting along the bottom of a watercourse exerts on the bottom an opposite force known as shearing stress (τ_o). On the other hand, the magnitude of the shearing stress determines the vertical velocity distribution, U_y. The velocity distribution can be approximated both by a logarithmic and an exponential function.

1° Logarithmic velocity distribution

Starting from a logarithmic velocity distribution and straight and parallel stream-lines, U_y can be expressed as (Fig. 2.4.7.1.).

$$U_y = \frac{U^*}{K} \ln \frac{y}{y_0} = 2.5\, U^* \ln \frac{y}{y_0} \qquad (1)$$

where y = distance from the bed, y_o = the point where U = 0, K = von Kármán's constant ≈ 0,4 and U* is called the 'shearing stress velocity' defined as

$$U^* = \sqrt{\frac{\tau_0}{\rho_w}} \qquad (2)$$

The bed shear stress can be also expressed as

$$\tau_0 = \rho_w g h i \qquad (3)$$

where h = water depth, ϱ_w = density of water, g = acceleration of gravity and i = hydraulic gradient of slope.
The average velocity is found by integrating the vertical velocity-distribution and will be approximately equal to

$$\bar{U} = \frac{U^*}{K} \ln\left(C_0 \frac{h}{y_0}\right) = 2.5 U^* \ln\left(0.4 \frac{h}{y_0}\right) = 5.75\, U^* \log\left(0.4 \frac{h}{y_0}\right) \qquad (4)$$

where $C_o = \frac{1}{e} = \frac{1}{2.718} = 0.368 \approx 0.4$

(U_y is equal to the mean velocity at $y \approx 0.4\, h$).

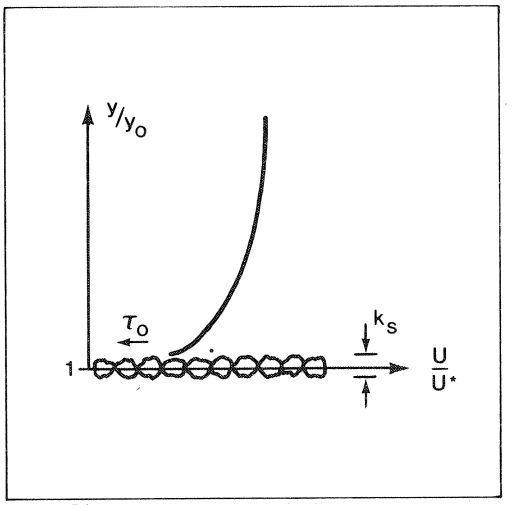

Figure 2.4.7.1 Definitions

For rough boundaries with uniform roughness Nikuradse found that $y_o = 0.033\, k_s$ in which k_s the size of the sand grains, is used as a roughness factor. In this case,

$$\bar{U} = 5.75\, U^* \log\left(12 \frac{h}{k_s}\right) \qquad (5)$$

However, this equation is only valid for the completely developed turbulent bottom layer. In the case of bed-roughness discontinuity, i.e. the point where the smooth part changes into a rough part, the magnitude of the bed shear stress at the beginning of the rough part can be much higher than at a certain distance further away because the velocity profile above the smooth bottom will be much less affected (the vertical distribution will be much closer to the rectangular one). Substitution of eqs.(2) and (3) into eq. (5) gives

$$\bar{U} = (18 \log 12\frac{h}{k_s})\sqrt{hi} \qquad (6a)$$

or

$$\bar{U} = C\sqrt{hi} \qquad (6b)$$

which is the well-known Chézy equation.

The roughness-value (k_s) can rougly be estimated as follows, [2,5]:

for uniform sediment k_s = (1 to 2).D (D = grain diameter)
for graded sediment k_s = (1 to 2) D_{90}
for a bed with ripples k_s = (0.5 to 1) h_{ripple}

The stability of a particle on the bed of a watercourse is disturbed if the resultant effect of the disturbing forces becomes greater than the stabilising forces such as gravity and cohesion. Cohesion is only important for sediments in the clay and silt or fine sands with an appreciable silt content.

The disturbing force (resulting from drag and lift forces) will be proportional to the bottom shear stress and the particle surface area (D^2). The stabilising gravity force is proportional to $(\varrho_s - \varrho_w)\, g\, D^3$. The quality of these forces gives the equation:

$$\alpha_1 \tau_0 D^2 \geq \alpha_2 (\rho_s - \rho_w) g D^3$$

or

$$\tau_0 \geq \Psi(\rho_s - \rho_w) g D \qquad (7)$$

The factor Ψ depends on the flow conditions near the bed, particle shape and the position of the particle in relation to other particles etc. The flow conditions near the bed can be described by the ratio of grain size to thickness of the viscous sublayer which ratio is proportional to $U^*D/\nu = R_e$,a Reynolds number based on grain size and shear velocity.
Under conditions that are critical for the material in question (i.e. initiation of movement), the above mentioned parameters can be expressed by Ψ_{cr} as,

$$\Psi_{cr} = \frac{\tau_{cr}}{\Delta \rho_w g D} = \frac{U^*_{cr}}{\Delta g D} = f(\frac{U^*_{cr} D}{\nu}) = f(R_e) \qquad (8)$$

where

$$\Delta = \frac{\rho_s - \rho_w}{\rho_w}$$

Relation (8) has been investigated by many authors especially by Shields [8] who did systematic tests and compared his results with results from other investigations(see Figure 2.4.7.2.). The difficulty in all tests is the definition of „initiation" of motion.Is it the movement of the first particle or of a certain number of grains? Shields correlated the rate of sediment transport with τ_0 and defined τ_{cr} by extrapolating to zero material transport [2].

For a large R_e (rough bed) it can be seen that U^*_{cr} varies with $\sqrt{D}$ (figure 2.4.7.3.). For equal values of $h/_D$ and therefore equal values of U/U* it follows that U_{cr}:: $\sqrt{D}$ and that the critical velocity of a stone (grain) is proportional to the 1/6 power of the weight of the stone (or stone weight proportional to $\bar{U}^6$).

Turning back to eq.(5), the condition of initial movement can be expressed as a function of mean velocity based on logarithmic vertical distribution as

$$\frac{\bar{U}_{cr}}{\sqrt{\Delta g D}} = 2.5\sqrt{\Psi_{cr}} \ln(12\frac{h}{k_s}) = 5.75\sqrt{\Psi_{cr}} \log(12\frac{h}{k_s}) \qquad (9)$$

2° Exponential velocity distribution.

In the case of the exponential function of vertical velocity distribution (i.e. Mannings formula), the above mentioned transformation will be as follows:
Mean velocity:

$$\bar{U} = \frac{1}{n} h^{2/3} i^{1/2} \qquad (10)$$

Normally, the value of n (roughness parameter)

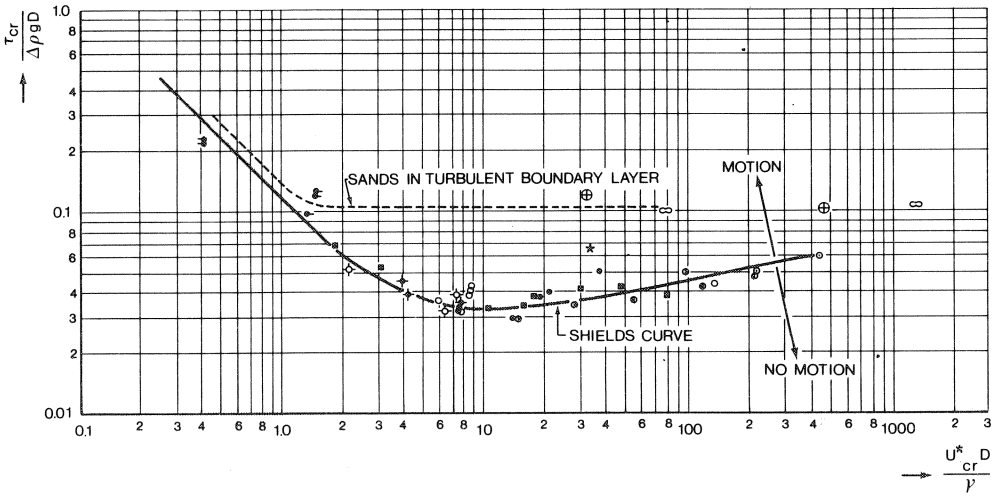

FULLY DEVELOPED TURBULENT VELOCITY PROFILE

SYM	DESCRIPTION		γ_s, g/cm^3
○	AMBER	(SHIELDS)	1.06
•	LIGNITE		1.27
◎	GRANITE		2.70
◉	BARITE		4.25
■	SAND (CASEY)		2.65
⊹	SAND (KRAMER)		2.65
+	SAND (U.S.W.E.S.)		2.65
⊙	SAND (GILBERT)		2.65

TURBULENT BOUNDARY LAYER

⊸	SAND (VANONI)	2.65
⊸	GLASS BEADS (VANONI)	2.49
⊕	SAND (WHITE)	2.61
∞	SAND IN AIR (WHITE)	2.10
*	STEEL SHOT (WHITE)	7.90

Figure 2.4.7.2 Shield's diagram; dimensionless critical shear stress vs, shear Reynolds number.

has been presented in a tabulated form as a function of the type of roughness [11]. However, it has been established that n is a function of D and may be taken as being equal to $n = 0.0525 D^{1/6}$ expressing D in meters, [3,6].

From equation (3), under „critical" conditions

$i = \frac{\tau_{cr}}{\rho w g h}$, which in combination with eq. (7) gives

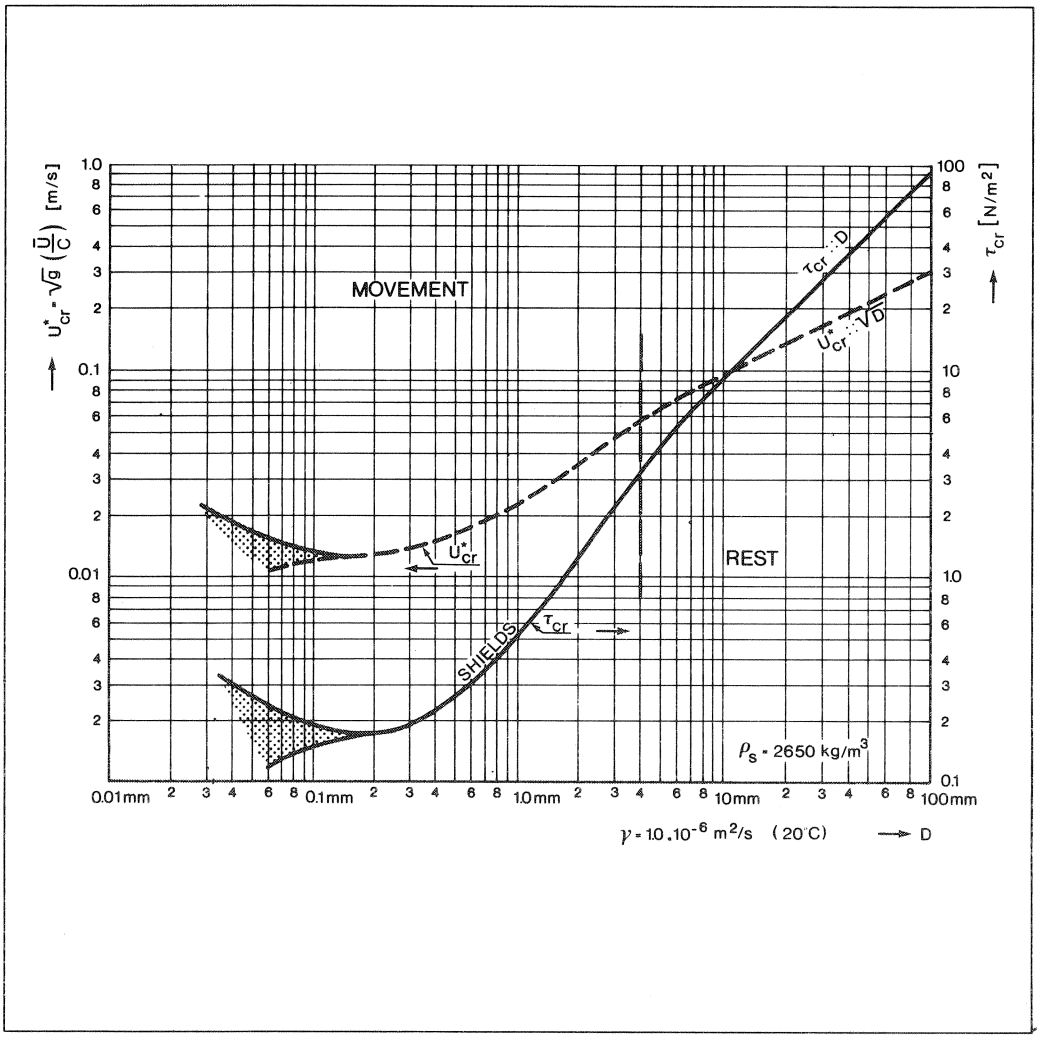

Figure 2.4.7.3 Critical shear stress and critical shear velocity as function of grain size for ϱ_s = 2650 kg/m³ (sand).

$$i = \frac{\Psi_{cr}\rho_w \Delta g D}{\rho_w g h} = \Psi_{cr}\Delta\frac{D}{h} \qquad (11)$$

Substituting the value of i from eq.(11) into eq.(10), for „critical" conditions at which sediment starts to move,

$$\bar{U}_{cr} = 19\sqrt{\Psi_{cr}}\sqrt{\Delta D}\,(\frac{h}{D})^{1/6} \qquad (12a)$$

or

$$\frac{\bar{U}_{cr}}{\sqrt{g\Delta D}} = \frac{19}{\sqrt{g}}\sqrt{\Psi_{cr}}\left(\frac{h}{D}\right)^{1/6} = 6.07\sqrt{\Psi_{cr}}\left(\frac{h}{D}\right)^{1/6} \qquad (12b)$$

The equations (9) and (12) suggest that when depth h is large in comparison with diameter D(or k_s), the velocity in the vicinity of the particles is less due to friction, so that the mean velocity must be greater for greater depths to produce the same critical shear stress on the stream bed. However, this conclusion is still insufficiently supported by experimental data.
The problem of defining the design stone diameter is still insufficiently solved. Different authors use different definitions for D. However, in most cases for diameter D, the average sieve value $D_{50\%}$ or the equivalent diameter D_s are used, where D_s is defined by:

$$\text{Volume} = \frac{\pi}{6} D_s^3 \text{ or } D_s = \left(\frac{6}{\pi}\text{ Volume}_{50\%}\right)^{1/3} = \left(\frac{6}{\pi}\frac{G_{50\%}}{\gamma_s}\right)^{1/3} \qquad (13)$$

where $G_{50\%}$ is the weight of stone, 50% of the particles in the total grain weight distribution are smaller than $G_{50\%}$.
For uniform flow, a criterion of a beginning of movement may be derived by taking a Shields Ψ-value of 0.06 ($= \Psi_{cr}$). However, because of the discovered unreliability of $\Psi = 0.06$ in most practical cases, it is advisable to use Ψ_{cr} equal to **0.03** or even less if one wishes to preserve a more reliable stability of stones.
It is clear that the critical value of τ_o will depend on the definition of the criterion for initiation of motion. To get an objective criterion Paintal [7] proposed to use the parameter Ψ as a function of the dimensionless transport-parameter q_s^*, where q_s^* is given by

$$q_s^* = \frac{q_s \rho_w^{1/2}}{\gamma_s D\sqrt{(\gamma_s - \gamma_w) D}} \qquad (14)$$

where: q_s = unit transport of sediment (= number of particles x volume of a particle x γ_s), ϱ_w = density of water, γ_s and γ_w = specific weight of sediment and water respectively, D = grain diameter equal to particle size of which 50% of the material is finer. Paintal recognized two transport areas; one area with a higher transport rate for $\Psi > 0.06$ and another area with a lower transport rate for $\Psi < 0.06$ (Figure 2.4.7.4.). He has measured very low rates of transport with coarse material down to $\Psi = 0.02$, thus well below the Shields value. Such presentation allows the choice of a value of Ψ for a permissible transport (= a number of stones) for each case in question.

2.4.7.2. Influence of various factors

Effect of particle shape
The shape factor is defined as

$$sf = \frac{c}{\sqrt{ab}} \qquad (15)$$

where a,b and c are the linear dimensions, maximum, intermediate and minimum respectively, of the three mutually perpendicular axes. Shields experiments were done with several types of material, but no systematic influence of shape has been observed. Tests at the Delft Hydraulics Laboratory with coarse material showed that the critical value of Ψ is roughly the same for various shapes (spheres, cubes, standard broken stones etc.) if the nominal diameter $D_n = (\text{Volume}_{50\%})^{1/3}$ is used for comparison, [10, 13, 14].

However, the results of the Hallmark and Smith work [4] showed that the shape factor of the particles affects the condition of the beginning of movement. Their tests showed that stones with low shape factor values (i.e. the flatter stones) move more easily, indicating a 30% increase in threshold velocity corresponding to an increase in shape factor from 0.5 to 0.7. It will be noted that the value of 0.7 normally corresponds with standard quarry stone. However, it generally requires, that the largest dimension shall not be greater than twice the smallest dimension.
The discussion implies that in some specific cases the shape factor can be an important factor in defining the stone stability.
The definite conclusion about this effect can still not be drawn.

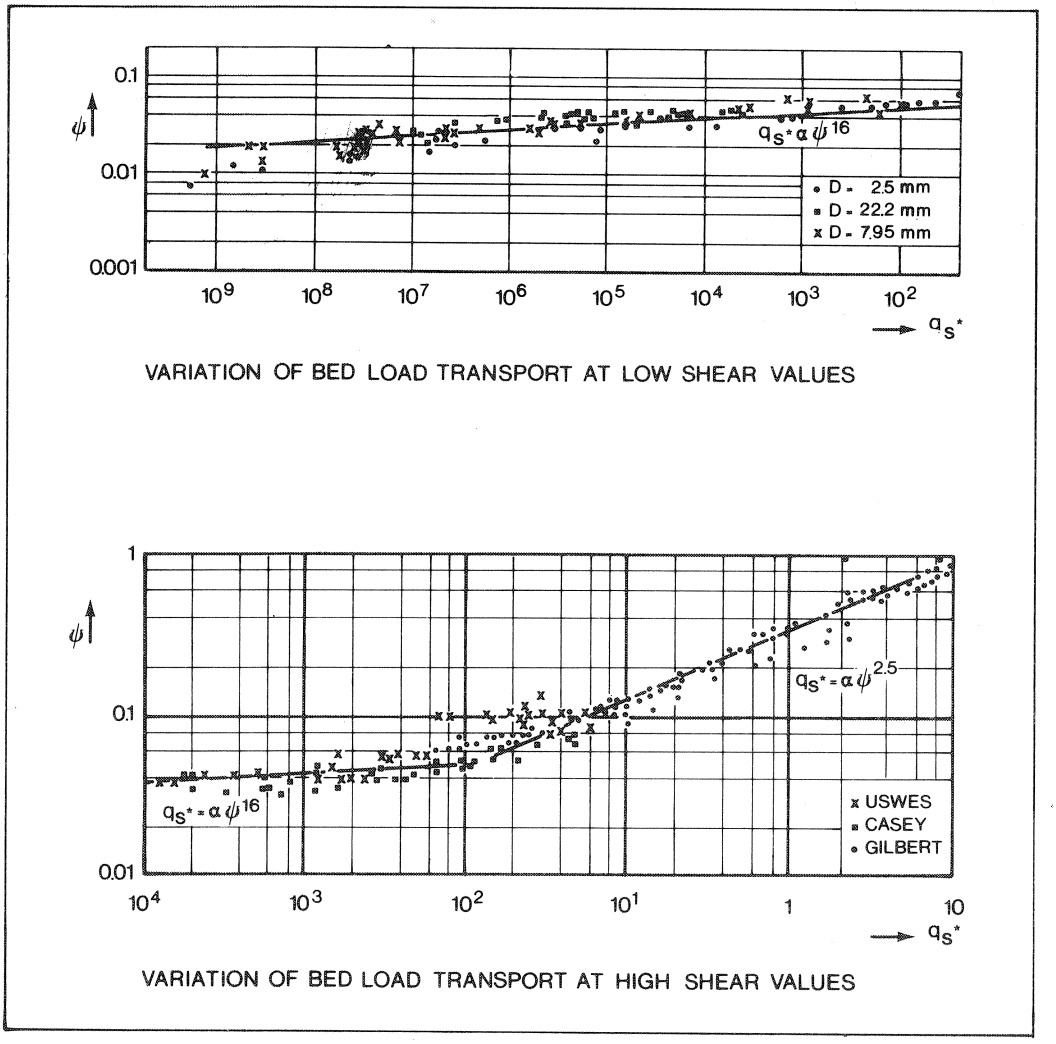

Figure 2.4.7.4 Ψ_{cr} vs. q^*_s according to Paintal.

Effect of gradation

It will be clear that a wide gradation will have an influence on τ_{cr} (or Ψ_{cr}). In practice, however, the gradation is only evident for $D_{95}/D_5 > 5$ because the larger grains are more exposed and smaller grains are shielded by the larger ones [14]. Therefore D_{50} is accepted to be a good measure for most samples, but the experience of the Delft Hydraulics Laboratory suggests the use of

D_n instead of D_{50}. For a wide particle gradation, the effect of armouring will occur which means that fine particles are eroded and an armour layer of coarse particles is formed, which protects the bed from further scour.

Effect of relative water-depth
For small values of h/D (waterdepth/particle diameter) a deviation from Shields graph is possible because τ_o is not representative in that case for the turbulent flow structure. The turbulence structure near the bed in an infinite fluid is defined completely by bed shear stress (τ_o)and roughness (k_s) but, for small values of h/D the water-depth also limits the size and frequency of large eddies. In that case the ratio of eddy duration and the time necessary to accelerate a particle decreases so that an influence of h/D may be expected (more stability with smaller h/D). Experiments by Ashida [1] have shown that Ψ_{cr} increases with decreasing h/D.
More studies must, however, still be done on this problem to arrive at an acceptable solution.

Influence of the bed slope. (Fig. 2.4.7.5.)
For a particle on a slope the value of τ_{cr} will be reduced.
For **a horizontal bed**, the relation

$$F(0) = G\tan\phi_r \tag{16}$$

is valid, in which Φ_r is an angle characteristic for the particle stability.
For a bed slope in the flow direction with angle α the following stability condition holds:

$$F(\alpha) + G\sin\alpha = N'\tan\phi_r = G\cos\alpha\ \tan\phi_r \tag{17}$$

and the reduction factor is equal to

$$K(\alpha) = \frac{F(\alpha)}{F(0)} = \frac{\sin(\phi_r-\alpha)}{\sin\phi_r} \tag{18}$$

For a side slope with angle β, the stability condition is

$$R = \sqrt{F(\beta)^2 + G^2\sin\alpha} = G\cos\beta\ \tan\phi_r \tag{19}$$

Figure 2.4.7.5 Forces acting on a non-cohesive particle on a bank.

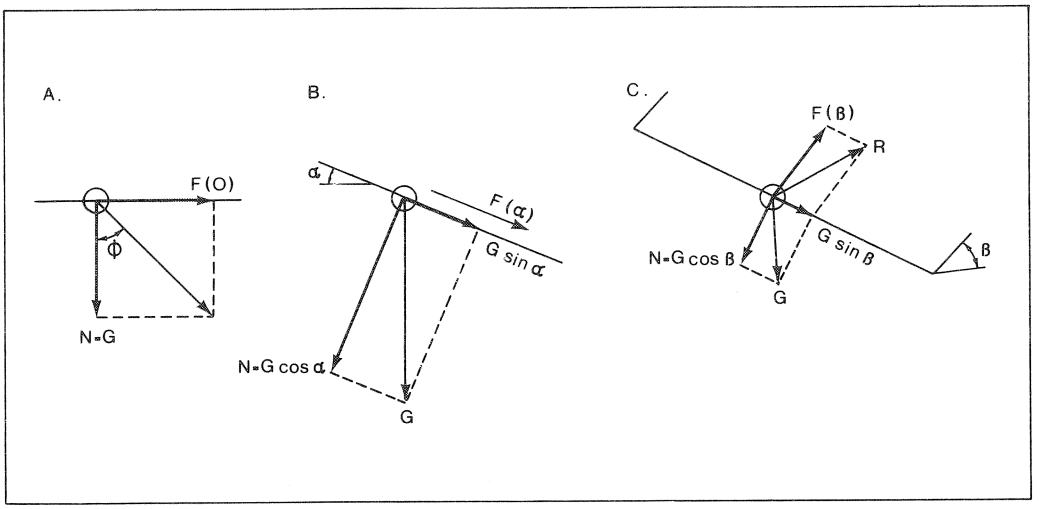

and the reduction factor is equal to

$$K(\beta) = \frac{F(\beta)}{F(0)} = \cos\beta\sqrt{1 - \frac{\tan^2\beta}{\tan^2\phi_r}} \qquad (20)$$

For a combination of a longitudinal and a side slope, the reduction factor $K(\alpha,\beta)$ becomes $K(\alpha,\beta) = K(\alpha).K(\beta)$.
Because $\tau :: F$ and $U^* :: \tau$ thus

$$\frac{U^*(\alpha)}{U^*(0)} = \sqrt{K(\alpha)} \text{ and } \frac{U^*(\beta)}{U^*(0)} = \sqrt{K(\beta)} \qquad (21)$$

In the derivation mentioned above the influence of the lift forces has been neglected. However, for slopes steeper than 1 on 3, the influence of the lift force becomes more evident and must therefore be taken into account to arrive at a more precise description of the lower limit of incipient motion [9] .
More information on stability of loose materials and sediment transport may be found in [15].

2.4.7.3. The maximum permissible velocity

Unprotected non-cohesive channels
In the past, attempts were made to define a mean velocity that would not cause erosion of the channel body (the so-called maximum permissible velocity, or the non-erodible velocity). However, it is now doubtful whether such a velocity actually exists. Ven te Chow [11] published the Russian values of maximum permissible velocities (data from 1936) above which scour would be produced in non-cohesive material of a wide range of particle sizes (Fig.2.4.7.6.). These data can be used for a first approximation of the permissible flow conditions for non-protected channels.

Grassed channels
The grass will on the one hand stabilize the body of the channel, consolidate the soil mass of the bed, and reduce erosion. On the other hand, the presence of grass will result in extra turbulence and retardation of flow. The design of the grassed channels is described in [11]. Permissible velocities for different vegetal covers, channel slopes, and soil conditions, recommended on

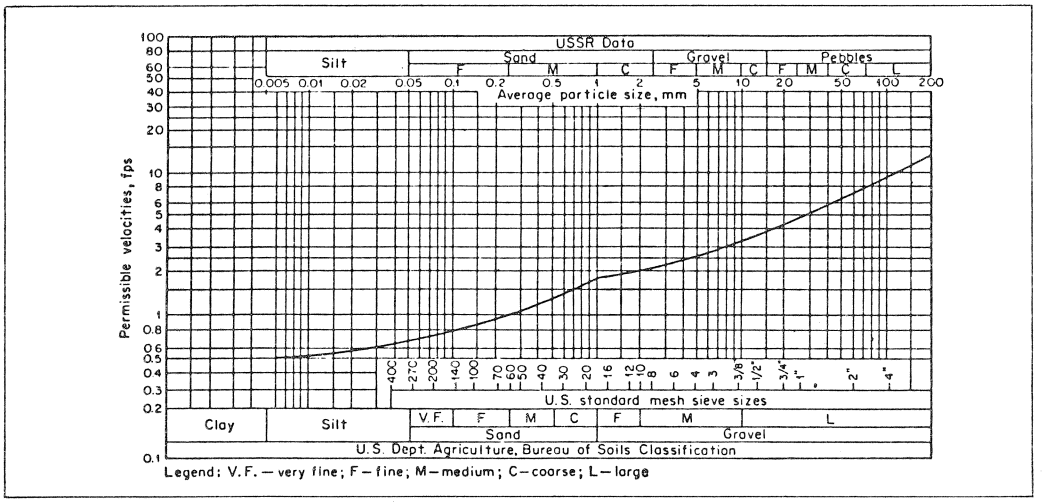

Figure 2.4.7.6 U.S. and U.S.S.R. data on permissible velocities for non-cohesive soils.

the basis of investigations by the U.S. Soil Conservation Service, are shown in the following table.

Table 1: Permissible Velocities for Channels Lined with Grass [11]

Cover	Slope range, %	Permissible velocity, fps: Erosion-resistant soils	Permissible velocity, fps: Easily eroded soils
Bermuda grass	0 – 5	8	6
	5 – 10	7	5
	> 10	6	4
Buffalo grass, Kentucky bluegrass, smooth brome, blue grama	0 – 5	7	5
	5 – 10	6	4
	> 10	5	3
Grass mixture	0 – 5	5	4
	5 – 10	4	3
	Do not use on slopes steeper than 10%		
Lespedeza sericea, weeping love grass, ischaemum (yellow bluestem), kudzu, alfalfa, erabgrass	0 – 5	3.5	2.5
	Do not use on slopes steeper than 5%, except for side slopes in a combination channel		
Annuals - used on mild slopes or as temporary protection until permanent covers are established, common lespedeza, Sudan grass	0 – 5	3.5	2.5
	Use on slopes steeper than 5% is not recommended		

Remarks. The values apply to average, uniform stands of each type of cover. Use velocities exceeding 5 fps only were good covers and proper maintenance can be obtained.

Cohesive soils

A cohesive character of a soil will increase the resistance against erosion.

For cohesive soils no theoretical approach exists as yet to determine the critical flow velocity. Instead empirical data obtained from experiments, usually performed in laboratory flumes, must be used. Some results of experiments carried out in the U.S.S.R. on critical mean velocities are given in table 2 [12].

The remaining subjective element is that one has to decide whether the material under consideration belongs to one of the categories.

In figure 2.4.7.7. an attempt is made to indicate the critical flow velocity U as a function either of n or of ϵ,[12]. In the diagram, all the known experiments are used whereas the Russian tests are shown separately. The figures are valid for a depth of about 1.0m, a horizontal bed, and a straight channel. For other depths, the correction factor has to be introduced according to the assumed velocity distribution. For slopes, the slope factor K (α,β) has to be applied.

One should keep in mind that, because of the arbitrary selection of the category to which the cohesive soil belongs, the above mentioned data should be used only to provide a first indication of the resistance of the soil against the

current. As soon as the application becomes important from a cost and risk point of view, it is recommended that the resistance of the material under consideration be checked on undisturbed samples in a laboratory.
Several authors have tried to correlate critical shear stress with mechanical properties of the soil [2]. From the data given it appears that, for cohesive soils with D_{50} = 10-100μ,a critical shear velocity U^*_{cr} of 3-4.5 cm/s is possible. However, for an exact determination of a critical shear stress of a cohesive soil, a special test for each soil will be necessary.

Table 2:

Material/compactness	Loose	Moderately compact	Compact	Very compact
heavy clayey soils	0.45m/s	0.9m/s	1.25m/s	1.70m/s
clay	0.35m/s	0.8m/s	1.20m/s	1.65m/s
lean clayey soils	0.30m/s	0.7m/s	1.05m/s	1.35m/s
Voids ratio, $\epsilon = \frac{n}{1-n}$	2.0-1.2	1.2-0.6	0.6-0.3	0.3-0.2

(n = voids/total volume)

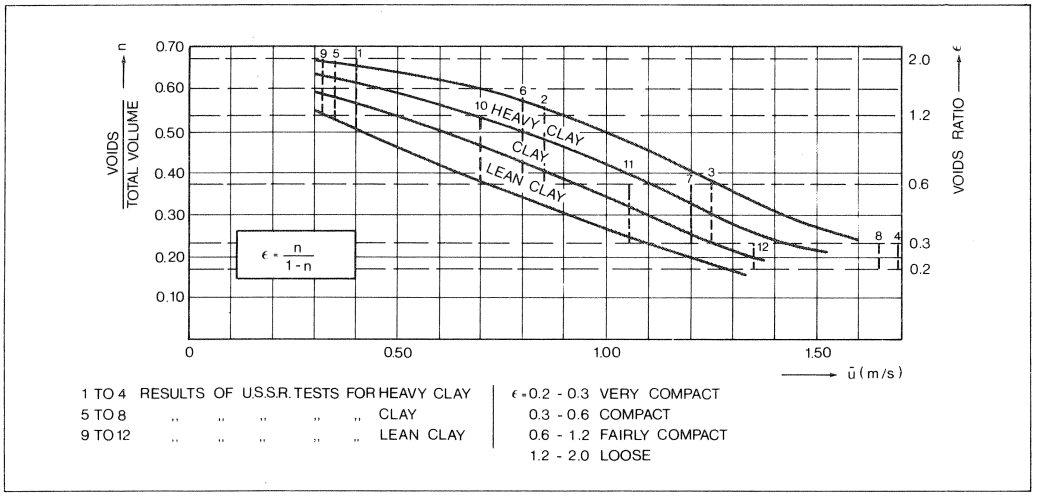

Figure 2.4.7.7 Critical flow velocity for cohesive soils.

References

1. Ashida, K. and Bayazit M., Initiation of Motion and Roughness of Flow in Steep Channels, **IAHR Conf.**, Istanbul, paper A58, 1973.

2. Breusers, H.N.C., Lecture Notes on Sediment Transport, **International Course in Hydraulic Engineering**, Delft 1979-1980.

3. Chang, Y.U., Laboratory investigations of the Flume Traction and Transportation, **Trans. ASCE, 65**, no.8, pt.2,1939.

4. Hallmark, D.E., Smith, G.L., Stability of Channels by Armorplating. **Jour. of the Waterways and Harbors Division**, WW3, August 1965.
(Discussions: WW1, February 1966 and WW3, August 1966).

5. Kamphuis, J.W., Determination of sand Roughness for Fixed Beds, **Journal of Hydraulic Research**, IAHR, Vol. 12, no.2, 1974.

6. Linford, A., Review of Literature on the Construction of Rockfill Dams by Dumping Stones in Running Water, **B.H.R.A. report TN873**, 1967.

7. Paintal, A.S., Concept of Critical Shear Stress in Loose Boundary Open Channels, **Journal of Hydraulic Research**, no.1. 1971.

8. Shields, A., Anwendung der Ahnlichkeitsmechanik der Turbulenzforschung auf die Geschiebebewegung, **Mitt. der Preusz. Versuchsanstalt für Wasserbau und Schiffbau**, Berlin, Heft 26, 1936.

9. Syunsuke Ikeda, Incipient Motion of Sand Particles on Side Slopes, **Journal Hydraulics Division**, HY1, January 1982.

10. Venis, W.A., Behaviour of Dumping Materials when Exposed to Currents and Wave Action, **De Ingenieur, 50, 1968** (The Netherlands).

11. Ven te Chow, **Open-channel Hydraulics**, McGraw-Hill Book Company, New York-London, 1959.

12. Zanen, A., Revetments, **Int. Courses in Hydraulic and Sanitary Engineering**. Delft 1976, The Netherlands.

13. Stability of Rockfill Dams (in Dutch), **Delfts Hydraulics Laboratory**, Report M731-VI., 1965.

14. A review of Literature on Incipient Motion of Sediments(in Dutch), **Delft Hydraulics Laboratory**.Report S159-I 1971 and S159-II, 1976.

15. Jansen, P.Ph. et al, **Principles of River Engineering**, The Non-tidal Alluvial River, Pitman, London-San Francisco-Melbourne, 1979.

K.W. Pilarczyk

2.4.8. Stability of rock-fill structures

2.4.8.1. Stability of stones exposed to currents. Practical applications

The stability of stones in revetments or on sills has been discussed by several authors [29, 32, 35, 42, 52]. However, the various formula which have been determined often differ greatly. Those that have been selected seem to be the most appropriate for practical application.

1°. General stability formula and recommended coefficients:

General equation:

$$\frac{U_{cr}}{\sqrt{g\Delta D_s}} = 6\sqrt{\Psi_{cr}}\left(\frac{h}{D_s}\right)^{1/6} = \varphi_1\left(\frac{h}{D_s}\right)^{1/6} \qquad (1)$$

or

$$D_s = \frac{1}{\varphi_1^3 (g\Delta)^{3/2}} \frac{U_{cr}^3}{\sqrt{h}} = \varphi_2 \frac{U_{cr}^3}{\sqrt{h}} \quad \text{(in m)} \qquad (2)$$

where: U_{cr} = critical velocity, g = acceleration of gravity, Δ = relative density of stones, ψ_{cr} = parameter defining the critical conditions of stone movement, h = water depth, D_s = equivalent diameter (sphere) of the average weight of stones, $G_{50\%}$, and φ_1, φ_2 = numerical coefficients.
In the case of a sill, the water depth has to be taken above the downstream part of the sill crest.
By choosing the appropriate values of the parameter Ψ_{cr} the following recommendatian can be given.

Coefficients:

No.	Ψ_{cr}	φ_1	φ_2	application ($\Delta = 1.6$ à 1.7)
1	0.06	1.5	0.005	horizontal bottom with no bed-roughness discontinuity and uniform flow (limited stone transport)
2	0.035	1.15	0.010	bottom protection (limited stone-transport); construction phases of a dam; a sill $B/h > 5$
3	0.0275	1.0	0.015	bottom protection (for absolute rest of stone) or a sill $B/h < 5$.

(B = width of the crest)

The formulas given do not take into account the influence of high turbulence generated by specific constructions such as spillways with a hydraulic jump.
In that case, the critical velocity calculated for a given stone diameter has to be reduced by a factor

$$\varphi_r = \frac{1.45}{1+3r} \qquad (3)$$

in which r is the relative turbulence intensity; a value r = 0.15 has been normally assumed in a uniform flow over a rough bed.
Directly downstream from a hydraulic jump (stilling basin), values of r in the order of 0.3 to 0.35 can be expected. This gives a value for φ_r of about 0.7. This agrees roughly with the design graphs given by Cox [17].

The influence of turbulence in the hydraulic jump on the erosion-capacity of the flow has also been studied by Kumin (33,53). For calculation of the stone diameter, Kumin proposes that the mean velocity be multiplied by a correction factor k, which value depends on the submergence-grade of the jump and the distance from the contracted section of the jump. It is apparent that the factor k is equal to $1/\varphi_r$. The graphical representation of the factor k is given in figure 2.4.8.1. The recommended formula for calculation of the stone diameter is of type (2) with $\psi = 0.035$ ($\varphi_2 = 0.01$).
A more sophisticated method of calculating the stone stability below spillways under action of a hydraulic jump is given by Zharkov [59].

For the stability of stones affected by vortex streets, it is difficult to give a generally valid recommendation. In most cases, a specific

model investigation is required. However, as a rough indication, in such extreme cases, the calculated permissible critical velocity has to be reduced by about 50%. Vortex streets can also be generated during the closing operations due to the presence of various abutments. These effects must therefore all be carefully examined in order to obtain a safe design of the protective structures.

Figure 2.4.8.1 Velocity correction-factor due to turbulence (hydraulic jump [53]).

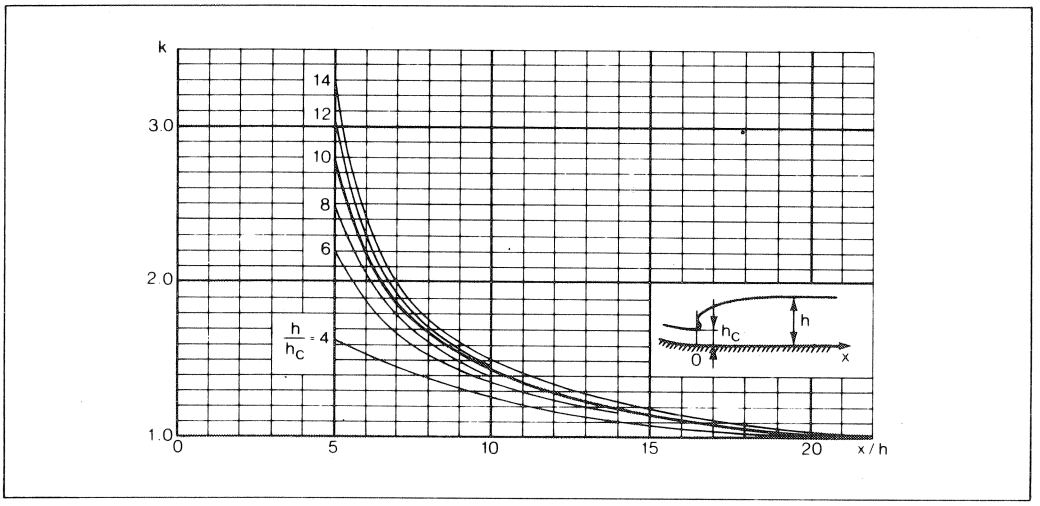

2°. Empirical formulas.

- Isbash [29] neglects the influence of h/D and gives the empirical relation for the stability of a stone in a bed (embedded between other stones) as,

$$U_{cr} = 1.2\sqrt{2g\Delta D_{50}} = 1.7\sqrt{g\Delta D_{50}} \qquad (4)$$

For a stone on the top of a dam (sill) or situations where no fully developed turbulent boundary layer exists (outlets) the critical velocity is reduced to:

$$U_{cr} = 0.86\sqrt{2g\Delta D_{50}} = 1.2\sqrt{g\Delta D_{50}} \qquad (5)$$

The formulas of Isbash can be successfully applied for the relative depths $h/D < 5$ or for outlets where no vertical adjustment of the velocity profile has taken place.

- The Delft Hydraulics Laboratory has established the following formulas which are applicable to the design of the closure stages of a vertically-built-up sill at $h/D > 5$ and submerged spillway-conditions [60a, 56, 19]:
For a broad-crested sill, $B/h > 5$

$$\frac{U_{cr}}{\sqrt{g\Delta D}} = 1.4 \log 3.5 \frac{h}{D} \qquad (6)$$

For a sharp-crested sill (side slopes 1:2)

$$\frac{U_{cr}}{\sqrt{g\Delta D}} = 1.4 \log 1.5 \frac{h}{D} \qquad (7)$$

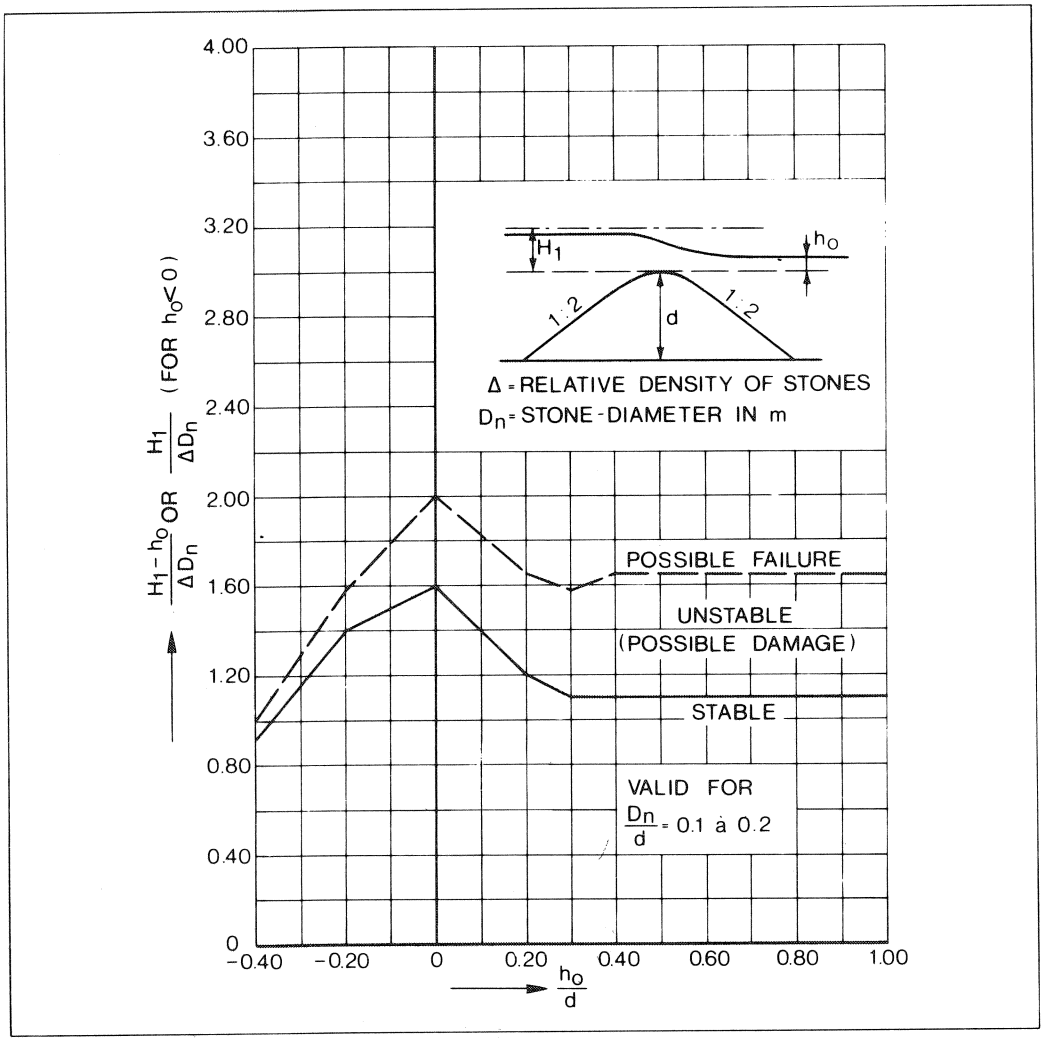

Figure 2.4.8.2 Critical head difference in relation to relative water depth.

Where diameter D (both for stones and blocks) is defined as a nominal diameter D_n = (volume$_{50\%}$)$^{1/3}$ = $(G_{50}/\gamma_s)^{1/3}$, representing the linear dimension of a cube of the material considered, the weight of which is exceeded by the individual weight of 50% of the total number of stones.

In the last stages of a closure, done by means of dumping e.g. rock (from a cableway), the dam

tends to develop a triangular shape. Because the determination of the velocity above a sharp-crested dam is usually very difficult, it is more practical to define the critical stability conditions by means of the head difference. Such a criterion has been established by Delft Hydraulics Laboratory for the different stone-sizes in a graphical form as is shown in figure 2.4.8.2.[60b, 56, 19]. The head difference is defined as $(H_1 - h_o)$ where H_1 denotes the energy level upstream and h_o the water level downstream, with reference to the crest of the dam. $H_1 - h_o$ develops into H_1 for $h_o < 0$. For the other parameter, the ratio h_o/d is chosen where d is the dam-height. Thus, this criterion can be used for designing the final closure-stages where free-spillway conditions are usually present.

- This last criterion has been evaluated using relation $H_o/\triangle D_n$ vs. h_B/D_n as it is shown in figure 2.4.8.3. $[60d]_1$ H_o. In this relation H_o is the upstream water depth above the crest.

- In case overtopped dams are also affected by wave-attack (combined effect of current and waves), the influence of the waves can roughly be taken into account by increasing the upper level by ⅓ H_s (H_s = significant wave-height).

- On both sides of a dam the bottom must be protected against scour in order to secure the stability of the dam structure.
From tests carried out on dam slopes varying from 1:2 to 1:8 under submerged flow conditions, it was found that the flow pattern downstream varies with the slope of the dam and with the depth of water over the crest. A gradual slope and a considerable depth produce a flow pattern without eddies, whereby the flow follows the dam. A steep slope ($ctg\alpha < 5$) and a shallow depth above the crest produce an eddy behind the dam (Fig. 2.4.8.4.).
Flow behaviour also depends on the permeability of the dam structure. If the structure is highly permeable, it is possible that no eddy will be formed even if the downstream slope is steep. With a well-developed eddy, the current attack on the bottom is maximal at the location where the main flow touches the bottom of the channel

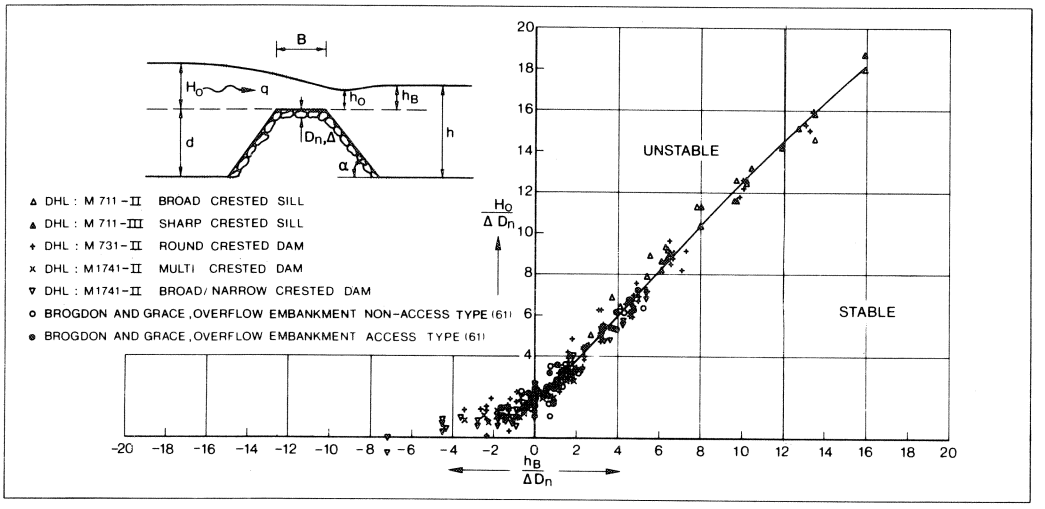

Figure 2.4.8.3 Critical overtopping height against $h_B/\triangle D_n$. Overall results [60d]

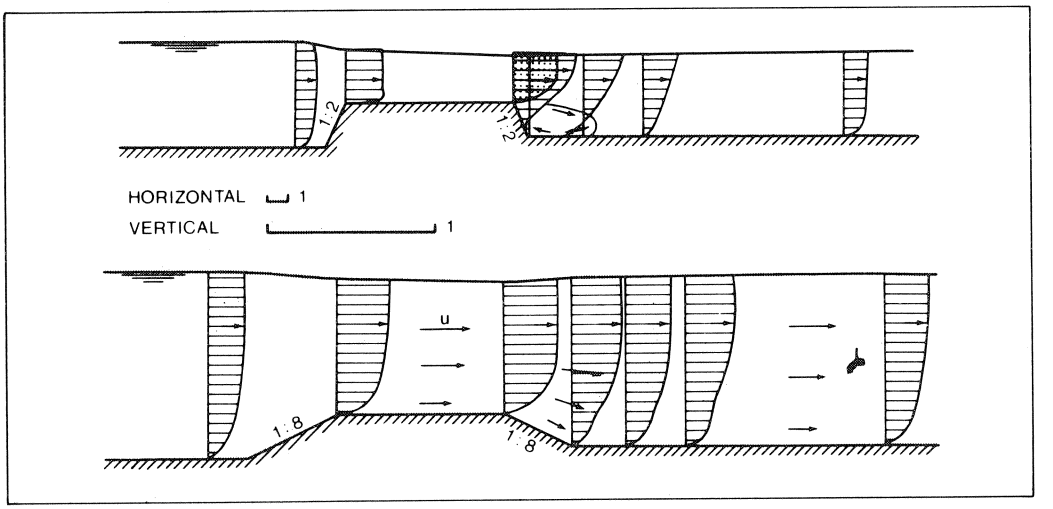

Figure 2.4.8.4 Velocity profiles for dams with steep and gradual slopes.

again. It is, however, not easy to define the exact location due to the heavy turbulence of the flow in this area.

Due to all these various factors, it is difficult to give a general quantification of the possible flow pattern below the dam during the different stages of execution. However, the major conclusion deduced from the results of investigation done by the Delft Hydraulics Laboratory is that, for the bottom protection below the dam under investigation, the same or less stone weight is required as for the critical building-stage of the dam [60].

If the dam has to work as a permanent over-flow dam, the protective top-layer of the dam and the bottom protection has to be checked with respect to the overflow conditions.

For the no-damage protection of the downstream slope of an overflow dam with a relatively impervious core and in the case of free flow conditions, the formula of Hartung and Scheuerlein [24] simplified by Knauss [32] can be applied. This formula defines the maximum unit discharge over the dam as a function of slope angle (α).

$$\text{max. } q = 0.84\sqrt{G_{50}}(1.9 + 0.8\phi - 3\sin\alpha) \quad \text{in } m^3/s.m \tag{8a}$$

or

$$\text{max. } q = \sqrt{g}\, D_s^{3/2} (1.9 + 0.8\phi - 3\sin\alpha) \tag{8b}$$

where D_s is the equivalent diameter and G_{50} is the average weight of stone in KN equal to $G_{50} = \varrho'_s.g.\pi/6\, D_s^3$.

The packing factor ϕ for the construction of the surface layer of rockfill should be estimated within the range of

$$1.125 \geq \phi \geq 0.625$$

(manual packing, placed embankment) (natural packing, dumped embankment)

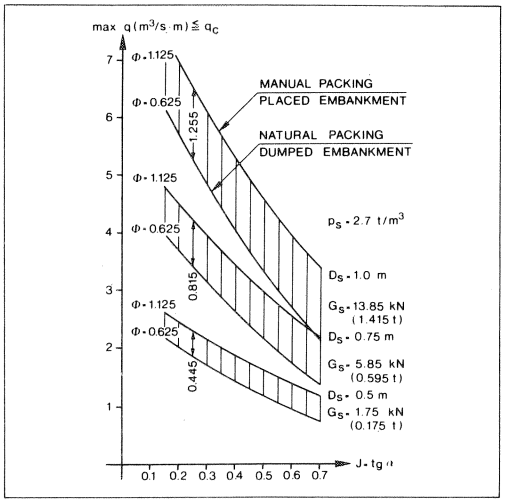

Figure 2.4.8.5 Maximum discharge versus downstream slope, size resp. weight of stones and packing factor [32].

Equation (8) is evaluated and plotted in fig. 2.4.8.5. for the limiting values of the packing factor and several selected stone sizes.It is advisable to use eq. 8 in the cases when the downstream water depth is lower than the dam height. In those cases when the downstream water depth is higher than the dam height eq. 8 is unnecessarily „safe". In such cases the stability criteria of the Delft Hydraulics Laboratory could be used (i.e. Fig. 2.4.8.3).

Other calculating methods and useful remarks and instructions pertaining to the necessary specific design considerations and to the construction procedure can be found in the papers of H. Olivier [42, 43], and also in [29, 52, 6 and 61]. The evaluation of the literature on the stability of stones for different stages of dam closure supplied by new additional investigations of the Delft Hydraulics Laboratory can be found in the report M1741-IV (60d). However, no uniform method of calculation of the stability of rock in closure dams has yet been developed.

4.8.2. Stability of alternative materials

Extensive research into the application of new materials was justified by the potential economic gains. For the closure of one of the sea-arms in the Netherlands (i.e. Grevelingendam), various types of materials were considered and tested [60, 56, 19].
Among the materials tested for applicability as dam-building material were: vacuum-packed plastic foil bags filled with dry or damp sand; nylon and jute bags filled with sand; bags filled with bituminous sand; and humps of sand asphalt manufactured by the warm-mixing method.

By drawing a vacuum within a plastic bag filled with sand, it is possible to increase stresses between the individual grains, thereby transforming the bag with loosely packed grains into a solid body. A disadvantage of this type of vacuum bag is its low specific weight. If sand is used, the bag's specific weight equals the weight of sand volume, i.e. about 1.6 t/m³ for dry sand and about 1.9 t/m³ for damp sand.
Furthermore, the plastic foil easily damages during the dumping process.

The applicability of ordinary sand-bags, made of a mixture of jute and nylon and filled with wet sand, was tested both in the laboratory and in the field. It was found in the model that optimal current stability results were obtained if the bags were filled to 80% of capacity, the degree of filling which in the protytype was found to be most easily accomplished. The tests showed that the loss of stability of sand-filled bags differs from the loss of stability of solid bodies. Before the bags as a whole began to move, the sand inside the bags shifted, causing a considerable change in shape.
The results of comparative tests on scales 1:20 and 1:5 are shown in fig.2.4.8.6.(a).These two tests clearly show a difference in outcome indicating that a scale-effect is involved.
To clarify the matter, a number of tests were

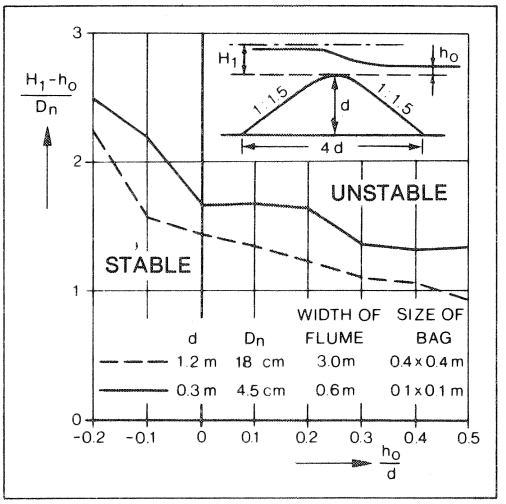

Figure 2.4.8.6(a) Test on sandbags.

Figure 2.4.8.6(b) Influence of ,,scale effect'' on current stability of sandbags.

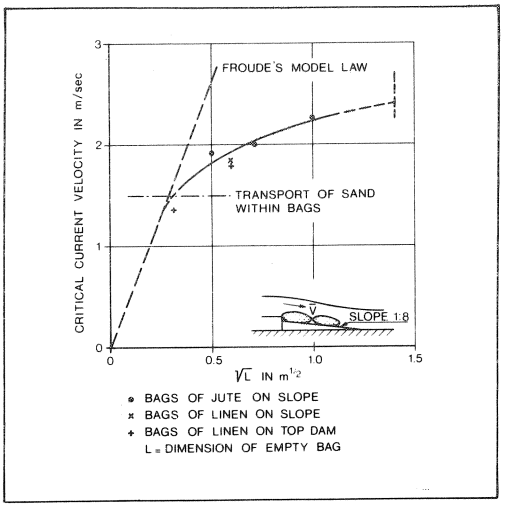

conducted on various scales using a schematized set-up. Results of these tests are shown in fig. 2.4.8.6.(b). in which the critical current velocity required to start movement of the bag is plotted against the square root of the length of the bag. If Froude's model law would be applicable, which is the case with normal materials retaining their shape, the result should be a straight line. This is not the situation at all, as is shown by the curved line in the diagram.
When transferring model tests to prototype conditions, using bags with L = 2m, a critical velocity of the order of 2.5 m/s was obtained. In the diagram, a horizontal line corresponding with a critical velocity of 1.5 m/s indicates the point at which the sand in the bags starts to shift.
The conclusion is that stability tests on sandbags should be undertaken at a scale of 1:1 or, if not possible, a series of scale-tests has to be done.
Due to the above mentioned difficulties, no generally valid design rules for the stability of sandbags have been established.

4.8.3. Stability of stones under wave attack

1° General stability formulas.

The most commonly used formulas to estimate the necessary weight of cover stones are the formulas derived by Iribarran [28] and Hudson [37]. The Iribarren formula is given by:

$$G = \frac{K\gamma_s H^3}{\Delta^3 (f\cos\alpha \pm \sin\alpha)^3} \qquad (9)$$

The Hudson formula may be similarly written as:

$$G = \frac{\gamma_s H^3}{K_D \Delta^3 \mathrm{ctg}\alpha} \qquad (10)$$

where:
G = median weight of armour unit
H = design wave height
Δ = relative density of armour unit;
$\Delta = (\varrho_s - \varrho_w)/\varrho_w$

ϱ_w = water density
ϱ_s = density of armour unit
γ_s = specific weight of armour unit
α = angle of slope
K, K_D = dimensionless stability coefficients
f = friction/interlocking factor of the armour units.

The Iribarren formula is derived in a theoretical way and has no restriction in use regarding the slope steepness. The corresponding values of f and K for riprap introduced in this formula are:

f = 2.38, K = 0.430 for equilibrium towards the bottom i.e. ($f \cos\alpha - \sin\alpha$)

and

f = 2.38, K = 0.849 for equilibrium towards the top i.e. ($f \cos\alpha + \sin\alpha$)

These two equilibrium-curves intersect for natural stones (riprap) at $\mathrm{ctg}\alpha = 3.64$. For slopes steeper than about $\mathrm{ctg}\alpha = 4$, the equilibrium condition towards the bottom is thus representative for estimating the necessary stone weight.

The above mentioned values of K relate to the no-damage conditions. Total failure will usually occur at a wave height 60% higher than the no-damage wave height.

The Hudson formula is based on the results of model tests on slopes of 1 : 1.25 to 1:5. For slopes flatter than 1:5, the use of armour weight as calculated for a slope of 1:5 is recommended. Table 2.4.8.1. shows recommended values of K_D for the no-damage conditions from [62]. It has to be pointed out that most K_D - values for quarrystone are established for rather uniform stone weight. The stones comprising the primary cover layer can range from about 0.75 G to 1.25 G with about 75 percent of the individual stones weighing more than G. For well-graded stone the K_{RR} - stability coefficient has to be used.In this case $G = G_{50}$, where G_{50} is the weight of the 50 percent size in the gradation. It is possible to use larger values of K_D if a few percent of damage is acceptable. In general, for a two-layer system of stones, the exceedance of the no-damage wave height up to 20 percent still provides „tolerable" damage without damage to the underlayer (without appreciable exposure of filter stone).

The stability coefficients K and K_D respectively in the formula of Iribarran and Hudson are determined by laboratory tests carried out with a regular train of waves. The height of the waves has been used in developing design formulas. In practice, the designer has to assume that the significant wave height or another characteristic wave height corresponds to the height of the regular wave train.
Neither of these formulas include any wave period influence. However, recent investigations [1, 2] have proved that the stability of the armour layer can be significantly influenced by the wave period (i.e. wave steepness and breaker type). Furthermore they refer to one-dimensional wave conditions (no directional spreading).
Because of the above mentioned shortages, neither of these formulas is universal and, therefore, they have to be treated with appropriate caution.

2° Influence of the wave period on riprap stability

The most extensive studies relating to the problem of the influence of the wave period on riprap stability have been performed by the Coastal Engineering Research Center (C.E.R.C.) of the U.S. Army Corps of Engineers [1].

The tests were performed in a large wave tank (regular waves) with wave periods ranging from 2.8 to 11.3 sec, wave heights for no damage conditions from 2 to 4 ft. and slopes from 1 : 2.5 to 1 : 5. This study showed that wave period has a strong effect on riprap stability. Ahrens [2] and Bruun and Günbak [7, 9] used data from these tests to show the influence of the surf similarity parameter, ξ, (and thereby the wave period or wave steepness and steepness of slope) on the stability expressed by parameter, N_{ZD}.
The surf similarity parameter identifies to some extent the way in which waves break. The limiting criteria of ξ can be strongly influenced by the roughness and porosity of slopes.

Table 2.4.8.1. Suggested K_D Values for Use in Determining Armor Unit Weight (62).

			No-Damage Criteria and Minor Overtopping				
Armor Units	n*	Placement	Structure Trunk K_D §		Structure Head K_D		Slope
			Breaking wave	Nonbreaking wave	Breaking wave	Nonbreaking wave	cot θ
Quarrystone							
Smooth rounded	2	random	2.1	2.4	1.7	1.9	1.5 to 3.0
Smooth rounded	>3	random	2.8	3.2	2.1	2.3	‖
Rough angular	1	random $	$	2.9	$	2.3	‖
Rough angular	2	random	3.5	4.0	2.9 2.5 2.0	3.2 2.8 2.3	1.5 2.0 3.0
Rough angular	>3	random	3.9	4.5	3.7	4.2	‖
Rough angular	2	special +	4.8	5.5	3.5	4.5	‖
Tetrapod and Quadripod	2	random	7.2	8.3	5.9 5.5 4.0	6.6 6.1 4.4	1.5 2.0 3.0
Tribar	2	random	9.0	10.4	8.3 7.8 7.0	9.0 8.5 7.7	1.5 2.0 3.0
Dolos	2	random	22.0 #	25.0 #	15.0 13.5	16.5 15.0	2.0 £ 3.0
Modified Cube	2	random	6.8	7.8	—	5.0	‖
Hexapod	2	random	8.2	9.5	5.0	7.0	‖
Tribar	1	uniform	12.0	15.0	7.5	9.5	‖
Quarrystone (K_{RR}) Graded angular	–	random	2.2	2.5			

* n is the number of units comprising the thickness of the armor layer.
$ The use of single layer of quarrystone armor units subject to breaking waves is not recommended, and only under special conditions for nonbreaking waves. When it is used, the stone should be carefully placed.
\+ Special placement with long axis of stone placed perpendicular to structure face.
§ Applicable to slopes ranging from 1 on 1.5 to 1 on 5.
‖ Until more information is available on the variation of K_D value with slope, the use of K_D should be limited to slopes ranging from 1 on 1.5 to 1 on 3. Some armor units tested on a structure head indicate a K_D-slope dependence.
\# Data only available for 1 on 2 slope.
£ Slopes steeper than 1 on 2 not recommended at the present time.

However, for one type of protection it has been proved that the parameter ξ is a very useful one for correlation of the external load (H,T), the geometry (ctgα), the run up (R) and the stability (N_{ZD}).
Below is shown the transition from one breaker type to another on smooth slopes [4] and riprap slopes [1, 9]. The surf parameter is defined as:

$$\xi = (\mathrm{ctg}\alpha\sqrt{H/L_0})^{-1} = \sqrt{\frac{g}{2\pi}}\, T\, \frac{\tan\alpha}{\sqrt{H}} \qquad (11)$$

where: α = angle of slope, H = wave height in front of the structure (slope), L_o = deepwater wave length and T = wave period.

The breaker types are shown in fig. 2.4.8.7.
The stability parameter N_{ZD} , called the zero damage stability number, is defined as:

$$N_{zD} = \frac{H_{ZD}}{\Delta (G_{50}/\gamma_s)^{1/3}} = \frac{H_{ZD}}{\Delta D_n} \qquad (12)$$

Breaker type		limiting criteria	
		Smooth slopes	Riprap slopes
Collapsing or surging	if	$3.3 < \xi$	$2 < \xi$
Plunging	if	$0.5 < \xi < 3.3$	$\xi < 2$
Spilling	if	$\xi < 0.5$	

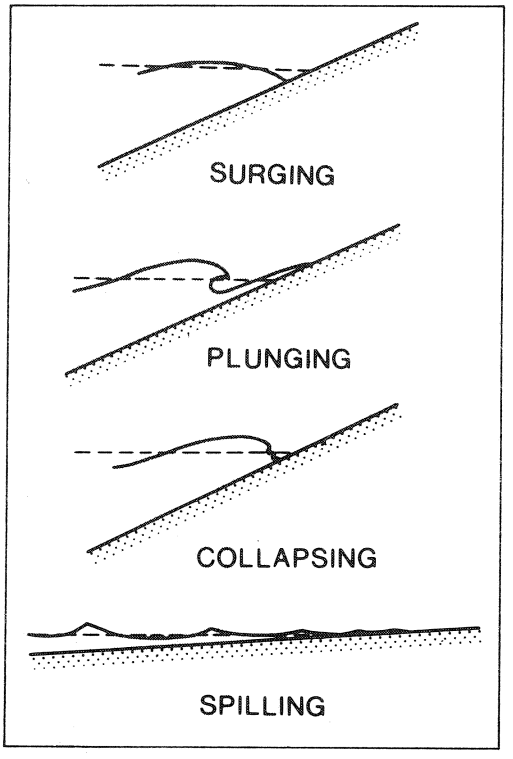

Where: H_{ZD} = zero damage wave height,
Δ = relative density and
D_n = nominal size of unit equivalent to the size of cube;
$D_n = (G_{50}/\gamma_s)^{1/3}$

The relationship between N_{ZD} and K_D or K_{RR} (Hudson formula) is:

$$N_{ZD} = (K_{RR}\,\mathrm{ctg}\alpha)^{1/3} \qquad (13a)$$

or

$$K_{RR} = \frac{N^3_{ZD}}{\mathrm{ctg}\alpha} \qquad (13b)$$

Figure 2.4.8.7 Breaker types.

The stability coefficients N_{ZD} calculated from the zero damage wave height for each test plotted versus the corresponding values of the surf parameter ξ, are shown in fig. 2.4.8.8. The significance of wave period is clearly apparent. Generally, the tests with the lowest stability fall between ξ -values of 2 and 3.3. which roughly corresponds with the collapsing breaker condition on the riprapped slope. Collapsing breaker

Figure 2.4.8.8 Wave period effect on N_{ZD} [9].

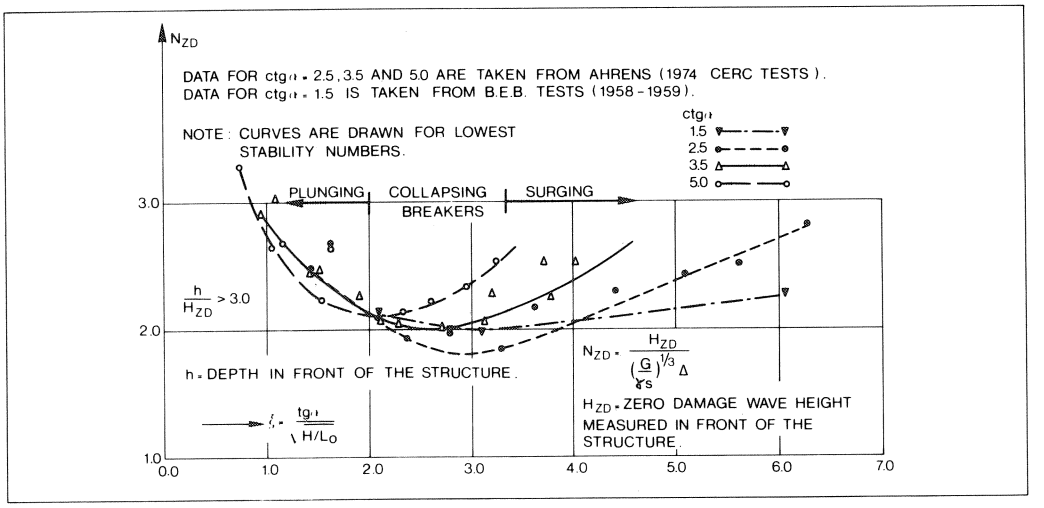

lies in the transition range between strong breaking (plunging) and no breaking (surging). These results underline the necessity of designing not only the riprap protection but also all kinds of rubble mounds and revetments based on design criteria which include wave period.

According to Ahrens [1], for wave conditions that produced the lowest zero-damage wave heights the lowest stability number $(N_{ZD})_{min.}$ can be predicted by the formula

$$(N_{ZD})_{min} = 1.54(ctg\alpha)^{2/9} \qquad (14)$$

Fig. 2.4.8.8. still shows some inconsistency in the N_{ZD} vs. ξ - relation, especially regarding the influence of the slope for the plunging-breaker range ($\xi < 2$). To analyse that, Pilarczyk [47] continued to replot Ahrens' data as shown in fig. 2.4.8.9.(a). For that purpose, he introduced the resistance parameter of slope given by

$$S_R = \mu\cos\alpha + \sin\alpha \qquad (15)$$

where: $\mu = \tan\phi_r$, ϕ_r = natural angle of repose.

For natural stones $\phi_r \approx 45°$ and $\mu \approx 1$, (20)
This slope resistance exists as long as no uplifting of stones take place.
When stones start to move on the slope (= damage), the resistance of the slope will probably change according to the general description given by the formula of Iribarren (i.e. f $\cos\alpha \mp \sin\alpha$).

The results of the analysis made by Pilarczyk regarding riprap stability can be summarized as follows.

- the lowest stability occurs at the critical wave steepness given by

$$\left(\frac{H}{L_0}\right)_{cr} \cong 0.05 \tan\alpha \qquad (16)$$

- the lowest stability number $(N_{ZD})_{min.}$ can be predicted from

$$(N_{ZD})_{min} = 1.1(ctg\alpha)^{0.25} S_R \qquad (17)$$

- for $H/L_o < (H/L_o)_{cr}$ (i.e. towards the weak and no-breaking waves), N_{ZD} is given by

$$N_{ZD} = 0.54 \left(\frac{H}{L_0}\right)^{-0.25} S_R \qquad (18)$$

- for $H/L_o > (H/L_o)_{cr}$ (i.e. towards strong breaking waves), N_{ZD} is given by

$$N_{ZD} = 2.25\, \xi^{-0.5} S_R = 2.25\sqrt{ctg\alpha}\left(\frac{H}{L_0}\right)^{0.25} S_R \qquad (19)$$

For practical purposes (safety), the numerical coefficient equal to 2.25 (the lower limit of N_{ZD}) is taken as the representative one instead of the average value equal to about 2.4.
(see fig. 2.4.8.9.(a)).

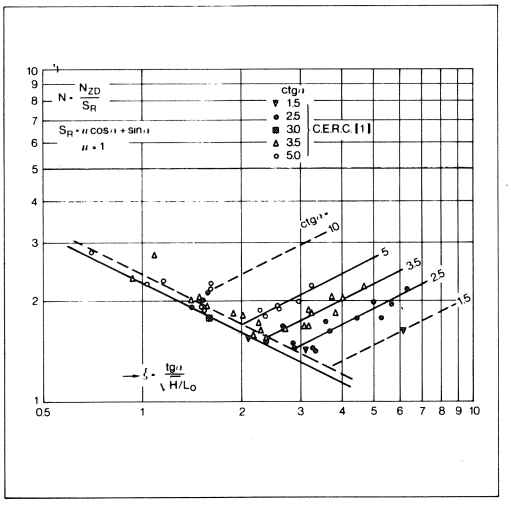

The relative run-up on riprap slopes based on data from [1] can be roughly expressed by equation (see fig.2.4.8.9.(b))

$$\frac{R}{H} = 0.8\xi^{0.5} \quad \text{for } 0.8<\xi<5 \qquad (20)$$

For smooth and impermeable slopes $R/H \approx \xi$ (breaking waves).

3° Design wave height. Effects of irregular wave trains

All the previously mentioned formulas related to stone-stability are based on tests carried out with uniform wave trains whereas, in nature, a wind-generated wave train consist of waves with a wide range of height and length. Since there is no established correlation between the destructive effects of a uniform wave train and a natural

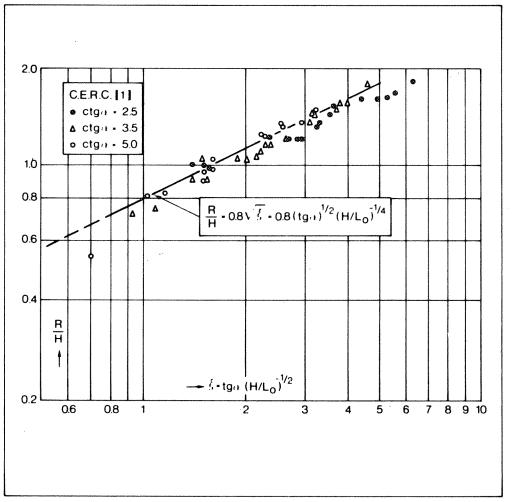

Figure 2.4.8.9(b) Relative run-up on riprap slopes [47].

Figure 2.4.8.9(a) Zero damage stability function vs. surf parameter [47].

wind-generated wave train, there is some doubt about the design wave-height to be used when prototype protection is based on tests with uniform waves. This problem is very difficult and still insufficiently solved. The reason for this is that the influence of the wave period is usually not included in the numerical values of the stability coefficients and because the number of comparative model tests with regular and irregular waves is still very limited.

For a rubble-mound structures, the design wave height is usually based on the significant wave height, that is the average of the one third highest waves in a given wave group, as damage to such a structure is progressive and a certain period of destruction action is normally required before the structure ceases to provide adequate protection. In such a case failure does not seem to occur from one maximum wave.

The problem of proper definition of the design wave height in the design formulas is more urgent for structures which are much more susceptible to immediate or complete failure. To such structures belong the block revetments on a permeable sublayer (filter) where, if one block is displaced, complete failure follows quite quickly. The results of the model tests showed also that block displacement can often occur under the action of a single wave. It follows that, since the highest is potentially the most damaging, the prototype block should be stable under attack by the highest wave anticipated.

Theoretical treatments and empirical studies (i.e. Bretschneider, Longuet-Higgins) have established the distribution of wave heights in a natural wind-generated wave train. These works make it possible to calculate the possibility of occurrence of a wave of a particular height. For a small (narrow) spectrum, the distribution of wave heights in ta wave train corresponds to a Rayleigh distribution. The main evaluation consists of determining the frequencies of occurrence of wave heights, from which it is possible to obtain the probability of exceedance of wave heights of a certain level with an irregular sea-state.
It is well known that the most probable value of the maximum wave height depends on the length of the record (i.e. duration of storm).

The ratio of the probable maximum wave-height, H_{max}, to the significant height, H_s, is related to the number of waves, N, in the manner shown in the following table (Rayleigh distribution):

N	H_{max}/H_s
1:10	1.07
1:100	1.52
1:1000	1.86
1:10000	2.15

Thus, the maximum wave-height at the structure face could be considerably greater than the significant wave-height. This example stresses once again the necessity of the proper definition of the design wave conditions.

Several investigations have been carried out on rubble-mound structures with regular and irregular waves. These older tests showed that, as a rule of thumb, the significant wave height could be used as the zero-damage wave height of regular waves in the Hudson formula.
However, the test results showed that the damage was dependent on the wave spectrum being used where the ratio of maximum wave height to the significant wave height and a wave grouping are important factors to be considered. Further information on this subject may be found in [5, 12, 21, 55, 63].
The results of the recent systematic investigation carried out by the Delft Hydraulics Laboratory with irregular waves(narrow spectrum) [74] indicate that the stability of rubble-mounds expressed by a significant wave height, H_s, is a factor 1.3 lower (for N = 3000 waves) than this for regular waves. This factor increases with the number of waves.
For the time being, the conclusion can be drawn that with respect to rubble-mound structures the wave height H in the relations (16) ÷ (19) (Fig. 2.4.8.9) has at least to be replaced by:
$H = 1.3\ H_s$ - for zero-damage conditions, and
$H = 1.0\ H_s$ - for "tolerable" damage (erosion depth $< 2\ D_n$)
Because of negligible variation of the resistance

parameter S_R (eq.15) for slopes with $ctg\alpha \geq 2$ (S_R = 1.1. ÷ 1.35), the stability formula (eq. 19) can thus be transformed to a more general form valid for irregular wave conditions (N = 3000 waves), viz.

For $\xi_z \leq 3$ (breaking waves; collapsing → plunging):

$\frac{H_s}{\triangle D_n} = 2.25\ \xi_z^{-0.5}$ — for zero damage contions, and

$\frac{H_s}{\triangle D_n} = 3.0\ \xi_z^{-0.5}$ — for "tolerable" damage

(exponent 0.5 is derived using data from [74])

where $\xi_z = (ctg\alpha\sqrt{H_s/L_o})^{-1}$ and $L_o = g\,\overline{T}_z^2/2\omega$ (T_z-mean wave period)

For $\xi_z > 3$ (no-breaking waves)

$\left(\frac{H_s}{\triangle D_n}\right)_{\xi_z = 3} \approx$ const.

will be a safe approximation.

However, for costly and important structures it is always advisable to test the final design in the model facility where the irregular waves (spectrum) can be simulated.

With respect to defining the design-wave conditons, Bruun and Günbak [7] stress that a particularly dangerous situation exists if "resonance" occurs between wave period and "downrushperiod", i.e. the situation which occurs when downrush is in its lowest position and collapsing-plunging wave breaking takes place simultaneously and repeatedly at or close to that location causing peak forces perpendicular to the slope. At the same time hydrostatic pressure from inside the mound maximizes. They conclude that it is not enough to select either a „design storm" or a specific „design spectrum". The design wave or the design spectrum gives a „load", which is sometimes regarded as the maximum exposure which can occur. This could, however, be far from the truth. To obtain the proper design conditions, they propose to examine a number of actual wave records from the site including analyses of extreme events [26] and trains of approximately regular waves with special reference to the correlation between succeeding waves as described in [41, 49]. Tests should then concentrate on combinations of certain waves and periods, which occur in the actual spectra, with particular reference to conditions which produce the most dangerous resonance phenomena. More detailed information on the subject of designing of rubble-mounds can be found in [10, 11, 45, 62, 63].

It is evident that the selection of the design wave becomes partly a statistical problem, based not only upon the statistics of wave occurrence but also on the probable damage resulting from any particular statistical wave occurrence. When a deterministic approach is used for designing a structure, one is faced with problems such as uncertainties about the probability of structural failure and uncertainties around the ultimate failure mechanism caused by poor understanding of the relationship between the failures of the different structural parts and thus of the total failure. These problems, among others, may hamper an economical and well-balanced design.

An approach that meets the problems mentioned above is the probabilistic approach, based on knowledge of statistical distributions of load and strength of the structure, stability and failure mechanisms [51].

The probabilistic approach has been widely applied to the design of the Eastern Scheldt Storm Surge Barrier in the Netherlands [64].

2.4.8.4. Wave Run-up

The run-up of waves is an important factor in the design of shore structures. It has been investigated in many studies, both theoretical and experimental. Because of the complexity of the problem (different slope-shapes, facings and permeability regular and irregular waves, wave spectra etc.) the data available on run-up are usually only valid incidentally and no generalization is yet possible.

A simple and reliable formula for the maximum run-up is given by Hunt [68], based on measurements with periodic waves breaking on smooth plave slopes. It can be written as:

$R = \sqrt{HL_0}\ \tan\alpha = 0.4T\sqrt{gH}\ \tan\alpha$

or

$\frac{R}{H} = \xi$ (for $\xi < 3$); $\xi = \frac{\tan\alpha}{\sqrt{H/L_0}}$ (= surf parameter)

and

$\frac{R}{H} = 2 \div 2.5$ (for $\xi \geq 4$)

in which R is the maximum height above the still water level reached by the periodic waves of height H and period T on the slope, ($\tan\alpha$), and L_o (deepwater wave length) is defined by $L_o = gT^2/2\pi$.
In the Dutch practice the so called „Old Delft" empirical formula is commonly used for calculation of 2% run-up on sea dikes. It can be written as:

$R_{2\%} = 8\ H_s \tan\alpha$

(for $\mathrm{ctg}\alpha \geq 3$, relatively smooth stone revetments and wave steepness of approximately 0.05).
The validity of this formula has been proved by Battjes in [67].

Van Oorschot and d'Angremond [71] suggest the following formula for run-up, based on model tests with irregular waves (plane and smooth slopes)

$R_{(n)} = C_{(n)}(\varepsilon)\hat{T}\sqrt{gH_s}\tan\alpha$

where: $R_{(n)}$ - run-up height, n-subscript: exceedance percentage, $C_{(n)}(\epsilon)$ - constant depending on the relative width of energy spectrum (ϵ), $\hat{T}$ - period of spectral component with maximum energy density (= top period).
The values for $C_{(n)} = C_{2\%}$ (run-up exceeded by 2% of waves) estimated from the measurements are roughly equal to:

$C_{2\%} = 0.55$ - small spectrum ($\epsilon \sim 0.3$)

$C_{2\%} = 0.70$ - wide spectrum ($\epsilon \sim 0.6$)

For typical North-Sea spectra with $\epsilon \sim 0.5$, $C_{2\%}$ is about 0.62.

Experimental results in [72] with irregular waves and different dike shapes and water depths at the toe of the dike give support to the relation given by Van Oorschot and d'Angremond. However for relatively shallow water at the toe the formula mentioned above has to be corrected in the following way (see Fig. 2.4.8.10):

$R_{2\%} = C'\hat{T}\sqrt{gH_s}\tan\alpha + \Delta h$

Some quantitative values concerning C' and Δh are tabulated below (applicable for $\hat{T}\sqrt{gH_s}\tan\alpha > 3$ m).

relative waterdepth at the toe	slope foreshore	C'	Δh
0.5	1 : 40	0,19	1.2 m
0.75	1 : 40/1 : 20	0,32	0.8 m
~1.0	1 : 40	0,45	0.6 m
≥1.5 à 2.0	1 : 40	0,62	0

The wave run-up as determined for plane and smooth slopes can be influenced by the roughness or permeability of a slope and by the shape of the latter. These factors may considerably reduce run-up.
Because the influence of roughness and permeability cannot be isolated, these effects must be considered jointly. The joint effects are expressed in the factor r_R and summarized below [9].

The shape of the slope must be considered as an independent variable. The influence of the shape cannot, however, be expressed easily in quantitative terms by a multiplication factor as may be used for the rough, plane slope, since in the case of non-plane slopes it is generally not clear what corresponding plane slopes should serve as a reference. However, as first proximation, Saville's equivalent gradient method can be applied for composite slopes [70, 73].
An exception is provided by slopes with a berm, provided that the gradients below and above the berm are identical. The corresponding plane slope is then defined as the limiting case in which the berm becomes zero. Various experiments have shown that the effect of a berm with a constant width (B) is maximum when the berm is situated approximately at the average water level. ($d_B < 0.5H$ see definition scheme). It

Source	Covering	r_R
Shankin	SMOOTH, IMPERMEABLE CONCRETE BLOCKS	1 0.9
H.L. Delft	BASALT COVERING) STONE BLOCKS))	0.85 to 0.9
Franzius	TURF	0.85 to 0.9
C.E.R.C.	1 LAYER OF RUBBLE	0.8
Shankin	SET STONE	0.75 to 0.8
Shankin	ROUND STONES	0.6 to 0.65
H.L. Delft	RUBBLE	0.5 to 0.6
H.R.S. Wallingford	RUBBLE	0.5 to 0.55
Shankin	BROKEN RUBBLE	0.5 to 0.55
C.E.R.C.	2 OR MORE LAYERS OF RUBBLE	0.5
Starozolszky	TETRAPODS	0.5

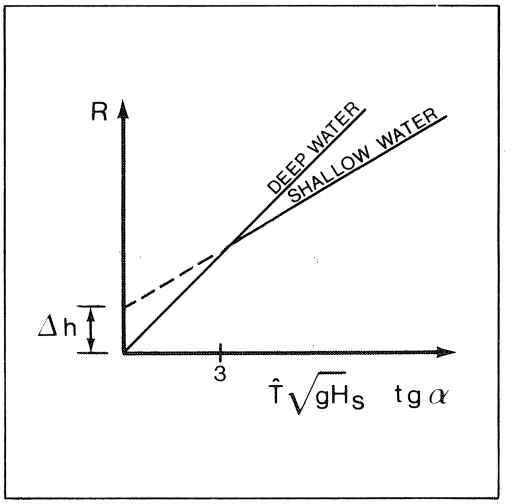

Figure 2.4.8.10 Schematic representation of run-up in deep- and shallow water

Figure 2.4.8.11 Definition scheme

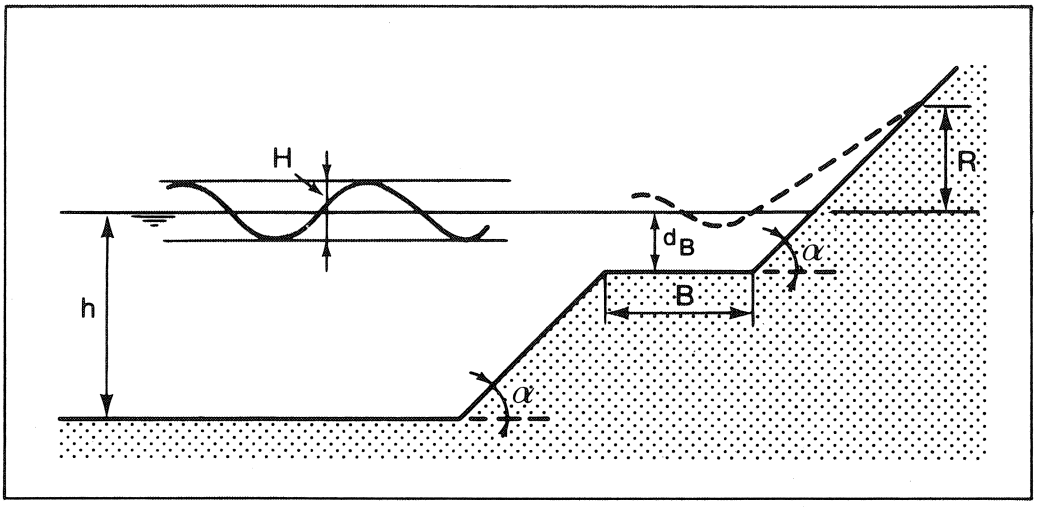

has furthermore been found that run-up diminishes with increasing berm-width although the reduction rapidly falls off once a certain minimum width is exceeded i.e. B ~ 0.25 L_o for non- and weak breaking waves, and B = 4 H for strong breaking waves, $H/L_o > 0.03$ (H = wave height, L_o = deepwater wave length, $L_o = gT^2/2\pi$, (see Fig. 2.4.8.11). The reduction factors r_B for the berm-width equal or larger than the minimum width mentioned above may be roughly derived from the experimental results in [5] (regular waves) and in [8] (irregular waves) as:

slope ctgα	r_B	($B \geqslant B_{min}$)
5 to 7	0.75	
4	0.6	
3	0.5	

The effective run-up on a dike or breakwater can be calculated as

$$R = R_{(n)}\ r_R\ r_B$$

More recent information hereabout can be found in [65], [66], [73] and [74].

References

1. Ahrens, J.P., Large Wave Tank Tests on Riprap Stability. **C.E.R.C. Technical Memorandum no. 51,** May 1975.

2. Ahrens, J.P. and McCartney, B.L., Wave Period Effect on the Stability of Riprap, **Proc.Civil Eng. in the Oceans,** Univ. of Delaware, June 9-12, 1975.

3. Ashida, K. and Bayazit, M., Initiation of motion and roughness of flow in steep channels, **IAHR - Istanbul,** paper A58. 1973.

4. Battjes, J.A., Surf Similarity, **14th Proc. Conf. on Coastal Eng.,** Copenhagen, 1974.

5. Bores, P.S., Earth dam wave protection, **10th Congress Large Dams,** Montreal, 1970. Vol.I. Question 36, Report 50.

6. Breusers, H.N.C., Lecture Notes on Sediment Transport, **International Course in Hydraulic Engineering,** Delft 1979-1980.

7. Bruun, P., Günbak, A.R., Hydraulic and Friction Parameters affecting the Stability of Rubble Mounds, **PIANC Bull.no.24,** 1976.

8. Bruun, P., Johannesson, P., Parameters Affecting Stability of Rubble Mounds, **J. of the Waterways, Harbors and Coast. Eng.,** Vol.102, WW2, May 1976.

9. Bruun, P., Günbak, A.R., Risk Criteria in Design Stability of Sloping Structures in Relation to, **Symposium on Design of Rubble Mound Breakwaters,** England, 1977. (also Coastal Engineering,1,1978)

10. Bruun, P., Common Reasons for Damage or Breakdown of Mound Breakwaters, **Coastal Engineering,**2,1979, (printed in The Netherlands).

11. Bruun, P., Kjelstrup, S., Practical Views on the Design and Construction of Mound Breakwaters, **Coastal Engineering,**5,1981.

12. Burcharth, H.F., The Effect of Wave Grouping on On-shore Structures, **Coastal Engineering,**2,1979.

13. Carstens, T., Torum, A. and Park, A.G., The Stability of Rubble- Mound Breakwaters against Irregular Waves, **Proc. 10th Coastal Eng. Conf.,** Tokyo, 1966.

14. Chang, Y.U., Laboratory Investigations of the Flume Traction and Transportation, **Trans. ASCE, 65,** no.8, Pt.2, 1939.

15. Cohen de Lara, G., A Study of Seepage in Rockfill Dykes, **Proc. 4th Hydr. Conf,** Societé Hydro de Paris, 1956.

16. Collins, I.J., Wave Statistics and Rubble Mound Structures, **Int. Symp. on Ocean Wave Measurement and Analyses,** New Orleans, Louisiana, U.S.A., Sept. 1974.

17. Cox, R.G., Velocity Forces on Submerged Rock, **U.S. W.E.S.** Vicksburg, Misc. paper no. 2-265, 1958.

18. Gerritsen, F., Bruun, P., Dutch and Florida Practices on Revetment Design, **9th Coastal Eng. Conf.,** Lisabon, 1964.

19. Gerritsen, F., Stability of Rock and other Materials against Current and Wave Action, **Topics in Ocean Engineering.**

20. Gravesen, H. Jensen, O.J. and Sorensen, T., Stability of Rubble Mound Breakwaters II, **Danish Hydraulic Institute,** 1978.

21. Gravesen, H., Stability of Main Armour Layer for Rubble Mound Breakwaters, **Danish Hydraulic Institute,** International note, 1979.

22. Hall, J.V., Stability Tests of Interlocking Block Revetment, **J. of the Waterways and Harbors Division,** WW3, August 1968.
(also 10th Coastal Eng. Conf. Tokyo, 1966).
Discussions by A. Fraetteberg, Frans Gerritsen and Per Bruun, and E.R. Köller in WW2, May 1969.

23. Hallmark, D.E., Smith, G.L., Stability of Channels by Armourplating, **Jour. of the Waterways and Harbors Division,** WW3, August 1965.
(Discussions: WW1, February 1966 and WW3, August 1966).

24. Hartung, F., Scheurlein, H., Design of Overflow Rockfill Dams, **Dixième congr. du Grands Barrages,** Montreal, 1970. Vol. 1, pp. 587 - 598.

25. Heteren van J., Bruinsma, J., A Method to Calculate the Probability of Exceedance of the Design Wave Height, **Coastal Engineering,** 5, 1981.

26. Houmb, V.G., Rye, H., Analysis of Wave Data from the Norwegian Continental Shelf, **Proc. 2nd Conf. of Port and Ocean Eng.** Reykjavik, 1973.

27. Hudson, R.Y., Laboratory Investigations of Rubble Mound Breakwaters, **Proc. ASCE,** 85, WW3, Sept. 1959.

28. Iribarren C., Formule pour le calcul des digues en enrochements naturels ou élément artificiels, **XXI Inter. Navig. Congress,** Stockholm 1965.

29. Izbash, S.V., Khaldre, Kh.Yu., Hydraulics of River Channels Closure, **Constr. Ind. Res. and Inf. Assoc.,** London Butterworths, 1976.

30. Jachowski, R.A., Interlocking Precast Concrete Block Seawall, **9th Coastal Eng. Conf.,** Lisbon, 1964.

31. Kamphuis, J.W., Determination of Sand Roughness for Fixed Beds, **Journal of Hydraulic Research,** IAHR, Vol.12 - no.2, 1974.

32. Knauss, J., Computation of Maximum Discharge at Overflow Rockfill dams, **13th Congr. du Grands Barrages New Delhi,** Q.50, R.9, p. 143-160, 1979.

33. Kumin, D.J., **Hydraulic Design of Bottom Protection below Spillways** (in Russian). Gosenergoizdat, 1956.

34. Linford, A., A Review of Literature on the Construction of Rockfill Dams by Dumping Stones in Running Water, **B.H.R.A. report TN 873,** 1967.

35. Lindford, A, Sauders, D.H., A Hydraulic Investigation of Through and Overflow Rockfill Dams, **B.H.R.A.,** RR 888, 1967.

36. Losada H.A., Gimenez-Curto, L.A., An Approximation to the Failure Probability of Maritime Structures under a Sea State, **Coastal Eng.,** 5, 1981.

37. Lysne, D.K., Tvinnereim, K., Scour Protection for Submerged Rockfill Sills, **Riv. and Harb. Auth.,** Bull. 13E, 1971.

38. McCartney, B.L., Ahrens, J.P., Stability of Gobi Block Revetments to Wave Attack, Technical Memorandum no.55, October 1975. **C.E.R.C. U.S. Army, Corps of Engineers.**

39. McCartney, B.L., Survey of Coastal Revetments Types, Miscellaneous Report no. 76-7, May 1976. **C.E.R.C. U.S. Army, Corps of Engineers.**
Giles, L.M., Evaluation of a Concrete Building Block Revetment, **Conf. Coastal Sediments,** 1977.

40. McCartney, B.L. and Ahrens, J.P., Overlay of Large Placed Quarrystone and Boulders to Increase Riprap Stability, **C.E.R.C.** Technical Paper no.76-19, December 1976.

41. Nolte, K.,. Hsu, F.H., Statistics of Ocean Wave Groups, **Proc. Offshore Tech. Conf.,** Houston, 1972.

42. Olivier, H., Through and Overflow Rockfill Dams - New Design Techniques, **Jour. Inst. Civil Eng.,** March 1967.

43. Olivier, H., Some Aspects of Major River Diversion During Construction, **Commission Int. des Grand Barrages,** Madrid 1973. (paper Q.41, R.63).

44. Ouellet, Y., Effects of Irregular Wave Trains on Rubble-mound Breakwaters, **Proc. ASCE. J. of the Waterways,** Harbours and Coastal Eng. WW1, February 1972.

45. Paape, A., Ligteringen, H., Model Investigations as a Part of The Design of Rubble-mound Breakwaters, **Delft Hydraulics Laboratory,** Publ.no. 246, Nov. 1980.

46. Paintal, A.S., Concept of Critical Shear Stress in Loose Boundary Open Channels, **Journal of Hydraulic Research,** no.1, 1971.

47. Pilarczyk, K.W. and K. den Boer, Stability and Profile Development of Coarse Materials and Their Application in Coastal Engineering, **Conference on Coastal and Port Engineering in Developping Countries,** Colombo, Sri Lanka, March 20-26, 1983.

48. Rogan, A.J., A Comparison of Regular and Wind-generated Wave Action on Rubble-mound Breakwaters, **Symp. Research on Wave Action,** Delft, Holland, 1969.

49. Rye, H., Wave Group Formation among Storm Waves, **14th Coastal Eng. Conference,** Copenhagen, 1974.

50. Sollitt, C.K., De Bok, D.H., Large Scale Model Tests of Placed Stone Breakwaters, **Proc. 15th Coastal Eng. Conf.** Honolulu, Hawaïï, 1976.

51. Stans, J.C., Model Investigations and Probabilistic Design, **Delft Hydraulics Laboratory,** Publication no.212, May 1979 (also Coastal Structures 1979, March 1979).

52. Stephenson, D., Rockfill in Hydraulic Engineering, **Developments in Geotechnical Engineering,** Vol. 27, Elsevier, Sc. Publ.Comp., Amsterdam - New York, 1979.

53. Stchavieliev, D.S., **Construction of Hydropower-plants,** Design and Calculation, Publ. Comp. 'Energia', Leningrad, 1967.

54. Syunsuke Ikeda, Incipient Motion of Sand Particles on Side Slopes, **Journal Hydraulics Division,** HY1, January 1982.

55. Torum, A., Hydraulic Aspects of Breakwater Design, Internal note 1980, **Norwegian Hydrodynamic Laboratories.**

56. Venis, W.A., Behavior of Dumping Material when Exposed to Currents and Wave Action, **De Ingenieur, 50, 1968** (The Netherlands).

57. Ven te Chow, **Open-channel Hydraulics,** McGraw-Hill Book company, New York -London, 1959.

58. Zanen, A., Revetments, **Int. Courses in Hydraulic and Sanitary Engineering,** Delft 1976, The Netherlands.

59. Zharkov, Yu.G., Stream Forces on Riprap Protection Downstream of the Hydraulic Structures and Method of Calculation, Izvestiya Vsesoyuznogo Nauchno-Issledovatelskogo, **Institute Gidrotekhniki 97,** 1971. 'Energia'. Leningradskoje otdelenje.

60. Stability of Rockfill Dams, **Delft Hydraulics Laboratory** (in Dutch):
a) Reports M711 , 1961-1966
b) Reports M731 , 1963-1966
c) Reports M1741 , 1981-1982
d) Konter, J.L.M. and Akkerman, G.J., Hydraulic Design Criteria for Rockfill Closure of Tidal Gaps, Vertical Closure Method, **Delft Hydraulics Laboratory,** Report on investigation, M 1741 - IV, July 1983 (in English).

61. Stability of riprap and discharge characteristics, Overflow embankments, Arkansas River, Arkansas, U.S.A., **U.S.A. Army Eng., W.E.S., Vicksburg,** Techn. Report 2-6500, 1964.

62. U.S. Army Coastal Engineering Research Center, **Shore Protection Manual,** 1975.

63. Final Report of the International Commission for the Study of Waves, **PIANC,** Annex to Bulletin no. 25 (Vol.III, 1976).

64. **Hydraulic Aspects of Coastal Structures,** Developments in Hydraulic Engineering related to the Design of the Oosterschelde Storm Surge Barrier in the Netherlands, Delft University Press, 1980.

65. Ahrens, J.P., Irregular Wave Run-up on Smooth Slopes, **U.S. Army Coastal Engineering Research Center,** CETA No. 81-17, December 1981.

66. Ahrens, J.P. and Titus, M.F., Wave Run-up Formulas for Smooth Slopes, Technical Note submitted to the **Journal of Waterway, Port, Coastal and Ocean Division,** ASCE, 1982.

67. Battjes, J.A., An old Run-up Formula considered from the Viewpoint of Modern Theories. (in Dutch) **De Ingenieur no. 45,** November 1970.

68. Hunt, I.A., Design of Seawalls and Breakwaters, **Proc. A.S.C.E.** Vol. 85, no. WW3, September 1959.

69. Pilarczyk, K.W. and Moret, B., Influence of Berm on Run-up of Regular Waves (in Dutch), **Delft Hydraulics Laboratory,** Report M1130, October 1976.

70. Saville, T., Wave Run-up on Composite Slopes, **Proc. 6th Conf. Coastal Eng.,** Gainesville, 1958.

71. Van Oorschot, J.H. and d'Angremond, K., The Effect of Wave Energy Spectra on Wave run-up, **Proc. 11th Conf. on Coastal Eng.,** London, Vol. I, 1968.

72. Van Oorschot, J.H. and Van Vliet, P., Run-up on a Dike with a Shallow Foreshore (in Dutch). **Delft Hydraulics Laboratory,** Report M1084, 1971.

73. _____ , Wave Run-up and Overtopping, **Technical Advisory Committee on Protection against Inundation,** Government Publishing office, The Hague 1974.

74. _____ , Hydraulic Aspects on Gravel and Riprap Slopes under Wave Attack (in Dutch), **Delft Hydraulics Laboratory,** Reports M 1809 and M1809/M1983, (be published in 1984).

Interaction Water Motion and Closing Elements

K.W. Pilarczyk

2.4.9. Local Scour

2.4.9.1. General Considerations

The construction of a dam, weir or (bridge) pier in a river or tidal estuary changes the sediment transport conditions and causes local scour.
The effects of local scour can be overcome by an increase in construction depth (bridge piers) or diminished by a bottom protection (Figure 2.4.9.1.).
Originally the development of scour in the fine material as a function of time is very fast, but eventually (generally much later) an equilibrium situation will be reached.
During the closing operations of a dam in an estuary or river, which take place within a limited time, equilibrium will not be attained. This renders it vital to know the development of the local scour as a function of time.
The problem of local scour is commonly solved by means of model investigations. For translating the model results to the prototype(= nature), however, a proper knowledge of the time-scale is needed.
For this reason, a systematic investigation of the time-scale for two- and three-dimensional local scour in loose sediments has been conducted by the Delft Hydraulics Laboratory and the Delta Department of the Rijkswaterstaat [18]. From model experiments on different scales and bed materials, relationships have been derived between time-scale and velocity, water depth and material density.
The final relationship allows the translation of the time-scour depth evaluation from model to prototype. This relationship was recently verified by means of prototype experiment (Brouwersdam, [6]).

2.4.9.2. Flow patterns and scouring process downstream of constructions

The study of the flow pattern can be helpful for obtaining some insight into the scouring process and also for the determination of the required length of the bottom protection, [2].
The flow downstream from dams is nearly always decelerating. From measurements on

Figure 2.4.9.1 Measures for protecting of sandbed in vicinity of structure.

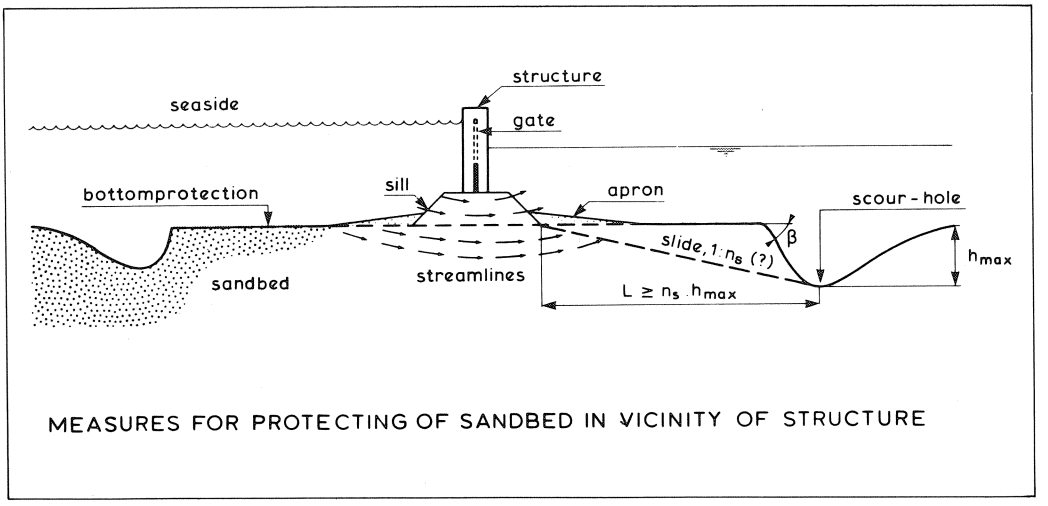

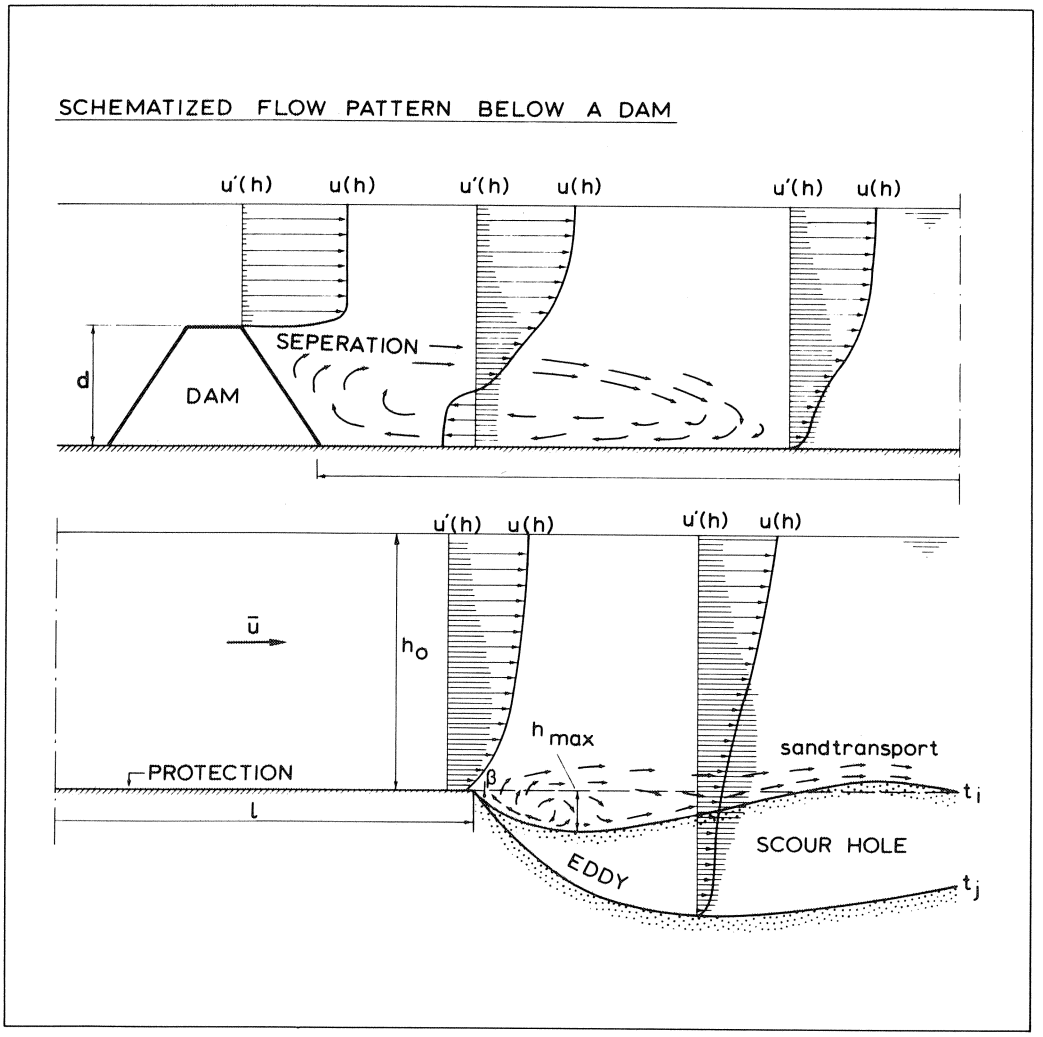

Figure 2.4.9.2 Schematized flow pattern below a dam.

diffusers and abrupt expansions it is known that turbulence intensities are high in regions with retarding flow due to the formation of layers with large velocity gradients.
After reattachment of the flow behind the dam an equalization of mean velocity and turbulence intensity takes place and the final distribution is gradually approached. From this type of

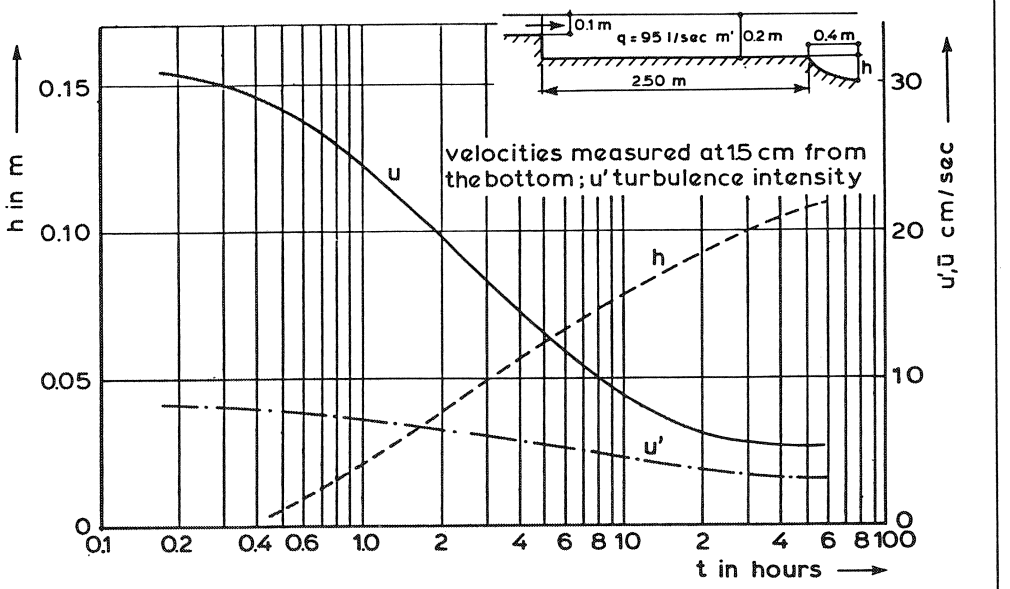

SCOURING DEPTH AND BOTTOM VELOCITY AS A FUNCTION OF TIME AT DISTANCE X

Figure 2.4.9.3 Scouring depth and bottom velocity as a function of time at distance x.

measurement an optimal length of bottom-protection can be deduced.
Behind the bottom protection a second region with decelerating flow is formed in the scour hole. An example of the velocity distribution is shown in Fig.2.4.9.2. For economic reasons the length of the bottom protection will generally be restricted to the minimum required for the

stability of the structure. The velocities and turbulence of flow will therefore generally still be large enough to carry along sediments downstream from the protected zone. A scour hole thus begins to form, which as it progresses, will modify the flow regime within it up to the point at which the flow is no longer capable of transporting sediments to beyond the hole, stabilisation thus being obtained.
The scour hole ends at the section where the flow has recovered the characteristics it had before the construction of the structure.
The mean velocity near the bottom decreases rapidly as the erosion depth increases whereas the turbulence intensity remains more constant (Fig. 2.4.9.3.) A schematized picture of the scouring process is given in Figure 2.4.9.4.
In order to obtain a detailed description of the scouring process many laboratory experiments have been performed with variable velocity, water depth, material and flow geometry [2, 11]. In general the following four phases can be distinguished in the evolution of a scour hole (Fig. 2.4.9.5.) viz.:

1st phase: the transport capacity of the flow results in sediment transport along the original bottom and hence gradual erosion downstream from the end of the bottom protection. This phase can be described by existing equations for sediment transport. The 1st phase is very short and is of little practical interest.

2nd phase: the scour hole is large enough to initiate flow separation, due to which a bottom eddy forms; the direction of the bottom velocity inside the eddy is toward the construction but outside it in the direction of the main flow. Because the velocities inside the eddy are lower than those outside it, stabilisation of the upper slope of the scour hole takes place earlier. The second phase generally lasts mostly much longer than the first and it is of great practical interest, especially with respect to dam closing operations.

3rd phase: the depth of the scour hole becomes so large that the bottom velocities nearly reach

Figure 2.4.9.4 Schematized picture of scouring process.

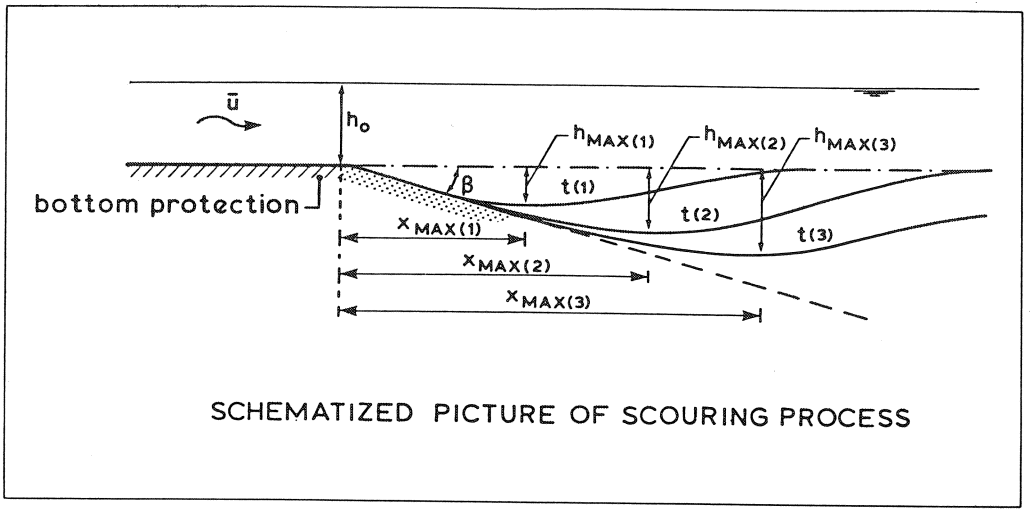

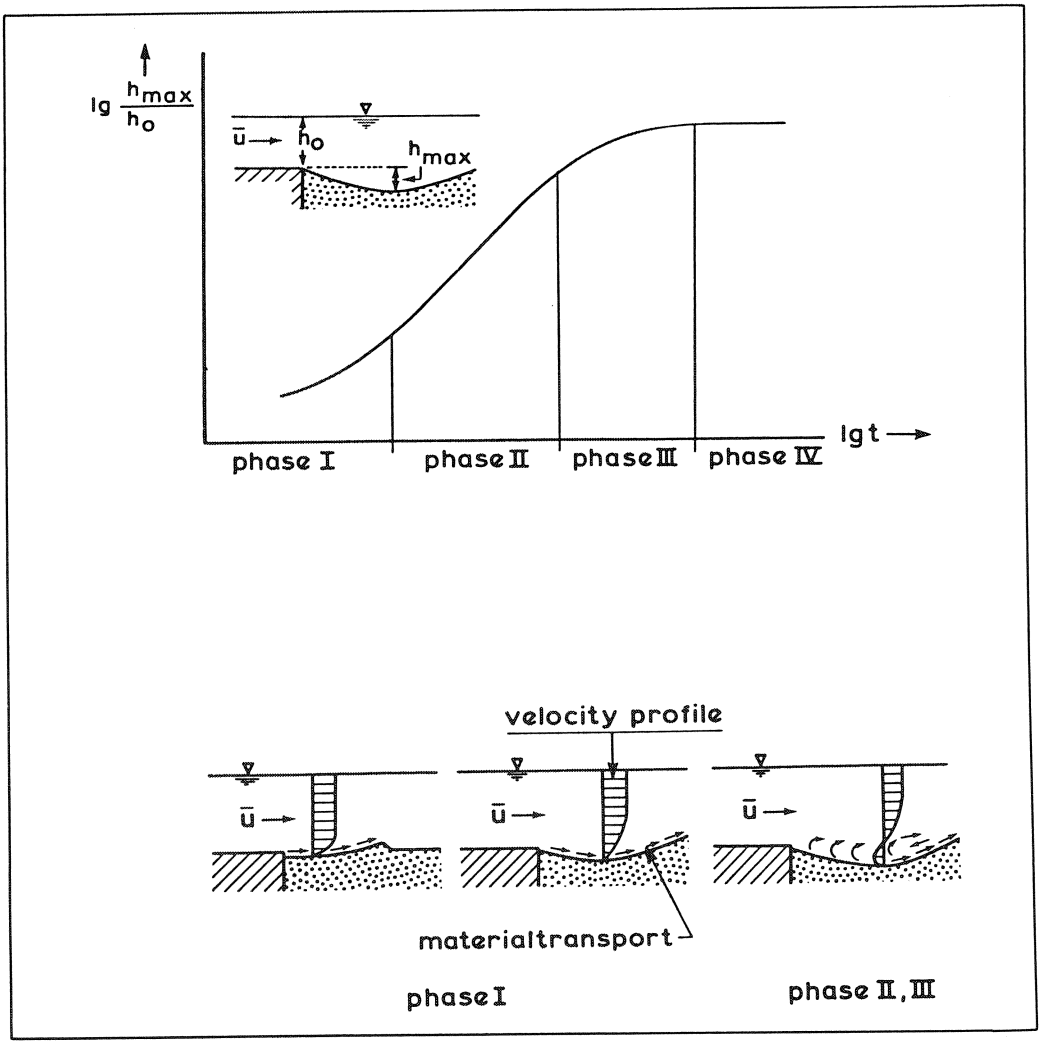

Figure 2.4.9.5 Phases of scouring process.

critical velocity at the beginning of motion of bottom sediment.
Sediment transport in this range of velocities is lower than at higher velocities. It can be qualitatively supported by the findings of Paintal [13] who recognised the lower and higher range of the transport capacity of flow.
Scour progress in this phase is generally very slow.

4th phase: the bottom velocity is nearly equal to the critical velocity of beginning of motion; a certain sediment transport along the bottom may still be present, however, the stream is not able to carry sediment outside the scour hole. A certain dynamic stabilisation of the scour hole is then achieved.
The conditions for reaching this state are strongly affected by the grade of turbulence introduced by the construction.
The maximum depth of the scour hole in this state is defined as the equilibrium depth. The equilibrium depth can be sometimes much less than might be deduced from the equality of the bottom velocity and the critical velocity of sediment.

The following section (2.4.9.3.) provides a quantitative description of the scour evolution for the 2nd phase. The 3rd phase and the prediction of the state of equilibrium will be described very briefly. It has to be pointed out that the relations presented in parts 2.4.9.3. and 2.4.9.4. are restricted to situations such as closing operations of dams and spillways and cohesionless materials. In fact only a limited number of experiments have been performed for cohesive soils. The scouring resistance of clay is of course larger than for sand.
Up to now, no general relationships can however be specified. For an example see [8]. The problem of local scour around the piers (obstacles) will be considered separately (part 2.4.9.8.).

2.4.9.3. Relationship between maximum scouring depth and time

From the experimental observations it appeared that for the 2nd phase of the scouring process the maximum scouring depth (h_{max}) increases exponentially with time,

$$\frac{h_{max}}{h_0} = f\left(\frac{t}{t_1}\right) \simeq \left(\frac{t}{t_1}\right)^p \qquad (1)$$

in which: h_{max} = maximum scour depth in m, h_o = waterdepth as defined below in m, t = time in hours, t_l = time in hours at the moment $h_{max} = h_o$, p = exponent. From a two- and three-dimensional systematic model investigation, it was deduced that the exponent „p" for the 2nd phase is nearly constant and equal to about 0.4 for two-dimensional flow conditions; the value of „p" for the three-dimensional conditions depends on the geometry of the construction (i.e. degree of turbulence) and has to be determined experimentally for each geometric arrangement.

Investigations have been made of the dependence of the characteristic scouring time t_l on the conditions of flow etc., or in other words the relationship between the times scale on the one side and the velocity scale, material scale, length scale and geometric situation on the other. The influence of the various factors on the rate of the scouring process can be described by the same general relationship for both two- an three-dimensional local scour:

$$t_1 = \frac{K\Delta^{1.7} h_0^2}{(\alpha\bar{U}-U_{cr})^{4.3}} \text{ (in hours)} \qquad (2)$$

in which: α = dimensionless scour factor involving the velocity distribution and the influence of the turbulence intensity due to the geometry of the structure, $\bar{u}$ = mean velocity in m/s = Q/A, Q = discharge in m³/s, A = wet cross-section at the end of the bottom protection = (B.h_o) in m², u_{cr} = critical velocity for initiation of motion in m/s, Δ = relative density of bottom material under water = $\rho_s - \rho_w / \rho_w$, K = numerical coefficient.
The value of K was originally determined as equal to 250 (see(11)).A recent evaluation of the previous data concluded a value of K of about 330 to be more appropriate (6).
By combining eq. (1) and (2), the following expression of „t" can be obtained:

$$t = \frac{330\left(\frac{h_{max}}{h_0}\right)^{1/p} \Delta^{1.7} h_0^2}{(\alpha\bar{U}-U_{cr})^{4.3}} \qquad (3)$$

Equations (2) and (3) may be converted in a dimensionless form leading to the following time scale, in which n denotes a scale relation:

$$n_t = n_\Delta^{1.7}\, n_h^2\, n_{(\alpha\bar{U}-U_{cr})}^{-4.3} \qquad (4)$$

From eq. (3) and p = 0.4 the following expression of h_{max} can be obtained:

$$h_{max}(t) = \frac{(\alpha\bar{U}-U_{cr})^{1.7} h_0^{0.2}}{10\Delta^{1.7}} t^{0.4} \quad \text{(in m)} \qquad (5)$$

From relation (5), it is evident that the influence of water depth on scour depth is rather negligi-

Figure 2.4.9.6 Scour relations (Phase [2]).

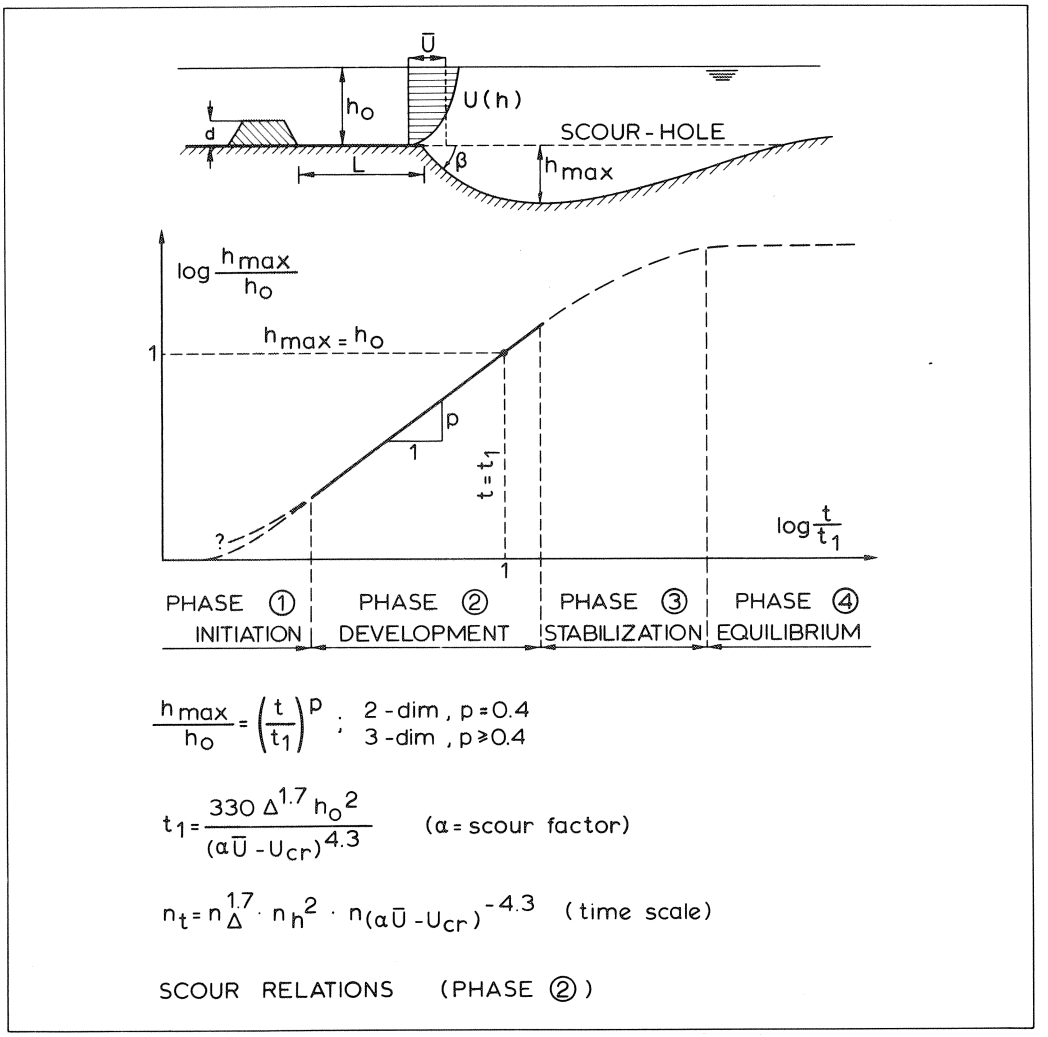

ble. The influence of the bed material is expressed by Δ and u_{cr}. It is also clear that the factor (α u - u_{cr}) is the dominant one in the scouring process. This factor mainly represents the influence of the flow velocity (u) and the geometry of the construction (α). It should be noted that all these relations are only applicable in situations where maximum (equilibrium) scour is still not reached.
The use of the relations mentioned above is illustrated in Figure 2.4.9.6.

The relationships which are valid for steady flow cannot always be used in practice because a number of significant factors are a function of time, such as the mean velocity u and the water depth h_o. The variation of u_{cr} as a function of time can generally be neglected. If one is not interested in reaching the equilibrium stage, the variation of "α" with the varying geometry due to variations in waterdepth is small, especially with respect to the 2nd phase, and can be left out of consideration. (In the 3rd phase "α" diminishes slowly with scour depth until a certain value is obtained for an equilibrium stage).
Equation (2) can be adapted into an equation for unsteady flow by taking into account a succession of infinite short-lasting steady situations. If the unsteady flow is cyclic (i.e. tidal movement) with cycle duration T, the value for the erosion time t_l then becomes

$$t_{l\,(tide)} = \frac{330\Delta^{1.7} h_0}{\frac{1}{T}\int_0^T \frac{[\alpha\bar{U}(t) - U_{cr}]^{4.3}}{h_0(t)}\,dt} \quad \text{(in hours)} \qquad (6)$$

where: u(t) = average velocity as a function of time, T = tidal period, h_o = average original water depth and $h_o(t)$ = variation of original water depth with time.
It has been proved by prototype test and model verification [6] that there is a reasonable similarity in scour development for model and prototype when using the time-scale relation according to eq.(6). The time-scour relation from this test for model and prototype is shown in Figure 2.4.9.7.

Figure 2.4.9.7 Model-prototype comparison acc. to [6, 20].

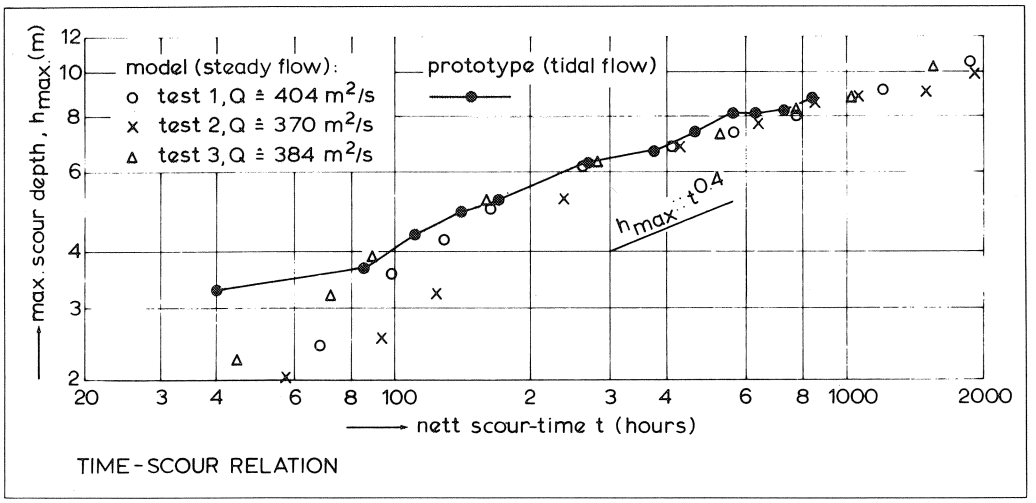

2.4.9.4 Remarks on three-dimensional local scour [11, 14]

The flow pattern and velocity distribution in both the vertical and the horizontal sense are the main governing factors for scour. In addition to the more or less important area governed by scouring which can be considered two-dimensional, there is usually also an area where the currents and consequently the scouring action produce a three-dimensional phenomenon-e.g. vortices during estuary closing operations. The vortices with vertical axis generated by the presence of abutments (especially vertical terminations) play a particularly important part. The bottom material, stirred up under the influence of current and turbulence, can be picked up by the rotating ascending current in the vortex and be thrown out sideways. The intensity of the vortex street may attain such magnitude as to seriously endanger the stability of the construction unless effective protective measures are taken.
For the sake of completeness it should be pointed out that vortex streets not only play an important part in the erosion of fine bed material, but that, under certain conditions, the bottom protection may even be affected.
The difference between two- and three-dimensional scour can be clearly seen in the respective values of the scour factor "α,, shown in Figure 2.4.9.8.
In general, because the scouring intensity of vortex streets is very high (i.e. a high value of "α,,), the state of equilibrium is reached more quickly in the case of three-dimensional than two-dimensional scour.
As has been already mentioned, the maximum scouring-depth in the case of 2-dim. scour can be described as a power-function of time (eq.1). During the investigation carried out on erosion by vortex streets, it appeared that the time/erosion-curves for the deepest points, especially for a scour depth $> 0.5\ h_o$, could often be better represented by the relationship (the same tendency being evident for 2-dim. scour in general for a depth $> h_o$; scour phases II→III):

$$\frac{h_{max}}{h_0} = 1 + A \log \frac{t}{t_1} \qquad (7)$$

where A = a constant and t_1 = time corresponding to $h_{max} = h_o$.

From the test results it appears that the value of the coefficient A depends to some extent on the height of the dam; however, for the first approximation the value of A = 0.7 can be used.
It must be emphasized that neither the beginning of the scouring process (starting phenomenon = phase I) nor its termination (phase III→IV) are covered by this equation(7) or by equation (1).
In the literature several approaches may be found for describing the equilibrium scour depth (phase IV). Some of these equations are summarized in [4] and [9]. It is not, however, possible to specify the real value of these relations.

Recently, Zanke [16] has established a somewhat different and more complicated equation for the time evolution of scour-depth than that given by eq.(3). A formula was also derived for the equilibrium stage. These equations were verified by means of two-dimensional model results only.

In observing the scouring action caused by vortex streets, a similarity may be recognized with two-dimensional action, viz. that the erosion is clearly influenced by the height of the dam and the length and roughness of the bottom protection.
With regard to the above criteria, which are important for the design, the general conclusion may be drawn that the degree of scour will decrease when the height of the dam is decreased and the length of the bottom protection increased, and that a rough protection will give less scour than a smooth protection.
The scouring capacity of vortex streets is furthermore dependent on the water depth at the location of the vortex street and in the immediate vicinity. Increasing depth causes greater flow which in turn facilitates vortex-street development.
Scour holes caused by vortex streets are in general characterized by steep slopes of up to 1 in 1.5, which can lead to geotechnical instability of the bed along the edge of the bottom protection (see part 2.4.9.7.).

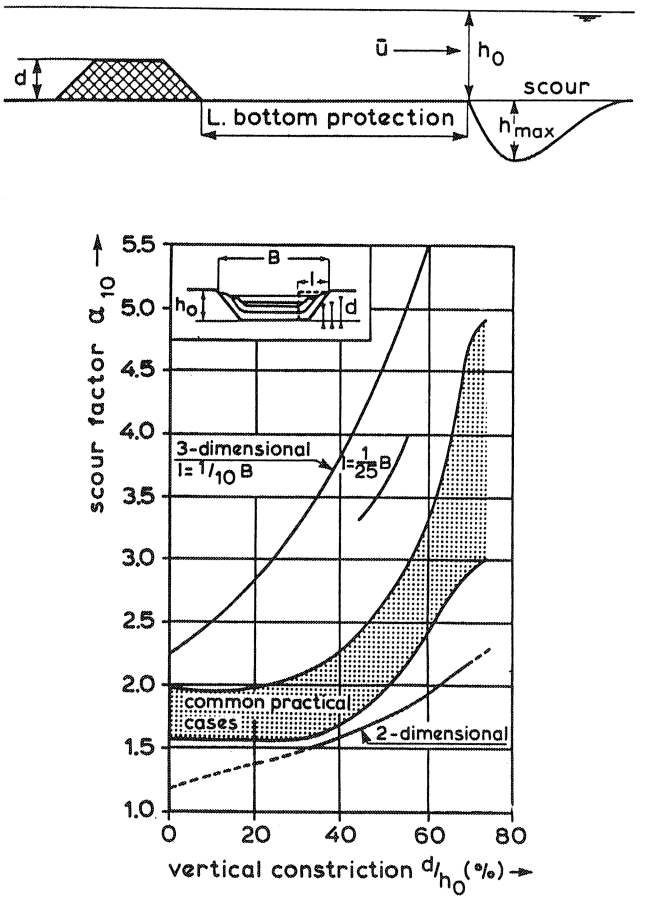

Figure 2.4.9.8 Quantifying of scour factor „α".

2.4.9.5 Influence of neglecting upstream material supply [11]

The model tests providing the basis for the equations mentioned in par. 2.4.9.3. and 2.4.9.4. were carried out in such a way that transport of bottom material could only take place downstream from the bottom protection. In practice, however, there will be a certain amount of material in

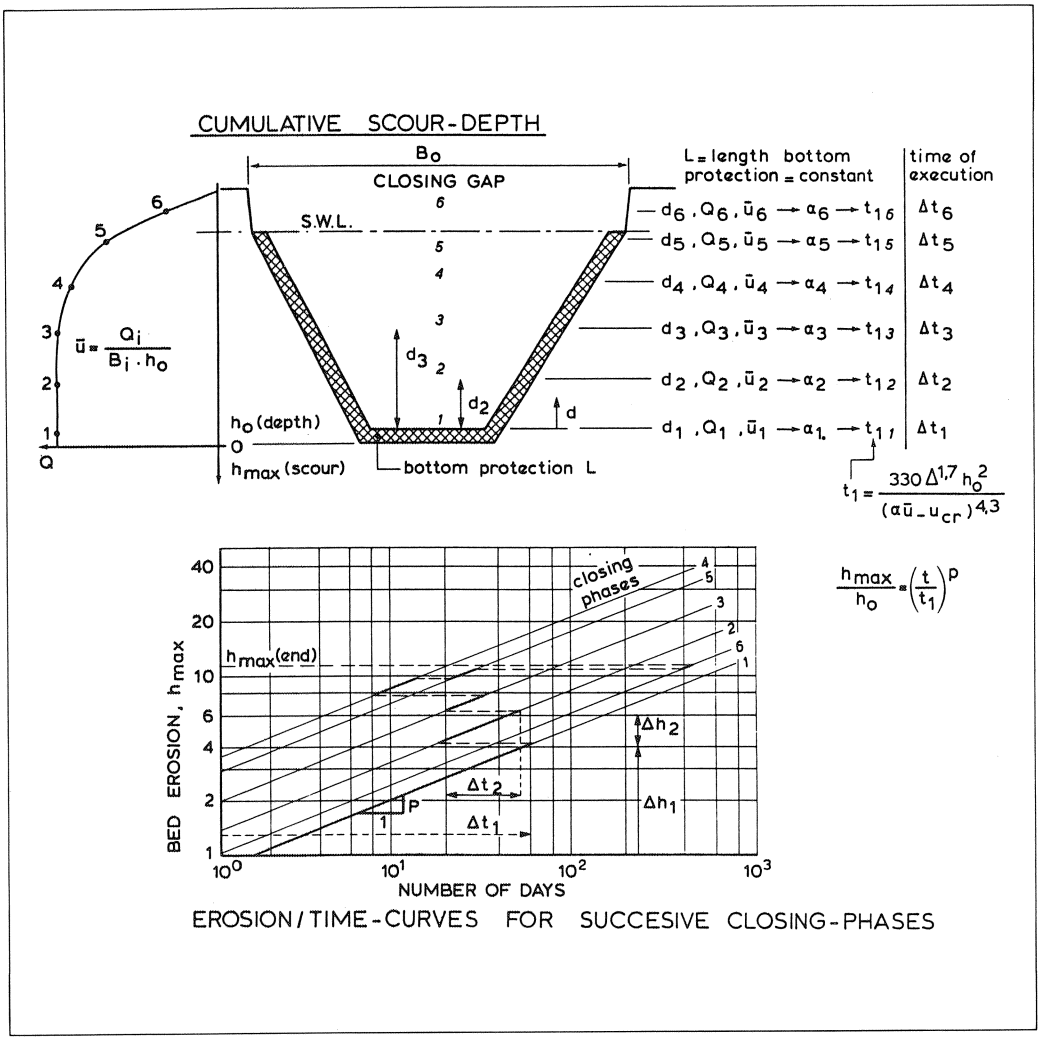

Figure 2.4.9.9 Erosion/time-curves for succesive closing-phases.

suspension, especially fine sediments. In this case a part of the transport capacity of the current will already be occupied, so that full transport capacity will not be available for the discharge of material thrown up from the scour hole. This means that less material will be taken away from the scour hole and that the scour holes will be smaller than in the model tests, where no upstream material supply was present.

This involves a reduction to the results of the model tests by means of computations for the capacity of the scour hole.

The contents of the scour hole per m. width can be approached by

$$I_t = bh^2_{max}(t) \quad (8)$$

in which b = shape factor and I_t = quantity of material discharged from the scour hole during time t from the beginning of erosion, if no upstream material is present.

If the upstream material supply is T_s per m width, the quantity of material which has been discharged from the scour hole will be:

$$I_{t,\ reduced} = I_t - T_s t \quad (9)$$

The reduced scouring depth follows then from:

$$h_{max}(t)_{,reduced} = \sqrt{h^2_{max}(t) - \frac{T_s t}{b}} \quad (10)$$

For the application of this method of reduction it will be necessary to determine the magnitude of T_s for various longitudinal sections. Measurements in prototype for this method are indispensable.
Moreover it has to be established whether all upstream material supplies will effectively reduce the dimensions of the scour hole.
The required insight can also be obtained with the aid of a small scale model. In the prototype there will hardly be any erosion after the bottom protections - the first step during the closing of estuaries - have been put in place. In the model without upstream material supply there will, however, be some erosion.
In order to obtain the results in nature (h_{max} = o) it can then be determined which value of T_s has to be used for the reduction of the model results.

2.4.9.6 Practical applications (prediction h_{max})

The extent of the necessary investigation of local scour depends on the type of the hydraulic structures and their dimension. In the case of large structures such as discharge sluices and large closure works, where the time history of the scouring process is of paramount importance, it will generally be necessary to predict the scour directly from movable bed models (to determine the variation of α in all phases of local scour for different locations = scour pattern). In the case of small structures or, in general, to make some preliminary predictions (first approximation) of local scour, the above equations (i.e. (1) and (2)) can be used satisfactorily.

In using these equations, however, the value of "α" should be estimated. In many cases it is possible to estimate "α" from previous model investigations for similar constructions to that in question (i.e.[17],[19],[20],[21].
As an example some indicative values of "α" will be presented for different stages of the closure dam. These values of "α,, are valid for the 2nd phase of the scour process.
Because the scour process during the various stages of construction of a dam chiefly takes place during the 2nd phase, the use of the presented values of "α" is justifiable.
Fig. 2.4.9.8. gives the relation between "α" and the dam height d in the case of a 10 h_o long bottom protection. The two-dimensional situation is a somewhat academic case, which may be regarded as a lower limit of "α". The three-dimensional situation is another extreme case, corresponding to a situation with an abutment on one side creating a strong vortex trail. The most common situations, such as spillways and closure dams, will lead to values of "α" situated in the hatched area. Especially where there are abutments on one or both sides of the stream, it is advisable to consider 25% of the stream on both sides as three-dimensional, while the 50% in the middle may be considered as „normal" (hatched area in Fig. 2.4.9.8). The influence of the length of the bottom protection is described by [21]:

$$\alpha = 1.5 + (1.57\alpha_{10} - 2.35)e^{-0.045L/h_0} \quad (11)$$
$$\text{for } L \geq 5h_0$$

where L = length of bottom protection in m, α_{10} = value of "α" for L = 10 h_o (Fig. 2.4.9.8.).

It appears that $\alpha = 1.5$ may be considered as a minimum value. The above estimations of "α" may then be used in equations (2), (3),and (12) to make a first approximation of the scouring process by means of equation (1) with $p = 0.4$, which appears to be a fair approximation in most common cases. It must be emphasised, however, that the values given below are coupled to the definition of the flow velocity and the other parameters given with equation (2).

The calculation of the total erosion during closure is illustrated in Fig.2.4.9.9. For each closure stage and chosen length of bottom protection ($-\alpha$) an erosion/time-curve has been determined. When the necessary time for executing of each stage is known, the total erosion can be determined by the superposition of the erosion (=scour depth) obtained during each stage (the erosion in the previous stage determines the starting point of erosion in the next stage). This procedure has to be repeated for different lengths of bottom protection until an acceptable total erosion (depth) is obtained.

In these instances where there is some initial sand transport the procedure described in part 2.4.9.5. must be adapted.
The problem however is how to obtain sufficient data on sand transport. In ideal circumstances the natural data will be available, but in most cases some rough estimations will have to be made.

2.4.9.7 Upstream slope of the scour hole, stability criteria

Besides the maximum scouring depth, the slope at the upstream end of the scouring hole (ß) is important for the stability of the bottom protection and the structure as whole. Observations show that the equilibrium of this slope is a dynamic one, achieved by equalization of the material transport governed by the back-flow currents and the rate of suspension of the bed-material. When this slope exceeds a certain critical value in non-cohesive sediments, a slide can occur or liquefaction of the soil under the bottom protection may even be possible.

From the systematic model investigation, it can be deduced that:

$$\cot g\beta = 5.5 \frac{w}{D}\left(\frac{\nu}{\Delta^2 g^2}\right)^{1/3} \left(2.5 + \frac{0.75}{\alpha - 1.32}\right) \qquad (12)$$

in which: ß = upstream slope of scour hole in radians, w = fall velocity of bottom material in m/s, D = mean diameter bottom material in m,ν = kinematic viscosity of water in m²/s, g = acceleration of gravity in m/s². From equation (12) it appears in particular that the values of "α" and w/D are of importance for the development of the upstream slope of the scour hole.
Equation (12) can be converted in a dimensionless form:

$$n_{\cot g\beta} = n_w n_D^{-1} n_\Delta^{-2/3} \qquad (13)$$

From equation (13) it may be concluded that the upstream slope cannot be exactly reproduced in a scale model when the bottom material differs from the prototype, which is generally the case. Furthermore, with more turbulent upstream conditions, much steeper slopes are found. Therefore, the value of "ß,, obtained from eq. (12) should be treated only as indicative and a certain reserve (safety) has to be allowed for the design. It is obvious that the allowed value of ß has always to be much less than the critical value of the natural slope of sediment in water.

The stability of the upstream slope is the result of the interaction between fluid motion and soil properties. The increasing power of fluid motion (velocity and turbulence) on that slope can produce disturbances in the ground mass. The properties of the sub-grade, which consists mostly of sand, are highly important in this aspect. The initial density of the sand is one of the determining factors in problems of this kind and is a measure of its looseness. There seems to be a critical value, meaning the porosity belonging to the so-called critical density [10].

If the value of the percentage of voids in nature is greater than the critical value the sand is said to be loosely packed. If shear stresses are exerted on sand of this kind its volume decreases. As the pores are full of water, pressure on it will

build up inside the mass of sand, diminishing the effective stresses and thus reducing the shear resistance. Not until sufficient water is drained out will the pore-water pressure decreases,thereby enabling the effective stresses as well as the shear resistance to build up once more.
The shear resistance in this period of high pore-water pressure is low and as a result sliding or even liquefaction may occur in the sand body. It is obvious that scouring will reduce the resistance of the construction base to sideways sliding. Sudden variations of overburden pressure, caused for instance by the placing of caissons, may be particularly risky, since over-pressured pore-water has no opportunity of flowing away in the short time available, so that stresses in the water do not diminish quickly enough.
The same thing occurs if there is a sudden sliding in the slope of a scouring pit beyond the sill.
If however the percentage of voids equals or exeeds below the critical value there is less to fear, since in that case the volume of voids increases as soon as a shear is exerted. The shear resistance also increases as a result. Hence, when making a design it is very important to know the critical density.
In general can be said that loosely packed sand with porosities as high as > 40% is sensitive to flow slide (liquefaction) while in well-packed sand a normal soil-mechanical slide can only occur.
The occurrence of flow slide is especially dangerous when the layer of the loosely packed sand extends until the construction; the flow slide initiated by the steep upper slope of the scour hole can then cause backward erosion under the bottom protection, which can reach the structure and undermine it, thus leading to a major structural failure.
The mechanism of flow slide is still not yet fully known. Nor are criteria for avoiding this phenomena as yet available. It will therefore be difficult to predict the damage and rate of backward erosion when a scour slide occurs.

The question to be answered thus concerns the critical conditions under which slides can occur, i.e. permissible max. depth and the upper slope of the scour hole.
The real answer depends largely on the soil mechanics of the bottom, in particularly the conditions under which a soil slide may take place, and the depth and slope of scouring required to cause a slide. It is also necessary to know the length of the bottom protection, and how well it maintains its integrity and its retarding effect given a soil slide.
While there is little information on the depth and slope of scouring that will result in a slide, it is still possible to establish some rough criteria on the occurrence of slides on the basis of field information on dike failures in the Eastern Scheldt area of the Netherlands [5],[15].
These criteria have been summarised in Figure 2.4.9.10. It should be noted that in these criteria on slide occurrence no retarding effect of the bottom protection has been allowed for. It may be expected that the presence of bottom protection can lead to somewhat shorter backward erosion (i.e. steeper end-slope after slide).
If it is known that the local sand has the potential to liquefy and to cause flow slides, some measures will have to be taken to avoid this. Protection of the construction in such a situation depends on reducing the scouring rate in the initial scour hole by extending the bottom protection so as to reduce the velocities to which the initial scour hole is exposed, and to localise the scour hole further away from the construction.
The general design requirements for bottom protection related to expected scour are summarized in Figure 2.4.9.11.
Protecting the slope of the scour hole by rock or slag, and full or local compacting (densification) or even replacement of the bottom soil, may increase the depth which must be scoured to cause the first slide, and thus protect the structure against unexpected conditions. The installation of a retaining wall, i.e. sheet piling at the edge of the bottom protection can also be taken into consideration. It is, however, always advisable frequently to monitor the development of the scour hole during construction and operation so as to be able to take the necessary measures in good time to avoid creating a dangerous situation.
For structures such as spillways, where scour

will also continue after construction, it is preferable to have as much scour rate as possible during construction rather than operation, since the slopes of the scour hole can then be stabilized once the scour has occurred (the necessary equipment and materials being directly available). This minimizes the amount of scour that may occur under operational conditions.

Figure 2.4.9.10 Permissible scour hole. Empirical criteria.

PERMISSIBLE SCOUR HOLE / EMPIRICAL CRITERIA

- MAX. SCOUR DEPTH , h_{max}
- MAX. UPPER SLOPE , β

DEFINITIONS :
(before slide)

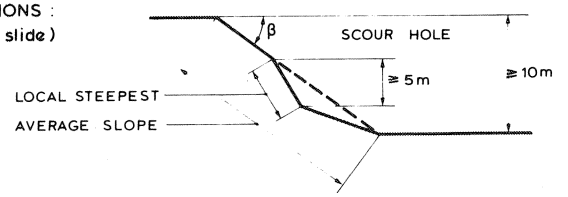

CRITERION OCCURANCE	BEFORE SLIDE				AFTER SLIDE
	STEEPEST		AVERAGE SLOPE		
	SLOPE ≥	DEPTH ≥	SLOPE ≥	DEPTH ≥	AVERAGE SLOPE ≥
FLOW SLIDE	1 : 4	5 m	1 : 7	10 m	1 : 15
NORMAL SLIDE	1 : 2	5 m	1 : 4	10 ÷ 15m	1 : 6

EXAMPLES :

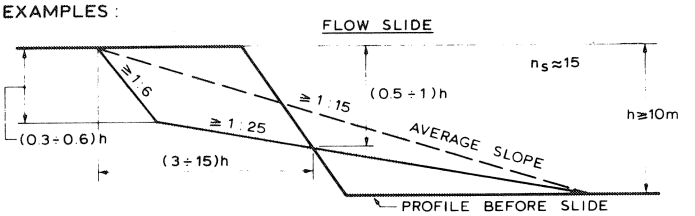

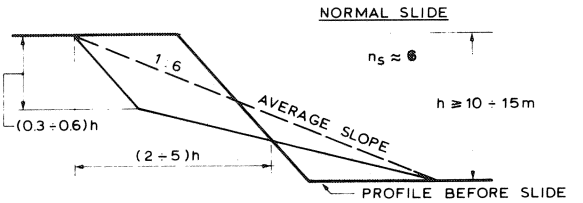

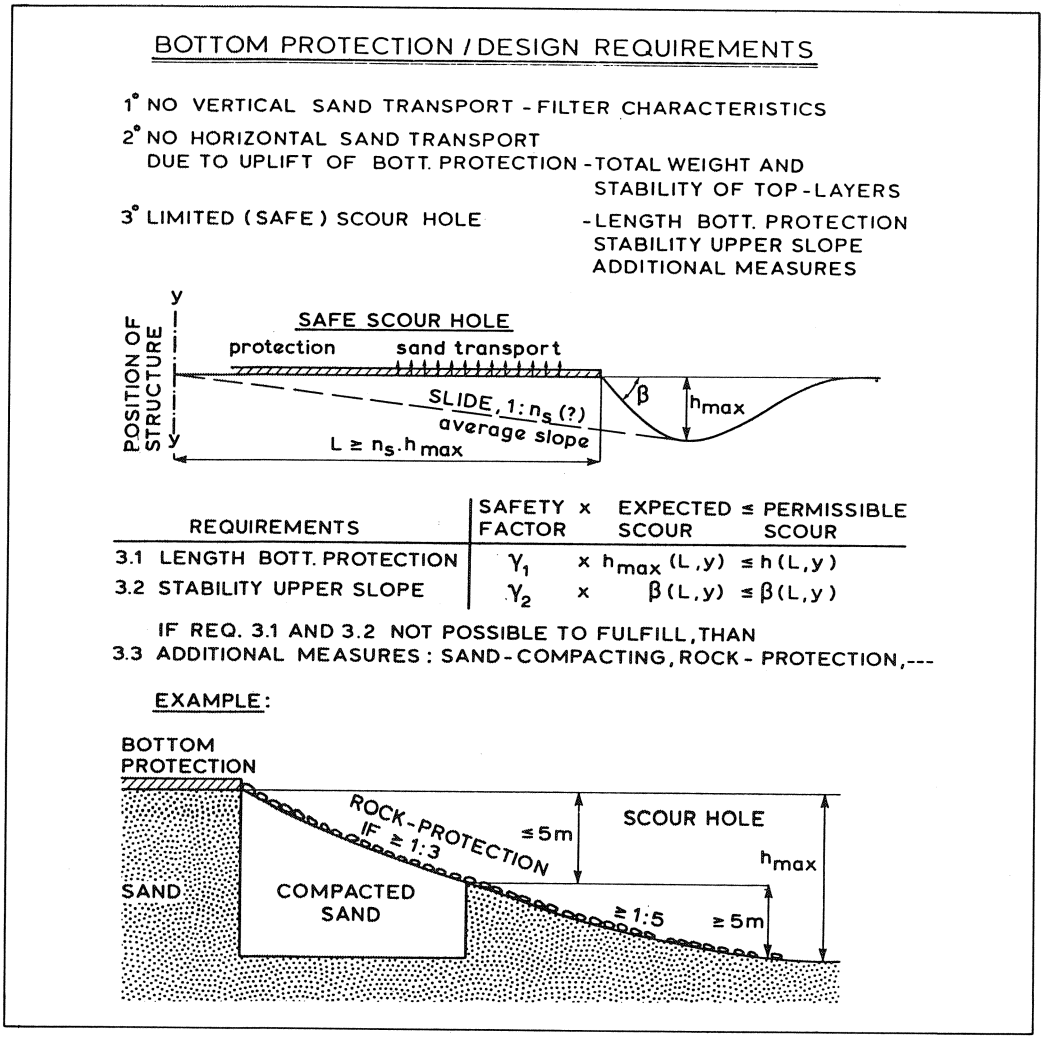

Figure 2.4.9.11 Bottom protection. Design requirements.

In the case of unreliable soils and/or high expected scour rates it is preferable to make an artificial scour hole beforehand and to protect the upper slope (1:2 à 1:3) by gravel or slag. This may be especially advisable in the case of a dry execution of bottom protection.
This will generally lead to a shorter and more reliable design of bottom protection.

The adaptation of the protective measures is illustrated in Figure 2.4.9.11. The bottom soil below the end of the bottom protection has been compacted. When the slope of the scour hole reaches the value of about 1 in 3 in the compacted area and about 1 in 5 in the original soil, both slopes have to be protected by rock or slag. In such cases filter construction will generally not be needed.

As a final conclusion with respect to the problem of flow slides, it may be stated that more authoritative quantity standards or criteria still need to be developed and applied as a part of the overall design. Additional research is needed for estimating slide failure probability and on measures for delaying a soil slide.
Furthermore, the inadequate state of knowledge concerning soil properties and the mechanics inside a soil body mean that one can never be certain about the effect of fluid motion on soil displacement during the scouring process.
This uncertain factor must be taken into account when planning hydrotechnical works and it is important that the studies be aimed at limiting this uncertainty as much as possible.

2.4.9.8 Scour around bridge piers [4]

Scour around bridge piers is due to a combination of three effects:
- local scour near the bridge pier caused by the disturbance of the flow field around the pier (see Fig.2.4.9.12. a, b).
- a lowering of the river bed in the cross-section of the bridge due to the contraction of the river profile at that section,
- a general lowering of the river bed in the river around the bridge site due to degradation or non-uniform river-bed changes during floods.

These last two aspects, together with practical experience for the situation of a bridge in a flood plain, are discussed in an excellent way by C.R. Neil [12].
The local scour near the bridge pier is discussed in detail in a review article by Breusers, Nicollet and Shen [3].
An analysis of existing data shows that the scour depth could be expressed as:

$$\frac{h_s}{b} = f_1\left(\frac{\bar{U}}{\bar{U}_{cr}}\right) 2\tanh\left(\frac{h_0}{b}\right) f_3(\text{shape})\, f_y\left(a\,\frac{1}{b}\right) \qquad (14)$$

h_s = scour depth (below original river bed)
b = width of pier
$\bar{U}$ = mean velocity
$\bar{U}_{cr}$ = critical mean velocity for beginning of motion
h_o = water depth
a = angle of attack
l = length of pier

For most practical situations: $\bar{U}/\bar{U}_{cr} > 1.0$ so that $f_1(\bar{U}/\bar{U}_{cr}) = 1.0$

f_3 (shape) = 1.0 for circular and round-nosed piers
= 0.75 for stream-lined piers
= 1.3 for rectangular piers
For f_y (a,l/b) = K(multiplying factors for angle of attack) see Figure 2.4.9.12.c.

If the river bed around the pier is protected with a revetment, it should be placed at or below the lowest river bed level to avoid extra obstruction. The stone size should be designed for a velocity 2.0 times the approach velocity U to account for the increase in velocities near the pier.
Generally speaking a flexible protection at some depth below the normal river bed will give the best results. The necessary stone size D for a given maximum mean velocity U_{max} can be obtained from:

$$\bar{U}_{max} = 0.5\,\bar{U}_{cr} = 0.43\sqrt{2g\Delta D}$$

or (15)

$$D = \frac{2.7}{g\Delta}\,\bar{U}^2_{max}, \text{ where } \bar{U}_{max} = 2\bar{U}$$

A good filter construction is necessary.
Rigid footings should be designed carefully and be placed at some depth below the level of general scour.
If the footing is exposed to the flow, scour depth will increase due to the greater effective width. Attention had to be given to the following special effects:

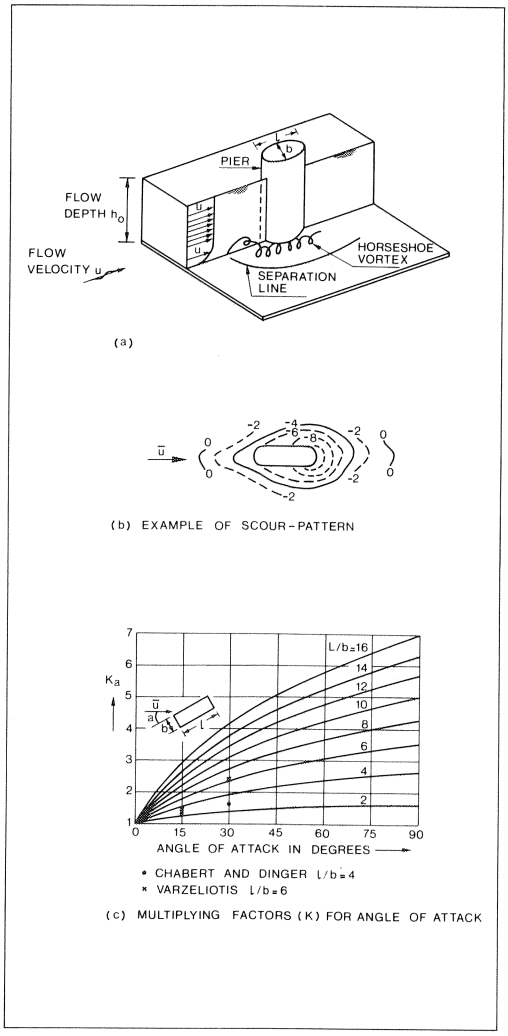

Figure 2.4.9.12 Scour around bridge piers.

- Debris and ice can increase the effective size of the piers and therefore the local scour.
- Flash floods can give a greater scour depth because of unsteady transport conditions.
- Dunes and sand waves can change the angle of attack and increase the local depth near the pier.
- A cohesive upper layer can be disturbed near the pier and cause an increase in scour depth because no upstream supply is present.
- General scour due to degradation, contraction, shifting channels, or level variations during floods has to be added to the local scour near the piers.
- Intensive suspension of sediment in large fine-bed rivers may invalidate the empirical relations.
- Bad placement of riprap can provoke scour.

References

1. Blench, T., **Regime Behaviour of Canals and Rivers,** Butterworths, London.

2. Breusers, H.N.C., Conformity and Time Scale in two-dimensional Local Scour, **Delft Hydraulics Laboratory,** Publication no.40, March 1965.

3. Breusers, H.N.C., Nicollet, G., Shen, H.W. Local Scour around Cylindrical Piers, **Journal of Hydraulic Research** 15(3), 1977.

4. Breusers, H.N.C., Lecture Notes and Local Scour, **International Institute for Hydraulic and Environmental Engineering,** Delft, 1979.

5. Davis, P.G.J., Interne nota betreffende optredings- en schadecriteria van zettingsvloeiingen en afschuivingen in zandgrond, **Internal Note Deltadienst,** RWS, April 1978.

6. Graauw, A.F.F., Pilarczyk, K.W., Model Prototype Conformity of Local Scour in Noncohesive Sediments beneath Overflowdam, **Delft Hydraulics Laboratory,** Publication no.242, November 1980. Also: XIX IAHR congress, New Delhi, Februari 1981.

7. Kotoulas, M., **Das Kolkproblem unter Besonderen Berücksichtigung der Faktoren Zeit und Geschiebemischung,** Diss. Braunschweig, 1967.

8. Kruchinina, Investigation Findings on Scouring Process in Cohesive Soils, **Comm. All. Union Scient. Res.,** Inst.B.E. Vedeneev, 88, 1969.

9. Lemos, F.O., General Report Subject: Non-steady Morphological Phenomena: Physical and Mathematical Modelling of Degradation (including local scour) and Aggredation, **XVIth congress IAHR, vol.6,** Sao Paulo, 1975.

10. Lindenberg, J., and Koning, H.L., Critical Density of Sand, **Géotechnique 31,** no.2, 1981.

11. Meulen, T. van der, Vinje, J.J., Three-dimensional Local Scour in Non-cohesive Sediments, **XVIth congress IAHR,** Sao Paulo, 1975.

12. Neill, C.R. (ed.), **A Guide to Bridge Hydraulics,** University of Toronto Press, 1973.

13. Paintal, A.S., Concept of Critical Shear Stress in Loose Boundary Open Channels, **Journal of Hydraulic Research,** 9(1),1971.

14. Vinje, J.J., Local Scour Caused by Vortex Streets, **Symposium on Closure of Estuarine Channels in Tidal Regions, De ingenieur, nr. 47,** 1968, The Netherlands.

15. Wilderom, M.H., Resultaten van het vooroever-onderzoek langs de Zeeuwse stromen (in Dutch), **RWS, Studiedienst Vlissingen,** nota nr. 75.2, Jan. 1979.

16. Zanke, V., Zusammenhänge zwischen Strömung und Sedimenttransport, Teil 2: Berechnung des Sedimenttransportes hinter befestigten Sohkenstrecken-sonderfall zweidimensionaler Kolk, **Franzius Institut,** Mitt.Heft 48, Hannover 1978.

17. Afsluiting Brouwershavense Gat (in Dutch). (Closure of Brouwershaven's Gap), **Delft Hydraulics Laboratory,** Report M675, 1970.

18. Systematisch onderzoek naar twee- en driedimensionale ontgrondingen (in Dutch). Systematic research on local scour, **Delft Hydraulics Laboratory,** Report M648/M863, 1972.

19. Hevels in de Grevelingendam. (Siphon spillway Grevelingendam) Stroombeeld en ontgrondingsonderzoek (in Dutch). **Delft Hydraulics Laboratory,** Report M1346, 1977.

20. Sluis Brouwersdam. Ontgrondingsproef (in Dutch). (Discharge sluice Brouwersdam), **Delft Hydraulics Laboratory,** Report M1533, parts I, II and III. 1979-1981.

21. Ontgrondingen (Local Scour), **Delft Hydraulics Laboratory,** nota II, M1001, June 1981 (in Dutch).

H. Speekenbrink

2.4.10 Stability of dredged trenches, erosion of ridges and impact of sand dumping

1. Introduction

The alluvial subsoil in tidal areas often consists of alternating layers of sand and clay or silt. The geotechnical conditions are therefore often too poor for the foundation of a closing structure. Often a soil improvement has to be made, usually by removing the original subsoil and then refilling the gap with other materials. The refill may consist of pure sand or a filter construction. The top level of the refill depends on the foundation depth of the closing structure. Local hydraulic conditions and, thus, sediment transports are affected during the soil improvement and afterwards if the top of the refill is below or above the original bed level. In trenches where the bed is below the adjacent bed level, sedimentation usually occurs, whereas embankments tend to erode.

2. Change of sediment transport due to variations of local conditions

2.1. General

The transport of non cohesive sediment is normally divided into separated bed load and suspended load. In many contexts, such a distinction is of minor importance but for the description of sedimentation and erosion this distinction is quite essential. The bed load adjusts itself very quickly to a change in conditions. However the adaptation of the concentration of sediments over the water depth may take quite some time, depending mainly on the particle fall velocity and the turbulence intensity.

A wide variety of sediment transport formulae can be found in technical literature. A compilation is given in the „Sedimentation Manual" (1).All formulae apply to uniform and steady flows, which means that they express the sediment transport capacity of the flow. As long as the transport capacity exceeds the actual transport, the bed will be eroded; where the capacity becomes less than the local transport, sedimentation will start (see fig. 2.4.10.1).

Figure 2.4.10.1 Erosion and sedimention due to changing flow velocities during a tide

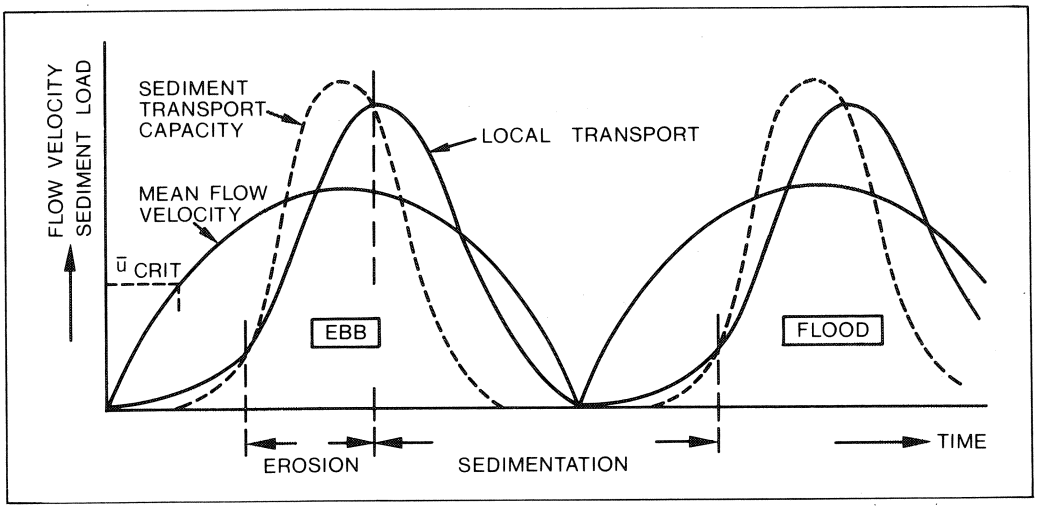

In tidal areas, the current velocities change continuously in place and time. It will therefore be obvious that the suspended load practically never equals the transport capacity, because of the time needed for adjustment. From an analysis of measured sediment transports and flow velocities in the Eastern Scheldt (2), a relation between suspended load and flow velocity could be deduced, which was mainly determined by the location of the measuring station and the velocity phase (accelerating or decelerating flow). It was found that, during the decelerating flow, the suspended load is far greater than during an accelerating flow for the same flow velocity. The deviations are significant (up to a factor 10). It is therefore unlikely that application of sediment transport formulae derived for uniform and steady flows will provide optimum results in tidal areas, unless the previous history of the flow with respect to sedimentation and erosion is taken into account. This however requires considerable computer time. The use of different formulae for accelerating and decelerating flows will be accurate enough, in most cases, for predicting the siltation rate in dredged trenches.

2.2. Bed load

Most bed load formulae may be expressed as a relation between a dimensionless transport parameter φ and a dimensionless flow parameter ψ. The transport parameter may be written as

$$\varphi = \frac{s}{d\sqrt{\Delta g d}} \qquad (1)$$

where:

s	=	transport in volume of grains per unit width	$m^3/m^1/s$
d	=	grain size	m
Δ	=	relative density of the sediment ($\Delta = (\varrho_s - \varrho)/\varrho$)	
ϱ_s	=	specific density of sediment	kg/m^3
ϱ	=	specific density of the fluid	kg/m^3
g	=	gravity	m^2/s

The flow parameter may be written as:

$$\psi = \frac{\tau_b}{\rho g \Delta d} \qquad (2)$$

where:

τ_b = shear stress acting at the bed

Shields investigated the initiation of motion and found that there is a critical value ψ_{cr} for the inception of the sediment transport.
Shields plotted his experimental results versus the grain Reynolds number Re* (see figure 2.4.7.1). The solid line in that figure, now known as the Shield curve, was found by Hunter Rouse. Since then, many more results have been added as a result of various experiments.
It has been shown that the bed shear stress may be divided into a shape drag and a roughness drag. The shape drag does not contribute to the transport, and only the roughness drag acts on the grains. Most transport relations therefore require a reduction of the total bed shear stress to a value that is relevant for the transport.
This reduction factor is called the ripple factor μ. Theoretically, one should expect:

$$\mu = \frac{\lambda_k}{\lambda} \qquad (3)$$

where:

λ = total bed friction coefficient (Darcy-Weisbach)

λ_k = bed friction coefficient with respect to the grain roughness.

Since sediment movement only starts after the threshold value is exceeded, the effective flow parameter ψ_* can be expressed as

$$\psi_* = \mu\psi - \psi_{cr} \qquad (4)$$

The shear stress, acting on a nearly horizontal bed for uniform flow conditions (parallel flow lines) may be written as:

$$\tau_b = \frac{1}{8}\rho\lambda\bar{u}^2 \qquad (5)$$

where

u = mean current velocity (over the depth) m/s

and hence it follows from equation (2), (3), (4) and (5) that

$$\psi_* = \frac{1}{8}\frac{\lambda_k}{g\Delta d}\bar{u}^2 - \psi_{cr} \qquad (6)$$

According to Alam and Kennedy (3) the λ_k in turbulent flow equals about 0.02; see figure 2.4.10.2.

The following simplified empirical relations for the sediment transport under uniform conditions can be found in literature:

$\varphi \approx :: \psi_*^2$ Du Bois (1879) (Bed load)

$\varphi \approx :: \psi_*^3$ Brown (1950) (Bed load)

Figure 2.4.10.2 Friction coefficient for flat bed flows in alluvial channels as function of the Reynolds number. The number by each point is R/d x 10^{-2}.

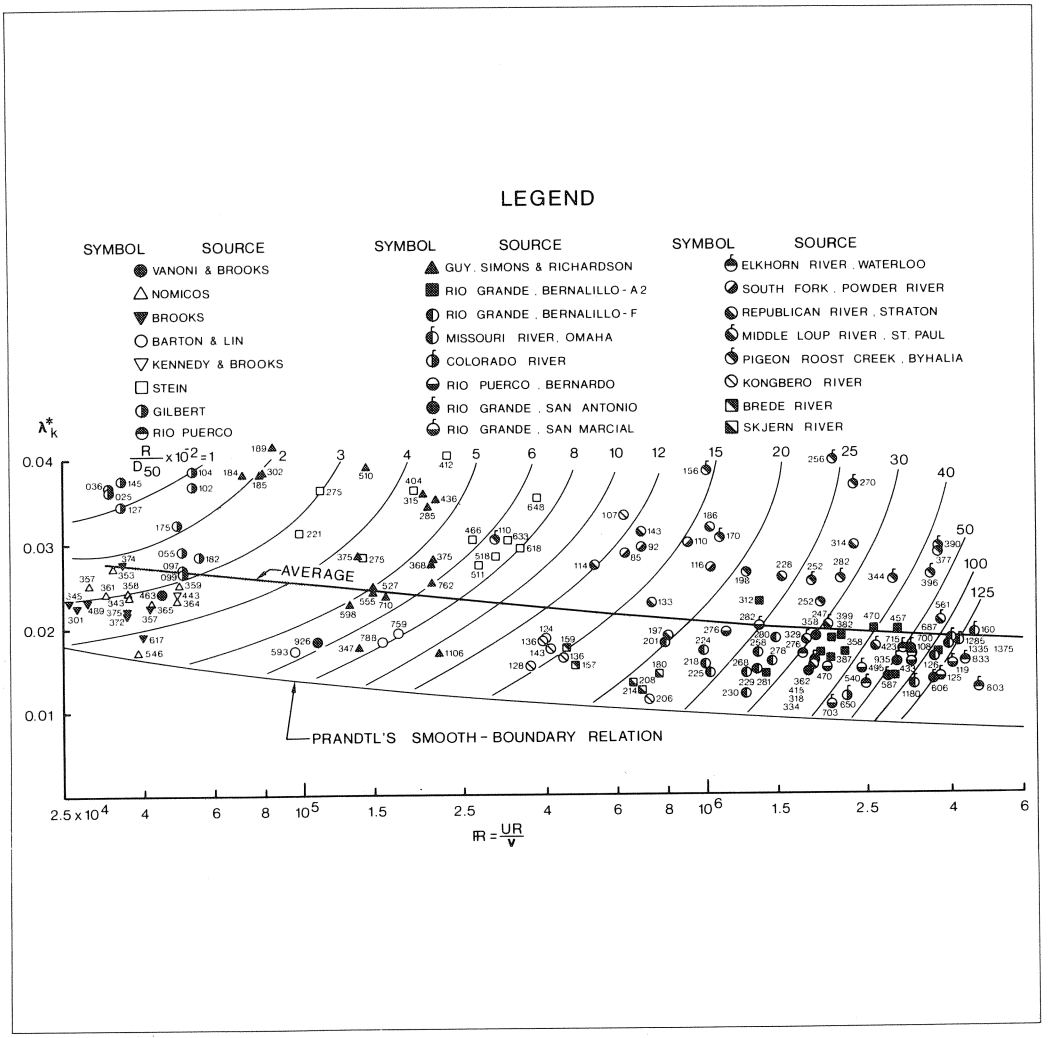

$\varphi \approx :: \psi_*^{3/2}$ Meyer Peter (1934) (Bed load)
$\varphi \approx :: \psi_*^{3/2}$ Bagnold (1956) (Bed load)
$\varphi \approx :: \psi_*^{5/2}$ Engelund-Hansen (1967) (Total load)
$\varphi \approx :: \psi_*^{5/2}$ Yalin (1963) (Total load)

As a simple relation we may assume that

$$\varphi = 20\ \psi_*^2 \qquad (7)$$

Figure 2.4.10.3 Comparison of bed load transport equations.

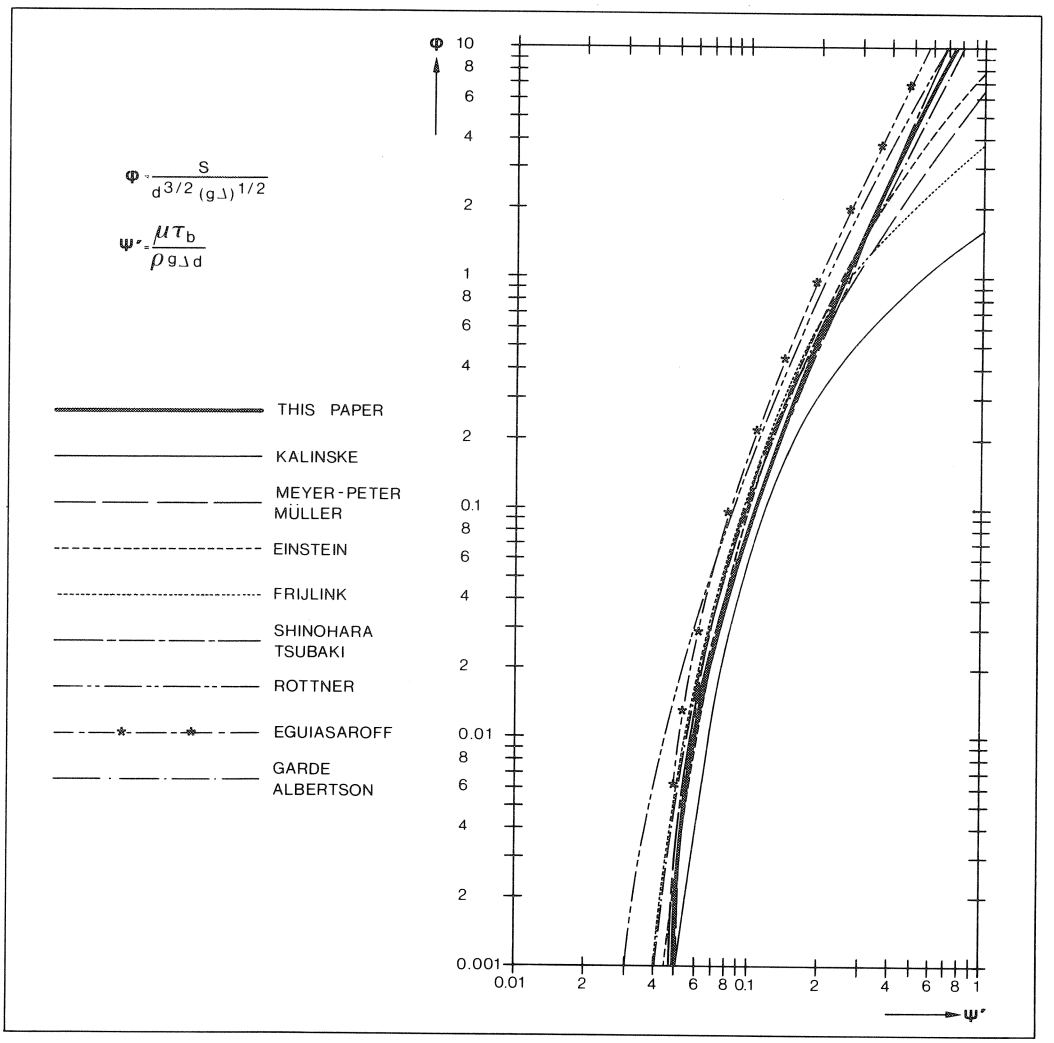

This relation is plotted in figure 2.4.10.3 for $\psi_{cr} = 0.04$ together with some other formulae. It can be seen that equation (7) agrees very well with these other formulae, since it remains within the envelope.

The bed load will vary when the sea bed level changes because of

1. gravity effects on the side slopes
2. variation in current velocity due to the changes in depth
3. effect of diverging or converging flowlines due to a change in bed slope.

re.1 The gravity effects reduce the critical Shields parameter ψ_{cr}, as is shown in chapter 2.4.7. Futhermore it will change the transport direction when the flow is not perpendicular to the slope axis

re.2 The variation in current velocities results in a variation of the flow parameter ψ.

re.3 The effects of diverging and converging flowlines change the shear stress applied to the bed and the turbulence intensity.

In „Stability of Loose and Cohesive Materials" (ch.2.4.7) it is shown that on a slope with angle α in flow direction the critical shear stress is reduced by a factor $K\alpha$

$$K\alpha = \frac{\psi_{cr_s}}{\psi_{cr_o}} = \frac{\sin(\phi-\alpha)}{\sin\phi} \qquad (8)$$

where:

ψ_{cr_s} = critical Shields parameter on a sloping bed

ψ_{cr_o} = critical Shields parameter on a horizontal bed

For gentle side slopes where $\cos\alpha \approx 1$ and $\sin\alpha \approx \tan\alpha$ equation (8) may be written as

$$\psi_{cr_s} = \psi_{cr_o}\left(1 - \frac{\tan\alpha}{\tan\phi}\right) \qquad (9)$$

Schlichting [4] deals with shear stresses in convergent and divergent flows for smooth boundaries. We now assume that the ratio of bed shear stress for uniform flow and the bed shear stress for diverging or converging flow is independent of wall roughness.

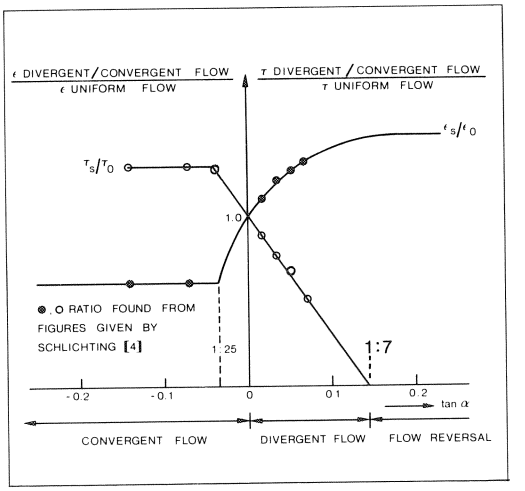

Figure 2.4.10.4 Ratio of shear stresses in convergent/ divergent and uniform flow for several slope angles. The ratio for the diffusion coefficient is also presented.

Based on figures by Schlichting, this ratio is determined for several slope angles and graphically represented in figure 2.4.10.4.
From this figure it can be seen that for convergent flow, the bed shear stress is 1.3 times the bed shear stress for uniform flow conditions on slopes steeper than 1:25. For divergent flow the bed shear stress drops to zero for an 1:7 slope. This slope coincides with the critical slope for flow separation and the start of flow reversal at the bed. Based on figure 2.4.10.4, it can now be derived that

$$\psi_s = K_\beta \psi_0 \qquad (10)$$

where

ψ_s = flow parameter on sloping beds

ψ_o = flow parameter on horizontal beds

$$\text{with } K_\beta = \left(1 - \frac{\tan\alpha}{\tan\beta}\right) \text{ for } \tan\alpha > -0.04 \quad (10a)$$

$$K_\beta = 1.3 \text{ for } \tan\alpha \leq -0.04 \quad (10b)$$

α = actual bed slope
β = critical slope for flow separation

Combining the equations (4), (8) and (10) finally yields the flow parameter for non-uniform conditions:

$$\psi_* = \xi K_\beta u^2 - K_\alpha \psi_{cr} \quad (11)$$

where $\xi = {}^1/_8 \frac{\lambda_k}{g\triangle d}$ (sediment parameter)

From equations (1), (7) and (11), the bed load variations for non-uniform conditions can be found by assuming that the bed load adjusts itself instantaneously to a change in ψ_*.

2.3. Suspended load

The distribution of suspended sediment in a vertical plane can be described by the sediment diffusion equation which, for a two dimensional approach reads:

$$\frac{\partial c}{\partial t} = \frac{\partial}{\partial x}\left(\varepsilon_x \frac{\partial c}{\partial x}\right) - \frac{\partial}{\partial x}(uc) + \frac{\partial}{\partial z}\left(\varepsilon_z \frac{\partial c}{\partial z}\right) \quad (12)$$

$$- \frac{\partial}{\partial z}(wc) + \frac{\partial}{\partial z}(w_s c)$$

where:

c	=	volumetric sediment concentration	
ϵ	=	diffusion coefficient	m^2/s
u	=	flow velocity in longitudinal direction	m / s
w	=	flow velocity in vertical direction	m / s
w_s	=	particle fall velocity of the sediment	m / s
x	=	coordinate in longitudinal (main flow) direction	m
z	=	coordinate in vertical direction	m

The longitudinal diffusion can be neglected with respect to the vertical diffusion, since it may be assumed that the diffusion coefficient in a single point is equal in all directions ($\epsilon_x = \epsilon_z$), whereas the vertical concentration gradient is much greater than the horizontal, due to gravity effects. The fall velocity may be considered as a constant over the depth ($\frac{\delta_{ws}}{\delta_z} = 0$) and the vertical flow velocities can normally be neglected. In steady flow, equation (12) now reads

$$\frac{\partial (uc)}{\partial x} - w_s \frac{\partial c}{\partial z} - \frac{\partial}{\partial z}\left(\varepsilon_z \frac{\partial c}{\partial z}\right) = 0 \quad (13)$$

For uniform flow and sediment transport conditions $\frac{\delta uc}{\delta x} = 0$ equation (13) is reduced to the familiar

$$w_s c + \varepsilon_z \frac{dc}{dz} = 0 \quad (14)$$

The first term $w_s c$ represents the settling tendency due to gravity and the second term $\epsilon_z \frac{\delta c}{\delta z}$ the diffusive action of the turbulence.

It is customary to use the same form for the sediment diffusion coefficient (ϵ_z) as for the diffusion coefficient for momentum (ϵ_m). Use of the logarithmic velocity law and the Prandtl mixing length-theory leads to

$$\varepsilon_z = \kappa u_* z\,(1 - z/h) \quad (15)$$

where

κ = Von Karman constant
μ_* = bed shear velocity
h = water depth

From sensitivity analyses, it could be concluded that in uniform flow the vertical sediment concentration distribution is only slightly influenced by the vertical distribution of the eddy diffusion coefficient but mainly by its maximum value (5).

The maximum value may be taken to be proportional to the mean value over the depth:

$$\varepsilon_{max} = \alpha\bar{\varepsilon}_z = \frac{\alpha}{6}\kappa u_* h \qquad (16)$$

Integration of equation (14), and assuming ϵ_z to be constant over the depth equal to its mean value, yields the vertical sediment concentration distribution for uniform flow conditions:

$$c(z) = c_b e^{-\frac{6w_s}{\kappa u_*}\frac{z}{h}} = c_b e^{-\frac{w_s z}{\varepsilon_z}} \qquad (17)$$

where
c_b = suspended load concentration at the bed boundary.

c_b has to be calculated from a sediment transport formula such as, for instance, the Kalinske-Kirkham formula (2);

$$c_b = \frac{A}{\sqrt{\pi}}\left\{\frac{ku_*}{\sqrt{2}w_s} e^{-\frac{w_s^2}{2k^2u_*^2}} - \frac{\sqrt{\pi}}{2}\,\mathrm{erfc}\left(\frac{w_s}{\sqrt{2}ku_*}\right)\right\} \qquad (18)$$

where
A = empirical constant = 0.0039
k = empirical constant = 0.28

Another way to calculate the bed concentration is by using the bed load equation (7) by assuming that c_b equals the mean concentration of the bed load, and that the bed load (s_b) is transported in a layer with thickness $a \approx k_s$, where k_s = specific bed roughness according to Nikuradse.

$$\text{Hence: } c_b = \frac{s_b}{au} \qquad (19)$$

The suspended load will vary across a bed level change because of
1. variation in current velocity due to changes in depth
2. variation in exchange coefficient ϵ due to converging/diverging flow.

The variation in ϵ can be determined in a similar way as was done for the variation in τ by assuming that the turbulent shear stress is proportional to the velocity gradient, on analogy to the viscous shear stress:

$$\tau = \rho\varepsilon_m \frac{\partial u}{\partial z} \qquad (20)$$

The ratio of the exchange coefficient for divergent/convergent flow and for uniform flow was again derived from figures given by Schlichting (4) and this ratio is also represented in figure 2.4.10.4. It can be seen that, for convergent flow, the turbulence is suppressed whereas, for divergent flow, the tubulence increases up to about a factor 1.5 for a 1:7 slope.

By integration of equation (13) over the depth, the variation in suspended load s_s can be derived

$$\frac{ds_s}{dx} = \int_0^h ucdz = w_s \int_0^h \frac{\partial c}{\partial z}\,dz + \varepsilon \int_0^h \frac{\partial^2 c}{\partial z^2}\,dz \qquad (21)$$

To solve this equation, the sediment distribution must be known. It can be determined from equation (13), by assuming that at x = 0, at the beginning of the bed disturbance, uniform flow conditions exist. Since equation (13) can not be solved analytically, numerical models have been developed (2,3).

2.4. Wash load

Wash load consists of very fine particles that, in general, tend to belong to the group known as cohesive materials. A small amount of turbulence will already be sufficient to prevent settling of the grains. The wash load is therefore almost entirely governed by the supply of fine-grained soils and not by the flow capability to transport it. Wash load is normally rather equally distributed over the depth, since the turbulence is far more important than gravity.

Only when the turbulence of the flow drops below a certain limit will siltation start. According to Reynolds' analogy, the tubulence in the flow is proportional to the bed shear stress.

Krone (6) derived a linear relationship between the sedimentation rate and the bed shear stress

expressed in shear velocity and checked the validity of this relationship by flume experiments. The equation as given by Krone can be written as

$$\frac{dM}{dt} = c_s w_s \{1-(\frac{u_*}{u_{*_L}})^2\} \qquad (22)$$

where

M	=	mass of siltation per unit of surface area	kg/m²
c_s	=	mass silt concentration in the flow	kg/m³
w_s	=	fall velocity of the silt particles	m / s
u_{*_L}	=	limiting shear velocity for inception of siltation	m / s

Krone derived an average value of 0.009 m/s for u_{*_L}.

When the bed shear velocity is greater than the critical value u_{*_L}, then $\frac{dM}{dt} < 0$, which would yield erosion. Due to consolidation after settlement, the cohesive resistance of the silt grains against erosion increases. Consequently the limiting shear velocity for erosion will increase too, depending on consolidation time. The increase factor already reaches a value of 3 to 4 after a short consolidation time of about one hour. In trenches, therefore, re-erosion of silt particles after siltation may be ignored.

To determine the amount of siltation from wash load, the upstream boundary silt concentration in the water must be known. Since this concentration is not governed by local conditions, measurements of the silt concentrations in the area have to be carried out.

The fall velocity of the silt grains may be determined by

$$w_s = \sqrt{\tfrac{4}{3}\frac{1}{C_D}\Delta g d} \qquad (23)$$

where C_d = drag coefficient

Schiller and Nauman (7) found for C_d

$$C_D = \frac{24}{Re^*}(1 + 0.15(Re^*)^{0.687}) \qquad (24)$$

where Re* = the Reynolds grain number = $\frac{W_s d}{\nu}$

For practical use, a fall velocity of 1 m/hr may be adopted.

3. Sedimentation in trenches

The rate of siltation in a trench depends on the supply of sediment, on the hydraulic conditions (wave and flow characteristics) and on the shape, size and alignment (relative to direction of flow) of the trench. These factors may vary in place and in time.

It can be shown that, for a quasi-steady two-dimensional sediment flow, the continuity equation is given by:

$$(1-n)\frac{\partial z_b}{\partial t} + \frac{\partial s}{\partial x} = 0 \qquad (25)$$

where:

n	=	porosity of the bed	
z_b	=	bed level	m
t	=	time	s
s	=	sediment transport in volume of grains per unit width of flow	m³/m¹/s
x	=	longitudinal coordinate (flow direction)	m

The sediment transport equals the total load, i.e. the suspended and bed load. These may be determined from equations (11) and (21).

The total sedimentation in the trench can be found as the difference between the load at the upstream boundary and the load at the downstream boundary.
When the trench is very wide, it may be assumed that equilibrium conditions will be reached within the trench and then it may be assumed that the total sedimentation equals the difference between the equilibrium load upstream and in the trench.

4. Erosion of underwater embankments

On the upstream slope of an embankment, the flow will converge and accelerate and, consequently the shear stress at the bed will increase and the turbulence be suppressed (see section

2). It may, therefore, be concluded that erosion will mainly be caused by an increase in bedload. The erosion rate may therefore be computed from equations (1), (7), (11) and (24).

5. Impact of sand dumping

When sand is discharged near the water surface, a distinction can be made between the behaviour of the sand discharge on its way to the bottom and its behaviour after impingement. Since there is only a little knowledge of the phenomena the mechanism involved will only be described in a qualitative way.
The sand-water stream released from the discharge point may accelerate in vertical direction due to gravity and in horizontal direction due to drag forces by the ambient flow in which it is discharged.
Due to the vertical acceleration, the flow velocity in the sand-water jet will increase and, thus, the velocity difference with the ambient water, since the vertical flow velocities in the ambient water may be assumed to be zero.
Due to this velocity difference, friction forces are mobilised and water is entrained in the jet from the ambient water.
The effects of the entrainment will only be discussed in a qualitative way since a treatment of entrainment is beyond the scope of this book. Reference can be made to (8) for a more detailed description of the entrainment functions.
By entrainment of water, the sediment concentration in the jet will decrease and, consequently, so will the gravitational forces. The friction forces may become predominant, causing the flow velocity in the jet to decrease again.
The final flow velocity in the impingement point (where the centre of the jet hits the bottom) will, therefore, be strongly dependent on the distance between the discharge point and the impingement point.
This distance will increase when the flow velocity of the ambient water increases. With increasing distance, the diameter of the jet will increase as well (continuity reasons) and, thus, so will the impingement zone.
Depending on the above effective distance and the initial flow velocity of the jet at the discharge point, the sand-water jet can reach values of several metres per second at the impingement point.
This high velocity causes high impact forces on the bed and, consequently, a crater is formed.
The depth of the crater depends on the strength of the impact forces and on the duration of the impact forces on the bed. In relation to the increasing depth of the crater, the impact forces will decrease until the distance to the discharge point is great enough to prevent impact forces from eroding the bed. In that case, however, the impingement zone will be very large and, in most cases beyond the limits of the dumping area.
The impact of the fluid jet generates a surge, which will spread out radially on horizontal flat beds when the ambient flow velocities are zero. When a trench is refilled, the surge will have predominant directions parallel to the trench axis whereas, when dumping on an embankment, the dominant surge direction will be perpendicular to the axis of the embankment. The front speed of the surge is initially very high and the flow from the impingement zone may be considered to remain supercritical. The thickness of the surge increases with the distance from the impingement zone due to continuous entrainment and, thus, its velocity decreases (continuity reasons) until a hydraulic jump will be formed, after which the flow becomes subcritical and sedimentation will start. The sediment concentration will now rapidly decrease until the phenomenon ceases to exist.

The above described behaviour of the sand is sketched in figure 2.4.10.5; the figures are based on measurements in the Eastern Scheldt (9).To avoid high impact forces and the consequent formation of deep craters, three possible solutions can be given.

1. By selection of a proper sequence of discharge locations, the crater formed by one dumping may be refilled by sedimentation during the following dumping when the distance between subsequent dumpings is about 30-50 m.
2. By discharging the sand through the suction pipe of the hopper with the discharge point

close to the bed. The effective distance to the impingement point will be too short for the outflow to reach supercritical flow conditions.

3. By horizontal discharge in the flow direction of the ambient water, the effective distance to the impingement zone will be very large and, consequently, the flow velocity in the jet at the impingement point will be too low to cause erosion.

The method with the suction pipe yields optimum results when small areas must be heightened, since the impingement zone will be very small compared with the other methods.

The method is, however, much more time-consuming than the first one.
Moreover, the workability under heavy weather conditions is much less for the suction pipe discharge than when hopper doors are used.
Finally, this method can only be applied during slack water.
The third method yields optimum results when the sand must be spread over a wide area and when the occurrence of bed disturbances must be kept within a minimum.

References

1. Vanoni, V.A. (ed) Sedimentation Engineering, ASCE **Manuals and Reports on Engineering Practice,** no. 54, 1975.

2. Speekenbrink H., Bliek A.J., Boon T.J., Svasek J.N., and Wijngaarden N.J. van, Sedimentation in Dredged Trenches, **Hydraulic Aspects of Coastal Structures,** Delft University Press, Delft 1980, pp. 215-235.

3. Alam A.M.Z., and Kennedy J.F., Friction Factors for Flow in Sand-Bed Channels, **Jour.Hydr.Div. ASCE,** HY6, 1969, pp. 1973-1992.

4. Schlichting H., **Boundary Layer Theory,** McGraw Hill 1968.

Figure 2.4.10.5 Sand dumping near the water surface.

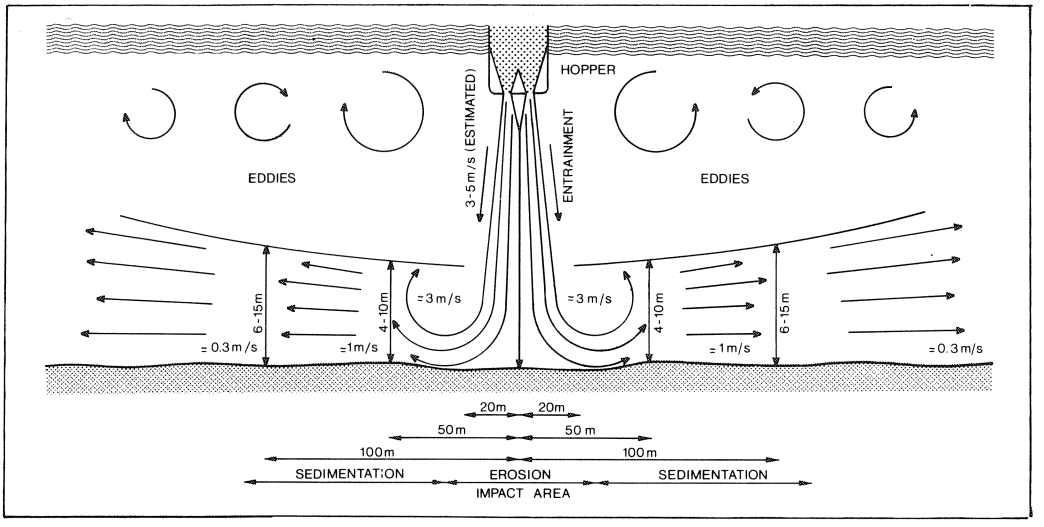

5. Delft Hydraulics Laboratory, **Sand Transport in Suspension,** Report R783-II (in Dutch), 1979.

6. Krone R.B., **Flume Studies of the Transport of Sediment in Estuarial Shoaling Processes,** University of California 1962.

7. Schiller L., Nauman A., Uber die Grundlegenden Berechnungen bei der Schwerkraftbereiting **Z.V.D.I.** Vol. 77, 1933.

8. Abraham G., Jet Diffusion in Stagnant Ambient Fluid, **Delft Hydraulics Laboratory,** publication 29, 1963.

9. Houweninge G. van, Leeuw R. de, Bliek A.J., Davis P., Execution of a Soil Improvement in the Oosterschelde, **Proc. WODCON IX,** Vancouver 1980.

Interaction Water Motion and Closing Elements

K.W. Pilarczyk

2.4.11. Stability of revetments

2.4.11.1. General information

Various types of revetments have been commonly used on sea- and river dikes, dams, sea-walls, breakwaters, banks of navigation channels and other protective works (fig. 2.4.11.1.).
In general, two main types of revetments can be distinguished; namely permeable and impermeable.
The permeable types have a (more or less) „open" surface whereby water may flow into and out of the structure. The impermeable types prevent water from flowing through the structure, so that hydraulic pressures may build up behind it. Such pressure forces are important factors in the design.
The permeable types generally require one or more layers of filter material to retain the soil particles. A granular filter may possibly be replaced by a synthetic filter. However, the need for a filter is only essential in the case of a sand underlayer.
Where permeable revetment-units are placed on clay, the use of a filter can very often be omitted or restricted to a synthetic filter.
The following principal types of permeable revetments can be considered:

- grassmats on a permeable sublayer
- open filter revetments
- stone pitching
- artificial block revetments

and the following impermeable types:

- grassmats on an impermeable clay-layer
- bitumen grouted stone, block or slab revetments
- asphalt revetments.

The design of most of these types of revetments tends still to be based on somewhat unspecific experience rather than on universally valid calculation methods. Very few model or prototype investigations exist, such as there are being chiefly limited to very narrow design conditions.

The problem of revetment stability in relation to current and wave attack is a complex one.
Whilst laboratory investigations provide a means for gaining further understanding of the interaction process between external factors (waves, current, tide etc.) and the protective structure, the solution of many practical coastal engineering problems cannot wait until a complete understanding of these processes has been obtained.
Therefore, however limited the existing knowledge on this subject, it is useful to systematize it and make it available to designers.

In this section a short review of existing knowledge on the design of different types of revetments will be presented. Where possible, the relevant calculation method and literature references will be mentioned.
There will also be some comparison of the different types of revetments with their advantages and disadvantages and suggestions regarding their practical application.

2.4.11.2. Functional requirements(23(b)).

By definition, a revetment is a slope protection designed to protect and stabilize a slope that may be subject to action by water currents and waves. A revetment must therefore be supported at the toe and provided with proper drainage unless it is laid on a slope consisting of an almost non-permeable material such as clay. This is, however, seldom the case in the United States but it happens for example in the Netherlands, Germany and England.
Normally, some settling may be expected and it is therefore important that the revetment be built flexibly to prevent it from being damaged by movements that open up the joints, thereby leaving part of the slope open to direct attack by wave-induced currents. Flexibility of the armour layer is a cardinal point in revetment design. The best block design is one which combines stability, flexibility and durability with hydraulic advantages such as relatively low uprush, little splash and at the same time, adequate drainage.
Stability means that the single block stays in place; flexibility on the other hand, means that a block is able to move independently (to a limited extent) of its neighbours without jamming.

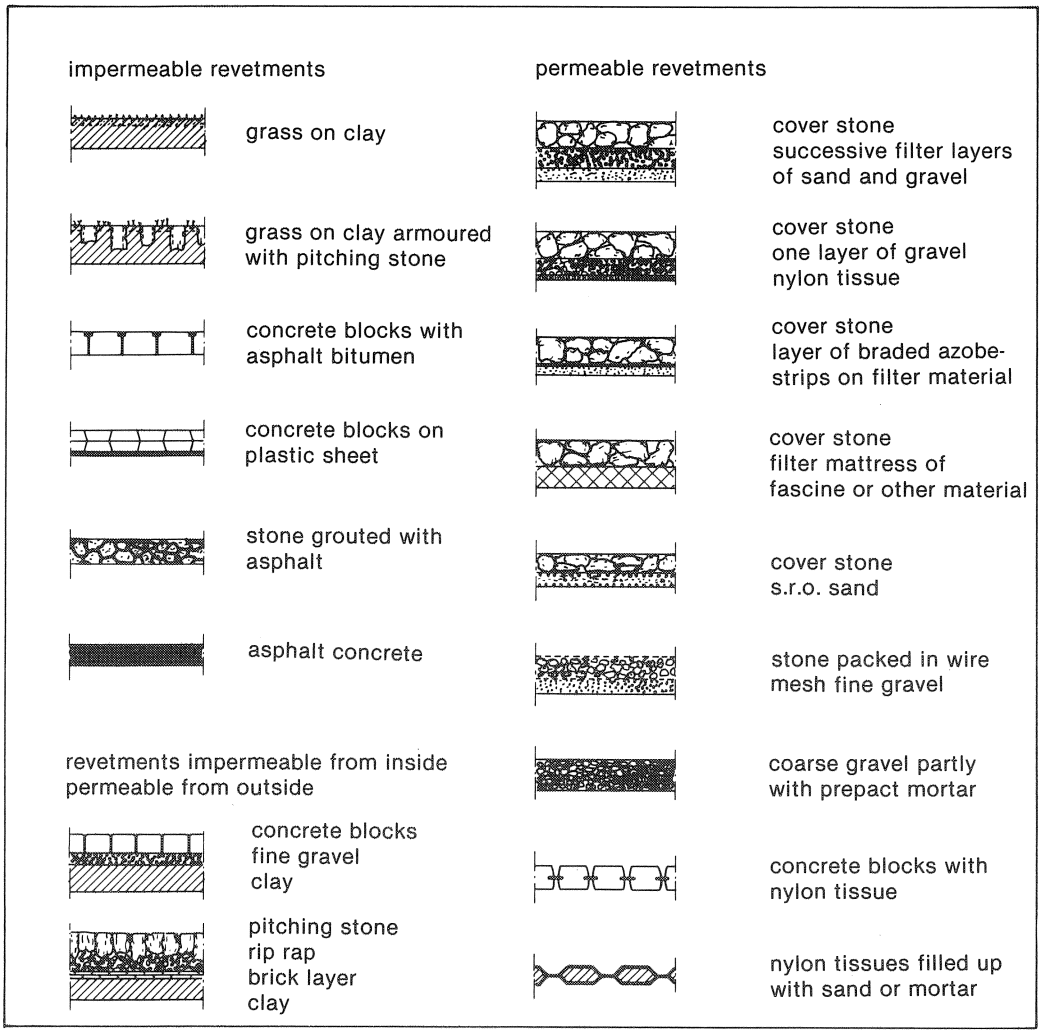

Figure 2.4.11.1 Examples of revetment constructions

Durability deals with the stability of the material itself against weathering of any kind.
Hydraulic aspects include possibilities for decreasing the uprush by friction elements integrated in the block, and draining, which may also be termed the „hydraulic ventilation" of the revetment.
Stability may be considered of primary importance in revetment design. One may distinguish

between external and internal stability. The former refers to the forces that act on the blocks themselves. The latter deals with the conditions of stability of the filter construction supporting the blocks. With respect to external stability, the following forces are involved: (a) Various pressure forces perpendicular to the slope, which may be downward or upward; in the latter case, they may cause lifting of the blocks from the revetment; (b) inertia and drag forces caused by flow parallel or perpendicular to the slope; (c) friction forces between individual blocks and between blocks and the sublayer; (d) forces in joints due to the effect of interlocking.
Because of the complexity of the problem, external stability has to be evaluated primarily by hydraulic model tests. In order to provide practical results, such tests must be based on a variety of realistic wave spectra.

Internal stability may be defined as the stability of the filter underneath the revetment blocks. In the first place, this implies that individual rock or gravel must be stable against hydraulic gradients in the direction of the slope between the blocks and the filter, so that these parts do not move. Next, individual filter material must not be sucked out through the joints by negative pressures. The size of the filter material must therefore be in proper relation to the size of the joints so that loss of filter material is largely or entirely prevented. In addition to the above criteria, which refer to the possibilities of leakage of filter material through the joints, it is also necessary for the original bank or core material below the filter not to move into the pores of the filter and finally to be lost through the joints. This requirement may be met either by selecting the proper ratio between the grains of the core material and the first filter layer or by means of a synthetic filter e.g., a woven plastic sheet to be placed between the core, which could be sand, and the filter construction.
An important aspect for overall stability is the relation between the revetment's armour layer and the condition of the core fill which it is placed upon. While a natural (eroding) slope may be well consolidated, new fill may be loose and must be well compacted to serve as a foundation for a new revetment. In addition, blocks have to be placed accurately which, in turn, means that they must be cast within narrow limits of tolerance.
Even the best design may fail as a result of poor workmanship.
Soil failures on revetments have occurred. A revetment's relation to its „footing" is also very important. A toe failure may prove to be fatal. This raises the question of which type of revetment behaves best when an initial damage occurs.

2.4.11.3. Load and strength aspects

Items which are important for the design of a structure can generally be related to loads on the one hand and to strength on the other hand [9, 63, 65, 66].

The questions concerning loads can be for example:
- What are the loads on the structure?
- Where do these loads occur?
- How do these loads vary in space and time?
- How can these loads be influenced?

as well as the questions concerning strength:
- Which factors influence the strength of the structure?
- How should strength vary along the structure?

Up till now, no generally valid description of this problem has been available. It can, however, be illustrated by the recent results obtained in the context of studies on the stability of blocks revetment [9] carried out by the Delft Hydraulics Laboratory (see figure 2.4.11.2.). The mathematical model developed for this purpose is also described briefly.

Loads and failure mechanisms
When in a wave-attack the run-up has reached its maximum value, the water on the slope starts to flow back due to gravity. During this stage water flows through the joints between the blocks into the filter layer, which may result in an increase of the water level in the filter laying depending inter alia on the permeability of the slope revetment k' and the filter layer k.
When the water on the slope flows back

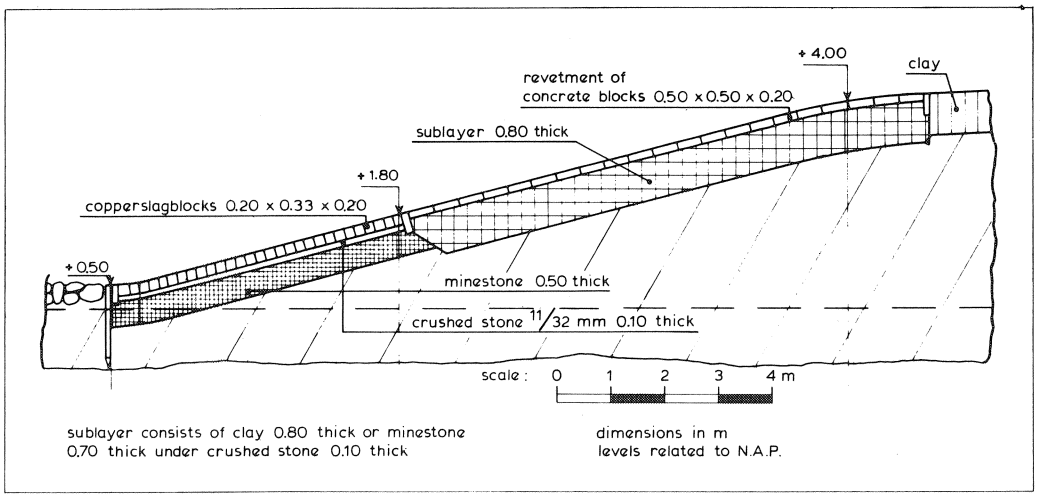

Figure 2.4.11.2 Cross-section Oesterdam.

pressures on the slope decrease. When a rough slope is present this back flow may result in drag forces, inertia forces and lift forces (failure mechanism a, see figure 2.4.11.3.).
Depending on k', k and the geometry, the water in the filter layer cannot follow immediately, which results in uplift pressures against the slope revetment (figure 2.4.11.4.). These uplift pressures may cause failure of the slope revetment (figure 2.4.11.3., failure mechanism b1). In general, wave run-up is larger than wave run-down. Therefore seepage into the dam takes place over a larger surface than seepage out of the dam, resulting in an elevation of the mean phreatic level and the pore pressures within the dam. This is a cumulative effect of a number of waves (mechanism b2, figure 2.4.11.3.).
When the next wave approaches the slope, an increase of pressures on the slope below this wave occurs. These pressures may be transmitted under the slope revetment just in front of the wave front, resulting in uplift pressures (figure 2.4.11.3. mechanism c).
These uplift pressures will be present over a very limited area in front of the wave front(figure 2.4.11.5.). At this stage considerable changes in the velocity field due to the approaching wave also occur (figure 2.4.11.3., mechanism d).

Depending on $\xi = tg\alpha/\sqrt{H/L_o}$ wave breaking may occur. A wave breaking on the slope will have an impact on the slope revetment. This causes a strong increase in pressures on the slope with a duration in the order of 0.1 s. These pressures on the slope may be transmitted under the slope revetment resulting in short duration uplift pressures (mechanism e, figure 2.4.11.3.).

After this short duration phenomenon a mass of water falls on the slope resulting in high pressures on the slope. These high pressures may propagate below the revetment just in front of the place where the wave breaks on the slope, thus resulting in uplift pressures on the revetment (mechanism f, figure 2.4.11.3.).
This phenomenon can be observed in figure 2.4.11.6.
After the wave hits the slope a strong reduction (even ,,negative,, related to atmospheric pres-

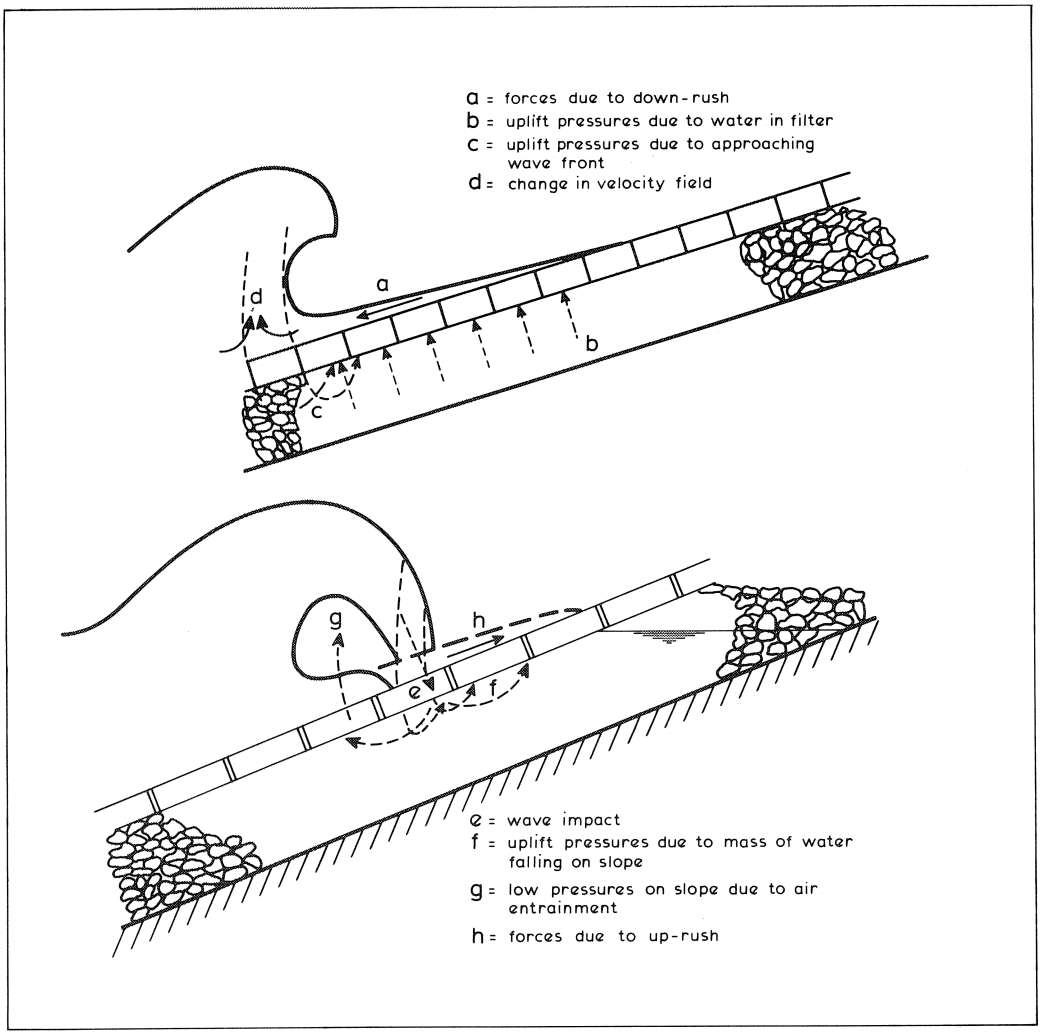

Figure 2.4.11.3 Schematic representation of failure mechanisms of slope revetment.

sures) of pressures in the slope may occur during a period in the order of 0.1 s. This phenomenon has been explained as being a result of oscillations of the air pocket entrapped in the breaking wave. These low pressure on the slope may cause failure (mechanism g, figure 2.4.11.3). This phenomenon was measured in the model tests and can be seen in figure 2.4.11.7.

After wave breaking, wave run-up occurs. During

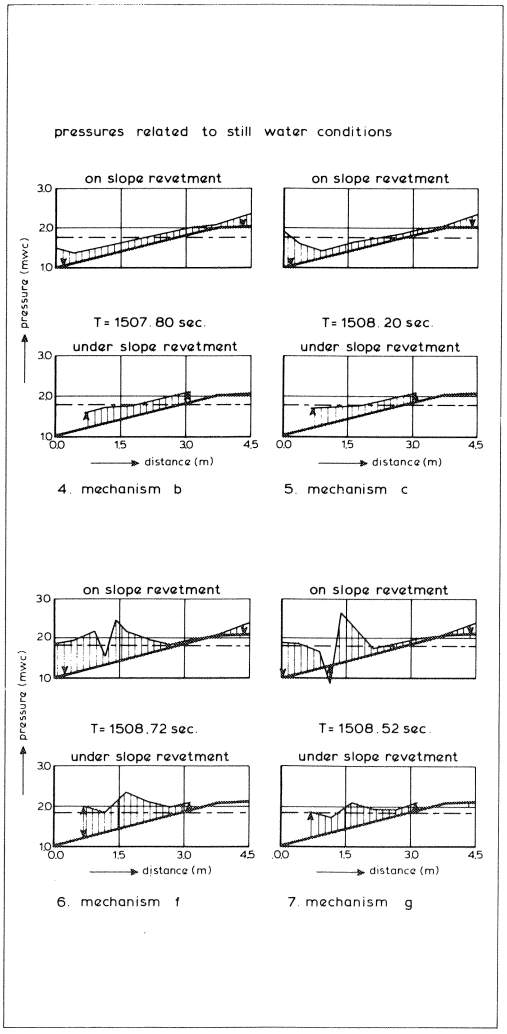

Figure 2.4.11.4-7 Pressure distributions.

this stage pressures on the slope revetment increase. At this stage no critical conditions are present, except when the slope is not smooth or when blocks have been raised, resulting in drag forces, inertia forces and lift forces (mechanism h, figure 2.4.11.3).
It should be noted that combinations of failure mechanism may occur.

Strength of the slope revetment

a) General considerations.

A slope revetment consisting of loose blocks derives its strength from the mass of each individual block. Friction between individual blocks increases the strength of the slope revetment.
Other factors also may contribute to the strength of a slope revetment, e.g. interlocking between blocks, clenching of the blocks, etc.

A slope revetment may also derive its strength from the sublayer. In the aforementioned study [9, 63c], for example, use of a sublayer of clay resulted in a stronger slope revetment than was the case with a sublayer of crushed stones.
When the strength of a slope revetment increases, other parts of the structure may become the weakest link, e.g. a sublayer or a transition between sublayers. For example when erosion of the clay occurs, the strength of the slope revetment decreases. In this case therefore, the strength of the clay (i.e. resistance against erosion) is the weakest link.

b) mathematical model.

A mathematical model has been developed for the calculation of pore pressures in the layer underneath the blocks. This model can cope with all quasi-static phenomena described in the previous section. The model is based on the solution of the equation for groundwater flow in the layer underneath the blocks, with leach terms to include the seepage through the revetment. The variation of the phreatic line within the dam is included by a simultaneous solution of the mass balance equation for the flow to and from the phreatic surface.
The use of a finite difference code creates the possibility of a realistic representation of the revetment as an alternation of blocks and joints.

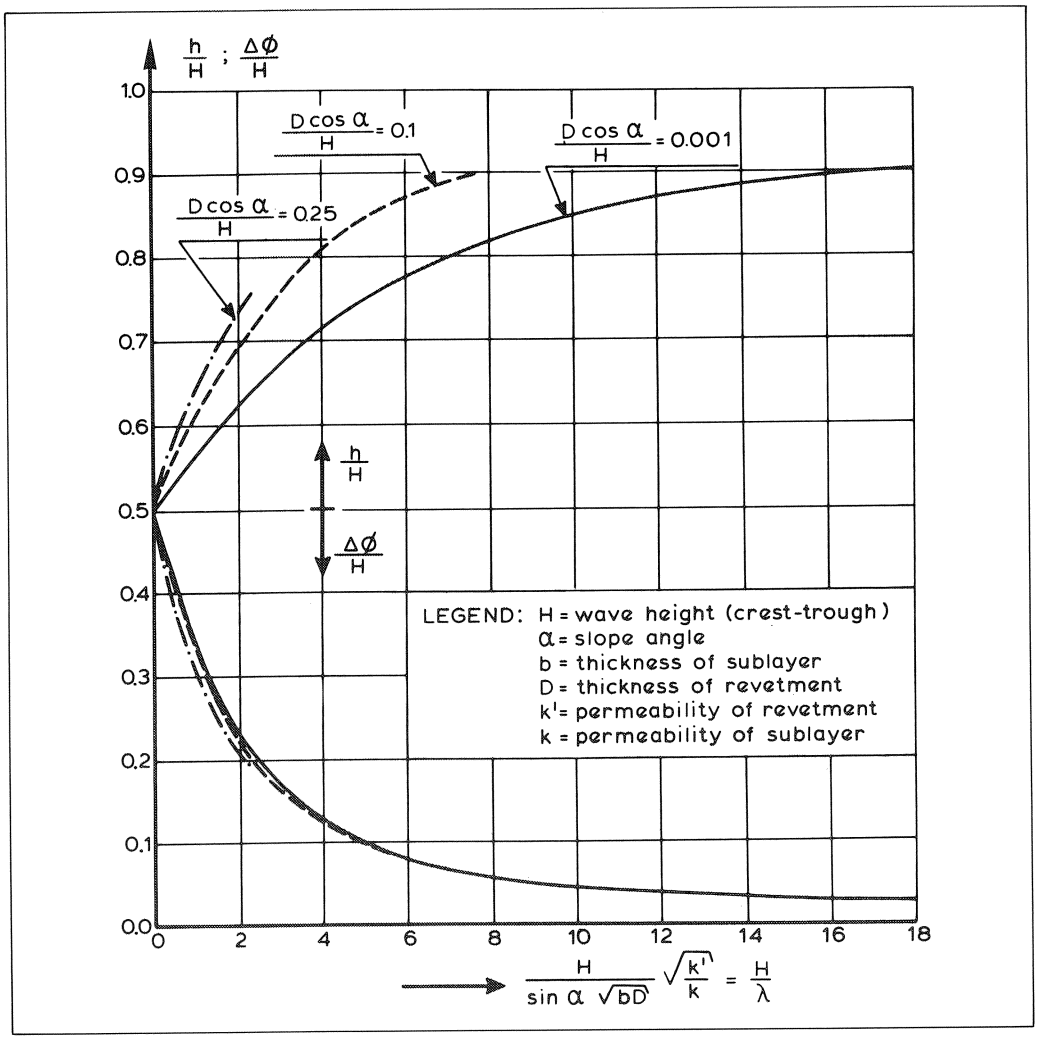

Figure 2.4.11.8 Elevation of phreatic line in sublayer (h) and lift forces on revetment (△φ) as function of leach length (λ). Sinusoidal waves (no run-up and run-down)

The permeability may be a function of the local gradient, thus allowing for turbulent or semi-turbulent flow. Formulae for flow in narrow joints were derived from special permeability tests.

The geometry of the dam may be rather arbitrary; a succession of different slopes is possible. The hydraulic boundary conditions may also be arbitrary, e.g. it is possible to use a tape with

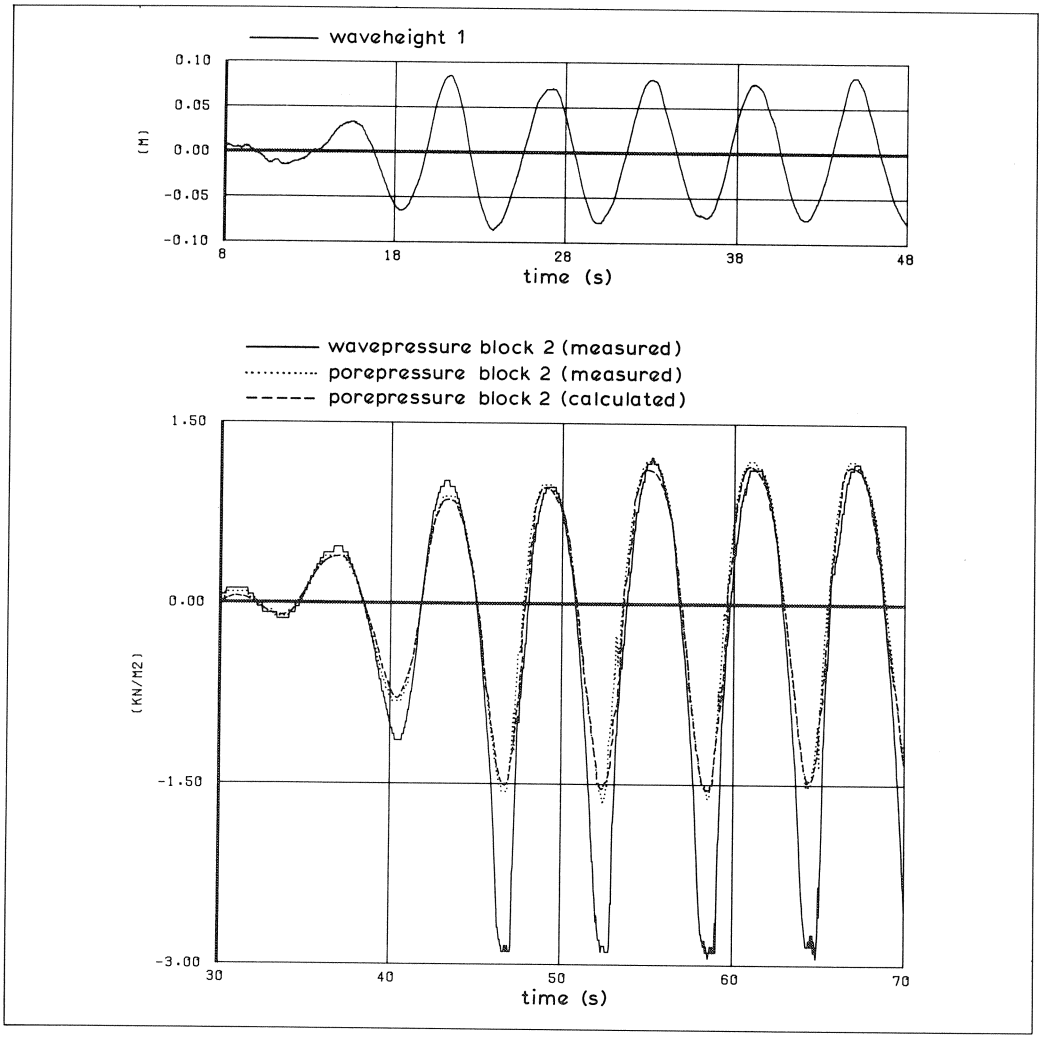

Figure 2.4.11.9 Comparison of measured and calculated pore pressure in sublayer (numerical model).

measured wave pressures as input for the programme.
The programme calculates both pore pressures and the phreatic level as a function of time and place. The following conclusions could be derived from the calculation study:

a. The risk of damage decreases as:
   - the revetment is more pervious

- the underlying (filter) layer is less pervious or thinner (or even completely absent).

b. The elevation of the mean level of the phreatic surface above its original position increases as the revetment is more pervious; however, the pore pressures are smaller in that case.

c. An important number for the determination of the quasi-static pressures underneath the revetment is the leach length, defined as:

$$\lambda = \sin \alpha \sqrt{bD \frac{k}{k'}}$$

where:

α = the slope of the dam
b = thickness of the (filter) layer underneath the revetment
D = thickness of the revetment
k' = permeability of the revetment
k = permeability of the filter layer

In figure 2.4.11.8 a pressure-difference curve is given, which was derived from the first analytical version of the calculation method. This curve is based on a horizontal free water surface, which varies sinusoidally in time.

The more recent numerical version of the calculation method can be applied for practical calculations (see figure 2.4.11.9). In this figure the measured pore pressure in the sublayer is given by a dotted line and the calculated pore pressure by a dashed line.

Further the wave pressure on top of the instrumented block is given (full line) which clearly deviates from the pore pressures in the sublayer. In this calculation the measured wave pressures were fed into the computer programme. Comparison with the measured wave height (upper figure) also shows that the elevation of the mean pore pressure caused by cumulative wave action (mechanism b2) is calculated quite well. Moreover the calculated values were compared with the results of an electric analogy study. Also in this case the agreement was good. This mathematical model might become an important tool in the design of revetments of dams and dikes.

2.4.11.4. Additional information regarding riprap revetments

There has been an increasing need for reliable information on the stability of riprap exposed to wave action. This need arises partly from an increase in the number and size of earth dams which must be protected from wave attack and partly from increased construction in coastal areas.
For countries with their own sources of stone, dumped quarrystone is usually the cheapest material per tonne which can be used for revetments exposed to waves. However, dumped stone has lower stability per unit weight to wave attack than most concrete armour units.
Because of these characteristics, dumped quarrystone can serve as a reference by which the stability and cost of other revetments may be judged.

The stability criteria of riprap against wave attack were examined in the previous section. This section, therefore, only provides some additional information regarding possible measures for increasing riprap stability and the influence of ship-waves.

Measures for increasing stability of riprap.
A riprap (also called 'open filter') revetment consists of several layers of filter material of different size covered by one or more layers of rock or rubble (thickness mostly 1.5 to 2 times the median diameter). Filter characteristics are determined by the fineness of the subsoil on the one hand and by the wave forces on the structure on the other.
However, the design criteria for filter revetments depend strongly on the hydraulic gradients induced by external loads (i.e.waves and currents)(43).
The weight of the individual rock or rubble forming the top layer has to be in accordance with the anticipated wave forces.
When rubble mounds, including artificial rubble, are placed „at random" no actual attempt is made to make them cooperate in resisting the forces to which they are subjected. They are instead supposed to support each other in all directions at random or incidentally by the

geometry they have. However, special measures may be taken in order to increase riprap stability, as shown below.

An analysis of several armour-stone gradation curves showed that stones with a diameter exceeded by 25% of the stones had a weight approximately 30% more than stones with a diameter exceeded by 50% of the stones. By selecting the larger stones for the top layer a factor of 1.3 could therefore be applied to K_D in Hudson's formula when computing stone weight based on the 50% stone size.
The practical application was demonstrated by Kirby et al.[30] for construction of a jetty where the supply of stones was limited in time. Since each stone had to be placed individually, it was possible to select the larger stones and place them in the outer surface of the armour layer.
McCartney and Ahrens [35] have done large-scale tests regarding revetment stability to wave attack for a single-stone-diameter- thick armour overlay.
The general conclusion of this investigation was that a one-layer stone overlay greatly improves riprap stability and can be useful for upgrading smaller existing riprap slope protections or as a cost-effective initial design. A 100-percent stone overlay coverage gives about the same stability, N_{ZD}, as a conventional two-layer armour stone thickness. However the reserve stability of an overlay is about half that, of the two layer system. This means that when the zero damage height is exceeded damage to the underlayer takes place earlier.

Another improvement of the stability of a riprap protection can be achieved by placing some of the largest stones as binders perpendicularly to the slope (fig. 2.4.11.10), [38]. Some of the stones may stick somewhat irregularly out of the „theoretical surface" but this will reduce uprush.In the case of placing the longest sides perpendicular to the slope the increase of stability can be roughly estimated by replacing D_n by the average longest side in the zero-damage stability number, N_{ZD}.
The efficiency of the latter method is supported by a small and large-scale model investigation done by Sollitt and De Bok [42].

In this case, the stability of placed quarry stones (if defined by N_{ZD}) was about twice the normal riprap stability of the same unit weight. However, in this case one should speak rather of stone pitching than of riprap (see figure 2.4.11.10 e).
A very traditional type of stone pitching (especially in the Netherlands) is the natural basalt prism revetment placed on a filter construction. Because of the lower porosity of the top layer (~ 15%) the filter requirements are somewhat less exacting than in the case of riprap. The stability number N_{ZD} is a function of ξ with the lowest value of about 4 for ξ = 2 to 3 and ctgα > 2. In order to increase the strength of the construction small sharp stones may be keyed in between the prisms. However, the best way substantially to increase the strength is to grout the prisms with graded crushed stones or copper (or phosphorous) slag as usually done in the Netherlands. Because of the high cost and shortage of natural basalt, an artificial concrete basalt-block (patented as „Basalton") has been developed in the Netherlands whose performance (if grouted) is even better than natural blocks (see fig. 2.4.11.10f). Recently full-scale tests have been performed on this type of revetment in the large Delta-Flume of the Delft Hydraulics Laboratory [64].
Due to the grouting the strength of the construction can increase up to $H/\triangle D \sim 15$ (see figure 2.4.11.13). With such strong slope revetments the stability of the filter layer may be more critical.

Influence of ship induced load on riprap stability.
Not only the load due to wind-waves but also the load induced by ship movement (waves and currents) is of major importance (fig.2.4.11.11). Design criteria concerning this aspect are very scarce in designing the bank protection of navigation channels and harbour entrances. However, with respect to inland vessels, systematic model and prototype research on this subject is being carried out by the Delft Hydraulics Laboratory [61]. For the stability of the upper part of a bank protection in the case of vessels sailing close to the bank, the load due to the transverse stern-wave (following the draw-

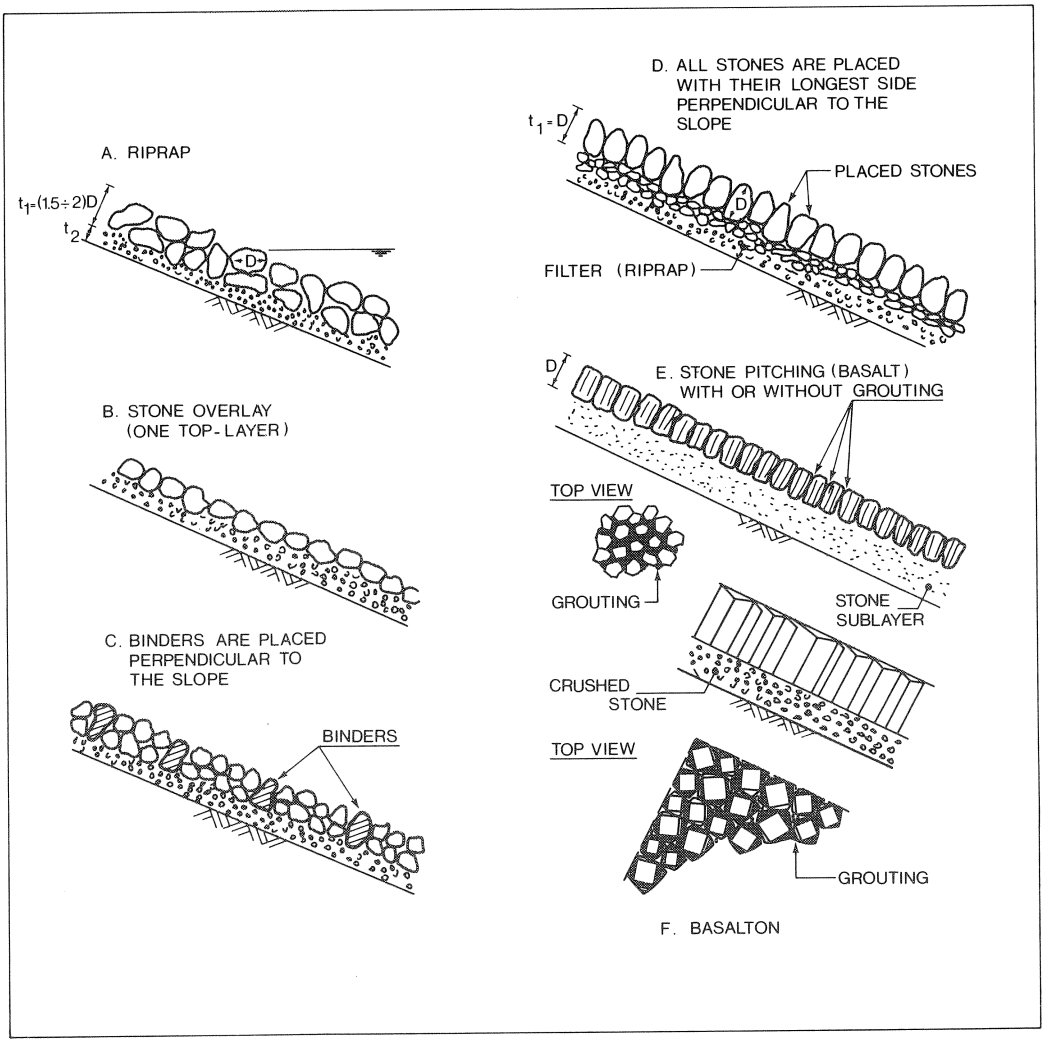

Figure 2.4.11.10 Riprap design and improving measures.

down of the water level) is generally of major importance. The stability parameter for this case, and of two-barge pushtow-units, as determined from a small-scale investigation (scale 1:10), for a slope 1:4 is equal to, [61,b].

$$\frac{Z_{max}}{\Delta D_{50}} = 2.3 \text{ or } \left(\frac{Z_{max}}{\Delta D_n} \simeq 2.75\right)$$

where Z_{max} is the height of the transverse stern-

wave (in first approximation equal to the maximum drawdown of the water level due to the passing of a ship), and $D_{50\%}$ and D_n are the characteristic stone diameters. This result is also supported by prototype observations. In the case of the stern-wave, the wave period is very long (each wave can be treated as an individual one), and its influence can therefore be ignored. In general, it can be said that the application of

Figure 2.4.11.11 Survey of phenomena around a ship in a channel.

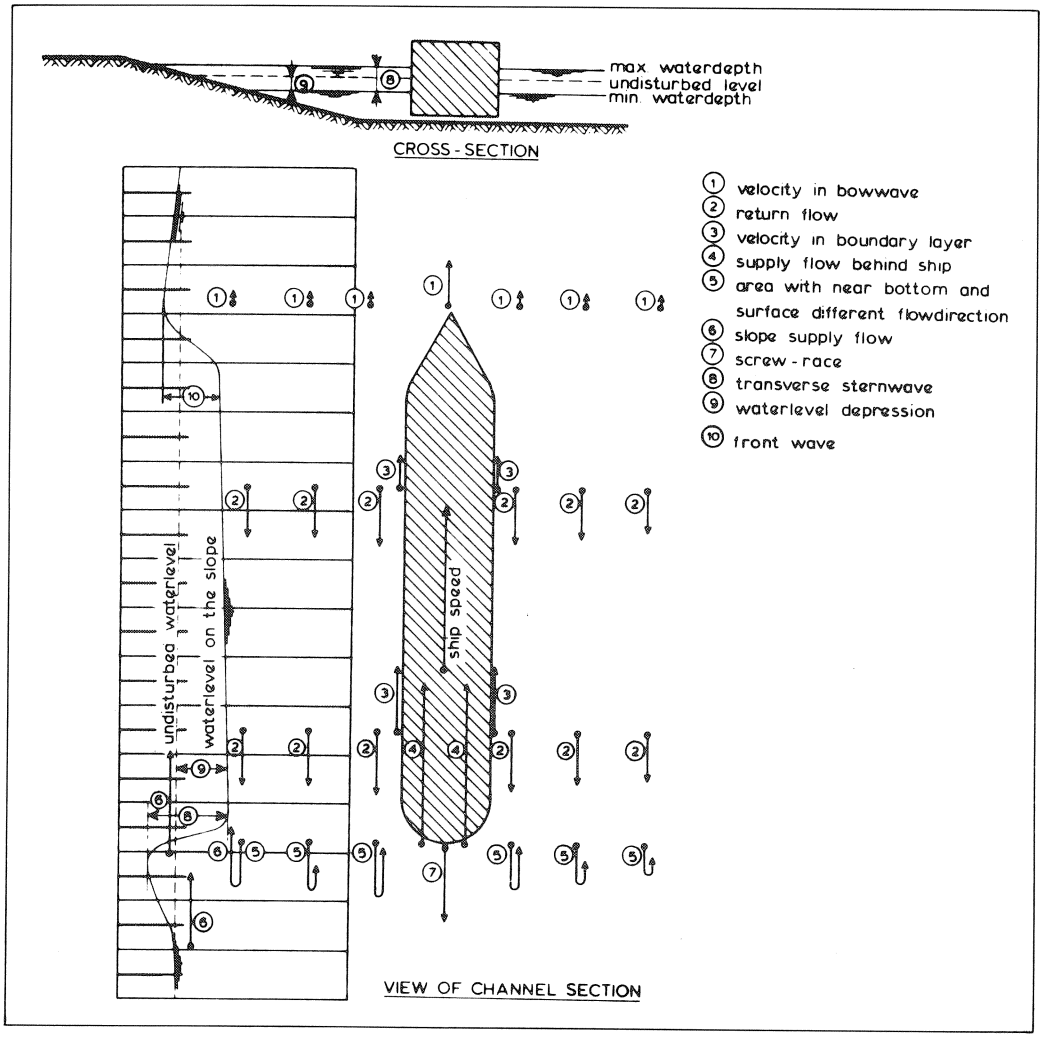

wind-wave stability criteria to ship-wave action leads to design overestimation (i.e. a greater safety margin).
The lower part of the bank protection of navigation channels is designed according to the combination of the natural currents in the channel and the return flow due to the passing of a ship. This generally leads to lighter protection measures than on the upper part.
Detailed analysis of design procedure for bank protection of navigation channels subject to waves and currents induced by ships may be found in [6, 8, 11, 18, 43, 61].

2.4.11.5. Block revetments.

Continued demand for relatively low-cost shore protection in estuaries and along the coasts has stimulated investigations into this subject. The reason for this has been, the increasing problems with respect to the defence of the coasts, harbours and banks of navigation channels and, the high cost and shortage of natural materials. This demand has resulted, inter alia, in the rapid development of artificial block revetments (see figure 2.4.11.12).
At the same time the quality of concrete blocks has been gradually improving with improvements in the manufacturing process, while the cost has diminished as the result of mechanical placing, so that concrete blocks of various shapes and sizes are at present being satisfactorily used for coastal protection and the protection of navigation channel banks under a variety of conditions.
Many different kinds of revetment blocks have been used.
These blocks are often provided with various kinds of joint arrangements, which include shiplaps, wedge-formed laps, single or double wedges for asphalt-filling, etc., or flexible joints by means of another (finer) material (grouting). Both these arrangements have their advantages and disadvantages.
With respect to artificial block revetments (concrete or copper-slag blocks, etc.) a distinction can be drawn between:

a) free blocks of different design
b) flexible interlocking blocks of different design
c) interlocked blocks of different design

All these blocks may be with or without roughness elements of different shape (→ reduction of run-up).
In all these cases, the type of sublayer (permeable/impermeable) and the grade of permeability of the blocks are very important factors for the stability of these blocks.
Concrete blocks are frequently used for the revetments of dikes, dams and banks in Holland and other European countries and in the United States. In general, no reliable design criteria are as yet available for this kind of construction. The design of the block-revetment was generally based upon experience in nature, sometimes supported by small scale- and in a few more recent cases large scale model investigations. However, as demonstrated by large scale tests in the USA and Holland [62,63] the reliability of the small scale model results is questionable, the main reason being the problem of scaling the sublayer and air entrainment in breakers.

On the other hand, the available data from investigations in the USA (mainly regarding interlocking blocks) and recent systematic research in Holland (on free blocks and flexible interlocked blocks, fig. 2.4.11.13), and some data from other countries (e.g. England, Norway, Germany) permit a preliminary attempt at defining the stability criteria. Most of these results are summarized by McCartney in [34].

Free block revetment
Rectangular blocks
This type of block is different from others in that only surface friction forces between individual blocks and between blocks and the sublayer are present (fig. 2.4.11.12a). The blocks are pushed together and there are only small joints between the blocks (mostly 1 to 2 mm).Moreover, in most cases, the joints are quickly filled up by silt and fine sand. Thus, the permeability of such a revetment is very low and there is a real danger of a build-up of pressure underneath the armour layer in the case of a permeable sublayer. This type of revetment has lower stability than those made with other block types (i.e. interlocked blocks) but, on the other hand, it is still more stable than riprap and is probably the cheapest

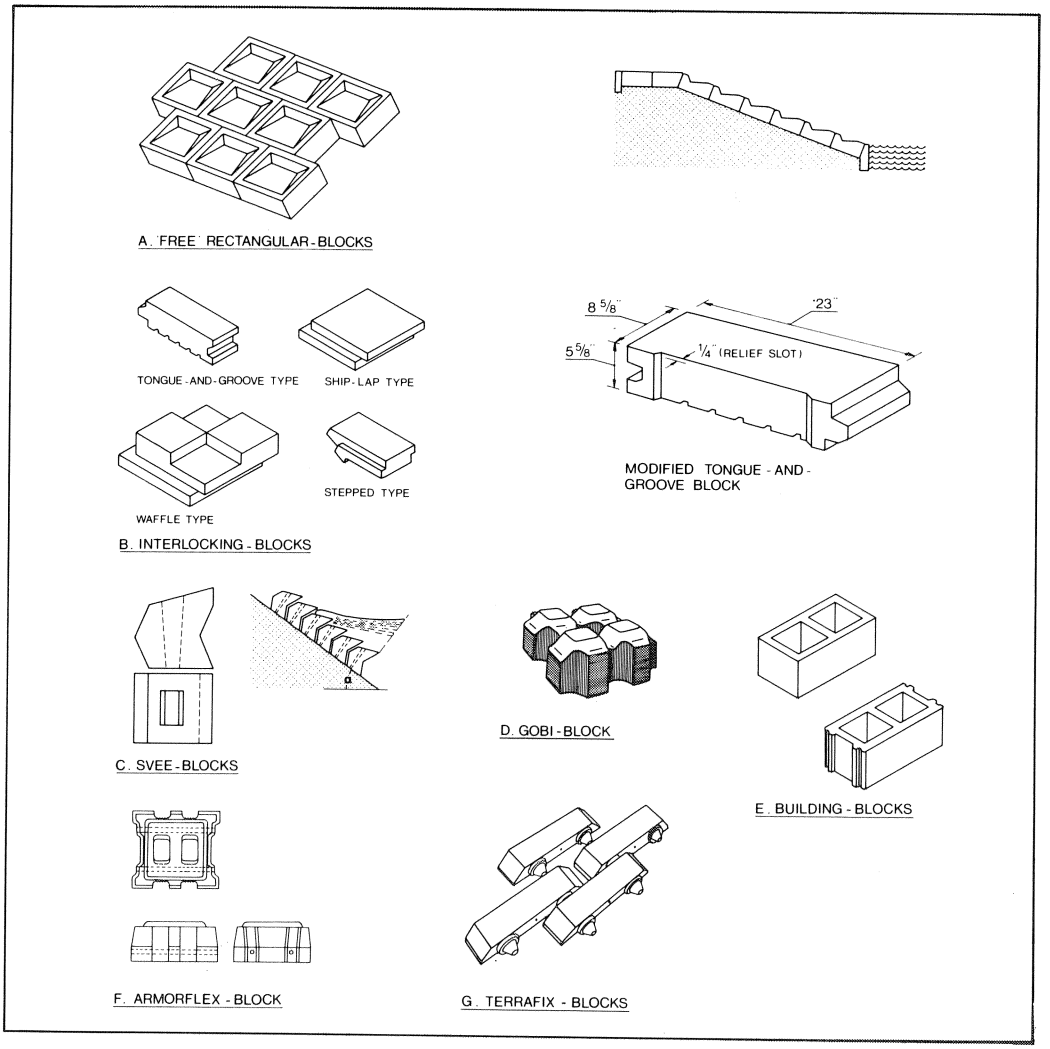

Figure 2.4.11.12 Examples of revetment-blocks

and most easily handled (i.e. easy mechanical placing) revetment. Its stability can be greatly improved by placing it on an impermeable sublayer (i.e. a clay-layer) or by increasing the permeability of the blocks. The filter requirements are the same as those for stone pitching: the size of the gravel (crushed stone) should be small enough to prevent washout of soil particles from underneath and large enough

not to pass through the joints between the blocks; a layer of 15-20 cm of graded gravel or fine crushed stone (1-50 mm) is usually sufficient. It is also possible to place these blocks on a sand-body, protected by a synthetic filtermat with or without a thin layer of crushed stone or gravel. In the latter case, the stability of the sandy-sublayer becomes more critical.
The stability of a free-block revetment depends mainly on the block thickness (D). The stability increases as the permeability of the blocks increases, and the thickness of the permeable sublayer decreases. However, this can be treated as a secondary improvement because of the practical limitations in filter thickness and composition(i.e. filter requirements regarding protection of the soil and inaccuracy of execution).
Large scale tests with regular waves and a 1:3 slope (63) revealed that the stability function for block revetments, related to the wave period, is similar to that for riprap. However, the minimum stability seems place at a lower value of the surf similarity parameter (ξ).

Some results of the large scale tests with irregular waves are presented in figure 2.4.11.13. The minimum stability number for this kind of block revetment can be taken roughly as $H/\triangle D = 2.5$ for $ctg\alpha > 2$. For H, the significant wave height H_s can be used.
These tests have shown that effective low-cost shore protection can be designed utilizing these rectangular units even if they are placed on a permeable sublayer. However, the stability of this block revetment can be greatly improved if there is an impermeable sublayer (clay-layer).

Clay as sublayer
In certain instances, concrete blocks can be placed on a layer of clay (without filter). In the Netherlands it is even obligatory to use clay as a sublayer for the protection of the sea-dikes (with or without a stone layer in between). This requirement was born in the past when no design criteria were available and clay as a sublayer was treated as a secondary defence when failure of the protective layer occurred.
This system requires accurate setting-out and precise dimensions of the blocks so that washout of clay particles through the joints does not occur. If such a revetment is frequently attacked by waves, some washout from underneath the blocks may be experienced. This occurs when clay quality is poor, i.e. if it contains only a small percentage of silt (less than 30%) or is not homogeneous (i.e. sand-lenses are present).
The large scale tests (scale 1 in 2) with regular and irregular waves done by the Delft Hydraulics Laboratory for the slope protection (1 in 4) of the Oesterdam (one of the secondary dams in the Eastern Scheldt in the Netherlands), have shown that rectangular blocks placed directly on clay form a very strong revetment [63c]. When there was good quality clay and no erosion of the sublayer it was impossible to create damage conditions within the range of possibilities of the wave generator (slope 1 in 4, blocks 25x25 cm 10 and 15 cm thick, max. $H_s = 2.0$ m - small spectrum).
The minimum stability number for this kind of revetment and good quality clay can be taken roughly as

$$\frac{H_s}{\triangle D} = 7 \text{ for } ctg\alpha \geq 3$$

(D = block thickness and $\triangle$ = relative density of block)

However, at the present state of our knowledge on this matter (especially regarding the performance of clay), it is not advisable to use a stability number higher than 6.

When the blocks are placed on a permeable sublayer, the exceedance of zero-damage wave height leads directly to great damage (whole sections of a revetment can be lifted out). If clay is used as the sublayer, the design will never be the same as for ideal clay. Therefore some reserve will always be involved. The damage will then be restricted to individual blocks (or a few of them) where erosion has taken place because of nonhomogenity of the clay.
A simple method of diminishing the chance of damage to a revetment on clay seems to be to equip the blocks with a small edge, a few centimeters in height, all round their lower edge. By

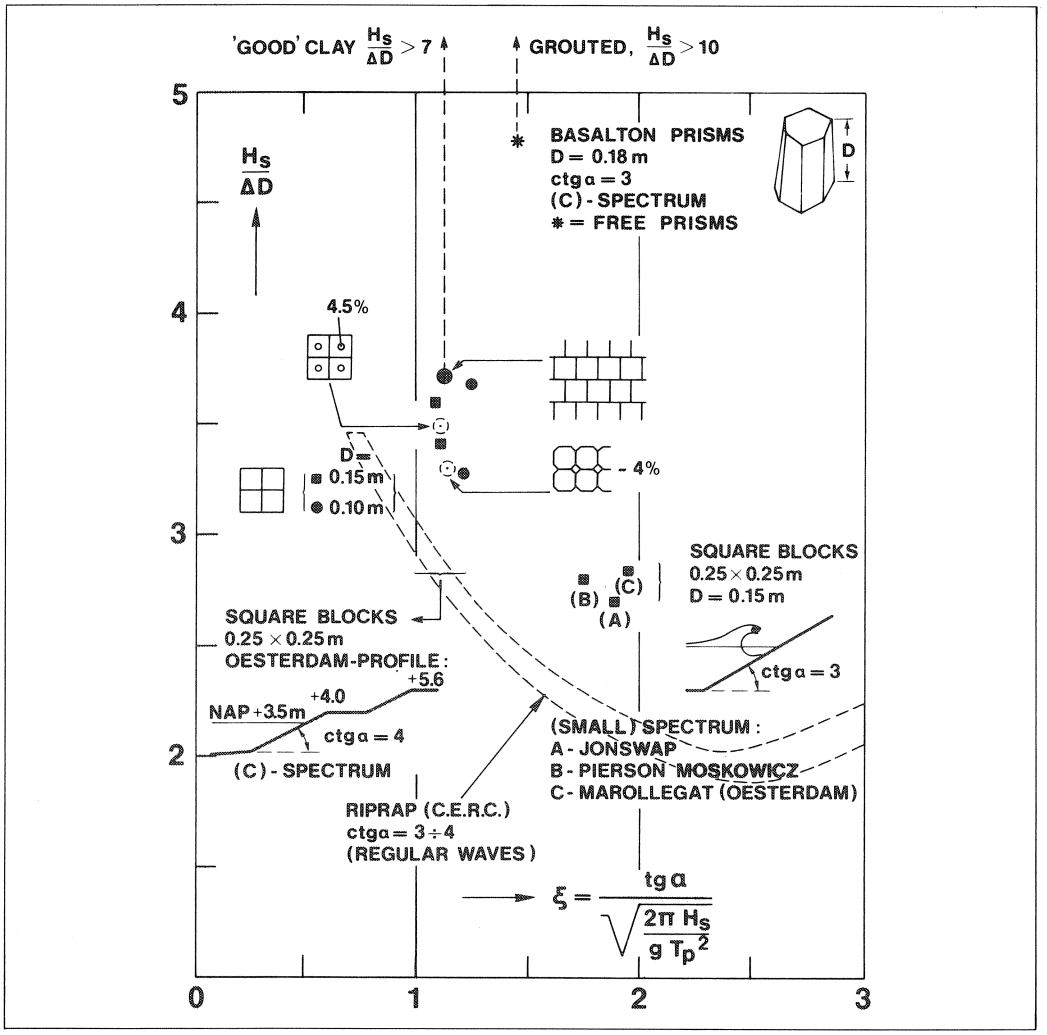

Figure 2.4.11.13 Stability numbers for block-revetments.

pushing the blocks into the clay, the area under the block will in most cases be sufficiently protected against erosion except, of course, when there is very high nonhomogenity. However, in this case, visual inspection during the execution of the work must be sufficient to detect this and to take the proper measures. Besides the requirement of good clay a very important execution requirement is the smoothing of the slope

before the placing of the blocks. If the blocks are to perform properly, they must adhere to the clay without the presence of too many interstices and cavities.

Gobi blocks
Gobi blocks are small, cellular unreinforced concrete blocks, mostly about 20x20cm and 10 cm high, which can be used as revetment units to protect against moderate wave action and as channel linings to resist erosion due to flow.
Two types of blocks are manufactured: one with straight (fig. 2.4.11.12d) and one with bevelled sides.
Straight-sided blocks are placed individually on filter cloth at a desired site. Bevel-side blocks are usually glued to a plastic filter at the factory and shipped to the site as a mat. These types of blocks have been extensively tested, on a small scale at the Delft Hydraulics Laboratory [31] and at prototype scale in a large wave tank at C.E.R.C., U.S.A. [33]. The large-scale tests were performed on a slope of 1 in 3.5 and with regular waves only.

The stability is a function of wave period (or ξ) with the minimum roughly equal to

$$\frac{H}{\Delta D} \simeq 3.5 \quad \text{(straight-sided blocks, } \operatorname{ctg}\alpha = 3.5\text{)}$$

The stability of blocks grouted with gravel is about 25% higher. The large wave tank tests showed that reserve stability comparable to dumped-stone riprap was clearly lacking in the Gobi block revetment. However, the use of gravel as dry mortar could retard the normally rapid deterioration of the revetment after the first block was removed.

Similar results have been obtained with cellular concrete building blocks (see figure 2.4.11.12e). Based on the large wave tank tests at C.E.R.C. [22], the minimum stability number can be roughly estimated as equal to:

$$\frac{H}{\Delta D} \simeq 4.5 \quad \text{(based on } \operatorname{ctg}\alpha = 5\text{)}$$

The weakest point during the tests with these revetments was the stability of the toe of the shallow foundation. In such cases, the strengthening of the toe can be achieved either by burying the toe or extending it into deeper water.

For whole building blocks of different dimensions, the stability number can be estimated using the data presented for the rectangular blocks.

Flexible interlocked block revetment.

Armorflex block slope protection mats.
The Armorflex block-mat system should be seen as the next step in developing the principles at the basis of the Gobi block mat system.

The interlocking Armorflex blocks of special shape (fig. 2.4.11.12F) are threaded with steel or nylon cables and bound together, thus forming a flexible and structurally integrated mat system. A filter cloth and/or graded filter is first spread over the slope to be protected, and the block-mat then overlaid. For structures with steep slopes, helix type corrosion resistant anchors are installed at the top of the slope to provide additional stability. Additionally, grouting material may be applied to the inter-block spaces to rigidify the mat once it is in place. Armorflex is placed by conventional construction equipment directly on the prepared subgrade of the structure as a system of factory pre-assembled mats.
Because of cabling, this system maintains its integrity in the event of subgrade deformation or severe dynamic loading upon a given exceedance of the design conditions. However, the latter also has a fundamental drawback, namely, the problem of repair in the case of erosion of the sublayer. Another weak point is the connecting of the mats lying next to each other.
The Armorflex block-mat system has been extensively investigated in a small scale model (scale 1 in 10) with respect to wave and current attack [55].
Because of the scale tested, the absolute reliability of these small scale results is difficult to judge. However, some indicative large scale tests on this block-system done by the Delft Hydraulics Laboratory[65] have shown that the minimum stability number can be taken as equal to

$\frac{H_s}{\Delta D} \simeq 5.8$ for $ctg\alpha \geq 3$

(cellular blocks on permeable sublayer)

However, due to the relatively large cell-dimensions, instability of the filter layer and/or sandy sublayer may take place earlier than that of the armour-layer. The proper design of the filter is thus of major importance. Grouting of these mats somewhat increases the stability, which can be treated as an extra stability reserve.

Basalton blocks (concrete prisms).
The excellent experience in the past with natural basalt revetment (stone pitching) on one hand and the high cost and shortage of natural basalt on the other, has resulted in the development in the Netherlands of artificial concrete prisms based on the shape of the natural blocks.
This system is characterized by a polygon connection and consists of various shapes of prisms of different weights which allow even a random-shaped revetment to be made (see Fig.2.4.11.10F). The blocks are produced in various heights and with various densities. The area of the inter-block space is equal to about 20% of the total surface area. The blocks are slighty tapered vertically (about 2 mm over the height around the block) so that the underneath surface is slightly larger than the upper area.
Because of this, the prisms may sink lower if there is any settlement in the soil-body or erosion of the sublayer, which is immediately evident. Moreover, because of this tapered shape, the prisms have a firm position in the slope and, after grouting the interstices between the blocks with, for example graded broken stone, silex or copper-slag (size 1-50 mm), the possibility of upward movement of the blocks is strongly reduced. Some mechanical tests gave an indication that the force needed to pull the block out from the grouted system is equal to at least 20 times the weight of the block. In common Dutch practice, the underlayer consists mainly of graded broken stone or silex-stone (a waste product of the cement industry) of 0-60mm and about 30cm thick. It is also possible to place basalton blocks on sand-soil with a filter cloth and ungraded stone in between.

The large scale tests in the Delta-flume of the Delft Hydraulics Laboratory [64] confirmed the positive practical experiences with this kind of revetment.
The tests were done on a 1 : 3 slope (mainly with grouted blocks) with regular and irregular waves. Some limited tests were also done on an ungrouted revetment. The critical stability number for free blocks was equal to

$\frac{H_s}{\Delta D} \simeq 4.8$ for $\xi = 1.45$

The grouted slope, with 15 cm thick blocks ($\triangle$ = 1.15), was tested with irregular waves (up to H_s = 1.8m) and with regular waves up to H = 2.6m. In all these cases, no instability in the revetment was observed. This means that the stability number for this type of revetment is

$\frac{H_s}{\Delta D} \geq 10$ or $\frac{H}{\Delta D} \geq 15$

However, with such strong slope revetments the stability of the filter layer may be more critical. The washing-out of the grouting material was, on average, restricted to a few centimetres in depth. In the first approximation, it could be expected that the maximum scour depth would be approximately equal to the dimension of the inter-block space.
Because the inter-block space varies very little with the height of the block, the relative depth of washing-out (scour depth related to block height) increases with a decrease in block height. This means that, despite the high stability value, the height of the block must not be less than about 10 cm to retain its stability performance.

Interlocking block revetment
The use of „rigid" interlocking concrete blocks is not a new concept for the improvement of the stability of revetments. They have been used extensively for some time in Europe and, more recently, in the United States. Typical blocks are generally rectangular slabs with ship-lap type interlocking joints. The later development of this type of block has resulted in a step-type interlocking block [28]. Another common group of interlocked blocks are blocks with a „rigid" tongue-and-groove connection (mechanical in-

terlocking); the tongue-and-groove connection can be wedged, bull-nosed, or circular in shape. However, the stability of any revetment constructed with a tongue-and-groove connection would depend on the strength and durability of the mechanical interlock because the block would not be stable by its weight alone. Some of these blocks are shown in figure 2.4.11.12B.
The stability of ship-lap blocks and bull-nosed tongue-and-groove blocks was investigated in the large wave tank with regular waves at the Coastal Engineering Research Center (C.E.R.C.), [23]. The step-type blocks, both with vertical and inclined face, were investigated by C.E.R.C. on a scale of 1 in 10 only [28]. The wedged-connection was applied in SVEE-blocks which were extensively tested on a small scale in Norway [46]. Only the results of the large scale tests (C.E.R.C.) will be discussed in detail below.

Ship-lap and tongue-and-groove blocks.
These two types of blocks were investigated on a slope of 1 : 2 [23]; one was a hand-produced ship-lap type weighing 68 kg (thickness 6" = 15.24 cm) and the other a machine-produced bull-nosed tongue-and-groove type weighing 34 kg (thickness 5 5/8" = 14.29 cm).
The embankment was composed of sand with a medium diameter of 0.4 mm covered by a filter cloth and a 15 cm layer of crushed stone with a medium diameter of about 12 mm.
As a result of these tests some improvements have been made in the design of the tongue-and-groove block. The relief slot (area), roughly equivalent to that provided by the spacers used in the test, was provided by depressing one side of each block by quarter of an inch (~ 6 mm) over about two-thirds the length of the block to reduce the uplift pressure. Observations made during the tests indicated that more flexibility should be built into the interlocking joint between blocks to prevent a rupture of the tongue or lips of the groove. In order to provide this flexibility, the shape of the tongue-and-groove was modified to provide a spur-gear type of mesh. The block as modified is shown in figure 2.4.11.12B.

After modifcation, the stability number (assuming $\triangle$ = 1.4) is equal to

$$\frac{H}{\Delta D} = 7.3 \text{ for } \xi = 2.43 \text{ (based on ctg}\alpha = 2)$$

Another question is the stability performance of the block when the relief slots clog up with sand and impurities, and, later on, with vegetation. It is possible that, in such a case, the stability value will decrease to the same as the situation without a relief slot. In this case, the stability number is equal to about 4, viz.:

$$\frac{H}{\Delta D} = 4.1 \text{ for } \xi = 2.07$$

In order to compare the stability of the tongue-and-groove block with the more generally used ship-lap block, the latter type was tested on the same slope. As in the previous tests, the need for spacers in the joints to relieve hydrostatic pressure beneath the revetment was immediately apparent. After installation of the spacers, the stability number was in this case equal to

$$\frac{H}{\Delta D} = 5.71 \text{ for } \xi = 3.4$$

The disadvantage of both types of revetment is that they could not adequately follow changes (erosion) as they occurred in the underlayer. The tongue-and-groove block would tend to bridge across the cavity or hole. This bridge may, for some time, stand up to the forces acting upon it but it may also fail without much forewarning.
The ship-lap revetment is more sensitive to the soil foundation.
If slope material for some reason or other is lost or is not well compacted initially, the blocks will settle. Extensive settling may make the available ship-lapping inadequate. For both types, repair works to the underlayer and the armour layer still remain a problem.
More detailled discussion of both types of revetment may be found in [23b, 24, 36].

2.4.11.6. Use of asphalt in revetment constructions.

In revetments, asphalt can be used for grouting stones and for (asphalt)lining.

Asphalt grouted revetments
The application of asphalt grouting can greatly improve the stability of stones or blocks. The purpose of grouting is to stabilize mounds

and/or layers of stones against heavy wave-attack by pouring hot mastic asphalt between the stones, thus keeping the stones in a fixed position. Asphaltic grouting has proved very effective for two reasons:

(i) when it has cooled down to ambient temperatures, mastic-asphalt behaves like a solid mass with a high elasticity modulus under short loading times such as wave-attack, and
(ii) as a plastic material of very high viscosity under prolonged loading times, it is able to follow subsoil settlements.

In the Netherlands it has been proved that the asphaltic-grouting technique is suitable for reducing the maintenance of stone pitching and even for replacing traditional stone-pitching. The asphaltic grouting technique has been adopted in the Netherlands as one of the standard methods of protecting dike slopes in tidal zones. Examples of this use can be found in [17, 50].
A distinction may be drawn between full grouting and pattern grouting (partial grouting). It should be realized that asphalt grouting in the interstices of stones or in the joints of blocks may change the character of a revetment from a permeable (i.e. pattern grouting) to an impermeable type (i.e. full grouting). In designing such revetments, consideration should be given to the possibility of excessive hydraulic pressures underneath the revetment. Drains may therefore be needed and may be placed at the toe.
A description of the general principles for design and the properties of asphalt mixtures for hydraulic application as developed in the Netherlands may be found in [53].
A satisfactory grouting mixture generally consists of a hot mixture of 7% bitumen 80/100, 8% filler, 42% sand and 50% chippings 5/15 (the mixture density about 2300 kg/m³). However, for grouting small joints e.g. between the blocks, the stone fractions may be replaced by sand (i.e. 71-72% sand) and the bitumen content may be increased to 15-20%.
Because full grouting can be equated with an asphalt revetment (impermeable type), pattern grouting only will be considered in this section. Pattern grouting was developed as the result of experience gained during the construction of several breakwater projects in the Netherlands. To avoid the problem of internal pressures originating from the impermeability of the stone-asphalt armour layer, a new concept was introduced with the idea of increasing the stability of an already fairly stable rock slope by local grouting with stone-asphalt in a regular pattern, thus maintaining the permeable character of the slope.
For pattern grouting of the armour layer of large sized stones, some additional principles are necessary [17].
Hydraulic model tests executed in the Delft Hydraulics Laboratory showed that filling up between 50 and 70% of the interstices seemed optimal for guaranteeing the overall permeability and a high increase in stability of construction [17]. Hydraulic model tests indicated that, due to grouting, the apparent weight of the armour stone could be „upgraded" at least 5 times as far as stability under wave attack is concerned, which manifests itself in a higher K_D value in the Hudson's formula.
The upgrading-factor F was defined as the ratio:

$$F = \frac{K_D \text{ for pattern grouted armour layer}}{K_D \text{ for non-grouted armour layer}}$$

A full scale test section was constructed at the head of the Separating Jetty in the harbour entrance of Europort Rotterdam. The prototype results confirmed the model expectations. Further details may be found in [50].

Führböter [19] found that inside water-filled cavities such as joints and cracks on slopes plunging breakers could cause high pressure shocks comparable with a waterhammer, producing a blasting effect.
These water pressures are proportional to the wave height. They occur just under still water level and, for slopes steeper than 1:6, depend little on the slope angle. These phenomena have probably been responsible for the damage at some breakwaters where grouting was applied.
The conclusion is that a closed surface is essential for heavy wave attack around still water

level. A fully-penetrated rubble revetment in this area is therefore recommended and measures should be taken to ensure that no even potential cracks are likely to occur. Among other things,this means that the slope should not be too steep (1 : 2.5 could be considered the limit), and that the mixture should be composed in such a way that optimum flexibility is combined with the necessary minimum stability on the slope.

As a new development in the construction of permeable asphalt revetment the Fixtone revetment can be mentioned [67]. Fixtone is prepared by mixing about 82% stones (16-56mm) with about 18% pre-mixed sand mastic (i.e. 64% sand, 16% filler and 20% bitumen 80/100), giving a material in which the stones are fixed firmly and form a stable, flexible and permeable (voids content 25% or more, pores up to 10 mm), construction material. The lining generally consist of a layer of 15 to 20 cm Fixtone on a filter layer. A more economical construction has recently been obtained with a layer of Fixtone on top of a fibre cloth which acts as a sand barrier. It is also produced in the form of Fixtone mats.
Fixtone surface is resistant to currents up to 6 m/s and waves up to 2m in height at least.
Due to the complicated visco-elastic behaviour of asphalt mixes, which cannot be scaled down, the assessment of resistance to wave attack can only be carried out on actual scale. In order to provide a design tool for designers, the experience from several projects has been compiled into a „rule of thumb", reading:

$$D = C\,H_s$$

in which: D = thickness of Fixtone layer, H_s = significant wave height and C = coefficient value being 1/6 in the case of Fixtone on filter cloth, and 1/10 on a sand bitumen filter.
This rule is also supported by the large-scale check-tests in the Delta-flume of the Delft Hydraulics Laboratory [67].
For other types of asphalt mats see also [18].

Impervious asphalt revetment
In designing impervious asphalt revetments, careful consideration should be given to the stability conditions of the asphalt (in various parts of the slope) and also of the soil underneath. If the subsoil consists of earth fill and is saturated with water, changes in water level are followed with a lag because of the low permeability of the subsoil. The accompanying uplift pressure can become dangerous when the changes of water level are slow, for only then can sufficient displacement of water and subsequent deformation and/or uplift of the revetment take place to cause rupture of the construction [53].
The material most commonly used for asphalt revetments is asphalt concrete or stone grouted with mastic asphalt; due to a large degree of porosity, the use of sand asphalt in earlier revetment design has proven less satisfactory, particulary below high-tidal level. Seawater and air penetrating into the pores finally lead to destruction of the material. The functional requirements and possible mixture compositions may be found in [53].
Asphaltic concrete for the revetment of sea dikes is mostly adopted above the tidal zone only because in the tidal zone:

- high pressures may be encountered requiring great thickness;
- the sliding criterion is difficult to satisfy
- steam formation, resulting from the emergence of tidal and pressure water from the warm asphalt-concrete mixture, may cause the asphalt revetment to become porous and lose its density. This increases the likelihood of stripping and aging.

A mild slope is favourable for asphalt revetments because better compaction results can be achieved; the slope gradient should not exceed 1 in 3 to avoid difficulty in compacting the asphalt.
In an area where the revetment is exposed to severe wave loads, strength considerations will make a thick layer of asphaltic concrete necessary. However, little experience has been gained so far with very thick asphalt revetments. Up to now, no all-round calculating methods regarding the necessary thickness of the asphalt cover on a sand core related to the wave load have been developed. However, analysis of this subject currently being carried out in the

Netherlands may well bring the problem close to solution.
The PIANC-Commission [57], based on experience, considers the following thicknesses as minimum values for watertight coverings on the seaward side:

Wave height H_s	Slope 1 in 3	Slope 1 in 6
3m	0.25m	0.15m
5m	0.60m	0.30m

In an area subject to severe wave loads, stone revetments (mostly two or three layers of stones) grouted with mastic asphalt have been the preferred solution up to now.
For the calculation of the uplift pressures resulting from tidal movement, an electric analogy is commonly used in the Netherlands, based on the analogy of Ohm's and Darcy's laws for electrical current and laminar groundwater flow respectively.
As the first approximation, and assuming that the position of the phreatic-line is known, and homogeneous soil the uplift pressures on slope 1 on n can be determined graphically (triangle-rule) as shown in figure 2.4.11.14a or by using analytical solutions for stationary and non-stationary groundwater flow given by Van der Veer [48].
The maximum uplift force at still water-level for $h/H_o < 0.8$ is then given by

$$P_{max} = a\ \phi_v$$

where ϕ_v is a position of the phreatic-line above still water level and 'a' is the lift-coefficient equal to:
1° stationary flow:

$$a_1 = \sqrt{1 - \left(\frac{h}{H_0}\right)^{\pi/\theta}}$$

2° non-stationary flow:

$$a_2 = \frac{1}{\pi} \arccos \left[2 \left(\frac{h}{H_0}\right)^{\pi/\theta} - 1\right]$$

3° triangle-rule:

$$a_3 = 1 - \left(\frac{h}{H_0}\right)$$

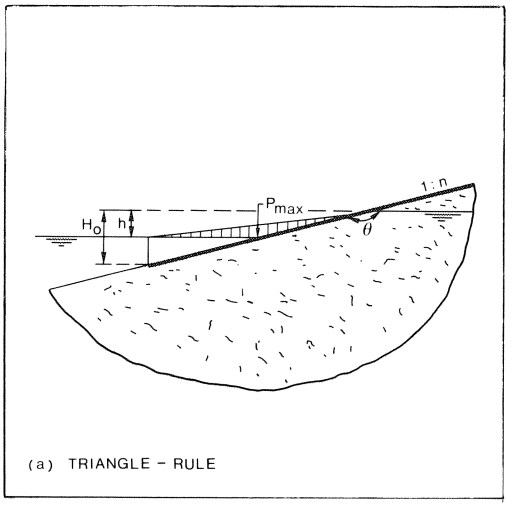

Figure 2.4.11.14 Pressure distribution on a slope.

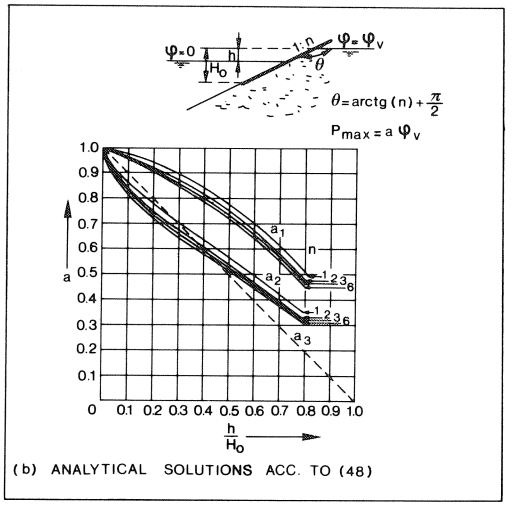

where θ = arctg(n) + $\frac{\pi}{2}$, h = the height of the phreatic-line above still water-level and H_o = the height of the phreatic-line above the toe of the asphalt layer.
The graphical representation of these solutions is given in figure 2.4.11.14b.
The revetment has also to be checked regarding its criterion for sliding(down).
This criterium can be expressed by

$$P \leq (1 - \frac{\tan \alpha}{\tan \phi}) D \Delta \cos \alpha$$

where:
ϕ = angle of internal friction of the soil material
P = uplift-force due to water pressure difference in water coloumn metres
α = angle of inclination of the bank
D = thickness of protection layer
Δ = relative density of protection-layer material;

The protection layer is lifted up as

$$P > D \Delta \cos \alpha$$

The submerged unit weight of revetment should be greater than the maximum uplift at design conditions. More information hereon may be found in [6] and [51]. At the same time drainage requirements for toe protection must be carefully evaluated with respect to the type of soil to be protected.
In the area above the highest wave crests (roughly above storm flood level under Dutch conditions), the asphaltic concrete only has a lining function; no heavy pressures or severe wave loading are encountered above storm flood level. In this area a single layer of asphaltic concrete (15-20cm) is generally sufficient. More practical information on use of asphalt for slope protection may be found in [3, 4, 17, 32, 50, 52, 53, 54].

2.4.11.7. Final remarks

It has to be pointed out that the present evaluation of the available data on stability of revetments still has many limitations regarding their practical use. This is due to:

1. Insufficient knowledge about performance mechanisms (external-internal interaction)
2. Scale effects, especially as regards small-scale tests
3. Restricted variety of slope gradients
4. The use generally of regular waves and two-dimensional conditions
5. Non-uniformity in presentation and definition of boundary conditions (i.e. wave-height definition, place and definition of instability, etc.)
6. Performance of stability tests within a narrow range of wave characteristics is generally insufficient for establishing the minimum value of the stability number.
7. Lack of proper investigation of stability and/or erosion aspects related to underlayer
8. Lack of proper (quantitative) examination under in situ conditions.

On the other hand, the data presented allow a first approximation to be made regarding the stability of different types of revetment, and thus to select an appropriate revetment with respect to available materials, stability and cost of construction. In many cases these data could be sufficient for design purposes, especially if some reserve stability were taken into account. It is also important to remember that the armour layer is only a part of a revetment. For the total stability the proper design of the underlayer (i.e. filter or clay), fixed enclosing at the toe and at the top of revetment and the proper design of the toe construction and the upper part of the slope (beyond the end of the revetment under consideration) are of essential value.
Considerably more study is required before definite answers on the selection of the best type of revetment for a variety of conditions can be given. Hydraulic model experiments, especially on a large scale and with the use of irregular waves (i.e. a spectrum of waves) supported by in situ examination, will be of immense value in solving some of the intricate problems associated with revetment design.

References/Bibliography

1. Ahrens, J.P., Large Wave Tank Tests of Riprap Stability, **C.E.R.C. Technical Memorandum no. 51,** May 1975.

2. Ahrens, J.P. and McCartney, B.L., Wave Period Effect on the Stability of Riprap, **Proc.Civil Eng. in the Oceans,** Univ. of Delaware, June 9-12, 1975.

3. Baron W.F. van Asbeck, **Bitumen in Hydraulic Engineering Vol. 1 and 2,** Elsevier Publishing Company, 1964.

4. Baron W.F. van Asbeck, **Modern Design and Construction of Dams and Dikes built with the use of Asphalt.**

5. Battjes, J.A., Surf Similarity, **14th Proc. Conf. on Coastal Eng.,** Copenhagen, 1974.

6. Bendegom van L. et al., Dutch paper on Revetments, presented at the **XXIInd International Navigation Congress,** Paris, 1969, Sec.1, Subject 6.

7. Berkeley Thorn, R. an Roberts, A.G., **Sea defence and Coast Protection Works,** London, Thomas Telford, 2nd., 1981.

8. Blaauw, H.G. and Kaa, E.J. van de, Erosion of Bottom and Sloping Banks caused by the Screw Race of Manoeuvring Ships, **Delft Hydraulics Laboratory, Publication no. 202,** Delft, 1978.

9. Boer K., den, C.J. Kenter and K.W. Pilarczyk, Large Scale Model Tests on Placed Blocks Revetment, **Delft Hydraulics Laboratory, Publ. no. 288,** January 1983 (also presented at „Coastal Structures '83", Washington March 9-11, 1983).

10. Bores, P.S., Earth Dam Wave Protection, **10th Congress Large Dams,** Montreal, 1970. Vol.I. Question 36, Report 50.

11. Bouwmeester, J., Kaa, E.J.van de, Nuhoff, H.A. and Orden, R.G.J. van, Recent Studies on Push-Towing as a Base for Dimensioning Waterways, **Delft Hydraulics Laboratory, Publication no. 194,** Delft, 1977.

12. Bruun, P., Günbak, A.R., Hydraulic and Friction Parameters affecting the Stability of Rubble Mounds, **PIANC Bull.no.24,** 1976.

13. Bruun, P., Johannesson, P., Parameters Affecting Stability of Rubble Mounds, **J. of the Waterways, Harbors and Coast, Eng.** Vol.102, WW2, May 1976.

14. Bruun, P., Günbak, A.R., Risk Criteria in Design Stability of Sloping Structure in Relation to . **Symposium on Design of Rubble Mound Breakwaters,** England, 1977. (also Coastal Engineering.1.1978)

15. Bruun, P., Common Reasons for Damage or Breakdown of Mound Breakwaters, **Coastal Engineering 2, 1979.** (printed in The Netherlands).

16. Bruun, P., Kjelstrup, S., Practical Views on the Design and Construction of Mound Breakwaters, **Coastal Engineering 5, 1981.**

17. D'Angremond, K., H.J.M. Span, J.van der Weide and A.J. Wenstenenk, Use of Asphalt in Breakwater Construction, **XIIth Coastal Engineering Conference,** Washington, 1970.

18. Della Luna, G. and R.Agostini, New Methods of Countering Erosion Generated by Vessels in Canals in Italy and other Countries. **XXVth International Navigation Congress,** Edinburgh, 1981.

19. Führböter, A., Der Druckschlag durch Brecher auf Deichböschungen, Heft 28, **Mitteilungen Franzius-Institut,** Hannover 1 (1966).

20. Führböter, A. et al., Response of Sea Dykes to Wave Impacts, **Coastal Engineering Conference,** Chapter 150, 1976.

21. Gerritsen, F., Bruun, P., Dutch and Florida Practices on Revetment Design, **9th Coastal Eng. Conf.,** Lisabon, 1964.

22. Giles, L.M., Evaluation of a Concrete Building Block Revetment, **Conf. Coastal Sediments,** 1977.

23a. Hall, J.V., Stability Tests of Interlocking Block Revetment, **J. of the Waterways and Harbors Division,** WW3, August 1968.

b. **Discussion** by F. Gerritsen and P. Bruun, WWZ, May 1969.

24. Hall J.V. and R.A. Jachowsku, Concrete Block Revetment near Benedict, Maryland, **CERC,** Miscellaneous paper no. 1-64, 1964.

25. Hedar A., Rules for the Design of Rock-fill Breakwaters and Revetments, **XXIst. Int. Navigation Congress,** Stockholm 1965.

26. Hudson, R.Y., Laboratory Investigations of Rubble Mound Breakwaters, **Proc. ASCE,** 85, WW3, Sep. 1959.

27. Hudson R.Y., Reliability of Rubble-Mound Breakwater Stability Models, **U.S.Army Engineer Waterways Experiment Station,** Vicksburg, Miscellaneous paper H-75-5, June 1975.

28. Jachowski, R.A., Interlocking Precast Concrete Block Seawall, **9th Coastal Eng. Conf.** Lisbon, 1964.

29. Jakobsen R., Per and A.H. Nielsen, Some Experiments with Sand-filed Flexible Tubes, **12th Coastal Engineering Conference,** 1970.

30. Kidby H.A., et al., Placed-Stone Jetty Weight Coefficients, **J. Waterways and Harbors D.V. ASCE,** November 1964.

31. Kostense, J.K., Gobi-Blocks as Slope Revetment Stability Under Wave Attack, Report 1184, **Delft Hydraulics Laboratory,** Netherlands, January 1973.

32. Kerkhoven, R.E., Recent Developments in Asphalt Techniques for Hydraulic Applications in the Netherlands, Paper to Annual Meeting, **Association of Asphalt Paving Technologists,** Philadelphic, 1965, Royal Shell-Laboratory, Amsterdam.

33. McCartney, B.L., Ahrens, J.P., Stability of Gobi Block Revetments to Wave Attack, Technical Memorandum no. 55, October 1975. **C.E.R.C. U.S. Army, Corps of Engineers.**

34. McCartney, B.L., Survey of Coastal Revetments Types, Miscellaneous Report no. 76-7, May 1976, **C.E.R.C. U.S. Army, Corps of Engineers.**

35. McCartney, B.L. and Ahrens, J.P., Overlay of Large, Placed Quarrystone and Boulders to Increase Riprap Stability, **C.E.R.C. Technical Paper no. 76-19,** December 1976.

36. Mohl E.V. and J.D.Brown, Flexible Revetment Using Interlocking Concrete Blocks, Tilghman Island, Maryland, **Shore and Beach,** October 1967.

37. Parsons D.A. and R.P. Apmann, Cellular Concrete Block Revetment, **J. Waterways and Harbors Div., ASCE,** May 1965.

38. Pilarczyk, K.W. and K. den Boer, Stability and Profile Development of Coarse Materials and their Application in Coastal Engineering, **Delft Hydraulics Laboratory,** Publ. no. 293, 1983 (also: Conference on Coastal and Port Engineering in Developing Countries, Colombo, Sri Lanka, March 20-26, 1983).

39. Price R.K., Some Ideas on Breakwaters, **Coastal Engineering Conference,** 1978.

40. Raichlen F., The Effect of Waves on Rubble-mound Structures, **Annual Review of Fluid Mechanics,** Vol.7, 1975.

41. Shirdan, L., Coastal Protection Employing Gabions, **XXIst. International Navigation Congress,** Stockholm, 1965.

42. Sollitt, C.K., De Bok, D.H., Large Scale Model Tests of Placed Stone Breakwaters, **Proc. 15th Coastal Eng. Conf.,** Honolulu, Hawaïi, 1976.

43. Span H.J.Th., et al., A Review of Relevant Hydraulic Phenomena and of Recent Developments in Research, Design and Construction of Protective Works, **XXVth International Navigation Congress,** Edinburgh, 1981, Vol.I.

44. Stephenson, D., Rockfill in Hydraulic Engineering, **Developments in Geotechnical Engineering,** Vol. 27, Elsevier, Sc. Publ.Comp., Amsterdam - New York, 1979.

45. Svee R., Formulas for Design of Rubblemound Breakwaters, **J.Waterways and Harbors Div. ASCE,** May 1962.

46. Svee, R., et al., The Stability Properties of the Svee-blok, **XXIst. International Navigation Congress,** Stockholm 1965.

47. Taylor K.V., Slope Protection on Earth and Rockfill Dams, **Int.Congress on Large Dams,** Madrid, 1973.

48. Veer, P.van der, Lift Forces under Impervious Revetment (in Dutch), **Polytechnisch Tijdschrift,** Pt-b 31 (1976), nr. 9-547.

49. Ven te Chow, **Open-channel Hydraulics,** McGraw-Hill Book company, New York-London, 1959.

50. Wenstenenk A.J., Use of Asphalt for Slope Protection on Earth and Rockfill Dams, **Int. Congress on Large Dams,** Madrid, 1973.

51. Zanen, A., Revetments, **Int. Courses in Hydraulic and Sanitary Engineering,** Delft 1976, The Netherlands.

52. Working Party on Sealed Dyke Revetments, Provisional Report 1961,(in Dutch), **Public Works Department** (Rijkswaterstaat).

53. Asphalt Revetment of Dyke Slopes, Committee on the Compaction of Asphalt revetments of Dyke slopes, **Rijkswaterstaat Communications No. 27,1977**

54. Asphalt in Hydraulic Structures, **The Asphalt Institute,** Maryland, March 1965 (Manual Series No.12).

55. Tetra Tech. Inc. Wave tests of Armorflex Block Slope Protection Mats, Technical report TC-3475, sep.1981, Pasadena, California. Prepared for **Armortec, Incorperated,** Atlanta, Georgia (also: Coastal Structures '83, Washington, March 9-11, 1983).

56. Wave run-up and overtopping, **Technical Advisory Committee on Protection Against Inundation,** 1974, Government Publishing Office, The Hague.

57. **Final Report of the International Commission for the Study of Waves,** PIANC, Annex to Bulletin no. 25 (Vol.III, 1976).

58. U.S. Army Coastal Engineering Research Center, **Shore Protection Manual,** 1975.

59. The Stability of Revetment Blocks under Wave Attack, **Hydraulics Research Station.** Report IT195, Wallingford, England, 1980.

60. Maritime and Riparian Uses of Gabions, **The Dock & Harbour Authority,** December 1965.

61. **Delft Hydraulics Laboratory.** Systematic Research on Erosion and Bank Protection of Navigation Channels, Reports M1115, 1974-1985.
    a) M1115-XB1, XB2: Erosion by return flow (1981, 1982)
    b) M1115-XC: Erosion and stability under attack of stern-wave (1983).

62. **Delft Hydraulics Laboratory,** Small Scale Investigation on Stability of Block Revetment (in Dutch):M 1507, 1970, M1410, 1980.

63. **Delft Hydraulics Laboratory,** Systematic Research on Stability of Block Revetments, M1795, 1982-84 (in Dutch).
    a) Review of Literature on Stability of Block Revetments, M1795-II, 1982

b) Review of Literature on Soil-mechanic Aspects of Stability of Revetments. M1795-III,1982.
c) Stability of Free Block Revetment of Oesterdam, M1795-VI,1982.

64. **Delft Hydraulics Laboratory,** Stability of Basalton Blocks (in Dutch). M1900, 1983.

65. **Delft Hydraulics Laboratory,** Stability of Armorflex Block Slope Protection Mats under Wave Attack, M 1910, May 1983.

66. Hydro Delft, Special Issue on Rubble-mound Breakwaters, No. 65, February 1983, **Delft Hydraulics Laboratory.**

67. **Delft Hydraulics Laboratory,** Fixtone: Stability under Wave Attack, report M1942, 1983.

Interaction Water Motion and Closing Elements

J.C. v.d. Burg, J.K. Nieuwenhuis

2.4.12. Groundwater flow

Introduction

The water in the hollow spaces between the weathered crust of the earth or in the pores in the case of soft soils is termed groundwater. Groundwater may either be stationary or in motion. In those cases where groundwater is in motion as a result of differences in the piezometric level, the velocity of propagation is generally extremely low. The most critical factor in this respect is the permeability of the soil.

In designing dikes, dams and other civil engineering structures it is essential when estimating the determining load situations to which the structure will be subjected, to take adequate account of the loads produced by groundwater flows.

These loads may be of two kinds:

- first, the flow itself, or discharge, also known as **seepage;**
- second, the impact in various ways on the stability of the structure.

The first of these categories, i.e. seepage problems, may include the following aspects:

- water loads (e.g. drainage, pumping or sluicing in polders and basins);
- drainage of construction pits during construction and execution stages;
- salt accumulation or pollution by seepage;
- leakages in constructions (well structures, sheet piling, tunnels);

Aspects affecting the stability of structures include:

- hydraulic pressures against structures or parts thereof (uplift of constructions, stability calculations for dike slopes, overpressure beneath watertight revetments, wave loads);
- flow pressures (damslopes, micro-stability);
- erosion problems (piping, filters).

In order to assess the design of a dike or other civil engineering construction during the design stage the groundwater flow patterns must be known. Various calculation methods may be used. In this respect a clear distinction should be drawn between groundwater calculations in the case of:

. steady state groundwater flows, and
. unsteady state groundwater flows.

The remainder of this chapter examines the theory of groundwater flow, the determination of permeability and the calculation methods. A number of practical applications are also discussed for both steady and unsteady state groundwater flows.

Theory of groundwater flow [1 - 7]

Groundwater flows from places of higher energy to places of lower energy. A difference in energy level between two places in the same aquifer will lead to groundwater flow. The energy level at a given point depends not only on the hydraulic pressure p at that point but also on the site elevation z in relation to a selected horizontal reference level. These provide the basis for the concept in groundwater mechanics of the groundwater head or simply the head h. The latter is expressed as the sum of the site elevation z and the hydraulic head $p/\varrho.g$, all terms expressed in water-column metres;

$$h = z + \frac{p}{\rho g}$$

in which:

h	=	piezometric head	(m)
z	=	elevation in relation to a reference level (e.g. MSL)	(m)
p	=	hydrostatic pressure at point z	(N/m^2)
ϱ	=	density of the fluid	(kg/m^3)
g	=	acceleration of gravity	(m/s^2)

In **groundwater statics** the following applies at all points of a saturated aquifer:

$$h = z + \frac{p}{\rho g} = \text{constant}$$

when there will be no groundwater flow.

Groundwater flow occurs if there is a difference in the piezometric level h, i.e. if there is a $\triangle h$.

The basic groundwater flow equation consists of Darcy's law of percolation discovered empirically in 1856. This equation establishes a linear relationship between the velocity of percolation of a fluid in a permeable medium and the hydraulic gradient: $u_f = - k.i.$

in which

u_f = velocity of percolation (m/sec)
k = coefficient of permeability of a porous medium (m/sec)
$i = \frac{dh}{ds}$ = hydraulic gradient of the aquifer (-)

The negative symbol indicates that the head declines in the direction of flow.
Groundwater motion is required to satisfy not just the motion equation but also the continuity equation. The latter is obtained when a mass balance is drawn up for the retention of groundwater in an elementary block of soil. In this respect a distinction needs to be drawn between:

Steady state groundwater flow and Unsteady state groundwater flow
In the case of steady state groundwater flow it is assumed that the same volume of water flows into an elementary block of soil as flows out. In the larger example of a dike this means that equally as much water enters the dike as leaves it. Over time, therefore, the dike and the subsoil do not provide any storage capacity for groundwater.
In the case of unsteady state groundwater flow, on the other hand, storage in the ground does take place. This may take the form either of specific storativity (i.e. an addition to unconfined groundwater) or of elastic storativity, i.e. the retention of water in an elementary block of soil as the result of the deformation properties of the grain skeleton and the groundwater.

Steady state groundwater flow
Steady state groundwater flow arises when:
- the difference in water level between the inner and outer sides of the dike or other civil construction is a constant over time or may be taken as a constant, and
- the groundwater is incompressible and the soil skeleton not subject to deformation, i.e. elastic storage in the soil does not take place or may be neglected.

In the two-dimensional case Darcy's motion equation combined with the continuity condition provides the basic differential equation for steady state groundwater flow:

$$k_x \frac{\partial^2 h}{\partial x^2} + k_y \frac{\partial^2 h}{\partial y^2} = 0$$

in which:
k_x = coefficient of permeability along the x-axis (m/sec)
k_y = coefficient of permeability along the y-axis (m/sec)
$\frac{\delta h}{\delta x} = i_x$ = hydraulic gradient along the x-axis (-)
$\frac{\delta h}{\delta y} = i_y$ = hydraulic gradient along the y-axis (-)

If the k value is equal along the x and y axes, we then obtain the shortened form, also known as Laplace's equation:

$$\frac{\partial^2 h}{\partial x^2} + \frac{\partial^2 h}{\partial y^2} = 0 \quad \text{or} \quad \nabla^2 h = 0$$

Unsteady state groundwater flow
Unsteady state groundwater flow occurs when:
- time-dependent piezometric head conditions arise along the boundaries in the form of head/time-curves;
- the storage of groundwater somewhere in the soil formation must be taken into account.

The time-dependent boundary conditions may be:
- quasi-static, i.e. relatively long-duration time curves such as tidal movement, stormsurge curves for sea-dikes and high-water discharge curves for river-dikes;
- dynamic, including brief-duration phenomena such as windwaves and shipwaves.

The storage of groundwater in a soil formation that needs to be taken into account includes:
- specific storativity, i.e. the storage of water in the soil pores above phreatic groundwater-table,
- elastic storativity due to the deformation properties of the soil.

In the case of an unconfined aquifer in a sand-dike body, unsteady state groundwater flow will generally consist of phreatic storativity only, this being the dominant form; the order of magnitude of the effective porosity is between 15 and 40%. The effective porosity n_e refers to that part of the actual pore space n that is periodically available for the storage of groundwater. $n_e < n$ as the result of trapped air and water retained against gravity.
Elastic storativity S is in the order of 0.001 to 0.00001 (unity m/m, see[2]), which may therefore be neglected.
In the case of a non-phreatic soil formation or confined aquifer, and given the existence of certain dynamic phenomena, elastic storativity becomes important and can by no means always be neglected.
For the derivation of the differential equation and the various calculation methods for unsteady state groundwater flow the reader is referred to the literature, e.g. [4]. It will suffice here to provide the basic differential equation for two-dimensional unsteady state groundwater flow where the horizontal and vertical permeability of the soil are equal to one another:

$$\frac{\partial^2 h}{\partial x^2} + \frac{\partial^2 h}{\partial y^2} = c_v^{-1} \frac{\partial h}{\partial t} \qquad \text{or} \qquad c_v \nabla^2 h = \frac{\partial h}{\partial t}$$

in which c_v represents the coefficient of consolidation in soil mechanics literature (see ref. [4]).
As a result of allowing for unsteady (time-dependent) piezometric head boundary conditions and for storage, damped, phased timecurves are obtained for the soil formation. In certain circumstances these can lead to hydrostatic over-pressure; see inter alia the section on over-pressure in the case of watertight revetments.

Determination of permeability
A vital soil parameter for the degree of groundwater flow is the coefficient of permeability k.
The speed at which water travels depends on the nature and permeability of the dike material and the composition of the subgrade. In the case of clayey materials, for example, the flow velocity is a factor of 10^5 to 10^6 smaller than in sandy materials. In a sand formation with a low silt percentage and a gradient of unity the velocity of propagation is in the order of 10^{-4} m/sec.
By way of orientation the approximate coefficients of permeability for a number of soil types are shown in table 2.4.12.1 below.

material	approximate k values (m/s)
clay	10^{-8} to 10^{-12}
peat	10^{-7} " 10^{-9}
clayey sand	10^{-5} " 10^{-8}
fine sand	10^{-4} " 10^{-6}
medium-fine sand	10^{-3} " 10^{-5}
coarse sand	10^{-2} " 10^{-4}
gravel	10^{-1} " 10^{-3}
limestone	10^{-6} " 10^{-9}
sandstone	10^{-5} " 10^{-8}

Table 2.4.12.1 Coefficient of permeability k for various soil types.

In the case of non-cohesive soils the coefficient of permeability k is related in a particular way to the representative diameter of the particular size distribution of the soil. This is often represented in terms of the mean (effective) diameter D_{50}. Some authors also use a different representative diameter, e.g. D_{10} (Allen Hazen).
Another factor of major importance for the permeability of a soil is the porosity or density; see [3], [5] and [6].

For sand, Kozeny's equation is often used:

$$k = \frac{1}{500} \frac{g}{\nu} D_{50}^2 \frac{n^3}{(1-n)^2}$$

in which:

k	=	coefficient of permeability of the soil	(m/sec)
g	=	acceleration of gravity	(m/sec²)
D_{50}	=	mean grain diameter of particle size distribution	(m)
ν	=	kinematic viscosity of the fluid	(m²/sec)
n	=	porosity of the sand	(-)

Apart from Kozeny's equation there are all sorts of other equations for determining the permeability of the soil, such as those of Hazen, Hooghoudt, Fair, Fahmy etc.
For sandy soils, the silt percentage has a major bearing on permeability; see e.g. [8].
In those instances where the result of groundwater calculations in a design are highly sensitive to the permeability of the soil, it will generally not be sufficient to rely on approximate estimates or calculations of permeability with the aid of formulae; laboratory or in situ research will be required as well. In a soil mechanics laboratory it is possible to test the permeability of both undisturbed and disturbed soil samples of varying densities.
There are various (generally expensive) in-situ techniques for determining permeability factors. The most important of these consists of conducting one or more pump tests (for a treatment of this subject see [9] and [10]. Indicative permeability research can also be conducted on site by means of remote-sensing techniques. These techniques only provide an indication of relatively large permeability differentials between various materials, e.g. they may be used to detect clay layers in sand formations. They may take the form of measurements taken either in the open or in an open borehole. Examples of such techniques include geo-electrical and geomagnetic research and gamma radiation and spontaneous potential analysis. Other indicative methods for site delimitation in geohydrology include seismic, geothermal and acoustic research and tracer techniques (for further details see the literature).

Calculation methods [4]
The following groundwater computation methods are available:

1. analytical solutions, including various complex mathematical techniques.
2. approximate methods, such as the graphical method using a (rectangular) flow net.
3. numerical solutions using computer programmes, based on the finite difference and finite element methods.
4. Analogue solutions such as parallel plate models and electric analogy models in the form of conductive paper models (using carbonized or „Teledeltos" paper) or electric network models (ELNAG).

Using analytical formulae, a good impression of the magnitude of seepage or groundwater pressure may often be obtained by means of simple hand calculations and rough schematizations.
Analytical solutions of this kind can, however, generally be used for simple cases. For complex cases more advanced calculation methods must be applied. This is the case if the geometry of the permeated soil formation is more complex and can no longer be schematized in rectangular form, if the composition of the soil is not homogeneous, if factors such as slope gradients, wet seepage surface areas, sheet piling and drain dimensions etc. have to be introduced, or if the potential boundary conditions are not constant but time-dependant, as for example in the case of tidal movement, stormfloods and waves. In these situations straight-forward analytical calculations by hand will generally no longer suffice.
The rapid developments in computer technology over the past few years have led to the development of a number of computer programmes for handling numerical solution methods for groundwater computations. There are now a large number of groundwater computer programmes, based on the finite difference, finite element and semi-analytical function methods. These have proved particularly useful for steady state groundwater calculations and for drainage problems. Where there are time-dependent potential boundary conditions, as in the case of sea-dikes with tidal, stormsurge or dynamic wave boundary conditions, computer calculations are often costly and electric model techniques may be superior, particularly if a large number of calculations for parametric research are involved.
In the Netherlands, the Rijkswaterstaat Delta Project Department has made frequent use since 1960 of electric analogue models based on the analogy between Ohm's law for the passage of an electric current through a conductor and Darcy's law for streamline groundwater flows. In the first few decades, electric analogue models relied exclusively on the use of conductive

paper. Since 1978, an advanced electric network analogue for groundwater flow (ELNAG) has also been used. This model enables anisotropy (i.e. the difference in horizontal and vertical permeability) and inhomogeneities in the soil (i.e. locally varying k values, as in dikes built up between parallel clay banks) to be incorporated into the calculations.
Apart from phreatic storage this technique can also be used for solving problems connected with internal or elastic storage such as the solution of the diffusion or heat equation in the case of dynamic potential boundary condition problems. For the application of the analogue technique the reader is referred to [2], [11] and [12].

Applications in steady state groundwater flow conditions

Groundwater uplift beneath a caisson
An example of an application in the case of steady state groundwater flow is the calculation of the total hydraulic uplift on the bottom of a caisson with a view to determining the latter's stability under extreme conditions: see Figure 2.4.12.1.
In this instance the application of the graphical approximation method can result in inaccuracies in the rectangular flow net pattern, especially around the corners of the caisson. A more precise solution may be obtained straightforwardly by taking measurements in a conductive paper model. Numerical models may also be used for the purpose.

Eastern Scheldt Barrier asphalt bottom protection
A second application for solving a groundwater problem under steady state flow conditions is the determination of the maximum anticipated over-pressures under a watertight (asphalt) bottom protection on the basin side of the sill of the Eastern Scheldt Barrier. The existence of a potential difference across the barrier means that groundwater flows under the asphalt bottom protection can give rise to over-pressures.
In order to prevent the revetment from being lifted up the asphalt layer may be ballasted

Figure 2.4.12.1 Distribution of groundwaterpotentials below a caisson in case of steady groundwaterflow.

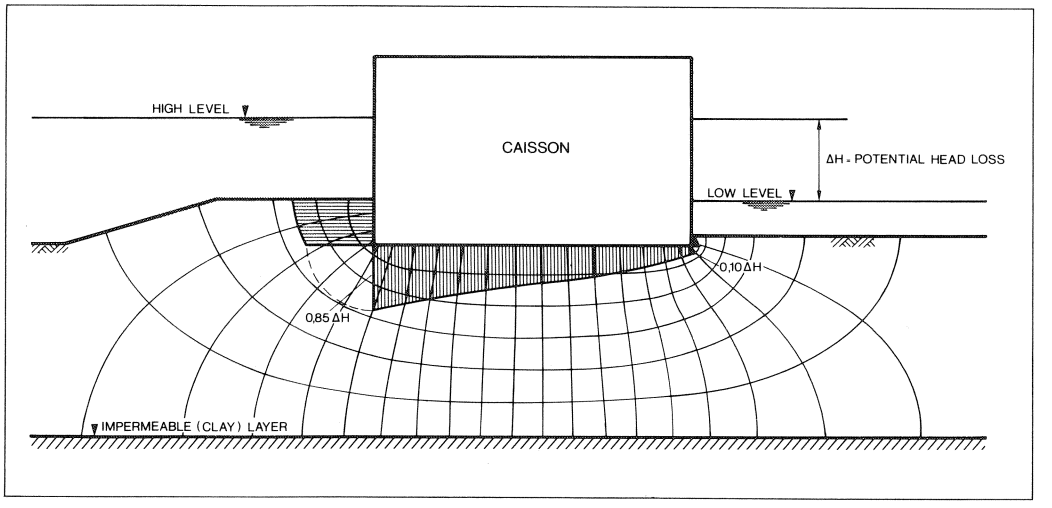

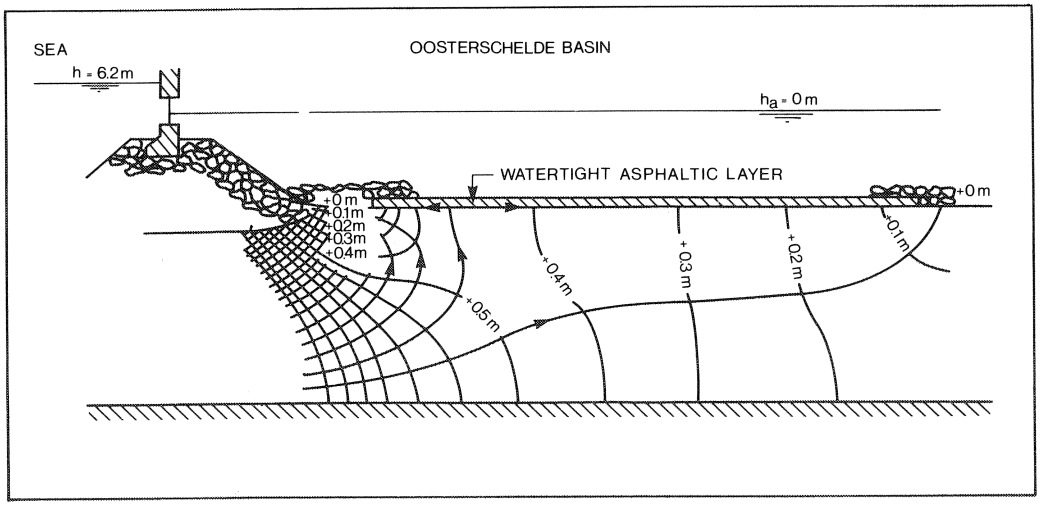

Figure 2.4.12.2 Pattern of flow-lines and equipotential lines below a watertight asphaltic layer on the basin side of the Eastern Scheldt Barrier.

Figure 2.4.12.3 Failure of a sheetpiling by piping.

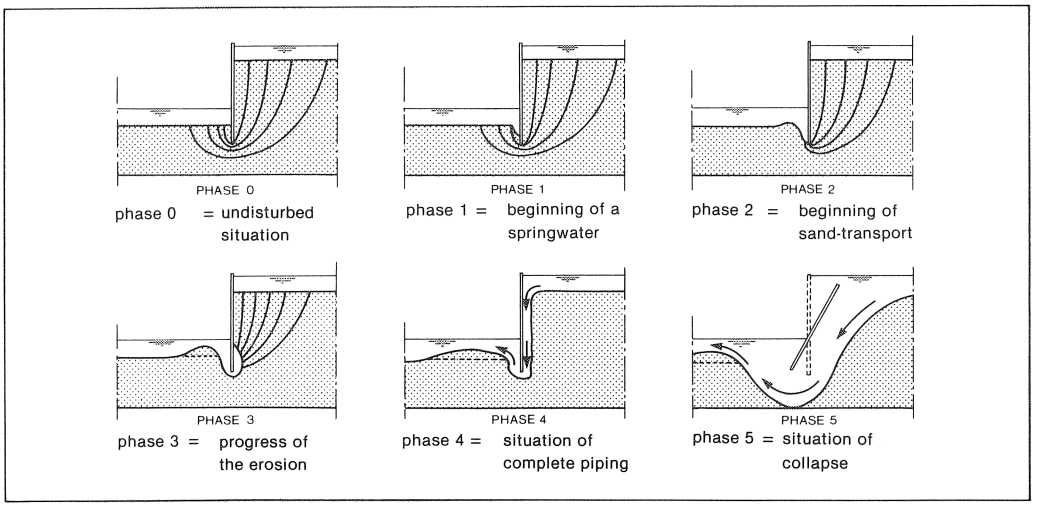

down. To select the required dimensions of the ballast the maximum over-pressures must be calculated under extreme boundary conditions. Detailed parameter research was conducted with the aid of an electric analogue model; Figure 2.4.12.2 shows by way of example a computed rectangular net in the form of a flow net and equipotential lines. In this case the results suggested a maximum over-pressure of 0.45 m water pressure or 4.5 KN/m². Further details on this particular piece of research may be found in [13]. The area or extensiveness of a watertight bottom protection will affect the potential configuration beneath it. In other words, there is an interaction between the design in a horizontal sense (extensiveness) and a vertical sense (weight and water-tightness). Thus in Figure 2.4.12.2 the section directly behind the sill has been constructed as a permeable stone formation. The groundwater potential beneath the water tight asphalt bottom protection downstream from this area is lower, so that it can be constructed more lightly.

Piping

A particular form of concentrated seepage at certain erosion-sensitive points beneath a dike or other engineering construction such as sluices and sheet piling consists of the phenomenon of piping.

When this happens, the groundwater seepage flow becomes concentrated in narrow passages or pipes. If the seepage flow builds up to the point that soil particles are transported it may even lead to the failure of the dike or construction.

Figures 2.4.12.3 and 2.4.12.4 illustrate how sheet piling or a dike may fail as the result of piping.

The literature indicates that piping may arise in one of two ways:

- suffusion or internal erosion, i.e. the erosion or disappearance of the finest particles from between coarse particles leading to the concentration of seepage and, possibly, to total erosion;
- regressive erosion, in which the erosion starts at a point where the slope exceeds the stability criterion, in general at the back of

Figure 2.4.12.4 Failure of a riverdike by piping.

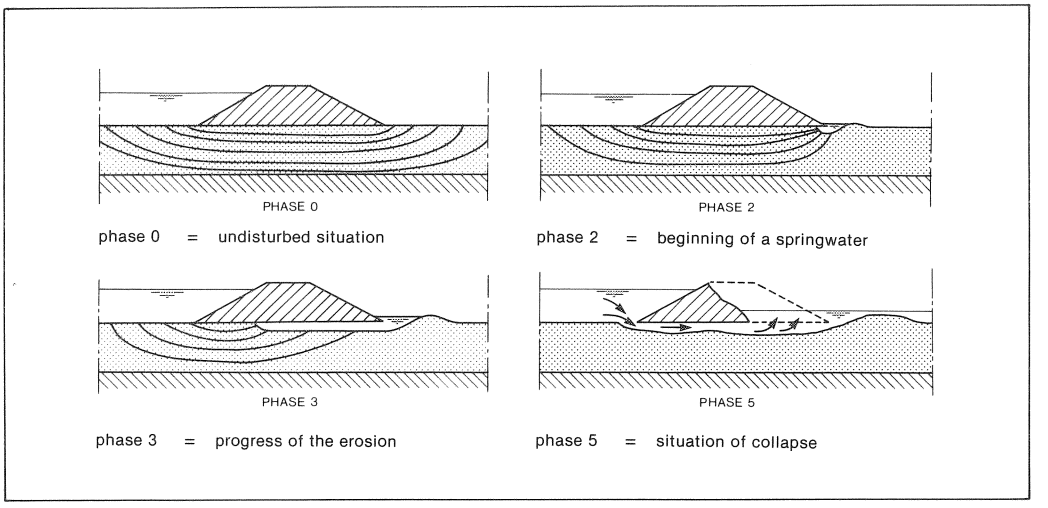

the dike or at the downstream side of the construction. If in these circumstances the first grains of sand start to disappear and erosion gets under way, the latter will establish itself, often regressively, as the hydraulic gradient in relation to the seepage length becomes steadily greater.

A considerable amount of research has been conducted in the past into the prevention of piping, and a number of design rules have been drawn up. A number of criteria have been established to prevent suffusion or internal erosion, a survey of which may be found in [14], [15] and [16]. A number of empirically determined design rules have been drawn up by Bligh, Griffith and Lane; see [17], [18] and [19] respectively. These rules all specify a relationship between the hydraulic gradient and the minimum seepage length in a dike or beneath a construction and is expressed as a c value depending on the grain size of the soil type. This may be expressed as:

$$L \geq c\,H$$

in which:

L = length of the shortest seepage path (m)
H = drop across the dike or construction (m)
c = constant per soil type (-)

Bligh and Lane defined the shortest seepage path L in a number of ways, a survey of which is provided in Figure 2.4.12.5

Table 2.4.12.2 provides a survey of the c values by both Bligh (c_b) and Lane (c_1) for various soil materials.

It has been realized in the Netherlands that it is theoritically incorrect to apply the piping criteria developed for different purposes, such as those of Bligh and Lane for barrages, to sea and river dikes. The form and duration of the stresses (e.g. the duration of high water) often vary considerably for various types of barriers or other civil engineering structures. For this reason the Soil Mechanics Laboratory in Delft has been carrying out basic research into piping since 1974 on behalf of the Rijkswaterstaat (Public Works

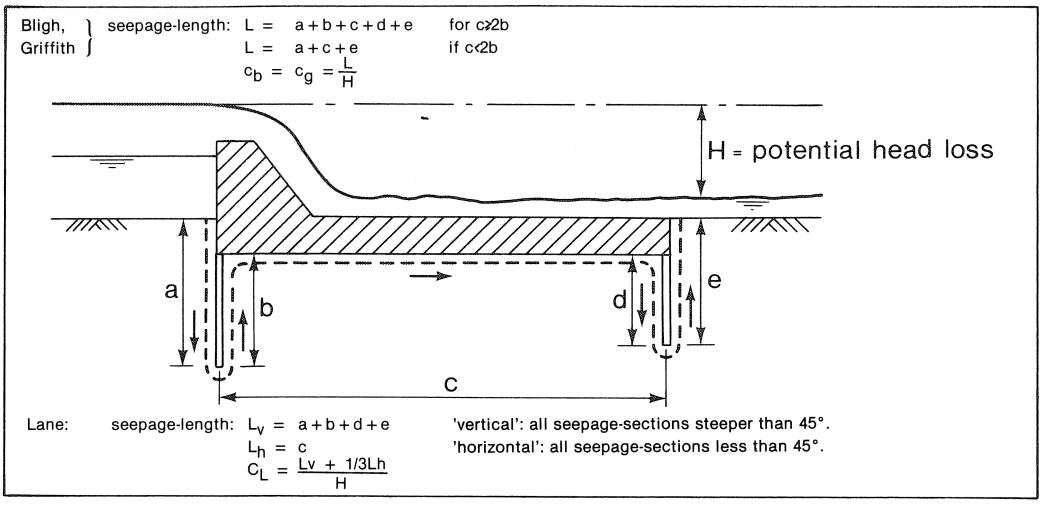

Figure 2.4.12.5 Definitions of seepage-length by Bligh, Griffith and Lane.

Department). This has included both scale model tests in the Laboratory and theoretical analysis of and calculation methods for the phenomenon of piping; see [20] and [21].

Material	Lane's creep ratio C_l	Bligh's value c_b
Very fine sand or silt	8.5	18
Fine sand	7.0	15
Medium sand	6.0	...
Coarse sand	5.0	12
Fine gravel	4.0	...
Medium gravel	3.5	...
Gravel and sand	...	9
Coarse gravel including cobbles	3.0	...
Boulders with some cobbles and gravel	2.5	...
Boulders, gravel and sand	...	4 to 6
Soft clay	3.0	...
Medium clay	2.0	...
Hard clay	1.8	...
Very hard clay or hard-pan	1.6	...

Table 2.4.12.2 Survey of c values for different soil materials.

Applications in non-steady state groundwater flow conditions

Over-pressures under watertight dike revetments

Apart from the fact that the dimensions of a sea-dike will depend on external loads imposed by currents and waves etc., the thickness of much of the revetment will be chiefly determined by the quasi-static water over-pressure that may be anticipated as the result of tidal and stormflood conditions. Even when a dike is being built and the revetment is still in the early stages of installation, account must be taken during dumping of protracted, high groundwater potentials in the body of the dike, which may lead to extreme water pressures beneath a watertight revetment. Water over-pressures are caused by unequal water levels outside and inside of the dam. In particular, the piezometric levels in the body of a dike can, as the result of damping and lags, be significantly higher than the rapidly declining water level on the seaward side in the period following high water or directly after a stormflood.

The magnitude of the over-pressures is affected by a large number of factors, including:

1. the height, duration and form of the time-dependent boundary conditions (tide, stormflood) on the seaward side of the dike and the potential at the back of the dike (i.e. level of the water-course, polder or basin).
2. the permeability of the soil, including internal variations, both in and beneath the body of the dike.
3. the geometry of the dike and especially of the toe construction such as the dimensions, embankment slopes, presence or absence of sheet piling, toe height, recessing of the toe, sanding up, and silt layers on tidal flats, etc.
4. the effective storativity of the soil above the phreatic groundwater level.
5. the elevation of any impermeable layers (e.g. clay) in the subsoil.

On account of this wide variety of governing factors it is not possible to lay down any universal guidelines for over-pressures.

The latter should be calculated by means of an unsteady state groundwater calculation method. This may either be a numerical computer programme or an electric analogue.

An application of analogue analysis of this kind is shown in Figures 2.4.12.6 to 2.4.12.9 in the case of the maximum anticipated over-pressures beneath an asphalt revetment in stormflood conditions. Figure 2.4.12.6 specifies the geometry of the analogue model of the sea dike with a watertight revetment.

Figure 2.4.12.7 illustrates the stormflood boundary conditions at a design level of 5.50 m above MSL for which the measurements were made. The measurement results are shown in Figure 2.4.12.8. These indicate that the over-pressures depend heavily on the coefficient of permeability k of the sand. The maximum over-pressure values have been read off from the k value graph and plotted as an enveloping line on the detail drawing of the embankment in Figure 2.4.12.9.

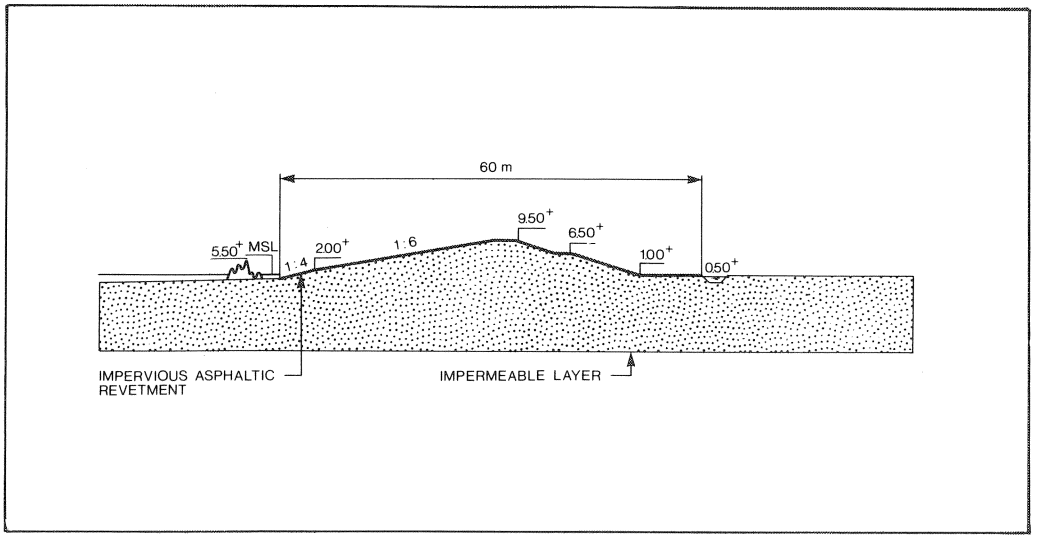

Figure 2.4.12.6 Sea dike with asphaltic revetment on which uplift waterpressures are measured using an electrical analogue model at stormsurge conditions.

This diagram also shows the uplift criterion line for the planned revetment, from which the extent to which the revetment agrees with of this criterion at the maximum calculated over-pressures may be seen.

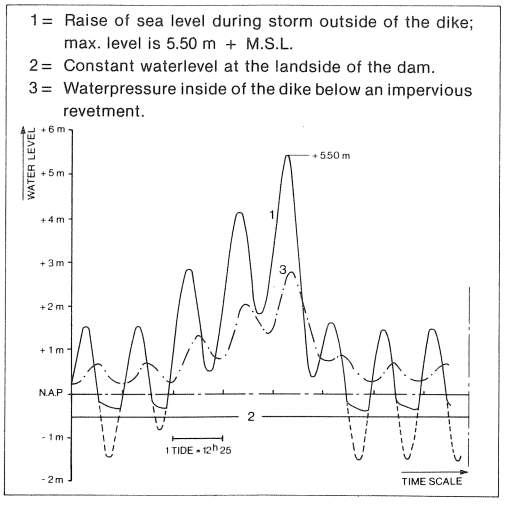

Figure 2.4.12.7 Design storm-surge curve and results of measured uplift waterpressures below a watertight revetment using an electrical analogue model.

Wave-induced groundwater stresses beneath a caisson or pier

In the case of a saturated, confined aquifer, the elastic storativity resulting from the compressibility of the soil cannot often be neglected. A confined aquifer of this kind may be created in a sea-arm by the installation of a caisson or pier. In order to prevent sub-soil scour due to both static water-level differences across the construction and dynamic wave

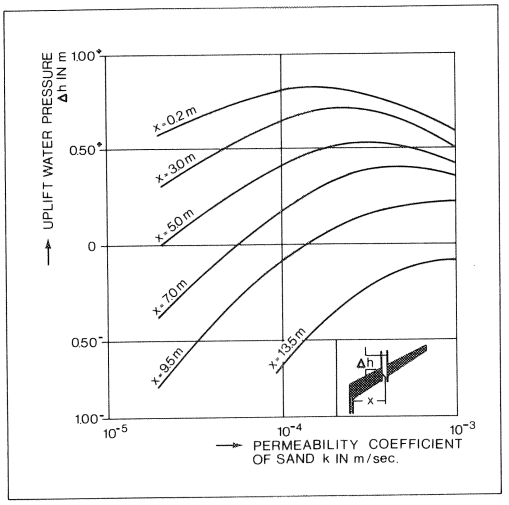

Figure 2.4.12.8 Dependence of the uplift waterpressures on the permeability (k-value) of the sand.

stresses on the structure, a granular filter must be installed between the bottom of the caisson or pier and the sub-soil. Wave penetration into the foundation layers and the cyclical movements of the caisson or pier in response to wave loads can, as the result of elastic storativity and consolidation effects in the porous media, result in damped and phase-shifted wave phenomena in the groundwater. In extreme cases this can lead to large hydraulic gradients in the foundation and filter layers, with the risk of migration of the foundation layer into the filter layer, or erosion of the filter layer. The required construction and strength of a filter to prevent erosion phenomena may be analysed by means of scale tests or various numerical calculation models. Research of this kind was carried out by the Delft Hydraulics Laboratory by means of a large scale-test in the Delta flume. This con-

Figure 2.4.12.9 Measured in electrical analogue model maximum uplift pressures on the impervious asphaltic revetment at maximum stormsurge.

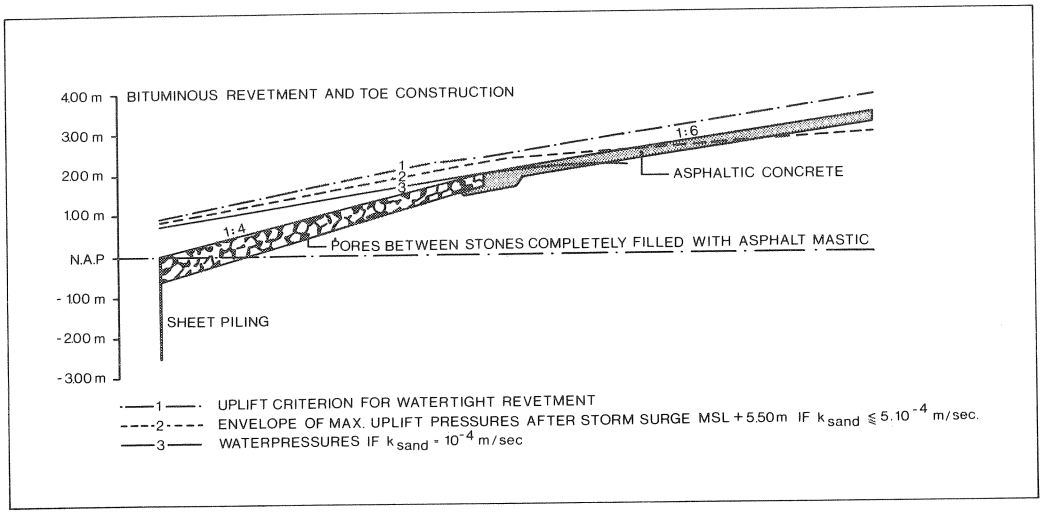

sisted of 1:6 scale model of a caisson subject to wave loads and resting on a sand subsoil.
Measurements included:

- water pressures against the front of the caisson;
- water pressures in the filter layer directly beneath the caisson; and
- water pressures at various depths and distances in the sand subsoil.

An example of these water pressure measurements is shown in Figure 2.4.12.10.
This clearly shows the damped, phased nature of the cyclical groundwater pressures. Ref. [22] provides further information on the Delta flume research and on the comparison made between the measured water pressures and those calculated by means of the numerical „SPONS" computation model.
SPONS is a numerical computer programme developed by the Delft Soil Mechanics Laboratory. It enables consolidation calculations to be carried out for a two-dimensional model under cyclical boundary conditions, assuming a flat (two-dimensional) deformation situation with linear elastic soil properties. The model is also capable of handling a heterogeneous composition of the subsoil. In this model the air-groundwater mixtures are compressible and groundwater flow occurs according to Darcy's law. Apart from any displacements this programm can also be used to calculate hydraulic pressures, either in digital form or in the form of equipotential or isochronous lines.
The SPONS programme was also used for analysing the cyclical water pressure gradients to be anticipated given maximum wave loads under the piers of the Eastern Scheldt storm-surge barrier. Figure 2.4.12.11 shows an example of the calculated iso-amplitude lines. Further details may be found in [23].

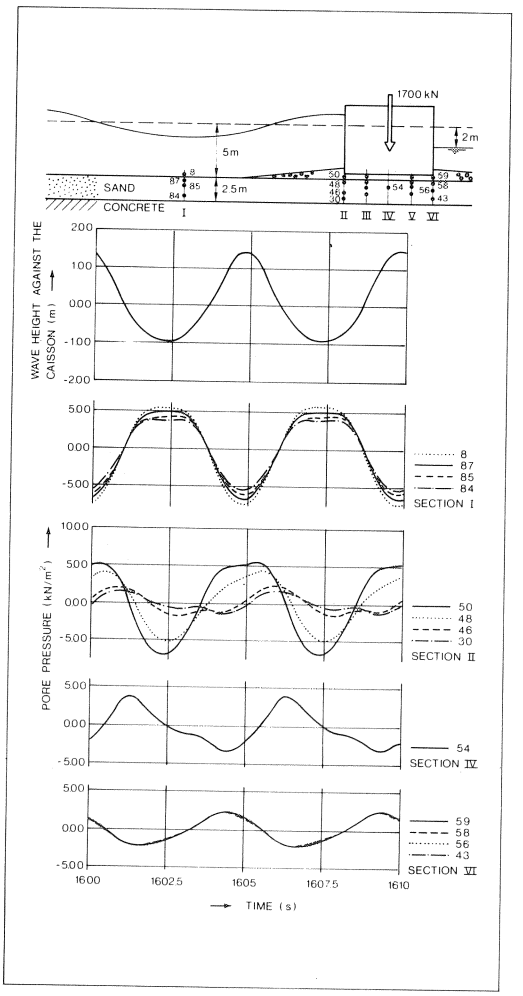

Figure 2.4.12.10 Measured pore pressures in the sand in front of and below the caisson.

Groundwater flow through coarse granular materials

A large potential difference across a coarse granular, porous structure such as a rubble dam, filter construction or filter layer and drain construction etc., can produce turbulent flows.
During the construction of a closure dam according to the sill-up method the resistance to the

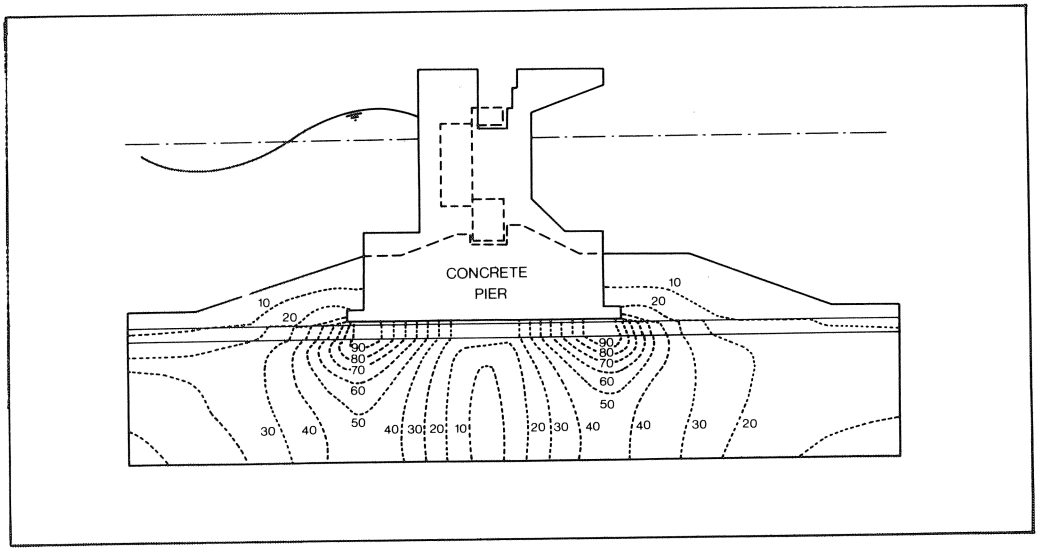

Figure 2.4.12.11 By computer program SPONS: calculated iso-amplitude lines of generated cyclic pore pressures in the subsoil below the piers of the Eastern Scheldt Barrier.

Figure 2.4.12.12 Various stages of a closure dam under construction at various tidal stages. Increasing potential drop over dam gives increasing groundwaterflow.

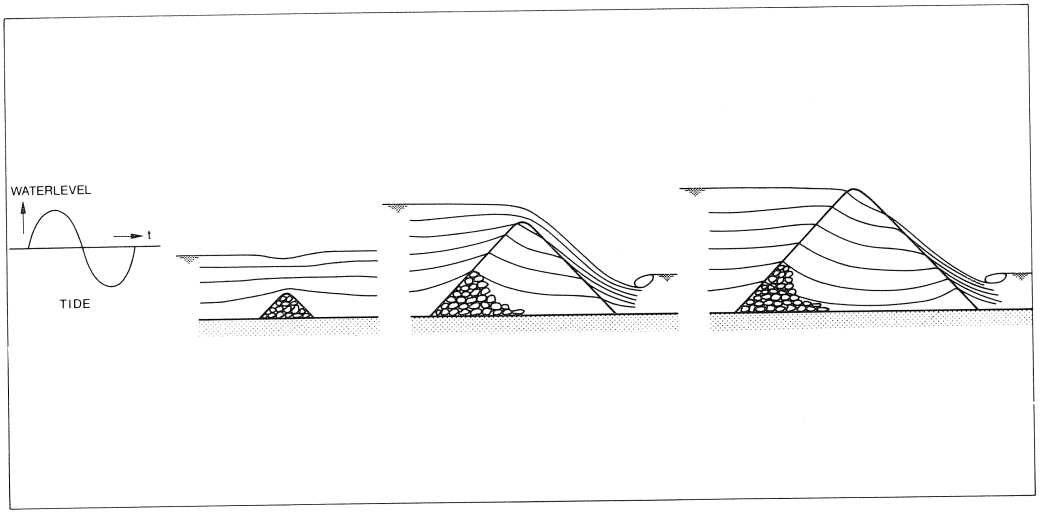

overflowing water as well as the potential drop over the dam increases. (See fig. 2.4.12.12 for various stages of execution of the dam).

The groundwater flow gradually provides a greater part of the discharge through the dam section and the character of the groundwaterflow may change from laminar into turbulent.
The gradient in the case of turbulent flow is no longer proportional to the resistance (or inversely, proportional to permeability). The gradient increases exponentially with increasing turbulent flow. As a consequence the load on the stones increases considerably. Particularly on the downstream side of the dam near the still water level where there is a concentration of flowlines the risk of instability of the stones increases. See fig. 2.4.12.13.

For calculations the actual turbulent flow is linearized, when the coefficient of permeability k^1 at each point is assumed to be dependent on the piezometric gradient i. The linearized coefficients of permeability k^1 of coarse granular materials are many times greater than those for sand, being in the order of 0.10 to 1 - 5 m/sec, varying from less coarse (gravel, cobbles etc.) to extremely coarse layers such as 1-10 tonne concrete blocks. In general the non-linearized relationship between the gradient and velocity of percolation is as follows:

$$U_f^n = a\, i$$

in which:
U_f = velocity of percolation (m/sec)
a = coefficient of permeability constant (m/sec)^n
n = exponential with:
n = 1: laminar flow
1< n < 2: transitional area from laminar to turbulent flow
n = 2: turbulent flow
i = piezometric gradient (-)

Figure 2.4.12.13 Difference in laminar and turbulent flownet. (The gradient increases in the direction of the flow).

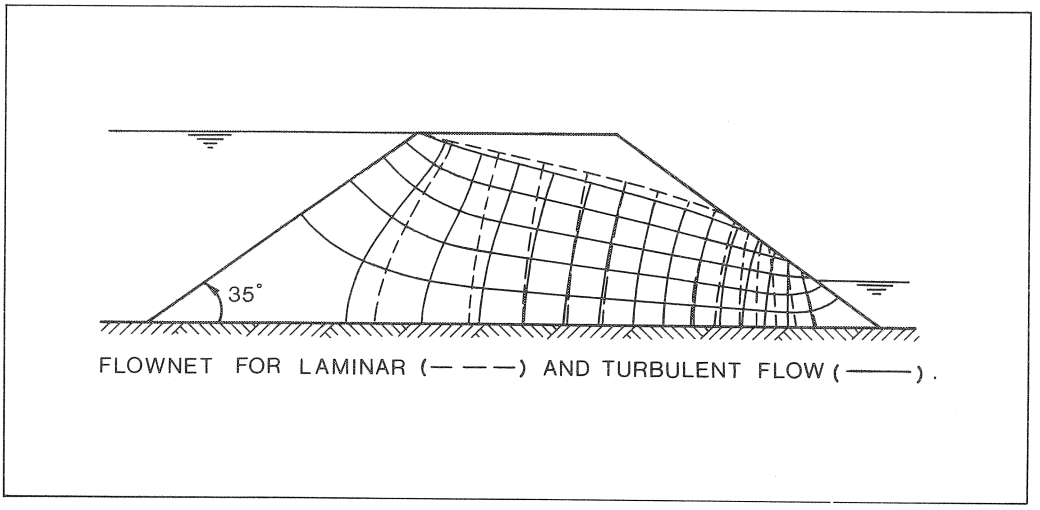

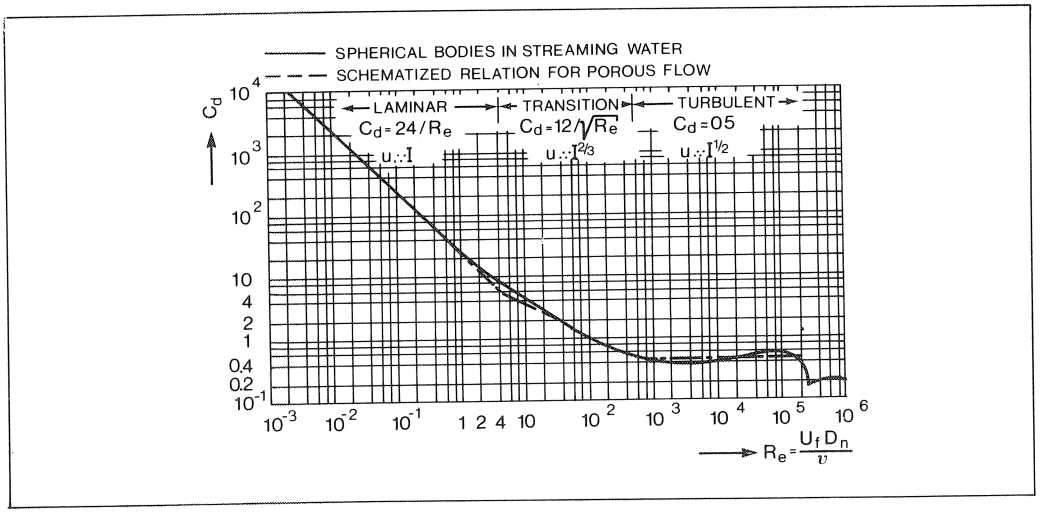

Figure 2.4.12.14 Coefficient C_d as a function of Reynolds number R_e.

Figure 2.4.12.15 Relation U_f^n = a.i. for various coarse materials as measured by the Delft Hydraulic Laboratory.

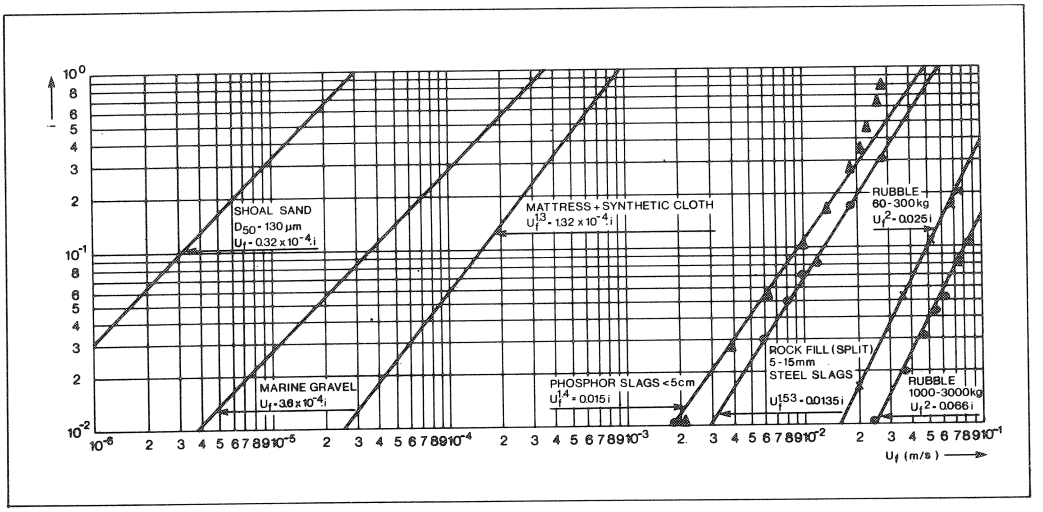

Linearization of the equation of motion and the Darcy equation gives:

$$U_f = k'i$$

which may then be written:

$$k' = a^{(\frac{1}{n})} i^{(\frac{1-n}{n})}$$

With the aid of the empirically determined Cohen de Lara formula

$$U_f^2 = 2g \frac{D_n}{C_d} n^5 i$$

in which:

U_f	=	velocity of percolation of water through the porous dam	(m/sec)
g	=	acceleration of gravity	(m/sec²)
D_n	=	determining diameter of the coarse material	(m)
n	=	porosity	(-)
C_d	=	dimensionless drag coefficient	(-)
i	=	piezometric gradient in the porous dam	(-)

and with the aid of the Reynolds number R_e in:

$$Re = \frac{U_f D_n}{\nu}$$

in which:

ν = kinematic viscosity of the fluid (m²/sec)

the coefficients of permeability a and the exponential n may be estimated on the basis of the coarseness properties of the material such as grain size D_n and the porosity n.

The drag coefficient C_d depends on the flow conditions and is characterized by the Reynolds number; see Figure 2.4.12.14. The relationship between the gradient and the velocity of percolation U_f^n = a.i has been measured for a wide variety of coarse materials by the Delft Hydraulics Laboratory; the results are set out in Figure 2.4.12.15. The linearization of these measured relationship U_f^n = a.i. to the linear Darcy flow equation $U_f = k^1.i.$ is shown in the table below.

An overall picture of the coefficient of permeability k for porous materials is provided in Figure 2.4.12.16. The Delft Soil Mechanics Laboratory has a number of numerical computer programmes (e.g. SEEP) with the aid of which the linearization of the flow equation from U_f^n = a.i, into the form $U_f = k^1.i$ can rapidly be incorporated in an iterative manner into the groundwater flow calculation process.
A more detailed treatment of this linearized calculation technique for groundwater flows in porous materials may be found in [23] and [24].

Drainage of construction pits

Another aspect of groundwater movement consits of the drainage of construction pits required for the building of engineering works such as locks or discharge sluices in barrier dikes and dams.

			k' (m/s) at a gradient of			
material	n	a	i:1.00	=0.50	=0.25	=0.10
stone 1000/3000 kg	2.0	0.066	0.25	0.36	--	--
stone 60/300 kg	2.0	0.025	0.16	0.22	0.3	--
steel slag	1.53	0.0135	0.060	0.076	0.097	--
phosphor slag	1.4	0.015	0.050	0.061	0.074	0.096
sandwich membrane	1.3	0.00013	0.0010	0.0012	0.0014	0.0018
sea gravel	1.0	0.00036	0.00036	0.00036	0.00036	0.00036
shallows sand	1.0	0.000032	0.000032	0.000032	0.000032	0.000032

Table 2.4.12.3. Measured relation U_f^n = a.i. to $U_f = k'.i.$ for various materials.

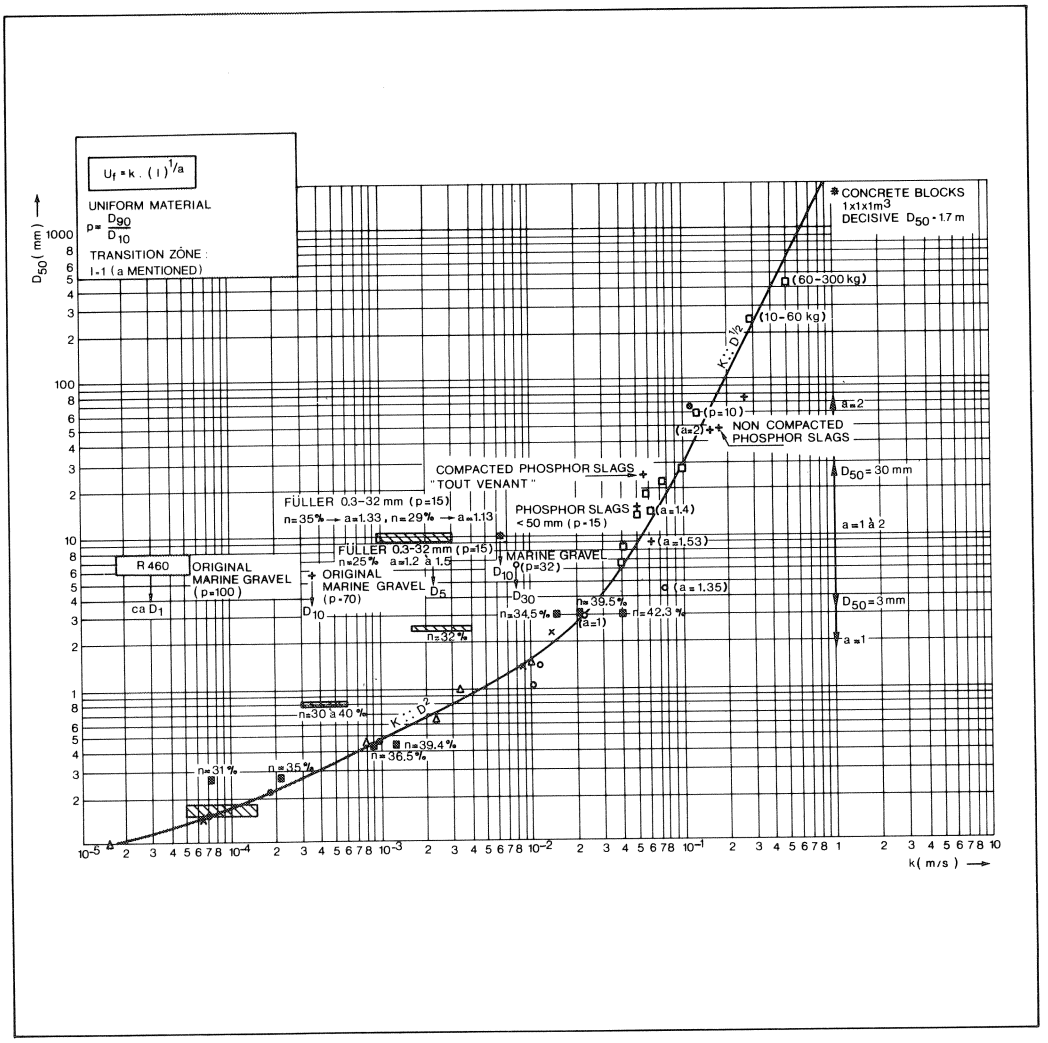

Figure 2.4.12.16 Permeability of porous media.

Drainage of a construction pit can have an effect on the surroundings and cause damage. Changes in the groundwater level can, for example, lead to undesirable settlement or to drying out in adjacent polders. The required capacity of the drainage system must be determined prior to installation. This is done by means of a groundwater computer program with a multi-layer system, in which the soil parameters and boundary

conditions have been incorporated. The soil parameters may best be determined by means of a pumping test; see [9] and [10]. The conditions in which a test of this kind is carried out should be comparable to those in the actual drainage situation. A comprehensive drainage plan is drawn up on the basis of the calculated results for the anticipated water discharge. Once a drainage system has been installed and is operative it is essential to monitor drawdown in the groundwater level by means of observation wells. This must be done not just in the construction pit itself but also for some distance outside it, since the influence of the drainage system will extend well beyond the pit itself. The range of influence depends closely on the soil parameters and the composition of the soil in the construction pit and the vicinity. In the case of sandy soils or when deep flow channels are located close to the pit, the range will be limited. If, however, a drained sand aquifer should be sealed off on top by a relatively impermeable clay layer, the impact on the surrounding will be much greater and may extend as much as several kilometres from the construction pit. With the aid of the soil parameters, groundwater calculations may be carried out to determine the sphere of influence of the drainage system.
For environmental reasons, it is necessary not only to measure the pumped discharges of a drainage system once it is in operation but also to take water samples in order to check for any impurities in the discharge.

Final remarks

The survey of various applications with respect to groundwater flow or seepage in the preceding sections makes no claims to being comprehensive. There are obviously a great many other groundwater problems susceptible to solution, both in the past and the future, to groundwater calculations based on Darcy's law. In the past in situ measurements and groundwater flow calculations were primarily concerned with quantitative aspects (e.g. the discharge Q, pressures and the gradient). For environmental reasons, close attention is also likely to be paid in the near future to quality, especially the quality of the groundwater. For example, it is necessary to determine the number and quantity of substances dissolved in the groundwater, where they are discharged, and in what quantities. There is a marked need for new measurement and calculation techniques to be devised with respect to the time such substances remain in the groundwater.
Increasing attention will have to be paid in the near future to various new types of groundwater problems. These include siltation, desalination, the release of heavy metals and pesticides transported in the water in general and from silt deposits in particular, and the pollution of groundwater by discharges and the storage of polluted fluids and materials, especially in relation to the supply of drinking water. Existing and still to be developed groundwater calculation methods may be helpful in this respect.

References

1. Bear, J., **Dynamics of Fluids in Porous Media,** American Elsevier, New York, 1972.
2. Bear, J., Irmay, S., Zaslavsky, D., **Physical Principles of Water Percolation and Seepage**; Unesco Parijs, 1968.
3. Polubarinova-Kochina, P.Ya., **Theory of Groundwater Movement,** Princeton Univ. Press., 1962.
4. Verruyt, A., **Theory of Groundwater Flow**; Mac. Millan, 1970.
5. Harr, M.E., **Groundwater and Seepage**; Mc Graw-Hill Book Company, Inc. 1962.
6. Wiest, R.J.M. de, **Flow through Porous Media**, Academic Press Inc. 1969.
7. Muskat, M., **The Flow of Homogeneous Fluids through Porous Media**, Mc Graw-Hill Book company, Inc. 1937.
8. Fahmy, M.I., **The Influence of Clay Particles on the Hydraulic Conductivity of Sandy Soils**, Diss. Wageningen, 1961.

9. Kruseman, G.P., De Ridder, N.A., **Analysis and Evaluation of Pumping Test Data,** International Institute for Land Reclamation and Improvement, Wageningen, The Netherlands, 1970.

10. Huisman, L., **Groundwater Recovery,** Macmillan, London, 1972.

11. Karplus, W.J., **Analog Simulation, Solution of Field Problems,** MacGraw-Hill Book Co., Inc. New York, 1958.

12. Huard de la Marre, P., **Publications scientifiques et techniques du Ministère de l'Air,** no 340, Paris, 1958.

13. Burg, J.A., Graauw A.F. de, Groot M.B. de, Bed Protection Adjacent to the Barrier, Proc. **Symp. on Hydraulic Aspects of Coastal Structures,** vol 2; Delft, 1980.

14. Kovács G., **Evaluation of Investigation related to Seepage through Earth Dams,** 1973.

15. Kovács G., **Characterization of the Grain Shape,** Studies Concerning Seepage, 1968.

16. Striegler W.I., Werner W., **Dammbau in Theorie und Praxis,** 1969.

17. Bligh E.W., **The Practical Design or Irrigation Works,** Londen, 1912.

18. Griffith, W.M., The Stability of Weir Foundations on Sand Soil subject to Hydrostatic Pressure, **Minutes of Proceedings J.C.E.** 1913-14. Vol 197. pt III.

19. Lane E.W., Security from Under-seepage Masonry Dams on Earth Foundations, **Trans. ASCE no. 100,** 1935.

20. Wit, J.M. de, Sellmeijer J.B., Penning A., Laboratory Testing on Piping, **Proceedings of the tenth international Confer. on Soil Mechanics and Foundation Engineering,** Vol. 1. Stockholm 1981.

21. Sellmeijer, J.B., Interpretation of Laboratory Tests on Piping, Publ. bij **Delft Soil Mechanics Laboratory L.G.M.**-mededelingen, part XXI, no. 2, 1980.

22. Lindenberg J., Swart J.H., Kenter C.J., Boer K. den, Wave Induced Pressures underneath a Caisson, A Comparison between Theory and Large Scale Tests, Publ. **Boss. Conference Behaviour of Offshore structures,** M.I.T. Cambridge, U.S.A., aug. 1982.

23. Barends, F.B.J., Thabet R.A.H., Groundwaterflow and Dynamic Gradients, **Proceed. International Symposium on Foundation Aspects of Coastal Structures,** Volume 2, part VI-1, Delft, 1978.

24. Barends, F.B.J., Advanced Methods in Groundwaterflow Computation; **Delft Soil Mechanics Laboratory,** L.G.M.-mededelingen no. XIX, part 1, 2, 3 and 4, 1978.

List of symbols

a	=	permeability coefficient of a non-Darcy-flow	$(m/sec)^n$
c_b	=	Bligh's safe weighted creep ratio	(-)
c_l	=	Lane's " " " "	(-)
c_d	=	dimensionless dragcoefficient.	(-)
c_v	=	Coefficient of consolidation	(m^2/sec)
D_{50}	=	Mean value in diameter of the grain-size diagram	(m)
g	=	gravitational acceleration	(m/sec^2)
h	=	piezometric head or potential = $z + p/\varrho g$.	(m)
H	=	loss of hydraulic head	(m)

i	=	piezometric gradient	(-)
k	=	faktor or coefficient of permeability of soils	(m/sec)
L	=	seepage-length	(m)
n	=	porosity, exponential	(-)
n_e	=	effective porosity	(-)
p	=	hydrostatic waterpressure	(N/m^2)
Re	=	Reynolds number	(-)
S	=	Specific (elastic) aquifer storativity	(-)
U_f	=	filter velocity	(m/sec)
z	=	elevation head	(m)
ν	=	kinematic viscosity of a fluid	(m^2/sec)
ϱ	=	density	(kg/m^3)

Interaction Water Motion and Closing Elements

K.W. Pilarczyk

2.4.13 Filters

2.4.13.1 Introduction

A filter, one of the most common elements in civil engineering practice, plays an important role in the total stability of hydraulic structures. Successive stone layers (granular filters) and recently also geotextiles (synthetic filters) are frequently applied in civil engineering. The primary function of a filter is to protect an underlaying layer, i.e. to prevent its particles from being washed out through the coarser top layer (see Fig.2.4.13.1.). One of the important requirements applying to the filters is that the filter should be permeable enough to avoid the development of uplift pressures.
The granular filter is widely accepted in practice and there is good experience with the maintenance of its permeability in the long-term. On the other hand, it is difficult to construct under water and it can be difficult to find the required material (see Fig. 2.4.13.2).
The synthetic filter can be applied almost everywhere. An obvious advantage is that it has tensile strength. Negative points of synthetic filters include a decrease in permeability in the longterm and bio-deterioration.

With respect to filter design, two specific aspects concerning its sand retaining function may be distinguished (see Figs.2.4.13.3-5). The first concerns the load conditions (acting hydraulic gradient,I), while the second aspect concerns the strength of the filter, i.e. its ability to withstand the exerted load and the possible erosion (settlement) that will take place if a certain (design) load is exceeded. A widely used strength parameter is the critical hydraulic gradient I_{cr} at which the filter starts to loose its sand-retaining function. The safety factor for the filter construction may be defined as a reserve in filter-strength related to the design load, viz.:

$$\text{safety factor } F_s = \frac{\text{strength}}{\text{load}} \text{ , e.g. } = \frac{I_{cr}}{I} \quad (1)$$

Except in certain cases, however (see section 13.4), the state of knowledge of filter strength does not permit the safety coefficient to be quantified. Further research is still needed to enable this to be done.

Because of the obvious physical difference between granular and synthetic filters, the strength of these filters will be discussed separately.
With respect to the strength of granular filters, some new developments regarding the influence of different load types (flow situations)will be mentioned.

Although the problem of designing a filter according to classical filter rules comes under the strength aspect, the general principles of classical rules will, in the interests of a better understanding of the problem, be discussed in combination with the functional requirements of filters (section 2.4.13.3).

2.4.13.2 Load conditions

The load conditions on filters are governed by the type of the external hydraulic load, which can be subdivided into:
- stationary hydraulic loading; dikes along canals and reservoirs,foundations of sluices and weirs and filters of well-points,
- semi stationary hydraulic loading (periods of a few hours or days); river and canal banks, shore and dike protection in tidal areas, drain trenches behind retaining structures, and sluices and weirs in tidal areas.
- cyclical hydraulic loading (waves); breakwaters, shore and sea-bed protections, foundations of offshore and coastal constructions, particularly the Eastern Scheldt Stormsurge Barrier (the combined effect of static pressure head and waves and the motion of the construction due to this effect may cause a strong cyclical flow in the foundation),
- dynamic hydraulic loading (wave impact and earthquakes); shore protection and foundations of constructions in areas with seismic activity.

In most cases there will be a combination of the above load conditions.

In the case of dynamic loading introduced by wave impact and earthquakes, inertial forces have an important effect on the grains of the

filter construction. As far as known, very little research has been carried out on the behaviour of filter under dynamic loading. This type of loading will therefore be left out of consideration here.

The hydraulic load on a filter may be defined as the stationary and/or cyclical gradient(s) (I) due to the stationary and/or non-stationary groundwater motion as influenced by the external load (waves, currents, water-level fluctuations etc.). It should be noted that the hydraulic gradients may cause the effective grain stress to diminish. The effective grain stress is one of the factors governing the strength of the filter (i.e. because of the increase in pore pressure, internal friction decreases).

The hydraulic gradient (I) is actually the seepage force on the grains. This force must be at least in equilibrium with the other forces in the grain skeleton, such as gravity and friction. When the external loading (waves and/or head loss) on the construction is known, the hydraulic gradients in the filter can be determined by means of the calculation methods given in chapter 2.4.12 and in [1]. In more specific or complicated cases, a model investigation may be applied.
If no erosion (settlement) of the filter layer is permitted, it is sufficient to calculate the hydraulic gradient for the extreme situation (waves and head loss). However, a limited settlement is often acceptable during the lifetime of the construction. Therefore the distribution of the hydraulic gradient over time must be established for both the normal and the extreme situation.

In view of the different types of external load and various geometrical aspects of a filter in a structure, the following groundwater-flow situations may be induced (see also Fig. 2.4.13.4):
a steady flow parallel to the interface;
b steady flow perpendicular to the interface;
c cyclical flow parallel to the interface;
d cyclical flow perpendicular to the interface
Combinations of these four situations may of course also occur.

The filter can therefore be loaded by the different hydraulic gradients resulting from the presence of one of these flow types or their combination. The relation between the strength of a filter and the various types of loading is discussed in the section 13.4.

2.4.13.3 Functional requirements and standard filter rules

Granular filters are designed in successively coarser layers proceeding outwards from the underlying (finer soil). The first layer should hold the base material (i.e. subsoil), while each following layer has to be able to hold the underlying one (see Fig. 2.4.13.1.). The outer layer must also be stable under the prevailing open boundary conditions. The number of layers will depend on the size of the underlying material and overlying top-layer and their gradations.
The stability against piping (that is, not allowing the soil to be washed out) and drainage (permeability) properties depends on the grain-size distribution of the filter and base material. The design of a filter thus requires a knowledge of the particle distribution diagram (sieve curve) of the in situ soil, and that of the filter materials available.
To define the filter requirements, sieve diameters D_{15}, D_{50} and D_{85} are generally applied. These correspond to particle diameters where 15%, 50% and 85% of the material (by weight) is finer than the sieve size (Fig. 2.4.13.2.). For specific requirements, however, sieve diameters D_{10}, D_{60} and D_{90} are also used.
To design a filter allowing water to pass through without allowing the soil to „pipe" (be washed out), the following three hydraulic criteria must generally be satisfied [15] [17]:
1°. The D_{15} filter < (5 x D_{85} base) Stability or Piping Criterion
2°. The D_{15} filter > (5 x D_{15} base) Permeability Criterion
3°. The D_{50} filter < (25x D_{50} base) Uniformity Criterion
NB. base = subsoil or under-layer of successive filter layer to be protected.
The first criterion governs the fine particle sizes of the filter. To prevent washing out of the underlying material into the filter, the smaller

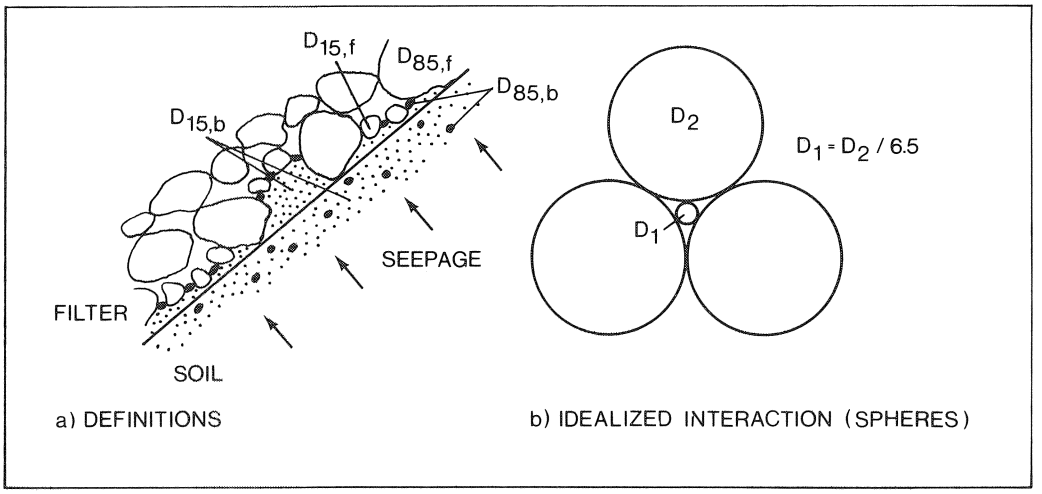

Figure 2.4.13.1 Filter-soil interface
a) definitions
b) idealized interaction (spheres).

Figure 2.4.13.2 Standard design method for granular filters.

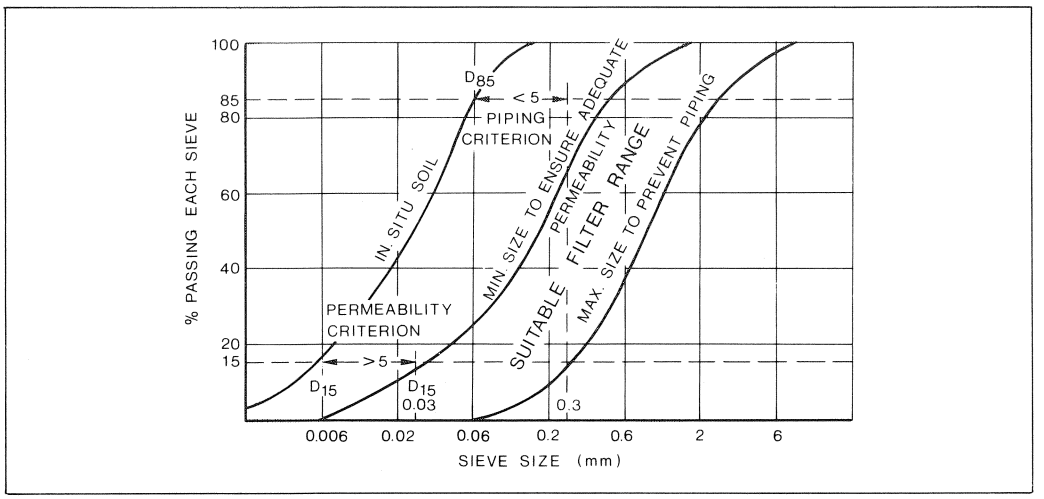

particles in the filter should be small enough to trap the larger particles of the underlying material. The concept is illustrated in Fig. 2.4.13.1. Three equal-sized spheres in contact will prevent spheres larger than 1/6.5 times the larger-sphere diameter from passing through the interstices of the larger spheres [17, 26]. For uneven-shaped natural materials, the first criterion ensures that at least 15% of the filter is of the same order of size as the coarser end of the soil distribution curve. Consequently the soil particles cannot move into the filter since there is a large number of fine filter particles available to hold them back [15].
The second criterion relates to permeability. This must operate effectively at the same time as the first, for although the filter is required to hold back soil particles as specified in the first criterion, it is also necessary that sufficient water be allowed out of the soil to prevent the build-up of uplift pressures within the soil itself. The permeability of the filter should therefore be sufficient for the hydraulic gradient through it to be negligible compared with that through the underlying material.

Since the overall permeability of the soil is similarly governed by its smaller particles for which the D_{15} size can be taken as representative, and the overall permeability of the filter is governed by its D_{15} size, then providing the filter's D_{15} is more than five times that of the soil, the filter will have ample excess permeability over the soil and will not sustain a backhead of water pressure. It will allow water to enter and flow freely through it [15].
The third criterion -which is rarely applied - is intended to ensure that the overall principles of overlapping filters and relative particle sizes are maintained relative to one another right across the particle distribution curve range. It implies therefore that the grading of each layer should be approximately parallel and not too far apart to minimize segregation (migration).
This criterion may be relaxed for plastic clays, which have high cohesion strength [17].

Once the particle distribution diagram of the natural soil is known, one can establish the criteria for a filter layer or even a series of filters to prevent 'piping' whilst still allowing adequate drainage. Multiple filters simply have a series of curves conforming to the above rules. Typical grading curves for successive filter layers are plotted in Fig. 2.4.13.2 where the application of the filter rules is also illustrated; such charts should be used in the design of filters.
The knowledge of the principles mentioned above is important not only for granular filters but also in the case of applying synthetic filter cloths (geotextiles) which are often used to replace one or more of the costly elements in multi-filter granular systems designed on the above basis (i.e. fulfilling the same functional requirements), [15].

The general criteria mentioned above (1°, 2° and 3°) are often referred to as the Terzaghi criteria (19). More recently, these criteria have been ex-

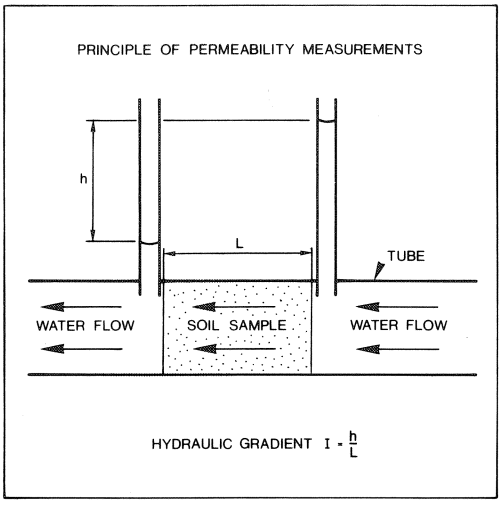

Figure 2.4.13.3 Principle of permeability measurement and definition of hydraulic gradient.

tended and strengthened by various authors for cases where almost absolute filter quality performance of filter is needed. These criteria can be used in special cases, for example if no settlement is allowed.
The standard filter requirements as developed up till now are summarized below.

Summary of standard filter criteria

I. Stability criterion:
The finer particles of an underlayer should be prevented from being washed out through the layer on top of it. The main criterion is:

Ia: $$\frac{D_{15,\ filter}}{D_{85,\ base}} < 5 \qquad (2)$$

Ib: According to [4], penetration of base material into the filter layer is prevented if:

$$D_{50,\ filter} \leq 3 \text{ to } 5\ D_{50,\ base} \qquad (3)$$

$$(\text{or } n_f D_{15,filter} \leq 1 \text{ to } 1.6\ D_{50,\ base})$$

where n_f = porosity of filter material. Factor 3 may be seen as a geometrical limit for penetration into the filter layer and is to be used in the case of strong cyclical flow. Factor 5 may be used only in the case of steady flow.

The above requirements are relative ones. The requirements developed experimentally by Kawakami and Esashi [7] have been based on the absolute dimension of the grains. The filter will be stable when:

$$\log\left[\frac{D_{10,filter}}{D_{10,base}} - 2\right] < \frac{1.9}{\log\left[D_{10,base} - 0.001)\,10^3\right]} \qquad (4)$$

where D_{10} is in millimeters.

II. Permeability criterion
The permeability of the filter should be sufficient for the hydraulic gradient through it to be negligible compared with that through the underlying material (i.e. without local build-up of hydraulic gradient concentrations). The main criterion is:

$$\frac{D_{15,filter}}{D_{15,base}} > 4 \text{ (or } 5) \qquad (5)$$

III. Uniformity criterion. Segregation and Internal Stability
IIIa. Segregation
The grading of each layer should be approximately parallel, and not too far apart to minimize segregation. This criterion is expressed as follows:

$$\frac{D_{50,filter}}{D_{50,base}} < 25 \qquad (6)$$

Internal stability
The grain-size distribution of each layer should preferably be approximately uniform to satisfy the internal stability of the filter layers(no internal migration of particles).
In the grain-size distribution no lack of intermediate grain-sizes may occur. As for the stability criterion the requirements for the internal stability have been based on the grain-size distribution:

$$U = \frac{D_{60}}{D_{10}} \quad (U = \text{coefficient of uniformity}) \qquad (7)$$

no migration	: $U < 10$
possible migration (depending on hydraulic conditions)	: $10 < U < 20$
migration	: $20 < U$

Specifications for two points of the grain-size distribution curve only are given above. Lubotshkow [10, 11] gives requirements related to a description of the whole grain-size distribution.

IV. Thickness criterion

Theoretically the minimum layer thickness is equal to roughly several times the nominal grain size (see also Wittman [32]).

However, due to irregularities in placing (especially in the case of dumping methods), the thickness of the layers is subject to a practical minimum, e.g.[27]:

coarse sand	:	d = 10 cm
gravel	:	d = 20 cm
dumped stone	:	d = 2 to 3 times the size of the largest stones

(d = thickness of the filter layer).

If the layers have to be placed under water or if the subsoil is uneven, it is a safe policy to increase the thickness of the layers. To prevent segregation of the material when dumped into water, it is often advisable to mix the material with a few percent of water beforehand and to place it in thin layers. According to Stephenson [17], the total filter thickness should be at least equal to 0.5 times the size of the overlying rock, to ensure it is not displaced when riprap is dumped on it.

It has to be pointed out that all these standard rules have been experimentally established under predominantly stationary conditions and generally meet the needs up to very high pressure gradients (absolute stability). A filter construction based on these requirements is thus independent of the hydraulic loading and there will be hardly any erosion of the interface of the filter. In most cases, this design procedure might lead to overdimensioning of the filter (very safe but often also very expensive and/or difficult to execute). In spite of this, these requirements are accepted all over the world and applied to more or less all types of structure.

In practice, the first mentioned criteria (1°, 2° and 3°) extended with the thickness criteria (regarding minimum thickness) will usually be sufficient for filter design. For further simplification of design, especially regarding filter revetment, Stephenson's remarks as given below will be of value.

For rockfill overlayer and rock/gravel filterlayers, the filter criteria may often be somewhat simplified (especially in the case of filter revetment) as given by Stephenson [17].

The size of rockfill will not vary much if it is selected and screened in a certain rock-class; the maximum nominal size is in fact normally about twice the minimum. Due to the narrow grading curve, the maximum size can replace the D_{85} and the minimum the D_{15} size. The stability criterion for stone filter layers becomes

$$D_{\text{overlayer}} < 10 \times D_{\text{underlayer}} \qquad (8)$$

where D refers to the nominal size. The permeability criterion and uniformity criterion are normally satisfied for rock.

Thus, to prevent underlying filter material washing into a stone layer, the nominal stone size of the overlying layer should not exceed ten times the nominal size of the underlying layer if it is rockfill or five times the D_{85} size if the underlying material is soil.

To prevent the filter or the riprap washing itself out, the maximum stone size in any layer should not exceed 10 times the minimum stone size in that layer.

In addition, the filter size should be fine enough to ensure that the water velocity within the voids will not scour the underlying material. Based on results for channel linings, Stephenson gives a stone size:

$$D = \frac{KV_v^2}{gi} \qquad (9)$$

where K is approximately 2 for gravel, „i" is the embankment slope, tan α (e.g.1/3), and V_v is the velocity in the rock voids which should not exceed the scour velocity of the underlying finer material. The equation is based on the premise that the rundown velocity will control this proces and reach an equilibrium value such that the friction gradient will equal the embankment slope.

In the case of a filter revetment or bottom protection below spillways or outlets, the top-layer of the filter is also the protective layer and has to resist the external loading (currents and wave forces). The stability of such a top-layer has to be designed using criteria mentioned in § 2.4.8. and 2.4.11.

2.4.13.4 Strength of granular filters

General

From the previous discussion it becomes obvious that the majority of current filter designs are based on rather conservative principles. Except in the case of steady flow parallel to the interface - the situation on which most of the information is available - designs are always based on geometrical considerations (size of base material relative to filter pore sizes) regardless of the flow intensity through the filter construction.
On the one hand this is due to the fact that there is a lack of information on the relationship between the flow in the filter (and subsoil) and the start of base material motion and, on the other hand, to the fact that the information available on the acting hydraulic gradient and its distribution as a function of time and space is usually scarce. Although the qualitative value of the current (standard)design rules cannot be doubted, savings in terms of quantity can certainly be achieved through the introduction of rules for filter design that take account of flow situations (see below). It has to be pointed out that such a design approach needs detailed information about the expected magnitude and time-history of load (I) and the (accurate) strength parameter of the filter (I_{cr}) for different load types. In most cases this information can be obtained from mathematical models, special tests or in-situ examinations on similar structures as that under consideration. For important and/or costly projects this leads to a most appropriate/safe design, and often to reduction of cost. An example of this can be found in [13], where the available filter materials, judged as not applicable according to standard rules, were found to satisfy the filter requirements when the strength of the filter was related to the actual load.
Although most filter constructions will still be designed according to the standard rules, the evaluation of the existing knowledge on the strength of filters under various flow conditions gives some information and better understanding about the strength mechanisms of the filter, and a general impression about the possible reserves of the filter.
However, in the absence of quantitative data on the hydraulic gradients it is advisable to design the granular filter layers according to the well-known standard filter rules as discussed in the previous section.

Strength definition

The strength of a filter may be characterized by the hydraulic gradient (fig. 2.4.13.3) at which the base material starts to migrate into or through the filter (usually denoted as I_{cr}).
This critical gradient is defined in the medium where the force responsible for the transport acts, and is different for gradients perpendicular to the interface and those parallel to it (see Fig. 2.4.13.4.). With flow parallel to the interface, the gradient is defined in the filter layer. With flow perpendicular to the interface, the gradient is defined in the base material(soil). A cyclical gradient perpendicular to the interface occurs due to amplitude and phase difference between the filter and base material.
If the hydraulic gradient I exceeds I_{cr}, the base material will be transported. The rate of „transport" is a function of $(I - I_{cr})$. In fact, there exists a certain range of $I > I_{cr}$ where the rate of transport is very small (Fig. 2.4.13.5.), [16]. Beyond this range, the transport becomes substantial. The designer should aim at keeping the hydraulic gradients under extreme conditions below a certain level of transport. Since the total amount of transport is the product of transport and time, and since the duration of the extreme conditions is by definition short, only a very small transport may result during the lifetime of the construction.
Transport of the soil under groundwater action will result in some settlement. As long as the total quantity remains small (one has to think in the order of a few millimetres within the lifetime of the structure in case of foundation elements of offshore and closing structures), such settlement is acceptable. In the case of slope-protective structures, the acceptable settlement can be even larger depending on the type of structure (a few centimetres settlement can be acceptable within the lifetime of riprap-protection structures).

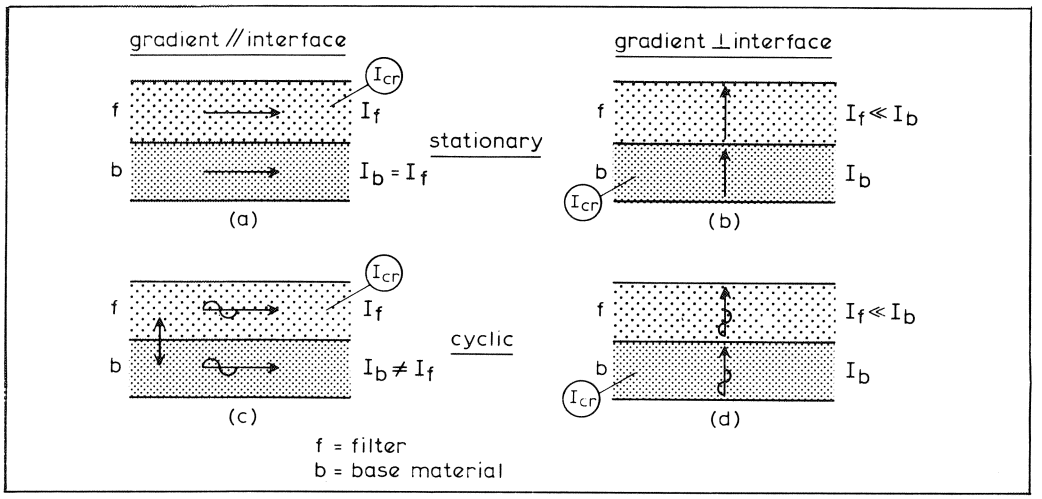

Figure 2.4.13.4 Definitions of gradienst.

Figure 2.4.13.5 Transport rate as a function of the hydraulic gradient.

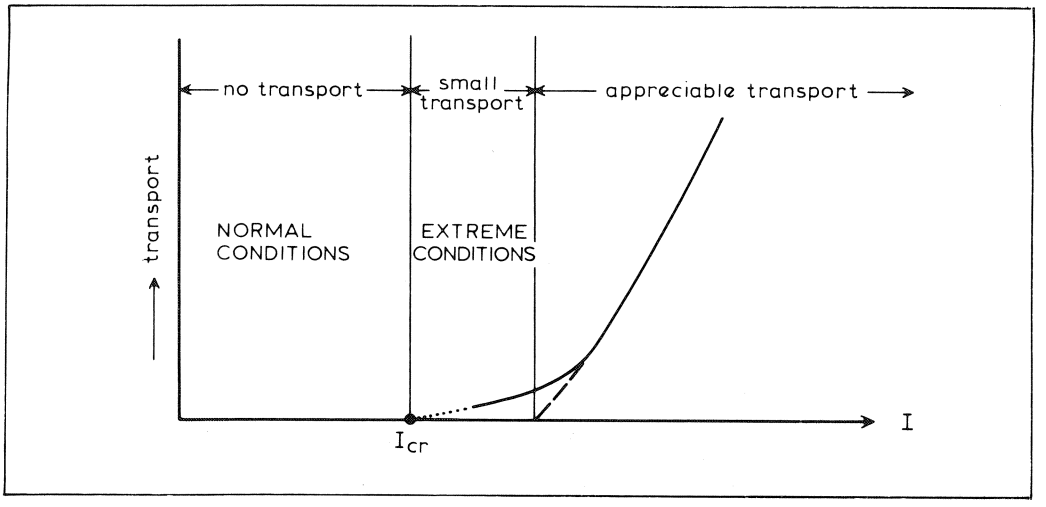

In general, the magnitude of I_{cr} is a function of [4,16]:

- characteristics of the base material: grain shape, size and size distribution, porosity and packing.
- type of flow, which is a function of the filter velocity and the physical properties of the porous material and the pore fluid, and may be characterized by the Reynolds number of the porous flow:

$$Re = \frac{u_f D}{\nu} \qquad (10)$$

where

u_f	=	filter velocity	(m/s)
D	=	characteristic size of the porous material	(m)
ν	=	kinematic viscosity of the fluid	(m^2/s)

In fact the Re-number is not entirely an independent parameter. The magnitude of the filter velocity depends firstly on the fluid boundary conditions (gradient I) and secondly on the characteristics of the filter or base material.

After combining and re-arranging the parameters, the following functional relationship is obtained for the critical gradient I_{cr}:

$$I_{cr} = f(D_{ib}, \frac{D_{if}}{D_{ib}}, n_b, n_f) \qquad (11)$$

where D_i is a characteristic grain diameter, n the porosity, index b denoting the base material and index f the filter layer. The choice of the characteristic grain diameter should involve the gradation of the material. The influence of the grain shape is considered to be of secondary importance and is thus eliminated in the above relation.
The effect of the Re-number is implicitly included in the other parameters. Although the elastic characteristics of the porous media influence the generated velocities and gradients, they are only of secondary importance as a parameter describing the critical gradient for a given combination of filter and base materials. A more or less similar relationship is valid for synthetic fabrics. It is obvious that I_{cr} will increase with decreasing D_{if}/D_{ib}, ultimately reaching the values given by the classical filter rules.

Finally, it should be noted that filter tests can only be carried out at a scale of I:I due to the influence of (the absolute magnitude of) D_{ib} and the role of the type of flow.
This condition rules out the scale model as a tool for the design of (the various layers of) bank protection and similar structures. A possible approach is to calculate the expected gradients by computational models and then to test the specific strength of the filter on a section at scale of I:I in an apparatus as described hereafter.
Next, some experimental results for granular filters are given, obtained during investigations carried out within the framework of the studies for the Delta works and in particular for the Eastern Scheldt Barrier (Oosterschelde).

Besides the cases shown in Figure 2.4.13.4., some other combinations of these cases were also investigated.

Behaviour of granular filters under static and cyclical loading

The comments are restricted to non-cohesive (base and filter) materials, and based on recent research carried out by the Delft Hydraulic and Soil-Mechanics Laboratories and the Delta Department of the Dutch Public Works Dept. as summarized in [4],[16],[30].
These results provided the data necessary for the design of the foundation of the Eastern Scheldt Barrier. A more systematic approach, however, is still needed to enable the establishment of design rules, in particular for the case of predominantly cyclical or dynamic loading (i.e. due to wave impact).

(a) Stationary flow parallel to the interface (see Fig. 2.4.13.6.) The tests were carried out with a few base materials and various filter materials (uniform materials).
The successive shift of the relation lines for the

various base-filter combinations reflects the effect of D_b (and Re) on the magnitude of I_{cr}. This result confirms, at least qualitatively, the results of Kawakami and Esashi[7].

It appears that, for a given ratio $n_f D_{15f}/D_{50b}$, the critical hydraulic gradient is greater in the case of fine base material then with coarse base material. However, the influence of the size of

Figure 2.4.13.6 Critical hydraulic gradient with steady flow parallel to interface.
a) Test rig in filter box en
b) Results

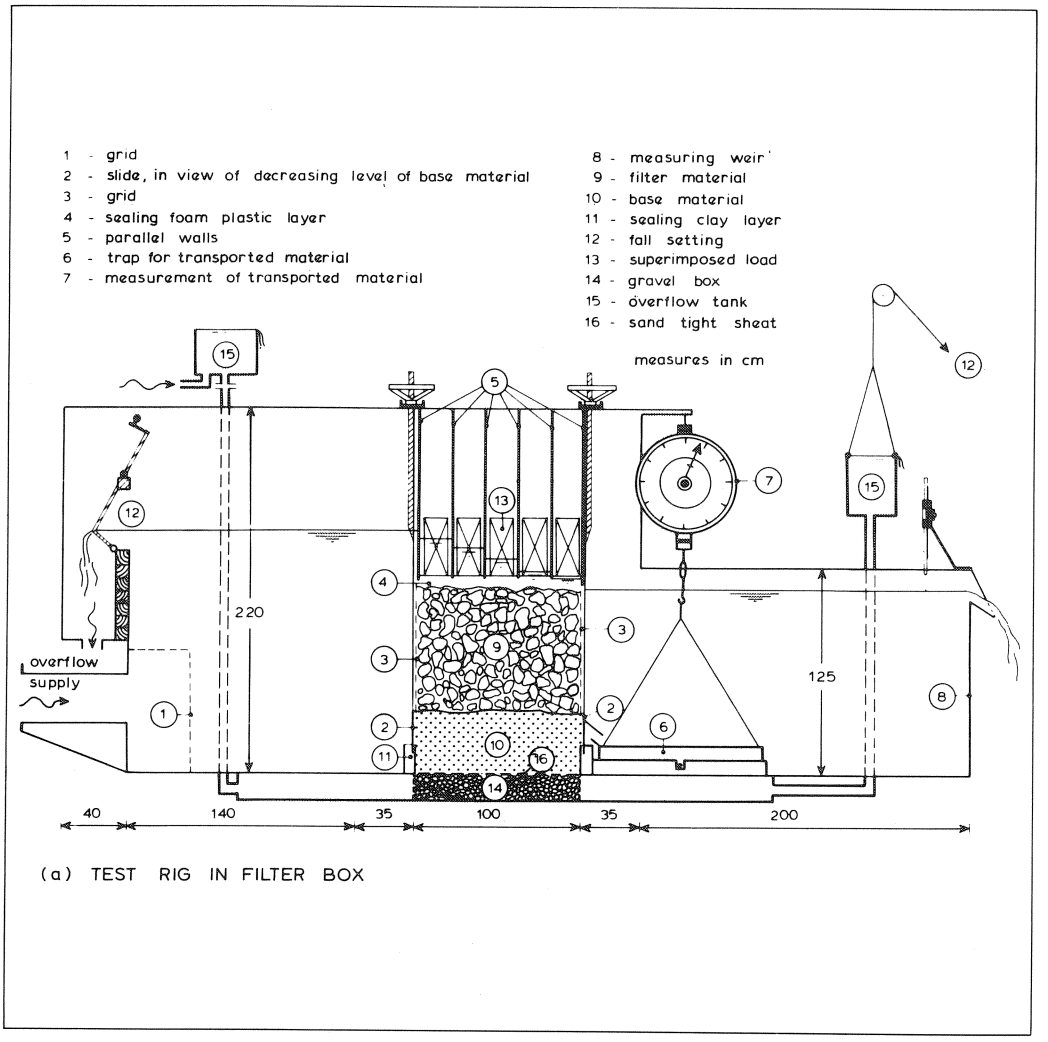

(a) TEST RIG IN FILTER BOX

the base material is negligible for gravel with $D_{50b} > 5$ mm. When characterized by means of D_{15}, the graded filter materials as well as the uniform filter materials may be described by the same function, as the points in figure 2.4.13.6 are fairly grouped for each base material tested. In the case of graded base material, it may be assumed that the base material will be better characterized by D_{85}.

Assuming an analogy between flow in pipes and porous media, an attempt was made at quantifying critical gradients through optimization using the tests results referred to above. Thus, the following empirical relation was found according to [4]:

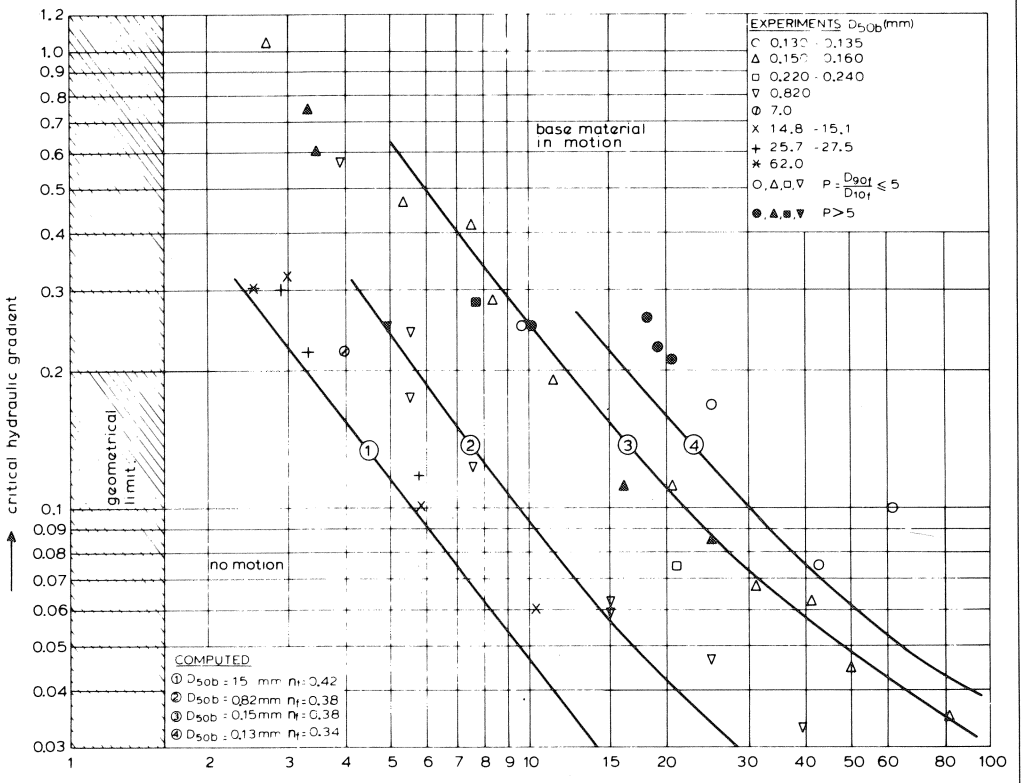

(b) RESULTS

CRITICAL HYDRAULIC GRADIENT WITH STEADY FLOW PARALLEL TO INTERFACE

$$I_{cr} = \left[\frac{0.06}{n_f^{3} D_f^{4/3}} + \frac{n_f^{5/3} D_f^{1/3}}{1000 D_b^{5/3}} \right] V^{*2}_{cr} \qquad (12)$$

where I_{cr} = critical hydraulic gradient parallel to interface; $D_f = D_{15}$ filter material (m); $D_b = D_{50}$ base material (m);
n_f = porosity of filter material; V^*_{cr} = critical

Figure 2.4.13.7 Critical hydraulic gradients with steady flow perpendicular to interface.
a) Test rig in filter cylinder
b) Results

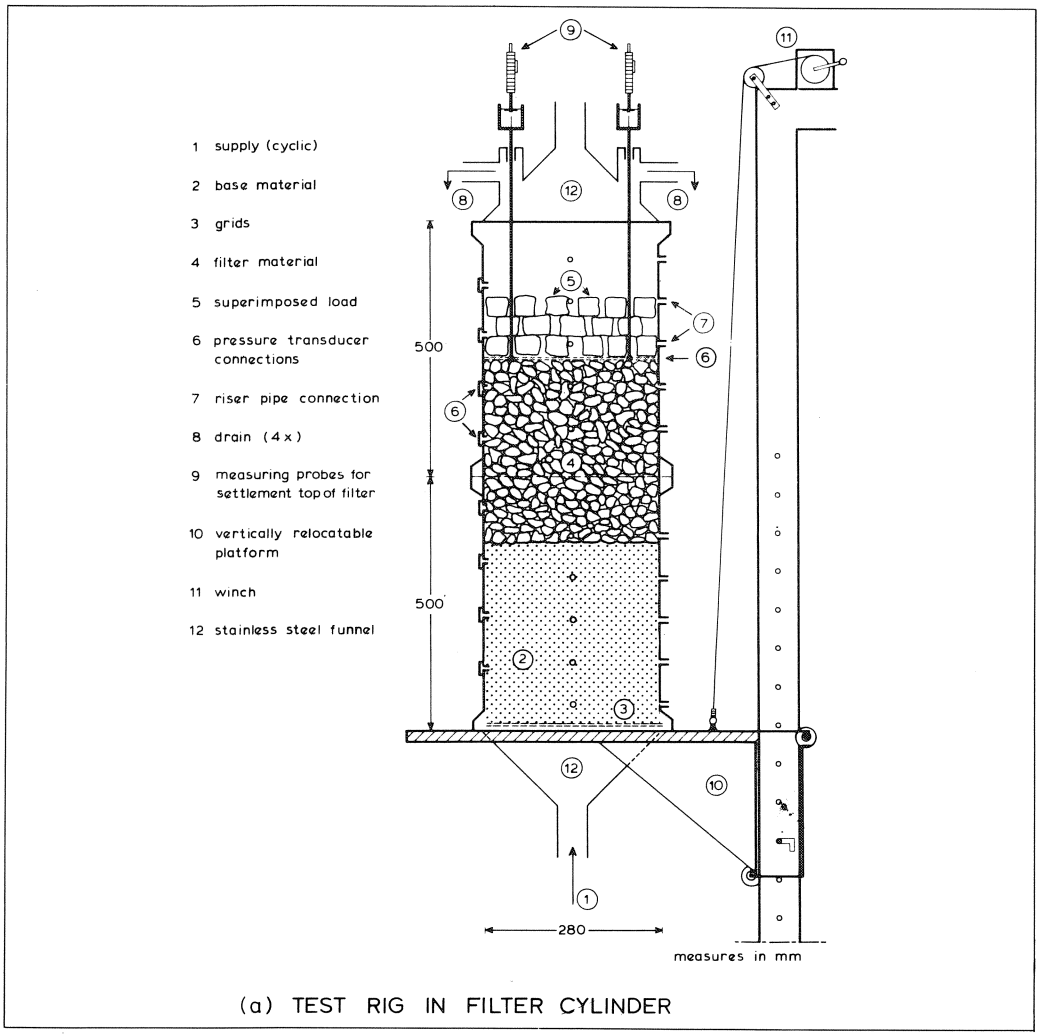

(a) TEST RIG IN FILTER CYLINDER

shear velocity of base material (m/s), approximated from Shield's diagram

$= 1.3\ D_b^{0.57} + 8.3\ 10^{-8} D_b^{-1.2}$ for sand.

The lines given in figure 2.4.13.6. are calculated from the above relation and provide a somewhat pessimistic impression of the hydraulic gradients. The physical significance of both terms of this relation is discussed in [4].

(b) Stationary flow perpendicular to the interface

(see Fig. 2.4.13.7). The trend with regard to the effect of the grain-size is the same as with flow parallel to the interface. The minimum critical gradient for upward flow is about 1 (minimum gradient to counteract the gravity force for sand of 2650 kg/m³ and n = 0.38). It is also referred to as the fluidization condition.

Combination of (a) and (b); stationary flow at an angle to the interface:

The tests were carried out in the apparatus of case (a), figure 2.4.13.6. Some of the results are shown in Fig. 2.4.13.8. It can be seen that the critical gradient for flow parallel to the interface is hardly affected by the vertical component of the flow. Close to the critical value of I perpendicular to the interface (about 1, see Fig. 2.4.13.7), the horizontal component of the critical flow drops rather suddenly.

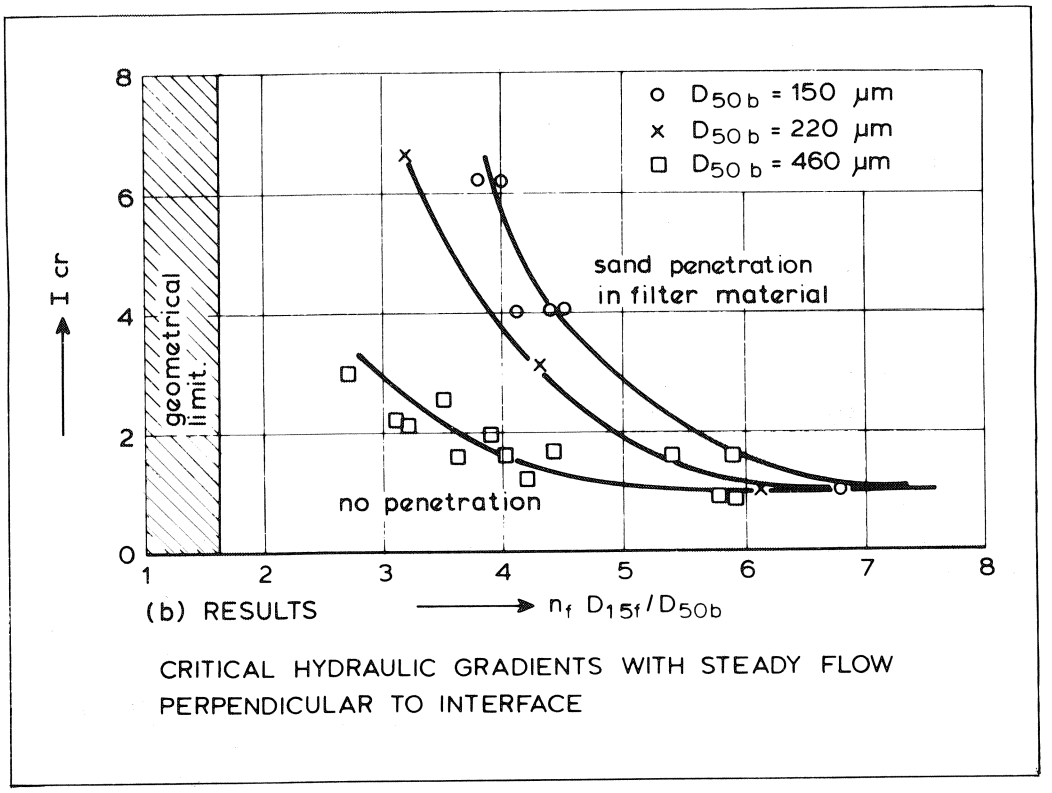

CRITICAL HYDRAULIC GRADIENTS WITH STEADY FLOW PERPENDICULAR TO INTERFACE

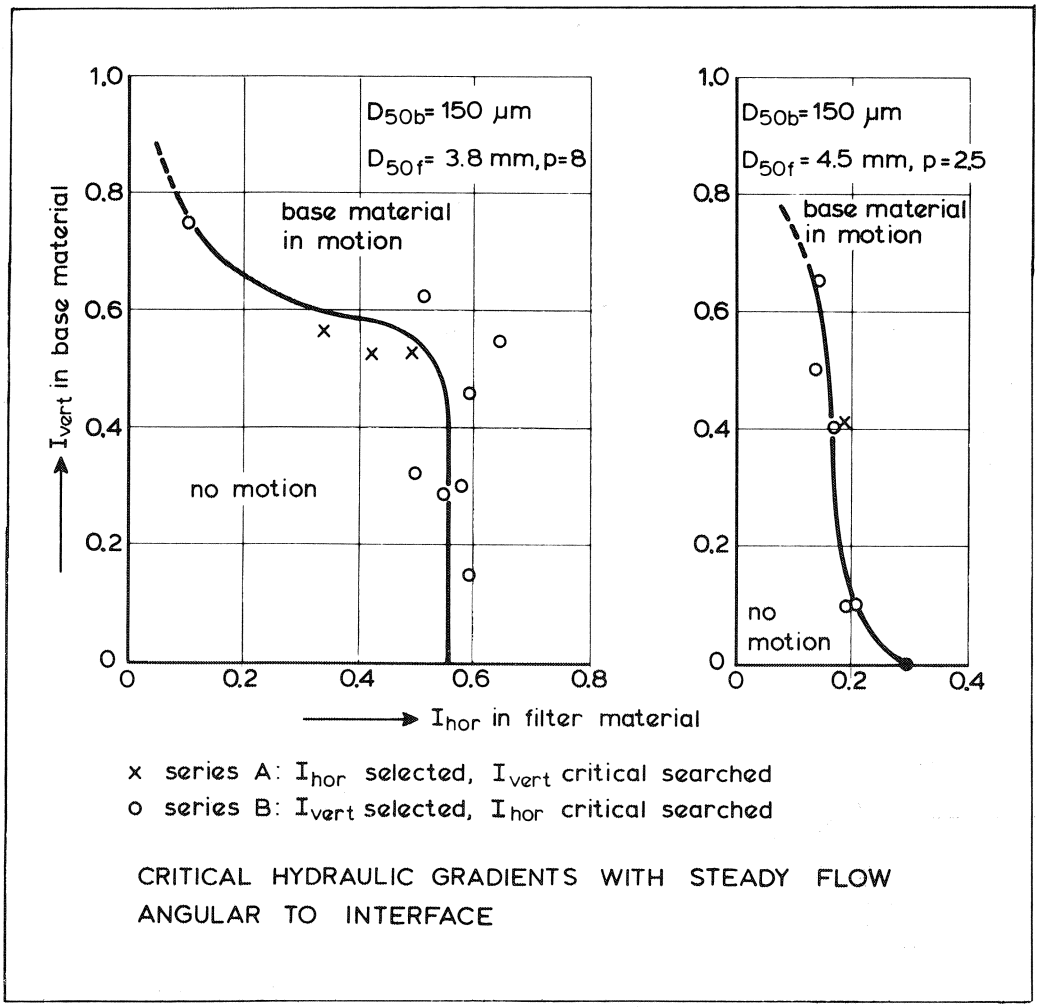

Figure 2.4.13.8 Critical hydraulic gradients with steady flow angular to interface.

Cyclical flow parallel to the interface

For this part of the investigations, use has been made of the water tunnel shown in Fig. 2.4.13.9. The critical gradient of the filter increased initially by decreasing the period of the cyclic flow. In the same time the packing of both the base material and the filter increased. Apparently the cyclical flow caused what might be called „hydraulic densification". The critical gradient for the densified materials proved to be indepen-

dent of the period, even up to stationary conditions (period T = ∞) (see Fig. 2.4.13.9). This result illustrates the influence of porosity on the magnitude of I_{cr}. Due to phase and amplitude differences of the cyclical pressures in the base and filter materials, a vertical cyclical gradient develops. Under certain conditions transport induced by these vertical gradients might occur earlier than transport induced by the horizontal gradients.

Cyclical flow perpendicular to the interface.
The tests were carried out in the apparatus shown in Fig. 2.4.13.6 after providing it with a device to generate cyclical flow. The period has been kept constant and equal to 10 seconds for all tests. The filter materials were graded, which is why D_{15} has been chosen to characterize its grain size. Some results are shown in Fig. 2.4.13.10, where the corresponding results for stationary conditions are also given for comparison. In the cyclical tests, the porosity of the filters n_f has been varied, thus making it possible to include its effect in the analysis of the results. The product $n_f \; D_{15f} \; / \; D_{50b}$ gave the best fit to the (few) results so far obtained.
It can be seen from Fig. 2.4.13.10 that cyclical conditions impose more severe demands on the filter than stationary conditions. A possible explanation of this is that under stationary conditions the flow (gradient) force must overcome the arching force of the grains of the base material before transport can take place (see Fig. 2.4.13.11a). This micro-arching effect increases with increasing (effective) grain stresses and decreasing porosity of the base material. Under cyclical conditions the gradient force is periodically reversed, thus creating unfavourable conditions for the development of grain arches.
In practice, the above applies only for relatively small ratios of D_{if}/D_{ib}. At larger ratios, the formation of arches vanishes and the transport takes place by another mechanism, as shown in Fig. 2.4.13.11b. The grains of the base material do not have any support in the local zone between the filter grains. When the flow force exceeds the submerged weight of the base material in this zone (which equals about 1 for $\varrho_{mat.} = 2650$ kg/m³ and $n_b = 0.4$), local fluidization (loss of intergranular contact) takes place, adjacent grains loose their lateral support and relative motion of base and filter materials is initiated. Under these conditions there should be no difference between stationary and cyclical loading. The migration of sand into the filter at upward gradients perpendicular to the interface cannot be measured directly. The settlement of the filter

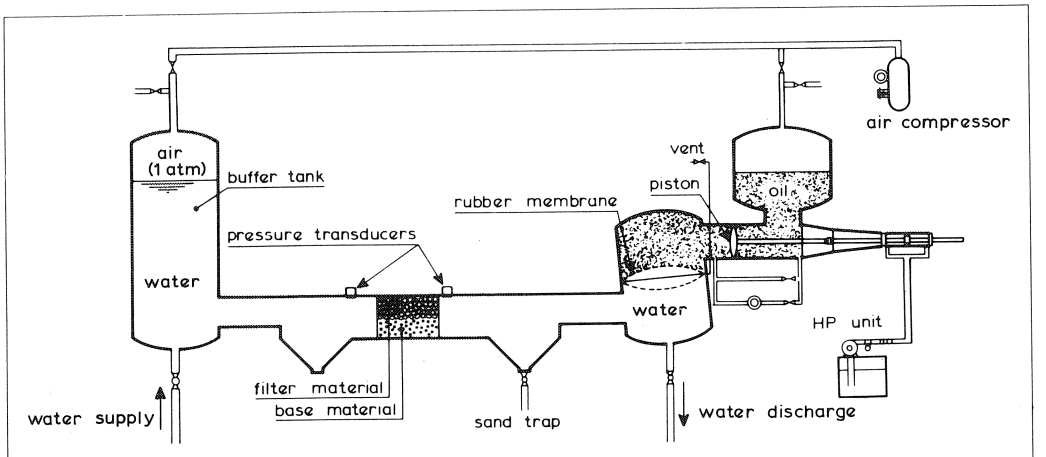

(a) TEST RIG IN PULSATING WATER TUNNEL

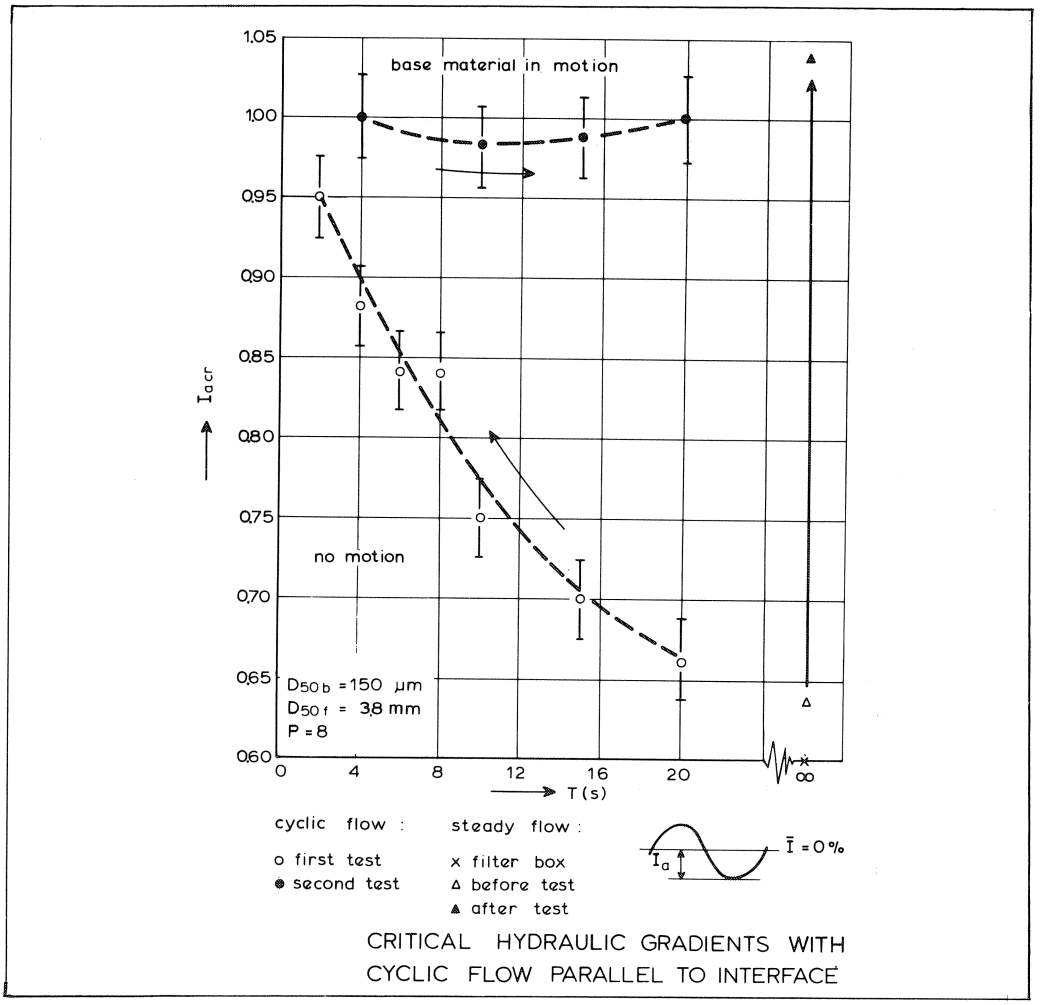

Figure 2.4.13.9 Critical hydraulic gradients with cyclic flow parallel to interface.
a) Test rig in pulsating water tunnel.
b) Results.

layer is usually taken as a measure of the transport. In fact, settlement is the type of information required for the design of bank and bottom protections and similar structures. Figure 2.4.13.12 shows the development of the settlement with time under cyclical loading. Similar results are obtained under stationary conditions though the magnitude may differ considerably.

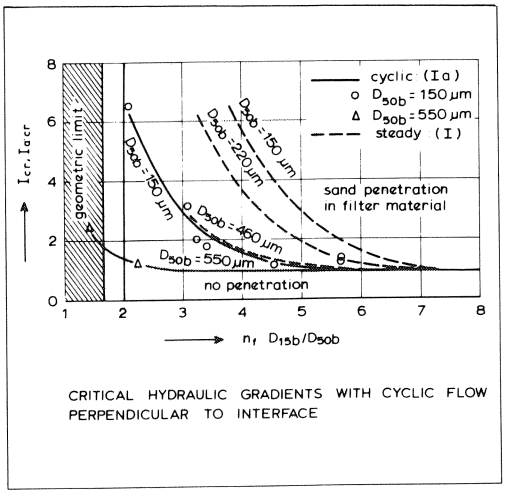

Figure 2.4.13.10 Critical hydraulic gradients with cyclic flow perpendicular to interface.

Figure 2.4.13.11 Mechanisms of transport for non-cohesive materials.

2.4.13.5. Synthetic filters (geotextiles)

General

Synthetic fabrics (also called geotextiles) have recently been used to great advantage in solving a variety of problems in civil engineering, and more specifically in geotechnical engineering [5, 8, 9, 25, 28]. Many of the uses are associated with long-term civil engineering structures, such as coastal defences, dams, road construction etc. For more detailed information on this subject the reader is referred to Rankilor's 'Membranes in Ground Engineering' [15]. This book is about recently developed uses of permeable fabrics in civil engineering, and covers their full range of applications, including the use of permeable geotextiles in filters.

Due to the developments mentioned above it is possible in many cases to substitute the granular filter by a synthetic one made from woven or non-woven (random packed) continous plastic fibre cloth. Its filtering ability (permeability and soil particle retention) can be designed to meet individual requirements. The synthetic filter is usually economical and easy to lay. Its effective life in various environments has however yet to be proved and its still insufficiently known clog-

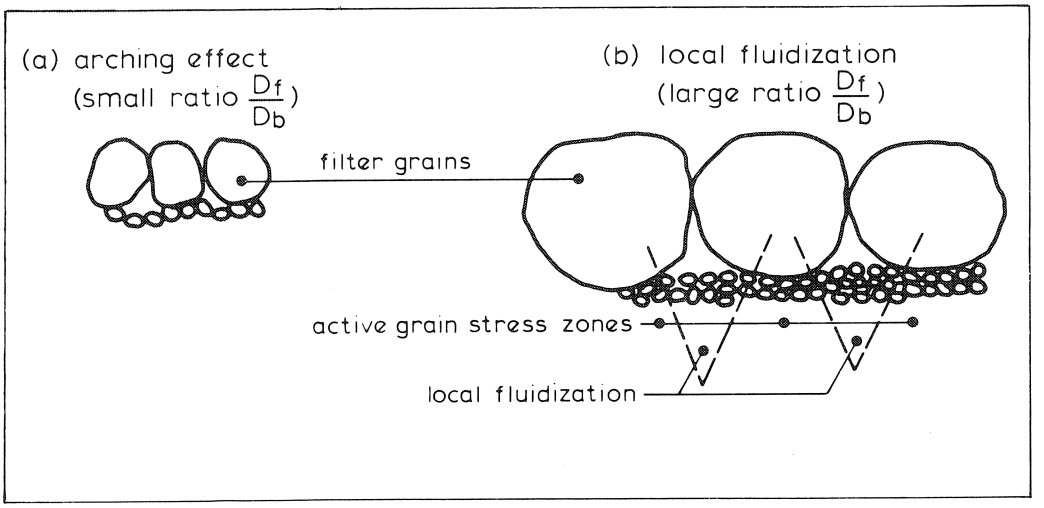

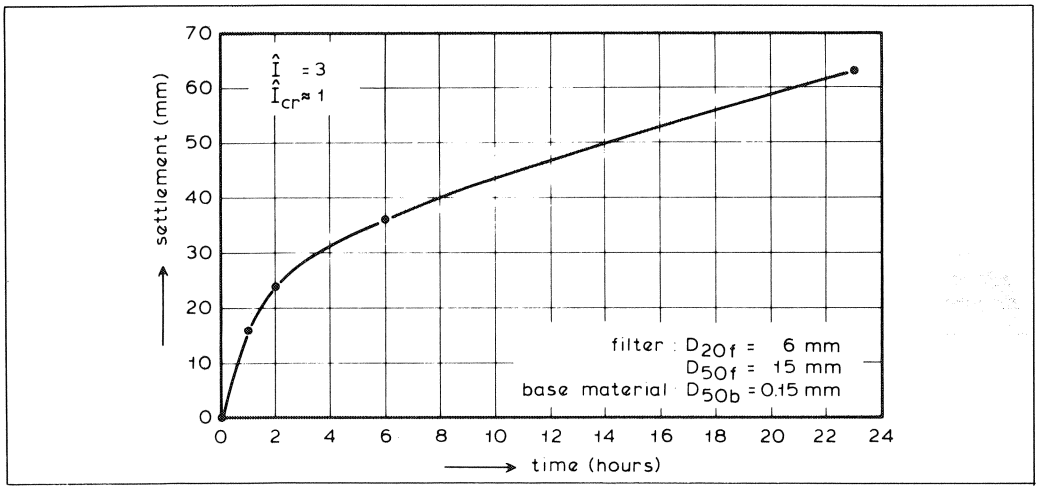

Figure 2.4.13.12 Settlement as a function of time under cyclical loading.

ging properties restrict the range of possible applications.
Important design considerations include: type of structure, weight and type of armour units, method of construction, and forces which the structure is designed to withstand (currents, wave action, head difference and hydraulic gradient oscillations). These variables determine the necessary abrasion resistance, tensile strength, puncture, and burst strengths of the synthetic filter cloth, as specified.

Classification of fabrics according to [14]

The fabrics on the market may be classified in terms of their appearance. In this publication the fabrics have been classified according to the structure of the threads and their composition. Five groups have been distinguished:
1. Mesh-nettings;
2. tape fabrics;
3. mats;
4. multi-filament fabrics; and
5. non-wovens.

Mesh-nettings are woven of thin, round single threads, so called round-yarn. These threads are mainly made of polyethene or polypropene. Characteristic of this group of fabrics is its regular pore size pattern and its large percentage of open area.

Tape fabrics may be distinguished from mesh-nettings by the typical flat shape of the threads. The threads have been shred from polypropene or polyethene film. Due to the flat shape of the threads, the percentage of open area of tape fabrics is small.

The threads of **mats** consist of a number of film fibres (as a result of the so called fibrilation process) which have been twisted. These threads have a typical round shape, as opposed to the tape fabrics. Nowadays mats are usually made of polypropene. Very characteristic of the mat structure is its irregular pore size pattern.

Multi-filament fabrics in general are woven of nylon yarn (polyamide, polyacryl)spun to very

fine synthetic fibres. These fabrics have a small thickness and little stiffness.

Finally, the **non-wovens**, as is expressed by the name, do not show any weave pattern; they have a very tumbled structure. Some non-wovens are strengthened by an armouring.

Combinations of these types of fabrics mentioned also appear.

An extensive outline of fabrics applied in hydraulic engineering has been given by Zitscher [28,29] and Rankilor [15]; the chemical composition and physical properties of the fabrics are also treated.

Filtering action of the geotextiles

Synthetic filter used to replace granular filters have to fullfil the same functional requirements. Thus the synthetic filter must be designed so that it will effectively retain soil (sand-tightness requirement) and remain permeable to water under both laminar and turbulent flow conditions. In a granular filter system, the filtering behaviour appears to be achieved by a mixing and grading at the interfaces between filter layers of different particle size, but the development of a filter in a soil adjacent to a permeable geotextile is distinctly different. Various research programmes showed that the geotextile itself did not filter the soil. However, by supporting the soil, it allowed an 'internal' filter to be built up as shown in figure 2.4.13.13.
Lawson [8] gives the following description of this process: „During an initial period immediately following the placement of the geotextile at the soil interface, the soil particles in the layer immediately adjacent to the geotextile, which are smaller than the pores in the geotextile, migrate into and through the geotextile under influence of soil water flow. Soil particles, which are larger than the pores in the geotextile and which lie immediately adjacent to it, orientate themselves against the upstream surface of the geotextile forming a bridging network. As soil water continues to pass through the geotextile, increasing amounts of the fine soil particles become trapped on this granular bridging network until such time as no soil particles can migrate across the boundaries of the geotextile".
More detailed information hereabout can be found in [5], [8] and [15].

Strength of the synthetic filters

If synthetic fabrics are used, the characteristics of the fabrics and their hydraulic strength are designed according to various ratios of 'O'/'D' where 'O' represents the diameter of holes (mesh size) in a fabric and 'D' the diameter of particles. Some definitions of characteristic sizes are given below:

O_{50} - corresponds to the average sand diameter of a sand fraction 50% of which remains on the fabric after a sieving time of 5 minutes.

Figure 2.4.13.13 Equilibrium soil conditions following formation of soil filter [8].

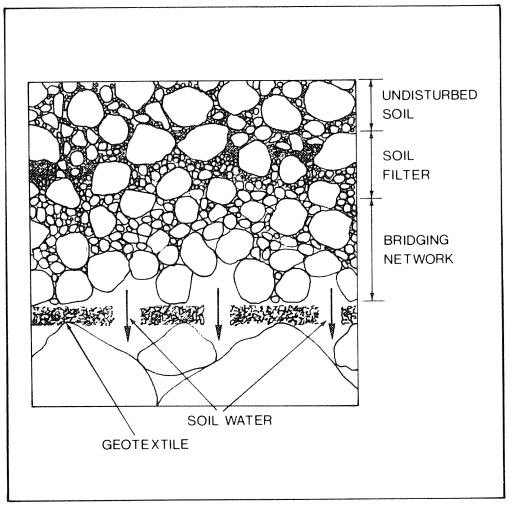

O_{90} - corresponds to the average sand diameter of a sand fraction 90% (or 98%) of which remains on the fabric after a sieving time of 5 minuters.

O_{98} - The quantity O_{98} gives a practical approximation of the maximum size of the fabric pores.

D_{90} - corresponds to the sieve size through which 90% of the total sand mass will pass.

Extensive investigations on the hydraulic characteristics of synthetic filters have been carried out by the Delft Hydraulics Laboratory [14]. Similar investigations have been carried out in the Federal German Republic [28], in the United States of America [3] and in the United Kingdom [18]. These results have been evaluated and summarized by Rankilor [15].
Some design criteria as established by Delft Hydraulics Laboratory [12,14] are mentioned below.

I. Stability criterion (sand-tightness)

The sand-tightness of a fabric depends on the grain-size distribution of the soil to be protected in relation to the size of the fabric pores. The investigations under static load conditions showed that the sand-tightness ratio is influenced positively by the arch effect of the sand particles around the filter pores. The dynamic load conditions which may ruin the arch, and possibly also the build-up of a natural filter, influence the sand-tightness ratio negatively.
The criteria are:

- Under static load conditions the woven fabrics (mats, mesh-netting, tape and multifilament fabrics) fulfil the sand-tightness requirement if:
  Ia: $O_{90}/D_{90} \leqslant 1.0$
  (O_{90}/D_{90} can be reduced below 1, but increasing hydrostatic pressures will be generated behind the membrane as it falls below 1).
- For non-woven fabrics the criterion is more favourable, viz.:
  Ib: $O_{90}/D_{90} \leqslant 1.8$.
- Under dynamic load conditions (alternating flow conditions with variation in hydraulic head, e.g. waves) the sand-tightness requirements are met if:
  Ic: $O_{98}/D_{15} \leqslant 1.0$
  Hereby it is assumed that the cyclical load conditions prevent the build-up of a natural filter immediately under the fabric and that a small percentage (15%) of the underlying sand may wash out.
  If the cyclical load permits the build-up of a natural filter, sand-tightness may occur if:
  Id: $O_{98}/D_{85} \leqslant 1.0$

N.B. The sand-tightness requirements, as mentioned above, are extremes. Under less strong cyclical or static load conditions, the requirements can be considerably more lenient. Additional laboratory research will be necessary to determine these requirements in each particular case (depending on type fabrics and load). Finally the above criteria are valid only for flow perpendicular to the interface.

II. Permeability criterion

Under a certain hydraulic gradient the permeability of the filter should be sufficient to prevent water over-pressure under the construction.

If geotextiles are designed according to the sand-tightness criteria only, some overdimensioning (too small openings of the fabrics) may result in respect to the required permeability. Under certain circumstances, the permeability of synthetic fabrics will be reduced, either by blocking or clogging, especially when the above rules are applied for fine soils [6]. Blocking is the partial closure of the fabric's pores by sand grains from the underlying bed. Clogging is the partial or total closure of the fabric's pores due to the deposition of very fine particles or chemical compounds. The fabric then tends to act as a watertight membrane, and this results in uplift pressures. If the weight of the structure is not sufficient to counteract the uplift, it will be raised up and in the case of a sloping structure, will progressively slide down the slope or, the soil underneath will be able to move along the geotextile causing uneven settlement of the structure.
In such cases it is advisable to determine the ac-

tual stationary and cyclic gradients and to introduce probabilistic considerations in the design. This may lead to a coarser fabric and limit the likelihood of clogging. If, in very fine or silty subsoils, these fabrics are not able to combine sufficient and permanent permeability with the required sand tightness, a coarser sand layer can be used as an intermediate filter. This type of construction, however, is vulnerable during construction.
Because of these various uncertainties, the required permeability of the fabrics has to be much higher than the permeability of soils. It is especially important for the fabric-mats in which a relatively large number of small apertures exist which are most sensitive to clogging.
Some indicative permeability criteria are given below:

k fabric > 2 k soil - for uniform soil
and (13)
k fabric > 5 k soil - for well graded soil
where k is permeability factor.
Further information on this subject may be found in [5, 8, 31, 32].

III. Mechanical and chemical requirements

Besides the hydraulic requirements which must be fulfilled by fabrics when used as synthetic filters, the composition of the fabrics must also satisfy certain long-term mechanical and chemical requirements. These can be requirements in relation to tensile stress, elasticity, abrasion resistance, rigidity, ultra-violet (U.V.) light stability and chemical stability, etc. The mechanical and chemical requirements have to be related to the type and life of the structure, method of execution (i.e. placing or dumping of stones), type of loading etc. Although the fabrics are normally highly resistant to puncturing by rock, it is common practice to cover the filter cloth with gravel before dumping riprap onto it. Further information on this subject and about test-methods may be found in [31] and [32]. A complete description of technical properties of over hundred different fabrics available all over the world is given in [15].
The use of geotextiles is constantly increasing and more information is becoming available on their durability under repeated current and/or wave action and various environmental conditions [32].

2.4.13.6. Composite and alternative filters

In the case of high hydraulic gradients it is not always possible or advisable to use a synthetic filter alone. For example, the armour layer of the sea-dike protection can be chosen in such way as to resist very heavy wave attack By placing such armour directly on a soil (sand) protected only by a geotextile, the protection may be insufficient.
Because of vibration of the protective top-layer due to the impact of breaking waves in combination with an excessively steep slope, some migration of sand along the slope at the soil-geotextile interface can be induced. In the long term and in conjunction with an unproperly designed footing of the slope protection (not sand-tight), this can lead to substantial damage-(erosion) and even total failure. To minimize the hydraulic gradients in such cases the thickness of the filter has to be increased by an extra layer of crushed stone.

In the absence of suitable stable filter material, or where the filter is to resist high pressure, it may be economical to replace the granular or synthetic filter with a relatively thin layer of sand bitumen which provides temporary protection apart from its excellent filtering capabilities. Sand bitumen consists of 96 to 97% sand (hot) mixed with 3 to 4% bitumen (percentages by weight). The Darcy k-value of sand bitumen (permeability) is almost equal to the k-value of the sand used for its production [16].

As an alternative to a non-cohesive top layer of rubble, a cohesive, bituminous permeable lining can be applied, such as permeable sand-asphalt and/or stone-asphalt. Another alternative consists of porous concrete [17], for which cement and gravel without fine aggregates are used. Care should be taken in designing the mix as excessive water or cement could cause blockage of the passages at the bottom. Fine underlying soils or filter cloths are prone to blocking with mortar.

References

1. Barends, F.B.J., Thabet, R.A.H. Groundwater Flow and Dynamic Gradients. Symposium on **Foundation Aspects of Coastal Structures**, Delft, 1978. Vol.2.

2. Belyashevskii, N.N. et al. Behaviour and Selection of the Composition of Graded Filters in the Presence of Fluctuating Flow. **Hydrotechnical Construction**, No.6, 1972 pp. 541-546.

3. Calhoun, C.C. Development of Design Criteria and Acceptance Specifications for plastic filter cloths, U.S. W.E.S. **Technical Report**, Vicksburg, Mississippi, USA, June 1972.

4. Graauw A. de., T. van der Meulen, M. van der Does de Bye. Design Criteria for Granular Filters. **Delft Hydraulics Laboratory**, Publication no. 287, January 1983.

5. Hoare D.J. Synthetic Fabrics as Soil Filters: a review, **J. of the Geotechnical Engineering**, ASCE, October 1982.

6. Hoogendoorn, A.D. and Meulen, T.v.d., Preliminary investigations on clogging of fabrics, **International Conference on the use of Fabrics in Geotechnics**, Paris, April, 1977.

7. Kawakami K. and Esashi, Y., On Drainage Filter for Earth Structure, Abstract of Papers 16th Ann. Meeting, **Jap.Soc. of Civ.Eng.**, 1961.

8. Lawson Ch. R., Filter Criteria for Geotextiles: Relevance and Use. **J. of the Geotechnical Engineering**, ASCE, October 1982.

9. Lee, T.T. Designs of Filters System for Rubble-Mound Structures, **Conf.Coastal Engineering**, Vancouver, 1972, Canada.

10. Lubotchkov, E.A., The Self Filtering Behaviour of Non-Cohesive Soils (in Russian) **Izvestia VNIGG** Vol.71, 1962.

11. Lubotchkov, E.A., Graphical and Analytical Methods for the determination of Internal Stability of Filters consisting of Non-Cohesive soil (in Russian), **Isvestia, VNIIG**, Vol.78, 1965.

12. Meulen, T.v.d., Testing of Fabrics for use in Hydraulic Structures, Index 78 Session 1: **Civil Engineering**, Amsterdam, April 1978.

13. Molenkamp, F., Calle, E.O.F., Heusden J.J., and Koenders, M.A., Cyclic filter Tests in a Triaxial Cell, **Design Parameters in Geotechnical Engineering**, BGS, London, 1979, Vol.2.

14. Ogink, H.J.M., Investigations on the Hydraulic Characteristics of Synthetic Fabrics, **Delft Hydraulics Laboratory**, Publication no. 146, May 1975.

15. Rankilor, P.R., **Membranes in Ground Engineering**, John Wiley & Sons, 1981.

16. Span, H.J.Th., Altink, H., Barends, F.J., Biemond, C., Biesheuvel, G.J., Huis in 't Veld, J.C., Thabet, R., Tutuarima, W.M., and Woestenenk, A.J., A Review of relevant Hydraulic Phenomena and of recent Developments in Research, Design and Construction of protective Works, XXVth **International Navigation Congress**, Edinburgh, 1981, Vol.1

17. Stephenson, D., Rockfill in hydraulic Engineering, **Developments in Geotechnical Engineering**, Vol.27, Elsevier, Sc.Pub.Comp., Amsterdam, 1979.

18. Sweetland, D.B. (M.Sc.Thesis), **The Performance of Non-Woven Fabrics as Drainage Screens** in Subdrains, University of Strathclyde, 1978.

19. Terzaghi, K and Peck, R.B., **Soil Mechanics in Engineering Practice**, 2nd ed. Wiley-Interscience, 1967.

20. Thanikachalam, V., and Sakthivadivel, R. Rational Design Criteria for Protective Filters, **Can. Geotechnical J.** 11 (1974) p.309.

21. Thanikachalam, V., and Sakthivadivel, R. Grain Size Criteria for Protective Filters -an Enquiry, **Soils and Foundations** Vol. 14 no. 4. Dec. 1974, Jap. Soc. of Soil Mechanics and Foundation Eng.

22. Thanikachalam, V., and Sakthivadivel, R. Design of Filter Thickness Based on the Application of Queing Theory, **Journ. of Hydr.Research**, vol.13,1975 no. 2. pp. 207-219.

23. U.S. Bureau of Reclamation (1963), **Earth Manual**, 1st. ed. revised. Washington D.C.

24. Vinjé, J.J. and Spaargaren, F., Some Aspects of Flow through and under Hydraulic Structures used for closing Estuaries, **Proc. 13th Congress IAHR**, Kyoto, 1969.

25. Welsh, J.P. and Koerner, R.M., Innovative uses of Synthetic Fabrics in Coastal Construction, **Coastal Structures** '79.

26. Wittman, L., The Process of Soil-Filtration-its Physics and the Approach in Engineering Practice, Proc. 7th European **Conference on Soil Mechanics and Foundation Engineering**, Brighton, 1979, Vol. I, paper b 42, pp. 303-310.

27. Zanen, A., Revetments, **Int.Course in Hydraulic and Sanitary Engineering**, Delft 1976, The Netherlands.

28. Zitscher, F.F., Kunststoffe für den Wasserbau, **Bauingenieur - Praxis**, Heft-125, Verlag von Wilhem Ernst und Sohn, Berlin, 1971.

29. Zitscher, F.F., Recommendations for the uses of Plastics in Soil and Hydraulic Engineering, Die Bautechnik,52(12) 1975.

30. State of the Art on Research into Granular Filters, **Delft Hydraulics Laboratory**, Report S469, July 1980.

31. **Proceedings 1st International Conference on Geotexiles**, Paris, April, 1977.

32. **Proceedings 2nd International Conference on Geotexiles**, Las Vegas, 1982, U.S.A.

Interaction Water Motion and Closing Elements

E.L. Birnbaum, R.J. Leewis

2.4.14. Environmental impact on marine structures

The impact of enigneering projects on the marine environment often receives critical attention and conversely the impact of a marine environment on the design and execution of such projects is also a subject that deserves serious consideration. A classic example is provided by the invasion of the Dutch coastline in the eighteenth century by the shipworm (Teredo navalis). The sea dikes, which had been reinforced with wooden materials (branches, trunks, etc.), were severely damaged by the newcomer and, as a result, harder materials such as stone had from that time to be used in place of wood. More recent examples are the reduction in cruising speed of ships due to fouled hulls and the reduction in cooling capacity of coastal power stations due to marine fouling in the cooling pipes. Recently critical attention has also been given to the effect of marine fouling on offshore gas and oil platforms in the North Sea [1]. The impact of fouling organisms on a structure, and the remedies available, depend largely on the type of structure and the environment in question. Widely applicable guidelines are difficult to formulate. A few examples provided by the Deltaproject in the Eastern Scheldt will be discussed here together with the strategies that haven been developed to deal with them.

One of the design alternatives originally considered for the storm surge barrier in the Eastern Scheldt consisted of paired gratings with horizontal openings for the exchange of water (see fig. 2.4.14.1.). To close the barrier, the position of the paired gratings could be adjusted so as to block the openings. Such a design would only function properly if marine growth on the gratings could be controlled.
The openings measured about half a metre; a layer of mussels of 10 to 20 cm thick around the edges, which is quite common in a productive estuary such as the Eastern Scheldt, would reduce the effective opening by more than half! As a result, this design had to be abandoned.

The marine environment also provided problems, which were less obvious at first, for the design of the sill construction, part of the barrier design. The sill consists of layers of rock, resulting in a porous construction through which water flows even when the barrier is closed. The sill is designed to remain intact even when barrier closure and a severe storm result in a large head of water exerting pressure differences over the sill. The calculations for the stability of the sill design in severe storms were carried out for a construction consisting of bare rock (see fig. 2.4.14.2a.). The rock is bare only in the initial phase shortly after construction is completed, but quite rapidly marine growth, consisting of barnacles, oysters, mussels etc. will begin. The total mass of living and dead organisms, primarily mussels, will after a few years be very considerable and probably fill a large fraction of the originally open space between the rocks. Provided the biomass is evenly

Figure 2.4.14.1. (Rejected) design of a storm surge barrier consisting of paired gratings with horizontal openings for the exchange of water; on the left in open position, on the right in closed position.

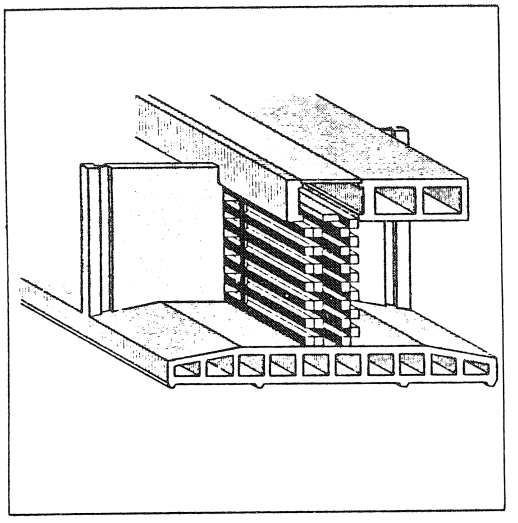

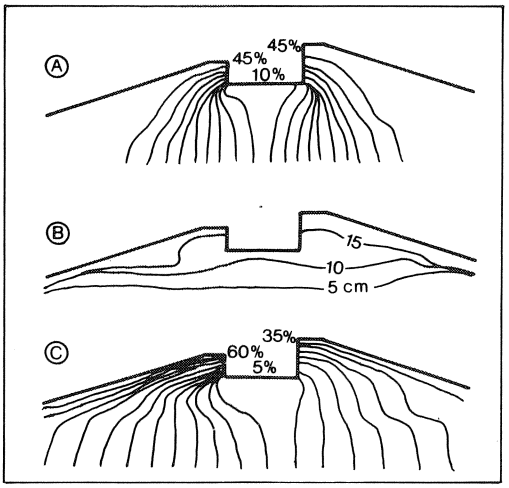

Figure 2.4.14.2a. Sill cross-section in initial phase with no mussels; a plot of the hydrodynamic loading forces acting on the construction. Each line represents 5% of the total head of water over the sill. A concentration of lines indicates a concentration of loading forces.
b. Maximum mussel concentrations in the sill, predicted by a model. 15 indicates that above that line mussel biomass can form a layer thicker than 15 cm on available surfaces; below the line a 15 cm layer is the maximum.
c. As for a, but for final phase with maximum mussel biomass.

distributed throughout the sill, the stability during a storm will not be affected. If the biomass is unevenly distributed, e.g. concentrated in the outer layers, the hydronamic forces acting within the sill during a storm can be greatly affected and sill stability may be reduced.
To cope with this problem a biological model was constructed in which the growth of mussels in the sill could be simulated. The model incorporated available biological data on the growth of mussels as a function of food level and was coupled to an existing computer program in which the flow of water through the sill and the resultant hydrodynamic forces were predicted. The model predicted that mussel growth would gradually become more and more concentrated on the outer layers of the sill as the food supply in the inner layers would eventually become too low to support further growth (see fig. 2.4.14.2b). As a result the outer layers, composed of 1 to 3 ton stones, might be subjected to greater hydrodynamic forces than originally planned for, and the stability during storms might become critical (see fig. 2.4.14.2c). Modifications of the sill design which quaranteed a greater stability in the case of extensive mussel growth were considered, and the model was then used to compare the effect of these modifications on mussel growth and overall stability. In this case the conclusion was that the modified designs afforded greater stability but that the safety factor provided by the original design was sufficient.

Another area in which marine growth can present considerable problems for the civil engineer is the design and operation of pipes or sewers through which seawater is transported. A well known example is that of cooling pipes in power stations using seawater as a coolant. Similar problems played a role in the design of the sluices for the partitioning dams in the Delta project. To minimize the exchange of saltwater and freshwater via the ship locks, the sluices are equipped with a system for replacing seawater in the lock with freshwater and vice versa. The seawater travels through a perforated concrete floor and sewers to a storage reservoir. Growth of mussels in the sewers and the perforated floor would probably be rapid and could lead to a reduction of the effective flow-through diameter,

higher energy costs and longer passage times for ships through the locks.

A study was made of the possible effect of marine growth in the Krammer Sluice on the operation of the locks. Three alternative strategies for minimizing the effects of marine growth were defined and evaluated. To facilitate a comparison between the alternatives the results were presented in tabular form, a simplified version of which is given in fig. 2.4.14.3. The use of anti-fouling compounds and mechanical removal of mussels are conventional solutions. The use of anti-fouling compounds has the advantage of providing a clean surface free of marine growth. Disadvantages are the limited duration of effective action (1-3 years; with special materials up to 10 years) and release of toxic compounds in the environment. Reducing the salinity within the sluices is a practical option due to the presence of an adjacent freshwater supply in a lake. The decision as to which control strategy to choose can be made after the locks have been in operation for a while and more experience has become available. The locks are so designed that there is access for machines and personnel to all places liable to be affected by marine growth.

For the construction of slopes often stone asphalt and rubble-stone mixed with asphalt is used. As a result of „mechanical erosion" (changes in temperature, wave-action, etc.) stones are sometimes loosened in these types of slopes. However,in addition the growth of barnacles also may play a role. As the surface of the slopes is uneven, due to protruding stones and hollows, it provides an excellent opportunity for the settlement and growth of barnacles. When the barnacles increase in size they might be able to push the stones out of the dumped stone-asphalt, resp. to widen the interstices which are often formed at the boundary between the dumped rubble-stone and the asphalt thus providing another cause for the stones becoming detached. Another source of damage can be the „boring animals", e.g. the boring mussel, which, when settling on sand-asphalt revet-

Figure 2.4.14.3. Evaluation of alternative fouling control strategies for the Krammer Sluice.

		finacial costs	shut-down time for lock	release of toxic compounds	type of control
ANTI-FOULING COM-POUNDS	perforated floor	high	ca.5days per yesr	Y	PRE-VEN-TIVE
	main sewers	high	ca.7 days per year	E S	
MECHA-NICAL REMO-VAL	perforated floor	low to moderate	0 to 4 d/y[1]	N	CURA-TIVE
	main sewers	low	1 to 3 d/y[1]	O	
REDUCED SALI-NITY	perforated floor	low	none	N	PRE-VEN-TIVE
	main sewers	low	none	O	

ments, could weaken the slopes. A possible solution would be to cover the slope with a fine gauze or filter-cloth (with a mesh of 50-100 μm), which would check settlement of larvae and prevent damage.

It should by now be clear that the design and realizationof engineering projects in a marine environment often require the engineers involved to possess a basic knowledge of the life forms present and their behaviour. It is no luxury and indeed often a necessity that biologists be consulted prior to the different stages of such projects.

Interaction Water Motion and Closing Elements

D.J. de Jong, R.J. Leewis, P.B.M. Storteldер

2.4.15. Some practical environmental points of attention

2.4.15.1. Introduction

In this section some points, that need particular attention when designing or constructing civil engineering projects in coastal areas, will be illustrated. Attention will be mainly focussed on environmental aspects, although it will be evident that the aspects mentioned are part of a much longer list. Large projects always go through certain phases of design, in the course of which the guiding principle is to progress in thinking from many rough alternatives on a large-scale to finally considering one detailed alternative or locality, while throughout this entire process, maintaining a consistent logical approach. As always reality is much more complex than the simplified world of examples. Nevertheless, some practical aspects will be described.
The items to be elaborated are:

- desalination in connection with the time of closure
- the impact of material selection and design on the environment
- the production of materials
- spoil dumps
- the co-use and re-use of dams and construction sites.

2.4.15.2. Desalination, in connection with the time of closure

„Desalination of a lake", means the lowering of the salt-content by supplying freshwater and discharging salt or brackish water. The desalination process will be discussed with the help of the following model of a lake (or part of it):

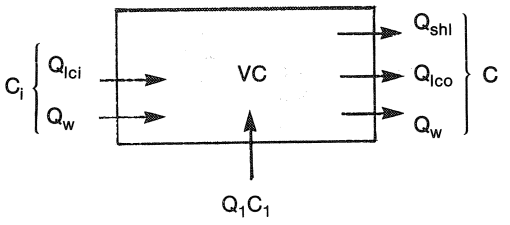

subscripts:

Q	-	discharge m³/day)
C	-	salt contents (g Cl^-/m^3)
V	-	volume (m^3)
l	-	local
lc	-	level control
shl	-	shipping locks
w	-	wash through
i	-	inlet
o	-	outlet

The process of desalination proceeds according to

$$\frac{d(VC)}{dt} = Q_{lci}C_i + Q_1C_1 + Q_wC_i - Q_{shl}C - Q_{lco}C - Q_wC \qquad (1)$$

The terms $Q_{lci}C_i$ and $Q_{lco}C$, indicated in (1), will occur in accordance with the direction of the water-transport required for the preservation of the waterlevel in the lake ($dV/dt = O$). For a further consideration of (1) it is assumed that the lake must be replenished and that therefore $Q_{lco} = 0$ and $Q_{lci} = Q_{lc}$.
Thus

$$V\frac{dC}{dt} = (Q_{lc} + Q_w)C_i + Q_1C_1 - (Q_{shl} + Q_w)C \qquad (2)$$

From the waterbalance ($\frac{dV}{dt} = 0$) can be derived that

$$Q_{lc} = Q_{shl} - Q_1 \qquad (3)$$

The solution of the equations (2) and (3), assuming the initial salinity in the lake to be C_o, is:

$$C(t) = \frac{(Q_{lc} + Q_w)C_i + Q_1C_1}{(Q_{shl} + Q_w)}\left[1 - \exp\{-(Q_{shl} + Q_w)\,t/V\}\right] + C_0 \exp\{-(Q_{shl} + Q_w)\,t/V\}$$

This equation requires some further explanation:

- the equilibrium concentration $t \rightarrow \infty$ is determined by the inlet content C_i and by local sources, provided their concentration differs from the inlet content. If $C_l > C_i$, then the equilibrium concentration is higher than C_i, if $C_l < C_i$, than the equilibrium concentration can be lower than C_i. The relative influence of local sources depends however on the ratio $Q_l/(Q_{shl} + Q_w)$. When flushing takes place (Q_w large) then the effect of local sources will be canceled out;
- the concentration in the lake will diminish from C_0 to about C_i. The desalination rate will be determined by the ratio $V/(Q_{shl} + Q_w)$, in other words, by the average residence time of the water in the lake. The residence time $\tau = V/(Q_{shl} + Q_w)$ can be considered to be a combination of two residence times via the relation
$$\frac{1}{\tau} = \frac{1}{\tau_{shl}} + \frac{1}{\tau_w}$$
in which τ_{shl} is the residence time without flushing, caused by the use of shipping locks and τ_w is the residence time of the water due to flushing.
- If $Q_w << Q_{shl}$ then $\tau = \tau_{shl}$: even without additional flushing the salinity can decrease rapidly, if τ_{shl} is sufficiently small. In that case gradual desalination will not be possible.

For the above-mentioned calculation it has been assumed that complete mixing has taken place; in this way an impression is gained of the average salinity for the entire lake. In practice, however, there will often be differences both vertically and horizontally. Additional models are therefore required for their definition. However, the methodology described usually yields sufficient information for a general approach.

Ecological consequences

As a result of the desalination after the closure, the original specific saltwater flora and fauna will completely die off, thus leading to a temporary deterioration of the water-quality. In particular, the oxygen concentration will decrease considerably as a result of the bacteriological decomposition of the dead organisms (mineralization), which can cause lack of oxygen (anaerobic conditions). Under these circumstances, anaerobic processes can result not only in obnoxious smells, but also at the time hamper the development of a new, adapted flora and fauna. It is clear that the total amount of dead organisms (the biomass) will also determine the probability of lack of oxygen.

Rate of desalination

To limit as much as possible the problems ensuing from complete desalination it may be preferable to opt either for relatively quick desalination (some weeks or months) or for very slow desalination (from 10 to 20 years).

Very slow desalination implies that the salt-water organisms will not all die at the same time due to their differing rates of salt-tolerance. During the long transitional phase, the flora and fauna will be able to adapt to the changed circumstances. Thus, the existing biotic community will gradually be transformed, via a brackish form, into a freshwater biotic community.
However, slow desalination is not always feasible as far as water management is concerned, for, as has been shown in the first section, desalination can occur quite rapidly just by the use of shipping locks.

A rapid desalination will limit possible problems to a very short period. Fig. 2.4.15.1 illustrates the oxygen concentration, oxygen demand and the density and thickness of the upperwater layer during a simulated desalination process in a basin in the South-West Netherland [2]. This simulation has been based on the oxygen demand as indicated in fig. 2.4.15.2. The model results show that during the desalination stage, two layers are formed, known as a „salt stratification": a fresher upper layer with a lower density on top of a saltier lower layer with a higher density. On account of lack of re-aeration of the lower layer and also because of the large quantity of dead matter that settles and decomposes on the bed, the oxygen-content in the lower layer will decrease rapidly causing anaerobic conditions which will continue until stratification ceases as a result of mixing.

The relation between desalination and the time of closure

In the case of a gradual desalination, it is difficult to define exactly when the process actually begins as it starts very slowly. However, under a rapid desalination-strategy, it makes difference when starting desalination. It appears that desalination during summer is considerably less advantageous than during winter, owing to the following factors:

- lower wind velocities in summer have adverse effects on the re-aeration process and limit vertical mixing;
- a higher temperature results in a lower saturation point for oxygen, whereby the oxygen supply via the re-aeration process is considerably limited:
- due to the higher temperature, oxygen consumption will increase as a result of increased speed of decomposition processes and soil respiration (oxygen demand of the soil);
- the increased biomass concentration in summer, by which larger amounts of organic matter has to be decomposed and therefore there is a greater possibility of lack of oxygen (and of the accompanying obnoxious smells)

But even a closure without desalination or a closure followed by gradual desalination will have a great impact on the original ecosystem and lead to the death of a part of the living organisms, owing to the fact that very abruptly both cease the tidal amplitude and the currents. It therefore seems that the most appropriate time to start a new situation is the period during which the existing biomass in the area to be closed off is at a minimum and at a time when the ecosystem is „dormant". In principle, both the low biomass and the „dormant period" occur during a season disadvantageous for the environment, which is usually in winter.

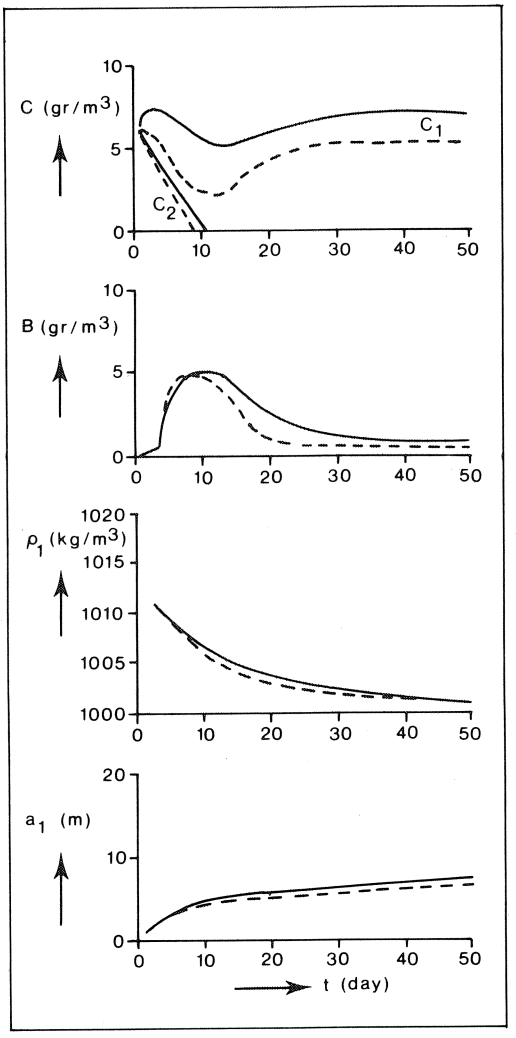

Figure 2.4.15.1. Simulations of oxygen concentration in the upper layer and the lower layer (C_1 and C_2 resp.), the biological oxygen demand (B), the density of the upper layer (ϱ_1) and the thickness of the upper layer (a_1) for an yearly averaged condition (——) and in june (- -). (Freshwater discharge 150 m^3/S, lake volume 249.10^6 m^3, mean depth 5.6 m). (After Anon, 1978 [2]).

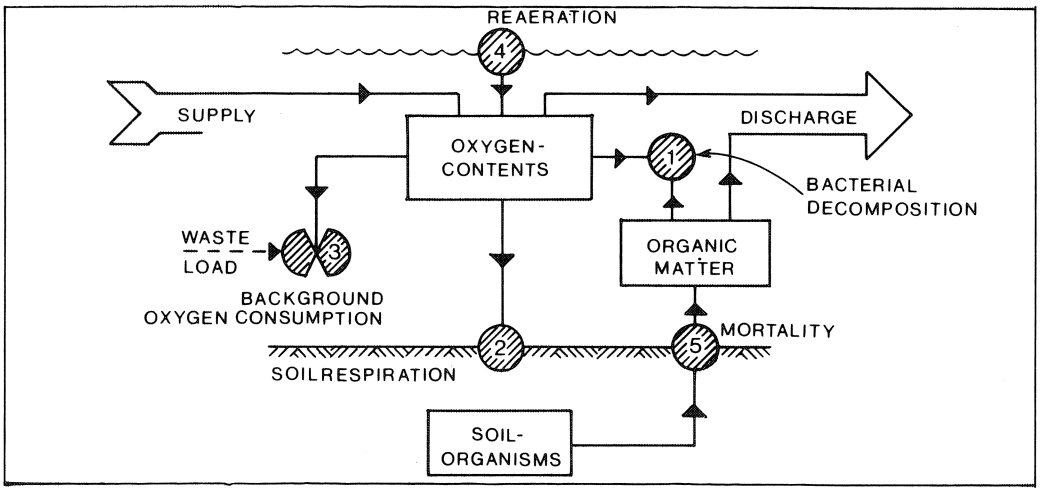

Figure 2.4.15.2. Simplified scheme of the oxygen budget during the desalination of a saltwater lake, as used in modelstudies (for some results see fig. 2.4.15.1.). (After Anon, 1978 [2]).

2.4.15.3. The impact of material selection and design on the natural environment

Most organisms have a relationship with the substratum; they either live in or on it or are fixed to it; they forage on it or extract food from it, etc. Each type of substratum harbours specific types of organisms: for instance, worms are particularly prevalent in soft, muddy or sandy soils, whereas sea-anemones are found on stony, solid substrata (see also 2.2.6).
The materials used for the building of civil engineering structures will, in principle, also be amenable to sustained settlement by all sorts of organisms. In addition to other factors, such as water-quality and current velocity, the nature of the used materials will determine, to a great extent, which organisms can live in or on them. Important aspects of the used materials are the coarseness of the materials and the density of the packing.
The coarseness of the materials, used for the construction of a dam or for the rubble-layer on a dike-foot, is an important factor for the survival of the organisms. It appears that, in running water, the smaller stones - in the Dutch Eastern Scheldt smaller than 10 centimetres in diameter -are generally less densily covered with vegetation than the larger stones. It is thought this is caused by the instability of the smaller stones as, because of their continuous movement, the overgrowth is rubbed off. This instability is even increased due to the fact that the overgrowth of organisms enlarges the area of impact for the currents.
In addition, the density of the packing of the dumped material is also important. Many organisms need cavities to hide in, to use as a base for hunting, or to build a nest. Under water, this need could be fulfilled by using stones with a diameter of at least 30 tot 40 cm and by dumping them, where possible, in several layers. This would provide such a variation in orientation and exposure of the stone's planes that a maximum number of different plant and animal species could live on (and „in") them.

Another important aspect is the toxicity of some materials, e.g. various types of blast-furnace slag and, depending upon its composition,

asphalt. Investigations into their effect on the water-quality have proven that, for instance, phosphorus slag is rather harmless, but that lead and copper slag release heavy metals into the water - particularly into saltwater. Even more serious - although there has been scarcely any research into this aspect - may prove to be the effect on animals and plants trying to settle on such slag. Their actions create a weathering locally and, as a consequence, the slag releases more toxic substances than when only exposed to the water. If these substances are taken up in the organism's tissues, it may well be that this will not only adversely affect the organism itself but all the organisms further up the foodchain, particularly when considering the accumulation in animals at the end of the foodchain.

A subsequent aspect is the speed with which the materials to be used disintegrate. For instance, does a certain fascine need to have a long or only a short life-span. In the latter case it is advisable to use materials that will degrade naturally, e.g. a fascine made from natural materials such as osiers and sisal rope and if necessary covered with natural cloth, rather than various types of synthetic materials.

Also above the water-surface widely differing interactions take place between the materials used, the design and the natural function. A method which is very often used to cover the crown of a dike is a bottom-layer suitable for the cultivation of grass. In addition to sowing grass it is, in principle, possible to grow other types of plants on these surfaces. Thereby, the management of such a dike (mowing or grazing) will influence to a great extent, not only the strenght and stability of the dike but also the composition of plantspecies (and animals) that will live on it.

Moreover, by creating environments which are rare in certain areas, organisms can be attracted which otherwise would not or hardly exist there. As an instance we cite the creation of stony (dike) slopes in the water, which form an artificial rocky coast on which flora and fauna, that are naturally attracted to these conditions, will settle.

At the moment, there is ample opportunity to consider the environmental aspects when selecting materials to be used. Apart from the more „passive" use of the relation between the substrata and overgrowth it is possible to use it „actively". This aspect is particularly evident in the combination of plant-growth with shore-revetments of different nature, the result of

Figure 2.4.15.3. Some examples of defense against shore-erosion by wave-attack in a new-formed lake.
a. reed in shallow freshwater
b. a layer of pebbles directly on the shore-line; the shore-processes are disturbed completely;
c. a ridge of pebbles at some distance of the shore-line; the shore-processes are less disturbed;
d. a ridge consisting of pebbles at the outer side and sand at the inner side.

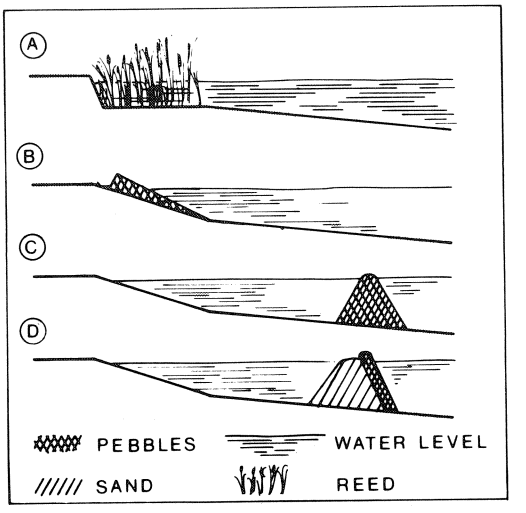

which could be both technically stronger and ecologically more stable and interesting. The reed-verges along freshwater lakes are already a familiar sight (see fig. 2.4.15.3a) but also along saltwater coasts there are plenty of opportunities to form an attractive and at the same time effective protection, depending on the actual location. Fig. 2.4.15.3 illustrates three ways of protecting an eroding shore of a stagnant lake. In fig. 2.4.15.3b the shore itself is protected with gravel (or asphalt) which results in a solid shore offering little or no possibility for the growth of vegetation and morphological processes. In fig. 2.4.15.3c a gravel-dam is built at some distance from the shore; this results in the creation of shallow and more or less sheltered water-zones in which benthic animals and waterplants can grow. In a freshwater lake, the shore itself can acquire a reed-vegetation. Finally, in fig. 2.4.15.3d this gravel-dam is built from both sand and gravel. In saltwater, the exposed area of such a dam - if low enough - will mostly remain bare and therefore, provide a breeding ground for certain species of birds; in freshwater reed-vegetation can occur, thus providing a more attractive landscape. Depending upon the local situation, many other possibilities are conceivable. See also [3].

2.4.15.4. Production of materials

Enormous quantities of building materials are required for the construction of large civil engineering structures; particularly such materials as gravel, sand and clay but also, for instance, marl (for cement). The production of these materials also affects the environment. Below the different environmental aspects will be discussed (briefly), particularly the dredging of sand as this usually takes place in the proximity of the structure to be built and is therefore directly related to the work. For more detailed information see [4, 5]. As to the environmental aspects, resulting from the excavation of these materials in other places, it can only be said that these will have to be assessed locally.

Winning of sand

Sand will usually be dredged in water, which will have its repercussions on morphology, waterquality, local flora and fauna and on - a human activity - fishery, particularly the cultivation of shellfish.

A first aspect of sand-winning is the change in the morphology, at least locally, but due to possible changes in the current pattern this can also occur at a greater distance from the actual winning-site. Whether the environment and also, for instance, the coastal defence will be adversely affected, will have to be examined in each case apart.

When large quantities of sand are dredged from one place, large sand pits will be created. If these deep pits remain after closure of the dam in a lake or in a quiet area of a tidal basin, where little or no currents occurs, this may easily result in stratification (see also 2.2.6.2). It is therefore advisable to prevent, whenever this is feasible, the creation of these deep pits. Dredging of sand can also be put to advantage, as far as stratification is concerned, by removing a shallow between two deep pits (or channels) that already exist. As a result of this the wind can generate an improved water- circulation in the deep sections or can cause a better circular flow (for instance, if a river debouches in the new lake). Thus, in principle, chances of stratification will be reduced in the pits. However, this must be done very carefully as, otherwise, the area that can be subject to stratification, will increase.
Next, it is important that the bed remains more or less level so as to prevent obstruction of the dredge-nets which are used by the fisheries.

A second aspect to be considered is that the benthic animals will be removed together with the top-layer of the dredged sand. These benthic animals are not evenly distributed over the bed. The biomass (i.e. the total amount) of benthic animals depends upon various factors. The largest quantities of biomass occur in the shallows and the intertidal areas; the biomass is smaller in deeper sections -and even less in the oceans, e.g.

ocean bed	1 g/m² dry organic material (d.o.m.)

North Sea (coastal sea) } some g/m² d.o.m.
Waddensea channels }
intertidal area in the Waddensea about 30 g/m² d.o.m.

A more abundant zone is also found in the shallow coastal seas which stretch some kilometres from the coast.
In addition, the composition of the sediment is important: in soils with a silt-content (fraction $<50\mu$) of less than 1% and over 25%, the biomass is smaller than in beds with a silt-content between 1% and 25%.
Attention must not only be paid to the disappearance of the biomass resulting from sand-dredging but also to the recovery period. The important factors here are the recovery of the bed-profile -and the new sediment composition. In a dynamic area - for instance, a tidal channel with high current velocities and dynamic coarse-grained sediment - the bed-profile as well as the original sediment-composition will recover more rapidly than in quieter areas, i.e. mudflats. Recolonization by animals will also take place more rapidly in a dynamic environment. Investigations, carried out in the Dutch Waddensea, show that an excavated area in a tidal channel recovers already within one year, whereas recovery in a sheltered mudflat area may take many decades. The conclusion to be drawn is that, in view of the much more rapid recovery in the tidal channels and the much larger biomass of benthic animals in shallow parts and on shoals, it must be recommended that dredging should only be allowed in channels and that areas which are no deeper than 5 metres below the mean low-water level should not be disturbed. Another point with regard to this is that, if shellfish cultivation is present, it is usually also concentrated in these shallow areas.

A third aspect of sand-winning is the water-quality. In addition to stratification attention must be paid to the perturbation of the silt which leads, in the first instance, to turbidity. Secondly substances such as heavy metals, persistent toxicants (i.e. CHCl) and nutrients, that normally lie dormant in the bed, can be stirred up. Moreover, an increased decomposition of dead organic matter can occur, resulting in a decrease of oxygen concentration in the water. These aspects may have important repercussions on the environment. Due to the activation of heavy metals and persistent toxicants in the water, these substances can strongly increase in the local benthic animals - even a doubling of the normal concentrations has been recorded.
As a result of the increased turbidity, the primary production (i.e. plant growth) can be restricted, while animals living in the water, who depend on their eyesight in their search for food can be hampered. In addition the feeding value of the matter in suspension (i.e. the proportion between digestible matter and indigestible silt) can decrease. As a consequence, animals subsisting upon matter in suspension will get down less food or will even „suffocate" on the regurgitated indigestible silt, resulting in decreased growth or even death.

The size of the affected area may vary greatly: e.g. at a sand-winning site in the Dutch Waddensea, an area of only one km² showed signs of being affected, whereas, in an adjacent area, the Eems estuary, containing finely grained sediment, an area of over 100 km² will probably be affected.
Therefore, it can be concluded that it is preferable to dredge sand in areas which contain coarse sand and where a satisfactory and rapid discharge of the stirred up silt is possible. Special attention must be paid to existing shellfish beds and to dredging activities in polluted silt.
Moreover, dredging in autumn and winter, when biological activities are reduced, will have less effect than in spring and summer. During the latter periods the biological activity is increased also because many animals breed and settle, as a result of which they are more vulnerable.

Excavation of clay

The excavation of clay will usually take place on land and may lead to the creation of deep pits. If these excavations are done with care and are properly finished off, the area can later be used for other purposes such as recreation and nature or also as drinking water basins or for fish-farming. When deciding on the site and

shape of the excavations, the future allocation of the area must be taken into account. If the area is intended to have a natural or fish-cultivation function, then the excavations should not be too deep to prevent stratification. For natural functions the slope of the fore-shore should be gentle (max. 1:10) to permit the growth of shore-plants, whereas for water-reservoirs excessive algae-growth is undesirable. However, the chance that this will occur is rather large as the incoming water is often rich in nutrients and the residence time in the basin is usually long. As indicated in 2.2.6.2 algae-growth is only possible up to a certain depth, known as the euphothic zone. Therefore, the algae biomass will be smaller in a deep reservoir than in a shallow one. Based on this information, it is preferable to opt for deep reservoirs when divising a construction plan [6] although, in these basins, there is a stronger possibility of stratification. The local situation will therefore determine the construction strategy.

2.4.15.5. Spoil dumps

Apart from the problem of winning of materials, there is the additional problem of the disposal of large quantities of unusable spoil. The spoil dumping can, in principle, be done in an environmentally consious manner by, for instance, using the material to create new intertidal areas. These new intertidal areas can compensate for the intertidal areas lost as a result of the construction activities, especially with regard to the important feeding functions of these areas for birds and fishes. Especially in the USA much research is done on this subject [7,3].
When the dredged material is pumped into certain areas it is important to ensure, that as little as possible of the sediment in suspension, particularly polluted sediment, drops into the water of the basin. The consequences, i.e. an increased turbidity of the water and its effects on the environment, have already been discussed in the former section. This implies that dumping of this waste spoil should, preferably, take place in an enclosed area. Depending upon the final situation and the future use of the spoil dump the temporary enclosure dike can be levelled after the completion of the project. In the case of spoil dumps also special attention should be paid to existing shellfish beds.

2.4.15.6. The co-use and re-use of dams and construction sites

The dimensions of dams and sluices, the possibilities of finishing-off and co-use of the dams and the finishing-off and re-use of the construction sites strongly depend on the local situation and the wishes of the local population and government. In the scope of this book, these points can only be discussed in general terms.

The dam and its auxiliary functions
When dimensioning and constructing the dam the technical requirements will be considered in the first place. In addition, a dam can fulfil all sorts of auxiliary functions. One obvious function is traffic (roads); other possible functions are recreation - e.g. shore recreation, sports-fishing -and the professional fishing industry -e.g. fish-traps and culture-beds. When dimensioning and designing the dam, if such auxiliary functions are being considered, they must be taken into account, for instance by constructing wide banks. The same applies when dimensioning and designing sluices; e.g. shipping locks, that in addition to the primary goal - shipping -can also be used to regulate the supply or discharge of fresh- or saltwater into a salt- or freshwater lake resp. When the salt-load is either too low or too high to maintain a desired salinity, solutions must be found, for instance by building smaller locks or a fresh-/saltwater separation system. When dimensioning and designing the discharge-sluices facilities could be provided to enable the import or export of organisms. This can be aimed at creating either an ecosystem as good and as varied as possible or specifically at the fishing industry. In addition, the size of the shipping locks and discharge-sluices greatly influences the possibilities of maintaining a wished water-level system and a good water-quality.
Sluices, that are either too small or too large can affect the basin negatively.

The construction sites
The construction of large civil engineering

works often requires the building of temporary working harbours and sites for the storage of materials and equipment. Usually such sites only have a temporary function and it is therefore possible after the works have been completed, to use them for other purposes such as a yachting harbour, an industrial site or for fish and shellfish cultures. As these new functions have specific requirements as to e.g. size, location and design of the former working harbour and sites, it is just sensible - if only from an economic viewpoint - to take these requirements into account from the outset.

If, at the time of construction of these sites and harbours, their future functions are still unknown, the plans must be so divised that there will be enough scope for as many realistic future options as possible.

Literature

1. Ralph, R. & K. Goodman, Foul play beneath the waves, **New Scientist,** June 21, pp. 1018-1021, 1979.

2. Anonymus, Oxygen model of the Zoommeer during its desalination, **Delft Hydraulics Laboratory R 1318**, 1978 (in Dutch).

3. Cronin, L.E. ed, **Estuarine Research**, Vol. I, II, Acad. Press Inc., New York, 1975.

4. May, E.B., Environmental Effects of Hydraulic Dredging in Estuaries, **Alabama Mar. Res. Bull. Vol. 9**, pp. 1-85, 1973.

5. Ierland, E.T. van & H.W. van de Veer, Study of literature with regard to the possible consequences of sand winning in the Dutch Waddensea, **Internal Reports of the Netherlands Institute for Sea Research**, Texel nr. 1982-5 (in Dutch).

6. Oskam, G., A Kinetic Model of Phytoplankton Growth and its Use in Algal Control by Reservoir Mixing, Int. Symp. on Man-made Lakes, their Problems and Environmental Effects, **Geophysical Monograph Series 17**, pp. 629-631, 1973.

7. Anonymus, Annual Reports of the Dredged Material Research Program. Environmental Laboratory, **U.S. Army Engineer Waterways Experiment Station**, Vicksburg, Mississippi.

Interaction Water Motion and Closing Elements

J. Stuip

2.4.16. Gates

Introduction

When a sea-arm is closed off whereas all or part of the river discharge must still be let through, the closure must incorporate a discharge sluice. In order to be able to regulate the water level in the basin behind the closure and/or the discharge through the sluice, the latter is generally fitted with regulating closure mechanism, namely gates. In some instances it may also be necessary for seawater to be admitted in order to regulate the level or quality (or both) of the water in the basin. This imposes particular requirements on the design of the sluice, gates and operating machinery. The gates in engineering works of this kind form part of permanent constructions and must therefore satisfy specified requirements in terms of durability and durable functioning. Where the gates in a structure are required to operate only temporarily, as in the case of a sluice caisson, they are subject to different demands with respect to durability and durable functioning. The requirements for opening and closing and the boundary conditions under which these operations must be able to take place will also differ. Gates in different structures do, however, share the common requirement of being able to keep out water in the closed position. This means in the first place that the gates must be able to cope with loads produced by the difference in water level and, where relevant, by waves. In addition the joint between the edge of the gate and the adjacent structural elements must be such as to limit leakage. It can happen that too tight a seal is sometimes aimed at, with the result that the sluice construction can be subjected to excessive shear and that the risk of a gate's jamming is increased. Apart from information on the geology and the load-bearing capacity of the bottom etc., it must also be decided when designing a sluice construction to what extent the following conditions must be satisfied for the structure to function satisfactory:

a. What discharge must be able to pass through at determining water levels? This might take the form of : at slack-tide, given no wind, a given number of m^3 must be capable of being discharged every 24 hours.
b. Is the flow in just one or both directions?
c. Are there special requirements with respect to holding back water?
d. Are there subsidiary functions, e.g. maintaining a constant basin-water level or a constant discharge, etc.?
e. Should it be possible to measure the discharge?
f. Does the water have to be aerated?
g. Does the discharge have to be withdrawn selectively from the upper or lower water layer? (e.g. in relation to discharging cooling water or salt penetration)
h. Must sand transport be permitted (or is sanding up anticipated)?
i. Passage of ice, suspended matter, etc. suspected?
j. What is the ice condition? (in relation to ice loads or to keep out ice floes)
k. Must the discharge or water level be automatically regulated? (i.e. self-regulating gates, automatic cut-in siphons, lever mechanism geared to water level etc.)
l. What are the determining wave conditions?
m. Is the passage of fish necessary?
n. Is there a risk of weed, algae, mussels, etc. growth?
o. Is there shipping in the vicinity? (e.g. prevention of vessels entering sluice, navigation problems caused by outflow discharge, waves generated by shipping)
p. Is the length of the sluice partly determined by the presence of a road on top, or is it incorporated in a dike?
q. What risks are acceptable (in relation to the number of openings, maintenance, single or double gates)?
r. Does shipping have access to the basin or seaward side in relation to the possible maintenance or repair of the scour protection after exposure to extreme conditions?
s. What are the maintenance and operating possibilities (of particular importance in developing countries).

A detailed discussion of the various types of gates would be beyond the scope of this book. The following sections examine a number of structural and hydraulic aspects.

Structural aspects

In principle a gate may be moved by either translation or rotation about three axes at right angles to each other. Combinations are also possible. In addition the translation and/or rotation axis may be situated at any point desired in the water-course. A number of basic possibilities are shown in Figure 2.4.16.1. Thus a horizontal axis may be placed on the bottom of a river, either above the water level or half in the water, while a vertical axis may be sited either in the middle or at the edge of a water-course or sluice.

It is not necessary that the axes of rotation should also form the supports for the gate in open or closed position. In the closed state, the supports on two, three or four sides of the gate may consist of concentrated bearing points taking the form of roller or slide bearings.

The loads resulting from the retained water and/or waves is transferred to these bearing structures. The loads resulting from opening or closing the gate generally operate in a different direction (vertical) from the (horizontal) water pressure, and are consequently absorbed in a different manner by the gate.

The design may also be such that the resultant water pressures upon opening and closing the gate are transferred through a single central bearing, as for example in a sector gate.

In order to switch from one bearing system (for opening and closing) to the other (closed or opened) a certain amount of free movement is required, which must then be nullified in the closed condition by water pressure resulting from the retained water or by a self-generated force. Freedom of movement of the gate can give rise to undesirable vibration; this will be examined in more detail later. Vibration is undesirable since large movements can produce excessive strains in the gate itself and structural elements near the moving gate can be damaged. The load on the gate must therefore always be exerted in the same direction so that the gate does not start vibrating.

The gate itself may be constructed in various

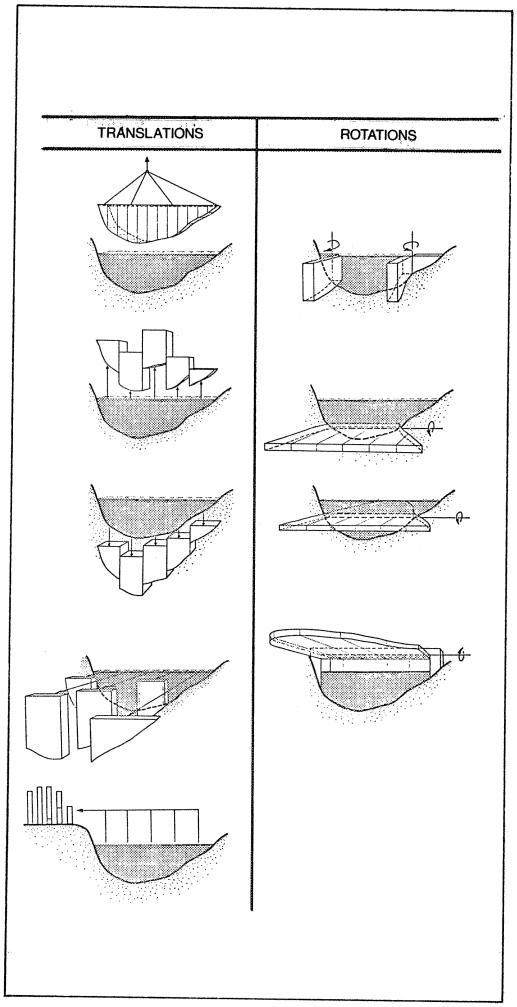

Figure 2.4.16.1 Possible techniques for the non-permanent closure of a water-course.

ways. In this way the barrage function may be separated from the force-transmission function. This is for example the case with a structure in which the plating transmits the horizontal water-pressure to a bearing structure consisting either of a box girder.

The barrier function may be combined with the force-transmission function by for example exploiting the high tensile strength of the steel plating of the gate and constructing the latter as a scale structure. The principle is illustrated in Figure 2.4.16.3, while Figure 2.4.16.4 shows a practical example in the form of the Hagestein barrage.

It is possible for the plating to be constructed not in the form of a single scale but of a number of smaller scales each supported by a bearing structure. The principle is illustrated in Figure 2.4.16.5, while Figure 2.4.16.6 shows a practical example in the form of the Eastern Scheldt Barrier.

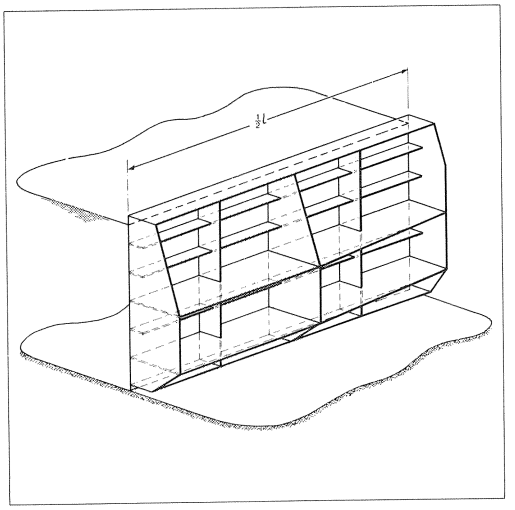

Figure 2.4.16.2 Plate girder.

It is not always necessary for gates to be made out of steel. In particular, closure systems which occupy a greater volume as a result of the method of closure can have a sufficient construction height for concrete to be used as the construction material. Figure 2.4.16.7 shows two examples of a concrete float and a concrete cylinder being used as the closure mechanism.

In a temporary structure such as a sluice caisson, a gate performs the function of holding back the water for a short period only (i.e. several days to several weeks). Apart from a number of test operations the gate will be moved only once, from the open to the closed position. The gate is not therefore required constantly to regulate a precisely-determined water level or to regulate discharges.

The choice between translational and rotational movement of the gate is inter alia determined by the forces on the supports and the stresses generated in them. The decision should be made on the basis of a comparative study into the

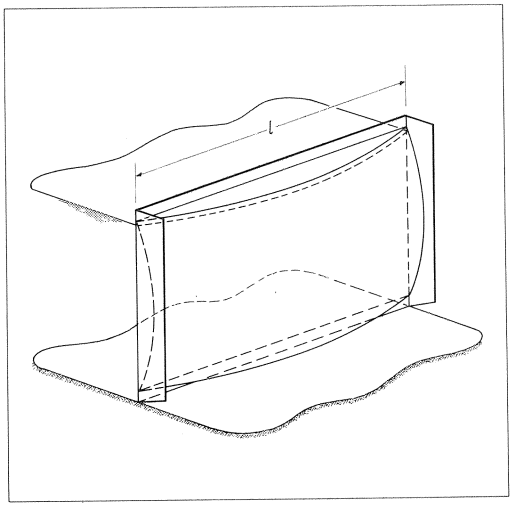

Figure 2.4.16.3 Mono-scale plating.

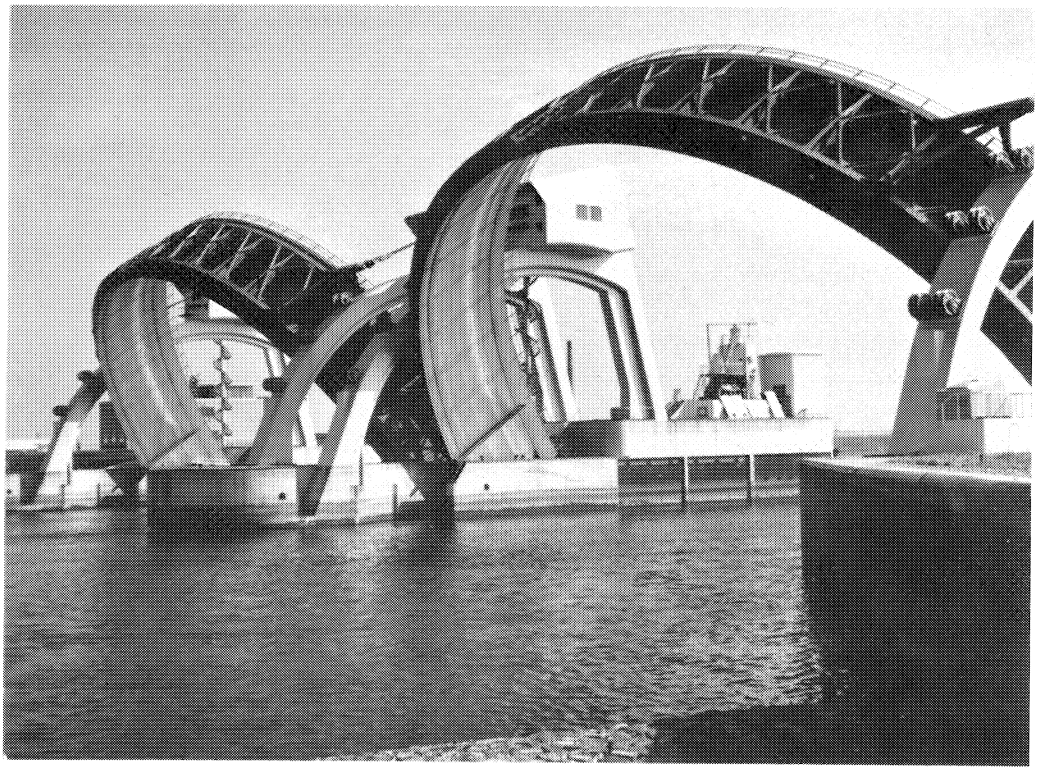

Figure 2.4.16.4 Visor barrage at Hagestein (Netherlands).

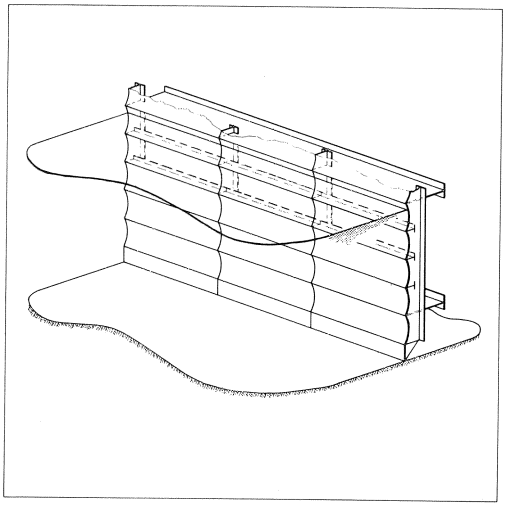

Figure 2.4.16.5 Multi-scale plating.

respective costs and also realiability of the structure. Account needs to be taken of the fact that operating machinery and supporting structures that are either large in size or made out of special materials cannot be manufactured in every country in the world and protectionist policies may prevent the work from being contracted out. Abroad local and national customs and capabilities need to be taken into account

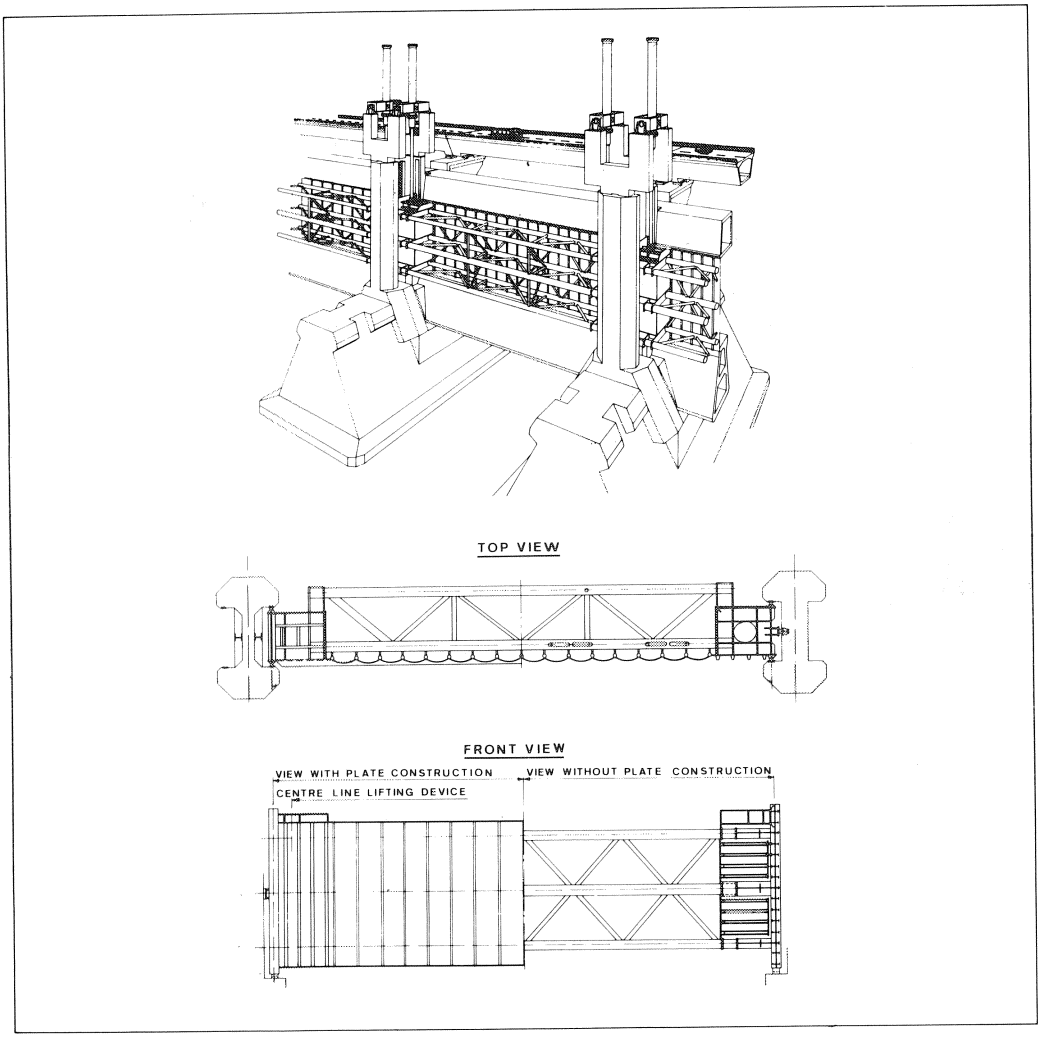

Figure 2.4.16.6 Eastern Scheldt barrier and gate construction

not just in respect of the maintenance but also the operation of gates.
When a gate is moved it rests on supports in order to prevent the stresses acting on the gate from producing uncontrolled movements.

In the case of lifting gates the choice between roller and slide bearings often falls in favour of the latter because a roller bearing has to be ad-

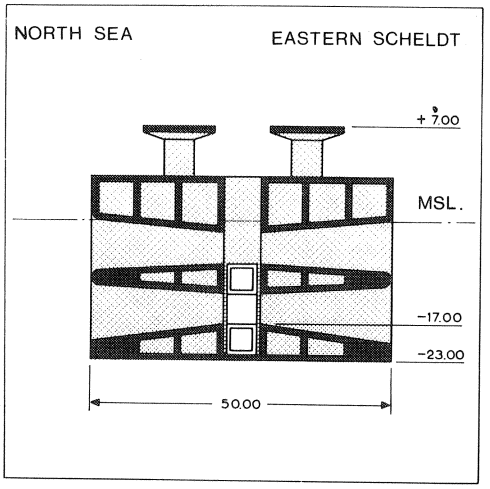

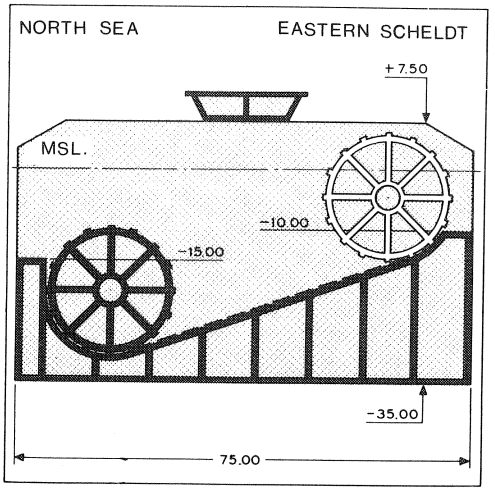

Figure 2.4.16.7 Concrete float and concrete cylinder as closure elements.

justed precisely in order to transfer the stress uniformly. Such adjustment takes extra time during design, assembly and maintenance and therefore increases costs. Slide bearings are moreover now available with very low coefficients of friction.

Operating machinery

Depending on the way in which the gate is operated, an external force or moment must be exerted on the gate in order to fully or partially close the flow gap.

The relevant forces during lifting generally include:

- the dead weight of the gate, armatures, ballast etc.
- weight of any clinging water, ice or sediment etc.
- the rolling or sliding friction in the bearings
- the weight of that part of the operating machinery affixed to the gate
- the rolling or sliding friction of the closure structure
- dead weight of counterweights
- upward force of buoyancy panels
- lifting power

When a gate with a friction bearing is operated, „slip-stick„ phenomena may occur, when the gate moves in jerks. This happens when the lifting force occasionally falls below the level required to keep the gate moving. The gate will then come momentarily to rest, whereupon the lifting force is able to increase again and re-start the movement of the gate. When the gate is moving the frictional resistance to be overcome is less than the lifting power, but the operating machinery is unable to follow the moving gate quickly enough, so that the lifting force declines and the gate momentarily comes to a halt again.

Various sources of energy may be used to supply the external forces, e.g. manual power or electric and diesel generators. The power may be transmitted either mechanically or hydraulically, or in combination. The table 2.4.16.1 sets out some of the advantages and disadvantages of the two methods.

The external force may also be mobilized by

Table 2.4.16.1 Comparison of gate moving systems

	advantages	disadvantages
mechanical transmission	- reliability	- large dimensions - difficult maintenance
hydraulic transmission	- ease of installation	- energy loss - cannot be manufactured or maintained in all parts of the world - too expensive for once-only use

means of the hydrostatic pressure on the floating body or by means of pressure differences from the flowing water. An example is shown in Figure 2.4.16.8

Figure 2.4.16.8 Examples of closure mechanisms operated by water power.

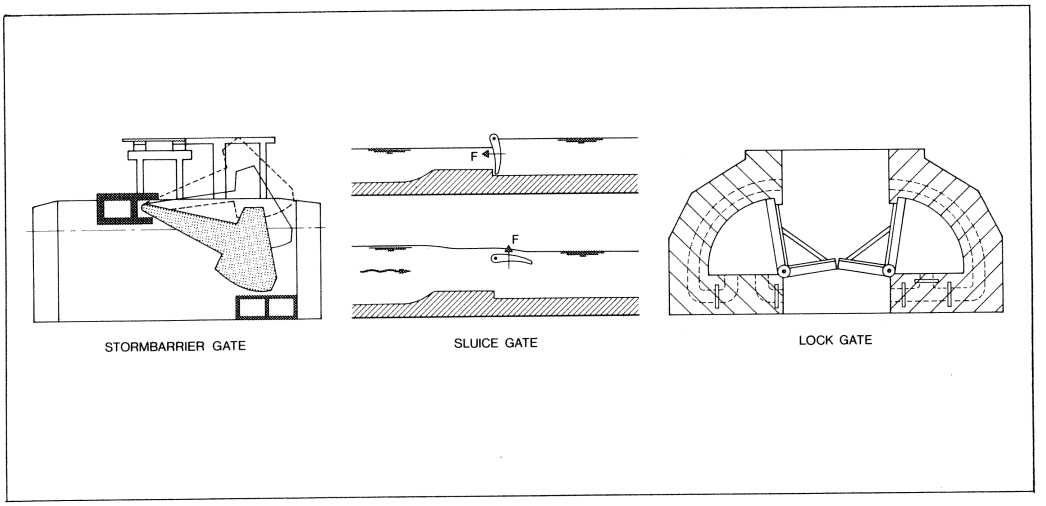

If the gates should form part of a sluice caisson and are situated in the middle, they can when closed increase the stability. The gate is working as a baffle-plate during towing the caisson from the construction dock to the closure dam. Stability requirements for the caisson during this transport stage or the sinking stage may call for lightweight operating machinery situated as low down as possible. This in turn may result in a split gate, such as those in the sluice caissons used for the Brouwershavensche Gat. (Fig. 2.4.16.9)

In this case the operating machinery will be very simple but at the same time highly reliable, if necessary designed in such a way that the gate can also be operated by hand. The gates should preferably be operated at a time when the

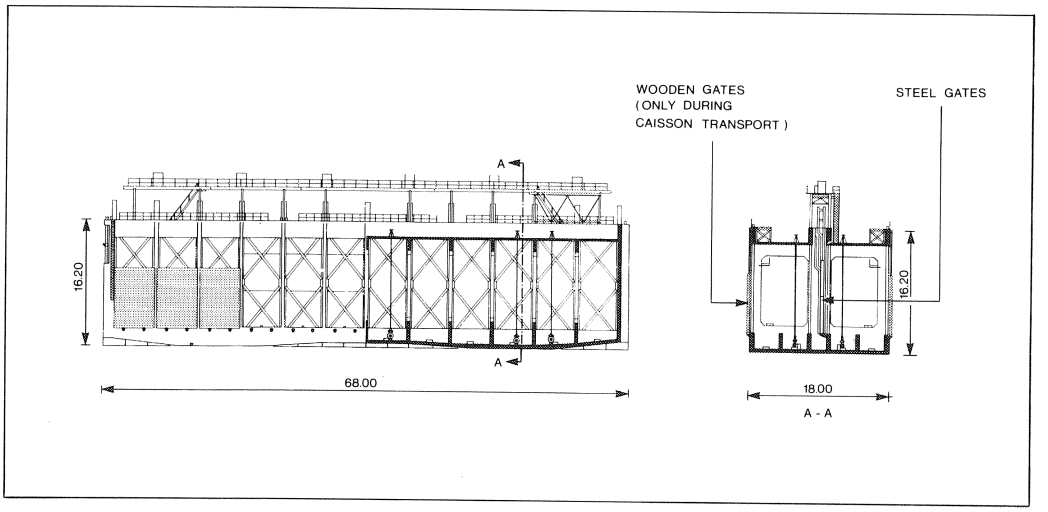

Figure 2.4.16.9 Gates in a Brouwershavensche Gat caisson.

stresses on them are limited, i.e. in tidal areas at the turn of the tide. If the closure operation should fail, i.e. if the gate should fail to move or get stuck half-way, it must then be possible for the gate, supports and operating machinery to bear the resulting loads. A second attempt at closing the gate can then be made at the next turn of the tide after rectifying the cause of failure. Measures should of course be taken at a much earlier stage to ensure that the gate itself and the bottom protection are able to withstand the consequences of a failure.

The type of gate, operating machinery and supports to be used depends on many factors. Reference has been made to the difference in requirements with respect to durability and long-term reliability. As far as ease of maintenance, energy supply and power transmission are concerned, different requirements will apply to a structure that is to be used only once from a structure that is required constantly to regulate the discharge and/or water level.
As regards the design of the gate and the adjacent elements, much the same hydraulic factors generally come into play.

Hydraulic aspects

Static and quasi-static loads

In the closed position a gate is subject to a distribution of hydrostatic forces as shown in Figure 2.4.16.10. The horizontal force is the sum of the resultant distribution of pressure over the height of the gate. For other types of gates the reader is referred to the literature, e.g. [1]. For the sake of simplicity an example is shown below of a lifting gate in a caisson.

$$F_h = \int_a^b \rho\, g\, (h_s - h_b)\, dh = \rho\, g\, (b - a)\, \Delta h$$

in which:

F_h = horizontal load per m of gate
ϱ = specific density of water
g = acceleration of gravity
a = height of the gate
h_s = water depth on seaward side (high-water mark)

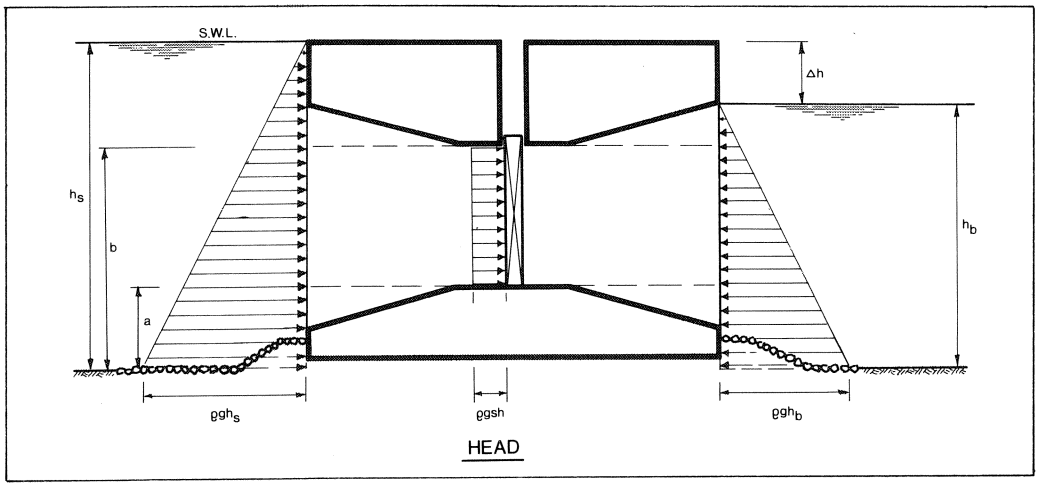

Figure 2.4.16.10 Pressure distribution resulting from potential drop across a caisson, gates closed.

h_b = water depth on basin side (low-water mark)
$\triangle h$ = potential drop across caisson

If linear wave theory is applied for calculating wave loads and if for the sake of simplicity wave pressure is assumed to be in linear relation to water depth, the horizontal wave load on the gate becomes:

$$\hat{F}_{peak} = \int_a^b [p_b + \frac{\rho g (1+\alpha) H - p_b}{h_s} . h] dh$$

$$\hat{F}_{peak} = p_b \int_a^b [1 + \frac{h}{h_s} (\cosh \frac{2\pi h_s}{L} - 1)] dh$$

in which:

$$p_b = \frac{\varrho g (1+\alpha) H}{\cosh \frac{2\pi h_s}{L}}$$

ϱ = specific density of water
H = incoming undisturbed wave height
α = reflection coefficient
L = wave length

$$\hat{F}_{trough} = \int_a^b [p_b + \frac{\rho g (1+\alpha) H - p_b}{h_s - \frac{(1+\alpha) H}{2}} . h] dh$$

$$\hat{F}_{trough} = p_b \int_a^b [1 + \frac{h}{h_s - \frac{(1+\alpha) H}{2}} (\cosh \frac{2\pi h_s}{L} - 1)] dh$$

At the passage of a wave peak the wave load acts in the same direction as the direction of propagation of the (undisturbed) waves while for a wave trough it acts in the opposite direction. Generally allowance is also made in this simplified Sainflou estimation for an increase in the intermediate height

$$h_0 = \frac{\pi H^2}{L} \coth \frac{2\pi h_s}{L}$$

Model analysis has indicated that where structures are subject to extensive breaking of waves over the top of the gate , as in the case of the

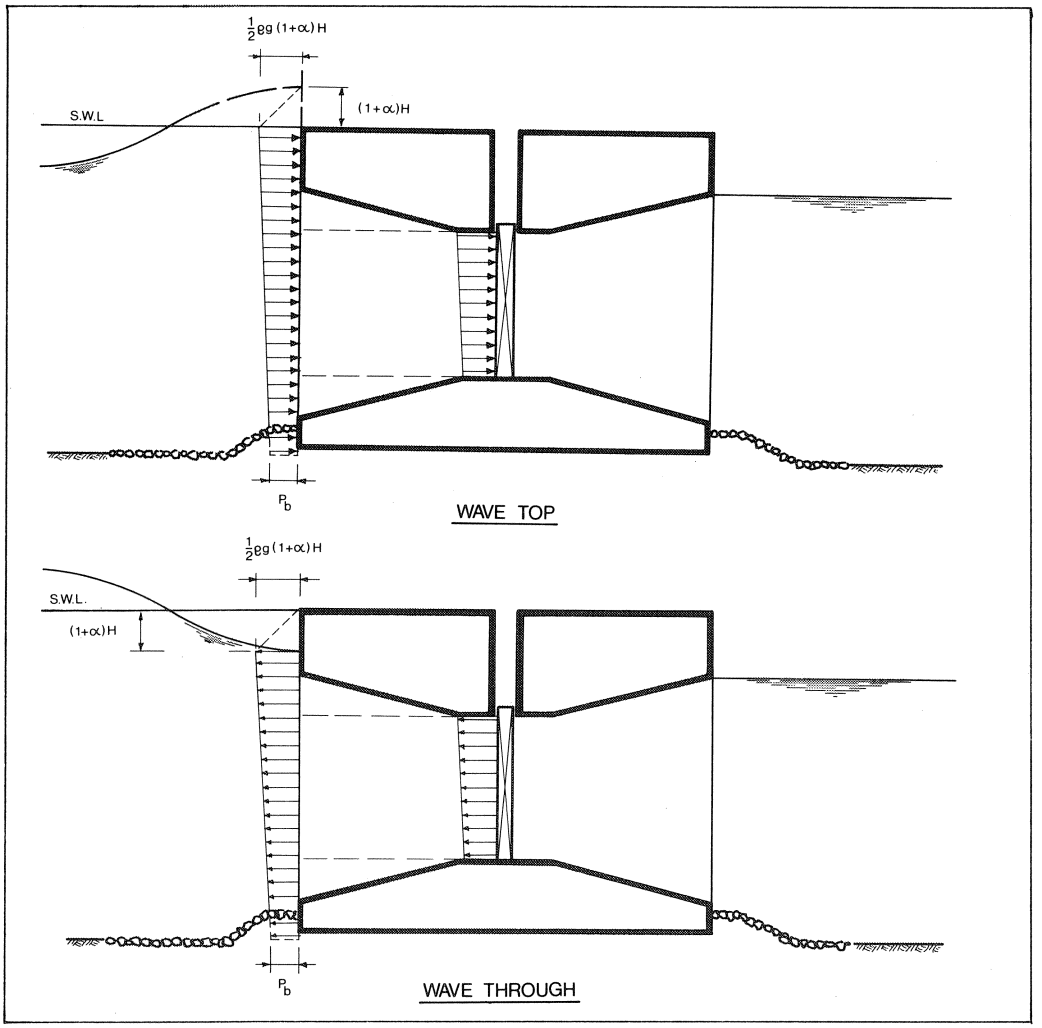

Figure 2.4.16.11 Pressure distribution resulting from wave loads at wave peak and trough.

above example, the increase in the height of the intermediate level is not measurable.

With reference to the subject of wave loads the sections should also be consulted that deal with wave loads on vertical faces. The wave and potential drop loads are superposed.

For partially closed or opened gates it is assumed for a first approximation that the wave form does not change and that the same pressure

distribution can consequently be used. In the case of larger openings, however, the wave will be sucked through under the gate, so that the wave form does alter distinctly. Wave reflection will decrease and the wave pressure be reduced. The direction of the wave pressures in a wave peak are opposite to those in a wave trough. In order to prevent a gate from rattling and hence to avoid possible damage to the gate or supports (or both) it should be ensured when operating the gate that, just as in the closed position, the resultant stresses on the gate act in one direction only. Apart from such quasi-static loads, local, extremely high stresses can be produced by wave shock, although these will be of very brief duration. An undulating water jump may even hit the structure at the rear and cause dynamic loading.
Phenomena of this kind occur in blind corners

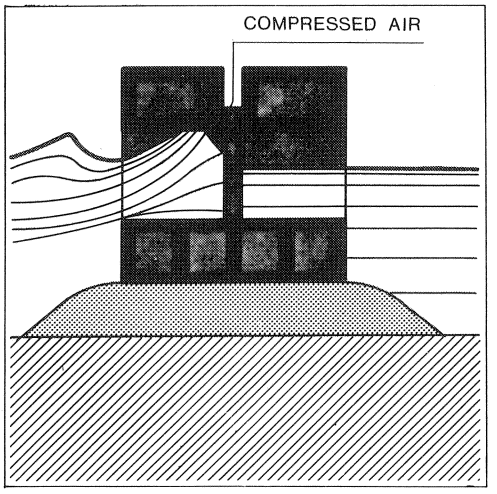

Figure 2.4.16.12 Piston-type wave shock due to compression of air in a blind corner in a caisson.

where the (reflected) wave is trapped (e.g. in a gate girder, sewer ceiling or underside of an upper compartment in a caisson). A thorough study of wave-impact phenomena would be beyond the scope of this book. In general, however, it may be stated that the designer should attempt as far as possible to prevent such wave-impact forces. The shape of the construction (gates, supports, superstructure etc.) should be designed in such a way as to prevent the sudden blocking or hitting of water masses. This means that there should be no horizontal structural elements around the still water line.

The load resulting from the potential drop across a partially opened gate differs substantially from that in the closed position, since the water flowing under the gate will produce a basic alteration in the distribution of pressure on the gate, particularly around the bottom edge and behind the gate. The horizontal force per metre on the gate is calculated as follows:

$$[\tfrac{1}{2}\,\rho\,g\,(h_s^2 - h_b^2) + F_h]\,dt = \rho\,Q\,(v_s - v_b)\,dt$$

in which:

$h_{s,b}$ = water depth on the seaward and basin sides resp.
F_h = horizontal load per m of gate
Q = discharge through opening
$V_{s,b}$ = velocity upstream and downstream from caisson resp. in area with straight flow-lines.

In the case of a gate in a sewer a pressure drop occurs across the gate reaching a maximum of

$$2\sqrt{\xi_s} \times \frac{v^2}{2g}$$

where ξ = loss resulting from contraction in the gate and v = current velocity in the sewer.

The drop in pressure across the upstream and downstream cross-sections 2 and 1 is equal to

$$\tfrac{1}{2}\,\rho\,v^2\,\xi_s$$

so that the total horizontal force per metre on the gate becomes:

$$F_h = \tfrac{1}{2}\rho v^2\,(\xi_s + 2\sqrt{\xi_s})\,h$$

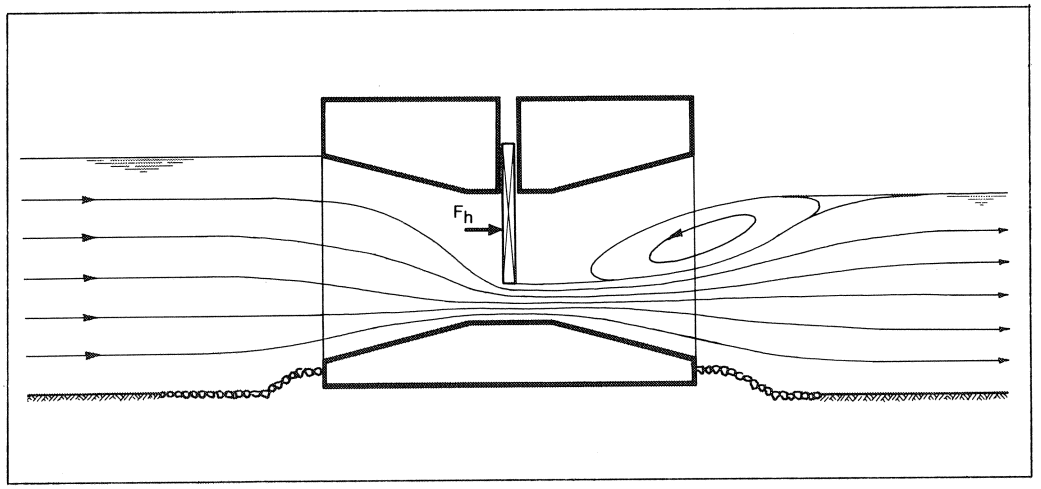

Figure 2.4.16.13 Flow pattern for a partially opened gate in a caisson (critical flow).

Figure 2.4.16.14 Flow pattern in a partially opened gate in a sewer (subcritical flow).

The under-pressure operates on all sides, including on the gate supports, which must therefore be taken into account in calculating the required lifting force. This vertical load may be reduced by perforating the horizontal girder. This will both reduce the area over which the forces are applied and enable an equalization with the lower pressure in the shaft to be achieved.

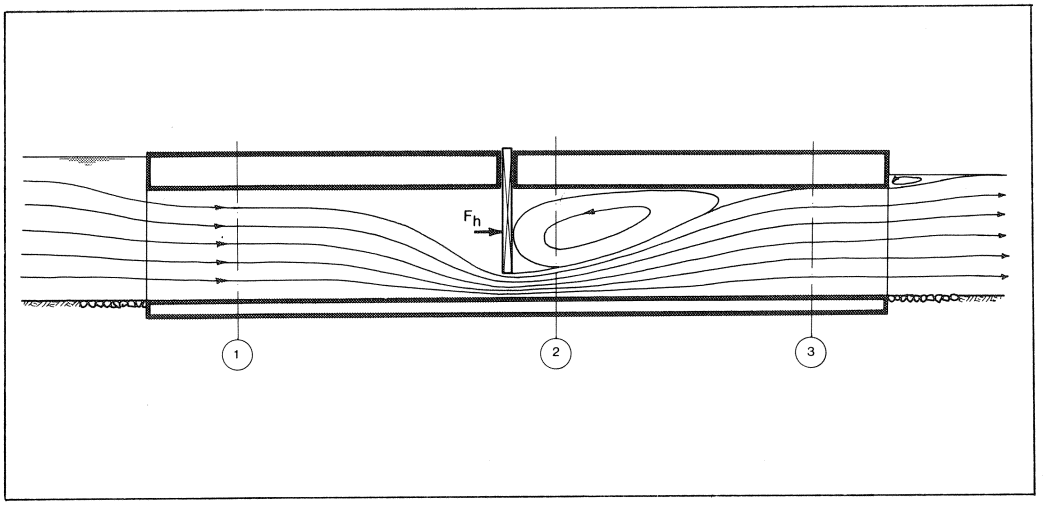

Due to the fact that the flow pattern around the edge of the gate is asymmetrical forces normal to the flow direction can be expected.
These forces are mainly suction forces that often fluctuate thus causing - mostly - impermissible vibrations.
Due to the flexible character of the gate and supports and the occaisionally fluctuating character of the waterflow over and/or under the gate, the structure can be considered as a mass-spring system with a certain damping property.

Gate vibrations can be classified into three types:

1. Vibration modes with flow-gap width variation due to gate vibrations.
2. Vibration modes with constant flow-gap width; high frequency. plate vibrations are often observed.
3. Vibrations occuring at gate position where the flow is wavering between reattachment and full seperation.

Fluctuating gap-vibration follows after phenomenon known as the bath tub plug analogue.
Due to a suction force the plug tends to close the bath tube. The continuous flow of the water in the drain pipe makes it difficult to stop the discharge immediatly. Holding the plug in place by hand (= spring) so as to leave a very small opening, always causes a vibration of the plug.
A suction force may be used as an indicator for evaluating the gate structure with respects to self excitations fig. 2.4.16.15 gives exemples of suction forces as an indicator for gate vibrations [3].

In the case of leakage flow throug the narrow gap between the gate and the adjacent structure the tendency of the pressure to increase or to decrease is an indicator for possible vibration.
If the presure tends to decrease then the situation is unstable.

To prevent gate vibrations, the following guidelines can be given for designing the shape of the gate, but these do not quarantee a problem free design.[3].

1. To prevent self-excitation
   a in cases of vibration modes in which the gap size fluctuates, suction forces (in general: forces tending to close the gap) should be prevented and/or structural damping properties should not bee low;
   b in all cases, unstable flow separation and/or rettachment zones should be prevented; if this is not complete possible then the gate edge or other gate elements should be designed in such a way that the fluctuating flow does not hit in phase the edge over a large length or area.
   c low-pressure regions should preferably be vented by admitting air or water from a high-pressure region;
   d the widht of leak gaps should be at least 1.5 times (preferably twice or more) the width of the gate edge;
   e when there is space formation no change in force direction should be permitted;
   f slender stop logs and gates should be carefully designed so that static and dynamic loads do not exceed over their weight.
2. Resonance frequencies of gate hoist systems and gate members should be well (3 to 10 times resonance frequency) above the dominant excitation frequencies.
3. Water surfaces, which are unstable, due to turbulence, waves, hydraulic jump, water colum seperation or cavitation, shoul be prevented from hitting structural surface, especially when these are parallel to the water durface or have blind corners.

In conclusion it is felt that flow-induced hydrodynamic forces should be thoroughly studied for the final design. In general, the studies are supported by physical model tests for the characteristic cross-section of the gates, and their support structure with a large range of hydraulic boundary conditions, and the opening position of the gate.

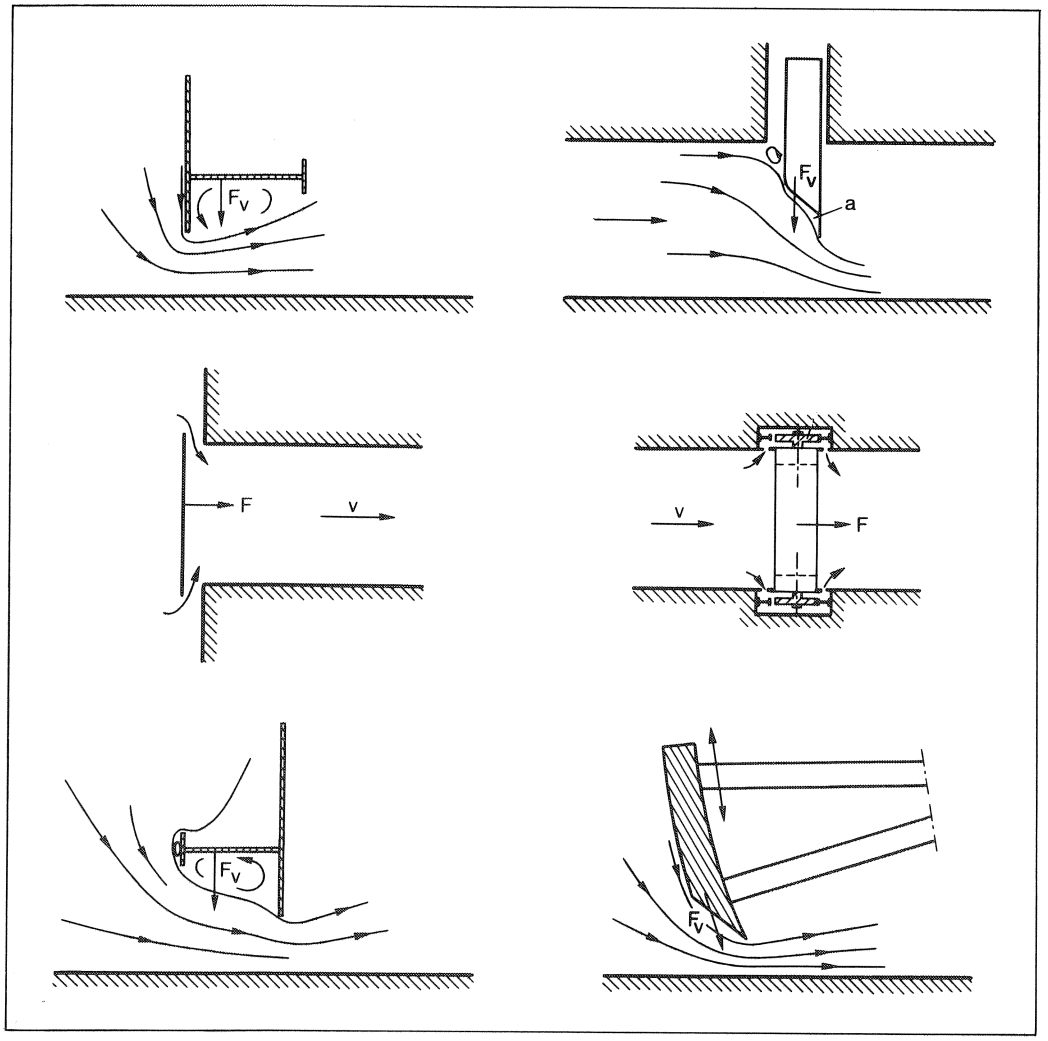

Figure 2.4.16.15 Suction forces on gates as an indicator for gate vibrations [Koltman (3)].

References

1. G. Wickert, G. Schmausser, **Stahlwasserbau,** Springer Verlag 1971
2. Naudascher, E. **Flow induced structural vibrations,** Symposium, Karlsruhe, 1972
3. Kolkman, P.A. **Flow induced vibrations,** Delft 1976

2.5. Impact on the Environment

The closure of a sea arm introduces a change in the environmental conditions not only in the vicinity of the works but also at larger distances.
This may arise gradually or as a shock effect. The impact may not only be present in the final stage but also already during execution stages. Short term actions (e.g. tidal periods) as well as long term operations (e.g. seasonal periods) during the execution may influence the natural conditions and also the way of execution.
Models to predict the short term and long term effects on the environment are the subject of this section.

Impact on the Environment

C.P. Ockhuysen

2.5.1 Hydraulic aspects

1.1. Introduction

This chapter examines the hydraulic aspects associated with the closure of breached dikes and estuaries. An indication is provided of the extent to which the various closure methods are dependent on the hydraulic conditions of the closure.

The first part of this chapter examines the repair of dikes after a breach. The second part deals with closures in estuaries. This division reflects the difference in geometry and starting points of the two situations. In the case of dike breaches there is generally no return to an equilibrium situation. Instead the size of the gap increases and channels are eroded, thus making it imperative for the gap to be closed as quickly as possible, often on the basis of rough estimates of pertinent data.
In the case of estuary closures, on the other hand, equilibrium conditions do prevail and there is time for data to be collected, thus permitting sophisticated analytical methods to be applied.

2.5.1.2. Hydraulic conditions in a flooded polder

2.1. Introduction

In drawing up a plan to close breaches in the dikes enclosing a flooded polder it is important to have a clear view of the hydraulic conditions. Such a survey should be compiled systematically, i.e. the breaches and inundated areas should be properly surveyed in terms of their hydraulic and geotechnical characteristics such as the surface area of the flooded basin during the various phases of the tide, the tidal prism, the hydraulic resistance of the polder and the consistency of the soil on the surface and in deeper layers. In addition a survey must of course be compiled as quickly as possible of threatened settlements and communication links. The inundation depth is the joint result of the elevation of the polder and the height of the water level If the inundation depth is great the water flows in and out of the polder with less resistance than if the depth is shallow.

These hydraulic factors are linked by relationships, which may be described with the aid of the mathematical formulations discussed below.

2.2. Water flow

The information on geometry, flow resistance, contraction coefficients necessary to calculate the flow in the breach and the polder, is dictated by the mathematical formulation of the elements referred to above. Calculations made by means of such formulations, equations, and, where appropriate generated by physical models are indispensable to arrive at a proper closure schedule. Even with computers the mathematical simulations, calibrations, computation and interpretation required for solving the complete 3-D equations is time consuming and expensive. For this reason the movement of water is assumed for calculation purposes to be one-dimensional with the ability where necessary to incorporate significant two-dimensional effects.
This approach will in general be acceptable because the flow in an inundated area will take place through scour channels or existing watercourses in the polder, and hence be of a one-dimensional nature.
The flow velocities in the inundated areas next to the channels are much lower; these areas simply serve as storage.
One-dimensional flows may be described by means of the equations of continuity and motion (figure 2.5.1.1).
Considering a unit width of channel the continuity equation is:

$$\frac{\partial \eta}{\partial t} + \frac{\partial u(h + \eta)}{\partial x} = 0 \qquad (1)$$

in which:

h	=	total depth at mean sea level	(m)
η	=	water elevation above or below mean sea level	(m)
u	=	average velocity in the cross-section	(m/sec)

Assuming a rectangular cross-section of breadth B, the continuity equation can be integrated to yield:

$$\frac{\partial Q}{\partial x} = - B \frac{\partial \eta}{\partial t} \qquad (2)$$

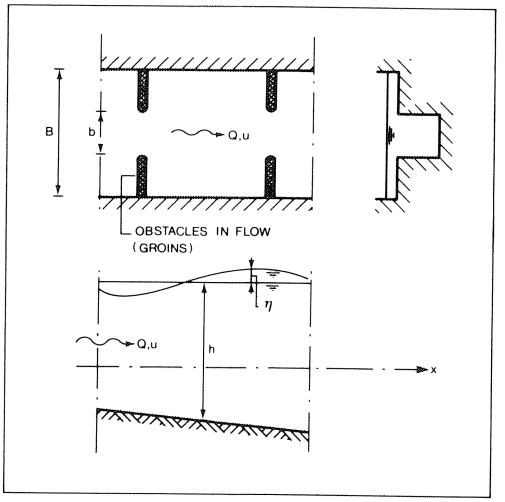

Figure 2.5.1.1. Schematized channel.

in which:

B = width of the channel (m)
Q = total discharge through the cross-section, positive in the flood direction (m^3/sec).

It is assumed in the above that $\delta\eta/\delta t$ is uniform across the breadth of the water-course.
The cross-section of the water-course will of course generally not be rectangular. In many cases a distinction will then have to be made between

- that part of the cross-section carrying the flow, and
- the overall cross-section

In case of a composite cross-section:
In the continuity equation, B is in case of a composite cross-section equal to the storage width. The continuity equation states that the difference in discharge between two cross-sections, X and X + dX, is in equilibrium with the accumulation or loss of water resulting from a rise or fall in the water level between the two cross-sections. The continuity equation for a non-rectangular profile is more complicated, and the reader is referred to the literature [2]. The general equation of motion for a one-dimensional long-period wave per unit of width is as follows:

$$\frac{\partial u}{\partial t} + u\frac{\partial u}{\partial x} + g\frac{\partial \eta}{\partial x} + g\frac{u|u|}{C^2R} - \beta\frac{W|W|}{(h+\eta)} = 0 \qquad (3)$$

in which:

C = Chezy coefficient ($m^{1/2}$/sec).
ß = wind stress coefficient
W = resultant of wind velocity in direction of the water-course (m/sec).
g = gravity acceleration (m/sec²)
R = hydraulic radius (m) = wetted area/wetted perimeter

Usually, instead of R the total waterdepth may be written in the equation of motion.
In the above it is assumed that:

. The fluid is incompressible and homogeneous
. The tide generating forces are negligible
. Vertical acceleration may be neglected with respect to the gravity acceleration.

The various terms in the equation of motion are as follows:

$\delta u/\delta t$ = local acceleration
$u\delta u/\delta x$ = advective acceleration (Bernouilli term) (4)
$\delta\eta/\delta x$ = water surface gradient
$\frac{\beta W|W|}{h+\eta}$ = wind stress per unit mass

For a channel with a rectangular cross-section the motion equation may be integrated over the width which yields the equation of motion in terms of :

$$\frac{1}{A}\frac{\partial Q}{\partial t} + \frac{\partial}{\partial x}\left(\alpha\frac{Q^2}{A^2}\right) + g\frac{\partial \eta}{\partial x} + g\frac{Q|Q|}{C^2A^2R} + \beta\frac{W|W|}{h} = 0 \qquad (5)$$

in which
α = coefficient taking the vertical and horizontal velocity profiles into account upon integration (usually 1).
A = wetted area, averaged over time (m^2)
For equations of motion in the cases of non-rectangular cross-sections the reader is referred to [2].
In a qualitative sence the following can be said about the terms in equation 5:
- In the inundated area the Bernouilli term can be neglected.
- For the flow in the breach the dominant terms in the equation of motion are the Bernouilli term and the water surface gradient term.

In general the equations 3 and 5 are solved using a numerical technique. For this purpose the flooded region is divided in an inlet channel encompassing the actual breach and existing and scoured water courses. The differential coefficients in the complete equations 2 and 5 or the simplified versions of the equations are written as difference quotients. In the calculations the main interest is in current speed in the breach.

To limit the computational effort and realizing that gradients in waterlevel and current speed in the polder decrease with increasing distance to the breach, the length of the space step is increased with increasing distance to the breach.

An example of sub-division and of water flows in the breach and the flooded polder is provided in figures 2.5.1.2. and 2.5.1.3. Both figures are taken from [3]
The foregoing implies that in a situation in which the Bernouilli term in the closure gap is of decisive importance - e.g. in the case of gradual decrease of cross-section of a breach - any uncertainty as to the friction factor becomes of subordinate importance.
As stated before the Bernouilli term and water surface gradient are the important terms. Retaining only these terms in equation 5 leads to the so called sub-critical flow formula:

$$Q = \mu A \sqrt{2g(H_1 - h_2)} \qquad (6)$$

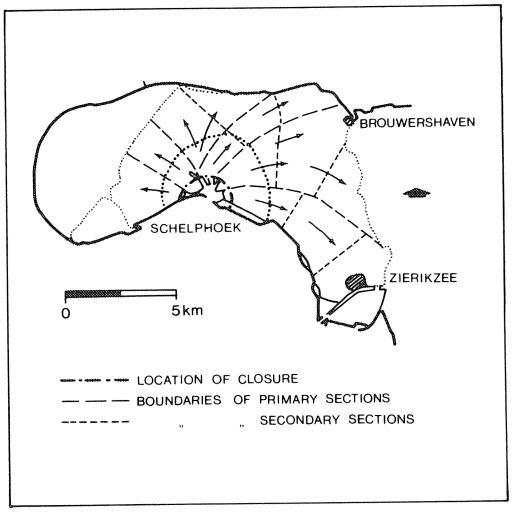

Figure 2.5.1.2. Dike breach at Schelphoek.

Figure 2.5.1.3. Tidal movement inside and outside the breached dike

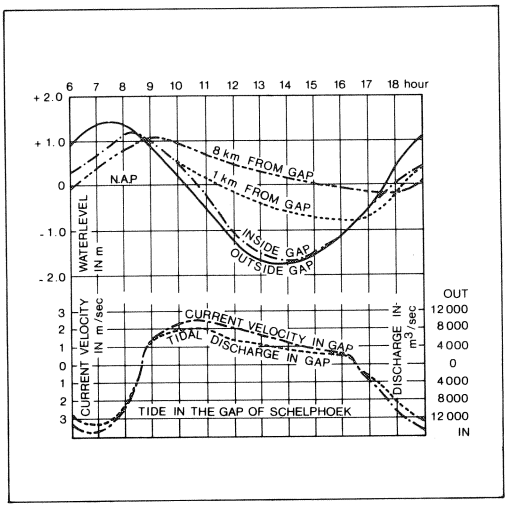

in which:
μ = discharge coefficient
H_1 = the head on the upstream side of the sill or construction in relation to the crest of it.(m)
h_2 = water level on the downstream side of the sill or construction in relation to the crest of it. (m)
A = discharge profile above the sill or in the constriction. (m^2).
The discharge coefficient is usually determined by means of model tests. This coefficient incorporates a variety of energy losses (i.e. exit- and entrance losses) and deviations resulting from a non-uniform velocity profile. Usually instead of $H_1 - h_2$ is written $h_1 - h_2$ in which h_1 = the water level on the upstream side of the sill or construction.
As the downstream water level lowers in relation to the upstream head, the discharge Q will increase.
The discharge is at a maximum if $h_1 - h_2 = 1/3\ h_1$. The current speed over the sill is critical, i.e. equal to $\sqrt{gh_2}$. Critical flow has then been obtained above the weir. The discharge Q equals:

$$Q = \frac{2}{3}\, m\, b\, H_1 \sqrt{\frac{2}{3}\, g\, H_1}$$

where:
m = discharge coefficient, which can have a different value from μ
b = width of the sill or constriction.(m)
In general the value of m will be about 1.
The phenomenon of critical flow is particularly important, as a means of restricting the current velocity to a maximum during the closure of a breach.
The situation of a local flow can also be dangerous. As a result of the downward vertical component of the current on the downstream side, the constriction will be heavily attacked. In the absence of a vertical component of the current the bottom scour will occur only at a much greater distance, where it will matter less.
If, because of losses due to friction on entrance-losses, the water head lowers, the critical flow will turn into a subcritical flow. In the so called transition zone, a hydraulic jump will be created. This hydraulic jump can occur on the downstream edge of the sill or constriction or some distance farther away. In the latter case the bottom has to be heavily defended against scour. Often an underwater levee is created to consume part of the energy of the water, thus lowering the head, stabling the hydraulic jump and creating subcritical flow.
Whether or not the flow is critical depends on the Froude number:

$$Fr = \frac{v}{\sqrt{gh}} \qquad (7)$$

in which
v = velocity of the water flow over the crest of the sill or through the constriction(m/sec.)
h = water depth at the edge of the sill (m)
Fr = Froude number

A Froude number of approximately 1.5 will lead to only a weak hydraulic jump, and a Froude number of around 10 to a very strong one. Other relevant factors include the relationship between the water depth - and to some extent the ground level - on the sill and directly downstream of the constriction.

Figure 2.5.1.4. (taken from [4]) provides an example of a hydraulic jump. Figure 2.5.1.5. (taken from [5]) shows in graph-form the relationship between various kinds of hydraulic jumps, and their dependence on the Froude number, the water level at the sill and the height of the sill. For a given Froude number, the downstream depth of a drop may fall in any of the five regions as shown in figure 2.5.1.5. The lower limit of region 1 is the depth at which the jump will begin to travel upstream. The upper limit of region 5 is the depth at which the jump will begin to travel downstream. Evidently the drop does not control the jump in these two regions. The jump is stable only in the regions 2 and 4. The intermediate region 3 represents an undular state of flow without a breaking front.

In figure 2.5.1.6. each curve for a given h/y_1 has two relatively straight limbs connected by a short straight portion near the middle.
The leftside limb represents the condition corresponding to region 2 and the rightside limb represents the condition corresponding to region 4.

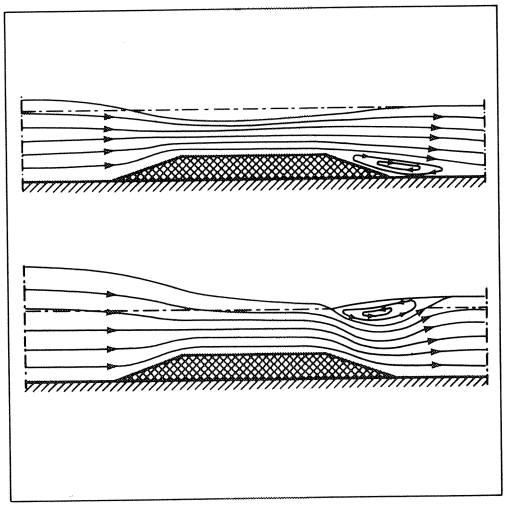

Figure 2.5.1.4. Various flow patterns above: non-diving jet with bottom eddy below: diving jet with surface eddy

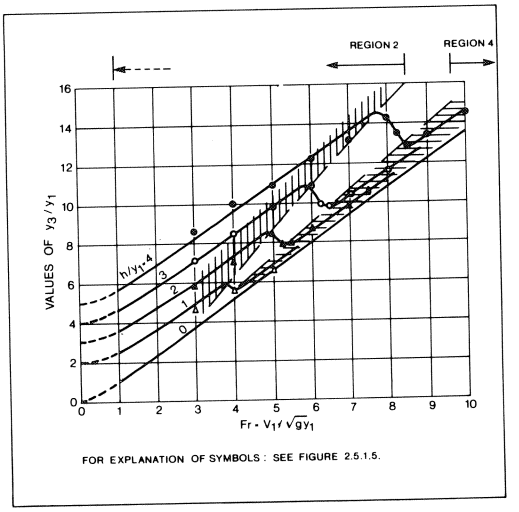

Figure 2.5.1.6. Experimental and analytical relations among Fr, y3/y1 and h/y1 for an abrupt drop (after E. Y. HSU, [6])

Figure 2.5.1.5. Various types of hydraulic jumps

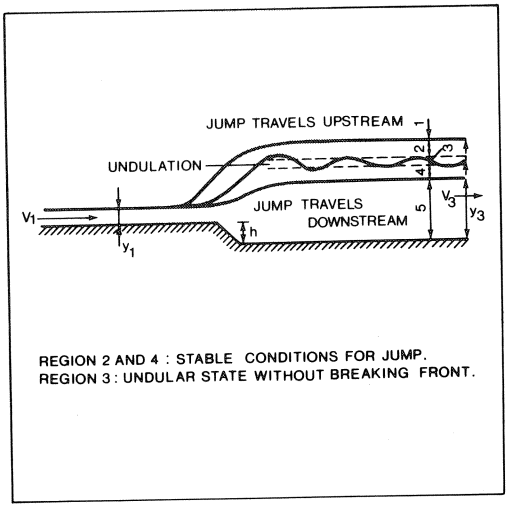

This diagram may be used for design purposes to determine the relative height of drop required to stabilize a jump for any given combination of discharge, upstream depth, and downstream depth (see [5]).

2.5.1.3. Hydraulic conditions in estuaries

3.1. Introduction

As with the repair of dike breaches, it is important to have a clear impression of the hydraulic conditions for the full or partial closure of an estuary. The hydraulic factors associated with the closure of dike breaches and polders display both similarities and dissimilarities. The mathematical hydraulic formulations describing the dynamics of the flow are the same in both cases, although the relative importance of these terms differs.

Other important differences between the repair of dike breaches and the closure of an estuary are.

a. The initial condition: in the case of a dike breach the morphology is not in equilibrium with the hydraulic conditions: The size of the gap in the dike continues to increase and the current rapidly scours channels in the flooded polder landscape behind the dike. In the case of estuary closures usually an equilibrium exists between the morphology and the hydraulic conditions: the size of the gap to be closed does not alter during the preparatory phase.
b. The hydraulic conditions: the longitudinal velocity gradients in the vicinity of the closure gap in the estuary are smaller than in the vicinity of the breach in the dikes. Also the maximum ebb and flood velocities in the closure gap are less than in the breach in the dike.
c. The maximum head difference: the maximum head difference over closure gaps in estuaries are smaller than the head differences for breaches in dikes. In the initial phase of the closing of the estuary hydraulic jump conditions do not arise; the Froude numbers at maximum ebb and flood currents being less than 1:
d. The relative importance of friction: The value of the Chezy coefficient in an estuary is some 60 $m^{1/2}$/sec, compared with approx. 30 $m^{1/2}$/sec, in a flooded polder.

3.2. Computation methods

In section 2.5.1.2. one method for an inundated polder was discussed; in this section various other methods are examined.
The selection of a particular method will depend on the extend to which the equations can be simplified and the availibility of high speed computers.

Storage basin-method

The basin is schematized to a closed end canal with a uniform cross- section. For a relatively short and deep basin the waterlevel in the basin may assume to fluctuate uniformly. The equation of motion may than be reduced to:

$$\frac{\partial \eta}{\partial x} = 0 \qquad (8)$$

The continuity equation may be written as:

$$\frac{\partial Q}{\partial x} = - B \frac{\partial \eta}{\partial t} \qquad (9)$$

The time during which the tidal wave travels through the estuary is short in relation to the tidal period

$$2\tau << T \qquad (10)$$

where:

τ = time, during which the tidal wave travels from the entrance till the end of the estuary (sec)
T = tidal period (sec)

with:

$$\tau = \frac{l}{c} \qquad c = \sqrt{g\frac{A}{B}} \qquad (11)$$

wherein

l = length of the estuary (m)
c = wave celerity (m/sec)
A = cross-sectional area (m^2)
B = storage width of the estuary (m)

When B and h do not depend on x, this gives:

$$Q_{(x,t)} = - B \frac{\partial \eta}{\partial t} (l-x) \qquad (12)$$

in which:
x = distance between the mouth and the cross-section in question of estuary (m)
In this respect it may be noted that the storage basin method is less often possible for flooded polders since the low water levels mean that the friction factor is more important in relation to the remaining terms than in the case of an estuary.
To illustrate non-linear effects a tidal wave in the Eastern Scheldt will be treated.
The length of the Eastern Scheldt is 50 km (approx. 1/10th the length of tidal wave), with an average depth of approx. 10 m, width of between 4 and 8 km and phase differences at mean tide between a point in the mouth and a point at the head of the basin of 77 minutes at high water and 55 minutes at low water.
Figure 2.5.1.7. illustrates water levels and current velocities for the mouth and basin of the Eastern Scheldt for a spring tide.

In this respect the following (qualitative) observations may be made:

a. at the mouth, the length of the flood period (i.e. with the current flowing in) is greater than the length of the ebb period (i.e. with the current flowing out).
b. in view of the fact that there is no discharge at the head of the basin, means that the current velocities in the mouth will on average during the flood period be lower then the corresponding ebb velocities.
c. at high water slack the non-linear terms in the motion equation will, on account of the higher water level, be of less account than at low water slack.

This in turn implies that the phase differences in the basin at high water slack are smaller than those at low water slack.

Figure 2.5.1.7. Tidal movement in the mouth and basin of the Eastern Scheldt.

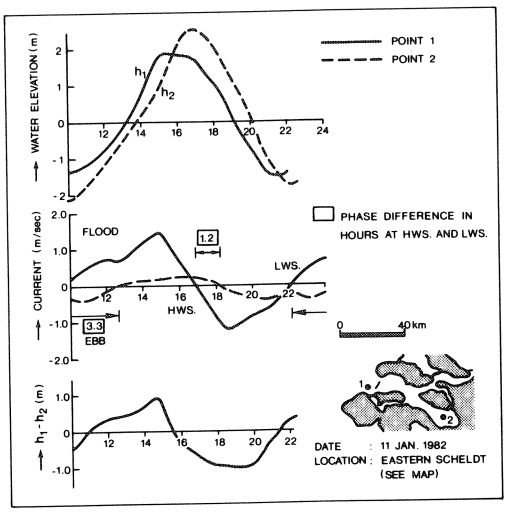

Harmonic method

In addition to the storage basin method a second analytical method to solve the equations of motion and of continuity is the harmonic method.

A condition for the application of the harmonic method is that the amplitude to depth ratio is much smaller than one. The flow is to be considered as one-dimensional.

In the harmonic method, the non-linear advective term in the equation of motion is neglected. The tidal wave is supposed to be decomposed into a number of harmonic functions, the most simple being a single sinusoidal wave.

Furthermore the friction term in the equation of motion is linearized. For simplicity the estuary is schematized to a channel having a prismatic profile. This method is extensively treated in [1].

The appropriate equation of motion is:

$$\frac{\partial u}{\partial t} = - g\left(\frac{\partial \eta}{\partial x} + M\, u\right) \qquad (13)$$

and the equation of continuity

$$\frac{\partial \eta}{\partial t} = - h\, \frac{\partial u}{\partial x} \qquad (14)$$

wherein

u	=	velocity in x-direction	(m/sec)
g	=	acceleration of gravity	(m/sec²)
η	=	vertical displacement of water surface from mean surface elevation	(m)
M	=	linearized friction coefficient	(sec/m)

M is defined by

$$M = \frac{8}{3\pi}\,\frac{u_{max}}{C^2 h} \qquad (15)$$

where

C	=	Chezy coefficient	($m^{1/2}$/sec)

The friction factor in the equation is linearized on the basis that the work done by friction over a tidal cycle must be the same whether determined by the quadratic resistance law or by a substitute linear approximation. The work done per unit of mass of fluid over a quarter-cycle equals:

$$\int_0^{\pi/2} \frac{u^2}{C^2 h}\, u\, dt = \int_0^{\pi/2} (M\,u)\, u\, dt \qquad (16)$$

using

$$u = u_{max} \cos \frac{2\pi}{T} t \qquad M = \frac{8}{3\pi} \frac{u_{max}}{C^2 h} \qquad (17)$$

The river discharge is zero.
Eliminating u in between the equations of motion and continuity yields:

$$c^2 \frac{\partial^2 \eta}{\partial x^2} = \frac{\partial^2 \eta}{\partial t^2} + g\, M \frac{\partial \eta}{\partial t} \qquad (18)$$

wherein

$$c = \sqrt{gh} \qquad (19)$$

A.T. Ippen [1] gives the solution of this equation for a closed end canal and for a canal connected to a tideless sea. Restricting attention to the problem of the closed end canal, the solution to equation 18 can be found by superposition of two waves: an incident wave of amplitude η_1 entering from the ocean and a reflected wave of amplitude η_2 travelling in the negative x-direction. The amplitudes η_1 and η_2 are functions of x and t and are at all times equal at the reflecting station at x = o. The time t is measured from the occurrence of high water at x = o. The tidal elevation at any time t, and at any station x in the channel is therefore:
(x = – l: ocean entrance, x = o: closed end of channel)

$$\eta = \eta_1 + \eta_2 = a_0 \left[e^{-\mu x} \cos\left(2\pi \frac{t}{T} - kx\right) + e^{\mu x} \cos\left(2\pi \frac{t}{T} + kx\right) \right] \qquad (20)$$

wherein:

k = wave number = $2\pi/L$ (m^{-1})
μ = damping coefficient (m^{-1})

To evaluate the damping coefficient μ from experimental tidal elevation the local maximum amplitude η_H is to be expressed in terms of the high water amplitude η_{oH} at x = o: ($\eta_{oH} = 2a_o$)

$$\frac{\eta_H}{\eta_{oH}} = \sqrt{\tfrac{1}{2}(\cos 2kx + \cosh 2\mu x)} \qquad (21)$$

The amplitude of the ocean tide η_{lH} is:

$$\frac{\eta_{lH}}{\eta_{oH}} = \sqrt{\tfrac{1}{2}(\cos 2kl + \cosh 2\mu l)} \qquad (22)$$

The time of high water at any station in the channel with respect to the time of high water at the end of the channel at x = o follows from:

$$\sigma_{tH} = \tan^{-1} (-\tan kx \tanh \mu x) \qquad (23)$$

where σ_{tH} = phase shift between high water at x and high water at x = o. In principal values of μ and k can be determined from equations 21 and 23. For details see Ippen [1].
Using one rectangular section from the entrance towards the end of the channel it follows in complex notation:

$$\frac{\hat{\eta}(x=-l)}{\hat{\eta}(x=0)} = \cosh rl \qquad (24)$$

and

$$\frac{A\, \hat{u}_{max}(x=-l)}{\frac{2\pi}{T} b\, l\, \hat{\eta}_{(x=-l)}} = \left|\frac{\tanh rl}{rl}\right| = \frac{Q(x=-l)}{\frac{2\pi}{T} B\, l\, \hat{\eta}\ (x=-l)} \qquad (25)$$

where

$$r = \pm \frac{2\pi}{T\sqrt{g\frac{A}{B}}} \sqrt{-1 + i\, M \frac{T}{2\pi} g} \qquad (26)$$

where
A = cross-sectional area (m^2)
B = channel width (m)

The factor $|\cosh rl|$ and $\left|\frac{\tanh rl}{rl}\right|$ are called the amplification factors for respectively the tide and the currents.

The factor $\left|\frac{\tanh rl}{rl}\right|$ can be regarded as the amplification factor of the discharge at the entrance of the channel computed by the harmonic method with regard to the discharge at the entrance, computed by the storage-basin method.
By means of the dimensionless parameters s_1, and s_2 where

$$s_1 = \frac{M}{\frac{2\pi}{T} g} \qquad s_2 = \frac{2\pi}{T} \frac{l}{\sqrt{g\frac{A}{B}}} \qquad (27)$$

the effect of alterations of resistance or channel length on the amplification factor can be computed.

The amplification of the tide and currents can be expressed in terms of s_1 and s_2 (see tables 2.5.1.2. and 2.5.1.3.).

An example of the use of these tables is the following: for a given shallow channel, length 20.000 m, a levee will be built halfway, so that the resulting channel has a length of 10.000 m. Such an estuary is located in Peru (Parachique-estuary). Computations were done by L. Voogt Rijkswaterstaat. The problem is to what extent the tidal wave in the channel and the velocities in the entrance will change.
The characteristics are:
$A = 300\ m^2$, $B = 500$ m, $R = 0{,}9$ m,

$C = 50\ m^{1/2}/sec$, $T = 44.700$ sec.
Halfway the channel $\hat{U}$ max ($x = 10\,000$) = 0.45 m/sec, with $l = 10.000$ m, it follows:

$$c = \sqrt{g\frac{A}{B}} = 2.4\ m/sec \qquad (28)$$

$$g_M = \frac{0{,}85\ \hat{u}(x = -10000)\ g}{C^2 R} = 15.10^{-4} sec^{-1} \qquad (29)$$

$$\left.\begin{aligned} s_{1_{old}} &= \frac{g_M T}{2\pi} = 10 \\ s_{2_{old}} &= \frac{1}{\sqrt{g\frac{A}{B}}}\frac{2\pi}{T} = 1.2 \end{aligned}\right\} \quad l = 20000\ m \qquad (30)$$

For the new situation

$s_{1new} = 10$)
$s_{1new} = 0{,}6$) $l = 10.000$ m.

From table 2.5.1.1 and 2.5.1.2., it follows that in the long channel ($l = 20.000$ m, old situation):

$$\frac{\hat{\eta}(x=0)}{\hat{\eta}(x=-1)} = 0.15 \qquad (31)$$

and

$$\frac{\hat{u}(x=-1)\,A}{\frac{2\pi}{T}\,B\,1\,\hat{\eta}(x=-1)} = 0.26 \qquad (32)$$

In the short channel ($l = 10.000$ m, new situation) these values are 0.60 and 0.61 respectively. It follows that by shortening the channel till it has the half of the original length, the tidal amplitude at the end of the estuary will be four times as high, and the velocities in the entrance will be amplified by ca. 20%.

There are a number of other methods apart from basin capacity analysis for calculating hydraulic conditions in an estuary with the aid of a one-dimensional schematization. These include the harmonic method, the exact method and the characteristic method, which are discussed in [2].

3.3 Other tidal models

The analytical methods discussed above were seen to have only a limited range of application. In the case of more complex geometries and/or problems not suceptible to basin capacity analysis, or where the frictional effect cannot simply be linearized, a number of other tidal models may be used, viz:
- mathematical models
- hydraulic models
- electric analogue models

The quality of the results obtained will always be limited by the quality of the model itself. A „bad" description or representation of an area or an engineering structure will produce imprecise results. The results will also depend on the precision of the boundary conditions used.

Mathematical models

These models provide a solution to the equations of continuity and of motion, either analytically or numerically. Before the advent of electronic calculators the equations had to be solved „by hand", which could only be done after considerable simplification. The leading hand-methods are one-dimensional harmonic and characteristic methods. A description of these methods may be found in [7]. Modern tidal computations done by computer can make use of the finite difference method, in which differential equations are converted into difference equations, which are then solved numerically. Other methods are the finite element method and the spectral method.

Table 2.5.1.1. Amplification factor for the vertical tide

S_2 \ S_1:	0.2	0.5	1.0	2.0	5.0	10.0	15.0
0.2	1.02	1.02	1.02	1.02	1.02	1.01	0.99
0.4	1.09	1.09	1.08	1.08	1.02	0.89	0.75
0.6	1.21	1.21	1.19	1.15	0.92	0.60	0.43
0.8	1.43	1.41	1.35	1.17	0.70	0.37	0.24
1.0	1.83	1.75	1.53	1.09	0.50	0.24	0.14
1.5	6.15	2.68	1.35	0.66	0.23	0.08	0.04
2.0	2.13	1.45	0.84	0.41	0.11	0.03	0.01
3.0	0.96	0.78	0.48	0.19	0.03	0.00	0.00
4.0	1.32	0.79	0.33	0.09	0.01	6.00	0.60
5.0	1.66	0.63	0.21	0.04	0.00	0.00	0.00

Table 2.5.1.2. Amplification factor for the horizontal tide

S_2 \ S_1	0.2	0.5	1.0	2.0	5.0	10.0	15.0
0.2	1.01	1.01	1.01	1.01	1.01	1.00	0.79
0.4	1.06	1.06	1.05	1.05	1.00	0.88	0.75
0.6	1.14	1.14	1.12	1.08	0.88	0.61	0.47
0.8	1.28	1.27	1.22	1.06	0.67	0.42	0.32
1.0	1.54	1.48	1.29	0.94	0.49	0.32	0.26
1.5	4.10	1.80	0.94	0.52	0.29	0.21	0.17
2.0	0.98	0.70	0.46	0.32	0.22	0.16	0.13
3.0	0.10	0.20	0.25	0.22	0.15	0.11	0.09
4.0	0.28	0.26	0.22	0.17	0.11	0.08	0.06
5.0	0.36	0.21	0.17	0.13	0.09	0.06	0.05

Hydraulic models
These models consist of a scaled-down reproduction of the area under investigation, in which the actual hydraulic conditions are simulated. In this case the flowing water fulfills the role of the integrator in differential equations. Scale rules ensure that the proper relationship between the terms in the equations of motion and continuity is maintained. The required information is obtained by taking measurements in the model in such the same way as in nature (see also [8]).

Electric analogue models
This type of model exploits the analogy between the movement of water and electric current. A description of this method may be found in [9].

Relative merits of the models
As yet there is no single model that manages to combine the full range of hydraulic aspects. Even if such a model were to exist it would be so complex that its use would only be economically justified for problems in which all those aspects were of real significance.

Each type of model thus has its advantages and limitations. The following general remarks may be made with respect to mathematical and hydraulic models.

Mathematical models provide the most insight into the physical mechanism. The share of each term in the equation of motion can be made apparent.
Hydraulic models help provide insight in a different way, in that the phenomena may be observed directly.

Once a computer-model programme has been drawn up, the impact of any variations in the geometry etc. can readily be determined. Given the time of calculation, this was certainly not the case with hand models, so that until the advent of the computer hydraulic models had the edge.

Mathematical models provide all sorts of information directly whereas in hydraulic models this has to be done by means of measurements in the model itself. For practical reasons measurements are confined to a limited number of places. On the other hand a hydraulic model also provides detailed information on flow patterns and current velocities etc.
Apart from one-dimensional mathematical models there are also two - and three-dimensional models. The three-dimensional mathematical models are however still in the gestation stage.

In view of all these factors the various models tend to be used for specialized purposes, although the division is not a strict one:
One-dimensional mathematical models are used in the case of a clear system of channels and when attention is focussed on water levels, total discharges and the like. The impact of wind can also be taken into account.
Two-dimensional mathematical models are used if there is no clear system of gullies and channels, e.g. in oceans and coastal areas, where the direction of flow is not determined by the bottom geometry (i.e. two-dimensional is used here in a horizontal sense). Nowadays these models can also be used to plot the dispersion of discharged substances, which is an important aid in solving problems in relation to water quality.
Hydraulic models are used if the bottom geometry is complicated (e.g. areas with channels and banks), particularly if data are required on current velocities and flow patterns. In this respect a hydraulic model is able to generate the boundary conditions for use in other (scale) models, as in the case of the scour model of the closure gaps in the Eastern Scheldt.
Although the flow in a hydraulic model is of course always three-dimensional, this does not necessarily mean that all aspects of the fluid flow will be accurately reproduced in all places.

3.4. General aspects of tidal models

Bottom schematization
The bottom configuration and roughness of the area under investigation must be simulated as accurately as possible. In mathematical models this is done by using the figures for basin capacity, resistance and flow profiles as input data in a computer programme. In a hydraulic

model the bottom configuration will be reproduced as faithfully as possible. The roughness of the bottom and banks will also be incorporated at the correct scale in the model. If the actual bottom configuration should change this will of course have to be copied in the model.

Boundary conditions
The equations used to describe tidal movement must be solved with the aid of boundary conditions. These may consist of water-level or flow-pattern data taken from nature. In a model of a basin such as the Eastern Scheldt the water level is generally used as the boundary condition on the seaward side, while for the basin boundaries a discharge boundary condition is set (often that discharge = 0).
On the sea boundary, the tidal wave coming from the North Sea is as it were simulated, while the condition of discharge = 0 at the boundary of the basin represents the impermeable dikes.
The location of the sea boundary should be elected in such a way that the tide there is scarcely if at all influenced by the engineering works in question.

Initial conditions
By setting the initial conditions a variable that changes over time is assigned a particular value at a given time.
This time is generally the time t = 0. An initial condition must be consistent with the boundary conditions and, in a mathematical model, be a solution of the system of differential equations of which the model is composed. The precise initial situation will not, however, be known throughout the area. In practice, the right choice of initial conditions is not critical since equilibrium will be established in the model between the driving force and resultant motion after a certain time has elapsed (i.e. the settling-down period). On account of the damping in the model the impact of any lack of accuracy in the starting condition will then be neutralized. In consequence the initial condition need do no more than provide the starting point for the computation. At the same time. however, the more closely the initial condition corresponds with the situation in the field, the less the settling-down period will be before reliable results are obtained.

An effective procedure for both models is to assume a state of complete rest, i.e. that all current velocities are equal to zero and that all water levels are equal to (for example) the average level. By allowing several tidal periods to elapse before the calculation or measurement-tide the model will have time to adjust to the situation as imposed by the boundary conditions. The model is then said to have settled down. Proper coordination of the commencing and boundary conditions will help cut down the length of the settling-down process.

Calibration
Before a tidal model can effectively be used it must be calibrated. In doing so any errors in bottom schematization, roughness and boundary conditions can be diagnosed.
Calibration is done on the basis of detailed field measurements, including water levels and currents.

3.5. Mathematical tidal models

Mathematical tidal models come in three forms, viz. one-dimensional, two-dimensional and three-dimensional. At this stage the three-dimensional models are barely operational. The one-and two-dimensional models were discussed briefly above. The number of dimensions depends on the number of directions in which the equations of motion and continuity are to be solved.
Figure 2.5.1.8. provides an example of the system of sub-division used in a one-dimensional model, applied to the Eastern Scheldt area.
Equations of motion and continuity are written in differential form and are solved for each compartment at each point in time. This may be done either explicitly or implicitly. Under the implicit method the equations are simultaneously solved for all the compartments and points at a given time, while under the explicit method the values of the unkown discharges and/or water levels for each compartment or node are determined proceeding from one of the boundaries.
The choice of the implicit or explicit method

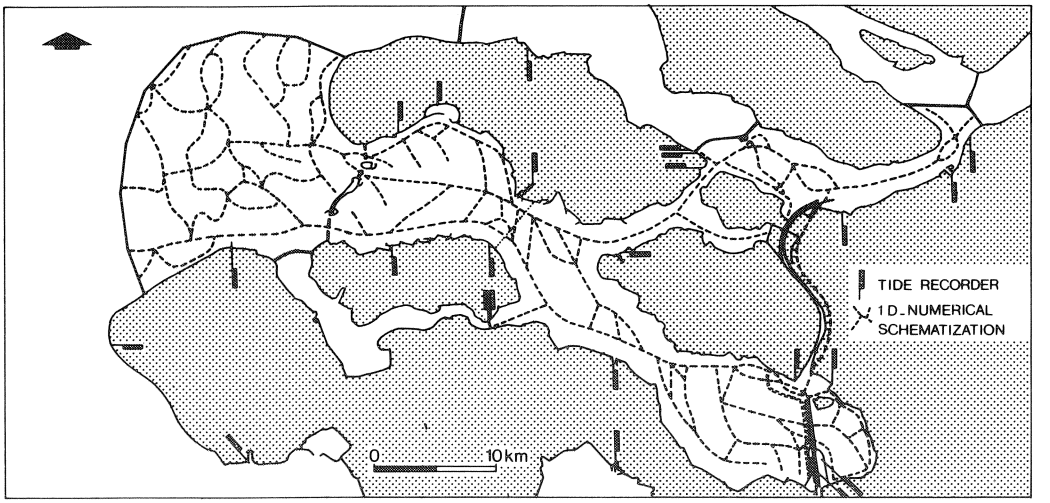

Figure 2.5.1.8. 1-D. Numerical Schematization of the Eastern Scheldt: Implic-model.

depends on the capacity of the computer in question, the desired accuracy of the results and the chance of possible computational instabilities. Detailed information on the use of numerical methods may be found in [10].

3.6 Hydraulic models

In those cases where the bottom geometry is complex and/or where comparatively detailed information is required (e.g. current velocity profiles) fluid flows may be studied in a hydraulic model. These models, in which currents are studied in open water-courses described by means of long-wave equations, are built according to the Froude scale, which assumes an equal Froude number for the model and the prototype at corresponding points in time.

The Froude number is defined as follows:

$$Fr = \frac{v}{\sqrt{gh}} \qquad (33)$$

where

Fr = Froude number
v = characteristic velocity (m/s)
h = characteristic water depth (m)
g = acceleration of gravity (m/s²)

This implies that the ratio between gravity and inertia in the model and prototype is equal. The derivation of the scaling rules may be found in various handbooks [1].
The Froude scale rule is as follows:

$$n^2_u = n_h \qquad (34)$$

where

n_u = current-velocity scale ratio
n_h = vertical scale ratio

It may be noted that there is no requirement under any scaling system for the horizontal and vertical scales to be the same. The model may in fact be distorted. The choice of the vertical scale is determined by the requirements that, as in the prototype, the current should be sufficiently turbulent and the water movement and depth measurable. For the Eastern Scheldt model a scale of n_h = 100 was adopted. If the current is

not turbulent, the resistance factor in the motion equation will no longer be proportionate to the square of the velocity. For the current to be turbulent the Reynolds number (Re = $\frac{u.h.}{\nu}$ where ν is the kinematic viscosity) must exceed 1000 to 2000. The value of ν depends on the type of liquid and on the temperature. For water, 20°C, ν = 0,98. 10^{-6} m²/sec.

Using the equation of motion it may be deduced that

$$n_c^2 = \frac{n_l}{n_h} \qquad (35)$$

where
n_c = roughness scale ratio
n_l = length scale ratio

A larger horizontal scale will not only produce a model with smaller horizontal dimensions but also a higher value for n_c. The C value in the model thus becomes smaller as n_l and hence n_c becomes larger. The hydraulic roughness of the model is therefore increased by means of small blocks. From this it follows that the viscous forces will have even less impact. If n_h and n_l should not be equal the model is referred to as **distorted,** the quotient of n_l and n_n being referred to as the **factor of distortion.**
The more distorted the model, however, the less accurate it becomes, especially where flow details over dams and around dam heads are concerned. On the basis of systematic research it was decided at the time that a factor of distortion equal to 4 would be acceptable for the Eastern Scheldt model.
From this it follows that n_l = 400.

2.5.1.4. Data collection

It will now be evident which hydraulic information is required in order to make a reasonably accurate forecast of hydraulic behaviour:

Qo = discharge through the flow gap, initial boundary condition for the compartment calculations, with the size of the flow gap and the flow pattern (contraction) being decisive for scour; (m³/sec)
h = water depth in relation to reference level (m)
a = ground-level elevation in relation to reference level (m)
b,B = current-bearing/storage breadth (m)
C = Chezy coefficient ($m^{1/2}$/sec.)

The extent to which the current will give rise to erosion and scour gullies depends heavily on the nature of the bottom. Instances have been recorded of a relatively thin clay layer at ground level having provided resistance for a full month, but once this layer had eroded away, a gap was eroded to a depth of some 20 m below ground level within a few days. In practice, therefore, care will have to be taken to maintain existing erosion-resistent clay layers, either by protecting them with bottom protection or by reducing the current velocities by widening the gap (provided the clay layer extends the fill width). Data on scour resistance will therefore be required.

Needless to say this should be done before a flood disaster occurs, since neither the time nor the manpower are likely to be available for data collection after the event, while the location itself is unlikely to be suitable for field research.

The above factors should be ascertained in the field by measurement. The discharge through the flow gap may be calculated by means of the discharge equation $Q = \mu A \sqrt{2g \Delta h}$ in which Δh (= head difference) has to be determined by means of water level observations, μ (= coefficient of discharge) has to be estimated with the aid of data from the literature (e.g. [5]) or calibrated by means of discharge measurements, and A (the discharge profile) must be gauged.
Ground-level elevation must be determined by means of topographical charts; these should of course be put together before a flood disaster.
The same applies to the current-bearing and storage capacities, which may be deduced from the elevation of the site, supplemented by water-level measurements during the flooding. The flows will often be concentrated in existing water courses and new scour gullies.
The system will be subject to particularly marked changes in the early stages, on which up-to-date data are vital. These may be obtained from

aerial photographs or in some cases by other remote sensing techniques.
The Chezy coefficient generally forms the balancing item for calibrations and computations. The water level and discharges are measured in the area for the existing situation; on account of the roughness of the inundated area the Chezy factor has a very low value, e.g. 30 $m^{1/2}$ sec^{-1} instead of 60 $m^{1/2}$. $sec.^{-1}$, i.e. the sort of value one might encounter in a river. An initial calibration can be carried out by measuring the water levels in the inundated area at HW- and LW-slack. The volume between the surfaces, at HW- and LW-slack, bounded by the edges of the area (as determined by aerial photography at the turn of the tide), provides the ebb and flood volumes (or ebb and flood capacities).
A great deal of information can be obtained at the turn of the ebb tide: as soon as the water level in the channels and gullies drops sufficiently, conditions of critical flow will be reached over the edges of the channels (i.e. small waterfalls). Once this happens the water level in the gully or channel ceases to exert any influence on the rate of discharge into it; the elevation of the site and the total length of the overfall (as determined by the channel configuration) are then the determining factors.
The discharge through the gullies and channels and current velocity in the closure gap may be calculated with the aid of detailed relief maps and aerial photographs. Now the edges of the gullies will act as sills with critical flow conditions before the low-water point outside the breached dike has been reached. Once the low-water point outside the dike has been reached, i.e. when the water level outside the dike begins to rise, it may be noted that the gullies will for some time continue to be filled with water flowing over the edges. This means that the low water slack in the closure gap will take place at the point when, at the beginning of the flood tide, the volume of water required per second to fill the gullies is precisely equal to the volume of water still running off into the gullies and channels. Beyond this moment the gullies will be filled from the area outside the dike, after it the low water slack in the polder will follow.

This pattern does not occur at the high water slack; the differences in the times at which the high tide turns outside the dike, in the closure gap and inside the dike are smaller than the corresponding differences at the turn of the ebb tide (see figure 2.5.1.9., taken from [3]).
The slack-tide interval (i.e. the period around the ebb and flood turns of the tide at which the velocities in the closure gap are sufficiently low for closure activities to be carried out) is therefore longer at low water slack than at high water slack. This forms the reason why channel closures in which a closure gap of reasonably large dimensions is sealed in a short space of time are completed at the turn of the ebb tide. It may, however, be noted that on account of their draught, caissons will often have to be manouevred into the closure gap at the turn of the highwater tide.
As the closure operation progresses and the

Figure 2.5.1.9. Vertical tide and corresponding duration of low-water slack and high-water slack outside the gap.

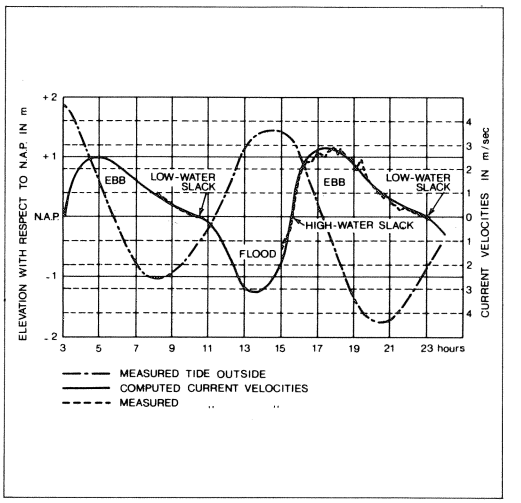

final gap narrows, the situation can be reached where the water level in the polder no longer corresponds with the water level outside the dike. In this case an absolute measure for the maximum current velocities (v) in the closure gap is provided by:

$$v = \sqrt{2g\ \Delta h} \qquad (36)$$

in which $\triangle h$ = the tidal difference, i.e. the difference between the high and low-water levels outside the dike or, better still, between high water within the dike and low water outside the dike or vice versa.

One further phenomenon associated with a channel closure that merits attention is the head effect, i.e. when the compressed current in the closure gap is bounded on both sides on the downstream side by eddies.
The motion at the boundary between an eddy and the main current is highly irregular, leading to greater bottom scour than anywhere else (see figure 2.5.1.10.). This effect is accentuated in the case of a vertical closure (where the height of the sill is increased in stages), when most of the rip-rap is placed in the axis of the channel. The current will then be deflected still further from the centre of the closure gap towards the four angular points, where head effects may occur (see figure 2.5.1.11.).

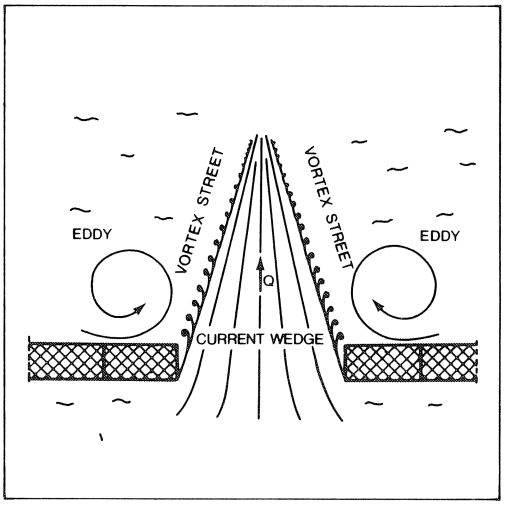

Figure 2.5.1.10. Generation of eddies and vortex streets.

Figure 2.5.1.11. Cross-section of closing gap.

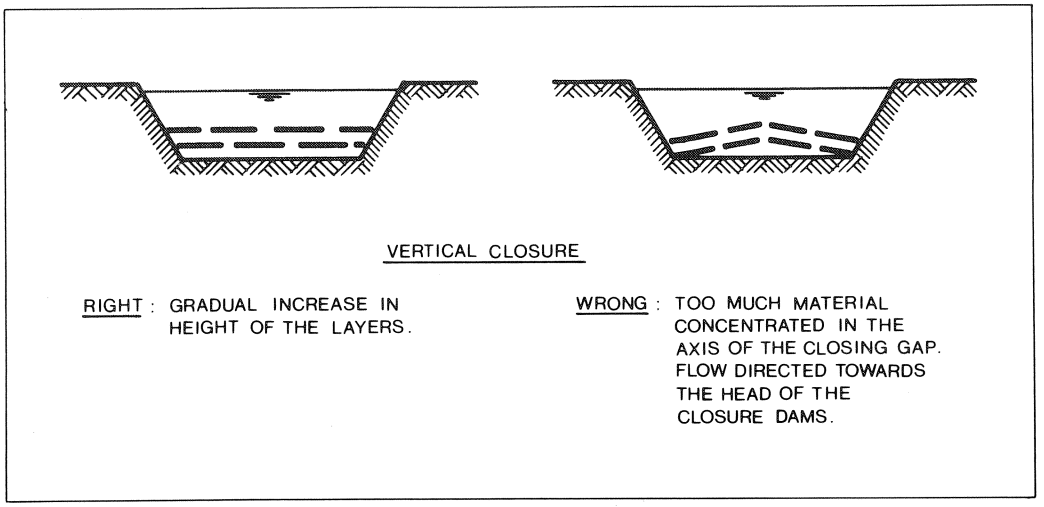

In general it may be said that the closure strategy adopted in the progressive repair of dike breaches will depend on many factors. These include:

1. Hydraulic aspects such as:
- the protection of scour-resistant (clay) layers (since emergency measures can limit the growth of the flow gap);
- priority to repairing inner dikes in order to decrease the area of the basin;
- making use of conditions of critical flow thus limiting the discharge;
- priority to closing deep channels (with critical flow) in order to achieve a substantial reduction in discharge before the current velocities in the channels begin to rise as the result of closure elsewhere;
- priority to the closure of upstream flow gaps in order to reduce the burden on downstream flow gaps;
- priority to the closure of small flow gaps in order to gain experience;
- design and execution support by means of computations, model analysis and prototype measurements.

2. organizational aspects such as
- independence of the design team and executive agency;
- supply of manpower, materials and equipment;
- communication facilities;
- foreign exchange policy.

Various closure strategies are discussed in detail in a number of publications from the 1950's [11, 12].

References

1. Ippen, A.T., **„Estuary and Coastline Hydrodynamics"**, McGrawhill, New York, 1966.

2. Dronkers, J.J., **Tidal Computations,** North Holland Publishing Company, Amsterdam, 1964.

3. Dronkers, J.J., „Het doel van getijberekeningen voor de afsluiting van de grote stroomgaten" (The object of Tidal Computations for Large Flow gaps), **De Ingenieur, no. 23,** 1954 (in Dutch).

4. Dibbitts, H.A.M.C., „Mededelingen over de afsluittechniek voor getijgeulen" (Notes on Closure Techniques for Tidal Channels), **De Ingenieur, no. 24,** 1956 (in Dutch).

5. Ven te Chow, **Open Channel Hydraulics,** McGraw Hill, 1959.

6. Eu-Yun Hsu, Discussion on Control of the Hydraulic Jump of Sills by John W. Forster and Raymond A. Skrindle, **Transactions of American Society of Civil Engineers,** 1951, vol. 115.

7. Silvester, R., **Coastal Engineering,** Parts I and II, Elsevier, Amsterdam, 1974.

8. Thijssen, J.Th., Het Deltamodel in het Waterloopkundig Laboratorium te Delft, (The Delta Model in the Delft Hydraulics Laboratory), **Report of the State Commission,** Part 5, contribution IV, Staatsuitgeverij, The Hague, 1960.

9. Schönfeld, J.C. and Stroband, H.J., Getijonderzoek door middel van de hydraulisch-electrische analogue (Tidal research by means of the Hydraulic-electrical Analogue), **Report by the Delta Commission, Part 4,** contribution IV.8, Staatsuitgeverij, The Hague, 1960.

10. Richtmeyer R.D. and Morton K.W., **Difference Methods for Initial Value Problems,** Interscience, New York 1967.

11. Royal Netherlands Institute of Engineers, Herstellings- en verbeteringswerken na de ramp van 1 februari 1953, (Repairs and Improvements following the Flood Disaster of 1 February 1953), Survey from **De Ingenieur nos. 22, 23, 24, 25, 29 and 30,** 1957.

12. Royal Netherlands Institute of Engineers, Het Deltaplan en zijn verschillende facetten, (The Delta Plan in its various Aspects), Reprint from **De Ingenieur, nos. 14, 20, 21, 23, 24 and 28,** 1956.

Impact on the Environment

D.J. de Jong, R.J. Leewis, R. Misdorp, P.B.M. Storteldер, J. Visser

2.5.2. Ecological aspects

2.5.2.1 Introduction

Complete closure of an estuary or sea-arm results in a strong decrease of the current velocities and the disappearance of the vertical tide. In addition, the exposed land areas and possible also the water will become desalinated.

Even when there is a permeable closure, as a consequence of which a reduced (or fake) tide is created, these changes, which can have a great impact on the original marine/estuarine ecosystem, will occur.

In the following pages, these changes will be described in four different variants (see also fig. 2.5.2.1):

1. a flowing freshwater system*
2. a stagnant freshwater system*
3. a stagnant salt or brackish water system
4. a salt (or brackish) water system with a reduced tide.

(The extent of the changes decreases from 1 to 4).

* Whether a closed estuary should be defined as a flowing or a stagnant freshwater system depends on the extent and the regularity of the river discharge. If the water discharge is high and constant it will be a flowing system, whereas, if the discharge is small, it will be a stagnant system (if the river discharge fluctuates, both possibilities can occur alternately).

In the description of the changes, in principle,

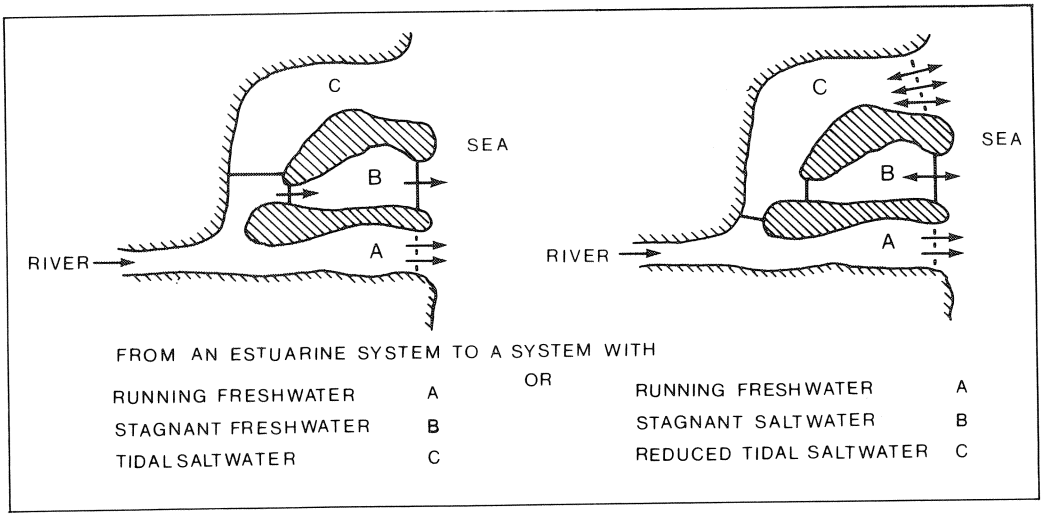

Figure 2.5.2.1. Some possible ways of closing an estuary

the subjects are dealt with in the same order as in 2.2.6. i.e.:

1. hydrological and chemical aspects;
2. morphological and soil mechanical aspects and
3. aspects of flora and fauna.

In addition, the morphological changes in the fore-delta, as a consequence of a (permeable) closure, will also be briefly discussed (2.5.2.5).

Desalination has already been dealt with in 2.4.15.2.

2.5.2.2 Transition into a flowing freshwater system (variant 1)

In this variant, the closed estuary maintains its main function as regards the river discharge; therefore discharge sluices have been included in the sluice-complex (fig. 2.5.2.1) (see also [10]).

1. Hydrological and chemical aspects

Immediately after the closure the salinity usually decreases rapidly, particularly with high river discharges. The water-quality in the entire basin will then be mainly determined by the quality of the inflowing river-water. In addition, subsidiary discharges and internal processes will also affect the quality (i.e. accumulation, algae-growth, self-purification, stratification, etc.).
A significant result of the great influence of the river is that the level in the new system is highly influenced by the rate of the river discharge; high river discharges will usually increase the mean water level. In addition, a minor form of tidal action can occur when the discharge sluices are open during periods of high river-water discharges. These level changes can have serious repercussions for the shores.

Another aspect is that the residence time of the river-water in the system and also the transparency of the water usually increases. In addition, the temperature of the water in summer can be higher than in the original system. These aspects can affect algae-growth and the future development of water-plants.
Just as there can be higher water temperatures in summer, lower temperatures can occur in winter which, in conjunction with the disappearance of the anti-freeze effect of saltwater, in temperate and cold climate areas can result in an enhanced possibility of ice-formation. The latter can lead in the shallow riparian zone to a periodical erosion of shore-vegetation and possible freezing of the benthic animals in this zone.

The reduction in the current velocity in the basin forms another aspect. This has as a major (and often negative) consequence an increased settlement of river-silt, particularly if the silt is polluted with certain heavy metals and other toxic substances originating from discharges into the river. Therefore, for all forms of matter, the proportion between the transports in dissolved and particulate form is of primary importance. As the rate of the particulate transport increases, the quantities of noxious substances in the accumulation area will also increase. In addition to this accumulation, resulting from a sudden reduction of the current velocity, other processes, such as adsorption to the particulate matter caused by an increase in the pH (rate of acidity) of the water, can also generate accumulation of polluted substances in the accumulation area. An increase in the pH can be induced by an abundant algae-growth, and moreover in a more or less natural situation the pH is somewhat higher in a lake than in a river. As a result of bed-erosion, caused by wind or very high river discharges, the accumulated polluted substances can be re-transported downstream. This phenomenon can be illustrated by the amount of heavy metals in two former Dutch estuaries, the Haringvliet and IJsselmeer (see fig. 2.5.2.2). Of the two, the present IJsselmeer belongs to the lake-category with a residence time of about six months, whereas the present Haringvliet has the character of a river with a residence time of only a few weeks. The figure shows that a large residue of both the particulate and the dissolved metals remains in the basins. Because of the nature of the IJsselmeer, the residue there is larger than in the Haringvliet. A total survey of the concentrations of various metals in the bed of the Delta waters in The South-West Netherlands has already been given in fig. 2.3.7.4. This also shows that the original Haringvliet estuary, through which a large portion of the river-water from the Rhine and Meuse flows through The Netherlands, has the highest concentrations in its bed due to the accumulation of particulate metals and the adsorption of dissolved metals to the particulate matter. For further information on this problem see [17].

The silt problem can also be important in the design stage, particularly with regard to the

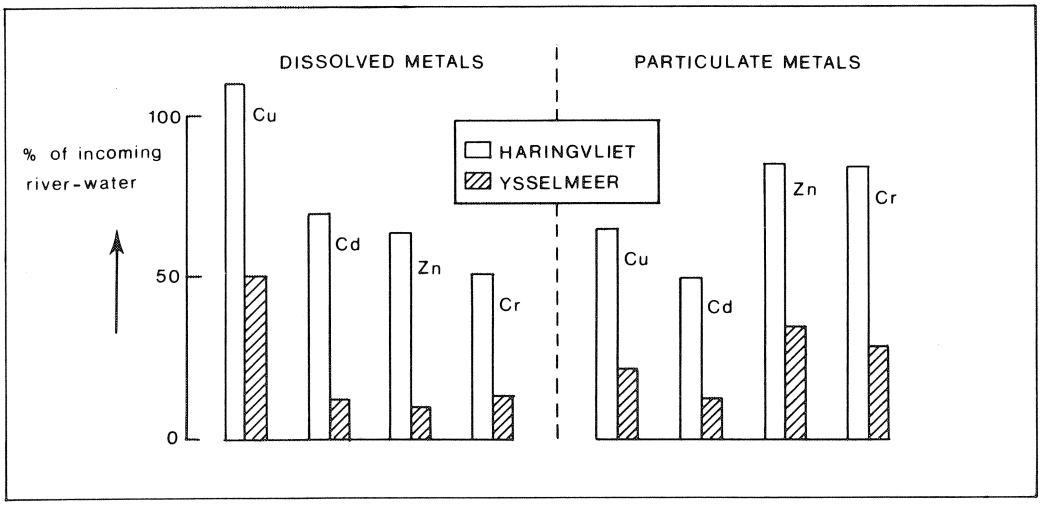

Figure 2.5.2.2. Concentrations of some dissolved and particulate metals in the water out-flow of two lakes in the Netherlands. Metal concentrations in the incoming river-water are 100% (after Salomons, 1981 [17]).

selection of the site where the dam, separating the river from the sea, will be built. If the position of the dam is some distance upstream, the river's cross-section is still small as a result of which only small quantities of polluted silt will settle on the bed. After the river-water has passed through the sluice-system, accumulation, possibly increased by flocculation, will take place on the seaward side. If such a site is selected, the river-silt can be transported towards the sea due to turbulence. Furthermore sea-silt will be able to penetrate far upstream, as a consequence of which the polluted river-silt will be mixed with clean sea-silt, resulting in lower concentrations of pollutants in the bed.

This option could conceivably have less harmful side-effects than those arising from structures built nearer to the sea.

2. Morphological and soil mechanical aspects

The distinctly different processes occuring on permanently exposed mudflats and shoals (land) and riparian zones are discussed separately.

Land

The major geomorphological process taking place on permanently exposed land is the drifting of sand of the initially bare mudflats and shoals (wind erosion). The principal soil mechanical processes are desalination and maturing of the soil.

Wind erosion can be induced by a great number of factors, which will be discussed briefly below (see also [2]). The figures quoted are based on experiences gained from closures in The Netherlands, but on the whole they can be applied to similar situations elsewhere.

- Wind velocity: if wind velocities are high material is displaced. Sandy soils with a low clay or humus content are apparently easily scattered when wind velocities exceed 7.5 m/s.
- Grain size: the 100 - 500 μ fraction is the most erosion-sensitive. Increasing concentrations of clay particles and organic matter will hamper erosion. The erosion-barrier is about

10% for clay particles and/or 7% for organic matter. An increase in the silt-content will also hamper erosion.

- Shells: the presence of shells and other coarser particles on the bed which cannot be dispersed by the wind means that, over the time, the quantities will progressively increase on the surface area. When the density on the surface area reaches 20 - 50%, the erosion will cease.
- Moisture: only dry sand-grains will be blown away by the wind. In humid soils, the capillary attraction is so high that the dispersal of sand will be prevented. Therefore, the groundwater level is of major importance.
- Soil-density: if the soil is closely compacted, the tendency to erode by wind will generally be less than in less tightly compacted soils, because of the increased cohesion and capillary forces.
- Sealing: this occurs when clay and silt particles are present in the soil which will adhere to one another. Thus, in dry periods, the upper layer of the soil hardens, forms a „crust", thus hampering the penetration of water and oxygen.
- Crust-forming: this is brought about by the adhesion of soil particles due to salt in the topsoil and/or a strong development of diatomes and blue-green algae on the surface of the bed.
- Uneven surface: an uneven surface obstructs the wind-influence at ground level and therefore reduces the erosion. For erosion-sensitive soils, however, this protection is only temporary as, due to high wind velocities, the tops of the uneven sections are rapidly levelled.

Densification of shell-layers, a decrease in the amount of erosion- sensitive materials, an increase in moisture due to lowering of the ground-level as well as increased vegetation (enhanced surface-roughness) will over a period of time decrease or even halt wind erosion. In the South-West Netherlands it was found that wind erosion generally stopped after two or three years; at the same time it was observed that ground level was lowered by 15 to 60 cm.

Usually, the eroded material does not travel large distances but accumulates, for the greater

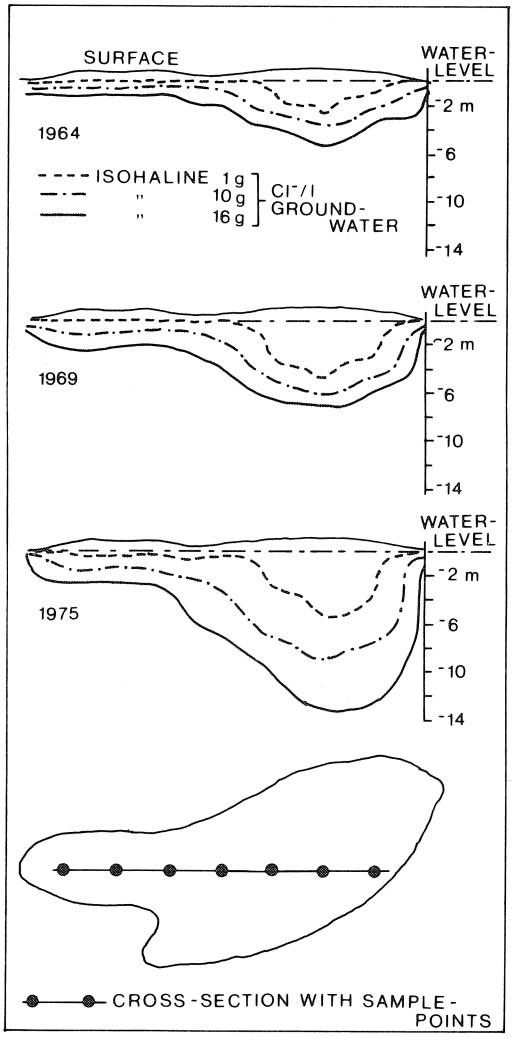

Figure 2.5.2.3. Cross-section of a former sandflat in Lake Veere (the Netherlands) showing the vertical desalination proces (lake-closure in 1961).

part, in another section of the region, often in the lee of various sorts of obstacles. Tussocks are particularly important in this matter. Cultivation measures (e.g. planting of lyme-grass) can promote the creation of small dunes which, depending on the extent of the sand-transport, can reach a height of several metres.
Another aspect to be taken into account is that the abundance of plant nutrients on the shoals and mudflats can decrease as a result of the sand erosion as partially assimilated organic matter (created by the massive mortality of the marine plants and animals) is blown away with the sand particles.
Desalination (see also [3]) occurs when the riparian shores are no longer washed periodically by saltwater and water is only supplied by rainfall. In principle desalination starts on the highest sections of shoals and mudflats where a freshwater pocket is formed in the salt groundwater.
Due to precipitation this freshwater pocket expands both vertically and horizontally until a certain balance is reached; see also fig. 2.5.2.3. and 2.5.2.4.
On the lower sections of the shoals desalination will progress more slowly as during most of the year the salt groundwater level is (nearly) at ground level, thus reducing percolation (penetration and underground flow of precipitation) to a minimum. Only small quantities of salt will diffuse from the saturated soil to the surface runoff. In addition to the elevation of the shoals or mudflats, the composition of the soil is also of major importance. Sandy soils desalinate more rapidly than clayey soils. The presence of layers with a low permeability less than 2 m. below surface-level can restrict desalination as they reduce the underground flow. Layers with a low permeability are those that consist of at least 8 to 12% clay particles and which are usually thicker than 10 cm.
Although the desalination-process in clay is slower than in sandy soils, the salt-content hardly fluctuates, once they have been desalinated, as the influence of capillary forces and groundwater fluctuations is not very high in clayey soils. However, in less desalinated sandy soils,

Figure 2.5.2.4. The horizontal desalination proces in the soil of a former sandflat in Lake Veere (the Netherlands) (lake-closure in 1961) (after Beeftink et al, 1971 [20]).

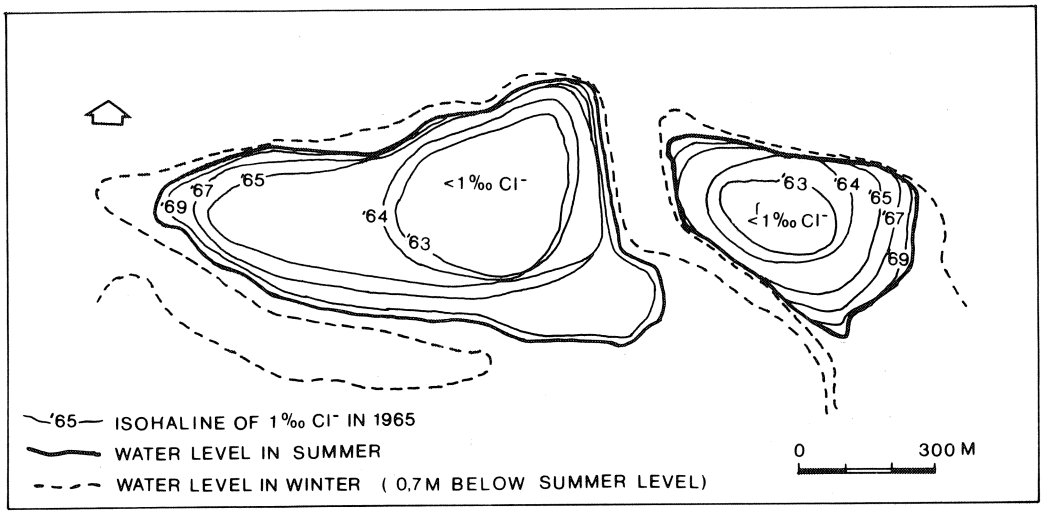

as a result of capillary attraction, the salt-concentration of the surface can sharply increase in dry periods. Desalination can be promoted by adequate draining of the soil (e.g. drain-pipes, ditches, trenches).

Maturing of the soil can be subdivided into three different categories, viz. physical, chemical and biological maturing (see also [3]).

After exposure, physical maturing occurs first. As the water is drained from the soil, the bed shrinks and cracks occur which can vary from extremely small ones in sandy soils to 10 cm wide cracks in clay-rich soils. When the soil dries out and also because of other processes, the bed will compact, i.e. it settles. The extent of the settling depends on the water content and the clay and organic-matter content present in the soil. Fig. 2.5.2.5. indicates the relation between settling and the clay content [4].

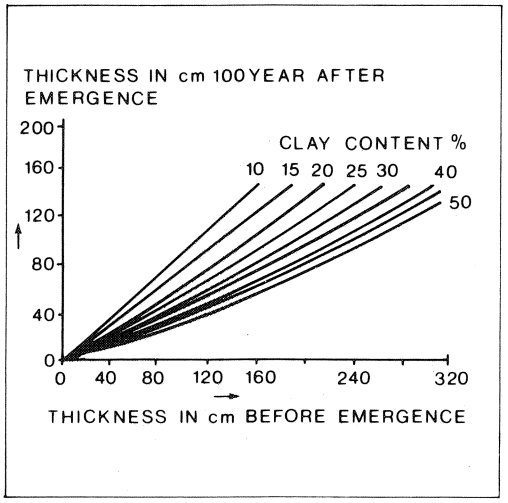

Figure 2.5.2.5. Relation between original thickness and thickness ± 100 years after emergence of naturally drained saltings in the SW Netherlands (after de Glopper, 1973 [4]).

The cracks resulting from shrinkage provide the main „access roads" for air and precipitation into the soil. As a result, various chemical processes are brought about, the most significant being the removal of salts, decomposition and changes in organic matter, and oxidation of sulphide compounds into sulphates. In organic matter, nitrogen compounds are the first to decompose as a result of which especially ammoniac and nitrates are released in the first period of mineralization; as a consequence, in the first phase, nitrophile plants establish themselves.

Biological maturing begins simultaneously with the chemical maturing, as living organisms come into being on and in the soil; consequently, organic matter is produced and decomposed thus making the soil more accessible for air and water.

Entrance of air into the soil can be impeded by sealing and/or crust-forming. The chance of sealing increases when there is little biological activity and a low humus-content in the soil.

Riparian zone (see also [2])

It has been assumed that the speed of the currents generated by the passage of freshwater is so small that it does not influence the morphological developments in the riparian zone. Therefore, changes in the riparian zone are only affected by wave action and the resulting currents on the shore. Those currents can attain velocities from 50 to 60 cm/sec.

In many places, the erosive impact of the waves is accompanied by a retreat of the shoreline, as a result of which small escarpments are shaped. The material, eroded by the waves, usually settles in the (shallow) fore-shores or in the deeper sections of the lake. However often a part of the material is transported along the shore, where it accumulates elsewhere in the shore zone and even may lead to the forming of spits. The rate of this longshore transport of material, usually attended by various forms of accumulation along the shore, depends on the frequency and time the waves run obliquely towards the shore, as well as on the presence of places along the shore where material can settle.

Erosion and accumulation can also occur simultaneously, i.e. accumulation of material can occur in places where the shore as a whole is retreating. As a result of these combined erosive and accumulative activities, the transitional zone between land and water can acquire a greatly diversified character. This diversity can lead to the development of a varied biotic community.

The extent of and speed at which these geomorphological changes occur depend upon many local factors. These are on the one hand the magnitude of the wave-energy, connected with wind-force, wind-direction and fetch, and on the other factors such as exposure of the shore, the contours of the (fore-)shore (slope, width and shape), the composition of the bed (grain diameter and structure), fluctuations in water level and the vegetation. The formation of an erosion escarpment as well as the speed with which the shore retreats will increase with increasing magnitude of waves (height/length) and duration of wave-action and when the sand density is loose and the fore-shore is small. E.g. on account of unfavourable conditions, it has been observed that the shoreline in Lake Grevelingen in The Netherlands has retreated some tens of metres annually (see fig. 2.5.2.6). It was found there, however, that if the slope of a fore-shore was very gentle, i.e. 1:1000, the shape of the shores hardly changed, while erosion was nearly absent.

As, in the course of time, vegetation develops on the initially bare shores, the wave-action is reduced considerably or even halted, thus strongly reducing morphological changes.

In the shallow fore-shores of a freshwater system, vegetation, i.e. wide belts of waterplants such as reeds and rushes, can develop and substantially affect the watersystem. However, strong wave attack can impede the development of these vegetation belts.

Level fluctuations occurring in this variant can influence the geomorphology of the shore in the sense that, as the fluctuations increase, the wave influence is distributed over a wider zone, whereas in stagnant waters the wave impact is

Figure 2.5.2.6. Shore erosion and the influence of pebble-ridges on it in a closed estuary (closure 1971).

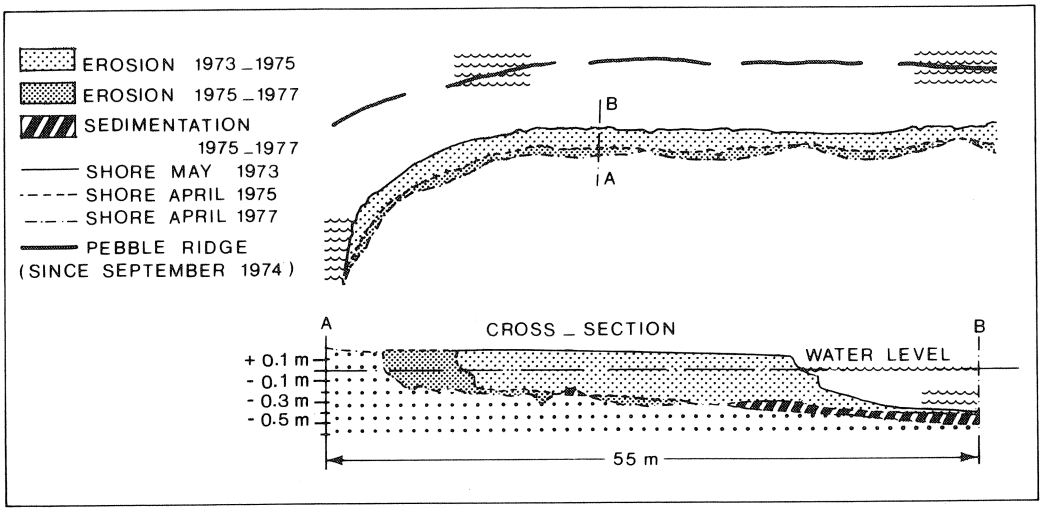

concentrated on one specific level. In the latter case, the changes are generally greater than in the former, whereby the frequency of fluctuations in water level also plays a part, particularly in relation to plant growth. If the water-level fluctuations are very irregular, the shore region remains practically bare, even in a freshwater system, which implies that the shore will be permanently and relatively heavily subjected to wave action. Therefore, protective measures must be taken in those places where, due to a retreating shoreline, the functions of the basin are impaired. It should not be forgotten, however, that the halting of erosion in one place may influence the rate of accumulation in other places.
Some of the many and varied measures to be taken are briefly described in 2.4.15.

3. Aspects of flora and fauna
The transition from a saline tidal system into a flowing freshwater system means, with regard to the plant and animal life that the tidal action is omitted, resulting in a clear division between land and water areas, separated by a shore zone. Another important change is the transition from saline into freshwater. Therefore a difference can be made in the processes occurring on land, in the water and in the shore zone.
The land areas will soon become dry. The animals living in this area, and who depend on a regular saltwater flooding, will die within a few days (or sometimes weeks). The halophile plants will also die although this usually takes considerably longer (1 - 10 years or more).
During this process the soil needs great quantities of oxygen and offensive odours can occur. In addition, desalination is taking place, the rate of which can vary locally (see also item 2). The result is in any case a gradual transition from an aquatic to a terrestrial ecosystem. Land vegetation will develop, gradually changing from open and low vegetations to woodlands or, if grazed, to grasslands. E.g. fig. 2.5.2.7 shows a vegetation-map of a former sandflat after ten years exposure; the shoal has been completely bare under normal tidal action but in ten years it has become covered by grass, herbs and willow saplings [3, 5, 6].
In the soil, a new micro-ecosystem comprising bacteria, fungi, worms, insects, etc. develops spontaneously; the vegetation growing on the surface provides food and/or refuge to earth-bound insects, mammals and birds.
In a flowing freshwater system, the shorezone is often less clearly defined as a result of fluctuations in the water level in the lake. If fluctuations are regular, the animal and plant life existing on the shore will be able to adapt to the situation; a type of freshwater tidal ecosystem will develop comparable to one that, in nature, can often be found along the lower reaches of rivers. Very irregular fluctuations will seriously impede the creation of a well-developed shore-ecosystem, as a result of which the shore can remain bare. The extent of erosion is also important for the development of a shore-ecosystem (see also item 2); substantial erosive action will seriously hamper the developments.

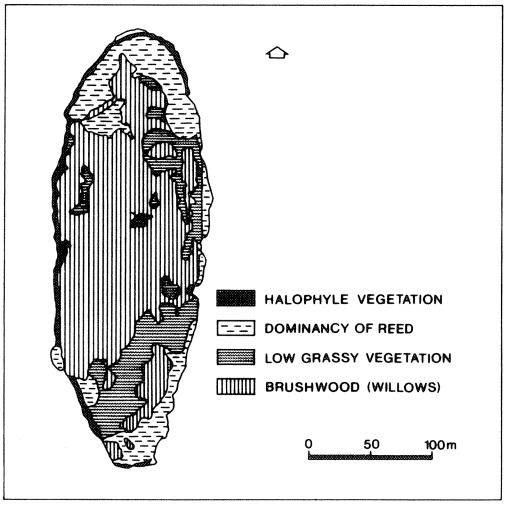

Figure 2.5.2.7. Vegetation map of a former sandflat in Lake Veere (the Netherlands), 12 years after closure. Immediately after closure the island was barren, 12 years later it has been overgrown with reed and brushwoods (after Saeijs & Bannink, 1978 [5]).

As a result of desalination, the existing plant and animal life in the aquatic area will completely disappear and will be replaced by communities of freshwater species. The speed of recolonisation by these organisms depends on the rate of desalination, which is very high in flowing freshwater systems, and the import-opportunities of new (freshwater) organisms. The ultimate composition of the new biotic community depends on the quality of the supplied water and the behaviour of the bed (chemical, morphological). Generally, it can be said that the flora and fauna in such a semi-river system are poorer than those that were present in the previous salt tidal system.

2.5.2.3. Transition into a stagnant freshwater system (variant 2)

The transition of an estuarine system into a stagnant freshwater system (lake) is possible if, in addition to the closure on the seaward side, a dam is also built on the river side, or when the supply of river-water is relatively small. As a result of the construction of a dam, the supply of river-water is or will be drastically restricted. A typical characteristic of a lake is that the residence time of water in a lake can last for several months or longer (fig. 2.5.2.1).

1. Hydrological and chemical aspects

In contrast with the situation in a flowing freshwater system (variant 1), the quality of the river-water fed into a freshwater lake plays a less dominant part, whereas the internal processes (algae-growth, settlement, exchange between water and sediment, etc.) as well as the discharge from adjacent land areas are relatively more important. For the water-quality, the following aspects merit attention: the water-quality during the desalination stage, the chloride-content and the algae-growth. The accumulation of toxic substances can also be important (see variant 1 on this subject).
A description of the desalination phase can be found in 2.4.15.2. The supply of fresh river-water into a lake is minimal. This implies that as a result of discharges of brackish polder-water, seepage through dams and dikes and, possible, the salt-load intruding via sluices the system can turn brackish on the borderline of fresh- and saltwater. This may hamper the development of a freshwater flora and fauna, and, moreover, this water will not be fit for human consumption or for irrigation in agriculture and horticulture.
These problems could be solved by increasing the flushing-discharge (provided sufficient water is available) and the construction of a fresh-/saltwater separation system in the sluices on the borderline of fresh- and saltwater. An increase of the flushing-discharge may, however, conflict with other water-quality aspects by producing adverse effects such as an increased load of undesirable substances - e.g. nutrients and toxic matter - depending on the extent of pollution in the river water.

Algae-growth may cause considerable problems when the water, supplied by the river, contains high concentrations of nutrients or if, due to other discharges, the nutrient load is too high. Besides, conditions for algae-growth are more favourable in lakes than in flowing water as the water remains for a longer period in the lake (as a result of which algae are discharged less rapidly), the penetration of light is better (a deeper euphotic zone) as silt and sand particles settle, and because of the greater influence of phosphorus released from the bed. If there are sufficient nutrients and algae-growth is only impeded by light, the maximum algae-biomass (in an ideal mixing-model) for differing residence times of the freswater, can be calculated as follows:

$$V \frac{dF}{dt} = QF_{in} - QF + \mu_{max} G(I) VF - rVF$$

with

$$G(I) = \frac{2f}{(k_o + \varepsilon F) H}$$

in which

Q : discharge (m^3/day)
V : volume of the lake (m^3)
t : time (day)
F : chlorophyll-a concentration (mg/m^3)
F_{in} : chlorophyll-a concentration in incoming water (mg/m^3)

ϵ : specific extinction coefficient (m^2/mg chlorophyll)
H : average depth of the lake (m)
μ_{max} : maximum gross growth rate (day^{-1})
f : relative day-length (-)
k_0 : background extinction coefficient (m^{-1})
r : respiration + mortality rate (day^{-1})
G(I) : light restriction factor for growth rate (-)

For the stationary situation ($dF/dt = 0$) and assuming that $F_{in} = O$

this means:

$$F = \frac{1}{\epsilon H} \frac{2f\ \mu_{max}}{\tau^{-1} + r} - k_0 H \quad \text{in which}$$

τ = residence time $(= \frac{V}{Q})$ (in day)

Fig. 2.5.2.8 shows the relation between F and the residence time τ of water. When applying this formula, it must be borne in mind that the quantities ϵ,μ_{max}, f, k_o and r may differ per basin or per region. These quantities can be approximated by taking measurements or by using reference books.
The level variation in such cases can often be managed within certain constraints. The choice of a fixed or a variable level can depend on such factors as agricultural water requirements in dry periods and discharge rates in wet periods. Some examples of this transformation are described in [7, 10].

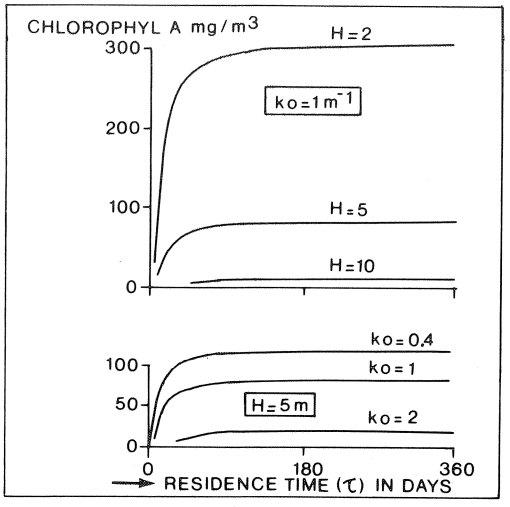

Figure 2.5.2.8. Relation between water residence time and chlorophyl-a concentration in a freshwater lake for different lake depths (H) and for different background extinction coëfficients (k_o).

2. Morphological and soil mechanical aspects
In the land areas the developments are fully comparable with those described in variant 1. The descriptions of these developments are given under that variant. The developments in the shore zone are, for the greater part, also comparable. The major factor that could lead to differences from a flowing system is the water level. In a lake it is usually easier to control the level and it is therefore often maintained more consistently at one level. On the one hand, this enhances the possibility of erosion, particularly on exposed shores - see 2.5.2.2, item 2; on the other hand, the possibility of shore vegetation increases on the sheltered shores as a result of which erosion is impeded. Which of these two alternatives dominates depends on the local situation, particularly on the exposure of land to waves and wind. Generally, the chance of shore vegetation will be greater at a fixed level than at an irregularly fluctuating level.

3. Aspects of flora and fauna
When a tidal area changes into a stagnant freshwater system, the existing animal and plant life will also change and distinct differences will be found in land, shore and aquatic areas.
In the land areas all the developments are comparable with those in variant 1; these are fully described under that variant.
As a rule, the shore zone in a stagnant freshwater system is clearly defined as the water level can be well-regulated. As a result of this fixed level the wave-attack is highly concen-

trated at a small height range, particularly on the shore regions exposed to the wind. As a result of this concentrated wave-attack on the very exposed regions it is hardly if at all possible for flora and fauna to develop. If the fore-shore slopes are steeply, this will also negatively influence the development of animal and plant life. By means of the shore defences, which are often necessary in these areas, it might be possible, depending on the local situation, to establish some form of biotic community. On the sheltered, shallow fore-shores there are, in principle, possibilities for the development of moderate or even well developed biotic communities by nature. Reeds and rushes are two of the important plant species in this zone.
In the aquatic area the previous community will be completely replaced by a freshwater community. The rate of development of this community depends mostly on the rate of desalination and the import possibilities of new organisms. The ultimate composition and abundance of the species depend on the water-quality and the behaviour of the bed. If algae-blooms occur, it exert a negative influence. Therefore, in large lakes with steep shores and a regularly occuring algae-bloom, a poorly developed biotic community can be expected.

2.5.2.4. The transition of an ecosystem into a stagnant saltwater system (variant 3)

The transition of an estuarine ecosystem into a stagnant saltwater ecosystem is possible if not only the estuary is closed off from the sea but if the freshwater supply is cut off as well. When a bay is closed off, the result will be the same, i.e. the formation of a saltwater lake without tidal action (fig. 2.5.2.1) (see also [7, 8, 11, 15]).

1. Hydrological and chemical aspects

Except for a decrease in larger matter in suspension as a result of settlement, the initial water-quality in the new situation is almost the same as it was in the former estuary and will remain so - provided there are no exchange or flushing possibilities - due to the long residence time of the water. Only internal processes and local discharges will affect the quality.
Lake Grevelingen in the Southwest Netherlands exemplifies the transition of an estuary into a stagnant saltwater lake. After closure of the estuary on the riverside and, subsequently, on the sea side, a saltwater lake has been created with a residence time of the water of many years.
Fig. 2.5.2.9 shows that the transparency increased from between 0.5 and 2.5 m to between 1.0 and 7.0 m and that the annual strongly fluctuating salinity in the estuary (10-17‰ Cl^-/l) became more stable. As a result of precipitation and discharges of brackish polder-water the salinity gradually decreased to 13‰ Cl^-/l in the sixth year after the closure.

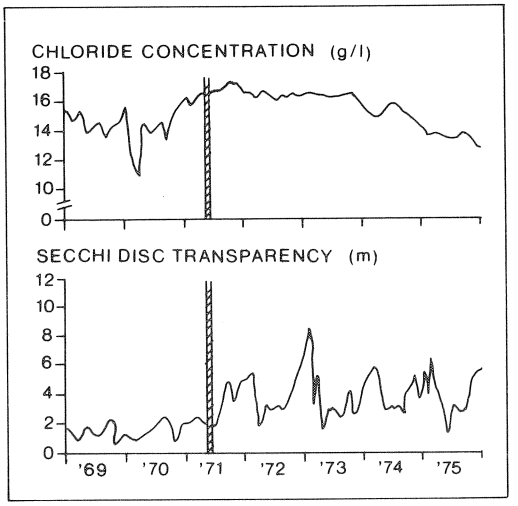

Figure 2.5.2.9 Differences in transparency and chloride concentration in Lake Gevelingen (the Netherlands) - a saltwater lake - before and after closure in 1971.

Immediately after the closure the orthophosphate concentration increased spectacularly which can partly be explained by the

mineralization of the great amount of dead organic matter due to the disappearance of the tide. Regular assessments of the nutrients content have shown that the annual increase of orthophosphate concentration is caused by the release of phosphorus compounds from the bed. Serious algae problems, such as greatly diminished transparency or strongly fluctuating and low oxygen concentrations, have not occurred in Lake Grevelingen, in spite of the relatively high phosphate concentrations. The mean annual chlorophyll concentration amounts to 8μg/l. It is remarkable that algae problems have not occurred in the salt lakes, while these do have arisen in the newly-formed freshwater lakes. A closely-reasoned explanation can not as yet be found for this phenomenon. The low nitrogen content in the saltwater lake may be a reason as well as the fact that shellfish (e.g. mussels, cockles and oysters) feed on phytoplankton (algae).

The gradual decrease in chloride-content is a threat to the marine flora and fauna (fig. 2.2.6.3 indicates that a decrease in salinity will result in a reduction in the abundance of species). For this reason, the management of saline lakes merits particular attention. This problem has been solved in Lake Grevelingen by building a discharge sluice (mean tidal capacity: 100 m^3/s) in the sea side dam which has made it possible to exchange lake-water with coastal-water and has led to an increase in the chloride content. However, during this exchange of water, there is a great chance that stratification will occur, as a result of the differences in density between coastal and lake-water. These differences in density can either be caused by differences in temperature or in chloride content. Fig. 2.5.2.10 shows that the saltier coastal-water (greater density) runs via the bed into the lake. In the course of time, this can result in quite a stable stratification in the lake.
When the temperature of the top layer (epilimnion) rises in spring, this stratification can even increase due to differences in temperature. A very negative effect of this form of stratification is the consequent lack of oxygen in the bottom layer (hypolimnion, see fig. 2.5.2.10). On the one hand oxygen deficiency results from oxygen consumption during mineralization of dead organic matter; this matter mainly comprises algae which lived in the toplayer, died and subsequently sunk. On the other hand, the amount of oxygen, supplied to the bottom layer, is limited as there is no re-aeration. As oxygen consumption is lower in winter (0-1 g/m^2/day) than in summer (2-3 g/m^2/day), as the rate of mineralization depends on the temperature, it may be worth to consider that water should only be exchanged in winter; moreover as in these months there is a greater possibility of storms, which enhances mixing [12]. A negative aspect of water exchange in winter is that the import of (new) organisms is often smaller during this season.
An extensive study of the consequences of the transitions of a tidal system into a salt stagnant one has been published in [8, 15].

2. Morphological and soil mechanical aspects
The developments on exposed land areas are similar to those in the previously described variants. On flat shore zones desalination can be retarded due to regular flooding by salt lake-water. As vegetation on the former mudflats and shoals will gradually expand towards the lake, the region that is being flooded will gradually decrease. As a rule, when a balance in the desalination process has finally been reached, only a narrow strip along the waterline will remain more or less saline. This saline zone is narrower on a high, steep shore than on a low flat one.
Because of the slower rate of desalination and the residual saline zone, the vegetation near the waterline will be minimal. The erosion in this zone will therefore continue over a much longer period.

3. Aspects of flora and fauna
The transition from a salt tidal system into a stagnant saltwater lake implies that a division will also be brought about in this variant between land and aquatic areas with specific developments in each area. In the land areas the developments can be compared more or less with those in variant 1; these are decribed under that variant. However, there are some differences: if, for instance, there is only a gentle

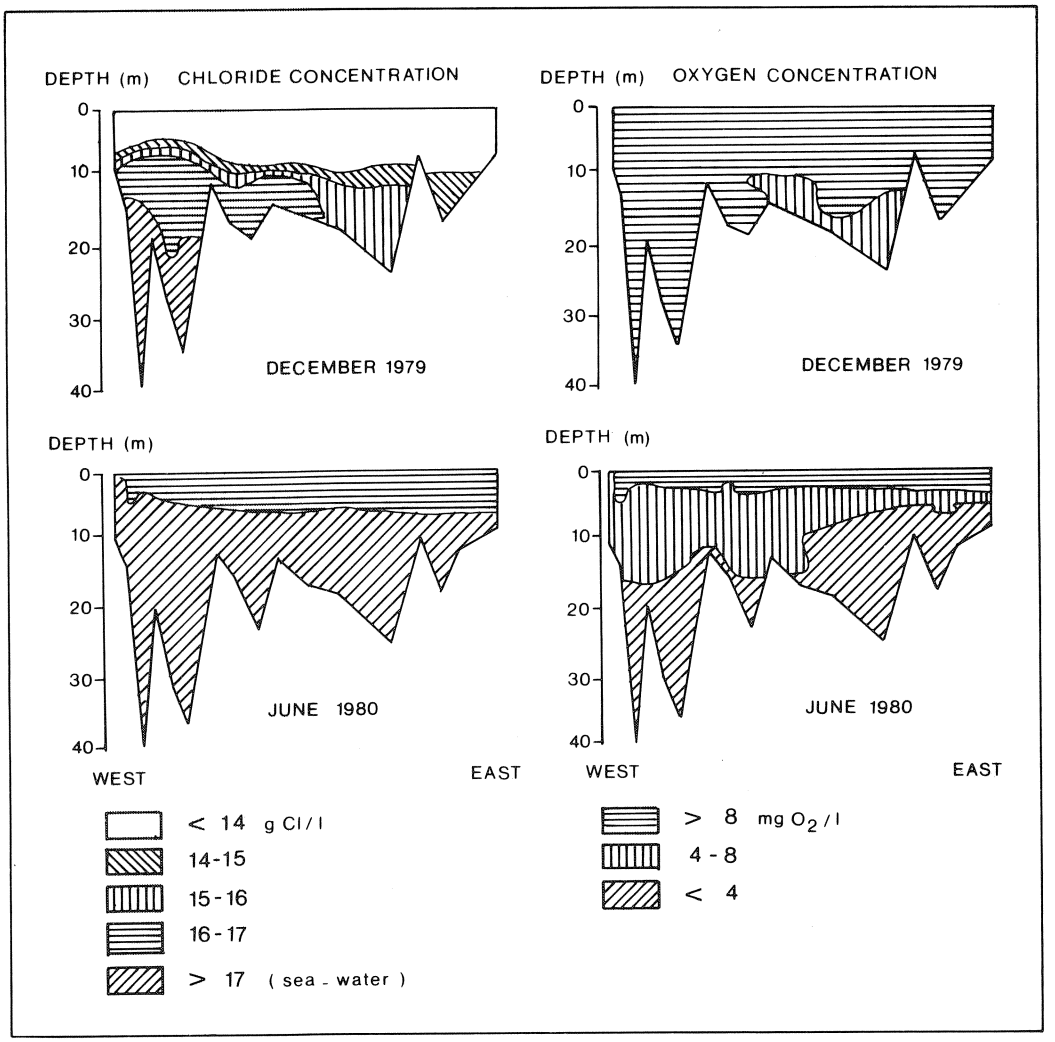

Figure 2.5.2.10 Diagrams of a transection of Lake Grevelingen (from west - sea side - to east) showing the influence of the inlet of sea-water on the chloride and oxygen concentration. Initial inflow of sea-water in December 1979. Due to the great difference in salinity and therefore in density - between the sea-water and the lake-water there is at first little mixing of the two types of water, resulting in salt stratification and lack of oxygen in the under layer. (After de Vos et al 1980 [12]).

slope on the shore zone the desalination may be retarded see also item 2). However, as the vegetation in this shore zone densifies, the lake-will flood less and less the former mudflat and, as a result, this zone will ultimately desalinate completely. Only in the immediate vicinity of the waterline a wider or narrower strip will remain saline and there the saline (halophile) vegetation will maintain its hold.

The changes in the aquatic system will be less extreme as, although the tidal action disappears, the salinity will be (more or less) unchanged. The changes that do occur are therefore, in particular, caused by the disappearance of the tidal current as only the - much smaller - wind-drift currents remain. This means that the living conditions of organisms dependent on the tidal current for transport, food and discharge of excretion products are drastically diminished. Most of the silt in suspension settles to the bed as do the many plankton species which can only remain in suspension in moving water. As a result, on the one hand, the water will become more transparent and, consequently, plants and phytoplankton can live at a greater depth. On the other hand, the composition of species of zoo- and phytoplankton changes substantially in such a way that only species that do not sink easily will remain. The „bed-animals" are also affected by this settlement. The „suspension-feeders" which subsist on food, filtered from the water, will find a decreased food supply in the water; the „sediment-eaters" who subsist on food particles in the mud will, on the other hand, have an increased supply. As a result, this group will probably increase in number whereas the suspension feeders will decrease until a new balance is reached.
As mentionned before the enhanced transparency of the water also implies that, in addition to algae, also many water-plants, such as seagrasses, can live in the water and both groups also to a greater depth. This can be very important as, due to the closing-off from the sea, the normally available import of nutrients from the sea will be cut off. As a result of the increase in the plant-biomass, the production of the lake can remain relatively high, although different animal species may benefit from this production. This is shown in fig. 2.5.2.11 [13], which indicates how the composition of the bird population in Lake Grevelingen has changed since its closure (from estuary to saline lake). Before the closure, the zoobenthos-eating birds (waders) -which fed on the vast mudflats and shoals -predominated; however, since the closure nearly all these birds have disappeared as the shoals and mudflats were either permanently submerged or exposed. Instead great numbers of plant-eating birds (such as ducks and swans) have taken their place. In addition, the number of fish-eating birds (grebes) has also strongly increased (fig. 2.5.2.12); this is a result of the greater transparency of the water, which made it easier for these birds to find their prey.
The exchange of lake-water with the sea is important, first, so as to maintain the salt concentration in the lake (for the managerial problems see item 1), and, secondly, because this enables

Figure 2.5.2.11. The response of birds in Lake Grevelingen on the closure (after Saeijs & Bannink 1978 [5], Saeijs & Baptist 1976 [13]).

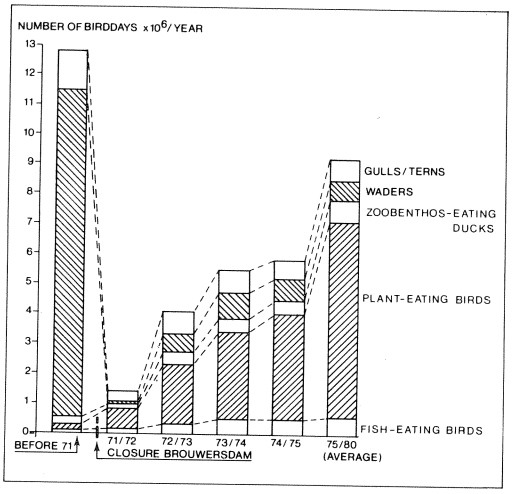

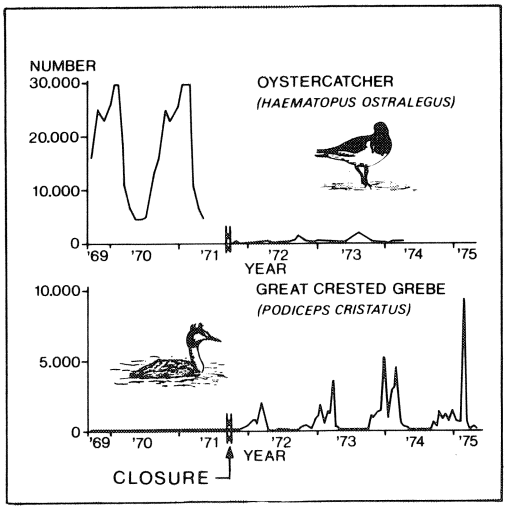

Figure 2.5.2.12. The response of two representative bird-species (a wader, resp a fish-eating bird) on the closure of Lake Grevelingen (after Saeijs & Bannink 1978 [5]).

all sorts of organisms to migrate to and from the sea, which is vital for the reproduction-cycle of many species.

2.5.3.5 Transition into a saltwater system with a reduced tidal action (variant 4)

The transition into a system with a reduced tidal action is possible if a structure is built in the mouth of the estuary - or sea-arm - through which a reduced tide can pass - a tide-reducer. Such a structure is often closable to retain stormfloods (see also [9]). If a tidal power station is included in this structure, a different tidal situation will arise, which, however, will not be dealt with here.

1. Hydrological and chemical aspects
If a tide-reducer is present, the tidal amplitude and volume will decrease. The current velocities will decrease in front of and behind the reducer, whereas in the vicinity of the structure they will increase. Finally the levels at which the maximum ebb and flood currents occur may change. The originally existing phase-differences between the tidal action in the basin and in the sea may also differ, which may have great consequences for the water-exchange (flushing) between basin and sea. For example, in the Eastern Scheldt, during ebb, the period of flow of the water from the basin with the tidal current on the North Sea in a northern direction is between 1½ and two times as long as in the southern tidal current during flood; as a result of this each tide a certain amount of „fresh" water arrives in the basin. After completion of the Eastern Scheldt barrier, the phase difference will shift, as a result of which at sea the north- and southward movement of the water coming from the Eastern Scheldt will last for about the same period. The water will then, as it were, „shuttle" back and forth in the mouth of the Eastern Scheldt thus leading to a strong decrease in the water-exchange. These processes may have important repercussions on the import and export of matter, such as the import of nutrients, and the export of freshwater and discharged matter from drainage.
On account of the lower current velocities in the basin, the water will become more transparent as the sand and silt will sink to a larger extent; consequently, algae-growth in the basin may increase. This means that a change may occur in the food-balance, i.e. the sum of the import and export of nutrients plus the primary production. If freshwater discharges take place in the basin (drainage, sluices), the salinity may decrease slightly, particularly if the net water-exchange between the basin and the sea decreases. All together discharges into and internal processes within the basin will affect the water-quality more than before. In addition, the extremes in temperatures may also be influenced by a reduced net water-exchange (warmer in summer, colder in winter).

2. Morphological and soil mechanical aspects
The geomorphological changes in the basin resulting from a tidal reduction depend to a great extent on the reduction-rate.
If the tide is only slightly reduced the geomor-

phological changes will be small or nil, however, if the reduction is so substantial that extensive land areas are created, the development will closely resemble the previously described state of the closed-off stagnant saline lakes. It is still not known whether the transition between both extremes is a gradual one in proportion to the reduction-rate or that there are certain threshold-values which may induce sudden, great changes.

A tidal reduction usually implies - at least for the channel system - that owing to the reduced tidal volume, the velocity of the tidal currents will decline. As the morphology and composition of the bed in a basin are, in principle, in equilibrium with the forces exerted on them (see also 2.2.6.4), the cross-sections of the channels will become „too wide" for the new tidal regime, which will mean that the channels will become shallower. The rate at which this occurs depends on the current velocity together with the transport capacity within the basin itself and the exchange of water and sediment between the basin and the sea. The highest velocities will occur in the reducer itself. It is expected, therefore, that with a reduced tide the sand will settle in the vicinity of the reducer whereas the finer-grained sand and silt will sink further upstream. Consequently, morphological changes will also occur more rapidly in the vicinity of the reducer than higher up in the basin.
The exchange of matter (particularly sand) between the basin and the sea is affected by the decelerating current velocities in the fore- delta; consequently the sand-transport capacity may reduce resulting in a decreased import of matter. The scour holes that will be created on either side of the reducer will also affect the sediment-transport between basin and sea. As the tidal current will decelerate in these scour holes a great part of the material will accumulate in them. Because of the fact that during flood the material will accumulate in the scour-hole on the sea-side of the reducer and during ebb on the basin-side, it seems that sand is not able to go from the fore-delta to the basin and the other way around.
This is not quite true because during storms one can expect that much more material is brought into suspension in the fore-delta than in the basin so that if not all the sand accumulates in the scour-hole and assuming that there is an equilibrium between the scour-hole and the threshold (see 2.5.1.), some of this material will accumulate on the threshold on the basin-side of the barrier. As a consequence the threshold will grow in an eastward direction.
Local differences can lead to spatial variations in this general pattern. If, for instance, another river debouches into the basin of an estuary, the sedimentation process can accelerate considerably, which may also result in a change in pattern of the differing forms of sedimentation.

As yet little is known about the exact influence of a tidal reduction on shoals and mudflats. In any case, because of the reduced tidal

Figure 2.5.2.13. The effect of tide-reduction on the sequential parts of the intertidal area; the intertidal area decreases, the shallow water zone and the zone above high tide increase. (M.H.T. : Mean High Tide; M.L.T. : Mean Low Tide)

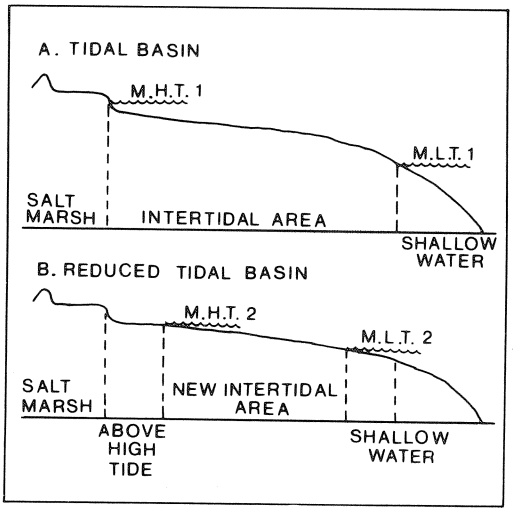

amplitude, the flooding frequency of the higher sections will decrease, while the lowest sections will be below the mean low-water level. Therefore, in the first instance, the extent of the intertidal area will decrease (see fig. 2.5.2.13). In which way this surface area will change in the future depends on the morphological adaptations of the shoals and mudflats to the new hydraulic conditions. These adaptations are determined by the cooperative effects of various processes, leading to either a decrease of the shoals and mudflats, or an increase. The adaptation-rate depends to a great extent on the rate of sediment transport:

- due to the tidal reduction, the effect of waves on the shoals will be concentrated on a narrower zone and probably cause erosion. Whether this happens, and where, depends on the combined action of waves and currents;
- a tidal reduction may cause a shift in the tidal phase, i.e. within the tidal cycle the levels at which the maximum flood and ebb current velocities occur may change. It may happen, for instance, that the maximum flood current occurs at a time when the shoals and mudflats have not yet been inundated. This may lead to an increased „current attack" at the level of the prevailing maximum currents; but it may also lead to a decreased supply of sediment on the shoals and mudflats.
  Conversely, a phase-shift of the ebb peak may result in a decreased export of matter from the shoals and mudflats towards the channel;
- a new shape of the tidal curve may lead to a prolonged period of slack-water. The resulting extension of the period with lower current velocities can cause increased sedimentation;
- as the presence of sand in the water decreases, primarily due to sedimentation near the reducer and in the channels, the remaining sediment will be finer, resulting in a richer silt content of the shoals and mudflats. This silt, which in itself is more erosion resistant, may, therefore, result in a decrease of the erosion, or even stop it, or lead to the creation of new or the increase of existing shoals and mudflats;
- changes in current velocities and sedimentation in the channels may result in different current patterns due to which the meandering pattern in the tidal channels may change. In combination with changes that will occur in the helical currents this may either lead to the accretion or erosion of shoals. Similarly, changes may occur in the pattern of ebb and flood channels, together with changes in the water levels between the channels. This process may further affect the transverse flows on the shoals often resulting in additional accretion, but erosional effects may occur as well.

The ultimate effect of these processes on the shoals and mudflats depends on the extent of the tidal reduction, and may vary geographically within the area.

Obviously, the lower high-water level and the consequent deminishing in flooding frequency will also effect the salt-marshes. If the highest sections are no longer be flooded, desalination and maturing of the soil will set in. On account of the reduced flooding frequency and the smaller quantities of water on the salt-marshes, the accretion pattern will shift towards the mudflats, whilst the accretion rate will probably decrease. The creeks will be too wide for the new tide and therefore will show a tendency to silt up. The salt-marshes could to a certain extent extend depending on the new mean high-water level, particularly in those places of the mudflats where conditions for accretion are favourable (i.e.a. large silt-supply, low current velocities and low wave-action). Those salt-marshes, which prior to a reduction of the tide already showed a tendency to extend, may increase even more rapidly under a reduced tidal regime. Even salt-marshes which are subject to erosion, as indicated by erosion-escarpments, may extend; however, if the escarpment erosion continues, no extension will take place. This erosive action could be continued if, as a result of the reduced tide, the mean high-water level would be at about the same level as the tip of the salt-marsh escarpment. The longer period that the water remains at that level may induce an increased wave-attack and consequent erosion.

3. Aspects of flora and fauna

When the tidal amplitude decreases, the highest sections of the tidal areas will less, or even no longer be flooded and become permanently exposed, whereas the lower sections may be flooded to a greater extent or even no longer be exposed. The total periodically-exposed surface area will thus decrease (see fig. 2.5.2.13). The result could be that their function as foraging areas for birds (mostly waders) diminishes. This implies that these birds will have to try and find other feeding grounds; if they do not succeed - because there are no such areas or because those are already being maximally used - these bird populations may decrease in number. On the other hand the highest sections, which after the tide-reduction will less or even no longer be flooded, may offer new possibilities as breeding grounds for certain bird species, so that the breeding function of the area for certain species may increase.

The composition of the vegetation on the salt-marshes, which is strongly determined by the flooding frequency, (see 2.2.6.6), will change; in general a tidal reduction will induce a shift of the vegetation-zones towards the lower sections of the marshes.

The increased transparency of the water enhances on the one hand the subsistence-possibilities for algae whereas, on the other hand, higher forms of plant life, for instance larger (multi-cellular) algae and sea-grasses, can live up to greater depths. The latter may also be enhanced by the reduced current.
An additional result of the increased accretion is a shift in the composition of the aquatic fauna; in principle, the chances of survival will decrease for current-dependent organisms i.e. „the filter feeders" such as sea-anemones, whereas the „sediment-eaters„ such as worms will increase. The changes are to a certain extent comparable to those in a stagnant saltwater lake, although less accentuated.
The settlement of silt in a large area of the basin may affect the composition of the local zoobenthos, but the fishery function of the basin may be influenced as well.
Finally, the tide-reducer itself may have a direct influence on plant and animal life; this applies particularly to the exchange possibilities for organisms between the basin and the sea. When this exchange decreases, this not only entails repercussions for the biotic communities but also for fisheries and even for the coastal region, if the basin has an important function for spawning or as a „nursery„ where larvae can mature.

2.5.2.6 Morphological developments in the fore-delta

The developments discussed above occur in the newly-created area behind the closure dam or the reducer. However, the area immediately in front of the dam/reducer, i.e. on the seaward side, will also be affected; this applies particularly to the morphology. In principle, there is little difference between the developments oc-

Figure 2.5.2.15 Erosion and sedimention on a yearly base after the closure of Haringvliet (A) and Brouwershavense Gat (B)

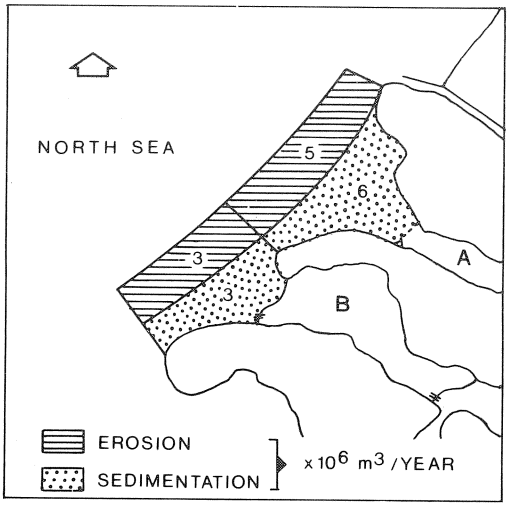

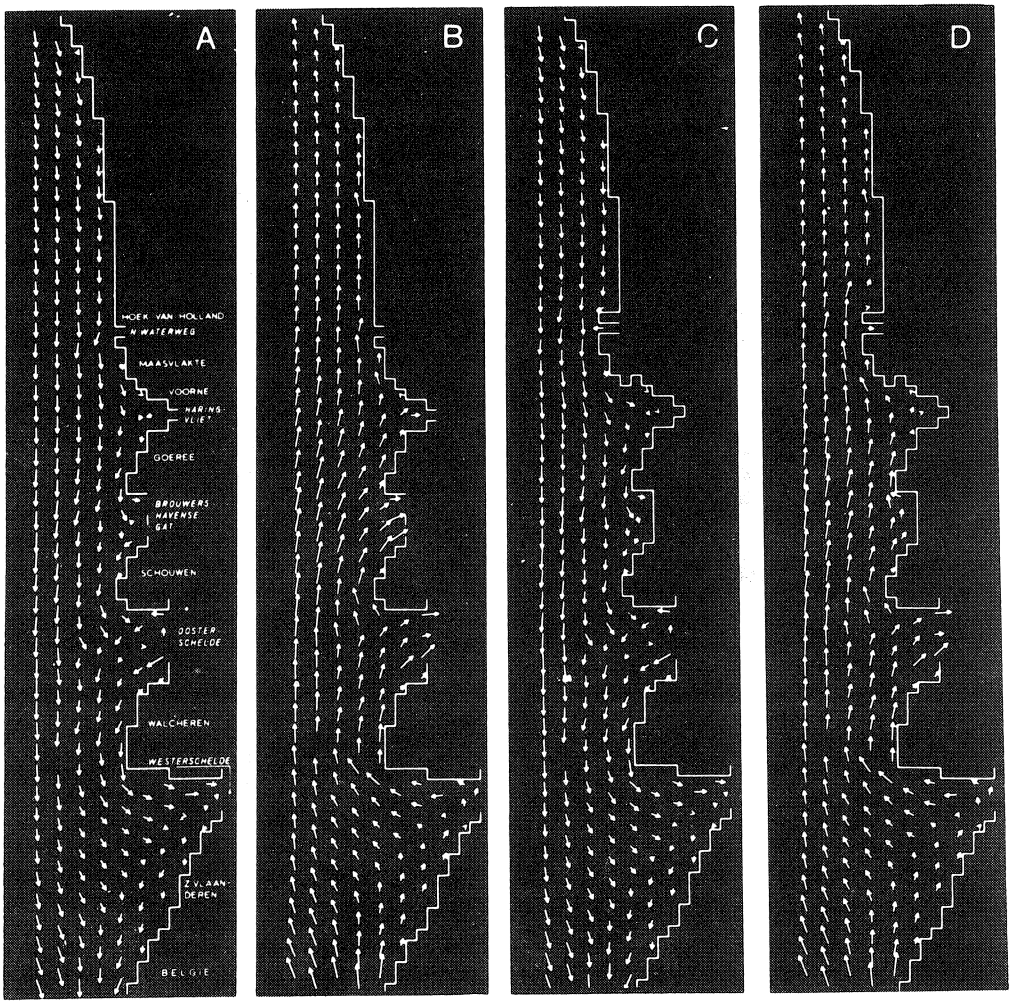

Figure 2.5.2.14 A and B represent the ebb and flood current pattern in the Haringvliet and Brouwershavense Gat before closure. C and D show the closed situation.

curring as a result of a closure dam or a reducer, although, with a reducer, the developments are less pronounced and slower. The morphology in the mouth of an estuary usually comprises a system of sandbars and channels. This system has been formed by a longterm proces of the in- and outgoing currents and has the form of a fan, which is called the underwater delta of the estuary or fore-delta (see 2.2.4). When in- and

outgoing currents are absent the morphology is more or less parallel with the general coastline configuration, due to the wave action and, if present, restcirculation along the coast. So in general it can be said that when an estuary is closed currents at an angle to the coast will disappear, possibly to be replaced by a more longshore oriented current. The latter is the case in the SW parts of The Netherlands (see fig. 2.5.2.14). The morphological consequences in this case have been broadly that the seaward part of the fore-delta erodes, while the eroded material accumulates to a large extent on the landward part (see fig. 2.5.2.15). The eroded material will also be transported in the direction of the restcirculation, i.e. for the S.W. Netherlands in a northern direction.
Ultimately it may be expected that the morphological pattern of the fore-delta will change into a morphology oriented parallel to the coastline.

Literature

1. Saeijs, H.L.F., **Changing Estuaries, A Review and New Strategy for Management and Design in Coastal Engineering.** Government Publishing Office, the Hague, 1982.

2. Buysrogge, R.A., J.J. Siereveld & J. Visser, Geomorfologische kartering van drooggevallen gebieden in de Grevelingen. (Geomorphological Maps of Newly Exposed Areas in Lake Grevelingen). **Rijkswaterstaat Deltadienst**, Milieu en Inrichting, nota 79-09, Middelburg, 1979 (unpubl. Report, in Dutch).

3. Joenje, W., **Plant Colonization and Succession on embanked Sandflats**. Thesis Groningen, 1978

4. Glopper, G.J. de, **Subsidence after Drainage of the Deposits in the Former Zuyderzee and in the Brackish and Marine Forelands in The Netherlands**. Van Zee tot Land no. 50, Tjeenk Willink, Zwolle, 1973.

5. Saeijs, H.L.F. & B.A. Bannink, Environmental Consideration in a Coastal Engineering Project, the Delta Project in the South-west of the Netherlands. **Hydrobiological Bulletin** 12: 3/4 pp. 180 - 202, 1978.

6. Jong, D.J. de & T.J. de Kogel, De vegetatieontwikkeling op de Slikken van Flakkee van 1972 - 1978. (Vegetation Development on a Former Mudflat and Salt-marsh in Lake Grevelingen), **Rijkswaterstaat, Deltadienst**, Milieu en Inrichting 79-11, Middelburg, 1979 (unpubl. Report in Dutch).

7. Proceedings First International Symposium on Integration of Ecological Aspects in Coastal Engineering Projects, Rotterdam. **Water, Science and Techn., Vol. 16, febr. 1984.** In which:

   8. Nienhuis, P.H. & J.C. Huis in 't Veld, **Grevelingen: from an Estuary to a Saline Lake.**

   9. Knoester, M., J. Visser, B.A. Bannink, C.J. Colijn & W.P.A. Broeders, **The Eastern Scheldt Project**.

   10. Ferguson, H.A., & W.J. Wolff, **The Haringvliet Project:The Development of the Rhine-Meuse Estuary from Tidal Inlet to Stagnant Freshwater Lake.**

   11. Meulen, J.H. v.d., J. Leentvaar & N.M. de Rooy, **Environmental Impact Statement on the Problem of a Fresh or Salt Lake Grevelingen.**

12. Vos, C.P. de, J.S.L. Vink, B.A. Bannink & J. Leentvaar, Water Quality Impacts Exchanging Water between Sea an a Closed Estuary. **Prog. Water Tech.**,Vol. 13 pp. 271-285, 1980.

13. Saeijs, H.L.F. & H.J.M. Baptist, Vogels in het Grevelingenmeer van 1971 - 1975 (Birds in a salt-water Lake of Estuarine Origin from 1971 - 1975). Nota 76-31, **Rijkswaterstaat, Deltadienst**, Middelburg, 1976 (unpubl. Report in Dutch).

14. Saeijs, H.L.F. & H.J.M. Baptist, Coastal Engineering and European Wintering Wetland Birds. **Biol. Conservation 17**: 1 page 63-83, 1980.

15. Saeijs, H.L.F. & P.B.M. Stortelder, Converting an Estuary to Lake Grevelingen: Environmental Review of a Coastal Engineering Project. **Environmental Management**, Vol. 6 no. 4, 1982.

16. Anonymus, **Het Delta Boek** (The Delta Book). Natuur en Techniek, Maastricht, 1982 (in Dutch).

17. Salomons, W., Impact of Civil Engineering on the pathways of Heavy Metals from Rivers to the Southern North Sea. **Proceedings International Conference Heavy Metals in the Environment**, pp. 359-362, Amsterdam, september 1981.

18. Visser, J. & H.L.F. Saeijs, Ecological Impact of the Delta Project in The Netherlands Landscape, Development and Ecological Possibilities of Terrestric Areas. **Land + Water Int.**, 42 pp. 9-16 Nedeco, The Hague, 1980.

19. Saeijs, H.L.F., Ecological Impact of the Delta Project in The Netherlands. **Land + Water Int.**, 40 pp. 20-34 Nedeco, The Hague, 1979.

20. Beeftink, W.G., M.C. Daane & W. de Munck, Tien jaar botanisch-oecologische verkenningen langs het Veerse Meer (Ten Years of Phytoecological Research on the Borders of Lake Veere). **Natuur en Landschap 25**, pp. 50 - 63, 1971 (in Dutch)

2.6. Performance Monitoring

If the construction of the structure is finished it is important to monitor its effect on the natural conditions in order to be able to judge wether the planned new situation is reached or not. If not and even more in the case of unexpected effects new strategies for managing the basin behind the structure have to be developed.
Also the condition of the structure itself should be monitored even under less severe conditions than the "design conditions". Only in this way a regular check, this means a prediction of the safety or probability of failure for future design conditions becomes possible.
This design philosophy is worked out in the following section.

Performance Monitoring

J.K. Nieuwenhuis

2.6. Performance monitoring

2.6.1. Introduction

As soon as a civil engineering work is planned a complete analysis of all the functions it will get in the future must be made. That analysis should not only comprise its primary function, i.e. a dike for retaining water, but also functions which are related to:

- conservation
- recreation
- fishery
- agriculture

It may then be that retention of water is not the most important function.If such a methodology is followed all kinds of alternatives with their consequences can be screened and may help avoid mistakes or not easily foreseen consequences with far-reaching effects. This may be the case with a dam in a large river (e.g. the Aswan dam in the river Nile) or the closure of an estuary (the Eastern Scheldt Barrier). Of course, concern for other functions will cost extra money, but on the other hand the usefulness of an area for the people will be greatly increased. In section 2.5.2. the impact of a major structure on society and the possibility of changing appreciation during planning, construction and after completion, were elaborated.
The following will deal with:

1. the technical aspects of performance, that is the structural behaviour
2. Environmental evaluation and control.

2.6.2. Technical performance

Performance and safety.
It will be clear that observing the behaviour of a structure is not a goal in itself. What should be done is to compare actual with predicted performance. After that conclusions must be drawn about the safety of the structure. These safety aspects are incorporated in the design and design criteria. Thus design, performance, instrumentation and performance evaluation should ultimately lead to an assessment of the safety or failure probability. More explicitely this relation is given below [1]:

1. Performance Criteria:
   a. Determine the consequences of failure.
   b. Select an acceptable level of risk.
   c. Establish criteria of performance.
   d. Ensure that the criteria meet appropriate legal requirements and accepted standards of practice.
2. Design Assessment:
   a. Check the design conditions, such as loads.
   b. Identify the critical mechanisms of performance.
   c. Identify typical and critical sections.
   d. Review the field and laboratory data used by the designer. Inspect the site and run selected tests that greatly affect the design.
   e. Examine the prediction methods employed by the designer. Check to see whether the designer's methods rest on mechanisms approximating the expected actual ones.
   f. Check the designer's predictions of performance and compare them with the performance criteria.
   g. Prepare a Design Summary which clearly states and references the loads used by the designer as well as his prediction methods and parameters, and portrays the predicted performance.
   h. Use the designer's methods and parameters to predict performance for conditions expected during the early life of the facility.
   i. Identify major uncertainties and critical aspects of performance.
3. Field Measurement System:
   a. Select appropriate field instruments and place them so they can measure critical aspects of performance.
   b. Install instruments which can reveal mechanisms and values of key parameters. The engineer should observe the installation of instruments to ensure that they are placed at the correct locations and that they read correctly.
   c. Periodically check and maintain field instruments.

4. Construction Assessment:
   a. Make periodic inspections of the facility during construction.
      Compare the actual construction with the design and document the significant features of construction, particularly those features which vary from the original design.
   b. Assess the significance for predicted performance of such departures from the design.
   c. Make frequent site visits where difficult site conditions prevail.
5. Surveillance:
   a. Make periodic visual inspections of the project, searching for any evidence of malfunction.
   b. Measure important aspects of performance.
   c. Obtain information on mechanisms and parameters.
   d. Portray (versus time) field measurements, significant events and predicted values.
6. Performance Evaluations:
7. Safety Assessment:
   a. Determine and indicate (in terms of safety factor or probability of failure) the degree of safety of the facility.
   b. State and evaluate any change in degree of safety during the period since the last safety assessment.
   c. State whether or not the existing degree of safety meets performance criteria.
8. Remedial Measures:
   a. Design and assist in executing remedial measures to bring the degree of safety to a satisfactory level if the safety assessment reveals an inadequate level of safety.
   b. Evaluate the effectiveness of remedial measures.
9. Contingency Plan:
   a. Develop a plan to limit the consequences of a failure.

To follow and work out all the steps in the way as indicated requires more effort by the designers than is generally given.
The advantages are that:
a. the design is more thorough;
b. the quality of the structure can be maintained and remedial measures taken, if necessary, to guarantee this quality during its lifetime
c. the possibility is given to the manager of changing the operation of the structure in its environment;
d. a learning effect is achieved, for the comparison of actual and predicted performance will lead to better designs.

All these considerations were thought of in the design of the barrier of the Eastern Scheldt estuary in the Netherlands (See fig.2.6.1)
This structure is technically complicated and required many studies, investigations and mathematical and physical models on both a small and large scale. Schematisation, extrapolation, wave spectra, failure mechanisms, probability of malfunctioning and failure led to the design criteria. All these aspects should be reviewed when the performance of the structure has been evaluated, not only after completion but also during construction. And not only the structure itself, also the environment has to be monitored. Changes of shallows and channels may well occur, which may influence the management operations of the barrier.
The Eastern Scheldt Barrier may be taken by way of illustration.

Surveillance and measurement of the barrier
In order to maintain the condition of the barrier, measurements are required. These measurements will consist of monitoring the sensors, installed in advance into or beneath the structure, and measurements with survey vessels or other inspection equipment (See fig.2.6.2 and 3)
Because of the fact that the design criteria, i.e. the superstorm which may occur once in 4000 years, will probably not be met, the method of measuring, processing and analysing the characteristics must be such that for less severe conditions, performance can still be evaluated well enough to assess the design.
The measurements can be divided into a number of groups:
a. Environmental conditions:
   Measurement of wave height and wave direction, water level and current.

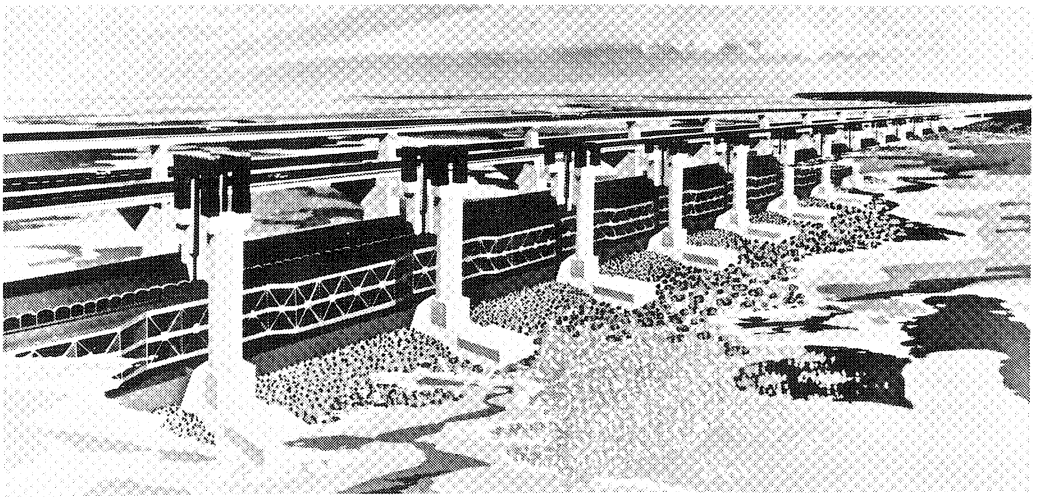

Figure 2.6.1 Eastern Scheldt Barrier, the Netherlands.

Figure 2.6.2 Main features of the Eastern Scheldt Barrier

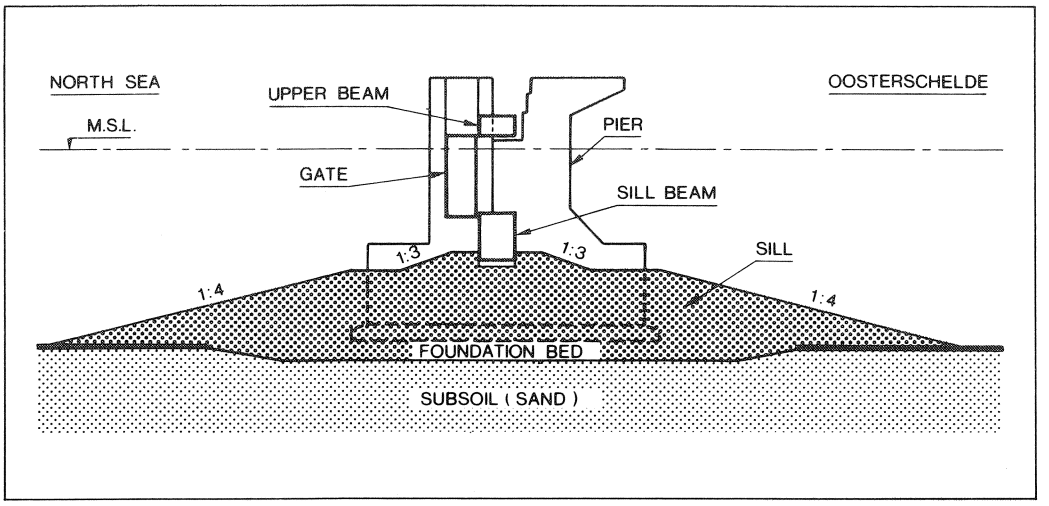

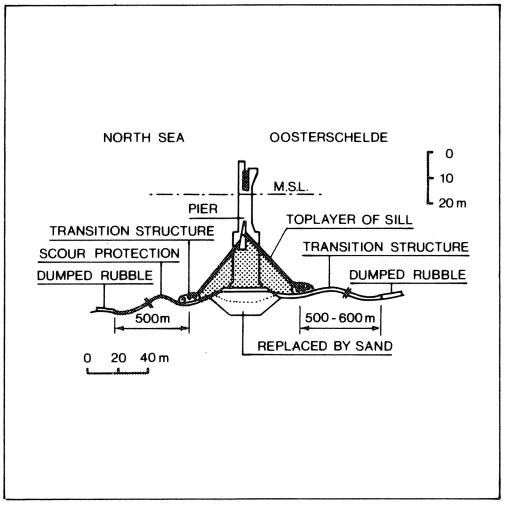

Figure 2.6.3 Underwater dam of the Eastern Scheldt Barrier

Figure 2.6.4 Forces on the foundation of the Eastern Scheldt Barrier

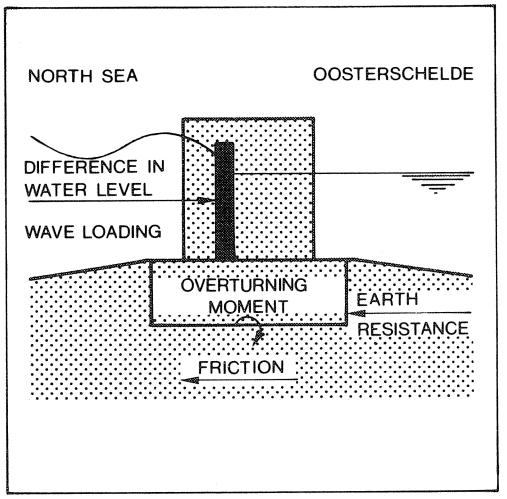

b. Concrete: piers: Beams for the steel gates and the road over the piers.
Measurement of stresses, translation and rotation, deflection (of the beams)
c. Steel: gates
Measurement of stresses, deflection, fatigue and corrosion
d. Foundation: sill, anti-scour mat, transition structure, rip-rap.(See fig. 2.6.3) Measurement of pore pressures, deformation, displacement (stones) and stability (scour holes).

Processing of measurements

Measurement of the environmental conditons is closely related to the collection of hydraulic data for the management of the barrier. These data will be registered and processed continuously under the responsibility of the manager. The same applies to the data, which yield direct information on the actual condition of the barrier. These data have an alarm-function for the manager so that remedial measures can be taken.

Evaluation of the design-criteria during condition surveillance aims at a better knowledge of the quality of the models and calculations which formed the basis of the barrier design.
The operational capacities of the structure can be made more pronounced and more certainty can be offered as to the effect of measures, which may have to be taken. Furthermore, new knowledge may be acquired, which can be used for other situations and designs.
This kind of evaluation can be divided into three parts. Of primary importance is that the wave condition, i.e. the amplitudal and directional

spectrum, is measured just in front of the barrier.
These parts are:
1. Checking the schematisation of the hydraulic conditions
2. Checking the wave-load transfer functions
3. Checking the soil-mechanics models

Re 1. By wave observation and measurements at a number of carefully selected points the reflection coefficients as measured in the model and the assumed wave direction can be verified. It will then become evident whether the wave criteria for the design were optimistic or pessimistic.

Re 2. The hydraulic criteria together with the transfer functions, adjusted with the help of results of model experiments are used as input for computerprogrammes, with which the forces acting upon the pier and foundation are calculated. By performing strain measurements at the gates and beams evidence can also be obtained as to wether the tranfer-function was optimistic or not. The forces and moments of the pier footing can moreover be determined more exactly. The latter forms the basis for the input of part 3.

Re 3. By installing a number of piezometers on the subsoil, a check on the variability of soil parameters can be made, i.e. compressibility, and permeability.
The registration of deformations gives direct information about the soil-structure model. Pore pressure measurements and deformation measurements will add greatly to the knowledge of the soil-structure interaction and thus the structure's behaviour in various conditions.

Evaluation and reliability of measurement
An important question is how a measurement can be evaluated for a conclusion to be drawn about design-criteria. In order to answer that question all aspects ranging from environmental conditons to that particular measurement have to be analysed step by step.
As an example the measurement of cyclic pore pressures beneath a pier of the Eastern Scheldt Barrier will be evaluated in theory.

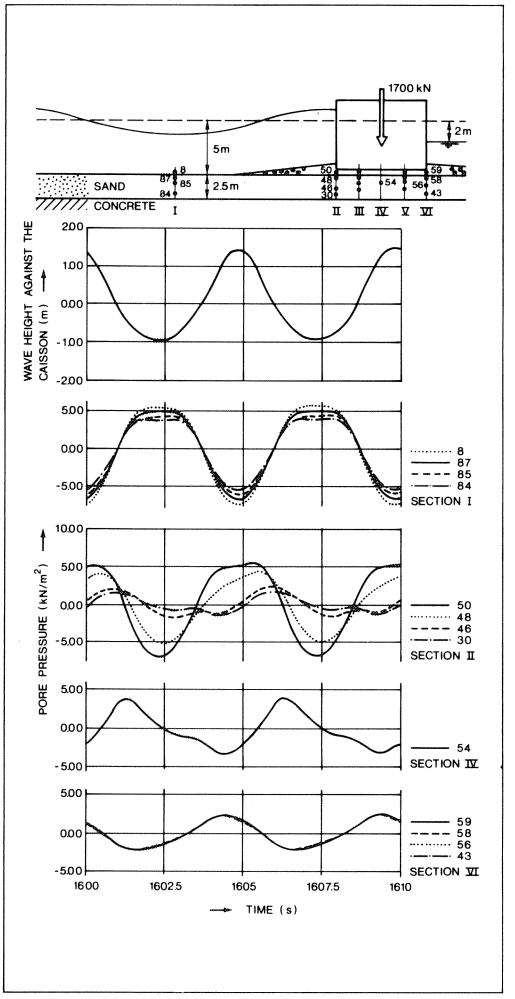

Figure 2.6.5 Measured pore pressures in the sand in front of and below the test-caisson for the Eastern Scheldt barrier design

	Factor	Type of information	Instrumentation	Variation
S :	Environment (wave spectrum)	- water level - wave height and direction	wave riders at representative locations, level-gauges not possible, theory only	5 % 15 %
T1 :	Transfer function(theory and model experiments)	- reflection coeff. - non-lineair effects when extrapolating		
P1 :	Total load spectrum on pier	- forces on gates, beams and pier giving: . hor. wave force . moment over pier footing . moment over pier footing	strain-gauges on gates, accellerometers pressure-meters load-cells (not feasible)	15 % (15 %) (15 %)
	P1 = S x T1 = 15%			
T2 :	Load distribution between pier and foundation	- forces from embedment (sill) on foundation and sill beam	theory	10 %
P2 :	Force distribution over pier footing (static and dynamic)	- dynamic reaction beneath footing	theory	20 %
	P2 = P1xT2 = 20%			
T3 :	Transfer-function (relation between wave spectrum and pore pressure)	- mathematical model - soil parameters (average and variation)	experiment with physical model lab.tests on bore hole samples	10 %
W :	Cyclic pore pressures	- pore pressures in subsoil underneath footing	piezometers	10 %

In this case the question was if the measured cyclic pore-pressures could confirm the design-criteria, i.e. the soil-parameters, with greater reliability than the laboratory tests could give. In the procedure list above one may see that the variations of P2 (force distribution on pier footing) is larger (20%) than the variation of the readings of the piezometers. This will give the opportunity to back-figure the soil parameters in the transfer function T3 with greater reliability.

Note that a high reliability of the mathematical model T3 could only be achieved by a large scale model test. Comparison of computed measurements and observed measurements of the model (See fig. 2.6.5) provided confidence that the computer programme can be also used for prototype conditions [3].

Instrumentation

Depending on the type of measurements an instrumentation program must be planned and carried out. This program depends on:

- the type of structure
- the experience with identical structures and conditions
- the failure probability of the structure or parts of it and consequences of failure for the structure and environment
- the feasibility of installation and measurement of instruments.

Table 2.6.1. summarizes an instrumentation plan for a concrete gravity structure for oil production [2].

Figure 2.6.6 shows a sketch of the Brent B gravity structure, within the North Sea, and the sensors installed.

Figure 2.6.7 presents the time-settlement record of another gravity structure. For the monitoring of dams a different instrumentation program is executed. Such a program is greatly affected by

Table 2.6.1 Instrumentation commonly used for performance measurements

Physical measurement	Use made of data	Accuracy required	Typical method of measurement	Relative success	
Tidal variation	To correct pore pressure measurements	0.1 m	- Graduated scales - Pressure transducers - Infrared or radar devices	Fair Good ?	Often damaged
Inclination of structure	To check long-term inclination of deck and differiental settlement of sub-structures	0.01°	- U-tubes - Spirit levels - Optical levelling - Electronic sensors	Fair Fair Fair Good	Depends on weather
Differential water pressure in skirt compartments	To determine uplift pressure underneath the base of the platform	4 kN/m²	- Absolute pressure transducers - Differential pressure transducers	Fair/Good Excellent	
Pore water pressure	Evaluate stability and rate of consolidation	5 kN/m²	- Pressure transducers embedded at different elevations in the foundation soil	Fair/Good	
Base contact stresses	Determine absolute pressure distribution under base, and variations with time	20 kN/m² to 30 kN/m²	- Earth pressure transducers	Excellent	Depends on details of base
Stresses in reinforcing steel and concrete	To determine static and dynamic stresses in special parts of structure	2%*	- Strain gauged reinforcement - Embedment strain gauges	Good Fair	
Linear and angular accelerations	To find dynamic response of structure, and structure/soil interaction	1×10^{-6} g 1×10^{-6} rad/sec²	- Linear servo accelerometers - Angular servo accelerometers	Good Fair/Good	
Long-term settlement	To measure consolidation settlement and secondary settlement of the structure	0.01 m	- Optical levelling from nearby piled structure - Closed hydraulic system - Tell-tale rod anchored in subsoil - Embedded radioactive bullets - Jointed casing and survey tool	Fair Fair Excellent Good Good	Seldom possible
Long-term horizontal displacement	To determine horizontal movements of structure relative to subsoil	0.02 m	- Inclinometer run in flexible casing beneath platform	Good	
Scour	Confirm need for, or effect of, erosion control	–	- Submarine inspection	Good	

Notes: Instrumentation for environmental and meteorological observations are not included in the table.
* denotes percentage of maximum design value.

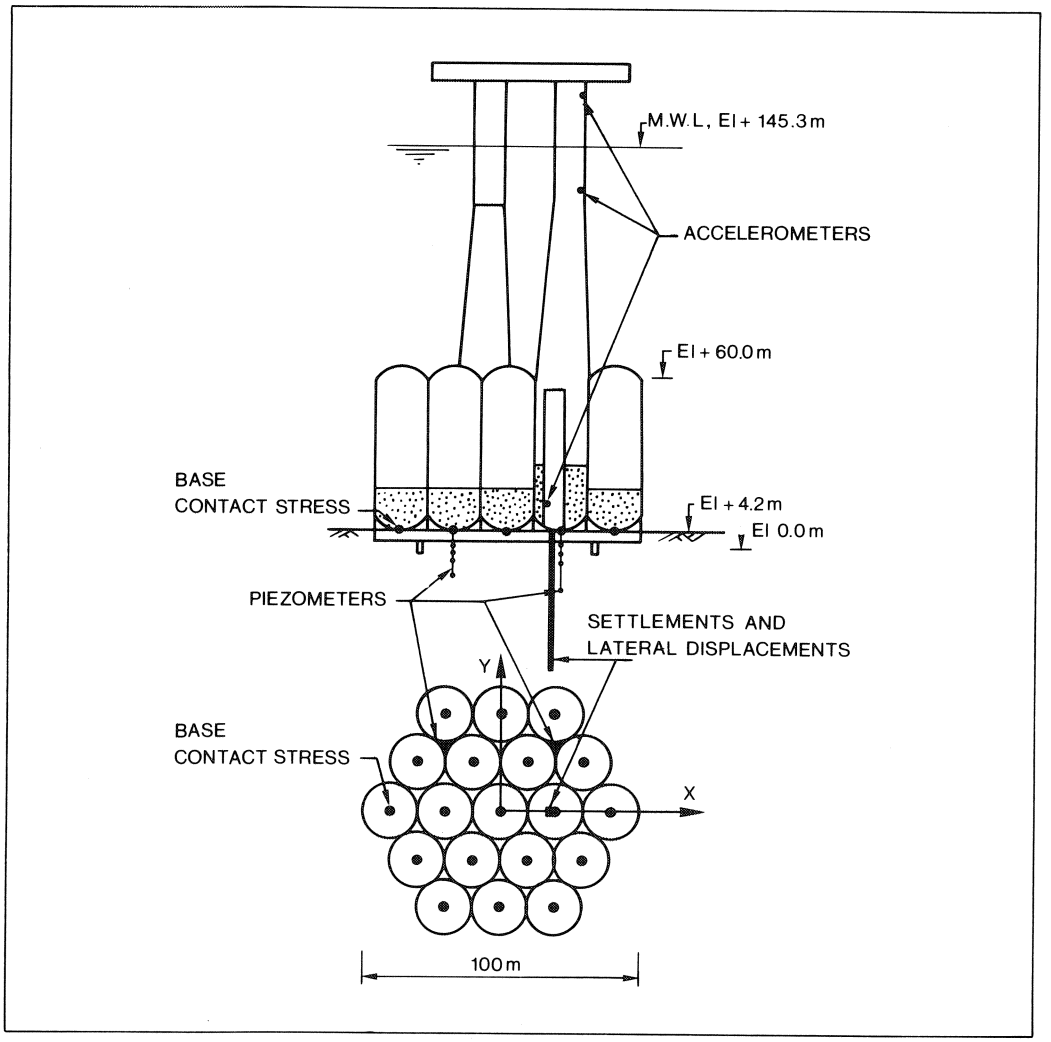

Figure 2.6.6 Geometry of the Brent B-structure and location of sensors monitored during the two-year research projects

the guidelines of the public organisation of the country where they are built. For instance in Norway the guidelines for routine dam structures require three basic types of measurements [4], namely:

- measurements of seepage to evaluate the long-term performance of the completed structure;

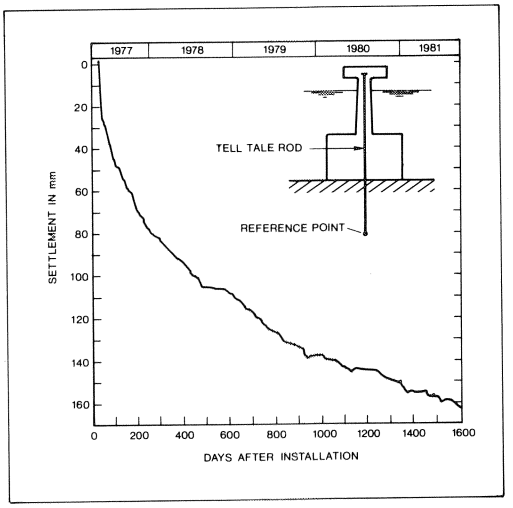

Figure 2.6.7 Time-settlement record for Stadfjord A platform

- measurement of deformations of the dam during construction and on a long-term basis as well by geodetic methods; and
- measurements of pore-water pressure in the core materials to verify that the embankment is being constructed at a safe rate.

The first two types of measurements are almost universally provided for, in that they are required for all high dams. Whether pore pressures will be monitored or not depends on the details of the particular dam.
Special situations do of course arise requiring the use of non-routine instrumentation.

Warning system.
Aside from monitoring leakage and downstream water levels the primary instrumentation in the public warning system is a dam failure detector. This consists of a minimum of three separate cables arranged as signal carrying loops which are securely attached at regular intervals to the crest of the dam and along its entire length. A dam failure, even a partial one, will cause a physical rupture of the signal wire resulting in an open circuit in the loops. So far, four concrete dams and one rockfill dam have been fitted with these devices in Norway.

Figure 2.6.8 Instrumented central cross-section of Svartevann dam, Norway

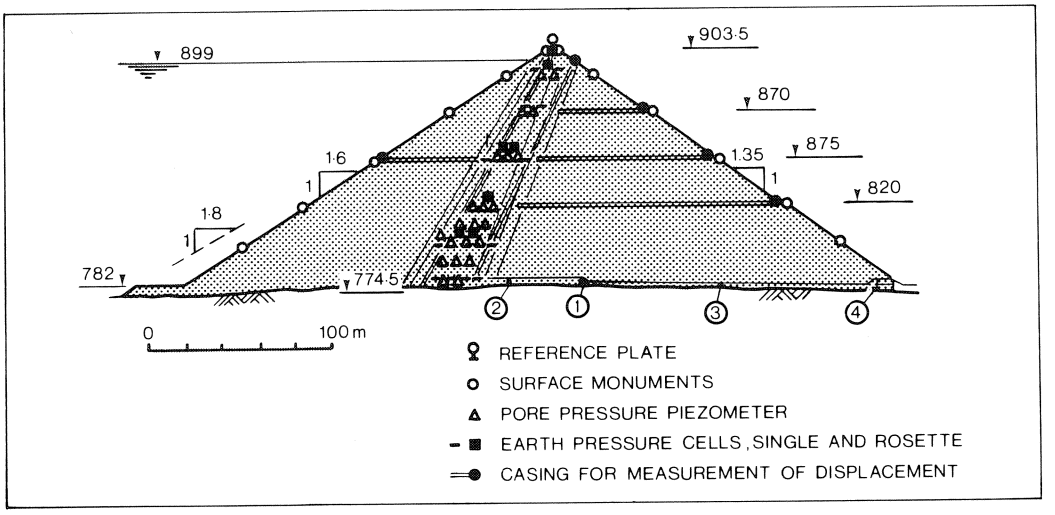

Extensive instrumentation program.
For non-routine dams a more extensive program must be carried out.
Fig. 2.6.8. shows the main instrumented cross section of the 129 m-high Svartevann dam, which was completed in 1976. The example shows the most comprehensive instrumentation programme carried out to date. The installations indicated in the figure are representative of the different types of instrumentation procedures used in Norway. Svartevann is an example of a new generation dam that was extensively instrumented because at the time of its conception in the early 1970s, its maximum height was forty per cent more than the highest existing dam in Norway. In addition it was the first of a number of dams of comparable size that were being planned for construction. The monitoring programme included: 141 surface monitors; 8 casings for measurement of displacements; 28 extensometers; 30 pore pressure piezometers; 60 soil stress instruments; 1 seepage monitoring installation; 3 downstream water level limit switches and 1 set of cables for detecting dam failure. As is to be expected, the types of instruments used to monitor the performance of dams in Norway have changed significantly through the years. The principal selection factors are robustness and proven reliability over long periods of time. The majority of the instruments are based on the principle of the vibrating wire strain gauge and have their origin in instruments developed at the Norwegian Geotechnical Institute.

2.6.3. Environmental inspection and control

Site utilization and management

The delivery of a dam or sluice etc. marks the end of the civil engineering phase. It is only at this point that the changes in the areas affected by the construction work really begin. The nature of these changes was broadly outlined in section 2.5.2.
The changes particularly concern the character of the ecosystem in question (salt-fresh, tidal-stagnant,tidal-reduced tidal) and the uses to which the area as a whole can be put by man. The extent and nature of these changes in the way the area can be used depend on the nature of the environmental intervention.
In many cases the possible uses of an area will be greatly enlarged, e.g. because it is made more accessible (by the construction of roads across dams), because the elements are brought under control (e.g. less or no tidal movement) or by an increase in the available surface area (as flats are laid dry, etc.). These changes should be taken advantage of in good time by means of planning. Changes to the ecosystem (which, as was noted, occur at the same time as the change in the range of human uses) should be managed very carefully: the ecosystem is at its most vulnerable during this period and the parameters within which the system will have to develop far into the future are also laid down at this time.
The dislocation of the environment can often lead to temporary but serious nuisances for human beings during the period in which the ecosystem is adapting to the new circumstances. Examples include mosquito plagues, algae growth and sand drifts. Failure to recognize these processes in good time (by forecasting) and to take timely decisions to control them (management planning) will often result in ad hoc measures being taken that are not concerned with managing the „ecosystem in change" but instead with dealing with the particular nuisance. Similarly it should be ensured that once the ecosystem has begun to evolve towards a new equilibrium state this process is not repeatedly interrupted by further major interventions. Interventions of this kind, such as the creation of nature reserves or recreation facilities, should in other words take place at the earliest possible stage. Otherwise, such ad hoc measures and interventions can lead to irreversible damage to the ecosystem. On the basis of the above it may therefore be said that a start should be made on preparing the policies for managing the affected areas at least several years before the work has been completed. This policy preparation should result in a plan for the utilization and management of the area. In principle an administrative plan of this kind may be drawn up along the following lines:

. First of all a forecast must be drawn up of the likely developments in the new situation.

. The ways in which the new areas are desired to be used (i.e. the policy proposals) must then be decided upon.

A comparison of the forecasts and the policy proposals will lead to the decision in what ways the various functions in the area can best come into their own; which functions are mutually incompatible, and which control measures might be required in order to permit various functions to co-exist. The responsible administrators can then make a choice between the various ways in which the new areas could be put to use. If such plans are drawn up in good time - i.e. during the design phase - it may in certain instances even be possible for certain wishes with respect to the control mechanisms (e.g. the size and/or location of a sluice) or siting (of an engineering work and/or ancillary sites) to be incorporated into the design. This can have important (e.g. financial) advantages. Apart from the timely drawing up of a policy plan in relation to the utilization and management of the new areas, control plans should also be drawn up specifying how the engineering works (which are in fact control mechanisms for these areas) should be used. It will be evident that these control plans must be drawn up in close collaboration with the policy plan for the area in question, and should in fact form part of it.

Evaluation studies

Because these plans, as well as the assessment of the impact of an environmental action, are based on forecasts of the new developments it is essential for these forecasts to be tested in practice. Then it will be possible to decide whether the site utilization and management plans can in fact be implemented as envisaged. If actual developments should deviate from those predicted often plans have to be adjusted. It means that the plan must be sufficiently simple for this to be done without difficulty. Procedures should therefore be adopted that provide for the regular adjustment of the utilization and management plans. The monitoring of developments is also essential in order to test the forecasts of the anticipated effects of the action. Any inaccuracies in the forecast effects can then be corrected, thereby enabling a superior forecast to be made when assessing the effects of another large civil engineering project.

The implementation of evaluation studies, as well as the compilation of policy plans for site utilization and management, therefore form a essential aspect of the realization of a civil engineering work.

Adaptation works

The realization of a civil engineering project and its consequences for the surrounding areas (e.g. the elimination of tidal movements) will often necessitate the adaptation of existing works such as sluices, harbours and drainage systems (e.g. debouchment sluices and pumping stations). In many cases these works will have to be completed in time for the new situation.

Apart from adjustment to the elimination or reduction of tides, consideration must be given to the reduction and/or increase of seepage to agricultural land situated in the vicinity of the basin in question.

References

1. Lambe T.W., Marr W.A., Silva F. Safety of a constructed facility: geotechnical aspects **Journal of the Geot. Eng. Division, ASCE,** March 1981 p.p. 339 - 352

2. Dibiagio E., Myrroll F., Borg Hansen S. How successful have Performance Monitoring Programs been for Gravity Base Structures, **Boss-Conference 1979,** paper 65

3. Lindenberg J., Swart J.H., Kenter C.J., den Boer K., Wave-induced Pressures underneath a Caisson: a comparison between theory and large scale tests, **Boss Conference 1982**

4. Nilsen K.Y., Dibiagio E., Andresen A., Norwegian Practice in Instrumenting Dams, **Water Power and Dam Construction,** November 1982 p.p. 34 - 38

5. Coppes, J.G.A., J.W. Verkuylen, J. Visci & M.J.J. de Waal Malefijt, A Policy Analysis for a Land-use Project, **Land + Water Int.,** 1980, 43 p.p. 11 - 20. Nedeco, The Hague, NI.

6. Saeijs, H.L.F., E.A. de Jong, The Oosterschelde and the protection of the environment; **Land + Water Int.** 46, 1981, p.p. 25 - 34. Nedeco, The Hague, NI.

3. Design and Operations of Closure Works

3.1. Approach

Design and Operations of Closure Works

J.C. Huis in 't Veld

3. Design and operations of closure works

3.1 Approach

3.1.1 General

From a technical point of view, the closure of dike breaches (in tidal areas) is not essentially different from the construction of dams in existing tidal waters.
In general, dike breaches must be closed as quickly as possible to avoid damage in the inundated regions. As a consequence, such a closure will be more provisional than the dam construction, since the latter can be extensively studied ahead of time by computations and model tests.

Before the decision is taken to close off a tidal basin, it is necessary to carry out a feasibility study of the project, including a forecast of future requirements, and an economic study of the plan which will give an insight into the viability of the project.
There are many different reasons for closing a tidal basin (see table 3.1). Whatever the purpose may be, there will be impacts on other aspects. For instance the closure of a tidal inlet for safety reasons may have (positive or negative) impacts on the ecology, commercial fishing, recreation etc. All these impacts have to be studied during the (feasibility) study phase. A scheme of the stages of analysis is given in fig. 3.1. During the feasibility study a preliminary layout must also be made.

After the decision to close off a tidal basin is made the planning phase follows.
During the planning phase preliminary designs and alternatives will be prepared for the closure dam, discharge sluice(s), lock(s) and various auxiliary facilities. A Design Interim Report will contain full information on the preliminary designs and alternatives, the design criteria and the materials and methods to be used for construction. Additional site investigations will be initiated and hydraulic model tests executed in

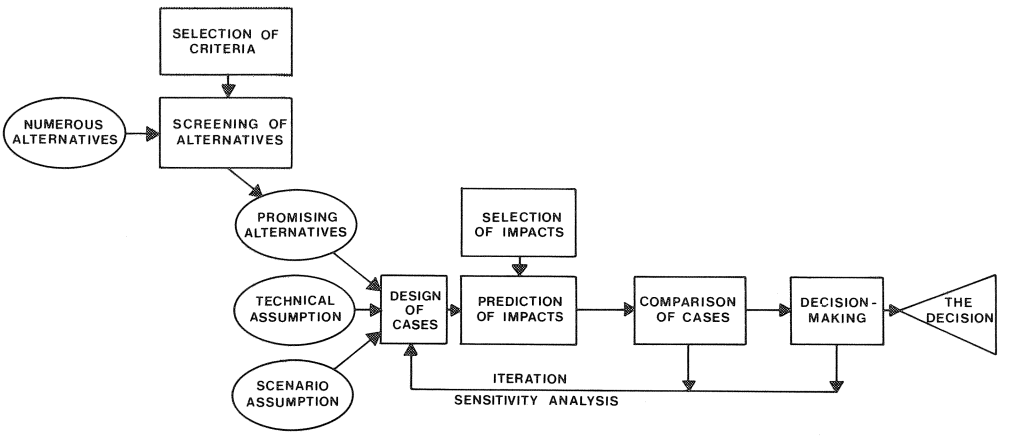

Figure 3.1 Stages of Analysis

order to obtain the required data for the design. The environmental, ecological and social impact of the project will be studied (see table 3.3.) such as:

- choosing a water level and permissible fluctuations in the enclosed basin
- choosing a fresh or salt water regime
- choosing a method for closing off the estuary and, in case of a fresh water body in future, for replacing salt with fresh water.

Table 3.1. Examples of purposes of closing a tidal basin

*	Land reclamation
-	Zuiderzee closing (Neth. 1932)
*	Protection against floods from the sea
-	Primary dams of the Delta Project (Neth. 1961-1986)
-	Eider (Germany 1970)
-	Keta Lagoon (Ghana 1969)
-	Eastern part of Finnish Gulf to protect the city of Leningrad (U.S.S.R. design phase).
-	Thames Barrier (London, England 1982).
*	Creating of fresh water reservoirs.
-	Zuiderzee closure (Neth. 1932)
-	Haringvlietdam (Neth. 1970)
-	Philips- and Oysterdam (Neth. 1987)
-	Plover Cove (Hong Kong)
-	Nakdong (Rep. of Korea 1988)
*	Production of tidal energy.
-	Rance (France 1960)
-	Severn Estuary (Wales/Engl. planning phase).
*	Closed sea harbours (behind locks)
-	Asan Bay (Rep. of Korea planning phase).
*	Creating a construction pit for locks, sluices etc. (closure of the ring embankment) or water supply basins.
-	Haringvliet (Neth. 1957)
-	Philipsdam (Neth. 1978)

These decisions are of great influence on the size of the discharge sluices. Considerations as to the nature of the landscape involved may influence the design of the dam as well. The objective of the design phase is to work out the best and most economical design for the closure dike, discharge sluice, lock and gates and various auxiliary facilities, including preparation of the technical specifications, quantity estimates and tender documents for bidding. The preliminary cost estimates and the required period for construction will be determined by the designers. Plans will be prepared for material testing, for construction supervision services and for procurement of major construction equipment. An operation and management plan will be prepared, including organization, personnel, required budget to assure effective operation, and management of the project after completion. If required, counter-measures will have to be devised against the adverse effects on the environment and ecology in the area.

3.1.2. Design phase

The design phase starts with a review and analysis of existing data.
Depending on the purposes of the project and on the circumstances, data in the following fields are necessary:

- meteorology
- oceanography
- hydrography and hydrology
- geotechnics
- topography
- geology
- construction materials and equipment
- labour
- environment
- land and fishery rights

Additional data will be searched for in the initial stages of the project. All available data will be reviewed and analysed; special attention will be paid to the quality and reliability of the data.
The data will serve as starting points for the layout and design of the structural elements of the project. As soon as possible after project commencement a programme for additional field investigations will be prepared.

During the design phase the broad outlines of the possible alternatives have to be worked out in more detail in order to evaluate the advantages and disadvantages of each alternative from a technical point of view as well as from an economic point of view.

Approach

For each alternative the following has to be prepared:
- a general plan and layout for all structural elements and marine works
- a longitudinal profile and cross sections
- major details
- a rough cost estimate
- an environmental impact statement.

When preparing the closure of a dike breach along tidal waters the decision how to execute the closure can be influenced by the positioning of the dam:
- reconstructing the damaged dike on its original course often involves the closing of gullies
- reconstructing a so called „horse shoe" dike around the gap on the land side, generally involves a wide gap at ground level.

After the evaluation of the site investigations the following main subjects will have to be studied:
- workability during the construction
- the availability of construction materials in quantity and quality
- the availability of labour and equipment
- the use of model investigations and/or numerical calculations
- the location and dimensions of temporary works, like building pits, work harbours, storage areas, cofferdams, etc.
- the cross section of the dam in the final position, which may have impacts on the materials to be used for the closure and for the final dam. The stability of the slopes and the seepage through the dam have to be considered.
- the wet cross-sectional area of the channel and the shape of the closure gap during the various construction stages. The closure gap is narrowed by building out construction pits of the locks and sluices, etc. The effects on this narrowing on the tidal velocities in the gap have to be considered.
- navigation requirements during execution
- the closure method

The influence on the design of available materials, labour equipment, sites, etc. are frequently underestimated by the designer. It often happens that the material required for marine works is either not available locally, or only in limited quantities. For instance: the quarry stone, often required for protection works in Holland, has to be imported from abroad. Therefore alternative constructions have been developed in recent years. In many countries there is only limited experience in the execution of closure works and consequently it may be a problem to find the necessary skilled labour. The employment of expatriate labour demands special attention with regard to housing, travelling and leave periods.
The possibility of training local labour therefore has to be thoroughly investigated. Also the utilisation of local equipment, adapted as necessary has to be investigated and should be compared costwise and equipment to be mobilised from abroad.
The provision of spare parts always asks for attention - especially if projects have to be carried out in remote places.
Site conditions may exert a considerable influence on the construction costs of the works. All these considerations should play a vital role in the selection of the appropriate design.

Investigations
Both the preliminary and final designs of the ultimate cross-section of the closure dam will be based on desk studies. As regards the closure operations, desk studies during the initial planning period will provide data to select the most appropriate method of closure. The type of model investigation required to support the final design depends largely on the chosen method of closure. (See table 3.2.).
When gradual horizontal or vertical closure is decided upon, the model studies will mainly deal with the stability of rubble and boulders used to build up the dam at various closure stages. Such studies can be performed in a discharge flume. A wider flume is required in the case of gradual horizontal closure than in the case of gradual vertical closure. The required width depends on the model scale, which in turn depends on the hydraulic boundary conditions and the size of the rubble. The hydraulic boundary conditions (head difference, discharge) will be obtained from the mathematical tidal model.

A scale model of the closure gap is required in the case of a sudden closure (caissons). This model, which will have a scale of 1:50 to 1:100, will provide detailed information on the current pattern for the various execution phases. The boundary conditions for operating the model will be obtained from the mathematical tidal model. If the thickness of the silt/sand layer, overlying the rockbed, is significant, local scour tests will become necessary to design optimal protection of the area or bed.

A scale model of the closure gap is required for these studies. Obviously it is advantageous to combine these and the above studies in a single model.

Important aspects which can be investigated in a (hydraulic) tidal model are the direction and sequence of construction of the dam-sections.
In connection with the extent of the sand loss as well as possible scouring of the bed, the criterion for the selection is determined by the way in which the flow-pattern develops directly in front of the sand-fill and in the remaining parts of the channel.
If a hydraulic model is not desirable, for instance in the case of small closures, the designer must be provided with sufficient data about local tidal currents. In addition, more insight will be required into the manner in which these currents will adjust to the changing geometry caused by the construction of the dams.

Table 3.2. Model type in relation to type of estuary and to data needed.

model / estuary	mathematical model 1 dim.	2.dim.	comb.	hydraulical scale model
short basin			*	
long basin	*	*		*
tidal river	*			

Model type in relation to data needed:

	mathematical model		hydraulic scale model	
Date needed	1 dim.	2 dim.	horizontal scale different from vert. scale	steady flow hor.scale = vert. scale
vertical tide	*	*	*	
discharges	*	*	*	
current pattern large scale		*	*	
current pattern small scale			*	*
phenomena, strongly influenced by vertical velocity distribution (3 dim. current pattern)				*

Environmental aspects of the design phase
In the following table the „design phase" is taken to include not only the primary dam (A) but also the discharge sluices (B), locks for ships (C) reinforcement of the shoreline (D), secondary dams (E) and obtaining sand (F) or modifications of shipping channels.

Usually an extreme current and an extreme wave height are separately considered.
An obvious disadvantage of the deterministic design approach is the lack of criteria for the choice of the „extreme loading".
Such a choice remains in fact a subjective one.
In recent years the conviction has grown marine

Table 3.3. Environmental aspects

Environmental aspects	design aspects	A	B	C	D	E	F
1.	Areas which will become dry						
1.1.	Purpose and function	-	-	-	x	o	x
1.2.	Vegetation	-	-	-	x	-	-
1.3.	Morphology (water level)	o	x	-	x	-	o
1.4.	Natural landscape	x	-	-	x	o	-
1.5.	Birds	-	-	-	-	-	-
2.	Water quality						
2.1.	Choice of fresh/salt water	-	x	o	-	o	-
2.2.	Stratification	-	o	-	-	x	x
2.3.	Toxic substances	-	-	-	-	-	-
2.4.	Replacing salt water by fresh water	-	x	-	-	o	-
2.5.	Sedimentation	-	x	-	-	o	x
3.	Fisheries						
3.1.	Present and future situation	-	-	-	-	-	-
3.2.	Raised levels of production, fish farming	-	-	-	-	x	-
4.	Surrounding area						
4.1.	Discharge to the sea	-	x	-	-	-	-
4.2.	River banks	-	-	-	x	-	-
5.	Water supply and control (water level)	-	x	o	-	o	-

x = closely interrelated during design phase
o = moderately interrelated during design phase
- = not interrelated during design phase

Design philosopy

On many places a deterministic approach has been utilized for the design of marine works. The design criterion is based on the prevention of instabilities under extreme load conditions.

works need not be designed to fully withstand the most extreme possible currents and waves.

In economic terms some damage can be accepted, especially in those cases where repair is not too costly. New studies must give better in-

sight into the incidence of extreme currents and waves in the probabilities of a coincidence of load combinations.

Apart from these studies the practical approach should not be forgotten, such as the construction of test sections in models and in situ.
The proposed design approach is a probabilistic one. To apply this approach information should be available not only about the frequency with which specific loads occur, but also about the response of the construction.
The response function is obtained either from hydraulic model tests or by applying known „transfer" relationships. If more than one type of loading is present, the summation of the damage should be computed by integration over the various load combinations.
The resulting total damage is a measure for the expected maintenance of the marine works for a given dimension.
A process of economic optimization, based on the costs of construction and maintenance, can further be carried out, leading to the selection of the optimum dimensions.
Besides this minimum integral costs criterion, one should also consider the „expected total damage" and the risk of progressive damage if repairs in good time should be impossible for technical, organizational or financial reasons.

3.2. Layout of a Closure Dam

Design and Operations of Closure Works

J.C. Huis in 't Veld

3.2. Layout of a closure dam

3.2.1. Positioning the dam

The factors contributing to the selection of the location of the dam alignment can be divided into two groups, viz. factors that are generally indicative and factors which determine in detail where the alignment should be.

The first group comprises the factors:
- purpose of the dam to be constructed
- hydraulic conditions during construction and after the dam has been completed
- water management conditions after the dam has been completed
- environmental aspects.

These factors have already been referred to.

The second group comprises factors such as:
a. the configuration of the bed in situ
b. the composition of the bed
c. the connection with the shores
d. the closure method

a. The configuration of the bed in situ

The position of channels and shoals in the area involved, and, in particular their evolution over time, are important. It will be evident that in determining the location of both the dam and the closure gap the existing pattern of channels and shallows should be utilized optimally.

Some of the postulates for the first provisional assessment of the respective positions are:
- that the deepest parts of the channels should be avoided for both economic and technical reasons;
- that the centre lines of the gaps to be closed should cross channels as nearly perpendicularly as possible, i.e. they should be as short as possible and be virtually perpendicular to the stream lines of both incoming and outgoing tides;
- that confluence or division of channels in the vicinity of the closure gap must be avoided as much as possible, since a stable current pattern and bed configuration will enable more accurate predictions to be made of the various construction stages.

If the location of a closure gap near a confluence or division proves to be necessary, then a choice must be made between the construction of one large closure gap and two smaller ones with an artificial work-island in between.
Placing the sections of the dam in the shallows would in general not seriously alter the current pattern, but can affect the distribution of the discharge over the various channels.
The boundaries of these dam sections in shallow parts are chosen in such a manner, as to take natural development into account (fig. 3.2.a).

Generally it can be assumed that the mouth of an estuary is in dynamic equilibrium (particularly where confluences and divisions are concerned).
However, the construction of dam-sections or working-islands will usually disturb this equilibrium. Of course, the consequences of this disturbance for the bed-configuration will depend strongly on its extent and duration.

b. The composition of the bed

Aspects relating to the composition of the bed include, the bearing capacity in connection with the stability of the dam sections to be constructed or the structures within the actual dam, and the availability of building materials (e.g. sand) for the dam.
The choice of location should, if possible, therefore avoid areas with a weak bottom composition. If this proves to be impossible, then soil improvement may be a solution.
This implies, that a trench must be dredged, new material supplied and, if necessary, the soil compacted to increase its bearing capacity.
If the available bed-material should not be suitable as a building material for the dam sections or for final sand-closure, additional costs for the supply of suitable sand will be incurred.

c. The connections with the shores

The connecting points of the dam with the shores may cause problems. These points may either be located „onshore" or „offshore".

Onshore problems often concern the existing infrastructure in the environs of the planned dam-

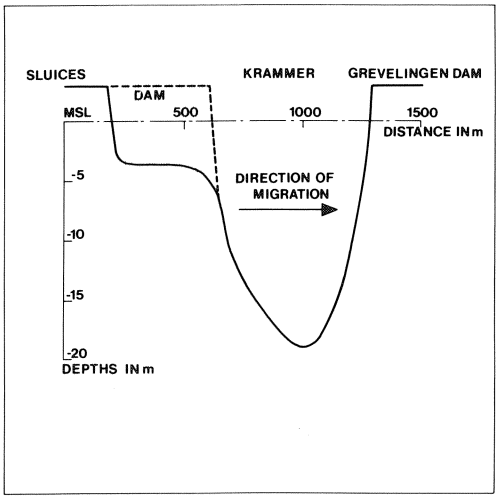

Figure 3.2a Dam section on shallows (dotted line)

Figure 3.2.b Sand dumping from right to left

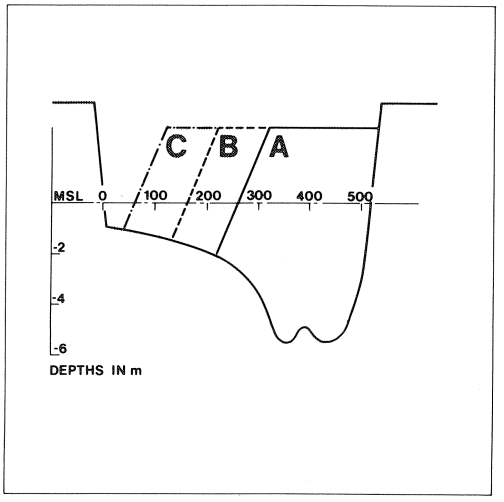

shore connection. Problems may arise concerning the connection between the carriageway over the newly-constructed dam with the existing infrastructure.

Offshore problems could include:
- trying to avoid locations where the channel runs close to the shore;
- trying to avoid places where the slopes of the shores are less stable (sensitive to liquefaction)
- trying to avoid, in general, connections in an outer-bend;
- trying to avoid as much as possible the disturbance of areas which are interesting from an environmental point of view (this also applies to the inner-dike sections).

Due to the prevailing boundaries of the closure-gap and (during construction) the building of the closure dam, the velocity of the current and the intensity of the turbulence will increase. In addition, the current will, due to the directional influence of the vertically-narrowed gap, tend to cross the crest of the closure-dam at right angles. As a result of this phenomenon, the higher current velocities will aggravate damage to the boundaries of the channel in an outside bend.

d. The closure method

The planned method of closure will play an important role in the actual design of the location of the dam and the closure gaps. The most conventional closure-methods are those which „follow" the shape of the gap in situ, e.g.:
- in case of a gradual closure, a wide and shallow closure-gap is to be preferred since the current will then be more diffused during the final closing procedure; a shallow gap therefore restricts the amount of filling material required.
- an attractive feature of the sand-closure method is, that from the sand-loss point of view, the execution of the final closure procedure is carried out at a relatively high ground level (the time to complete the sand-fill will be shorter and the loss of sand less). This means that one boundary of the gap must be at some distance from the channel's deepest parts. (fig. 3.2.b.).

- in case of a caisson-closure (sluice caissons), a relatively narrow and deep gap is to be preferred since the number of placing-manoeuvres will be limited (which are complicated and risky) while at the same time the water depth above bottom and sill remains relatively deep in order to maintain an adequate wet cross-section; the boundaries of the closure gap must be placed in relatively deep water in order to limit dredging near the shores.
- When preparing the closure of a dike breach the decision how to realise the closure can be influenced by the positioning of the dam:
  - reconstructing the damaged dike on its original course often involves the closing of gullies
  - reconstructing a so called „horse-shoe" dike round the gap on the land side, generally involves a wide gap at groundlevel (see fig. 3.8).

3.2.2. The location of structures in the dam

Questions relating to this aspect include (i) how will the structure function after it has been completed; and (ii) how can the structure be built without causing too much disturbance of the tidal action?

In the final stage nautical aspects and preservation of the water quality will influence the choice of the location of a lock or a discharge sluice.
In the construction stage of a lock or a sluice a construction pit will generally be necessary.
By construction of an earth embankment, built with local materials, a construction pit will be formed. This construction pit will have to be kept dry by means of a drainage system. Investigations and study of hydrological and geological data could necessitate a review of the location and call for special construction methods and ways of draining the construction pit.
From a constructional point of view, building on shoals will always be preferable as the costs will be lower and there will be little disturbance of the tidal action. However, for the final stage additional costs will generally be incurred for dredging the approach channels.
Conversely, for the final stage, construction in the channels could be more favourable although this would mean that during the construction additional problems could arise due to erosion (with constriction of the cross-section in the closure gap resulting in an increase of the current-velocities); moreover the construction costs could be extremely high.

Discharge sluices
The main function of a discharge sluice is to pass excess water from the basin into the sea after the completion of an enclosure dam.
Not only will it be necessary to maintain the water level in the basin within certain limits, but irrigation schemes upstream of the sluices will also require the proper regulation of the water levels in the basin.
In view of possible damage from flooded fields, critical maximum levels in the basin will have to be determined.

The discharge capacity of the sluice will have to be determined based on the maximum floods from the rivers debouching into the area, and taking into account permissible water levels in the reservoir, the storage capacity of the reservoir, local rainfall and the tidal water levels. The above will be determined by calculations.
From the required discharge capacity the main dimensions of the sluice can be determined. Depending on the aperture of the discharge sluices a part of the tidal motion can be allowed to pass through them during the final stage of the closing works. In this way it may be possible to reduce that head difference across the dam during the closing operation.

Navigation requirements
The shipping sector can have special requirements. One of these will be for navigation to be hampered as little as possible during the construction of the dam. During the dam construction certain demands can come from shipping which normally use the route across, and/or others from shipping normally using a route running more or less parallel with the dam. If a dam is provided with a lock, this lock will allow the passage of floating equipment during the works.

Modern lock systems are increasingly equipped with centralized operation systems. Such a system is costly and requires highly qualified personnel.
Depending on the operation system, the location and layout of a central control building and satellite control buildings must be determined. In all cases the basic requirement will be an unobstructed view of and over the total lock complex.
Workshops and stores will be required for maintenance of the various mechanical and electrical components. Storage will have to be provided for the spare gates, the larger parts of the beacon system, etc.

For the shore-based part of the navigational aid system, an adequate building may have to be provided.

Figure 3.3. Cross section of mouth of the Eastern Scheldt after construction of dam sections and work islands, creating 3 closure gaps.

To monitor the water level fluctuation, additional hydrometric stations will have to be established within the basin.

3.2.3. The shape of the closure gap

Concerning the shape of the closure gap the following factors are important:
- the location and orientation of the closure-gap;
- the dimensions of the closure gap;
- the shape of the boudaries (heads);
- the absence or presence of a sill and its dimensions.

The impacts of the above-mentioned factors are interrelated and cannot be designed for separately. The resulting flow-pattern in or near a closure gap will be determined by a combination of all these factors. In practice, initial designs will be made in which all factors are included, and subsequent selections of the most appropriate design will be carried out by means of desk studies.
The application of desk studies has become possible on the basis of the widespread experience which has been gained in the last three decades during the execution of closure work. To enable this, data should be available on the

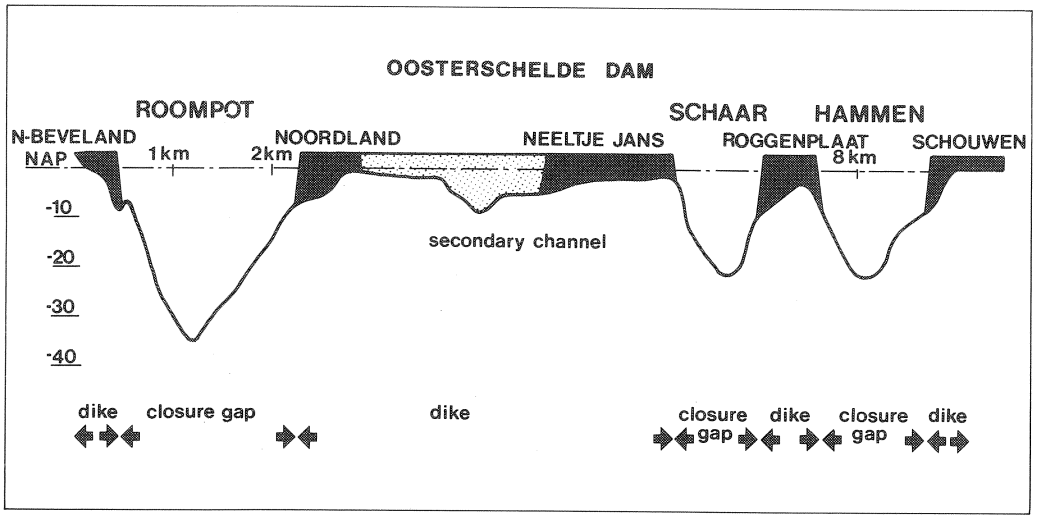

tidal motion before, during (various stages of) and in the ultimate stage of the construction. Such information can be obtained by means of a mathematical tidal model. The necessity for and type of model investigation required to support the final design depend largely on the chosen method of closure.

Location and orientation of the closure gap

The factors determining the location of the dam-position and hence of the closure gaps have already been discussed. In order not to change the tidal action too much during the construction of the dam-sections, a closure gap will be made in each (main) channel. The number of closure-gaps will therefore be equal to the number of channels feeding the estuary. If any sizable, secondary channels exist in the alignment-area and are included in the dam-sections well before the closure-operation, the current velocities in the closure gaps will increase (see fig. 3.3).

If the bottom should consist of loosely packed material, some scouring will occur. In that case, it is recommended that a bottom protection in the closure gaps be constructed as early as possible.
If, however, the scourings form a critical part in the design, the secondary channels will have to be kept open until just before the final closure of the main channel(s), or until the scouring process has been completed.

It was mentioned before that the closure gap should be designed at right angles to the flow-direction (in particular during and around the maximum flow-velocity). A current approaching the closure-gap at an angle will cause turbulence and consequently attack the bottom downstream severely.
In addition these peak-velocities, that are coupled with increased turbulence, will form an additional threat to the dam under construction.
Due to oblique currents, sedimentation problems may occur in those areas where eddies are formed near the edges of the closure-gaps. If an oblique approach be alleviated by the choice of an appropriate shape for the boundaries of a closure gap.

Dimensions of a closure gap

The tidal volume flowing in or out of the estuary will hardly be affected by the construction of the dam-sections during the early stages of construction. A possible (limited) discharge-function of the shoals (for instance at HW), will be taken over by the closure gap, just as is the case with the closure of secondary channels already described above. The average current velocity through the closure gap will, apart from the effect of tidal and estuarine characteristics (tidal volume), be determined by the size of the wet cross-section.
In addition, the (horizontal) velocity-distribution in the closure gap will be important. This factor will be determined by the location and the current approach to the closure gap and the position and shape of the dam-heads.
The actual current-velocities are important for the stability of the dumping operations, excavations and the use of floating equipment. It should be noted that the increase in velocity of the current has an important bearing on scouring and erosion, since it determines the extent to which the absorption capacity of the current exceeds the sediment-supply.

In contrast, as far as the stability of the dumped material and the current-loads on floating equipment are concerned, it is the absolute magnitude of the velocity which is important.

In estuaries adjoining seas with high tides, the tidal discharges will be relatively high even in an indisturbed situation. In this case, the closure gap will have to be designed as wide as possible with regard to workability (floating equipment/caissons). This implies that the amount of the material required for the closure will increase.

Therefore, a dam-section projected too far into the channel (with relatively) low current velocities in the indisturbed situation will result in an increase in velocity in the remaining part of the closure gap.
In addition, the adjoining part of the closure gap will be obliquely approached by the current resulting in separation of the current and generation of vortex streets, a phenomenon

which occurred in the Hammen-closure gap in the mouth of the Eastern Scheldt (fig. 3.4.).
An important aspect is the natural development of the sea-bed to be taken into account in the design of the boundaries of the closure gap. This means that if a channel should migrate towards a dam-section, measures will have to be taken to ensure that this dam-section is not engulfed by the channels during the construction period, as this would require additional defence structures. If a channel does move away from a dam-section, it will have to be constructed on the boundary between channel and shoal. If the pace of the migration of the channel is high, then it may prove necessary to extend the actual dam-section (a relatively cheap operation) shortly before the final closing procedures, in order to obtain an adequate boundary of the closure-gap.

Figure 3.4 Scour in Channel Hammen with and without damsection

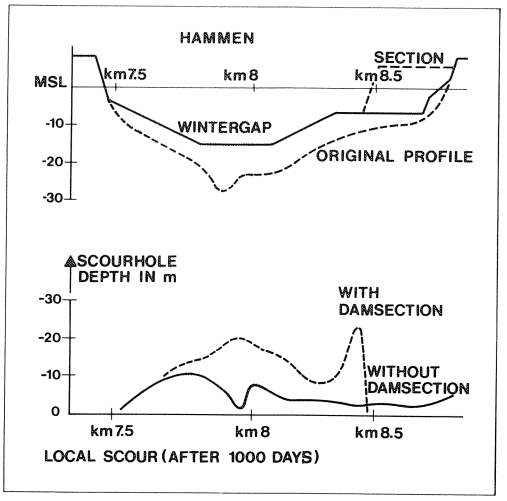

Shape of the boundaries
The current-pattern near and in the closure gap will, to a great extent, be affected by the shape of the boundaries of the closure gap (or the heads of the dam-sections). With relatively long dam-sections, in particular, the current velocities along the toe of these dams will, to a great extent, be determined by the shape and size of the dam-heads. In these cases, it is often necessary to build an extensive construction or constructions to ensure that the current is more or less directed straight towards the closure gap. There are numerous examples of directional constructions, such as the dam-head „Noordland" and the „Neeltje Jans" in the mouth of the Eastern Scheldt (fig. 3.3.).
These constructions are so enormous that they provide ample room for working or refuge-harbours to be built within them.

However, it is not always necessary to build such extensive directional dams. The position of the closure gap can be such, that a simple dam-head construction will suffice. The designer can compensate for its effects (the effective width of the closure gap is diminished) and extend the bottom-protection locally.

A sill in the closure gap
A sill is in fact part of the closure-construction of the gap. From the work-planning aspect it is, however, often necessary to build the sill during a previous season.
A caisson-closure, for instance, requires the crest of the sill to be absolutely level. Since this is a lengthy undertaking, endeavers should be made to build the sill at least one season before the final closure. In case of a gradual closure, an advance sill-construction means that a large part of the material will already have been dumped in the closure gap (largest volume, uniformity in height). The necessity for an early construction is however less evident in this case, depending on the length of the „working season" and the available dumping capacity. It should be noted, however, that completion activities must take place in the same working season. In particular, with a relatively shallow closure gap, the prior construction of the sill can or even should be avoided. In this case, the

presence of the sill would constitute an important constriction of the closure gap, which would require large grained dumping material (in order to survive the winter season) and a longer bottom-protection (because of greater scouring).
A sill in the closure gap is usually favourable for an even lateral distribution of the current. The applied obstruction promotes an even current-distribution and, as such, an efficient use of the wet cross section.
The higher the sill, the higher the equalization effect. On the other hand, scouring will increase the proportion of the height of the sill. Efforts must be made to find an optimal solution which will combine the advantages of both effects.

Finally, some more information about the shape of the sill.
The longitudinal cross-section (transversing the channel) strongly depends on the closure-method to be applied. For a caisson-closure the crest of the sill has, in general, to be horizontal (and flat).
For a gradual closure, the cross-section of the crest may follow the original channel-profile, which may prove advantageous for current-distribution on the downstream side of the closure gap (see fig. 3.5.a).

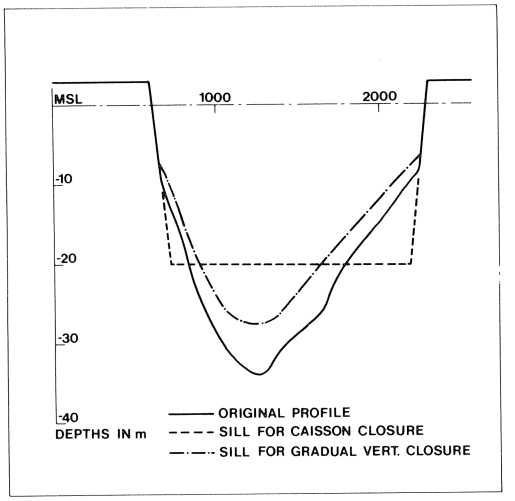

Figure 3.5a Shape of a sill in a closure gap

Figure 3.5b Development of cross sections of closure dams in the Netherlands

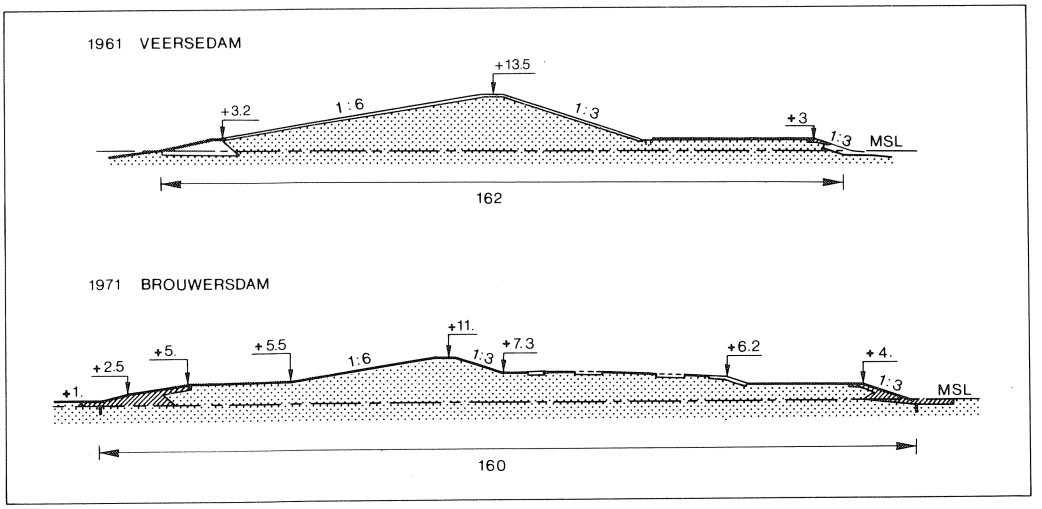

3.2.4. Cross-section of the dam

The cross-section of the final dam depends on several factors:

- the hydraulic parameters (water levels, waves, ice)
- the necessity for a road over the dam and the intensity of the traffic
- requirements about the sealing of the dam (a division of salt and fresh water)
- environmental conditions (landscape, recreation etc.)
- available construction materials, methods and period
- the used materials and method for the closure operation

The cross-section of the final dam would have to be designed to withstand the tidal difference over the dam and wave or ice attack.

For a given storm surge level and wave height, the wave run-up and hence the crest height of a dike are determined by the slope gradient and the width of the wave-breaking berm (if a berm is built - see fig. 3.5.b).
Other conditions being equal, the necessary crest height of a dike with a faint slope on the seaward side, broken by a berm will be less than for a dike with an uninterrupted or steep slope. This follows from the formula:

$$R_{2\%} = C(\varepsilon)\,\tilde{T}\,\sqrt{gH_s}\,\mathrm{tg}\alpha$$

where

$R_{2\%}$ = run-up exceeded by 2% of the waves
$C(\epsilon)$ = a coefficient dependent on the width of the wave spectrum
$\tilde{T}$ = period of spectral component with maximum energy density
H_s = significant wave height (m)
α = slope gradient

A faint slope is favourable for an asphalt revetment and better compaction results can be achieved [1].
The most economical method is to make the inward slope as steep as possible.

The cross-section of the final dam may affect the materials used for the closure.
If the closure embankment is a temporary structure it may be interesting to check the possibility of recycling the used materials. Recycling the materials will be easier when applying rubble, rock or concrete blocks then when caissons are used.
If the sand closure method is applied an interesting alternative is to create a dune and beach profile.
When using „sluice" caissons, which are virtually floating sluices, it is possible to consider them as temporary structures that stay in the core of the final dam, but it is also possible to design them as the definitive sluices, storm surge barriers or turbine cassons for tidal-power energy.

3.3. Construction Methods

Design and Operations of Closure Works

J.C. Huis in 't Veld

3.3. Construction methods

3.3.1 Closure methods

When building a dam to close off a tidal basin, the inflow and outflow through the narrowed gap will be reduced, causing a decrease in the tidal range in the basin, but higher current velocities through the remaining opening. As a consequence, the scouring effect on the bottom near the dam will be increased, which endangers the stability of the riverbottom and thus the foundation of the new seawall to be built on it. This implies that the bottom, when consisting of easily erodable sand, must be protected by current-resistant material. Naturally, these problems will not be encountered where the bottom is rocky.

A special problem arises from the method of closure. In the beginning the velocities will usually be low; therefore, relatively cheap materials may initially be used to narrow the gap - if possible (and if available) sand, and otherwise small-sized rubble (gravel) or clay. The gap is narrowed by building out from the sides and by heightening the sill. If the velocities become higher than 2 to 3 m/s, heavier material must be used. The difficulties in effecting the closure will increase for still higher velocities because navigation in the gap will not be possible during the whole tide, and the scouring effect will become more serious. To close the final gap there are three groups of closure methods: (see fig. 3.6)

1 : the gradual closure
2 : the sand closure
3 : the „sudden" closure

1.a. Gradual horizontal closure

If a closure gap with a low sill is horizontally constricted the current velocities increase in proportion to the gradual decrease of the cross-section area. Very heavy material will therefore be needed to close the last gap since the bed protections will be heavily attacked.
This method of closure is not applied on a large scale for the closing of tidal basins in areas with a large tidal range.

Figure 3.6 Closure methods

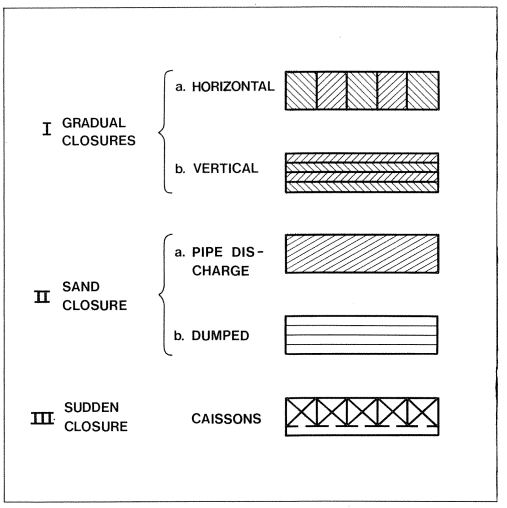

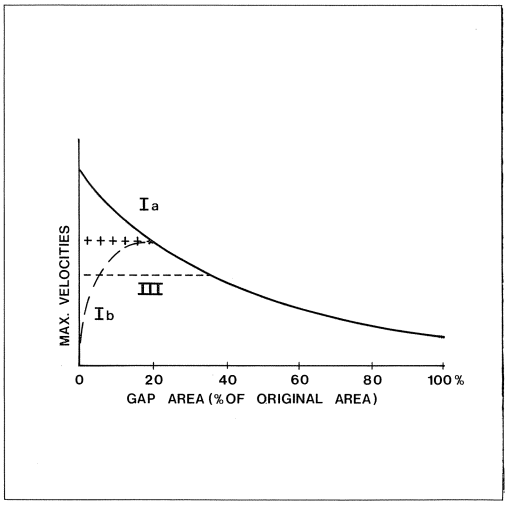

When closing a gap with a high sill, the sill is raised to such a height that a situation of a clear overfall is reached, this is to say, that the current velocity over the sill will be determined by the height of the sill and not be influenced by the head difference over the barrier.
The horizontal constriction of a closure gap with a high sill can be done by dumping glacial clay, bags filled with either sand or clay and rubble, or by placing box-type caissons.

1.b. Gradual vertical closure

A gradual vertical closure is usually applied as follows.
First, after the bottom has been protected, the dam is built out from one of the banks. Generally this becomes a damsection on relatively shallow part. This process can be continued until the velocity of the current in the remaining gap is 2 to 3 m/s, depending on the materials used in these damsections.
The closure gap is then built up in horizontal layers. As a consequence, the velocity increases and the weight of the stones to be used must also increase. There are various methods of dumping stones, such as by floating equipment, a cable way, a bridge or helicopters. During the closure period, the velocities may increase greatly.
By heightening the dam, the total quantity of water flowing over the crest is decreased and the velocities on the river bottom may become lower and the scouring effect weakened.
Usually the largest velocities are found immediately below the water surface. Velocities will reach a maximum when the flow over the crest of the embankment becomes critical during maximum flow. Further heightening the embankment will result in a decrease of the maximum velocity until the dam has attained its full height.

2. Sand closure

A requirement for a gradual or sudden closure is that the material to be used should have sufficient weight to resist erosion, whereas for a sand closure the material (sand) has to be supplied in such large quantities that the main portion is not carried away by the current. If current velocities in the closing gap reach high values (in the order of 3 m/s or more) large-scale efforts are necessary. Due to the high velocities, expensive bottom protection works are required. If the current velocities are of moderate magnitude (2,5 m/s or less) local sand may be used. A part of this material will be lost during the closure operation.
However, the costs of the expensive bottom protection are saved.
Therefore, the losses of sand may well be acceptable in the overall economics of the works.
Recently, a number of tidal channels, both in the Netherlands and in Germany, were closed successfully by pumping sand into the gap.
This was mainly possible because of the high capacity of modern suction dredgers.

3. Sudden closures

This method deals with structures which allow the whole gap to be closed rapidly. Normally, these structures are caissons which are placed in the gap during a slack-water period and thus close the whole gap at once.
Another solution is the use of sluice caissons which are positioned during several successive slack-water periods and kept open during the period in which all the sluice caissons are positioned.

After the placement of the final caisson, all the caissons are closed at the same slack-water period by means of gates. Sluice caissons should be used when the gap to be closed is a large one and the tidal motion is considerable. Closed caissons are useful in small gaps, say no larger than one to three caissons, or in areas where there is only a very small tidal motion. A characteristic feature of a sudden closure by means of sluice caissons is to maintain the widest possible effective wet area in the closure gap until all the caissons are sunk in position on the sill.

By using open caissons, a great increase of the velocity in the gap is avoided, so that, provided the flow pattern is not excessively influenced by the walls of the caissons, strong scouring does not occur.

3.3.2 Bottom protection works

The scouring which takes place in the vicinity of a closure dam is the time-integrated resultant of the progressively increasing current velocity.

If the seabed is composed of loose sediments, a certain part of it under and on both sides of the dam will have to be protected in order to ensure its stability. This aspect can be disregarded in the case of a rocky bed or when the silt/sand cover on the rock base is in the order of only a few metres. Initial designs and subsequent selection of the most appropriate type of bottom protection will have to be carried out.

The main distinction between permeable and impermeable bottom protection is not always clear.

The distinction depends not only on the construction itself, but also on the characteristics of the load variaton and the properties of the subsoil.
This means that the same construction may be permeable for slow-changing water pressures but act as impermeable for rapidly-changing water pressures.
Subject to this proviso, the following tabulation may give a general indication of the various options open to the designer (see table 3.4).

Table 3.4. Various bottom protection methods

using permeable materials	prefabricated construction	with loose ballast	Fascine mattresses with quarry stone
			combined fascine/polypropylene mattresses with quarry stone
		with fixed ballast	mattresses with concrete blocks
			mattresses with gravel tubes
			mattresses with stone asphalt
	construction in situ	cohesive materials	sand asphalt
			stone asphalt
		non-cohesive materials	filter layer systems
using impermeable materials	construction in situ	natural stone	loam
			clay loam
		with asphalt	asphalt concrete
			mastic asphalt
			mastic grouted quarry stone
		with concrete	concrete slabs
			injected concrete (stabilisation)
		impermeable cloth	plastic sheet with protection layer and ballast
			bituminous membrane

The technical realisation of bank and bed protection works will be determined by a number of factors. The most important of these can be formulated as follows:
- availability of construction materials;
- availability of labour and equipment;
- external boundary conditions at the site;
- interrelationship between labour, equipment and material cost.

The present possibilities of laboratory investigations are such that new concepts of bottom protection can be designed and tested in a relatively short period.

3.3.3 Temporary works

The temporary works envisaged for an enclosure project consists of for instance:
- access roads
- labour camps
- construction harbour(s) with storage areas
- construction jetty
- building pit for a lock, a discharge sluice or caissons, etc.

An adequately designed road must be provided to facilitate the transport of men, equipment and materials to the construction site: a careful assessment must be made of the maximum size of equipment and maximum loads to be transported to arrive at an economical design of the access road.

The size of the labor camps is determined by the number of men to be housed. Special attention must be paid to the lay-out, so that accessability, drainage fire-protection, sanitation, power and water supply are realized at minimum cost. The catering service and recreational facilities must be located in the camps.

A construction harbour is envisaged to serve as a base for the storage and delivery of construction equipment and materials. This equipment may be required for the construction of a lock, discharge sluice or enclosure dam. In many cases construction harbours have to be built on artificial islands at the end of dam sections in the shallows. Construction sites where elements of the dam are prefabricated (e.g. bottom protection mattresses) must be situated in the proximity of a construction harbour.

A construction jetty may be required in addition to the construction harbour. The location of both the construction harbour and the jetty must be subject of an intensive study taking into consideration the requirements of the enclosure dam, the construction of a lock and a discharge sluice.

The construction pit for the lock is a major construction job. In conjunction with the possible alternative locations of the lock a careful economic evaluation must be made to arrive at the most economical solution. Special care must be taken to ensure proper drainage under all circumstances. The influence of the construction pit on the remaining enclosure gap must also be studied. The same applies to the construction pit of a discharge sluice or caissons (i.e. sudden closure).

3.4. Gradual Closures

J.C. Huis in 't Veld

3.4 Gradual closures

3.4.1 Hydraulic conditions

The gradual closures can be subdivided into three methods, such as:

- horizontal constrictions with a low sill
- horizontal constrictions with a high sill
- vertical constrictions

Figure 3.7 Influence of closure method on hydraulic conditions

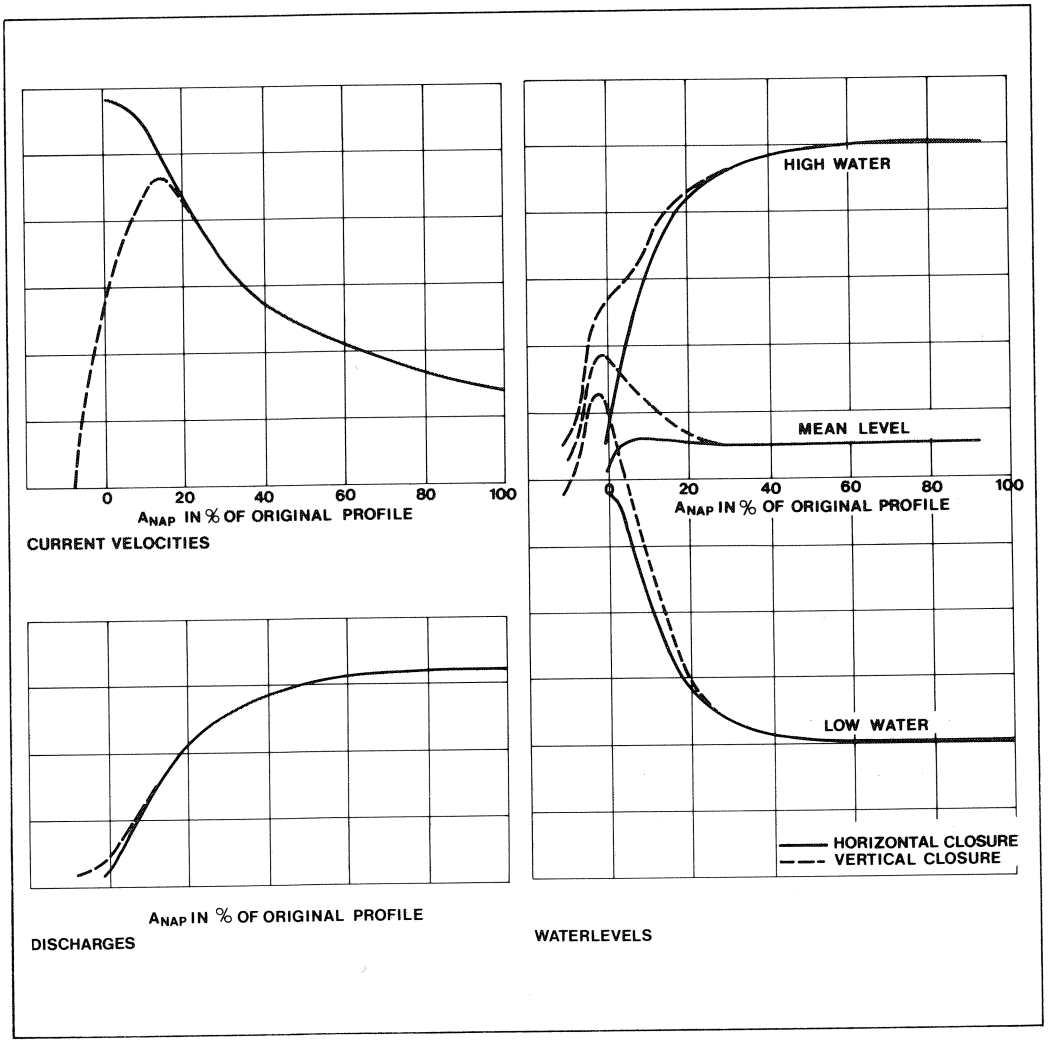

The most significant difference between these methods is the current velocity in the closure gap when the size of the wet cross-section decreases during the closure (see fig. 3.7).
This figure shows that, particularly during a gradual horizontal closure with a low sill, the current velocity can increase considerably. This method can therefore only be applied provided the head over the closure gap is not too great.
With gradual horizontal constriction on a high sill, the current velocity follows from the formula for sub-critical flow: $V = m \sqrt{2g(H-h)}$
where:

V	=	average current velocity in the closure gap	(m/s)
m	=	discharge coefficient	(-)
g	=	acceleration of gravity	(m/s²)
H	=	water level upstream	(m)
h	=	water level downstream	(m)

With a gradual horizontal constriction on a high sill, the sill is raised to a height at which a clear overfall is reached. This means that the current velocity over the sill will be determined by the height of the sill, and not be influenced by the head difference over the barrier.
This follows from the formula for super-critical flow:

$$V = m \sqrt{\frac{2}{3} gH},$$

where H = height of the waterlevel upstream above the crest of the sill (m)

Characteristic for a gradual vertical closure is the building up of the embankment over its whole length. It is possible to build up in horizontal layers, but also to follow the shape of the cross-section of the channel to be closed.
During the closure period, the velocities may greatly increase. As a consequence the weight of the materials to be used must also increase.
The increase in the maximum velocity will stop when the flow over the crest of the embankment becomes critical during maximum flow. The situation of a clear overfall has been reached. Further heightening the embankment will result in a decrease of the maximum velocity until the dam has attained its full height.
An advantage of this method of closure is the diminution of the velocities at the riverbottom during the heightening of the embankment; depending on the height of the sill and the water depth, the largest velocities are usually found in the upper layers of the vertical velocity distribution.

3.4.2 Construction methods

The materials and equipment that can be used in gradual closures depend strongly on the scale and local circumstances.
As far as possible local methods and materials should be used for closing tidal basins.

The following methods can be applied:
- horizontal constriction (narrowing the gap from the sides):
  - dumping gravel, clay, rubble or bags filled with either sand or clay, over the head of dam-sections by manual labour, trucks or cranes
  - placing tight box-type caissons
- vertical constriction:
  - dumping rocky materials (gravel, stones, concrete blocks or rock units), clay or sandbags by
  - manual labour or trucks over a causeway
  - floating equipment, such as stone dumping vessels or floating cranes
  - cableway
  - helicopters

Horizontal constriction by means of manual labour
This method was used to repair the dike on the isle of Tholen (Neth.) in February and March 1953 after the flood disaster, when bags filled with sand and clay were used as filling material. About 3,400 people were required to carry the sand bags manually. A high capacity was obtained by circuit walking. Within a fortnight 1,75 million sand-bags were transported and in total 2,35 million bags were used in this operation. As the normal methods of supplying these bags would have required too much time, they were dropped by aeroplanes at various places.

Another example is the method developed in Bangladesh (Bay of Bengal) to close small channels.

The local method involves the horizontal constriction of dams from both banks. The dams are composed of compartments of widely-spaced timber piles filled with large rolls of straw, palm leaves and clay.
The rolls generally do not disintegrate in the current and the clay is retained. This method is suitable provided that the ultimate closure-gap is sufficiently small to be closed during one low water period, while still being sufficiently large to avoid very high water velocities, which would cause scouring of the channel bottom and the dam heads.

Horizontal constriction using closed caissons
This method was used for the secondary dams (S.W. Netherlands) in the Zandkreek (1960) and the southern channel of the Grevelingen Dam (1962). A gradual horizontal constriction was achieved on a sill with a depth of M.S.L. - 5 m, by placing compact caisson units (concrete, box-like elements approx. 11 m long, approx. 7.5 m wide and approx. 6 m high). As no tidal basins were closed here, the differences in water level over the retaining dam were limited to a few decimeters only. Consequently, the maximum current velocities did not increase by more than approx. 2m/s in the final closure gap.

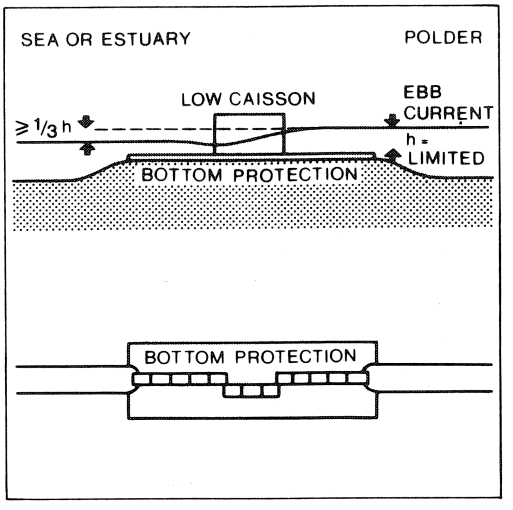

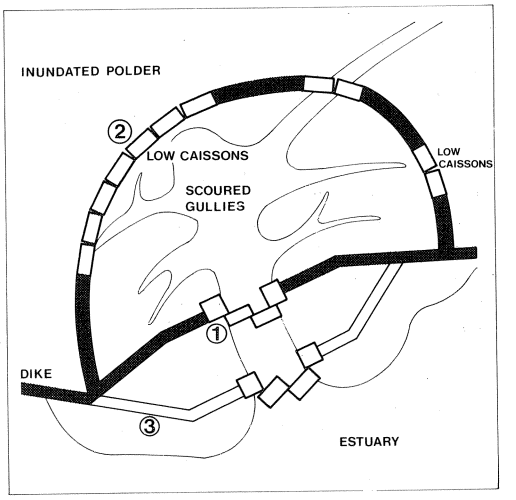

1. By reconstructing the damaged dike along its original course, which involves the closing of gullies.
2. By constructing a „horseshoe" dike round the gap on the land side, which involves a wide gap at ground level.
3. By constructing a „horseshoe" dike along the shallows outside the original dike, which involves the closure of gullies.

Figure 3.8a Closing of dike breaches

Figure 3.8b Closure gap with a high sill at ground level, situation of critical flow.

In 1953 caisson units were built for the first time as a means of closing the dike breaches caused by the flood disaster earlier that year.
At that time it was impossible to determine at short notice the dimensions and the necessary number of caissons.

When a dike breach occurs, the closure can be done either at the flow gap or behind the flow

gap at ground level (see fig. 3.8.). The reconstruction of the damaged dike along its original course involves the closure of gullies.
The construction of a „horseshoe" dike round the gap on the land side involves a wide gap at ground level.
A striking example of the application of „standard" or „unit" caisson on a high „sill" was the closure at ground level at Schelphoek in August 1953.
At Schelphoek, the breach in the coastal dike formed a flow gap 525 m long, with maximum depth of 37 m. This gap was closed by a „horseshoe" shaped (inter-section) dike 4 kilometers long for which, in total, 235 standard caissons were used.
To prevent seepage under the generally narrow bottom protection (40 to 50 m) the closure of ground level gaps had to take place at high speed. When closing the gap at Schelphoek, 462 meters of caissons (42 units, 11 m long) were placed within 24 hours. While closing the gap at ground level, it appeared that the soil in situ, sandy clay, needed a bed protection of fascines, which in turn caused the current velocity at ground level to increase up to 1,5 to 2 m/s. The intention was to select a sill with such a height that, at peak low-water level, current velocities of 3 m/s would not be exceeded. However, because of the altitude of the ground level and the thickness of the fascines, these demands could not always be met; the velocities exceeded the 3 m/s standard.
The bed protection was not, however, severly damaged.

Vertical constrictions
A gradual vertical closure is generally divided into the following main construction stages:

1. a stable, scour-resistant seabed is required at the gap and protection of the sea bottom is the first stage, if the bed consists of loosely-packed sediment.
2. in most cases building up a sill with the function of pressure distribution in the suboil (if necessary) or to act as a filter between the bottom protection and the materials of the closure embankment.
3. closure materials are dumped into the sea, thus gradually forming an embankment along the length of the gap. The embankment is heightened evenly along its length of the gap, until it emerges above the H.W. level.
4. when the closure embankment has been built up sufficiently to stop the tide, the permanent dam is built around it.

Equipment for a gradual vertical closure
1. Manual labor or trucks over a causeway.
   advantages:
   - building up in horizontal layers depending on the construction of the causeway
   - relatively cheap

   disadvantage:
   - only applicable in relatively shallow channels

2. Stone dumping vessels or floating cranes
   advantages:
   - building up the embankment in horizontal layers;
   - less materials needed in the final critical closing stage
   - relatively cheap

   disadvantage:
   - low capacity (decreasing until zero when using vessels) in the last stage (from about 3 m below L.W.), because the vessels can only cross the embankment at H.W. and when the current velocities are sufficiently low.
3. Cableway, helicopter, trucks over a bridge
   advantage:
   - high capacity during all stages

   disadvantages:
   - expensive
   - many stones or concrete blocks to be dropped in the final stage
   - more scouring
4. First: stone-dumping vessels
   Later: cranes, trucks, cableway or helicopters
   advantage:
   - high capacity during all stages

   disadvantage:
   - two types of closure equipment

Floating equipment
On a smaller scale a vertical constriction of the

closure gap can be achieved by dumping clay, sandbags or small-grained rubble. As early as 1870, the Sloe (the Netherlands) was closed off by the classical method of sinking matresses on top of each other. A disadvantage of this method, however, is that at the final closure the slack-water period is too short for the sinking manoeuvres. The building up of the closure embankment only with glacial clay has the disadvantage that the clay with a height from five up to eight meters or more will show a tendency to slump. To transport and dump huge quantities of rubble and concrete blocks, stone-dumping vessels and floating cranes may be used. An advantage of using this equipment is that the retaining dam can be built up in horizontal layers, thus avoiding the need for large quantities of rubble to be dumped in the closure gap at the final critical closing stage (see fig. 3.9). The side slopes of a retaining dam, consisting of rubble, have a gradient of broadly 1:1.5. This implies that with a low-lying sill, approximately 80% of the materials will already have been dumped before a situation of critical flow is generated.

On the other hand, the capacity of the floating equipment will be hampered and reduced in the final stages of closure. Due to their draught and the highly increased current velocities, stone-dumping vessels are able to float over the retaining dam at high tide only.

Floating cranes have a relatively low dumping capacity and are unable to anchor behind the closure gap due to the high current velocities without special mooring pontoons or anchor poles. The use of floating equipment, such as split barges, elevator barges or stone-dumping vessels, to close a channel vertical is quite an easy and cheap solution until the crest of the embankment reaches about 2 to 3 m below L.W. The use of floating equipment has to be adapted during the final stage of a gradual closure for the increasing current velocities (see fig. 3.10).

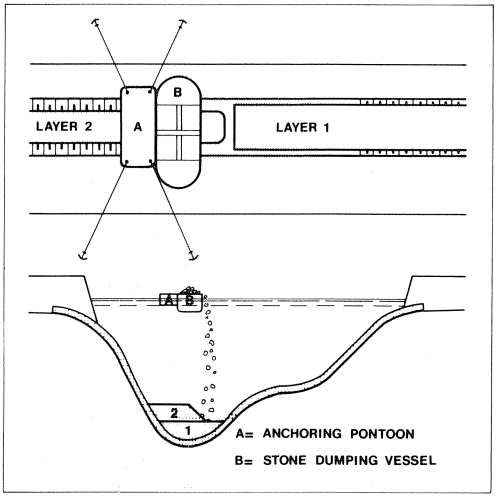

Figure 3.9 Floating equipment

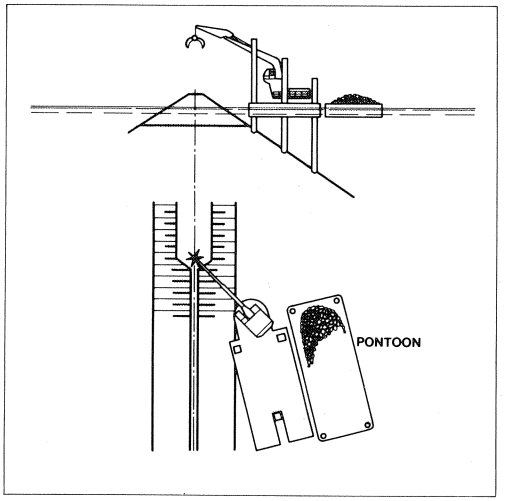

Figure 3.10 Floating cranes during final closure stage

Example:
Stone dumping vessel data:

carrying capacity	700 to 800 ton
load draught	2,5 m
length	55 m
beam	11 m
flow resistance = $\frac{1}{2} C_w \varrho_w v^2 A \approx$	80-110 v^2 (kN)*
skin friction = $\frac{1}{2} C_f \varrho_w v^2 S \approx$	3- 4 v^2 (kN)
Energy gradient force $\approx \varrho \sin \alpha \approx$	1- 10 v^2 (kN)
	85-115 v^2 (kN)*

* = data for transverse flow
v = current velocity (m/s)

Depending on the anchoring system, stone dumping from the vessel is possible up to current velocities of:
* 1,5 to 1,8 m/s under transverse current attack
* 2,5 to 3 m/s under head current attack

If the distance from the dumping site to the depot is about 1 km, the average cycle period of a stone-dumping vessel of 700 tonnes carrying capacity will be approximately 4,5 hours.
The capacity of a single vessel will be about 2700 tonnes/day provided that dumping is possible during the whole tidal cycle.
If, however, the draught of the vessel and the current velocities make dumping possible only during slack H.W., the capacity of a vessel decreases to 1400 tonnes/day (with a semi diurnal tide).
If the tidal range is 3,5 m, the maximum height of the crest that can be constructed by using stone dumping vessels will be approximately 1,5 m to 2 m below M.S.L., when critical state for maximum ebb and flood will have been reached (i.e. clear overfall).

The final closure will then take place by narrowing the gap from the sides, e.g. by placing caissons on the sill or by using stones. In that case the maximum velocities will remain constant for similar tides. If stones are used to narrow the gap horizontally, floating cranes or backhoe dredgers can be used.
This combined vertical and horizontal closure is, in fact, a horizontal closure on a high sill (see fig. 3.11).

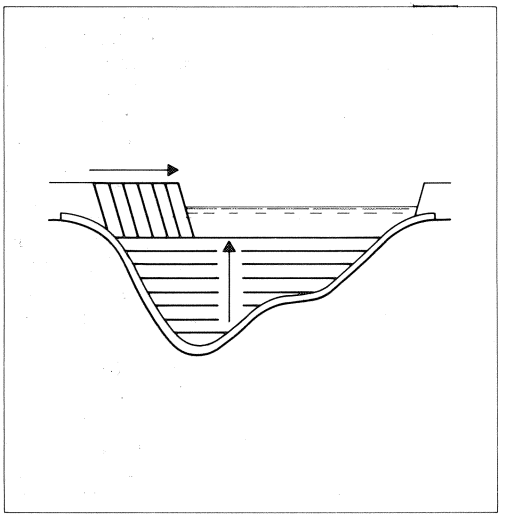

Figure 3.11 Combined vertical and horizontal closure

Another possibility is to close the final stage vertically with stones by using hydraulic cranes on the crest of the closure embankment during low water.

Cableway
In view of the disadvantages of floating equipment, cableways were used for closing the Grevelingendam (1963), the Haringvlietdam (1970) and the southern channel of the Brouwersdam (1971) in the Netherlands.
During the gradual closures in the Haringvliet and the Grevelingen the tidal differences were rather small: respectively 60 and 90 cm.

In relation to the tidal differences in these waters the drop in head over the embankments was comparatively small; in the Grevelingen this was due to the fact that the area at the rear was

not closed off, whereas in the Haringvliet the tidal range could be limited by opening the large discharge sluices.
In the Brouwershavense Gat the tidal range and consequently the current velocities were considerably higher since the closure took place in an area sealed off at the rear; there was a close relation between the tidal difference and the tidal range. Many model tests were carried out to determine the best dumping material. Because rubble is hardly available in the Netherlands, most of these tests were carried out using concrete blocks; the cube appears to be the most appropriate shape for these blocks.

As may be seen from Table 3.5, it was possible for dumping capacity to be increased in three gaps by means of cableways.

Table 3.5. Closures in South-west Netherlands by means of cableways

	material	dumping capacity
Northern channel Grevelingendam 1963	rubble 60 - 300 kg in loading nets	120 tonnes/h.
Rak of Scheelhoek Haringvlietdam 1970	4 concrete blocks of 2,5 ton per telpher (own weight 20 tonnes)	300 tonnes/h.
Southern channel Brouwersdam 1971	6 concrete blocks of 2,5 ton per telpher (own weight 17 tonnes)	1.000 tonnes/h.

A cableway consists of a fixed rail structure on each side of the gap to be closed (see fig. 3.12a). Two cables are then stretched between these structures (in the Haringvliet closure the cables were approx. 92 mm thick and 6 m apart). At the Haringvlietdam and Brouwersdam cableways, the distance between the two rail structures was divided into four by three intermediate supports, with resultant spans (at Haringvliet) of 80, 560, 580 and 110 m.

The cables were independent of each other, and were anchored at one end and tensioned at the other end by a tensioning weight or counterweight.
Anchorage was achieved by means of a heavy concrete block, pre-tensioning cables and a cast-steel anchorage seating.
The average working tension of 300 tonnes in a cable was maintained by a 300 tonnes weight that was able to move vertically in a shaft on one of the shores. The cables slid over supports fitted with bronze linings through the fixed rail structures and towers.

Depending on the size of the load and the position of the load in the span, the cable would sag to a certain extent and so had to be able to move to and from over the points of support. As a result of the variable cable lengths required in the spans for conveying one or more loads, the counterweight would move up or downwards in the shaft.
The construction of a cableway generally enables only one telpher to travel along a span at a time. To get a high dumping capacity, loading points are required on each shore.
These loading points are installed in the fixed rail structures, where the telphers pass along the flange of a rail section.
The telphers could travel a circuit, i.e. making the outward trip along one cable, describing a half-circle turn at the other end and returning on the other cable (see fig. 3.12b).
The vehicles used for transporting the concrete

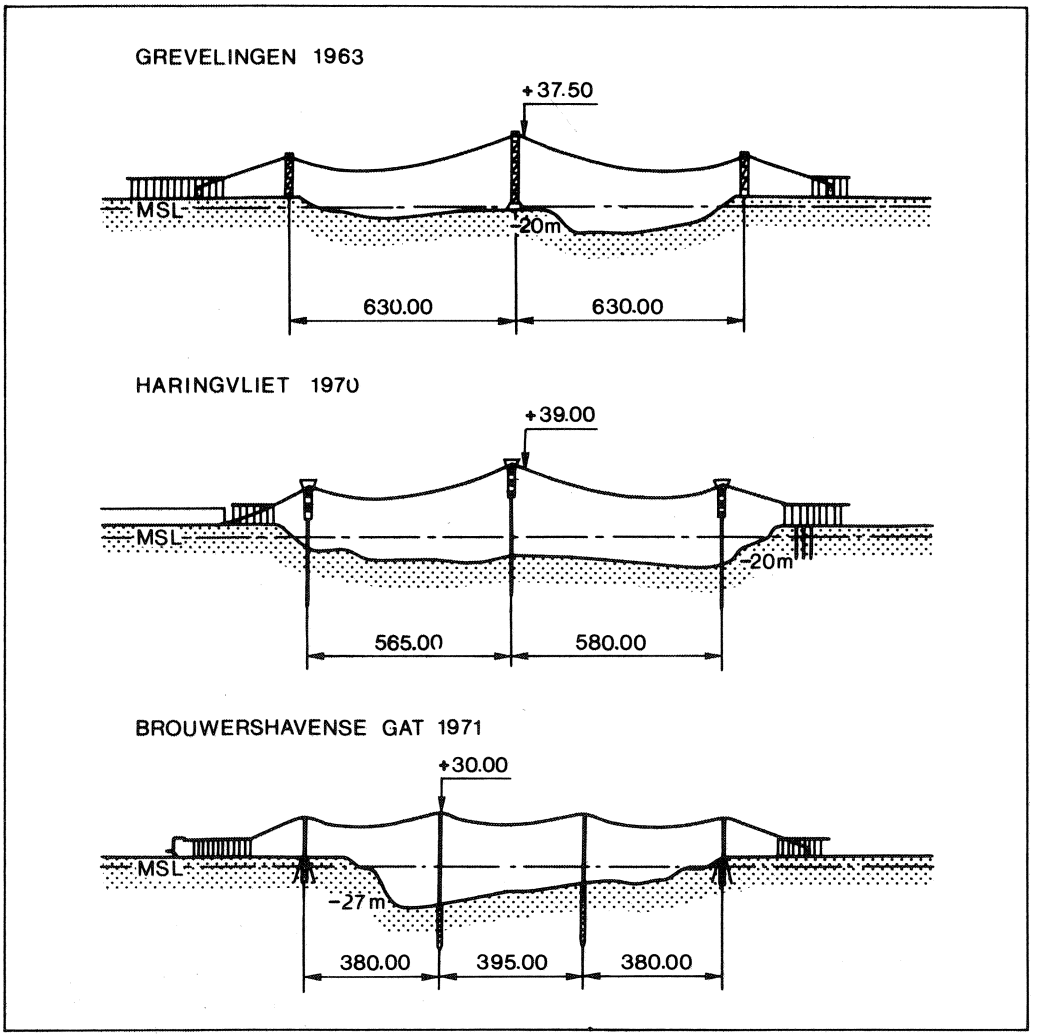

Figure 3.12a Examples of cable way closures

blocks, measuring 1,04 m3 and weighing 2,5 tonnes each, from the depot to the loading points are standard trucks, but whose body must be replaced by a special frame for receiving the blocks.

If a single-crested closure embankment is stable enough and the telphers describe a circuit and load on both shores, it will not of course be possible to make a continuous crest. Around the

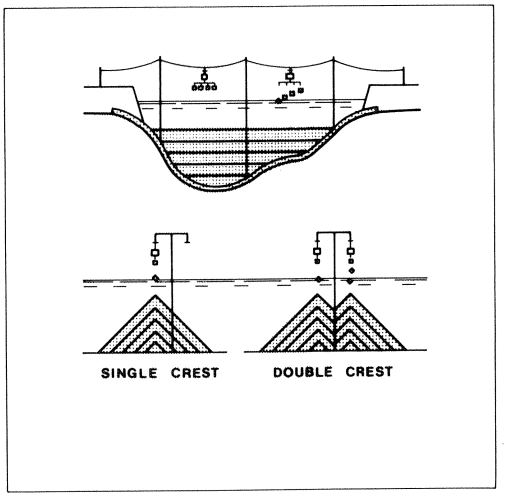

half-way point a connection section (6 to 7 m) must then be made, this being the distance between the cables. For capacity reasons the circuit operation should be maintained for as long as possible.

For determining the exact position at which the telpher has to drop its load, use may be made of a metrecounter in the telpher and a specially developed guide-light system. The guide-light system is suitable for the telpher operations, except for the odd occasion when this is impossible.

Figure 3.12b Gradual vertical closure by cable way

3.5. Sand Closure

Design and Operations of Closure Works

J.C. Huis in 't Veld

3.5 Sand closure

Sand closure general

The sand closure is carried out by supplying sand either by hopper dredger or split barge from which the sand is dumped, or by pipeline taking a water sediment suspension to the head of the dam.

The suspension runs off over the sandfill, where the sand will be deposited with the decelerating water velocities and thus build out the dam.

The narrowing of the closure gap, which will cause increasing tidal velocities, and the fact that a part of the sediment supplied by the pipe will reach the closure gap in suspension, will mean some loss of sand. A distinction is made between gross and net loss of sand. The gross loss is the sand that deposits outside the closure dam profile and is of importance for the time involved in the closure operation. The net loss is the sand taken beyond the profile of the final dam and determines the actual loss.

In the case of an upper discharge the ebb flow will be stronger than the flood below and will hold longer during a tidal cycle. By shifting the axis of the closure dam against the direction of the upper-discharge, the net loss can be minimised (see fig. 3.13).

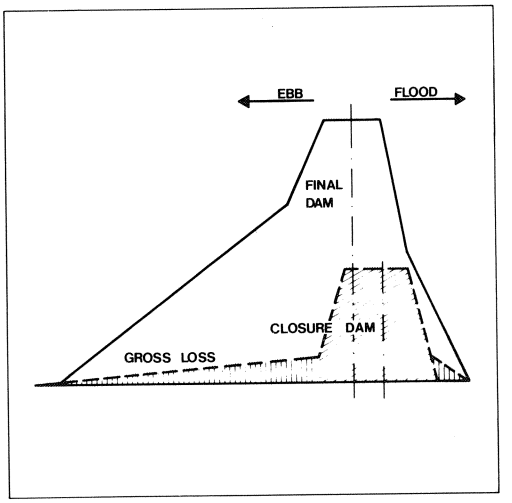

Figure 3.13 Sand loss of closure dam within cross section of final dam

The crest-elevation of the closure dam depends on the astronomical tide, the wind configuration and the run up.

When preparing a sand closure, determination of the crest width of the closure dam is very important for the following reasons.

A minimum crest width is favourable with respect to:

1. Reducing the net loss. The larger the difference in cross-section between the final dam and the closure dam the smaller the net loss will be.
2. Reducing the gross loss. A closure dam with a small crest needs a smaller sand volume during the closing operation. For this reason the time involved during the critical stage of the operation will be shorter and so the gross loss of sand will be reduced.

A wider crest however is more advantageous with respect to the available working space for equipment at the fill.

If sand is supplied only by pipe (not dumped) the pipes will have to be lengthened during the operation. The pipes should be used in pairs: one for the actual filling, while the other can be lengthened by connecting a new pipe section.

Pipes with a diameter in the order of 0.7 m are still easy to handle. The sand discharge capacity of such a pipe is about 2000 m³/hour. The slopes of the dam in the tidal zone will vary from 1:30 till 1:100 depending on the wave action. The slopes under low water will become in the order of 1:15, depending on the mean grain size of the sand. The side slopes of the dam above M.S.L. are mostly created by bulldozers and can be taken as equal to 1:5.

3.5.1 Sand-fill by horizontal pipe discharges

Based on the experience gained with the first

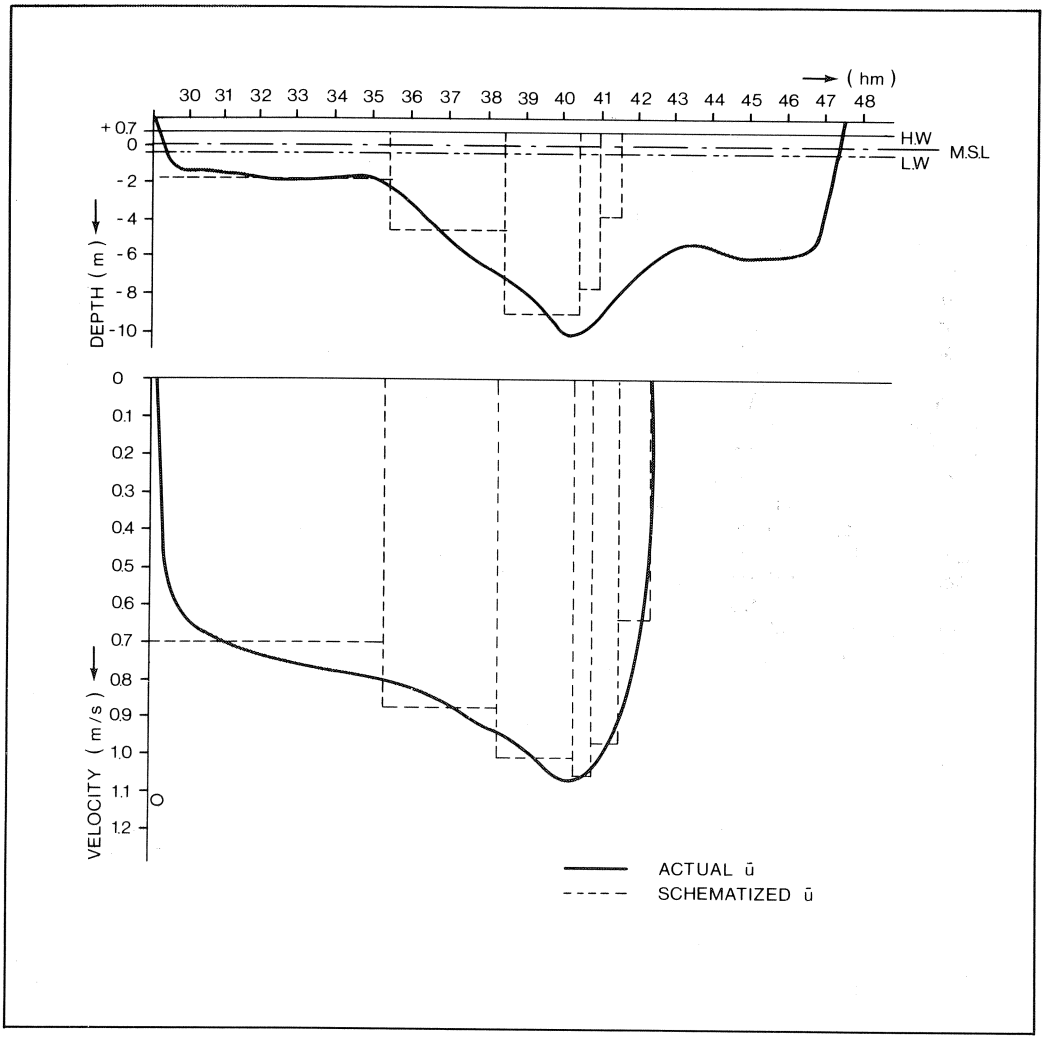

Figure 3.14 Schematisation of closure gap

sand closures of tidal channels a rough calculation method was developed for sand closings. The developed calculation method for losses of sand was tested in practice with later sand closings.

The applied calculation method is based on the calculated sand transport in suspension. As for all completed sand closings, relatively fine sand

(diameter up to 250 micron) has been used. In this case only sand transport in suspension has to be taken into account; bed transport can be neglected. If a coarsely-grained type of sand is used, for instance with a diameter of over 300 micron, bed transport must then be taken into account.
The suspended sediment loss can be calculated using the Kalinske-Kirkham formula, which was introduced in the Netherlands by Morra.
The equation, describing the suspended sediment load, applies to steady flow in a condition of equilibrium between erosion and sedimentation.
The condition of steady flow is not satisfied and the current velocity curve during the tide is therefore schematized in time-intervals (0.5 or 1 hour).
The equilibrium of erosion and sedimentation is also not satisfied, since the flow needs distance to adapt to its new conditions.

The hydraulic and geotechnical parameters for the calculation of sand loss (q_{cap}) are:

- V_m = average current velocity over the vertical (m/s)
- h = waterdepth (m)
- D_{50} = mean diameter of both the sand to be supplied and that of the bed material in the gap (mm)
- n = Manning coefficient (.) for the bottom roughness or C - Chézy coefficient: average value of n for Dutch coast: 0.024.

The cross-section of the channel has to be schematized as well as the velocities per width over which constant depth is assumed.

These schematisations over width and time step may differ for ebb and flood situation. An example is given in figure 3.14.

The representative grainsize for a more or less homogenious gradation of sand can be assumed equal to D_{50}. For sand with a wide range of gradation, the representative grainsize can be established in a way as shown in figure 3.15 for each grainsize the transport capacity can be calculated taking into account the percentage material present in that particular fraction. The cummulative gives the total sand transport for that grainsize distribution. Furthermore the sand transport capacity can also be calculated for each fraction assuming a uniform grain diameter. The representative diameter is the abcis that belongs to the intersection of the lines in figure 3.15.

The total sediment transport is the sum of bottom and suspended transport. The bottom transport is usually small compared to the suspended transport in tidal channels and may therefore be neglected. Then the total sediment transport can be calculated by Integration of the

Figure 3.15 Representative grainsize

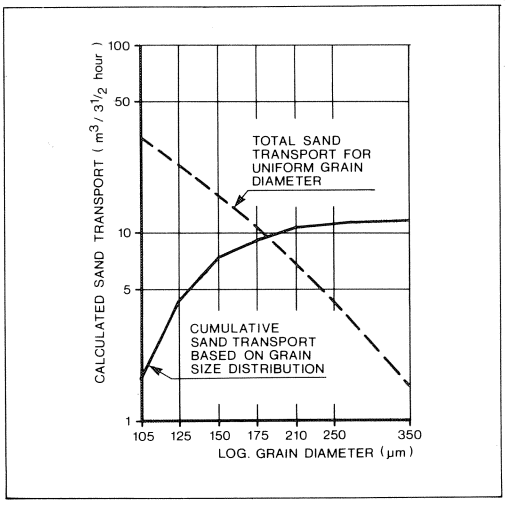

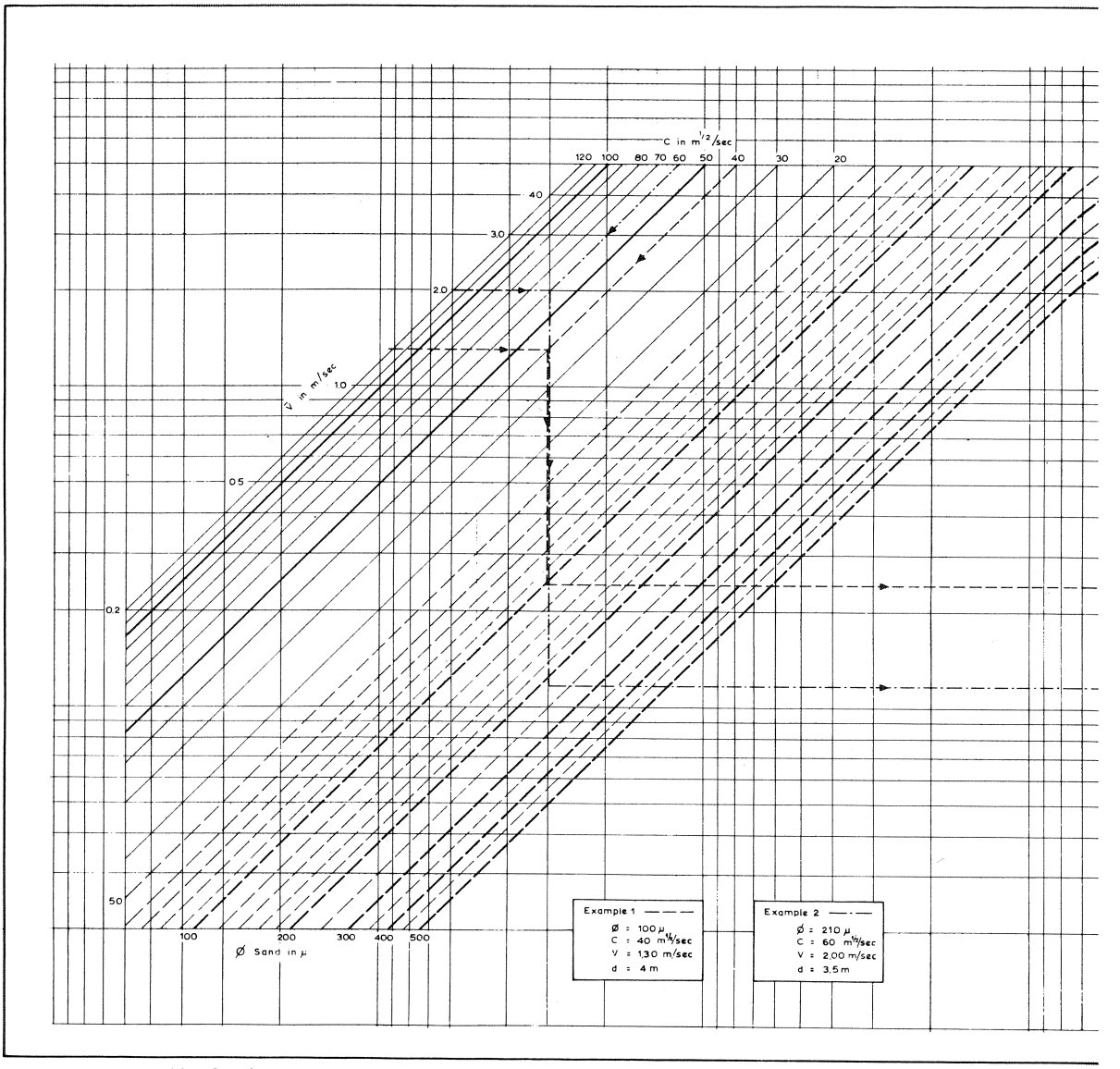

Figure 3.16 Sand concentration as function of grain diameter, roughness, velocity, and water depth (acc. to Morra)

Sand Closure

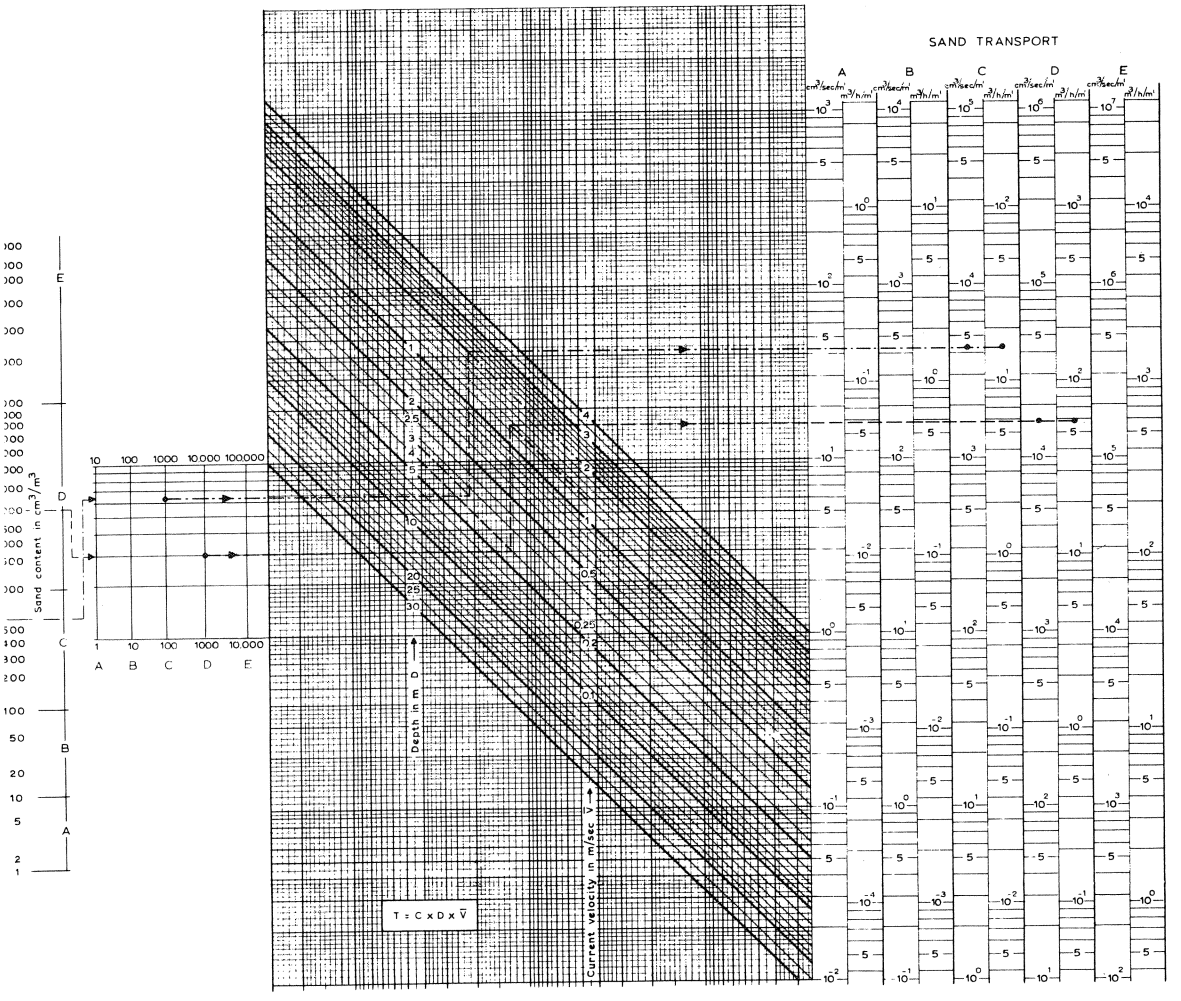

sediment concentration over the water depth and unity of width and time as:

$$T_c = \int_0^h C(Z)\,U(Z)\,dZ$$

where:
T_c = suspended load transport per unit width (capacity),
c = sediment concentration,
u = velocity, h = water depth and
z = vertical coordinate.

For calculating the vertical sediment concentration. Morra [5] has adapted the Kallinske formula for a Rouse vertical distribution.
Because of their complicated form these equations have been solved numerically and presented as a diagram (figure 3.16.). Some numerical values of T_c integrated for three different depths and velocities (under the assumption that u(z) = u = const.) are presented in figure 3.17. The above mentioned deviations in respect to the theoretical assumption (steady flow and equilibrium-stage of sediment transport) are compensated for in the calculation method by the overall experience factors A and B, as explained later.

The closure gap may be divided into two areas: the sloping head of the fill and the part of the channel outside this head.
The increase in sand transport capacity (q_{cap}) along the streamlines of the gap will result in a certain amount of erosion.
If q_{ld} represents the transport on the head of the fill in tidal direction and q_{le} (the transport outside) this zone, Svasek et. al assumed the following propotionality factors:
$q_{ld} = B\,q_{cap}$ where B = 2
$q_{le} = A\,q_{cap}$ where A = 0,25

The total sandloss in the closure gap is equal to $Q_t = \xi\, q_{ld} + \xi\, q_{le}$ (summation over the width of the characteristic areas).
To make progress in the dam building the supply capacity Q_s integrated per tide or day has to be greater than the integrated sand-transport capacity Q_t.

If the transport capacity on the head of the fill exceeds in a certain time interval the sand supply a reduction factor of 0.5 or even 0.25 may be applied for the interval of exceedance, as shown in figure 3.18.

An additional factor must be brought into the calculation, the distinction of spring, normal and neap conditions. This is done by using tidal coefficients. For all the phases of the closure operation each calculation step must be carried out for these tidal coefficients.
By integrating over the steps of tide for each coefficient a loss per tide can be calculated as a function of the width of the gap and a graph results as given in figure 3.19

The actual losses will be somewhere between the extremes and depend on the tidal condition during a certain phase of the closure. An example of this is represented in figure 3.19 by the dashed line.

If a good estimate can be made of the progress of the closure and thus the tidal conditions during a certain stage, the time of closure can be estimated with the formula:

$$T = \frac{V(1 + P/100)}{Q}$$

where:
T is time of closure,
V is volume of closure dam,
P is percentage of loss and
Q is the dredge output.

A large output, which involves faster work will reduce the overall loss by limiting the number of tides.

The last phase of the operation, where the actual closure is effected, must be carried out under neap conditions when, the maximum water level will be limited and the chance of a breakthrough reduced.
In order to reduce the sand loss in the final stage of the closure the remaining gap should be situated in a shallow part of the channel, as less sand will have to be brought in to make the same

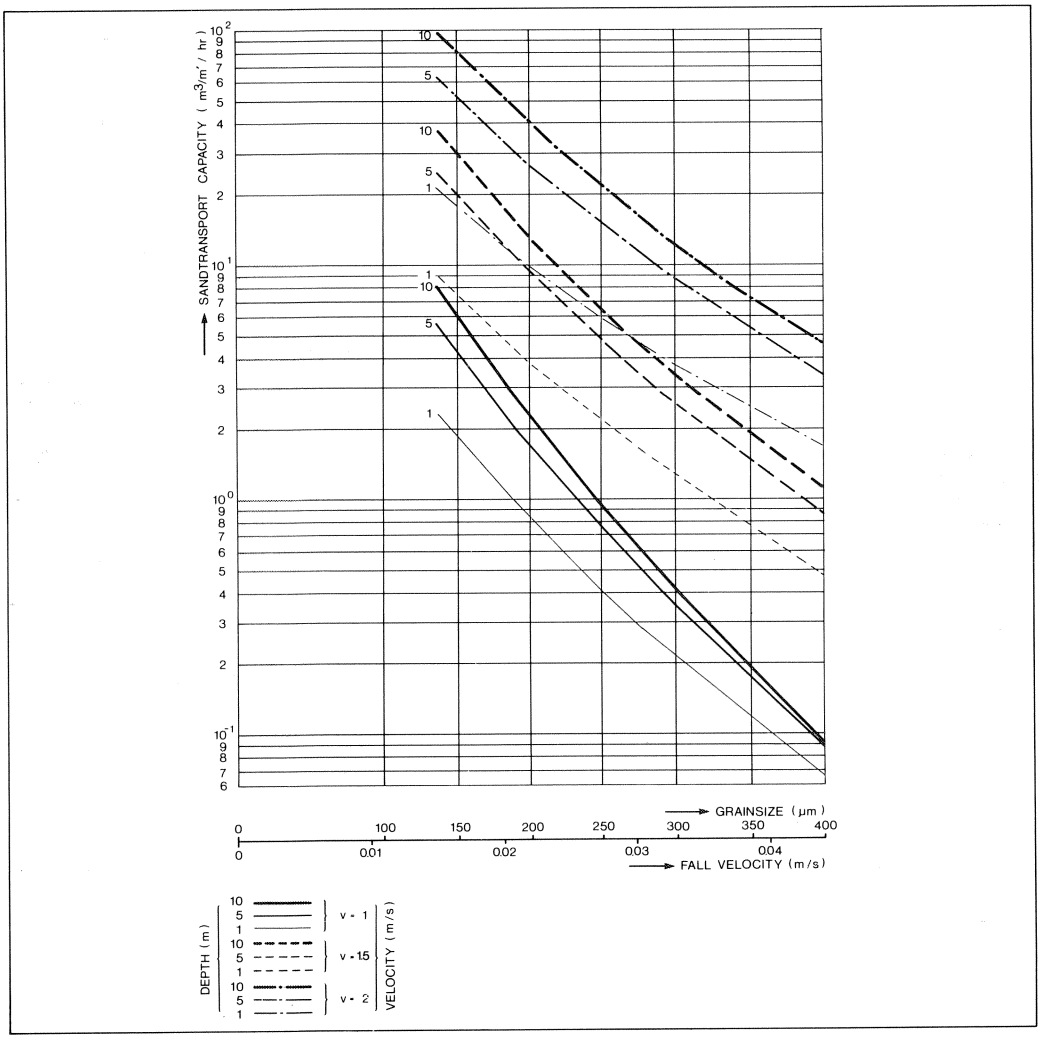

Figure 3.17 Relation between sand transport capacity, grain diameter, velocity and waterdepth (acc. to Morra and RWS)

progress than in the case of a deeper gap.
In the final gap bulldozers and draglines operate on the fill to control sand deposition above the water level. A special problem consists of controlling the pumped water so as to prevent it from eroding channels while running down the fill.
The duration and cost of the operation depend on the location of the sand to be borrowed for

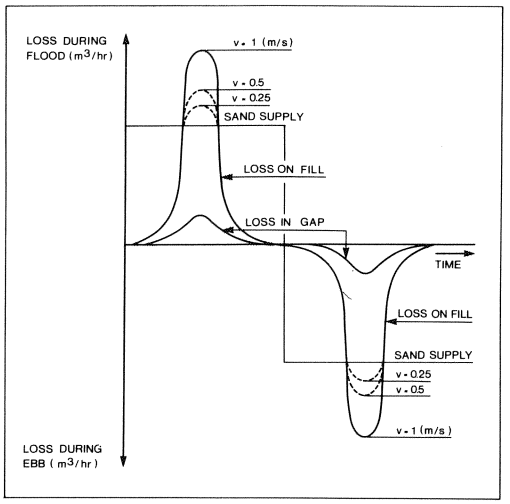

Figure 3.18 Integration of sand-loss during a tidal cycle

Figure 3.19 Total sand-loss during closing operation (example)

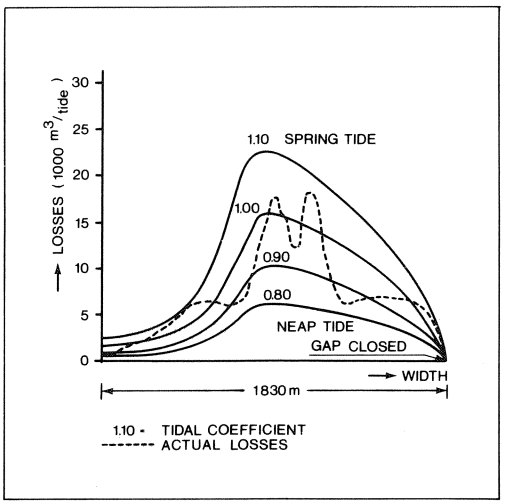

the dam. Travel distances should be kept as short as possible. Borings are needed of both the dredging area and the channel.

Some examples of the influence of the parameters:

1. Influence of grain size (D 50)
   Given : V_m = 1.00 m/s
   h = 6.00 m
   n = 0.024

Table 3.6. Influence of grain size

D_{50}	q_{cap} $m^3/m^1/h$	loss of sand ($m^3/m^1/h$) head of fill B = 2	bottom A = 0,25
0,150	6.29	12.58	1.57
0,175	3.96	7.92	0.99
0,200	2.58	5.16	0.65

2. Influence of bottom roughness (n):
   Given : V_m = 1,00 m/s
   h = 6,00 m
   D_{50} = 0,175 mm

Table 3.7. Influence of bottom roughness

n	q_{cap} $m^3/m^1/h$	loss of sand ($m^3/m^1/h$) head of fill B = 2	bottom A = 0,25
0.026	5.06	10.12	1.27
0.024	3.96	7.92	0.99
0.022	3.00	6.00	0.75

3. Influence of dredger output
   Dam through Springerdiep - Brouwersdam (1970)
   Tidal range : 2.6 m; length of the gap: 1000 m; max. depth 6 m - MSL;
   volume of closure dam V = 6 10^6 m^3, D_{50} = 0.20 mm.

Table 3.8. Influence of dredger output

Assumed dredger output m³/week	Length of closure operations (weeks)	Calculated loss of sand (10^6 m³)	Observed loss of sand (10^6 m³)
230,000	5	0.50	
300,000	3.5	0.35	0.25
350,000	2.5	0.25	

From some closure operations in the Netherlands data are available to compare predicted, calculated and observed sand losses. Table below gives the results. In figure 3.20 the dredgerproduction and the observed sand losses as function of time are illustrated.
It may be concluded that in most cases the calculated and observed sand losses are of the same order of magnitude. The predicted sand losses deviate in most cases considerably from

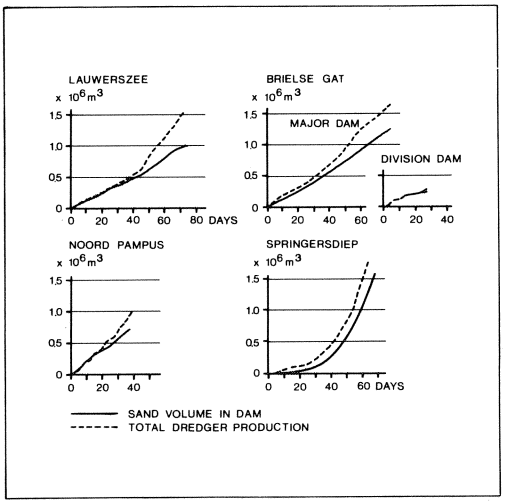

Figure 3.20 Examples of sand-closures for various projects in the Netherlands

Examples of sand-closures for various projects in the Netherlands

	tot.dredger production 10^6m³	Observed loss 10^6m³	Predicted loss 10^6m³	Calculated loss 10^6m³
Lauwerszee	1.56	0.52	0.90	0.45
Brielse gat.div.dam	0.27	0.06	—	0.10
Brielse gat,maj.dam	1.72	0.53	—	—
Noord Pampus	0.97	0.22	0.20	0.06
Springersdiep	1.87	0.25	0.70	0.35

the observed losses. This indicates that much care should be given to the data on which the prediction is based.

3.5.2 Sand-fill by dumping

In recent years experience has been gained in the procedures for highly accurate sand-fill by dumping. This formed part of the soil improvement, required for the pier foundation of the Eastern Scheldt Barrier (figure 3.21).

The refill of dredged trenches was carried out by using hopper dredgers with a capacity of approx. 3000 m³.
The refill consisted of sand with a mean grain

size of approx. 0.2 mm (0.35 mm apart). The maximum layer thickness to be replaced amounted to 12 metres, the minimum thickness 6 metres. The water depth varied between 18 and 39 m below MSL.

In the middle of the flow channels, where the water depth was greater than the foundation level of the piers to be installed, the original bottom level had to be raised. Because of the high current velocities (up to 2.0 m/s at springtide) these artificial sills were subject to erosion during the project.
Once constructed the sills were covered with current-resistant material (gravel).

Application of hopper doors
At the start of the refill operation only one placement method was used viz. the dumping of sand through the doors in the bottom of the hopper dredger.
Due to the waterdepth (30 to 40 metres), the sand losses were very great (50% or more). In the optimalization process other installation methods were considered as well, especially the dumping of sand through suction pipes in an inverse direction to the bottom.
Sand installation takes place alongside a mooring pontoon. The positioning of the dredger during dumping is relative to the position of this pontoon. From the measurement results the following conclusions about the physical process may be derived.

On its way from the doors to the bottom, the sand/water stream accelerates. In the meantime the sand concentration drops due to the entrainment of the surrounding water. Close to the bottom he sand/water jet has a downward front speed of approx. 3 to 5 m/s (estimated, not measured).
This jet causes high impact forces on the sandy bottom and consequently a crater is formed (depth approx. 1 m.). The impact of the fluid jet generates a surge which spreads outwards; due to the irregular shape of the bottom and the presence of tidal velocity, this surge does not spread radially. The front speed of the surge is

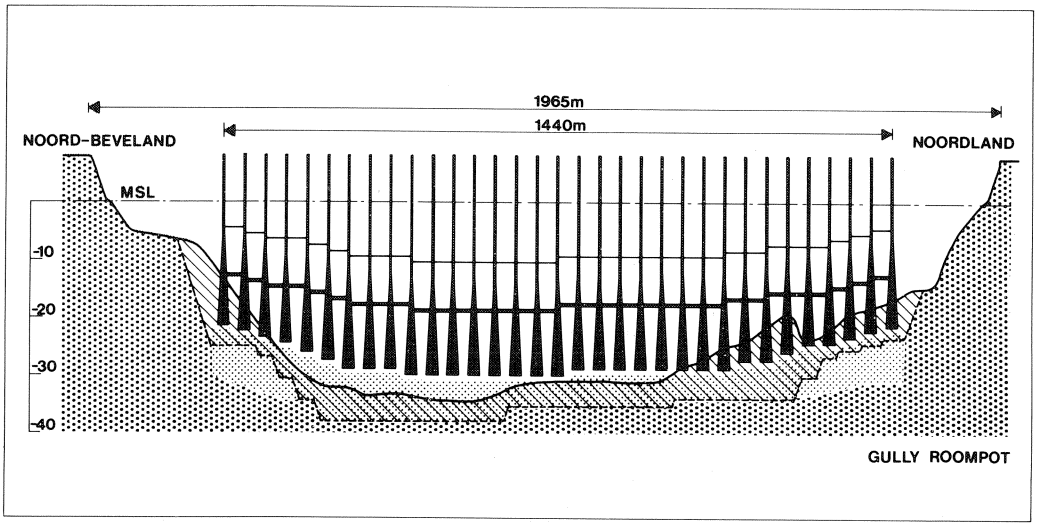

Figure 3.21 A sand sill as foundation for the Eastern Scheldt Barrier

initially very high; at approx. 20 metres from the hopper a front speed of 3 m/s has been measured.
The sediment concentration at a distance of approx. 20 m varies between 2000 and approx. 5000 p.p.m.
At a distance of approx. 150 m. from the point of impact the energy and the sand contents of the surge are so low that the phenomenon ceases to exist.
Eddies reach the upper water layers from the impact area and the high turbulence surge. Deposition of sand from the surge starts at approx. 20 m. from the centre of the impact area and reaches a maximum at a distance of approx. 50 m.

Suction pipe technique
Dumping time using a suction pipe is approx. one hour, while the technique using the hopper doors only takes ten minutes. Furthermore, the suction pipe technique is much less easy to use than the hopper technique in turbulent water conditions.
Workability depends strongly on the anchoring and manoeuvring capabilities of the pontoon. In the beginning in contrast with the hopper doors, dumping through the suction pipe can only take place at slack water (current limitation of 1-1.2 m/s for efficiency reason).
On the other hand, echo soundings for the suction-pipe method showed that higher net efficiencies could be obtained with this method than with hopper doors.

In general the sand losses using the suction-pipe method are dependent on:
- distance between the mouth of the suction pipe and the bottom
- sand discharges per unit of time
- tidal velocities in relation to the anchored pontoon.

In a later stage successful trials were carried out using the suction pipe alongside a large pontoon moored with six anchors. In this way, it is possible to use the suction pipe up to current velocities of 1,5 m/s.

It is also possible to apply this method in combination with a gradual closure. If the foundation of a closure embankment of rock-units can be raised above the original bottom level less rock will be needed for the closure. In particular, when many rock-units (rubble or concrete blocks) have to be dropped during the final closing stage, this stage will cause more scour

Table 3.9. Summary of the sand fill by dumping method

Subject	Dumping through hopper doors	Dumping through suction pipe
Net efficiency	30 - 60%	60 - 80%
Under water gradients	1:10 - 1:15	1:4 - 1:6
Dumping time	10 minutes	1 hour
Restrictions	to avoid craters and uneven surfaces a special procedure is necessary	normally done at slack water; net efficiency depends highly on the navigation of the track; with an adapted anchoring pontoon filling possible during whole tidal cycle
sphere of sedimentation	fine sand : 100 - 150 m coarse sand: 70 - 120 m	10 - 30 m

where the bottom protection ends. The use of a sand sill can therefore reduce total scouring during a gradual (horizontal or vertical) closure operation.
If the toe of the sand sill still falls inside the cross section of the final dam, the losses of sand are much more likely to be accepted in the overall economics of the project.
This alternative is being considered for the closure of the Oesterdam (a compartmentalization dam in the Eastern Scheldt) (figs. 3.22 and 3.23).

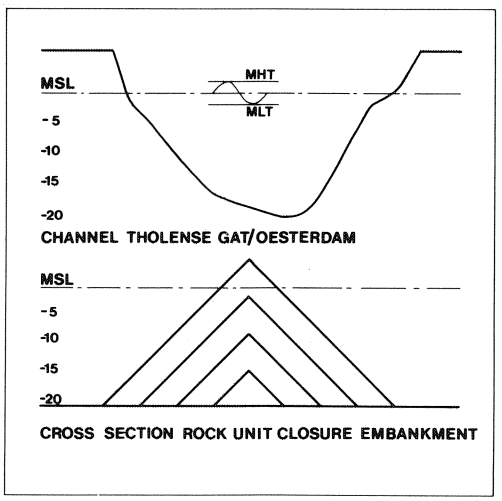

Figure 3.22 Cross section Rock unit closure embankment

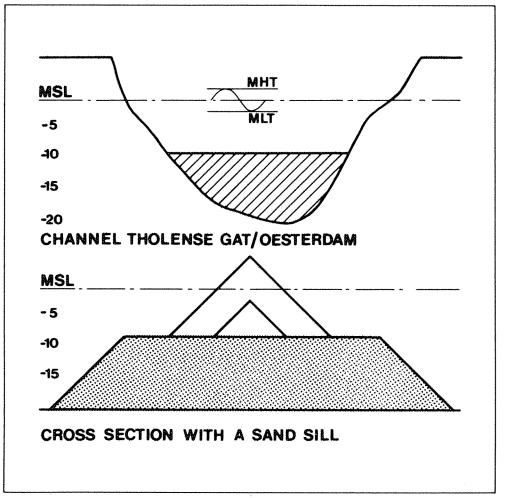

Figure 3.23 Cross section with a sand sill

3.6. Sudden Closure

J.C. Huis in 't Veld

3.6 Sudden Closure

By means of caissons

General

This method deals with structures which allow the whole gap to be closed suddenly. Normally these structures consist of caissons which are placed into the gap during a slack water period and thus close the whole gap at once. Another solution is the use of „sluice" or „culvert" caissons which are placed during several successive slack-water periods and kept open throughout placement of the remaining sluice caissons. After the placement of the final caisson, they are all closed at the same slack-water period by means of gates. Sluice caissons should be used when the gap to be closed is a large one and the tidal motion is considerable.

Closed caissons are useful in small gaps, say not larger than one to the three caissons, or in areas where only a very small tidal motion occurs. A characteristic feature of sudden closure by means of sluice caissons is the maintenance of the widest possible effective wet area of the closure gap until all the caissons have been sunk in position on the sill. By using open caissons, a great increase in the velocity in the gap is avoided.

Provided the flow pattern is not too greatly influenced by the walls of the caissons, this will prevent strong scour.

Advantages:

- The sluice caissons have the advantage that they do not strongly influence the tide, and that the velocities in the gap can be kept below a certain limit before being changed in a short time to zero.
- If the closure gap comes under strong wave or ice attack during a great part of the year, it may be a solution to pre-fabricate these large concrete structures in milder climatological zones in a year-round operation. These structures can then be towed to their final destination whenever circumstances permit.

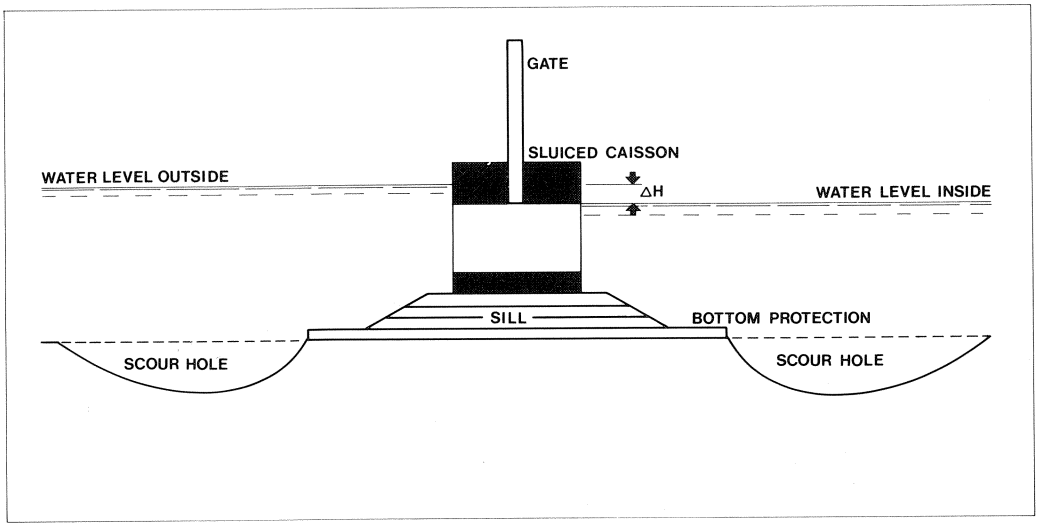

Figure 3.24 Construction stages of caisson closure

Disadvantages:
. The placement operation is a critical one, and is highly sensitive to weather conditions
. The use of caissons needs a slack-water period long enough for placing at least one caisson (i.e. the final caisson during a neap tide).

A sudden closure by means of sluice caissons is generally divided into the following construction stages (fig. 3.24).

1. A flat, stable sill structure with vertical or oblique abutments is constructed on a stable, scour-resistant sea bed, protected by a bottom revetment.
2. a) Rigid concrete caissons are floated into position, successively, across the gap.
   b) When a caisson has been sunk into position on the sill, wooden boards along the sides of it are opened (in fact totally removed), so that the tide can flow through.
3. When all caissons are in position, their gates are closed simultaneously at slack water, thus effecting the closure.
4. The permanent dam is then built around the caissons, if these have only a temporary function.

There are two ways in which to use sluice caissons. First, they can be used as temporary structures: after closure they are incorporated in an impermeable dike-body of sand with revetments. The other possibility is to use the caissons as definite elements of the barrage, without covering them with other material. These elements have to be stronger than the temporary ones but, in some cases, the absence of large amounts of sand and revetments makes the total structure cheaper.
On the other hand, the permeability causes problems.
The side connections of the caissons cause minor problems; the permeability of the sill is a more difficult problem and has to be solved, for example by undergrouting.

The „winter" closure gap
The shape of a „winter" closure gap (fig. 3.25), to be closed in the following spring or summer by means of caissons, calls for special attention.

The height of the sill determines:
- the scouring action;
- the dimensions of the caissons;
- the current velocities during placement of the caissons.

The shape of the abutments determines:
- the origin of vortex streets and local scour.

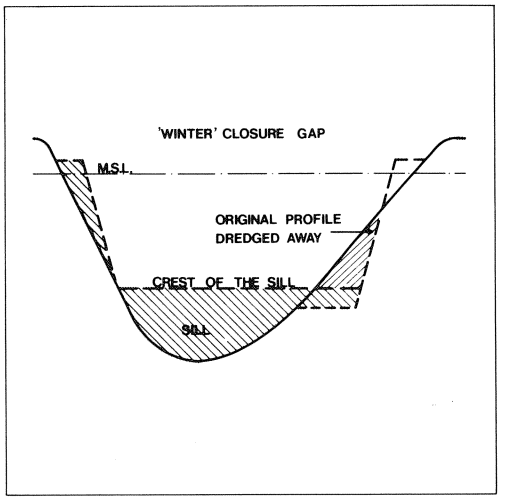

Figue 3.25 Shape of a closure gap for a caisson closure

The **height of the sill** is important because a closure by the caisson method calls for the construction of the sill one or more years preceeding the final closure and the depth and starting angle of the scour holes increase over time.
A deeply positioned caisson sill limits the increase of the current velocities and thus avoids deep scouring. Another advantage of a deeply-

placed sill is that there are more and better opportunities during the turn of the tide for floating and sinking the caissons.
On the other hand, greater depths mean that a reasonable levelling of the caisson sill will become more difficult and the costs of the caisson will rise.
The **shape of the abutments** has to be designed to minimize vortex streets. Downstream from an abutment, with a vertical head on a sill, a strong string of vortices will occur, which cause deep scouring.
A better solution consists of filling the triangular space between the first caisson and the slope with a specially adapted caisson with a sloping bottom (Volkerak and Brouwersdam closures, see fig. 3.26). Placing and consolidating this caisson take no more than a few days, a factor that will greatly reduce scouring.

Figure 3.26 Caisson with sloping bottom, first caisson between abutment and first regular caisson

The interaction between sill and caisson
Caissons used for closures of tidal basins are generally placed on a sill, constructed as a graded filter structure. For stability reasons, the upper layer of the sill generally consists of rubble. For the design of the sill as a foundation for caissons the following factors are of importance:
- the transference of horizontal loads;
- the transference of vertical loads;
- the stability of the upper layer of the sill;
- the flatness of the surface of the sill.

Transferring horizontal loads
For caissons that are placed on top of a surface and are not embedded, the horizontal force will have to be transferred to the subsoils by friction of the base over the sill surface.
Due to the fact that the vertical force is low, the surface immediately under the structure is often a critical failure plane.
This is even more so when, in this plane, a poor contact medium has to be accepted such as asphalt or loose sedimentary sand, or when contact is limited to only a few points of a surface consisting of large stones.
This quite often means that the angle of friction or the H/V value of this layer is low, thus dic-

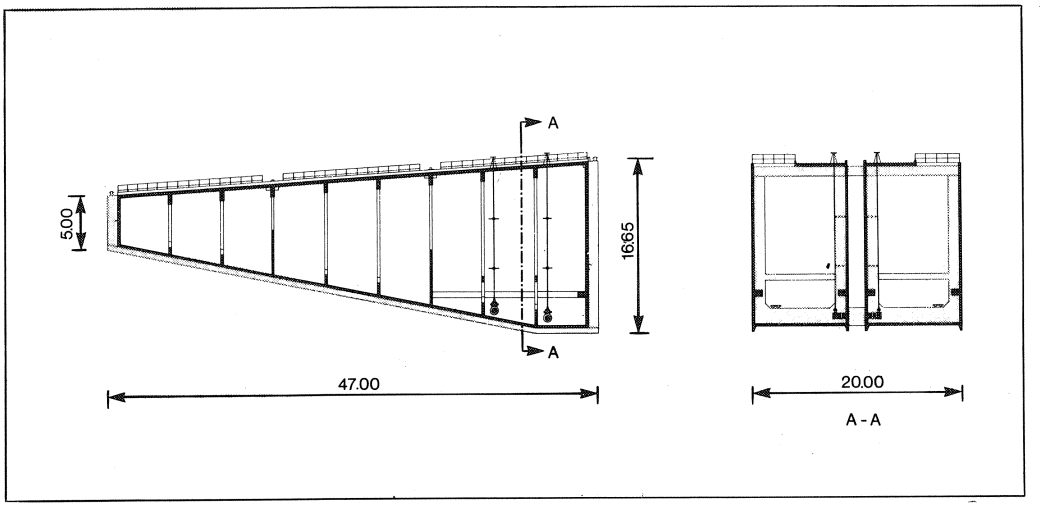

tating the required effective weight of the structure (see figure 3.27).
The required weight of the caissons is a very important factor in the total design and cost of a caisson closure. For this reason much attention has to be paid to trying to find a solution with a high friction coefficient between sill material and the bottom of the caissons.

Transferring vertical loads
The vertical forces that are transmitted to the foundation are the dead weight of the structure (including water displacement, sand ballast, gates, sill, etc) and the vertical components of the wave loads (see figure 3.27).
It should be mentioned that the rotational moment due to the water head and wave loading influence the pressure line of the vertical forces.
One of the important requirements of the sill is to ensure a reasonably even stress distribution under the base of the structure.
Tests indicate that, when a flat stiff surface (e.g. the bottom of a caisson) makes contact with an uneven surface of a layer consisting of compacted gravel or stones, very high local stress peaks can occur and hardly any flattening or redistribution takes place. In the floor of the caissons, places can be indicated where high local stress peaks give no problem at all (mainly under the walls and spans), while local stress peaks at other points can give serious problems (mainly between the walls).

For the **stability of the upper layer** it is necessary to examine the situation when the last caissons have to be placed. It can then be found out what the critical flow will be for the top layer of the sill, which has to be built as a filter. The head walls and bottoms of the caissons cause trains of eddies that may be a critical factor in the stability of the materials. If the eddies are very strong, they may carry off the stones at much lower average velocities through the closure gap than a normal current with straight flow-paths would do. If there is a real danger of the critical flow being reached, two solutions are possible:
- the sill can be finished off with a heavier material (Volkerakdam);
- the original material may be consolidated by

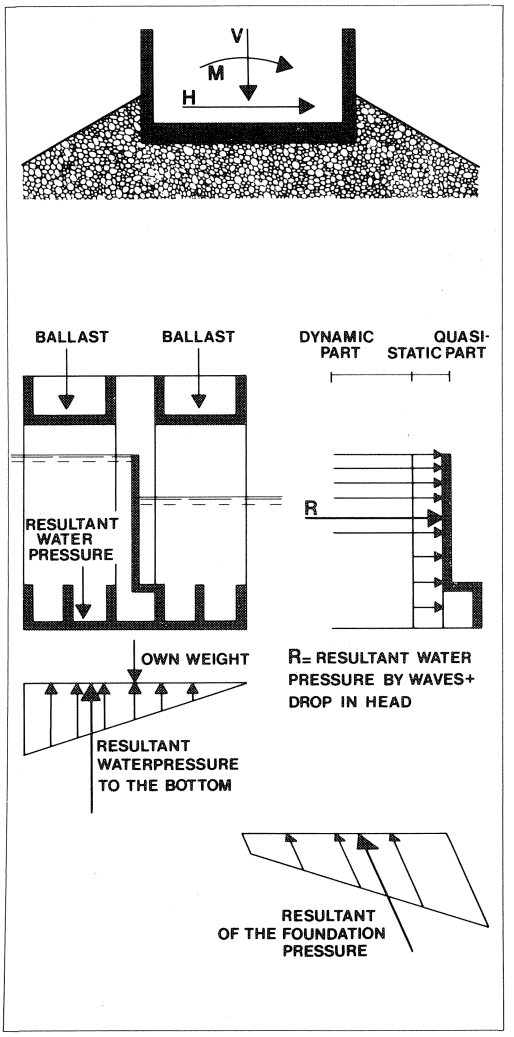

Figure 3.27 Transferring horizontal and vertical loads from the caisson to the sill

means of an asphalt filling (nothern channel Brouwersdam).

Both measures have an effect on the design and completion of the closure.

The coarser and heavier the sill material, the more difficult it is to give the sill a regular, even surface. One possible consequence is the greater risk of seepage after the closure with caissons bearing on an uneven finish of the sill. Filling of the sill may affect the design of the caissons.

In the design, the horizontal load resulting from waves and difference of head is estimated, while the maximum shear resistance is calculated by using the friction coefficient between sill material and the bottom of the caissons. The risk is great that the value of the friction coefficient will be reduced as a result of the filling-up process. This means that a heavier caisson would have to be designed.

To determine the value of the friction coefficient, prototype tests with a concrete slab on a rubble mound with flat surface and on asphalt-jointed stone pitching were carried out.

The conclusion reached from the tests is that the asphalt filling does indeed cause a fairly serious reduction of the friction coefficient, depending on the quantity of the asphalt used in the filling and on the specific pressure under the concrete slab.

The higher the specific pressure and the greater the quantity of asphalt used, the greater the reduction in value of the friction coefficient.

In the case of a flat caisson bottom on a sill of rubble a friction coefficient of 0.5 may be assumed. In the case of a jointed sill, the value may be taken as a maximum of 0.4.

If the bottom plate of the caissons is ribbed, the value of the friction coefficient increases to 0.6 in case of a normal rubble sill and to 0.5 in the case of a jointed sill.

Sill surface flatness

As already mentioned, a large stone size in the upper layer will mean that the sill will not always be completely level. If caissons are placed on the sill, gaps under the caissons will be present with a height at least as great as the diameter of the rubble, depending on the method of execution. For example when using only stone-dumping vessels to construct the sill, the irregularities will be approximately 0.5 to 0.7 m (rock 60-300 kg); after finishing off the surface by means of a bucket dredger, these unevenness will possibly be reduced to 0.2 to 0.3 m.

The consequences of these irregularities are:

- the caissons will not be fully supported along their entire bases;
- seepage will arise.

The bottom of the caissons for the closures of the Veerse Gat and the Volkerak was completely flat. In these cases, it was uncertain where the caissons rested on the sill. To be certain, of the points at which the caissons for the Brouwersdam were supported, the bearings, which had a height of 0.5 m, were situated at 1/4 and 3/4 of the length in order to prevent the caisson from resting on its outer ends or in the middle.

The first plans for a permanent caisson dam in the mouth of the Eastern Scheldt were to put caissons on a square net of ribs and skirts or on a temporary three-point support and to undergrout the rest of the bottom of the caisson before ballasting.

Another proposed solution was to put each caisson on a three-point support in the permanent situation. These supports had and area of 15 x 15m² and were to be grouted.

High velocities can occur in the gaps under the caissons as a result of the head difference over the caissons during the closing operation.

This can endanger the stability of the rubble on top of the sill, and thus the structure as a whole. Therefore, two measures can be taken:

- place narrow ribs under the caissons, which allow them easily to penetrate the sill. The ribs have a function of sealing and increasing the friction. They do not have a bearing function.
- dump stones against the walls of the caissons. If these structures consist of rubble dams, the stability of the dam - especially the downstream one - must be assured (fig. 3.28).

A distinction should be made between the

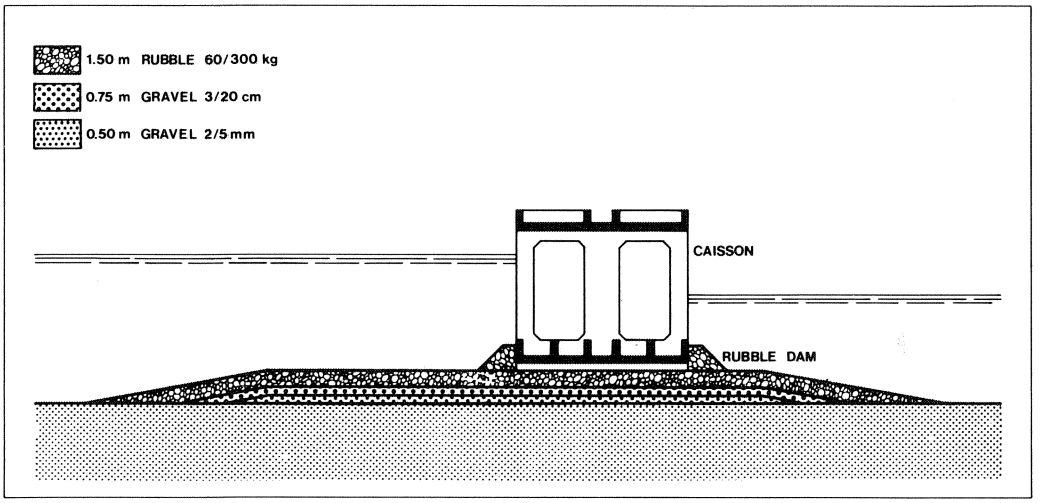

Figure 3.28 Caisson with rubble dam on a sill

stability of the rubble dam as a whole and the stability of the individual stones.
Comparing both stabilities, it can be stated that the stability of the downstream rubble dam as a whole is significant.

For the determination of the volume of the rubble dam to be dumped against the walls of the caissons, it is necessary to know the distribution of the head-loss over the dam(s) and the gap under the caisson.
Model tests have been carried out to obtain insight into this matter. During the tests, the course of the water pressure along the surface of the sill was measured, so that the distribution of the head-loss could be determined.
It can be concluded that the stability of the rubble depends on:
- the porosity;
- the weight of the material
- the head-loss.

The total head-loss over the downstream rubble dam is strongly influenced by the presence of the upstream rubble and the gap height.
Porosity of the material depends on the grading. No significant influence of the diameter of the rubble could be determined.

If the predicted settlement and deformations of the caissons are too big, a densification of the sill is necessary. Experience with these methods has been gained in the Eastern Scheldt Barrier.

The design of the caissons
A caisson has to be constructed in such a way as to be strong enough to be towed from the construction pit towards the closure gap, where it will be sunk and must find a stable place on the sill.
The design considerations concern:
- hydraulic aspects;
- manoeuvring aspect;
- structural/constructional aspects.

Hydraulic aspects
In the case of a sudden closure, it is necessary to maintain as wide as possible a wet cross-section during caisson placement.

The effectiveness of the sluice caissons increases in proportion to the depth of the sill on which they rest.

1) Design the wet cross-section of each caisson as large as possible:
   - large spans between the walls: apply steel diagonals to give the caissons enough torsional strength;
   - thin bottom;
   - place the ballast bunkers required to obtain enough friction between sill and caisson bottom in the caisson superstructure.

2) Design the discharge coefficient as high as possible:
   - streamline the diagonals within the spans (fig. 3.31);
   - apply downstream and upstream rubble dams on the crest of the sill (fig. 3.28) and give these dams a streamlined shape.

Figure 3.29 Crosss section of caisson, energy head and waterlevels

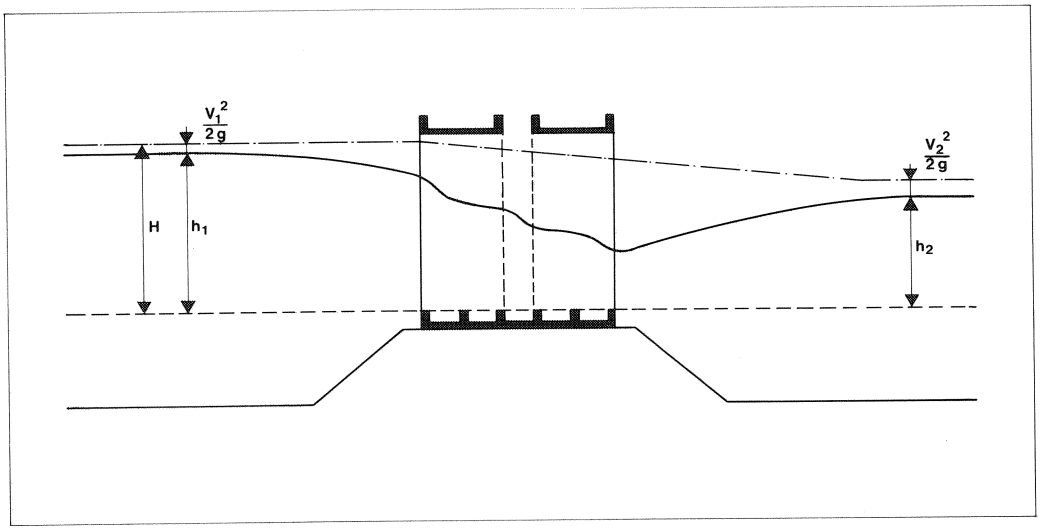

Table 3.10. Survey of some caisson closures

	Depth of sill with regard to M.S.L.	Discharge coefficient sluice caissons
Veerse Gat 1961	– 8 m	not measured
Lauwerszee 1969	– 6 m to – 6,5 m	0,6
Volkerak 1969	– 7 m	0,75
Brouwersdam 1971	– 10 m	0,82
Caissons designed for the closing of the Eastern Scheldt	– 20 m	1,0

Navigation aspect
From a working point of view, it is advantageous to minimize the number of caisson placements at a closure. In addition it is desirable, from a nautical point of view for the relationship between the width and length of the caisson to be 1 : 3 or 1 : 4.
Based on these considerations, caissons longer than 50 m are to be preferred.

The most important navigation conditions affect:
- draught: depends on the waterway and the depth above the sill
- manoeuvrability: if L/B > 3, it is possible to tow two caissons in a row
- flow resistance and immersed volume: number and strength of the tugs
- the stability of a floating caisson.

Flow resistance

$$W_w = C_w \tfrac{1}{2} \rho_w v^2 A$$

$$W_L = C_L \tfrac{1}{2} \rho_w v^2 A$$

W = resistance force (Newton)
L = lift force (Newton)
ϱw = density of water (kg/m³)
v = current velocity, measured about 150 m upstream from the caisson and 3m below water surface (m/s)
A = area of the water plane perpendicular to the flow direction (m²)
h = water depth (m)

Stability of a floating caisson
It is desirable that the caisson maintain its vertical position during transport and sinking. This can best be achieved by building it symmetrically around its longitudinal axis.
The sluice caisson used for closing the Veerse Gat lacked a symmetrical form since gates were suspended on the one side and wooden boards on the other.
To increase stability during the sinking process, a temporary stabilizing board was fixed in the centre of the caisson. With the sluice caisson for the Volkerakdam and the northern channel in the Brouwersdam, wooden boards were used on both sides at the floating stage. The steel gates were placed in the centre. During towing and sinking these also served as stabilizing boards.
A floating unit (caisson) is stable if the centre of buyancy C is above the centre of gravity G.
C = centre of buyancy
G = centre of gravity

$$MC = \frac{I}{V} = \frac{\frac{1}{12} LB^3}{V}$$

M = transverse meta centre
I = transverse moment of inertia of the waterplane
L = length of the caisson (m)
B = breadth of the caisson (m)
V = immersed volume (m³)
MG = h_M = height of transverse meta centre above centre of gravity
MG = MC - CZ

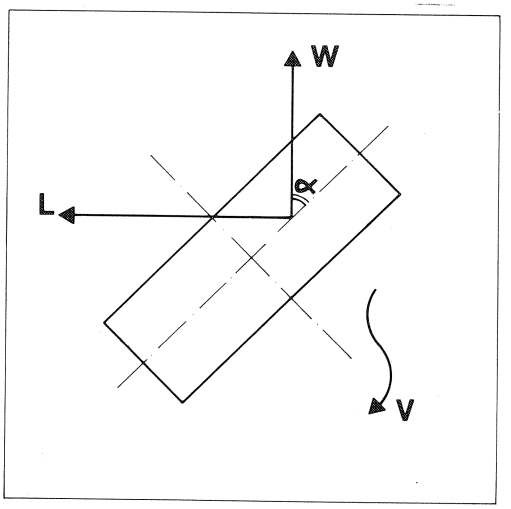

Figure 3.30 Current induced load on floating caisson. Definitions.

Constructional aspects

Using sluice caissons has the advantage that they are independent units, each with its own gates.

The caissons must be rigid so that the gates can always be closed, even if there is unequal settlement.

To pick up a displacement between two adjoining caissons, a space for filling with rubble is required between the head of the caissons.

The caissons allow for deformations as long as the caisson floor is strong enough to withstand pressure differences.

Due to the fact that a small water displacement is advantageous for navigation, and a high own weight is required for obtaining enough friction between caisson floor and sill surface, ballast bunkers are used. These bunkers are filled with sand or pour concrete immediately after positioning the caisson on the sill.

Dimensions of the sluice-caissons

The transport and positioning of a caisson is a costly operation as it requires much equipment and labour. To a certain extent, the costs per caisson depend on its size. The number and/or power of the tugs to be used, form no exception to this rule as the number and power will increase in proportion to the water displacement of the element. On the whole, however, the costs of a closure will decrease when a smaller number of caissons is used; or, in other words, if the longest caissons possible are used. By limiting the number of positioning activities the total operation time will be reduced and, at the same time, the risks due to unfavourable weather and tidal conditions will also decrease. However, it must be noted that increasing the caisson size increases the risk of an individual caisson operation.

The width of the caissons is defined by their stability whilst they are in tow and during positioning. During the latter phase, the bottom area of the caisson must be so large that the forces due to horizontal head differences and to waves can be transferred to the subsoil without causing too much deformation either to the foundation or to the caisson itself.

The length of the caissons is, to a large extent, determined by the degree of eveness of the sill on which they are placed. The vertical load that must be transferred to the subsoil must be evenly distributed over the bottom area of the caisson. The vertical load equals the weigth of the caisson and of the ballast reduced by the upward water-pressure. If the sill surface is finished evenly and the weight of the caisson is evenly distributed over its foundation, then no bending moments will be induced into the caisson. During the placing of the first (sluice)-caisson in the Veerse Gat (1961), differences in sill-level of up to 0.50 m ocurred over the total length of the caisson. An equal distribution of the forces on the bottom of the caisson over its entire length was thereby out of the question.

The bottom surfaces of the caissons used in the Veerse Gat were flat i.e. without ribs or bearings. As a certain unevenness of the sill was expected (the exact values were at that time unknown), two models were made to simulate and calculate the moments. In the first model, the caisson was only supported at both ends. Each bearing surface was assumed to have a length equal to 1/8 of the total length of the caisson. The central part, i.e. 6/8 of the caisson, was thus not supported. In the second model only 2/8 of the caisson was supported at the centre. This means that 3/8 of the total length on either side was unsupported. Investigations of the prototype caisson after placing showed that the situation was indeed similar to that of the second model. The calculations made with the aid of the models showed rather large bending moments as a result of which the lengths of the caissons had to be limited. Therefore, the caissons used for the closure of the Veerse Gat were only 45 m long. Based on this experience, the caisson-bottom profile was varied in order to obtain well-defined bearing surfaces and to limit the moments so as to be able to increase the length of the caisson as much as possible. As a result, longer caissons (60 m) could be used for the closure of the Brouwershavensche Gat in 1971. Figure 3.31 shows that the caisson bottom is curved. By curving the bottom by more than 0.50 m (the maximum expected uneveness of the sill), it is guaranteed that only the bearing area is

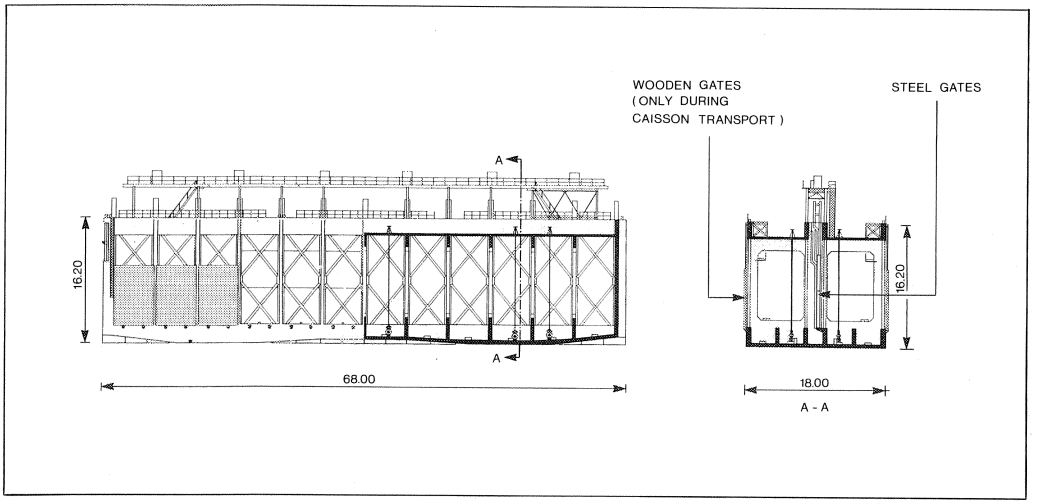

Figure 3.31 Long caisson, used in Brouwershavense gat, longitudinal and cross-section (1971)

Figure 3.32 Caisson towing

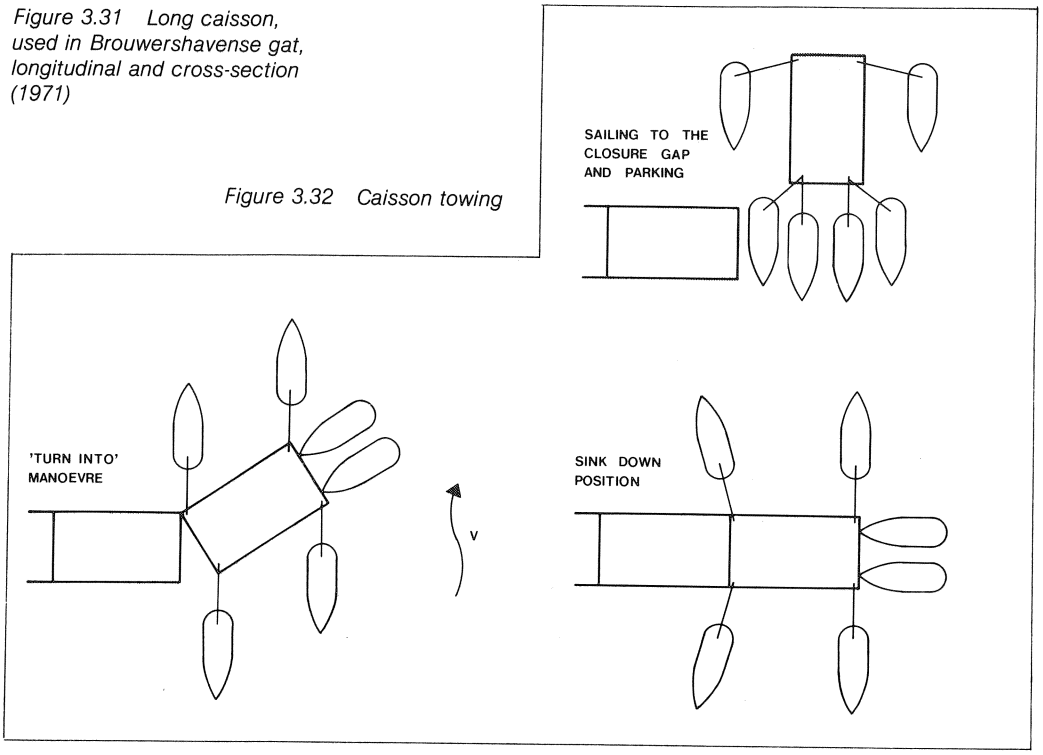

in contact with the sill. The transfer of forces will therefore be concentrated on the lowest sections of the caisson bottom, i.e. those that are at 1/4 from both ends. In this way, a girder is created which is supported favourably so that the moments are minimal in the longitudinal direction of the caisson. The girder is formed by the ribs. The ribs will furthermore seal the space between the caisson and the sill and also increase the friction resistance against horizontal loads caused by differences in water level and wave forces. The „local" supports not only decrease the moments but they also determine in advance in which sections the largest forces are exerted on the bottom slab of the caisson. If the bottom is completely flat, each section of the floor must be able to withstand the maximum expected load.

Positioning of caissons

In general, a caisson will be parked near the closure gap before commencing the placement manoeuvre. When the current velocities have dropped sufficiently, the caisson is towed to the sill and moored.

After placing in position, the valves are opened and the caisson is sunk onto the sill.

Preferably, the caissons will be sunk in position onto the sill just before slack water, so that the flow forces on the caisson and the tugs are maintained as long as possible.

L.W. slack is favourable for placing the caissons, because then:

- the required time for sinking the caisson in position onto the sill is less than at H.W. slack.
- the temporary wooden floating boards can be lower.

But, if:

- there is a longer slack water period at H.W.;
- the water depth above the sill is too small at L.W. (e.g. and abutment caisson); and
- for capacity reasons, two caissons are being placed per day, then H.W. slack may be favourable too.

The required time for placing a caisson depends on the duration of each necessary step. From

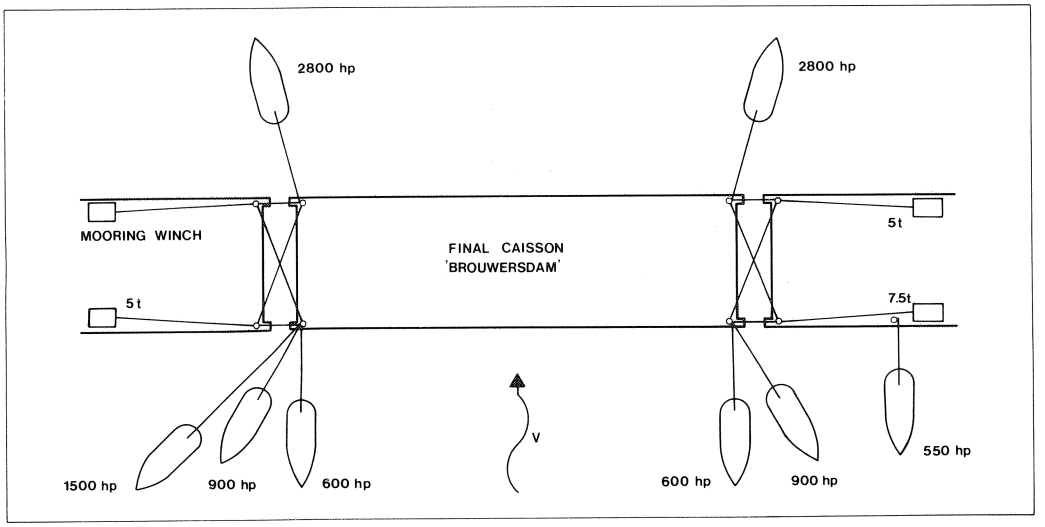

Figure 3.33 Tug configuration during positioning

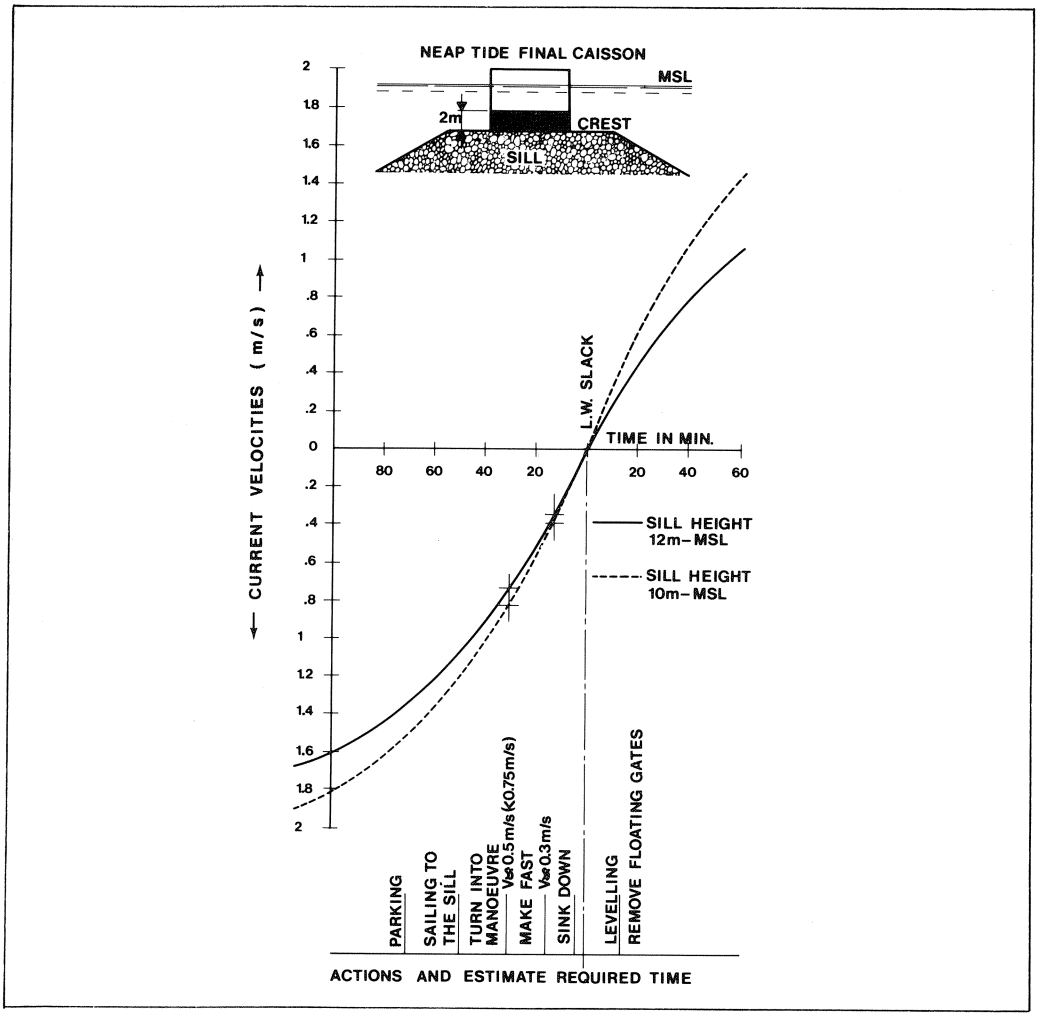

Figure 3.34 Manoeuvring stages of caissons before and after LW slack

earlier caisson closures the following placement operation periods were found for a tidal range of approx. 3 m (Table 3.11) For caisson closures, under circumstances with a tidal range of 6 to 8 m, the placement operation will have to start, when the current velocity is e.g. 2 m/s and stop when the velocity is 0.5 m/s in the opposite direction. In this case, about one hour will be for carrying out the operation during mean tide.
Placement will of course be easier during a neap tide. In these cases, one hour will be enough to carry out an accurate positioning, provided that anchored pontoons equipped with tension winches or fixed anchor points, in addition to tugs, are used (see figure 3.33).

Caisson placement procedure
An example of caisson placement operations is given by the table below.

The duration of the critical phase is determined by the length of the steps 6, 7 and 8 and amounts to 25 min (see figure 3.34).
For mooring the caisson the desired current velocity above the sill is about 0.5 m/s (max. allowed 0.75 m/s.)
As a consequence of the placing of a caisson, local velocities will increase.

The available slack water period is influence by the height of the sill (fig. 3.34)

References

1. Asphalt Revetments of Dike Slopes, **Rijkswaterstaat Communications no. 27.**

2. The Dutch Delta, **A Compromise between Environment and Technology in the Struggle against the Sea (1982),** Royal Netherlands Academy of Arts and Sciences.

3. Closure of Estuarine Channels in Tidal Regions, **Koninklijk Instituut van Ingenieurs (1968),** The Hague.

4. P.H. Nienhuis and J.C. Huis in 't Veld, Grevelingen: From an Estuary to a Saline Lake, **Integration of Ecological Aspects in Coastal Engineering Projects,** Rotterdam, 1983.

5. Svasek, et.al., Sand Transport during Closure of Tidal Channals, **Proc. 13th Conf. Coastal Engineering,** Voll. II, PD865-881, 1972.

Table 3.11

	Action subject	Time before/ after L.W. slack (min.)	Velocity above sill (m/s)
1.	Sailing to gap		
2.	Parking outside	– 130	
3.	Preparing	– 100	
4.	Sailing to the sill	– 70	
5.	„Turn into" manoeuvre	– 55	
6.	Make fast	– 30	0,50 (0,75)
7.	Open valves (sink down)	– 13	0,30
8.	Caisson on the sill	– 5	
9.	L.W. Slack	0	0,0
10.	Levelling		
11.	Remove wooden floating gates	+ 10	
12.	Stone dumping beside + ballast	+ 60	
13.	Open gates	+ 80	

4. Case Studies

4.1. Introduction

Case Studies

J.M. van Westen

4. Case studies

4.1 Introduction

In this chapter three different types of closure methods will be dealt with as „case studies". Two of these originated from the 1953 stormflood disaster in the Netherlands, which cost 1,800 lives and caused considerable damage.
The first case study relates to the repair in 1953 of some dike breaches in the moles at Zierikzee. The second relates to the closure of a sea-arm or estuary - the Brouwershavense Gat - between 1965 and 1971 as part of the Delta Project. This Project was initiated to provide the Netherlands with adequate protection against „future" stormfloods.
The third case study relates to the closure of a flowgap in the Ganges Delta in Bangladesh.

The points of correspondence between these three closures are less extensive than the differences. Points of correspondence include the object of the projects, namely the improved protection of the hinterland and the character of the soil. In all three cases the bottom consisted of material that was subject to erosion at even fairly low current velocities, which meant that the bottom had to be protected against scouring over a sufficient area at the site where closure was to take place. The differences are more numerous and relate to design, research and implementation.
In the Netherlands, the large closures of the Delta Project executed since 1953 or still being carried out were thoroughly prepared beforehand on the drawing board and during preliminary studies in laboratories and in the field. In addition, new methods were developed for the execution of these works. The projects were made accessible by the construction of infrastructural works such as harbours, construction harbours and roads, etc. This meant that these closures had to be implemented with appropriate materials and suitable equipment and executed within a tight time-frame. In the case of closures resulting from calamities such as the 1953 stormflood disaster, the time element is decisive. In the beginning, the size of the breach is in most cases fairly small. The gap is, however, increased with each tidal movement.

This makes it necessary to improvise and to use whatever material or equipment is available locally, with the sole aim of closing the gap as quickly as possible. In this respect the insight and experience gained from previous closure works is of major importance. The experience gained during the large closures in 1953 showed model research to be an invaluable aid. On the other hand, provisional closures at an early stage may be assumed to prevent the need for larger closures at a later stage. The closure in Bangladesh forms part of a greater number of closures of flow gaps in the Ganges Delta. These may, as far as the structures themselves are concerned, be very similar to the ones provided for in the Delta Act in the Netherlands, but their execution is characterized by a more improvised approach. This improvization is caused on the one hand by a lack of hydraulic data, which makes it difficult to predict the consequences of such a closure, and by a lack of practical experience on the other.

4.2. Closure of Flow Gaps in the Harbour Moles at Zierikzee

Closure of Flow Gaps in the Harbour Moles at Zierikzee

J.M. van Westen

4.2 Case 1 closure of flow gaps in the harbour moles at Zierikzee in 1953

4.2.1 Causes and generation of the flow gaps

The Storm

On January 31st, 1953 a heavy storm rose over the North Sea area.
Initially, the wind was south to south-westerly, i.e. an offshore wind in the southern part of the North Sea. Later the wind veered to north-west and west-north-west. Gradually the situation worsened. At 1800 GMT that day, the water was being driven over the whole length of the North Sea, i.e. a stretch of nearly 1,000 km, towards the coasts in the southern part. The water level rose steadily as the force of the wind field increased. This weather phenomenon resulted in extremely high water levels along the coasts of the North Sea (see figures 4.1 and 4.2). The storm occurred two days after full moon and coincided with the spring tide of February 1st, 1953.
Figure 4.2 provides an impression of the water levels during the floods throughout the entire disaster area, while figure 4.1 shows the water levels in the Eastern Scheldt.

The moles of the Zierikzee entrance canal (see fig. 4.3.)
Of the two moles of the entrance canal at Zierikzee, the crown of the western mole was the lowest, i.e. approximately 4.20 m. above MSL. The crown of the eastern mole was approximately 4.40 m. above MSL. Figure 4.4 shows a cross-section of the western mole. A comparison of the heights of the crowns of the moles with the maximum recorded water levels at Zierikzee (see fig. 4.1), indicates the maximum water level to have been nearly as high as the crown of the eastern mole and even higher than that of the western mole. It is therefore not surprising that both moles were badly damaged. On the inner slope, which was often steeper than 1:2, the water flowing and breaking over the top caused large-scale erosion. In some instances the erosion was so severe as to affect the outer slope as well. This was the characteristic pattern throughout the disaster area. Where the dikes were too low the water breaking over the top caused erosion on the inner, i.e. polder, side of the dike. In instances of severe erosion on the inner side a breach would sometimes be caused, either as the dike continued to be eaten away or as the remaining part of the dike gave way under the water pressure (or as the result of both). In the beginning these breaches were generally no lower than the adjoining ground level. But since virtually the entire disaster area was below sea level, each tidal movement would erode the breach still further.

In this way two flow gaps were created in both the western and the eastern moles. It proved possible to seal one of the gaps in the western mole at an early stage with sandbags. The enlargement and closure of the three remaining flow gaps are discussed below.

4.2.2 Location of the flow gaps

The western mole formed part of the sea defence of the (at that time undivided) Schouwen polder with a surface area of 8,860 ha. The location of the flow gaps is shown in fig. 4.5, while figure 4.6 provides an impression of the size the flow gaps had reached by May 1st, 1953. The eastern mole formed part of the sea defence of the Zuidhoek polder with a surface area of 300 ha.

4.2.3 Enlargement of the flow gaps

In the early stages the flow gaps were not deep and were limited in size. The enlargement of the two flow gaps in the eastern mole is discussed under 4.2.5, where the closure of these gaps is described. The enlargement of the flow gap in the western mole needs to be viewed in conjunction with the other flow gap in the sea defence of the Schouwen polder, namely the Schelphoek gap. The filling and emptying of the Schouwen polder took place almost entirely through the larger Schelphoek flow gap. The large distance -approx. 10 km. - between the two flow gaps and the large area of the Schouwen polder resulted in a big difference in phase and amplitude between the water movement on the harbour and polder sides of the flow gap in the western mole

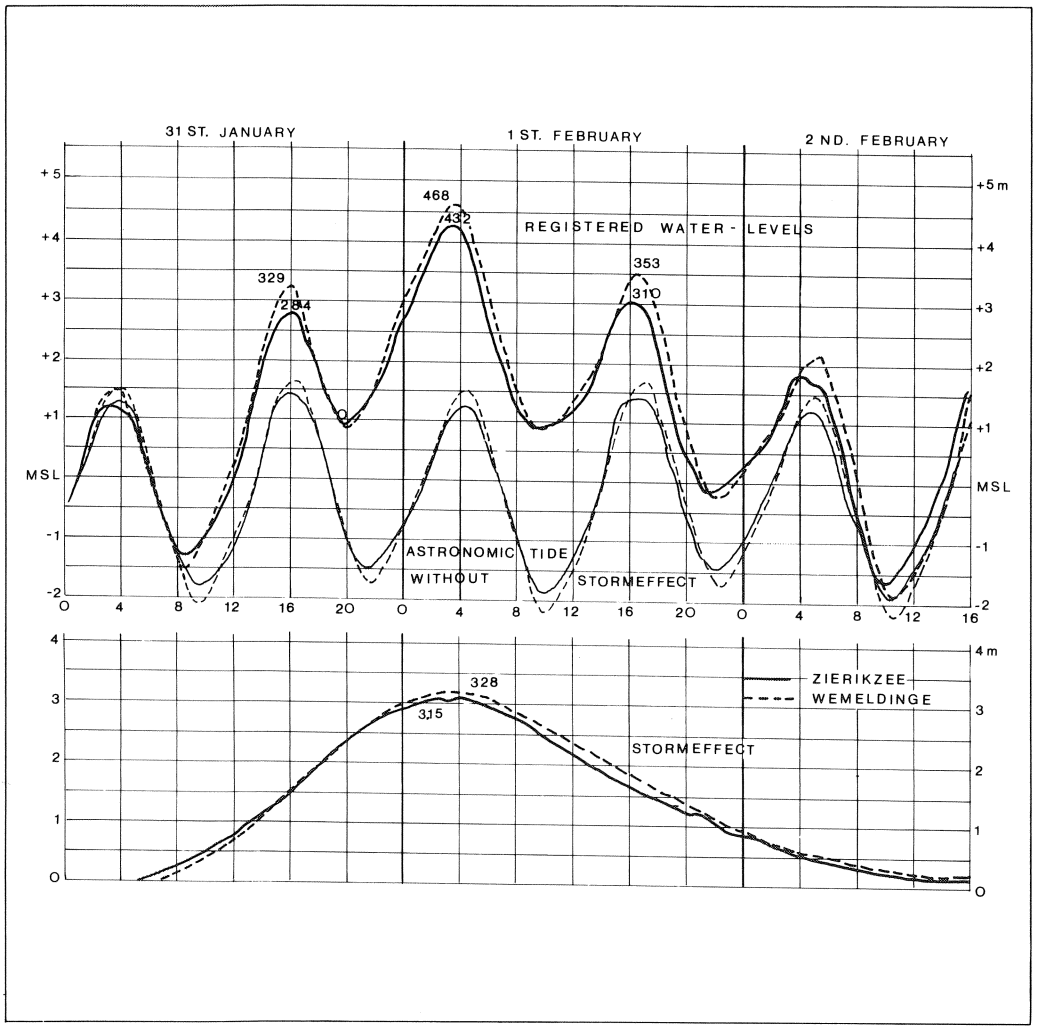

Figure 4.1. Eastern Scheldt, registered water-levels and stormeffect

(see fig. 4.7). The largest difference between the water levels on the polder and harbour sides was approx. one metre on March 23rd. A strong current was generated through the flow gap, thus increasing its size and depth. As a result of this development the flow gap had already attained a width of 60 m and a depth of 20 m by the beginning of March. In addition, part of the bed in the entrance canal between the flow gap and the

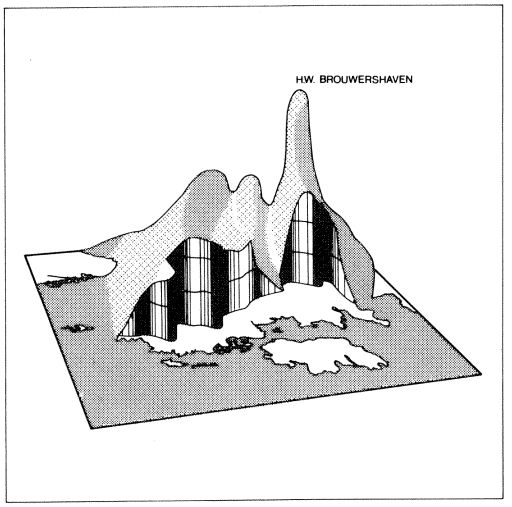

Figure 4.2. Model of the height of the sea level on February 1st as opposed to mean sea level at High Water under normal conditions in Brouwershaven.

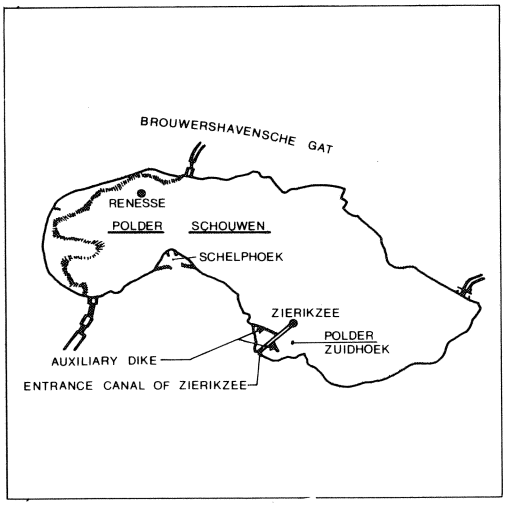

Figure 4.3. Location of the Zierikzee Entrance Canal.

Figure 4.4. Cross section of the western mole of the entrance canal of Zierikzee.

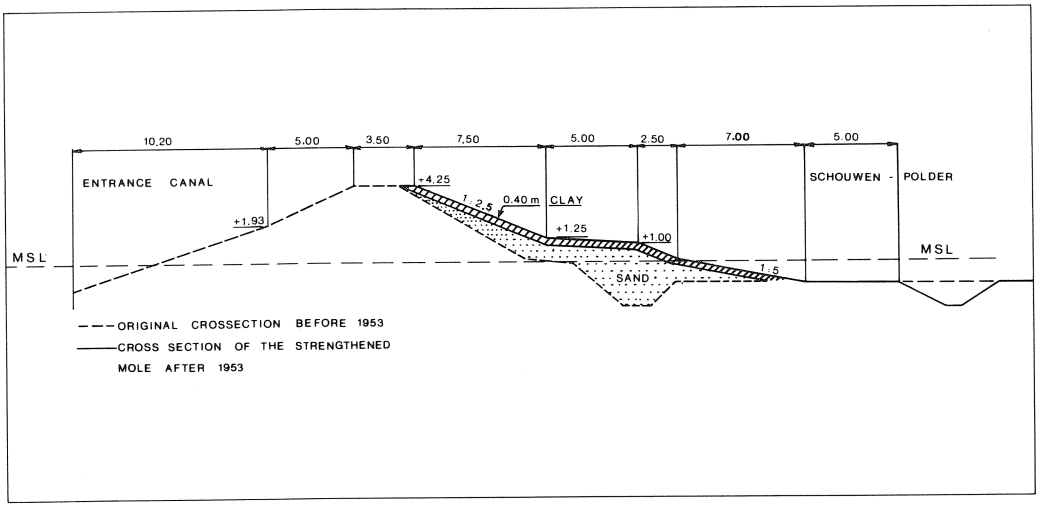

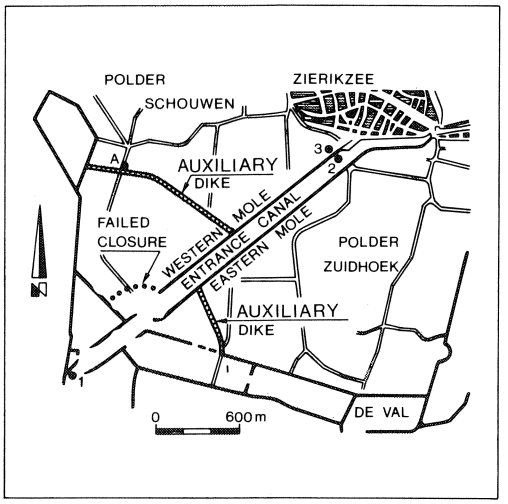

Figure 4.5. Entrance canal of Zierikzee. Measurements of water levels and currant velocities ware taken at sites A, 1, 2 and 3 (see figure 4.7)

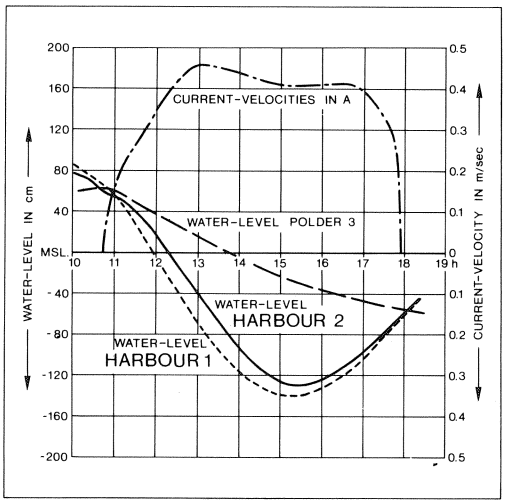

Figure 4.7. Measurements of water levels and current velocities on March 23th 1953. For the sites where measurements were carried out see figure 4.5

harbour mouth was deeply eroded. An additional consequence that deserves to be mentioned is the fact that shipping traffic through the entrance harbour was badly impeded by the strong cross-currents flowing through the gaps in the two moles.

When one considers that practically all transport to and from Zierikzee - at that time the crisis centre for a large area - had to take place by water, it will be appreciated that there was more than one reason for a speedy closure of the flow gaps.

4.2.4 Closure of the flow gap in the western mole

The first attempts

Initially, the closure of the flow gap was of a rather improvised nature. Attempts were made with the means available, initially from the immediate surroundings and later from other places, to close the flow gap at an early stage. When these attempts failed, the closure of the gap was eventually achieved by using a planned approach and with the aid of physical model research.

Immediately after the night of the disaster, attempts were made to close the gap with sacks filled with clay and/or sand. These efforts failed as the sacks were not sufficiently stable to withstand the force of the current and were carried away.

This is not so surprising when it is considered that the stability of the dumped rubble depends on the dimensions (i.e. diameter) and density of the material under the water surface. Material such as sandbags which must be handled manually generally weigh no more than 300 or

Photo KLM AEROCARTO

Figure 4.6. The condition of the Zierikzee moles on May 1st 1953. On the left the western mole and on the right the eastern mole.
The picture shows the flow gaps in the moles very well.

400 N and, as a result, can never be large. In addition, clay and sand are low-density materials when compared for example with rubble.

The following formula illustrates the fact that the clay and sandbags used were far too small to be stable in the current velocities encountered:

$$\Delta D > \alpha \frac{v^2}{2g}$$

where:
$\triangle$ = relative specific density;
D = D_{50};
α = coefficient
v = velocity
g = acceleration of gravity;

$$\Delta = \frac{\rho_c - \rho_w}{\rho_w} = \frac{1800 - 1020}{1020} = 0.76$$

where:
ϱ_c = specific density of clay;
ϱ_w = specific density of salt water

D = average diameter (D_{50}) of the material in metres.
If the clay bags are assumed to have been spherical the equivalent diameter D becomes

$$D = \sqrt[3]{\frac{6G}{n\,\rho_c\,g}}$$

where:
D = equivalent diameter of the clay bag in m.;
G = weight of clay bag = 400 N.;
ϱ_c = specific density of clay = 1800 kg/m³;
g = acceleration of gravity.

$$D = \sqrt[3]{\frac{6 \times 400}{n \times 1800 \times 9.81}} = 0.35$$

The coefficient α depends on the degree of turbulence.
A common value is 1.1, or for highly turbulent flows 1.4.
v = current velocity in m/s. In view of the drop in height of approx. one metre referred to in 4.2.3, the current velocity will be $\sqrt{2\,gh} = \sqrt{2 \times 9.81 \times 1} = 4.4$ m/s. It is however possible for the gap to act as a clear overfall, thus reducing the current velocity. Assuming an average high-water level in the entrance channel of 1.50 m above MSL and the crest of the breach to be 1.50 m. below MSL and disregarding the velocity head, $H \cong 3.0$ m and $V_{max} = \sqrt{2.g\ 1/3\ H} \cong \sqrt{2.g.1} = 4.4$ m/s.
In other words, the calculated current velocity of 4.4 m/s is also equal to the critical flow.

$$0.76\ D > 1.4\ \frac{4.4^2}{2g};\ D > 1.84\ m$$

This indicates that the clay bags used, with their average diameter of 0.35 m, would not be stable at high current velocities.
When this attempt to close the breach failed, a local contractor began to construct a cofferdam. At that time the breach was still so shallow that it could be waded through at low water.
The construction of the cofferdam (see figure 4.8) entailed the gradual horizontal closure of the breach. As noted in Chapter 3, two cases may be distinguished, namely:
a) the crest of the breach is high and a situation of clear overfall is reached;
b) the crest of the breach is low and clear overfall is not obtained.

When the cofferdam was first being built case a) applied and $V_{max} = \sqrt{2g.1/3H} = 4.4$ m/s. At this velocity the foundation of the breach proved unstable and eroded. The deepening of the breach increased the current velocity. The result was that such substantial channels were created that the attempt had to be abandoned.
Subsequently, efforts were made to close the breach with boulder clay taken from Lake IJssel. Boulder clay is highly cohesive and this material was successfully used in 1932 when the Zuiderzee was closed off by the Afsluitdijk (Closure Dam). The tidal difference near the Afsluitdijk, in the nothern part of the Netherlands, is however much smaller than in the south-west of the country. This attempt also failed because the material could not withstand the force of the current in the flow gap and because boulder clay embankments exceeding 7-8 m. in height have a tendency to sag. Before more extensive closure methods were undertaken, a final attempt was made to close the breach in the beginning of March by sinking several ships at a short distance behind the breach.
It was, however, inevitable that openings remained between the ships, resulting in local flow concentrations. Attempts were made to close those openings with rubble. Rubble dumping is rather timeconsuming, however, while a concentrated current can erode the bed considerably in a very short period of time. This attempt therefore also failed.

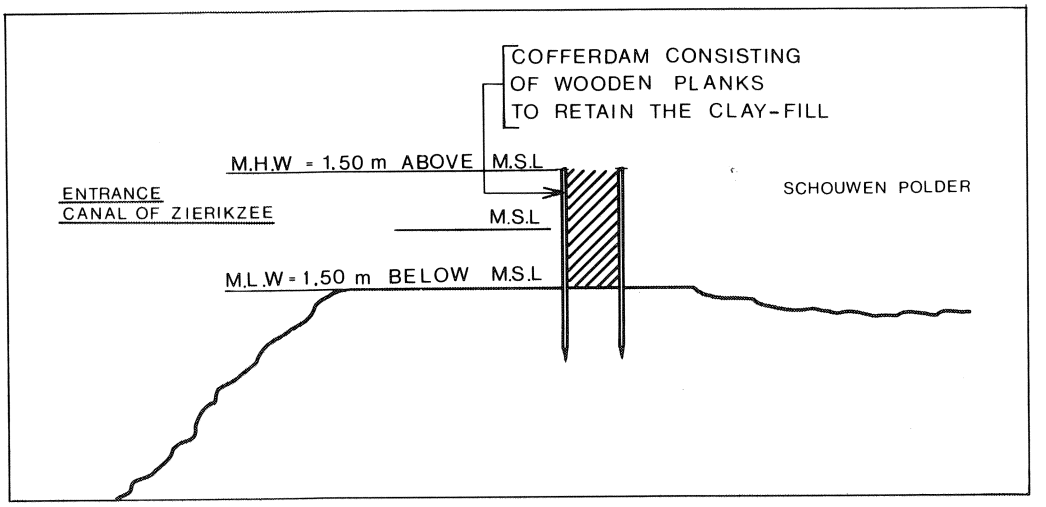

Figure 4.8. A first attempth to close the gap in the western mole.

The final closure method used

A. Location of an auxiliary dike with a closure gap.

Finally it was decided that closure would not take place in or near the alignment of the breach but further inland. For this purpose it was decided to build an intersection dike, as shown in figs. 4.3 and 4.5. The underlying conditions for this decision are explained below.

Instead of executing the closure in unstable circumstances, i.e. in the ever-deepening and widening flow gap, a location was chosen where the actual dimensions of the gap could be determined and controlled. With this method the closure dimensions were such that, during the time required for the closing operation, no flow velocities were to be expected that would endanger the construction. More specifically, this meant that if the erosion of the subsoil in a closure gap were limited by placing a bed protection - which in 1953 still consisted of osierwood mattresses weighted with layers of rubble or quarry stones - then the occurring flow velocities would have to be such that neither the stability of the mattress (fascine) and rubble nor the structure would be endangered by erosion along the edges of the bed protection.

The danger of erosion can obviously be minimised by extending the length of the bed protection, so that the erosion (i.e. scouring holes) along the edges of the bed protection will take place further away from the closure construction.

The auxiliary dike was built on a relatively high site (see fig. 4.9), and its alignment was not traversed by channels, unlike at Schelphoek. This type of closure is called a „ground level" closure (see chapter 3). The closing structure was relatively long so as to maintain as wide as possible a wet cross-section and thus to prevent unacceptably high flow velocities.

The auxiliary dike, which was approximately 1,170 m long, was aligned longitudinally in three sections (see figs. 4.5 and 4.10a.)

The first section running from the western mole was 65 m long and consisted of boulder clay excavated from Lake IJssel. The second section, which equalled the actual length of the breach,

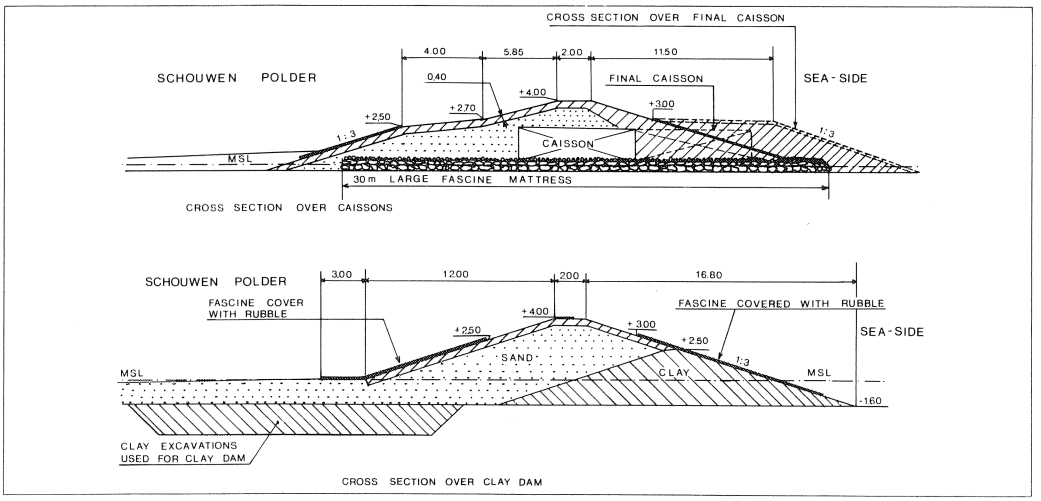

Figure 4.9. Cross sections of the auxiliary dike

was 515 m long, while the third, 590 m in length, was a clay dam behind which hydraulic sandfill was pumped (see fig. 4.9).

B. Means used for the closure.

Although consideration was initially given to closing the gap in layers with mattresses weighted with rubble, it was finally decided on a caisson closure instead. The reasons behind this decision were:

- the desire to gain experience for the subsequent closure of the Schelphoek flow gap with caissons;
- to carry out a rapid closure with large units constructed elsewhere;
- the large number of fascine workers required for a closure using mattresses could not have been spared from other places, or only with great difficulty.

Caissons had been previously used on several occasions for the closure of flow gaps, namely for the reclamation of Walcheren (1945 - 1946) and the damming of the Brielse Maas (1950) and Braakman (1952). In 1953 the Netherlands still had one BX type caisson, that had been stored in a harbour at Sluiskil, and a number of Phoenix caissons of the largest type (AX) were made available by the U.K. Admiralty.

It was however evident from the outset in 1953 that the available caissons would not go nearly far enough. For this reason a decision was taken early in the piece to construct a large number of „standard" or „unit" caissons measuring 11 x 7.5 x 6 m (length x width x height), with a 2 m capping unit to provide extra height. By combining these units in various configurations, the caissons could be used for the construction of auxiliary dikes at ground level, the formation of abutments or for blocking channels. The standard caissons proved to have too great a draught for sealing the final gap in the auxiliary dike, for which reason some of the capping units were fitted with bottoms and used as caissons. The dimensions of these caissons were 11.00 x 7.50 x 2.12 m (length x width x height). The draught was 0.88 m and each caisson weighed 80 tonnes (see fig 4.11).

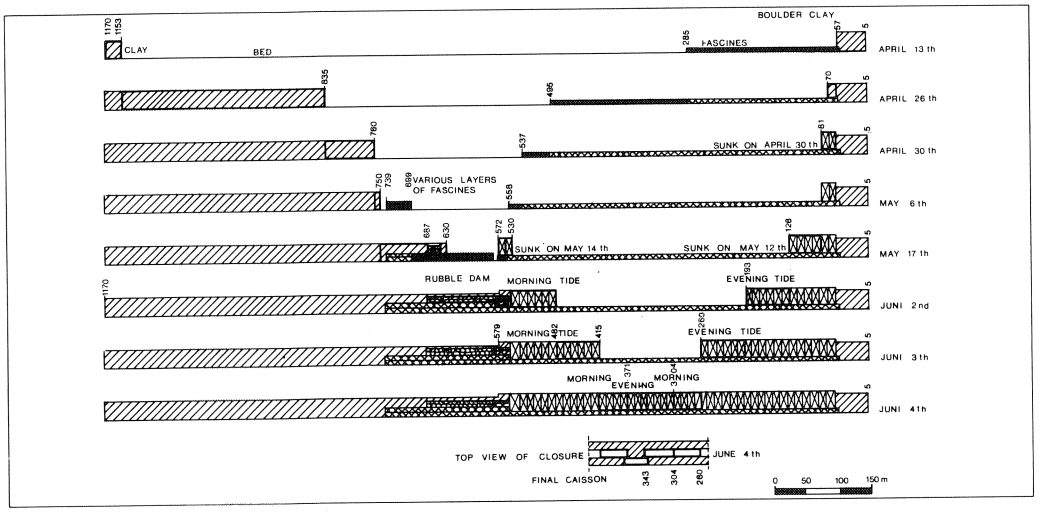

Figure 4.10a Closure scheme auxillary dike

Figure 4.10b. Scheme for lowering caissons

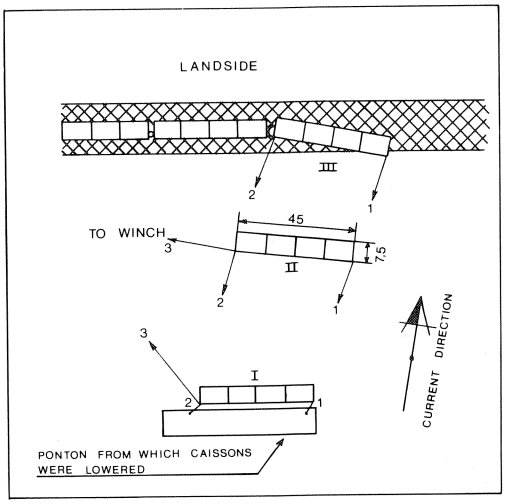

Figure 4.11. Caisson 11.00 m long 7.50 m wide and 2.12 m high.

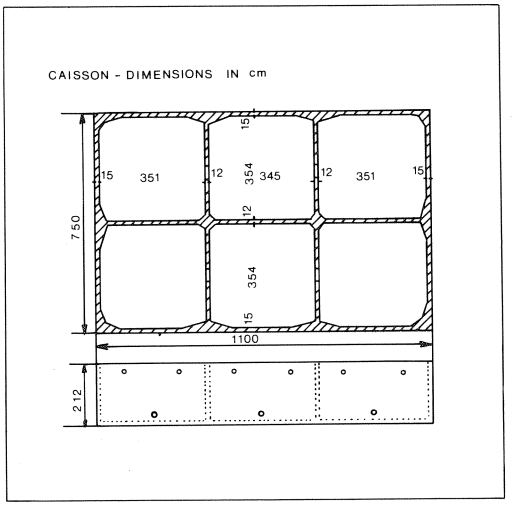

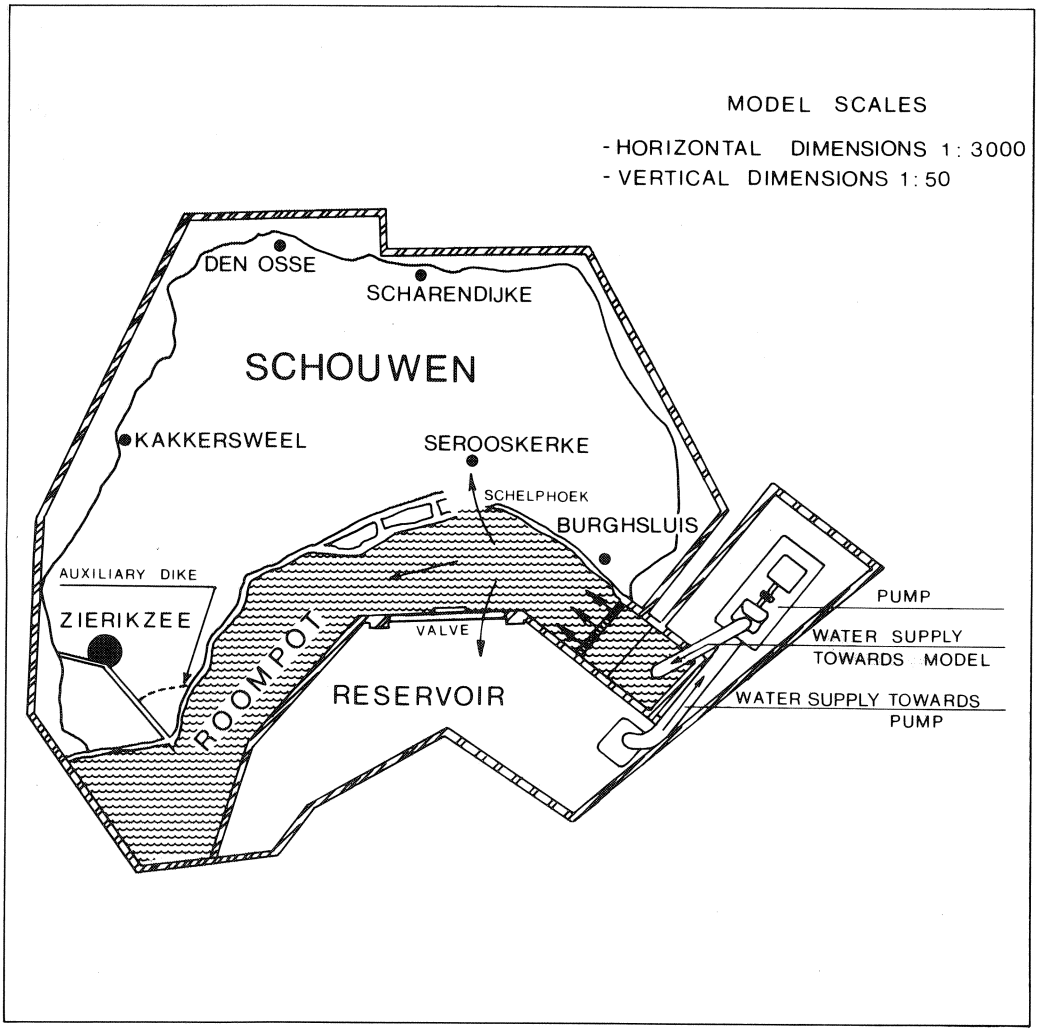

Figure 4.12. Tidal model Schouwen.

C. Hydraulic research

Flow measurements and gauge observations were made between March 22nd and 25th by way of preparation for the closure plan. The points where the observations were made are shown in Fig. 4.5; points 1 and 2 are located in the entrance canal, point 3 in the Schouwen polder and point A in the Schouwen polder and in the alignment of the auxiliary dike.

Fig. 4.7 lists the measurements taken on March 23rd. At points 1, 2 and 3 the water levels were measured and, at point A, the current velocities. The maximum current velocity proved to be 0.6 m/s, the ebb prism 6.7 million m^3 and the flood prism 12.4 million m^3.
In the Delft Hydraulics Laboratory, a tidal model was built to study the tidal action in the Schouwen polder as affected by the two breaches at Schelphoek and Zierikzee (see fig. 4.12). In this model, the manner in which the tidal action and currents in the breaches would change as a consequence of the progress of the activities prior to and during the closure of the gap was examined.
For the horizontal dimensions the scale of the model was 1 : 3000 and for the vertical dimensions 1 : 50. In addition, a detailed model was built to a scale of 1 : 50 of the breach in the western mole and a model to a scale of 1 : 50 for the manoeuvring of small caissons singly or in combination for ground-level closures.
These models proved to be valuable not only for the actual data they provided but also because they offered a possibility to study and practise the manoeuvres prior to or during the closure in the presence and with the collaboration of the persons who would be actively involved with the execution of the works.

D. Activities carried out prior to the final closure

The progress of the works is shown schematically in figure 4. 10a. The construction of the eastern and the western abutments and the installation of bed protection were started simultaneously. The eastern abutment consisted of boulder clay and the western abutment of clay, whereas the bed protection at the closure gap consisted of fascines (i.e. flexible layers of brushwood weighted down by stones). The fascines or mattresses were 30 m long and 20 m wide and were placed lengthwise in the direction of the current. The construction of the boulder clay abutment as well as the installation of the bed protection at the closure gap progressed speedily and was completed on May 7th.
The construction of the clay abutment proved to be more troublesome. On May 7th 160 m still remained to be built. As a result of the increase in the current velocities, two fascines were placed over this length of the ground level to prevent scouring. On April 30th and May 14th respectively, abutment-caissons were placed on the bed protection. The abutment caissons comprised two linked-together caissons of the same sizes as mentioned under B. These abutments served as connecting structures between the abutments and the caissons to be places in the closure gap created in this manner.

In the meantime, the work on the clay abutment had progressed some tens of metres and thus, on May 14th, the aperture towards the western abutment had been reduced from 160 to 125 metres. Because of the ever-decreasing wet cross-section, the flow velocity had increased to such an extent that a more resistant material than clay had to be used. Quarry stones and rubble were therefore used for the remainder of the western abutment.

E. The final closure

What still remained to be done was the closure with caissons of the aperture between the two abutments. The length of time for positioning closure caissons is usually very short since prolonged exposure of the bed protection to the ever-increasing current velocities must be avoided. (The caissons used in 1953 consisted of one-piece closed units.) It should be noted, however, that with the relatively high position of the sill in a ground-level closure, and a tidal range of about 3 m, clear overfall conditions are generated. The current velocity and the tidal prism occurring in the closure gap are shown schematically in figure 4.13 as a function over time.

After clear overfall conditions have been reached, the flow velocity will no longer increase even though the aperture of the closure gap is further restricted in a vertical direction. The gap in the auxiliary dike was closed by positioning a number of linked caissons at slack water before high tide. Due to the in situ position of the ground level, the first set of four linked caissons was positioned during the springtide high water of May 12th. The other caissons were positioned

on June 2nd, 3rd and 4th in accordance with table 4.1.

Table 4.1. Dates of positioning the caissons

dates of positioning	western side mornings	evenings
June 2nd	6 × 11 m	
June 3rd	6 × 11 m	
June 4th	4 × 11 m	3 × 11 m (closing-caisson)
dates of positioning	**eastern side mornings**	**evenings**
June 2nd		6 × 11 m
June 3rd		6 × 11 m
June 4th	4 × 11 m	4 × 11 m

The height of the ground level and of the sill made it impossible to perform the positioning manoeuvres by tugs. Instead the caissons were carefully lowered by winches fixed to an anchored pontoon and guided in the flood-stream towards the sill (see fig. 4. 10b).
An additional winch was set up to manoeuvre the caissons in the longitudinal direction of the closure.

The exact timing for the positioning of the caissons had to satisfy certain conditions, such as:

- at or around the time of HW in connection with the draught of the caissons and the height of the ground level and the sill;
- as close as possible to the slack-water period before HW, as the velocity of the current is then at its lowest, thus minimising the load on the cables between the pontoon and the caissons, but still sufficiently before the HW turn of the tide to ensure sufficient tension on the wires.

During the closure dates of June 2nd, 3rd and 4th, the water levels and current velocities were constantly monitored in order to keep the closure operators well-informed of the ongoing situation.
Fig. 4.14 shows the difference in level during

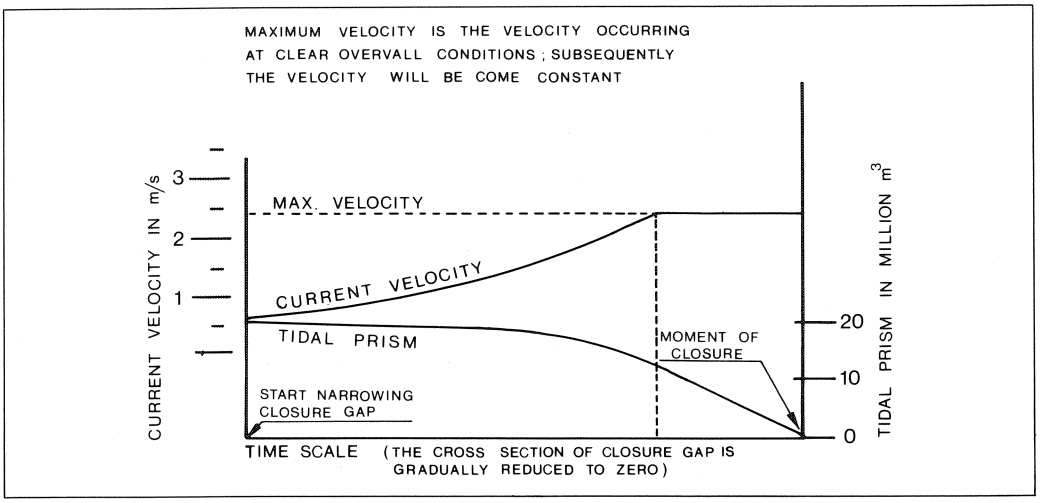

Figure 4.13. The current velocity and the tidal prism as a function of time.

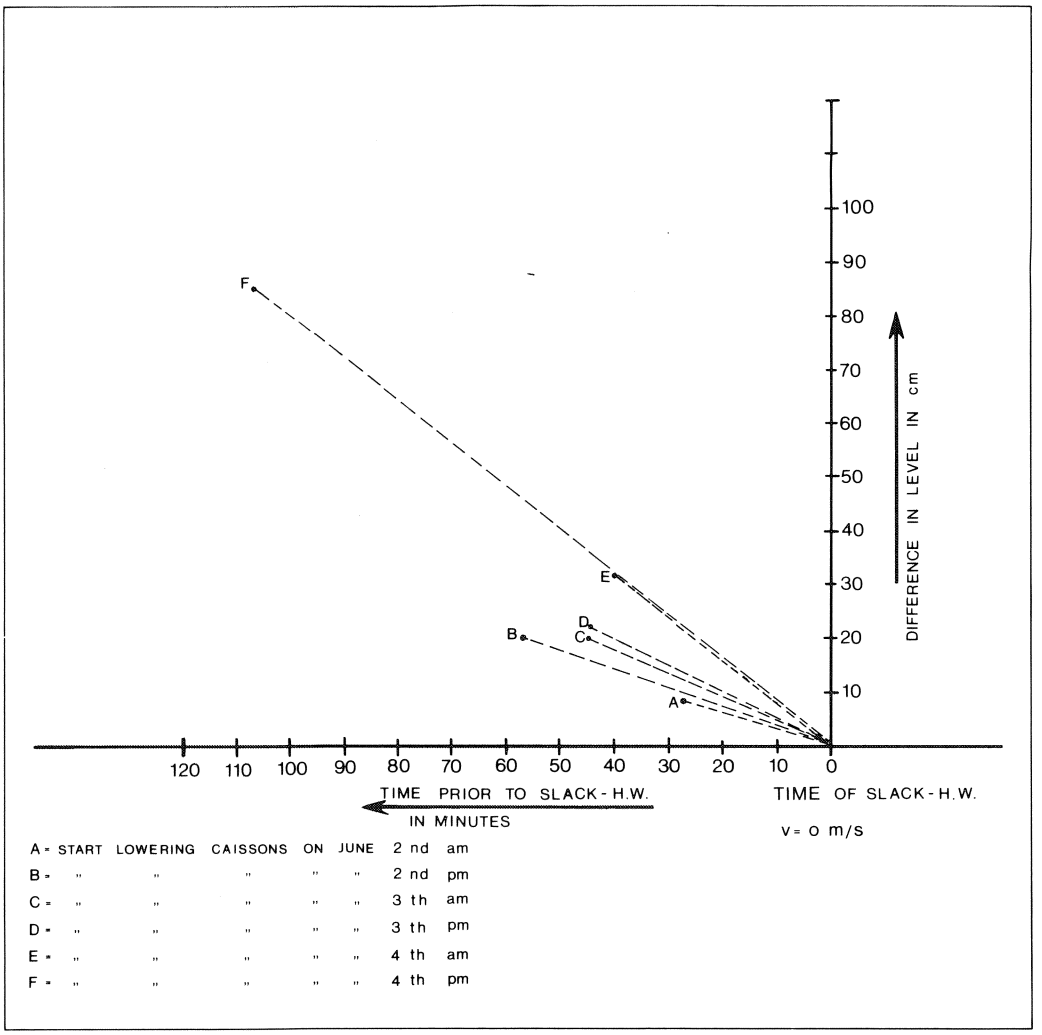

Figure 4.14. Start of lowering caissons in relation to the time of slack HW and the rate of difference in level.

which the caisson-installation was started and the decrease in the difference in level per unit of time throughout the operation. The figure shows that the positioning of the caissons on June 2nd A.M. was started just before the turn of the tide. On the other hand, on June 4th P.M., the positioning started some time before the turn of tide at a difference in level of 0.85 m. The probable reason for this early start was that the two last

caisson units had to be placed during the same slack water period and there had also to be sufficient time for placing the caissons, which were actually to seal off the gap. Immediately after the caissons were positioned they were ballasted with sand. This caused differential settlement. After they were placed, pore pressure occured under the caissons, which was countered by constructing a clay dam on the seaward side of the caissons. The problem was only completely solved, however, after sandfill was pumped behind the caissons on the polder side.

F. Completion of the auxiliary dike
The auxiliary dike was finally finished according to the cross-sections shown in fig. 4.9.

4.2.5 Closure of the flow gaps in the eastern mole

As a result of two breaches in the eastern mole, the Zuidhoek polder (see fig. 4.3 and 4.5) was connected to the entrance channel.
The Zuidhoek polder had a surface area of some 300 ha. The breaches were initially about 30 and 40 m long, with a depth of approx. 1.50 m below MSL (mean low water). The maximum current velocities in the breaches were not initally determined by the basin area (300 ha) but by the situation of clear overfall in the gaps. At an average high water of 1.50 m above MSL, $v_{max} = \sqrt{2}\ g.1/3H = 4.4$ m/s. The resultant current velocities led to the widening and deepening of the breaches.

This process would have continued until a situation of equilibrium had been reached, i.e. a wet cross-section area of such size that the resultant current velocities no longer caused erosion. The bed material in the breaches meant that an equilibrium situation was reached at a current velocity of approx. 1 m/s. The surface of the wet cross-section of the breaches at which this current velocity occurs may be calculated from the average maximum rise and fall of the tide per unit of time and the size of the basin to be filled. The average maximum rise and fall of the tide was approx. 1 m/hour and the size of the basin 300 ha.

The resultant discharge is $\frac{3.10^6}{3600} = 833$ m³/s.
At an acceptable current velocity of 1 m/s the combined wet cross-section of the two breaches would therefore have to have amounted to around 830 m² in order to prevent further erosion. It is not known whether the breaches in fact attained this size.

Once again closure was effected by means of an auxiliary dike (figs. 4.3 and 4.5). The auxiliary dike consisted of bottom protection of mattresses weighted down with a stone dam. As the stone dam was built up, the current velocity increased until a situation of clear overfall was reached. The crest of the sill was approx. 1 m below MSL.

$$v_{max} = \sqrt{2g \times 1/3\ H} = \sqrt{2g\ \frac{2.50}{3}} = 4.0 \text{ m/s}$$

The D_{50} of the stone required may be calculated from

$$D_{50} > \frac{\alpha\ v^2}{2g\ \Delta}$$

where:

D_{50} = the average diameter of the stone material in m;
α = a coefficient the size of which depends on the degree of turbulence, in this case 1.4;
v = current velocity in m/s;

$$\Delta = \frac{\rho_s - \rho_w}{\rho_w} = \frac{2650 - 1020}{1020} = 1.6$$

ϱ_s = specific density of stone;
ϱ_w = specific density of water.

$$D_{50} > \frac{1.4 \times 4.0^2}{2g \times 1.6};\ D_{50} > 0.73 \text{ m}$$

If the stone is assumed to be spherical this means a G_{50} of $1/6\ \eta.\ D^3.\varrho_s.g = 1/6\ \eta \times 0.73^3 \times 2650 \times 9.81 = 5300$ N.

Given for example a stone assortment of 300 – 1000 kg.
The two breaches in the eastern mole were then sealed with pumped sand. The construction of

the auxiliary dike had reduced the tidal basin behind the breaches from approx. 300 ha to approx. 20 ha. During the final stage of the closure, as the flow velocities in the ever-decreasing gaps increased, increasing amounts of sand were carried away by the current. However, the comparatively small surface area of the basin enabled the breaches to be sealed with sand without undue difficulty.

4.2.6 Contractual arrangements for the 1953 closure works

It will be evident that a flood disaster such as that of February 1st, 1953 leaves no time for the proper preparation of construction works that have to be undertaken totally unexpectedly and in a large number of places at the same time. There is no opportunity to make tender documents and drawings beforehand or to draw up estimates and an operating plan. This also means that it is not possible to put the work out to tender. The work must instead be got under way using suitable contractors and the equipment and materials available. Nevertheless it was considered desirable in 1953 to reach prior financial agreements wherever possible. These took the form of so-called cost-plus contracts. These contracts were primarily designed to lay down regulations between the contracting parties concerning payment. The cost-plus contracts used in 1953 for works in the disaster area contained the following provisions:

a. equipment was paid for on the basis of hourly rates specified in the cost-plus contracts. Different rates were laid down for equipment in use or idle equipment;
b. deliveries and payments commissioned by the governement were reimbursed at cost price plus 8%;
c. employees' wages and travel and accomodation expenses were reimbursed at cost price plus 13%;
d. in the case of sub-contracted work, the principal contractor was reimbursed for the cost of the sub-contracted work plus 4%.

The premiums were intended to cover risks, profits and general expenses; these factors were also designed to be covered by the rates referred to in point a.

4.3. Closure of the Brouwershavenschegat by the Construction of the Brouwersdam

Case Studies

J.M. van Westen

4.3 Closure of the Brouwershavensche gat by the construction of the Brouwers dam

4.3.1 Location of the Brouwers dam in the Delta Plan (see fig. 4.15)

The Brouwers dam is the approximately 6.5 km long dam in the south-west of the Netherlands, connecting the heads of the islands of Goeree-Overflakkee and Schouwen-Duiveland. The construction of the Brouwers dam and, in particular, the closure of its two final gaps in 1971, was the last major closure before the construction of the Oosterschelde dam.
Before the start was made with the construction of the Brouwers dam the construction of the Grevelingen dam to the east was completed.
The basin area closed off by the Brouwers dam is the present Lake Grevelingen between the Brouwers dam and the Grevelingen dam. It has a total surface area of some 13,500 ha, of which 10,000 ha are below and some 3,500 ha above MSL.

4.3.2 Siting the dam

Alignment investigations were commenced as early as 1961, ten years before the closure. The choice was eventually narrowed down to four possible alignments for further investigation, as shown in figure 4.16. The respective merits of these alignments were assessed on the basis of data drawn from:

* hydraulic and geotechnical site investigations;
* desk research and preliminary laboratory studies;
* cost estimates.

The hydraulic and geotechnical site investigations consisted of:

- soundings of the entire Brouwershavensche Gat area;
- current measurements, consisting of two series of simultaneous current-velocity, current direction and water-level measurements;
- wave measurements made with the self-recording wave measurement post B.G.1 installed in 1958 (see fig. 4.16) and with a floating tank;
- ground borings and cone penetration tests.

* The desk research and preliminary laboratory studies consisted of:
  - model analysis in a scale model built to a horizontal scale of 1:300 and a vertical scale of 1:100;
  - mean tide calculations for conditions after the closure of the Grevelingen dam (in 1961 the Grevelingen dam was still open).

The prototype current measurements carried out in the Brouwershavensche Gat provided data on the situation as it was with Grevelingen still open. With the aid of tide calculations and model analysis, flow data were obtained for later conditions of greater relevance for the Brouwers dam, i.e. upon the closure of the Grevelingen.

The cost estimates were obtained by making a rough estimate of the materials required for each of the possible alignments, multiplying these by a unit price and then aggregating the costs thus obtained.
Certain additional costs were added to the results, such as the need to heighten and strenghten the dike section between Den Osse and West-Repart in the case of Alignment IV.

On the basis of the above data a final alignment selection was made.
After weighing a variety of considerations, especially technical factors, the choice eventually fell on Alignment I. The following general observations may be made about this assessment process.

All four dam alignments were designed in such a way as to cross the direction of flow in the Brouwershavensche Gat, Kous and Springersdiep at right angles for two reasons. In the first place it was at that time (1961) still assumed that the channels would be closed with sluice caissons. In order to disturb the flow pattern through the open caissons as little as possible it is desirable for the direction of flow to be crossed at right angles.

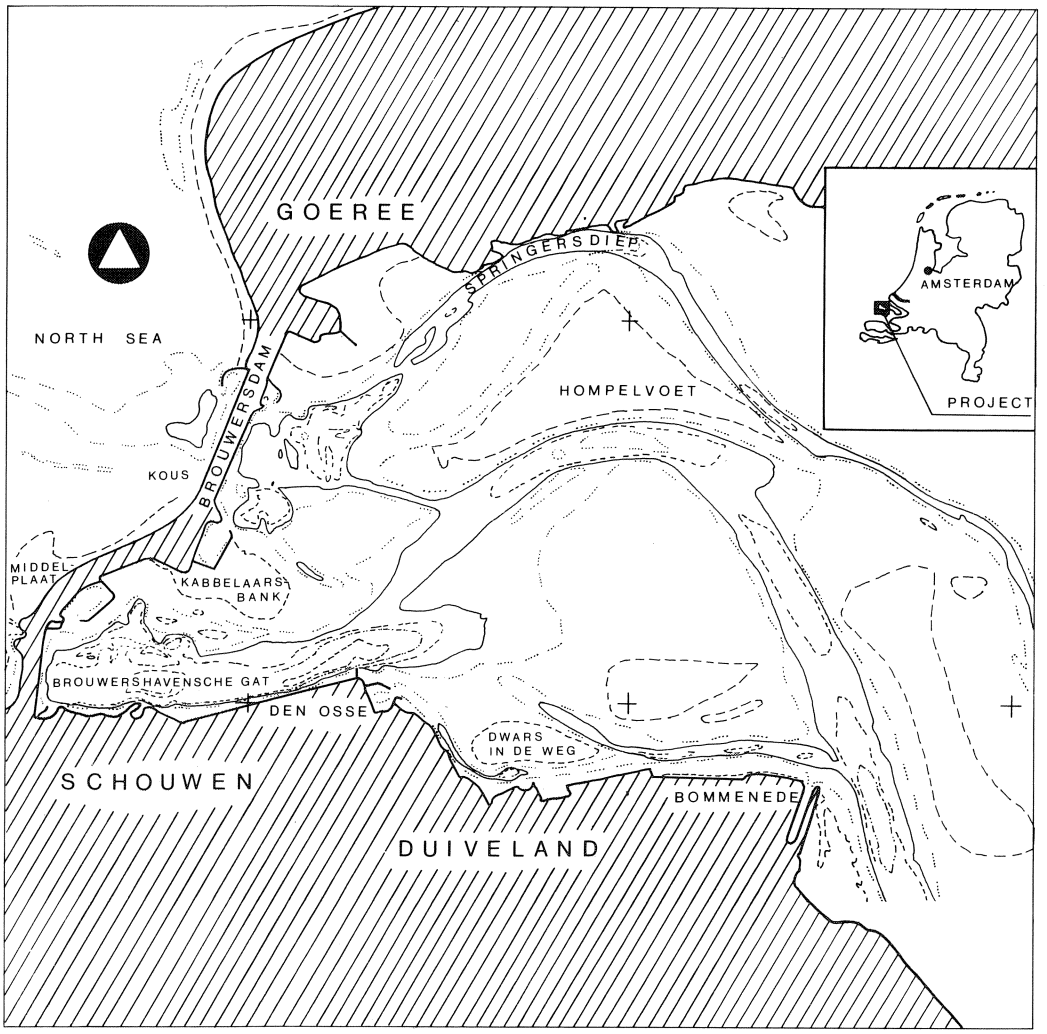

Figure 4.15. The Brouwers Dam that connects the (former) Schouwen-Duiveland and Goeree-Overflakkee islands in the South Western part of the Netherlands.

Another consideration was the need to prevent the current attack from being concentrated in the Brouwenshavensche Gat on the Schouwen shore during the construction stage.
Secondly, a perpendicular crossing of the flow direction makes for the shortest possible dam length in the channels; since these are easily the most expensive sections of the dam, the overall cost of the dam is thus kept to a minimum.

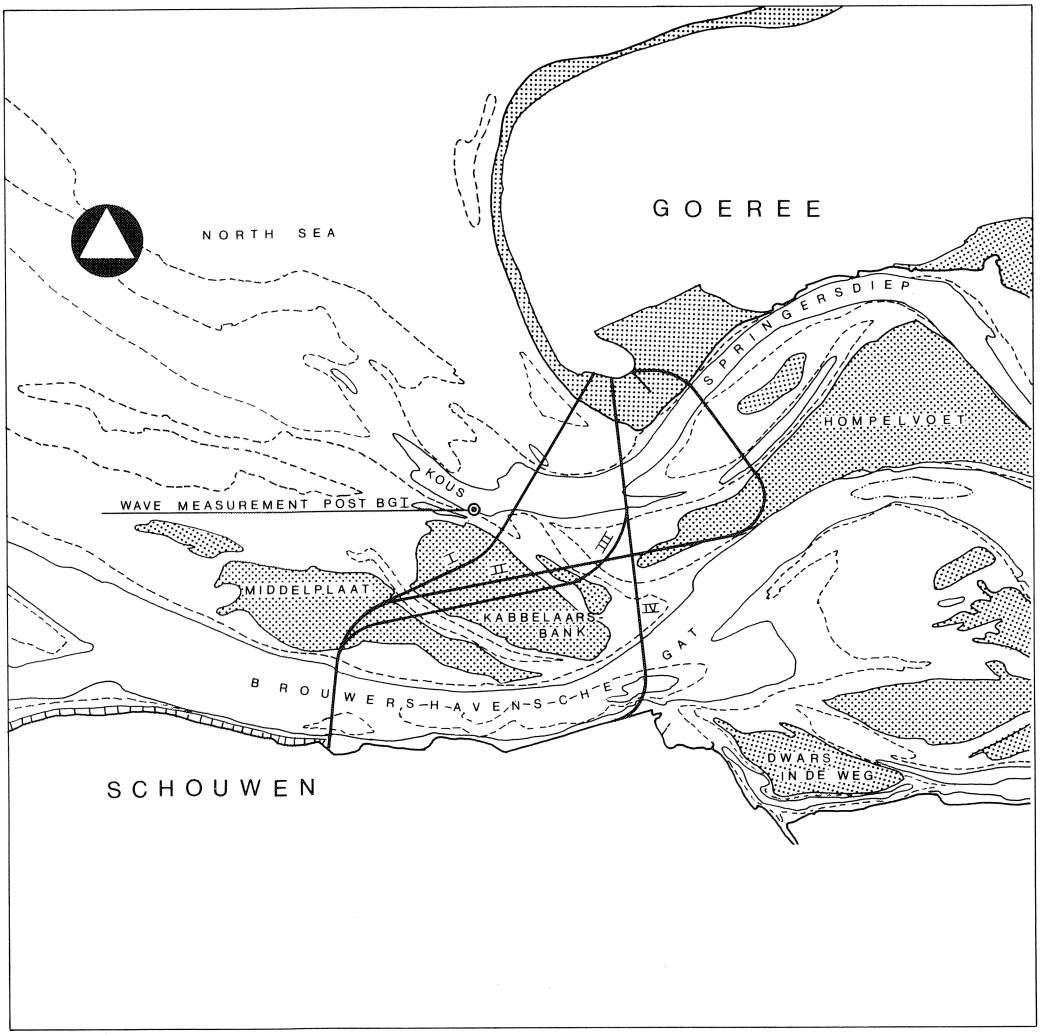

Figure 4.16. The four investigated alignments of the dam.

As regards ease of working in wave conditions during the construction stage there was little to choose between the four alignments. The maximum wave heights in the final stage were however higher in the case of Alignment I than for the more easterly locations, meaning that a dam at Alignment I would have to be higher than dams in the other alignments.
On account of the fact that the Springersdiep

and Kous channels virtually formed a single channel at the location of Alignment I, only two gaps would have to be closed in this case. The other three dam alignments crossed all three channels and would therefore have entailed three separate closures. This, together with its shorter length, made the estimated cost of Alignment I the lowest.
Alignment IV was particularly unattractive because it afforded no protection to the heavily attacked sea-dike between Den Osse and West-Repart. This dike-section would then have had to be raised to delta level, but the deep channels with their steep banks close to the dike would still have posed a danger. The southernmost channel - the Brouwershavensche Gat - is also much deeper (40 m below MSL) in the case of Alignment IV than in the case of the three other sites (25 m below MSL). The vast majority of the above considerations argued in favour of Alignment I, and this was the location that was eventually recommended and adopted.

4.3.3 Design of the dam

A number of factors have to be taken into account in cross-section design. In the case of the Brouwers dam these were as follows:
* safety;
* transport;
* recreation.

*** Safety**
The Delta Plan is based on water levels and wave heights with a probability of exceedance of 10^{-4} per year. This applies to the densely-populated and industrialized heart of the Netherlands. In other areas an economic reduction of 2.5 applies, thus enlarging the probability of exceedance to 2.5×10^{-4} per year (1 in 4000). On the basis of this frequency, the cross-section of the Brouwers dam had to be designed so as to take account of a stormsurge level of 5 m above MSL at the Hook of Holland and of the waves encountered at this level, assuming a design wave 7 m in height with a period of 12 seconds at the Goeree lightship.
In the light of these data the following basic values were arrived at (at that stage still deterministically) for the allignment of the dam:

- a stormsurge base level (i.e. design level) of 5.35 m above MSL at the southern connection of the dam to the island of Schouwen and of 5.15 m above MSL at the northern connection to Goeree;
- a wave height of 5 m at the foot of the dam, as determined on the basis of refraction patterns for the 7 m high design wave at the Goeree lightship.

West-Repart - the point at which the dam was to join Schouwen - the following tidal conditions obtained during the construction stage:

	spring tide	mean tide
mean HW	MSL + 1.41 m	MSL + 1.19 m
mean LW	MSL − 1.22 m	MSL − 1.17 m

	slack tide
mean HW	MSL + 0.91 m
mean LW	MSL − 1.07 m

For the sake of convenience the above values were applied tothe entire Brouwersdam during the construction stage.

*** Transport**
The Brouwers dam was required to be wide enough for the construction of a dual carriageway motorway and a parallel road for slow traffic.
The width of the motorway is 2 x 7.25 m, the carriageways being separated by 10 m wide median strip. The parallel road is 6 m wide (see figure 4.17).

*** Recreation**
Where possible recreation facilities were to be provided on both the seaward and lake sides of the dam.

Design of the dam
The dam was built up with sand. This material, with grain sizes ranging between 175 and 250 μm, is abundantly available in the delta area of the Rhine, Meuse and Scheldt as well as the North Sea, and is inexpensive. The sand body can be constructed on such a scale that a given

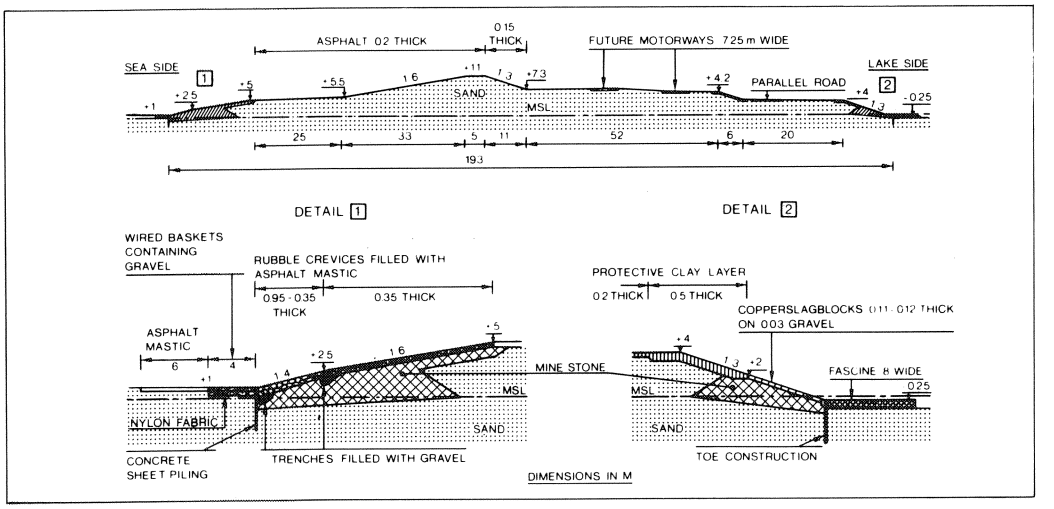

Figure 4.17. Cross section of the southern part of the Brouwersdam (length about 5.5 km) the dam consists of sand with a protective layer of asphalt, stones, clay or other materials.

minimum cross-section may be expected to survive even a heavy storm. This is known as a dune dam. The sand body can also be minimized by using a protective material against erosion and sand loss. Both types were used in the Brouwers dam. The northern section of the dam (a length of approx. 1 km) adjoining the dune coast of the island of Goeree was constructed as a dune dam, while the remaining section (some 5.5 km) consists of sand covered with protective material.

The dune dam

The dune cross-section of the northern part of the Brouwers dam is shown in figure 4.18. The gradient of the beaches in the south-west of the Netherlands is generally between 1:30 and 1:50 below the foot of the dunes (generally around 3 m above MSL), while the slope of the dunes themselves is about 1:3.

During a storm tide, heavily attacked coastal sections may be subject to dune erosion. After a storm flood it may often be observed that the beach, while retaining its former gradient of between 1:30 and 1:50, now reaches byond the original foot of the dune.

This phenomenon has given rise to a design criterion.

This criterion stipulates that, in a very heavy storm with extreme high-water levels (the design level), it must be possible for a beach to be formed with a gradient of 1:50 reaching to a height of 5.50 m above MSL while still leaving a sufficiently heavy body of sand to act as a defence.

The highest part of such a beach is at much the same height as the design level. In these circumstances little or no allowance need be made for waves above the heighest point of the beach, since virtually all the energy of the waves will have been dissipated on its long, gentle slope.

Figure 4.18 shows the cross-section of the northern part of the Brouwers dam, which was constructed as a dune dike. The dune shown in the figure with a crown height of 8.50 m above MSL is designed as a supplement. In addition this dune has a landscaping purpose, being designed to blend in with the line of dunes at the Goeree heads.

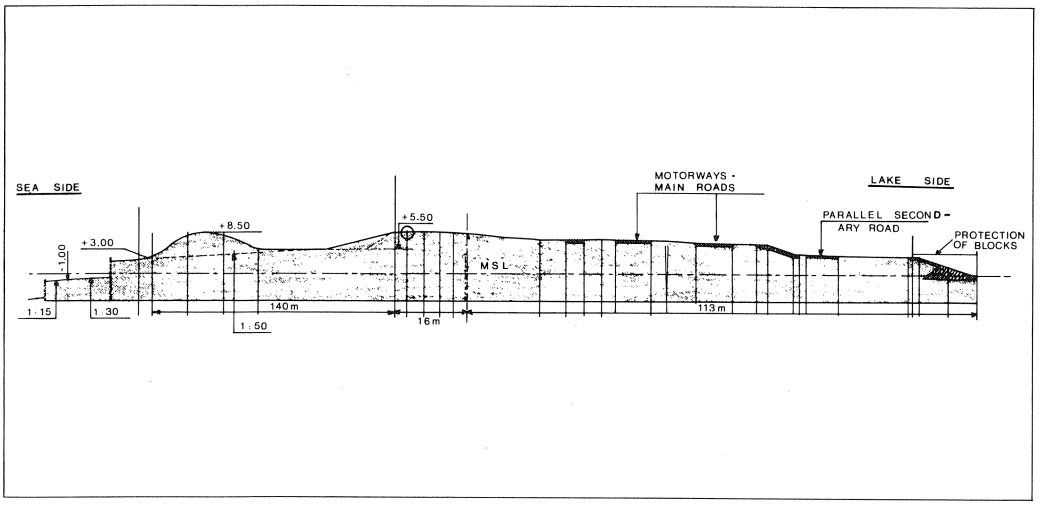

Figure 4.18. Cross section of the northern part of the Brouwers Dam (length about approximately 1 km) the dam consists of sand without protective layers at the sea-side.

Figure 4.19. Calculation of crest height based on various factors such as wave run-up, water level etc.

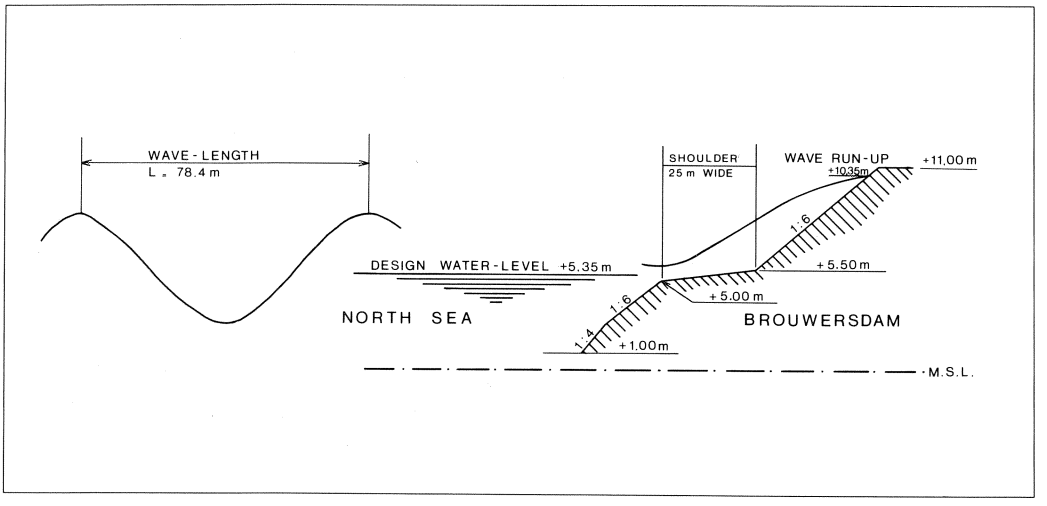

The protected dam
Figure 4.17 shows the cross-section of the dam. The dimensions of the cross-section had to be selected in such a way as to satisfy the functional requirements of the dam, while optimalizing the required dimensions with a view to cost. Thus a number of possible combinations of crest height and outer-slope gradient were compared with one another, viz:

a. crest height 16 m above MSL, outer slope 1:4, no berm;
b. crest height 13 m above MSL, outer slope 1:6, no berm;
c. crest height 11.5 m above MSL, outer slope 1:8, no berm;
d. crest height 11 m above MSL, outer slope 1:6, berm at storm-tide level.

In calculating the crest height in case d. it was assumed that the wave run-up with such a cross-section would be equal to three-quarters of the wave run-up on an uninterrupted slope, provided that the width of the berm was at least a quarter of the maximum anticipated wave length (see figure 4.19).

Wave run-up against a smooth slope may be calculated using the formula $Z = 8H \tan \alpha$
where:

Z = wave run-up in metres exceeded by 2% of the waves.
H = significant wave height at the foot of the slope in metres.
According to the above, H = 5 m, ignoring the fact that a wave of this height would find itself in the breaker area at the 1 m above MSL foot.
α = gradient of the slope.
Z = 3/4 (8.5.1/6) = 5 m (in which 3/4 is the previously mentioned reduction factor).

In the light of the factors that would give rise to a frequency of once in 4,000 years, the height of the dam would then have to be at least equal to:

- the height of the water level in these circumstances and its maximum in the vicinity of the connection of the dam to the coast of Schouwen, namely MSL + 5.35 m
- the wave run-up + MSL + 5.00 m

MSL + 10.35 m

The resultant height of 10.35 m above MSL was then rounded off to 11.00 m above MSL.

In order to apply the reduction factor of three-quarters for determining the wave run-up, it is essential for the width of the berm (25 m) to be at least equal to one quarter of the maximum anticipated wave length.
The wave length may be calculated using the formula L = c.T.,
where:

L = wave length in metres;
c = propagation velocity of the wave in m/s, where
c = $\sqrt{gh}$, in which h is the water depth at the foot of the slope in metres. In this case:
c = $\sqrt{gh} = \sqrt{9.81 \times 4.35} = 6.53$ m/s.

The wave length then becomes:
L = c.T.
L = 6.53 x 12 = 78.4 m.
The berm width therefore satisfies the condition that it must exceed 1/4 L.

The costs of these four alternaties, each of which was equivalent in safety terms, were estimated, with configurations b. and d. turning out to be somewhat cheaper than a. and d.
Option d. (see figure 4.17) was finally settled on since a berm on the seaward side could also be used for constructing a road, which was advantageous from the viewpoint of both maintenance and recreation.

4.3.4 Choice of closure method

Introduction
In 1965, when a decision about the means of closing the Brouwers dam had to be made, experience had been acquired with closures using sluice or culvert caissons (i.e. sudden closure) and with closures using rubble conveyed by a cableway (gradual closure).
A choice between these two methods had to be made for the closure gaps in the Brouwers dam. The dominant consideration in deciding on the most appropriate closure method was the stability of the Schouwen shore, which had to be safeguarded as best as possible.
In making the choice various data were available, such as:

Hydraulic
- data on the horizontal and vertical tidal

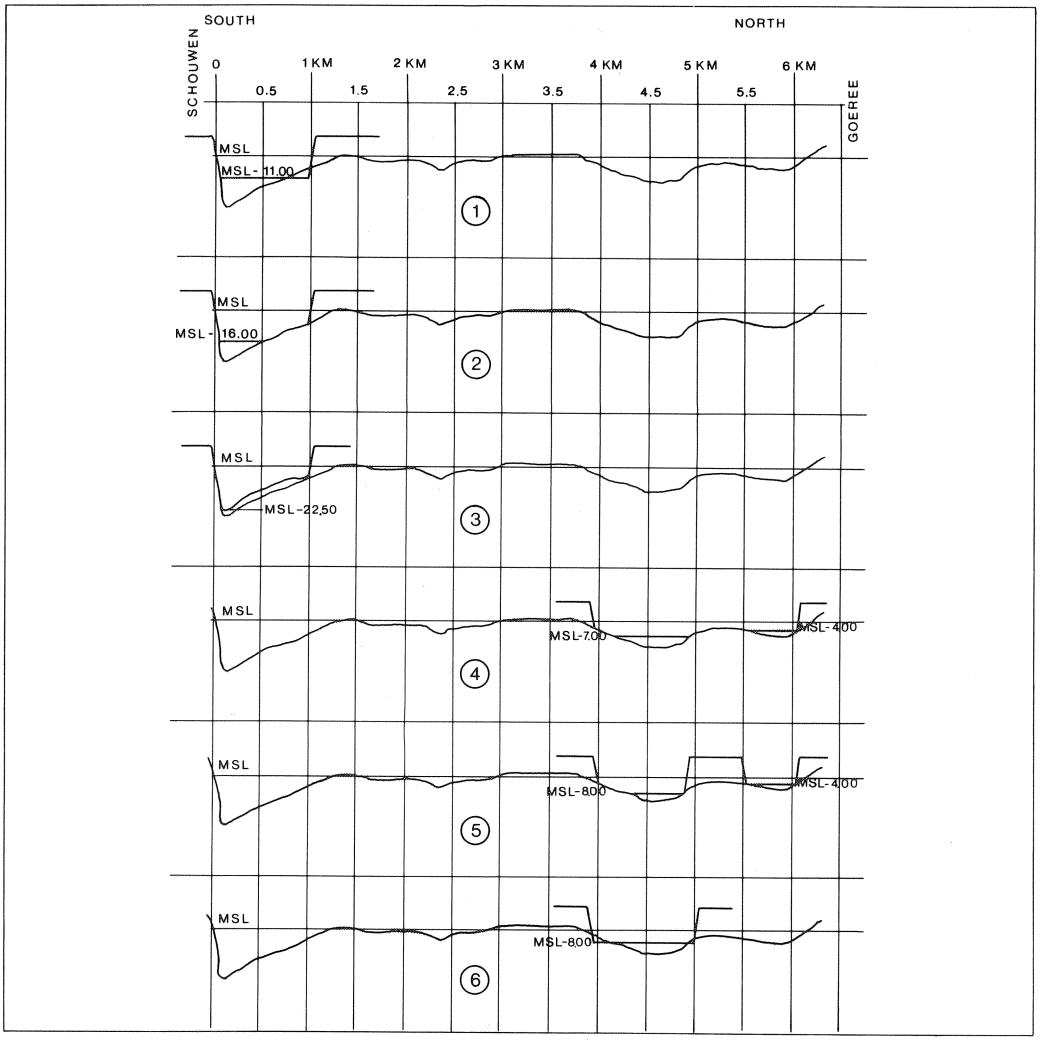

Figure 4.20. Alternative plans for closing the channels crossing the dam-alignment.

movements in and around the closure gaps as a function of the flow gap;
- data on the stability of various kinds of rubble in flowing water;
- a permanent scale model (with a fixed bottom) of the Brouwershavensche Gat (with a horizontal scale of 1:300 for the closure gaps and a vertical scale of 1:100);

Figure 4.21. The wave height at several points in the Brouwershavensche Gat in relation to the prevailing wave. height at BGIII in onshore wind conditions.
Wind directions between SW and NE.

- a permanent detail model (with a moveable bottom) of the southern closure gap (scale 1:60);
- calculations of erosion downstream from a bottom protection.

Hydrometeorological
- data on the incidence of fog, poor visibility,

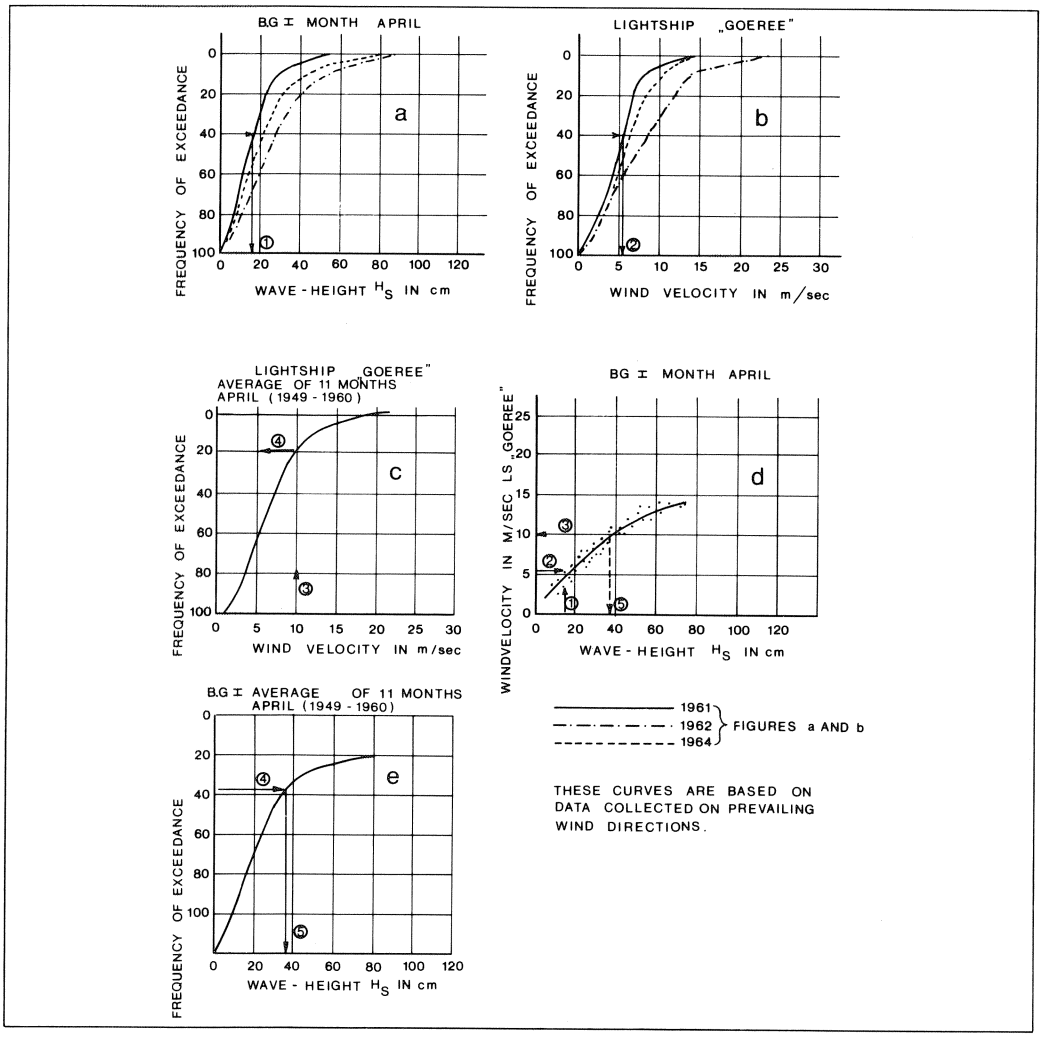

Figure 4.22. Method of analysing the wind and wave data.

wind and waves in the Brouwershavensche Gat.

Design data

- rough plans for sluice caissons and cableways.

Geotechnical

- ground borings and cone penetration tests.

Geomorphological
Hydrographic

On the basis of model analysis the desirability rapidly emerged of narrowing both closure gaps by an equal percentage amount.
This was related to:
- the risk of a transverse gradient across the sand-banks;
- the discharge distribution between the two closure gaps;
- erosion on both sides of the closure embankments.

If the closure of one of the gaps were to get ahead of the other, a transverse gradient would be introduced, with a substantial risk of a short-circuit channel being formed from north to south through the sand-flats.
The constructors were anxious to preserve the flats and were also concerned that a gully of this kind could arise near the foot of the dam, thus threatening its stability.
Unequal closure would moreover have led to a disproportionate increase in the current velocity in one of the gaps, with the result that greater erosion could have been expected in that gap.

Subsequent analysis therefore consistently assumed an equi-proportionate narrowing of the two closure gaps.

Boundary conditions

Of the two closure gaps the southern channel was the deeper. The deepest point of the dam alignment was approx. 27 m below MSL, at a point close to the Schouwen shore. The Schouwen shore where the dam was to be built had a slope of 1:3 to 1:4 to a depth of 17 m below MSL, after which the slope was approx. 1:10.
The deepest point of the dam alignment in the northern closure gap was located some 2 km from the shore of Goeree, the depth being some 14 m below MSL (see fig. 4.20). In both gaps the bottom consisted mainly of loosely-packed sand with grain sizes ranging from 175 to 250 μm.

Research was carried out into working conditions in both gaps. Working conditions were characterized by the specification of fog, winds and waves to be expected during the period of construction.

Data on the incidence of fog and on wind patterns were available from the Royal Netherlands Meteorological Institute (KNMI).
Of greater importance for workability and especially the stability of the closure dike was the wave pattern. Fog and wind were unlikely to create variations in the working area, whereas waves were. Figure 4.21 indicates relative wave heights at the wave measurement post BG III and other points in the working area in onshore wind conditions. These wave differentials, together with wave height exceedance frequency figures as registered by the two wave measurement posts BG I and BG III, provided a means of obtaining a comprehensive picture. The observation series made at the two posts, however, covered only a few years, namely 1961, 1962 and 1964.
Analysis of the data from the wave measurement posts BG I and BG III and the wind observations taken by the Goeree lightship indicated the existence of a usable correlation of the two, on the basis of which representative exceedance curves for wave heights could be obtained.

Table 4.2 Frequency of exceedance of significant wave heights at the closure gaps.

Frequency of exceedance	Heights in cm.	
	Northern gap	
	April - July	winter
2.5%	65	85
5%	55	70
10%	45	55
	Southern gap	
	April - July	winter
2.5%	80	110
5%	60	95
10%	50	70

Figure 4.22 indicates the method of analysing the wave and wind data. The diagram below indicates how the data (i.e. the wave height measurements at wave measurement post BG I in 1961, 1962 and 1964 and wind velocity recordings at the Goeree lightship between 1949 and 1960 and in 1961, 1962 and 1964) were used to reconstruct wave heights at the wave measurement post BG I during the period 1949 to 1960. The results of this analysis are shown for the closure gaps in table 4.2.

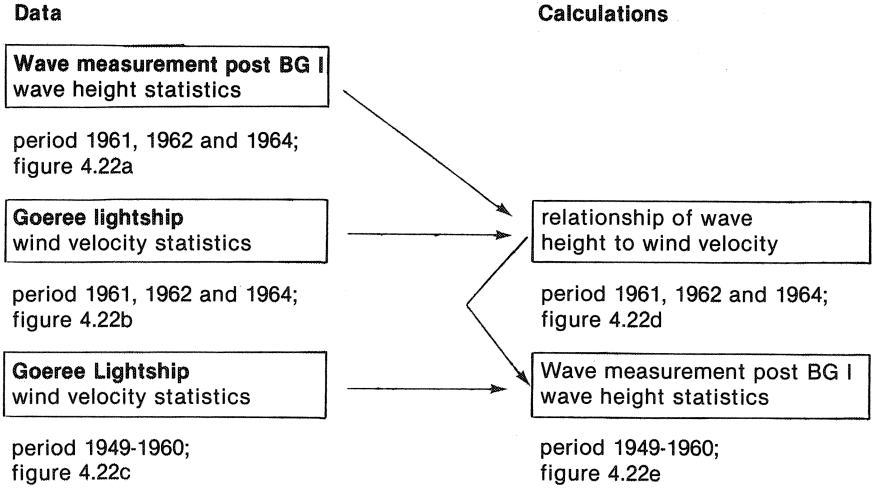

The tidal circumstances during the construction stage are recorded in section 4.3.3.

The closure gaps

The main criterion in choosing the means for closing the gaps - especially the southern gap - was the stability of the Schouwen shore.
For this reason particular attention was paid in the case of the southern gap to the impact that the various means of closure would have on the degree of erosion close to the Schouwen shore, while in the case of the closure of the 2,000 m channel on the Goeree side one of the chief considerations was whether to work with a single closure gap of 2,000 m (figure 4.20, no. 4) or two gaps (figure 4.20, no. 5), or a single gap of 1,000 m (figure 4.20, no. 6).

*** The southern closure gap**

The winter closure gap was to be formed by a sill constructed on bottom protection, bordered on one side by the Schouwen shore and by a dam section on the other. For both a caisson and a gradual closure, the length of the bottom protection on both sides of the path of alignment was put at seven to eight times the height of the dam at that stage of the gradual closure when the increase in scour would be at its peak (see also 4.3.5 and figure 4.31).

The erosion research for a caisson closure assumed a horizontal sill with a crest width of 45 m, slopes of 1:6 and varying crest heights. The erosion measured at the end of the winter closure period as a function of sill height is shown in table 4.3.

In terms of execution the sills with the highest crests were the most attractive. The ability to work at less great depths would have made it easier to level the sill off using available materials, while the required caisson height

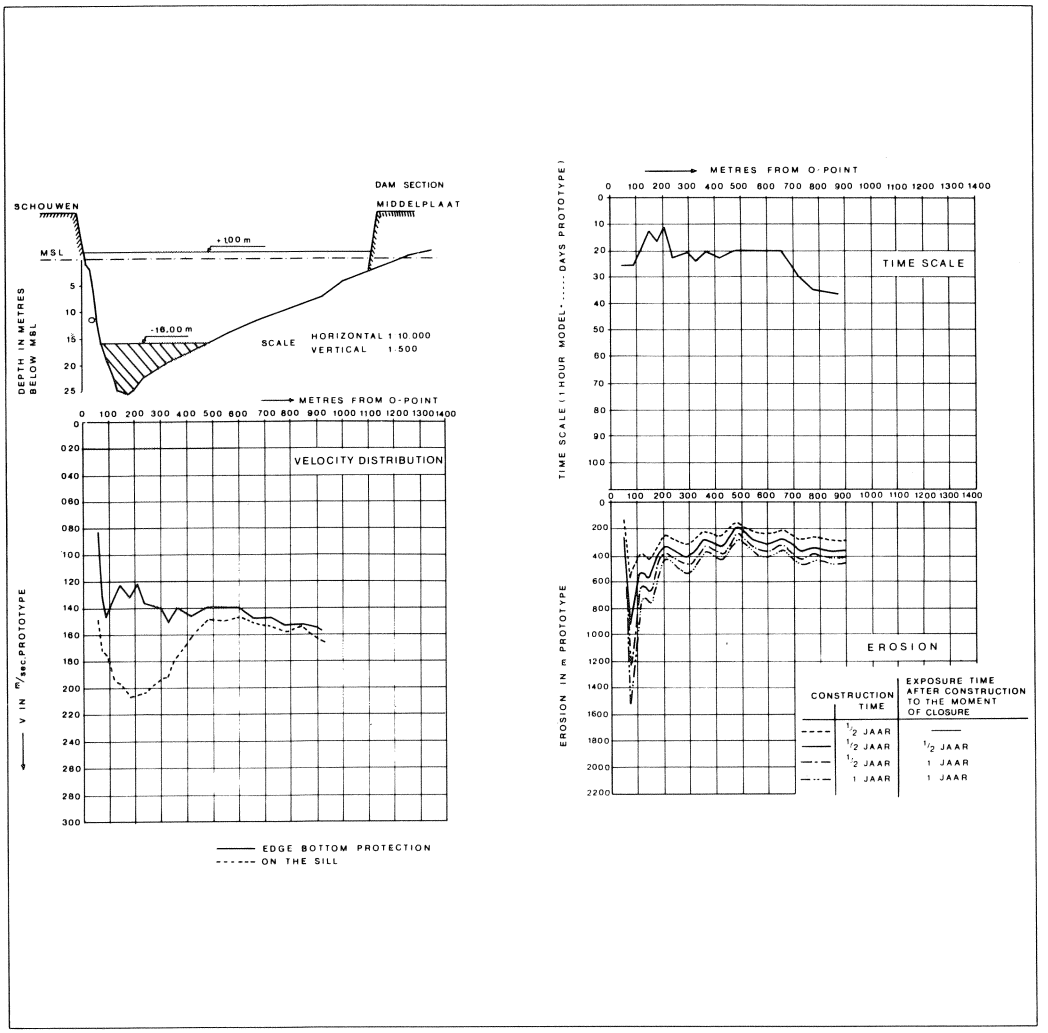

Figure 4.23. Southern closure gap.
Erosion in winter closure gap
Caisson closure.

decreases the higher the crest of the sill. On the other hand, as indicated in Table 4.3, erosion increases with the height ot the sill, while the periods of low current velocities at the turn of the tide, when caisson placement has to take place, become shorter.

On account of these drawbacks the sills with crest heights of 12.75 m and 11.00 m below MSL had to be ruled out as too risky.

Table 4.3. Depth erosion at the end of the winter closure period

Sill height in relation to MSL	Erosion depth in relation to bottom	Erosion depth in relation to MSL	Figure
- 20.00 m	5.50 m	- 30.00 m	
- 17.50 m	10.50 m	- 35.00 m	
- 16.00 m	12.50 m	- 37.00 m	4.20-2
- 12.75 m	18.00 m	- 42.50 m	
- 11.00 m	21.50 m	- 46.00 m	4.20-1

Of the remaining sills considered, that with a crest height of 20.00 m below MSL would have caused the least erosion. The final levelling of the sill at such a depth would, however, have presented formidable problems, while the transportation and installation of a caisson of the dimensions and draught required for such a low sill would also have been a major difficulty. This left the sills with crest heights of 17.50 m and 16.00 m below MSL. Since there was no significant difference between the depth of the erosion created with these two sills, a sill height of 16.00 m below MSL had the most in its favour.

Figure 4.23 shows the velocity profile and erosion measured in the research at this sill height. According to the model analysis, closure of the gap with a caisson closure would, on account of the brief period required, not result in substantially greater erosion depths than those already created during the winter period before closure of the gap, provided that due care was paid to the formation of the abutments. Flow pattern analysis revealed that the best results would be obtained with an abutment caisson initially positioned against the Schouwen shore and which fitted in with the underwater slope of the shore without any passage openings (i.e. without sluices).

In the case of a **gradual closure** the sill does not have to be levelled off. In fact the sill needs only satisfy the following conditions:

- to be sufficiently sand-tight to prevent sand escape from the bottom;
- to be resistant - i.e. to remain sufficiently sand-tight - when rubble is dumped on the sill;
- to be resistant to passing current.

Research was carried out on two sills with differing crest heights but the same length of bottom protection (see figure 4.24).
Model tests revealed that the lower of the two sills (no. 1 in the figure) produced half as deep scouring holes as the higher (no. 2 in the figure). The results are shown in the table below.

Table 4.4. Erosion depth during construction as a function of sill height

	Maximum erosion depth in relation to bottom	Maximum erosion depth in relation to MSL
Sill 1	5.50 m	- 30.00 m
Sill 2	11.00 m	- 35.50 m

It was therefore decided to work with sill 1 in further analysis.

In building up the closure embankment with rubble in a gradual vertical closure, the dumping procedure turned out to have a major bearing on the degree of erosion. If the rubble were built up in more or less even layers across the sill, the protracted duration of an unfavourable flow pattern resulted in an enourmous increase in scour. A favourable result was achieved by initially dumping rubble starting at the MSL point on the Schouwen shore and working out onto the sill at a gradient of 1:25 (see figure 4.24). By means of this dumping procedure the point of maximum erosion could be displaced towards the middle of the closure gap, with beneficial results for the stability of the Schouwen shore.
In view of the above it was concluded that a caisson closure with a sill height of 16.00 m below MSL (figure 4.23) would cause deeper scour than a gradual closure with a sill height of 22.50 m below MSL (see figure 4.24). In addition, the latter method of closure would also mean that the point of maximum scour would be pushed towards the middle of the closure gap.

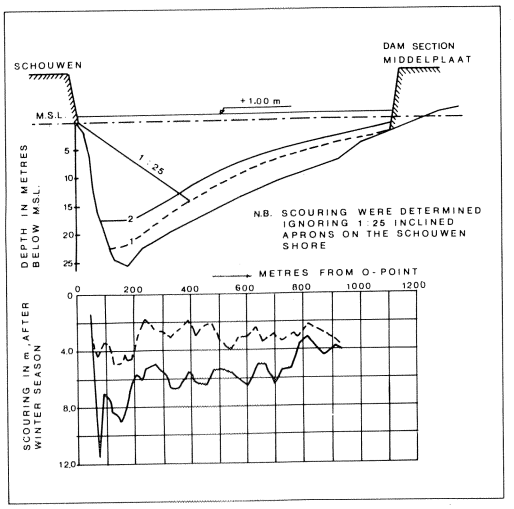

Figure 4.24. Southern closure gap.
Scouring in winter closure gap.
Gradual closure.

Moreover, the construction of a caisson sill with a level surface at a depth of 16.00 m below MSL was seen as presenting considerable difficulties. For these reasons it was decided to adopt the gradual closure method for the southern gap.

*** The northern closure gap**

Since the northern closure gap was less deep, so that a relatively low sill could be used for either a caisson or a cableway closure, the anticipated scour was much less deep than in the southern gap. In addition, the major bottom depths were far out from the Goeree shore.

For this reason the erosion criterion was much less decisive for the selection of closure technique than it was for the southern gap.

Given the great length of the closure embankment, a gradual closure of the Kous and Springersdiep channels would have been expensive and drawn-out. The possibility was therefore investigated of limiting the length of the closure gap. Three alternatives were considered:

a. a 2,000 m closure gap (figure 4.20, no. 4);
b. two closure gaps (figure 4.20, no. 5);
c. a 1,000 m closure gap (figure 4.20, no. 6).

The following observations may be made about these three alternatives:

re. a: As far as flow patterns and velocity profiles were concerned any other situation would have been inferior to a 2,000 m closure gap. The costs of the closure materials for a 2,000 m gap were higher than those for a 1,000 m gap. In the northern section, bottom protection and a sill would have been required where there was a comparatively shallow channel, the execution of which presented problems because this part of the gap was navigable only at high water.

re. b: At high tide, which was spread over the full width of the northern gully area, the central island would form a distinct obstacle. This would produce two head actions of considerable intensity, thus increasing the degree of scour. The cost of the closure materials was higher than for a 1,000 m closure gap and, in the case of a gradual closure, higher even than for a 2,000 m closure gap.
Here again bottom protection and a sill would be required in the shallow northern section, although over a shorter distance than for alternative a.

re. c: The entire inflow and outflow of the northern area would be channelled throught the Kous. This meant that a severe vortex street could be anticipated on the Goeree side at high tide.
The cost of the closure materials was less than for either a. or b. No bottom protection or sill was required in the relatively shallow northern section.

In weighing the pros and cons of these three alternatives, the twin-gap model (b. above) turned out to be inferior to the single, 2,000 m gap model in terms of hydraulic aspects, and to offer little if any advantage in terms of costs and execution.

This alternative was therefore rejected.
In assessing the respective merits of the two remaining models, the constructional objections and higher cost of a 2,000 m closure gap were considered of greater importance than the head actions produced by a 1,000 m closure gap. In this respect it was taken into consideration that the erosion resulting from the head actions would pose a risk only for the stability of the sill and the abutments. This risk could be reduced by increasing the area of bottom protection. The cost differential between a 1,000 m and 2,000 m gap was sufficiently great to cover such an extension.

The selection therefore fell on a 1,000 m closure gap through the Kous. This of course left the closure of the Springersdiep channel. This took place in 1969, when the Springersdiep dam section was constructed, prior to the final closure of the Kous and Brouwershavensche Gat channels in 1971. The closure of the Springersdiep in 1969 took the form of a sand closure, details of which are provided in Chapter 3.
The question then remained of deciding between the two closure methods for the Kous gap.
A major consideration in this respect consisted of the severe vortex street likely to be formed on the Goeree side of the closure gap. The scour caused by this vortex street could be limited by leaving the construction of the dike section from Goeree to the last possible moment. This could best be achieved by a caisson closure; the building up of the firm shore section and an anchorage point for a cableway would have required the early construction of this dam section. Another factor in the choice of closure technique was the desirability of obtaining experience with both systems (i.e. cableway and caisson closures), since it was assumed that the Eastern Scheldt would be closed by one or both of these methods;

To sum up, a gradual closure of the southern gap was desirable for ensuring the stability of the Schouwen shore, while there were also practical reasons in its favour. In the case of the northern closure gap, on the other hand, a caisson closure offered the best prospects for limiting or overcoming the hydraulic problems.

The schedule as envisaged in 1965 for the two closures - which did not in fact take place until 1971 - is shown schematically in figure 4.25, with the winter closure gaps being indicated on the top line.

Dumping material used for the southern gap
The gradual closure of the southern gap in 1971 was effected with 1 m^3 concrete cubes weighing 2.5 tonnes. The optimum size for these blocks was determined by model analysis. These tests were based on embankments with slopes of 1:1, with either a single crest (constructed with a single cable) or a double crest (constructed with two cables set 6.25 m apart). This analysis was based on the criterion that no unacceptable damage to the closure dike should occur during the adverse current and wave conditions, experienced in the closure period. In analysing these conditions, allowance was made for a storm with a probability of exceedance of once in a hundred years (i.e. 10^{-2} per year), while damage not concentrated at a single point and which could be repaired within a reasonable period of time (i.e. within a week) was regarded as acceptable. Concrete blocks rather than rubble were selected for their superior stacking qualities and relative ease of transport.

Rubble could of course also have been used as dumping material.
In the early stages (in 1965) investigations were carried out to see whether a sufficiently stable closure dike could be built up with the rubble grades in use at that time. In doing so two factors were taken into account:
1) a combined attack of current and waves during the construction of the closure dike;
2) wave attack upon completion of the closure dike.

Model tests indicated that the use of rubble of between 300 and 1000 kg could result in a crest settlement during the construction of the closure dike as the result of currents and waves within the limits laid down as acceptable. As regards wave attack upon completion of the closure dike, it was known from the closure of the Grevelingen in 1964 that 10/300 kg rubble with a specific density of 2.7 t/m^3 could be used

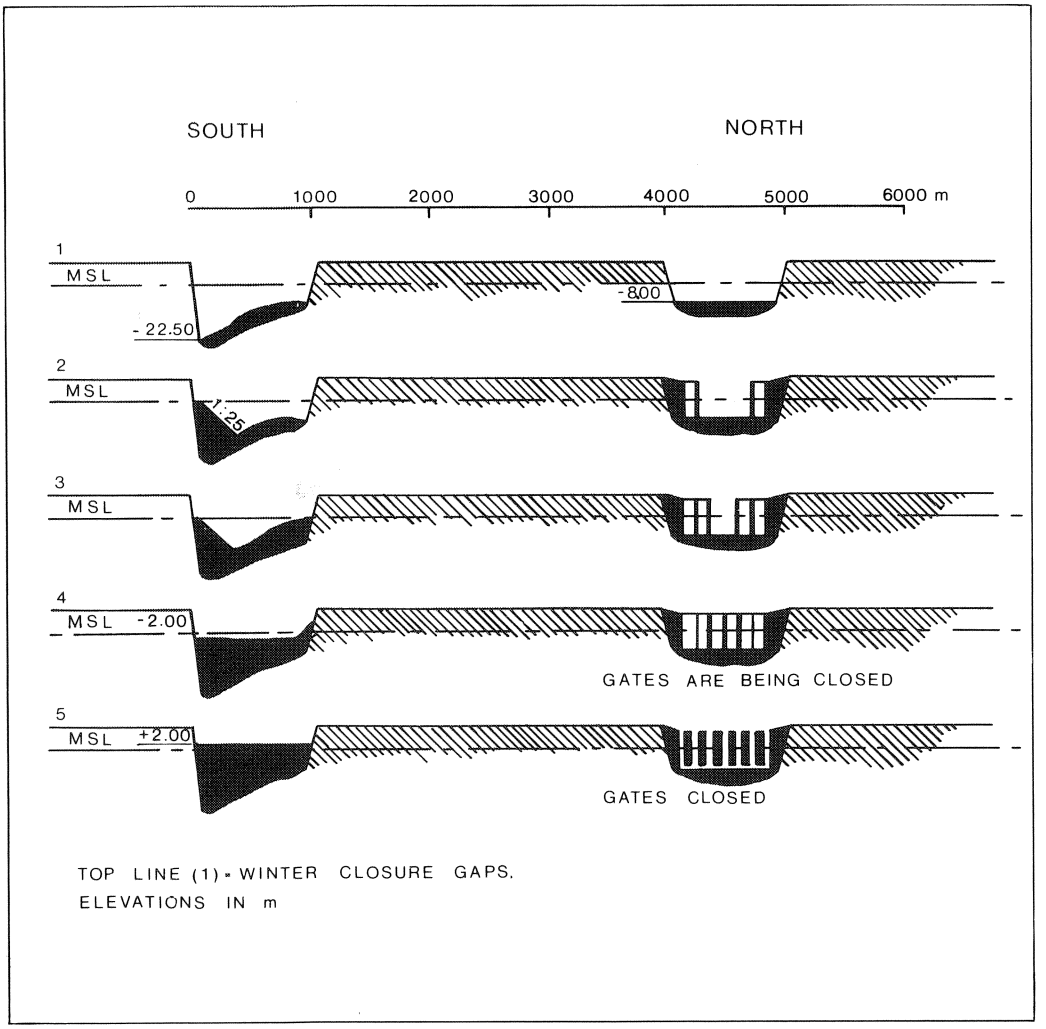

Figure 4.25. Schedule as envisaged in 1965 for the two closures.
— in the south : gradual closure
— in the north : caisson closure

given dike slopes of 1:1.1 and a crest height of 3 m above MSL. Maximum attack occurred at normal high-water levels. The design wave height was 0.8 m.

The question was which rubble grade could be regarded as stable for the closure of the southern gap given:

a. slopes of 1:2 and 1:1.1 respectively;
b. a design wave height of 2.00 m (1.86 x Hs).

The problem may be approached using Beaudevin's formula:

$$G = k.H^3 \frac{\rho_s}{(S_s - 1)^3} \left[\frac{1}{t - 0.8} - 0.15\right] \text{ or}$$

$$G = k \frac{H^3}{\Delta^3}.\rho_s \left[\frac{1}{\text{cotg}\alpha - 0.8} - 0.15\right]$$

in which
G = average stone mass in tonnes;
k = coefficient = $\sim$ 0.25;
H = wave height in m;
ϱ_s = specific density of stone in t/m³;
ϱ_w = specific density of water in t/m³;

$$S_s = \frac{\rho_s}{\rho_w} \; ; \; \Delta = \frac{\rho_s - \rho_w}{\rho_w}$$

t = cotgα in which α = slope gradient

This formula may be applied as:

$$\frac{G}{H^3} \qquad \frac{(S_S - 1)^3}{\varrho_S} > 4.10^{-3}$$

The comparison between 10/300 kg rubble (index 1) and the rubble to be calculated (index 2) may be written:

$$\frac{G_1}{G_2} = \frac{H_1^3}{H_2^3} \frac{\frac{\rho_{s1}}{(S_{s1} - 1)^3} \left\{\frac{1}{t_1 - 0.8} - 0.15\right\}}{\frac{\rho_{s2}}{(S_{s2} - 1)^3} \left\{\frac{1}{t_2 - 0.8} - 0.15\right\}}$$

a. In the case of a 1:2 slope and a wave height of 2.00 m, the required average stone weight at equal specific densities for the two grades becomes:

$$\frac{0.135}{G_2} = \frac{0.8^3}{2^3} \frac{\frac{1}{1.1 - 0.8} - 0.15}{\frac{1}{2 - 0:8} - 0.15}$$

60/300 kg rubble; G_1 = 0.135 ton
G_2 = 480 kg

This requirement will be satisfied by a rubble grade of 300/1000 kg with an average unit weight of 600 kg.

$$\frac{G}{H^3} \frac{(S_s - 1)^3}{\rho_s} = \frac{0.480}{2^3} \frac{(2.65 - 1)^3}{2.7} =$$

$$= 0.10 > 4.10^{-3}$$

b1. In the case of a 1:1.1 slope and a wave height of 2.00 m, the required average stone weight at equal specific densities for the two grades becomes:

$$\frac{0.135}{G_2} = \frac{0.8^3}{2^3}$$

G_2 = 2110 kg

This requirement is satisfied by a rubble grade of 3/6 tonnes with an average unit weight of approx. 4.5 tonnes.

b2. As for b1, but in this instance with a specific density of the required rubble of 3 t/m³ (i.e. basalt), and a specific density of sea water of 1.02 t/m³.

$$\frac{0.135}{G_2} = \frac{0.8^3}{2^3} \cdot \frac{\frac{2.7}{(2.65 - 1)^3}}{\frac{3}{(2.94 - 1)^3}}$$

G_2 = 1500 kg

This requirement is satisfied by a rubble grade of 1/3 tonnes with an average unit weight of 1.9 tonnes.

4.3.5 Preliminary works

Introduction

The closure of the Brouwershavensche Gat occurred in stages. To begin with sections of the closure dam were constructed in the more elevated parts of the dam alignment. This resulted in little change to the flow conditions in the remaining openings (i.e. the closure gaps), since the cross-section of these openings was

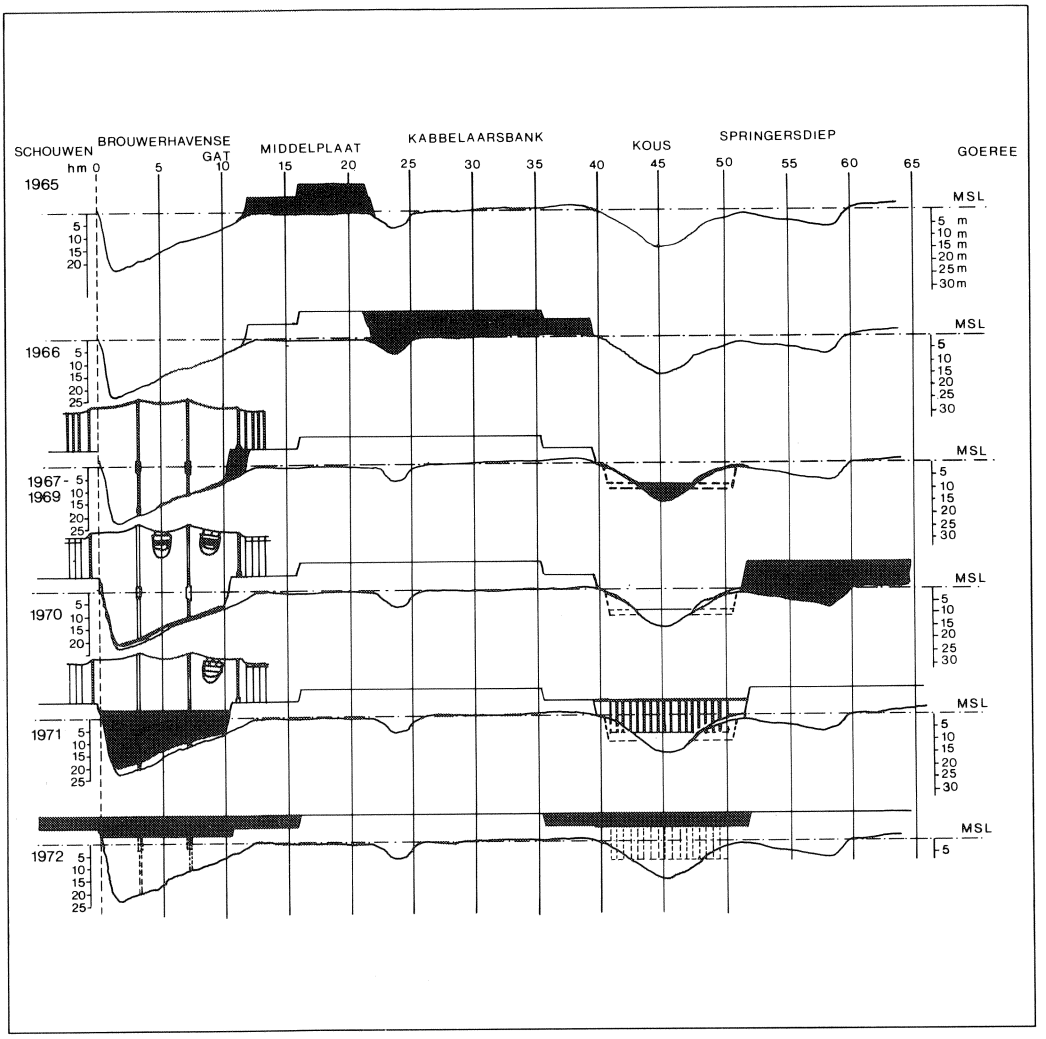

Figure 4.26. Construction stages Brouwers Dam.

not greatly altered. The next stage consisted of the installation of bottom protection in the closure gaps, together with the sills forming the foundation for the closure means employed. These were required in order to protect the sandy bottom against scour given the increase in current velocities and the turbulence in the closure gaps.

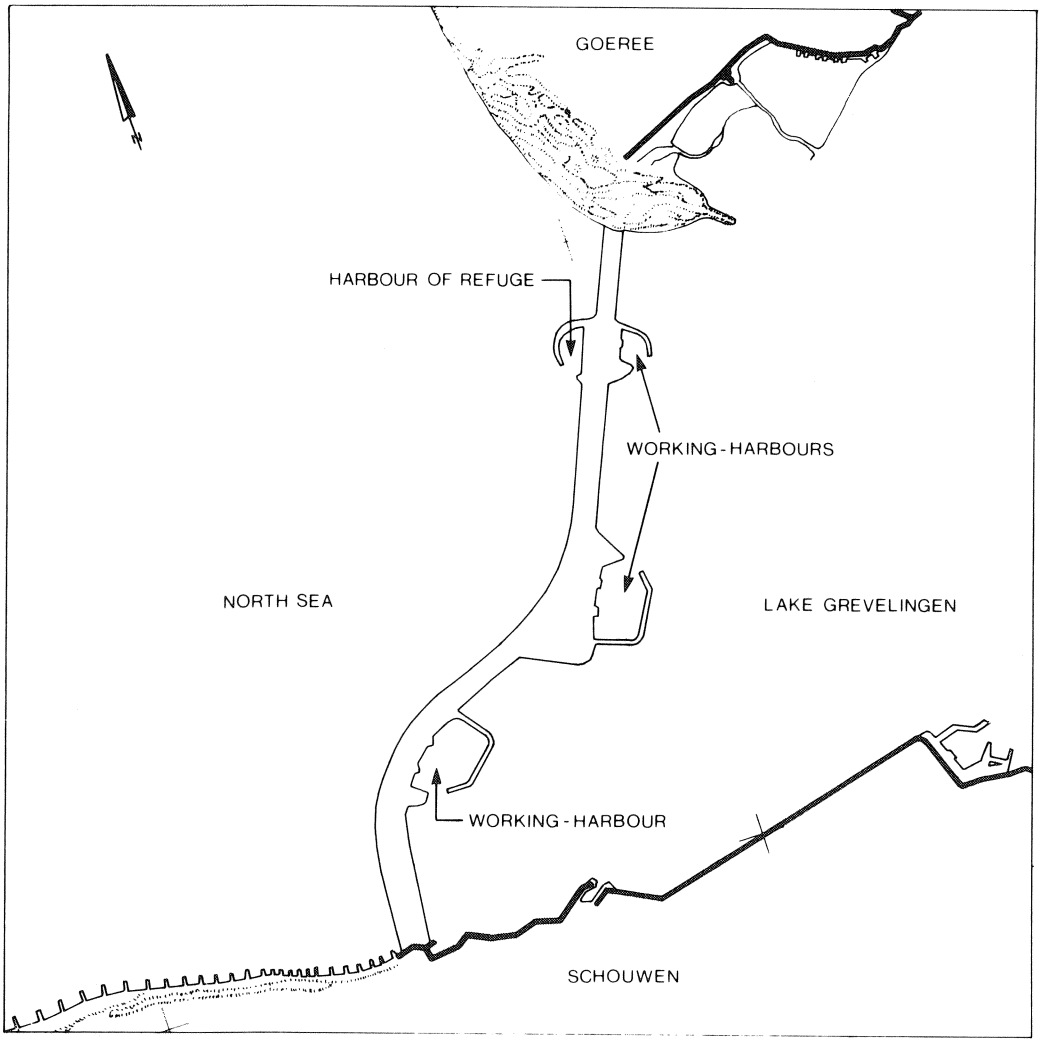

Figure 4.27. Situation Brouwers Dam.

Depending on the closure technique in question, the sills were also required to satisfy certain supplementary requirements. In the northern gap, the sill for the caisson closure had to be levelled off at a given height, while in the southern gap the sill for the gradual closure had to be able to withstand the dumping of rubble and concrete blocks.

The closure materials were constructed at the same time as these works were carried out, the caissons being built in a construction dock not far from the closure itself.
The concrete blocks for use in the gradual closure were manufactured, and stored in depots on both sides of the southern gap. A cableway was also installed in this southern gap.
The closure of the gaps followed these preliminary works. The actual closure is discussed in the next chapter, while the preliminary works are discussed below.

Dam sections and working harbours
The various stages of the construction of the Brouwers dam are shown schematically in figure 4.26. From this it may be seen that three dam sections were built prior to the closure in 1971, namely:
- the Middelplaat dam section in 1965;
- the Kabbelaarsbank dam section in 1966;
- the Springersdiep dam section in 1970.

These three dam sections had a combined length of some 4.5 km. This left the two closure gaps, each about 1 km in length.

As indicated in figure 4.27, a working harbour was built for each of these sections. These served various objectives, being required to:
a. provide berthing space for vessels with material and equipment for the construction of the dam sections and for the closure, together with landing quays for unloading these vessels;
b. provide berthing space for vessels for conveying staff and employees of both the contractor and the works management, as well as suitable jetties and footbridges;
c. provide berthing space for the floating equipment of the contractor;
d. provide space for the storage and transshipment of rocky materials in the wet.

The working harbours had to cover a considerable area in order to meet all these requirements. This was not as expensive as it might first appear since the working harbours

Figure 4.28. Dam section in the Springersdiep.

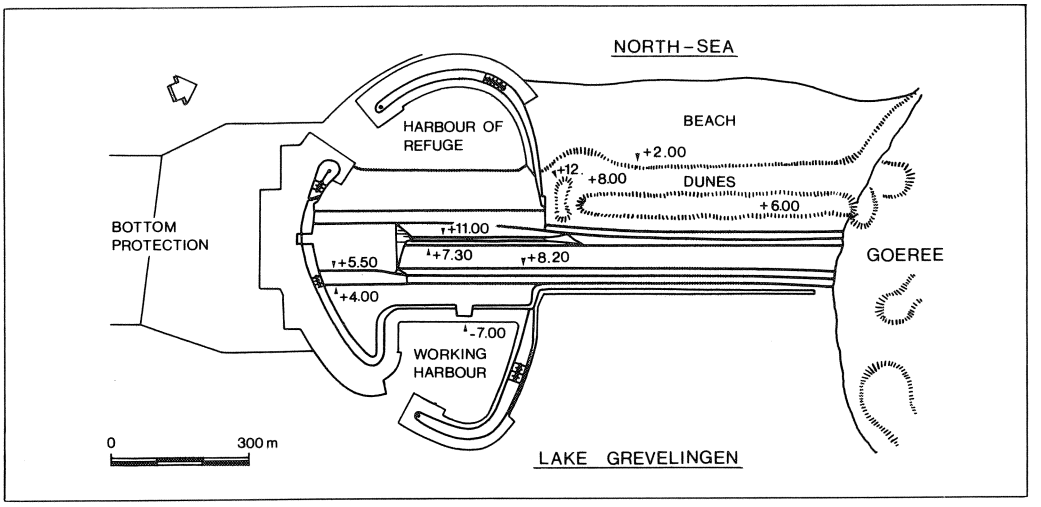

were used as a source of sand, thus making a virtue of necessity.
In some instances the harbour dams were also designed to conduct the flow (see for example the shape of the Springersdiep dam section in fig. 4.28).

Bottom protection and sills

1a Dimensions of the bottom protection and the sills
For economic reasons, it is assumed when determining the size of the required bottom protection that there wll be a scouring hole along the edge of the protection, but that the geometry of the hole will not create a risk of earth slide such as might endanger the stability of the closure dam.

1b Northern gap bottom protection
The required width of the bottom protection for the northern closure gap was determined by means of model tests. These test were based on the criterion that no unacceptable erosion could be allowed to occur (see figure 4.29). If the development of an erosion hole along the edge of the bottom protection and increased loads on the bottom or loss of support caused by a steep-sided hole caused settlement flow, this could not be allowed to endanger the dam.
On the basis of practical measurements and tests if was assumed that a slope of 1:15 could arise beginning at the lowest point of the erosion hole as the result of settlement flow. A slope of this kind, shown in the figure with a dotted line, must not be allowed to disturb the sill construction.
In this way the required width of the bottom protection in the northern closure gap on either side of the sill-axis was decided to be 130 m over an uneven surface of bottom protection. The bottom protection consisted of mastic asphalt covered with rubble. This width was determined allowing for highly adverse circumstances, viz. extreme high water (the stormsurge level of April 1943 of 3.20 m above MSL) with all caissons in position but the sluices still open and the dam of blocks in the southern gap built up to MSL height.

Figure 4.29. Northern closure gap.
Cross section bottom protection, sill and caisson.

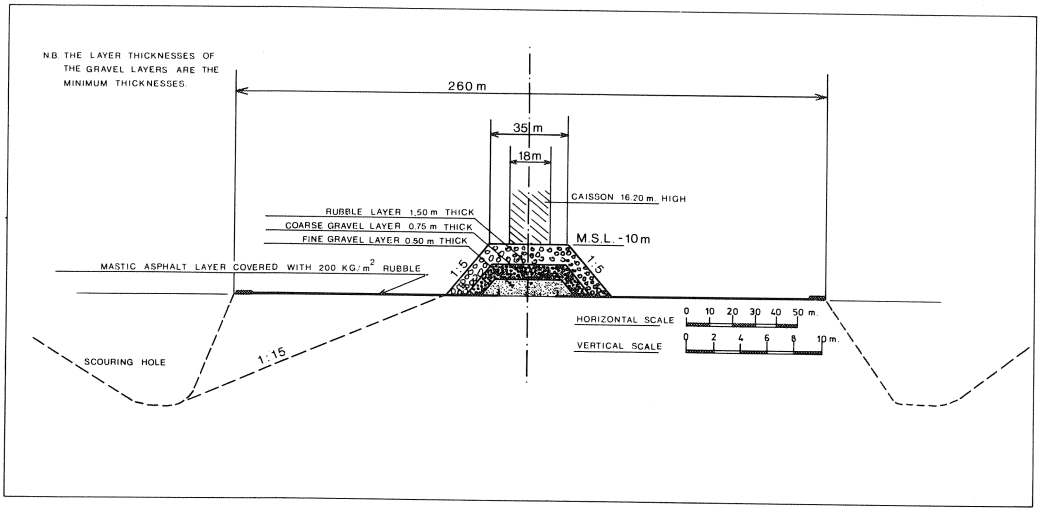

On the seaward side of the heads an extension to 160 m from the centre of the sill proved necessary (see figure 4.30).

1c Northern gap sill

The caisson sill in the northern gap was given a crest width of 35 m and a crest height of 10 m below MSL. This crest width was sufficient for placing the 18 m wide caissons while leaving room for the dumping of stones or slag on one or if necessary both sides of the caissons. The crown height of 10 m below MSL was determined so that the distribution of the discharge between the two (winter) closure gaps was virtually the same as that before the commencement of closure works.

1d Southern gap bottom protection

The method used for the southern gap is outlined in figure 4.31 and was based on the following.

As long as a situation of clear overfall has not been obtained, the heightening of a closure dam will lead to an increase in flow velocity over the embankment and in the degree of turbulence. At this stage there is still relatively little decline in the discharge.

Once the closure dam reaches the height at which a situation of clear overfall is obtained the flow velocity over the embankment will be at a maximum. Any further heightening of the embankment will lead to a decline in both the flow velocity and the discharge. The height of the closure dam marking the transition from submerged to clear overfall is a critical height, since the flow velocities over the dam are then at their greatest. For the determination of the width of the bottom protection this height was assumed to be roughly three-quarters of the original water depth (see figure 4.31).

The width of the bottom protection was selected in such a way as to ensure that the bottom would be protected at the point where the water flowing over an embankment of this height would hit the bottom.

The current over the embankment is only able to touch the bottom behind the eddy at a distance of six to eight times the embankment height.

In order to limit the depth of the erosion and to

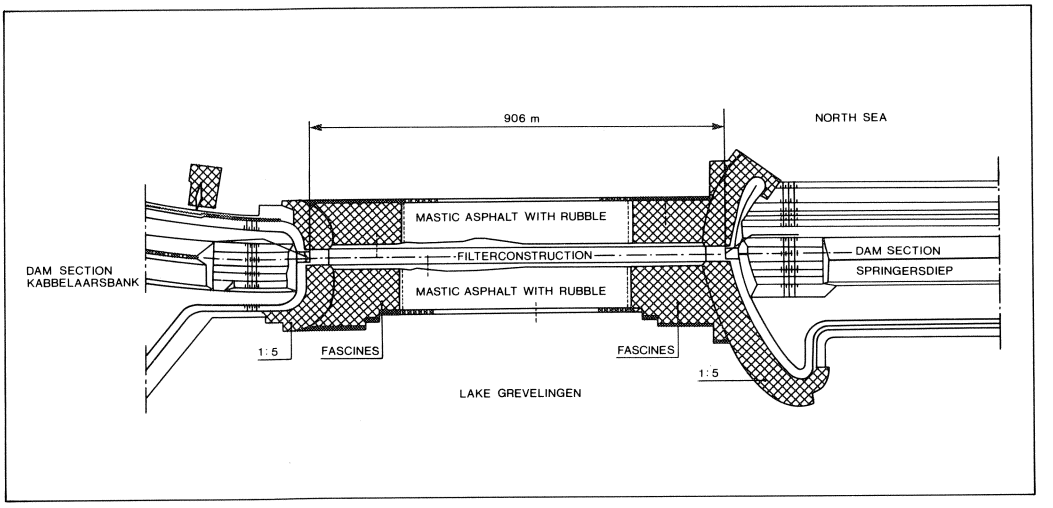

Figure 4.30. Bottom protection northern closure gap.

prevent scour from occurring too close to the sill, the protection of the channel bottom must be extended beyond the end of the eddying. If this is done the current flowing over the crest of the dam will always reach the bottom before the end of the protection. The design allowed for a reserve of at least 20 m, thus determining the dimensions of the bottom protection (see figure 4.32).

In practice these simple rules have proved applicable for temporary works only; for more permanent works (such as the stormsurge barrier in the Eastern Scheldt) these rules cease to hold good and extensive model analysis is required.

1e Southern gap sill

The southern gap sill consisted of a layer of rubble approx. 1.75 m thick and 2 x 10 m wide plus the basic width of the closure embankment. The basic width varied with the water depth. The purpose of this excess width of the sill was to enable the embankment to be built with a gentler slope than originally planned.

Figure 4.31. Southern closure gap.
Cross section bottom protection;
Sill and closure dam.

2a Construction of the bottom protection and means of installation

At the time the bottom protection was built in 1967 three types were available, namely:
- filter construction;
- mattresses;
- mastic asphalt.

All three of these bottom protection methods were used for the Brouwers dam.
The various kinds of bottom protection are set out in table 4.5. All these types of bottom protection were in the process of development and were refined in the course of construction of the Eastern Scheldt dam. Thus the bottom protections referred to under numbers 4 and 5 in table 4.5 were not used in the Brouwers dam but first developed for the Eastern Scheldt dam. In the case of the Brouwers dam, mastic-asphalt bottom protection was, after initial hesitation, used in the construction of the Grevelingen dam on a large scale for the first time, while mattresses evolved from the conventional brushwood kind to the so-called „sole" piece.

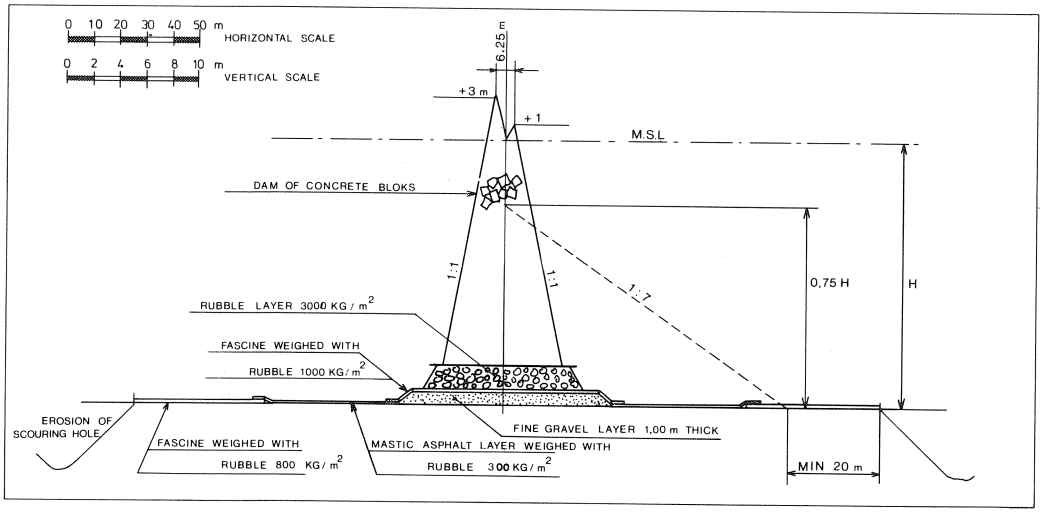

Table 4.5 Survey of types of bottom protection for the Brouwersdam

No	Type of bottom protection	construction	Principal components material	quantity	Quantity used in Brouwersdam
1	Filter (loose grained)	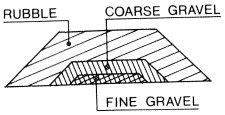	- rubble - coarse gravel - fine gravel	1.5 m layer 0.75 m layer min. thickness 0.50 m layer min. thickness	Over a length of 907 m with a 35 m crest in the n. gap
2	conventional mattress	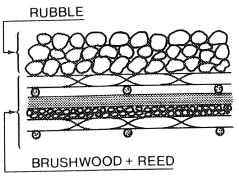	- rubble - brushwood - reed	800 kg/m² 4 bundles/m² 0,5 bundles/m²	**a.** at right angles to current 155,000 m²* **b.** in direction of flow 290,000 m²*
3	sole piece	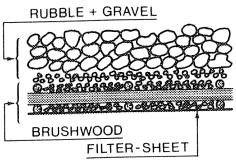	- rubble - gravel - brushwood - filter-sheet	600 kg/m² 200 kg/m² 2 bundles/m² 1.05 m²/m²	in direction of flow 140,000 m²*
4	block mat	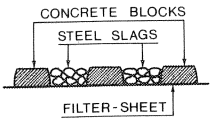	- steel-slag - conc blocks - filter-sheet	200 kg/m² 200 kg/m² 1.05 m²/m²	not used
5	concrete asphalt mats	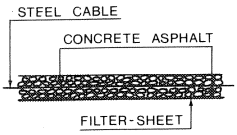	- concrete asphalt - filter-sheet	1.05 m²/m²	not used
6	mastic asphalt	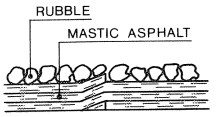	rubble mastic asphalt	s.gap:350 kg/m² n.gap:200 kg/m² in 3 layers up to total thicknesses of 30 and 24 cm	110.000 ton

* These quantities are the sum of the combined surface areas of the sunken mattresses

Table 4.6 Properties of different types of bottom protection

bottom protection / properties	mattresses with rip-rap		mastic asphalt	filter
	conventional	sole piece		
permeability	good	fair	none at all	good
sand-tightness	up to a gradient of c. 4%	up to a gradient of c. 25%	completely sand-tight	depending on constuction, up to v. steep gradients
suitability for use on slopes	good	good	On account of wet fluid applic. usable only on gentle slopes (up to 1:5 to 1:7). Able later in hardened condition to follow slopes.	Can be applied on slopes of up to c. 1:4. Once applied will not readily follow slopes.
surface nature	hydraulically rough	hydraulically rough	hydraulically smooth	hydraulically rough

The particular characteristics of the various kinds of bottom protection are shown in table 4.6.
The three types of bottom protection used are discussed in more detail below.

2b Filter construction
A loose-grained filter consists of layers of stony material of ascending grain size, constructed in such a way that the grains of one layer are unable to escape through the interstices between the grains of the layer above. The top layer of the filter is designed to retain granular stability against passing currents. The structure of a filter is determined according to the rules discussed in chapter 3. From bottom to top the sill in the northern gap was therefore constructed as follows (see figure 4.29):
- 2-5 mm gravel, av. layer thickness 0.50 m;
- 30 mm gravel, av. layer thickness 0.75 m;
- 10/300 kg rubble, layer thickness 1.50 m.

In determining the required layer thicknesses of the filter the various tolerances have to be taken into account in order to decide the acceptable minimum thicknesses. The filter must remain able to carry out its function at these minimum thicknesses. In the case of tolerances of 10 cm for the bottom and for the two gravel layers and 30 cm for the rubble layer, the minimum layer thicknesses employed were as follows:
- 2-5 mm gravel, 0.30 m;
- 30 mm gravel, 0.55 m;
- 10/300 kg rubble, 1.10 m.

The high-water level attained during the storm-flood of April 1943 (3.20 m above MSL) was taken as the design boundary condition for both the sand-tightness of the filter and the stability of the rubble in the upper layer. The frequency of such a water level is once a century. A water level of this order could, immediately after closure with the sluices shut, lead to a dif-

ference in level alternating in both directions of between 2.5 and 3 m (i.e. the boundary condition for determining sand-tightness).
The same high-water level with all caissons but one in position was taken as the boundary condition for determining the stability of the rubble in the upper layer of the filter. Model analysis indicated 10/300 kg rubble to be sufficiently stable to satisfy this boundary condition.
The gravel layers were installed by means of hoppers positioned alongside a moored pontoon, which were drawn along the sill at a given speed while discharging their load. This was done at the turn of the tide at current velocities of up to 0.30 m/s. The top of the gravel layer was dredged level at a depth of 11.50 m below MSL, with a permitted tolerance of 10 cm either way. The layer of rubble was then placed on top by means of stone dumpers. This 1.50 m thick layer was not dumped in one go but gradually, so that the depth could be monitored progressively and the sill kept level as required.

The dumping of the stone was possible in current velocities of up to 0.50 m/s. The crest of the sill had to be finished off level at a depth of 10 m below MSL, with a permitted tolerance of 30 cm either way. Over a large section of the sill the dumping technique in itself ensured that the required flatness was achieved.
In those cases where the depth variations exceeded the 30 cm limit, stone either had to be added or levelled off. The latter presented the most difficulties. To begin with a heavy steel frame attached to a cable was dragged over the sill in the expectation that this would have a levelling effect. The results were however disappointing, and better results were obtained with a carefully adjusted, slowly revolving bucket dredger.

2c Mattresses

Sand-tightness of mattresses
One of the conditions that bottom protection must satisfy is that of sand-tightness. Conventional mattresses (fig. 4.33) proved insufficiently

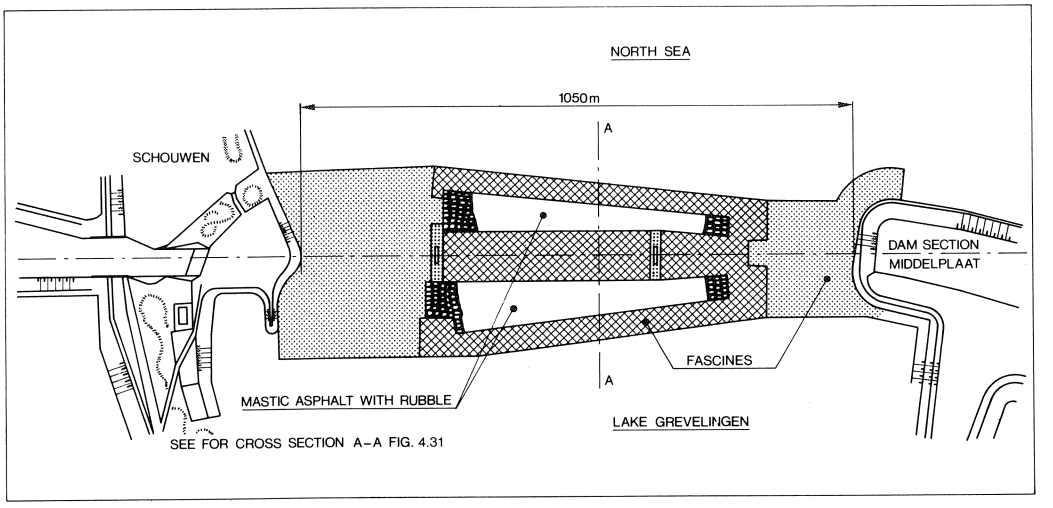

Figure 4.32. Bottom protection southern gap.

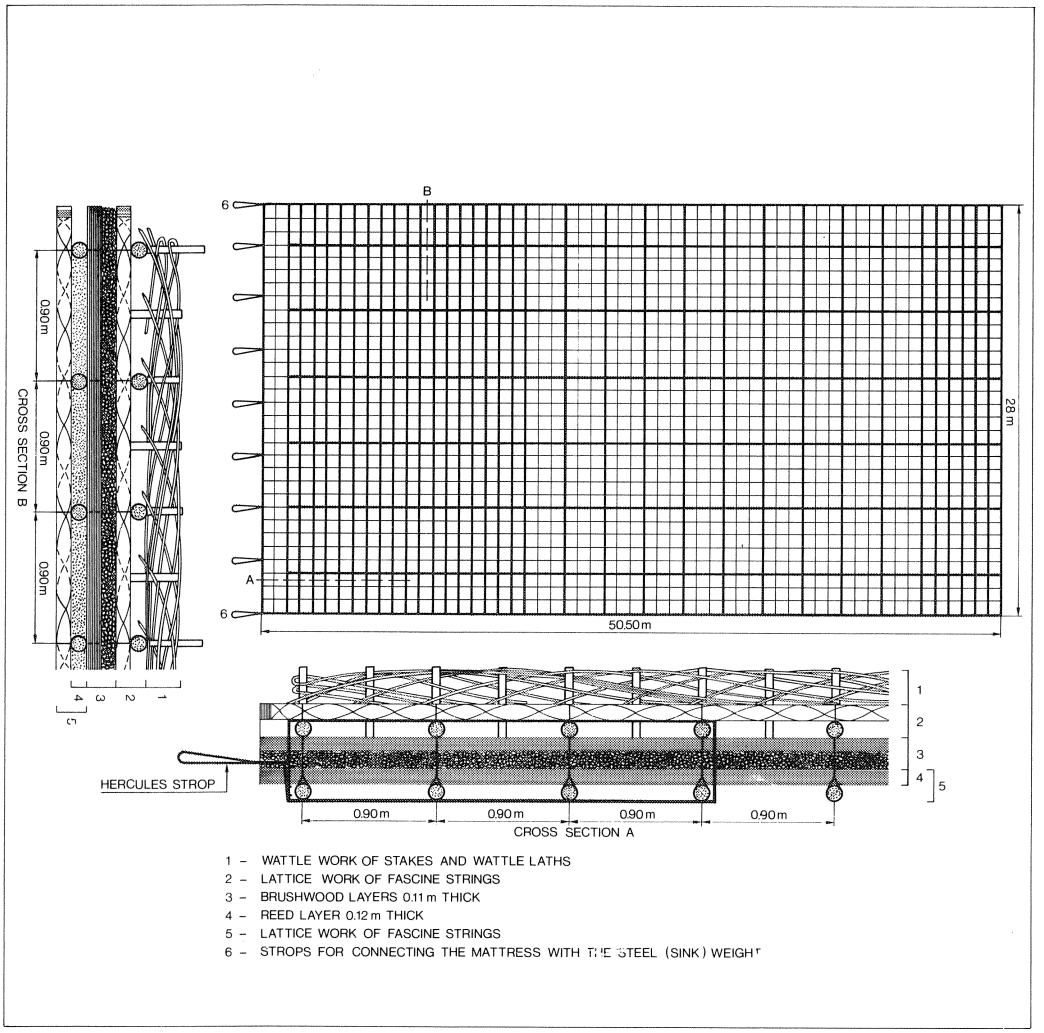

Figure 4.33. Construction of a conventional mattress.

sand-tight under the boundary conditions noted above, for which reason a „sole piece" was developed in which the bottom layer of the mattress was replaced with a sand-tight fabric (fig. 4.34). The sole used was of the „coconut matting" type, namely a polypropylene monophyletic fabric which, when applied in the right place in the mattress, has the property of being

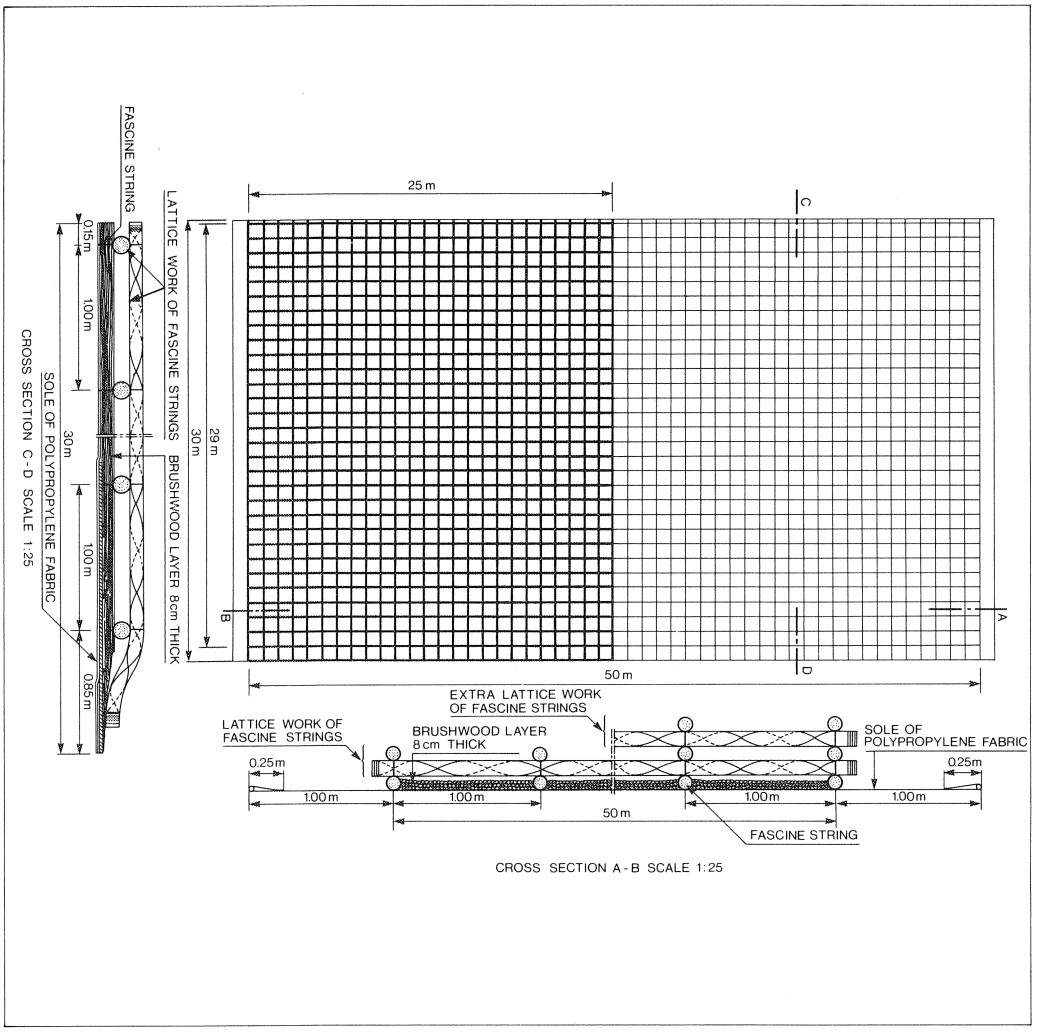

Figure 4.34. Construction of a matress with a "sole" of polypropylene fabric.

sufficiently sand-tight while also being completely permeable.

The latter is important since differences in permeability (e.g. at seams in the mattress or where two pieces overlap) give rise to concentrated water flow-off, which can result in large local sand-losses.

Rip-rap and edge weighting

The rip-rap is designed to sink and hold the mattress in place. In the case of a conventional mattress the rip-rap also serves to enhance sand-tightness. It must remain stable when exposed to current attack.

In the case of the current attack to which the rip-rap in the Brouwershavensche Gat was exposed, this condition was satisfied by limestone with a density of 2.65 t/m³ and a unit size of 10/300 kg. The current velocities with which this stone can cope may be calculated with the formula

$$\Delta . D_{50} > \alpha \frac{v^2}{2g}$$

in which:

D_{50} = average diameter of the stone material in m;

α = a coefficient varying with the degree of turbulence, in this instance 1.4;

v = current velocity in m/s;

$$\Delta = \frac{\rho_s - \rho_w}{\rho_w} = \frac{2650 - 1020}{1020} = 1.6$$

g = acceleration of gravity

ϱ_s = specific density of stone = 2650 kg/m³

ϱ_w = specific density of seawater = 1020 kg/m³

The mean diameter D_{50} may be calculated using

$$1/6 . \eta . d^3 . \varrho_s . g = G_{50}$$

in which:

d = D_{50}

G_{50} = average unit weight of the stone in N; in the case of 10/300 kg rubble, c. 1500 N.

In this instance $d = D_{50}$ = 0.48 m. The stone turns out to be stable: filling in the above formula we obtain $1.6 \times 0.48 > 1.4 \times \frac{v^2}{2g}$ from which it follows that the stone is stable at a current velocity of v = max. 3.3 m/s. The velocity encountered under the design boundary conditions was approx. 2.5 m/s.

In order to increase the stability of the rip-rap on the mattresses, an upright woven structure, (a wattle work of stakes and wattle laths) is installed on conventional brushwood mattresses. This could not, however, be done with sole pieces, since the posts would have damaged the fabric. For this reason an extra latticework of fascine-strings was added in the case of sole pieces. These did not, however, cover the full surface area of the mattress but 25 m wide strips along the edges.

The mattresses were weighed down with the following stone and gravel layers.

The preliminary ballasting was designed to reduce the buoyancy of the traditional mattresses, thereby reducing the angle of inclination of the mattress when sinking it at low current velocities.

The difference in stone size for sinking and final ballasting had two causes:

	conventional mattresses	sole pieces
prelim. ballasting with 10/60 kg stone	25 kg/m²	
sinking with 10/60 kg stone	200 kg/m²	
sinking with coarse gravel	–	200 kg/m²
final ballasting with 10/300 kg stone	+ 575 kg/m²	+ 600 kg/m²
total weight	800 kg/m²	800 kg/m²

- a stone dumper's load must be spread as evenly as possible during sinking, and with the stone dumper in question this proved easier using light stone;
- the points of overlap should not be weighed down with large stones since these will prevent a proper join between the mattresses.

The second factor has even more force in the case of sole pieces, since the aim is to cover the entire bottom with the fabric. For this reason the sole pieces were sunk with coarse gravel. Apart from the fact that coarse gravel effects a better join between adjoining mattresses, it is also cheaper and easier to spread evenly than rubble. Conventional mattresses might also have been sunk with gravel except for the fear that the gravel would have worked its way through the mattress; in the case of sole pieces the dense sole rules this out.

Tests carried out around 1970 indicated that in order to resist high current velocities, the edge of the mattress needed to be weighted down with some 800 kg of stone per m². At first sight this presented no problem since the quantity of stone used for weighting the mattress was in any case of that order, but if local scour were to occur along the edge of the mattress so that the edge ended up on a steep scour-hole slope, there would be a real risk of all or some of the stone rolling off the mattress. To prevent this the edges of the sole pieces were given extra weighting by means of concrete beams attached to the fabric with glue and ties (figure 4.35).

Mattress sinking

Between 1965 and 1967 a number of conventional brushwood mattresses were still sunk along traditional lines. This entailed transporting the mattress well before the turn of the tide to the place where it was to come to rest, where it was then achored. The actual sinking to the bottom was effected by mooring a number of barges loaded with 10/60 kg stone around the mattress, the stones then being transferred to the mattress by hand. This method of application was used for mattresses on steep slopes whose longitudinal axis was at right angles to

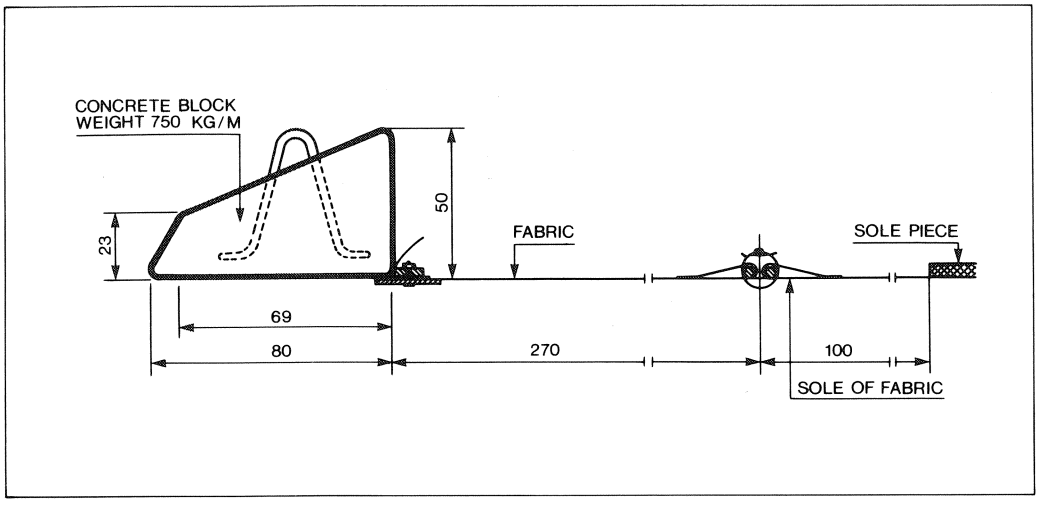

Figure 4.35. Attachment concrete blocks to sole of fabric.

Figure 4.36. Upstream lowering of fascine. Stone dumping vessel ,,Pieter'' preparing to moor in opening between pontoon and fascine.

the direction of flow. From 1967 onwards a different method was employed.
With this method the stones were no longer transferred to the mattress by hand but by means of special stone-dumping vessels known as stone dumpers, which released their load onto the mattress mechanically (figure 4.36). In order to enable a stone dumper to transfer its load to a mattress, the latter had first of all to be

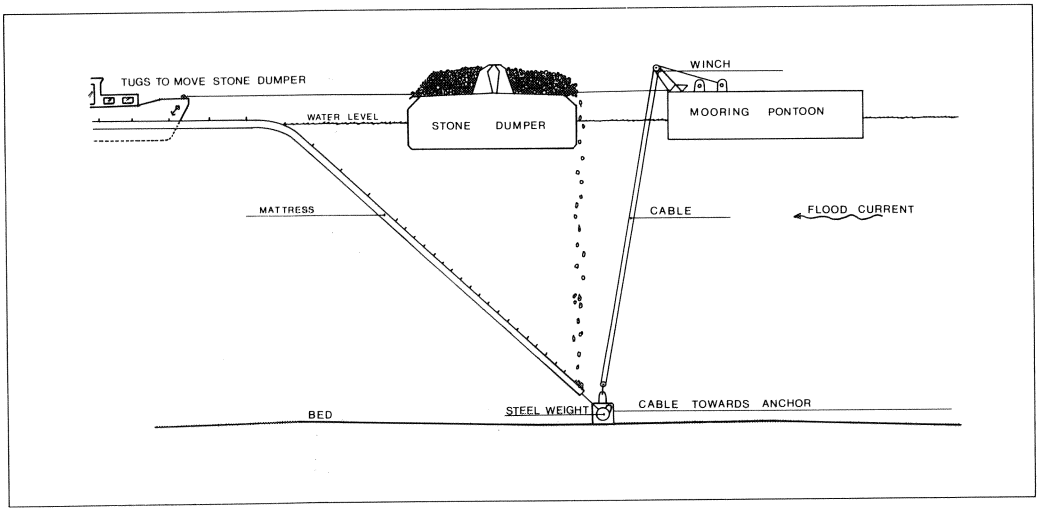

Figure 4.37. Lowering a mattress by stone dumping.

pressed down to the bottom in some manner. This was done by attaching a weight to one of the narrow ends of the mattress (the head), for example a hollow steel pipe which could be filled with water, so that the edge of the mattress would be carried down to the bottom (figure 4.37). This operation was carried out at the turn of the tide, with the mattress ending up more or less vertically in the water. In order to create sufficient space between the mattress and the moored pontoon from which the steel pipe was winched down, the angle of the mattress had first to be reduced. This was initially done by making use of the current pressure. Later, tensile force was also exerted on the tail of the mattress („stretched" sinking). The advantage of this method was that it cut the time required for the sinking manoeuvre and that it also enabled mattresses to be sunk the longitudinal axis of which was not in the direction of flow, e.g. along the natural levees.

2d Mastic asphalt

Beneath a continous mastic-asphalt layer overpressures may be produced.

The size of these overpressures and hence of the thickness of the mastic-asphalt layer are to a large extent determined by the difference in water level an by the width of the mastic-asphalt layer.

The thickness of the mastic-asphalt layer may be reduced by covering it with a layer of rubble. The combined weight of the mastic-asphalt and the rubble must be at least equal to the overpressure on the asphalt revetment. The rubble layer more over provide the mastic-asphalt with a hydraulicly rough surface, with has a favourable effect on the depth and slope of the scourhole.

The mastic-asphalt used as bottom protection consisted on average of:

- 17.2% by weight of asphalt bitumen;
- 20.8% by weight of very weak filler;
- 62% by weight of sand.

This mixture was the result of systematic laboratory research into the hollow space of sand-filler mixtures and the overfilling degree of this mineral aggregate.

An important criterion consisted of the application viscosity, which had to be between 700 and 800 poises in order to ensure that the mastic

Figure 4.38. Sinking by making use of the current pressure in the southern closure gap.
In front, a stone dumping barge loaded with about 600 tonnes of stone.
In the centre, the mattress anchored between two pontoons.
At the upstream side, the mattress is already submerged.
At the back the Isle of Schouwen.

Figure 4.39. Sinking by making use of the current pressure in the southern closure gap.
In front the mattress between two pontoons. Behind it, the loaded stone dumping barge.
Left: two pylons for the cableway.
At the back: the working island Middelplaat.

asphalt would flow properly through the feed pipe on the „Jan Heymans", a barge fitted with an asphalt plant (figure 4.42).
In the southern gap the design thickness of the mastic-asphalt layer was 30 cm, the latter then being covered with 300 kg of 10/60 kg rubble per m². The purpose of the rubble was to ensure that, together with the mastic-asphalt layer, sufficient weight would be obtained to counter possible overpressure against the bottom of the mastic-asphalt layer. The mastic asphalt was laid in 5 m wide/0.15 m thick strips overlapping one another by 2.50 m like roofing tiles. The strips were laid in the direction of flow, with the vessel moving from east to west. In order to obtain a good join with mattresses adjoining the mastic-asphalt layer, a 5 m overlap was allowed for. The depth at which the asphalt was laid varied between 8 and 25 m below MSL.
No gaps in the mastic-asphalt layer, were observed. Once the asphalt had been laid it was covered with a layer of rubble by means of the stone-dumpers.
In the northern gap the design thickness of the mastic-asphalt layer was 24 cm, which was then covered with 200 kg of 10/300 kg rubble per m². The rubble served a dual purpose, namely (i) helping ensure that, as in the southern gap, sufficient ballast would be obtained to counter possible overpressure against the bottom of the mastic-asphalt layer, and (ii) the formation of a hydraulically rough surface.
The 24 cm thick mastic-asphalt layer weighted down with 200 kg of rubble proved sufficient to compensate for any overpressure on the layer. This did not, however, hold good for the edge of the bottom protection, where the ballasting proved inadequate. By increasing the ballasting along the edge of 800 kg per m², the bottom protection proved in tests to resist folding back and flipping over even in circumstances similar to those of the design storm of April 1943 (a storm with a frequency of occurence of once in a hundred years). This greater ballasting could have been obtained with stones, but measures would than have had to be taken to ensure that they did not roll off the mat if the latter came to rest on the slope of a scour hole.
For this reason the mastic-asphalt layer was weighted along its edge with 500 kg of rubble bound together with 300 kg of asphalt per m² (fig. 4.43). The mastic-asphalt itself was not applied in one go to a thickness of 24 cm but in three 8 cm layers. There were two reasons for doing so. The first of these was to limit the extent of hot flow (which increases at greater thicknesses), which is relevant if the asphalt has to be applied over a sand ripple or some other irregularity on the bottom; the second was to obtain a more uniform thickness of the bottom protection.

Figure 4.40. Manufacture of a mattress
The fascine strings of willow brushwood are lashed with lanyard to the „sole" of polypropylene fabric.

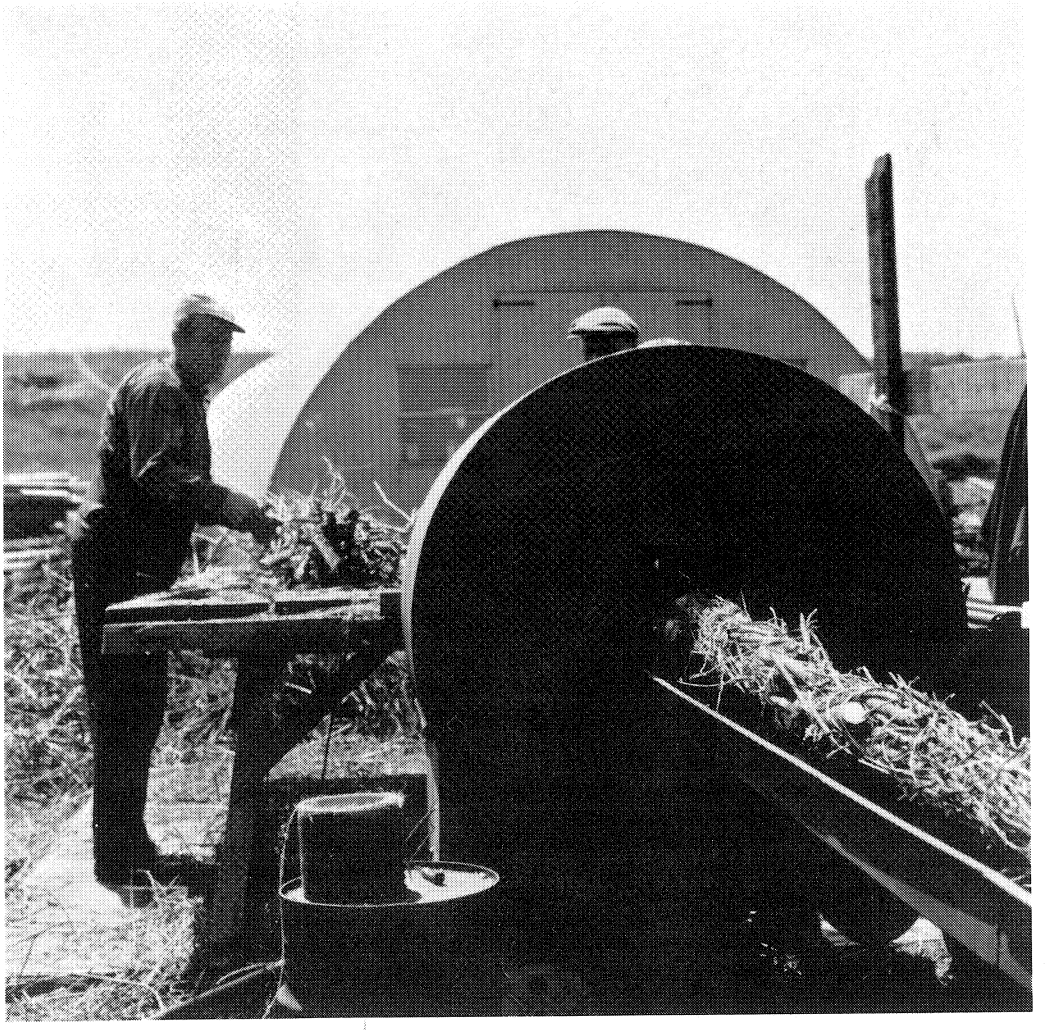

Figure 4.41. Mechanical producing of fascine strings of willow branches.

In order to ensure that the bottom would be fully covered with an asphalt mat consisting universally of at least two layers. the 8 cm thick strips were laid in roofing-tile fashion, each strip overlapping the last by two-thirds its width. The possibility existed of sand deposits being formed on a given strip before the next strip had been laid, thus preventing a proper join between the two. Tests revealed however that, given the

Figure 4.42. The asphalt vessel „Jan Heymans".

width of overlap, there was no need for concern that sand might be washed out throught the open „gills", besides which these „gills" served to reduce overpressure under the asphalt mat.

Required quantities, fabrication and storage of concrete blocks for closure of the southern flow gap

For the closure of the southern gap concrete

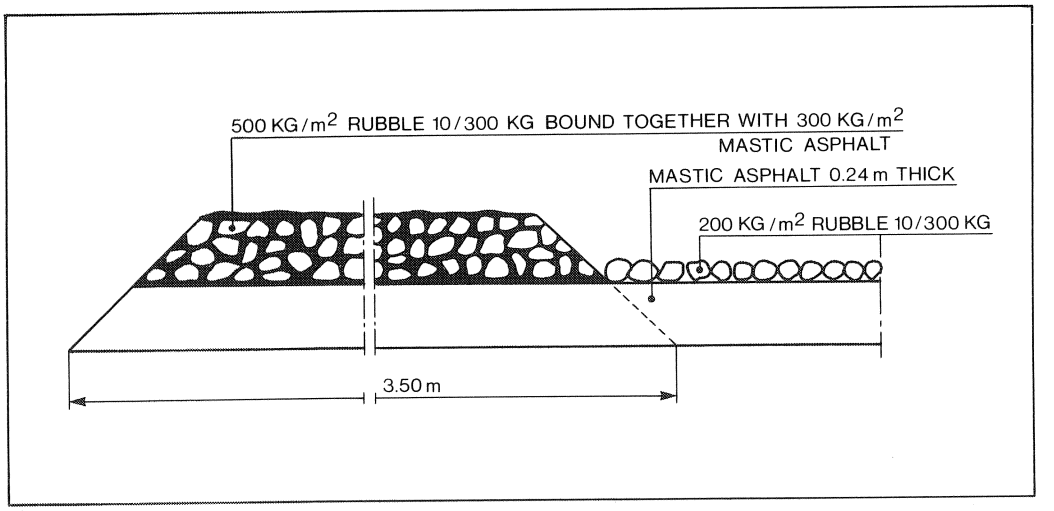

Figure 4.43. Strengthening along the edge of the mastic asphalt layer.

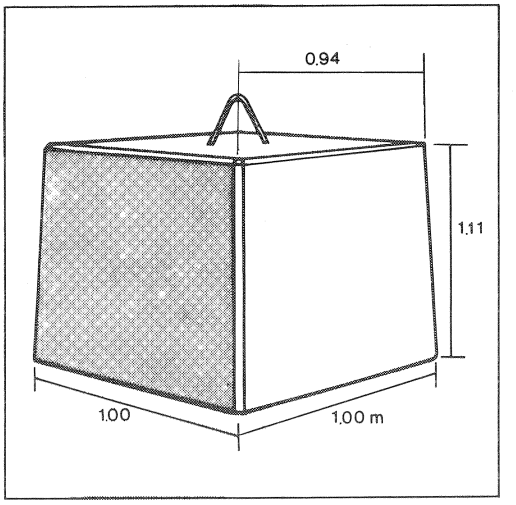

Figure 4.44. Example of a concrete block used for the closure of the Southern flow gap.

blocks were used, with dimensions as specified in figure 4.44. These blocks were 1.04 m³ in volume and weighed around 2.5 tonnes. A hook was incorporated into each block by means of which it could be transported and ultimately fastened to the cableway gondolas.

Assuming 40% hollow space between the concrete blocks of the block-dam the required quantity was calculated as follows:

a. in the body of the block-dam (fig 4.31)	187,510 units
b. as a result of anticipated settlement	9,550 units
c. in the strengthening of the block-dam against the Schouwen shore (fig. 4.56)	4,500 units
d. storm damage calculated at 19 units per metre	+ 19,000 units
	220,560 units
e. 7% damage	+ 15,440 units
TOTAL	235,900 units

On the basis of these estimates, and allowing for the fact that a number of blocks would be left over after the closure of the Rak van Scheelhoek,(a closure gap in another delta-dam, which was closed in 1970) an order was placed for the fabrication of 210,000 blocks.
In the event these calculations proved on the pessimistic side. Thus it was concluded from the data obtained from the closure of the Rak van Scheelhoek that the hollow space did not amount to 40% but 43%, with allowance for damage already being included in the latter figure.
The number of blocks left over after the closure of the Rak van Scheelhoek was 46,000, and no storm damage occurred during the closure of the southern Brouwers dam gap. The number of blocks theoretically required for the block-dam on the basis of these subsequently obtained data then became:

a.	in the body of the block-dam	178,130 units
b.	as a result of anticipated settlement	9,070 units
c.	for the strengthening against the Schouwen shore	+ 4,280 units
	Number of blocks required	191,480 units
d.	left over from closure of the Rak van Scheelhoek	– 46,000 units
	Number of new blocks required	145,480 units

The latter figure is not far off the number of blocks actually installed in the dam by means of the cableway, viz. 149,439 units. The blocks left over from the closure of the Rak van Scheelhoek were not brought to the dam by cableway but transported by ship from the Haringvliet dam to the Brouwers dam in the year prior to closure and directly off-loaded by crane into position in the dam.
The blocks were fabricated at a site with deep-water access at Dinteloord in North Brabant, some 50 km from the Brouwers dam.
From there the concrete blocks were transported to the Brouwers dam by ship.
The concrete composition of the blocks was as follows:

- 30-80 mm coarse gravel	1,010 kg
- 5-30 mm concrete gravel	550 kg
- 0-5 mm concrete sand	700 kg
- Hoogoven A-B cement	200 kg
- water	60 kg
TOTAL	2,520 kg

The concrete was mixed with the aid of two special concrete-mixers with a volume of 1500 l dry matter each and a capacity of approx. 230 m³/hour. The concrete was then transported to a set of 12 steel boxes, into which it was poured. The concrete was next vibrated for one minute by means of two high-frequency vibrators (9000 revs/min.).

Immediately after vibration the blocks were withdrawn from the boxes, which were then repositioned for a further filling with concrete.

As noted above, the blocks left over from the closure of the Rak van Scheelhoek were transported by ship to the Brouwers dam and off-loaded directly into the dam cross-section.
The blocks fabricated at Dinteloord were conveyed by ship to the working harbours at Middelplaat and Schelphoek, where they were unloaded onto lorries and transported to the two depots - those from the Middelplaat harbour to the nearby depot a kilometre away on the Middelplaat dam section and those from the Schelphoek harbour to the depot on Schouwen at a distance of 6 km.

The blocks were stored on either side of the southern closure gap: 90,000 units on the Middelplaat dam section and 110,000 units at the Schouwen depot (figure 4.46). Storage took place in large, specially-prepared sites with a sand-cement stabilization. The blocks were stacked in such a way that they could be picked up in the depots in horizontal rows of six, this being the capacity of the gondolas, given the space limitations the blocks were stacked seven or eight high (see figure 4.45). It was particularly important in stacking to ensure that the hooks in the blocks were spaced at 1.10 m intervals, this being the spacing of the suspension points on the gondola.

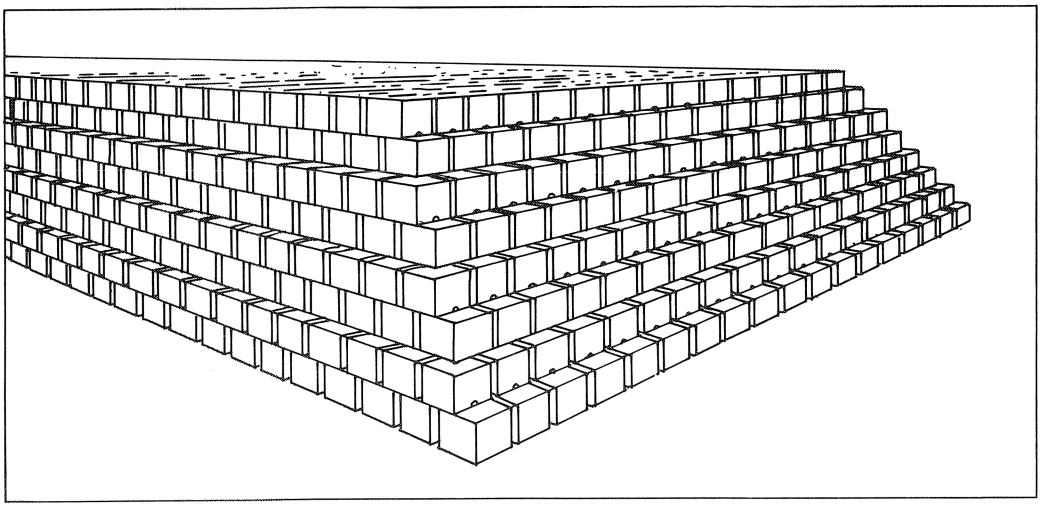

Figure 4.45. The stacking method of the concrete blocks.

Figure 4.46. The cableway in the southern flow gap and stores of concrete blocks.

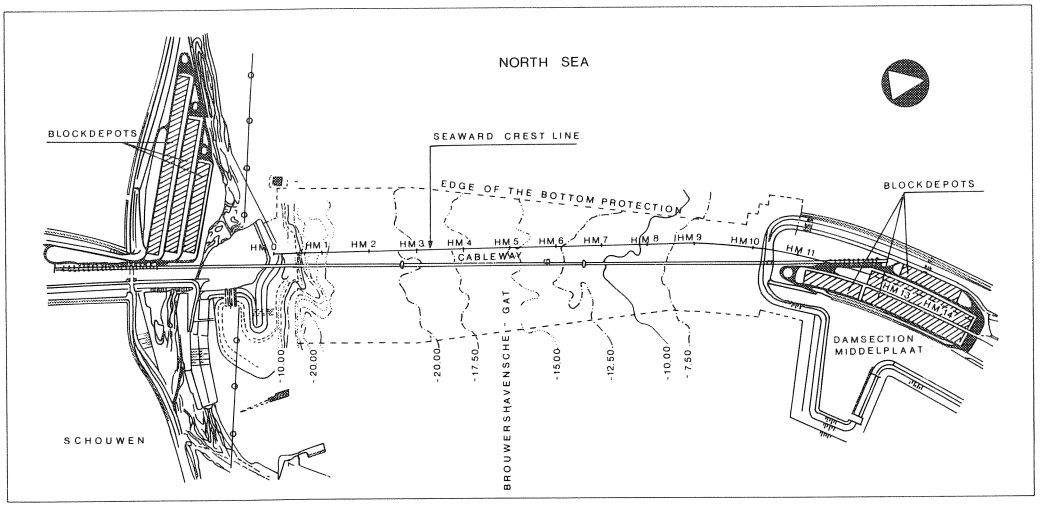

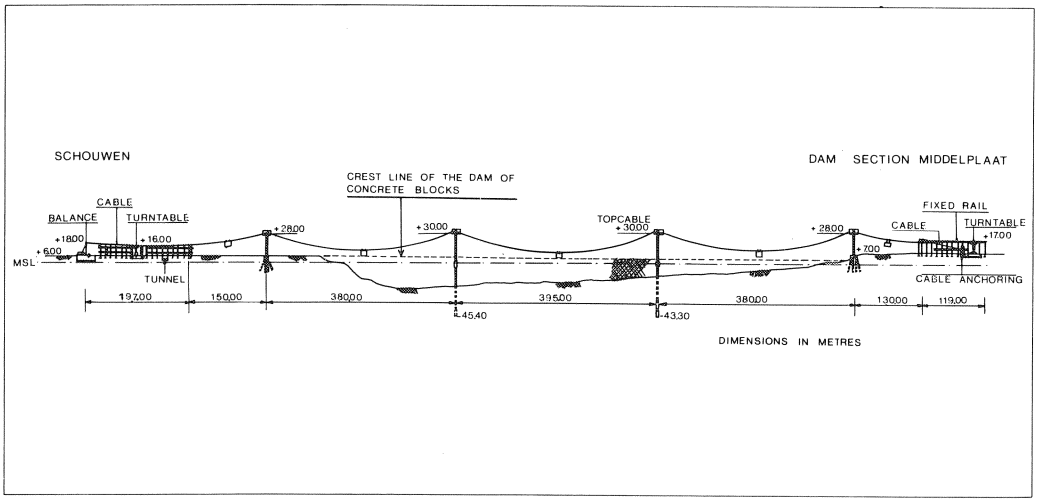

Figure 4.47. Outline of cableway.

Figure 4.48. Loaded and dropping cable caps (gondolas) passing.

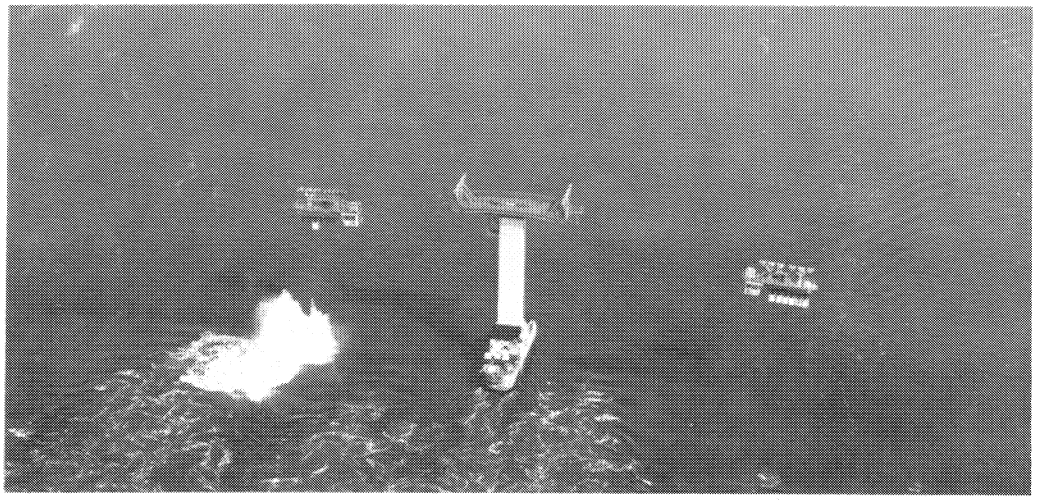

Cableway design

The design of the cableway is shown in figure 4.47. The gondolas used for transporting the concrete blocks along the cableway to their final location in the closure dam were equipped with a turbine (fig 4.48).

The own weight of the gondolas was 17 tonnes and their effective carrying capacity 15 tonnes. In order to limit damage to the blocks, they were not allowed to be dropped from more than 10 m above water level or the dam itself where the latter was above water level.

This meant that at certain points of cableway -particularly near the supporting towers, where the cable was fitted at a height of 30 m above MSL - the load had first of all to be slackened off before the blocks could be discharged. The easing off and dumping could be carried out as successive steps while the gondola was in motion. The gap between the supports was greatest in the middle span, namely 395 m. The diameter of the cables was 106 mm, while the tensile force on the cables was 350 tonnes.

With this design it was possible for two loaded gondolas to be carried per span at the same time, provided they were separated by at least 100 m. The height of the supports was such that the gondola loads would always be above the crest of the block-dam (3m above MSL).

The cable was tensioned by a counterweight on the Schouwen side (figure 4.49). This consisted of two tiltable weights exerting a tensile force of 350 tonnes on the cables. On the Middelplaat side the cable was attached to a reinforced concrete anchoring block (figure 4.50). The cable was able to move freely to and fro over all the support and restraining points of the fixed rail construction as well as over all the bearing points in the towers. Depending on their position and whether or not they were laden, the gondolas caused varying degrees of sag in the cable, and the tensile force on the cable had continually to be kept in balance with the mobile weight. This meant that the cable was continually in motion, with the counterweight going up and down.

The cable did not move smoothly but in jerks. This was brought about by the frictional force at

Figure 4.49. Balance with tiltable weights.

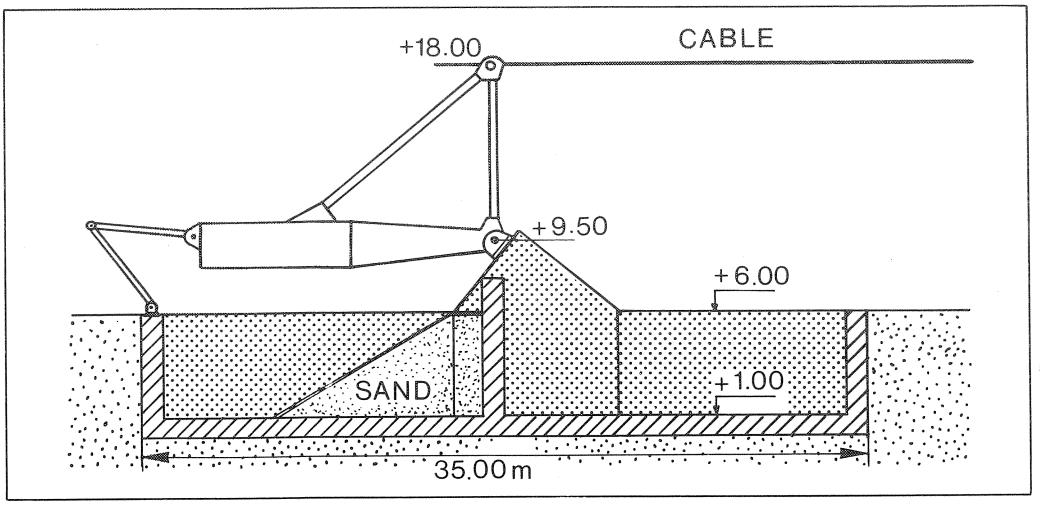

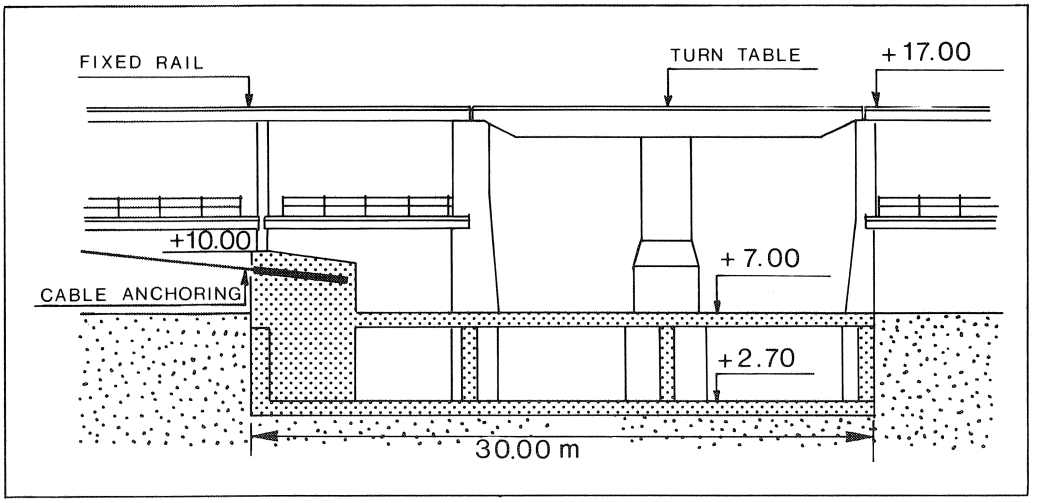

Figure 4.50. Reinforced concrete anchoring block.

the bearing points. The difference between the horizontal component of the tensile force on the cable either side of a bearing point had first to exceed the frictional force at the bearing point before the cable would jerk through in the direction of greater force. The cable would return to rest once the altered angles of the cable had reduced the horizontal component of the tensile force in the cable to below the frictional force.
The high pre-tensioning on this self-supporting cable enabled variations in the degree of sag to be kept comparatively small.
Similarly the slopes of cables as they approached the high bearing points was kept limited, thus reducing the required turbine capacity of the gondolas.
The boundary condition for the desired working capacity of the cableway was determined by the speed with which it was desired to narrow the wet cross-section during the most critical phase of the closure. In this case the most critical phase was regarded as the stage in which the original wet cross-section was to be reduced to values between 75% and 90%. As discussed previously, this phase was also the decisive one for determining the width of the bottom protection. Hydraulic research had indicated that in the critical phase the cross-section had to be narrowed at a given minimum rate for scour to be kept within acceptable bounds. On account of the layered construction of the dam, however, raising the level of the closure dike required a greater number of concrete blocks during this phase and hence more time than in the preceding phases. The cableway capacity required for executing this critical stage sufficiently quickly therefore determined the capacity of the cableway in general.
During the critical phase a weekly capacity of 90,000 tonnes was required, i.e. an average hourly capacity of 1,000 tonnes given a 90-hour working week.

The cableway consisted of three spans, 380 m, 395 m, 380 m in length, while the side spans were 130 m and 150 m long. The spans rested on four pylons. Two of these were placed in the water, with the cables at a height of 30 m above MSL, and two on land, with the cables at 28 m above MSL. These dimensions enabled two gondolas

to be carried on each span. Fixed rail sections were constructed on the shore-ends of the two side spans. These sections included the turntables used for switching the gondolas from one track to the other.
On the Schouwen side a 60 m garage track was constructed behind the turntable. The track, which was largely roofed over, enabled maintenance and minor repairs to the gondolas to be carried out in all sorts of weather. In the case of major repairs gondolas were removed from the track and placed on a specially constructed carrier. On the Middelplaat side there was a short 14 m run-out beyond the turntable. This enabled a gondola to be quickly shunted out and prevented it from running off the turntable if, as result of faulty manoeuvring, it had failed to come to rest upon entering the turntable.
The gondolas travelled in circuits over the two cables, which were set 6.25 m apart. The gondolas were loaded up on one side (e.g. Schouwen), travelled along one cable to the dumping point, and then proceeded to the opposite shore (Middelplaat). After being re-loaded the gondola would then travel back along the other cable to the dumping point, ultimately returning to the loading station on the Schouwen side. The overall circuit length was 3,267 m.

Based on (i) the so-called velocity characteristics of the turbine, and (ii) the loading time, the time required to travel a complete circuit was calculated at 1100 seconds. The net number of gondolas required was then calculated with the aid of the formula:

$$\text{net number of gondolas} = \frac{T.C.}{2.L.WC}$$

in which:
T = calculated time taken to complete circuit in seconds;
C = average hourly capacity of the cableway in tonnes /second;
L = effective carrying capacity of a gondola in tonnes;
WC = working coefficient, by which was understood

$$\frac{\text{actual capacity}}{\text{theoretical capacity}}$$ of the cableway, i.e. a figure between 0 and 1.

If the magnitude of WC is put at 0.75, the net number of gondolas required becomes:

$$\frac{1100.\frac{1000}{3600}}{2\times15\times0.75} = 13.58 \text{ or (rounded off) } 14 \text{ gondolas}$$

If the gondolas are taken as having an operating coefficient of 0.9, meaning that 90% of the gondolas would on average be in effective use, the total number of gondolas rises to a minimum of 16. The total number of gondolas with which the cableway was equipped was one less, i.e. 15 gondolas.

1 Caisson design and caisson construction in a construction dock
Hydraulic research had indicated the required size of the northern closure gap below MSL to be approx. 8,000 m². This area was determined on the basis of the proportionate narrowing of the two closure gaps, since a disproportionate narrowing of one gap in relation to the other could have produced a transverse water-level gradient with the risk of a short circuit between the two gaps. The selected sill depth of 10 m below MSL and the associated sill length were derived from the required wet cross-section surface area of 8,000 m², with attention being paid to the bottom configuration of the closure gap and manageable caisson dimensions.

2 Sluice caisson design (figure 4.51)
The Brouwershavensche Gat is exposed to swell from the North Sea. The ability to work at sea is in fact more affected by swell than by wind waves. In order to be able to place all the caissons within the appointed time it was important to minimize the number required.
Caisson length was determined by (i) the magnitude of the stress to which the caissons would be subject from their own weight and from the ballast, and (ii) the means by which they were supported from underneath on the sills.
In practice it turned out that height variations of

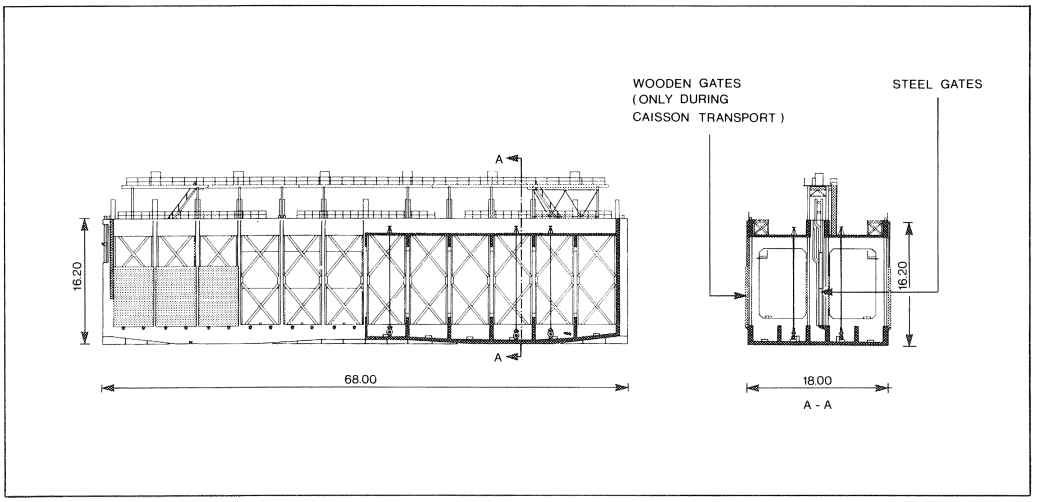

Figure 4.51. Sluice caisson.

approx. 30 cm were still encountered in a sill that had been „levelled off" by dredging.
By fitting the caisson with a „camel back" on the bottom, it could be assumed that the load would be taken by the two „humps" resting on the sill.
By positioning the humps in such a way that when they took the weight the moments in the caisson bottom were minimized, the length of the caisson could be set at 68 m. This meant that the number of sluice caissons required was twelve. On account of stability requirements during towing and sinking the width was set at 18 m. The height of the caissons was 16.20 m, their draught 6.10 m and displacement some 7,000 m³. Each caisson had twelve sluices or culverts 5 m in width. Each of these openings could be closed off by two gates placed along the length of the caisson. During the sinking operation the bottom gate was lowered and served as a shifting board for increasing the caisson's stability. During towing and sinking the openings were closed by wooden gates which increased the displacement of the caissons to the point that they could be towed afloat. Each caisson was fitted with sixteen 50 cm diameter valves for filling the caissons during sinking.
On the basis of laboratory tests, the steel sections criss-cross behind the openings were provided with a semi-circular edge to improve the flow. This measure enabled the discharge coefficient to be increased from its original level of 0.73 to approx. 0.82.

3 Sluice caisson calculation principles (figure 4.52)

The centre of gravity of the caissons lies at 0.43 x the height calculated from the bottom. Their weight by volume was low, namely 0.377.
The load on a sunk caisson takes three forms, viz.:

- static;
- quasi-static;
- dynamic.

The static load is formed by the dead weight of the caisson (80 tonnes/m) and the ballast (45 tonnes/m); the quasi-static load by the relatively slow-changing water pressures resulting from difference in water level, long (swell) waves (60 tonnes/m) and the dynamic load by wave im-

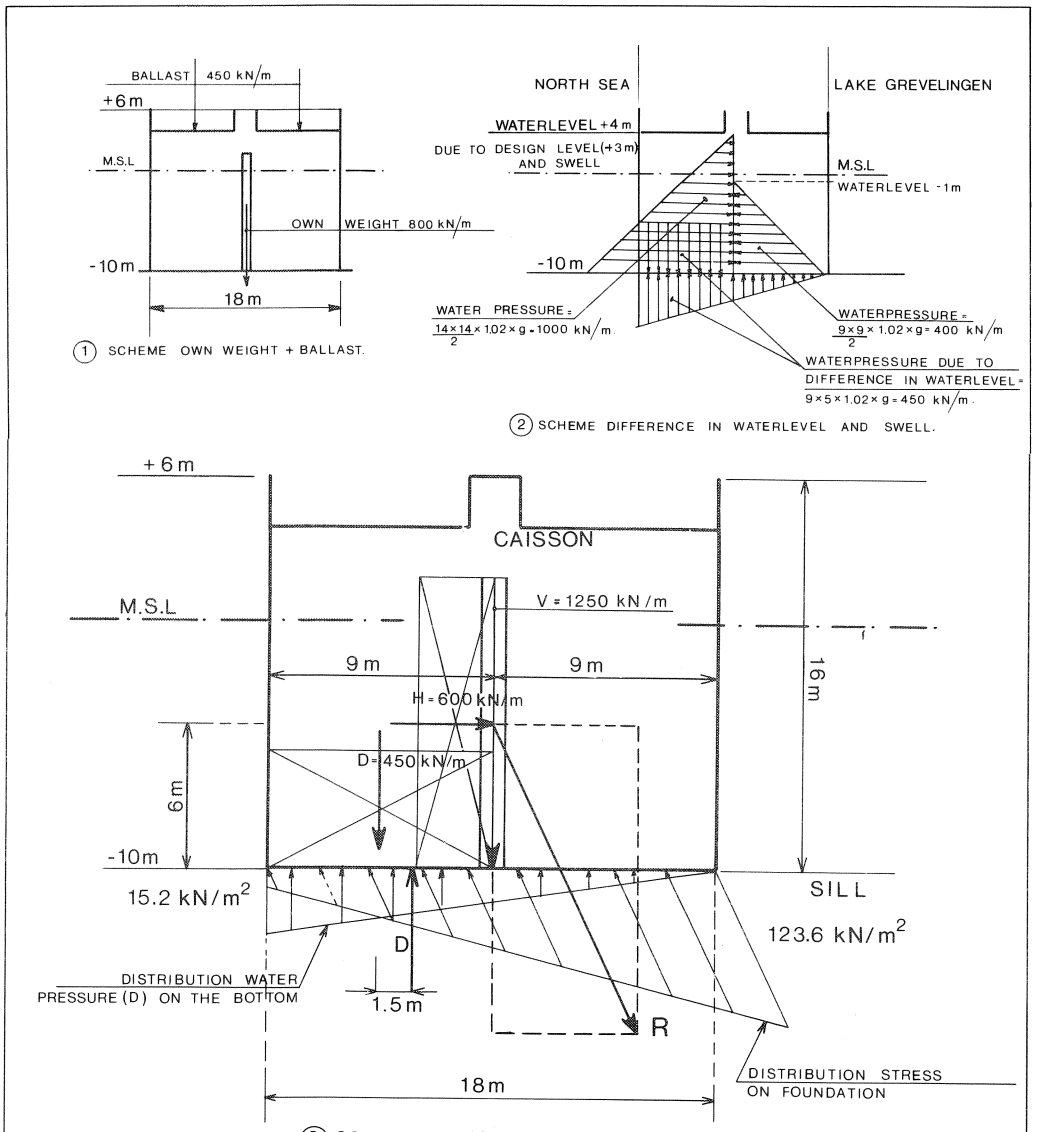

Figure 4.52. Loads on caissons.

pacts caused by wind waves (82 tonnes/m). The first two types of loads extend the full length of the caisson and must therefore be in equilibrium with the foundation pressure or with the grain stress between the stone sill and the caisson bottom. With the exception of dynamic load, figure 4.52 provides a survey of caisson stress. The grain stress between the stone sill and the caisson bottom is (see figure 4.52):

$$\sigma = \frac{P}{F} \pm \frac{M}{W}$$

in which:
- σ = grain stress in KN/m²;
- P = vertical load in KN;
- F = base surface area bearing the vertical load P in m²;
- M = moment of all the loads acting on the caisson in KN/m;
- W = moment of resistance of base in m³.

$$\sigma = \frac{1250}{18} \pm \frac{6 \times 600 - 1.5 \times 450}{1/6 \times 1 \times 18^2}$$

$$\sigma_{max} = 69.4 + 54.2 = 123.6 \text{ kN/m}^2$$

$$\sigma_{min} = 69.4 - 54.2 = 15.2 \text{ kN/m}^2$$

This stress may be resolved into a vertical component and a horizontal frictional force. These loads then determine the strength which the caisson as a whole is required to possess.
The dynamic load exerts a local influence on the upper gates and is decisive for the required strength of the gates, gate tracks and cross-girders, but not for the stability of the caisson as a whole.

Because the flat sections of the caisson bottom may rest on a flat sill, a coefficient of friction of 0.5 was assumed. Given a normal force of V = 1250 KN/m this means a horizontal force of 0.5 x 1250 = 625 KN/m, or just sufficient to cope with the quasi-static load of 600 KN/m. If this load is exceeded the caisson will not only start shifting but also setting, i.e. forcing its way into the stone sill. If this happens the ribs will start bearing part of the frictional resistance, as a result of which the coefficient of friction can rise to an estimated 0.85.
From the above it is evident that given the loads shown in fig. 4.52, a coefficient of friction of at least $\frac{H}{V} = \frac{600}{1250} = 0.48$ is required in order to prevent shifting.

This means that the safety coefficient against shifting $\gamma = \frac{H(\text{available})}{H(\text{actual})} = \frac{625}{600} = 1.04$

At higher loads, if the ribs also begin to bear some of the load, $\gamma = \frac{0.85}{0.48} = 1.77$

4 Abutment caissons (figure 4.53)
The closure gap was bordered on both sides by slopes with a gradient of 1:5. On these slopes caissons had to be placed the bottoms of which were at the same angles as the slopes. These caissons lacked any sluices but were fitted with six 50 cm diameter valves.

5 Reserve caisson
A Phoenix caisson dating from the Second World War was used as a reserve. This caisson, of the Phoenix type, measured 62.06 m (l) by 13.42 m (w) by 12.20 m (h). In order to prepare it for possible use a number of modifications were carried out at a drydock in Vlissingen.

Before the closure the caisson was transported to the port of refuge at Zijpe at the eastern end of Schouwen-Duiveland, from where it could have been brought to the closure gap at short notice if needed. To compensate for the fact that it was some 4 m lower than the sluice

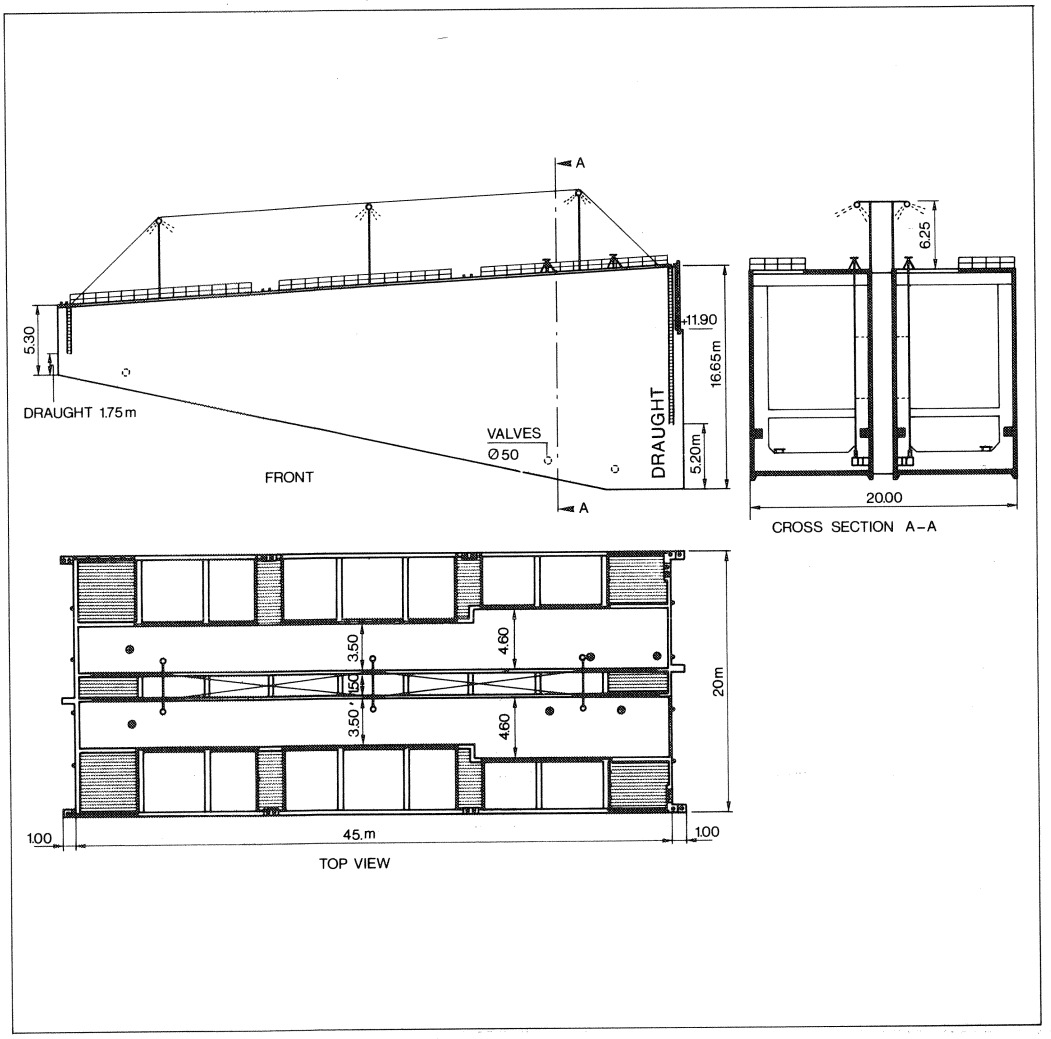

Figure 4.53. Abutment caisson.

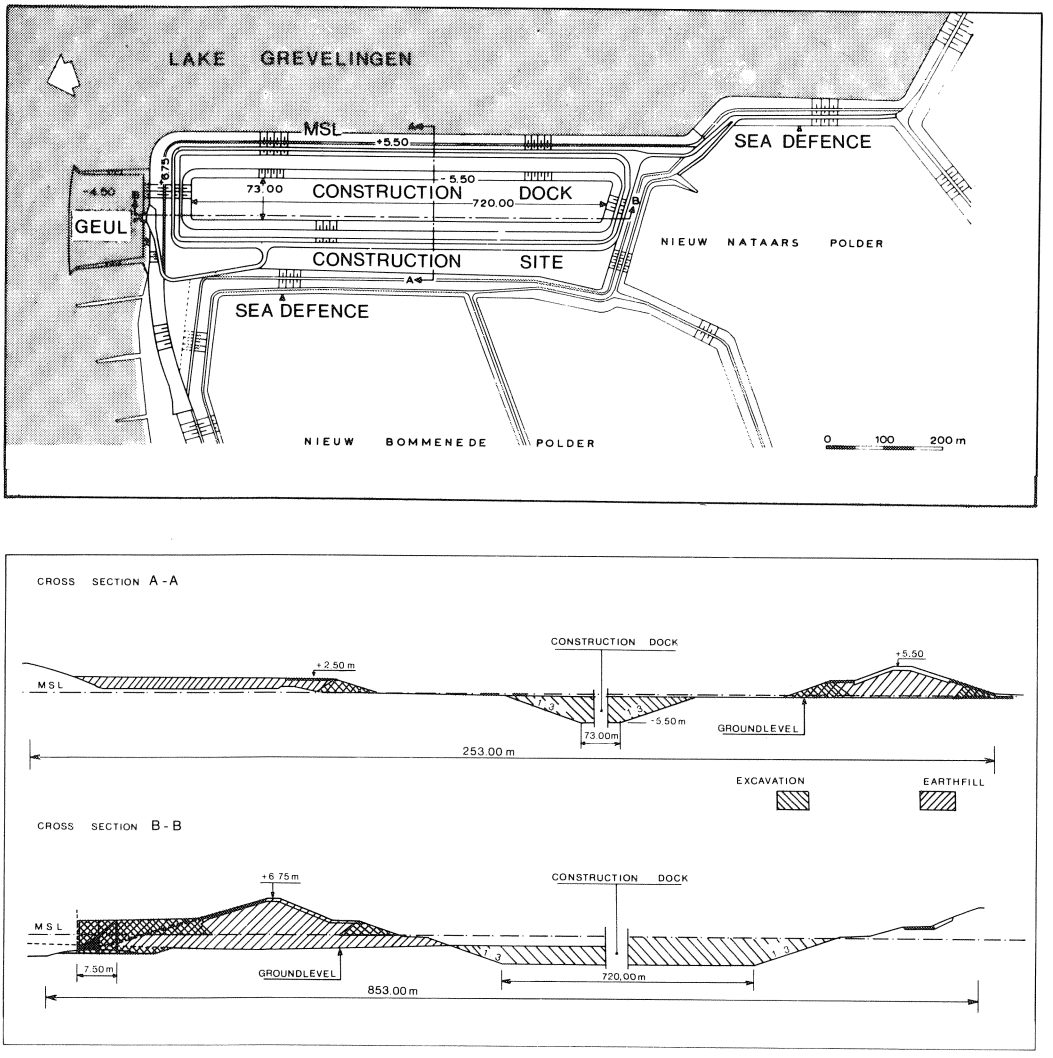

Figure 4.54. Construction dock of the caissons.

caissons, it was planned to construct a Bailey bridge after the caisson had been installed. In the event the caisson was not used in the closure.

6 Construcion dock

The twelve sluice caissons and two abutment caissons had to be built in a dock that (i) was not too far removed from the Brouwers dam; (ii) had deep-water access; and (iii) was easily accessible by land.

A site satisfying these conditions was found in an area outside the sea-dikes of the Nieuw Bommenede and Nieuw Nataars polders to the east of Brouwershaven on the island of Schouwen-Duiveland.

A constructon dock was built of sufficient size (figure 4.54) for the construction of the caissons, storage of materials and building acess roads to the caissons.

After the construction of the enclosing dike as shown in figure 4.54, drainage was installed consisting of 30 pumps each with a capacity of 50m³/hour at a 25 metre head. The bottom was then excavated in the dry to the required depth. At the site where the caissons themselves were to be built the bottom was excavated a further 0.5 m to a depth of 6 m below MSL. Filters were placed in these recessions consisting of:

- 35 cm of 3-15 cm gravel;
- 5 cm of 1-3 cm gravel;
- 5 cm of sand (concrete sand).

The filters were designed to maintain water beneath the caisson bottoms in order to prevent suction or sticking when they were to be floated off. Concrete tiles measuring 55 cm x 55 cm and 5 cm thick were placed on top of the filters. Gaps of 5 cm were left between the tiles which were grouted with concrete sand. Waterproof hardboard sheets were then placed on top and anchored in the concrete of the caisson bottoms. This was done in order to ensure that later, during the floating and towing of the caissons, loose sheets would not be able to block valve openings and stop them from working properly.

When the caissons had been built the construction dock was flooded and the northern section of the enclosing dike dredged away. A connecting channel was also dredged between the construction dock and the deep waterway, with a draught of 8 m below MSL.

4.3.6 Closure of the Brouwershavensche Gat

Relationship between the simultaneous closure of the two gaps

In 1971 the two closure gaps of the Brouwers dam were closed simultaneously. Prior to the closure three schemes for simultaneous closures were tested (see fig. 4.55). The hallmarks of these schemes were:

scheme II	-	closure of the northern gap running ahead of the closure of the southern gap;
scheme III	-	closure of the southern gap running ahead of the closure of the northern gap;
scheme I	-	in between schemes II and III.

Under schemes II and III higher current velocities and hence local scour were expected in one of the two final gaps than under scheme I, which allowed for the two gaps to be narrowed in equal proportion.
In the event scheme I was decided on, with the closure of the southern gap taking place slightly ahead of the closure of the northern gap.

Closure of the southern gap with concrete blocks

The blocks had to be transported from the depots on either side of the southern gap for dumping in the gap. To this end the blocks were taken six at a time from the depot by means of a portal crane and transferred onto lorries. The lorries then drove from the depot to the cableway loading terminal. A gondola would then be positioned over the lorry and pick up the six blocks by means of loading beam. The gondola would then travel along the cableway to the dumping point, which was marked by a special guide light. The blocks were evenly spread out over

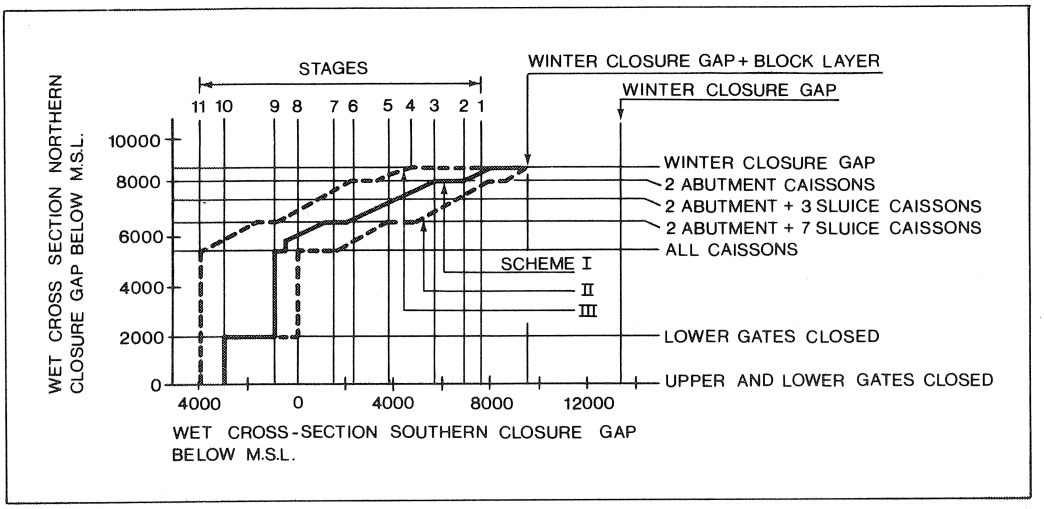

Figure 4.55 3 schemes for simultaneous closure both gaps.

Figure 4.56 Dumping pattern concrete blocks in southern closure gap

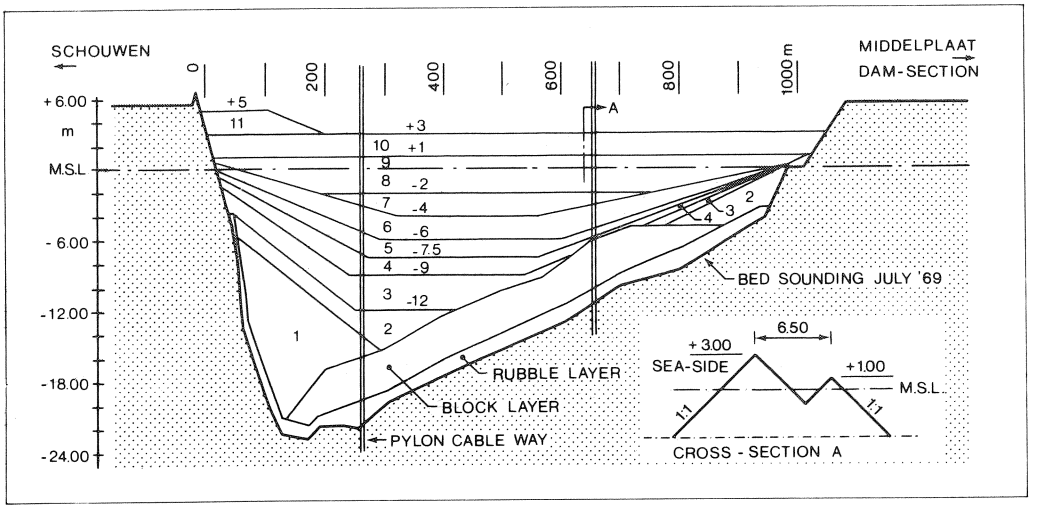

20 m dumping sections, with the gondola travelling at 3-4 m/s.

The acceleration to which the manned gondola was subject upon discharging its load did not exceed 0.15 g m/s². Higher acceleration and, in particular, higher incidence of acceleration, would have induced sea-sickness sensations among the gondola crew.
After discharging the blocks the gondola proceeded in the same direction to the loading terminal at the other end, where it was re-loaded.
The blocks were dumped in a systematic pattern (see fig. 4.56). The rubble cover and block layer shown in figure 4.56 were installed prior to the closure. During the closure the blocks were positioned in 11 stages. These stages, numbered from 1 to 11 in figure 4.56, were designed to ensure that the closure gap would be narrowed evenly and that the current would as far as possible be diverted from the steep Schouwen bank during closure. The level of the crest was monitored upon the completion of each stage. Any discrepancies in excess of one metre from the theoretical crest height were corrected for in the next stage.

The block dam was finished on 27 May 1971. The hourly output of the cableway turned out to be lower than initailly assumed. There were a number of reasons:
- the circuit time was 1700 instead of 1100 seconds. This was because the speed at which the gondola travelled had to be restricted to 3 m/s in order to prevent undesirable vibration when the cable passed over the bearing points and upon entering the fixed rail sections on the abutments. Occasionally the automatic speed governor on one of the gondolas would also malfunction, with flow-on effects on the other gondolas on the circuit;
- the working coefficient was 0.65 instead of 0.75 as envisaged;
- the operating coefficient was 0.91, i.e. virtually equal to the envisaged level of 0.9.

Filling these data in the formula specified in 4.3.5 the average hourly capacity of the cableway may be calculated as follows:

$$C = \frac{n.2.L.Wc.Oc}{T}$$

in which
C = average hourly capacity of the cableway in tonnes/s.
n = number of gondolas
L = effective carrying capacity of a gondola in tonnes.
Wc = working coefficient.
Oc = operating coefficient.
T = time to complete a circuit in seconds.

$$C = \frac{15 \times 2 \times 15 \times 0.65 \times 0.91}{1700}$$

C = 0.16 t/s or 564 t/hour.
This is of course a mean figure over a longer period.

The block dam was highly porous and consequently let a lot of water through. Model analysis indicated that the filter velocity through the block dam at a drop in height of 1.50 m was such that the sand deposited at smaller drops in height would erode away. This applied to both the sand that had settled in the openings of the block dam and, depending on the ebb or flood conditions, the sand deposited along a length of several dozen metres alternately on one side and the other of the block dam. In the model it proved possible by filling the interstices between the concrete blocks with 30/100 mm gravel to reduce the discharge through the block dam to 1-2% the level before plugging.

It also proved feasible in practice to fill the gap between the blocks with 30/100 mm gravel. This was done by discharging the gravel from ships with a crane and conveyor belts. In doing so the gravel was discharged on that side of the dam where the water level was highest so that it would be carried into the body of the dam by the current.

By way of experiment the gravel filling was omitted in a number of places, first of all along 20 m lengths and later along 50 m lengths.
No erosion of any size was observed in these test sections, from which it may be concluded that it might also have been possible to add the sand without the gravel plugging.

Closure of the northern gap with caissons

1 Preparation of the caissons in the construction dock

Before the caisson placement got under way, a number of modifications and facilities were fitted to the caissons in the construction dock (see figure 4.54).
After being floated the caissons were moored alongside a pontoon.
This provided easy access to the caissons and enabled equipment to be brought aboard conveniently.

After the construction dock was flooded the sluice caissons were individually allowed to float and then sunk again in the same place. This exercise was particularly designed to test whether the temporary wooden gates at both sides of the openings were sealing off the openings effectively.
Following these floating and sinking tests with the sluice caissons more extensive tests were carried out on a single caisson. These tests were designed to determine how the list in the caissons could be corrected by manipulating the valves during the sinking operation. The list was caused by the asymmetrical design of the caissons, in that the closed gates divided the caissons into compartments of unequal width.
A floating caisson was estimated to have a list of 2-3°. In practice the presence of leakage water in the caissons caused a somewhat greater list. However, as indicated by model tests carried out in the Netherlands Ship Model Basin, it was possible to reduce the list appreciably by keeping two valves in the narrowest lengthwise compartment closed over a long period.

The preparation of the sluice caissons (see fig. 4.51) prior to final placement consisted of a number of measures designed in essence to (i) get the caisson afloat; (ii) keep it afloat for a short period; and (iii) permit it to be sunk rapidly. In order to float a caisson some 8,300 m^3 of water had to be pumped out. On average this took between five and six hours. Once the difference in water level inside and outside the caisson had been built up to around one metre, the temporary wooden gates would seal off by pressing with their stops against the concrete wall of the caisson. The caisson would be afloat approximately an hour after low water. The time of low water was deliberately chosen so as to limit the water pressure on the temporary wooden gates, pressures much in excess of 4 m being considered unacceptable.
The eight „butt" panels (four on each side of the caisson) were already raised during pumping. These hardwood panels, measuring 1.5 x 1.5 metres and 0.1 metres thick, were positioned across the concrete frames of the caisson with the bottom edge 0.5 metres above the waterline, against the temporary wooden gates. The panels enabled tugs to exert pressure on the caisson without risk of the temporary wooden gates shifting or being damaged.
After the caisson had been towed to the mooring jetty it was stationed at a dead anchorage where the necessary materials and equipment could be brought on board.

The abutment caissons (see fig. 4.53) were closed concrete containers without sluices and hence also without temporary wooden gates and butt panels.
Instead the locations of the transverse beams in the caisson were marked with paint, indicating where the tugs could press against the caissons.
On account of their inclined bottoms the floating abutment caissons had a tendency to „nod", i.e. the high front would rise while the low back would sink down. To enable the back of the caisson to dip down the foundation was locally excavated before the construction dock was flooded.
Since the abutment caissons were completely sealed containers, no bilge pumps were required after the caissons had been pumped out, although they were in fact installed as a precautionary measure.

The reserve (Phoenix) caisson was towed from Vlissingen to the port of refuge at Zijpe, where it was grounded. Since hydrological research had shown that a sealed caisson (i.e. one without sluices) would have a deleterious effect on scour, it was decided that if the caisson had to

be used, it would be the last to be placed. In that case the sluices in the other caissons would have been left open and then shut as quickly as possible once the Phoenix caisson was in position.
The reserve caisson was shorter than the sluice caissons. The planning was to plug the gaps between the reserve caissons and the adjacent sluice caissons with rubble and/or concrete blocks. After the closure of the Kous gap, when it was clear that it would not be required, the reserve caisson was towed to the Schelphoek working harbour and beached there.

2 Navigation route

The Brouwershavensche Gat consisted of two sets of channels (see figure 4.57). In the northern section of the area these channels discharged through the Springersdiep and the Kous into the Kous closure gap, and in the southern part of the area through the actual Brouwershavensche Gat into the southern closure gap.
Between these two principal sets of channels there were a number of sand-flats crossed by a number of transverse channels, all of which were however of limited depth and breadth.
Three possible solutions were analysed in the Delft Hydraulics Laboratory for deepening and widening one of the transverse channels so that it would be used for caisson transportation. In two instances the flow pattern proved highly unfavourable, cutting across the channels, thus making it unlikely that they would retain sufficient draught during the closure and immediately preceding period following the completion of dredging.
In addition the tug-master expressed major reservations about sailing through a comparatively narrow channel subject to cross-currents.
The third possibility consisted of cutting through the western spur of the Hompelvoet, where troughs had consistently been observed in recent years, giving rise to the impression that a channel was in the proces of being formed. This would make a towing secion of 12 km, while the channel would have to be deepened over a length of 1800 m from some 3 m below MSL to 10 m below MSL, involving the excavation of at least 1,200,000 m³. The direction of flow proved to be parallel to the channel throughout the tidal cycle.
The current velocities were sufficiently high to remove the risk of silting up on a significant scale. In view of all these considerations it was decided to dig out the Hompel channel. The channel was designated as a sand-extraction area for the Public Works Department of the Province of South Holland, which at that time required sand for road construction on Goeree-Overflakkee. Calculations had indicated that the channel would have to be dredged to a depth of at least 10 m below MSL across a width of 50 m. Because the Province of South Holland was able to use some 2,000,000 m³ of sand it was possible to dredge a wider channel than strictly necessary. The channel ended up 65 m wide across the bottom at 12 m below MSL, with slopes of approximately 1:10. The entire naviga-

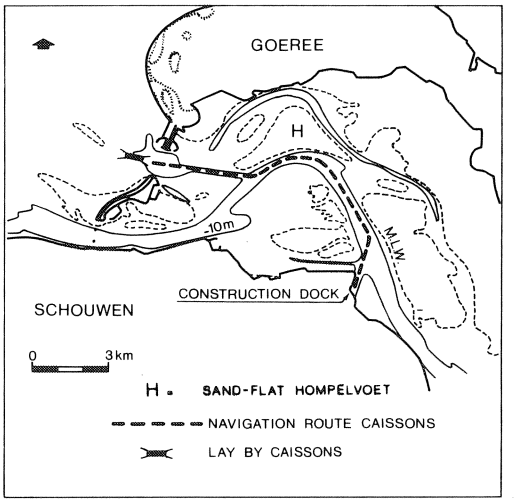

Figure 4.57. Navigation route caissons.

tion route from the construction dock to the closure gap was fitted with buoys where required.

3 Tugs

Prior to the placement of the sluice caissons in the Volkerak model analysis was carried out into the towing resistance of caissons during transport and manoeuvring. Part of the research, relating to towing resistances at various water depths, was repeated with a model of the Kous sluice caissons. This research indicated that, depending on the water depth and the angle between the longitudinal axis of the caisson and the towing direction, the forces specified in table 4.7 were required for towing a caisson at a given speed in relation to the water.

The positioning of the caissons at the turn of the tide involved a number of actions. In order to allow enough time for these to be carried out it appeared advisable in deciding upon the required power of the tugs to assume that the caissons would have been swung into position some 30 minutes before the turn of the tide (being defined as the point at which the current velocity was less than 0.5 m/s). After taking account of variations in the time at which the tide turned, the astronomical tide and the planned situation of the southern channel, allowance had to be made for current velocities of up to 0.75 m/s. In this case a force of 250 kN would be required to keep the caisson at right angles to the current.
In order to prevent play between the ends of adjacent caissons as the result of wave action, a force of approximately 200 kN needed to be exerted against the pivoting point of the floating caisson, thus keeping it hard up against its neighbour.

Tests revealed that a tug would produce a pulling force of some 10 kN for every 100 hp power in conditions where the propellor water was able to flow away unimpeded and the boat was stationary, i.e. the „pulling force at the post". In the

Table 4.7 Towing force (KN)

angle between longitudinal axis of caisson and direction of tow in degrees	water depth in m	towing force at speed of V = 1.5 m/s in relation to water		towing force at speed of V = 2.0 m/s in relation to water		towing force at speed of V = 2.5 m/s in relation to water	
		R	L	R	L	R	L
0	7.25	190	–	330	–	530	–
0	8.25	120	–	210	–	330	–
0	15.00	100	–	170	–	270	–
15	7.25	290	330	540	590	840	940
15	8.25	220	260	390	460	600	720
15	15.00	160	120	290	200	470	320

R = resistance of the caisson in direction of tow
L = resistance of the caisson at right angles to direction of tow.

The underlined values apply to the shallowest, critical part of the towing section, viz. the Hompel channel.

case of a positioning manoevre it is safer to assume a relationship of 6 kN pulling force for every 100 hp in power. On this basis and also taking account of the experience gained with previous closures, it was decided that six tugboats with a combined power of 8,600 hp would be required for the positioning of a sluice caisson. This power could have been supplied with a smaller number of tugs, but six provided a greater degree of flexibility when it came to towing, turning in and holding the caissons in place. The power of the tugs was determined in such a way that they would be able to supply the necessary power for the placement manoeuvre, although winches were also used. The tugs were, however, required to manoeuvre the caissons into the required position before winches could be hooked up. By way of reserve the tugboat „Spitsbergen", which had been used for various operations in the construction dock, was on stand-by. Table 4.8 provides a survey of the tugboats used. The last of these, the **Azië** was only used in conjunction with the others for positioning the final caisson.

4 Placement plan

The actual placement sequence is shown in figure 4.58. The originally planned sequence is shown in brackets, under which the caissons were to have been placed alternately on the southern and norhtern sides of the closure gap. On account of the severe scour that arose after the placement of caisson K 5 the following caissons were all placed on the southern side of the still open part of the closure gap.

5 Towing of the caissons

The abutment caissons left the constructon dock at the low-water turn of the tide and were towed against the current towards the closure gap. In the first few hours after the turn of the tide, however, the tide did not run with any force, and only the first four of the tugs listed in table 4.8 were required for towing the caissons. The position of the tugs is indicated in figure 4.59. During the journey the tugs „Brielsche Bank" and „Breedbank", both with Voith-Schneider propulsion, were positioned at the back.

The abutment caissons were drawn across the current towards the end of the flood-tide and pushed into position. On account of the limited draught on the landward side of the caissons the foremost tugs had little room. The lack of draught also formed the reason why these caissons had to be sunk at the high-water turn of the tide. It proved difficult to keep the caissons in position until the winch cables from four firmly-embedded winches on the shore had been secured to the caisson bollards and the slack taken up. Once this has been done the caissons could be held steady in the current. The fairly heavy swell, particularly when the first caissons were being positioned, meant that the caissons moved up and down, thus brushing against the face of the abutment with their corners, but not to the point of breaking loose.

Table 4.8 Survey of tugboats used for placing caissons

tugboat name	type of propulsion	power	cable mounting
Brielsche Bank	Voith-Schneider	2800 hp	bitt or towing winch
Breedbank	" "	2800 hp	" "
Italië	Propellor	900 hp	bitt
Volharding 12	"	900 hp	"
Amerika	"	600 hp	"
Frankrijk	"	600 hp	"
Spitsbergen in const. dock and on stand-by	"	550 hp	"
Azië for placing final caisson	Voith-Schneider	1500 hp	"

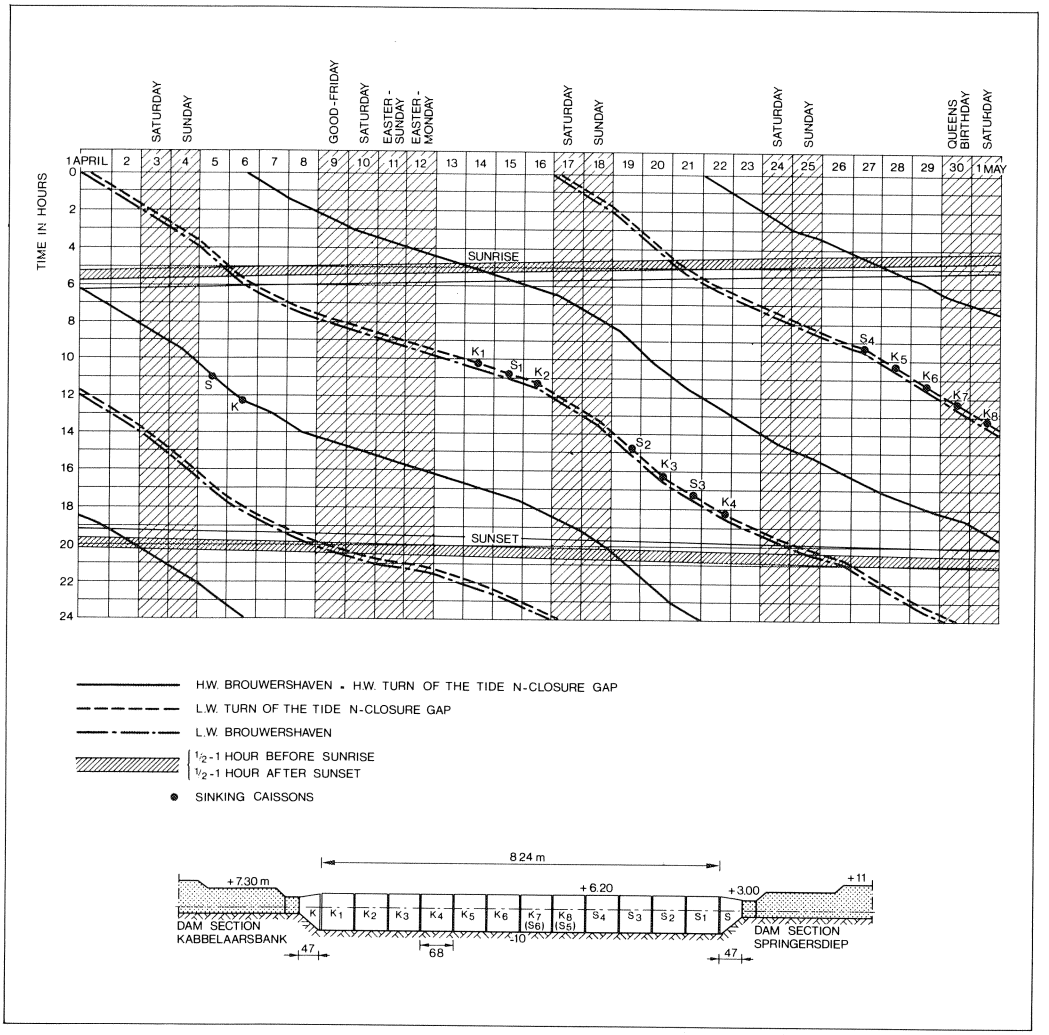

Figure 4.58 Placement plan caissons northern closure gap.

With the exception of the final one, all sluice-caissons left the constrution dock at the high-water turn of the tide preceding the low-water turn of the tide when they were to be positioned. Because the caissons, with the exception of the last, were transported on the ebb tide it was important in the narrow Hompel channel and in the closure gap itself to have sufficient power at the back of the caisson to enable it to be steered

and if necessary braked or stopped.
For this reason the two most powerful tugs, the „Brielsche Bank" and the „Breedbank", were placed at the back of the caissons during the towing operation.
These two highly manoeuvrable tugboats with Voith-Schneider drive were also the most suited for towing the caissons to the pivoting point.
This meant that the „Brielsche Bank" and the „Breedbank" made fast to that side of the caisson that was to abut an existing caisson upon placement and that during towing and placement this side would act alternately as the back or the front of the tow (see figure 4.59).
On the other short side of the caisson four tugs were made fast, namely the „Italië", „Volharding 12", „Amerika" and „Frankrijk". The combined power of the tugs was designed to maintain a speed of 1.5 - 2 m/s in relation to the water.
The tug convoy was preceded by a measuring barge fitted with communications and navigation equipment, current-velocity meters and echo sounders. In addition a pontoon equipped with a radar unit was moored at the western extremity of the Hompel channel. Before the departure of the convoy the tug „Spitsbergen" would

Figure 4.59 Position of the tugs

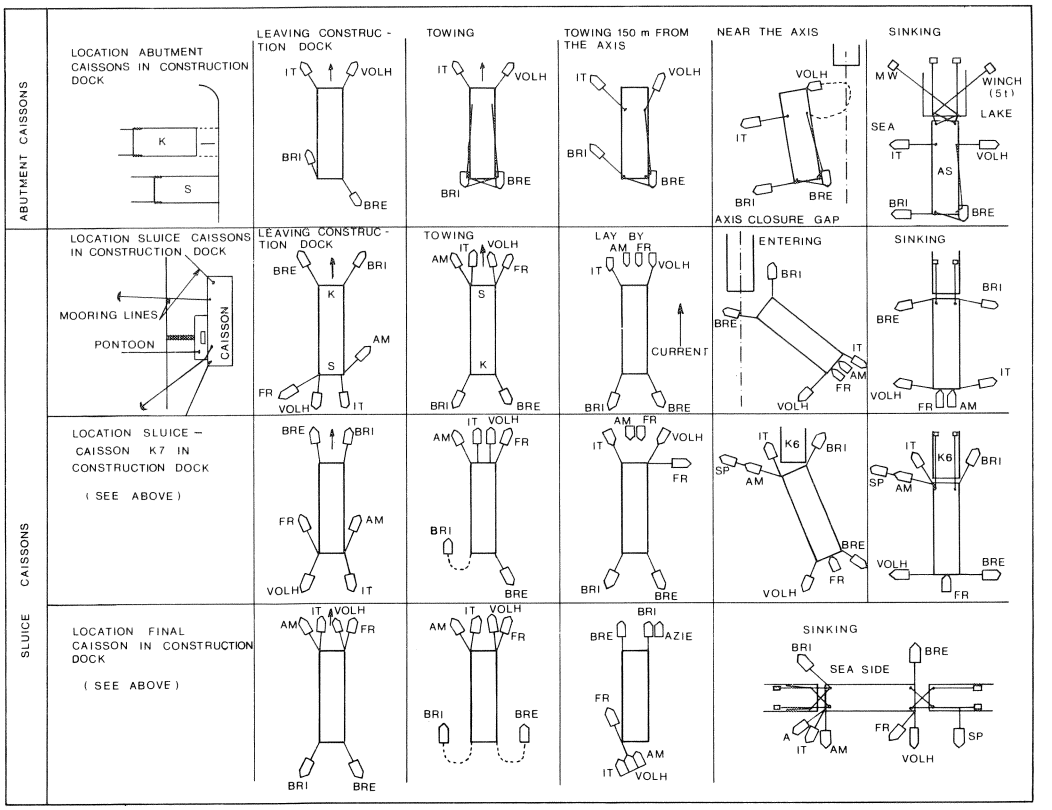

proceed to the pontoon, where it remained on stand-by. The measuring barge that preceded the convoy proved particularly valuable in misty and dark weather. The support provided by the radar pontoon was in fact superfluous.
The direction of flow in the mouth of the Hompie channel was tested upon each placement. In most cases the direction of flow was parallel to the longitudinal axis of the channel, the only exception being at the beginning of the ebb tide, when the current at the eastern extremity of the channel cut across the channel axis at an angle of 15-20°. The result was that the caissons tended to slew round and hence required a greater width of water. The depth and breadth of the channel proved, however, adequate.
The journey from the construction dock to the closure gap took two to three hours. The caisson arrived some two to three hours before the commencement of the placement manoeuvre, approximately one hour before the low-water turn of the tide. During the waiting period the caisson was parked at a distance of 200-300 m from the closure gap, generally on the seaward side. While a caisson was parked a number of preparatory operations were carried out, e.g. the butt panels were removed, the pumps hoisted on deck and the locking hooks of the temporary wooden gates checked and if necessary adjusted.
As soon as the caisson had been brought to a halt by the tugs „Brielsche Bank" and „Breedbank", the tugs „Amerika" and „Frankrijk„ were cast off. The latter two were then lashed together and to the caisson as pushing boats (figure 4.59).
Some 45 minutes before the low-water turn of the tide, at current-velocities of around 0.9 m/s, the parking operation was ended and the caisson was towed to the place where it was to be sunk. On arrival the caisson was swung in until it was at an angle of 60° to the sill axis. As soon as the seaward head rib lay against the corresponding rib of the in situ caisson and a hinge had been formed, the remaining tugs steadily pushed the caisson athwart the last of the ebb-tide until it was above the sill. The „pushing boats", i.e. the „Frankrijk" and „Amerika", ensured that the caisson remained hard up against the face of the in situ caisson. In doing so they were assisted by two longitudinal cables that were secured once the hinge had been formed.

The first sluice caissons fitted against the abutment caissons, which, at 20 m, were 2 m wider than the sluice caissons, the ribs of which slotted in exactly provided the caisson was floating vertically. This was, however, never the case and, even if it had been, the current and tugboats, acting as they were in opposite directions and hence producing a substantial torque, would have pulled the caisson out of true.
Positioning the sluice caissons was therefore extremely difficult and time-consuming. It would in future be advisable to increase the gap between the ribs on the abutment caisson or to space the caisson ribs evenly.

6 Achoring and sinking the caissons
After a caisson had been brought into position, it was secured by cables from winches mounted on previously positioned caissons (see fig. 4.59). With the exception of the final caisson, two cables were used running the length of the caissons. These cables were able to absorb forces along the longitudinal axis of the caissons, with forces at right angles to the axis being absorbed by the head ribs of the caissons. The cable to the seaward side was attached to a self-tensioning or mooring winch, which was able to haul in or pay out a cable at a constant, pre-determined tension.
In the case of the abutment caissons two transverse cables were also employed since these caissons had flat ends and lacked the head ribs for absorbing forces at right angles to the longitudinal axis of the caisson.
The final sluice caisson was anchored at both ends with two longitudinal and two transverse cables. This was because the caisson had to be shorter than the remaining gap for it to be swung into position.
The final caisson was placed in the middle of the gap, i.e. clear of the head ribs of the adjacent caissons.

The length of the gap for the final caisson was worked out beforehand.
Apart from this gap adequate flexibility was

built into the entire system to ensure that if two caissons should fail to abut closely they would still leave enough room for the last caisson. At the same time, the generous spacing design meant that if all the caissons were positioned hard up against one another, the gap left for the final caisson would have become very large. For this reason wooden buffers were used with which a certain amount of space could be created between each pair of caissons. By using wooden buffers of varying thickness the spaces between the caissons could be regulated in such a way as to leave precisely the right size gap for the final caisson.

In positioning the caissons the aim was for the middle of the caisson bottom on the short side that did not adjoin an already positioned caisson to be lined up with the axis of the sill. To facilitate this the axis was indicated on both sides of the closure gap by means of illuminated marker poles on the shore and by lights mounted on mobile tripods stationed on previously positioned caissons on either side of the one being brought in.
The position of the other short side of the caisson was determined by squeezing the headribs of the caisson being brought in against the head ribs of the previously positioned caisson.
Once the caisson had been anchored and correctly positioned the valves were opened at low current velocities. This was done by rotating the valve wheels two full turns every ten seconds.
After six minutes most of the valves were completely open, although a number of valves were deliberately kept throttled in order to combat listing. After about seven minutes the caisson would be resting on the sill.
With the caisson standing on the sill the temporary wooden gates were removed and towed away, first on the seaward and then on the landward side.
This was done to eliminate the risk of the gates being pressed immovably into position as the incoming tide gathered force. After that the valves were re-closed.

7 Finishing off the caisson closure

After a caisson had been sunk a number of further operations had to be carried out. These fell into the following steps:

a. the partial dismantling of the caissons;
b. filling the ballast compartments with sand;
c. filling the openings between the caissons and building up a rubble and slag surround;
d. opening the sluice gates of a caisson once the above operations had been carried out;
e. measuring up the caisson with a view to positioning subsequent caissons;
f. at the moment of final closure, shutting all the caisson sluice gates at the same time.

Once a caisson had been sunk in position on the sill and the temporary wooden gates removed, the equipment used was loaded onto a barge and taken back to the construction dock.
The next step consisted of filling the two ballast compartments with sand. This was done with lorries, which brought the sand required (approx. 2 x 850 m^3 per caisson) across the previously installed caissons. The sand was designed to increase the weight of the caissons and so provide them with the necessary stability. The abutment caissons did not have any ballast compartments but consisted of hollow concrete containers, which were one third filled with sand. Just before the dumping of the ballast sand the gap between the last and the previous caisson was filled with 40/80 mm lead slag and 300/1000 kg rubble.
The lead slag was filled in a 2 m layer from the top of the sill and then covered with the rubble to a height of at least 3 m above MSL. The filling, which was designed to prevent piping around the caissons, was held in position between the head ribs of the caissons. The lead slag ((of small dimension but high density) was designed to fill any gaps in the rubble layer of the sill. The openings on either side of the final caisson were too large for the rubble to be held in place by the ribs. To this end chain nets were installed, which were attached on either side of the gap to special recesses in the ribs (see figure 4.51).
As soon as the caisson had been stationed on the sill, rip-rap consisting of 40/80 mm lead slag was installed on the seaward side of the caisson by means of a stone-dumper. At the following high-water turn of the tide the slag was covered with 10/300 kg rubble. The lead slag/rubble rip-

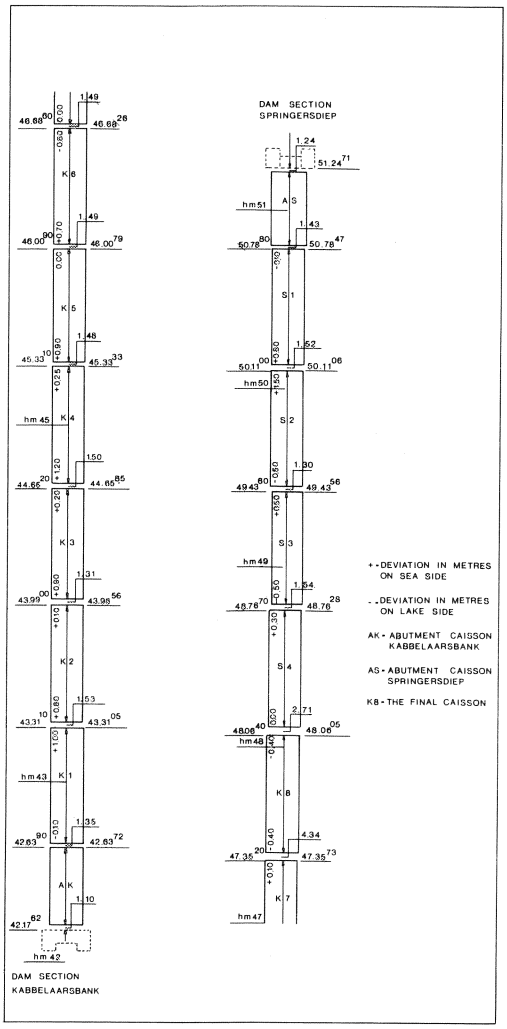

Figure 4.60. Position caissons after placement.

rap was designed to prevent piping under the caisson.

Once the rip-rap was in place the caisson sluice gates were raised.
This had to be done before the current velocity had reached 0.5 m/s.
The sluice gates were not raised until the rip-rap had been dumped along the caisson for two reasons, viz.:

- to facilitate manoeuvring with the stone-dumper beside the caisson;
- to prevent slag or stones getting caught in the gates and thus preventing the sluices from being closed later on.

Once a caisson had been positioned the height of the four corners was measured. The measurement was repeated after the caisson had been ballasted and daily for the next fortnight, and then at fortnightly intervals.
These measurements were designed to obtain an impression of the height of the top of the caisson and of the extent of settlement.
Measurements were then made by theodilite of the two angular points of the caisson on the Lake Grevelingen side. The positions after placement are shown in figure 4.60.

Following the placement of the final sluice caisson on 1st May, 1971, the sluice gates were closed on 3rd May, 1971 around the low-water turn of the tide.
The current velocity was measured on the land side, viz. the Lake (Grevelingen) side of the caissons with the aid of six measuring barges. As soon as one of these barges had recorded a current velocity of less than 0.4 m/s the sluices of the nearest caissons were closed. The expectation that current velocities of this order would occur approximately one hour sooner in the northern than in the southern part of the gap was not borne out in practice. Closing all the sluice gates took around 45 minutes.
A visual inspection at the subsequent high water (i.e. when the difference in water level was at its greatest) revealed no leakages through the dam of any significance.
The closure of the northern gap was an accomplished fact.

4.3.7 Contractual arrangements for the construction of the Brouwers dam

The contract for the construction of the Brouwers dam was awarded in 1965 to N.V. Aannemingmaatschappij Dijksbouw, a consortium of four large Dutch contracting firms.
The contract took the form of a framework agreement between the Dutch government and the contracting consortium Dijksbouw. Since a good deal of research had to be carried out during the construction period itself (1965/1972) before the design could be worked out in detail it was not possible for the entire project to be covered in detail in the framework agreement. Instead the agreement laid down a number of general rules and the work was divided into sub-projects. Each of these sub-projects was covered by a separate agreement, with the costs estimated by both the State and the contractor. Among other things the framework agreement specified:

- which part of the overall project was covered by the framework agreement and which parts were not;
- the tendering procedure to be followed for each sub-project.

The framework agreement covered the construction of the Brouwers dam with the exeption of:

- road surfacing other than as required for the execution of the project;
- the delivery of materials commisioned by the State from parties other than the contractor;
- the hydraulic structures to be built in the Brouwers dam;
- the steel and concrete works (e.g. the construction of the caissons, cableway and concrete blocks for the closure of the southern gap);
- regular maintenance;
- land development projects.

As noted above, the cost of each sub-agreement was estimated by the State on the one hand and the contractor on the other. These estimates were compared at a given point before project commencement.

Depending on the percentage difference between the State estimate (S) and the contractor's estimate (C), the framework agreement provided as follows:

1. If $C \leqslant 1.06S$ the work specified in the sub-agreement was awarded to the contractor for sum C;
2. if $C > 1.06S$ but $C \leqslant 1.14\ S$ the work specified in the sub-agreement was awarded to the contractor for a sum equal to $\frac{1}{2}(C + 1.06\ S)$;
3. if $C > 1.14\ S$ the estimates were compared and if necessary adjusted and negotiations held between the two parties. On the basis of the revised estimates arrived at, the work specified in the sub-agreement could be awarded to the contractor:
   - for a mutually agreed contract price before commencement of the work;
   - for a contract price to be finalized upon completion of the work on an actual cost basis.

4.4. Closure of Rivers and Tidal Channels in Bangladesh

Case Studies

J.M. van Westen

4.4 Closure of rivers and tidal channels in Bangladesh

4.4.1 General

Bangladesh comprises the delta of two large rivers, the Ganges and the Brahmaputra (see fig. 4.61). The country is bordered on its western, northern and eastern side by India. To the south-east it borders Burma, while the southern, coastal area adjoins the Bay of Bengal. Behind the coast there is an enormous swamp area known as the Sunderbans.
Virtually the entire country consists of flat, low-lying land, covered with a thick layer of silt. In the border area with Burma in the south-east there are mountain chains ranging in height from 500 to 1000 m above sea level.
The land is fertile, with the majority under cultivation. In view of the population of some 80 million and the rate of population growth of some 3% p.a., the maximum agricultural area is required for food production. For this reason it is important for the low-lying land to be protected against high water levels and salt penetration.
In Bangladesh a system of dikes has, as in the Netherlands, been constructed in order to improve water management. In those instances where the polder includes a tidal channel, the latter must be closed.
Bangladesh has been grappling with the closure of these channels for many years, with varying success. In recent years assistance has been provided by the Netherlands.

Figure 4.61 Map of south Bangladesh

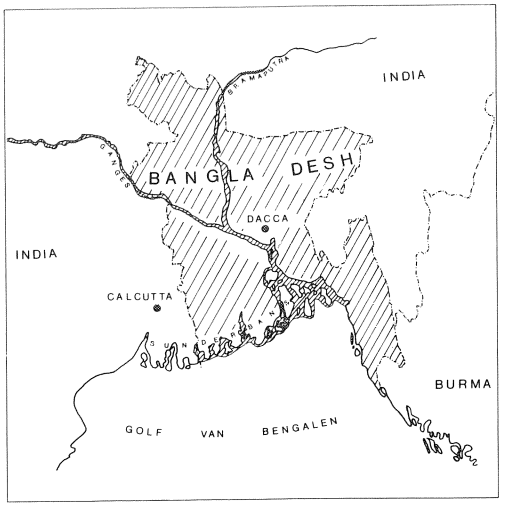

4.4.2 Materials

In the past, closures of tidal channels in the Netherlands were largely effected with materials available in the Netherlands or in neighbouring countries. Examples include sand, clay, brushwood and stone. These works were highly labour-intensive; sealing a channel with brushwood mattresses was solely a matter of manual labour, as far as both the construction and the sinking of the mattresses was concerned.
In recent decades, however, closure works in the Netherlands have been marked by increasing mechanization. Bottom protection is now manufactured in factories and laid by large specialized vessels. The use of brushwood mattresses in several layers has been replaced by that of caissons and the dumping of concrete blocks with a cableway, etc.
These developments in the Netherlands and in rich countries in general are of no relevance for closure works in Bangladesh, which is one of the poorest countries in the world. Manual labour is cheap and machine-work expensive. Materials cannot be transported over long distances but must be locally available. The materials must also be the sort that can be applied by hand.

Locally available materials in the delta area of south-west Bangladesh suitable for closure works include:
- clay;

- jute of rope and bags, the bags being filled with clay;
- palm leaves;
- reed, bound together in bundles with a circumference of c. 0.60 m;
- bamboo pieces;
- brushwood;
- straw.

4.4.3 Role of Dutch technicians

The Dutch Government started in 1975 by offering funds for studying and improving local methods for the closure of tidal channels as a part of embankment projects in the coastal areas of Bangladesh. The programme falls within the framework of „Early Implementation Projects on Flood Control and Irrigation in Bangladesh", a joint undertaking of the Bangladesh Water Development Board and the Technical Assistance Programme of the Ministry of Foreign Affairs of the Netherlands.

The programme is being carried out with the assistance of a team of Dutch experts, including a consulting engineer, an international contractor and (officials of) the Ministry of Transport and Public Works.
The Dutch assistance was not designed to find ready-made Dutch solutions to closure works in Bangladesh. Instead familiarity was first acquired with the methods that had been evolved in Bangladesh for the closure of creeks and channels. From this it became evident that these methods were suitable for small creeks and channels but that they fell short when extrapolated for the closure of larger creeks and channels.
It was then sought to devise methods that were suitable for the closure of larger channels, drawing on locally available materials, the large stock of indigenous labour and Dutch know-how and experience.

4.4.4 Methods of closure

Original horizontal method for relative small channels
In Bangladesh, tidal channels are closed using the so-called horizontal method. The gaps are dammed (narrowed) in stages by means of filling rectangular structures (similar to cells of sheet-piles used for coffer dams).
These cells, which are called compartments, are rectangular in shape and are built out from both banks, one in front of the other, by driving in rows of poles using (hand-operated) pile driving derricks.
Once one compartment is finished, it is filled up to mean water level with the „sausages" (mata) which have been prepared for this purpose from palm leaves, brushwood and clay. These sausages may be up to 30 metres long and are about 1 metre thick. The mata which are strong enough to withstand the tidal flow are rolled into the gap. The compartments are raised above the highest water level with bundles of brushwood and clay (see figure 4.62). It should be remembered that all this clay is carried with monotonous regularity to the site in baskets by thousands of men, women and children.
In the end, there is one final gap (12-15 metres wide) which remains open with ebb and flood rushing through it. This gap must now be sealed within one single tidal period. This work normally requires the labour of many people, working day and night. The aspect of the work which amazed the Dutch experts was that the bed of the creek did not become eroded away during the gradual process of narrowing the creek. The reason appeared simple: the bottom consisted of soft, but erosion-resistant clay. Throughout the process this clay tends to move down through the filled compartments as a result of the load from above. One way and another, this results in horizontal and vertical shifts in the compartments and the foundations. The bed of the channel is thus forced upwards, and whilst the initial depth of the bed may have been around 10 metres, the final may amount to only 4 to 6 metres, and this can quite feasibly be closed in one operation. This is actually a highly interesting method of closure which would not be possible in Holland, with its easily erodable soil.
The local method might, under circumstances, fail, the two principal technical reasons for the failure being:
- the development of deep scour holes in the closure gap which results in the undermining and loss of dam heads,

- the overtopping or breaching of the final closure which can occur due to:
- lack of earth-fill at the crucial construction stage. This fill can only be delivered to the dam by hand and often the delivery rate is too low for the limited period of time available for the final closure, around low water;
- settlements which reduce the effective crest level and cross-section of the final closure dam.

Overtopping or breaching generally only occur with larger closures involving large tidal volumes. As the matas will not withstand high tidal velocities, the final closure gap has to be rather large which, in turn, requires a high delivery rate of earth-fill during the limited period between the stoppage of flow by placing matas around low water slack and the next highest water. The limiting tidal volume for which the local method can still be used is in the range of 5 to 10 million m^3 depending on the tidal range. In order to eliminate these two principal reasons for failure, i.e. scour and overtopping and/or breaching, it was decided to develop a closure procedure based on the matamethod and traditional Dutch methods. One approach would be to study the problem in a small-scale hydraulic model; alter-natively full-scale tests could be carried out in the field. The cost of small-scale tests in the Netherlands is of the same magnitude as the cost of full-scale tests in Bangladesh and therefore, on the principe that „practice is the best teachter", it was decided to carry out full-scale tests in Bangladesh, these having the additional advantage that local employment would be created in the project area and a successful closure would produce the necessary benefits. The local enthusiasm to commence immediately with a large and probably difficult closure, with only limited experience, has to be guarded against in view of the greater risks of failure involved.

Use of bottom-protection mattresses

Protection of the river bottom by means of mattresses, common practice in the Netherlands,

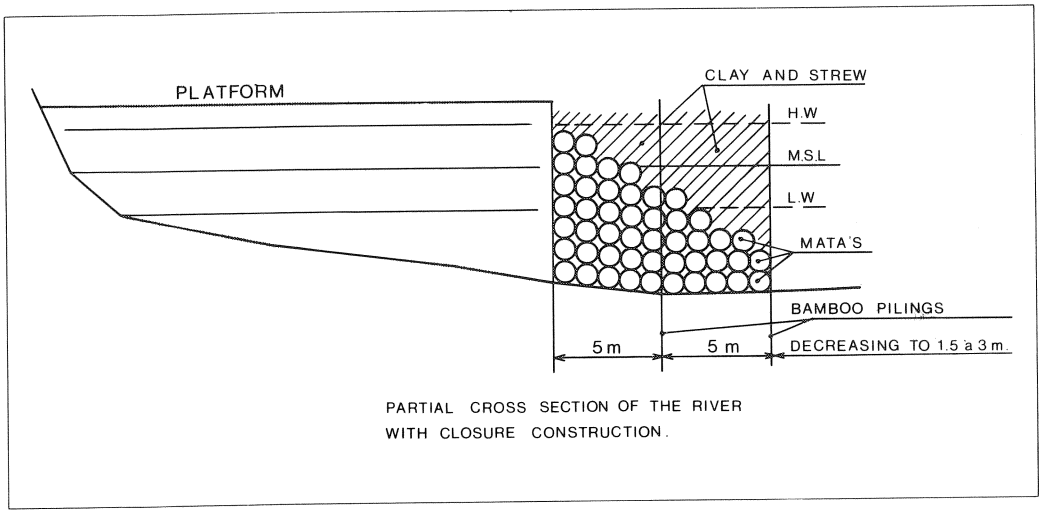

Figure 4.62. Bangladesh closure method.

can prevent bottom scour and thus eleminate one principle reason for closure failure. The traditional Dutch bottom-protection mattress was made of fascines of willow brushwood layed in a grid, incorporating layers of brushwood and, if required, layers of reeds, depending on the function of the mattress and the characteristics of the channel bed material. The combination of layers of fascines, brushwood and reed formed a sufficiently dense filter layer so that little if any bed materials was lost through the mattress and water over-pressures, which could result in uplift of the mattress, could not develop.
Mattresses used today in the Netherlands and elsewhere comprise a synthetic fibre sheet, forming the filter layer and a grid of fascines made from willow brushwood to give the required stiff ness and buoyancy, necessary when positioning prior to sinking. The willow brushwood used in the traditional Dutch mattress was grown in the fresh water delta of the River Rhine. This material is, however, not available in the delta area of Bangladesh. There is a brushwood in the mangrove forests which, however, does not float and cannot therefore be used. A local material which, however, is suitable and readily available is bamboo. The floating capacity is mainly provided by the air in the hollow core.
„Full" bamboo, i.e. unsplit, is, however, too stiff and a mattress made solely from full bamboo would tend to act as a stiff slab and could not be readily sunk. Neither would it be sufficiently flexible to adjust to irregularities in the channel bottom. Alternatively a split-bamboo mattress could be used which, however, would not float so readily and would be relatively expensive.
A suitable filter materials is formed by the leaves of a dwarf palm, known as goal-pata, which is used locally as a roofing material.

In the Netherlands' situation in the past mostly boulders, coarse gravel or rock were used as ballast with which to sink the mattress.
These materials, however, do not occur in the delta area of Bangladesh and are only found at a considerable distance from the closure site. As an alternative for the ballasting of the mattresses, clay-filled jute bags have therefore been used, second hand jute bags being readily available in Bangladesh, the main producer of the world's jute. The required life-time of the ballast units is only about 2 months, i.e. the closure construction period, after which bottom protection is no longer necessary.
An alternative fill for the jute bags is sand. The sand which is available locally is very fine and losses from the jute bags would be unacceptably large. Clay has therefore been used to fill the bags.
Bottom protection works were carried out for the first time as an experiment in the winter of 1977/1978, in connection with a closure project commissoned for execution by a local contractor using the local closure method.
The tidal river to be closed was the Madargong, a river with the following characteristics:

- a channel width about 150 m;
- channel bottom level about 6 m below mean water level;
- spring tidal range 5.0 m, Neap tidal range 2.5 m;
- tidal volume between 3 and 7 million m^3.

The Madargong is the only tidal river entering a polder of 20,000 hectares. Low embankments along the river, total length 30 km, provide an unreliable protection against flooding during extreme high tides.
The, much higher, embankments surrounding the polder as well as drainage sluices were already completed before 1970.
In the first month of the project, the team was involved with tests on the preliminary mattress design and with the arrangements for the closure. The bamboo grids were adjusted so that the mattresses were sufficiently stiff for the required sinking while remaining sufficiently flexible to follow irregularities of the channel bed. A grid with a longitudinal spacing of 0.75 m and transverse spacing of 0.90 m was eventually selected. The thickness of the layer of palm leaves was 0.05 m, this being sufficient to ensure an adequate bearing capacity for the ballast and also a correct filter function.
The cross connections between the upper and lower bamboo grids were made with jute ropes with a tensile strength of about 100 kg. The lower grid was assembled on a platform inside the low embankments and was then carried to a

platform outside the polder area which was liable to flood at high water. Final manufacture of the mattress, as described below, had to be completed during one low water period.
The rope connections were tied to the tops of pegs, so that they were not lost during the laying of the palm leaves. The palm leaves were then laid in three layers onto the lower bamboo grid. The upper bamboo grid was then fixed to the lower grid using the ropes of the lower grid for the cross-connections. About 50 labourers were required to execute this work.
The palm leaves proved to have only a limited floating capacity and as a result the floating capacity of the whole mattress was also limited. The grid spacing of the mattress could not be reduced to increase the buoyancy as the mattress would then have become too stiff for the required sinking procedure. Reeds, the material used in the Netherlands to ad buoyancy to the mattress, were not available in the project area. A traditional Dutch willow brushwood mattress would require ballasting with rubble at about 200 to 300 kg per m². In view of the lower specific weight of clay, a ballast weight of the order of 325 kg per m² was selected. For the present case, the ballast weight was achieved using a total of 3400 clay-filled bags, each weighing 50 kg, for a mattress of 15 x 30 m². These bags were loaded onto the flat-topped barge, used for the sinking, prior to the commencement of the sinking operations.

Sinking of mattresses was achieved in the following stages (see figure 4.63):

1. the mattress was pushed off the manufacturing platform at high water and temporarily anchored along the bank. The platform was situated upstream of the closure site to enable positioning of the mattress on the outgoing tide and sinking at low water slack.
2. the five anchor hawsers of the barge were connected to the anchor blocks. The barge was then moved alongside the mattress to which it was connected, along one side, by 5 ropes. The barge and the mattress were then floated towards the closure location on the ebb current by slackening off the anchor

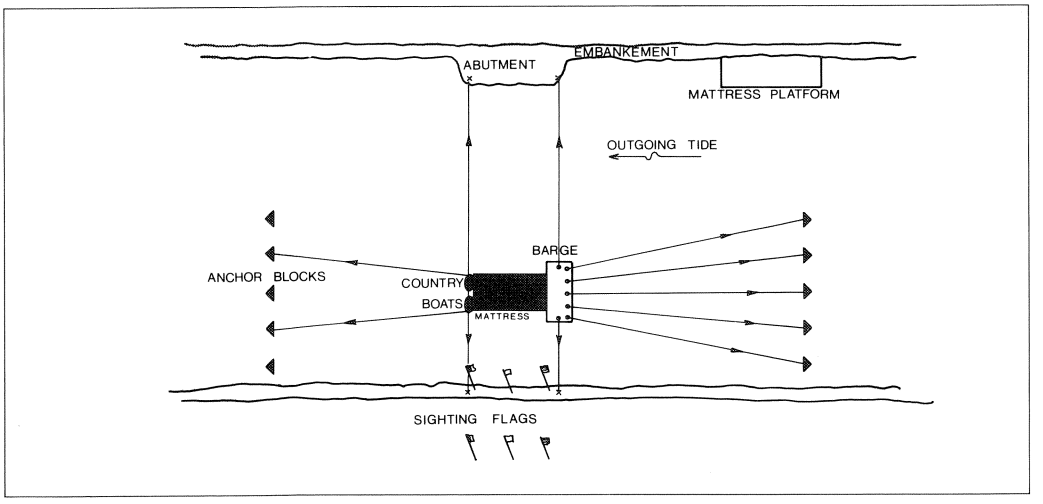

Figure 4.63. Schematic arrangement of mattress, barge and anchor hawsers. (Madargone)

Figure 4.64. Ballasting a mattress by clay-filled jute bags. (Chakamaya)

hawses. In the meantime the tail end of the mattress was attached by ropes to two country boats.,

3. on arrival at the closure location, the tail and side anchor hawsers were laid out and the mattresses were anchored by means of anchor hawsers. Steel anchors were not available locally and therefore concrete blocks, 1 m^3, were used,

4. ballasting commenced by placing the clay-filled jute bags, carried by head-load, on the mattress, working from the centre towards the barge, until the mattress was completely under water. The central part of the mattress was already, at this stage, submerged to a considerable depth (see fig. 4.64),
5. ballasting continued by throwing bags from the barge till the load was sufficient to ensure rapid sinking on release of the ropes. After this release the barge moved over the mattress towards the tail boats by either the ebb current, or by pulling on the ropes connecting it to the tail boats, 16 mattresses were sunk in a period of one month to eliminate scouring in the closure gap and around the dam heads. In addition 3 mattresses were sunk, in a row, to give bottom protection over 90 m in the direction of the flow.

Subsequently, closure was attempted by using the local „horizontal" method. This attempt failed.
The closure failed due to breaching of the final closure dam. Although stoppage of flow was achieved successfully at low water, the earth-fill dam in the closure gap could not withstand the following highwater conditions.
The principle reason for failure are considered to have been:

- weakness of compartments due to a shortage of timber piles,
- the late date of the closure attempt (3 days after neap tides, i.e. the chance of success would have been better on the very lowest range tide),
- the late time of the stoppage of flow (two hours after lowest water, which reduced the time available in which to complete the primary closure dam).

Poor labour management was also considered to be a contributory factor to the failure.
During the spring tide preceding the closure, current velocities in the closure gap attained about 3.5 m/s.
During the final closure operations, the current velocities rose to over 4 m/s. No damage to the mattresses or scouring could be detected however during the closure operations. Immediately after breaching, currents reached 6 m/s in the closure gap and a hydraulic jump occurred damaging the mattresses up and downstream of the breach. The damage was however restricted in area and only limited scouring occurred.
A repeated closure attempt could therefore be made during the following neap tides, which, however, also failed in the same way as the first attempt. Three months after the failures, the maximum depth in the closure gap was 6 m below the original bed level. Scour took place in the form of a deep gully, the width of which was only 25 m and was probably limited by the remaining bottom protection mattresses which were still in good order. Therefore, although the closures had failed, due to breaching, the installation of mattresses had been successful.

Vertical closure method
The introduction of mattresses had eliminated one of the two main failure reasons, but the remaining failure reason, overtopping, caused the failure of the closure. It was therefore decided to replace the local horizontal closure method by a new method, which allows a complete control during all stages of the closure. In view of the aim, namely that the next method to be developed should in principe enable the closure of much larger tidal channels, it was decided that the new method should be a vertical closure method.
The method of closing in the case of a vertical closure is independent of the width of the tidal channel. Only the quantities of the required materials are influenced by the width. The principles of a vertical closure are:

- decreasing of the width of the channel to such an extent that the current velocities in the closure gap do not exceed a given limit at any stage of the closure;
- the gradual raising of the sill in the remaining gap in such a way that the sill level is as horizontal as possible. The sill should be constructed in such a way that the resulting water velocities can be withstood. The maximum level up to which the sill is raised depends of the method of construction of the sill and the dam on top of the sill which will stop the flow;

- the construction of a dam on top of the sill with materials, which are not washed away by the current;
- increasing the cross section of the closure dam by earth fill till the section can withstand the design highest water level and the design waves.

The main technical principle of the vertical closure is that the current velocities over the sill reach a maximum when flow conditions just become critical. The current velocities decrease when the sill is raised further.
The main practical difference from the existing local method is that a large part of the work has to be done waterborne. The availability of waterborne equipment for transporting building materials is essential.
If waterborne transport equipment is unavailable, transportation must be achieved by means of a jetty or cableway accross the channel. The width which can be reached is however restricted to the width of these constructions, as only manual labour can be employed. The Bangladesh Water Development Board fortunately has several self-propelled flat-top barges with a carrying capacity of 150 tons.
As with bottom protection mattresses, the actual development of the closure method was done in practice, because the cost of small scale tests in the Netherlands is of the same magnitude as the cost of full scale tests in Bangladesh. Practice is moreover the best teacher.
The first closure project taken up in the winter of 1978/1979 was the closure of the Chakamaya Khal with a tidal volume of 10 million m^3 and a tidal range of 3.3 m at springtide, a width of 210 m and an average depth of 5 m below mean water level (see figur 4.65). This first project was rather large, due to local pressure to go for large projects, making it difficult to develop new techniques by experimenting with alternatives. The Chakamaya Khal was closed successfully.

Mattresses

The size of the mattresses was increased up to 16 x 46 m^2 in view of delays in the start of the project and the availability of two self-propelled

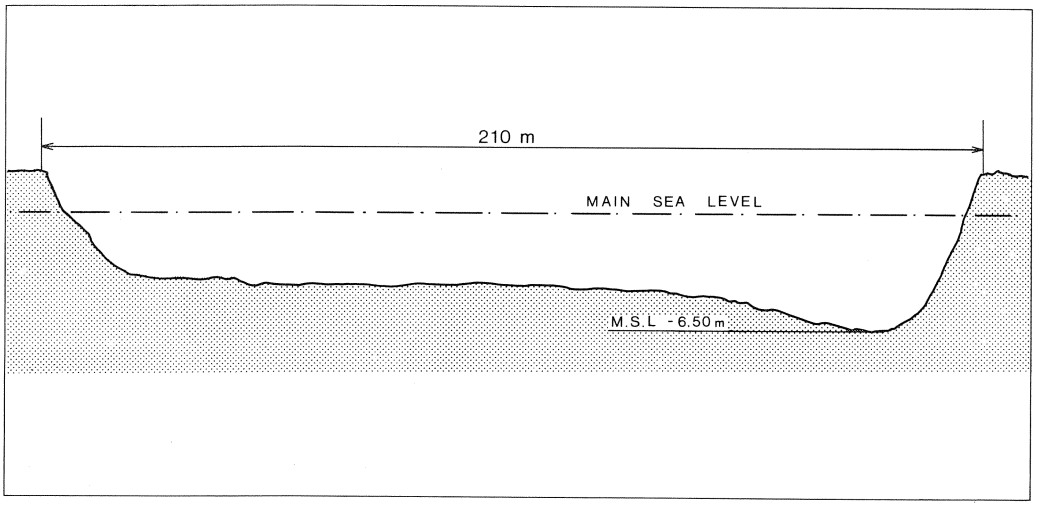

Figure 4.65. Cross section of the Chakamaya river.

barges. The second barge could be used as tail-barge in stead of country-boats and could be loaded with the additional bags required for a larger mattress. About 5500 bags were required for the sinking while one barge can only load 3500 bags. The increased size caused no problems.

Construction of sill

The cross-section of the sill is dependent on the hydraulic conditions, the available construction materials and equipment, and the loads due to the dam on top and the water pressures after stopping the flow.

The sill construction material should satisfy four main requirements:

1. cheapness;
2. sufficient resistance against the prevailing currents;
3. sufficient internal stability to allow for large loads on top of the sill due to the final closure dam;
4. sufficiently impervious so that no flow of any importance will occur through the sill.

Clay satisfies 1 and 4 and 2 only partly. Fine sand satisfies 3, 1 and 4 only partly. Stone rubble or river boulders satisfies 2 and 3.

The cheapest way to transform the most promising material, clay, into a material meeting requirements 2 and 3 is to use clay-filled jute bags. Second-hand jute bags are readily available in large quantities at reasonable cost in Bangladesh. Cement bags or other bags of similar size were used having a filled weight of about 50 kg. The higher the sill can be made the easier the final closure. Current velocities increase however with higher levels till critical flow conditions are reached.

The current resistance of layers of clay-filled jute bags was not known and could not be derived from the literature. It was assumed that a sill made with clay-filled jute bags with a level not too much below lowest water required a protective cover to withstand the high current velocities during springtide.

The top of the sill including the cover should be completed during a neap tide period when protected bags will not wash away so easily, on account of the much smaller velocities. The tidal range during neap tide in southwest Bangladesh is about 40% of the range during springtide. The protective cover was designed as a bottom-protection mattress, with a kind of wattlework in order to prevent the washing away during springtide of the ballast, composed of clay-filled gunny bags. The raising of the sill level above lowest low water is also increasingly difficult because the time available for dumping decreases considerably. The current velocities should not exceed 1 m/s during dumping, which only occurs around highest water slack.

The experience gained from the Chakamaya closure showed that it was possible to raise a sill up to a level of 1.5 m below Datum, or 0.3 m below lowest low water. Fig. 4.66 shows the designed sill construction with an upper sill level of 2.15 m below Datum. The last sill mattress could be sunk at the proper level, although bags partly washed away at the unprotected spot during the low water prior to the sinking. The wattle-work was formed by reed rolls with a diameter of 0.3 m. The 10 sill mattresses were ballasted with 5,500 bags each. Two springtide periods passed between the completion of the sill and the stopping of flow. High currents during springtide of 2.5 m/s damaged the ballast slightly due to the washing away of bags after a large part of the contents was washed out. The clay was rather liable to washing out due to the high silt content of about 80%.

A proper ballast could however be maintained by dumping additional bags.

The building of an underwater sill by dumping clay-filled jute bags by barge proved to be no problem. The sill was built with 400,000 bags. It was possible to dump 20,000 bags daily with two barges. The crest of the sill should have a proper flatness, so that no hollow space occurs underneath the sill and an uniform crest level is created. An acceptable flatness can only be achieved by alternately dumping the bags with the barge parallel to and then accross the current, while regularly taking soundings to check the flatness.

Jetty

The uncertainties regarding the resistance of clay-filled jute bags against scouring by water

current and the restricted capacity to dump bags by barge at levels above lowest low water led to the decision to construct a jetty on top of the sill across the tidal channel. A jetty (see the figures 4.66 and 4.67) enables the dumping of large numbers of bags independently of the tide. The dumping capacity is determined by the number of walkways and the production capacity of each labourer.
The jetty also ensures access independent of the tide at any part of the sill crest (see the figures 4.68 and 4.69). Provisions can be made in combination with the jetty to reduce or eliminate the possible scouring of bags meant to form the final closure dam.
The building of the jetty should not have created any problem, because the driving of piles from the water and the building of jetties and walkways with timber and bamboo is well-known in Bangladesh. However, it proved very difficult for the jetty to be built sufficiently strongly. The purchase of timber piles of 10 m or more proved rather difficult. The use of two half sawn timber piles as girders was not successfull. Sized timber should be used in future.
The walkways with a width of about 1.50 m had a restricted capacity for dumping bags. About 100 labourers on a walkway coming from one bank is the maximum before congestion occurs. The limitations on capacity are partly due to the fact that the labourers demand to be paid on the basis of tokens received on the spot when a bag is dumped. The capacity of a walkway was about 1700 bags per hour, depending on the walking distance. This rate could be maintained for four hours by one gang without rest.

Final closure dam

Because it was not known which current velocity could be resisted by a layer of well-placed clay-filled jute bags, the design of the final closure dam on top of the sill was rather flexible.
Provision was made for 1200 bamboos to be placed vertically along the jetty to form a lattice-work in order to prevent the possible scouring of bags by the current. The practice showed that bags dumped around high-water slack and levelled out during lowest water could withstand

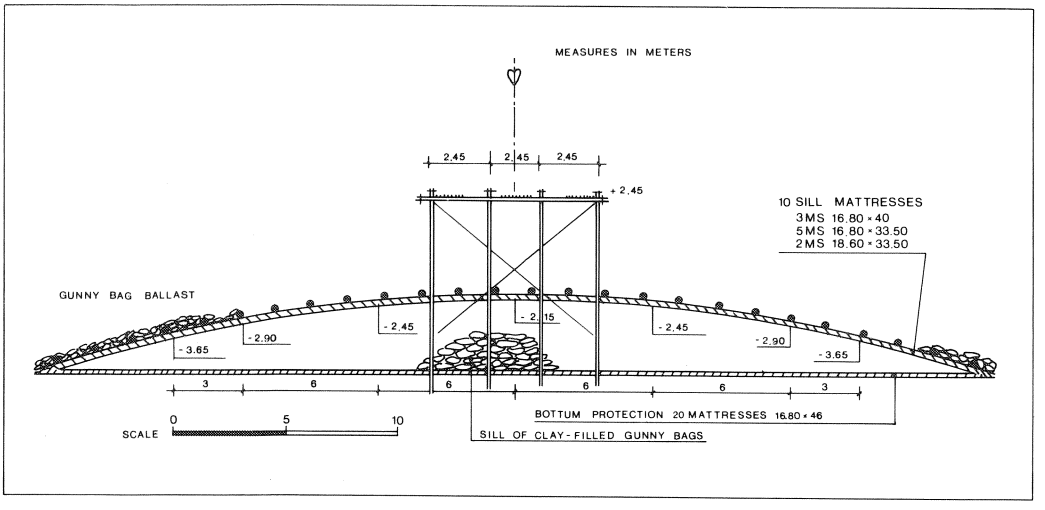

Figure 4.66. Cross section sill construction with jetty.

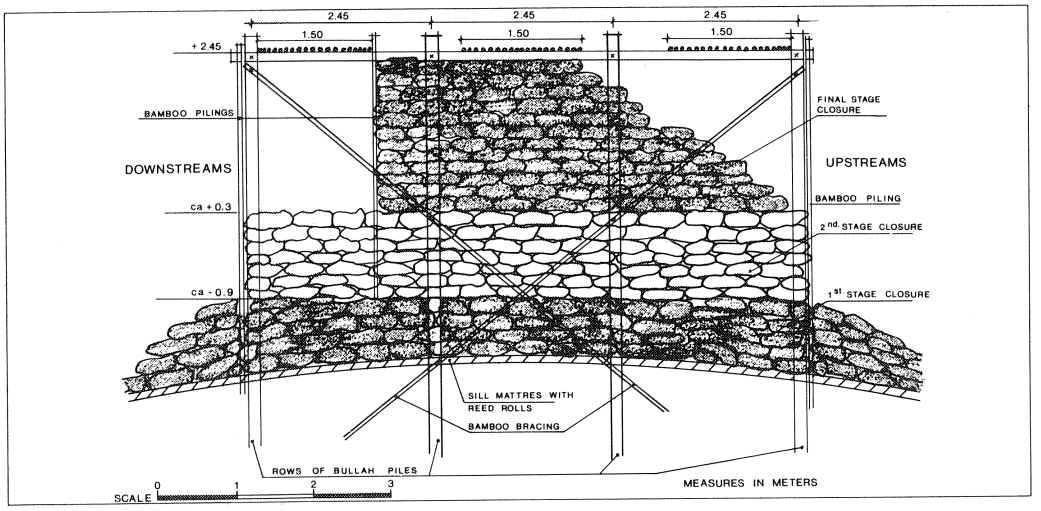

Figure 4.67. Cross-section jetty and coffer-dam.

Figure 4.68. Transportation of gunny bags over the jetty.

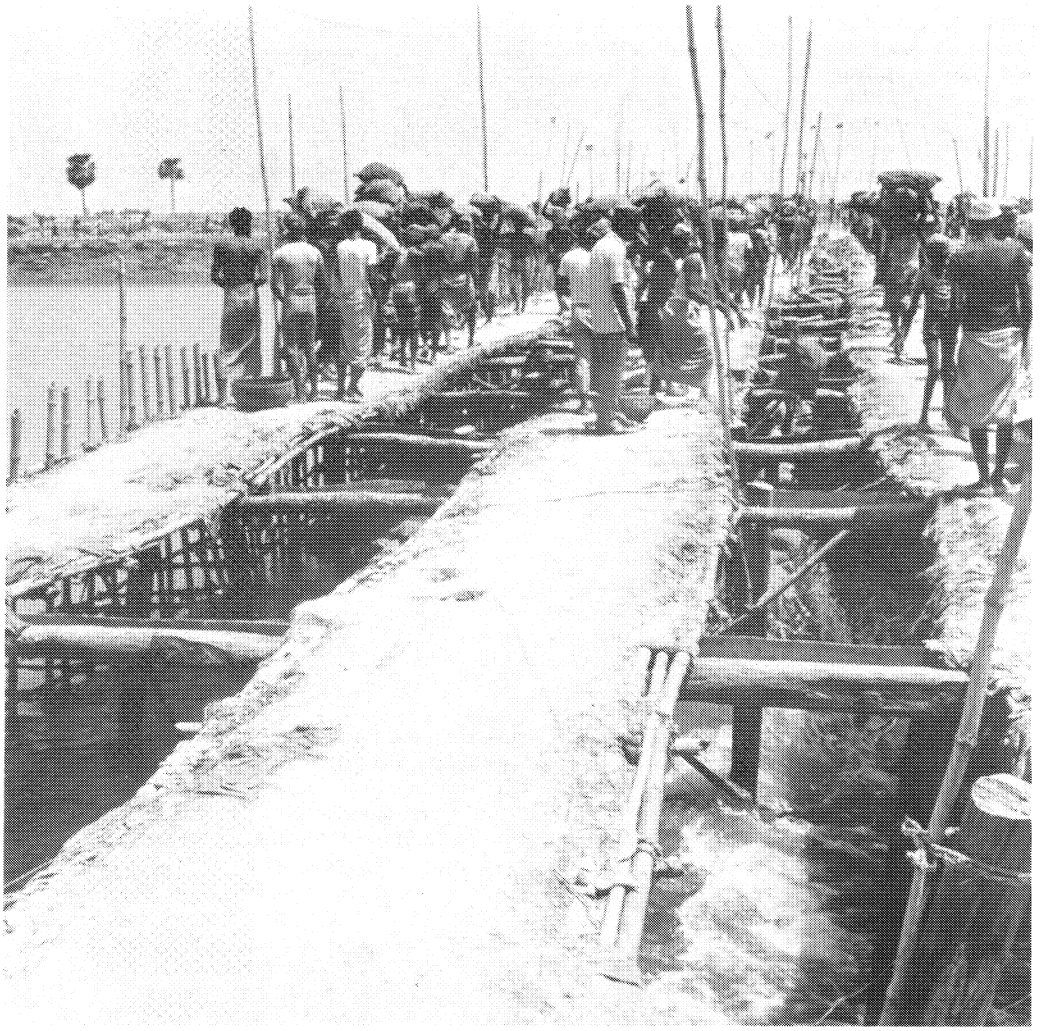

Figure 4.69. The jetty and the coffer-dam.

currents up to 2.5 m/s. The weak point of such an unprotected cross dam was the downstream slope. The bags could not be properly placed and levelled out on this slope, leading to the loss of bags due to rolling-away. It was decided on the second day of the final closure operation to use the 1200 bamboos to form a kind of coffer-dam of lattice-works formed by bamboo-pilings. A third row of bamboos was installed after the

final closure dam was raised above mean water level to decrease the load on the downstream outer bamboo piling.
The system of filling a cofferdam formed with bamboo pilings and a jetty with clay-filled jute bags to achieve the final stopping of the flow proved to be a reliable and easy method. Some scouring downstream of the most downstream piling caused by a waterjump gave some problems. This scouring could possibly have undermined the stability of the foot of the bamboo piling. Dumping of more bags on the place of scouring prevented this. The level of the walkways was such that the girders were just incorporated in the dam section, which resulted in leakage when the dam settled and the jetty did not. A total of 305,000 bags was dumped in four days by 1000 labourers to stop the flow.

Fill for final cross-section
The normal method of earth-fill in Bangladesh is the carrying of the fill material in baskets on the head. A gang of labourers forms a line between the borrowing pit and the fill area. Each member of the gang carried the filled baskets along a certain lead. The maximum distance of lead was about 30 m. The delivery rate is largely dependent on the distance between the borrowing pit and fill area and for a distance of about 150 m is about 1.5 m^3 per man per day. A reasonable production is only possible if the labourers walking to and fro are not obstructing each other. Each row of labourers requires a path width of about 1.5 m.
Each labour gang is paid on the basis of the quantity of excavation measured in the borrowing pit. The rather low production of each labourer makes it necessary to employ large numbers who require a lot of walking space. The walkways of the jetty must temporarily be used by the labourers carrying the earth-fill, after stopping the flow till the crest width of the dam is sufficiently large.

4.4.5 Contractual arrangements

Closure works in Bangladesh were carried out on the basis of the „no cure-no pay" principle. This rule had, however, a number of major drawbacks, such as:
- it plunged contractors responsible for a number of failed closures into great financial difficulty;
- it caused contractors to invest as little as possible in a closure in order to minimize their risks in the event of failure - although this of course also increased the chance of failure;
- it meant that the management in fact had no control over the way in which the work was carried out;
- it dissuaded banks and other financiers from providing backing.

The closure of the River Madargong was effected according to this principle. In the case of the closure of the Chakamaya-khal, for which the Dutch experts wished to introduce a different method, it was essential for a different contractual form to be employed if there was to be any assurance that the proposed method would be carried through.
For this closure a contract was drawn up that broadly corresponded to the customary contractual arrangements in the Netherlands, whereby a number of contractors are invited to tender.
The contract provided for payment in instalments, with a given percentage of the contract price being paid out as soon as the work had reached a certain stage. In order to ensure that contractors would not abandon the project prematurely, a bank guarantee was sought at the beginning of the work which was returnable upon project completion.